Structural Composite Materials

F.C. Campbell

ASM INTERNATIONAL®
The Materials Information Society

Structural Composite Materials

F.C. Campbell



ASM International®
Materials Park, Ohio 44073-0002
www.asminternational.org

Copyright © 2010
by
ASM International®
All rights reserved

No part of this book may be reproduced, stored in a retrieval system, or transmitted, in any form or by any means, electronic, mechanical, photocopying, recording, or otherwise, without the written permission of the copyright owner.

First printing, November 2010

Great care is taken in the compilation and production of this book, but it should be made clear that NO WARRANTIES, EXPRESS OR IMPLIED, INCLUDING, WITHOUT LIMITATION, WARRANTIES OF MERCHANTABILITY OR FITNESS FOR A PARTICULAR PURPOSE, ARE GIVEN IN CONNECTION WITH THIS PUBLICATION. Although this information is believed to be accurate by ASM, ASM cannot guarantee that favorable results will be obtained from the use of this publication alone. This publication is intended for use by persons having technical skill, at their sole discretion and risk. Since the conditions of product or material use are outside of ASM's control, ASM assumes no liability or obligation in connection with any use of this information. No claim of any kind, whether as to products or information in this publication, and whether or not based on negligence, shall be greater in amount than the purchase price of this product or publication in respect of which damages are claimed. THE REMEDY HEREBY PROVIDED SHALL BE THE EXCLUSIVE AND SOLE REMEDY OF BUYER, AND IN NO EVENT SHALL EITHER PARTY BE LIABLE FOR SPECIAL, INDIRECT OR CONSEQUENTIAL DAMAGES WHETHER OR NOT CAUSED BY OR RESULTING FROM THE NEGLIGENCE OF SUCH PARTY. As with any material, evaluation of the material under end-use conditions prior to specification is essential. Therefore, specific testing under actual conditions is recommended.

Nothing contained in this book shall be construed as a grant of any right of manufacture, sale, use, or reproduction, in connection with any method, process, apparatus, product, composition, or system, whether or not covered by letters patent, copyright, or trademark, and nothing contained in this book shall be construed as a defense against any alleged infringement of letters patent, copyright, or trademark, or as a defense against liability for such infringement.

Comments, criticisms, and suggestions are invited, and should be forwarded to ASM International.

Prepared under the direction of the ASM International Technical Book Committee (2009–2010), Michael J. Pfeifer, Chair.

ASM International staff who worked on this project include Scott Henry, Senior Manager, Content Development & Publishing; Steven R. Lampman, Content Developer; Eileen De Guire, Senior Content Developer; Ed Kubel, Technical Editor; Ann Britton, Editorial Assistant; Bonnie Sanders, Manager of Production; Madrid Tramble, Senior Production Coordinator; Diane Whitelaw, Production Coordinator; and Patricia Conti, Production Coordinator.

Library of Congress Control Number: 2010937090
ISBN-13: 978-1-61503-037-8
ISBN-10: 0-61503-037-9
SAN: 204-7586

ASM International®
Materials Park, OH 44073-0002
www.asminternational.org

Printed in the United States of America

This book is dedicated to my youngest granddaughter, Matilda,
who is so little yet is so brave and strong.

"*This page left intentionally blank.*"

Contents

Preface xi
About the Author xv

Chapter 1 Introduction to Composite Materials 1
1.1 Isotropic, Anisotropic, and Orthotropic Materials 4
1.2 Laminates 7
1.3 Fundamental Property Relationships 8
1.4 Composites versus Metallics 10
1.5 Advantages and Disadvantages of Composite Materials 14
1.6 Applications 18

Chapter 2 Fibers and Reinforcements 31
2.1 Fiber Terminology 31
2.2 Strength of Fibers 32
2.3 Glass Fibers 33
2.4 Aramid Fibers 39
2.5 Ultra-High Molecular Weight Polyethylene Fibers 41
2.6 Carbon and Graphite Fibers 42
2.7 Woven Fabrics 49
2.8 Reinforced Mats 52
2.9 Chopped Fibers 52
2.10 Prepreg Manufacturing 52

Chapter 3 Matrix Resin Systems 63
3.1 Thermosets 64
3.2 Polyester Resins 65
3.3 Epoxy Resins 67
3.4 Bismaleimide Resins 70
3.5 Cyanate Ester Resins 71
3.6 Polyimide Resins 72
3.7 Phenolic Resins 74
3.8 Toughened Thermosets 75
3.9 Thermoplastics 81
3.9.1 Thermoplastic Composite Matrices 82
3.9.2 Thermoplastic Composite Product Forms 87
3.10 Quality Control Methods 90
3.10.1 Chemical Testing 91
3.10.2 Rheological Testing 92
3.10.3 Thermal Analysis 94
3.10.4 Glass Transition Temperature 97
3.11 Summary 99

Chapter 4 Fabrication Tooling **101**
4.1 General Considerations 101
4.2 Thermal Management 104
4.3 Tool Fabrication 111

Chapter 5 Thermoset Composite Fabrication Processes **119**
5.0 Lay-up Processes 119
5.1 Wet Lay-Up 119
5.2 Prepreg Lay-Up 122
5.2.1 Manual Lay-Up 123
5.2.2 Flat Ply Collation and Vacuum Forming 124
5.2.3 Roll or Tape Wrapping 125
5.2.4 Automated Methods 125
5.2.5 Vacuum Bagging 131
5.2.6 Curing 133
5.3 Low-Temperature Curing/Vacuum Bag Systems 137
5.4 Filament Winding 141
5.5 Liquid Molding 146
5.5.1 Preform Technology 148
5.5.2 Resin Injection 162
5.5.3 Priform Process 164
5.5.4 RTM Curing 166
5.5.5 RTM Tooling 167
5.5.6 RTM Defects 170
5.5.7 Vacuum-Assisted Resin Transfer Molding 172
5.6 Resin Film Infusion 174
5.7 Pultrusion 175

Chapter 6 Thermoplastic Composite Fabrication Processes **183**
6.1 Thermoplastic Consolidation 183
6.2 Thermoforming 186
6.3 Thermoplastic Joining 192

Chapter 7 Processing Science of Polymer Matrix Composites **201**
7.1 Kinetics 202
7.2 Viscosity 206
7.3 Heat Transfer 207
7.4 Resin Flow 209
7.4.1 Hydrostatic Resin Pressure Studies 214
7.4.2 Resin Flow Modeling 217
7.5 Voids and Porosity 219
7.5.1 Condensation-Curing Systems 226
7.6 Residual Curing Stresses 226
7.7 Cure Monitoring Techniques 232

Chapter 8 Adhesive Bonding **235**
8.1 Theory of Adhesion 235
8.2 Surface Preparation 235
8.2.1 Composite Surface Preparation 237
8.2.2 Aluminum Surface Preparation 239
8.2.3 Titanium Surface Preparation 242
8.2.4 Aluminum and Titanium Primers 243
8.3 Epoxy Adhesives 244
8.3.1 Two-Part Room-Temperature Curing Epoxy Liquid and Paste Adhesives 245
8.3.2 Epoxy Film Adhesives 247

8.4 Bonding Procedures 248
8.4.1 Prekitting of Adherends 249
8.4.2 Prefit Evaluation 249
8.4.3 Adhesive Application 250
8.4.4 Bondline Thickness Control 251
8.4.5 Bonding 252

Chapter 9 Sandwich and Integral Cocured Structure 255
9.1 Sandwich Structure 255
9.2 Honeycomb Core Sandwich Structure 255
9.2.1 Honeycomb Processing 264
9.2.2 Cocured Honeycomb Assemblies 267
9.3 Foam Cores 271
9.3.1 Syntactic Core 272
9.4 Integrally Cocured Unitized Structure 273

Chapter 10 Discontinuous-Fiber Composites 285
10.1 Fiber Length and Orientation 285
10.2 Discontinuous-Fiber Composite Mechanics 287
10.3 Fabrication Methods 289
10.4 Spray-Up 289
10.5 Compression Molding 290
10.5.1 Thermoset Compression Molding 290
10.5.2 Thermoplastic Compression Molding 295
10.6 Structural Reaction Injection Molding 296
10.7 Injection Molding 297
10.7.1 Thermoplastic Injection Molding 298
10.7.2 Thermoset Injection Molding 304

Chapter 11 Machining and Assembly 307
11.1 Trimming and Machining Operations 307
11.2 General Assembly Considerations 309
11.3 Hole Preparation 311
11.3.1 Manual Drilling 311
11.3.2 Power Feed Drilling 314
11.3.3 Automated Drilling 315
11.3.4 Drill Bit Geometries 316
11.3.5 Reaming 317
11.3.6 Countersinking 317
11.4 Fastener Selection and Installation 318
11.4.1 Special Considerations for Composite Joints 320
11.4.2 Solid Rivets 322
11.4.3 Pin and Collar Fasteners 323
11.4.4 Bolts and Nuts 323
11.4.5 Blind Fasteners 326
11.4.6 Interference-Fit Fasteners 328
11.5 Sealing and Painting 329

Chapter 12 Nondestructive Inspection 333
12.1 Visual Inspection 333
12.2 Ultrasonic Inspection 335
12.3 Portable Equipment 341
12.4 Radiographic Inspection 342
12.5 Thermographic Inspection 345

Chapter 13 Mechanical Property Test Methods **351**
13.1 Specimen Preparation 351
13.2 Flexure Testing 352
13.3 Tension Testing 353
13.4 Compression Testing 354
13.5 Shear Testing 356
13.6 Open-Hole Tension and Compression 357
13.7 Bolt Bearing Strength 358
13.8 Flatwise Tension Test 361
13.9 Compression Strength After Impact 361
13.10 Fracture Toughness Testing 362
13.11 Adhesive Shear Testing 364
13.12 Adhesive Peel Testing 364
13.13 Honeycomb Flatwise Tension 367
13.14 Environmental Conditioning 367
13.15 Data Analysis 369

Chapter 14 Composite Mechanical Properties **373**
14.1 Glass Fiber Composites 374
14.2 Aramid Fiber Composites 376
14.3 Carbon Fiber Composites 379
14.4 Fatigue 383
14.5 Delaminations and Impact Resistance 388
14.6 Effects of Defects 393
14.6.1 Voids and Porosity 393
14.6.2 Fiber Distortion 397
14.6.3 Fastener Hole Defects 398

Chapter 15 Environmental Degradation **401**
15.1 Moisture Absorption 401
15.2 Fluids 411
15.3 Ultraviolet Radiation and Erosion 411
15.4 Lightning Strikes 412
15.5 Thermo-Oxidative Stability 415
15.6 Heat Damage 416
15.7 Flammability 417

Chapter 16 Structural Analysis **421**
16.1 Lamina or Ply Fundamentals 421
16.2 Stress-Strain Relationships for a Single Ply Loaded Parallel to the Material Axes ($\theta = 0°$ or $90°$) 425
16.3 Stress-Strain Relationships for a Single Ply Loaded Off-Axis to the Material Axes ($\theta \neq 0°$ or $90°$) 427
16.4 Laminates and Laminate Notations 429
16.5 Laminate Analysis—Classical Lamination Theory 430
16.6 Interlaminar Free-Edge Stresses 439
16.7 Failure Theories 440
16.8 Concluding Remarks 446

Chapter 17 Structural Joints—Bolted and Bonded **449**
17.1 Mechanically Fastened Joints 449
17.2 Mechanically Fastened Joint Analysis 450
17.3 Single-Hole Bolted Composite Joints 455
17.4 Multirow Bolted Composite Joints 459
17.5 Adhesive Bonding 463

17.6 Bonded Joint Design 464
17.7 Adhesive Shear Stress-Strain 466
17.8 Bonded Joint Design Considerations 475
17.9 Stepped-Lap Adhesively Bonded Joints 479
17.10 Bonded-Bolted Joints 481

Chapter 18 Design and Certification Considerations 489
18.1 Material Selection 489
18.2 Fiber Selection 490
18.3 Product Form Selection 491
18.3.1 Discontinuous-Fiber Product Forms 492
18.3.2 Continuous-Fiber Product Forms 493
18.4 Matrix Selection 494
18.5 Fabrication Process Selection 496
18.5.1 Discontinuous-Fiber Processes 496
18.5.2 Continuous-Fiber Processes 497
18.6 Trade Studies 498
18.7 Building Block Approach 499
18.8 Design Allowables 501
18.9 Design Guidelines 503
18.10 Damage Tolerance Considerations 508
18.11 Environmental Sensitivity Considerations 512

Chapter 19 Repair 517
19.1 Fill Repairs 517
19.2 Injection Repairs 517
19.3 Bolted Repairs 520
19.4 Bonded Repairs 523
19.5 Metallic Details and Metal-Bonded Assemblies 533

Chapter 20 Metal Matrix Composites 537
20.1 Aluminum Matrix Composites 540
20.2 Discontinuous Composite Processing Methods 542
20.3 Stir Casting 542
20.4 Slurry Casting—Compocasting 544
20.5 Liquid Metal Infiltration 545
20.5.1 Squeeze Casting 545
20.5.2 Pressure Infiltration Casting 545
20.5.3 Pressureless Infiltration 546
20.6 Spray Deposition 546
20.7 Powder Metallurgy Methods 548
20.8 Secondary Processing of Discontinuous MMCs 549
20.9 Continuous-Fiber Aluminum MMCs 550
20.10 Continuous-Fiber Reinforced Titanium Matrix Composites 554
20.11 Continuous-Fiber TMC Processing Methods 557
20.12 TMC Consolidation Procedures 560
20.13 Secondary Fabrication of TMCs 562
20.14 Particle-Reinforced TMCs 566
20.15 Fiber Metal Laminates 567

Chapter 21 Ceramic Matrix Composites 573
21.1 Reinforcements 575
21.2 Matrix Materials 578
21.3 Interfacial Coatings 580
21.4 Fiber Architectures 580

21.5 Fabrication Methods 581
21.6 Powder Processing 581
21.7 Slurry Infiltration and Consolidation 583
21.8 Polymer Infiltration and Pyrolysis (PIP) 584
21.8.1 Space Shuttle C-C Process 585
21.8.2 Conventional PIP Processes 587
21.8.3 Sol-Gel Infiltration 588
21.9 Chemical Vapor Infiltration (CVI) 589
21.10 Directed Metal Oxidation (DMO) 592
21.11 Liquid Silicon Infiltration (LSI) 594

Appendix A Metric Conversion Factors 597
Index 599

Preface

Composite materials are pervasive throughout our world and include both natural and man-made composites. For example, in nature, wood is a composite consisting of wood fibers (cellulose) bound together by a matrix of lignin. Composite materials have been used by mankind for thousands of years; many of the sun-dried mud brick buildings of the earliest known civilization in Mesopotamia at Sumer were reinforced with straw as early as 4900 B.C. However, with the advent of high-strength man-made fibers and the tremendous advances in polymer chemistry during the twentieth century, in many instances composite materials now can be made that offer advantages comparable to those of competing materials. The advantages of these advanced composites are many, including lighter weight, the ability to tailor composites for optimum strength and stiffness, improved fatigue life, corrosion resistance, and, with good design practice, reduced assembly costs due to fewer detail parts and fasteners. The specific strength (strength/density) and specific modulus (modulus/density) of high-strength fiber-reinforced composites, especially those with carbon fibers, are higher than those of comparable metal alloys. This translates into greater weight savings, resulting in improved performance, greater payloads, longer ranges (for vehicles), and fuel savings.

This book is intended primarily for technical personnel who want to learn more about modern composite materials. It would be useful to designers, structural engineers, materials and process engineers, manufacturing engineers, and production personnel involved with composites.

The book deals with all aspects of advanced composite materials: what they are, where they are used, how they are made, their properties, how they are designed and analyzed, and how they perform in service. It covers continuous- and discontinuous-fiber composites fabricated from polymer, metal, and ceramic matrices, with an emphasis on continuous-fiber polymer matrix composites. The book covers composite materials at the introductory to intermediate level. Throughout the book, practical aspects are emphasized more than theory. Because I spent 38 years in the industry, the information covers the current state-of-the-art in composite materials.

The book starts with an overview of composite materials (Chapter 1) and how highly anisotropic composites differ from isotropic materials, such as metals. Some of the important advantages and disadvantages of composites are discussed. Chapter 1 wraps up with some of the applications for advanced composites. Chapter 2 examines the reinforcements and their product forms, with an emphasis on glass, aramid, and carbon fibers. Chapter 3 covers the main thermosetting and thermoplastic resin systems. Thermoset resin systems include polyesters, vinyl esters, epoxies, bismaleimides, cynate esters, polyimides, and phenolics. Thermoplastic composite matrices include polyetheretherketone, polyetherketoneketone, polyetherimide, and polypropylene. The principles of thermoset resin toughening are also presented, along with an introduction to the physiochemical tests that are used to characterize resins and cured laminates.

Chapters 4 through 11 describe the progression of composite fabrication steps. Chapter 4 covers the basics of cure tools. This is followed by a discussion of thermoset composite fabrication processes (Chapter 5). Important thermoset lay-up methods include wet lay-up, prepreg lay-up, automated tape laying, fiber placement, filament winding, and pultrusion. Vacuum bagging in preparation for cure is also discussed, along with the cure processes for both addition and condensation curing thermosets. Thermoset liquid molding covers preforming technology (weaving, knitting, stitching, and braiding) followed by the major liquid molding processes, namely, resin transfer molding, resin film infusion, and vacuum-assisted resin transfer molding.

In Chapter 6, thermoplastic composite consolidation is covered, along with the different methods of thermoforming thermoplastics. Finally, the joining processes that are unique to thermoplastic composites are discussed. After these processing fundamentals are fully described, Chapter 7 deals with some of the detailed processing issues unique to thermoset and thermoplastic composites. The concept of cure modeling is introduced along with the importance of both lay-up and cure variables, hydrostatic resin pressure, chemical composition, resin and prepreg, debulking, and caul plates. Residual cure stresses and exothermic reactions are also covered, followed by a brief description of in-process cure monitoring.

Adhesive bonding, sandwich, and integrally cocured structures are introduced in Chapters 8 and 9. The basics of adhesive bonding are covered, along with its advantages and disadvantages. The importance of joint design, surface preparation, and bonding procedures is discussed, along with honeycomb bonded assemblies, foam bonded assemblies, and integrally cocured assemblies. Large, one-piece composite airframe structures have demonstrated the potential for impressive reductions in part counts and assembly costs.

The properties and fabrication technology for discontinuous-fiber polymer matrix composites are addressed in Chapter 10, with an emphasis on spray-up, compression molding, structural reaction injection molding, and injection molding.

Assembly (Chapter 11) can represent a significant portion of the total manufacturing cost, as much as 50 percent of the total delivered cost. In this chapter, the emphasis is on mechanical joining, including the hole preparation procedures and fasteners used for structural assembly. Sealing and painting are also briefly discussed.

Chapters 12 through 15 cover the test methods and properties for composite materials. Important nondestructive test methods (Chapter 12) include visual, ultrasonics, radiographic, and thermographic inspection methods. Mechanical property test methods (Chapter 13) include tests for both composite materials and adhesive systems. In Chapter 14, the strength and stiffness for both discontinuous and continuous reinforced composites are compared. Chapter 15 covers the important topic of environmental degradation, including moisture absorption, fluids exposure, ultraviolet radiation and erosion, lightning strikes, thermo-oxidative behavior, heat damage, and flammability.

Chapters 16 through 19 cover the analysis, design, and repair of composites. Structural analysis (Chapter 16) starts with analysis at the lamina, or ply, level and then uses classical lamination theory to illustrate the analysis methods for more complex laminates. The concept of interlaminar free edge stresses is introduced. Four failure theories are discussed: the maximum stress criterion, the maximum strain criterion, the Azzi-Tsai-Hill maximum work theory, and the Tsai-Wu failure criterion. The important topic of analysis of composite joints, both bolted and bonded, is covered in Chapter 17. Chapter 18 deals with composite design and certification considerations, including materials and process selection, design trade studies, the building block approach to certification, design allowables, and design guidelines. Considerations for handling damage tolerance and environmental issues are also discussed. Repair of composites (Chapter 19) includes fill repairs, injection repairs, bolted repairs, and bonded repairs.

Metal matrix composites (Chapter 20) offer a number of advantages compared to their base metals, such as higher specific strengths and moduli, higher elevated-temperature resistance, lower coefficients of thermal expansion, and, in some cases, better wear re-

sistance. On the downside, they are more expensive than their base metals and have lower toughness. Because of their high costs, commercial applications for metal matrix composites are limited. As with metal matrix composites, there are few commercial applications for ceramic matrix composites (Chapter 21), also because of their high costs, as well as concerns for reliability. Carbon-carbon composites have been used in aerospace applications for thermal protection systems. However, metal and ceramic matrix composites remain an important material class, because they are considered enablers for future hypersonic flight vehicles.

The reader is cautioned that the data presented in this book are not design allowables. The reader should consult approved design manuals for statistically derived design allowables.

I would like to acknowledge the help and guidance of Ann Britton, Eileen De Guire, Steve Lampman, and Madrid Tramble, ASM International, and the staff at ASM for their valuable contributions. I would also like to thank my wife, Betty, for her continuing support.

F.C. Campbell
St. Louis, Missouri
July 2010

"*This page left intentionally blank.*"

About the Author

F.C. Campbell's 38-year career at The Boeing Company (retired 2007) was closely divided equally between engineering and manufacturing. He worked in the engineering laboratories, manufacturing research and development, as well as engineering on four production aircraft programs, and in production operations. At the time of his retirement, he was a Senior Technical Fellow in the field of structural materials and manufacturing technology. He is knowledgeable about a large number of materials, fabrication, and assembly processes for airframe structural materials. Previously, he was director of manufacturing process improvement (1995–2000), and from 1987–1995, he was director of manufacturing research engineering. Earlier in his career, he worked in materials and process development with responsibility for composite related research and development programs. He has also worked on the F-15, F/A-18, AV-8B, and C-17 aircraft programs, conducted manufacturing research on composite and metallic materials, and worked as a laboratory engineer doing process development on both metal matrix and organic matrix composite materials.

"*This page left intentionally blank.*"

Copyright © 2010, ASM International®
All rights reserved.
www.asminternational.org

CHAPTER 1

Introduction to Composite Materials

A COMPOSITE MATERIAL can be defined as a combination of two or more materials that results in better properties than those of the individual components used alone. In contrast to metallic alloys, each material retains its separate chemical, physical, and mechanical properties. The two constituents are a reinforcement and a matrix. The main advantages of composite materials are their high strength and stiffness, combined with low density, when compared with bulk materials, allowing for a weight reduction in the finished part.

The reinforcing phase provides the strength and stiffness. In most cases, the reinforcement is harder, stronger, and stiffer than the matrix. The reinforcement is usually a fiber or a particulate. Particulate composites have dimensions that are approximately equal in all directions. They may be spherical, platelets, or any other regular or irregular geometry. Particulate composites tend to be much weaker and less stiff than continuous-fiber composites, but they are usually much less expensive. Particulate reinforced composites usually contain less reinforcement (up to 40 to 50 volume percent) due to processing difficulties and brittleness.

A fiber has a length that is much greater than its diameter. The length-to-diameter (l/d) ratio is known as the *aspect ratio* and can vary greatly. Continuous fibers have long aspect ratios, while discontinuous fibers have short aspect ratios. Continuous-fiber composites normally have a preferred orientation, while discontinuous fibers generally have a random orientation. Examples of continuous reinforcements include unidirectional, woven cloth, and helical winding (Fig. 1.1a), while examples of discontinuous reinforcements are chopped fibers and random mat (Fig. 1.1b). Continuous-fiber composites are often made into laminates by stacking single sheets of continuous fibers in different orientations to obtain the desired strength and stiffness properties with fiber volumes as high as 60 to 70 percent. Fibers produce high-strength composites because of their small diameter; they contain far fewer defects (normally surface defects) compared to the material produced in bulk. As a general rule, the smaller the diameter of the fiber, the higher its strength, but often the cost increases as the diameter becomes smaller. In addition, smaller-diameter high-strength fibers have greater flexibility and are more amenable to fabrication processes such as weaving or forming over radii. Typical fibers include glass, aramid, and carbon, which may be continuous or discontinuous.

The continuous phase is the matrix, which is a polymer, metal, or ceramic. Polymers have low strength and stiffness, metals have intermediate strength and stiffness but high ductility, and ceramics have high strength and stiffness but are brittle. The matrix (continuous phase) performs several critical functions, including maintaining the fibers in the proper orientation and spacing and protecting them from abrasion and the environment. In polymer and metal matrix composites that form a strong bond between the fiber and the matrix, the matrix transmits loads from the matrix to the fibers through shear loading at the interface. In ceramic matrix composites, the objective is often to increase the toughness rather than the strength and stiffness; therefore, a low interfacial strength bond is desirable.

The type and quantity of the reinforcement determine the final properties. Figure 1.2 shows that the highest strength and modulus are obtained with continuous-fiber composites. There is a practical limit of about 70 volume percent reinforcement that can be added to form a composite. At higher percentages, there is too little matrix to support the fibers effectively. The theoretical

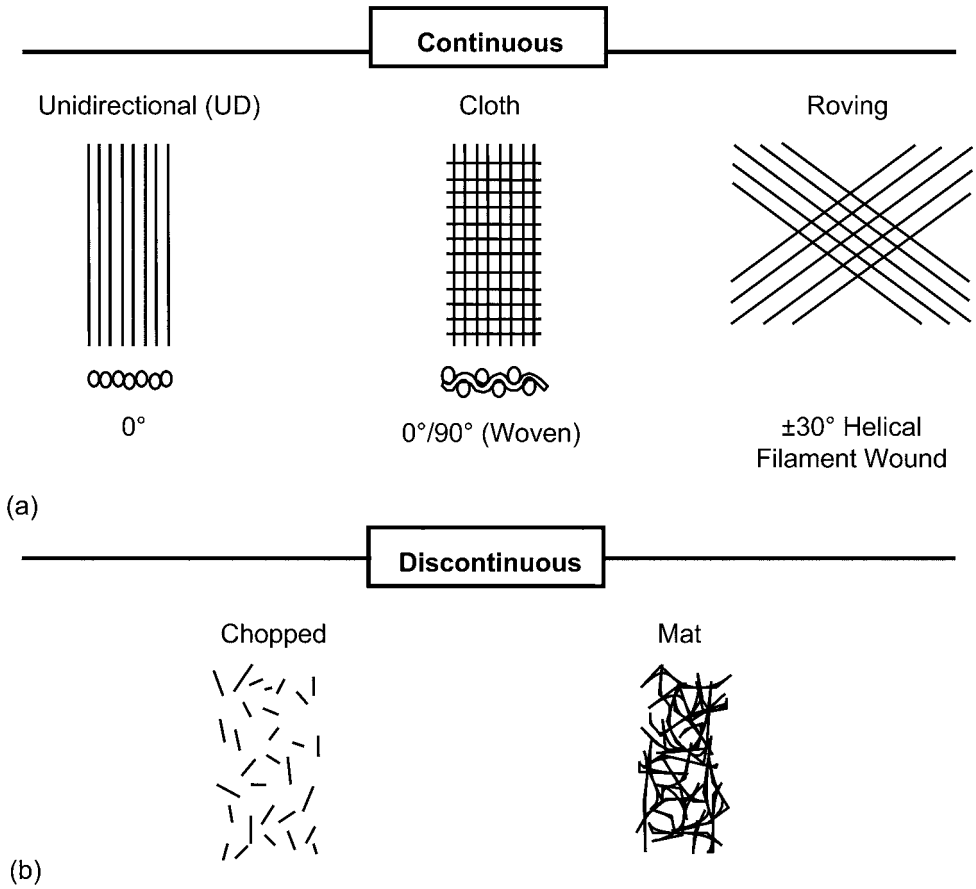


Fig. 1.1 Typical reinforcement types

strength of discontinuous-fiber composites can approach that of continuous-fiber composites if their aspect ratios are great enough and they are aligned, but it is difficult in practice to maintain good alignment with discontinuous fibers. Discontinuous-fiber composites are normally somewhat random in alignment, which dramatically reduces their strength and modulus. However, discontinuous-fiber composites are generally much less costly than continuous-fiber composites. Therefore, continuous-fiber composites are used where higher strength and stiffness are required (but at a higher cost), and discontinuous-fiber composites are used where cost is the main driver and strength and stiffness are less important.

Both the reinforcement type and the matrix affect processing. The major processing routes for polymer matrix composites are shown in Fig. 1.3. Two types of polymer matrices are shown: thermosets and thermoplastics. A thermoset starts as a low-viscosity resin that reacts and cures during processing, forming an intractable solid. A thermoplastic is a high-viscosity resin that is processed by heating it above its melting temperature. Because a thermoset resin sets up and cures during processing, it cannot be reprocessed by reheating. By comparison, a thermoplastic can be reheated above its melting temperature for additional processing. There are processes for both classes of resins that are more amenable to discontinuous fibers and others that are more amenable to continuous fibers. In general, because metal and ceramic matrix composites require very high temperatures and sometimes high pressures for processing, they are normally much more expensive than polymer matrix composites. However, they have much better thermal stability, a requirement in applications where the composite is exposed to high temperatures.

This book will deal with both continuous and discontinuous polymer, metal, and ceramic matrix

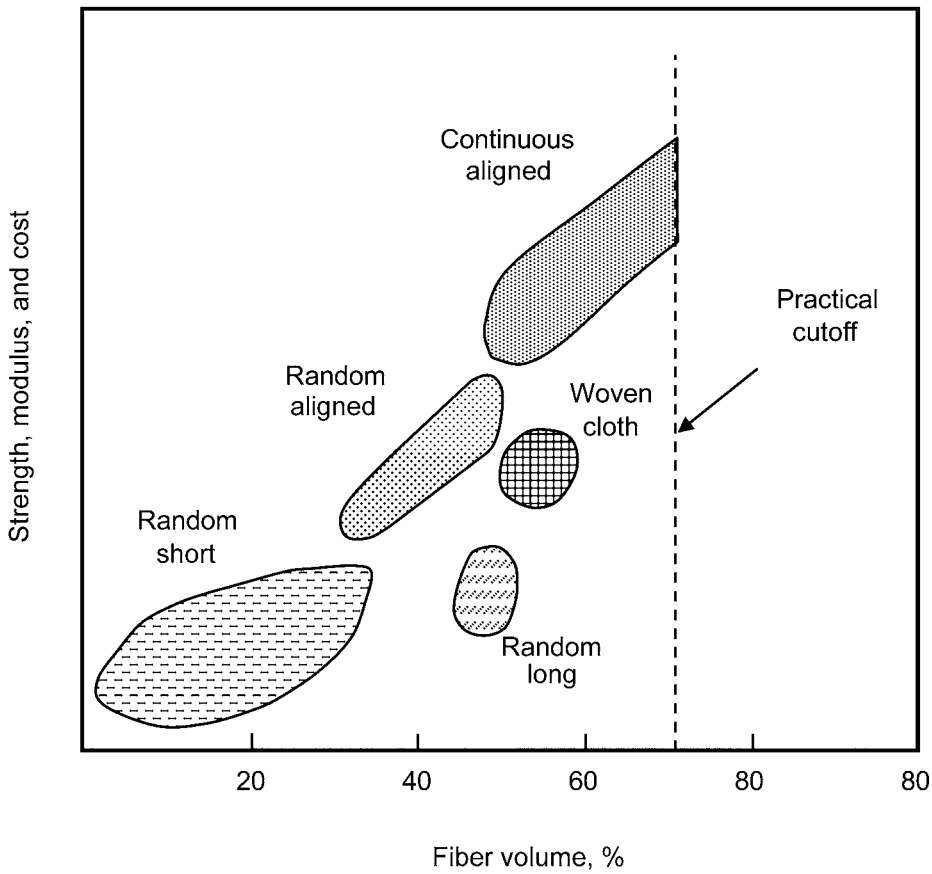


Fig. 1.2 Influence of reinforcement type and quantity on composite performance

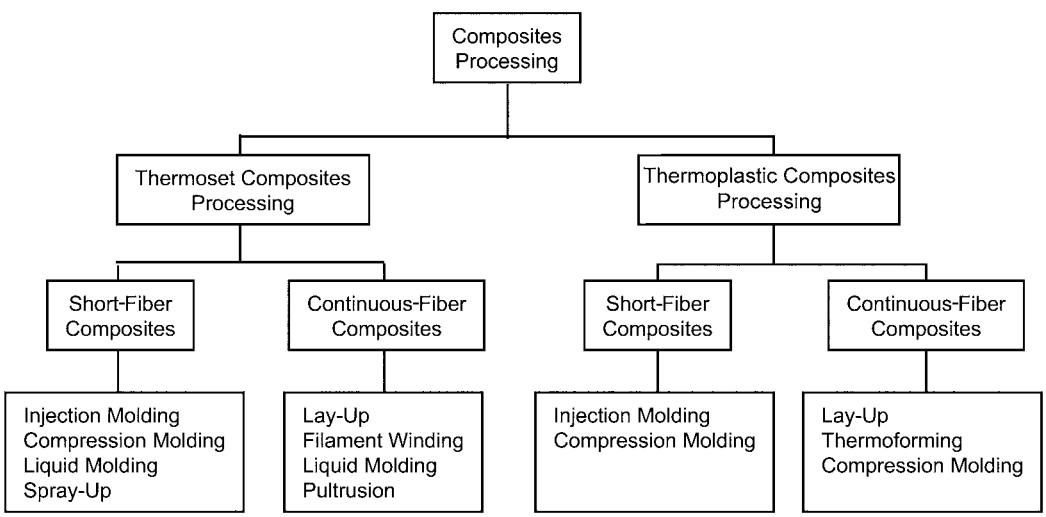


Fig. 1.3 Major polymer matrix composite fabrication processes

composites, with an emphasis on continuous-fiber, high-performance polymer composites.

1.1 Isotropic, Anisotropic, and Orthotropic Materials

Materials can be classified as either isotropic or anisotropic. Isotropic materials have the same material properties in all directions, and normal loads create only normal strains. By comparison, anisotropic materials have different material properties in all directions at a point in the body. There are no material planes of symmetry, and normal loads create both normal strains and shear strains. A material is isotropic if the properties are independent of direction within the material.

For example, consider the element of an isotropic material shown in Fig. 1.4. If the material is loaded along its 0°, 45°, and 90° directions, the modulus of elasticity (E) is the same in each direction ($E_{0°} = E_{45°} = E_{90°}$). However, if the material is anisotropic (for example, the composite ply shown in Fig. 1.5**)**, it has properties that vary with direction within the material. In this example, the moduli are different in each direction ($E_{0°} \neq E_{45°} \neq E_{90°}$). While the modulus of elasticity is used in the example, the same dependence on direction can occur for other material properties, such as ultimate strength, Poisson's ratio, and thermal expansion coefficient.

Bulk materials, such as metals and polymers, are normally treated as isotropic materials, while composites are treated as anisotropic. However, even bulk materials such as metals can become anisotropic—for example, if they are highly cold worked to produce grain alignment in a certain direction.

Consider the unidirectional fiber-reinforced composite ply (also known as a *lamina*) shown in Fig. 1.6. The coordinate system used to describe the ply is labeled the *1-2-3 axes*. In this case, the 1-axis is defined to be parallel to the fibers (0°), the 2-axis is defined to lie within the plane of the plate and is perpendicular to the fibers (90°), and the 3-axis is defined to be normal

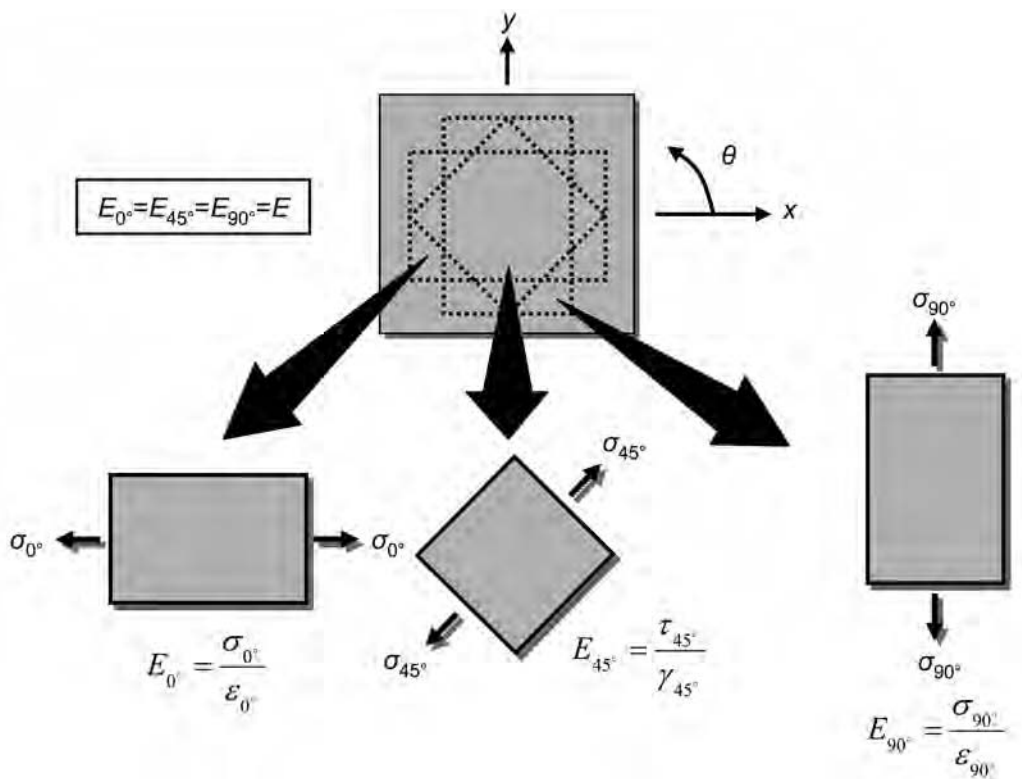


Fig. 1.4 Element of isotropic material under stress

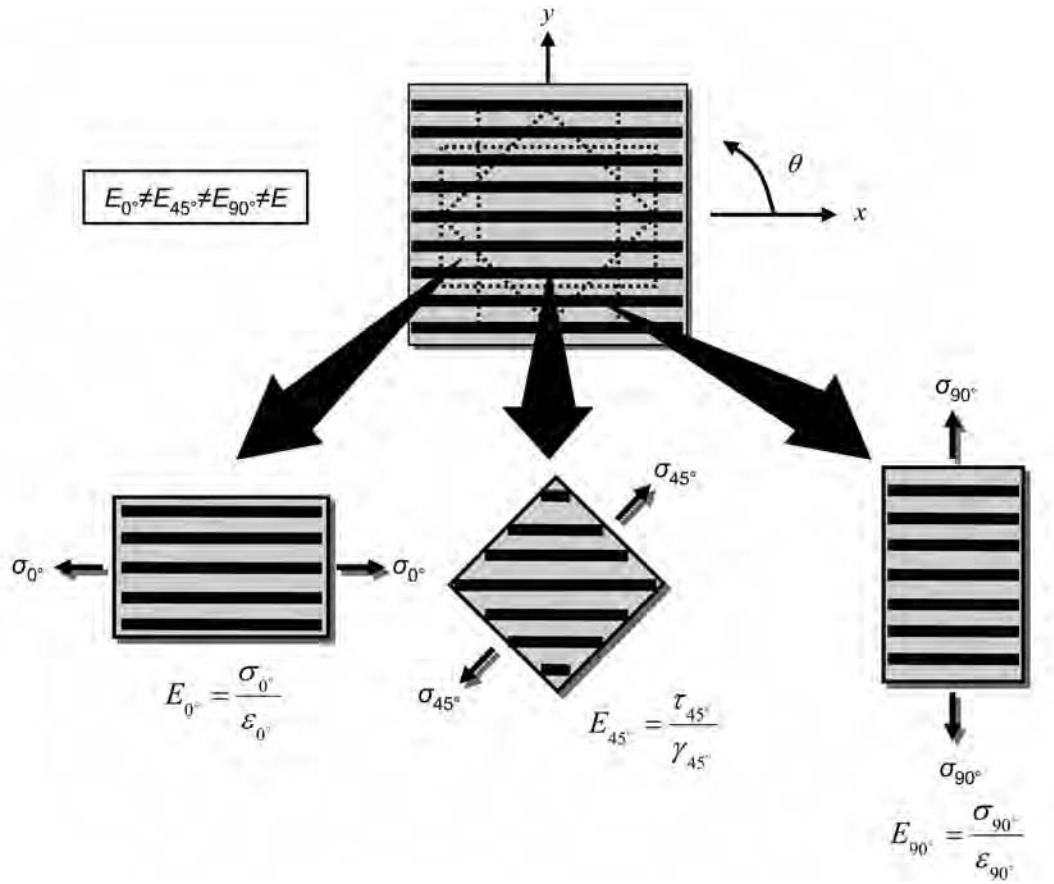


Fig. 1.5 Element of composite ply material under stress

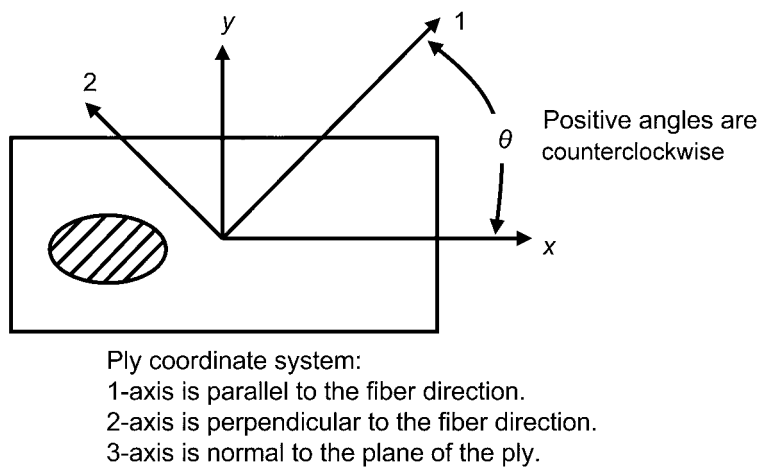


Fig. 1.6 Ply angle definition

to the plane of the plate. The 1-2-3 coordinate system is referred to as the *principal material coordinate system*. If the plate is loaded parallel to the fibers (one- or zero-degree direction), the modulus of elasticity E_{11} approaches that of the fibers. If the plate is loaded perpendicular to the fibers in the two- or 90-degree direction, the modulus E_{22} is much lower, approaching that of the relatively less stiff matrix. Since $E_{11} >> E_{22}$ and the modulus varies with direction within the material, the material is anisotropic.

Composites are a subclass of anisotropic materials that are classified as orthotropic. Orthotropic materials have properties that are different in three mutually perpendicular directions. They have three mutually perpendicular axes of symmetry, and a load applied parallel to these axes produces only normal strains. However, loads that are not applied parallel to these axes produce both normal and shear strains. Therefore, orthotropic mechanical properties are a function of orientation.

Consider the unidirectional composite shown in the upper portion of Fig. 1.7, where the unidirectional fibers are oriented at an angle of 45 degrees with respect to the *x*-axis. In the small, isolated square element from the gage region, because the element is initially square (in this example), the fibers are parallel to diagonal AD of the element. In contrast, fibers are perpendicular to diagonal BC. This implies that the element is stiffer along diagonal AD than along diagonal BC. When a tensile stress is applied, the square element deforms. Because the stiffness is higher along diagonal AD than along diagonal BC, the length of diagonal AD is not increased as much as that of diagonal BC. Therefore, the initially square element deforms into the shape of a parallelogram. Because the element has been distorted into a parallelogram, a shear strain γ_{xy} is induced as a result of coupling between the axial strains ε_{xx} and ε_{yy}.

If the fibers are aligned parallel to the direction of applied stress, as in the lower portion of

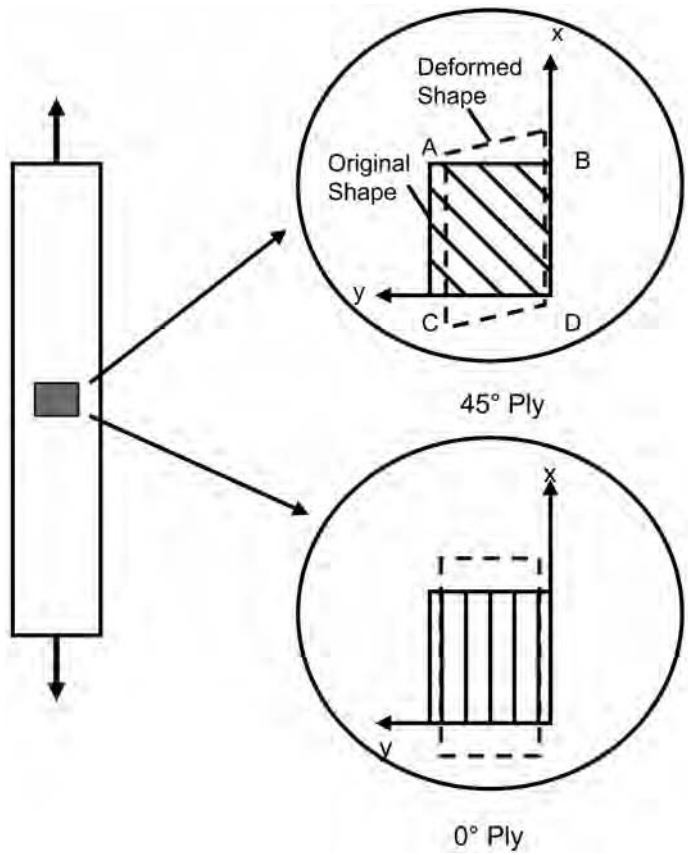


Fig. 1.7 Shear coupling in a 45° ply. Source: Ref 1

Fig. 1.7, the coupling between ε_{xx} and ε_{yy} does not occur. In this case, the application of a tensile stress produces elongation in the *x*-direction and contraction in the *y*-direction, and the distorted element remains rectangular. Therefore, the coupling effects exhibited by composites occur only if stress and strain are referenced to a non–principal material coordinate system. Thus, when the fibers are aligned parallel (0°) or perpendicular (90°) to the direction of applied stress, the lamina is known as a *specially orthotropic lamina* ($\theta = 0°$ or 90°). A lamina that is not aligned parallel or perpendicular to the direction of applied stress is called a *general orthotropic lamina* ($\theta \neq 0°$ or 90°).

1.2 Laminates

When there is a single ply or a lay-up in which all of the layers or plies are stacked in the same orientation, the lay-up is called a *lamina*. When the plies are stacked at various angles, the lay-up is called a *laminate*. Continuous-fiber composites are normally laminated materials (Fig. 1.8) in which the individual layers, plies, or laminae are oriented in directions that will enhance the strength in the primary load direction. Unidirectional (0°) laminae are extremely strong and stiff in the 0° direction. However, they are very weak in the 90° direction because the load must be carried by the much weaker polymeric matrix. While a high-strength fiber can have a tensile strength of 500 ksi (3500 MPa) or more, a typical polymeric matrix normally has a tensile strength of only 5 to 10 ksi (35 to 70 MPa) (Fig. 1.9). The longitudinal tension and compression loads are carried by the fibers, while the matrix distributes the loads between the fibers in tension and stabilizes the fibers and prevents them from buckling in compression. The matrix is also the primary load carrier for interlaminar shear (i.e., shear between the layers) and transverse (90°) tension. The relative roles of the fiber and the matrix in detemining mechanical properties are summarized in Table 1.1.

Because the fiber orientation directly impacts mechanical properties, it seems logical to orient

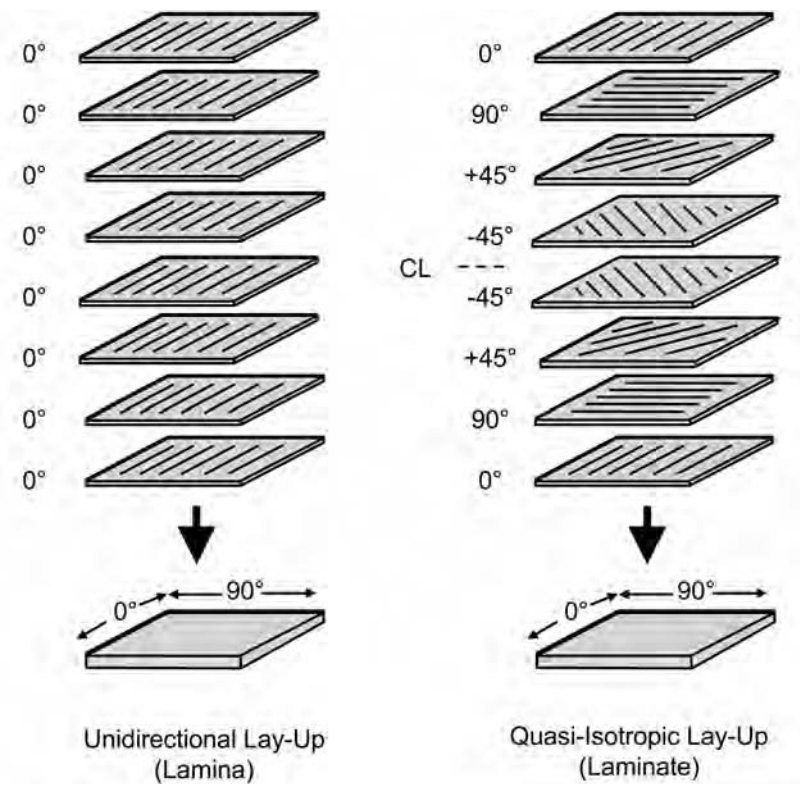


Fig. 1.8 Lamina and laminate lay-ups

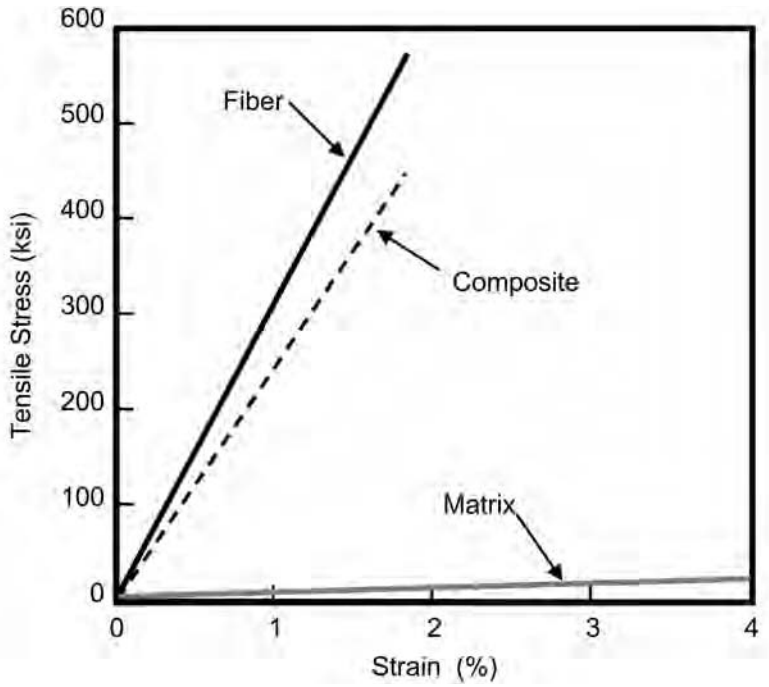


Fig. 1.9 Comparison of tensile properties of fiber, matrix, and composite

Table 1.1 Effect of fiber and matrix on mechanical properties

	Dominating composite constituent	
Mechanical property	**Fiber**	**Matrix**
Unidirectional		
0° tension	√	…
0° compression	√	√
Shear	…	√
90° tension	…	√
Laminate		
Tension	√	…
Compression	√	√
In-plane shear	√	√
Interlaminar shear	…	√

as many of the layers as possible in the main load-carrying direction. While this approach may work for some structures, it is usually necessary to balance the load-carrying capability in a number of different directions, such as the 0°, +45°, –45°, and 90° directions. Figure 1.10 shows a photomicrograph of a cross-plied continuous carbon fiber/epoxy laminate. A balanced laminate having equal numbers of plies in the 0°, +45°, –45°, and 90° degrees directions is called a *quasi-isotropic laminate*, because it carries equal loads in all four directions.

1.3 Fundamental Property Relationships

When a unidirectional continuous-fiber lamina or laminate (Fig. 1.11) is loaded in a direction parallel to its fibers (0° or 11-direction), the longitudinal modulus E_{11} can be estimated from its constituent properties by using what is known as the *rule of mixtures*:

$$E_{11} = E_f V_f + E_m V_m \quad \text{(Eq 1.1)}$$

where E_f is the fiber modulus, V_f is the fiber volume percentage, E_m is the matrix modulus, and V_m is the matrix volume percentage.

The longitudinal tensile strength σ_{11} also can be estimated by the rule of mixtures:

$$\sigma_{11} = \sigma V_f + \sigma_m V_m \quad \text{(Eq 1.2)}$$

where σ_f and σ_m are the ultimate fiber and matrix strengths, respectively. Because the properties of the fiber dominate for all practical volume percentages, the values of the matrix can often be ignored; therefore:

$$E_{11} \approx E_f V_f \quad \text{(Eq 1.3)}$$

$$\sigma_{11} \approx \sigma V_f \quad \text{(Eq 1.4)}$$

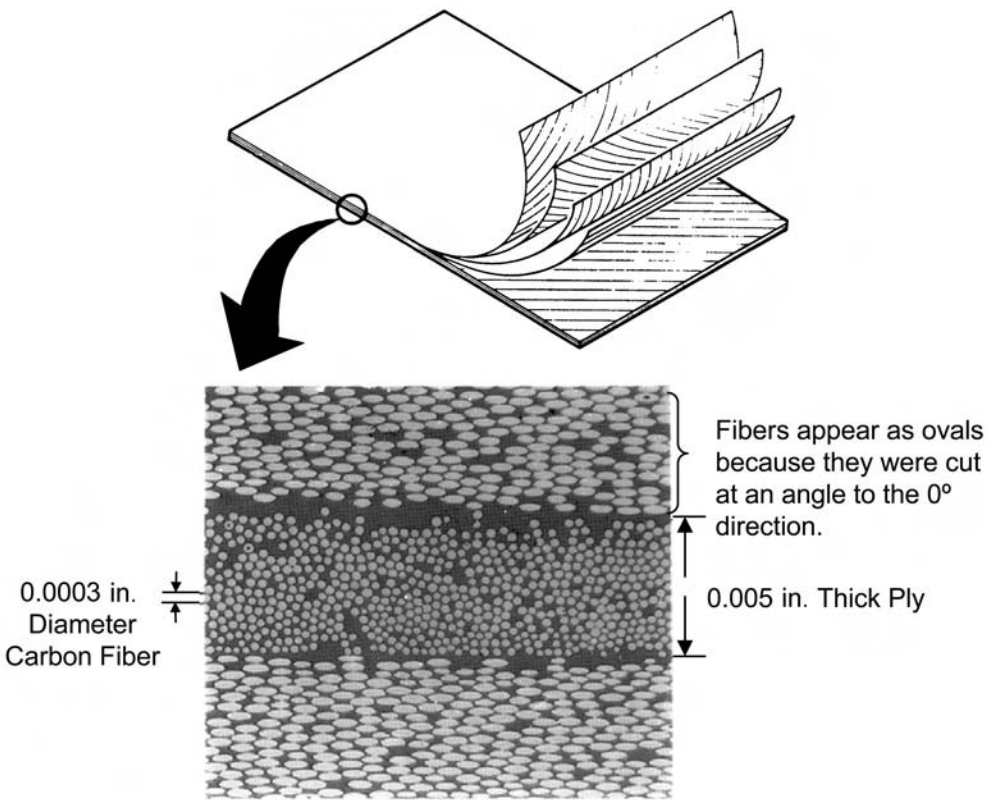


Fig. 1.10 Cross section of a cross-plied carbon/epoxy laminate

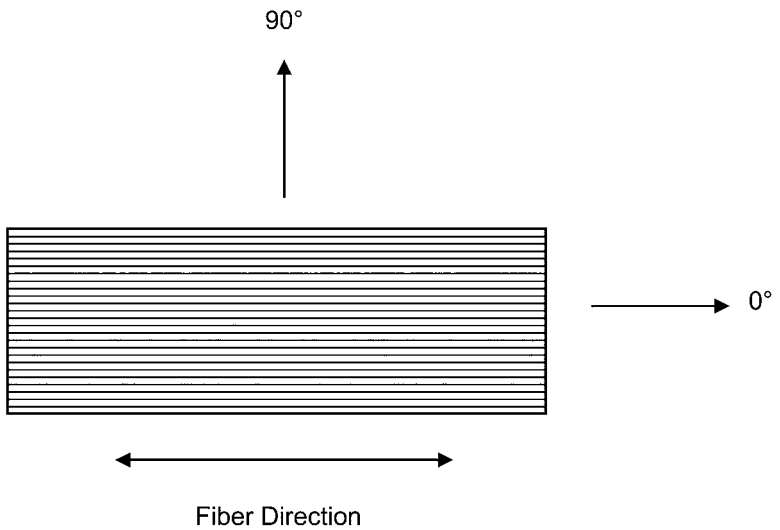


Fig. 1.11 Unidirectional continuous-fiber lamina or laminate

Figure 1.12 shows the dominant role of the fibers in determining strength and stiffness. When loads are parallel to the fibers (0°), the ply is much stronger and stiffer than when loads are transverse (90°) to the fiber direction. There is a dramatic decrease in strength and stiffness resulting from only a few degrees of misalignment off of 0°.

When the lamina shown in Fig. 1.11 is loaded in the transverse (90° or 22-direction), the fibers and the matrix function in series, with both carrying the same load. The transverse modulus of elasticity E_{22} is given as:

$$1/E_{22} = V_f/E_f + V_m/E_m \quad \text{(Eq 1.5)}$$

Figure 1.13 shows the variation of modulus as a function of fiber volume percentage. When the fiber percentage is zero, the modulus is essentially the modulus of the polymer, which increases up to 100 percent (where it is the modulus of the fiber). At all other fiber volumes, the E_{22} or 90° modulus is lower than the E_{11} or zero degrees modulus, because it is dependent on the much weaker matrix.

Other rule of mixture expressions for lamina properties include those for the Poisson's ratio ν_{12} and for the shear modulus G_{12}:

$$\nu_{12} = \nu_f V_f + \nu_m V_m \quad \text{(Eq 1.6)}$$

$$1/G_{12} = V_f/G_f + V_m/G_m \quad \text{(Eq 1.7)}$$

These expressions are somewhat less useful than the previous ones, because the values for Poisson's ratio (ν_f) and the shear modulus (G_f) of the fibers are usually not readily available.

Physical properties, such as density (ρ), can also be expressed using rule of mixture relations:

$$\rho_{12} = \rho_f V_f + \rho_m V_m \quad \text{(Eq 1.8)}$$

While these micromechanics equations are useful for a first estimation of lamina properties when no data are available, they generally do not yield sufficiently accurate values for design purposes. For design purposes, basic lamina and laminate properties should be determined using actual mechanical property testing.

1.4 Composites versus Metallics

As previously discussed, the physical characteristics of composites and metals are significantly different. Table 1.2 compares some properties of composites and metals. Because composites are highly anisotropic, their in-plane strength and

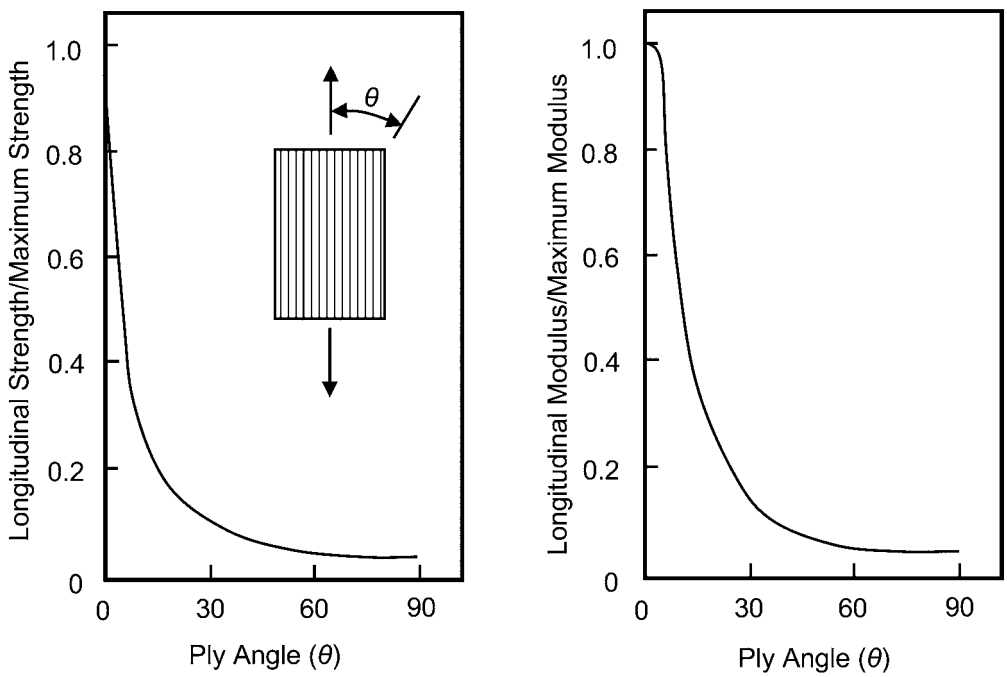


Fig. 1.12 Influence of ply angle on strength and modulus

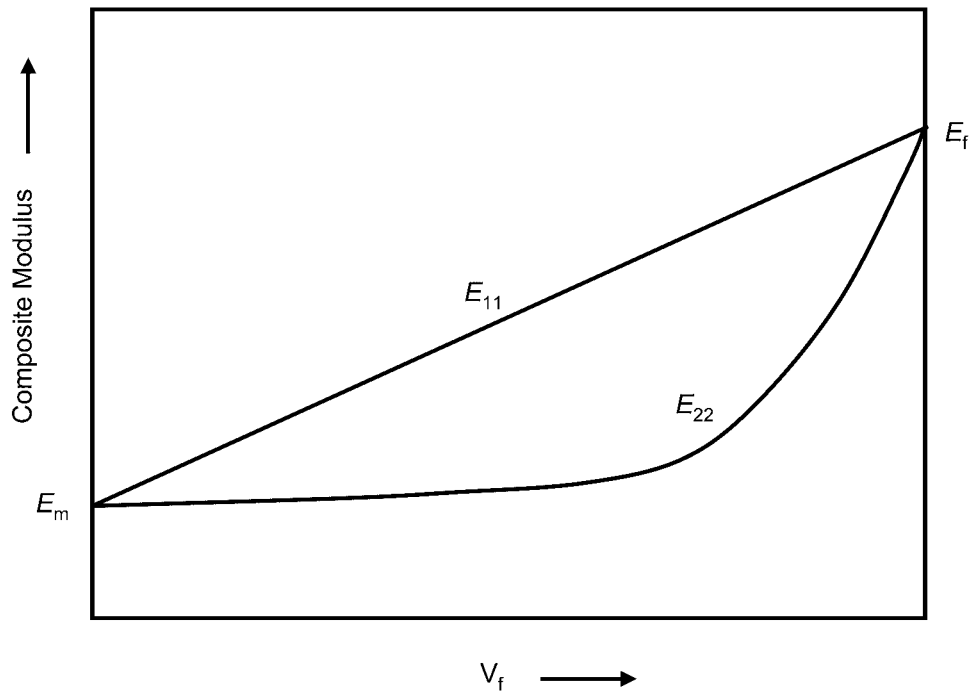


Fig. 1.13 Variation of composite modulus of a unidirectional 0° lamina as a function of fiber volume fraction

Table 1.2 Composites versus metals comparison

Condition	Comparative behavior relative to metals
Load-strain relationship	More linear strain to failure
Notch sensitivity	
Static	Greater sensitivity
Fatigue	Less sensitivity
Transverse properties	Weaker
Mechanical property variability	Higher
Fatigue strength	Higher
Sensitivity to hydrothermal environment	Greater
Sensitivity to corrosion	Much less
Damage growth mechanism	In-plane delamination instead of through thickness cracks

Source: Ref 2

stiffness are usually high and directionally variable, depending on the orientation of the reinforcing fibers. Properties that do not benefit from this reinforcement (at least for polymer matrix composites) are comparatively low in strength and stiffness—for example, the through-the-thickness tensile strength where the relatively weak matrix is loaded rather than the high-strength fibers. Figure 1.14 shows the low through-the-thickness strength of a typical composite laminate compared with aluminum.

Metals typically have reasonable ductility, continuing to elongate or compress considerably when they reach a certain load (through yielding) without picking up more load and without failure. Two important benefits of this ductile yielding are that (1) it provides for local load relief by distributing excess load to an adjacent material or structure; therefore, ductile metals have a great capacity to provide relief from stress concentrations when statically loaded; and (2) it provides great energy-absorbing capability (indicated by the area under a stress-strain curve). As a result, when impacted, a metal structure typically deforms but does not actually fracture. In contrast, composites are relatively brittle. Figure 1.15 shows a comparison of typical tensile stress-strain curves for two materials. The brittleness of the composite is reflected in its poor ability to tolerate stress concentrations, as shown in Fig. 1.16. The characteristically brittle composite material has poor ability to resist impact damage without extensive internal matrix fracturing.

The response of damaged composites to cyclic loading is also significantly different from that of metals. The ability of composites to withstand cyclic loading is far superior to that of metals, in contrast to the poor composite static strength when it has damage or defects. Figure 1.17

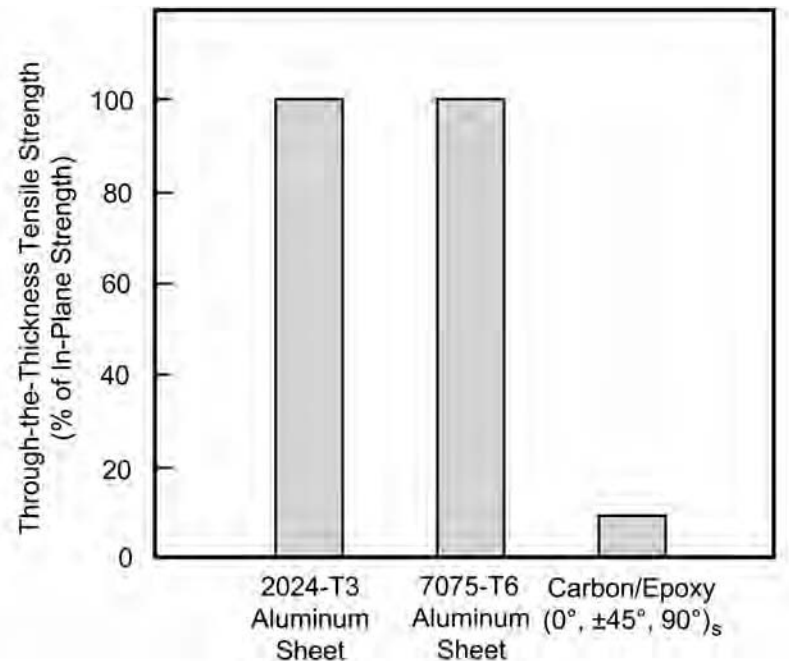


Fig. 1.14 Comparison of through-the-thickness tensile strength of a composite laminate with aluminum alloy sheet. Source: Ref 3

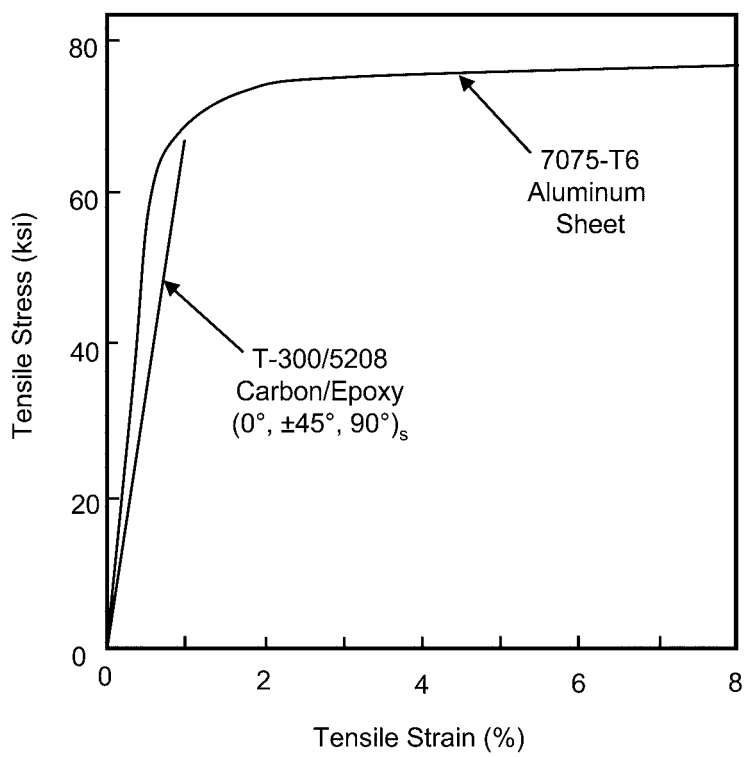


Fig. 1.15 Comparison of typical stress-strain curves for a composite laminate and aluminum alloy sheet. Source: Ref 3

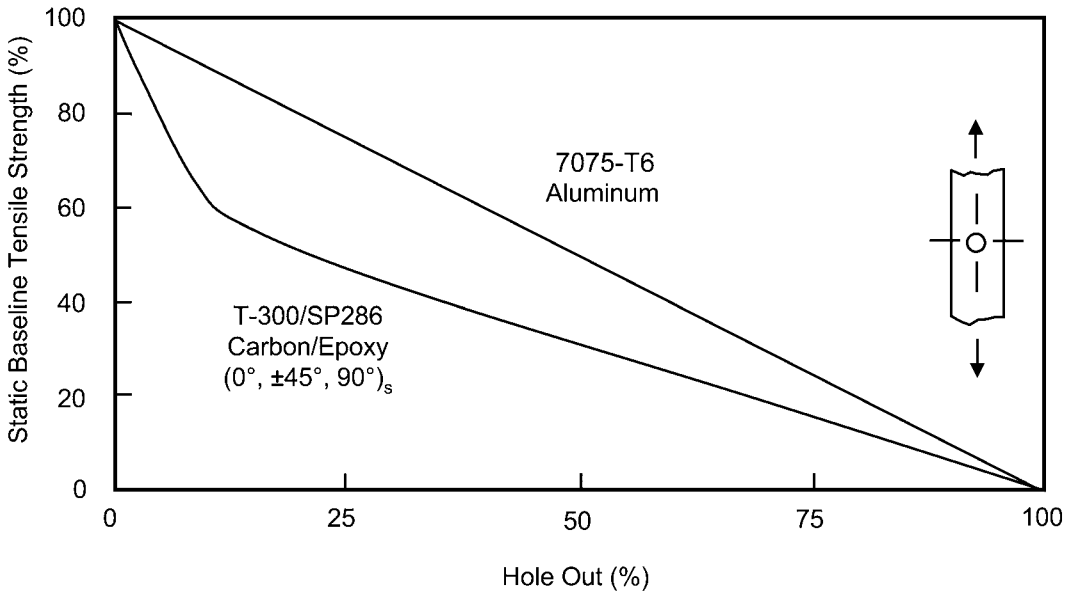


Fig. 1.16 Compared with aluminum alloy sheet, a composite laminate has poor tolerance of stress concentration because of its brittle nature. Source: Ref 3

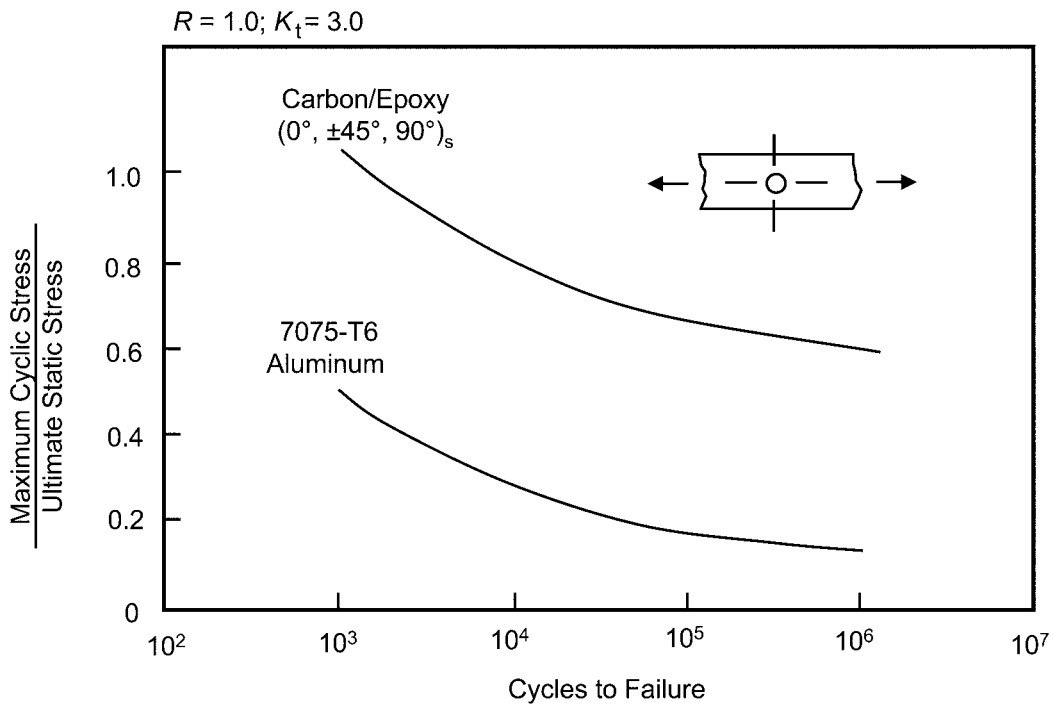


Fig. 1.17 Comparative notched fatigue strength of composite laminate and aluminum alloy sheet. Source: Ref 3

shows a comparison of the normalized notched specimen fatigue response of a common 7075-T6 aluminum aircraft metal and a carbon/epoxy laminate. The fatigue strength of the composite is much higher relative to its static or residual strength. The static or residual strength requirement for structures is typically much higher than the fatigue requirement. Therefore, because the fatigue threshold of composites is a high percentage of their static or damaged residual strength, they are usually not fatigue critical. In metal structures, fatigue is typically a critical design consideration.

1.5 Advantages and Disadvantages of Composite Materials

The advantages of composites are many, including lighter weight, the ability to tailor the layup for optimum strength and stiffness, improved fatigue life, corrosion resistance, and, with good design practice, reduced assembly costs due to fewer detail parts and fasteners.

The specific strength (strength/density) and specific modulus (modulus/density) of high-strength fibers (especially carbon) are higher than those of other comparable aerospace metallic alloys (Fig. 1.18). This translates into greater weight savings resulting in improved performance, greater payloads, longer range, and fuel savings. Figure 1.19 compares the overall structural efficiency of carbon/epoxy, Ti-6Al-4V, and 7075-T6 aluminum.

The chief engineer of aircraft structures for the U.S. Navy once told the author that he liked composites because "they don't rot [corrode] and they don't get tired [fatigue]." Corrosion of aluminum alloys is a major cost and a constant maintenance problem for both commercial and military aircraft. The corrosion resistance of composites can result in major savings in supportability costs. Carbon fiber composites cause galvanic corrosion of aluminum if the fibers are placed in direct contact with the metal surface, but bonding a glass fabric electrical insulation layer on all interfaces that contact aluminum eliminates this problem. The fatigue

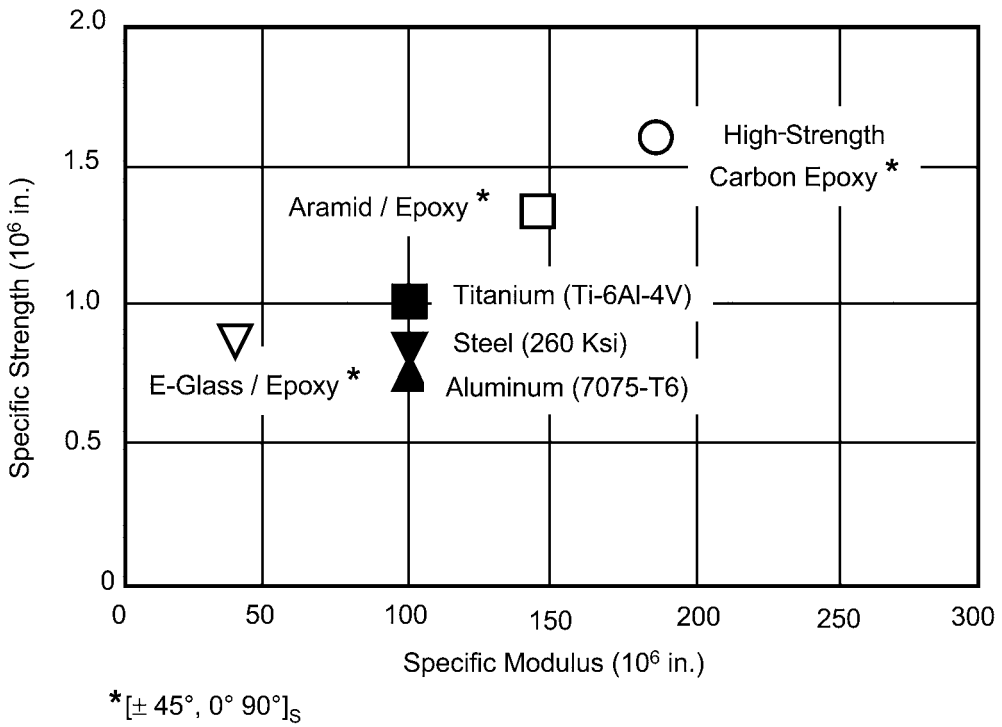


Fig. 1.18 Comparison of specific strength and modulus of high-strength composites and some aerospace alloys

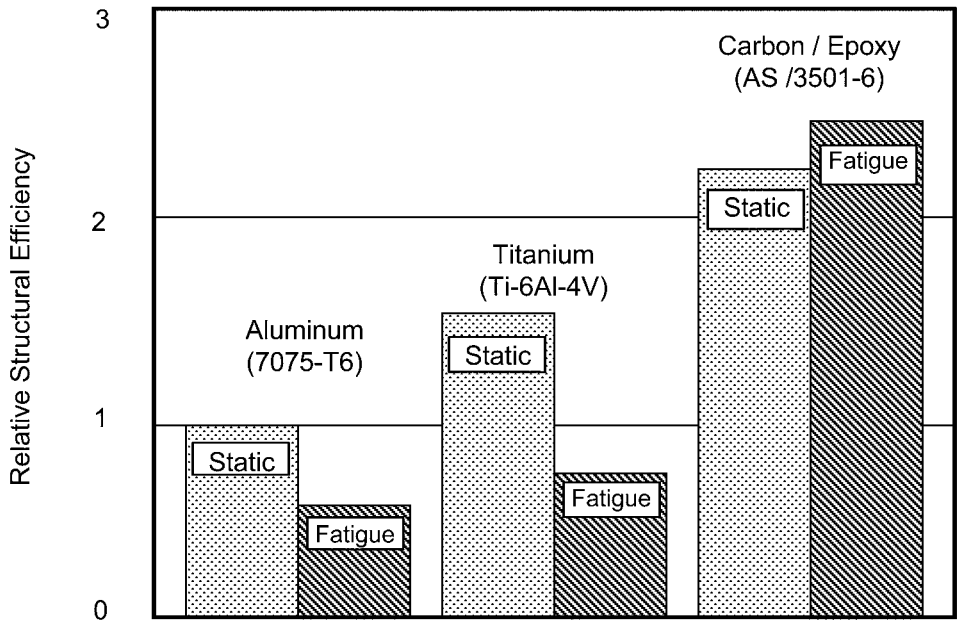


Fig. 1.19 Relative structural efficiency of aerospace materials

resistance of composites compared to high-strength metals is shown in Fig. 1.20. As long as reasonable strain levels are used during design, fatigue of carbon fiber composites should not be a problem.

Assembly costs can account for as much as 50 percent of the cost of an airframe. Composites offer the opportunity to significantly reduce the amount of assembly labor and the number of required fasteners. Detail parts can be combined into a single cured assembly either during initial cure or by secondary adhesive bonding.

Disadvantages of composites include high raw material costs and usually high fabrication and assembly costs; adverse effects of both temperature and moisture; poor strength in the out-of-plane direction where the matrix carries the primary load (they should not be used where load paths are complex, such as with lugs and fittings); susceptibility to impact damage and delaminations or ply separations; and greater difficulty in repairing them compared to metallic structures.

The major cost driver in fabrication for a composite part using conventional hand lay-up is the cost of laying up or collating the plies. This cost is generally 40 to 60 percent of the fabrication cost, depending on part complexity (Fig. 1.21). Assembly cost is another major cost driver, accounting for about 50 percent of the total part cost. As previously stated, one of the potential advantages of composites is the ability to cure or bond a number of detail parts together to reduce assembly costs and the number of required fasteners.

Temperature has an effect on composite mechanical properties. Typically, matrix-dominated mechanical properties decrease with increasing temperature. Fiber-dominated properties are somewhat affected by cold temperatures, but the effects are not as severe as those of elevated temperature on the matrix-dominated properties. Design parameters for carbon/epoxy are cold-dry tension and hot-wet compression (Fig. 1.22). An important design factor in the selection of a matrix resin for elevated-temperature applications is the cured glass transition temperature. The cured glass transition temperature (T_g) of a polymeric material is the temperature at which it changes from a rigid, glassy solid into a softer, semiflexible material. At this point, the polymer structure is still intact but the crosslinks are no longer locked in position. Therefore, the T_g determines the upper use temperature for a composite or an adhesive and is the temperature above which the material will exhibit significantly

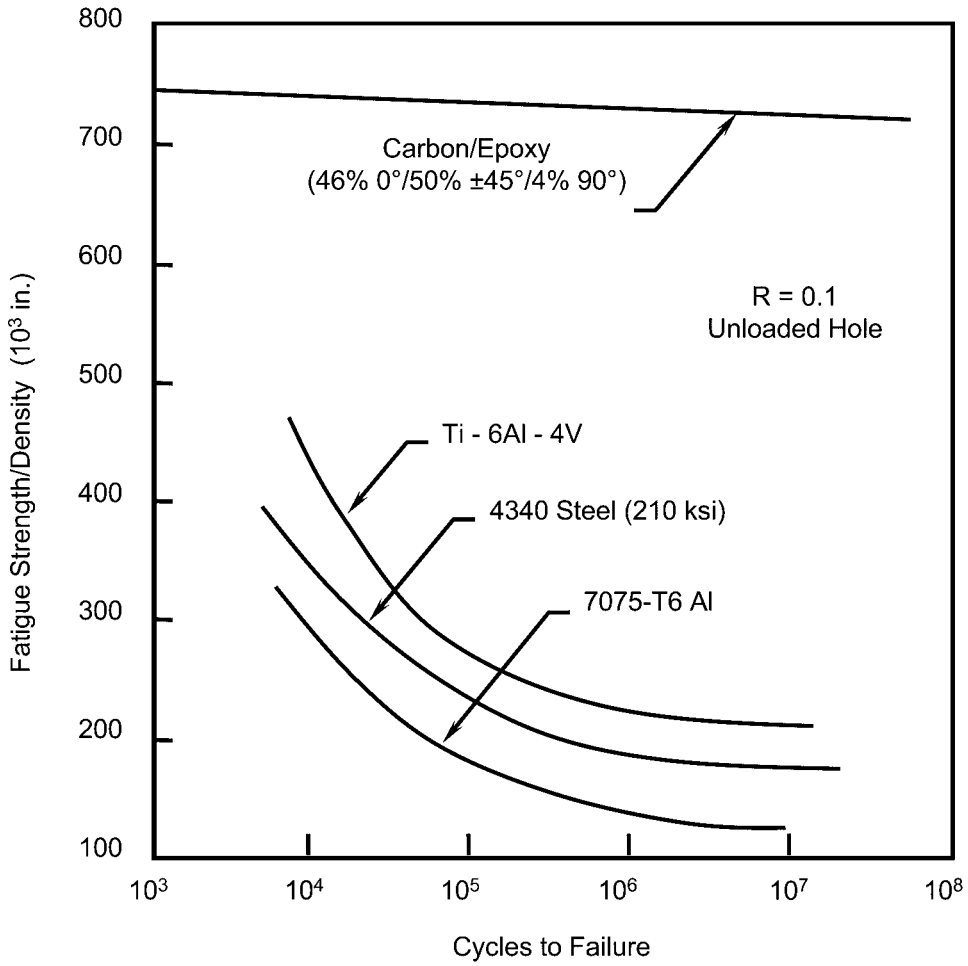


Fig. 1.20 Fatigue properties of aerospace materials

reduced mechanical properties. Since most thermoset polymers will absorb moisture that severely depresses the T_g, the actual use temperature should be about 50 °F (30 °C) lower than the wet or saturated T_g.

$$\text{Upper Use Temperature} = \text{Wet } T_g - 50\ °\text{F} \qquad \text{(Eq 1.9)}$$

In general, thermoset resins absorb more moisture than comparable thermoplastic resins.

The cured glass transition temperature (T_g) can be determined by several methods that are outlined in Chapter 3, "Matrix Resin Systems."

The amount of absorbed moisture (Fig. 1.23) depends on the matrix material and the relative humidity. Elevated temperatures increase the rate of moisture absorption. Absorbed moisture reduces the matrix-dominated mechanical properties and causes the matrix to swell, which relieves locked-in thermal strains from elevated-temperature curing. These strains can be large, and large panels fixed at their edges can buckle due to strains caused by swelling. During freeze-thaw cycles, absorbed moisture expands during freezing, which can crack the matrix, and it can turn into steam during thermal spikes. When the internal steam pressure exceeds the flatwise tensile (through-the-thickness) strength of the composite, the laminate will delaminate.

Composites are susceptible to delaminations (ply separations) during fabrication, during assembly,

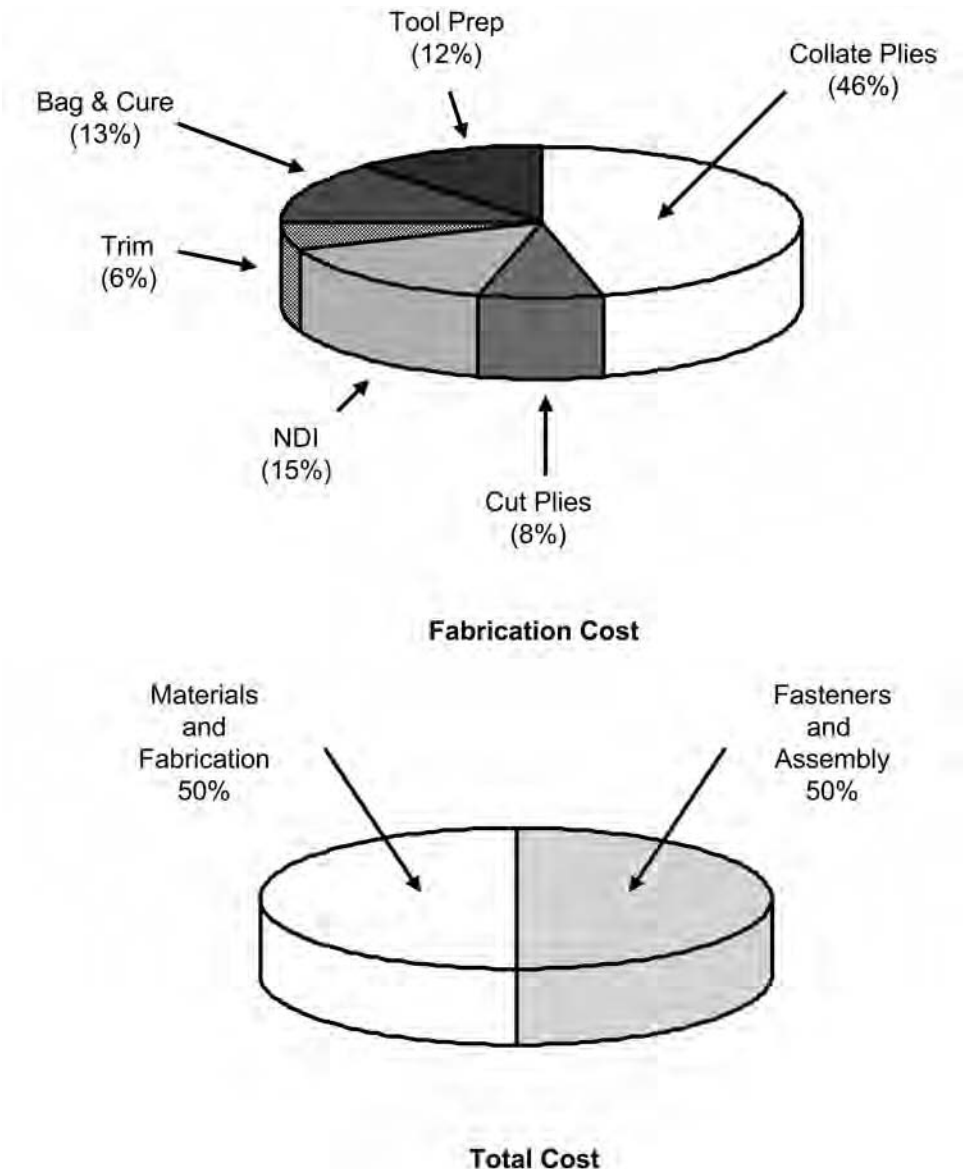


Fig. 1.21 Cost drivers for composite hand lay-up. NDI, nondestructive inspection

and in service. During fabrication, foreign materials such as prepreg backing paper can be inadvertently left in the lay-up. During assembly, improper part handling or incorrectly installed fasteners can cause delaminations. In service, low-velocity impact damage from dropped tools or forklifts running into aircraft can cause damage. The damage may appear as only a small indentation on the surface but it can propagate through the laminates, forming a complex network of delaminations and matrix cracks, as shown in Fig. 1.24. Depending on the size of the delamination, it can reduce the static and fatigue strength and the compression buckling strength. If it is large enough, it can grow under fatigue loading.

Typically, damage tolerance is a resin-dominated property. The selection of a toughened

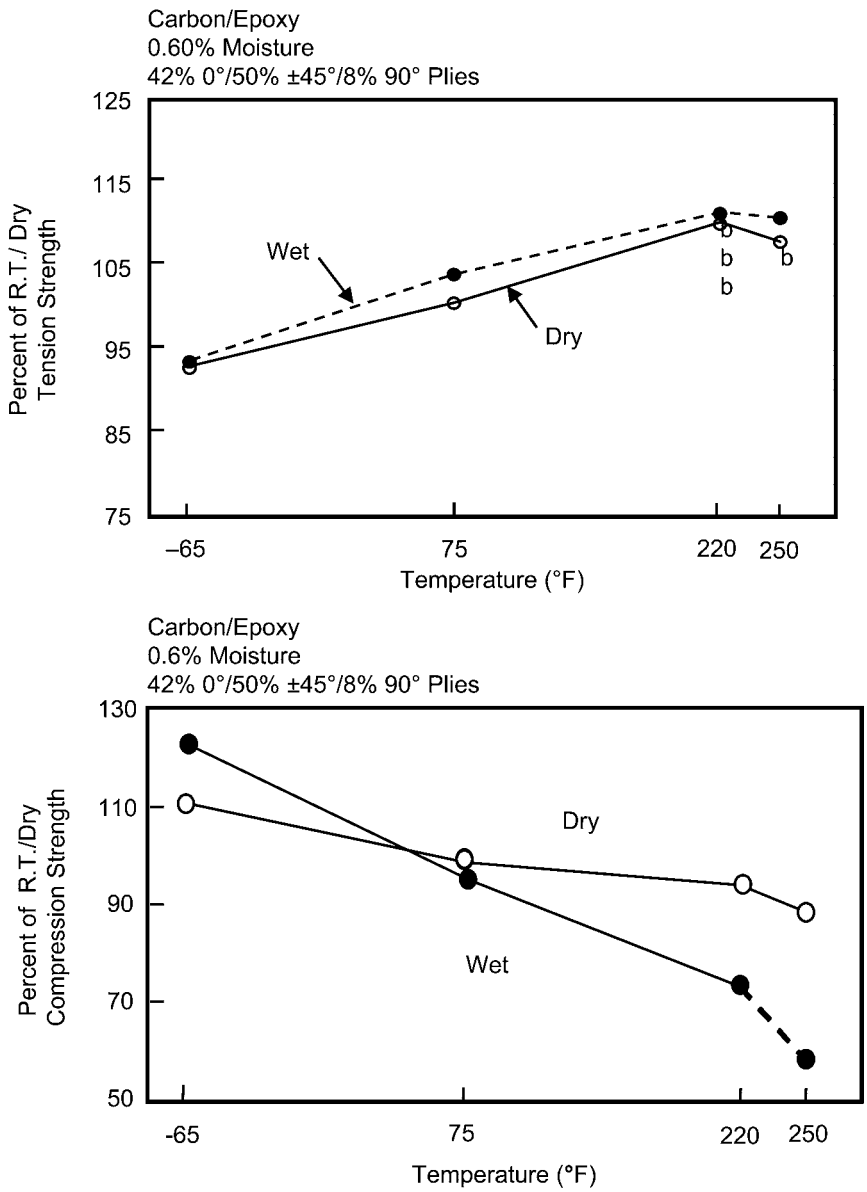


Fig. 1.22 Effects of temperature and moisture on strength of carbon/epoxy. R.T., room temperature

resin can significantly improve the resistance to impact damage. In addition, S-2 glass and aramid fibers are extremely tough and damage tolerant. During the design phase, it is important to recognize the potential for delaminations and use sufficiently conservative design strains so that a damaged structure can be repaired.

1.6 Applications

Applications include aerospace, transportation, construction, marine goods, sporting goods, and more recently infrastructure, with construction and transportation being the largest. In general, high-performance but more costly continuous-carbon-fiber composites are used

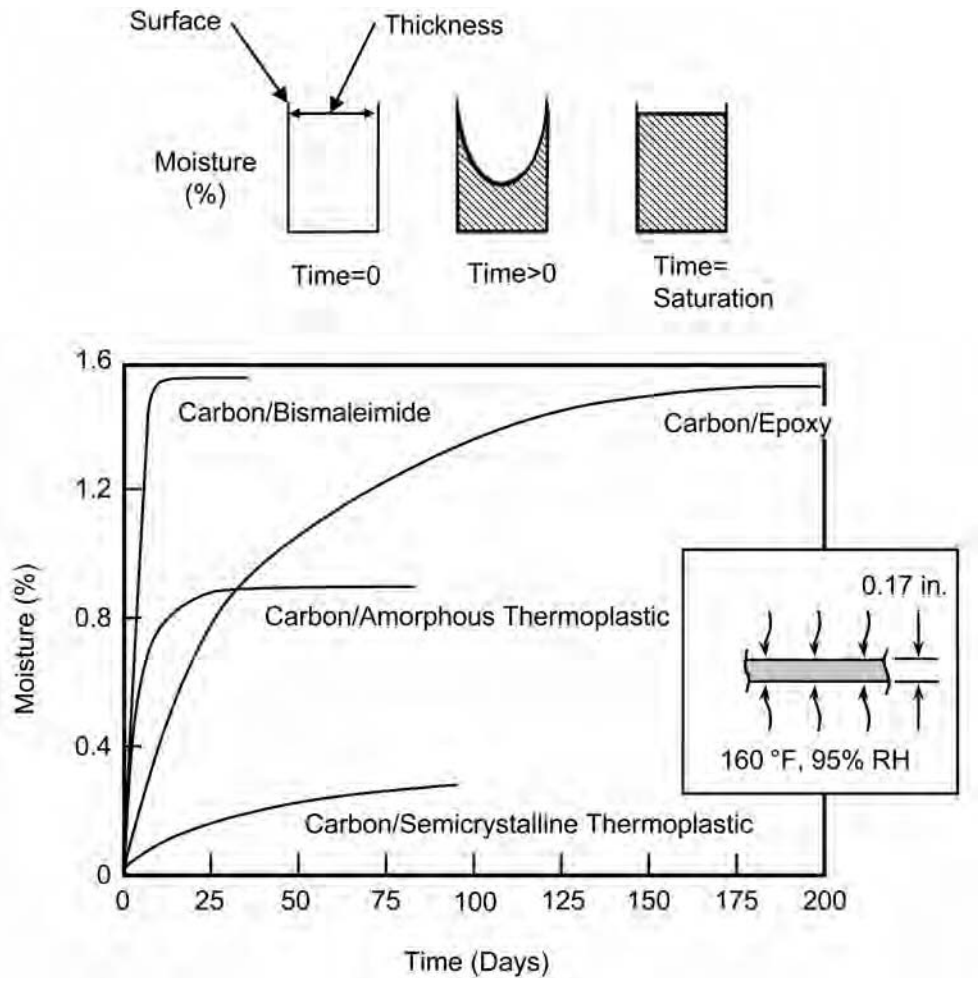


Fig. 1.23 Absorption of moisture for polymer matrix composites. RH, relative humidity

where high strength and stiffness along with light weight are required, and much lower-cost fiberglass composites are used in less demanding applications where weight is not as critical.

In military aircraft, low weight is "king" for performance and payload reasons, and composites often approach 20 to 40 percent of the airframe weight (Fig. 1.25). For decades, helicopters have incorporated glass fiber–reinforced rotor blades for improved fatigue resistance, and in recent years helicopter airframes have been built largely of carbon-fiber composites. Military aircraft applications, the first to use high-performance continuous-carbon-fiber composites, drove the development of much of the technology now being used by other industries. Both small and large commercial aircraft rely on composites to decrease weight and increase fuel performance, the most striking example being the 50 percent composite airframe for the new Boeing 787 (Fig. 1.26). All future Airbus and Boeing aircraft will use large amounts of high-performance composites. Composites are also used extensively in both weight-critical reusable and expendable launch vehicles and satellite structures (Fig. 1.27). Weight savings due to the use of composite materials in aerospace applications generally range from 15 to 25 percent.

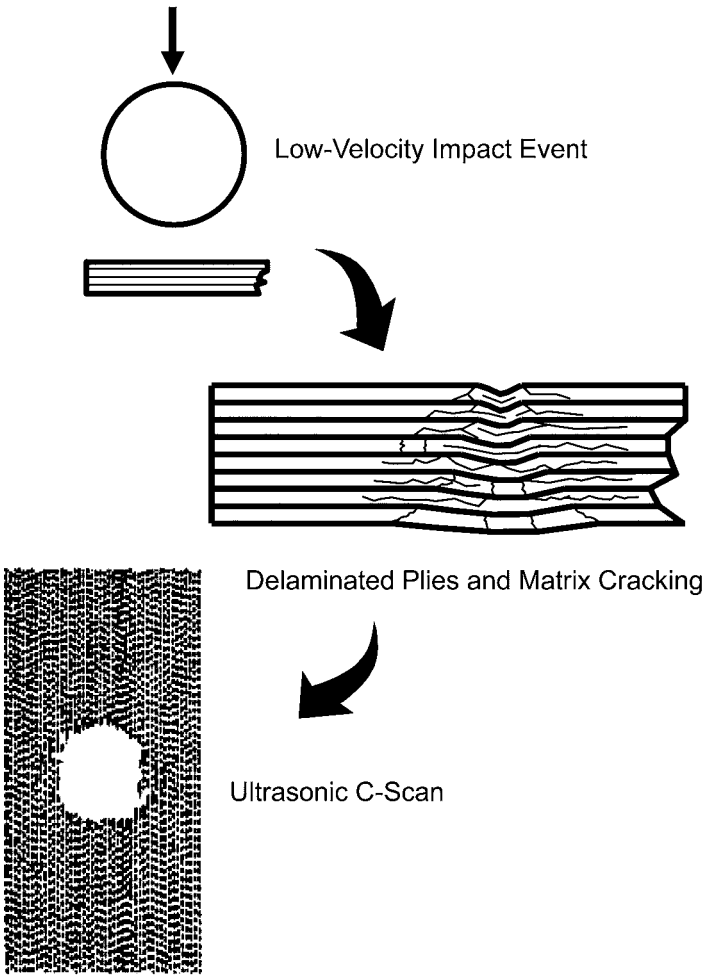


Fig. 1.24 Delaminations and matrix cracking in polymer matrix composite due to impact damage

The major automakers (Fig. 1.28) are increasingly turning to composites to help them meet performance and weight requirements, thus improving fuel efficiency. Cost is a major driver for commercial transportation, and composites offer lower weight and lower maintenance costs. Typical materials are fiberglass/ polyurethane made by liquid or compression molding and fiberglass/ polyester made by compression molding. Recreational vehicles have long used glass fibers, mostly for their durability and weight savings over metal. The product form is typically fiberglass sheet molding compound made by compression molding. For high-performance Formula 1 racing cars, where cost is not an impediment, most of the chassis, including the monocoque, suspension, wings, and engine cover, is made from carbon fiber composites.

Corrosion is a major headache and expense for the marine industry. Composites help minimize these problems, primarily because they do not corrode like metals or rot like wood. Hulls of boats ranging from small fishing boats to large racing yachts (Fig. 1.29) are routinely made of glass fibers and polyester or vinyl ester resins. Masts are frequently fabricated from carbon fiber composites. Fiberglass filament-wound SCUBA

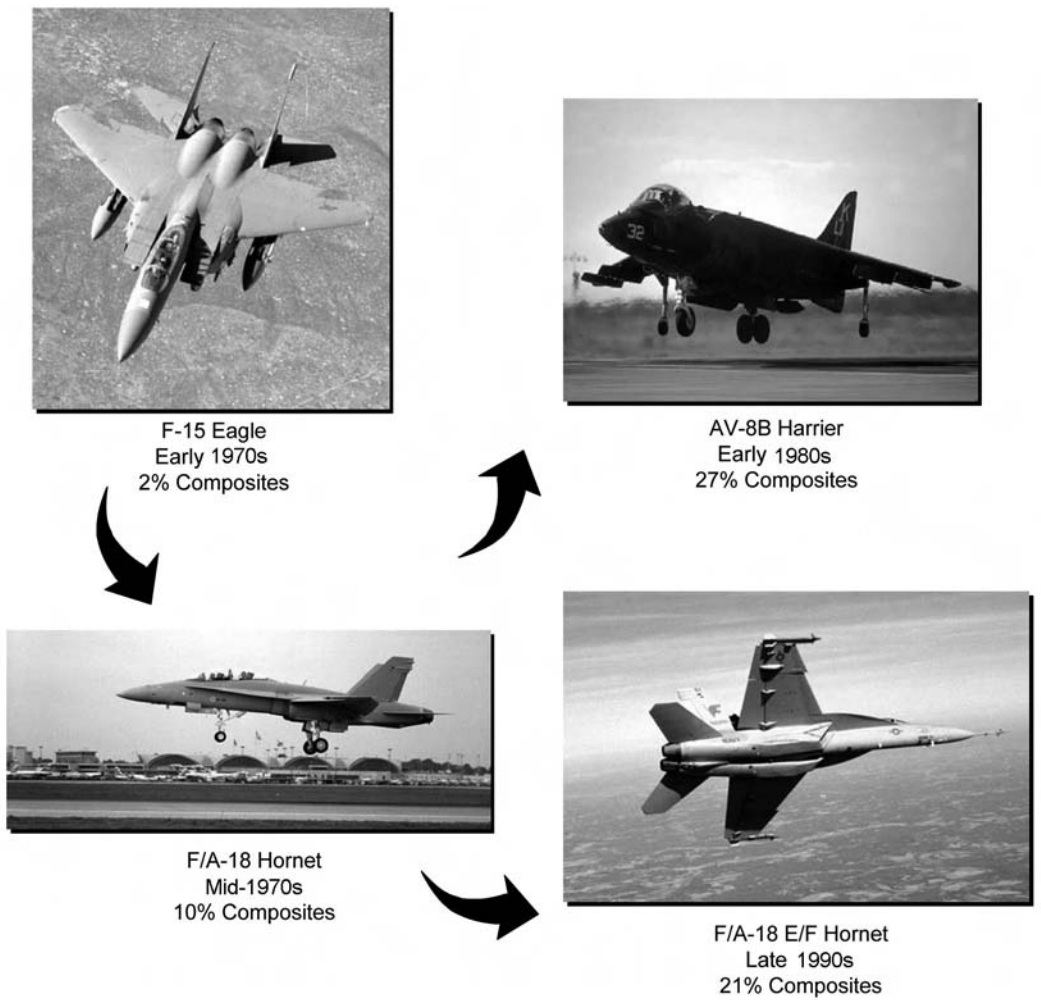


Fig. 1.25 Typical fighter aircraft applications. Source: The Boeing Company

tanks are another example of composites improving the marine industry. Lighter tanks can hold more air yet require less maintenance than their metallic counterparts. Jet skis and boat trailers often contain glass composites to help minimize weight and reduce corrosion. More recently, the topside structures of many naval ships have been fabricated from composites.

Using composites to improve the infrastructure (Fig. 1.30) of our roads and bridges is a relatively new, exciting application. Many of the world's roads and bridges are badly corroded and in need of continual maintenance or replacement. In the United States alone, it is estimated that more than 250,000 structures, such as bridges and parking garages, need repair, retrofit, or replacement. Composites offer much longer life with less maintenance due to their corrosion resistance. Typical processes/materials include wet lay-up repairs and corrosion-resistant fiberglass pultruded products.

In construction (Fig. 1.31), pultruded fiberglass rebar is used to strengthen concrete, and glass fibers are used in some shingling materials. With the number of mature tall trees dwindling, the use of composites for electrical towers and

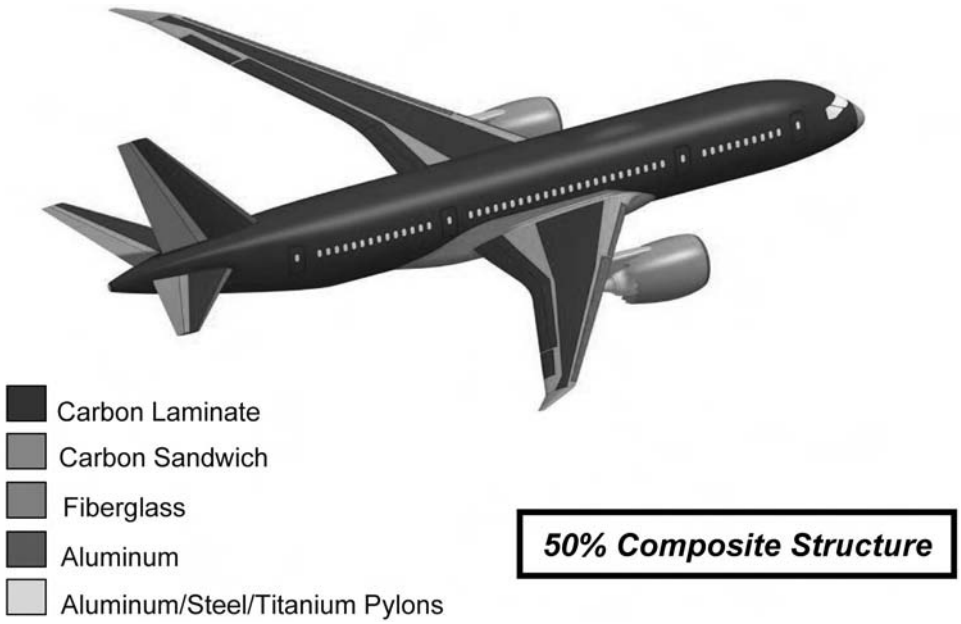


Fig. 1.26 Boeing 787 Dreamliner commercial airplane. Source: The Boeing Company

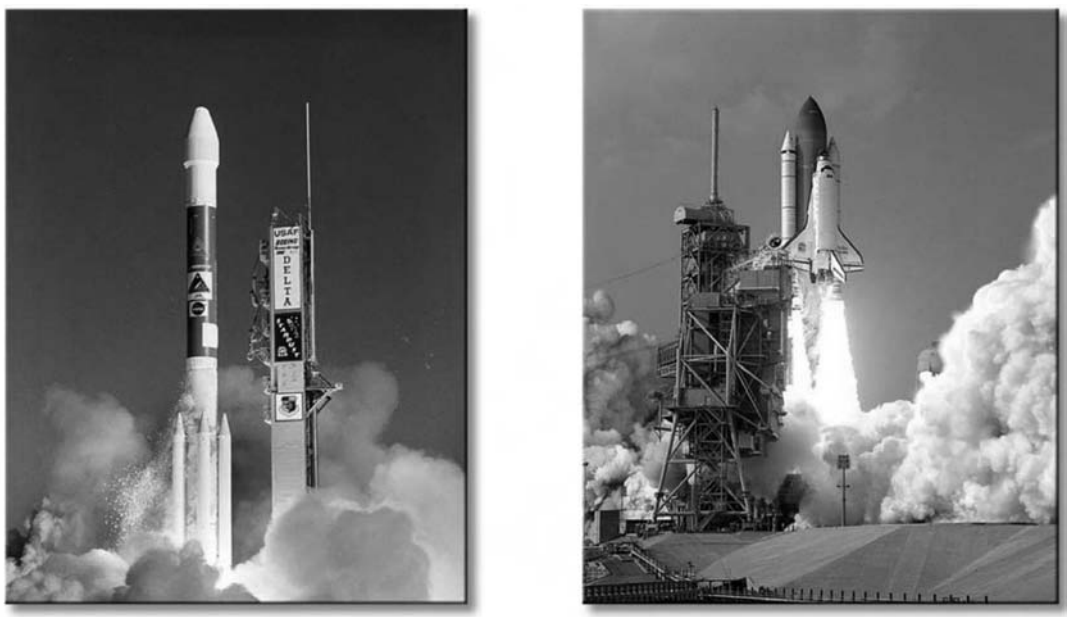
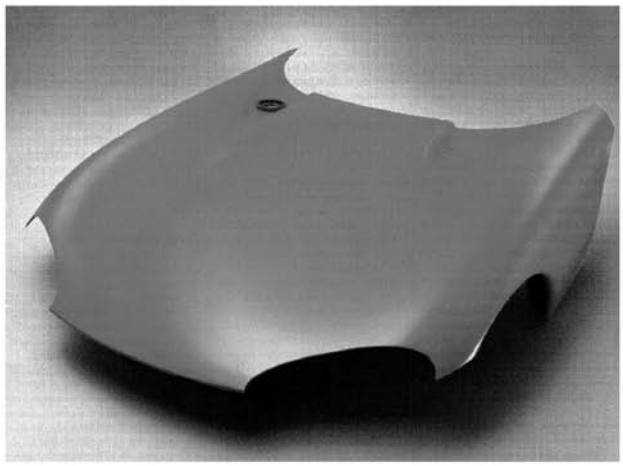


Fig. 1.27 Launch and spacecraft structures





Composites are used in both trucks and cars to reduce weight and Increase fuel efficiency.

Recreational vehicles have long used fiberglass composites, mostly for its durability and weight savings over metal.





Fig. 1.28 Transportation applications

light poles is greatly increasing. Typically, these are pultruded or filament-wound glass.

Wind power is the world's fastest-growing energy source. The blades for large wind turbines (Fig. 1.32) are normally made of composites to improve electrical energy generation efficiency. These blades can be as long as 120 ft (37 m) and weigh up to 11,500 lb (5200 kg). In 2007, nearly 50,000 blades for 17,000 turbines were delivered, representing roughly 400 million pounds



Rigid and flexible oil gas tubulars





Maintenance and corrosion in either fresh or salt water can be major headaches and expenses. Composites help minimize those problems.





Racing sailboat hulls and equipment

More recently, composites are being used for major components In naval ships.

Fig. 1.29 Marine applications

(approximately 180 million kg) of composites. The predominant material is continuous glass fibers manufactured by either lay-up or resin infusion.

Tennis racquets (Fig. 1.33) have been made of glass for years, and many golf club shafts are made of carbon. Processes include compression molding for tennis racquets and tape wrapping or

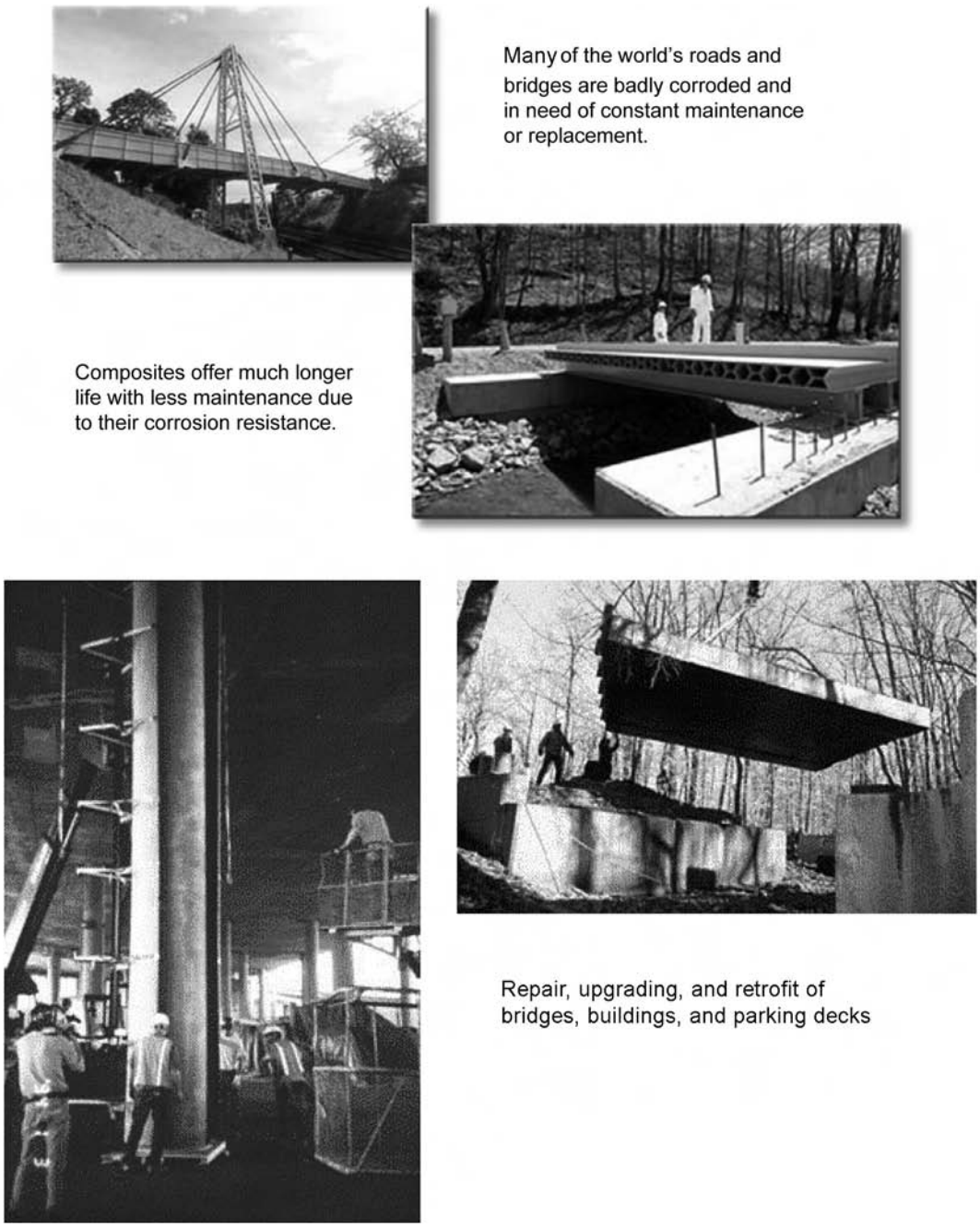


Fig. 1.30 Infrastructure applications

filament winding for golf shafts. Lighter, stronger skis and surfboards also are possible using composites. Another example of a composite application that takes a beating yet keeps on performing is a snowboard, which typically involves the use of a sandwich construction (composite skins with a honeycomb core) for maximum specific stiffness.

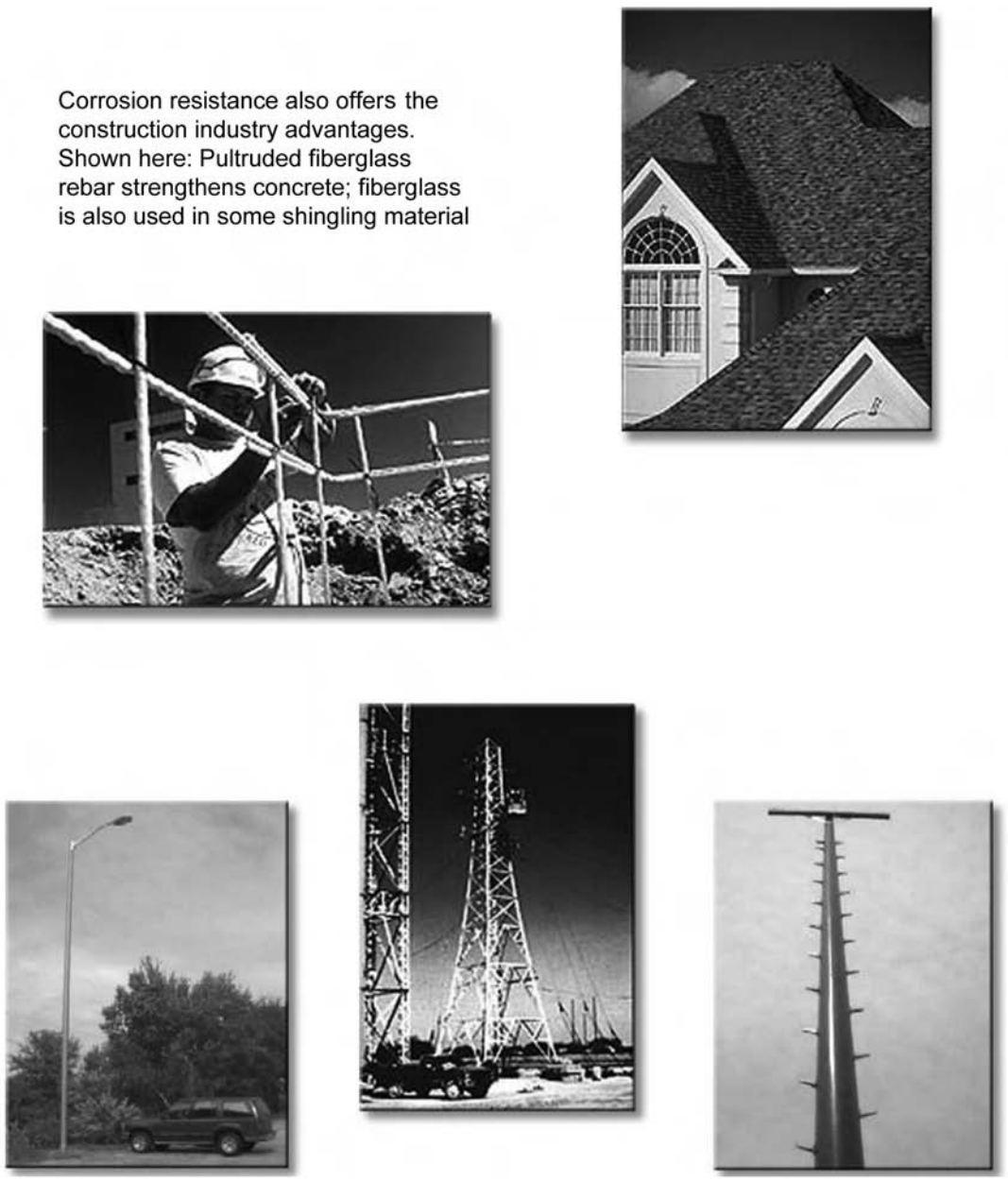


Fig. 1.31 Construction applications

Although metal and ceramic matrix composites are normally very expensive, they have found uses in specialized applications such as those shown in Fig. 1.34. Frequently, they are used where high temperatures are involved. However, the much higher temperatures and pressures required for the fabrication of metal and ceramic matrix composites lead



Composites are being used for wind turbine blades to improve energy generation efficiency and reduce corrosion problems.

Fig. 1.32 Composite clean energy generation

to very high costs, which severely limits their application.

Composites are not always the best solution. An example is the avionics rack for an advanced fighter aircraft shown in Fig. 1.35. This part was machined from a single block of aluminum in about 8.5 hours and assembled into the final component in five hours. Such a part made of composites would probably not be cost competitive.

Advanced composites are a diversified and growing industry due to their distinct advantages over competing metallics, including lighter weight, higher performance, and corrosion resistance. They are used in aerospace, automotive, marine, sporting goods, and, more recently, infrastructure applications. *The major disadvantage of composites is their high cost.* However, the proper selection of materials (fiber and matrix), product forms, and processes can have a major impact on the cost of the finished part.

REFERENCES

1. M.E. Tuttle, *Structural Analysis of Polymeric Composite Materials*, Marcel Dekker, Inc., 2004

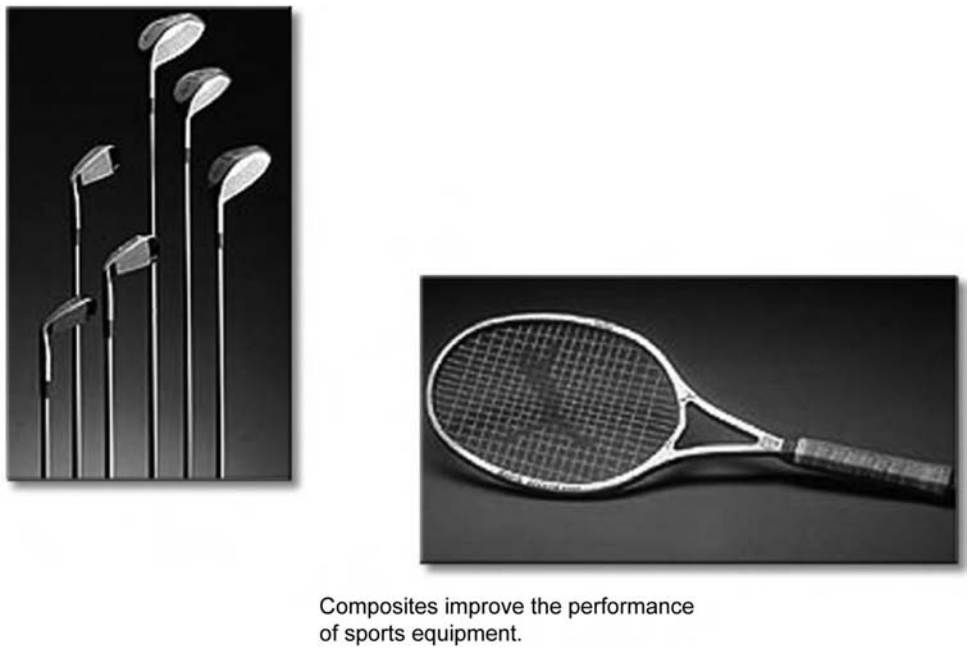


Fig. 1.33 Sporting goods applications

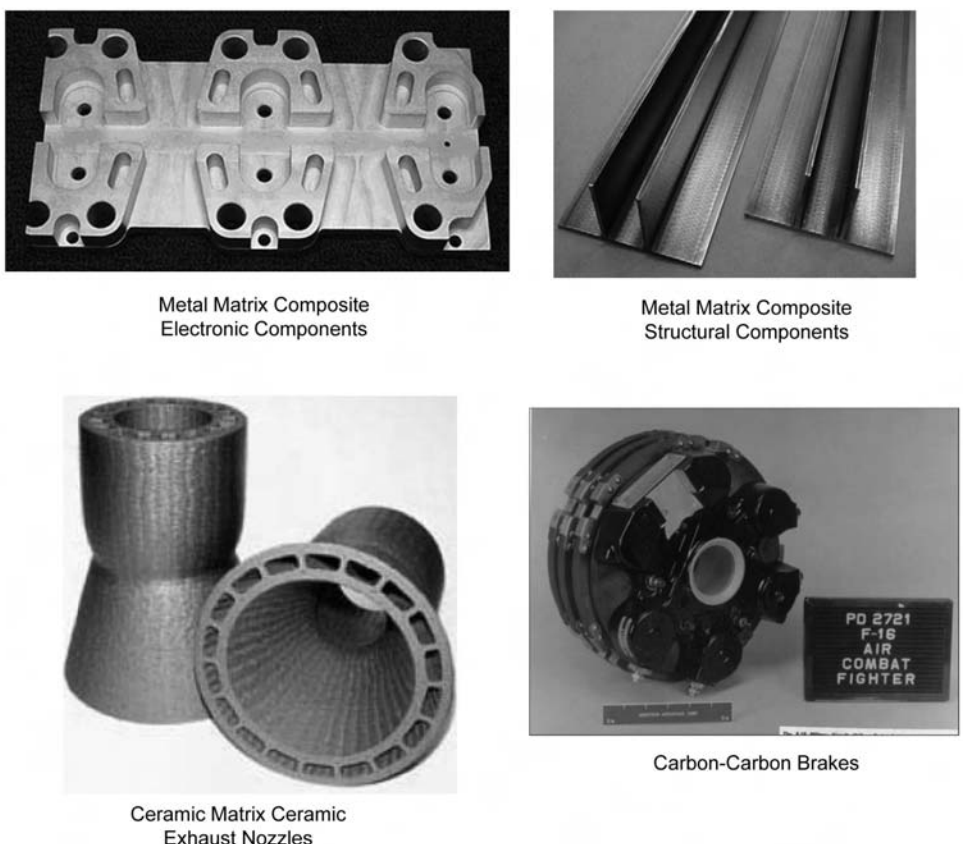
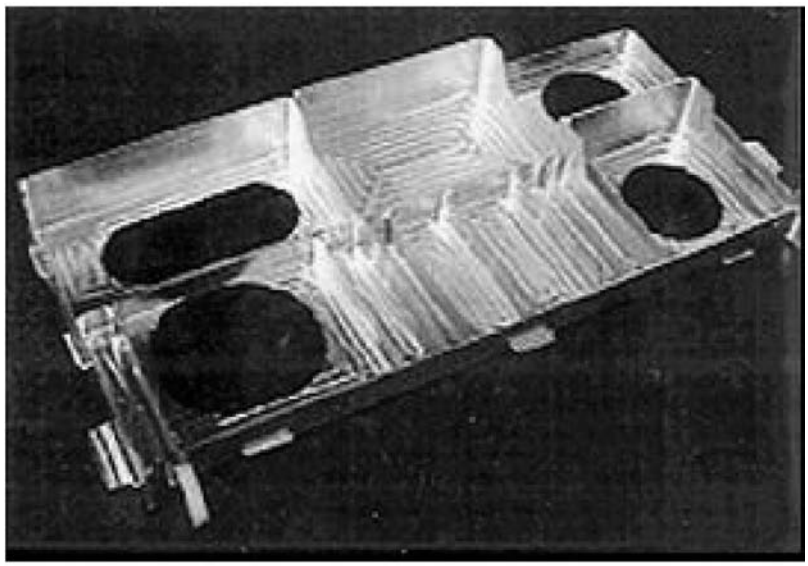


Fig. 1.34 Metal and ceramic matrix composite applications



Number of Pieces	6
Number of Tools	5
Design and Fabrication hr (Tools)	30
Fabrication hr	8.6
Assembly Man-hours	5.3
Weight (lb)	8.56

Fig. 1.35 Composites are not always the best choice. This avionics rack machined from an aluminum alloy block would not be cost-competitive if made of composites. Source: The Boeing Company

2. M.C.Y. Niu, *Composite Airframe Structures*, 2nd ed., Hong Kong Conmilit Press Limited, 2000
3. R.E. Horton and J.E. McCarty, Damage Tolerance of Composites, *Engineered Materials Handbook*, Vol 1, *Composites*, ASM International, 1987

SELECTED REFERENCES

- *High-Performance Composites Sourcebook 2009*, Gardner Publications Inc
- S.K. Mazumdar, *Composites Manufacturing: Materials, Product, and Process Engineering*, CRC Press, 2002

"*This page left intentionally blank.*"

Copyright © 2010, ASM International®
All rights reserved.
www.asminternational.org

CHAPTER 2

Fibers and Reinforcements

REINFORCEMENTS for composite materials can be particles, whiskers, or fibers. Particles have no preferred orientation and provide minimal improvements in mechanical properties. They are frequently used as fillers to reduce the cost of the material. Whiskers are single crystals that are extremely strong but are difficult to disperse uniformly in the matrix. They are small in both length and diameter compared to fibers. Fibers have a very long axis compared to particles and whiskers. They are usually circular or nearly circular and are significantly stronger in the long direction because they are normally made by either drawing or pulling during the manufacturing process. Drawing orients the molecules so that tension loads on the fibers pull more against the molecular chains themselves than against a mere entanglement of chains. Due to the strength and stiffness advantages of fibers, they are the predominant reinforcement for advanced composites. Fibers may be continuous or discontinuous, depending on the application and manufacturing process.

This chapter covers the fibers used for organic matrix composites, with an emphasis on continuous fibers. Fibers used for metal- and ceramic-matrix composites are discussed in Chapters 20 and 21, "Metal Matrix Composites" and "Ceramic Matrix Composites," respectively.

2.1 Fiber Terminology

Before examining the various types of fibers used as composite reinforcements, the major terminology used for fiber technology will be reviewed. Fibers are produced and sold in many forms.

- *Fiber*—A general term for a material that has a long axis that is many times greater than its diameter. The term *aspect ratio*, which refers to fiber length divided by diameter (l/d), is frequently used to describe short fiber lengths. Aspect ratios are normally greater than 100 for fibers.
- *Filament*—The smallest unit of a fibrous material. For spun fibers, this is the unit formed by a single hole in the spinning process. The term *filament* is synonymous with *fiber*.
- *End*—A term used primarily for glass fibers that refers to a group of filaments in long parallel lengths.
- *Strand*—Another term associated with glass fibers that refers to a bundle or group of untwisted filaments. Continuous strand rovings provide good overall processing characteristics through fast wet-out (penetration of resin into the strand), even tension, and abrasion resistance during processing. They can be cut cleanly, and they disperse evenly throughout the resin matrix during molding.
- *Tow*—Similar to a strand of glass fiber, *tow* is used for carbon and graphite fibers to describe the number of untwisted filaments produced at one time. Tow size is usually expressed as *X*k; for example, a 12k tow contains 12,000 filaments.
- *Roving*—A number of strands or tows collected into a parallel bundle *without* twisting. Rovings can be chopped into short fiber segments for sheet molding compound, bulk molding compound or injection molding.
- *Yarn*—A number of strands or tows collected into a parallel bundle *with* twisting. Twisting improves the handleability and makes processes such as weaving easier, but the twist also reduces the strength properties.
- *Band*—The thickness or width of several rovings, yarns, or tows as it is applied to a

mandrel or tool; a common term used in filament winding.

- *Tape*—A composite product form in which a large number of parallel filaments (such as tows) are held together with an organic matrix material (such as epoxy) commonly referred to as *prepreg* (preimpregnated with resin). The length of the tape in the direction of the fibers is much greater than the width, and the width is much greater than the thickness. Typical tape product forms are several hundred feet long, 6 to 60 in. (15 cm to 1.5 m) wide, and 0.005 to 0.010 in. (125 to 255 μm) thick.
- *Woven Cloth*—Another composite product form made by weaving yarns or tows in various patterns to provide reinforcement in two directions, usually zero and 90 degrees. Typical two-dimensional woven cloth is several hundred feet long, 24 to 60 in. (60 cm to 1.5 m) wide, and 0.010 to 0.015 in. (255 to 380) μm thick. Woven cloth is normally supplied either without resin (dry) or as prepreg with resin.

Additional fiber and textile terminology will be introduced as different fiber types, processes, and product forms are discussed.

The physical and mechanical properties of some commercially important fibers are given in Table 2.1, and a graph of specific strengths versus specific moduli is given in Fig. 2.1. Several types of fibers are used for polymeric composites, with glass, aramid (for example, Kevlar), and carbon being the most common. Boron fiber was the original high-performance fiber before carbon was developed. It is a large-diameter fiber made by pulling a fine tungsten wire through a long, slender reactor, where it is coated with boron using chemical vapor deposition. It is very expensive because it is made one fiber at a time rather than thousands of fibers at a time. Due to its large diameter and high modulus, it has outstanding compression properties. On the negative side, it does not conform well to complicated shapes and is very difficult to machine. Other high-temperature ceramic fibers, such as silicon carbide (Nicalon), aluminum oxide, and alumina boria silica (Nextel), are frequently used in ceramic-based composites but rarely in polymer-based composites. The stress-strain curves in Fig. 2.2 show that high-strength fibers are usually linearly elastic up to the point of failure. Figure 2.3 shows some relative fiber costs versus performance data. Carbon and graphite fibers are the most expensive, followed by aramid, S-2 glass, and E-glass. Because E-glass is a very affordable high-performance fiber, it is the most widely used and dominates in commercial composite applications.

2.2 Strength of Fibers

Fibers generally exhibit much higher strengths than the bulk form of the same material. The probability of a flaw per unit length present in a sample is an inverse function of the volume of the material. Since fibers have a very low volume

Table 2.1 Properties of some commercially important high-strength fibers

Type of fiber	Tensile strength, ksi	Tensile modulus, msi	Elongation at failure, %	Density, g/cm^2	Coefficient of thermal expansion, 10^{-6} °C	Fiber diameter, μm
Glass						
E-glass	500	10.0	4.7	2.58	4.9–6.0	5–20
S-2 glass	650	12.6	5.6	2.48	2.9	5–10
Quartz	490	10.0	5.0	2.15	0.5	9
Organic						
Kevlar 29	525	12.0	4.0	1.44	–2.0	12
Kevlar 49	550	19.0	2.8	1.44	–2.0	12
Kevlar 149	500	27.0	2.0	1.47	–2.0	12
Spectra 1000	450	25.0	0.7	0.97	…	27
PAN-based carbon						
Standard modulus	500–700	32–35	1.5–2.2	1.80	–0.4	6–8
Intermediate modulus	600–900	40–43	1.3–2.0	1.80	–0.6	5–6
High modulus	600–80	50–65	0.7–1.0	1.90	–0.75	5–8
Pitch-based carbon						
Low modulus	200–450	25–35	0.9	1.9	…	11
High modulus	275–400	55–90	0.5	2.0	–0.9	11
Ultra-high modulus	350	100–140	0.3	2.2	–1.6	10

Note: Representative only. For specific properties, contact the fiber manufactures. PAN, polyacrylonitrile

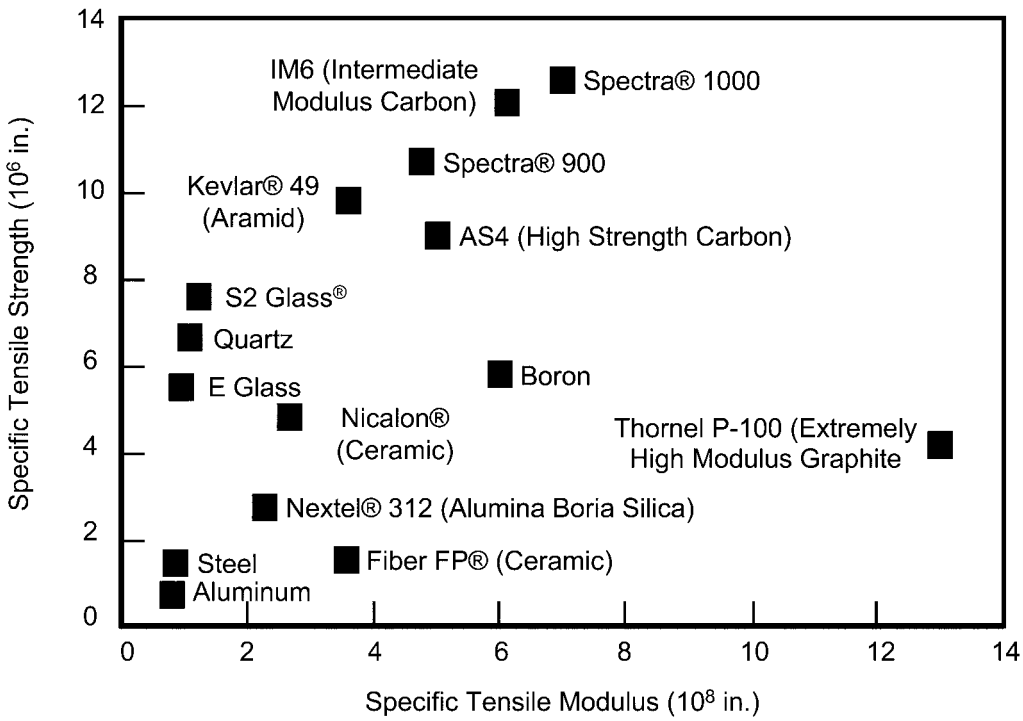


Fig. 2.1 Specific strength and modulus of some commercially important fibers. Source: Ref 1

per unit length, they are much stronger on average than the bulk material, which has a high volume per unit length. On the other hand, because a bulk material has a much higher content of weakening flaws, it exhibits much lower variability in strength. Thus, the smaller the fiber diameter and the shorter its length, the higher the average and maximum strength but the greater the variability. The effect of fiber diameter on the strength of glass fibers is shown in Fig. 2.4. Therefore, fibers have higher strength than their bulk counterparts, but they have greater scatter in their strength. The variability in the strength of fibers is a function of the flaws they contain and, in particular, the flaws they contain on the surface. Flaws can be minimized by careful manufacturing processes and the application of coatings to protect them from mechanical and environmental damage. Precursors used in fiber manufacturing processes must be of high purity and free of inclusions.

Many fiber manufacturing processes involve drawing or spinning operations that impose very high degrees of orientation parallel to the fiber axis, thus producing a more favorable orientation in the crystalline or atomic structure. In addition, some processes involve very high cooling rates that produce ultrafine-grained structures, which are not achievable in most bulk materials.

2.3 Glass Fibers

Due to their low cost, high tensile strength, high impact resistance, and good chemical resistance, glass fibers are used extensively in commercial composite applications. However, their properties do not match those of carbon fibers in high-performance composite applications. Compared to carbon fibers, they have a relatively low modulus and inferior fatigue properties. Although there are many types of glass fibers, the three most commonly used in composites are E-glass, S-2 glass, and quartz. E-glass is the most common and least expensive, providing a good combination of tensile strength 500 ksi (3.5 GPa) and modulus 10.0 msi (70 GPa). S-glass, which has a tensile strength of 650 ksi (4.5 GPa) and a modulus of 12.6 msi (87 GPa), is more expensive, but is 40 percent stronger than E-glass and retains a greater percentage of its strength at elevated temperatures. Quartz fiber is a rather

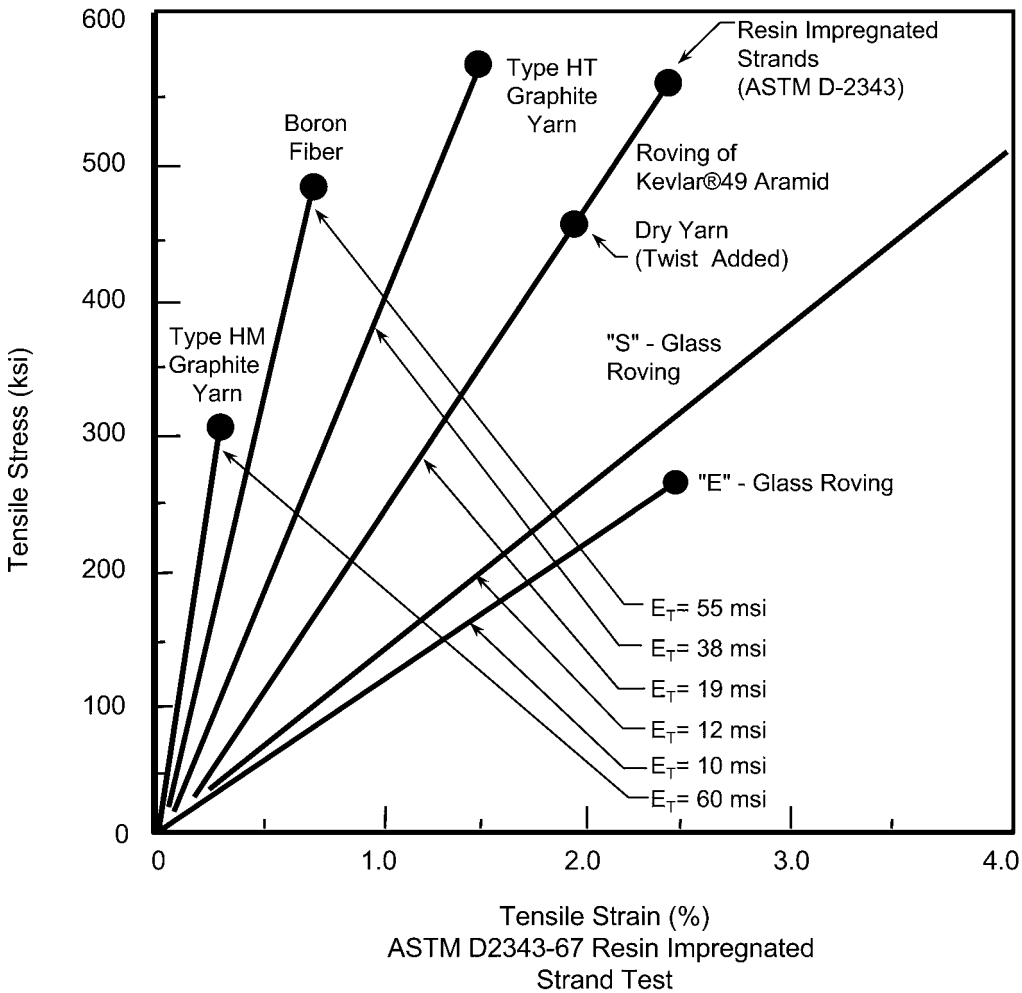


Fig. 2.2 Comparison of stress-strain curves of high-strength fibers. Source: Ref 1

expensive ultrapure silica glass that is a low-dielectric fiber and is used primarily in demanding electrical applications.

High-strength glass fibers were first developed in the 1930s and today represent a worldwide structural composite reinforcements market of roughly four to five million tons (3630 to 4540 kg) per year. Glass is an amorphous material that consists of a silica (SiO_2) backbone with various oxide components to give specific compositions and properties. Glass fibers are made from silica sand, limestone, boric acid, and minor amounts of other ingredients such as clay, coal, and fluorspar. Silica, which melts at 3128 °F (1720 °C), is also the basic element in quartz, a naturally occurring rock. However, quartz is crystalline with a rigid, highly ordered atomic structure and is 99 percent or more silica. If silica is heated above its melting temperature and slowly cooled, it crystallizes and becomes quartz. On the other hand, glass is produced by altering the temperature and cool-down rates. If pure silica is heated above 3128 °F (1720 °C) and then quickly cooled, crystallization can be prevented and the process yields a glass with an amorphous, or randomly ordered, atomic structure. Although the process is refined and improved continuously, today's glass fiber manufacturers combine this high-heat/quick-cool strategy with other steps in a process that is basically the same as that developed in the 1930s.

High-strength glass fibers are made by blending raw materials, melting them in a three-stage furnace, extruding the molten glass through bushings in the bottom of the forehearth, cooling

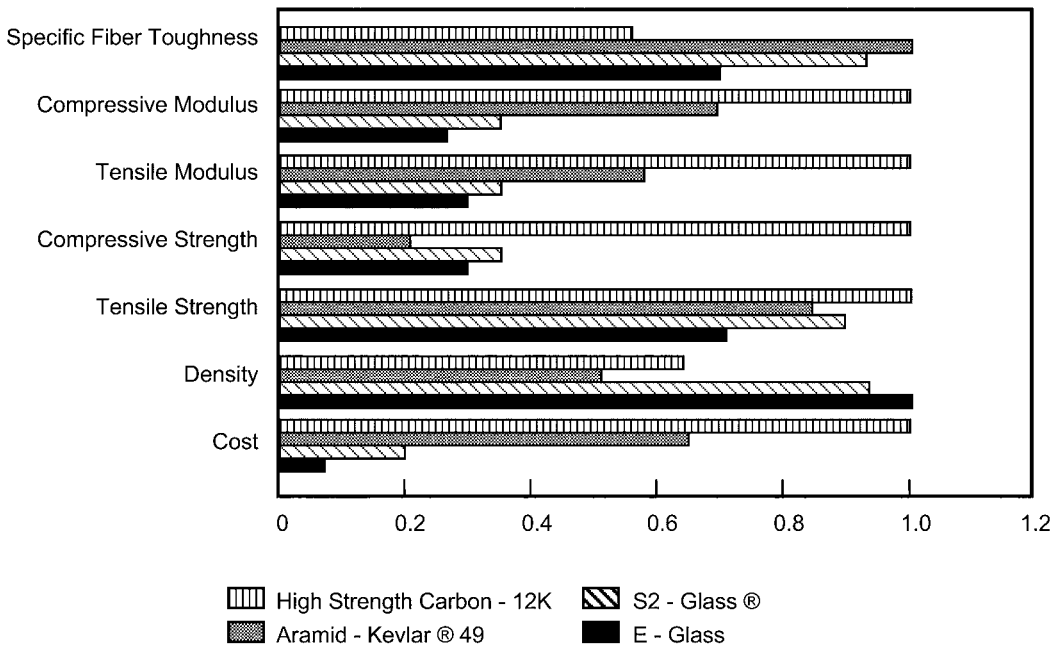


Fig. 2.3 Relative fiber cost and performance of some high-strength fibers. Source: Ref 1

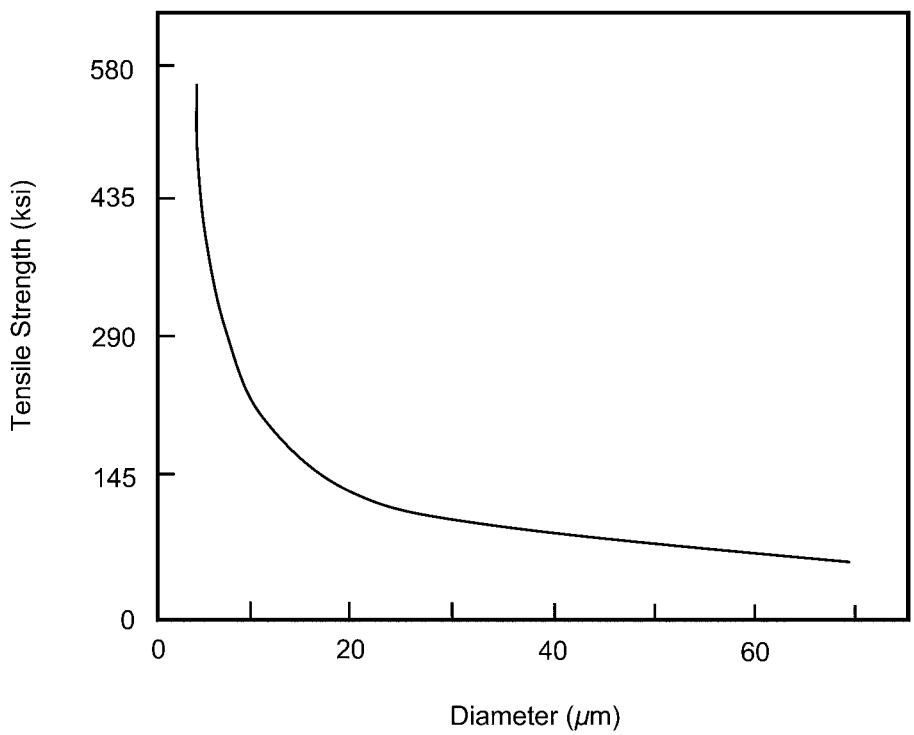


Fig. 2.4 Effect of fiber diameter on strength of glass fibers. Source: Ref 2

the filaments with water, and applying a chemical size. The filaments are gathered and wound into a package. The production process can be broken down into five basic steps: batching, melting, fiberization, coating, and drying/packaging.

Batching. Although a viable commercial glass fiber can be made of silica alone, other ingredients are added to reduce the working temperature and impart other properties that are useful in specific applications. For example, originally targeted for electrical applications, E-glass with a composition including silica, alumina (Al_2O_3), calcium oxide (CaO), and magnesium oxide (MgO) was developed as a more alkali-resistant alternative to the original soda-lime glass. Later, boron oxide (B_2O_3) was added to increase the difference between the temperatures at which the E-glass melted and then formed a crystalline structure to prevent clogging of the nozzles used in fiberization. S-glass fibers, developed for higher strength, are based on a silica-alumina-magnesium oxide formulation but contain higher percentages of silica for applications in which tensile strength is the most important property. The maximum use temperature of glass fibers ranges from 930 ºF (500 °C) for E-glass up to 1920 ºF (1050 °C) for quartz.

Batching consists of weighing the raw materials in exact quantities and thoroughly mixing them. Batching is automated using computerized weighing units and enclosed material transport systems. Each ingredient is transported by pneumatic conveyors to its designated multistory storage bin (silo), which is capable of holding 70 to 260 ft³ (2 to 7.5 m^3) of material. Directly beneath each bin is an automated weighing and feeding system that transfers the precise amount of each ingredient to a pneumatic blender in the batch-house basement.

Melting. From the batch house, another pneumatic conveyor sends the mixture to a high-temperature, approximately equals 2550 ºF (1400 °C), natural gas–fired furnace for melting. The furnace is typically divided into three sections with channels that aid glass flow. The first section receives the batch, where melting occurs and uniformity is increased, including the removal of bubbles. The molten glass then flows into the refiner, where its temperature is reduced to 2500 ºF (1370 °C). The final section is the forehearth, beneath which is located a series of four to seven bushings that are used to extrude the molten glass into fibers. Large furnaces have several channels, each with its own forehearth. Control of oxygen flow rates is crucial because furnaces that use the latest technology burn nearly pure oxygen instead of air; pure oxygen helps the natural gas fuel to burn cleaner and hotter, melting glass more efficiently. It also lowers operating costs by using less energy and reduces nitrogen oxide (NO_x) emissions by 75 percent and carbon dioxide (CO_2) emissions by 40 percent.

Two processes used to make high-strength glass fibers are the marble process and the direct melt process. In the marble process, the glass ingredients are shaped into marbles, sorted by quality, and then remelted into fiber strands. Alternatively, molten glass is introduced directly to form fiber strands. In the marble process, molten glass is sheared and rolled into marbles roughly 0.6 inches in diameter, which are cooled, packaged, and transported to a fiber-manufacturing facility where they are remelted for fiberization. The marbles allow visual inspection of the glass for impurities, resulting in a more consistent product. The direct melt process transfers molten glass in the furnace directly to fiber-forming equipment. Because direct melting eliminates the intermediate steps and the cost of forming marbles, it has become the more widely used method.

Fiberization. Glass fiber formation, or *fiberization*, involves a combination of extrusion and attenuation. After being heated to approximately 2200 ºF (1200 °C), the molten glass flows or is extruded from the forehearth through an electrically heated platinum-rhodium alloy bushing or spinneret containing a large number (200 to 8000) holes in its base to form filaments, which are immediately quenched with water or an air spray to yield an amorphous structure (Fig. 2.5). Bushing plates are heated electrically, and the temperature is precisely controlled to maintain a constant glass viscosity. *Attenuation* is the process of mechanically drawing the extruded streams of molten glass into fibrous elements called *filaments*. A high-speed winder catches the molten streams and, because it revolves at a circumferential speed of approximately two miles per minute (much faster than the molten glass exiting the bushings), tension is applied, drawing them into thin filaments.

Nozzle diameter determines filament diameter, and the number of nozzles equals the number of ends. Fiber diameter (typically around 5 to 20 μm) is controlled by hole size, draw speed, temperature, melt viscosity, and cooling rate. In typical glass fiber terminology, a number of individual strands (or ends) are usually incorporated into a roving to provide a convenient form for subsequent processing. Rovings are preferred

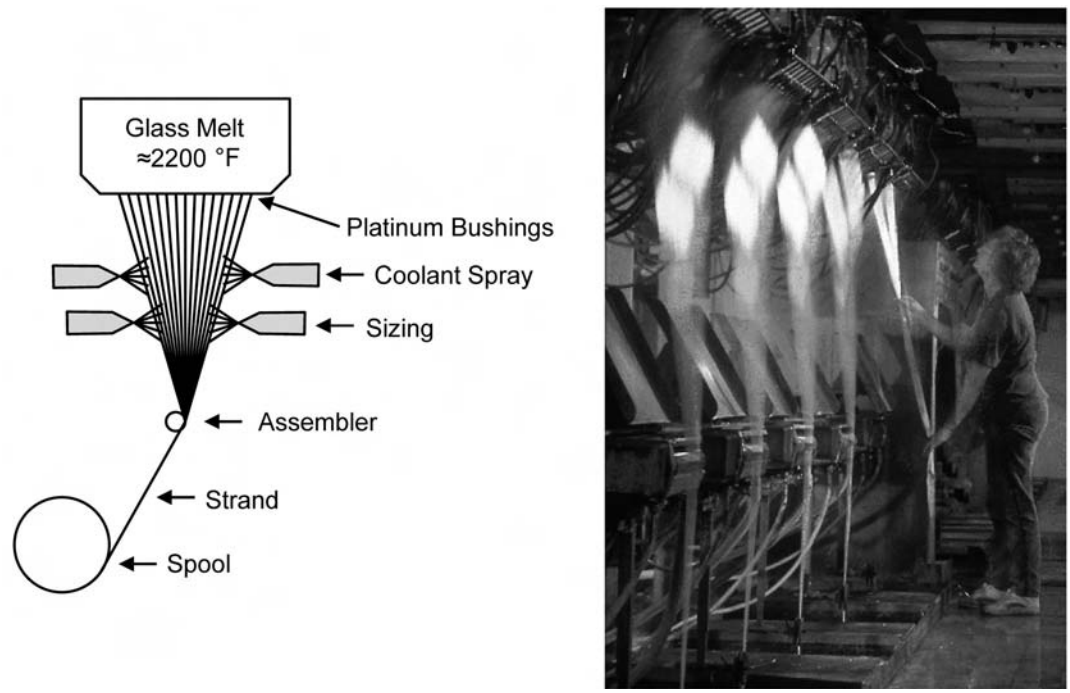


Fig. 2.5 Manufacturing processes for fiberglass fibers

for most reinforcements because they have higher mechanical properties than twisted yarns. Rovings are wound onto individual spools (Fig. 2.6) containing 20 to 50 lb (9 to 23 kg) of fiber. If the material is to be used for weaving, it is usually twisted into a yarn to provide integrity during the weaving operations. The strands are specified by their yield (yd/lb) or *denier* (the weight in grams of 9000 m of fiber). Another textile term frequently encountered is *tex*, which is the weight in grams of 1000 m of fiber.

Coating. Because glass fibers are monolithic, linearly elastic brittle materials, their high strength depends on the absence of flaws and defects. Flaws are nanometer-size submicroscopic inclusions and cracks. Tensile strength depends on the internal stresses at the surface, which are different than in the interior due to the very high cooling rates on solidification. Although this surface layer is only about one nanometer thick, it is on the order of the flaw size that controls the strength of glass fibers. Virgin glass filaments are very susceptible to degradation from exposure to both air and mechanical abrasion. The tensile strength of as-drawn fibers can be reduced by more than 20 percent after contact with air during drawing under normal ambient conditions due to absorption of atmospheric moisture into microscopic flaws, which reduces the fracture energy. Therefore, a sizing is applied immediately after manufacturing to prevent scratches from forming on the surface during spooling and from mechanical damage from weaving, braiding, and other textile processes. Sizings are extremely thin coatings that account for only about one to two percent by weight. The sizing (usually a starch and a lubricant) can be removed by either solvents or heat scouring after all mechanical operations are completed.

After the sizing is removed, it is replaced with a surface finish that greatly improves the fiber-to-matrix bond. For example, organosilane coupling agents have one end group that is compatible with the silane structure of the glass and another end group that is compatible with the organic matrix. The silane molecule on hydration in water can be represented by the following simplified formula:

$$R \ldots Si(OH)_3$$

The silane bonds with the oxide film at the surface of the inorganic fiber glass, while the organic functional group R is incorporated into the organic matrix during its cure. Coupling agents are critical to the performance of the glass-reinforced

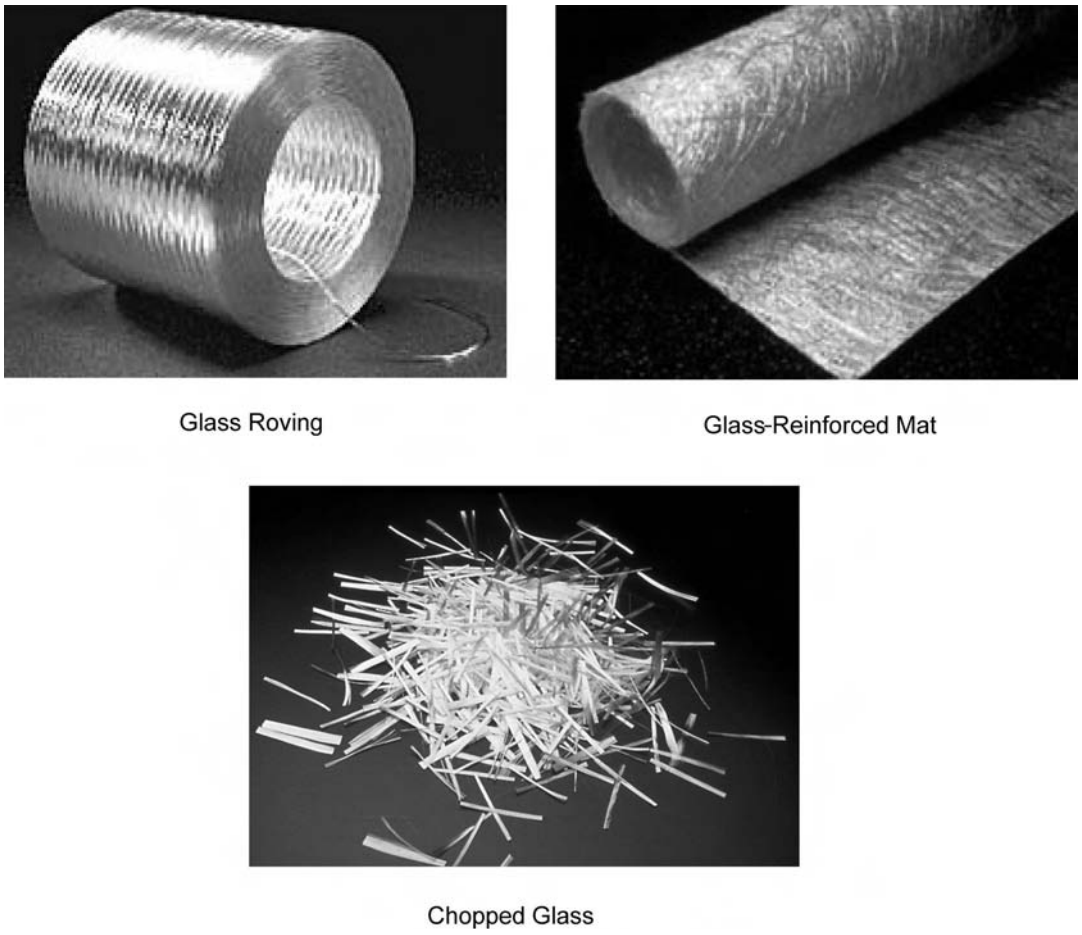


Fig. 2.6 Typical glass fiber product forms

composites. Improvements of over 100 percent have been demonstrated in composite tensile, flexural, and compression strength. The coupling agent also helps to protect the glass fiber from attack by water. Some sizings also function as coupling agents, and therefore remain on the fiber throughout the manufacturing process. The organic functional group R must be a group that is chemically compatible with the matrix resin. For example, for an epoxy resin, an epoxy silane may be used. Many different types of sizings/finishes are available, and it is important that the one selected is compatible with both the fiber and the matrix. A partial list of some of the coupling agents for various resins include vinyl silane (methacrylate silane) used for polyester resins; Volan (methacrylate chromic chloride) used for polyester and epoxy resins; amino silane used for epoxy, phenolic, and melamine resins; and epoxy silane used for epoxy and phenolic resins.

Antistatic agents and lubricants can also be used to improve handling and processing characteristics such as hardness and softness. If the glass fiber will be chopped into short lengths for fiber spraying, hardness is a desirable property because it improves the ability to be chopped. On the other hand, if the fiber will be used in a lay-up operation where drapablility and forming are important, then softness is a desirable property.

Drying/Packaging. Drawn, sized filaments are collected together into a bundle, forming a glass strand consisting of 51 to 1624 filaments. The strand is wound on a drum into a forming package. Forming packages, still wet from water cooling and sizing, are dried in an oven, after which they are ready to be palletized and shipped

or further processed into chopped fiber, roving, or yarn. Roving is a collection of strands with little or no twist. For example, an assembled roving might be made from 10 to 15 strands wound together into a multi-end roving package. Yarn is made from one or more strands, which are twisted to protect the integrity of the yarn during subsequent processing operations such as weaving.

While glass has a high tensile strength comparable to that of some high-strength carbon fibers, its modulus and fatigue properties are inferior to those of carbon. In addition, glass fibers are susceptible to static fatigue in which their strength decreases with time under a static tensile load. While glass fibers do not absorb water into their bulk, water molecules can attach to their surface, forming a very thin, softened layer. This adsorbed layer can have an important effect on fiber strength because water and other surface active substances lead to surface microcracks. Humid environments reduce the strength of glass fibers under sustained loading, as the moisture adsorbed onto the surface of the flaw reduces the surface energy, thus promoting slow crack growth to a critical size.

2.4 Aramid Fibers

Aramid fibers are organic fibers with stiffness and strength intermediate between those of glass and carbon. Dupont's Kevlar fiber is the most prevalent. These aromatic polyamides are part of the nylon family. Aramid fibers are based on the amide linkage formed by the reaction between carboxolic acid and the amine group. When the linkage occurs between straight-chained saturated molecules, aliphatic amides known commercially as *nylon* are formed. When the linkage occurs between unsaturated benzene rings, aromatic amides called *aramids* are formed (Fig. 2.7). The aromatic ring structure contributes high thermal stability, while the para configuration leads to stiff, rigid molecules that contribute high strength and high modulus.

Kevlar is made by reacting para-phenylene diamine with terephthaloyl chloride in an organic solvent to form polyparaphenylene terephthalamide (aramid). This is a condensation reaction that is followed by extrusion, stretching, and drawing. The polymer is washed and then dissolved in sulfuric acid. At this point, the polymer is a partially oriented liquid crystal. The polymer solution is then extruded through small holes (spinnerets). The fibers are oriented in solution and during spinning and are further oriented as they pass through the spinneret. The fibers are then washed, dried, and wound up.

The structure of aramid fibers (Fig. 2.8) consists of highly crystalline, aligned polymer chains separated into distinct zones or fibrils. The aromatic rings provide thermal stability and result in a crystalline, rigid, rod-like structure held together by strong covalent bonds. However, the bonds between the chains are relatively weak hydrogen bonds, which result in defibrillation failures in tension and kink band formation in compression (Fig. 2.9). The compression strain-to-failure is only about 25 percent of the tensile value. As a result of this compression behavior, the use of aramid fibers in applications that are subject to high-strain compressive or flexural loads is limited. However, the compressive

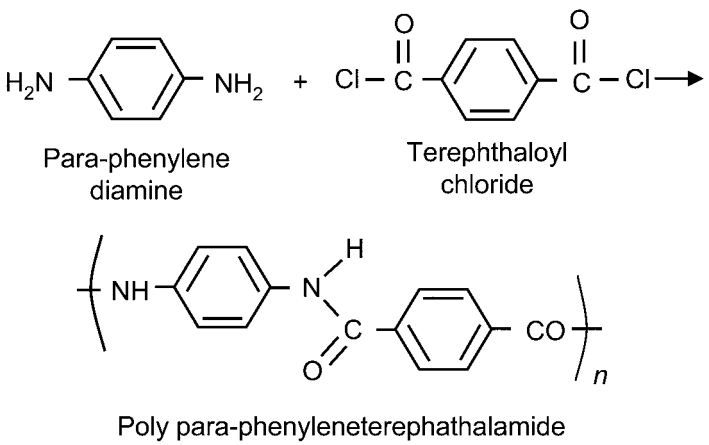


Fig. 2.7 Chemical structure of para-aramid. Source: Ref 3

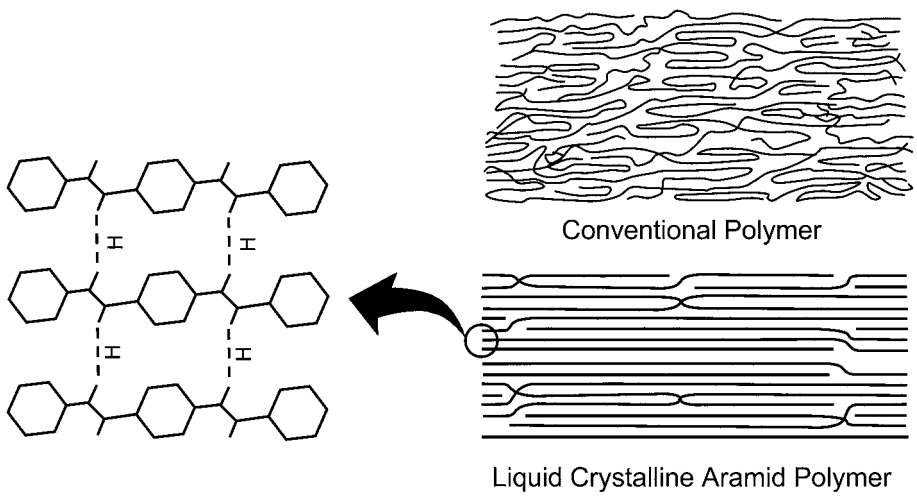


Fig. 2.8 Conventional polymer and liquid crystal–like aramid polymers. Source: Ref 3

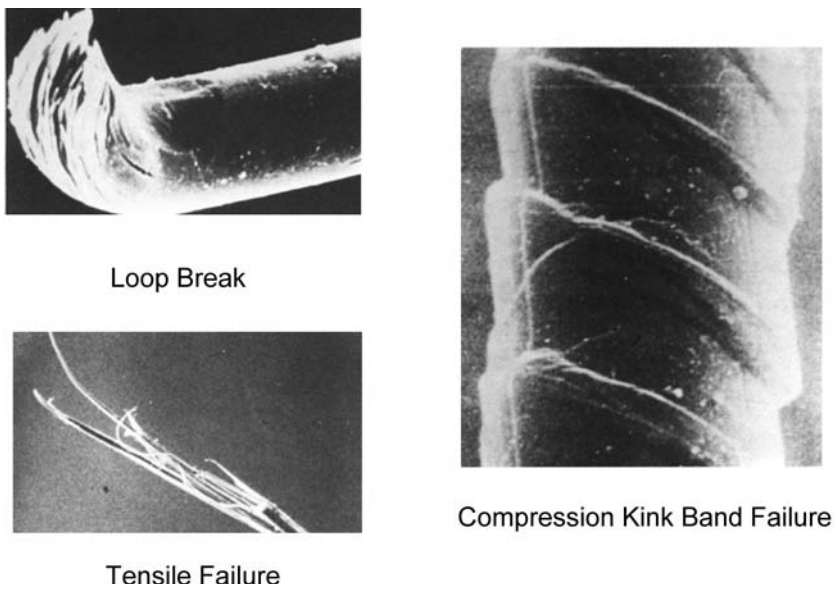


Fig. 2.9 Aramid fiber failure modes. Source: Ref 3

buckling characteristics have led to the development of crashworthy structures that rely on the fail-safe behavior of aramid composites under sustained high compressive loading.

Due to their extreme toughness, aramid fibers are often used for ballistic protection. A major advantage of aramid fibers is their ability to absorb large amounts of energy during fracturing, which results from their high strain-to-failure values, their ability to undergo plastic deformation in compression, and their ability to defibrillate during tensile fracture. The Kevlar fibrillar structure and compressive behavior contribute to composites that are less notch sensitive and that fail in a ductile, nonbrittle, or noncatastrophic manner, as opposed to glass and carbon.

Unlike glass and carbon, or graphite, fibers, aramid fibers are not surface treated because no acceptable surface treatment for aramid fibers has been developed to date. Sizings are used when the fiber will be woven, made into rope, or used in ballistic applications. Aramid fibers are

lightweight and have a combination of good tensile strength and modulus, excellent toughness, and outstanding ballistic and impact resistance. However, due to the lack of adhesion to the matrix, they exhibit relatively poor transverse tension, longitudinal compression, and interlaminar shear strengths. Like carbon and graphite, aramid fibers exhibit a negative coefficient of thermal expansion.

The three most prevalent aramid fibers are Kevlar 29 (low modulus, high toughness), Kevlar 49 (intermediate modulus), and Kevlar 149 (high modulus). The property differences in the different grades of Kevlar are due to changes in process conditions that promote additional crystallinity in the intermediate- and high-modulus fibers. The tensile modulus of Kevlar fibers is a function of molecular orientation. Kevlar 29 has a modulus of 12 msi (83 GPa) that is slightly higher than that of E-glass 10 msi (70 GPa). Heat treatment under tension increases crystalline orientation, and the resulting fiber (Kevlar 49) has a modulus of 19 msi (130 GPa). Kevlar 149 has an even higher modulus approximately 27 msi (185 GPa); and is available on special order. Normal bundle size ranges from 134 to 10,000 filaments per bundle.

Like carbon fibers, aramid fibers are available in tows or yarns of various weights that can be converted to woven cloth or chopped fiber mat. However, because the fibers are extremely tough, they are more difficult to cut, which causes some handling problems. Because aramid yarns and rovings are relatively flexible and nonbrittle, they can be processed in most conventional textile operations, such as twisting, weaving, knitting, carding, and felting. Yarns and rovings are used in filament winding, prepreg tape, and pultrusion processes. Applications include missile cases, pressure vessels, sporting goods, cables, and tension members. Aramid paper used in honeycomb sandwich constructions is made of Nomex aramid fiber. Nomex is chemically related to Kevlar, but its strength and modulus are considerably lower, more like those of conventional textile fibers.

The aromatic chemical structure of aramid fibers imparts a high degree of thermal stability. They decompose in air at 800 °F (425 °C) and are inherently flame resistant, with a limiting oxygen index of 0.29. They can be used at a temperature range of −330 to +390 °F (−200 to +200 °C), but they are not generally used for extended periods at temperatures above 300 °F (150 °C) because of oxidation. Aramid fibers are resistant to most solvents except strong acids and bases, and they have a strong tendency to absorb moisture. At 60 percent relative humidity, Kevlar 49 absorbs about four percent moisture and Kevlar 149 absorbs around 1.5 percent moisture due to its higher crystallinity. The effect of moisture on tensile strength at ambient temperatures is not significant. Aramid fibers are prone to significant short-term creep even at modest temperatures, but long-term creep is negligible. Aramid fibers are also prone to stress rupture under prolonged static loading, but they are much less sensitive to this mode of failure than glass fibers. Aramid fibers are degraded in strength by prolonged exposure to ultraviolet radiation, and while this can be a serious concern with cables that have exposed fibers, it is not a significant problem for aramid composites because the fibers are protected by the resin matrix.

2.5 Ultra-High Molecular Weight Polyethylene Fibers

Gel-spun polyethylene fibers are ultra-strong, high-modulus fibers based on the standard polyethylene molecule. Gel-spun polyethylene fibers are produced from polyethylene having a very high molecular weight (UHMWPE). This material is chemically identical to normal high-density polyethylene, but the molecular weight is higher than that of the commonly used polyethylene grades. The chemical nature of polyethylene remains in the gel-spun fiber, which can be both an advantage and a limitation; abrasion and flex life are very high, but the melting point is sometimes too low for use in many applications.

UHMWPE fibers are commercially produced under the trade names Dyneema in the Netherlands and Japan and Spectra in the United States. In the gel-spinning process, the molecules are dissolved in a solvent and spun through a spinneret. In solution, the molecules become disentangled and remain in that state after the solution is spun and cooled to produce filaments. Because of its low degree of entanglement, the gel-spun material can be drawn to a very high extent (super-drawn). As the fiber is superdrawn, a very high level of macromolecular orientation is attained (Fig. 2.10), resulting in a fiber with a very high strength and modulus. Gel-spun fibers are characterized by a high degree of chain extension, parallel orientation greater than 95 percent, and a high level of crystallinity (up to 85 percent).

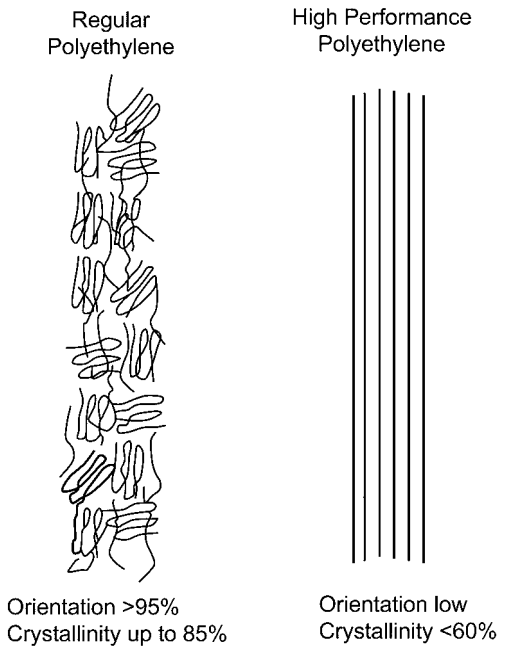


Fig. 2.10 Macromolecular orientation of ultra-high molecular weight (UHMWPE) and normal polyethylene (PE). Source: Ref 4

Owing to their low density and good mechanical properties, their performance on a weight basis is extremely high. At a density of 0.97 g/cm^3, they are even lighter than aramid fibers; they are so light that they will float on water. They have high impact resistance and attractive electrical properties (in this case, low dielectric constant and low loss tangent), and they have exceptional chemical resistance and low moisture absorption characteristics.

Due to the relatively low melting point of polyethylene, UHMW-polyethylene fibers are limited to a maximum use temperature of 200 °F (95 °C). For example, Spectra melts at a temperature of around 300 °F (150 °C). On a specific basis, polyethylene fibers have tensile properties exceeding those of most other fibers, including aramid. Like aramid fibers, polyethylene fibers exhibit low compression strength and fail under compression through kink band formation. Also, they do not form a strong bond to the matrix, which results in poor transverse tension and compression strengths.

Because they are thermoplastic, polyethylene fibers are subject to creep under continuous loading, even at modest temperatures, which limits their use in applications involving high, prolonged static loading. Creep occurs in part because the fibers cannot be drawn to their full extent in commercial production. However, sliding of the polymer chains encouraged by the weak interchain bonding also makes a significant contribution.

2.6 Carbon and Graphite Fibers

Carbon and graphite fibers are the most prevalent fiber forms used in high-performance composite structures. They can be produced with a wide range of properties. They generally exhibit superior tensile and compressive strength, have high moduli, have excellent fatigue properties, and do not corrode. Although the terms are often used interchangeably, *graphite fibers* are subjected to heat treatments above 3000 °F (1650 °C), have three-dimensional ordering of their atoms, have carbon contents greater than 99 percent, and have elastic moduli (E) greater than 50 msi (345 GPa). *Carbon fibers* have lower carbon contents (93 to 95 percent) and are heat treated at lower temperatures.

The graphite structure consists of carbon atoms arranged in a lamellar structure of hexagonal layers (Fig. 2.11). The high strengths and moduli of carbon and graphite fibers are a result of the strong covalent bonds (≈525 kJ/mol) along the basal planes (in this case, the *ABABAB* stacking sequence). Carbon fibers actually consist of graphite and nongraphitic carbonaceous material. The graphitic phase is in the form of crystallites with discrete dimensions that can be oriented differently from each other, with high-stiffness carbon fibers containing a large portion of graphite aligned in the fiber direction. As the graphitization heat treatment temperature increases, the planes become oriented more parallel to the fiber axis. Carbon and graphite fibers are extremely anisotropic. Because the covalently bonded basal planes are held together by rather weak van der Waals forces (≈10 kJ/mol), the transverse strength and modulus of the fiber are much less than the longitudinal values. For example, the longitudinal modulus can be as high as 145 msi (1000 GPa), while the transverse modulus may only be approximately 5 msi (35 GPa).

Carbon and graphite fibers can be made from rayon, polyacrylonitrile (PAN), and petroleum-based pitch precursors. Although PAN fibers are more expensive than rayon fibers, PAN is used extensively for structural carbon fibers because the carbon yield is almost double that of rayon fibers. The pitch process produces fibers that

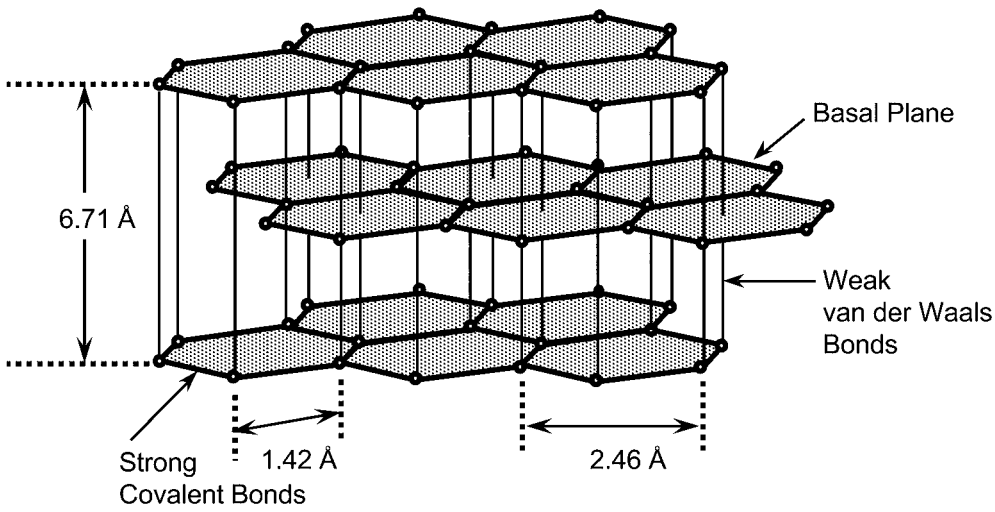


Fig. 2.11 Structure of graphite crystal

have lower strength than those produced from PAN, but it can produce high-modulus fibers 50 to 145 msi (345 to 1000 GPa). The generalized manufacturing processes for PAN and pitch-based carbon fibers are shown in Fig. 2.12.

Rayon-Based Carbon Fibers. Rayon-based fibers originate from wood pulp in which the cellulose is extracted and the tows are produced by wet spinning. The fibers are then heat treated at 400 to 800 °F (205 to 410 °C) to start the conversion process to carbon. Unlike PAN- and pitch-based fibers, rayon-based fibers do not require a stretching and heat-setting process prior to carbonization; they can be carbonized without melting. During carbonization and graphitization, there is a gradual ordering of the structure. However, the alignment is rather poor compared to that of PAN- and pitch-based fibers. To improve the strength and modulus of rayon-based fibers, it is necessary to hot stretch the graphitized fibers up to 50 percent at 5000 to 5500 °F (2760 to 3040 °C), which increases the orientation of the basal planes; they rotate toward the fiber axis, and the porosity within the fibers is reduced. The disadvantages of rayon-based carbon fibers are (1) the decreasing availability of a suitable rayon precursor; (2) a low yield, only 15 to 30 percent; and (3) problems with hot stretching the fiber at the end of the cycle. However, rayon-based carbon fibers work well in carbon-carbon and carbon-phenolic composites, where fibers produced with low moduli minimize microcracking of the matrix during fabrication.

PAN-Based Carbon Fibers. Polyacrylonitrile-based fibers exhibit a high degree of orientation in the raw precursor form and have much higher yields of approximately 50 percent than rayon-based fibers. The production process of PAN-based carbon fibers can be divided into five steps:

1. Spinning and stretching the PAN copolymer to form a fiber
2. Stabilization and oxidation in air at 390 to 570 ºF (200 to 300 °C) under tension
3. Carbonization in an inert atmosphere at 1800 to 2900 ºF (980 to 1595 °C)
4. Graphitization in an inert atmosphere at 3600 to 5500 ºF (1980 to 3040 °C)
5. Surface treatment and sizing

Polyacrylonitrile is formed by the polymerization of the acrylonitrile monomer, an olefin derived from the substitution of the nitrile group for a hydrogen. Because PAN decomposes before melting, it is necessary to make a solution using a solvent such as dimethyl formamide to be able to spin the material into a fiber. The spinning operation can be done either dry, where the solvent evaporates in a spinning chamber, or wet, where the fiber is placed in a coagulating bath solution. In dry spinning, the rate of solvent removal is greater than the rate of diffusion within the fiber, and the surface of the filament hardens faster than the interior, resulting in its collapse and the formation of a dogbone cross section. In wet spinning, the fiber dries uniformly and the cross section is circular. Of the two processes,

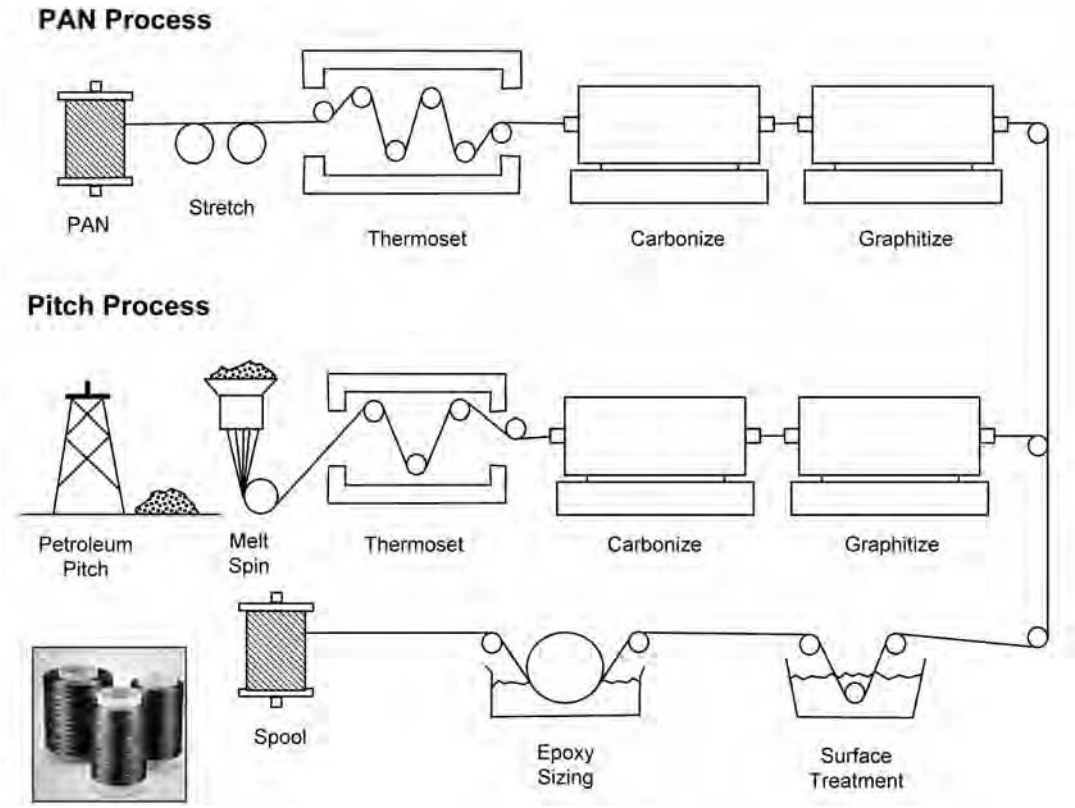


Fig. 2.12 Polyacrylonitrile (PAN) and pitch-based carbon fiber manufacturing processes

only wet-spun PAN is currently used for carbon-fiber precursors. The spun fiber is composed of a fibrillar, or ribbon-like, network, which acquires a preferred orientation parallel to the fiber axis, provided that the fiber is stretched either while it is still in the coagulating bath or subsequently in boiling water. Stretching results in an elongation of 500 to 1300 percent, and is an essential step in obtaining high-strength fiber.

Heat setting or oxidation crosslinks the PAN and stabilizes the structure so that it will not melt during the carbonization process. The heat-setting process converts the thermoplastic PAN into a nonplastic cyclic or ladder compound capable of withstanding the high temperatures used during carbonization. The PAN fibers are heated to 390 to 570 ºF (200 to 300 °C) in air for one to two hours while the fibers are under tension. Sufficient tension, causing elongation of 300 to 500 percent, is used to unfold the tightly folded chain molecules. The oxidizing environment causes the unfolded chains to crosslink with oxygen molecules, replacing hydrogen molecules on adjacent chains. Hydrogen combines with excess oxygen and is evolved as water vapor. Oxidation causes the formation of C=C bonds and the incorporation of hydroxyl (-OH) and carbonyl (-CO) groups in the structure, which promotes crosslinking and thermal stability. The product at this stage is often referred to as *oxy-PAN*.

Carbonization is conducted in a nitrogen atmosphere at 1800 to 2900 ºF (980 to 1595 °C) and converts the PAN to carbon. During carbonization, the fibers shrink in diameter and lose approximately 50 percent of their weight. As the PAN is slowly heated to the carbonization temperature, approximately equals 40 °F/min (22 °C/min), considerable amounts of volatile by-products are released, including water, carbon dioxide, carbon monoxide, ammonia (NH_3), hydrogen cyanide (HCN), methane (CH_4), and other hydrocarbons. The carbon yield is 50 to 55 percent. The circular morphology of the fiber is maintained, and the final diameter varies from 5 to 8 μm, which is approximately half that of the precursor PAN fiber. The removal of nitrogen occurs gradually over a range of temperatures: Nitrogen evolution starts at 1110 °F

(600 °C), reaching a maximum at 1650 °F (900 °C), approximately six percent remains at 1830 °F (1000 °C), and only 0.3 percent remains at 2380 °F (1305 °C). Carbonization results in a carbon network of hexagonal ribbons, known as *turbostatic graphite*, that tends to align parallel to the fiber axis (Fig. 2.13). The crystal structure is very small, which contributes to its high strength.

If a true graphite fiber is desired, the fiber is graphitized at temperatures between 3600 and 5500 °F (1980 and 3040 °C), which produces a more crystalline structure and a higher elastic modulus. The final carbon content is greater than 99 percent. This treatment completes the conversion of the remaining carbonaceous material to graphite. The graphite tends to align the basal planes in the direction of the fiber. However, during the process, the crystallite size can increase. The increase in graphite content results in increased stiffness, while the increase in crystallite size lowers the strength.

Carbon-fiber costs reflect the cost of heat treatment (Fig. 2.14). Higher-modulus fibers require higher heat-treating temperatures to produce the greater amounts of aligned graphite. Graphitization improves the degree of alignment of one ribbon to the next along the fiber axis. As the final graphitization temperature increases, the elastic modulus increases, while the strength reaches a maximum and then decreases in the manner shown in Fig. 2.15.

When carbon fibers were first introduced in the 1960s, it was soon realized that the as-manufactured carbon fiber did not bond well to epoxy resins. The importance of the effect of a proper surface treatment on fiber-to-matrix adhesion is shown in Fig. 2.16. Untreated carbon fibers exhibit almost no adhesion to the epoxy matrix. While poor adhesion does not affect 0° tensile strength, it does adversely affect matrix-dependent properties such as 90° tensile strength, 0° compressive strength, and interlaminar and in-plane shear strength. Therefore, in the next to last production step, the carbon fibers are subjected to an electrolytic oxidation that removes weak surface layers, etches the fibers,

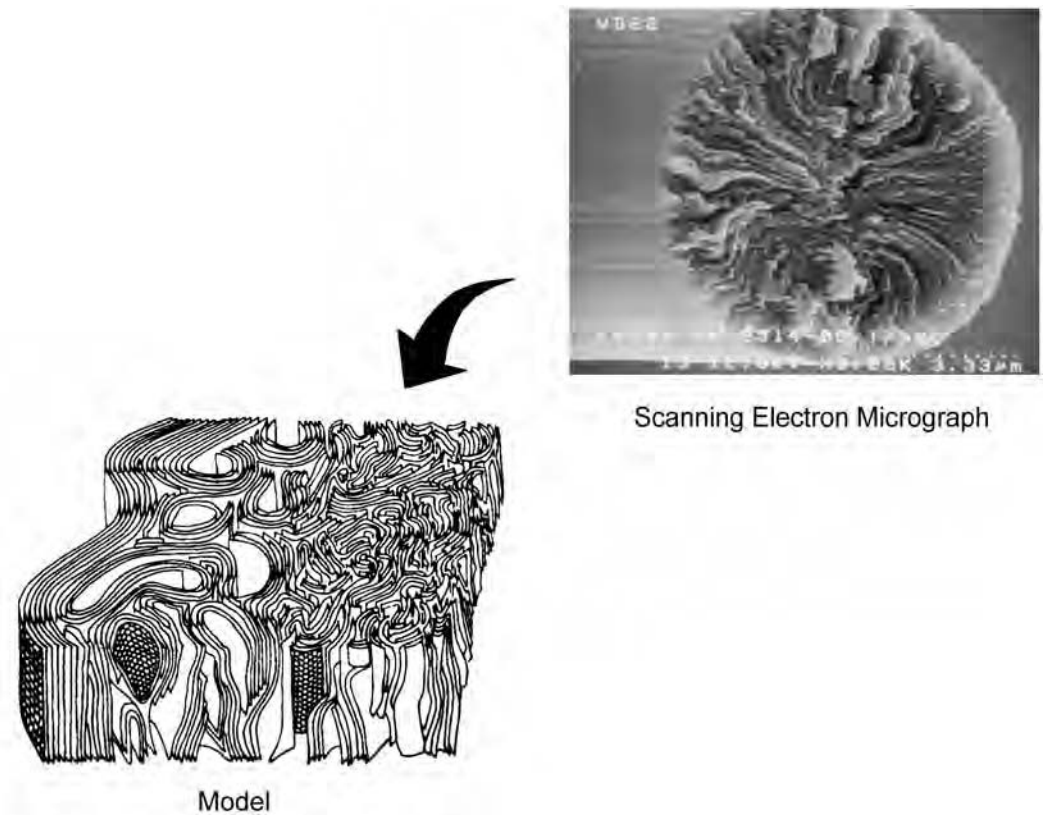


Fig. 2.13 Carbon fiber structure. Source: Ref 5

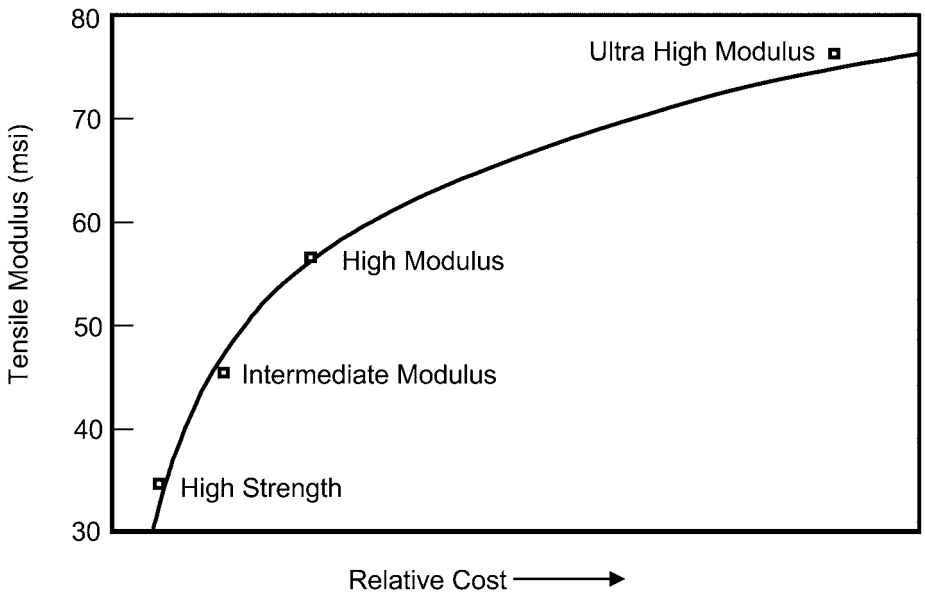


Fig. 2.14 Carbon fiber cost increases with the heat treatment used to obtain a higher modulus. Source: Ref 1

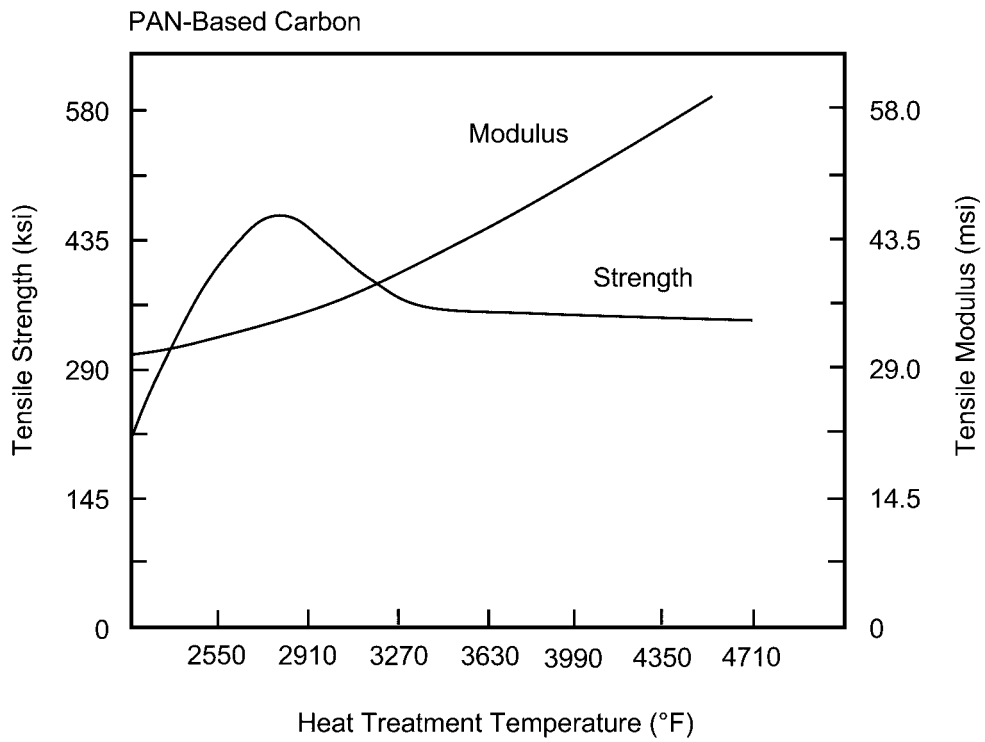


Fig. 2.15 Effect of heat treatment on the strength and modulus of PAN-based carbon fiber. PAN, polyacrylonitrile. Source: Ref 6

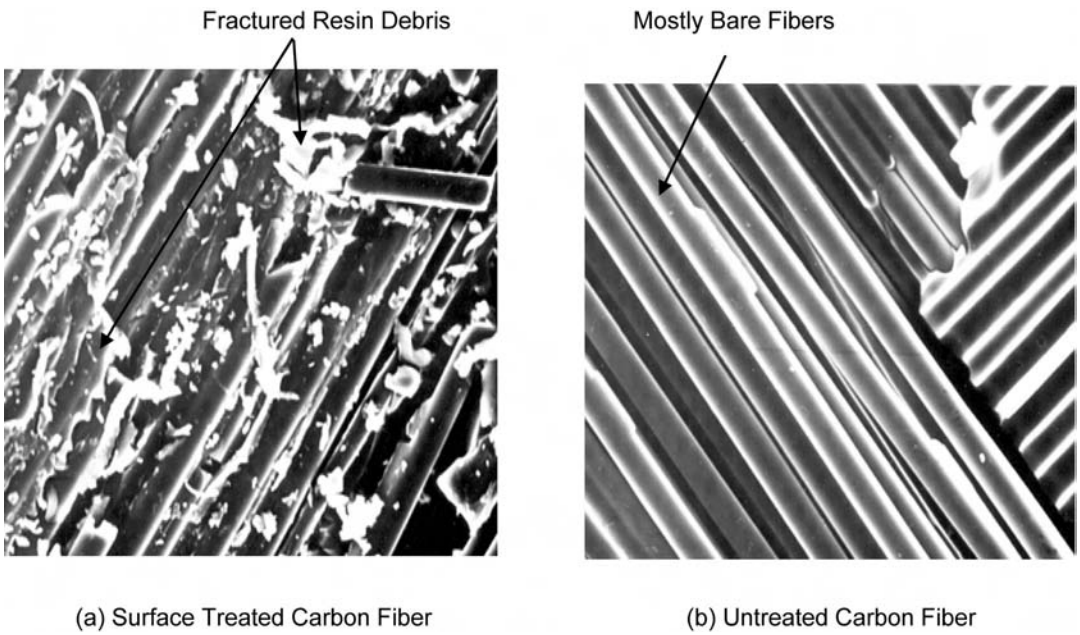


Fig. 2.16 Effect of surface treatments on fiber-to-matrix bonds: (a) good bond; (b) poor bond. Source: Ref 7

and generates reactive, or polar, groups. The surface treatment attaches carboxyl, carbonyl, and hydroxyl groups to the fiber surface, which can bond to the polymeric matrix.

The fiber emerges from the heat-treating furnace and passes around a positively charged roller (anode) and into an aqueous electrolytic cell. Various electrolytes, such as sodium hydroxide (NaOH), are used to conduct current and to create surface groups. The fiber is washed and dried before it enters the size-application bath. The surface generated by this treatment greatly improves adhesion to thermosets and to some thermoplastic resins.

The last step is the application of a protective material called *sizing* to the carbon fiber. If the fiber will be woven, sizes (usually uncatalyzed epoxy) are applied to the fiber to protect the fiber surface from mechanical abrasion. *Size, sizing,* and *finish* are all names for coatings applied to carbon fibers to make them easier to handle. The size protects the small filaments from damage by holding them together and reducing friction. Only a small amount of sizing is used, typically 0.5 to 1.5 percent. It should be noted that sizes for carbon fibers are not coupling agents, as are silane compounds used with glass fibers.

Pitch-Based Carbon Fibers. Pitch-based carbon and graphite fibers are made by heating coal tar pitch for up to 40 hours at 800 °F (425 °C), forming a highly viscous liquid having a high degree of molecular order known as a *mesophase*. The mesophase is spun through a small orifice that aligns the molecules along the fiber axis. Pitch-based fibers are then processed following the same basic steps used in PAN-based fiber manufacturing, namely, carbonization, graphitization, and surface treatment.

Pitch is a by-product of the distillation of coal, crude oil, and asphalt. Its carbon yield can exceed 60 percent, which is appreciably higher than the yield of PAN approximately 50 percent. The composition of pitch includes four generic fractions in variable proportions: (1) saturates, which are aliphatic compounds having a low molecular weight similar to that of wax; (2) napthene aromatics, which are low molecular weight compounds having a saturated ring; (3) polar aromatics, which are medium molecular weight compounds with some heterocyclic molecules; and (4) asphaltenes, which have a high molecular weight and a high degree of aromaticity. The higher the ratio of asphaltene, the higher the softening point, thermal stability, and carbon yield.

Pitch-based fibers can be divided into two groups: isotropic pitch fibers, which have low mechanical properties but are relatively low in cost, and mesophase pitch fibers, which have

very high moduli but are more expensive. Low-cost carbon fibers are produced from an isotropic pitch with a low softening point. The precursor is melt spun, thermoset at a relatively low temperature, and carbonized. The resulting fibers generally have low strength and a low modulus. Carbon fibers from mesophase pitch have medium strength and a high modulus. The processing of mesophase pitch fibers is similar to that of PAN fibers, except that the stretching step during heat treatment is not necessary. The processing steps can be summarized as follows:

1. Polymerization of the isotropic pitch to produce mesophase pitch
2. Spinning the mesophase pitch to obtain a *green fiber*
3. Thermosetting the green fiber
4. Carbonization and graphitization to obtain a high-modulus carbon or graphite fiber

The pitch is heated to approximately 750 °F (400 °C) and is transformed from an isotropic to a mesophase, or liquid crystal, structure consisting of large polyaromatic molecules with oriented layers in parallel stacking. The mesophase pitch is melt spun in a mono- or multifilament spinneret heated to 570 to 850 °F (300 to 455 °C) and pressurized with inert gas. It is drawn at a speed greater than 400 ft/min (122 m/min) with a draw ratio of approximately 1000 to l to a diameter of 10 to 15 μm (0.4 to 0.6 mil). The draw ratio is an important factor in the control of the orientation of the fiber structure; the higher the draw ratio, the greater the orientation and uniformity. At this stage the fiber is thermoplastic, and a thermosetting operation is needed to avoid relaxation of the structure and to prevent the filaments from fusing together. This thermosetting operation is carried out in an oxygen atmosphere or in an oxidizing liquid at approximately 570 °F (300 °C), causing oxidation crosslinking and stabilization of the filament. Temperature control during this thermosetting step is critical, because a temperature that is too high will relax the material and eliminate its oriented structure. The thermoset fibers are then carbonized at temperatures of up to 1830 °F (1000 °C). This is done slowly to prevent rapid gas evolution and the formation of bubbles and other flaws. Carbonization is followed by high-temperature graphitization at 5000 to 5500 °F (2760 to 3040 °C).

Pitch-based graphite fibers have a higher modulus and lower strength than PAN-based carbon fibers. In addition, pitch-based fibers tend to have more flaws such as pits, scratches, striations, and flutes. These flaws are detrimental to tensile properties but do not necessarily affect the modulus and thermal conductivity. As with PAN-based fibers, as the heat treatment temperature during carbonization/graphitization is increased, the fiber strength increases to a maximum and then decreases, while the modulus continues to increase. The higher temperatures used in the graphitization process for graphite fibers result in more orientation of the graphite cystallites parallel to the fiber axis. The better the alignment of the crystallites, the higher the modulus of the fiber. However, high crystallinity also causes the fiber to be weak in shear, which results in lower compressive strength. Therefore, high-crystalline graphite fibers do not exhibit balanced tensile and compressive mechanical properties. Pitch-based, high-modulus graphite fibers having a modulus between 50 and 145 msi (345 and 1000 GPa) are often used in space structures requiring high rigidity.

In addition to their high modulus and low thermal expansion, pitch-based graphite fibers have high values of thermal conductivity—for example, 900 to 1000 W/mK compared to only 10 to 20 W/mK for PAN-based carbon fibers. The large crystallites in graphite fibers are structurally close to the perfect graphite crystal and well aligned along the fiber axis, offering few scattering sites for phonons. This means that these fibers have high thermal conductivity along the fiber axis. Fibers with the highest degree of orientation, such as the pitch-based fibers, have the highest thermal conductivity. Their conductivity along the axis is higher than that of even the best metal conductor. Polyacrylonitrile-based fibers have much lower thermal conductivity because of their more pronounced isotropic structure. These high thermal conductivities are used to remove and dissipate heat in space-based structures. High-modulus graphite fibers can also be manufactured using the PAN process. However, the highest modulus attainable is around 85 msi (585 GPa).

The strength of carbon and graphite fibers depends on the type of precursor used, the processing conditions during manufacturing such as fiber tension and temperatures, and the presence of flaws and defects. Flaws in the carbon fiber microstructure include internal pits and inclusions, external gouges, scratches, and stuck filament residues, as well as undesirable characteristics such as striations and flutes. These flaws can have a considerable impact on fiber tensile strength but have little, if any, effect on modulus,

conductivity, and thermal expansion. Both carbon and graphite fibers usually have a slightly negative coefficient of thermal expansion, which becomes more negative as the modulus of elasticity increases. One consequence of using high and ultrahigh-modulus carbon fibers is the increased possibility of matrix microcracking during processing or environmental exposure due to the larger mismatch in the coefficients of thermal expansion between the fibers and the matrix.

Carbon fibers are available from a number of domestic and foreign producers having a wide range of strength and moduli. Polyacrylonitrile-based carbon fibers having strengths ranging from 500 to 1000 ksi (3.5 to 7 GPa) and moduli ranging from 30 to 45 msi (205 to 310 GPa) with elongations of up to two percent are commercially available. Standard-modulus PAN fibers have good properties with lower cost, while higher-modulus PAN fibers are higher in cost because high processing temperatures are required. Heating the fibers to 1800 °F (980 °C) yields PAN fibers containing 94 percent carbon and six percent nitrogen, while heating to 2300 °F (1260 °C) removes the nitrogen and raises the carbon content to around 99.7 percent. Higher processing temperatures increase the tensile modulus by refining the crystalline structure and the three-dimensional nature of the structure. Carbon fiber diameters usually range from 0.3 to 0.4 mil (7.6 to 10 μm).

Carbon fibers are provided in untwisted bundles of fibers called *tows*. Tow sizes can range from as little as 1000 fibers/tow up to more than 200,000 fibers/tow. A typical designation of "12k tow" indicates that the tow contains 12,000 fibers. Normally, as the tow size decreases, the strength and cost increase. Due to its cost, the small 1k tow size is normally not used unless the property advantages outweigh the cost disadvantages. For aerospace structures, normal tow sizes are 3k, 6k, and 12k, with 3k and 6k being the most prevalent for woven cloth and 12k for unidirectional tape. It should be noted that there are very large tow sizes greater than 200k, which are primarily used in commercial applications and are normally broken down after manufacturing into smaller tow sizes such as 48k for subsequent handing and processing. The cost of carbon fibers depends on the manufacturing process, the type of precursor used, the final mechanical properties, and the tow size. Costs can vary from less than $10 per pound for large-tow commercial fibers to several hundred or even several thousand dollars per pound for small-tow, ultra-high-modulus, pitch-based fibers. The maximum use temperature of carbon and graphite fibers in an oxidizing atmosphere is 930 °F (500 °C).

The ideal engineering material would have high strength, high stiffness, high toughness, and low weight. Carbon fibers combined with polymer matrices meet these criteria more closely than any other material. Carbon fibers are elastic to failure at normal temperatures, creep resistant and not susceptible to failure; are chemically inert except in strong oxidizing environments or in contact with certain molten metals; and have excellent damping characteristics. Some disadvantages of carbon fibers are brittleness and low impact resistance, low strains-to-failure, lower compressive strengths than tensile strengths, and higher in cost than glass fibers.

2.7 Woven Fabrics

Two dimensional woven products (Fig. 2.17) are usually offered as a 0º, 90º construction. However, bias weaves (45º, 45º) can be made by twisting the basic 0º, 90º construction. Weaves are made on a loom by interlacing two orthogonal (mutually perpendicular) sets of yarns (warp and fill). The warp direction is parallel to the length of the roll, while the fill, weft, or woof direction is perpendicular to the length of the roll. Textile looms (Fig. 2.18) produce woven cloth by separation of the warp yarns and insertion of the fill yarns. Most weaves contain similar numbers of fibers and use the same material in both the warp and fill directions. However, hybrid weaves (Fig. 2.19), such as carbon and glass, and weaves dominated by warp yarns can also be produced. These hybrid weaves can be used to obtain specific properties, such as mixing carbon with aramid to take advantage of the toughness of aramid, or to reduce costs, such as mixing glass with carbon fibers. Woven broadgoods may be purchased either as a dry preform or preimpregnated with a B-staged resin. In most applications, multiple layers of two-dimensional weaves are laminated together. As with tape laminates, layers are oriented to tailor the strength and stiffness.

Weaves may be classified by the pattern of interlacing, as shown in Fig. 2.20. Probably the two most prevalent weaves used in high-performance composites are the plain and satin weaves, which are compared in Fig. 2.21. The simplest pattern is the plain weave, in which every warp and fill yarn goes alternatively over and then under

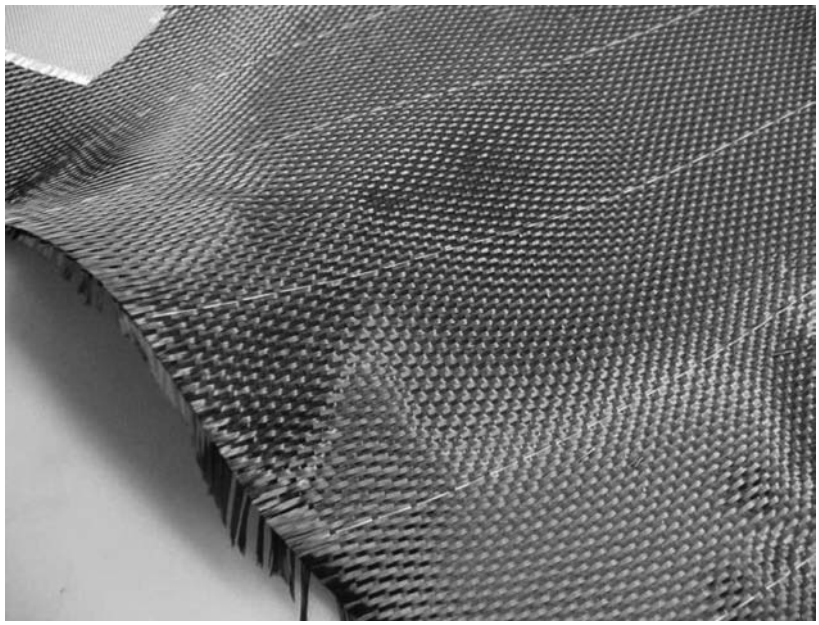


Fig. 2.17 Two-dimensional dry woven carbon cloth

successive warp and fill yarns, respectively. Plain weaves have more interlaces per unit area than any other type of weave, and therefore the tightest basic fabric design, and are the most resistant to in-plane shear movement. Therefore, plain weaves resist distortion during handling but may be difficult to form on complex contours. They are also more difficult to wet-out during impregnation. Another disadvantage of the plain weave is the frequent exchanges of position from top to bottom made by each yarn. This waviness, or yarn crimp, reduces the strength and stiffness of the composite.

The basket weave is a variation of the plain weave in which two (or more) warp and two (or more) fill yarns are woven together. An arrangement of two warps crossing two fills is designated as a *2×2 basket*, but the arrangement of fibers need not be symmetrical; it is possible to have 8×2, 5×4, and other variations. The basket weave has less crimp than the plain weave and is therefore somewhat stronger.

Satin weaves are characterized by a minimum of interlacing and, therefore, have less resistance to in-plane shear movement and have the best drapablility. Plain weaves are often used for less curved parts, while harness satin weaves are used for more highly contoured parts. In the four-harness satin weave, the warp yarns skip over three fill yarns and then under one fill yarn. In the five-harness satin weave, the warp yarns skip over four fill yarns and then under one fill yarn. In the eight-harness satin weave, the warp yarns skip over seven fill yarns and then under one fill yarn. Due to less fiber crimp, satin weave fabrics are stronger than plain weave fabrics. They also provide smooth part surface finishes at a minimum per ply thickness. The eight-harness satin weave has the best drapablility of this group. However, five-harness weaves normally use a 6k carbon tow, which is less expensive than the 3k carbon tow used for eight-harness satin weaves. The trend in industry has been to move toward greater use of the less expensive five-harness satin weaves.

Twill weaves are occasionally used because they have better drapablility than the plain weaves and are known for their extremely good wet-out during impregnation. In this weave, one or more warps alternately weave over and under two or more fills in a regular repeating manner, producing the visual effect of a straight or broken "rib" to the fabric.

The leno and mock leno weaves are rarely used for structural composites. The leno weave is also a form of the plain weave in which the adjacent warp fibers are twisted around consecutive fill fibers to form a spiral pair, effectively locking each fill in place. This construction produces an extremely open fabric with a low fiber

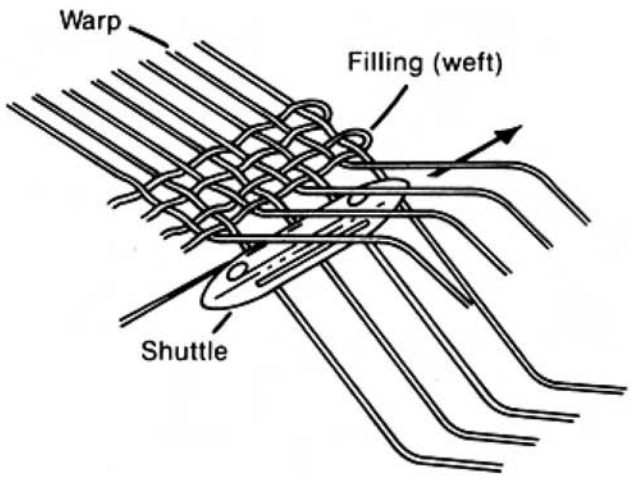




Fig. 2.18 Weaving glass cloth on a textile loom

content. The leno weave is frequently used to tie the edges of dry fabric together so that it will not unravel during handling. The mock leno (also a version of the plain weave) has occasional warp fibers at regular intervals but several fibers apart, which deviate from the alternate under-over interlacing and instead, interlace every two or more fibers. This happens with similar frequency in the fill direction, and the overall result is a fabric having increased thickness, a rougher surface, and more porosity.

Woven fabrics often contain tracer yarns. For example, yellow aramid tracers are often woven on two-inch (50 mm) spacings in carbon cloth

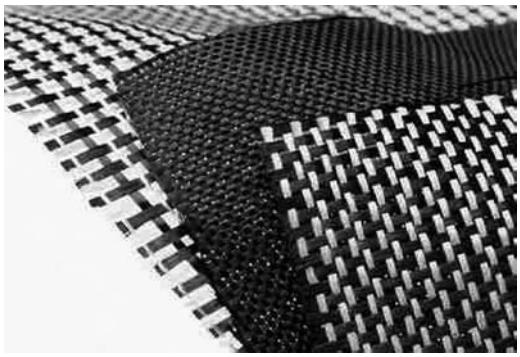


Fig. 2.19 Examples of hybrid weaves

along the warp direction to help fabricators identify warp and fill direction during composite part lay-up.

The selection of a weave involves manufacturing considerations as well as final mechanical properties. The weave type affects dimensional stability and the conformability (or drape) of the fabric over complex surfaces. For example, satin weaves exhibit good conformability. Unfortunately, good conformability and resistance to shear are mutually exclusive. Thus, while woven fabrics are frequently the material of choice for complex geometries, the designer must be aware that specified material directions may be impossible to maintain on compound contours and other complex shapes; that is, initially orthogonal yarns may not remain orthogonal in the finished product. Commonly used weave styles for high-performance composites are shown in Table 2.2.

2.8 Reinforced Mats

Reinforced mats (Fig. 2.6) are made of either chopped strands or continuous strands layed down in a swirl pattern. Mats are generally held together by resinous binders. They are used for medium-strength parts having uniform cross sections. Both chopped and continuous-strand reinforcing mats are available in weights varying from 0.75 to 4.5 oz/ft^2 (240 to 1430 g/m^2) and in various widths. Surfacing mats, or veils, are thin, lightweight materials used in conjunction with reinforcing mats and fabrics to provide good surface finish. They are effective in blocking out the fiber pattern of the underlying mat or fabric. Combination mats, consisting of one ply of woven roving chemically bonded to chopped strand mat, are available from several processors of glass reinforcements. These products form a drapable reinforcement that combines the bidirectional fiber orientation of woven roving with the multidirectional fiber orientation of chopped strand mat. This saves time in hand lay-up since two layers can be placed in the mold in a single operation. Other combinations are available for surface finish improvement as well as for multilayer reinforcement.

2.9 Chopped Fibers

Chopped fibers (Fig. 2.6) produce higher strength in compression and in injection-molded parts. Chopped fibers are usually available in lengths ranging from 0.125 to 2 in. (3.2 to 50 mm), although shorter milled fibers and longer fibers are available. They are blended with resins and other additives to prepare molding compounds for compression or injection moldings, encapsulation, and other processes. Chopped-glass reinforcement is available with many surface treatments to ensure optimum compatibility with most thermosetting and thermoplastic resin systems. The shorter chopped reinforcements are best suited for blending with thermoplastic resin systems for injection molding. Longer chopped reinforcements are blended with thermosetting resins for compression and transfer molding. Milled fibers combine reinforcing properties with processing ease in encapsulation or injection molding. Milled fibers are 0.03125 to 0.125 in. (0.8 to 3.2 mm) lengths of fibrous glass. They are used to reinforce thermoplastic parts where strength requirements are low to moderate and for reinforcing fillers in adhesives.

2.10 Prepreg Manufacturing

Prepreg is an important product form in which either unidirectional fibers or woven cloth is impregnated with a controlled amount of resin. The resin is staged or advanced (B-staged) to the point where the resin in the prepreg is a tacky semisolid, which allows the layers to be layed up to form a laminate that can be cured. A resin goes through several stages in the manufacturing process. Resins are normally made by batch manufacturing, in which the ingredients are placed in mixers (Fig. 2.22) and slowly heated to the A-stage condition, or initial mixed state, where the resin has a very low viscosity, which allows

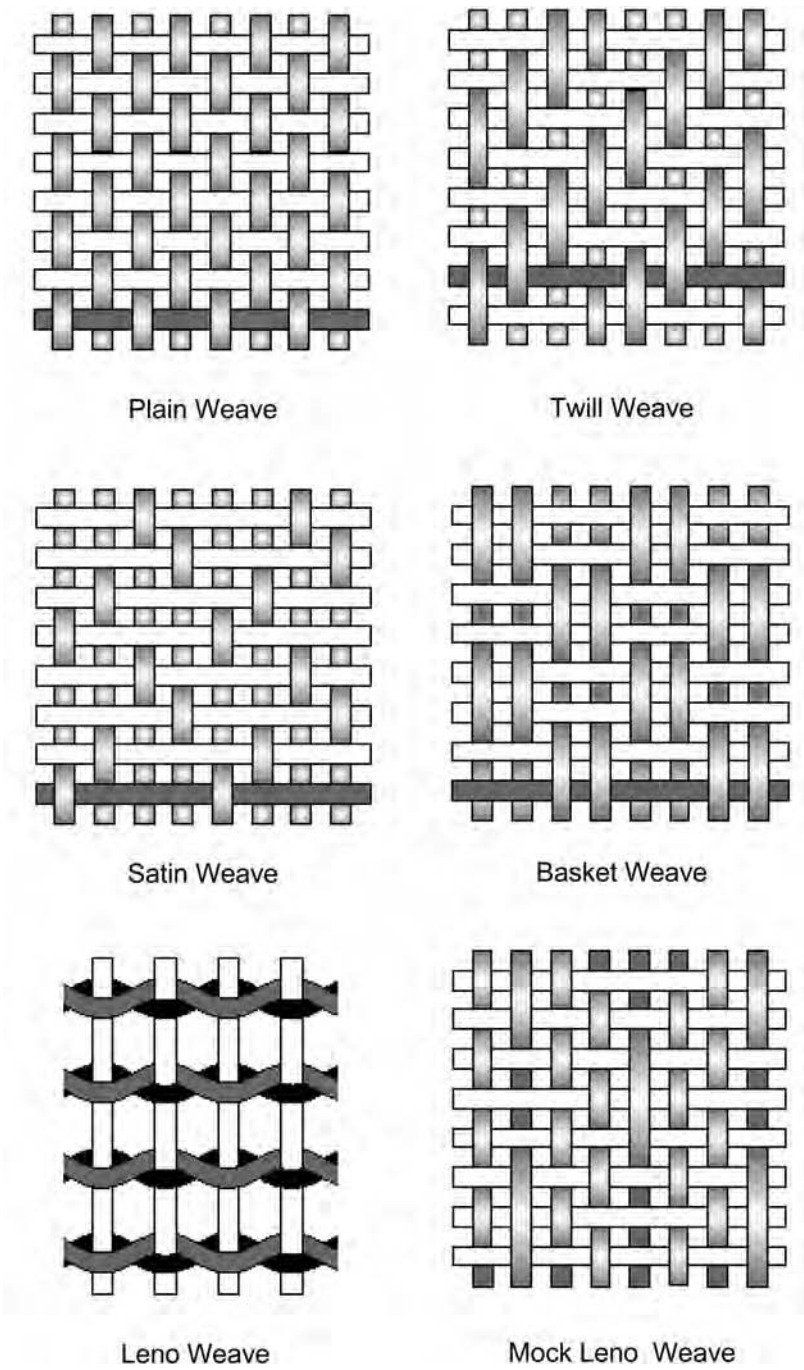


Fig. 2.20 Common two-dimensional weave styles. Source: Ref 8

flow and impregnation of the fibers. Because the resins and curing agents used in composite matrices can be quite reactive, careful temperature control during mixing is critical to prevent an exothermic reaction, which could result in an explosion or a fire. Some components may require premixing before being added to the main mix. After mixing, the resin is usually placed in plastic bags and frozen until it is needed for prepregging or until it must be shipped for processes

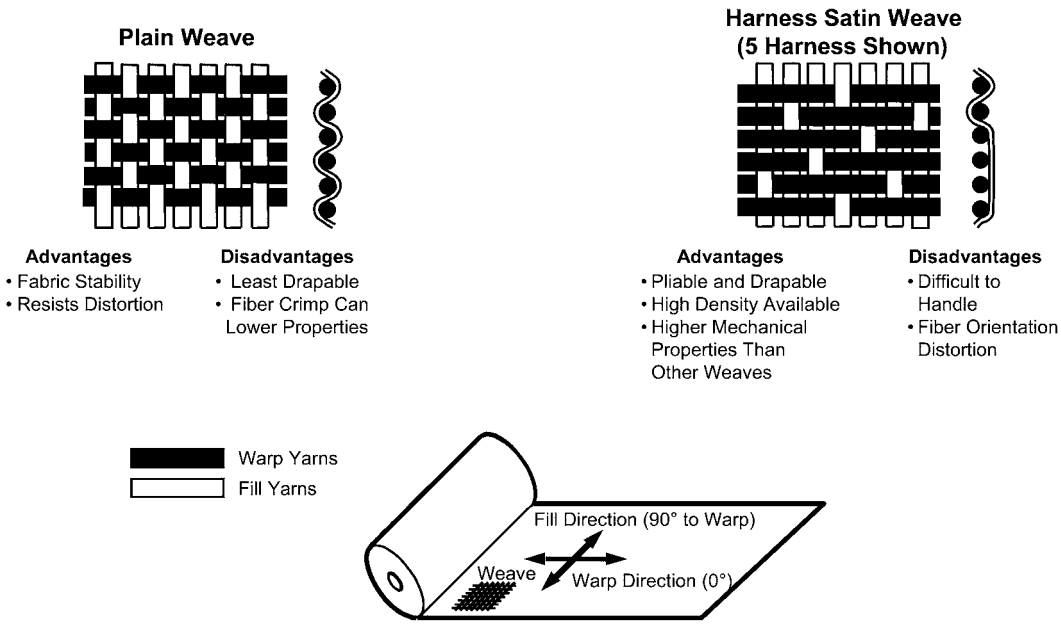


Fig. 2.21 Plain and satin weave cloths are most often used in high-performance composites. Source: Ref 1

Table 2.2 Common weave styles used in high-performance composites

Weave	Type of fiber	Construction yarns/in. warp × fill	Fiber areal weight, g/m²	Approximate cured per ply thickness(a), in.
Style 120	E-glass	60 × 58	107	0.005
Style 7791	E-glass	57 × 54	303	0.010
Style 120	Kevlar 49	34 × 34	61	0.004
Style 285	Kevlar 49	17 × 17	17	0.010
8-harness satin	3K carbon	24 × 23	370	0.014
5-harness satin	6K carbon	11 × 11	370	0.014
5-harness satin	1K carbon	24 × 24	125	0.005
Plain	3K carbon	11 × 11	193	0.007

(a) Actual cured per ply thickness depends on resin system, resin content, and processing conditions.

such as wet filament winding, liquid molding, or pultrusion.

Prepreg is the most prevalent product form used in advanced composite manufacturing. It usually consists of a single layer of fibers embedded in a B-staged resin (Fig. 2.23). During prepregging, the resin advances to a B-stage condition in which it is a semisolid at room temperature, and remelts and flows during the cure cycle. The B-staged resin normally contains some tack, or stickiness, to allow it to adhere to itself and tooling details during the lay-up operation. Because the resin is in a state of continual advancement (i.e., reaction), the degree of advancement and the resultant tack and flow behavior will change unless it is kept refrigerated when not in use.

Variables that define a prepreg are fiber type, fiber form (such as unidirectional or woven), resin type, fiber areal weight (FAW), prepreg resin content, and cured per ply thickness. Fiber areal weight is simply the weight of the fibers in a given area and is usually specified in g/m^2. Prepreg resin content specifies the percentage of resin by weight in the prepreg; this is not necessarily the resin content of the cured part. Some resins are prepregged with excess resin (e.g., 42 percent), which will be bled off (removed) during cure to yield a final cured resin content of 28 to 30 percent by weight. Other resins, called *net-resin-content prepregs*, will be prepregged to almost the same resin content as the final cured part; therefore, no bleeding of excess resin is required for this product form. Cured per ply thickness is specified as the thickness of each ply in inches. It should be noted that the final cured per ply thickness is strongly dependent on part configuration (especially part thickness) and the user's processing conditions.

Prepreg is usually supplied as narrow unidirectional tape, roving (or towpreg), wide unidirectional tape, and woven cloth called *broadgoods* (Fig. 2.24). Prepreg rovings or tows are bundles of fibers that are used primarily for filament winding or fiber placement. As the name

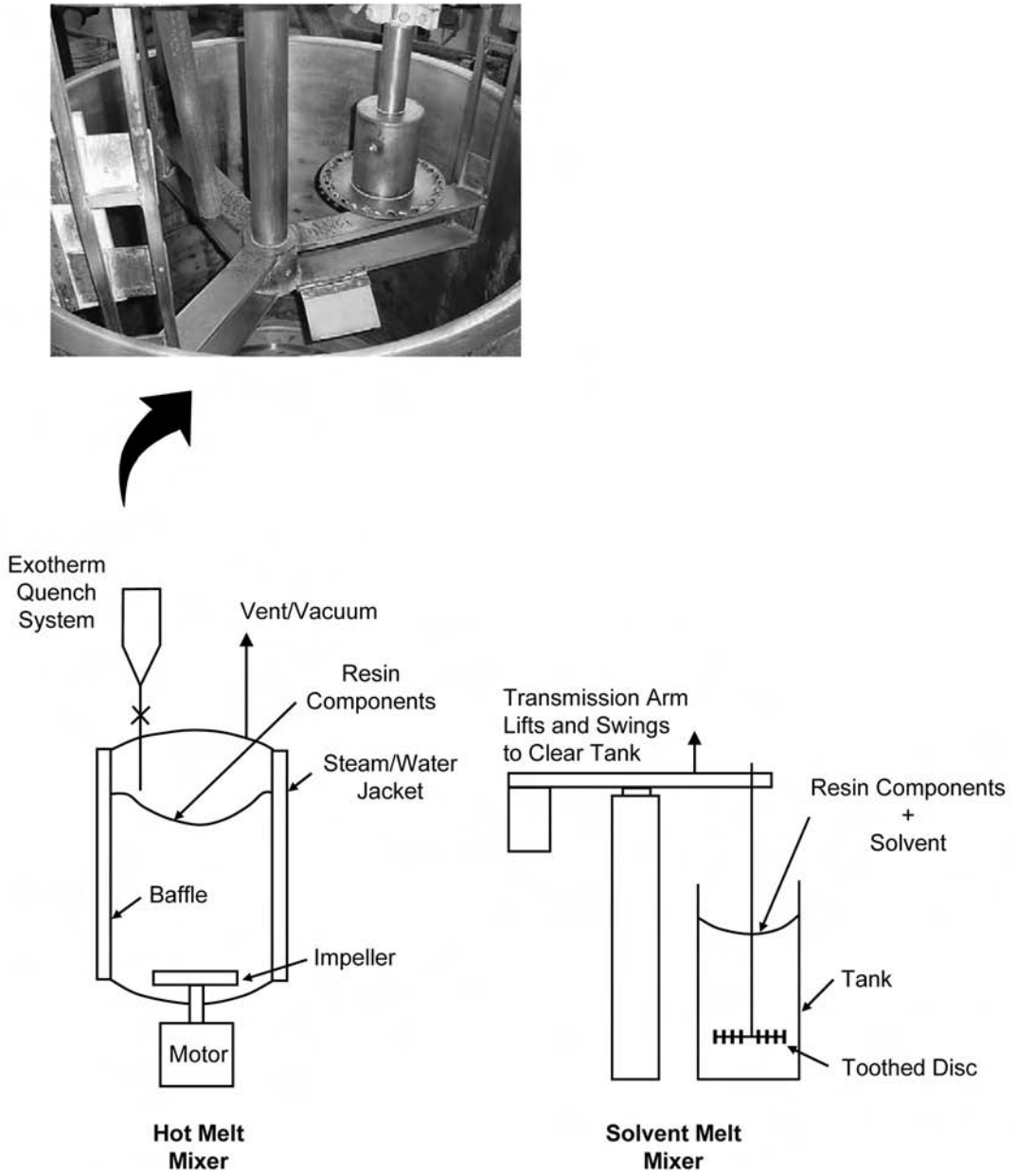


Fig. 2.22 Resin-mixing schematics. Sources: Photo, Cytec Engineered Materials; figure, Ref 9

implies, a single bundle of fibers is impregnated with the resin during prepregging. The cross section of both product forms is a flat rectangle with a width between 0.100 and 0.250 in (2.5 to 6.4 mm). The material is supplied in long lengths, up to 20,000 ft (6100 m), on a single spool. Unidirectional tape prepreg is a combination of multiple tows aligned in parallel that are impregnated with resin. Typical FAWs range from as low as 30 to as high as 300 g/m^2, with typical values being 95, 145, and 190 g/m^2, which correspond to cured per ply thicknesses of 0.0035, 0.005, and 0.0075 in. (0.09, 0.13, and 0.19 mm), respectively. Widths range from 6 to 60 in. (15 cm to

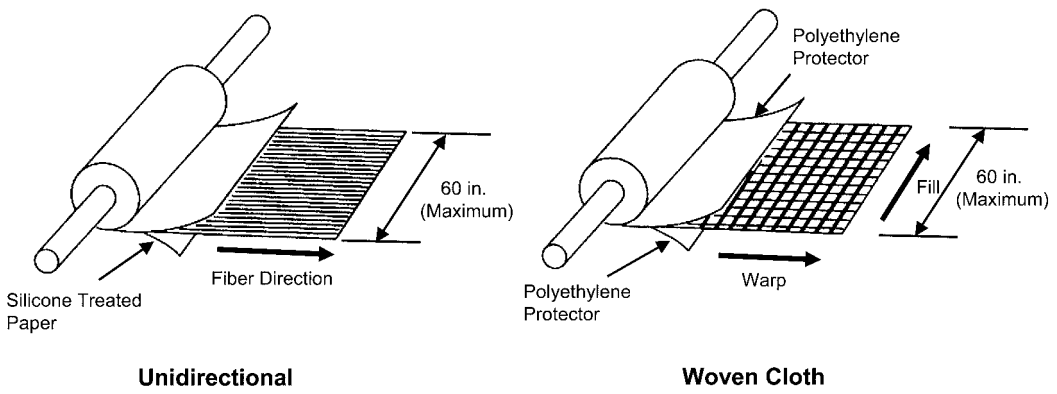


Fig. 2.23 Unidirectional and woven cloth prepreg. Source: Ref 10

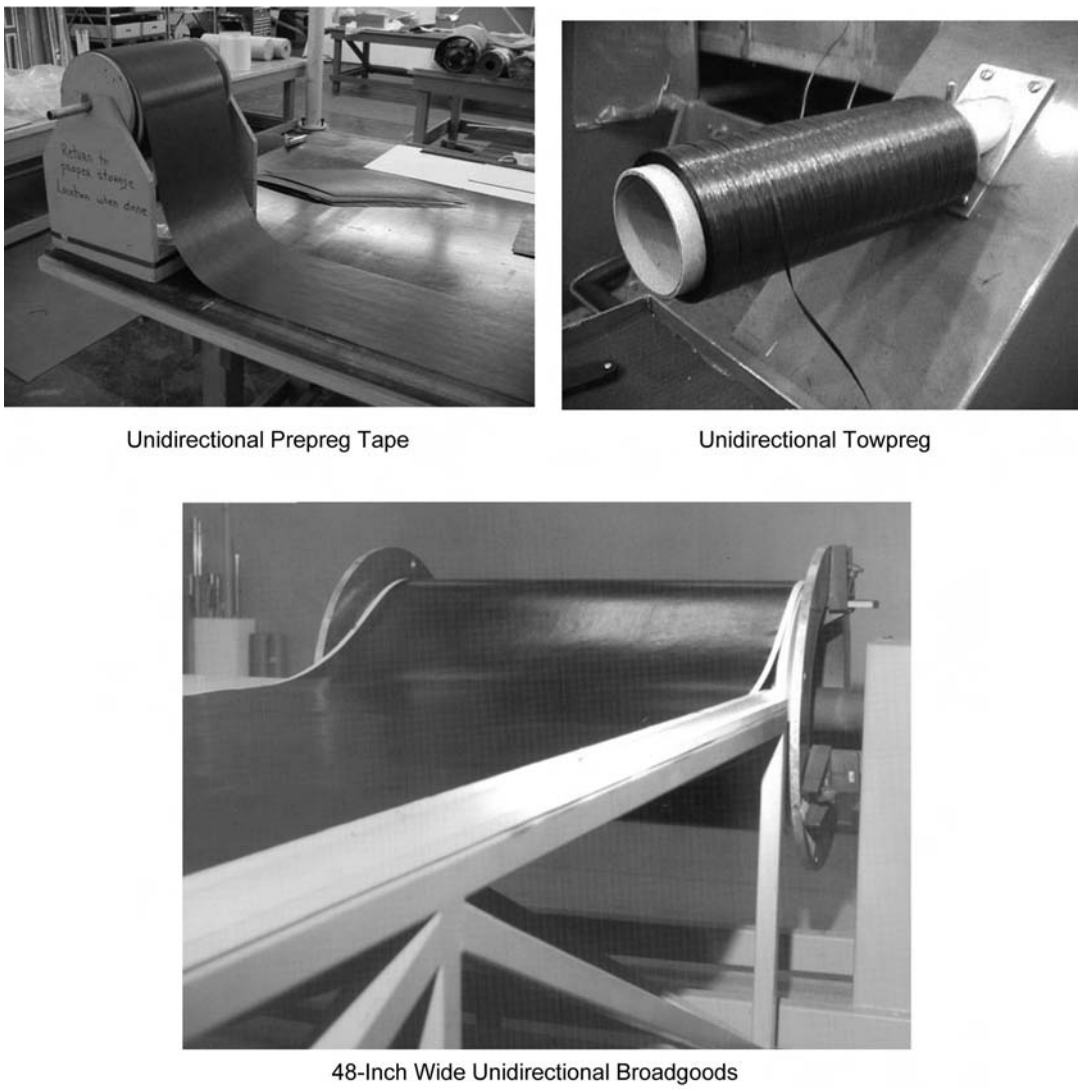


Fig. 2.24 Unidirectional prepreg tape, towpreg, and broadgoods (unidirectional tape and woven cloth). Source: The Boeing Company

1.5 m). Automated tape-laying machines usually use 6 or 12 in. (15 or 30 cm) wide material, while the wider 48 to 60 in. (1219 to 1524 mm) broadgoods are machine cut into ply shapes and used for hand lay-up. Fabric prepregs consist of a woven fabric impregnated with a resin. Because fabric prepregs are primarily used for hand lay-up, the material is usually supplied as wide rolls (up to 60 in. (1.5 m) wide) to minimize the number of splices required in a part. Fabric prepregs usually have higher FAWs than unidirectional tape and thicker cured per ply thickness such as 0.014 in./ply. Prepregs normally produce the highest laminate strengths when they are layed up and autoclave cured. Some typical cured carbon/epoxy properties for unidirectional tape materials are shown in Table 2.3, and woven cloth laminate properties are given in Table 2.4.

Prepregging can be accomplished by hot melt impregnation, resin filming, and solvent impregnation. In the original hot melt process (Fig. 2.25), fibers are fed from a creel, collimated, impregnated with the melted resin, and immediately cooled prior to spooling on the roll. The newer resin filming process consists of two operations. The resin is first filmed to a controlled thickness on backing paper, as shown in Fig. 2.26. The spooled film can then be either taken directly to the prepregging operation or frozen for future use. The majority of prepreg is currently made by the filming technique, because it allows better control of resin content and FAW. Typical filming weights are in the range of 0.06 to 0.25 oz/ft^2 (20 to 80 g/m^2) with speeds of up to 40 ft/min (12 m/min). When the resin film is ready for impregnation, it is conducted on a separate machine (Fig. 2.27) in which the fiber web is protected on both surfaces with a backing paper. Impregnation is achieved by the application of heat and nip-roll pressure as the fibers, resin film, and upper and lower backing papers are pulled through the line. After the material passes through the second set of nip rollers, it is immediately chilled to raise the resin's viscosity and produce the semisolid prepreg. At the exit, the upper paper sheet is removed and discarded, the edges are trimmed straight with slitter blades, and the finished prepreg is rolled up on the spool. This process runs at the rate of about 8 to 20 ft/min (2.5 to 6 m/min) in widths of up to 60 in. (1.5 m).

A third method, solvent impregnation (Fig. 2.28), is used almost exclusively for towpreg, woven fabrics, and high-temperature resins (e.g., polyimides) that are not amenable to hot melt prepregging and must be dissolved in solvents. A disadvantage of this process is that residual solvent may remain in the prepreg and cause a volatile evolution problem during cure. Therefore, the recent trend has been to use hot melt or resin film methods for both unidirectional and fabric prepregs. The solution process is operated with a treater line. The fabric web is drawn off a reel into a dip tank containing the resin solution (acetone is a common solvent for epoxies) and pulled through a controlled set of nip rollers to set the resin content. Typical speeds are 10 to 15 ft/min (3 to 4.5 m/min) for 60 in. (1.5 m) wide material. The web moves to a hot-air oven that serves to both evaporate the bulk of the solvent and advance the resin for tack control. At the end of the oven, the material is spooled up with a layer of plastic film applied to one side to

Table 2.3 Typical properties of 0° tape carbon/epoxy laminates

	Fiber type			
	AS-4	AS-4	IM-6	AS-4
	Resin type			
Property	3502	3501-6	3501-6	8552
0° tensile strength, ksi	275	310	350	330
0° tensile modulus, msi	20.3	20.5	23.0	20.4
0° compression strength, ksi	240	240	240	221
Interlaminar shear, ksi	18.5	17.5	18.0	18.6
Compression after impact, ksi	22	22	22	33

Source: Ref 11

Table 2.4 Typical properties of woven carbon/epoxy cloth laminates

Style weave	A193-P plain	A280-5H 5-harness satin	A370-5H 5-harness satin	A280-5H 8-harness satin	1360-5H 5-harness satin
Fiber type	AS-4	AS-4	AS-4	AS-4	IM-6
Tow size	3K	3K	6K	3K	12K
Areal weight, g/m^2	193	280	370	370	360
Tensile strength, ksi	100	100	100	100	146
Tensile modulus, msi	10.0	10.5	10.5	10.0	14.0
Interlaminar shear, ksi	9.5	10.0	10.0	10.0	10.2
Cured per ply thickness, mils	6.9	10.0	13.2	13.2	12.8

Source: Ref 11

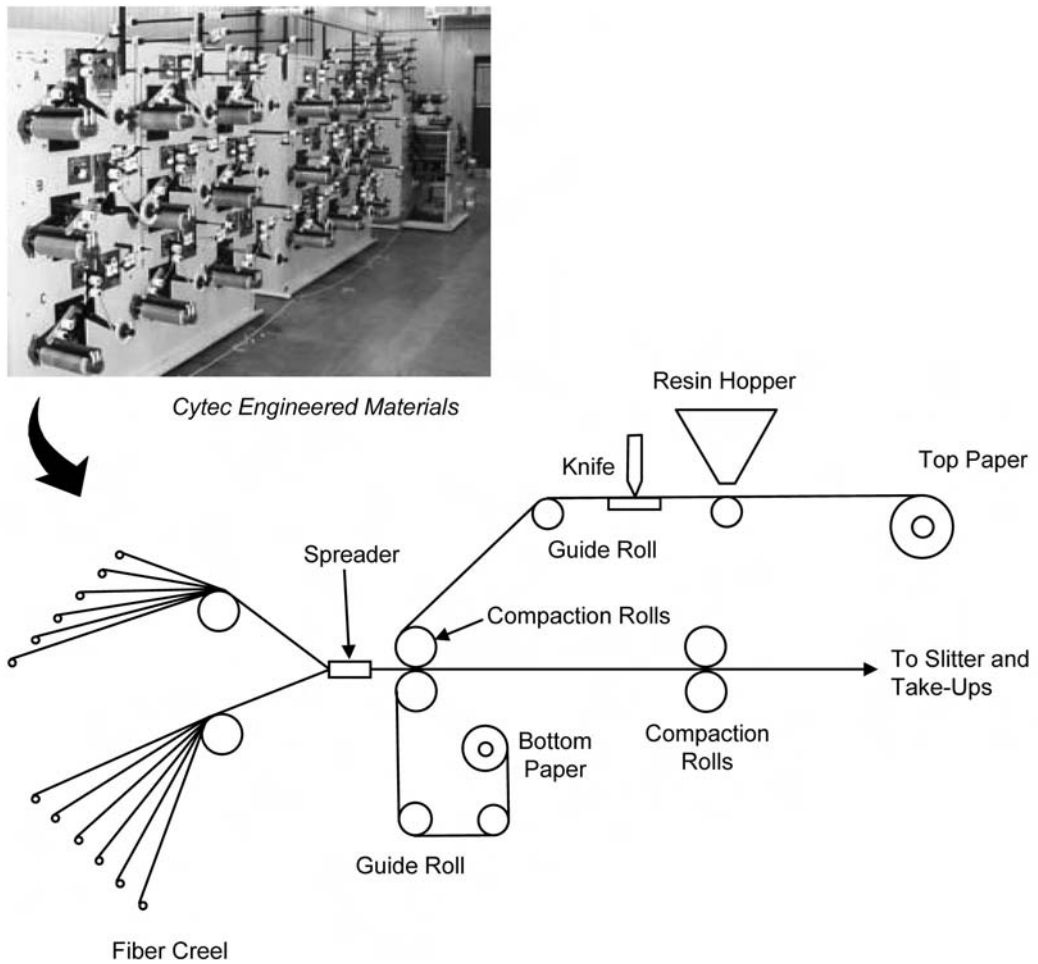


Fig. 2.25 Hot melt resin impregnation process. Source: Ref 9

provide a separator. Some products require compaction at this stage to close the weave. Others may be distorted during the passage through the treater line and require reworking in a tenter, which pulls and straightens the fabric to restore alignment.

REFERENCES

1. R. Bohlmann, M. Renieri, G. Renieri, and R. Miller, Training course notes given to Thales in the Netherlands entitled "Advanced Materials and Design for Integrated Topside Structures," 15–19 April 2002
2. A.G. Metcalf and K.G. Schmitz, *ASTM Proc*., Vol 64, 1075, 8, 1974
3. K.K. Chang, Aramid Fibers, *ASM Handbook*, Vol 21, *Composites*, ASM International, 2001
4. J.L.J. Van Dingenen, Gel-Spun High-Performance Polyethylene Fibres, *High-Performance Fibres*, CRC Press, 2000
5. S.C. Bennett and D.J. Johnson, Structural Heterogeneity in Carbon Fibers, *Proceedings of the 5th Carbon and Graphite Conference*, Vol 1, Society for Chemical Industries, 1978, p 377–386
6. W. Watt, *Proc. R. Soc*., Vol A319 (No. 5), 1970
7. L.T. Drzal, Interfaces and Interphases, *ASM Handbook*, Vol 21, *Composites*, ASM International, 2001
8. SP Systems "Guide to Composites"

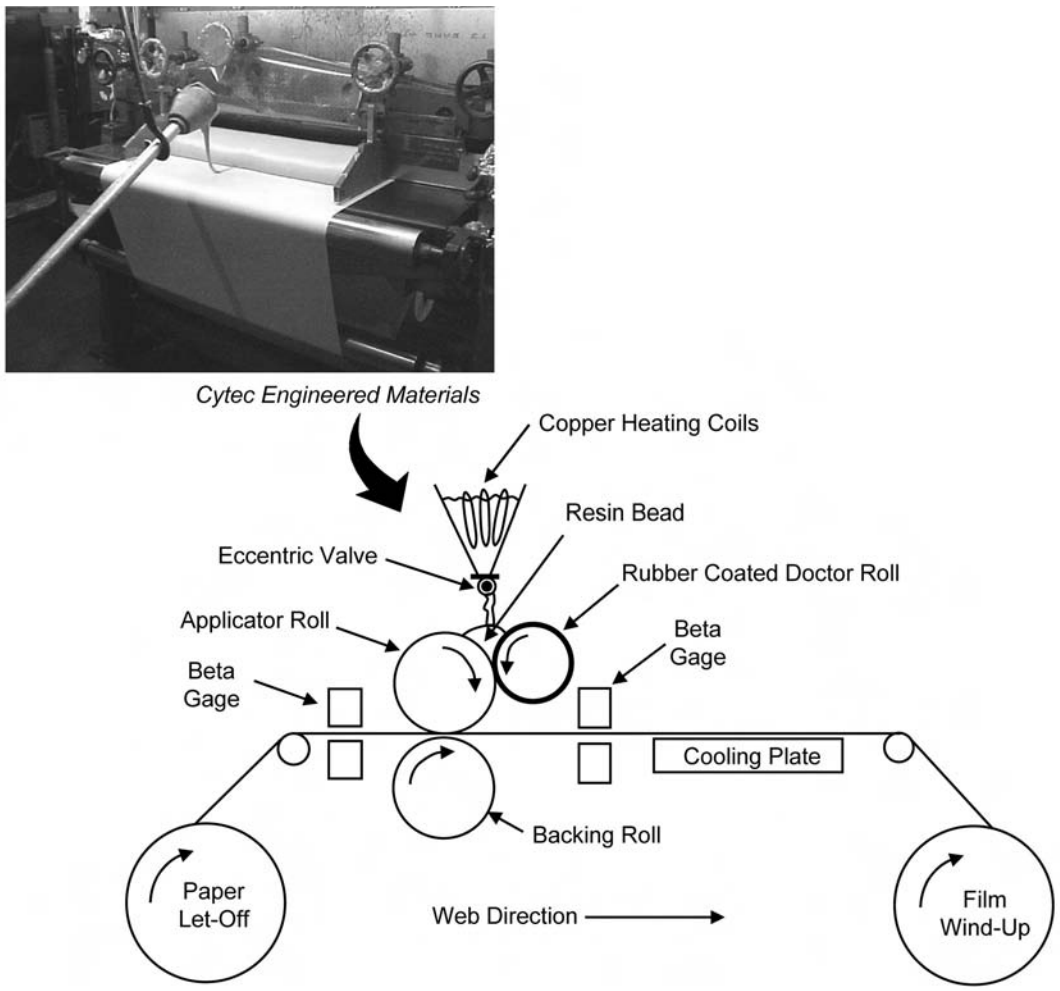


Fig. 2.26 Resin filming process. Source: Ref 9

9. C. Smith and M. Gray, ICI Fiberite Impregnated Materials and Processes—An Overview, unpublished white paper
10. Hexcel Product Literature, "Prepreg Technology," 1997
11. Hexcel Product Literature, "Graphite Fibers and Prepregs," 1988

SELECTED REFERENCES

- S. Backer, Textiles: Structures and Processes, *The Encyclopedia of Materials Science and Engineering*, Pergamon Press, 1986
- K.K. Chawla, *Fibrous Materials*, Cambridge University Press, 1998
- Fabrics and Preforms, *ASM Handbook*, Vol 21, *Composites*, ASM International, 2001, p 59–68
- T.G. Gutowski, Cost, Automation, and Design, *Advanced Composites Manufacturing*, John Wiley & Sons, Inc., 1987
- P. Morgan, *Carbon Fibers and Their Composites*, Taylor & Francis, 2005
- Pitch Fibers Take the Heat (Out), *High Perform. Compos.*, September/December 2001
- T.L. Price, G. Dalley, P.C. McCullough, and L. Choquette, "Handbook: Manufacturing Advanced Composite Components for Airframes," Report DOT/FAA/AR-96/75, Office of Aviation Research, April 1997

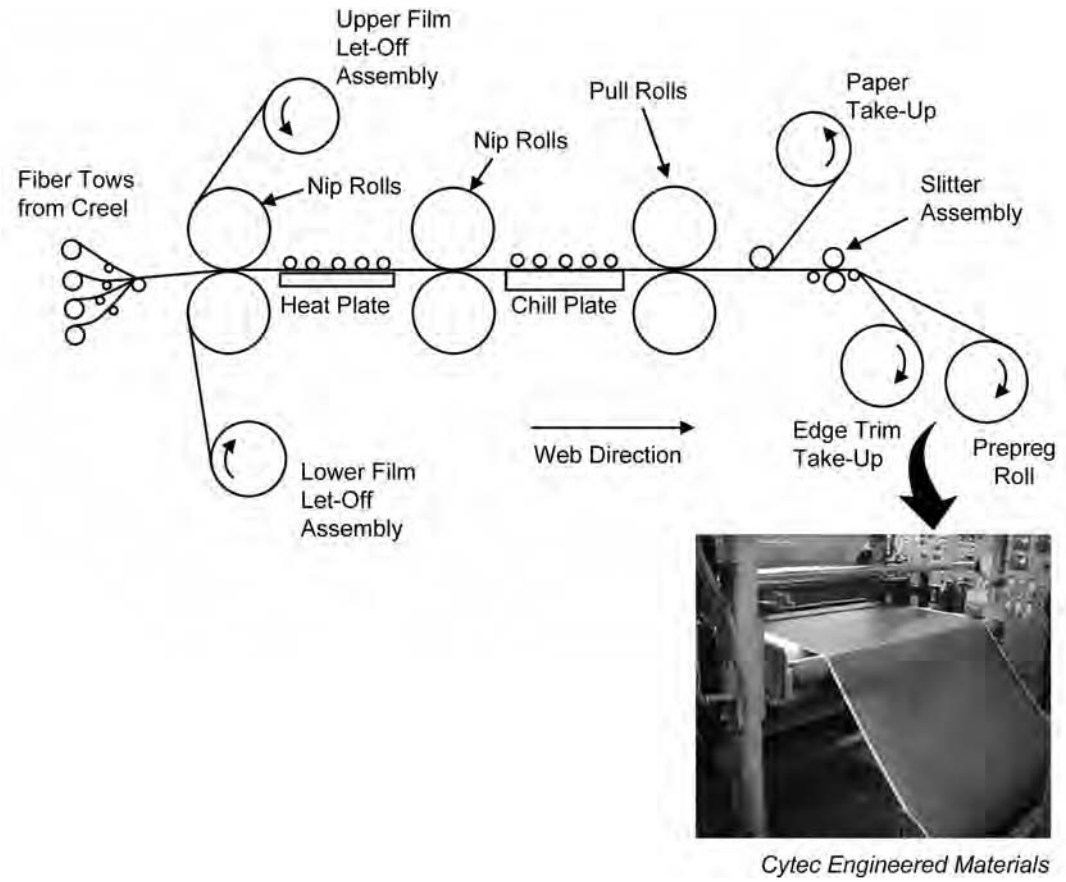


Fig. 2.27 Process for producing hot melt tape from resin film. Source: Ref 9

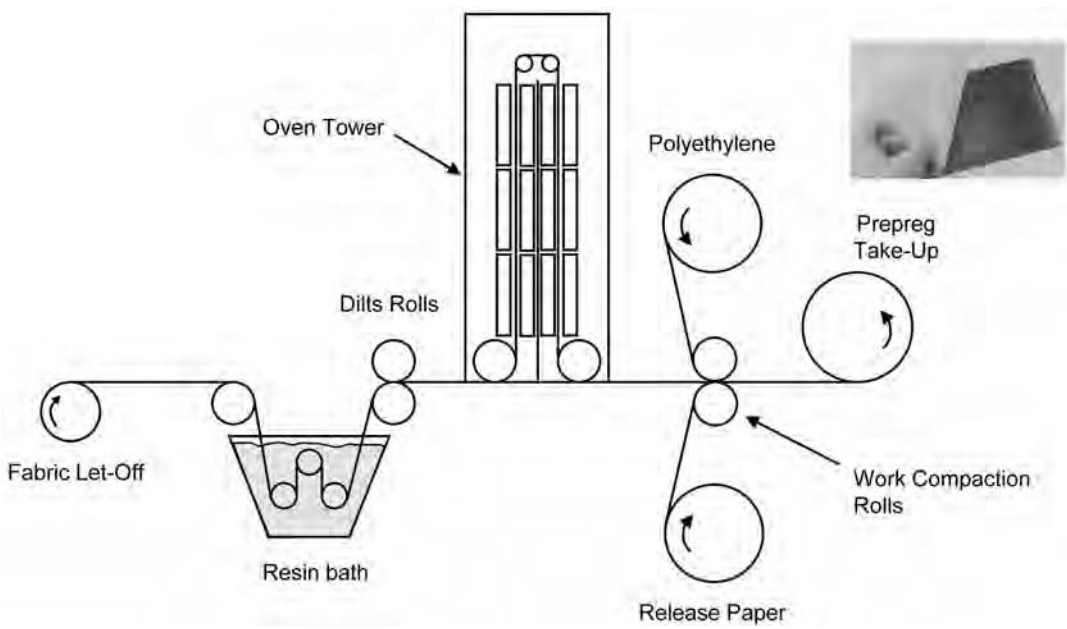


Fig. 2.28 Solution impregnation line for producing prepreg

- S. Rebouillat, Aramids, *High-Performance Fibres*, CRC Press, 2000
- D.A. Schultz, Advances in UHM Carbon Fibers, *SAMPE J*., March/April 1987
- A.B. Strong, *Fundamentals of Composite Manufacturing: Materials, Methods, and Applications*, SME, 1989
- A.B. Strong, Practical Aspects of Carbon Fiber Surface Treatment and Sizing
- J.-S. Tsai, Carbonizing Furnace Effects on Carbon Fiber Properties, *SAMPE J*., May/June 1994
- P.J. Walsh, Carbon Fibers, *ASM Handbook*, Vol 21, *Composites*, ASM International, 2001

"*This page left intentionally blank.*"

Copyright © 2010, ASM International®
All rights reserved.
www.asminternational.org

CHAPTER 3

Matrix Resin Systems

BINDING THE FIBERS together in an orderly array and protecting them from the environment is the role of the matrix. The matrix transfers loads to the fibers and is critical in compression loading in preventing premature failure due to fiber microbuckling. The matrix also provides the composite with toughness, damage tolerance, and impact and abrasion resistance. The properties of the matrix also determine the maximum usage temperature, resistance to moisture and fluids, and thermal and oxidative stability.

Polymeric matrices for advanced composites are classified as either thermosets or thermoplastics. Thermosets are low molecular weight, low viscosity monomers (≈2000 centipoise) that are converted during curing into three-dimensional crosslinked structures that are infusible and insoluble. Crosslinking (Fig. 3.1) results from chemical reactions that are driven by heat generated either by the chemical reactions themselves for example, exothermic heat of reaction, or by externally supplied heat. As curing progresses, the reactions accelerate and the available volume within the molecular arrangement decreases, resulting in less mobility of the molecules and an increase in viscosity. After the resin gels and forms a rubbery solid, it cannot be remelted. Further heating causes additional crosslinking until the resin is fully cured. This progression through cure is shown in Fig. 3.2. Since cure is a thermally driven event requiring chemical reactions, thermosets are characterized as having rather long processing times. In contrast, thermoplastics are not chemically crosslinked with heat and therefore do not require long cure cycles. They are high molecular weight polymers that can be melted, consolidated, and then cooled. Since thermoplastics do not crosslink, they may be subsequently reheated for forming or joining operations; however, due to their inherently high

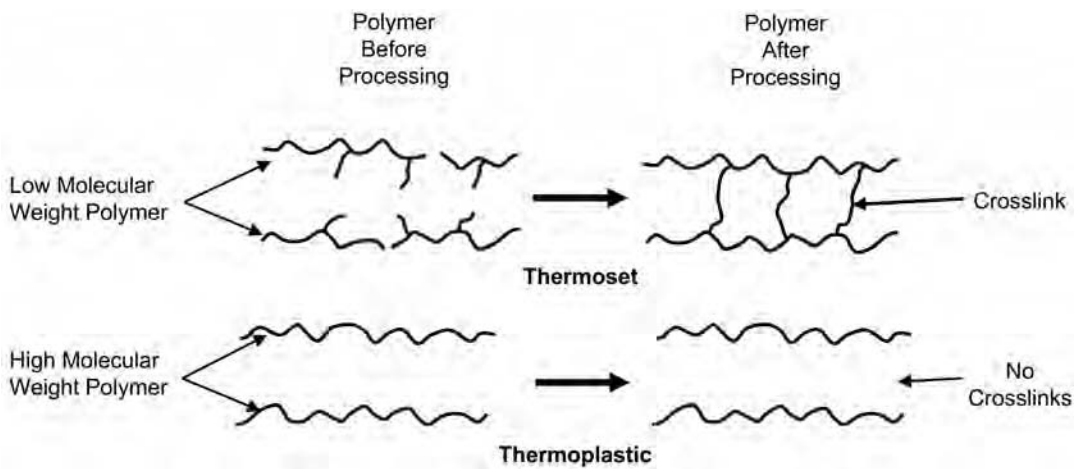


Fig. 3.1 Comparison of thermoset and thermoplastic polymer structures

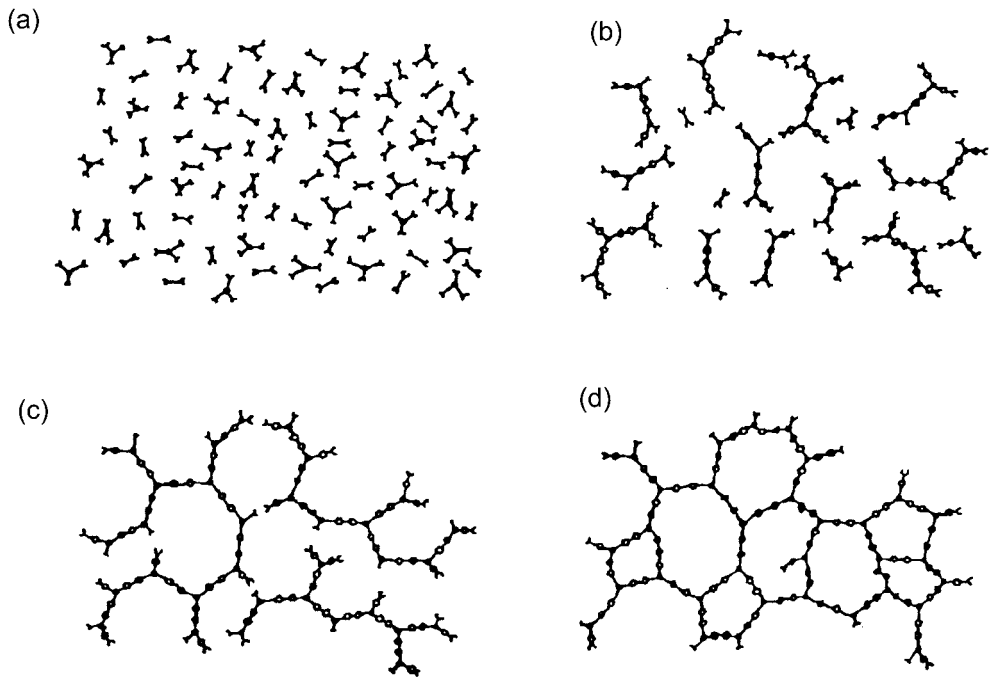


Fig. 3.2 Stages of cure for thermoset resin. (a) Polymer and curing agent prior to reaction. (b) Curing initiated with size of molecules increasing. (c) Gelation with full network formed. (d) Full cured and crosslinked. Source: Ref 1

viscosity and high melting points, high temperatures and pressures are normally required for processing.

3.1 Thermosets

Thermoset composite matrices include polyesters, vinyl esters, epoxies, bismaleimides, cyanate esters, polyimides, and phenolics (Table 3.1). Epoxies currently are the dominant resins used for low and moderate temperatures (up to 275 °F or 135 °C). Bismaleimides are used primarily in the temperature range of 275–350 °F (135–175 °C). For very-high-temperature applications (up to 550–600 °F or 290–315 °C), polyimides are typically the material of choice. Polyesters and vinyl esters, which can be used at approximately the same temperatures as epoxies, are used extensively for commercial applications but rarely for high-performance composite matrices because of their lower mechanical properties and somewhat poorer environmental resistance. Cyanate esters are a relatively new class of resins that were designed to compete with both epoxies and bismaleimides. These newer resins offer some advantages in lower moisture absorption and have attractive electrical properties but at a significantly higher price. Phenolics are high-temperature systems that offer outstanding smoke and fire resistance and are frequently used for aircraft interior components. Due to their high

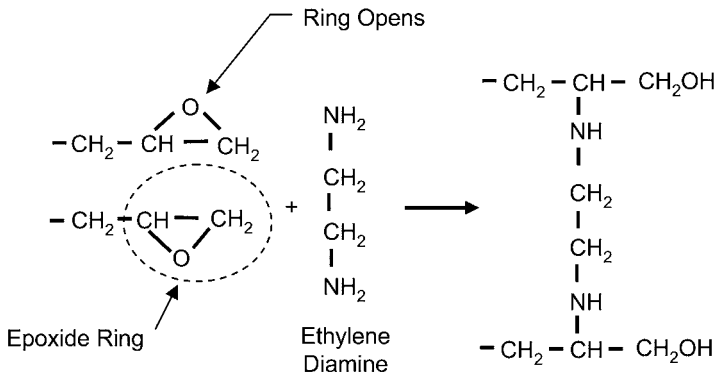
Table 3.1 Relative characteristics of thermoset resin matrices

Polyesters	Used extensively in commercial applications. Relatively inexpensive, with processing flexibility. Used for continuous and discontinuous composites.
Vinyl Esters	Similar to polyesters, but are tougher and have better moisture resistance.
Epoxies	High-performance matrix systems for primary continuous-fiber composites. Can be used at temperatures up to 250–275 °F. Give better high-temperature performance than polyesters and vinyl esters.
Bismaleimides	High-temperature resin matrices for use in the temperature range of 275–350 °F with epoxy-like processing. Requires elevated-temperature postcure.
Cyanate Esters	High-temperature resin matrices for use in the temperature range of 275–350 °F with epoxy-like processing. Requires elevated-temperature postcure.
Polymides	Very-high-temperature resin systems for use at 550–600 °F. Very difficult to process.
Phenolics	High-temperature resin systems with good smoke and fire resistance. Used extensively for aircraft interiors. Can be difficult to process.

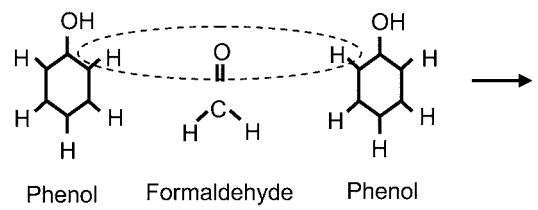
char yield, they can also be used as ablators and as precursors for carbon-carbon (C-C) components. Polyesters, epoxies, bismaleimides, and cyanate esters are all classified as addition-curing polymers, while polyimides and phenolics are condensation-curing systems. The most distinct difference between the two types of reactions is that condensation reactions give off water or alcohol, while addition-curing reactions do not give off a by-product. This difference is illustrated in Fig. 3.3, which compares a reaction for an addition-curing epoxy with one for a condensation-curing phenolic. The evolution of water and/or alcohols during curing presents a volatile management problem. If these by-products are not removed prior to the resin gelling or setting up, voids and porosity in the cured matrix will occur. Thus, condensation-curing systems are much more difficult to process than addition-curing systems.

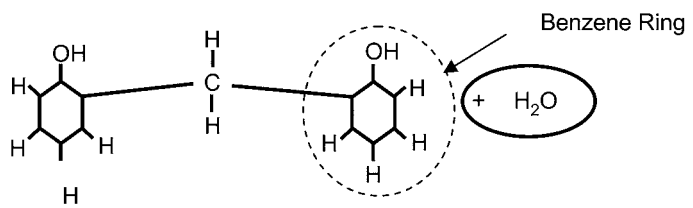
3.2 Polyester Resins

Polyesters are used extensively in commercial applications but are limited for use in high-performance composites. Although lower in cost than epoxies, polyesters generally have lower temperature capability, lower mechanical properties and inferior weathering resistance, and they exhibit more shrinkage during cure. Polyesters cure by addition reactions in which unsaturated carbon-carbon double bonds (C=C) are the locations where crosslinking occurs. A typical



Addition Reaction to Form Crosslink





Condensation Reaction to Form Crosslink

Fig. 3.3 Comparison of addition and condensation reactions

polyester consists of at least three ingredients: a polyester; a crosslinking agent such as styrene; and an initiator, usually a peroxide such as methyl ethyl ketone peroxide or benzoyl peroxide. Styrene acts as the crosslinking agent and also lowers the viscosity to improve processability. Styrene is not the only curing agent (crosslinker); others include vinyl toluene, chlorostyrene (which imparts flame retardance), methyl methacrylate (improved weatherability), and diallyl phtalate, which has low viscosity and is often used for prepregs. The properties of the resultant polyester are strongly dependent on the crosslinking or curing agent used. One of the main advantages of polyesters is that they can be formulated to cure at either room or elevated temperature, allowing great versatility in their processing.

The basic chemical structure of a typical polyester (Fig. 3.4) contains ester groups and unsaturated or double bond reactive groups (C=C). Polyesters are usually viscous liquids consisting of a solution of polyester in a monomer, usually styrene. Styrene in amounts up to 50 percent reduces the viscosity of the solution, thereby improving processability, and reacts with the polyester chain to form a rigid crosslinked structure. Since polyesters have a limited pot life and will set or gel at room temperature over a long period of time, small quantities of inhibitors, such as hydroquinone, can be added to slow the reaction rate and extend the out-time. A solution of polyester and styrene alone polymerizes too slowly for practical purposes; therefore, small amounts of accelerators or catalysts are always added to speed up the reaction. Catalysts are added to the resin just prior to use to initiate the polymerization reaction. The catalyst does not actually take part in the chemical reaction but simply activates the process. Accelerators, such as cobalt napthenate, diethyl aniline, and dimethyl aniline, can also be added to speed up the reaction. A wide variety of monomers and curing agents are available that yield a broad range of physical and mechanical properties. For example, the bulky benzene ring improves rigidity and thermal stability.

Vinyl esters are very similar to polyesters but only have reactive groups at the ends of the molecular chain (Fig. 3.4). Since this results in

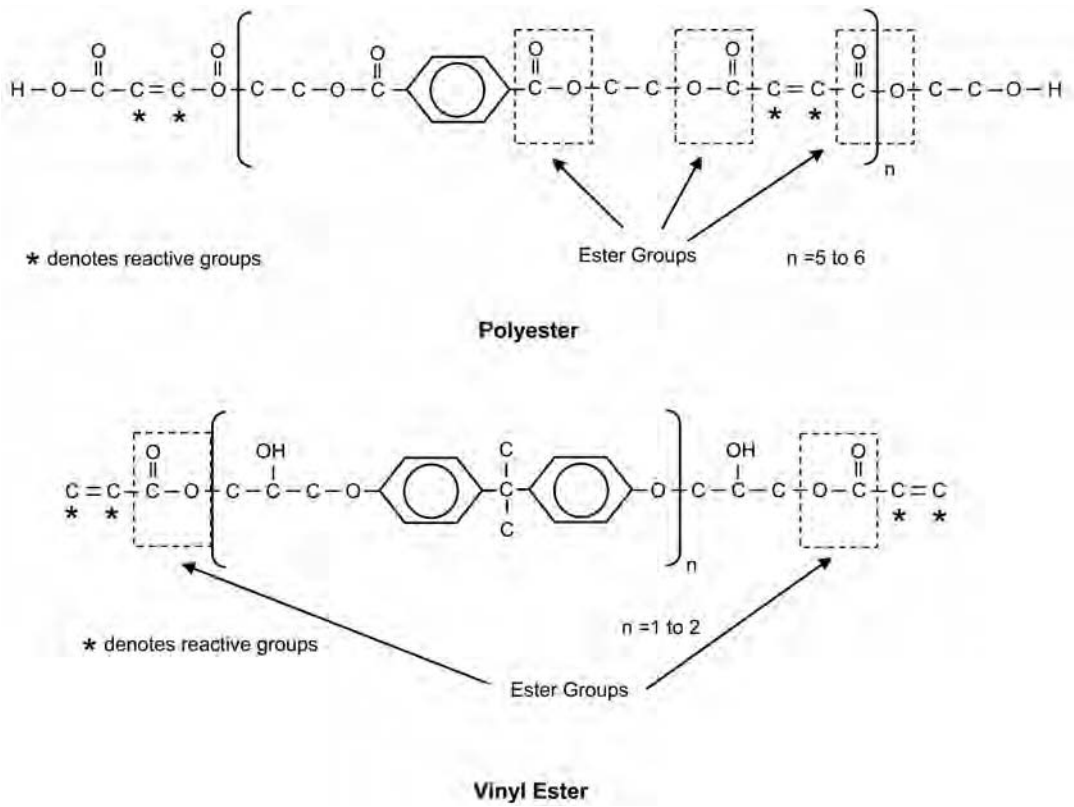


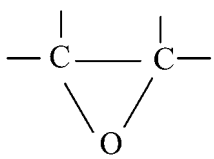
Fig. 3.4 Typical polyester and vinyl ester structures. Source: Ref 2

lower crosslink densities, vinyl esters are normally tougher than the more highly crosslinked polyesters. In addition, since the ester group is susceptible to hydrolysis by water and since vinyl esters have fewer ester groups than polyesters, they are more resistant to degradation from water and moisture.

3.3 Epoxy Resins

Epoxies are the most common matrix material for high-performance composites and adhesives. They have an excellent combination of strength, adhesion, low shrinkage, and processing versatility. Commercial epoxy matrices and adhesives can be as simple as one epoxy and one curing agent; however, most contain a major epoxy, one to three minor epoxies, and one or two curing agents. The minor epoxies are added to provide viscosity control, impart higher elevated temperature properties, provide lower moisture absorption or to improve toughness. Two main major epoxies are used in the aerospace industry. The first is diglycidyl ether of Bisphenol A (DGEBA), which is used extensively in filament winding, pultrusion, and some adhesives. The second is tetraglycidyl methylene dianiline (TGMDA), also known as tetraglycidyl-4,4″-diaminodiphenylmethane (TGGDM), which is the major epoxy used for a large number of the commercial composite matrix systems.

The epoxy group, or oxirane ring, is the site of crosslinking:



The cure of epoxy resins is based on the oxirane ring opening and crosslinking with the curing agent. The epoxide group has unfavorable bond angles, which makes it chemically reactive with a variety of substances that can easily open the ring to form a highly crosslinked structure. The crosslinking may occur through the epoxy groups or the resulting hydroxy groups. The three-member epoxy group is usually present as either a glycidyl ether or a glycidyl amine or as part of an aliphatic ring. Glycidyl ethers and amines are normally used for composites, while cycloaliphatics are used extensively in electrical applications or as a minor epoxy in composite matrix systems. With amine curing agents, each hydrogen is reactive and can open one epoxide ring to form a covalent bond (Fig. 3.5). When the amine nitrogen contains two hydrogens, each reacts with a different epoxide ring. The reaction between epoxide and amine produces a carbon-nitrogen (C-N) bond. It should be emphasized that the properties of a cured epoxy are strongly dependent on the specific curing agent used. Like polyesters, they may be formulated to cure at either room or elevated temperatures.

The most widely used epoxy type is DGEBA (Fig. 3.6). Since it is a difunctional epoxy (such as two epoxy end groups that can react) that can be either a liquid or a solid; and is available as a liquid at several viscosities, it is frequently used for filament winding and pultrusion. If the repeat unit (*n*) is between 0.1 and 0.2, it is a liquid with a viscosity in the range of 6000 to 16,000 cps.

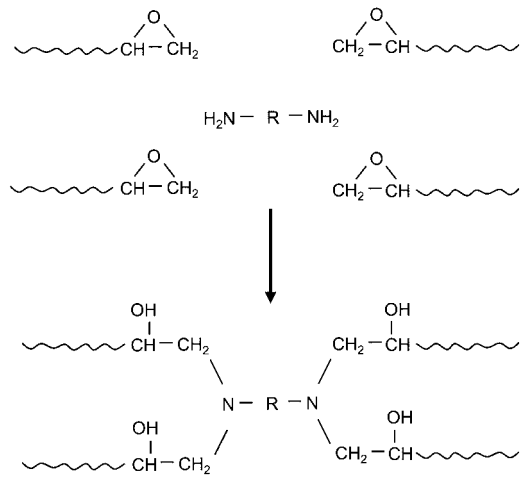


Fig. 3.5 Amine crosslinking reaction with epoxies

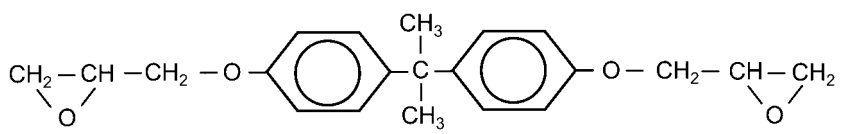


Fig. 3.6 Diglycidyl ether of Bisphenol A (DGEBA)

The effect of the repeat unit on viscosity is shown in Table 3.2. As *n* approaches two, it becomes a solid. For *n* values greater than two, it is not useful as a matrix material because the crosslink density becomes too low.

Glycidyl amines contain higher functionality (such as three or four reactive epoxy end groups) because the resins are based on aromatic amines. The most important glycidyl amine is TGMDA or TGGDM. This resin, shown in Fig. 3.7, is the base resin used in the majority of composite epoxy matrix systems. Its high functionality (four) provides highly crosslinked structures that exhibit high strength, rigidity, and elevated temperature resistance. In some adhesive systems, where toughness (such as peel strength) is an important property, suppliers will mix difunctional DGEBA with tetrafunctional TGMDA to help provide more flexibility in the cured adhesive. If a lower crosslink density is desired, there are also trifunctional epoxies available, such as the triglycidyl derivative of *p*-aminophenol (TGAP), shown in Fig. 3.8.

Minor epoxies are frequently added to improve processability (viscosity), elevated-temperature performance, or other properties of the cured resin system. Typical minor epoxies include amine-based phenols, novolacs, cycloaliphatics, and others.

Table 3.2 Effect repeat unit on weight per epoxide (WPE) and viscosity for DGEBA resins

Repeat unit *n*	Weight per epoxide(a)	Viscosity or melting point
0	170–178	4–6000 cps
0.07	180–190	7–10000 ops
0.14	190–200	10–16000 cps
2.3	450–550	65–80 °C
4.8	850–1000	95–105 °C
9.4	1500–2500	115–130 °C
11.5	1800–4000	140–155 °C
30	4000–6000	115–165 °C

(a) Epoxy prepolymers are characterized by the epoxide content or weight per epoxide (WPE), which is the weight of resin containing one mole of epoxide groups.

The composition of a typical epoxy matrix system is:

Component	Total percent (*wt*)
Tetraglycidyl methylenedianiline (TGMDA)	56.4
Alicyclic diepoxy carboxylate	9.0
Epoxy cresol novolac	8.5
4,4' Diaminodiphenyl sulfone (DDS)	25.0
Boron trifluoride amine complex (BF_3)	1.1

In this case, TGMDA is the major epoxy, while the alicyclic diepoxy carboxylate and epoxy cresol novolac are the two minor epoxies. The curing agent is DDS, and BF_3 is a catalyst.

Diluents are sometimes added to epoxy resin systems to reduce viscosity, improve shelf and pot life, lower the exotherm, and reduce shrinkage. They are normally used in small amounts (three to five percent) because higher concentrations degrade the mechanical and thermal properties of the cured system. Typical diluents include butyl glycidyl ether, cresyl glycidyl ether, phenyl glycidyl ether, and aliphatic alcohol glycidyl ethers.

There are a wide variety of curing agents that can be used with epoxies; the most common ones for adhesives and composite matrices include (1) aliphatic amines, (2) aromatic amines, (3) miscellaneous and catalytic curing agents, and (4) anhydrides. A number of these different types of curing agents are shown in Fig. 3.9.

Aliphatic amines are very reactive, producing enough exothermic heat given off by the reaction to cure at room or slightly elevated temperature. In fact, if they are mixed in large mass, the exotherm can be large enough to cause a fire. However, since these are room-temperature curing systems, their elevated-temperature properties are lower than those of the elevated-temperature cured aromatic amine systems. Aliphatic amine systems form the basis for many room-temperature curing adhesive systems. Their elevated-temperature performance can sometimes be improved by initially curing at room

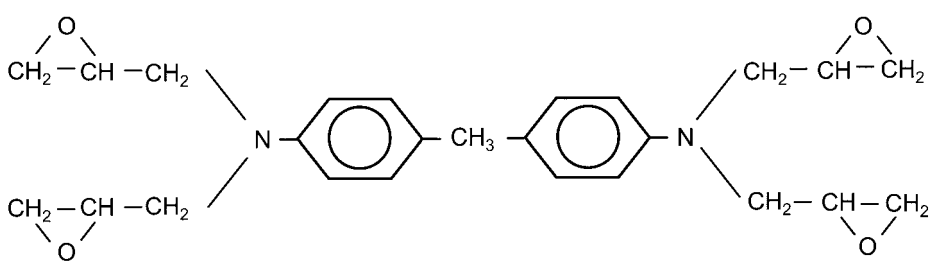


Fig. 3.7 Tetraglycidyl methylene dianiline (TGMDA)

temperature followed by a second cure cycle at elevated temperature to increase crosslink density.

Aromatic amines require elevated temperatures, usually 250 to 350 °F (120 to 175 °C), to obtain full cure. These systems are widely used for curing matrix resins, filament winding resins, and high temperature adhesives. Aromatic amines produce structures with greater strength, lower shrinkage, and better temperature capability but less toughness than aliphatic amines. Aromatic amine curing agents are usually solids at room temperature that must be melted, although some low melting point eutectic liquids are available. Diaminodiphenyl sulfone (DDS) is by far the most common curing agent used in epoxy composite matrices and in a high percentage of the high-temperature adhesive systems. It should be noted that methylene dianiline, the curing agent used in the high-temperature polyimide PMR-15, and occasionally used with epoxies, is a suspected carcinogen that can either be inhaled or absorbed through the skin.

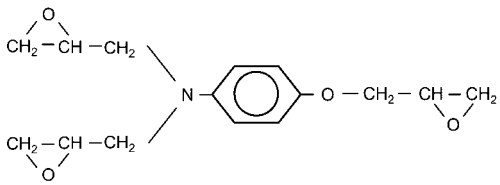


Fig. 3.8 Triglycidyl derivative of *p*-aminophenol (TGAP)

Catalytic curing agents, such as BF_3, promote epoxy-to-epoxy or epoxy-to-hydroxyl reactions. They do not serve as crosslinking agents; however, they produce very tightly crosslinked structures and are characterized by long shelf lives.

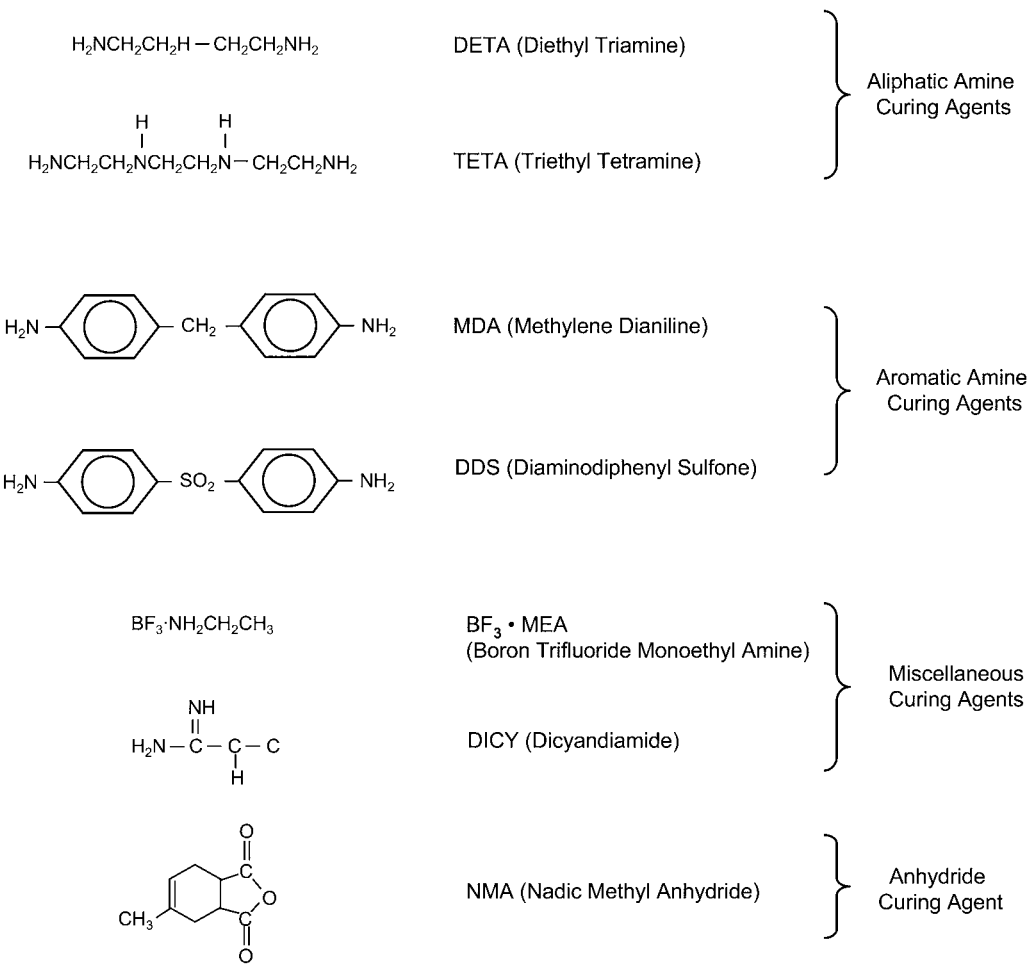


Fig. 3.9 Curing agents for epoxy resins

A typical catalytic curing agent is boron trifluoride mono ethyl amine (BF_3-MEA), which is a Lewis acid. It is normally used along with another curing agent (for example, DDS) in small amounts (1 to 5 phr) to reduce the flow and improve the processability of the composite matrix. It is a latent curing agent with a long pot life that requires a temperature of 200 °F (95 °C) or higher to initiate cure. However, once cure is initiated, it proceeds at a very rapid rate. Dicyandiamide (dicy) is also a very important latent curing agent used in both prepregs and adhesives. It is a solid powder that must be thoroughly mixed into the resin to provide uniform cures.

Anhydride curing agents require high temperatures and long duration cures to achieve full cure. They are characterized by their long pot lives and low exotherms. They yield good high-temperature properties, chemical resistance, and electrical properties. They can be blended with epoxies to reduce viscosity. Anhydride curing agents generally require the addition of a catalyst to proceed at a rapid rate. One anhydride group reacts with one epoxy group during cure. However, anhydride curing agents are susceptible to moisture pickup, which can inhibit the cure reaction. Nadic methyl anhydride is the most frequently used anhydride curing agent.

The curing of an epoxy resin system consists of low molecular weight resins and curing agents reacting under heat at room or elevated temperature to yield high crosslinked structures. The important points to remember are:

- Commercial matrix resins and adhesives are usually a blend of two or more epoxies combined with one or two curing agents. The principal epoxy in the majority of epoxy matrix systems and high-temperature adhesives is TGMDA. Frequently two, or sometimes three, minor epoxies are added to control viscosity or influence the final cured properties, such as modulus or toughness. The major curing agent used in matrix resins and many adhesives is DDS. Catalytic curing agents can be added to reduce flow and accelerate the cure. Epoxy resins for both composite matrices and adhesives are truly engineered systems to yield the best combination of processability and final properties.
- Higher cure temperatures and long cure times give the highest glass transition temperatures, T_g. When these are combined with high functionality (for example, four reactive end groups), the highest possible crosslink densities are achieved, which yield strong, stiff, but somewhat brittle structures. The resin is frequently toughened by a number of different means, but this often results in lower usage temperatures. The use of flexibilizing units (either the epoxy or the curing agent) gives higher elongation and impact strength at the expense of T_g, tensile and compression strength, and modulus. However, recent advances in epoxy chemistry and formulation have allowed much tougher resin systems with acceptable elevated-temperature performance.
- Epoxy matrices and adhesives—in fact, almost all thermoset resins—will absorb moisture from the atmosphere that degrades their elevated-temperature matrix-dependent properties (Fig. 3.10). However, the moisture problem is well understood and can be accounted for in the structural design process. The effect of moisture absorption on composite properties is covered in more detail in Chapter 15, "Environmental Degradation."

3.4 Bismaleimide Resins

Bismaleimides (BMIs) were developed to bridge the temperature gap between epoxies and polyimides with dry T_g in the range of 430 to 600 °F (220 to 315 °C) and use temperatures of 300 to 450 °F (150 to 230 °C). They process very similarly to epoxies by curing through addition reactions at 350 to 375 °F (175 to 190 °C). To obtain their high-temperature properties, they are given freestanding post cures at 450 to 475 °F (230 to 245 °C) to complete the polymerization reactions. Bismaleimide composites can be processed by autoclave curing, filament winding, and resin transfer molding. The tack and drape of most BMIs are quite good due to the liquid component of the reactants. Since BMIs process at the same temperature (such as 350 °F or 175 °C) and pressures (in this case 100 psig) as epoxies, conventional nylon bagging films, bleeder and breather materials, and other expendables can be used. In contrast, the higher-temperature traditional polyimide materials usually require higher temperature cures (600 to 700 °F or 315 to 370 °C) and higher pressures (in this case 200 psig or higher), resulting in more expensive and difficult tooling and bagging materials.

Bismaleimide chemistry is quite varied, with many potential paths to producing matrix materials. Both BMIs and polyimides contain the imide group shown in Fig. 3.11. Bismaleimide

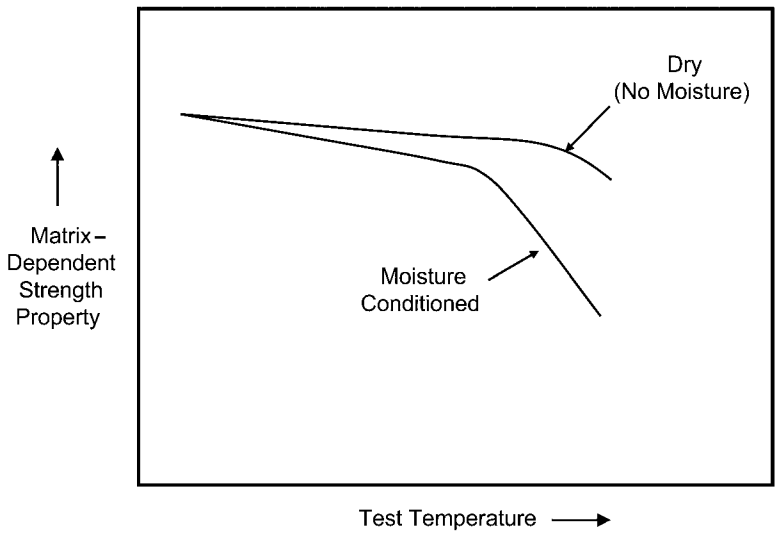


Fig. 3.10 Effect of moisture absorption on hot-wet matrix mechanical properties

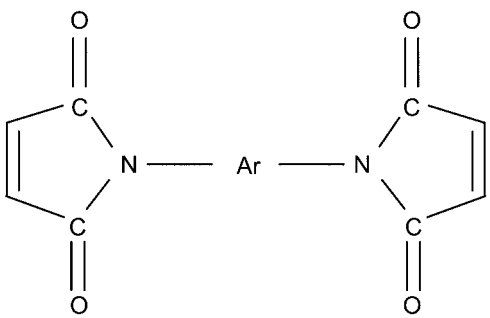


Fig. 3.11 Bismaleimide chemical structure

monomers are synthesized by reacting a primary diamine with maleic anhydride. The most prevalent BMI base monomer for matrices and adhesives is 4,4′-bismaleimidedodiphenylmethane. Commercial BMIs are usually one of five forms: (1) BMIs or mixtures of different BMIs, (2) blends of BMIs and BMI-diamines, (3) BMI and olefinic monomers and/or oligomeric blends, (4) BMI and epoxy blends, or (5) BMI and 0,0′-dicyanobisphenol A mixtures. Although early BMI materials were characterized as being hard to process (low tack and short out-times) and possessing low toughness (brittle), the BMI materials being produced today have much better tack and long out-times. In addition, some BMIs (such as Cytec 5250-4) are almost as tough as some toughened epoxies. Bismaleimides can also readily be processed by using liquid molding processes such as resin transfer molding (RTM).

One potential usage problem with BMIs, and with any polymer containing the imide end group, is a phenomenon known as *imide corrosion.* This is a form of hydrolysis that results in degradation of the polymer itself. It was originally observed in the aerospace industry with carbon fiber/BMI composites galvanically coupled to aluminum in a sump environment (in this case, a stagnant mixture of salt water and jet fuel). If the aluminum corrodes, the composite, because it is electrically coupled to the aluminum through the carbon fibers, becomes the cathode. Water reduction in the presence of oxygen occurs at the cathode, leading to the formation of hydroxyl ions that attack the imide-carbonyl linkage of the BMI. The mechanism is shown schematically in Fig. 3.12. No corrosion occurs with nonconductive fibers such as glass or aramid, nor does corrosion occur if the metal is galvanically similar to carbon, such as titanium or stainless steel. Studies have shown that increases in temperature and bare exposed carbon edges accelerate the deterioration. Electrically isolating the carbon from the aluminum will prevent the problem, which can be accomplished by curing a layer of fiberglass on the composite faying surface and then sealing the edges with a polysulfide sealant.

3.5 Cyanate Ester Resins

Cyanate esters are often used in applications requiring low dielectric loss properties, such as

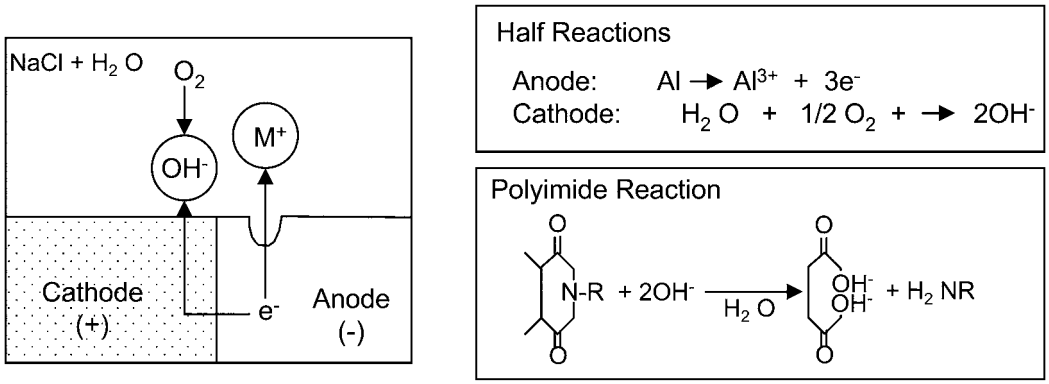


Fig. 3.12 Galvanic corrosion mechanism for imide linkage. Source: Ref 3

antennas and radomes. They are potential substitutes for both epoxies and BMIs with dry T_gs ranging from 375 to 550 °F (190 to 290 °C). However, due to a rather limited market and an inherently expensive monomer, they are expensive materials. The prepreg is also susceptible to moisture pickup that can produce carbon dioxide during cure. Their adhesion, or bondability, is inferior to that of epoxies. The cured laminates exhibit lower moisture absorption than epoxies or BMIs and are inherently flame resistant.

Cyanate esters are bisphenol derivatives containing a ring-forming cyanate functional group. This family of thermosetting monomers and their prepolymers are esters of bisphenols and cyanic acid that cyclotrimerize to substituted triazine rings upon heating (Fig. 3.13). During cure, three-dimensional networks of oxygen-linked triazine rings and bisphenol units crosslink by addition reactions. The high aromatic content of the triazine and benzene rings provides a high T_g. The single-atom oxygen linkages function somewhat like ball joints to dissipate localized stresses. Moderate crosslink densities contribute to toughness. In addition, both rubber and thermoplastic toughening mechanisms have successfully been used with cynate esters to further enhance toughness.

The attractive electrical properties, low dielectric constant, and dissipation factor are a result of the balanced dipoles and the absence of strong hydrogen bonding. This lack of polarity, along with the symmetry of the triazine rings, makes cyanate esters more resistant to water absorption than most epoxies and BMIs. The low moisture absorption (in the range of 0.6 to 2.5 percent) creates less outgassing, a critical factor in the dimensional stability required for space structures.

3.6 Polyimide Resins

Polyimides are high-temperature matrix materials intended for usage temperatures as high as 500 to 600 °F (260 to 315 °C). Polyimides can be thermoplastics or thermosets. They are normally condensation-curing systems. The condensation systems give off water or water and alcohol, which causes a severe volatile management problem during cure. If the volatiles are not removed prior to resin gellation, they become entrapped as voids and porosity that lower the matrix-dependent mechanical properties. In addition, polyimides are usually formulated with high-temperature solvents, such as dimethylformamide (DMF), dimethylactamide (DMAC), *N*-methylpyrrolidone (NMP), or dimethylsufoxide (DMSO), which must also be removed either prior to or during the cure cycle.

Polyimides are much more difficult to process than epoxies or BMIs. They require high processing temperatures (such as 600 to 700 °F or 315 to 370 °C), long cure cycles, and higher pressures (such as 200 psig). Volatiles and voids are always potential problems when processing polyimides. Even the so-called addition-curing systems can exhibit volatile problems as the low molecular weight monomers are usually dissolved in solvents during manufacturing.

The best known of the addition-curing polyimide materials is PMR-15. It's a *polymeric monomer reactants* with a molecular weight of 15,000. In PMR-15, three types of monomers (Fig. 3.14) are mixed together along with a solvent, usually methyl or ethyl alcohol. However, one of the monomers, 4,4′ methylene dianaline (MDA), is a suspected carcinogen that can be absorbed through the skin or inhaled if used as a

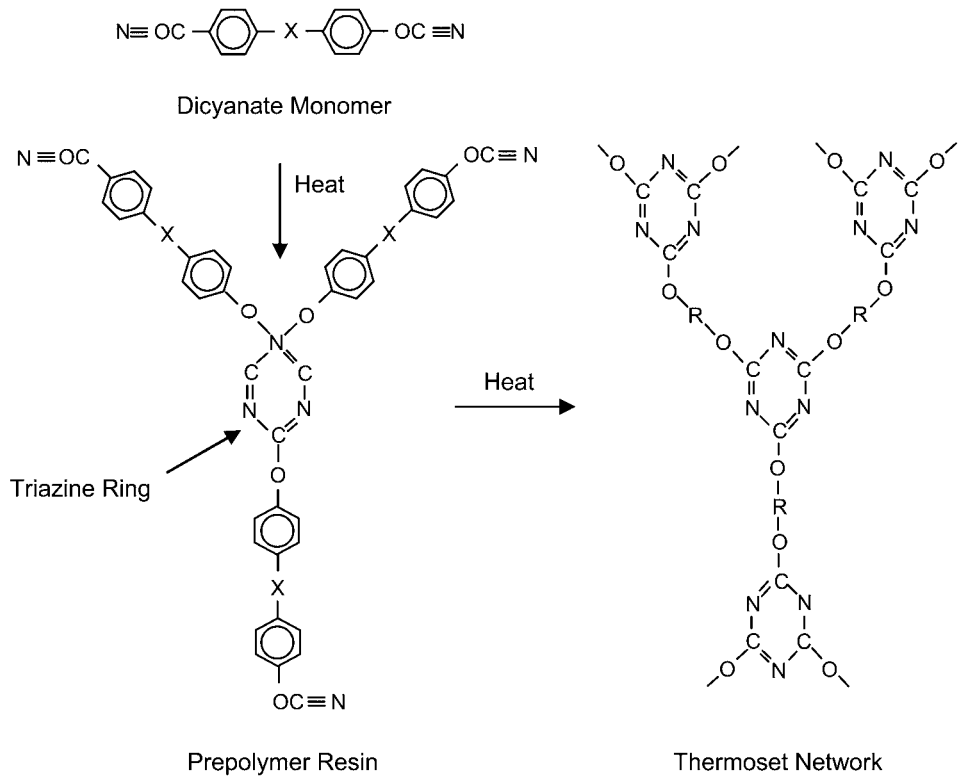


Fig. 3.13 Cure of cyanate resins

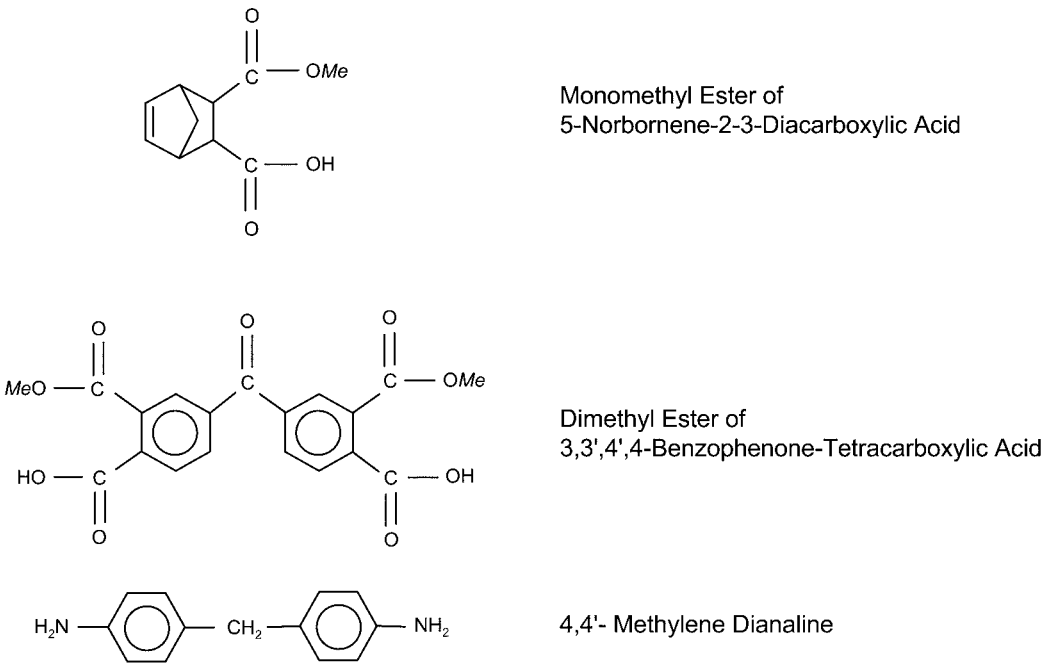


Fig. 3.14 Components of PMR-15

spray. Several non-MDA polyimides have been formulated and sold; however, their elevated-temperature performance is not as good as that of the original formulation. Even though PMR-15 is classified as an addition-curing reaction, it undergoes condensation reactions early in the cure cycle during the imidization stage that creates a volatile management problem, and the impregnation solvent must be removed before the resin gels; otherwise, the solvent will result in voids and porosity. PMR-15 has a usage temperature of 550 to 600 °F (290 to 315 °C) for 1000 to 10,000 hours, depending on the specific use temperature. The main disadvantages of PMR-15 are the potential for voids, poor tack and drape, inadequate resin flow for fabricating thick and complicated structures, a tendency toward microcracking, and the health and safety concerns regarding MDA.

Considerable effort has been expended over the last 25 years on the development of high-temperature polymers that have good thermal-oxidative behavior in the 500 to 600 °F (260 to 315 °C) range yet are easy to process. Much of this effort has either been led or funded by the National Aeronautics and Space Administration (NASA), most recently to support the High Speed Civil Transport program conducted during the mid-1990s. The goal was to develop a resin system capable of withstanding a temperature of 350 °F (175 °C) for 60,000 hours. After screening of the available materials, the most promising resin developed was PETI-5, a phenylethynyl terminated imide. A matrix resin, an adhesive, a RTM grade, and a resin film infusion grade of PETI-5 were developed during the program. As with other high-temperature resin systems that use high- boiling-point solvents for manufacturing—NMP in this case—management of volatiles during cure is a major consideration. However, successful demonstration parts were fabricated using all of these product forms.

3.7 Phenolic Resins

Phenolics are normally very brittle and exhibit large shrinkage during cure. Their primary use is for aircraft interior structures because of their low flammability and low smoke production. They are also used for high-temperature heat shields, due to their excellent ablative resistance, and as the starting material for C-C composites because of their high char yield during graphitization.

Phenolics are made by a condensation reaction with phenol and formaldehyde that gives off water as a by-product. A typical phenolic reaction is shown in Fig. 3.15. Phenolics are usually classified as either resoles or novolacs. If the phenol-formaldehyde reaction is carried out with an excess of formaldehyde and a base catalyst, the result is a low molecular weight liquid resole. If the reaction is carried out with an excess of phenol and an acid catalyst, the result is a solid novolac. Resoles are normally used for phenolic prepregs.

Phenolics are one route to the production of high-temperature-resistant C-C composites. The phenolic is charred, or pyrolized, to produce a carbon matrix. Since the charring process produces a porous structure due to the vaporization of the organics in the phenolic, the process has to be repeated several times. Before each subsequent pyrolization, the porous structure is impregnated with either pitch, phenolic resin, or directly with carbon by chemical vapor deposition. This is a slow process that must be done with great care to prevent delaminations and severe matrix cracking. Quite frequently, three-

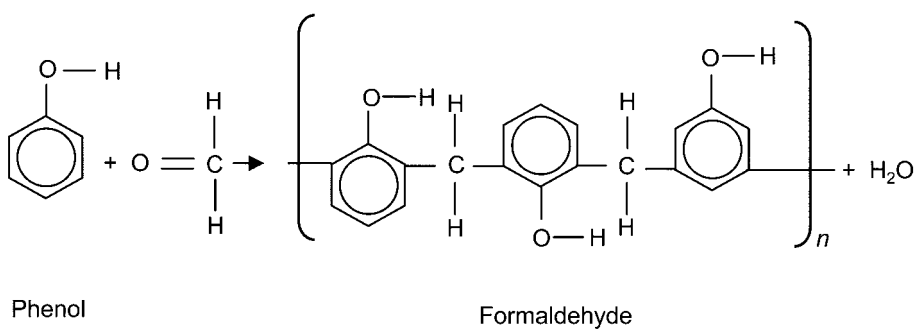


Fig. 3.15 Typical phenolic condensation reaction

dimensional reinforcements will be used to resist ply delaminations. Carbon-carbon composites can also be made directly using chemical vapor deposition. A carbon preform is impregnated with a methane gas. Since there is a tendency for the deposited carbon to seal off internal voids and porosity, intermittent machining operations are required to remove the surface layer to allow the carbon deposit access to the internal structure. Carbon-carbon composites are dealt with in more detail in Chapter 21, "Ceramic Matrix Composites."

3.8 Toughened Thermosets

The toughness limitation of the thermoset matrix is a direct result of the rigid, highly crosslinked, glassy polymer structures that form during cure. These rigid structures have both advantages and disadvantages. The main advantages are high-temperature capability and the ability of the rigid matrix to stabilize the reinforcing fibers during compression loading. The greatest disadvantage is their susceptibility to delaminations when impacted. Of particular concern are low-velocity impacts causing internal delaminations that cannot be detected during visual walk-around inspections.

Since the early 1980s, a large amount of effort has been expended to develop resin systems that are tougher and less susceptible to impact damage. Two candidates emerged in the mid-1980s: (1) damage-tolerant thermoplastic composites and (2) toughened thermoset composites. Although these systems are radically different in chemical structure, their resultant properties are somewhat similar. Both have improved resistance to low-velocity impact damage, resulting in greater load-carrying capability after being impacted. Also, compared to the stiff thermoset systems, both have a somewhat lower resin modulus and therefore exhibit lower compression strengths. Although it is certainly not true in every case, the tougher systems generally have less heat resistance than the rigid glassy thermosets.

Due to the inhomogeneous nature of these systems, where the properties vary in many directions, toughness is more complicated for composites than for homogeneous metallic materials. In composite structures, in-plane loading is controlled primarily by the reinforcing fibers, while out-of-plane loading is dominated by the properties of the resin matrix. Therefore, composite structures are intentionally designed so that the load paths are stiff and are primarily in-plane. However, out-of-plane loading can occur. Out-of-plane loads develop during in-plane compressive buckling but, more important, out-of-plane loads are induced by a variety of design features. Five of the more common design details that can cause out-of-plane loading are shown in Fig. 3.16. Even under normal in-plane loading conditions, interlaminar shear and normal stresses develop at these locations. These indirect loads can act either alone or in combination with direct

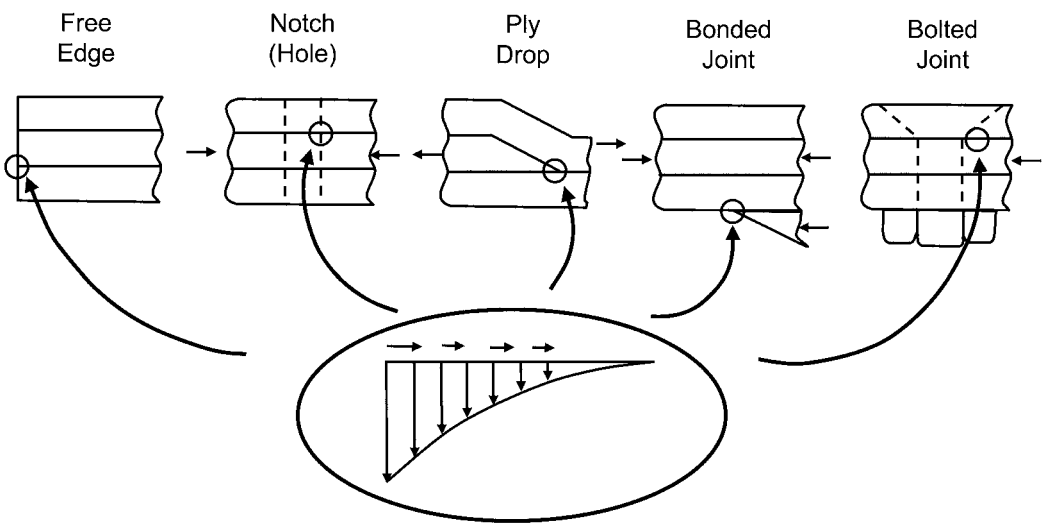


Fig. 3.16 Design details that cause out-of-plane loads

out-of-plane loads, such as fuel or air pressures. If the out-of-plane loads become large enough, interply delaminations can form and propagate. Fortunately, current design criteria are conservative enough that even if a small delamination is present, either from a manufacturing defect or from service abuse, it will normally not propagate.

Crosslinks are the chemical ties between two or more polymer chains that give the cured polymer its strength, rigidity, and thermal resistance. As shown conceptually in Fig. 3.17, the higher the crosslink density (in this case, the number of crosslinks per unit volume) and the shorter the polymer chain lengths between the crosslinks, the more constrained the chain motion, and thus the stiffer and more thermally resistant the molecular structure. Further stiffening can be imparted by the use of stiffener backbones in the main chains. However, this rigidity results in brittleness, low strain-to-failure, and poor impact and postimpact properties. Highly crosslinked rigid structures usually exhibit good thermal stability due to their ability to restrict the relative motion of the polymer chains by the chemical bonds holding them together. Since the crosslink bonds are primary covalent bonds, they retain a large portion of their strength as the temperature is increased. When the crosslink density is high and the bond lengths are short, acceptable properties are maintained up to near the glass transition temperature of the resin. Above the glass transition temperature, the rigid solid polymer converts to a softer rubber-like material as the main backbone chains themselves soften. Therefore, highly crosslinked polymers possess moderate to high strength and stiffness and excellent temperature resistance. However, being rigid and glassy structures, they are somewhat brittle and susceptible to impact damage.

The molecular structure of a thermosetting polymer determines how it processes and its resultant properties. Examples of properties that are a function of molecular structure include glass transition temperature, moisture absorption, strength, modulus, elongation, and toughness. By altering the molecular structure, it is possible to alter these performance properties. The molecular structure is controlled by its backbone structure (in this case the main polymer chains) and its network structure (in this case the number and types of crosslinks). The chemical structure of the main monomer defines the backbone structure and to some extent the network structure. The network structure is also influenced by the type of curing agent, or hardener, used in the curing reaction. Resin formulators have expended a significant amount of effort to develop new molecular structures that result in polymers with improved toughness.

The improved postimpact compression strength of the toughened systems is a direct result of the amount of damage inflicted during the impact event. As shown in Fig. 3.18, the toughened systems (Hexcel's IM-7/8551-7 in this example) experience much less internal damage when impacted. Therefore, when the specimens are subsequently loaded to failure, the toughened systems have a larger cross-sectional area of undamaged material to help support the compression load.

To impart greater toughness to the crosslinked thermoset polymers, a number of different approaches have evolved. Some are used by themselves, while others are often combined to further enhance toughness. Four toughening approaches will be discussed: (1) network alteration, (2) rubber elastomer second phase toughening, (3) thermoplastic elastomer toughening, and (4) interlayering.

Network Alteration. Since the brittleness of thermosetting polymers is a direct consequence of their high crosslink densities, one method of

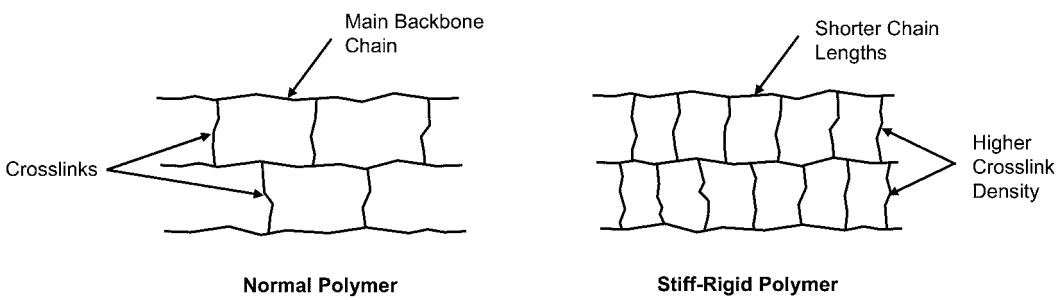


Fig. 3.17 Effect of crosslink density on rigidity

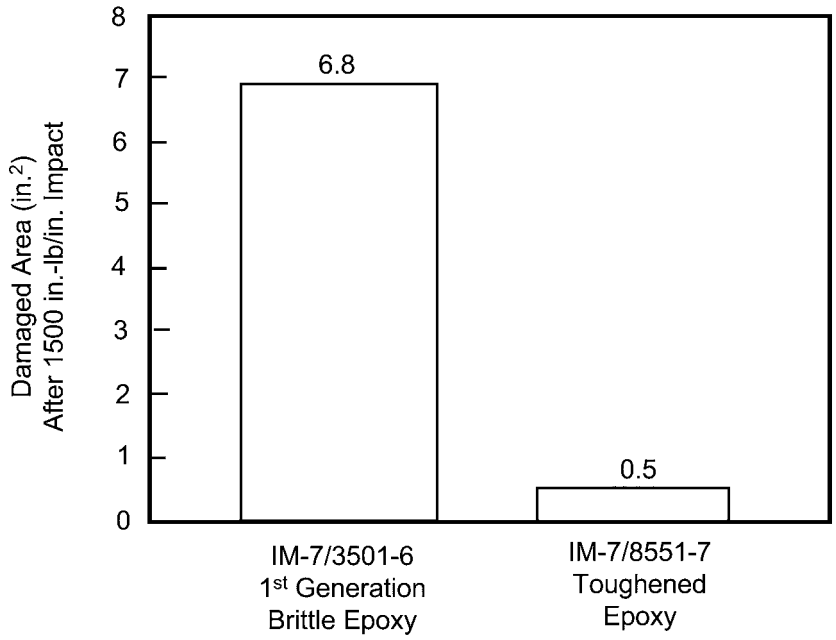


Fig. 3.18 Damage comparison during low-velocity impact

toughening a thermoset polymer is to lower the crosslink density. This approach, when taken to the extreme case in which there are no more crosslinks, results in a thermoplastic polymer. Since amorphous thermoplastic polymers are inherently tough, the more the crosslink density is reduced, the tougher the resulting polymer. However, the decrease in crosslink density is also accompanied by a decrease in desirable properties such as the glass transition temperature and the resin modulus.

There are three well-known methods for reducing the crosslink density of thermoset polymers (Fig. 3.19). The first is to alter the main monomer backbone chain by increasing the molecular weight between crosslinks with long-chain monomers. The resulting decrease in glass transition temperature can be somewhat offset by constructing a long-chain monomer with rigid bulky side groups, such as benzene rings. The decreased mobility of the polymer chains will somewhat compensate for the loss in glass transition temperature due to the lower crosslink density.

A second method is to lower the monomer functionality. Most highly crosslinked thermosetting polymers have a functionality of four, which means that there are four reactive end groups that can react and crosslink during cure. If a portion of the polymer mix contains a monomer with a functionality of two, there are fewer available sites for crosslinking during cure and the toughness will therefore be improved due to the lower crosslink density. However, the heat resistance is again affected, as evidenced by the lower glass transition temperatures of difunctional monomers.

A third method is to incorporate flexible subgroups into the main chain backbone of either the resin or the curing agent. Although these subgroups are depicted as "springs" in Fig. 3.19, in actuality more flexible aliphatic segments are used in preference to the more rigid and bulky aromatic groups that contain the large benzene ring. As with the other approaches described above, there is a trade-off in glass transition temperature. This can be minimized by using some stiff segments along with the flexible ones.

Rubber Elastomer Second Phase Toughening. When a crack begins in a brittle glassy solid, it requires very little energy to propagate. In fiber-reinforced composites, the fibers will prevent in-plane crack growth. However, if the crack is interlaminar or between the plies, the fibers are of no help in preventing crack propagation. One way of reducing crack propagation is to use second-phase elastomers. Discrete rubber particles help to blunt crack growth by promoting greater plastic flow at the crack tip, as shown in Fig. 3.20.

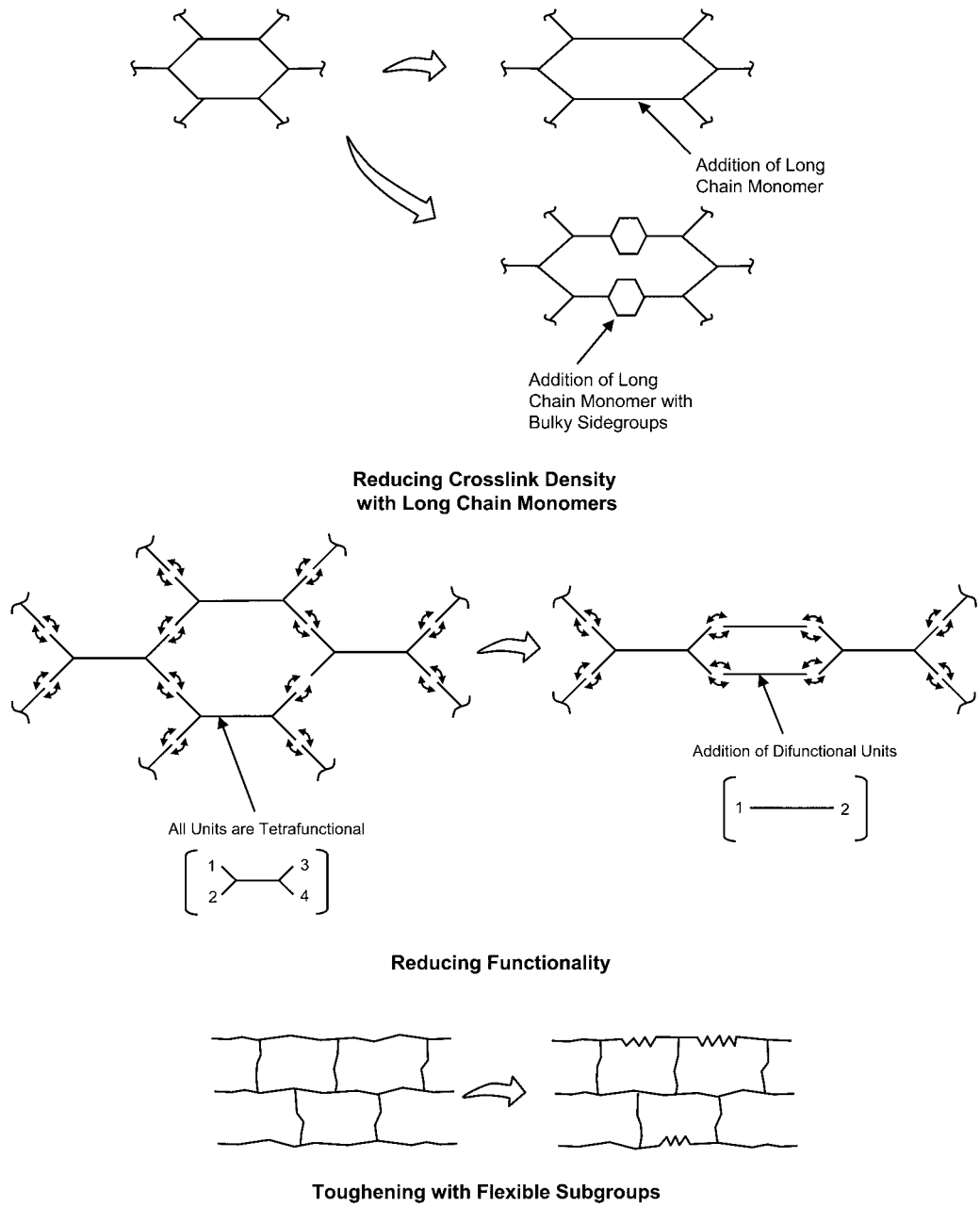


Fig. 3.19 Network alteration toughening mechanisms

The size of the elastomeric domains is a critical factor in determining the microdeformation processes that control toughening. Rubber particles, usually round, having domain diameters of 100 to 1000 Å, initiate shear yielding, while larger domains (10,000 to 20,000 Å) are generally believed to lead to crazing. Very small domains are used to enhance the shear deformation processes. However, if the crosslink density permits the use of larger domain sizes, bimodal distributions (such as a mixture of large and small domains) of the elastomer will result in both crazing and shear. Since these mechanisms complement each other, the toughening effect can be nearly doubled.

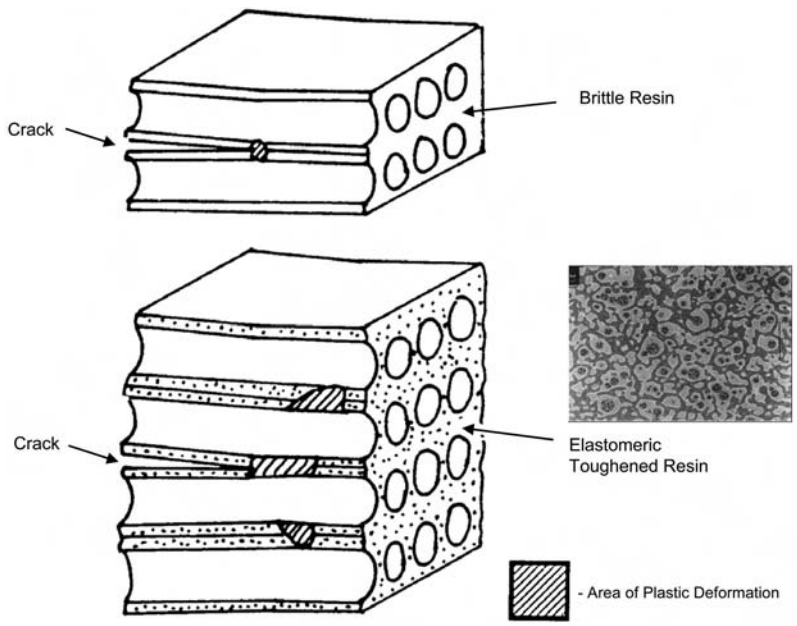


Fig. 3.20 Elastomeric toughening

A finely dispersed phase of elastomer-rich domains can be obtained by using either (1) preformed rubber particles or (2) a rubber elastomer system that is initially soluble in the liquid resin but then phase separates (i.e., precipitates) during cure. Preformed particles are advantageous because they can be used as additives or fillers. Also, their domain size is easier to control than when a phase separation process is used. Unfortunately, commercially available preformed rubber particles are suitable only for toughening some of the lower-temperature thermosets. When elastomer domains are to be precipitated during cure, it is necessary to use a rubber with suitable solubility. The rubber must be initially soluble in the resin and then phase separate into the desired small domains during the cure process. An elastomer that is too soluble will remain in solution too far into cure, and significant quantities will be trapped in solution when the resin gels. The trapped elastomer will then act as a plasticizer and subsequently will lower the glass transition temperature and the hot-wet properties. On the other hand, if the elastomer is not soluble enough, a stable solution with the resin will not be possible and a fine dispersion of particles will not be obtained. If just the right amount of compatibility exists, then the elastomer will initially remain in solution, and once the resin begins to cure, small particles will precipitate uniformly into the resin matrix. Early and complete phase separation is necessary to maintain good hot-wet matrix performance.

In epoxy-based composites and adhesives, reactive liquid polymers, such as carboxyl terminated butadiene-acrylonitrile (CTBN) rubber, are often used to provide the desired solution and compatibility characteristics. Functional carboxyl groups, such as CTBN rubbers, are usually blended and prereacted with one of the epoxy monomers to provide the desired solubility. In addition, the carboxyl groups react with some of the epoxy groups to form light crosslinks that increase the cohesive strength of the elastomeric domains. Good bonding between the elastomer domains and the continuous resin phase is important. If the bond is poor, the elastomer can debond from the resin during cooling and form voids.

The elastomer itself must have good rubbery characteristics. Specifically, the elastomer-rich domain must have a T_g lower than about –100 °F (–75 °C) so that when a crack travels rapidly through the material, the domains still act as elastomers. If the T_g is too high (in this case, too close to room temperature), then at high deformation rates it will behave in a glassy manner and the desired toughening effect will not be achieved. Another requirement is that the elastomer must be thermally and thermally-oxidatively stable. If unstable rubbers are used, they are likely

to crosslink or degrade when oxidized, which would embrittle the elastomeric domains.

Elastomeric second phase toughening is not always effective. If the resin is too highly crosslinked, then the resin will lack the ability to deform locally. In the absence of some localized deformation, the addition of an elastomeric second phase is largely ineffective. As the crosslink density is lowered, the benefits of second-phase elastomeric toughening rapidly increase. In epoxy resins, it has been shown that the relatively small gains in toughness, obtained by modification of the monomer stiffness or length, or by altering the network structure, can be greatly amplified by the use of second-phase toughening.

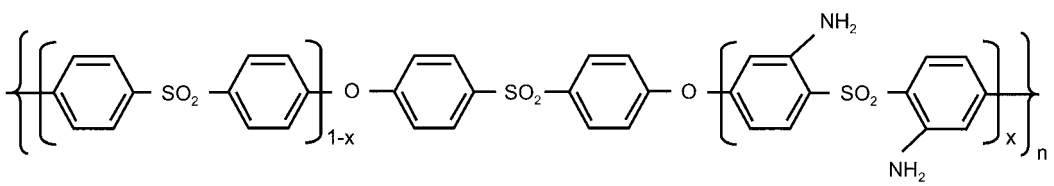
Thermoplastic Elastomeric Toughening. A number of important commercially available toughened thermoset composite systems are based on thermoplastic toughening, which can exhibit four distinct morphologies in the cured composite: (1) homogeneous (single phase), (2) particulate (thermoplastic particles in a continuous thermoset matrix), (3) cocontinuous (both the thermoplastic and thermoset are continuous), and (4) phase inverted (the thermoplastic is continuous and the thermoset is discontinuous). It has been shown that the cocontinuous morphology results in the greatest toughness improvements. Polyetherimide, polyethersulfone, and polysulfone have all been evaluated.

In a cocontinuous structure, the thermoplastic increases the toughness, while the crosslinked thermoset helps to retain a high glass transition temperature and hot-wet performance. A thermoplastic with a high T_g helps to maintain the final T_g, since the T_g is at least the average of those of the separate components. The selection of the optimum thermoplastic component depends on its compatibility, heat resistance, and thermal stability. Chemical compatibility is required so that the thermoplastic will remain in solution (i.e., not phase separate) until the thermoset network has gelled. In addition, the viscosity of the ungelled resin must be controlled so that it remains low enough to allow fiber wetting and ply bonding during cure. Finally, the thermoplastic must have good heat resistance and be thermally stable to maintain the hot-wet performance.

As an example, functionalized polyaromatic thermoplastic toughening agents can be produced that allow the thermoplastic to bond covalently to the thermosetting resin during cure. The use of an amino functionalized polyethersulfone (Fig. 3.21) at even low content (10 phr) is useful in improving the toughness of an epoxy resin.

Interlayering. A "mechanical" or "engineered" approach to toughness can be achieved by incorporating a thin layer of a tough, ductile resin between the individual prepreg plies. As shown in Fig. 3.22, this layer is usually thin (0.001 in. (0.025 mm) or less) and must remain fairly discrete during the composite curing operation. The rationale behind this approach is that the stiff, brittle matrix will support the carbon fibers in compression and thus help to maintain the hot-wet performance, while the tough interlayers provide the desired increase in resistance to low-velocity impact. Since the tough interlayer has a high strain-to-failure, it helps to reduce the interlaminar shear and normal forces that can induce delaminations.

The original development work was conducted using tough film adhesives that were simply placed between the prepreg plies during lay-up. More recently, discrete thermoplastic toughening particles have been added to the surfaces during the prepregging operation. The particles are larger than the fibers and therefore remain on the interlayers during prepregging and cure. The interlayering approach can be used with either brittle or toughened resin systems. Although a toughened resin system used in combination with interlayers will provide better impact resistance, the hot-wet compression strength will decrease



4: x = 0
5: x = 0.05
6: x = 0.20

Fig. 3.21 Amino functionalized polyethersulfone. Source: Ref 4

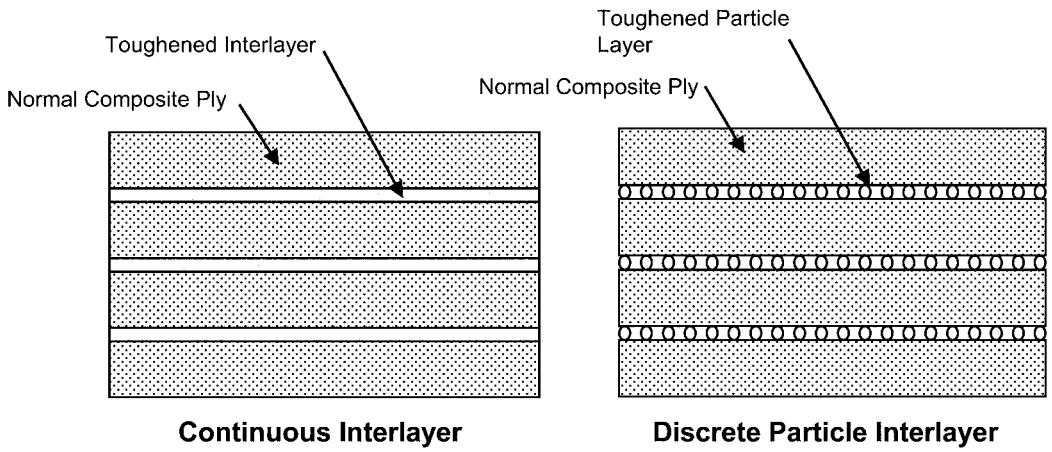


Fig. 3.22 Interface toughening

somewhat compared to that of a stiff, brittle matrix used by itself.

3.9 Thermoplastics

During the 1980s and early 1990s, government agencies, aerospace contractors, and material suppliers invested hundreds of millions of dollars in developing thermoplastic composites to replace thermosets. Despite all of this investment and effort, continuous fiber thermoplastic composites account for only a handful of production applications for commercial and military aircraft. In this section, we will examine the potential advantages of thermoplastics and discuss why they failed to replace thermoset composites in the aerospace industry.

Before considering the potential advantages of thermoplastic composite materials, it is necessary to understand the difference between a thermoset and a thermoplastic. As shown in Fig. 3.1, a thermoset crosslinks during cure to form a rigid, intractable solid. Prior to cure, the resin is a relatively low molecular weight semisolid that melts and flows during the initial part of the cure process. As the molecular weight builds during cure, the viscosity increases until the resin gels and then strong covalent bond crosslinks form during cure. Due to the high crosslink densities obtained for high-performance thermoset systems, they are inherently brittle unless steps are taken to enhance their toughness. Thermoplastics, by contrast, are high molecular weight resins that are fully reacted prior to processing. They melt and flow during processing but do not form crosslinking reactions. Their main chains are held together by relatively weak secondary bonds. However, since they are high molecular weight resins, the viscosities of thermoplastics during processing are orders of magnitude higher than those of thermosets (for example, 10^4–10^7 poise for thermoplastics vs. 10 poise for thermosets). Since thermoplastics do not crosslink during processing, they can be reprocessed. For example, they can be thermoformed into structural shapes by simply reheating to the processing temperature. On the other hand, thermosets, due to their highly crosslinked structures, cannot be reprocessed and will thermally degrade and eventually char if heated to high enough temperatures. However, there is a limit to the number of times a thermoplastic can be reprocessed. Since the processing temperatures are close to the polymer degradation temperatures, multiple reprocessing will eventually degrade the resin, and in some cases it may crosslink.

The structural difference between thermosets and thermoplastics yields some insight into the potential advantages of thermoplastics. Since thermoplastics are not crosslinked, they are inherently much tougher than thermosets. Therefore, they are much more damage tolerant and resistant to low-velocity impact damage than the untoughened thermoset resins used in the early to mid-1980s. However, as a result of improved toughening approaches for thermoset resins, primarily with thermoplastic additions to the resin, the thermosets available today exhibit toughness somewhat comparable to that of thermoplastic systems.

Since thermoplastics are fully reacted high molecular weight resins that do not undergo

chemical reactions during cure, the processing for these materials is theoretically simpler and faster. Thermoplastics can be consolidated and thermoformed in minutes (or even seconds), while thermosets require long cures (hours) to build molecular weight and crosslink through chemical reactions. However, since thermoplastics are fully reacted, they contain no tack and the prepreg is stiff and boardy. In addition, competing thermoset epoxies are usually processed at 250 to 350 °F (120 to 175 °C), while high-performance thermoplastics require temperatures in the range of 500 to 800 °F (260 to 425 °C). This greatly complicates the processing operations, requiring high-temperature autoclaves or presses and bagging materials that can withstand the higher processing temperatures. Another advantage of thermoplastic composites involves health and safety. Since these materials are fully reacted, there is no danger to the worker from low molecular weight unreacted resin components. In addition, thermoplastic composite prepregs do not require refrigeration, as thermoset prepregs do. They have essentially an infinite shelf life but may require drying to remove surface moisture prior to processing.

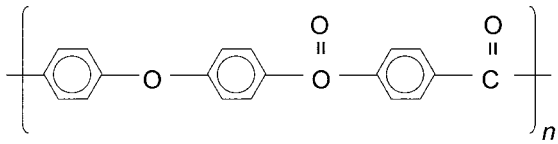
Another potential advantage of thermoplastics is their low moisture absorption. Cured thermoset composite parts absorb moisture from the atmosphere, which lowers their elevated temperature (hot-wet) performance. Since many thermoplastics absorb very little moisture, the design does not have to take such a severe structural "knockdown" for lower hot-wet properties. In contrast, thermosets are highly crosslinked and are resistant to most fluids and solvents encountered in service. Some amorphous thermoplastics are very susceptible to solvents and may even dissolve in methylene chloride, a common base for many paint strippers, while others, primarily semicrystalline thermoplastics, are quite resistant to solvents and other fluids.

Since thermoplastics can be reprocessed by simply heating them above their melting temperature, they offer advantages in forming and joining applications. For example, large, flat sheets of thermoplastic composite can be autoclave or press consolidated, cut into smaller blanks, and then thermoformed into structural shapes. Unfortunately, this has proven to be much more difficult in practice than originally anticipated. Press forming processes are limited to relatively simple geometric shapes because of the inextensible nature of the continuous fiber reinforcement. If a defect (such as an unbond) is discovered, the part can often be reprocessed to heal the defect, but in practice such repairs are rarely practical without undesirable fiber distortion and the associated structural property degradation. The melt fusible nature of thermoplastics also offers a number of attractive joining options such as melt fusion, resistance welding, ultrasonic welding, and induction welding, in addition to conventional adhesive bonding and mechanical fastening.

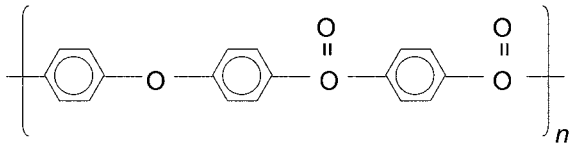
3.9.1 Thermoplastic Composite Matrices

During the 1980s, dozens of thermoplastic matrices and product forms were available to industry. The number commercially available today is much more modest. The five most important materials are shown in Fig. 3.23. Polyetheretherketone (PEEK), polyetherketoneketone (PEKK), polyphenylene sulfide (PPS), and polypropylene (PP) are semicrystalline thermoplastics, while polyetherimide (PEI) is an amorphous thermoplastic. PEEK, PEKK, PPS, and PEI are normally used for continuous fiber-reinforced thermoplastic composites, while PP is a lower-temperature resin that is used extensively in the automotive industry as a discontinuous glass fiber stampable sheet product form called *glass mat reinforced thermoplastic*. High-performance thermoplastics, such as PEEK, PEKK, PPS, and PEI, have high T_gs with good mechanical properties, much higher than those of conventional thermoplastics, but are also more costly. High-performance thermoplastics are usually aromatic, containing the benzene ring (actually, the phenylene ring), which increases the T_g and provides thermal stability. Also, when n (i.e., the number of units in the molecular chain) is large, there is a high degree of orientation in the liquid state that helps promote crystallinity during freezing. Highly aromatic thermoplastics exhibit good flame retardance because of their tendency to char and form a protective surface layer.

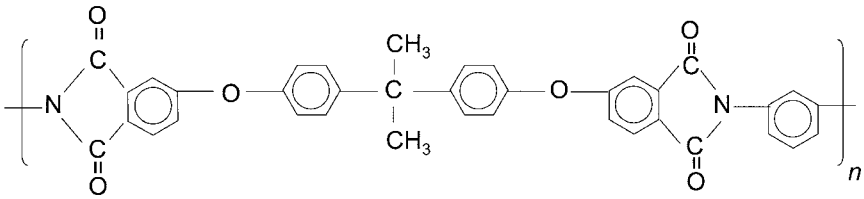
The differences between an amorphous and a semicrystalline thermoplastic are shown in Fig. 3.24. An amorphous thermoplastic contains a massive random array of entangled molecular chains. The chains themselves are held together by strong covalent bonds, while the bonds between the chains are much weaker secondary bonds. When the material is heated to its processing temperature, it is these weak secondary



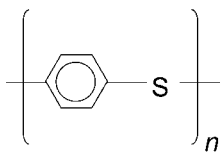
Polyetheretherketone (PEEK)
T_m= 653°F
T_g= 290°F
Processing Temperature= 680-750°F



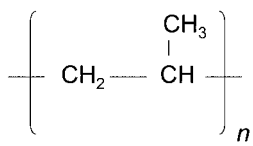
Polyetherketoneketone (PEKK)
T_m= 590°F
T_g= 313°F
Processing Temperature= 620-680°F



Polyetherimide (PEI)
T_m= Not Applicable (Amorphous)
T_g= 424°F
Processing Temperature= 600-680°F



Polyphenylene Sulfide
T_m= 545°F
T_g= 190°F
Processing Temperature= 625-650°F



Polypropylene
T_m= 338°F
T_g= 25°F
Processing Temperature= 375-435°F

Fig. 3.23 Chemical structure of several thermoplastic resins

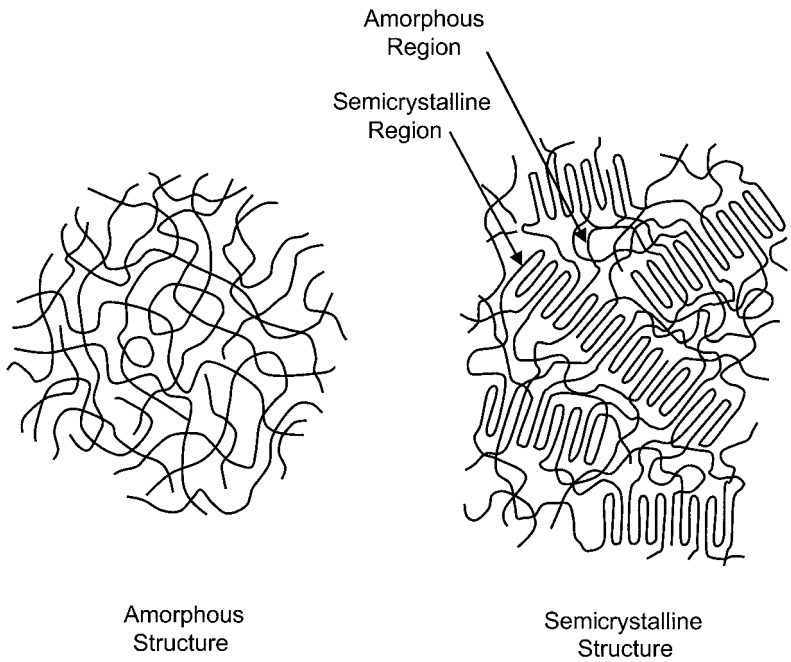


Fig. 3.24 Comparison of amorphous and semicrystalline thermoplastic structures

bonds that break down and allow the chains to move and slide past one another. Amorphous thermoplastics exhibit good elongation, toughness, and impact resistance. As the chains get longer the molecular weight increases, resulting in higher viscosities, higher melting points, and greater chain entanglement, all leading to higher strength.

Semicrystalline thermoplastics contain areas of tightly folded chains (crystallites) that are connected together with amorphous regions. As shown in Fig. 3.25, amorphous thermoplastics exhibit a gradual softening on heating, while semicrystalline thermoplastics exhibit a sharp melting point when the crystalline regions start dissolving. As the polymer approaches its melting point, the crystalline lattice breaks down and the molecules are free to rotate and translate, while noncrystalline amorphous thermoplastics exhibit a more gradual transition from a solid to a liquid. In general, the melting point T_m increases with increasing chain length, greater attractive forces between the chains, greater chain stiffness, and increasing crystallinity. The glass transition temperature T_g increases with lower free volume, greater attractive forces between the molecules, decreasing chain mobility, increasing chain stiffness, increasing chain length, and, for thermosets, increasing crosslink density. Crystallinity provides the following attributes to a thermoplastic resin:

- Crystalline regions are held together by amorphous regions. The maximum crystallinity obtainable is about 98 percent, whereas metallic structures are usually 100 percent crystalline and exhibit much more ordered structures.
- Crystallinity increases density. The density increase helps to explain the improved solvent resistance of semicrystalline thermoplastics since it becomes more difficult for the solvent molecules to penetrate the tightly packed crystallites.
- Crystallinity increases strength, stiffness, creep resistance, and temperature resistance but usually decreases toughness. The tightly packed crystalline structure behaves somewhat like crosslinking in thermosets by decreasing and restricting chain mobility.
- Crystalline polymers are either opaque or translucent, while transparent polymers are always amorphous.
- Crystallinity can be increased by mechanical stretching.
- Crystallinity is an exothermic process in which heat is given off to obtain the lowest free energy state.

In general, thermoplastics used for composite matrices contain 20 to 35 percent crystallinity. It

should also be noted that all thermoset resins are amorphous but are crosslinked to provide strength, stiffness, and temperature stability. As a general class of polymers, thermoplastics are much more widely used than thermosets, accounting for about 80 percent of all polymers produced.

Crystallites form from the melt as spherulites during cooling by a nucleation and growth process, as shown in Fig. 3.26. Spherulites are families of crystallites radiating from a single nucleation point. If carbon fibers are present, they will frequently nucleate on the surface of the fibers and grow outward until they impinge on another spherulite. The degree of crystallinity is dependent on the cooling rate. As shown in Fig. 3.27, it is possible to quench a semicrystalline thermoplastic from the melt at very high cooling rates and form a primarily amorphous structure. Slow cooling rates are required to provide the time necessary for the nucleation and growth process. The optimum cooling rate for PEEK is in the range of 0.2 to 20 °F/min (0.1 to 11 °C/min),

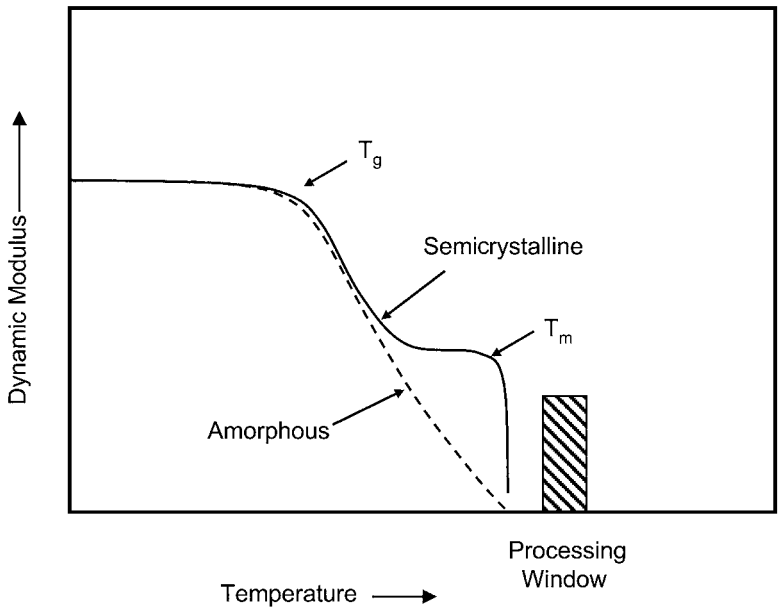
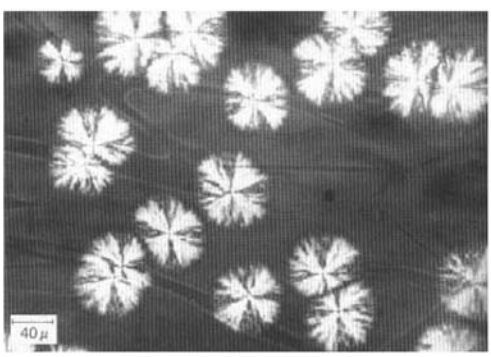
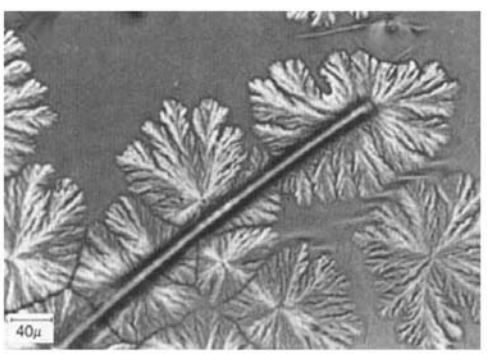


Fig. 3.25 Matrix stiffness versus temperature



Nucleation of Spherulites
in Pure PEEK Resin



Nucleation of Spherulites
on Carbon Fiber Surface

Fig. 3.26 Nucleation and growth of spherulites in PEEK

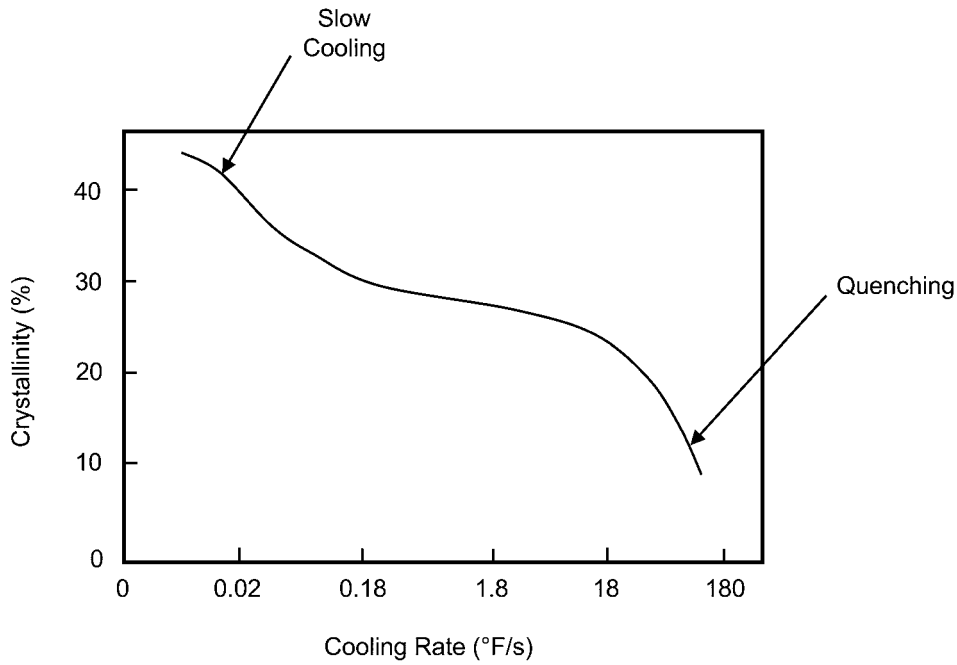


Fig. 3.27 Crystallization versus cooling rate for carbon/PEEK laminate. Source: Ref 5

which will yield a crystalline content of 25 to 35 percent. If the material is quenched to produce an amorphous structure, the proper amount of crystallinity can be established by a short (1 min) annealing cycle at 430 to 520 °F (220 to 270 °C). The rate of crystallization is also dependent on the specific annealing temperature. As shown in Fig. 3.28, the peak rate lies at about the midpoint between the glass transition temperature (T_g) and the melt temperature (T_m). The specific volume-versus-temperature curve of Fig. 3.29 illustrates the reduction in free volume that occurs during crystallization and helps to explain the superior solvent resistance of semicrystalline thermoplastics. Since there is no step change in density for amorphous thermoplastics, they have less tendency to warp or distort during rapid cooling, as residual stresses are typically lower.

It should be pointed out that many condensation polyimides are also thermoplastics. Some, like Avimid K-III, are often classified as pseudo-thermoplastics because they can undergo light crosslinking during processing. These materials can be supplied in either low or high molecular weight forms. When supplied as a low molecular weight prepreg, they process in a manner similar to that of thermoset prepregs; that is, long processing cycles are required to achieve the molecular weight buildup. Low molecular weight thermoplastic polyimide prepregs are normally produced using conventional thermoset prepregging equipment. Thus, both unidirectional and woven data product forms are readily available. However, due to the chemical inertness of some of the resin components, they must be dissolved in high boiling point solvents (such as NMP) to facilitate prepregging. Although some of the solvent is removed in a subsequent drying operation, an appreciable amount remains (as much as 12 to 18 percent in Avimid K-III). This residual solvent can cause problems with volatile evolution resulting in voids during elevated temperature processing. In addition, the condensation reactions give off water and ethanol, further contributing to the void problem. Extensive use of breather and vacuum porting arrangements can facilitate volatile removal. Although these materials do possess tack and drapability, their handling properties are inferior to those of production grades of carbon/epoxy prepreg. High-temperature heat guns and respirators are required when forming the prepreg to complex contours. The high molecular weight forms are somewhat easier to process; however, voids can also be formed in some of these materials through additional high-temperature reactions evolving carbon dioxide.

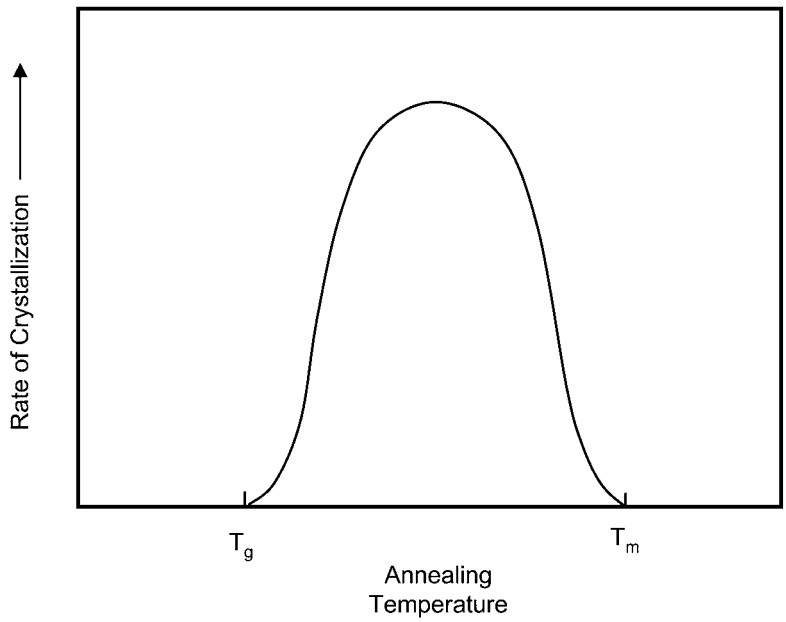


Fig. 3.28 Crystallization rate dependency on annealing temperature. Source: Ref 5

The low molecular weight thermoplastic polyimide prepregs are processed in a manner similar to that of thermoset composite parts but at much higher pressures and temperatures. The prepregs can be layed up, bagged, and autoclave processed. The processing cycles are necessarily long, and high temperatures such as 650 to 700 °F or (345 to 370 °C) are required to build up the required final molecular weight and allow time for volatile removal. The processing is complicated by water, alcohol, and solvent evolution. These volatile by-products can cause voids in the final laminate; therefore, they are very difficult to process. After consolidation, they can be reheated and formed in a press; however, the viscosity remains high, and high pressures must be used to form even simple structural shapes. K-polymers, such as Avamid K-III), based on the polyamideimide family, are actually prepolymers with tack that first polymerize to a powdery solid, which allows removal of volatiles before finally melting and fusing. In addition, since many of them have a tendency to lightly crosslink (approximately 10 to 15 percent), their formability is much less than that of the true melt-fusible thermoplastics. As such, they are not true thermoplastics. Even this small amount of crosslinking makes them much more difficult to reprocess and thermally form. The crosslinking does, however, impart added solvent resistance. The remainder of this section will deal with true melt-fusible thermoplastics.

3.9.2 Thermoplastic Composite Product Forms

Thermoplastic composite materials can be supplied in a number of different product forms, several of which are shown in Fig. 3.30. Unidirectional tape, tow, and woven cloth prepregs are boardy and contain no tack. If the resin is amorphous (such as PEI), it can be dissolved in solvents and prepregged similarly to thermoset prepregs. A distinct disadvantage of this process is that the solvent must be removed prior to laminate consolidation. Even trace amounts of solvent have been shown to reduce the T_g and properties of the composite due to the plasticizing effect of the solvent. One investigation reported that T_g decreased from 400 to 250 °F (205 to 120 °C) as the residual solvent increased from zero to 3.7 percent.

Hot melt impregnation of thermoplastics, a requirement for the semicrystalline materials that will not dissolve in solvents, is much more difficult than the equivalent process for thermosets. Much higher temperatures are required to melt the high molecular weight resins, and even at their melt temperature their viscosities are orders of magnitude higher than those of thermoset resins. This makes uniform fiber impregnation

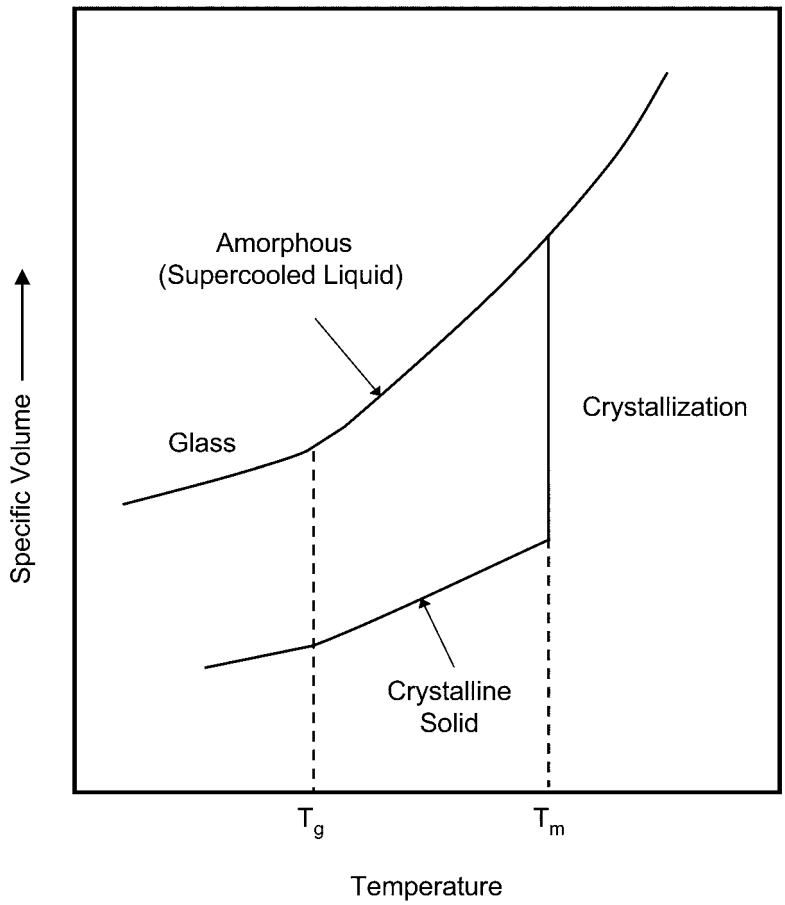


Fig. 3.29 Cooling behavior of amorphous and semicrystalline thermoplastics

very difficult, and those who have mastered the process consider it a closely guarded trade secret. References to flowing the resin through a series of porous heated spreader plates combined with nip rollers to push the resin into the fiber tows followed by an extrusion die are reported in the literature. The extrusion die produces shear thinning (in this case, reduces viscosity by several orders of magnitude) by forcing the resin through a heated die that creates large shear stresses. Hot melt prepregging with viscous polymers requires high pressures, slow speeds, and thin fiber beds. A well-impregnated hot melt tape usually contains resin-rich surface layers.

An alternative method developed for impregnating carbon tows is called *powder coating.* Here a fluidized bed is used to introduce powder onto the carbon fiber surface, which is then fused to the fibers in an oven. The powder is charged and fluidized, while the tow is spread and grounded in order to pick up the charged powder. Other processes, such as electrostatic dry powder and slurry coatings, have also been developed.

Comingled fiber prepreg is another method of making a drapable product form. Fine fibers of the thermoplastic resin are extruded and then comingled with the carbon fiber tows. Both the powder-coated and the comingled tows are then normally woven into a tackless but very drapable product form. It should be pointed out that the fiber distribution for powder-coated and comingled product forms will not be as uniform as the fiber distribution achievable by prepregging; therefore, it is difficult to achieve consistent fiber volume contents during consolidation. In addition, there is considerable bulk in these product forms. This bulk, combined with the extensive drapability, can also result in wrinkling and buckling of fibers during material placement and consolidation.

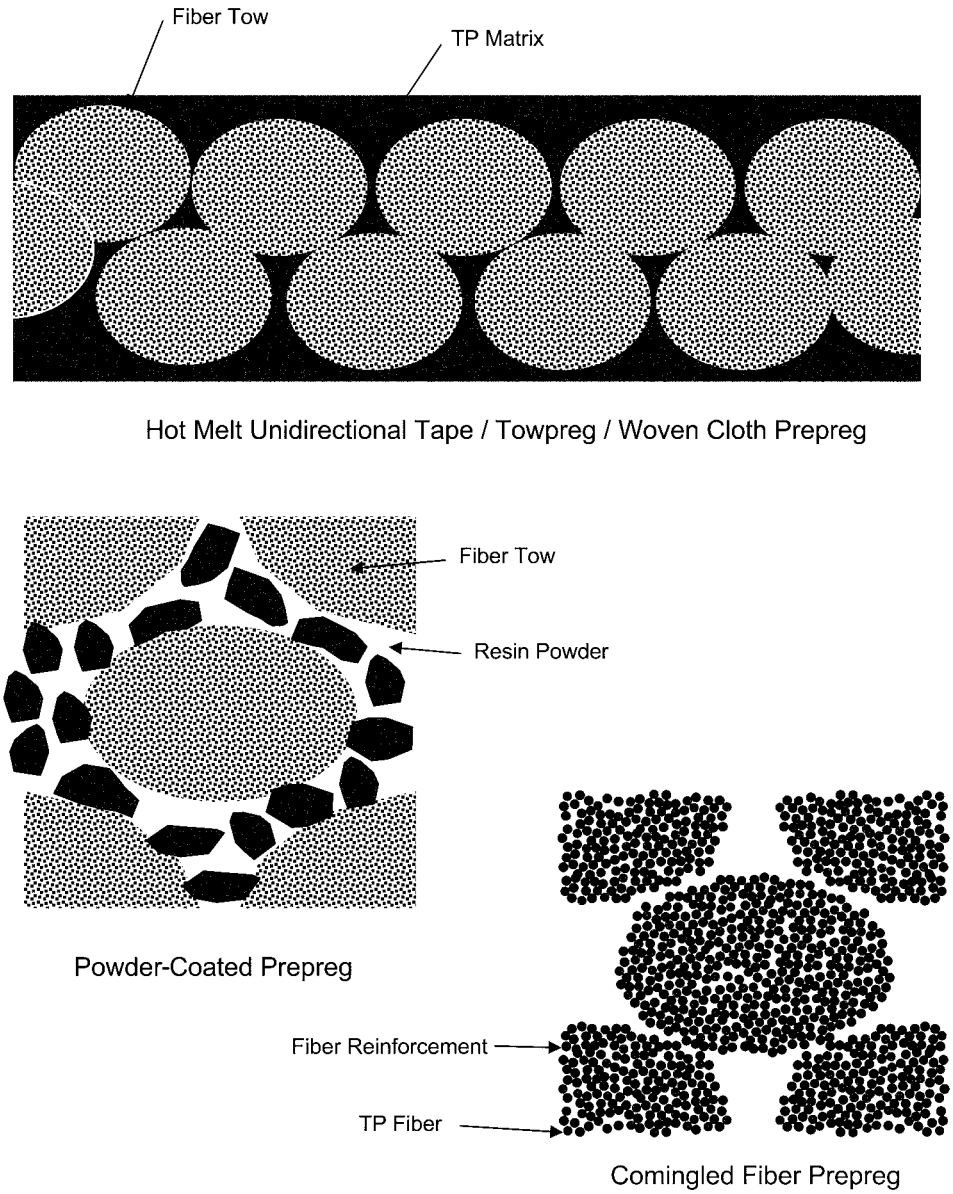


Fig. 3.30 Forms of thermoplastic composite prepreg

Thermoplastic consolidation occurs by a process called *autohesion*, as depicted in Fig. 3.31. When two interfaces come together, they must achieve intimate contact before the polymer chains can diffuse across the interface and obtain full consolidation. Due to the low flow and tow height nonuniformity of thermoplastic prepregs, the surfaces must be physically deformed under heat and pressure to provide the intimate contact required for chain migration at the ply interfaces. To obtain intimate contact and autohesion, the material must be heated above the T_g if it is amorphous, and above the T_m if it is semicrystalline. In general, higher pressures and higher temperatures lead to shorter consolidation times.

Autohesion is a diffusion-controlled process in which the polymer chains move across the interface and entangle with neighboring chains. As the contact time increases, the extent of polymer

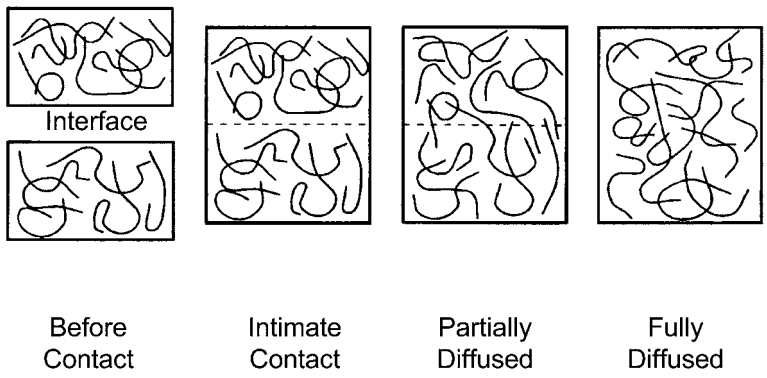


Fig. 3.31 Autohesion at thermoplastic interfaces

entanglement increases and results in the formation of a strong bond at the ply interfaces. Consolidation times are usually longer for amorphous thermoplastics since they do not melt and generally maintain higher viscosities at the processing temperature; however, shorter times can be used if higher pressures are employed. The time required for autohesion is directly proportional to the polymer viscosity; therefore, a certain amount of bulk consolidation must occur at the interfaces prior to the initiation of autohesion. Consolidation is also aided by resin flow due to the applied pressure that aids in ply contact and eventually leads to 100 percent autohesion. The process is essentially complete when the fiber bed is compressed to the point at which it reacts with the applied processing pressure.

Thermoplastic composites offer some definite advantages compared to thermoset composites; however, in spite of large investments over the last 25 years, very few continuous-fiber thermoplastic composites have made it into production applications. Compared to thermoset composites, thermoplastic composites offer the potential for short processing times, but their inherent characteristics have prevented them from replacing thermoset composites in the aerospace industry:

- High processing temperatures (500 to 800 °F or 260 to 425 °C) increase the cost of the prepreg and complicate the use of conventional processing equipment.
- The lack of tack and boardiness of the prepreg results in expensive manual handling operations.
- Thermoforming of continuous-fiber reinforced thermoplastics has proven to be much more difficult than anticipated due to the tendency of the fibers to wrinkle and buckle if not maintained under tension during the forming operation.
- The early claims of superior toughness and damage tolerance have largely been negated by the development of much tougher thermoset resins.
- Solvent and fluid resistance properties remain major barriers to the use of amorphous thermoplastic composites.

In the author's opinion, two criteria must be met to take advantage of continuous-fiber thermoplastic composites: (1) there must be a demand for a large quantity of parts and (2) the process must be automated to remove almost all manual operations. Unfortunately, neither of these criteria has been met in the aerospace industry, where lot sizes are small and production rates cannot justify the investment in highly sophisticated automated equipment. However, it is interesting and insightful that glass mat thermoplastics (GMTs) have made significant inroads in the automotive industry, where the demand for parts is large and the process has been almost totally automated.

3.10 Quality Control Methods

Composites are unlike metals in that their final properties are dependent upon chemical reactions. Since the fabricator cures the part, methods must be used to control fabrication, and physical, chemical, and thermal testing must be performed on the starting materials rather than on just the finished product. The quality of a composite part can be assured by either postfabrication testing of "tagalong" or "process control"

test specimens fabricated with the production hardware, using the same materials, or by being certain that the proper raw materials were used and processed correctly. In the early phases of integrating a new material into production, both approaches are usually used. The supplier will run a battery of physical, chemical, and mechanical property tests before shipping the material. When the fabricator receives the material, these tests are often repeated. During part fabrication, the same material that is used in the part will also be used to fabricate tagalong (or process control) specimens. After fabrication, the part is normally subjected to nondestructive testing and the process control specimens are destructively tested. As more confidence is gained in the material and processing, it is normal practice to reduce this rather expensive battery of testing. Frequently, the material supplier is given the responsibility for all testing of the raw material and supplies certification sheets to the user. As the fabricator gains more experience and confidence, it is normal practice to scale back on the number of in-process control specimens fabricated with the production part.

Physiochemical testing is a series of chemical, rheological, and thermal tests used to characterize both uncured resins and cured composites. These tests are useful in evaluating new resins, developing processing parameters, and ensuring the quality of incoming materials. The major factors that must be considered to ensure the uniformity of a resin include the types and purity of the ingredients, the concentration of the individual ingredients, and the homogeneity and advancement of the resin mix.

3.10.1 Chemical Testing

Chromatographic methods can be used to ensure that the correct ingredients are present in the resin in the prescribed ratios. These methods accomplish separation of the resin by the interaction of soluble resin components with a flowing liquid or mobile phase and a solid stationary phase. Frequently, they are used in conjunction with spectrographic methods to identify and quantify the specific components in the resin. High-performance liquid chromatography (HPLC) uses a mobile liquid phase and a solid stationary phase. A resin sample is dissolved in a suitable organic solvent, injected into the chromatograph, and then swept through a column packed with fine solid particles. A detection device senses the presence of each molecular fraction. The detector monitors the concentrations of the separated components, and its signal response, recorded as a function of the time after injection, provides a "fingerprint" of the resin's chemical composition. If the components are known and sufficiently well resolved, and if standards are available, then quantitative information can be obtained for the sample. A chromatograph of the epoxy resin system 3501-6 is shown in Fig. 3.32. Peak locations are associated with the chemical structure of the individual components, and the areas under the peaks are proportional to the amounts of each component. A subset of HPLC is gel permeation chromatography (GPC), in which the components are separated based on molecular size. In GPC, the components are separated by their permeation through a porous packing gel.

Infrared (IR) spectroscopy is based on molecular vibrations in which a continuous beam of electromagnetic radiation is passed through or reflected off the surface of the sample. Individual molecular bonds and bond groupings vibrate at characteristic frequencies and selectively absorb IR radiation at matching frequencies. The amount of radiation absorbed or passed through unchanged depends on the chemical composition of the sample, and the resultant curve is known as an *infrared spectrum*, as shown in Fig. 3.33 for 3501-6 epoxy resin. Another use of IR spectroscopy is for identifying the specific ingredients by comparing the sample with a computerized spectrum search. Computerized libraries of spectra for common materials exist for direct comparison and identification of the resin ingredients. Infrared spectroscopy is sensitive to changes in the dipole moments of vibrating groups of molecules, which yields useful information about the identity of resin components. It also provides a "fingerprint" of the resin composition and may be used with gases, liquids, or solids. Fourier transform infrared spectroscopy (FTIR) is a computer-assisted method in which Fourier transformation of the IR spectra is used to enhance the signal-to-noise ratio and provide improved spectra for interpretation. For metallic catalysts such a BF_3, atomic absorption is a useful test.

The equivalent weight or weight percent epoxide is a measure of the number of active sites available for crosslinking. Knowing the equivalent weight allows one to calculate the amount of curing agent required to fully cure the resin. Equivalent weight is usually determined by titration that utilizes a known concentration of one

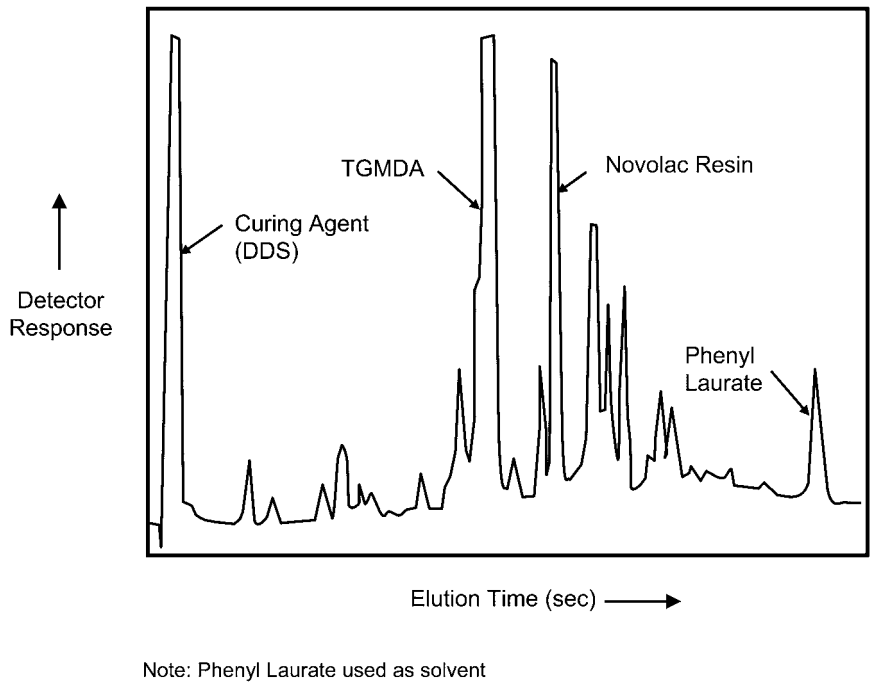


Fig. 3.32 HPLC Curve for 3501-6 epoxy resin. DDS, diaminodiphenyl sulfone; TGMDA, tetraglycidyl methylene dianiline. Source: Ref 6

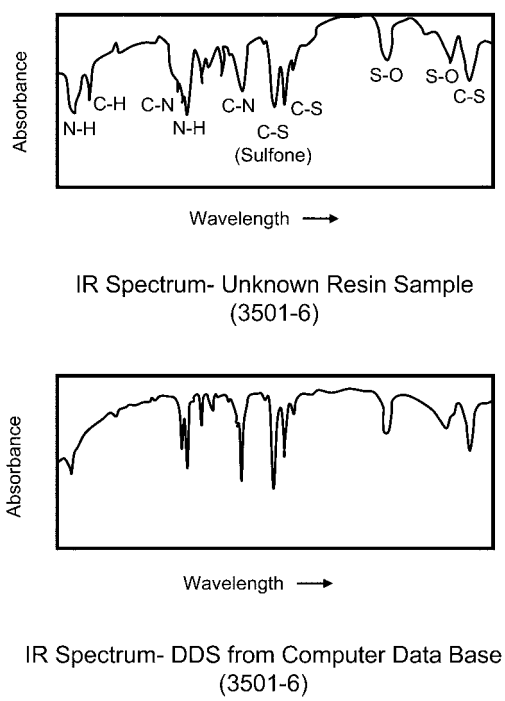


Fig. 3.33 IR identification of DDS curing agent. Source: Ref 7

substance to react with and detect the amount of reaction species in the unknown sample.

3.10.2 Rheological Testing

Rheology is the study of deformation and flow. It is frequently used to determine the flow (viscosity changes) of uncured resins. The viscosity of an uncured resin is usually determined by a parallel plate rheometer in which a small sample is placed between two oscillating parallel plates and then heated. During curing, the resin is converted from an uncrosslinked liquid or semisolid into a rigid crosslinked solid. As shown in the viscosity curves in Fig. 3.34, as heat is applied, the semisolid resin melts and flows. At this point in the cure process there are two competing forces: (1) as the temperature increases, the resin melts, the mobility of the molecules increases, and the viscosity falls; and (2) as the temperature increases, the molecules start to react and grow in size, leading to an increase in viscosity. On further heating, the crosslinking reactions cause the viscosity to rise rapidly, and eventually the resin gels and transforms from a liquid to a rubbery state. Gellation is the point in

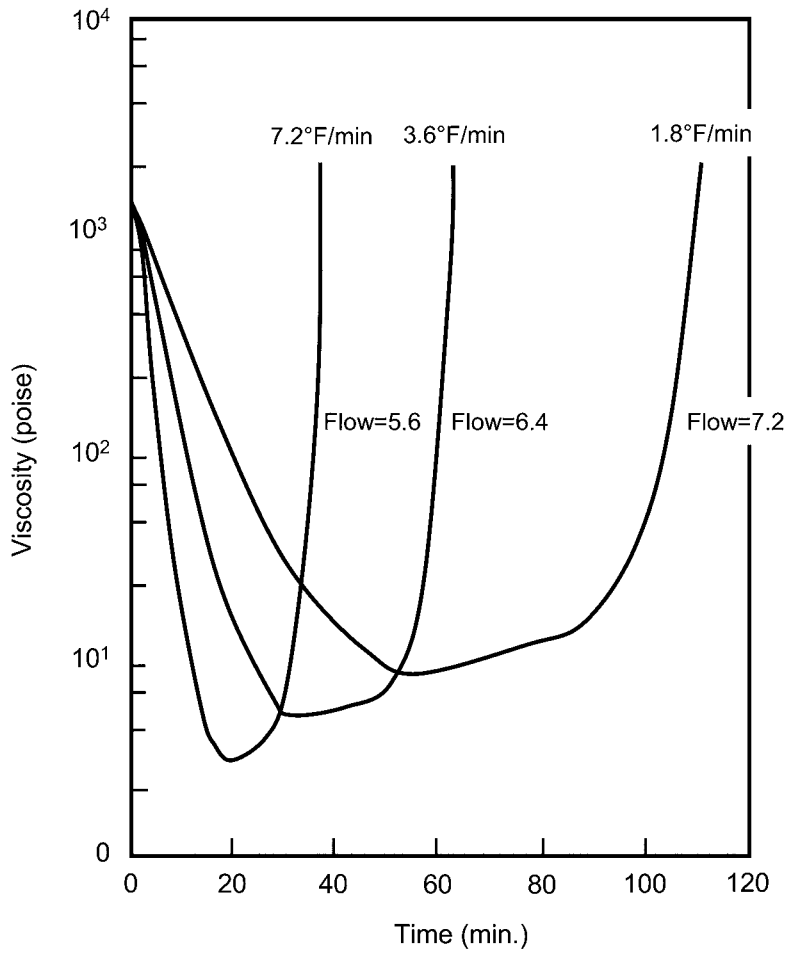


Fig. 3.34 Viscosity curves at three different heating rates

the cure process at which the reacting molecules have become so large that no further flow can take place. At gellation, the resin is normally about 58 to 62 percent crosslinked. The gel point is the point at which the viscous liquid becomes an elastic gel and the beginning of an infinite crosslinked network. Flow behavior affects the way in which the resin can be processed, and gellation marks the end of flow. Gellation is often arbitrarily taken as the point where the resin reaches a viscosity equal to 1000 poise. The resin is then held at the cure temperature, usually 250 to 350 °F or 120 to 175 °C, until the crosslinking reactions are completed and the resin is fully cured. Further heating above 480 °F (250 °C) results in resin degradation for a typical epoxy resin.

Rheology is a valuable tool in characterizing new resins and developing cure cycles. For example, note in Fig. 3.34 that if the same resin was heated at different heat-up rates, the sample heated at the fastest rate (7.2 °F/min or 4 °C/min) obtained the lowest viscosity and gelled in the shortest time, while the sample heated at the slowest rate (1.8 °F/min or 1 °C/min) had the highest minimum viscosity and took the longest time to gel. Since the sample with the slowest heat-up rate took a lot longer to gel, it remained at a low viscosity for a significantly longer time. To quantify viscosity behavior, a flow number was calculated for each viscosity curve where the flow number is defined as the reciprocal of viscosity (η) when integrated as a function of time between the starting time (t_0) and the time to gellation (t_{gel}):

$$\text{Flow Number} = \int_{t_0}^{t_{gel}} \frac{dt}{\eta} \qquad \text{(Eq 3.1)}$$

The larger amount of flow for the slowly heated sample would allow more time for resin flow and bleeding than the sample with the faster heat-up rate.

The chemical composition of the resin can also significantly affect viscosity. Viscosity curves for three different epoxy matrix resins are shown in Fig. 3.35. All three resins contain TGMDA as the main epoxy and DDS as the curing agent. The resin that also contains the BF_3 catalyst reacts more quickly than the unmodified resin, resulting in higher minimum viscosity and less total flow. When tougheners are added to a resin, there is normally a significant increase in viscosity. However, since almost all of these newer systems are net resin content prepregs, less resin flow is needed, as there is no bleeding of excess resin during the cure.

3.10.3 Thermal Analysis

Thermal analysis is the general term given to a group of analytical techniques that measure the properties of a material as it is heated or cooled. Techniques such as differential scanning calorimetry, thermal mechanical analysis, and thermogravimetric analysis are used to determine the degree of cure, the rates of cure, heats of reactions, melting points of thermoplastics, and thermal stability.

Differential scanning calorimetry (DSC) is the most widely used method for obtaining the degree of cure and reaction rate. It is based on the measurement of the differential voltage, converted into heat flow in a calorimeter, necessary to obtain thermal equilibrium between the resin sample and an inert reference. A small sample of

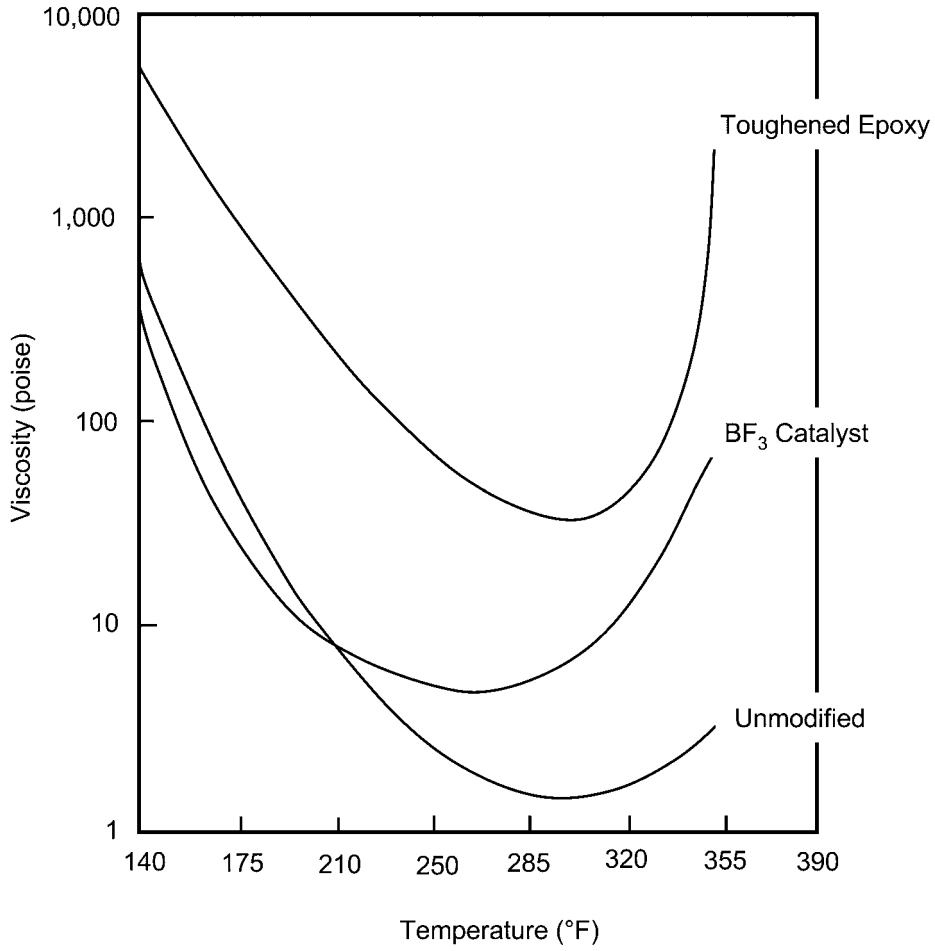


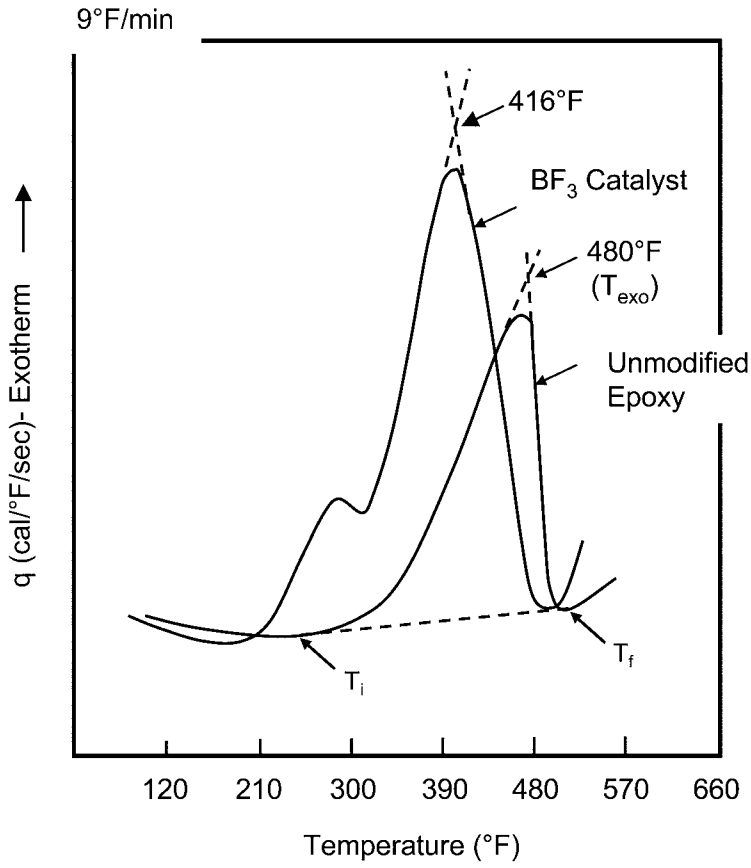
Fig. 3.35 Viscosity comparison of toughened and untoughened epoxies

resin is placed in a sealed packet and then inserted into the calorimeter heating chamber along with a known standard of material. The temperature is increased and the amount of heat given off (exothermic) or taken in (endothermic) is compared to a known standard. Heating modes used to run DSC can be either isothermal or a dynamic. In the isothermal mode, it measures the thermal changes as a function of time at a constant temperature. In the dynamic mode, it measures the thermal changes as a function of temperature at predetermined heating rate. A typical dynamic DSC scan is shown in Fig. 3.36. The two resins shown in this scan are the same unmodified (TGMDA + DDS) and BF_3-added (TGMDA + DDS + BF_3) samples shown in the viscosity curves of Fig. 3.35. The initial exotherm peak on the resin with the catalyst is due to the BF_3 addition, which is only added at 1.1 percent. Similar to the indication on the viscosity curves, the catalyst addition causes the resin to react faster and reach its peak exotherm (414 °F or 215 °C) at a lower temperature.

Critical points on the curve are:

- T_i, the initiation or onset temperature of the reaction indicating the beginning of polymerization
- T_{exo}, the major exotherm peak temperature
- T_f, the final temperature, indicating the end of heat generation and the completion of cure

As the resin cures, the T_g rises until it becomes fixed. The extent of cure at any given time can be defined as the degree of cure α. Since cure of



T_i- Onset Temperature or Beginning of Polymerization
T_{exo}- Peak Exotherm Peak
T_f- Final Cure

Fig. 3.36 DSC scans for epoxy matrix resins

thermoset resins is an exothermic process, α can be related to the heat released during the cure reaction:

$$\alpha = \frac{\Delta H_t}{\Delta H_R} \qquad \text{(Eq 3.2)}$$

where: ΔH_t = heat of reaction at time t
ΔH_R = total heat of reaction

For a 100 percent cure, the degree of cure $\alpha = 1$. The degree of cure progression during a typical cure cycle is depicted in Fig. 3.37. During the initial portion of the cycle when the resin melts and reaches its minimum viscosity, the rate of degree of cure is low but then rises as the resin gels and starts to crosslink. It eventually slows down with longer and longer times, producing only slight increases in the degree of cure. Composite matrix systems usually attain a degree of cure of 90 to 95 percent. Higher degrees of cure take excessively long times and may cause the resin to become too brittle.

As previously stated, DSC can be conducted isothermally or dynamically. Two methods are commonly used for isothermal DSC measurements. In the first method, the resin sample is placed in a previously heated calorimeter, or in an unheated calorimeter, and the temperature is raised as quickly as possible to the cure temperature. In the second method, the resin sample is cured for various times until no additional curing can be detected and the sample is then scanned at a heating rate of 2 to 20 °C/min to measure the residual heat of reaction (ΔH_{res}). The degree of cure can be calculated from:

$$\alpha = \frac{\Delta H_R - \Delta H_{res}}{\Delta H_R} \qquad \text{(Eq 3.3)}$$

DSC can also be used with thermoplastic resins to measure the melting point and determine whether a semicrystalline thermoplastic is in an amorphous or a semicrystalline state. The differences between an amorphous and a semicrystalline C/PEEK laminate are shown in the DSC scans in Fig. 3.38.

Thermogravimetric analysis (TGA) measures the weight gain or loss of a material as a function of temperature as it is heated isothermally or dynamically. The TGA unit is a sensitive microbalance within a precision-controlled furnace. As the material is heated, various changes in weight are recorded as a function of either temperature (isothermal) or time (dynamic). Thermogravimetric analysis is used to measure the amount of moisture which will evolve at 212 °F (100 °C), the total volatiles in the sample, and the temperature and rate of thermal decomposition. It's often used in conjunction with mass spectroscopy so that as the gases evolve from the sample, they can be collected and analyzed for their composition. One of the most important uses of TGA is in determining the thermal degradation profile of a composite as it is heated to higher and higher temperatures.

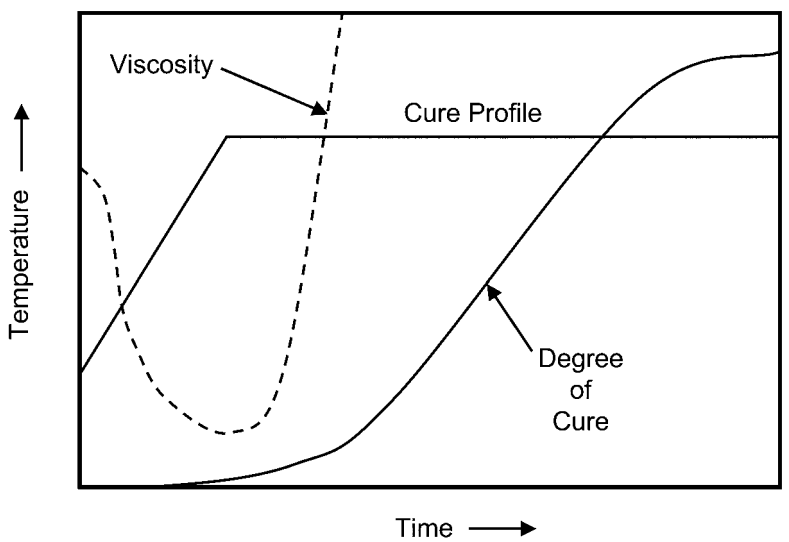


Fig. 3.37 Degree of cure progression

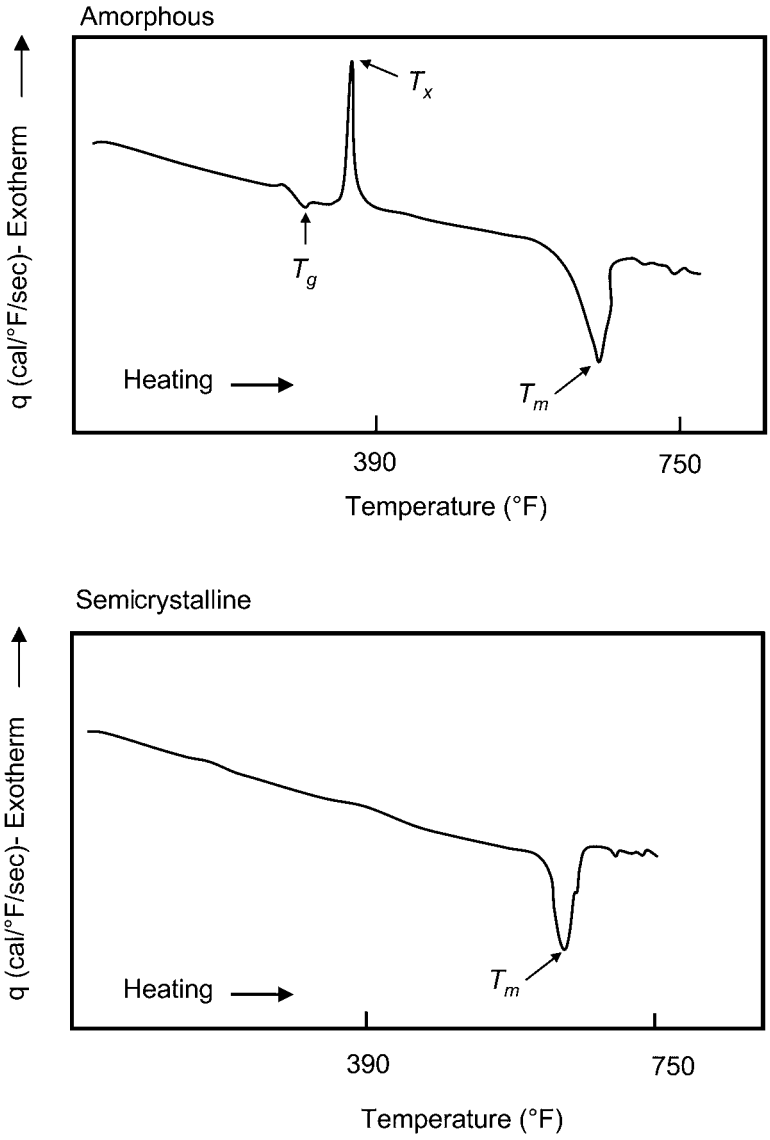


Fig. 3.38 DSC Scans for C/PEEK. Source: Ref 8

3.10.4 Glass Transition Temperature

As explained in Chapter 1 "Introduction to Composite Materials", the cured glass transition temperature (T_g) of a polymeric material is the temperature at which it changes from a rigid glassy solid into a softer, semiflexible material. At this point, the polymer structure is still intact but the crosslinks are no longer locked in position. The T_g determines the upper use temperature for a composite or an adhesive, above which the material will exhibit significantly reduced mechanical properties. Since most thermoset polymers will absorb moisture that severely depresses the T_g, the actual service temperature should be about 50 °F (30 °C) lower than the wet or saturated T_g. The cured glass transition temperature can be determined by several methods, such as TMA, DSC, and DMA, all of which give different results because each measures a different property of the resin. Idealized schematic outputs from these three methods are shown in Fig. 3.39.

Thermal mechanical analysis (TMA) measures the thermal expansion of a sample as it is

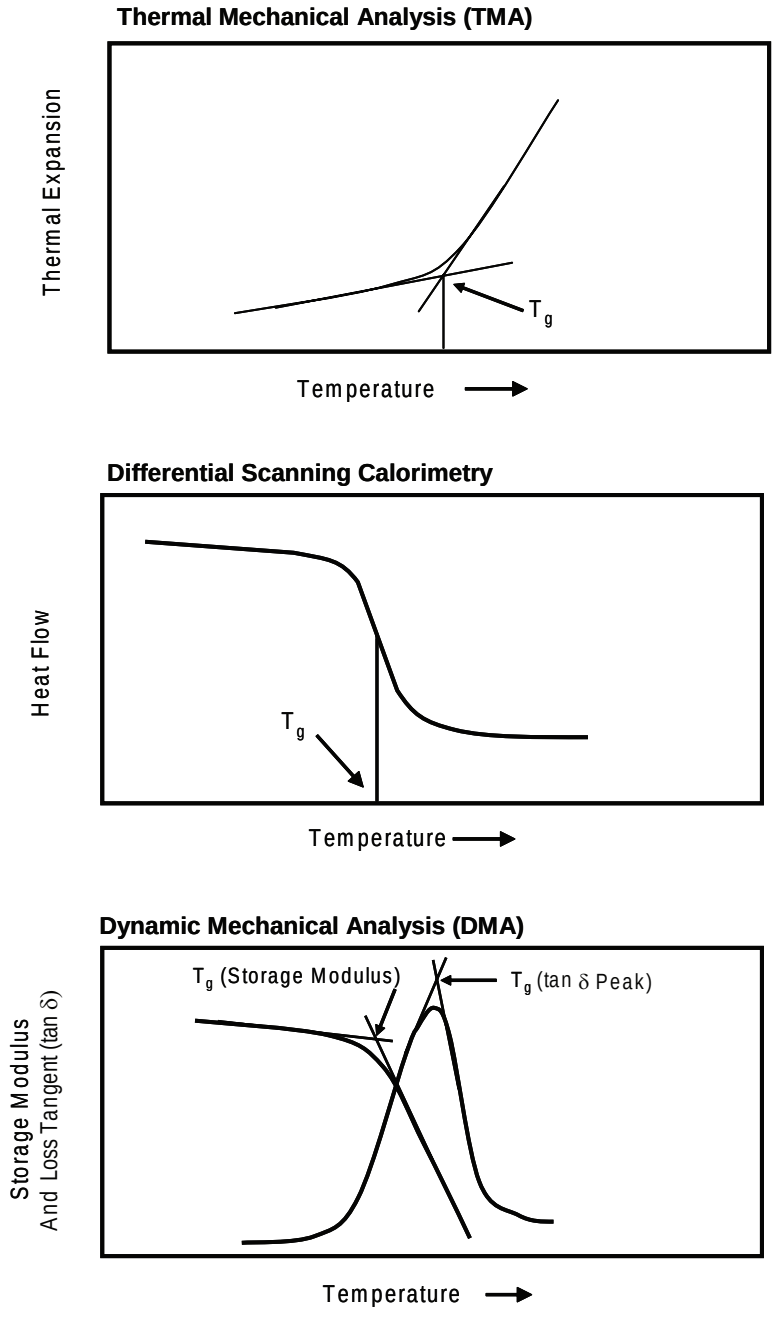


Fig. 3.39 Schematics T_g curves

heated. The slope of the thermal expansion-versus-temperature curve changes at the T_g due to changes in the coefficient of thermal expansion as it passes through the T_g. Materials below their T_g expand linearly at a lower rate than above their T_g, where the material is more mobile; the molecules are moving more rapidly, and as a result, the material's expansion rate increases dramatically. Cured thermosets usually exhibit two linear regions. The first is associated

with the glassy state and is followed by a change at the T_g to a second linear region of higher slope associated with the rubbery state.

The T_g can also be measured by DSC since the glass transition is an exothermic reaction. Although DSC is an accepted method of determining T_g, it is sometimes difficult to accurately determine the T_g from the curve, especially for high crosslinked resin systems. An advantage of DSC is that a small sample size (25 mg) can be used to determine the T_g.

Dynamic mechanical analysis (DMA) measures the ability of a material to store and dissipate mechanical energy upon deformation. Therefore, DMA is a mechanical measure of the T_g in which a cured sample is loaded under a sinusoidal stress and the displacement is measured. The T_g is the point where the storage modulus (G' or E') or stiffness drops by several orders of magnitude. The loss modulus (G'' or E'') is usually associated with the viscosity or toughness of the material. The specimen may be loaded in either torsion or flexure. In a typical DMA test, a small bar of cured composite is either twisted (torsion) or flexed (tension) while it is being heated. Two properties are normally reported: (1) the torsional (G') or bending (E') storage modulus and (2) the loss tangent (tan δ). As the material nears its T_g, it loses stiffness and G' (or E') drops rapidly with increasing temperature, as shown in Fig. 3.39. The loss tangent is a measure of the energy stored in the polymer's structure as a result of its viscoelastic behavior. This stored energy rises to a sharp peak and then drops rapidly. The peak in the tan δ curve is often reported as the glass transition temperature, but this gives artificially high values. A more realistic T_g is the intercept of the two tangent lines on the storage modulus curve because this represents the point at which the composite starts exhibiting a significant loss in mechanical stiffness. The complex modulus (G^*), the storage modulus (G'), the loss modulus (G''), and the loss tangent (tan δ) are mathematically related by the following equations:

$$G^* = G' + G''$$
$$\text{Tan } \delta = G''/G' \qquad \text{(Eq 3.4)}$$

3.11 Summary

In general, the specific resin chemistries and their formulation practices are closely held trade secrets of the material suppliers. However, these suppliers will work with their customers to select the right material system for the required application and will help to develop the composite characterization methods and processing cycles. It is important to seek their help early and often when implementing any new material system. Since uncured resin systems can contain materials that are potentially hazardous to the health and safety of the workers, it is again important to coordinate with the material supplier and closely examine the Material Safety Data Sheet (MSDS) for any new material.

REFERENCES

1. R.B. Prime, Chapter 5, *Thermal Characterization of Polymeric Materials*, E.A. Turi, Ed., Academic Press, 1981
2. SP Systems, "Guide to Composites"
3. M.I. Rommel, A.S. Postyn, and T.A. Dyer, Accelerating Factors in Galvanically Induced Polyimide Degradation, *SAMPE J.*, Vol 30 (No. 2), Mar/Apr 1994, p 10–15
4. G. Di Pasquale, O. Motta, A. Recca, J.T. Carter, P.T. McGrail, and D. Acierno, New High-Performance Thermoplastic Toughened Epoxy Thermosets, *Polymer*, Vol 38 (No. 17), 1997, p 4345–4348
5. B.T. Astrom, *Manufacturing of Polymer Composites*, Chapman & Hall, 1997
6. T.A. Sewell, Quality Assurance of Graphite/Epoxy by High-Performance Liquid Chromatography, *Composite Materials: Quality Assurance and Processing*, ASTM STP 797, 1983, p 3–14
7. J.F. Carpenter, Assessment of Composite Starting Materials: Physiochemical Quality Control of Prepregs, *AIAA/ASME Symposium on Aircraft Composites: The Emerging Methodology for Structural Assurance*, San Diego, CA, 24–25 March 1977
8. F.N. Cogswell, *Thermoplastic Aromatic Polymer Composites*, Butterworth-Heinemann Ltd., 1992

SELECTED REFERENCES

- G.R. Almen, R.M. Byrens, P.D. MacKenzie, R.K. Maskell, P.T. McGrail, and M.S. Sefton, 977—A Family of New Toughened Epoxy Matrices, *34th International SAMPE Symposium*; Reno, NV; 8–11 May 1989, p 259–270

- A. Bottcher and L.A. Pilato, Phenolic Resins for FRP Systems, *SAMPE J.*, Vol 33 (No. 3), May/June 1997, p 35–40
- V.M.A. Calado and S.G. Advani, Thermoset Resin Cure Kinetics and Rheology, *Processing of Composites*, Hanser, 2001, p 32–107
- J.F. Carpenter, Physiochemical Testing of Altered Composition 3501-6 Epoxy Resin, *24th National SAMPE Symposium*, San Francisco, CA, 8–9 May 1979
- J.F. Carpenter, "Processing Science for AS/3501-6 Carbon/Epoxy Composites," Technical Report N00019-81-C-0184, Naval Air Systems Command, 1983
- J.M. Criss, C.P. Arendt, J.W. Connell, J.G. Smith, and P.M. Hergenrother, Resin Transfer Molding and Resin Infusion Fabrication of High-Temperature Composites, *SAMPE J.*, Vol 36 (No. 3), May/June 2000, p 31–41
- H.H. Gibbs, Processing Studies on K-Polymer Composite Materials, *30th National SAMPE Symposium*, 1985, p 1585–1601
- H.J. Harrington, Phenolics, *Engineered Materials Handbook*, Vol. 2: *Engineering Plastics*, ASM International Inc., 1988, p 242–245
- P.M. Hergenrother, Development of Composites, Adhesives and Sealants for High-Speed Commercial Airplanes, *SAMPE J.*, Vol 36 (No. 1), Jan/Feb 2000, p 30–41
- M.L. Huang and J.G. Williams, Mechanisms of Solidification of Epoxy-Amine Resins During Cure, *Macromolecules*, Vol 27, 1994, p 7423–7428
- B.Z. Jang, Fibers and Matrix Resins, *Advanced Polymer Composites: Principles and Applications*, ASM International Inc., 1994, p 24
- D.C. Leach, F.N. Cogswell, and E. Nield, High Temperature Performance of Thermoplastic Aromatic Polymer Composites, *31st National SAMPE Symposium*, 1986, p 434–448
- D. Lesser and B. Banister, Amorphous Thermoplastic Matrix Composites for New Applications, *21st SAMPE Technical Conference*, 25–28 Sept 1989, p 507–513
- V.P. McConnell, Tough Promises from Cyanate Esters, *Adv. Compos.*, May/June 1992, p 28–37
- J.D. Muzzy and J.S. Colton, The Processing Science of Thermoplastic Composites, *Advanced Composites Manufacturing*, John Wiley & Sons, Inc., 1997
- J. Muzzy, L. Norpoth, and B. Varughese, Characterization of Thermoplastic Composites for Processing, *SAMPE J.*, Vol 25 (No. 1), Jan/Feb 1989, p 23–29
- J.W. Park and S.C. Kim, Phase Separation and Morphology Development During Cure of Toughened Thermosets, *Processing of Composites*, Hanser, 2000, p 108–136
- R.H. Prater, Thermosetting Polyimides: A Review, *SAMPE J.*, Vol 30 (No. 5), Sept/Oct 1994, p 29–38
- S. Robitaile, Cyanate Ester Resins, *ASM Handbook*, Vol. 2, *Composites*, ASM International Inc., 2001, p 126–131
- S.L. Rosen, *Fundamental Principles of Polymeric Materials*, John Wiley & Sons, 1971
- D.A. Scola, Polyimide Resins, *ASM Handbook*, Vol 21, *Composites*, ASM International, Inc., 2001, p. 107
- W. Smith, Chapter 3, Resin Systems, *Processing and Fabrication Technology*, Vol. 3, *Delaware Composites Design Encyclopedia*, Technomic Publishing Company, Inc., 1990, p 15–86
- H. Stenzenberger, Bismaleimide Resins, *ASM Handbook*, Vol 21, *Composites*, ASM International Inc., 2001, p. 97
- A.B. Strong, *Fundamentals of Composite Manufacturing: Materials, Methods, and Applications*, Society of Manufacturing Engineers, 1989
- A.B. Strong, *High Performance and Engineering Thermoplastic Composites*, Technomic Publishing Co., Inc., 1993
- Vantico, Inc. Data Sheets for MY-720 and MY-721

Copyright © 2010, ASM International®
All rights reserved.
www.asminternational.org

CHAPTER 4

Fabrication Tooling

TOOLING FOR COMPOSITE FABRICATION is a major up-front nonrecurring cost. It is not unusual for a large bond tool to cost as much as $500,000 to $1,000,000. Unfortunately, if the tooling is not designed and fabricated correctly, it can become a recurring headache, requiring continual maintenance and modifications and, in the worst-case scenario, replacement. This chapter will cover some of the basics of bond tools for composites, primarily for autoclave curing. As other composite manufacturing processes are introduced in later chapters, additional tooling information specific to those processes will be presented.

Tooling for composite structures is a complex discipline in its own right, based largely on years of experience. It should be pointed out that there is no single correct way to tool a part. There are usually several different approaches that will work, with the final decision based largely on knowledge of what has and has not worked in the past. The purpose of the bond tool is to transfer the autoclave heat and pressure during cure to yield a dimensionally accurate part, and there are a number of alternatives that will usually work. Although this chapter provides an introduction to tooling, the interested reader is referred to Ref 1 for much more comprehensive coverage. A shorter review of some of the key principles of Ref 1 can be found in Ref 2 to 4.

4.1 General Considerations

There are many requirements a tool designer must consider when selecting a tooling material and a fabrication process for a given application; however, the number of parts to be made on the tool and the part configuration are often the overriding factors in the selection process. For instance, it would not make good economic sense to build an inexpensive prototype tool that would only last for several parts when the application calls for a long production run. Part configuration or complexity will also drive the tooling decision process. For example, while welded steel tools are often used for large wing skins, it would not be cost effective to use steel for a highly contoured fuselage section due to the high fabrication cost and complexity.

One of the first tooling choices that must be made is which side of the part should be tooled—the inside or outside surface, as shown in Fig. 4.1. Tooling a skin to the outside or outer moldline (OML) surface provides the opportunity to produce a part with an extremely smooth outside surface finish. However, if the part is going to be assembled to substructure, with mechanical fasteners for example, tooling to the inside or inner moldline (IML) surface will provide a better fit, with fewer gaps and less shimming required. An example is the wing skin shown in Fig. 4.1, which was tooled to the IML surface to ensure the best possible fit to the substructure during assembly. A caul plate is used on the bag side during cure to provide an acceptable OML aerodynamic surface finish. The part shown in Fig. 4.1 contains severe thickness transitions on the IML surface. If the part were constant in thickness or contained little thickness variation, then it might have been more sensible to tool it to the OML surface. Ease of part fabrication is another tooling concern. Depending on part geometry, it may be easier to lay up the plies on a particular surface. In general, it is normally easier to collate plies on a male tool rather than down inside a female tool cavity.

Selection of the material used to make the tool is another important consideration. Several key properties of various tooling materials are

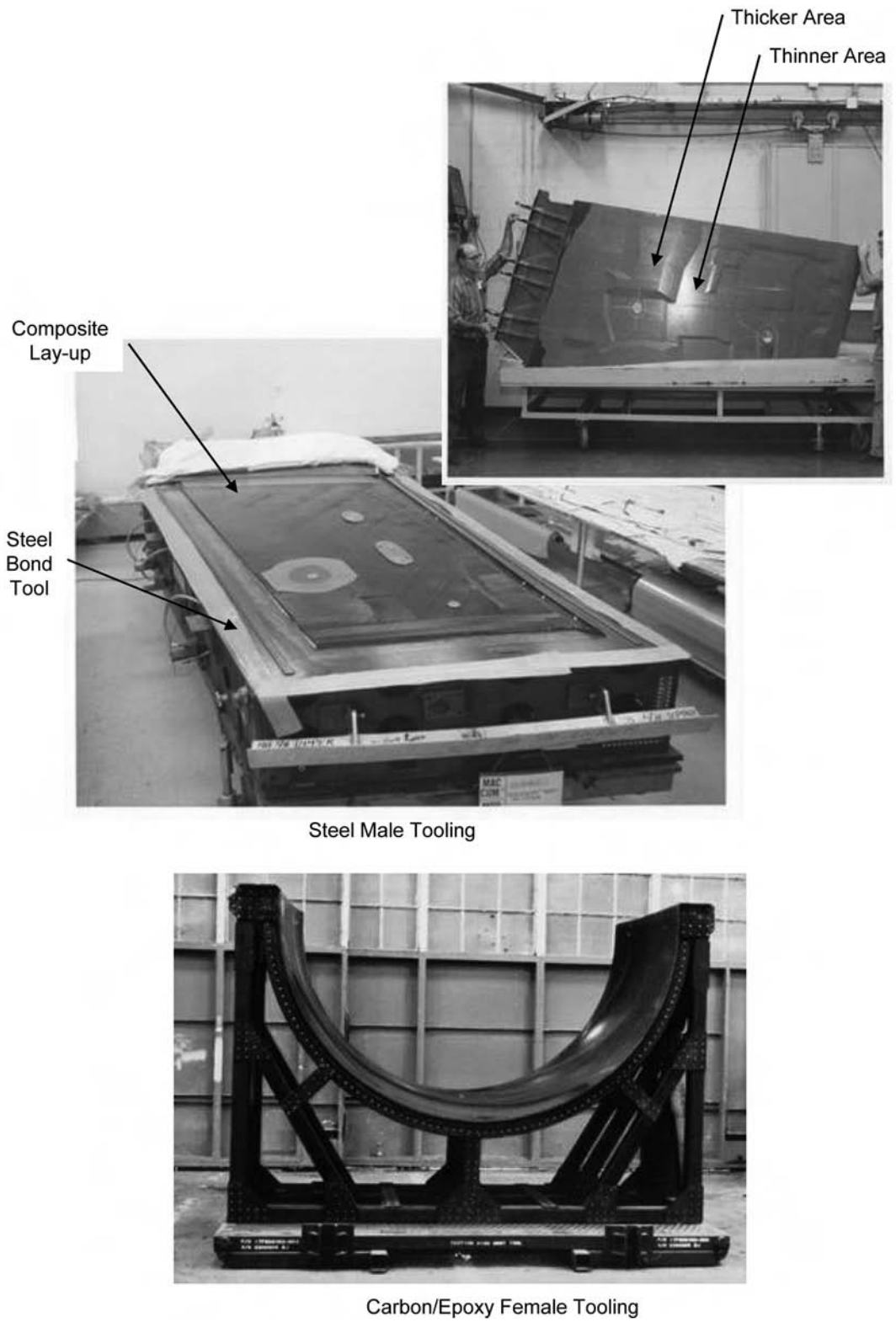


Fig. 4.1 Male and female tooling. Source: The Boeing Company

presented in Table 4.1. Normally, reinforced polymers can be used for low to intermediate temperatures, metals for low to high temperatures, and monolithic graphite or ceramics for very high temperatures. Tools for autoclave curing traditionally have been made of either steel or aluminum. Electroformed nickel became popular in the early 1980s, followed by the introduction of carbon/epoxy and carbon/bismaleimide composite tools in the mid-1980s. Finally, in the early 1990s, a series of low-expansion iron-nickel alloys was introduced under the trade names Invar and Nilo.

Steel is a fairly inexpensive material with exceptional durability. It is readily castable and weldable and has been known to withstand more than 1500 autoclave cure cycles and still be capable of making good parts. However, steel is heavy, has a higher coefficient of thermal expansion (CTE) than the carbon/epoxy parts usually built on the tool, and for large, massive tooling it can have slow heat-up rates in an autoclave. When a steel tool fails in service, it is usually due to a cracked weldment.

Aluminum, by contrast, is much lighter and has a much higher coefficient of thermal conductivity and and a much higher CTE. It is also much easier to machine than steel, but it is more difficult to produce pressure tight castings and weldments. The two biggest drawbacks of aluminum are that (1) it is a soft material and thus rather susceptible to scratches, nicks, and dents; and (2) it has a very high CTE. Aluminum tools are frequently hard anodized to improve durability. However, hard anodize coatings tend to spall and flake off as the aluminum temper ages during multiple thermal cycles. Due to its light weight and ease of machinability, aluminum is often used for what are called *form block* tools. As shown in Fig. 4.2, a number of aluminum form block tools can be placed on a large, flat aluminum project plate. This plate is then covered with a single vacuum bag for cure, a considerable cost savings compared to bagging each individual part. Another application for aluminum tools is matched-die tooling, where all surfaces are tooled, as shown for the spar in Fig. 4.3. An advantage of aluminum for matched-die tools is that the aluminum will shrink away from the part during cool-down, making part removal much easier.

Electroformed nickel has the advantage that it can be made into complex contours and does not require a thick faceplate. When backed with an open tubular-type substructure, this kind of tool has excellent heat-up rates in an autoclave. However, to make an electroformed nickel tool, a mandrel must be fabricated to the exact contour of the final tool. The mandrel is then placed in a bath for the electroplating operation.

Carbon/epoxy or glass/epoxy tools (Fig. 4.1) also require a master or mandrel for lay-up during tool fabrication. A distinct advantage of carbon/epoxy tools is that their CTE can be tailored to match that of the carbon/epoxy parts they build. In addition, composite tools are relatively light and exhibit good heat-up rates during autoclave curing, and a single master can be used to fabricate duplicate tools. On the downside, there has been a lot of negative experience with composite tools that are subject to 350 ºF (175 ºC) autoclave cure cycles: The matrix has a tendency to crack, and with repeated thermal cycles it can develop leaks. Another consideration when specifying composite tools is that the surface is somewhat soft and easily scratched. If plies are cut directly on the tool, it is necessary to place a metal shim between the ply and the tool to

Table 4.1 Properties of typical tooling materials

Material	Max service temp., °F	Coefficient of thermal expansion $\times 10^{-6}$/°F	Density, lb/in.^{3}	Thermal conductivity, Btu/h · ft · °F
Steel	1500	6.3–7.3	0.29	30
Aluminum	500	12.5–13.5	0.10	104–116
Electroformed nickel	550	7.4–7.5	0.32	42–45
Invar/Nilo	1500	0.8–2.9	0.29	6–9
Carbon/epoxy 350 °F	350	2.0–5.0	0.058	2–3.5
Carbon/epoxy RT/350 °F	350	2.0–5.0	0.058	2–3.5
Glass/epoxy 350 °F	350	8.0–11.0	0.067	1.8–2.5
Glass/epoxy RT/350 °F	350	8.0–11.0	0.067	1.8–2.5
Monolithic graphite	800	1.0–2.0	0.060	13–18
Mass cast ceramic	1650	0.40–0.45	0.093	0.5
Silicone	550	45–200	0.046	0.1
Isobutyl rubber	350	≈ 90	0.040	0.1
Fluoroelastomer	450	≈ 80–90	0.065	0.1

Note: For reference only. Check with material supplier for exact values.

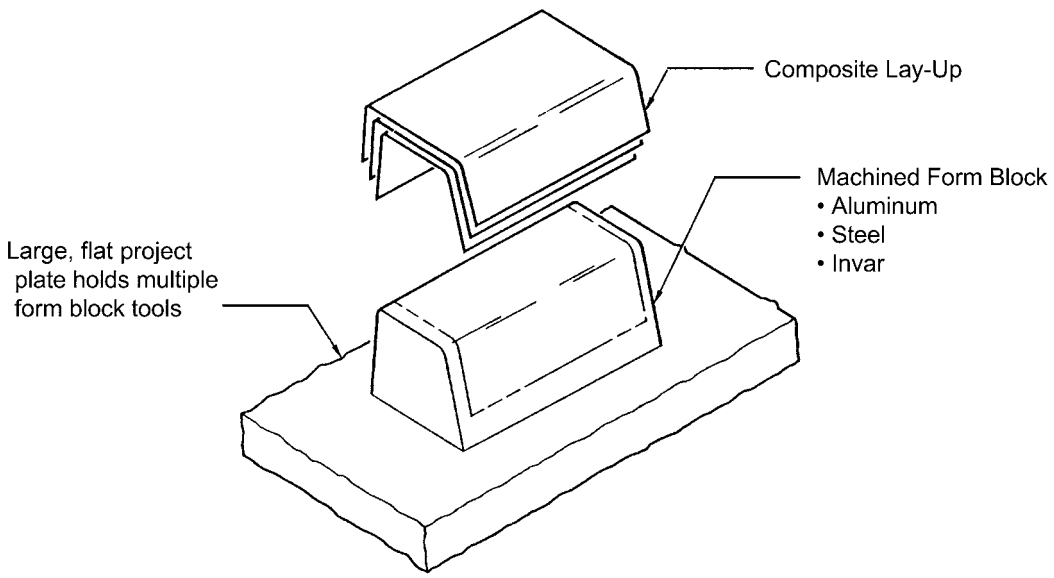


Fig. 4.2 Typical form block tooling

prevent scouring of the tool surface. In general, this is a bad practice since it increases the chance of the shim being left in the lay-up through cure, producing a possible repair or scrap condition. An additional consideration is that composite tools will absorb moisture if not in continual use. It may be necessary to dry tools slowly in an oven after prolonged storage to allow the moisture to diffuse out. A moisture-saturated tool placed directly in an autoclave and heated to 350 °F (175 ºC) could very easily develop blisters and internal delaminations due to the absorbed moisture.

Invar and the Nilo series of alloys were introduced in the early 1990s as the answer for composite tooling. Being low-expansion alloys, they very closely match the CTE of the carbon/epoxy parts. Their biggest disadvantages are high cost and slow heat-up rates. The material itself is very expensive, and it is even more difficult to work with than steel. It can be cast, machined, and welded. It is used for premium tooling applications such as wing skins.

4.2 Thermal Management

Since many common tooling materials, such as aluminum and steel, expand at greater rates than the carbon/epoxy part being cured on them, it is necessary to correct their size or compensate for the differences in thermal expansion. As the tool heats up during cure, it grows or expands more than the composite laminate. During cool-down, the tool contracts more than the cured laminate. If not handled correctly, both of these conditions can cause problems ranging from incorrect part size to cracked and damaged laminates. Thermal expansion is normally handled by shrinking the tool at room temperature using the calculation method shown in Fig. 4.4. For example, an aluminum tool producing a part 120.0 in. (3.05 m) in length might actually be made as 119.7 in. (3.04 m) long, assuming that it will be cured at 350 °F (175 ºC).

Another correction required for tooling for parts with geometric complexity is spring-back. When sheet metal is formed at room temperature, it normally springs back, or opens up somewhat, after forming. To correct for spring-back, sheet metal parts are overformed. The opposite phenomenon occurs in composite parts: They tend to spring in, or close up, during the cure process. Therefore, it is necessary to compensate for angled parts, as shown in Fig. 4.5. The degree of compensation required is somewhat dependent on the actual lay-up orientation and thickness of the laminate. A great deal of progress has been made in calculating the degree of spring-in using finite element analysis, but it still usually requires some experimental data for the particular material system, cure conditions, orientation, and thickness to establish tool design guidelines.

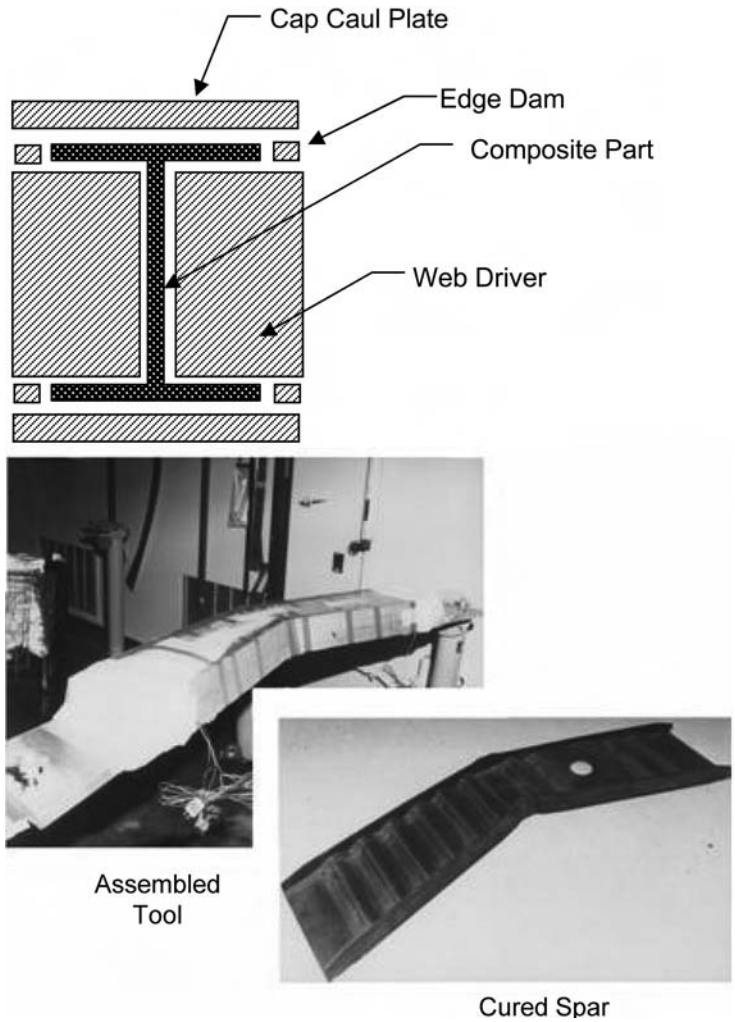


Fig. 4.3 Example of a matched-die aluminum tool. Source: The Boeing Company

Cool-down from cure can also cause problems because now the tool shrinks or contracts at a faster rate than the part. Several potential problem areas are illustrated in Fig. 4.6. For a tooling material with a large CTE such as aluminum, the tool can actually bind the part, causing ply cracking or delaminations. For skins and other parts, Teflon shear pins are often used to prevent damage. It is possible to hard pin a tooling detail at one or possibly two locations on the bond tool, but the detail must be allowed to contract freely and separate from the bond tool upon cooling. Another example is the draft that is needed in a tool pocket to allow the part to be pushed out from the pocket during cool-down, avoiding the possibility of ply cracking.

Unless the tool is a form block tool that can be placed on a project plate, it generally requires a substructure to support the faceplate. Two examples are shown in Fig. 4.7. The design of the substructure is important because it can affect the gas flow to the tool during autoclave curing. In general, the more "open" the substructure, the better the gas flow and the faster the heat-up rate. In one study (Ref 5), three different tool designs were compared for their heat-up rates during autoclave processing. The designs, shown in Fig. 4.8, consisted of a steel faceplate with a welded eggcrate substructure, a numerical controlled (NC) machined aluminum form block tool placed on an aluminum project plate, and an electroformed nickel tool with an open tubular substructure.

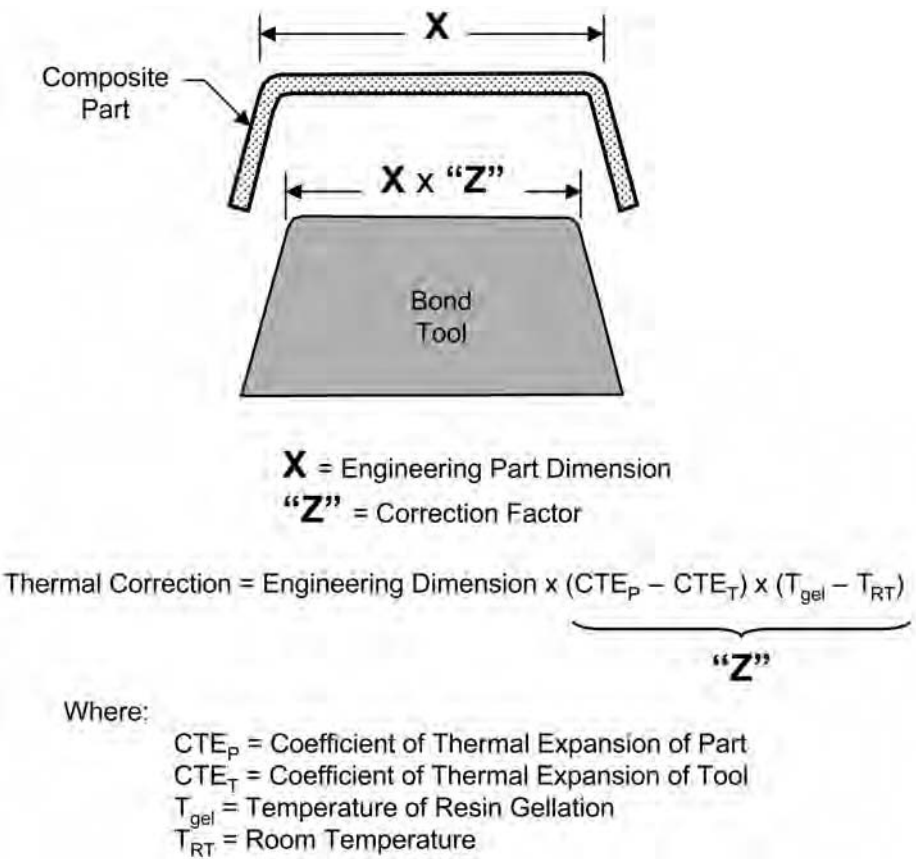


Fig. 4.4 Thermal expansion correction for tooling

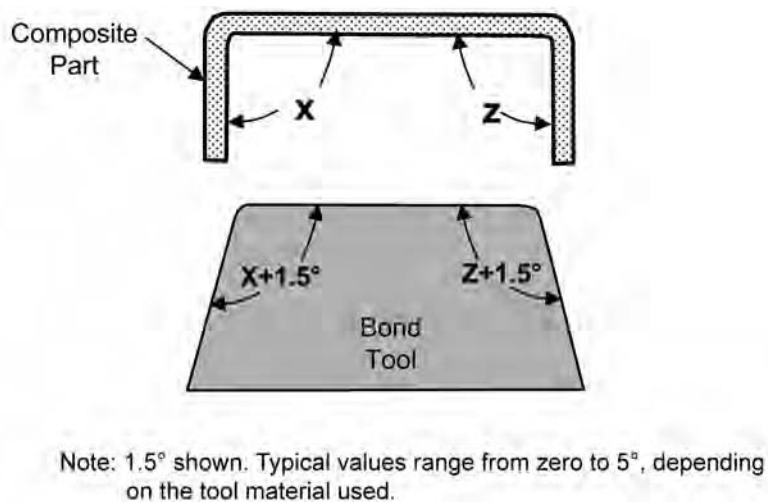
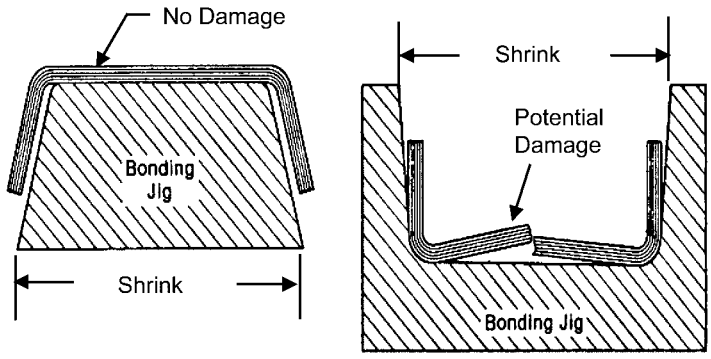
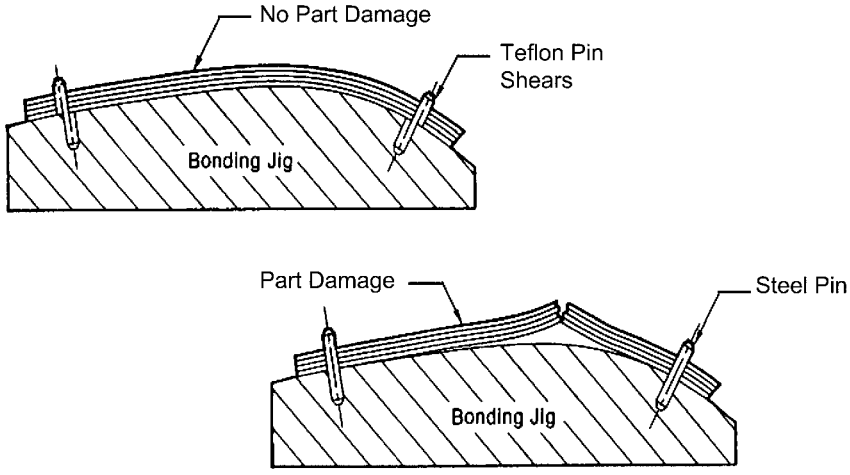


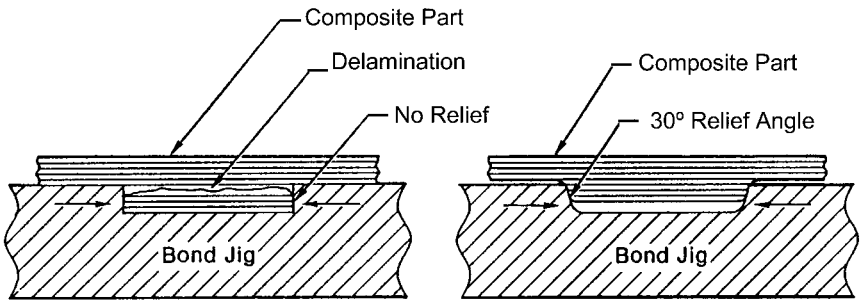
Fig. 4.5 Spring-in correction



Potential Effects of Tool Shrinkage on Part Quality



Shear Pins Used to Eliminate Tool Shrinkage Damage



Cool-down shrinkage of bond tool may cause delamination of plies during removal of part

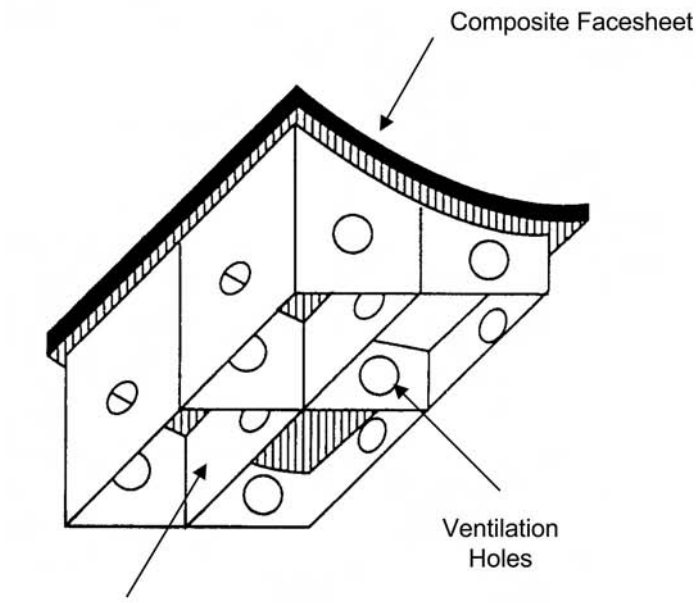
Cool-down shrinkage of bond tool causes part to lift up from bond tool, avoiding damage

Draft Used to Prevent Tool Shrinkage Damage

Fig. 4.6 Potential thermal contraction issues



Eggcrate for Metallic Bond Tool



Eggcrate for Composite Bond Tool

Fig. 4.7 Eggcrate structures for bond tools. Photo Source: The Boeing Company

The steel and aluminum tools were used to produce the same part configuration, a wing panel, while the electroformed nickel tool was used to produce a highly contoured fuselage sidewall panel containing cocured hat stiffeners on the inside surface. The faceplate on the steel tool was 0.45 to 0.55 in. (11.4 to 14.0 mm) thick. The welded steel eggcrate support contained circular cutouts to improve autoclave gas flow. This tool was identified as Tool "A." The NC machined aluminum project plate tool was identified as Tool "B." Although it is used to make the same aircraft part as Tool "A," the design concept is entirely different. Tool "B" consists of a thick

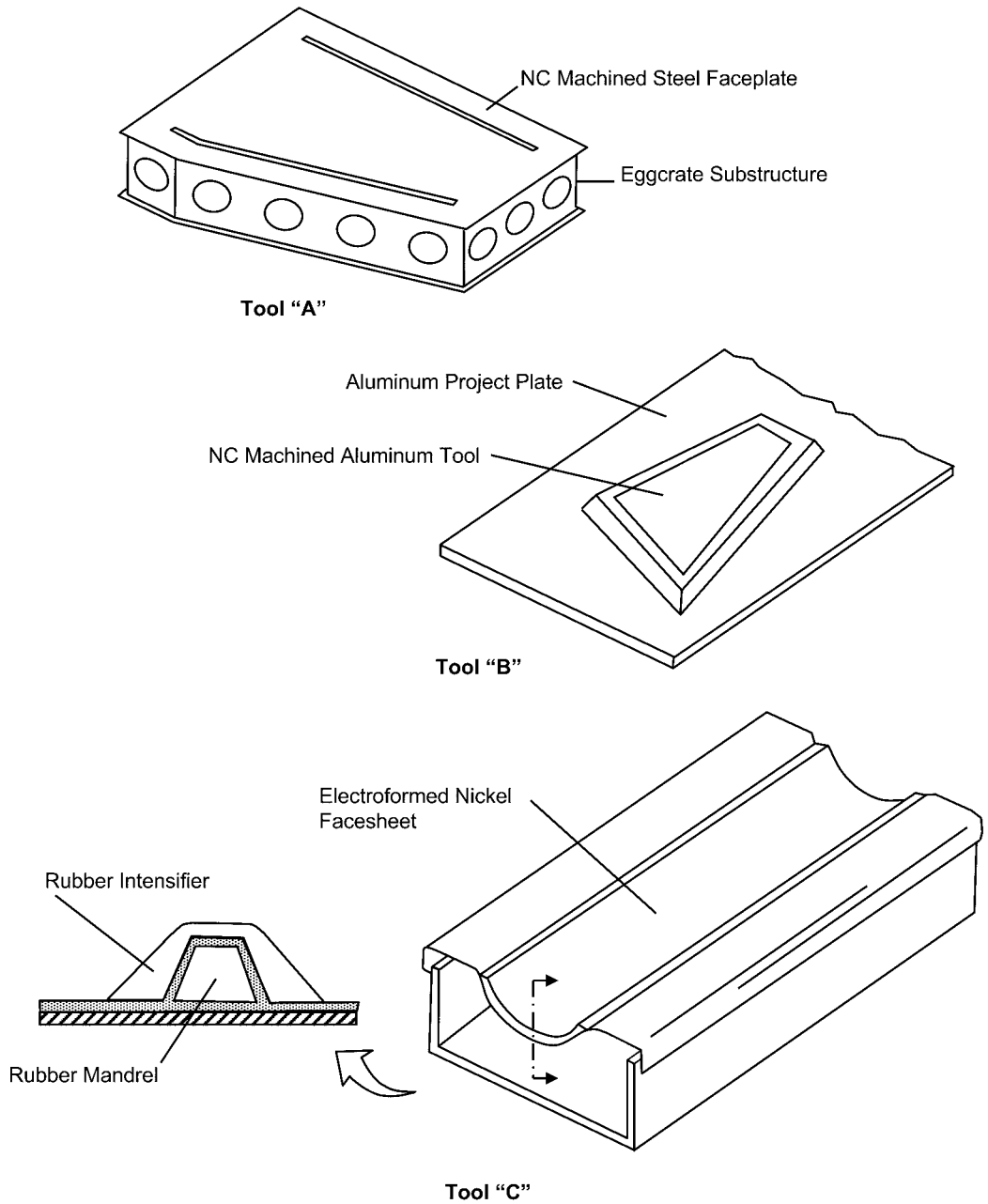


Fig. 4.8 Tools used for autoclave heat-up tests. NC, numerical control. Source: Ref 5

aluminum slab 2.2 to 2.3 in. (56 to 58 mm) that was NC machined to the moldline contour on one surface and flat on the other surface. During autoclave curing, it was placed on a standard 1.0 in. (25.4 mm) thick aluminum project plate. Normally, a number of these types of tools are placed on each project plate. The electroformed nickel bond tool, identified as Tool "C," consisted of a relatively thin 0.25 to 0.38 in. (6.4 to 9.7 mm) electroformed nickel shell supported by an open support structure. Rubber mandrels and pressure intensifiers were used at locations requiring cocured hat stiffeners.

The nesting positions (autoclave locations) for the three batches were predetermined simply by rotating the tool position for each batch.

The same production autoclave was used for all three batches. After the tools were vacuum bagged and leak checked, they were nested in the autoclave using the positions shown in Fig. 4.9 to 4.11. Additional thermocouples were then placed above the tool surfaces to measure the autoclave free air temperature. The autoclave was pressurized to between 85 and 100 psig for each run. The tools were then heated through a typical cure cycle profile to 350 °F (175 ºC) while thermocouple data were recorded during heat-up and cool-down.

The autoclave characterization tests revealed three significant findings:

1. The aluminum project plate tool (Tool "B") exhibited a slower heat-up rate than either the steel tool (Tool "A") or the electro-

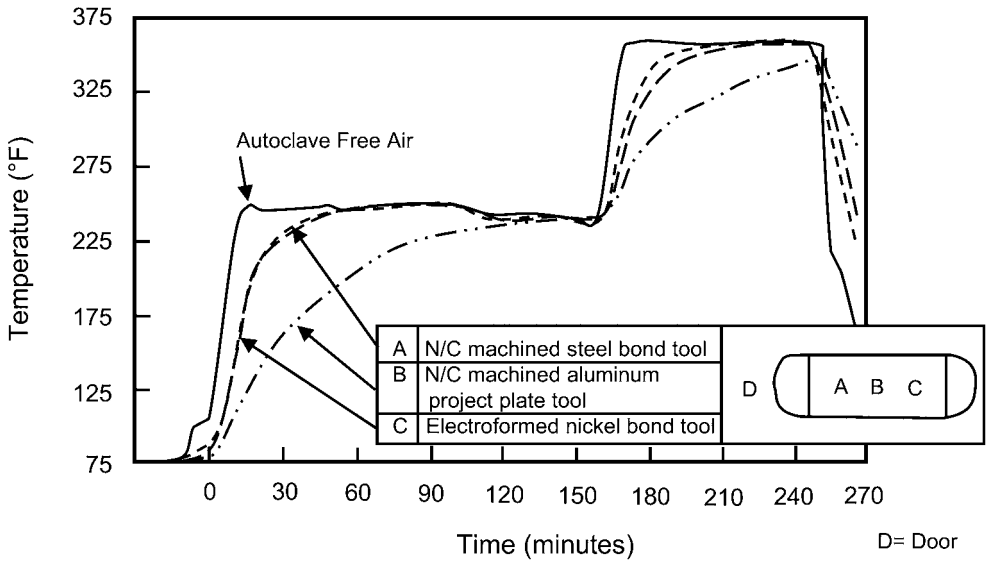


Fig. 4.9 First autoclave heat-up rate test. NC, numerical control. Source: Ref 5

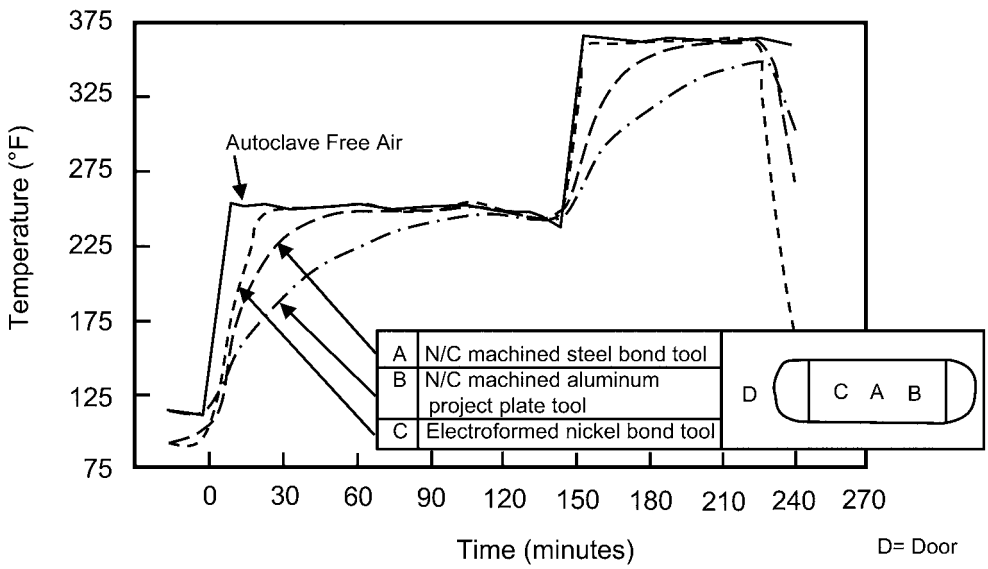


Fig. 4.10 Second autoclave heat-up rate test. NC, numerical control. Source: Ref 5

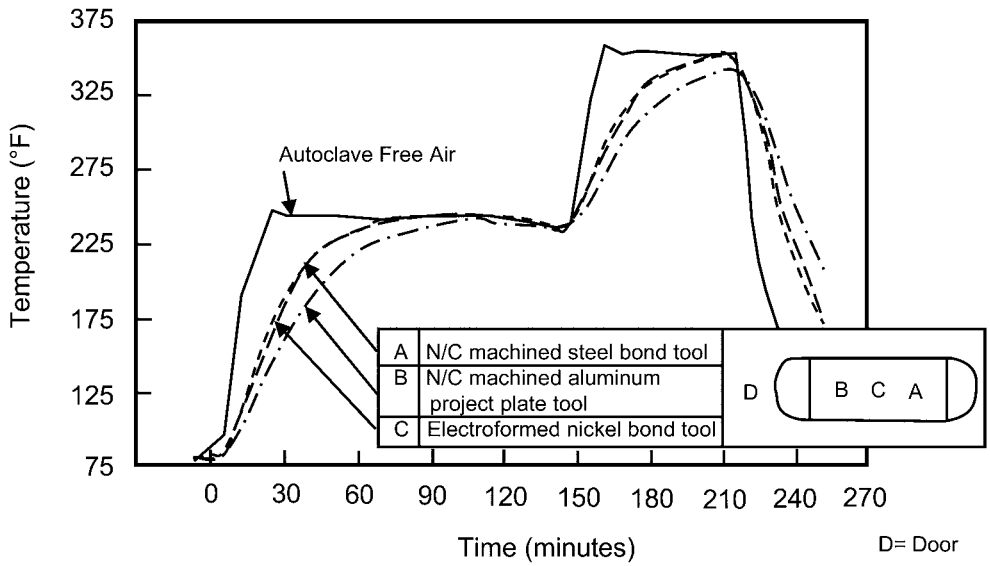


Fig. 4.11 Third autoclave heat-up rate test. NC, numerical control. Source: Ref 5

formed nickel tool (Tool "C"). This slower heat-up rate was a function of the large thermal mass of the thick aluminum tool. However, the heat-up rate for the aluminum tool improved when it was located at the front of the autoclave (Fig. 4.11), where higher gas velocity increased the heat transfer rate from the autoclave free air to the tool.

2. The electroformed nickel tool (Tool "C") exhibited the fastest thermal response; however, the rubber mandrels used to support the cocured hats created localized cold spots on the tool due to their heat sink effect and insulative qualities.
3. The heat-up rate for the steel tool (Tool "A") was about the same, irrespective of nesting in the front, middle, or back of the autoclave. A possible explanation is that the thick eggcrate support structure acted as a flow blocker and minimized the effects of autoclave gas velocity differences.

4.3 Tool Fabrication

The fabrication sequence for a typical large steel bond tool is shown in Fig. 4.12. Prior to the start of fabrication, the steel faceplate sections are formed, rolled, or machined to contour. The eggcrate substructure is made from steel plates that are welded together. The faceplate sections are then welded to sections of the eggcrate, and the final contour of the faceplate is NC machined. Finally, if the tool is very large, like the one shown in Fig. 4.12, the sections are welded together. All welds are ground smooth, the faceplate is finished to give a smooth surface, and the tool is vacuum leak checked. Normally, this type of tool will have integral vacuum manifolds incorporated around the periphery of the tool with multiple lines for vacuum and static readings. At a minimum, two manifolds are required: one for the dynamic vacuum and one for the static gauge. As a rule of thumb, vacuum ports should be located no farther than 6 to 10 ft (1.8 to 3.0 m) apart. To make production easier, most vacuum and static ports are equipped with quick-disconnect fittings. Thermocouples are normally welded to the back side of the tool. Handling provisions, such as casters with wheels and tow bars, are provided for movement. The fabrication approach for Invar-type tools is very similar to that for steel tools except that more cast shapes are used that are then welded to final contour. If the contour is simple, it may be possible to roll a metal faceplate to contour and attach it directly to the substructure. For tools with thin faceplates, it is common practice to use threaded connectors so that adjustments can be made to the faceplate contour.

Electroformed nickel and composite tools require that a master model be made prior to tool fabrication; that is, it takes a tool to make a tool. Master models must have the correct shape and

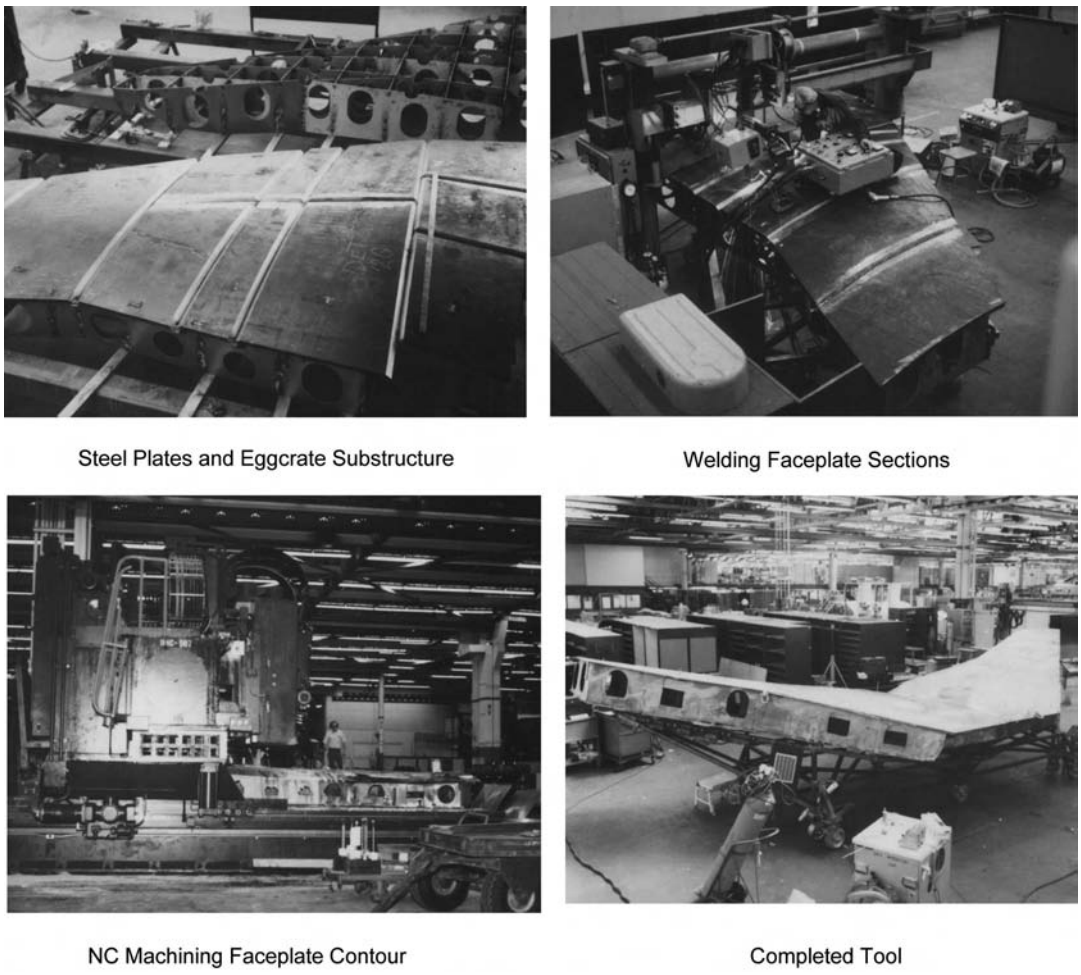


Fig. 4.12 Manufacturing sequence for large NC machined steel bond tool. NC, numerical control. Source: The Boeing Company

a smooth surface finish, be able to withstand the processing temperature for tool curing, be leak free, have a sealed surface, and be mold released prior to use. There are many methods for making master models. However, with the advent of more powerful computer-aided design/manufacturing computer packages, masters are generally NC machined directly from materials such as mass cast epoxies, foams, plasters, wood, and laminated polyurethane tooling boards, as shown in Fig. 4.13. Once the master model is complete, a plastic-faced plaster (PFP) is usually made off of the master. Plastic-faced plasters can be made of pure plaster, have epoxy faces backed by plaster, or have fabric-reinforced faces backed by plaster. Higher-temperature intermediate or facility tools can also be fabricated off of the master or the PFP, depending on the processing temperature required for the final tool. The number of steps involved in fabricating a composite tool can be numerous, as shown in Table 4.2, depending on which surface is the work surface and what material system is used. Note that some accuracy is lost each time the tool surface is replicated, primarily due to material shrinkage during cure.

The use of a PFP to fabricate an electroformed nickel tool is shown in Fig. 4.14. The PFP or plaster splash is used to make a laminated tool, usually glass/polyester 0.4 to 0.5 in. (10.2 to 12.7 mm) thick, that is then coated with a thin layer of silver so that it will be conductive when placed in the electroforming bath. It is important that the electroforming mandrel remain stable during the plating process. If the tool is large, the plating mandrel is frequently supported with

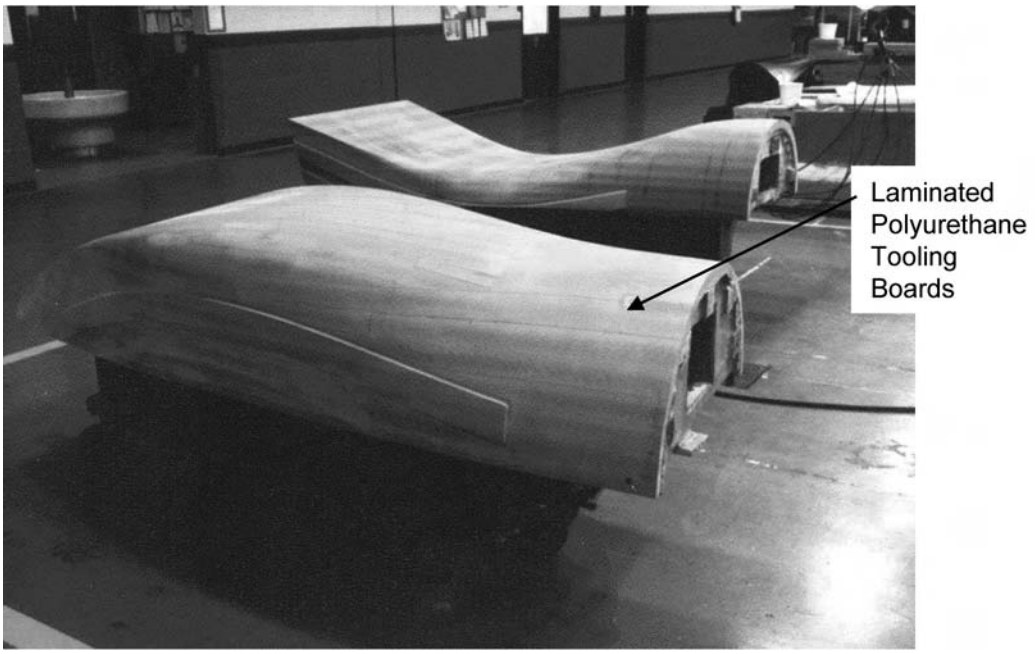


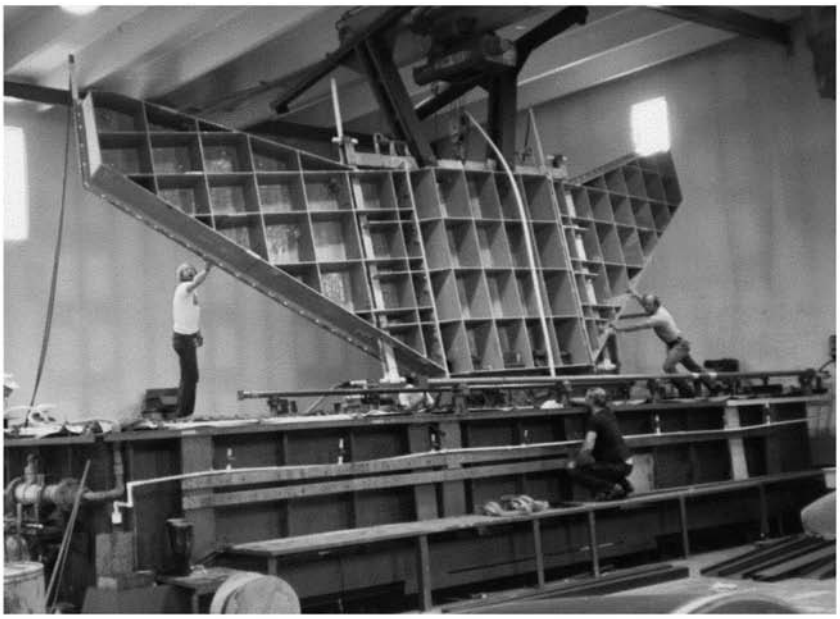
Fig. 4.13 Numerical control (NC) machined master models. Source: The Boeing Company

a substructure to ensure stability. The surface of the plating mandrel must be as smooth as that of the desired tool, since the plating procedure will reproduce the mandrel's smoothness. The electroforming procedure usually takes several weeks to build up the required faceplate thickness, usually around 0.2 to 0.4 in. (5.1 to 10.2 mm). The plating bath temperature is approximately 120 °F (50 ºC). After removal, the faceplate is attached to the substructure before the plating mandrel is

Table 4.2 Options for making composite tools

Accuracy	Number of steps	Master pattern	Master mold	Intermediate or production tool		
Most accurate	1 step		RT/HT prepreg mold			
	2 steps		PFP	200 °F prepreg mold		
	3 steps		PFP	RT/HT intermediate mold	250 °F or 350°F prepreg mold	
	3 steps		Splash	PFP	200 °F prepreg mold	
Least accurate	4 steps		Splash	PFP	RT/HT intermediate mold	250 °F or 350 °F prepreg mold

PFP, plastic-faced plaster; RT/HT, room temperature/high temperature. Source: Ref 5.



Lowering the Tool into the Plating Tank

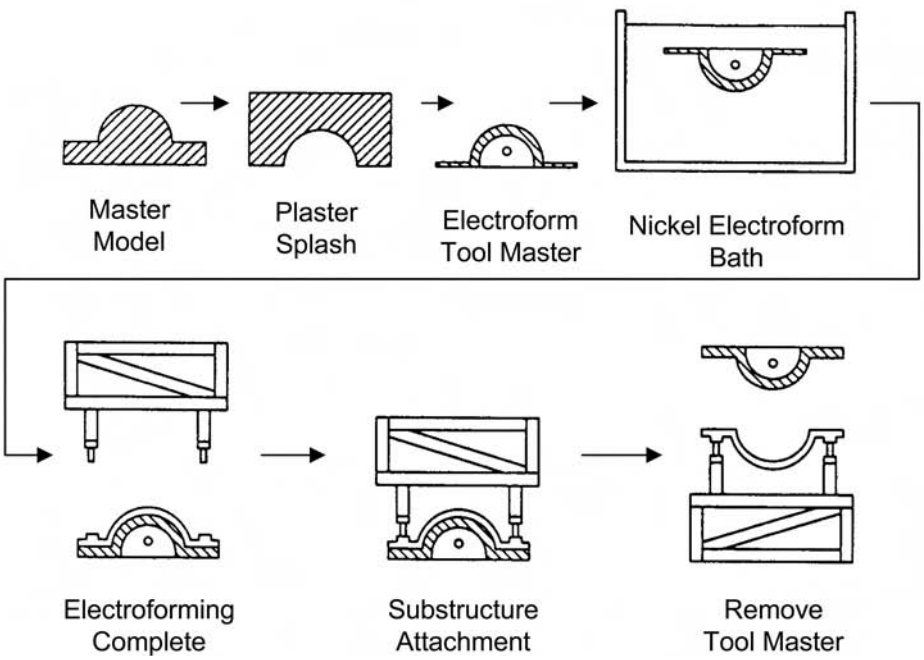


Fig. 4.14 Process flow for electroformed nickel tools. Source: Photo, the Boeing Company; figure, Ref 7

removed. Electroforming is capable of making quite large tools, essentially limited by the size of the plating bath. Tools with more than 200 ft^2 (18.6 m^2) of surface area have been fabricated. Sharp corners and recesses are difficult to plate uniformly; the plating tends to build up excessively in these areas. Fittings, tooling pin locators, vacuum connectors, and threaded pins for

attaching the substructure can be embedded during the plating operation to provide vacuum- and pressure-tight connections. In general, nickel has better damage tolerance than aluminum or composite tools and is more scratch resistant. Electroformed nickel tools can be repaired by soldering or brazing; however, this is generally more difficult than the weld repair of a steel or Invar tool. The lead in some repair solders can react with the nickel, causing joint cracking and leaks. If a superior surface hardness is required, the tool surface can be chrome plated. After plating, the tool is polished to give a smooth laminating surface.

For the fabrication of a composite tool, a PFP is used to lay up and cure a carbon or glass laminate. For aerospace tools, epoxies are normally used, while polyesters and vinyl esters dominate commercial applications. The predominant reinforcements are twill, plain, or satin weave carbon or glass fabrics. Balanced, symmetric quasi-isotropic lay-ups are normally used where the plies are cut into large rectangles and then butt spliced during lay-up. Finer fabrics can be used on the surface to improve the surface finish, while heavier fabrics are used internally to reduce lay-up time. For vacuum bag–cured tools, gel coats may also be useful in improving the surface finish, while prepreg films or adhesive layers are often used for autoclave-cured tools. Periodic vacuum debulking to consolidate the lay-up generally improves tool quality. Several different material systems have been used for fabricating composite tools: (1) wet lay-up in which a liquid resin is used to impregnate dry cloth layer by layer, which is cured at room or elevated temperature; (2) high-temperature/high-temperature (HT/HT) prepregs in which the tool is again layed up layer by layer and then cured at elevated temperatures such as 350 °F (175 ºC) followed by elevated-temperature postcure such as 350 °F (175 ºC); and, more recently, (3) low-temperature/high-temperature (LT/HT) prepreg that is layed up and cured at low temperatures such as 150 °F (65 ºC), followed by a high-temperature such as 350 °F (175 ºC) postcure. If the cures are conducted at an elevated temperature, curing can be accomplished in either an oven or an autoclave, although autoclave curing produces higher-quality tools.

The highest-quality tools are made using either HT/HT or LT/HT prepregs that are autoclave cured to give maximum compaction and low void contents. Voids need to be avoided in tool facesheets because they can serve as initiation points for microcracks that will eventually propagate through the thickness, resulting in potential leak paths. The biggest advantage of LT/HT systems is that they can initially be cured on low-temperature-capability PFPs and then removed from the PFP for the elevated-temperature postcure. By contrast, HT/HT prepregs require an intermediate or facility tool with greater temperature tolerance than a PFP. To prevent distortion during the postcure, the eggcrate support structure is usually attached to the faceplate prior to postcure. (Details of a typical eggcrate support structure are shown in Fig. 4.7.) The eggcrate support structure can be made from honeycomb laminates or carbon/epoxy tooling board or constructed from carbon/epoxy prefabricated tubes. Alternatives to eggcrate support systems include stiffeners molded to the back side of the tool and tubular support systems. To help protect the edges of the faceplate from handling damage, they should either be even, slightly recessed, or have rolled edges. A typical faceplate is usually about 0.25 in. (6.4 mm) thick, which, in the author's opinion, causes one of the major problems during service: leakage. The author thinks that thicker faceplates would have less tendency to develop leaks. Another potential leakage problem is due to the creation of holes in the faceplate for vacuum connections and manifolds. Although molded-in pass-throughs are better than ones that are potted in after cure, an even better approach is to never put a hole in a composite faceplate and instead use through-the-vacuum-bag fittings for evacuation and static readings. Thicker faceplates with no penetrations are more tolerant of both handling damage and thermal cycling. When a leak does develop in a composite tool, it can be extremely difficult to locate and repair. The leak may start at an edge or a surface, propagate in a winding path down through the laminate layers, and exit several feet away from where it started.

If high processing temperatures are required, for example 500 to 700 °F (260 to 370 ºC) for high-temperature polyimides or thermoplastic composites, either steel or Invar 42 tooling can be used. Monolithic graphite and mass cast ceramics are options as well. Blocks of monolithic graphite can be bonded together and then NC machined to final contour, while mass cast ceramics are mixed, poured, and cured. Both of these materials have excellent temperature capability and low CTEs. Monolithic graphite is lightweight, easy to machine (but messy), has a high thermal conductivity, and can be used at temperatures up to 800 °F (425 ºC) in air. Ceramics are also relatively lightweight; however, their thermal

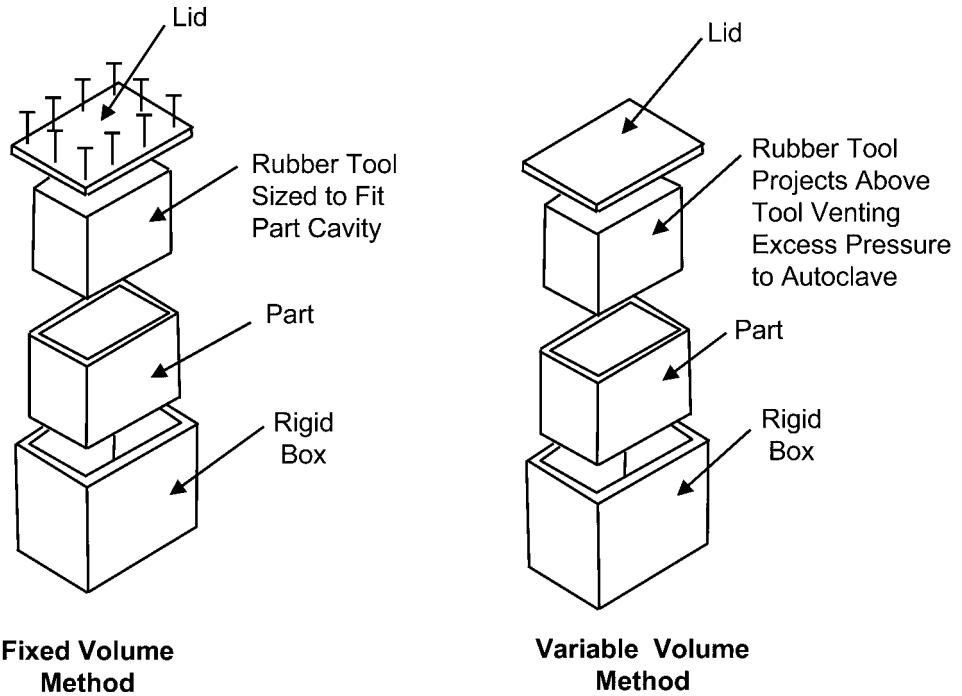


Fig. 4.15 Fixed-volume and variable-volume elastomeric tooling methods. Source: Ref 7

conductivities are lower, and they must be thoroughly surface sealed prior to use. Ceramic tools are also more difficult to fabricate than monolithic graphite due to their slow cure rates and their tendency to crack during cure. Reinforcing bars or grids are often embedded in the casting to strengthen it. The biggest drawbacks to both monolithic graphite and cast ceramics are that they are very brittle materials and are susceptible to breakage and handling damage.

Elastomeric tooling materials, such as silicone rubber, butyl rubber, and fluoroelastomers, are frequently used for caul pads and pressure intensifiers. They are used to either intensify pressure or redistribute pressure during the cure cycle. They are frequently used in areas where it is difficult to vacuum bag and there is a danger of the bag bridging, such as radii in corners. Elastomers can be used in one of two ways (Fig. 4.15): (1) the fixed-volume method, in which the elastomer is totally contained within a hard tool and expands during heating to apply pressure to the part; or (2) the variable-volume method, in which the elastomer is allowed to vent or release excess pressure against the autoclave pressure (usually 85 to 100 psi).

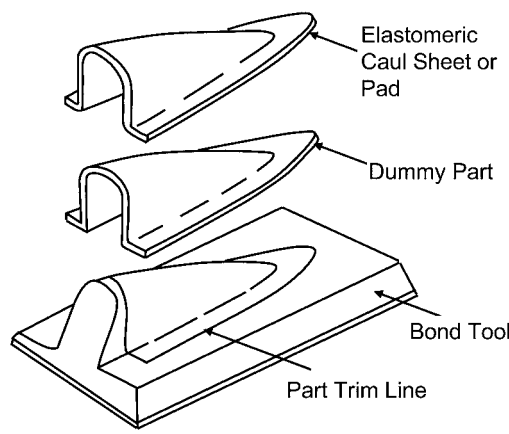


Fig. 4.16 Method for making a conforming caul sheet or pad

The problem with the fixed-volume method is that it requires quite precise calculations of the volume of rubber required; otherwise, it can result in either too much or too little pressure. Methods for calculating the required amount of rubber can be found in Ref. 7.

The fabrication sequence for a typical caul pad is shown in Fig. 4.16. In this sequence, the

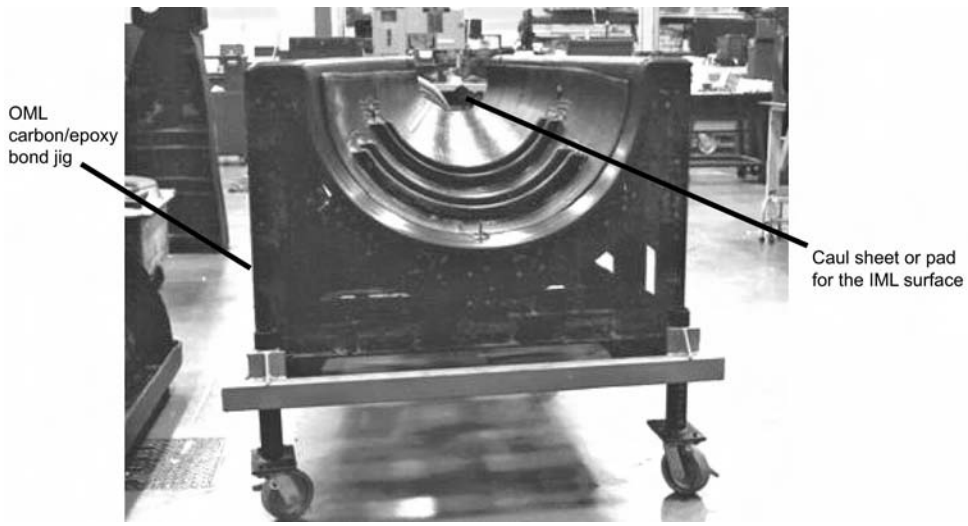


Fig. 4.17 Elastomeric caul plate or pad. IML, inside moldline; OML, outside moldline. Source: The Boeing Company

caul pad is made from a calendered elastomeric sheet stock that is placed over a "dummy" part and cured on the bond tool. A dummy part is simply a first article part made on a tool without an intensifier. After cure, any surface wrinkles are filled and splined smooth. The dummy part is then used to make the caul pad. If a dummy part is unavailable, the part thickness can be built up with layers of special tooling waxes. Elastomeric tooling materials generally come as either calendered sheet stock or liquids that can be cast to shape in molds and room temperature vulcanized or cured. A composite tool with an elastomeric caul plate is shown in Fig. 4.17. In this application, the elastomeric caul plate covers both the stiffeners and the skin.

The life of elastomeric tooling details is limited, usually to fewer than 30 autoclave cycles. Resins tend to attack some elastomers and the continual heat cycling causes shrinkage and embrittles them, leading to cracking and tearing. Layers of carbon cloth are often embedded in elastomeric intensifiers to provide local stiffening and improve durability. Elastomers also have low thermal conductivities and can act as heat sinks if large masses are used in a local area.

For flat or mildly contoured parts, it is common practice to use a caul sheet or caul plate on the nontooled surface (in this case, the bag side) to provide improved surface finishes. Caul plates can be made from metal, reinforced glass or carbon, or elastomers. It is important that the caul plate be flexible enough so that local surface bridging does not occur. The caul plate may be perforated to allow air evacuation and, in some cases, resin bleeding.

REFERENCES

1. J.J. Morena, *Advanced Composite Mold Making*, Van Nostrand Reinhold Company, 1984
2. J.J. Morena, Mold Engineering and Materials—Part I, *SAMPE J.*, Vol 31, (No. 2), March/April 1995, p 35–40
3. J.J. Morena, Advanced Composite Mold Fabrication: Engineering, Materials, and Processes—Part II, *SAMPE J.*, Vol 31 (No. 3), May/June 1995, p 83–87
4. J.J. Morena, Advanced Composite Mold Fabrication: Engineering, Materials, and Processes—Part III, *SAMPE J.*, Vol 31 (No. 6), November/December 1995, p 24–28
5. J.M. Griffith, F.C. Campbell, and A.R. Mallow, Effect of Tool Design on Autoclave Heat-Up Rates, *SME Composites in Manufacturing*, Vol 7, December 1987
6. J.J. Morena, *Advanced Composite Mold Making*, Van Nostrand Reinhold Company, 1988
7. *Engineered Materials Handbook*, Vol 1, *Composites*, ASM International, 1987

SELECTED REFERENCES

- *ASM Handbook*, Vol 21, *Composites*, ASM International, 2001
- "The Nilo Nickel-Iron Alloys for Composite Tooling," Inco Alloys International, 1994
- S. Black, Epoxy-Based Pastes Provide Another Choice for Fabricating Large Parts, *High-Perform. Comp.*, January/February 2001, p 20–24
- M.C.Y. Niu, *Composite Airframe Structures: Practical Design Information and Data*, Conmilit Press, Hong Kong, 1992

Copyright © 2010, ASM International®
All rights reserved.
www.asminternational.org

CHAPTER 5

Thermoset Composite Fabrication Processes

THE MAJOR THERMOSET composite fabrication processes for continuous-fiber composites, including lay-up, vacuum bagging, and curing are covered in this chapter. Three lay-up processes are discussed: wet lay-up, prepreg lay-up, and low-temperature/vacuum bag curing prepreg. Wet lay-up is used extensively in commercial industries to fabricate fiberglass/polyester parts. Prepreg lay-up and autoclave curing is the predominant fabrication method used in the aerospace industry to make carbon/epoxy parts. The third lay-up process, low-temperature/vacuum bag curing prepreg, was originally developed for making carbon/epoxy tools. However, due to material and process improvements, it is now viewed as an alternative to autoclave curing when the part count is small and the cost of autoclavable tools is too high.

Filament winding and pultrusion are two other processes with deep roots in commercial part fabrication. While filament winding can be conducted using liquid resins and prepreg, by far the majority of parts are fabricated using the liquid resin method. Pultrusion is a high-rate commercial process used primarily to make long fiberglass/polyester parts of constant cross section.

Liquid molding includes resin transfer molding, vacuum-assisted resin transfer molding, and resin film infusion**.** These processes use a dry preform that is then injected with a liquid resin to form the part. Preforms can be manufactured by textile processes such as weaving, knitting, stitching, and braiding. Although structural reaction injection molding is used to make continuous-fiber parts, this process is more frequently used to make discontinuous-fiber parts and is therefore covered in Chapter 10, "Discontinuous-Fiber Composites."

5.0 Lay-up Processes

Lay-up processes are ideally suited for the manufacture of low-volume, medium-sized to large parts. However, manual lay-up processes are labor intensive, and part quality is strongly dependent on worker skill. Three lay-up processes will be covered: (1) wet lay-up, (2) prepreg lay-up, and (3) low-temperature curing/vacuum bag prepreg lay-up.

5.1 Wet Lay-Up

Wet lay-up is capable of making very large parts with minimal tooling costs, such as custom-built yacht hulls. In the wet lay-up process, shown schematically in Fig. 5.1, a dry reinforcement, usually a woven glass cloth, is placed manually on the mold. A low-viscosity liquid resin is then applied to the reinforcement by pouring, brushing, or spraying. Squeegees or rollers are used to densify the lay-up, thoroughly wetting the reinforcement with the resin and removing excess resin and entrapped air. The laminate is built up layer by layer until the required thickness is obtained. E-glass is the most prevalent material, but S-2 glass, carbon, or aramid can be used where the improved properties justify the higher costs. Heavy glass woven rovings (500 g/m^2) can be used to build up the thickness quickly and reduce labor costs, yielding a part with approximately 40 percent glass content. Although heavy woven rovings reduce lay-up times, these heavy weaves are more difficult to impregnate than the lighter-weight glass cloths. Where the high strength of woven roving or glass cloth is not required, glass mats can be used to reduce costs. Glass mats can

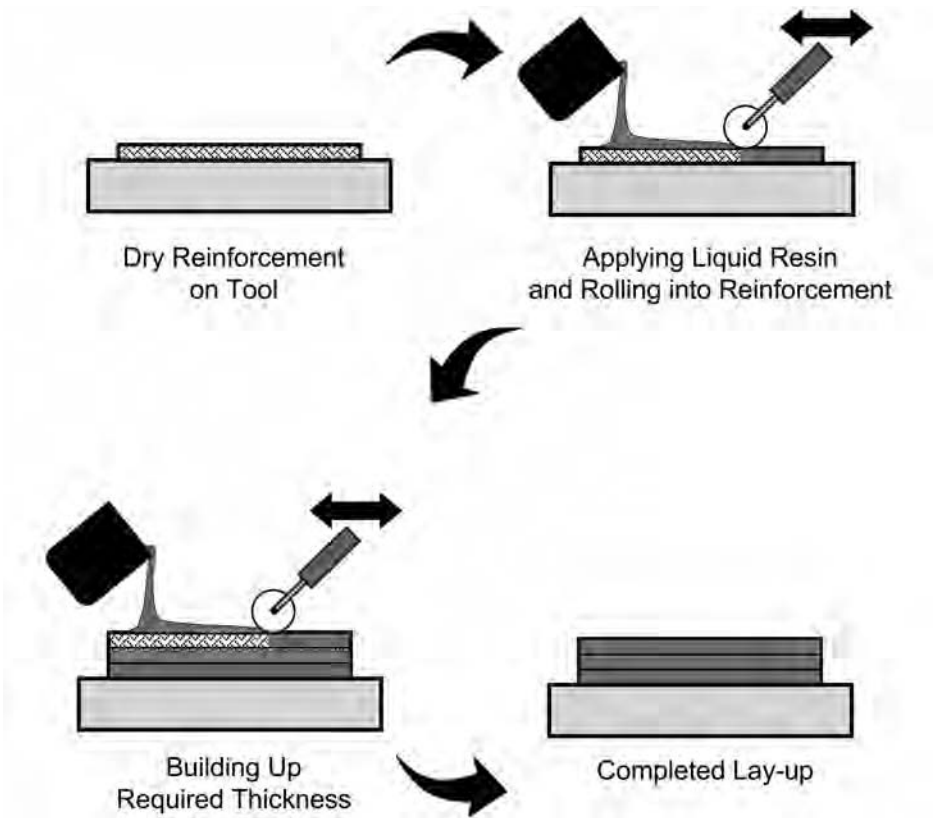


Fig. 5.1 Typical wet lay-up operation

be either continuous strand mats, in which continuous strands of glass are swirled onto a moving carrier and then tacked with a binder, or chopped strand mats, in which chopped fibers approximately 1 to 2 in. (25.4 to 50.8 mm) are sprayed onto a moving carrier and again heat tacked with a liquid, spray, or powder binder. Frequently, to reduce weight and save labor costs, core materials such as honeycomb, balsa, or foams are added to produce a sandwich construction, which, in the case of a boat hull, can also help provide flotation. In general, foam cores should be sealed prior to lay-up to reduce excessive resin absorption. Since impregnation is done by hand, voids, resin-rich, and resin-starved areas can be a problem. Improvement in the impregnation consistency can be obtained by preimpregnating the reinforcement before it is placed on the tool. This can be accomplished by placing a layer of biaxially oriented polyethylene teraphthalate (boPET: a clear sheet of polyester made from stretched polyethylene teraphthalate) on a flat bench, covering the boPET with the dry reinforcement, applying a predetermined amount of resin, covering with another layer of boPET, and then thoroughly rolling the resin into the reinforcement. (BoPET is known by several trade names, the most common being Mylar by DuPont.) The boPET sheets can then be used to support the preimpregnated ply as it is moved to the lay-up. Some manufacturers improve the quality and productivity by building their own impregnation machines. One simple example is shown in Fig. 5.2, in which a dry reinforcement is being impregnated through rollers with a liquid resin.

To provide a smooth surface finish on the tool side, a gel coat is often applied to the mold-released tool prior to the start of lay-up. Gel coats, which are specially formulated resins that provide a resin-rich surface on the cured laminate, can be applied by either brushing or spraying. The normal thickness for a gel coat should be 0.020 to 0.040 in. (0.5 to 1.0 mm). If it is too thick, resin crazing and cracking can development in service. Usually lay-up can begin after the gel coat cures to a tacky condition. Gel coats

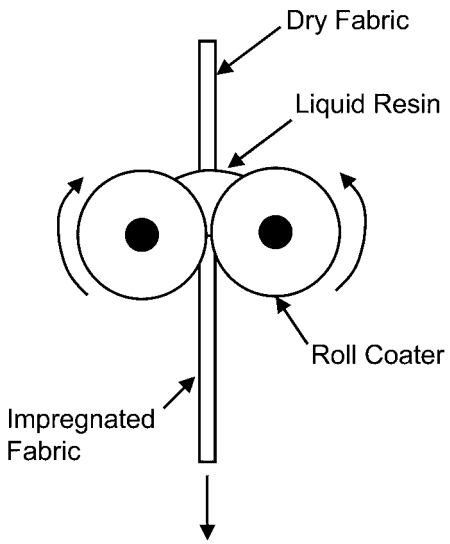


Fig. 5.2 Example of a simple impregnation process

can be formulated for improved flexibility, blister resistance, stain resistance, weatherability, and toughness. Tough, resilient gel coats can provide impact and abrasion resistance to the laminate surface. Gel coats can also be pigmented to provide the cured part with a variety of colors. Some manufacturers also use a fine mat or woven cloth (veil) as the first ply to further enhance surface finish. Veils, which are used primarily for surface plies, consist of thin weaves with very fine fibers to enhance the surface finish.

If the part is cured at room or low temperatures, extremely inexpensive tooling can be fabricated from wood, plaster, sheet metal, or glass laminates. These tooling approaches make this process attractive for large parts where the size of the part and the expense of autoclave curing would not be practical. The process is also good for making prototype parts where the design may change prior to production. Typically, wet lay-up molding is done on an open single-sided tool. The tool configuration can be designed to control the internal shape and surface finish (male tool) or the outside shape and surface finish (female tool). Cured parts will have one finished surface (i.e., the tool surface) that is essentially as smooth as the tool itself, while the untooled surface will be somewhat rougher.

Wet layed-up parts are usually cured at room temperature without a vacuum bag. Although a vacuum bag increases costs, it provides better consolidation and more uniform laminates. A vacuum bag cure also produces laminates with higher reinforcement contents, more uniform thicknesses, and better surface finishes. Vacuum bags can also be used for intermediate debulks during the lay-up process. If the part is cured at a slightly elevated temperature, for example less than 200 °F (95 °C), heat lamps are often used or a simple forced air convection oven can be built around the part. The ovens are frequently constructed of plywood with foam insulation and heated with hot-air blowers. If this process is used, it is a good idea to conduct a trial heat cycle on the tool prior to part fabrication to identify any hot or cold areas. Thermocouples can be attached to the tool to monitor the cure cycle.

Polyesters and vinyl esters are the predominant resins used for wet layed-up glass fiber reinforced parts. In fact, polyesters are the most commonly used thermoset resins for all commercial composite parts. These resins provide a balance of good mechanical, chemical, and electrical properties, dimensional stability, ease of handling, and low cost. They can be formulated for low- or high-temperature usage, for room or high-temperature cure, and for flexible or rigid products. Additives can be incorporated to provide flame retardance, superior surface finishes, pigmentation, low shrinkage, weather resistance, and other properties. Vinyl esters, although somewhat most costly than regular polyesters, offer some advantages in toughness and weathering resistance (i.e., lower moisture absorption). Vinyl esters can also be formulated for higher-temperature resistance.

Polyester resins are usually supplied in liquid form as a mixture of resin and a liquid monomer, usually styrene. The amount of monomer is the major determinant of resin viscosity. The addition of a catalyst and its subsequent activation (usually by heat) cause the crosslinking reaction. Completion of the reaction is dependent on both the formulation and the cure cycle for the selected formulation. In room-temperature curing systems, an accelerator can be used to promote a catalytic reaction. Inhibitors can also be added to provide slower cures and a longer working life (i.e., pot life), an important consideration when laying up large parts. Since polyester resins are more susceptible to exotherm than epoxies, the cure temperature must be properly controlled.

Polyester resins can be formulated to provide special processing characteristics:

- Hot strength allows hot parts to be removed from the tool or die without losing their dimensional stability or shape.

- Low exothermic heat is used for thick laminates to minimize the heat given off during cure, an important consideration for parts with extremely thick sections.
- Extended pot life is necessary for large, complex parts where resin flow is needed for some time during the lay-up and cure process.
- Air drying provides a tack-free cure at room temperature, which again is useful when fabricating very large parts such as boat hulls and pool liners.
- Thixotropy, a property of the resin that causes it to resist flowing or sagging on a vertical surface, is important when laying up boat hulls or pool liners.
- Additives for special end use requirements can be added to the resin formulation to provide the finished part with special properties dictated by end use requirements. These include the following additives:

  1. Pigments are available that can provide almost any color and shade for the finished part. Pigments can also be added to gel coats.
  2. Fillers are usually inorganic or inert materials that can improve the surface appearance, processability and some mechanical properties, and reduce costs.
  3. Flame retardants are often used when interior parts are being manufactured and toxic fumes from a fire are a concern.
  4. Ultraviolet absorbers can be added to the resin to improve resistance to extended sunlight exposure.
  5. Mold release agents can either be applied directly to the mold or blended with the resin to facilitate part removal.
  6. Low-shrink and low-profile additives, usually thermoplastic types, give the cured part minimum surface waviness and low shrinkage.

Epoxies exhibit better temperature resistance than polyesters. They have good to excellent mechanical strength-to-weight ratios and better dimensional stability than polyesters. Epoxies are ideal for applications requiring elevated temperatures. However, they are not as economical as polyesters, but their extended range of properties can make them cost effective in certain applications. Flame retardants, pigments, and other additives can also be added to epoxies. They can be formulated for room-temperature cure, but more commonly heat is used to cure epoxies if high mechanical properties are required.

If higher mechanical properties are required, the following methods may be used to reduce voids and porosity and ensure consistent glass contents:

- *Vacuum Bag*: A flexible film (e.g., nylon) is placed over the completed lay-up or spray-up, its joints are sealed, and a vacuum is drawn. Bleeders and breathers can be used to remove excess resin and promote the evacuation of air. The vacuum bag pressure helps minimize voids in the laminate and forces excess resin and air from the lay-up. The addition of pressure also yields higher reinforcement concentrations and provides better adhesion between the layers.
- *Pressure Bag*: A tailored rubber sheet is placed against the finished lay-up, and air pressure is applied between the rubber sheet and a pressure plate. Steam may be applied to heat the resin to accelerate cure. Pressure eliminates voids and drives excess resin and air out of the laminate, increasing the density and improving the surface finish.
- *Autoclave*: Either a vacuum bag or a pressure bag process can be further improved by using an autoclave, which provides additional heat and pressure capabilities, producing greater laminate densification. This process is usually employed in the production of high-performance laminates using epoxy resin systems in aircraft and aerospace applications. However, either a pressure bag or an autoclave usually increases the costs substantially and negates many of the cost advantages of the wet lay-up process.

The main advantages of the wet lay-up process are that it is a simple method offering low-cost tooling and simple processing, and it is capable of producing a wide range of part sizes. There is a minimum investment in equipment; however, skilled operators are needed to produce consistent part quality, and the processes are somewhat messy and labor intensive. There are also growing environmental and health concerns about using polyesters that contain styrene in open molding processes.

5.2 Prepreg Lay-Up

Automated ply cutting, manual ply collation or lay-up, and autoclave curing is the most widely used process for high-performance composites in the aerospace industry. While manual

ply collation is expensive, this process is capable of making complex and high-quality parts. Since cost has become a major driver, a number of other processes such as automated tape laying, filament winding, and fiber placement are used for certain classes of parts. In addition, other low-cost processes, such as liquid molding and pultrusion, are either in limited production or are emerging as production-ready processes. The fabrication of sandwich and cocured structures creates the ability to make large structures that incorporate many smaller parts into a single assembly, which can eliminate a significant portion of the final assembly costs.

Cutting and manual ply collation are the major cost drivers in composite part fabrication; normally, they account for 40 to 60 percent of the cost, depending on part size and complexity. Ply collation can be accomplished by hand, automated tape laying, or fiber placement. Hand lay-up is generally the most labor-intensive method, but it may be the most economical if the number of parts to be built is limited, the part size is small, or the part configuration is too complex to automate.

5.2.1 Manual Lay-Up

Manual hand collation is conducted using either prepreg tape (24 in. (0.6 m) maximum width) or broadgoods (60 in. (1.5 m) maximum width). Prior to actual lay-up, the plies are usually precut and kitted into ply packs for the part. The cutting operations are normally automated unless the number of parts to be built does not justify the cost of programming an automated ply cutter. However, if hand cutting is selected, templates to facilitate the cutting operation may have to be fabricated. In addition, if the lay-up has any contour of the plies, the contour will also have to be factored into the templates.

Automated ply cutting of broadgoods, usually 48 to 60 in. (1.2 to 1.5 m) wide, is the most prevalent method used today. Both reciprocating knives and ultrasonically driven ply-cutting methods are currently used in the composites industry. The reciprocating knife concept originated in the garment industry. In this process, a carbide blade reciprocates up and down, similar to a saber saw, while the lateral movement is controlled by a computer-controlled driven head. The bed supporting the prepreg consists of nylon bristles that allow the blade to penetrate the prepreg during the cutting operation. With a reciprocating knife cutter, normally one to five plies can be cut during a single pass.

The ultrasonic ply cutter operates in a similar manner; however, the mechanism is a chopping rather than a cutting action. Instead of a bristle bed that allows the cutter to penetrate, a hard plastic bed is used with the ultrasonic method. A typical ultrasonic ply cutter, shown in Fig. 5.3, can cut at speeds approaching 2400 fpm (approximately 730 m/min) while holding accuracies of ± 0.003 in. (0.08 mm). One of the primary advantages of all automated methods is that they can be programmed off-line, and nesting routines are used to maximize material utilization. In addition, many of these systems have automated ply labeling systems in which the ply identification label is placed directly on the prepreg release paper. A typical ply label will contain both the part number and the ply identification number. This makes sorting and kitting operations much simpler after the cutting operations are completed. Modern automated ply cutting equipment is fast and produces high-quality cuts.

Prior to ply collation, the tool should have either been coated with a liquid mold release agent or covered with a release film. If the surface will be painted or adhesively bonded after cure, some lay-ups also require a peel ply on the tool surface. Peel plies are normally nylon, polyester, or fiberglass fabrics. Some are coated with release agents and some are not. It is important to thoroughly characterize any peel ply material that is bonded to a composite surface, particularly if that surface will be structurally adhesively bonded in a subsequent operation.

The plies are placed on the tool in the location and orientation specified by the engineering drawing or shop work order. Prior to placing a ply on the lay-up, the operator should make sure that all of the release paper has been removed and that there are no foreign objects on the surface. Large boPET (clear polyester film) templates are often used to define ply location and orientation. However, these are quite bulky and difficult to use and are rapidly being displaced by laser projection units. These units, shown schematically in Fig. 5.4, use low-intensity laser beams to project the ply periphery on the lay-up. They are programmed off-line using computer-aided design (CAD) data for each ply and, with advanced software, are capable of projecting ply locations on both flat and highly contoured lay-ups. The accuracy is generally in the ± 0.015 to 0.040 in. (0.4 to 1.0 mm) range, depending on the projection distance required for the part. Ply location accuracy requirements are normally specified on the engineering drawing or applicable process



Fig. 5.3 Large ultrasonic ply cutter. Source: The Boeing Company

specification. For unidirectional material, gaps between plies are normally restricted to 0.030 in. (0.8 mm), and overlaps and butt splices are not permitted. For woven cloth, butt splices are usually permitted but require an overlap of 0.5 to 1.0 in. (12.7 to 25.4 mm). The engineering drawing should also control the number of ply drop-offs at any one location in the lay-up.

The lay-up should be vacuum debulked every three to five plies or more often if the shape is complex. Vacuum debulking consists of covering the lay-up with a layer of porous release material, applying several layers of breather material, applying a temporary vacuum bag, and pulling a vacuum for a few minutes. This helps to compact the laminate and remove entrapped air from between the plies. For some complex parts, hot debulking, or prebleeding, in an oven under a vacuum or autoclave pressure at temperatures of approximately 150 to 200 °F (65 to 95 °C) can be useful for reducing the bulk factor. Prebleeding is similar to hot debulking except that prebleeding intentionally removes some of the resin with the addition of bleeder cloth, while in hot debulking no resin is intentionally removed.

5.2.2 Flat Ply Collation and Vacuum Forming

To lower the cost of ply-by-ply hand collation, in which plies are placed directly on the contour of the tool, a method called *flat ply collation* was developed in the early 1980s. This method, shown schematically in Fig. 5.5, consists of manually collating the laminate in the flat condition and then using a vacuum bag to form it to the contour of the tool. If the laminate is thick, this process may have to be done in several steps to prevent wrinkling and buckling of the ply packs. Heat (<150 °F (65 °C)) can be used to soften the resin to aid in forming if the contour is severe.

This process has also been used successfully to make substructure parts, such as C-channels. Normally woven cloth is used and the parts are flat ply collated, placed on a form block tool, covered with a release film, and then vacuum formed to shape using a silicone rubber vacuum bag. Note that it is important to keep tension in the fibers during the forming process. If compression occurs, the fibers will wrinkle and buckle. To maintain uniform tension during the forming

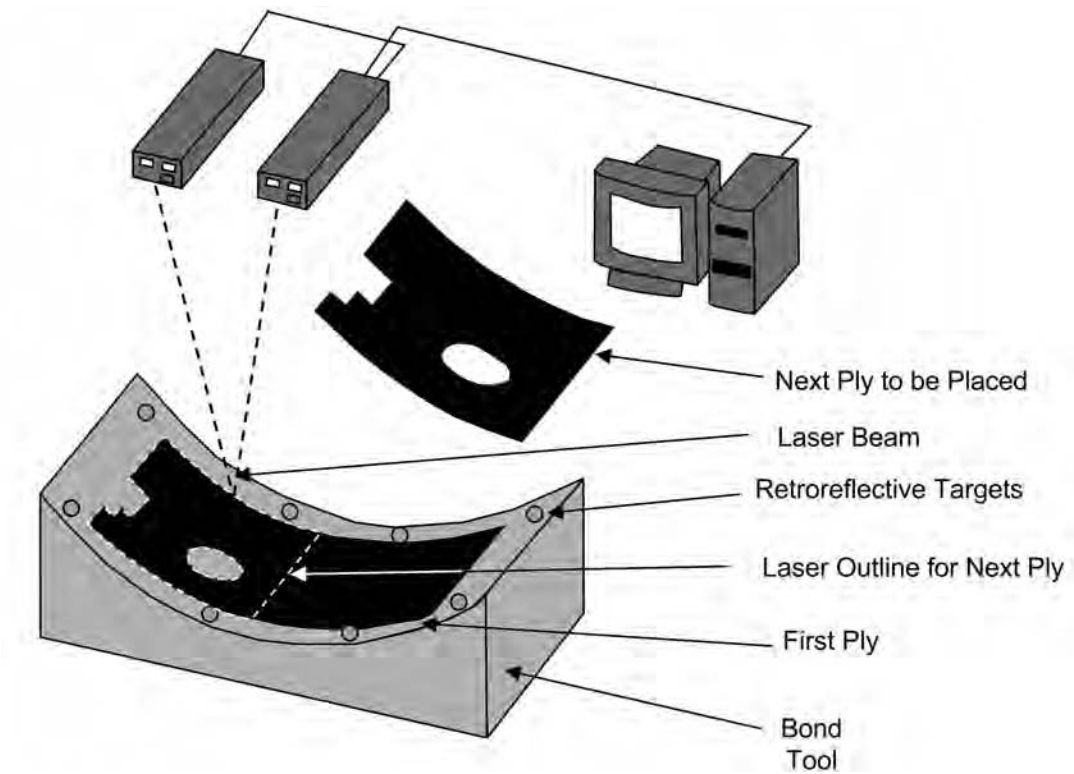


Fig. 5.4 Principle of laser ply projection. Source: Ref 1

operation, a double diaphragm forming technique can be used, in which the plies are sandwiched between two thin, flexible diaphragms pulled together with a vacuum. The application of low heat to soften the resin and aid in forming is quite prevalent. After cure, these long parts can be trimmed into shorter lengths, thus saving the cost of laying up each part on its individual tool.

5.2.3 Roll or Tape Wrapping

Small-diameter, hollow cylindrical parts, such as golf club shafts and fishing rods, are made by a process called *roll wrapping*. Rectangular or triangular prepreg plies, called *flags*, are cut and then roll wrapped at various angles on mold-released steel mandrels. Specialized rolling tables are used to provide some degree of automation, which also improves the quality of the lay-up. The lay-up is then wrapped with shrink tape and hung in an oven for cure. During cure, the tape shrinks and provides some compaction to the plies. The mandrels are normally tapered to facilitate part removal after cure. Since the shrink tape produces a rather rough surface finish, the parts are cylindrically ground after cure.

5.2.4 Automated Methods

A number of automated ply collation methods, primarily automated tape laying and fiber placement, have been developed to reduce the costs of composite part fabrication. Automated tape laying is advantageous for flat or mildly contoured skins, such as large, thick wing skins. Fiber placement is a hybrid process that possesses some of the characteristics of automated tape laying and filament winding. It was developed to allow the automated fabrication of large parts that could not be fabricated by either tape laying or filament winding alone.

Automated tape laying (ATL) is a process that is very amenable to large, flat parts such as wing skins. Tape layers usually lay down 3, 6, or 12 in. (7.6, 15.2, or 30.5 cm) wide unidirectional tape, depending on whether the application is for flat structure or mildly contoured structure. Automated tape layers are normally gantry-style

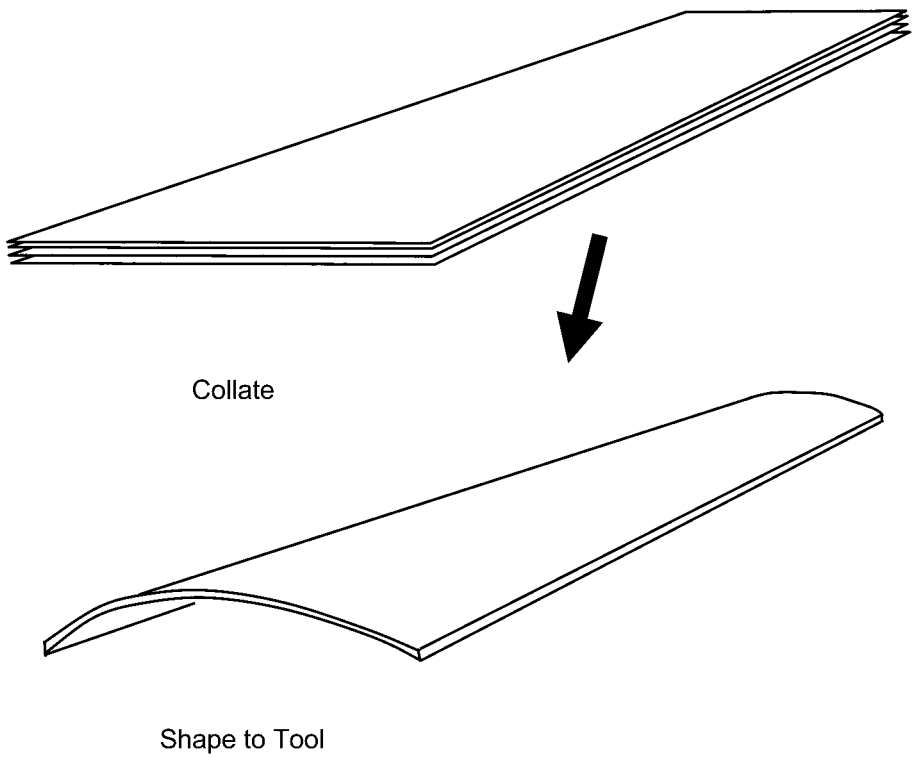
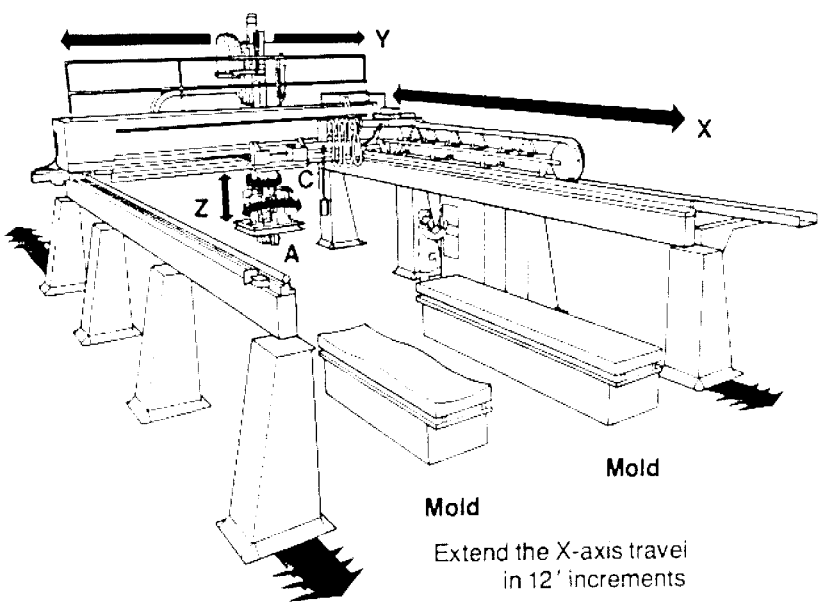


Fig. 5.5 Flat ply collation



Note: X, Y, Z, A, and C denote axes of movement.

Fig. 5.6 Typical gantry-style tape-laying machine. Source: Ref 2

machines (Fig. 5.6) that can contain up to 10 axes of movement. Normally, five axes of movement are associated with the gantry itself and the other five axes with the delivery head movement. A typical tape layer consists of a large floor-mounted gantry with parallel rails; a cross-feed bar that moves on precision ground ways; and a ram bar that raises and lowers the delivery head, which is attached to the lower end of the ram bar. Commercial tape layers can be configured to lay either flat or mildly contoured parts. Flat tape-laying machines (FTLMs) are either fixed-bed machines or open-bay gantries, while contour tape-laying machines (CTLMs) are normally open-bay gantries. The tool is rolled into the working envelope of the gantry and secured to the floor, and the delivery head is initialized onto the working surface.

The delivery heads (Fig. 5.7) for both FTLM and CTLM are basically the same configuration and will normally accept 3, 6, or 12 in. (7.6, 15.2, or 30.5 cm) wide unidirectional tape. To facilitate the tape-laying process, the unidirectional tape purchased for ATL applications is closely controlled for width and tack. The FTLMs use either 6 or 12 in. (15.2 or 30.5 cm) wide tape to maximize material deposition rates for flat parts, while most CTLMs are restricted to 3 or 6 in. (7.6 or 15.2 cm) wide tape to minimize tracking errors (gaps and overlaps) when laying contoured parts. The CTLM process currently applies to mild contours that rise and fall at angles up to about 20 percent. More highly contoured parts are normally made by processes such as hand lay-up, filament winding, or fiber placement, depending on the geometry and complexity of the part. Material for ATL comes in large-diameter spools, some containing almost 3000 lineal ft (900 m) of material. The tape contains a backing paper that must be removed during the tape-laying operation.

The spool of material is loaded onto the delivery head supply reel (reels as large as 25 in. (0.64 m) in diameter are used) and threaded through the upper tape guide chute and past the cutters. The material then passes through the lower tape guides, under the compaction shoe, and onto a backing paper take-up reel. The backing paper is separated from the prepreg and wound onto a take-up roller. The compaction shoe makes contact with the tool surface, and the material is laid onto the tool with compaction pressure. To ensure uniform compaction pressure, the compaction shoe is segmented so that it follows the contour of the lay-up. The segmented compaction shoe is a series of plates that are air pressurized and conform to lay-up surface deviations, maintaining a uniform compaction pressure. The machine lays the tape according to a previously generated numerical control (NC) program and cuts the material at the correct length and angle. When a length (course) is completed, it lays out tail, lifts off the tool, retracts to the course start position, and begins laying the next course.

Modern tape-laying heads have optical sensors that will detect flaws during the tape-laying process and send a signal to the operator. In addition, machine suppliers now offer a laser boundary trace in which the boundary of a ply can be traced by the operator to verify the correct position. Modern tape-laying heads also contain a hot-air heating system that will preheat the tape (80 to 110 °F (25 to 45° C)) to improve the tack and tape-to-tape adhesion. Computer-controlled valves maintain the temperature in proportion to the machine speed; that is, if the head stops, the system diverts the hot-air flow to prevent overheating the material.

Software to drive modern tape layers has improved dramatically in the last 10 years. All modern machines are programmed off-line with systems that automatically compute the "natural path" for tape laying over a contoured surface. As each ply is generated, the software updates the surface geometry, eliminating the need for the designer to redefine the surface for each new ply. The software can also display detailed information about the fiber orientation of each course and the predicted gaps between adjacent courses. Once the part has been programmed, the software will generate NC programs that optimize the maximum quantity of composite tape laid per hour.

Part size and design are key drivers for composite tape layer efficiency. As a general rule, larger parts and simpler lay-ups are more efficient. This is illustrated in Fig. 5.8 for a FTLM. If the design is highly sculptured (many ply drop-offs) or the part size is small, the machine will spend a significant amount of time decelerating, cutting, and then accelerating back to full speed.

Fiber placement, shown conceptually in Fig. 5.9, is a hybrid between filament winding and tape laying. A fiber placement, or tow placement, machine allows individual tows of prepreg to be placed by the head. The tension on the individual tows normally ranges from zero up to about 2 lb (0.9 kg). Therefore, true zero degree

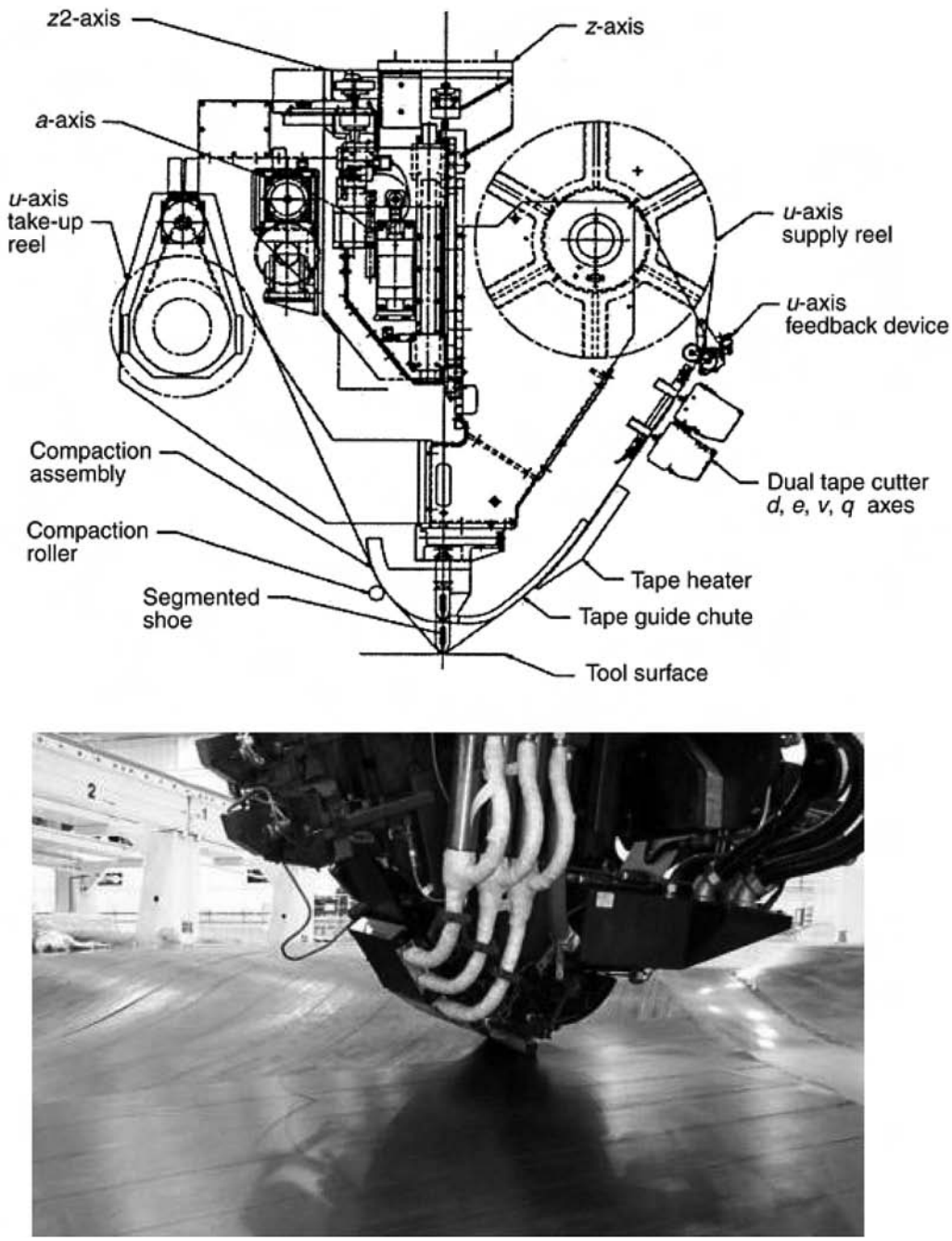


Fig. 5.7 Composite tape layer delivery head. Source: The Boeing Company

(longitudinal) plies pose no problems. In addition, a typical fiber placement machine (Fig. 5.10) contains 12, 24, or 32 individual tows that may be cut separately and then added back in during the placement process. Since the tow width normally ranges from 0.125 to 0.182 in. (3.2 to 4.6 mm), bands as wide as 1.50 to 5.824 in. (38.1 to 148.0 mm) can be applied, depending on whether a 12- or 32-tow head is used. The adjustable tension employed during this process

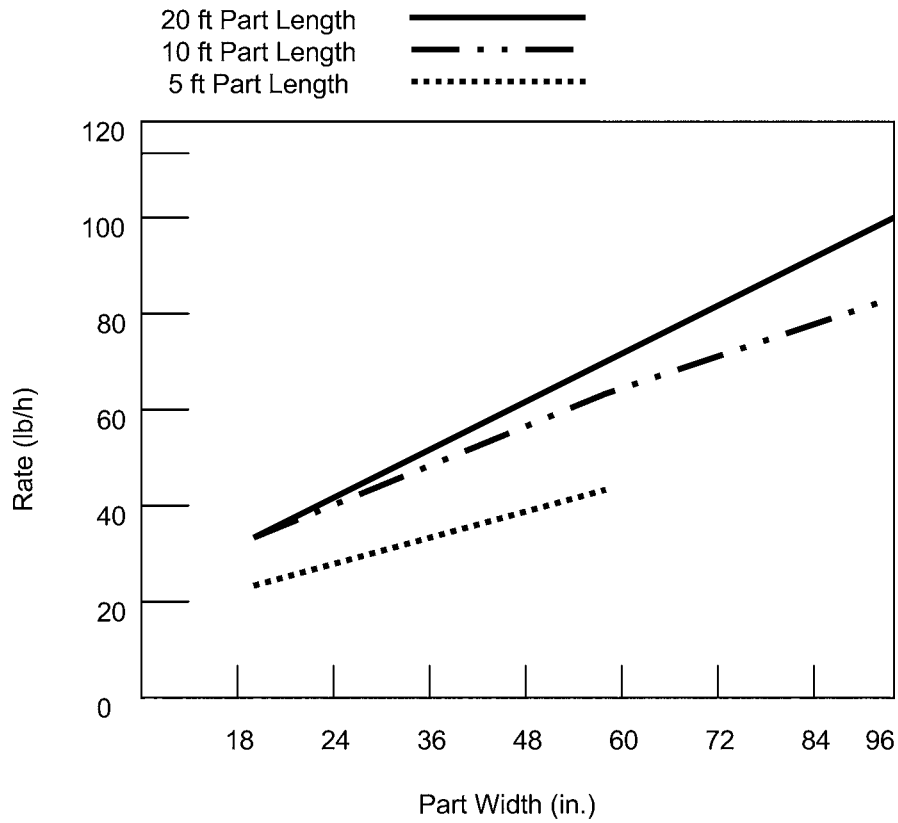


Fig. 5.8 Tape-laying efficiency versus part size. Source: Ref 3

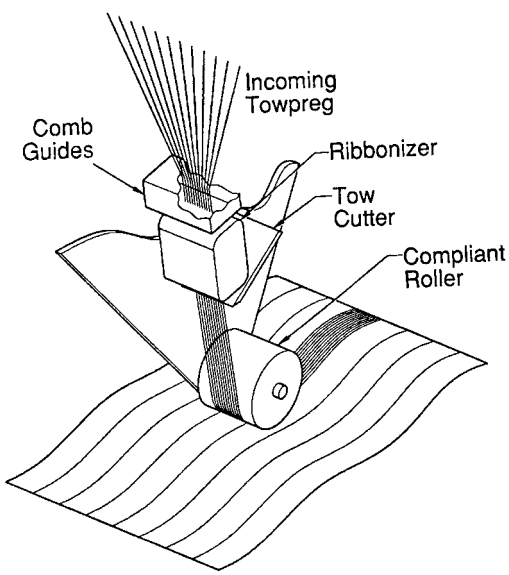


Fig. 5.9 Fiber placement process

also allows the machine to lay tows into concave contours, limited only by the diameter of the roller mechanism. This allows complicated ply shapes similar to those that can be obtained by hand lay-up. In addition, the head contains a compliant compaction roller that applies pressure in the range of 10 to 400 lb (4.5 to 180 kg) during the process, effectively debulking the laminate during lay-up. Advanced fiber placement heads also contain heating and cooling capability. Cooling is used to decrease the towpreg tack during the cutting, clamping, and restarting processes, while heating can be used to increase the tack and compaction during lay-down. For the current generation of fiber placement heads, a minimum convex radius of approximately 0.124 in. (3.1 mm) and a minimum concave radius of 2 in. (5.1 cm) are obtainable. One limitation of the fiber placement process is that there is a minimum course (or ply) length, normally about 4 in. (10.2 cm). This is a result of the cut-and-add process. A ply that is cut or added must then pass under the compliant roller, resulting in

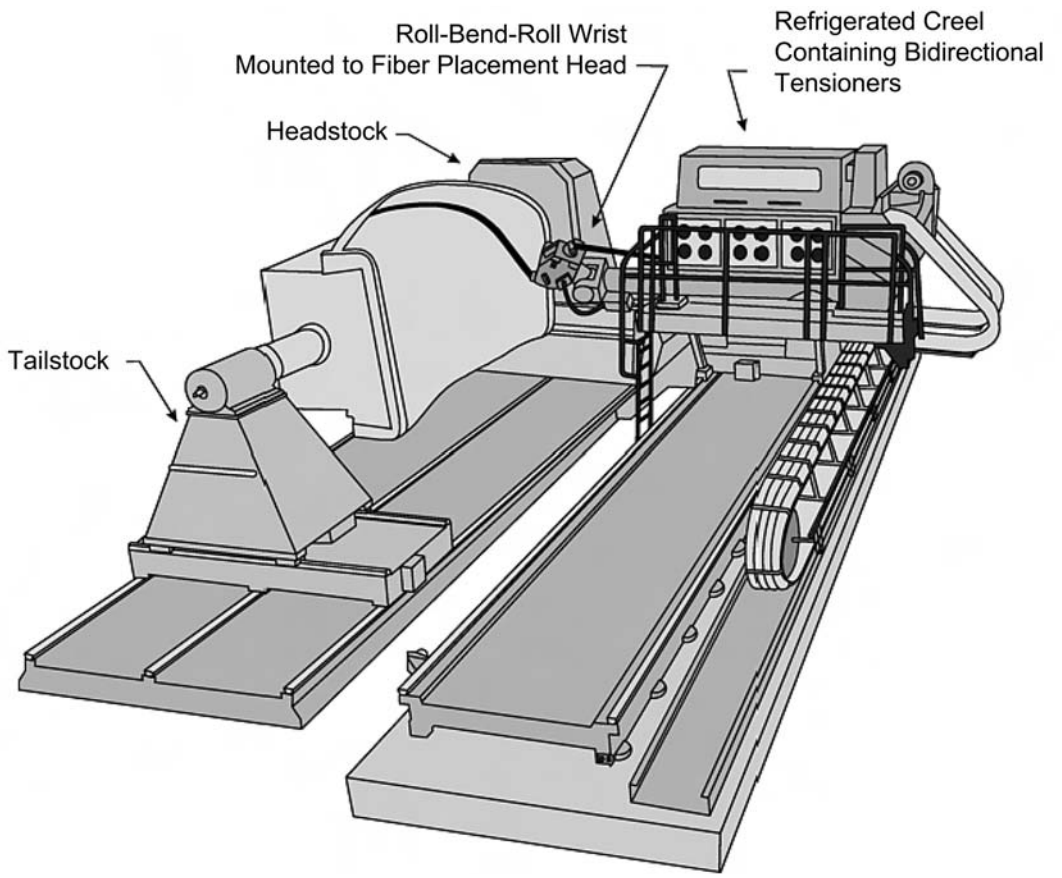


Fig. 5.10 Fiber placement machine. Source: Ref 4

a minimum length that is dependent on the roller diameter.

Fiber placed parts are usually autoclave cured on carbon/epoxy, steel, or low-expansion Invar™ tools to provide dimensionally accurate parts. Typical applications for fiber placement are engine cowls, inlet ducts, fuselage sections, pressure tanks, nozzle cones, tapered casings, fan blades, and C-channel spars. The aft section of a V-22 fuselage, in which the skin is fiber placed over cocured stiffeners, is shown in Fig. 5.11.

Extensive testing has shown that the mechanical properties of fiber-placed parts can be essentially equivalent to those of hand layed-up parts. As with hand layed-up parts, gaps and overlaps are typically controlled to 0.030 in. (0.8 mm) or less. One difference between fiber-placed and hand layed-up plies is the *stair-step* ply terminations obtained with fiber placement, since each tow is cut perpendicular to the fiber direction. Again, this stair-step ply termination has been shown to be equivalent in properties to the smooth transition obtained with manual lay-up. In fact, some parts have been designed so that either fiber placement or manual hand lay-up may be used for fabrication. Since the tows are added in and taken out as needed, there is very little wasted material; scrap rates of only two to five percent are common in fiber placement. In addition, since the head can "steer" the fiber tows, there is the potential for the design of highly efficient load-bearing structure.

The software required to program and control a fiber placement machine is even more complex than that required for an automated tape layer or a modern filament winder. The software translates CAD part and tooling data into five-axis commands, developing the paths and tool rotations for applying the composite tows to the part's curved and geometric features while keeping the compaction roller normal to the surface. A simulator module confirms the

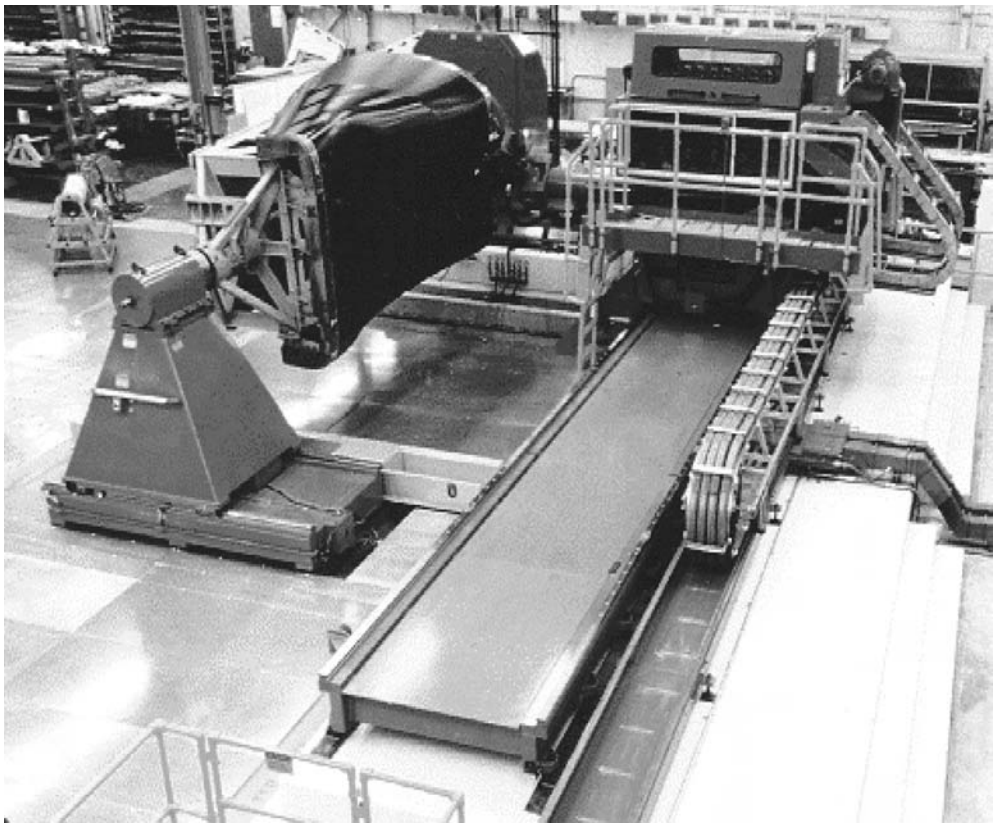


Fig. 5.11 V-22 aft fuselage. Source: The Boeing Company

part program with three-dimensional animation, while integrated collision avoidance post-processing of the NC program automatically detects interferences.

Modern fiber placement machines are extremely complex and can be very large installations. Most machines contain seven axes of motion (cross-feed, carriage traverse, arm tilt, mandrel rotation, and wrist yaw, pitch, and roll). The larger machines are capable of handling parts up to 20 ft (6 m) in diameter and 70 ft (20 m) long, with mandrel weights up to 80,000 lb (36.3 metric tons). They typically contain refrigerated creels for the towpreg spools, towpreg delivery systems, redirect mechanisms to minimize twist, and tow sensors to sense the presence or absence of a tow during placement.

Although complex part geometries and lay-ups can be fabricated using fiber placement, the biggest disadvantages are that the current machines are very expensive and complex and the lay-down rates are slow compared to most conventional filament winding operations.

5.2.5 Vacuum Bagging

After ply collation, the laminate is sealed in a vacuum bag for curing. A typical bagging schematic is shown in Fig. 5.12. To prevent resin from escaping from the edges of the laminate, dams are placed around the periphery of the lay-up. Typically, cork, silicone rubber, or metal dams are used. The dams should be butted up against the edge of the lay-up to prevent resin pools from forming between the laminate and the dams. The dams are held in place with either double-sided tape or Teflon pins.

If the surface will be bonded or painted, a peel ply may be applied directly to the laminate surface. Then a layer of porous release material, usually a layer of porous glass cloth coated with Teflon, is placed over the lay-up. This layer allows resin and air to pass through the layer without the bleeder material bonding to the laminate surface. The bleeder material can be a synthetic material (e.g., polyester mat) or dry fiberglass cloth, such as style 120 or 7781 glass. The amount

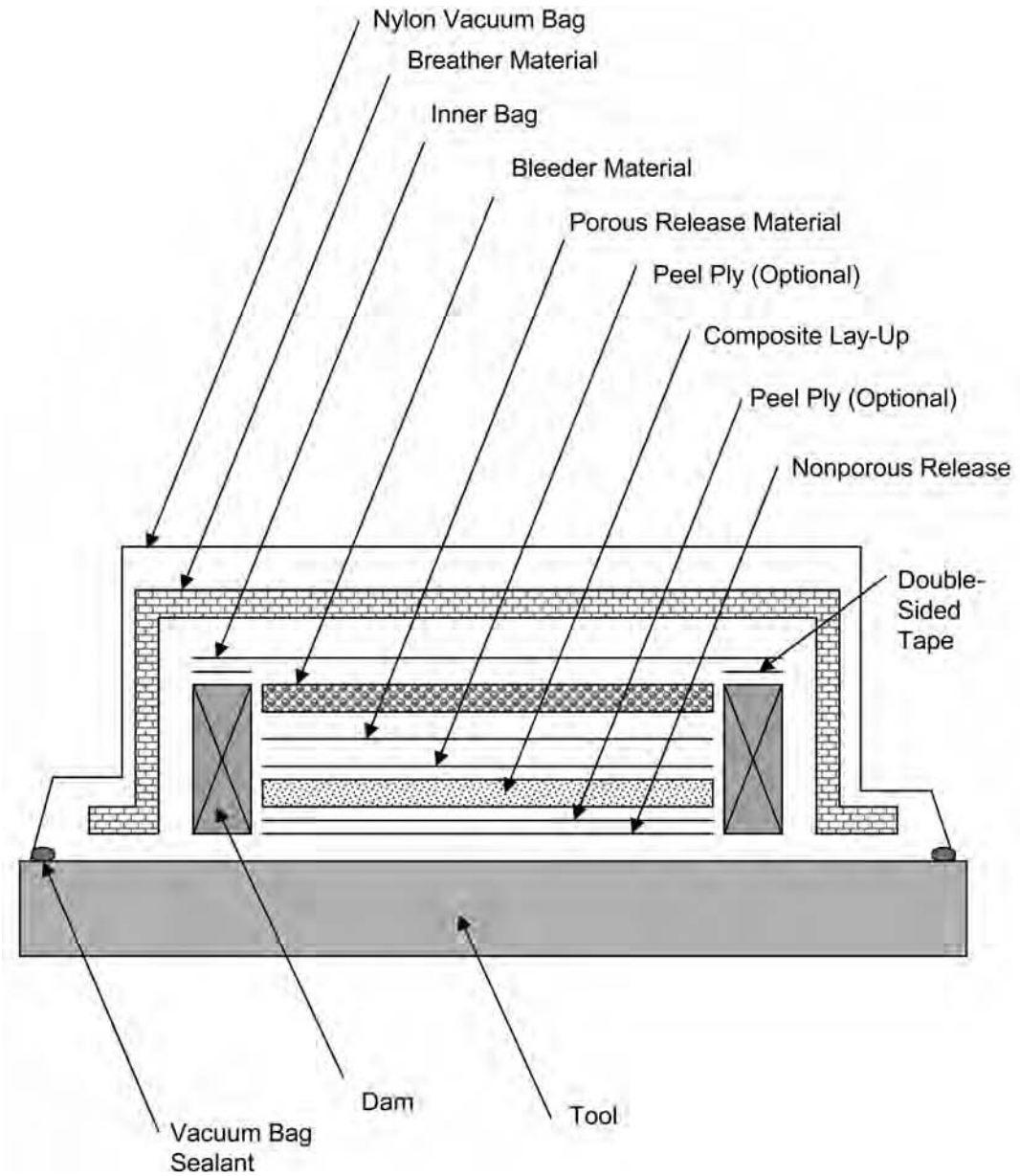


Fig. 5.12 Typical vacuum-bagging schematic

of bleeder material depends on the laminate thickness and the desired amount of resin to be removed. For the newer net resin content prepregs, bleeder cloth is not required since it is not necessary to remove any excess resin.

After the bleeder is placed on the lay-up, an inner bag made of boPET (polyester, e.g., Mylar), polyvinyl fluoride (e.g., Tedlar), or polytetrafluoroethylene (e.g., Teflon) is placed over the lay-up. The purpose of the inner bag is to let air escape while containing the resin within the bleeder pack. The inner bag is sealed to the edge dams with double-sided tape and then perforated with a few small holes to allow air to escape into the breather system. The breather material is similar to the bleeder material; either a synthetic mat material or dry glass cloth can be used. If dry glass cloth is used, the last layer next to the vacuum

bag should no coarser than style 7781 glass. Heavy glass fabrics, such as style 1000, have been known to cause vacuum bag ruptures during cure. As a result of autoclave pressure, the nylon bagging material can be pushed down into the coarse weave of the fabric and rupture. The purpose of the breather is to allow air and volatiles to evacuate out of the lay-up during cure. Therefore, it is important to place the breather over the entire lay-up and extend it past the vacuum ports.

The vacuum bag, which provides the membrane pressure to the laminate during autoclave cure, is normally a 0.1 to 0.2 in. (3 to 5 mm) thick layer of nylon-6 or nylon-66. It is sealed to the periphery of the tool with a butyl rubber or chromate rubber sealing compound. Nylon vacuum bags can be used at temperatures up to 375 °F (190 °C). If the cure temperature is higher than 375 °F (190 °C), a polyimide material (such as DuPont's Kapton film) can be used up to approximately 650 °F (345 °C), along with a silicone bag sealant. Still higher temperatures usually require the use of a metallic bag (e.g., aluminum foil) and a mechanical sealing system. It should be noted that polyimide bagging films are stiffer and harder to work with than nylon. Some manufacturers have invested in reusable silicone rubber vacuum bags to reduce costs and lessen the chance of a leak or bag rupture during cure. These bags normally require some type of mechanical seal to the tool. Also, if the part is large, reusable rubber vacuum bags become heavy and difficult to handle, so they may require an overhead handling system to facilitate their installation and removal. There are suppliers who sell both of the materials to make silicone rubber vacuum bags or provide a complete bag and sealing system ready for use.

Caul plates, or pressure plates, can be used to provide a smoother part surface on the bag side. Caul plates are frequently made of mold release coated aluminum, steel, fiberglass, or glass-reinforced silicone rubber. They range in thickness from 0.060 in. (1.5 mm) up to about 0.125 in. (3.2 mm). The design of a caul plate and its location in the lay-up are important considerations in achieving the desired surface finish. The caul plate may be placed above or within the bleeder pack, but close to the laminate surface to provide a smooth surface. However, it will then require a series of small holes (e.g., 0.060 to 0.090 in. (1.5 to 2.3 mm) diameter) to allow resin to pass through the caul plate into the top portion of the bleeder pack. It should be noted that a caul plate containing holes is not placed next to the laminate surface, because the holes will mark off on the laminate surface. In general, the farther the caul plate is from the laminate surface, the less effective it is in producing a smooth surface due to the cushioning effect of increasing amounts of bleeder material.

The current trend in the composites industry is to use net or near-net resin systems (32 to 35 percent resin by weight), which require little or no bleeding, in contrast to the more traditional 40 to 42 percent resin systems. Since the labor and cost of the bleeder material are eliminated, the bagging system is simplified. However, when using this type of system, it is even more important to seal the inner bag system properly to prevent resin loss during cure or resin-starved laminates may result. The edges are a particularly critical area, where excessive gaps or leaks in the dams can result in excessive resin loss and thinner than desired edges. In addition to eliminating the need for a bleeder pack, net resin content prepregs produce laminates with a more uniform thickness and resin content. The problem with the traditional 40 to 42 percent resin content prepregs is that as the laminate gets thicker (i.e., the number of plies increases), the ability to bleed resin through the thickness decreases. As more bleeder is added, the plies closest to the surface become overbled, while those in the middle and on the tool side of the laminate are underbled.

5.2.6 Curing

Autoclave curing is the most widely used method of producing high-quality laminates in the aerospace industry. An autoclave works on the principle of differential gas pressure, as illustrated in Fig. 5.13. The vacuum bag is evacuated to remove the air, and the autoclave supplies gas pressure to the part. Autoclaves are extremely versatile pieces of equipment. Since the gas pressure is applied isostatically to the part, almost any shape can be cured in an autoclave. The only limitations are the size of the autoclave and the large initial capital investment required to purchase and install it. A typical autoclave system, shown in Fig. 5.14, consists of a pressure vessel, a control system, an electrical system, a gas generation system, and a vacuum system. Autoclaves lend considerable versatility to the manufacturing process. They can accommodate a single large composite part, such as a large wing skin, or numerous smaller parts loaded

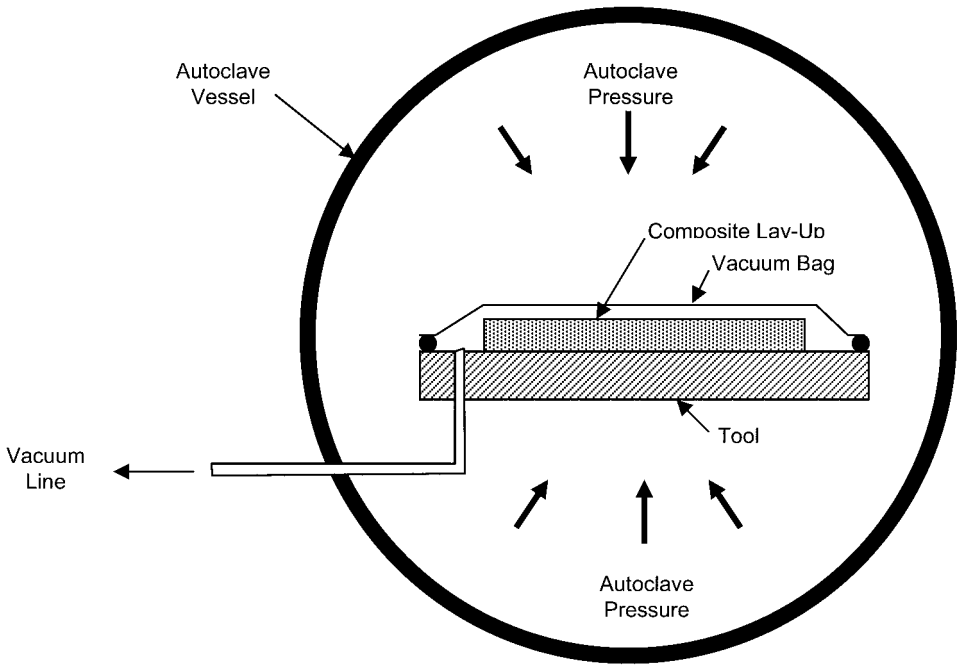


Fig. 5.13 Principle of autoclave curing



Fig. 5.14 Typical production autoclave

onto racks and cured as a batch. While autoclave processing is not the most significant cost driver of the total part cost, it does represent a culmination of all of the previously performed manufacturing operations, because final part quality (per ply thickness, degree of crosslinking, and void and porosity content) is often determined during this operation.

Autoclaves are normally pressurized with inert gas, usually nitrogen or carbon dioxide. Air can be used, but it increases the danger of a fire within the autoclave during the heated cure cycle. The gas is circulated by a large fan at the rear of the vessel and passes down the walls next to a shroud containing the heater banks, usually electrical heaters. The heated gas strikes the front door and then flows back down the center of the vessel to heat the part. There is considerable turbulence in the gas flow near the door, which produces higher velocities that stabilize as the gas flows toward the rear. The practical effect of this flow field is that higher heating rates are encountered for parts placed close to the door; however, the flow fields are dependent on the actual design of the autoclave and its gas flow characteristics. Another problem that can be encountered is blockage, in which large parts can block the flow of gas to smaller parts located behind them. Manufacturers typically use large racks to ensure uniform heat flow and maximize the number of parts that can be loaded for cure.

Composite parts can also be cured in presses or ovens. The main advantage of a heated platen press is that much higher pressures such as 500 to 1000 psi (3400 to 6900 kPa) can be used to consolidate the plies and minimize void formation and growth. Presses are often used with polyimides that give off water, alcohols, or high boiling point solvents, such as *N*-methylpyrrolidone. On the other hand, presses usually require matched metal tools for each part configuration and are limited by platen size to the number of parts that can be processed at one time. Ovens, usually heated by convective forced air, can also be used to cure composite flow (bleed) and allow volatiles to escape. However, since pressure is provided only by a vacuum bag ≤14.7 psia (101 kPa), the void contents of the cured parts are normally much higher (for example, five to ten percent) than those of autoclave-cured parts (less than one percent).

Addition Curing Thermoset Composites. A typical cure cycle for a 350 °F (175 °C) curing thermoset epoxy part is shown schematically in Fig. 5.15. It contains two ramps and two isothermal holds. The first ramp and isothermal hold, usually in the range of 240 to 280 °F (115 to 135 °C), is used to allow the resin to flow (bleed) and volatiles to escape. The imposed viscosity curve on the figure shows that the semisolid resin matrix melts on heating and experiences a dramatic drop in viscosity. The second ramp and hold is the polymerization portion of the cure cycle. During this portion, the resin viscosity initially drops slightly due to the application of additional heat, and then rises dramatically, as the kinetics of the resin start the crosslinking process. The resin gels into a solid and the crosslinking process continues during the second isothermal hold, usually at 340 to 370 °F (170 to 185 °C) for epoxy resin systems. The resin is held at this cure temperature for normally four to six hours, allowing time for the crosslinking process to be completed. It should be noted that as the industry has moved towards net resin content systems, the use of the first isothermal hold which allows time for resin bleeding, has been eliminated by many manufacturers, resulting in a straight ramp-up to the cure temperature.

Even though high pressures such as 100 psi (690 kPa) are commonly used during autoclave processing to provide ply compaction and suppress void formation, porosity and voids can be problems, even with addition-curing thermosets. A detailed discussion of the causes of voids and porosity is presented in Chapter 7, "Processing Science of Polymer Matrix Composites."

Condensation Curing Systems. The chemical composition of a thermoset resin system can dramatically affect volatile evolution, resin flow, and reaction kinetics. Addition-curing polymers, in which no reaction by-products are given off during crosslinking, are, in general, much easier to process than condensation systems. Because of the reaction by-products and solvents that evolve during processing, condensation systems, such as phenolics and polyimides, are extremely difficult to process without voids and porosity.

Condensation curing systems, such as polyimides and phenolics, give off water and alcohols as part of their chemical crosslinking reactions. In addition, to allow prepregging, the polymer reactants are often dissolved in high-temperature boiling point solvents, such as dimethylformamide, dimethylactamide, *N*-methylpyrrolidone, or dimethylsufoxide**.** Even the addition-curing polyimide PMR-15 uses methanol as a solvent for prepregging. The eventual evolution of these volatiles during cure creates a major volatiles management problem, which can result in high void and porosity percentages in the cured part. Unless a heated platen press or a hydroclave with extremely high pressures for example, 1000 psi (6900 kPa) is used to keep the volatiles in solution until gelation, they must be removed during cure heat-up when resin viscosity is low. In addition, since

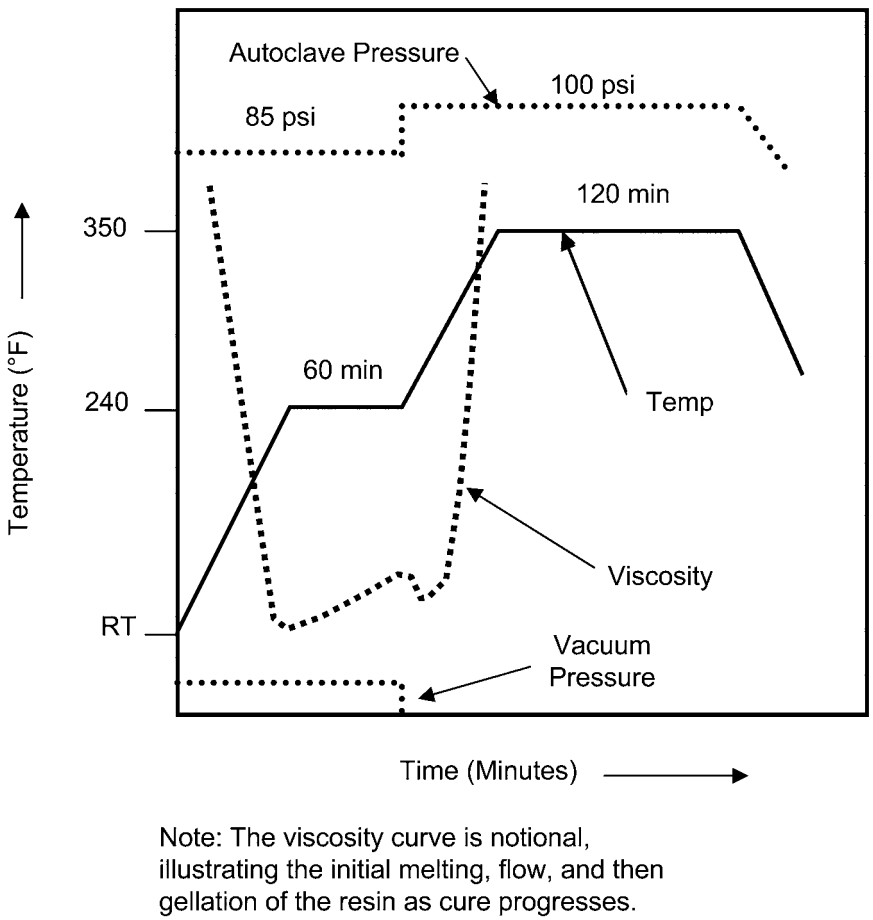


Fig. 5.15 Typical autoclave cure cycle. RT, room temperature

these materials boil or condensate at different temperatures during heat-up, it is important to know the point(s) during the cycle when the different species will evolve.

There are three strategies for volatile management: (1) use a press or a hydroclave with an applied hydrostatic resin pressure greater than the volatile vapor pressure to keep the volatiles in solution until the resin gels; (2) remove the volatiles by laying up only a few plies at a time and hot debulking under vacuum bag pressure at a temperature higher than the volatile boiling point; or (3) use slow heat-up rates and vacuum pressure during cure, with intermediate holds, to remove the volatiles before resin gelation. It should be noted that more than one of these strategies can be used at the same time. The advantage of a heated platen press or hydroclave is that high pressures can be used to suppress volatile evolution. However, the tooling must be designed to withstand the higher pressures, and special damming systems must be incorporated to prevent excessive resin squeeze-out. The second method, intermediate hot debulks under vacuum pressure, is effective but very costly and labor intensive, since the ply collation operation has to be interrupted every several plies and the part must be bagged and moved to an oven, hot debulked, and then cooled before further collation. The last method, as shown in Fig. 5.16 for a typical autoclave cure cycle for PMR-15, incorporates multiple holds under vacuum during heat-up to evacuate the volatiles during various points in the cure cycle. Frequently, only a partial vacuum is used during the early stages of cure, with a full vacuum applied later in the cycle. After all of the volatiles have been evacuated, full autoclave pressure is applied. Although the

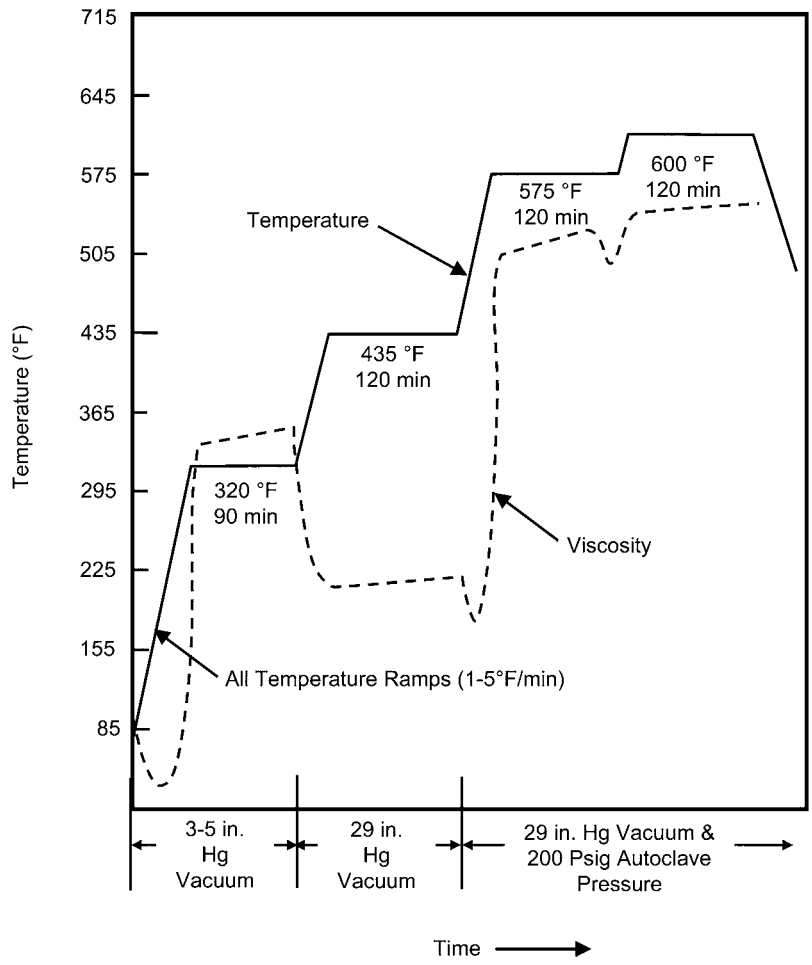


Fig. 5.16 Typical PMR-15 cure cycle

final cure of PMR-15 is an addition reaction, it undergoes condensation reactions early in the cure cycle during the imidization stage, which creates a volatile management problem. The difficult part to this approach is determining the optimum times and temperatures for the hold periods and the heat-up rates to use. Physiochemical test methods can be used in helping to design these cure cycles. To obtain full crosslinking, polyimides often require extended postcure cycles. Note that even the postcure cycle incorporates multiple hold periods during heat-up to help minimize residual stress buildup and reduce the likelihood of matrix microcracking.

5.3 Low-Temperature Curing/Vacuum Bag Systems

Low-temperature curing/vacuum bag (LTVB) prepregs were originally developed for building composite tooling. However, over the last 15 years, they have evolved to the point where they are useful for making composite structural

parts. They are normally supplied as carbon fabric prepregged with a low-temperature curing epoxy resin; however, other reinforcements and even unidirectional material forms are available. These materials have several advantages over wet lay-up: (1) because they are prepregs, the resin content is much more tightly controlled; (2) there is no chance for mixing errors that can occur with liquid resins; (3) much higher fiber volumes are obtainable (in this case, 55 to 60 percent versus 30 to 50 percent for a typical wet lay-up); (4) these materials are net resin content prepregs that do not require bleeding of excess resin during cure; and (5) they are available in both unidirectional tape and woven cloth product forms. Their disadvantage is that they cost as much as conventional 250 to 350 °F (120 to 175 °C) curing prepregs; however, much of the additional material cost is offset by the labor involved in wet lay-up to mix the resin, impregnate the dry plies, and then roll out air and excess resin. As for wet lay-up, the main driver for using LTVB materials is the ability to make large parts with minimal tooling investment. These prepregs have been successfully used in a number of low-rate-prototype aerospace programs.

Since these materials are formulated to initially cure at temperatures in the range of 100 to 200 °F (35 to 95 °C), they contain very reactive curing agents, and their working life is normally short compared to that of conventional prepregs. In general, the lower the cure temperature, the shorter the out-time. For example, there are materials that initially cure at temperatures as low as 100 °F (35 °C) for 14 hours under vacuum bag pressure, but the total out-time for the material is only two to three days. On the other hand, if tooling can be designed to tolerate temperatures of 150 °F (65 °C) for 12 hours, the out-time increases to five to seven days at room temperature. A typical cure and postcure cycle is shown in Fig. 5.17. The manufacturing approach is to initially cure the part at low temperatures such as 175 to 200 °F (80 to 95 °C) for four to six hours under a vacuum bag on an inexpensive tool. Low-cost tooling can be made from plywood, plaster, syntactic core, tooling dough, or other materials. Heat for cure can be provided by placing the part in an oven or by building a low-cost foam oven with hot air blowers around the part. The initial low-temperature cure produces a

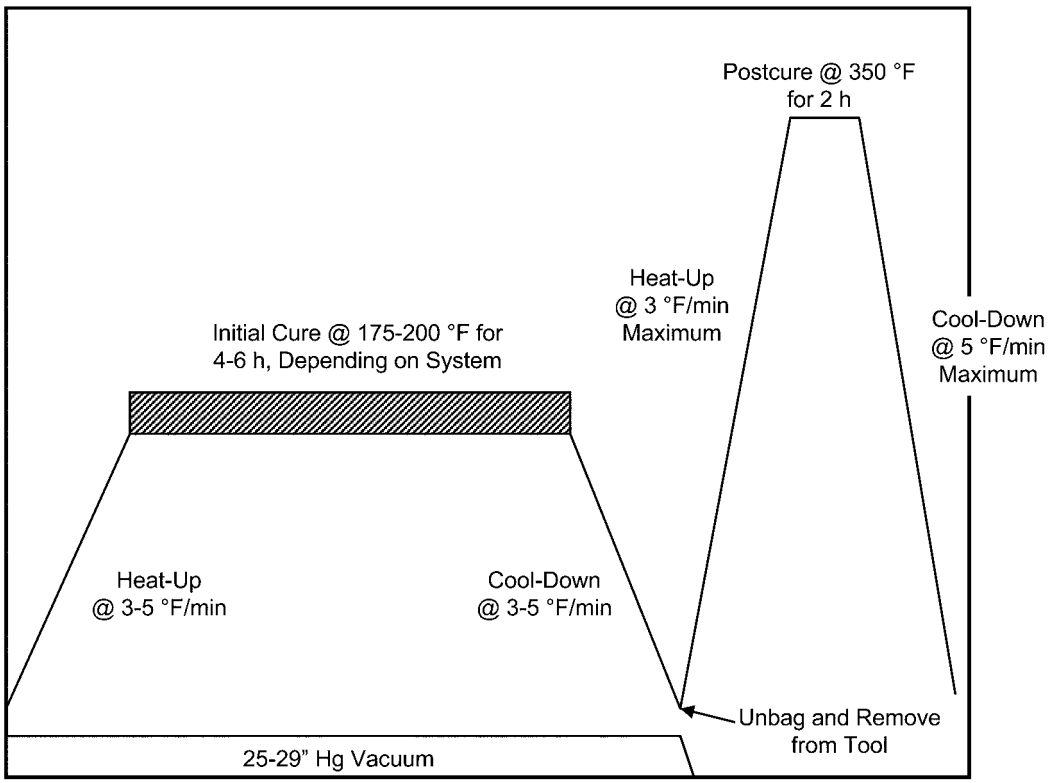


Fig. 5.17 Notional cure cycle for low-temperature curing/vacuum bag prepreg parts

part that is approximately 40 to 50 percent cured. After the initial cure, the part is removed from the tool and postcured at 350 °F (175 °C) to optimize its mechanical properties and elevated-temperature resistance. Lower-temperature postcures can be used if the service temperature is lower. During the initial cure, the part develops enough green strength to prevent it from sagging or warping during postcure. As the part heats up to the postcure temperature, the glass transition temperature T_g steps ahead of the postcure temperature to prevent part distortion. Since the initial cure is done at low temperatures less than 212 °F (100 °C) water and volatile vapor pressure should not be a problem, as they can be for the 250 to 350 °F (120 to 175 °C) curing systems.

When LTVB materials were first developed for use on aerospace prototype vehicles, excessive porosity was a problem. Depending on the material (for example, fabric style) and lay-up orientation, porosity levels as high as three to five percent were occasionally experienced. This is not surprising, since the only consolidation pressure during cure is vacuum pressure less than 15 psia (103 kPa). Since the initial cure is done at low temperatures less than 212 °F (100 °C), water and volatile vapor pressure should not be a problem, as they can be for the 250 to 350 °F (120 to 175 °C) curing systems. It should be noted that a conventional 350 °F (175 °C) curing prepreg cured under only vacuum pressure will contain five percent or more porosity due to the combination of entrapped air and volatiles such as water coming off during cure. However, air entrapped during lay-up can be a major problem for the low-temperature curing materials. Attempts were made to reduce porosity by reducing the viscosity of these resins. While this approach was partially successful, porosity remained a problem since the viscosity was constantly changing as the material aged during lay-up. To reduce or eliminate the porosity problem, manufacturers developed three methods to allow the air to escape during the initial portion of cure. The first method is a partially impregnated prepreg that was originally developed for 350 °F (175 °C) curing prepregs to help eliminate porosity. In partially impregnated prepregs, the resin is placed on the surfaces of the prepreg and contains some "dry fiber" in the middle to provide a path for the air to escape. On further heating during the initial cure, the resin flows in behind the evacuating air to fully impregnate the plies. A photomicrograph of a carbon/epoxy tape laminate made using this technique (Fig. 5.18**)** shows essentially no significant porosity. The second method is to coat only one surface of the prepreg with resin, which allows entrapped air to evacuate from the uncoated surface, and the resin again subsequently flows through the fiber bed to impregnate the plies. The third method consists of leaving narrow, unimpregnated bands 0.50 to 1.50 in. (12.7 to 38.1 mm) wide to allow the air to evacuate. These methods have been successful in reducing the porosity contents to less than one percent, essentially equivalent to those of autoclave-processed parts.

The success of making good parts with these materials is providing an escape route for air

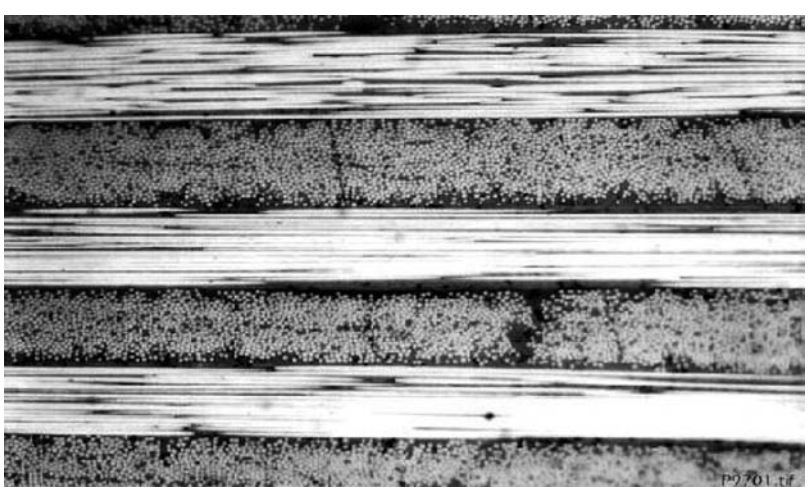


Fig. 5.18 Low-temperature vacuum bag (LTVB) cured laminate. Source: Ref 5

during the initial evacuation and cure; therefore, several precautions need to be taken during lay-up and bagging. During lay-up it is important to work as much air out of the lay-up as possible. When laying plies, one should tack them in the middle first and work outward toward the edges. Extreme care should be taken to make sure that there is no "bridging" or gaps between the plies, especially at the inside radii of stiffeners. The number of vacuum debulks should be minimized during lay-up, as these can often seal off the edges, making it harder to remove entrapped air. If debulks are required, edge breathers should be placed around the part and the vacuum bag should not pinch off at the edges. A recommended bagging schematic for debulking and cure is shown in Fig. 5.19, illustrating the importance of edge breathing and avoiding vacuum bag pinching during evacuation. Since the only source of pressure for consolidation of the plies is a vacuum, it is important to have a vacuum bag with no leaks and to pull as good a vacuum as possible during cure. The minimum acceptable vacuum is in the range of 25 in. (635 mm) of mercury or higher. Some manufacturers recommend that once the final bag is applied, the part should remain under vacuum for four to eight hours to allow all air to be evacuated. During cure, it is important not to exceed the manufacturer's recommended heat-up rates. These resins contain extremely reactive curing agents, and an exothermic reaction may occur if they are heated too rapidly.

It should be noted that these materials can also be processed in an autoclave. Since the initial cure temperature is low, many of the low-cost tooling approaches can still be used; however, the tool must be capable of withstanding autoclave pressures of 50 to 100 psi (345 to 690 kPa). While an autoclave may not always be available, it does provide positive pressure and allows more complex configurations to be made than a vacuum bag alone.

As shown in Fig. 5.20, the tooling cost for a large production program is minimal when it is amortized over a large number of parts; however, if only a few to several parts will be fabricated, tooling can be a substantial cost of the

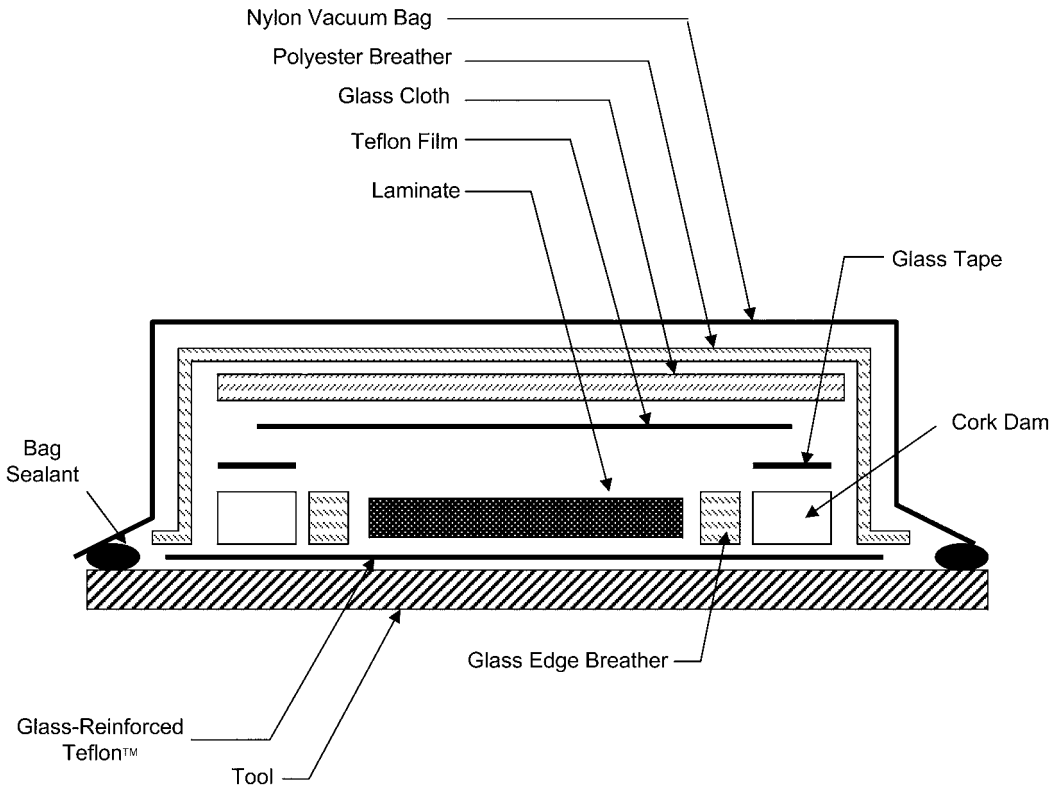


Fig. 5.19 Low-temperature vacuum bag (LTVB) bagging schematic. Source: Ref 5

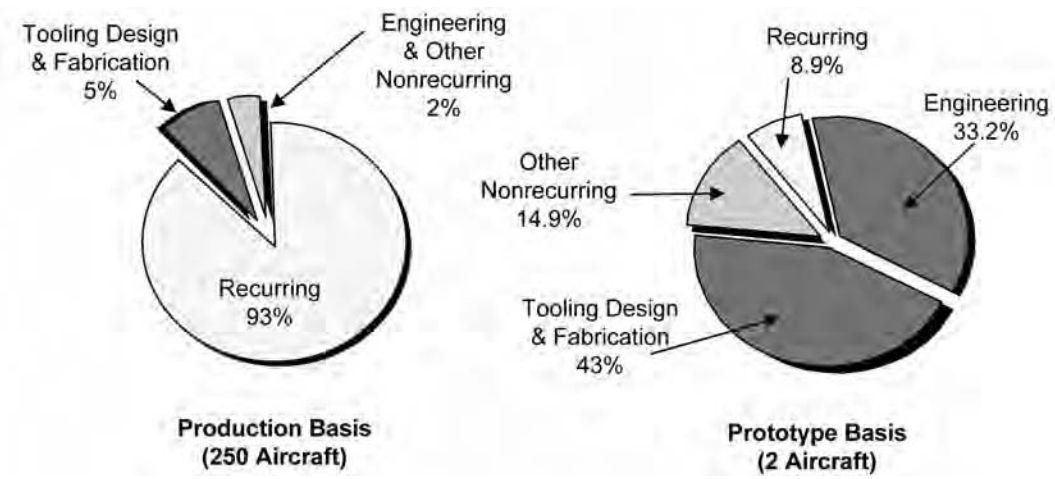


Fig. 5.20 Tooling cost comparison: production versus prototype program

total program—up to 40 percent if conventional autoclavable tooling is produced. These tooling approaches can be used for wet lay-up methods and low-temperature curing/vacuum bag prepregs.

Low-cost molds can be fabricated by a number of approaches, several of which are shown in Fig. 5.21. A number of facesheet materials can be used with a plywood substructure, including thin aluminum, drapable plywood, or wet layed-up or sprayed-up fiberglass if a master model is available. Many parts can be fabricated directly off of a master model constructed from plaster, NC machined polyurethane, or syntactic foams. Simple aluminum headers can be used if a full computer-aided design (CAD) model of the part is not available. For very large parts, the mold can be built in sections (Fig. 5.22) and then bonded together, splined smooth, and surface sealed.

5.4 Filament Winding

Filament winding is a high-rate process in which a continuous fiber band is placed on a rotating mandrel. Lay-down rates as high as 100 to 400 lb/h (45 to 180 kg/h) are not uncommon. Filament winding is also a highly repeatable process that can fabricate large and thick-walled structure. It is a mature process, having been in continuous use since the mid-1940s. It can be used to fabricate almost any body of revolution, such as cylinders, shafts, spheres, and cones. Filament winding can also fabricate a wide range of part sizes; parts smaller than 1 in. (25.4 mm) in diameter (for example, golf club shafts) and as large as 20 ft (6 m) in diameter have been wound. The major restriction on geometry is that concave contours cannot be wound, because the fibers are under tension and will bridge across the contour. Typical applications for filament winding are cylinders, pressure vessels, rocket motor cases, and engine cowlings. End fittings are often wound into the structure, producing strong and efficient joints.

A typical filament winding process is shown in Fig. 5.23. Dry tows are drawn through a bath containing liquid resin, collimated into a band, and then wound on a rotating mandrel. To deliver the fiber tows from the spool to the part, the band must pass through a series of guides, redirects, and spreader bars. During the entire delivery process, tension on the tows is minimized to preferably 1 lb (0.5 kg) or less. Low tension helps to reduce abrasion to the fibers, minimizes the possibility of tow breakage, and helps to spread the band as it passes over the spreader bar. Many modern filament winding machines are equipped with automatic tensioning devices to help control the amount of tension during the winding process.

Filament winding equipment costs can be low, moderate, or high, depending on part size, the type of winder, and the sophistication of the control system (mechanical or NC control). For high-rate applications, some winders have been designed with multiple pay-out systems and multiple mandrels so that several parts can be fabricated simultaneously. Filament-wound parts are usually cured in ovens rather than autoclaves, with

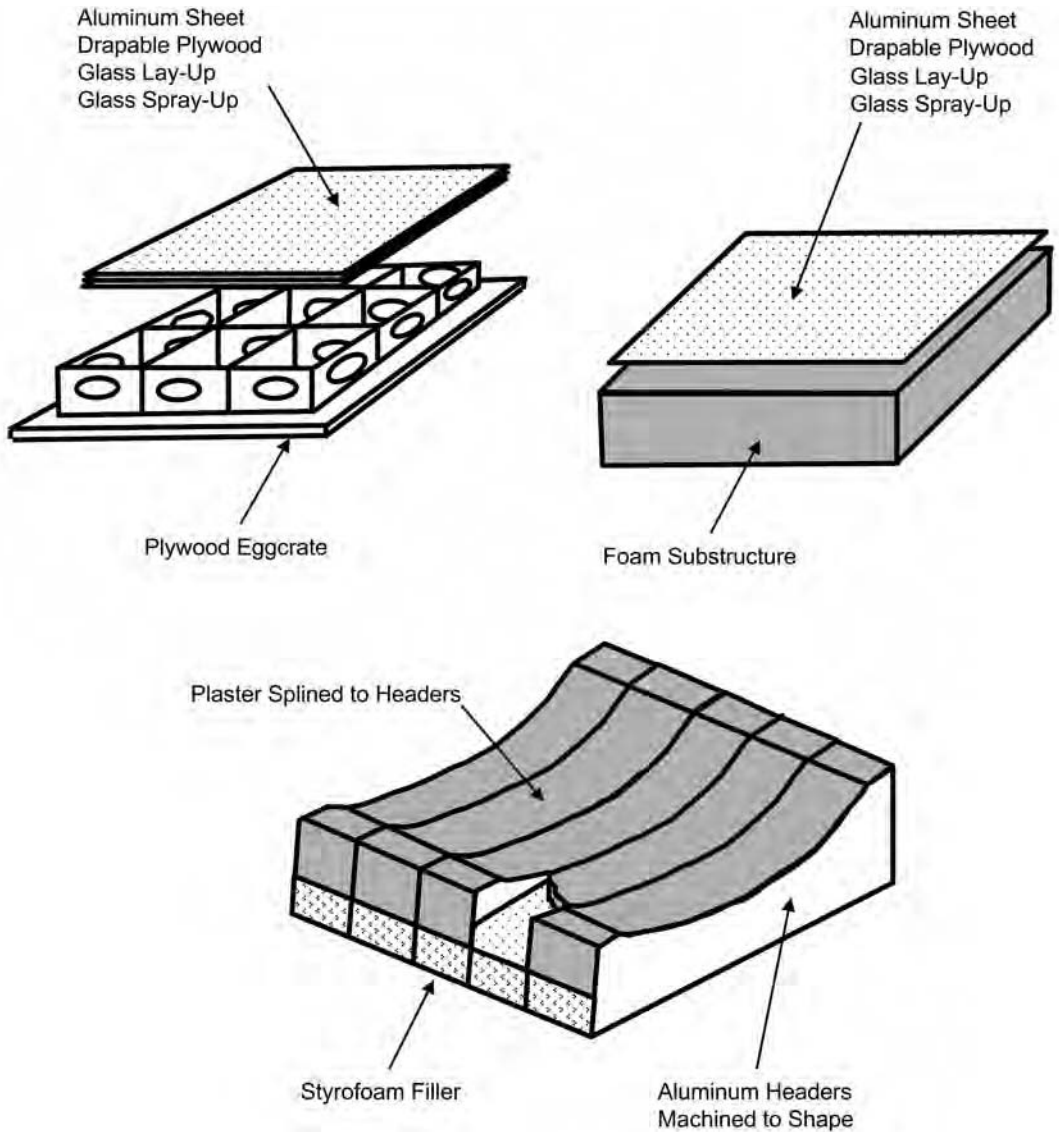


Fig. 5.21 Low-cost skin tools

the compaction pressure provided by mandrel expansion and fiber tension on the lay-up. Circular windings, separated from the part by caul plates or separator sheets, can also be used to provide compaction during cure. Forced-air convection ovens are the most common curing equipment. Others, such as microwave ovens, are faster but result in higher equipment costs.

Mandrel costs can be moderate to high, depending on part size and complexity. The mandrel must be able to be removed from the part. This is often accomplished by shrinkage of the mandrel during cool-down; incorporation of a slight draft or taper; and wash-out, plaster breakout, inflatable, or, for complex parts, segmented mandrels, which can be removed from the inside of the part in sections. While the inner surface (mandrel side) of the part is usually smooth, the outer surface can be quite rough. If this presents a problem, it is possible to wind sacrificial layers on the outer surface and then grind, or machine, the outer surface smooth after cure.

Fiber orientation can be a problem for some filament-wound designs; the minimum fiber angle that can usually be wound is 10 to 15 degrees due to slippage of the fiber bands at the mandrel ends.

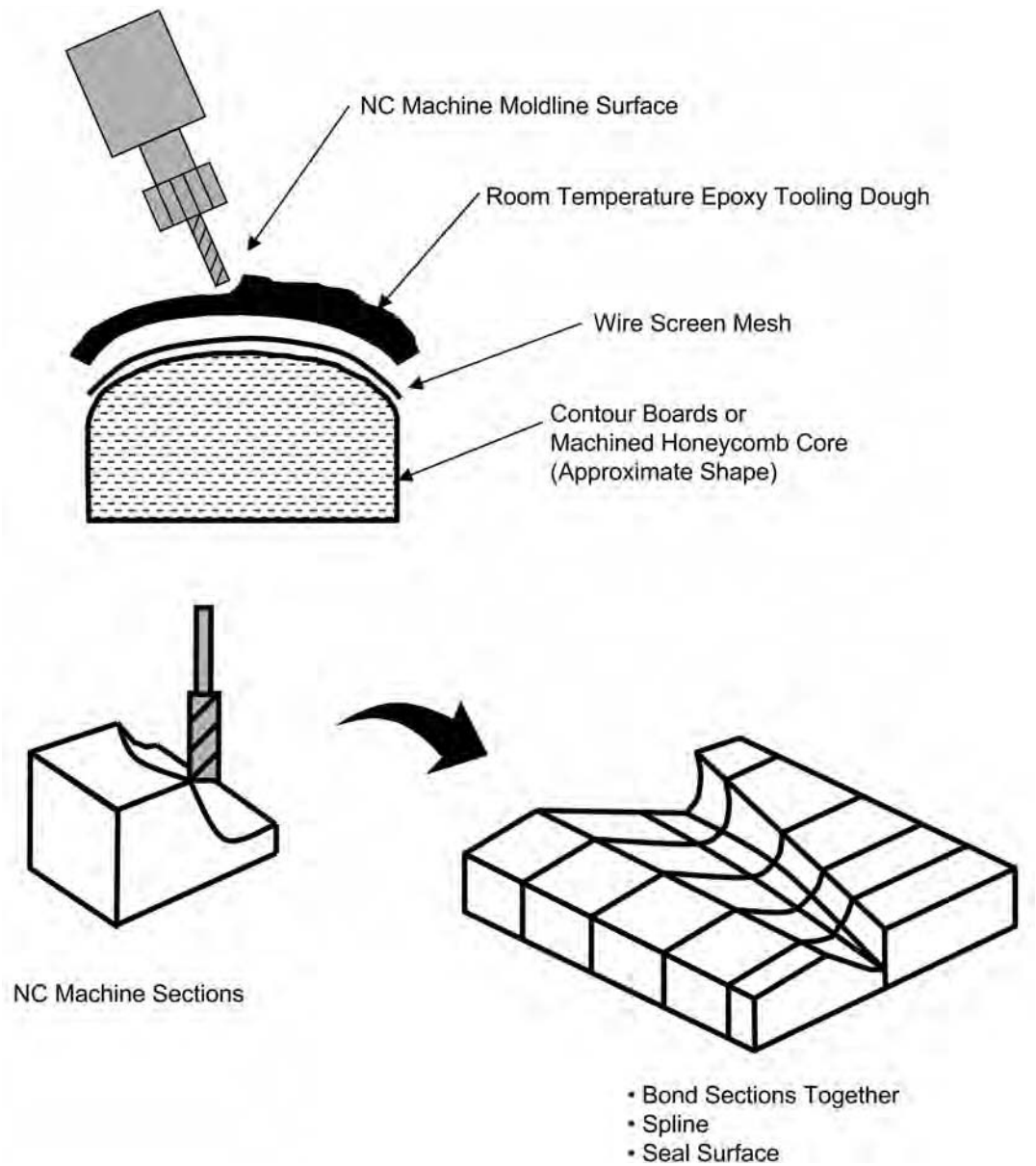


Fig. 5.22 Fabrication of large prototype lay-up tools. NC, numerical control

However, schemes such as inserting temporary pins in the mandrel ends during winding can sometimes be used to overcome this limitation.

Helical, polar, and hoop are the three dominant winding patterns used in filament winding (Fig. 5.24). Helical winding is a very versatile process that can produce almost any combination of length and diameter. In helical winding the mandrel rotates, while the fiber carriage traverses back and forth at the speed necessary to generate the desired helical angle (θ). As the band is wound, the circuits are not adjacent and additional circuits must be applied before the surface begins to be covered with the first layer. This winding pattern produces band crossovers at periodic locations along the part, which can be controlled somewhat by the newer NC-controlled winding machines. Due to this crossover winding pattern, a layer is made up of a two-ply balanced laminate. If the end dome openings are

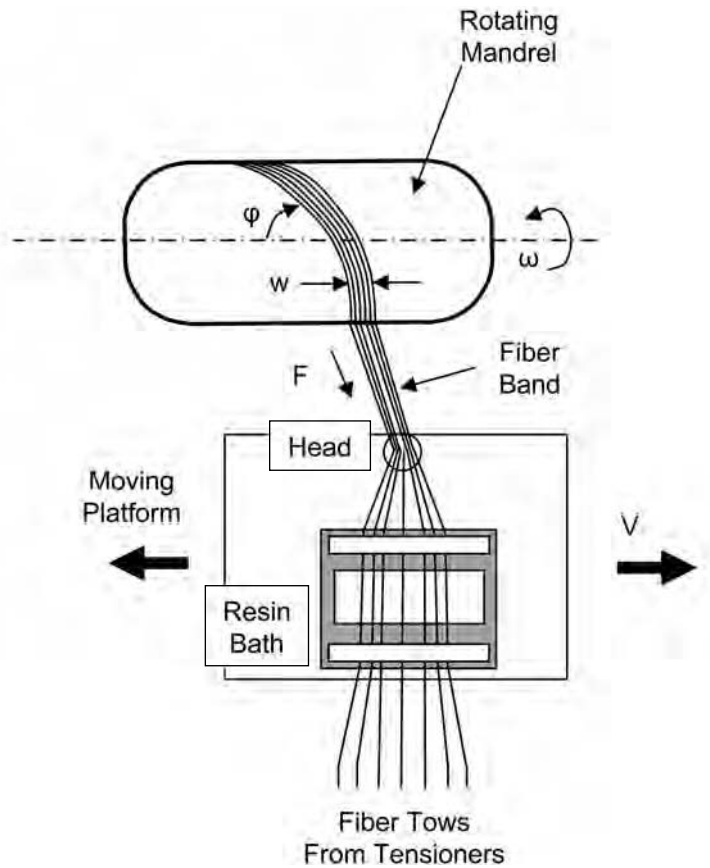


Fig. 5.23 Filament winding process. Source: Ref 27

the same size, a geodesic wind pattern may be used. This pattern produces the shortest band path possible and results in uniform tension in the filaments throughout their length. An additional advantage of the geodesic pattern is that it produces a no-slip condition; that is, there is no tendency for the bands to slip or shift on the mandrel surface.

Polar winding is somewhat simpler than helical winding in that (1) a constant winding speed can be used; (2) it is not necessary to reverse the carriage during winding; and (3) the bandwidths are laid adjacent to each other as the part is wound. Polar winding is an excellent method for fabricating spherical shapes. In this process, the bands pass tangentially to the opening at one end of the part, reverse direction, and then pass tangentially to the opening at the opposite end of the part. The lay-down is planar, with the bandwidths adjacent to each other since the winding arm generates a great circle during each pass. Simple polar winders have only two axes of motion, the mandrel and the winding arm. Polar winding machines are generally much simpler than helical winding machines, but they are also somewhat limited in their capabilities. For example, the length-to-diameter ratio must be less than 2.0. Polar winding machines are frequently used to wind spherical shapes by utilizing a continuous step-out pattern. A variation of the polar winder is the tumble winder, in which the mandrel is mounted at an inclined axis and tumbles in a polar path, while the roving strands remain stationary. While tumble winders are very efficient for spherical shapes, they are usually limited to diameters of 20 in. (0.5 m) or less.

Hoop winding, also known as *circumferential* or *circ winding*, is the simplest winding process. This winding action is similar to that of a lathe, where the mandrel speed is much greater than the carriage travel. Each full rotation of the mandrel advances the carriage one full bandwidth so that the bands are wound adjacent to each other. During part fabrication, hoop winding is often

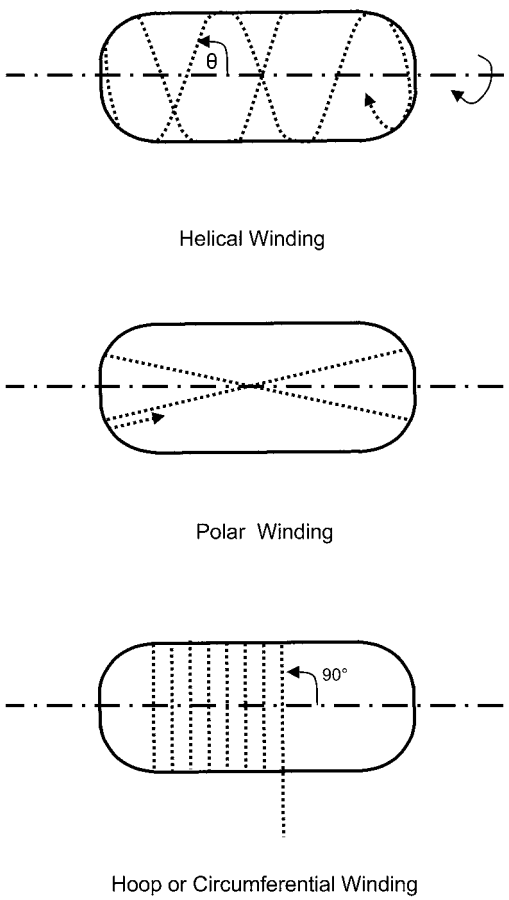


Fig. 5.24 Filament winding patterns. Source: Ref 7

combined with longitudinal (helical or polar) winding to provide adequate part strength and stiffness. The hoop windings are applied to the cylindrical portion of the part, while the longitudinal windings are applied to both the cylindrical and domed portions. It should again be pointed out that the minimum wind angle for longitudinal winding is generally about 10 to 15 degrees to preclude slippage of the bands at the ends of the mandrel.

There are three main variants of the filament winding process: (1) wet winding, in which the dry reinforcement is impregnated with a liquid resin just prior to winding; (2) wet-rolled prepreg winding, in which the dry reinforcement is impregnated with the liquid resin and then rewound prior to filament winding; and (3) towpreg winding, in which a commercially impregnated tow is purchased from a material supplier. The majority of filament winding fabricators formulate their own resin systems for both wet winding and wet-rolled prepreg. If a prepreg product form is specified, then they will normally purchase the preimpregnated tow from one of the major prepreg suppliers. Viscosity and pot life are two of the main factors in selecting a resin for wet winding. Low viscosity, generally around 2000 centipoise, is desirable to help wet the fibers, spread the band, and lower the friction over the guides during the winding process. Pot life is primarily a function of the time it takes to wind the part; larger and thicker parts require a longer pot life than smaller and thinner parts. A number of premixed wet winding resin systems are also available from material suppliers. While preimpregnated tow (towpreg) is more expensive than wet winding resin systems, it has several important advantages: (1) a qualified fiber and resin system can often be prepregged onto a tow; (2) it allows the best control of resin content; (3) it allows the highest winding speeds because there is no wet resin that will be thrown off during winding; and (4) the tack can be adjusted to allow less slippage when winding shallow angles.

Wet winding is accomplished by pulling the dry tows either through a resin bath or directly over a roller that contains a metered volume of resin controlled by a doctor blade. The resin content of wet-wound parts is difficult to control, being affected by resin reactivity, resin viscosity, winding tension, pressure at the mandrel interface, and mandrel diameter. For example, a resin with too low viscosity will impregnate the strands thoroughly but will tend to squeeze out during the pressure of the winding operation, resulting in an excessively high fiber content. At the other extreme, a resin with too high viscosity will not sufficiently impregnate the strands, and there will be a tendency for the cured part to contain excessive porosity. Due to the generally low viscosity of wet winding resins, it is not uncommon to have parts with higher fiber volume percentages (70 percent and sometimes higher) than are normally found in composite parts fabricated with higher-viscosity prepreg resins (approximately 60 volume percent).

To circumvent some of the problems of controlling a direct wet winding process, wet-rolled prepreg is sometimes manufactured by wet impregnating the strands in the normal manner and then respooling them prior to winding. There are two main advantages to this process: (1) the fabricator can conduct off-line quality assurance testing on the wet-wound prepreg prior to use; and (2) the fabricator can control the viscosity

and tack somewhat by room temperature staging. Staging at room or slightly elevated temperature is commonly called *B-staging*. The objective is to advance the resin to increase the viscosity and tack. On the negative side, wet-wound prepreg has to be packaged and refrigerated for storage unless it is immediately used for winding.

Commercially supplied prepregs offer the best control of resin content, uniformity, and bandwidth control but are also the most expensive of the product forms, usually 1.5 to 2 times the cost of wet winding materials. While prepreg tows are the predominant prepreg form used in filament winding, some aerospace manufacturers specify slit prepreg tape to ensure extremely tight control of the bandwidth, and the resultant gaps, during the fiber placement or filament winding of flight-critical hardware. Prepreg tows for filament winding generally (1) have the longest pot lives; (2) allow higher winding speeds because there is less chance of "resin throw" during the winding process; and (3) allow winding angles closer to longitudinal (zero degrees) because they contain higher tack than most wet winding systems and do not tend to slip as much at the ends.

The choice of a mandrel material and design is to a great extent a function of the design and size of the part to be built. Many materials have been used for filament winding mandrels. Dissolvable mandrels are often used for parts with only small openings. This type of mandrel includes water-soluble sand, water-soluble or breakout plaster, low-temperature eutectic salts, and occasionally low-melting-point metals. After cure, the disposable mandrel is dissolved out with hot water, melted, or broken into small pieces for removal. An alternative to these approaches is to use an inflatable mandrel that can be either left inside the part as a liner or extracted through an opening. Reusable mandrels can either be segmented or nonsegmented. Segmented mandrels are required when the geometry of the part does not allow it to be removed by simply sliding it off the mandrel after cure. Segmented mandrels are generally more expensive to fabricate and use than nonsegmented mandrels. Nonsegmented mandrels usually have a slight draft or taper to ease part removal after cure.

After the winding operation is complete, wet-wound parts are often B-staged prior to final cure to remove excess resin by heating the part to a slightly elevated temperature but below the resin gel temperature. Frequently, the part is heated with heat lamps and the excess resin is removed as the part rotates. The majority of filament-wound parts are cured in an oven (electric, gas-fired, or microwave) without a vacuum bag or any other supplemental method of applying pressure. As the part heats up to the cure temperature, the mandrel expands but is constrained by the fibers in the wound part. This creates pressure that helps to compact the laminate and reduce the amount of voids and porosity. Since the majority of filament-wound parts are cured in ovens rather than autoclaves, filament winding is capable of making very large structures, limited only by the size of the winder and the curing oven available.

Autoclave curing may also be used to further reduce the amount of porosity; however, the compaction pressure applied by an autoclave can also induce fiber buckling and even wrinkles in the part. The use of thin caul plates that are allowed to slip over the surface may help to alleviate some wrinkling on cylindrical surfaces, but these plates are prone to leaving mark-off on the part surface where they terminate. Caul plates with circumferential windings over their outside surface have also been used in oven-cured parts to improve compaction and provide a smoother surface finish. Occasionally, the part will be wrapped with shrink tape to provide compaction pressure, a common method employed in manufacturing carbon fiber golf club shafts.

5.5 Liquid Molding

Liquid molding comprises a number of composite fabrication processes that are capable of fabricating extremely complex and dimensionally accurate parts. One of the main advantages of liquid molding is part-count reduction, in which a number of parts that would normally be made individually and either fastened or bonded together are integrated into a single molded part. Another advantage is the ability to incorporate molded-in features, such as the incorporation of a sandwich core section in the interior of a liquid-molded part. Resin transfer molding (RTM), the most widely used of the liquid molding processes, is a matched mold process that is well suited to fabricating three-dimensional structures requiring tight dimensional tolerances on several surfaces. Excellent surface finishes are possible, mirroring the surface finish of the tool. The major limitation of the RTM process is the relatively high initial investment in the matched-die tooling. Sufficient part quantities, usually in the 100 to 5000 range, are necessary to justify

the high nonrecurring cost of the tooling. A summary of the advantages and disadvantages of the RTM process is presented in Table 5.1.

The RTM process consists of fabricating a dry fiber preform that is placed in a closed mold, impregnating with a resin, and then cured in the mold. The basic RTM process, shown in Fig. 5.25, consists of the following steps:

1. Fabricate a dry composite perform.
2. Place the preform in a closed mold.
3. Inject the preform with a low-viscosity liquid resin under pressure.
4. Cure the part at elevated temperature in the closed mold under pressure.
5. Demold and clean up the cured part.

Over the past several years many variations of liquid molding processes have been developed, including resin film infusion and vacuum-assisted resin transfer molding**.** The objective of all of these processes is to fabricate near-net molded composite parts at low cost. In this section, we will examine the basic RTM process and some of the major variants that have evolved over the past several years. A comparison of

Table 5.1 Resin transfer molding (RTM) process advantages and disadvantages

Advantages	Disadvantages
• Best tolerance control—tooling controls dimensions	• Mold and tool design critical to part quality
• Class A surface finish possible	• Tooling costs can be high for large production runs
• Surfaces may be gel coated for better surface finish	• Mold filling permeability based on limited permeability data base
• Cycle times can be very short	• Mold filling software still in development stages
• Molded-in inserts, fittings, ribs, bosses, and reinforcements possible	• Preform and reinforcement alignment in mold is critical
• Low pressure operation (usually less than 100 psig)	• Production quantities typically range from 100 to 5000 parts
• Prototype tooling costs relatively low	• Requires matched, leakproof molds
• Volatile emissions (e.g., styrene) controlled by close mold process	…
• Lower labor intensity and skill levels	…
• Considerable design flexibility: reinforcements, lay-up sequence, core materials, and mixed materials	…
• Mechanical properties comparable to autoclave part (void content <1%)	…
• Part size range and complexity make RTM appealling	…
• Smooth finish on both surfaces	…
• Near net molded parts	

Source: Ref 8

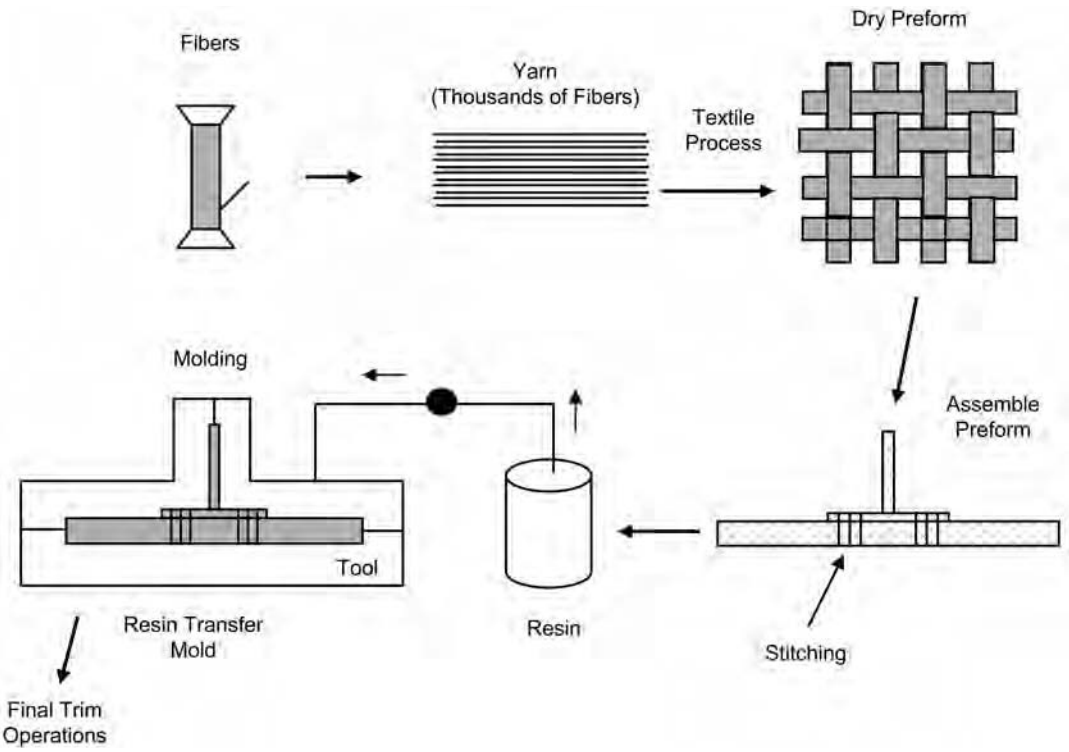


Fig. 5.25 Conceptual process flow for resin transfer molding (RTM). Source: Ref 9

the three major types of liquid molding processes is presented in Table 5.2. However, many variations of these processes are in development and use.

5.5.1 Preform Technology

The most important types of preforms for liquid molding processes are (1) woven, (2) knitted, (3) stitched, (4) braided, and (5) nonwoven mats. In many cases, conventional textile machinery has been modified to handle the high-modulus fibers needed in structural applications and to reduce costs through automation. In addition, to meet the growing demand for three-dimensional reinforced preforms, manufacturers have developed specialized machinery. A large variety of advanced textile architectures is possible, several which are shown in Fig. 5.26.

Fibers. Textile machines have been adapted to handle most of the fibers commonly used in structural composites, including glass, quartz, aramid, and carbon. The main limitation is that most textile processes subject yarns to bending

Table 5.2 Comparison of major liquid molding processes

Process terminology	Process attributes
Resin transfer molding (RTM)	• Resin injected into matched mold under pressure • Vacuum assistance may or may not be used • Excellent surface finishes on both surfaces • Can obtain high fiber volumes (59–60 v/o) • Tooling costs can be high
Vacuum assisted RTM (VARTM)	• Single sided tool normally used • Vacuum pulls liquid resin into perform (no applied pressure) • Resin distribution media used to facilitate perform infiltration • Requires low viscosity resins • Excellent surface finish on tool side • Tooling less expensive than RTM • Lower fiber volumes normally obtained (50–55 v/o)
Resin film infusion process (RFI)	• Resin film placed in bottom of tool and autoclave heat and pressure used to melt and force resin into preform • Normally requires matched die tools for complex parts • Variations include individual resin layers placed between preform layers • Capable of producing high quality parts, depending on the tooling

Source: Ref 8

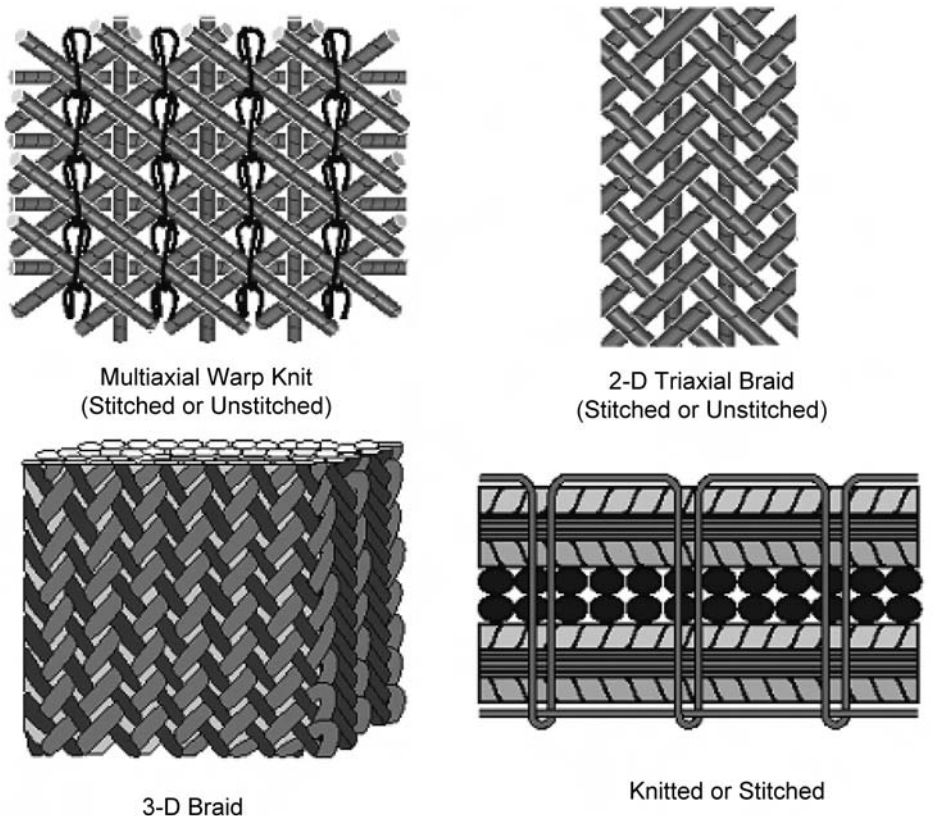


Fig. 5.26 Advanced textile material forms. 2-D, two-dimensional; 3-D, three-dimensional. Source: Ref 10

and abrasion. Although machines have been modified to minimize fiber damage, in many processes exceptionally brittle or stiff fibers will suffer significant strength degradation. In general, the higher the modulus of the fiber, the harder it is to process and the more prone it is to damage. Strength reductions can vary, depending on the property being measured and the textile process used to fabricate the preform. Polymeric sizings are usually applied to fibers to improve their handling characteristics and minimize strength degradation during processing. The sizing may be removed after processing or left on the fibers for the lamination process. If the sizing remains on the fibers, it is important that it be compatible with the matrix resin. A surface treatment is normally used to improve the adhesion between the fibers and the matrix.

In traditional textile processes, yarns are usually twisted to improve handling, structural integrity, and their ability to hold shape. However, twist reduces the axial strength and stiffness of the fibers, which is paramount in structural applications. Therefore, yarns with minimal or nominally zero twist (strands and tows) are preferred. Different processes and weaves require different strand or tow sizes. In general, the smaller the tow size, the more expensive the material will be on a per unit weight basis, particularly for carbon fiber.

Woven fabrics are available as two-dimensional (2-D) reinforcements (*x*- and *y*-directions) or three-dimensional (3-D) reinforcements (*x*-, *y*-, and *z*-directions). When high in-plane stiffness and strength are required, 2-D woven reinforcements are used. The various types of 2D weaves are described in Chapter 2, "Fibers and Reinforcements;" however, it should be noted that 2-D woven products can be supplied as either a prepreg or a dry cloth for hand lay-up, preforming, or repair applications. Two-dimensional weaves have the following advantages: (1) they can be accurately cut using automated ply cutters; (2) complicated lay-ups with ply drop-offs are possible; (3) a wide variety of fibers, tow sizes, and weaves are commercially available; and (4) 2-D weaves are more amenable to thinner structures than 3-D weaves.

Three-dimensional reinforced fabrics are normally used to (1) improve the handleability of the perform; (2) improve the delamination resistance of the composite structure; or (3) carry a significant portion of the load in the composite structure, such as a composite fitting that would be subject to complex load paths and major out-of-plane loading. If improved handleability is the objective, usually *z*-direction fiber volumes as low as one to two percent will suffice. Major improvements in the delamination resistance of composite structures can be obtained with as little as three to five percent *z*-direction fiber; however, as the amount of *z*-direction fiber is increased, the delamination resistance and durability increase. If the application calls for major out-of-plane loading, as much as 33 percent *z*-direction fiber reinforcement may be required. The fibers will then be arranged with roughly equal load-bearing capacity along all three axes of a Cartesian coordinate system.

Three-Dimensional Woven Fabrics. Historically, composite designs have been restricted to structure that experiences primarily in-plane loading, such as fuselage or wing skins. One of the key reasons for the lack of composite structures in complex substructure, such as bulkheads or fittings, is the inability of 2-D composites to handle complex out-of-plane loads effectively. The planar load-carrying capability of composites is primarily a fiber-dominated property requiring well-defined load paths. Unfortunately, the planar loads must ultimately be transferred through a 3D joint into adjacent structure (e.g., a skin attached to a bulkhead). These 3-D joints are subject to high shear, out-of-plane tension, and out-of-plane bending loads, all of which are matrix property–dominated properties in a traditional composite design. Since loading the matrix with large primary loads is a totally unacceptable design practice, metallic fittings are used to attach composite structure to metallic bulkheads with mechanical fasteners. With the introduction of high-performance 3-D textiles, both woven and braided, this barrier to composite designs has the potential to be eliminated. Other design benefits include stiffening concepts for monolithic composite aircraft skins in which the stiffeners are woven integral with the skin structure. This eliminates the need for mechanical or bonded stiffener attachment, reducing the part count and cost for the assembly.

Three-dimensional woven fabrics are usually produced on rather complex multiwarp looms such as the one shown in Fig. 5.27. In a conventional 2-D loom, harnesses alternately lift and lower the warp yarns to form the interlacing pattern. In a multiwarp loom, separate harnesses lift different groups of warp yarns to different heights, so that some are formed into layers while others weave the layers together to form the net shape preform. A 3-D weave contains

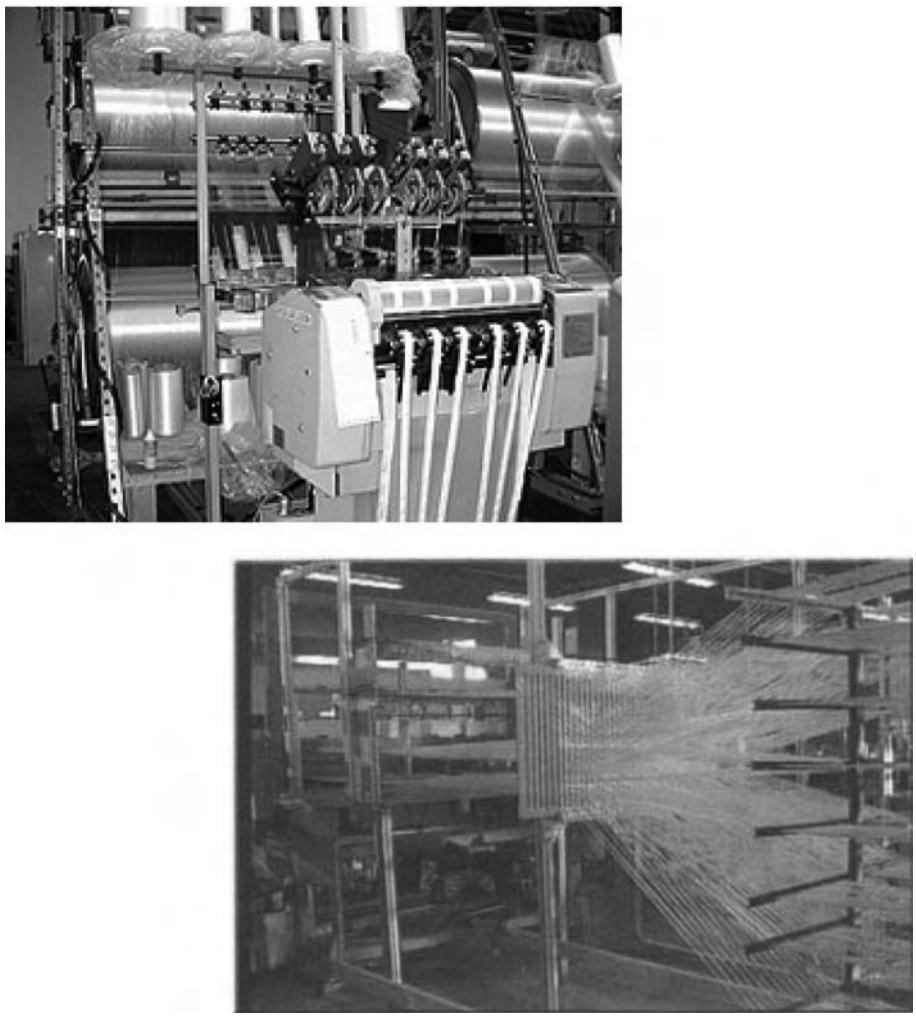


Fig. 5.27 Three-dimensional weaving equipment

multiple planes of nominally straight warp and fill yarns that are connected together by warp weavers to form an integral structure. The most common classes are shown in Fig. 5.28. Within each class, there are several parameters that can be varied. Angle interlock weaves can be categorized by the number of layers that the warp weavers penetrate. A through-the-thickness interlock fabric, in which the warp weavers pass though the entire thickness, is shown in Fig. 5.28a. Figures 5.28b and c show layer-to-layer interlock patterns, where a given weaver connects only two planes of fill yarns but the weavers collectively bind the entire thickness. Various intermediate combinations can be fabricated with the weavers penetrating a specified number of layers. In orthogonal interlock weaves, the warp weavers pass through the thickness orthogonal to both in-plane directions, as shown in Fig. 5.28d. Interlock weaves are sometimes manufactured without straight warp yarns (stuffers) to produce a composite reinforced predominantly in one direction. They may also be fabricated with fill rather than warp yarns used for interlock. A major limitation of 3-D weaves is the difficulty of introducing bias direction yarns to achieve in-plane isotropy. One solution is to stitch additional 2-D fabric plies oriented at ± 45 degrees onto the woven preform. Three-dimensional weaving is capable of producing a wide variety of architectures, several of which are shown in Fig. 5.29.

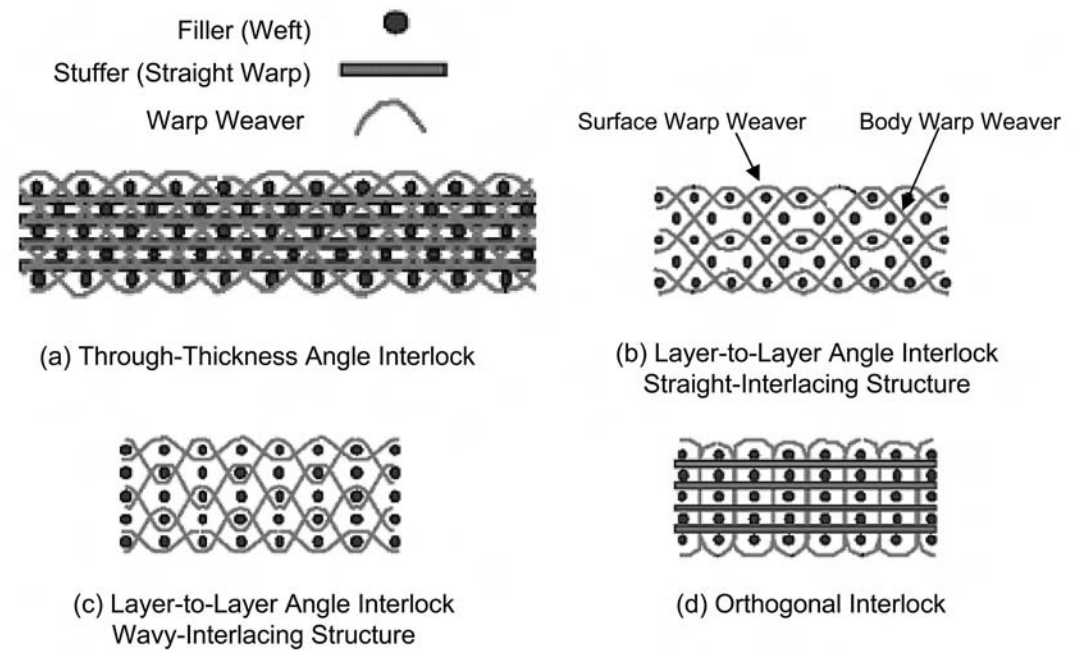


Fig. 5.28 Three-dimensional weave architectures. Source: Ref 9

While 3-D woven preforms have the potential to fabricate complex net-shaped preforms, the setup time is extensive and the weaving process is slow. In addition, small tow sizes, which generally increase the cost, must be used to achieve high fiber volume percentages and eliminate large resin pockets that are susceptible to matrix microcracking during cure or later when the part is placed in service.

Multiaxial Warp Knits. Traditional knitted fabrics, such as the weft and warp knits, are highly flexible and conformable fabrics, but the extreme crimp of the fibers results in low structural properties. However, knitting can be used effectively to produce multiaxial warp knits (MWKs), also called *stitch bonding*, which combines the mechanical property advantages of unidirectional tape with the handling and low-cost fabrication advantages of fabrics. Multiaxial warp knitting (Fig. 5.30) consists of unidirectional tows of strong, stiff fibers woven together with fine yarns of glass or polyester thread. The glass or polyester thread, which normally amounts to only two percent of the total weight, serves mainly to hold the unidirectional tows together during subsequent handling. An advantage of this process is that the *x*- and *y*-tows remain straight and do not suffer as much strength degradation as woven materials, in which the tows are crimped during the weaving process.

The MWK process is used to tie tows of unidirectional fibers together in layers with 0, ± θ, and 90 degree orientations (where θ is the off-axis orientation). During knitting, the polyester threads are passed around the primary yarns, and around one another, in interpenetrating loops. Selecting the tow percentage in each of the orientations can be used to tailor the mechanical properties of the resulting stack. The MWK stacks form building blocks two to nine layers thick that can be laminated to form the desired thickness of the structure (Fig. 5.31). Multiple layers of MWK are often stitched together in a secondary operation to form stacks of any desired thickness, which can be stacked, folded, and stitched into net shapes. The stitching operation also greatly improves the durability and damage tolerance of the cured composite. Multiaxial warp knitting has the advantages of being fairly low cost, having uniform thicknesses, capable of being ordered in prefabricated blanket-like preforms, and being very amenable to gentle or no contour parts, such as large skins. The MWK material is supplied by the Saertex Company in Germany. The Saertex material can typically be supplied as either

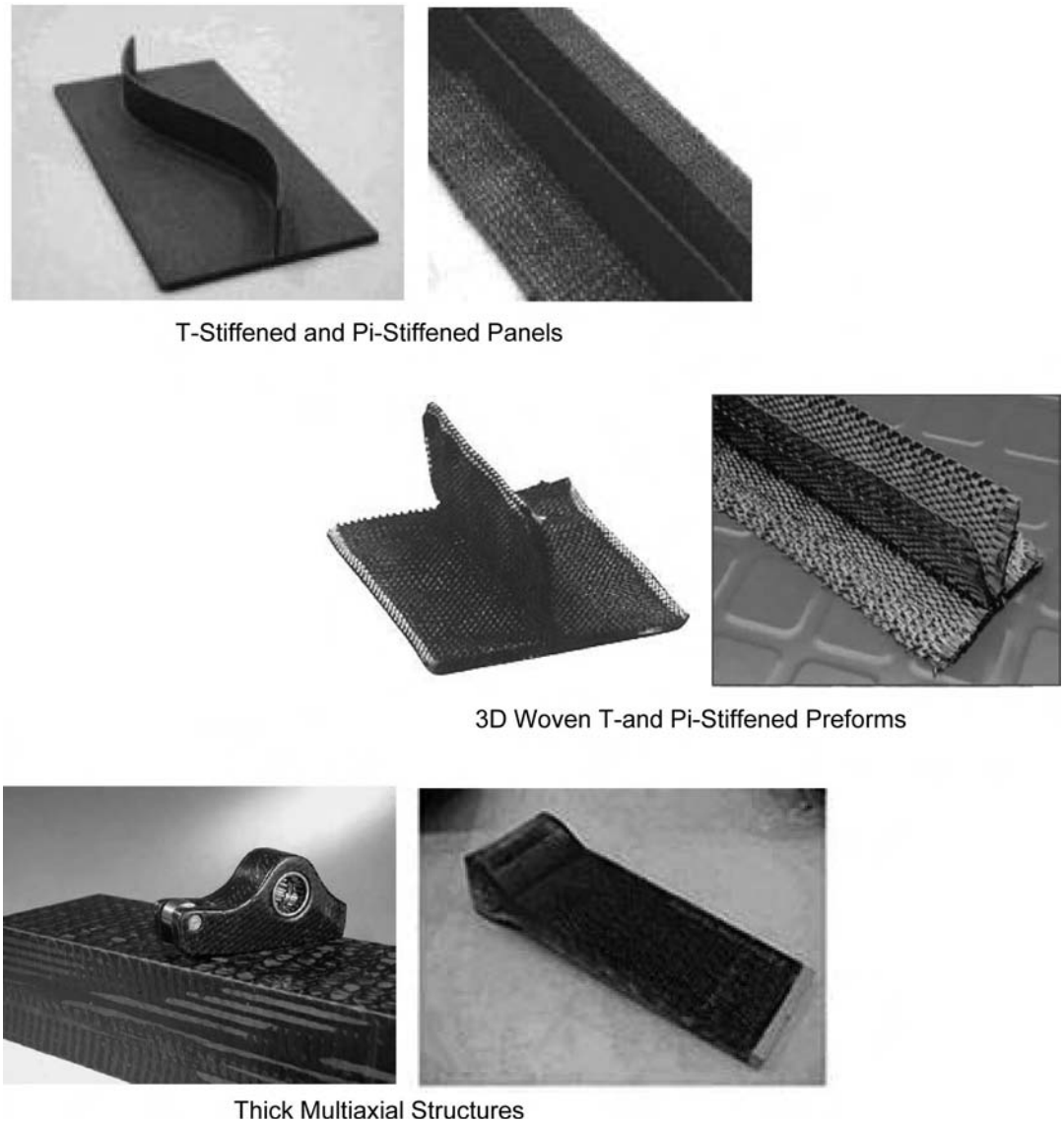


Fig. 5.29 Three-dimensional (3D) woven preforms

seven- or nine-layer-thick material with typical orientations of 0°, ± 45°, and 90°. This material is made on a Libra warp knitting machine (Fig. 5.32) that uses a 72 denier polyester thread to hold the stack-ups together.

Stitching has been used for more than 20 years to provide through-the-thickness reinforcement in composite structures, primarily to improve damage tolerance. The major manufacturing advance in recent years has been the introduction of liquid molding processes that allow stitching of dry preforms rather than prepreg material. This increases speed, allows stitching through thicker material, and greatly reduces damage to the in-plane fibers. In addition to enhancing damage tolerance, stitching aids fabrication. Many textile processes generate preforms that cannot serve as the complete structure. Thus, stitching provides a mechanical connection between the preform elements before the resin is introduced, allowing the completed preform to be handled without shifting or damage. In addition, stitching compacts (debulks) the fiber preform closer to the final desired thickness. Therefore, less

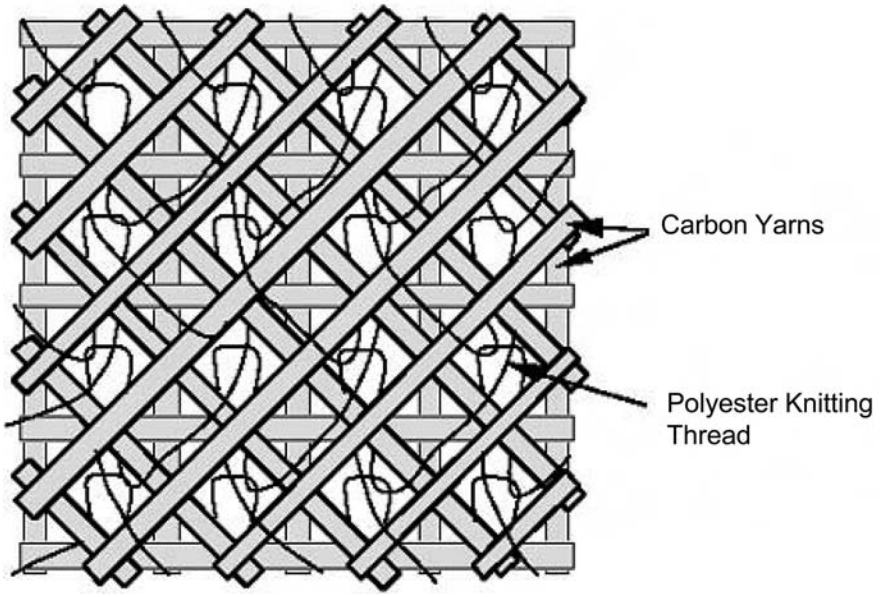


Fig. 5.30 Multiaxial warp knit architecture. Source: Ref 9

mechanical compaction needs to be applied to the preform in the tool.

Two forms of stitching are normally employed for structural applications: the modified lock stitch and the chain stitch (Fig. 5.33). The chain stitch uses only one stitching thread, while the lock stitch requires a separate bobbin and needle thread. In the modified lock stitch, the thread tension is adjusted so that the knot forms on the outer surface of the laminate rather than internally, helping to minimize distortion of the laminate. Important stitching parameters include the pitch between penetrations, the spacing between parallel rows of stitching, the stitching material, and the weight of the stitching yarn. Robotic 3D stitching machines are available that can perform one-sided stitching using either a lock stitch or a tuft. In tufting, a loop is inserted from one side and folds over on the back side to secure the reinforcement.

Various stitching materials have been successfully used, including carbon, glass, and aramid, with Kevlar 29 (aramid) being the most popular. Yarn weights for Kevlar of between 800 and 2000 denier have been used. Stitching that contributes around three to five percent of the total areal weight of the completed fabric has usually been found to impart satisfactory damage tolerance (such as compression strength after impact). However, one disadvantage of aramid is that it absorbs moisture and can sometimes exhibit leaks through the skin at the stitch locations.

Braiding is a commercial textile process dating from the early 1800s. In braiding, a mandrel is fed through the center of the machine at a uniform rate, and fiber yarns from moving carriers on the machine braid over the mandrel at a controlled rate. The carriers work in pairs to accomplish an over/under braiding sequence, as shown schematically in Fig. 5.34. Two or more systems of yarns are intertwined in the bias direction to form an integrated structure. Important parameters in braiding include yarn tension, mandrel feed rate, braider rotational speed, number of carriers, yarn width, perimeter being braided, and reversing ring size.

Braided preforms are known for their high level of conformity, torsional stability, and damage resistance. Either dry yarns or prepregged tows can be braided. Typical fibers include glass, aramid, and carbon. Braiding normally produces parts with lower fiber volume fractions than filament winding, but it is much more amenable to intricate shapes. The rotational speed of the yarn carriers relative to the traversing speed of the mandrel controls the orientation of the yarns. The mandrel can vary in cross section, with the braided fabric conforming to the mandrel shape. Typical braiding machines contain anywhere from 3 to 144 carriers. An actual braider in operation and a schematic of a large 144-carrier braider

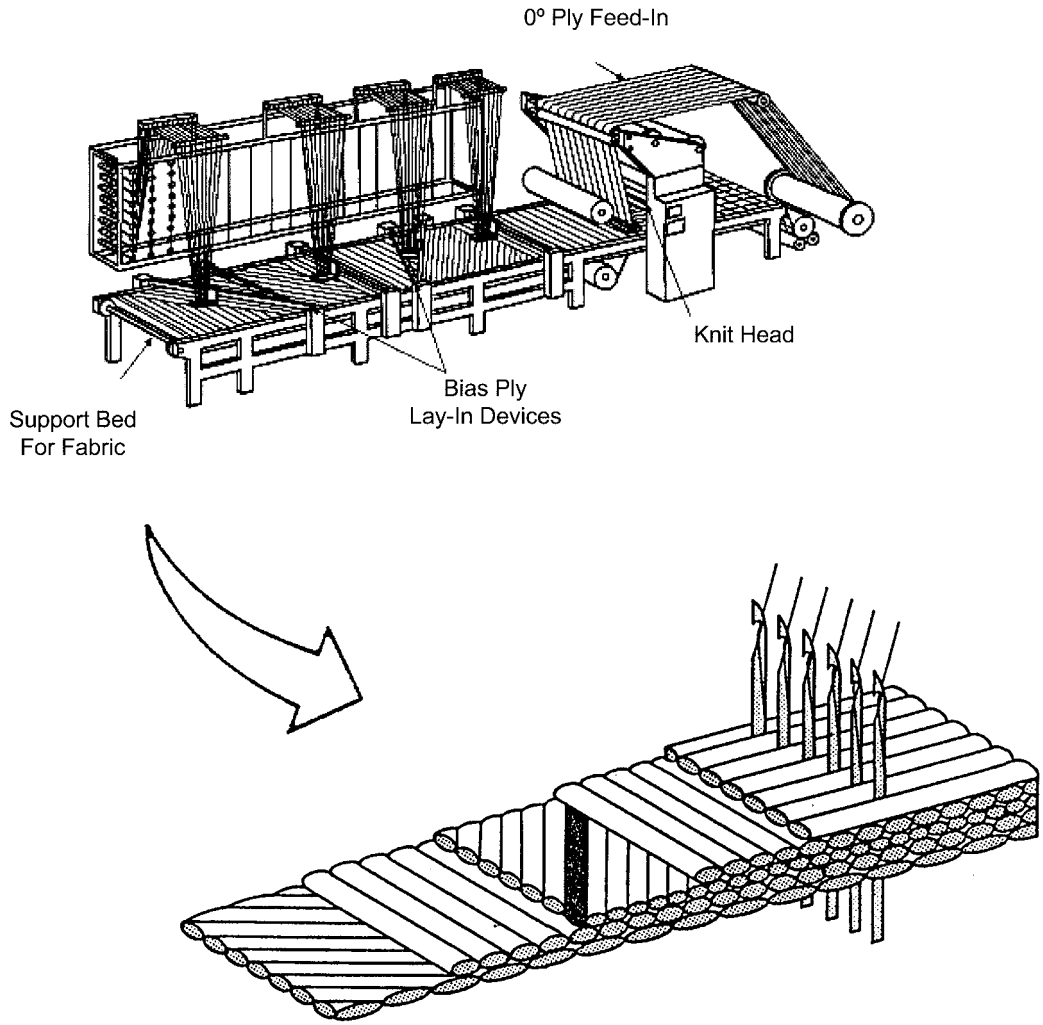


Fig. 5.31 Libra™ warp knitting machine and typical product form produced. Source: Ref 11

are shown in Fig. 5.35. State-of-the-art braiding equipment provides full control over all of the braiding parameters, including translational and rotational control of the mandrel, vision systems for in-process inspection, laser projection systems to check braid accuracy, and, in some instances, integrated circumferential filament winding.

Yarn width and the number of carriers determine the approximate braid angle for a given part perimeter in accordance with the relationship:

$$\sin\theta = \frac{WN}{2P} \qquad \text{(Eq 5.1)}$$

where:

θ = braid angle
W = yarn width
N = number of carriers
P = part perimeter

If the number of carriers and the braiding speed are controlled, the orientation of the braid angle and the diameter of the braid can be controlled. The total thickness of a braided part can be controlled by overbraiding, in which multiple passes of the mandrel are made through the braiding machine laying down a series of nearly identical layers similar to a lamination. Possible fiber orientations are $\pm\theta$ or $0/\pm\theta$ degrees with no 90-degree layers unless the braider is fitted with filament winding capability.

A number of braided preforms are shown in Fig. 5.36. Due to the material conformity inherent in a braided product form, braided socks can



Fig. 5.32 Libra™ warp knitting machine

be removed from the braiding mandrel and formed over a mandrel of a different shape for curing. In other situations, the braided part is cured directly on the mandrel. Both permanent and water-soluble or breakout mandrels can be used. Fixed, straight axial yarns (0°) can also be introduced at the center of orbit of the braider yarn carriers. The braider yarns lock the axial yarns into the fabric, forming a triaxial braid, that is, a braid reinforced in three in-plane directions. Cutting the cylindrical sheet from the mandrel and stretching it out flat can form a flat braided sheet.

Three-dimensional braiding can produce thick net section preforms in which the yarns are so intertwined that there may be no distinct layers. Three-dimensional braided socks can also be shaped into a preform suitable for use in joints and stiffeners. Due to the nature of braiding, a bias or 45° fiber orientation is inherent in

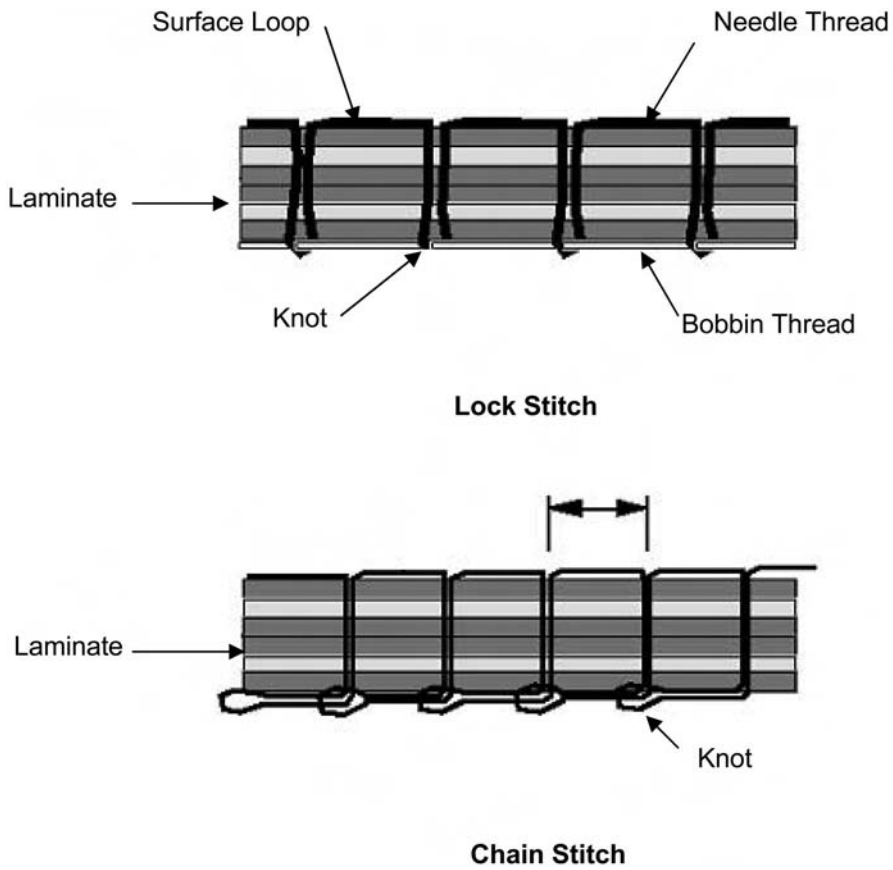


Fig. 5.33 Modified lock and chain stitches for stitching preforms. Source: Ref 9

the braided preform and theoretically allows the preform to carry high shear loads without the necessity of 45 degrees hand layed-up overwrap plies. A 3-D braiding machine can be set up to produce a near-net shape to the cross section of the final part. Examples of the complex fiber architectures that can be produced by 3-D braiding are shown in Fig. 5.37. The disadvantages of 3-D braiding are similar to those of 3-D weaving, namely, complicated setups and slow throughput. Again, resin microcracking can be a problem with maximum fiber volumes of 45 to 50 percent obtainable.

Random Mat. Many preforms for commercial applications that do not require high mechanical properties can be made from random mat using either discontinuous chopped fiber or swirled fiber mat. This is a very economical approach that allows complex shapes with compound contours. Since the fiber volume is about 40 percent maximum, mats are also easy to infuse by a variety of liquid molding processes.

Preform Advantages and Disadvantages. Textile preforms will continue to play an integral role in the composites industry due to their ability to improve damage resistance and their potential to reduce composite part costs.

1. Textile preforms have a handling advantage compared to unidirectional products forms. They are manufactured as dry fiber preforms that are held together without any polymer or matrix material. A textile preform can be shipped, stored, draped (within limits that depend on the kind of fabric), and pressed into shaped molds. The finished product can be cured in a mold by liquid molding.
2. Separate preforms can be easily joined by cocuring if joints of moderate strength suffice or by stitching if joints must be stronger. Textile product forms allow designers

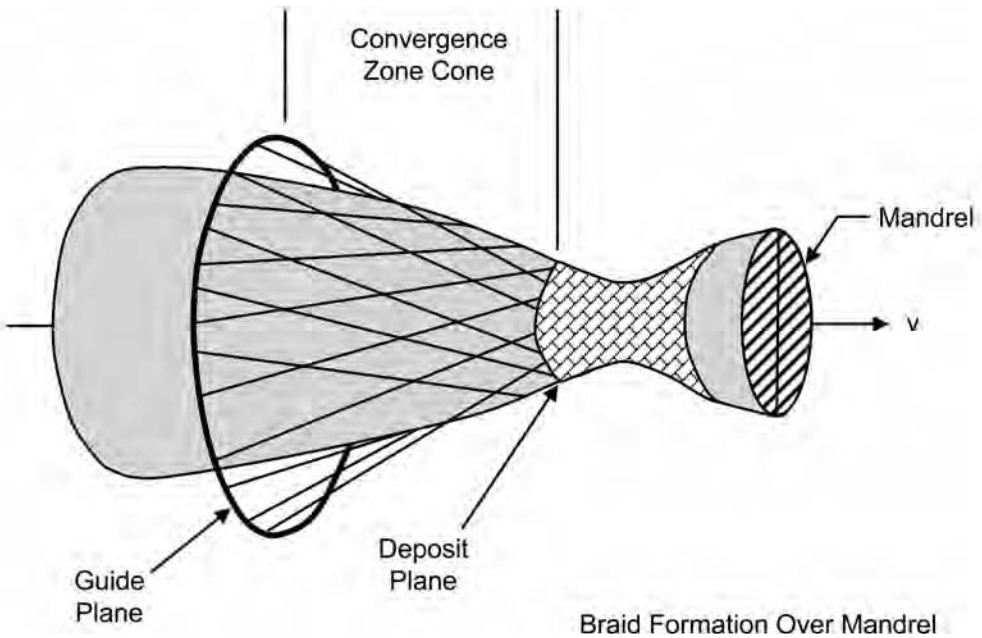


Fig. 5.34 Principle of braiding. Source: Ref 12

to step beyond conventional laminate concepts. For example, with conventional tape lay-up, a laminate skin is stiffened to prevent buckling by nonintegral ribs, which must be attached in a separate process, such as cocuring, bonding, or mechanical fastening. Textile preforms and liquid molding processes allow the manufacture of net shape integral parts. The skin and stiffeners can be manufactured as one piece. Net shape manufacturing of integral structures provides considerable potential cost savings over prepreg lay-up because forming complex shapes through hand lay-up is difficult and integral structures eliminate joining steps. Integral structures are also superior in performance because, given a correct design, failure by delamination of the attached parts should be eliminated as a failure mechanism.

3. Preforming eliminates the high-cost matched metal molding die in the resin transfer molding (RTM) process from everything but loading, curing, and unloading. It is common practice to use lower-cost preforming tools to lay up and heat set the preform to shape.

With the exception of improved damage tolerance and possibly lower cost, most preform products exhibit lower mechanical properties than unidirectional products. The lower properties are a combination of several factors:

1. Any time high-strength fibers are handled or bent, particularly carbon fibers, their properties are degraded. In many of the textile processes described above, there is considerable mechanical abrasion and bending of the tows or yarns.
2. In weaving and braiding, the interlocking nature of the fiber architecture creates crimp or bending in the fibers that is not present in a laminate made from unidirectional material. There is also considerable pinching of the tows or yarns at the crossover points in the weave. Knitted or stitched unidirectional preforms generally behave more like unidirectional material.
3. When a flat woven preform is formed to a tool with a complex compound contour, the fiber orientation will change and the original orthogonal construction will become distorted. In braided products, changes in the mandrel diameter will generally result in changes in the braid angle. For 3-D woven products, during compaction the *z*-direction reinforcement can become compressed and lose its straightness.
4. In general, the more complex the preform becomes (such as 3-D woven preforms), the

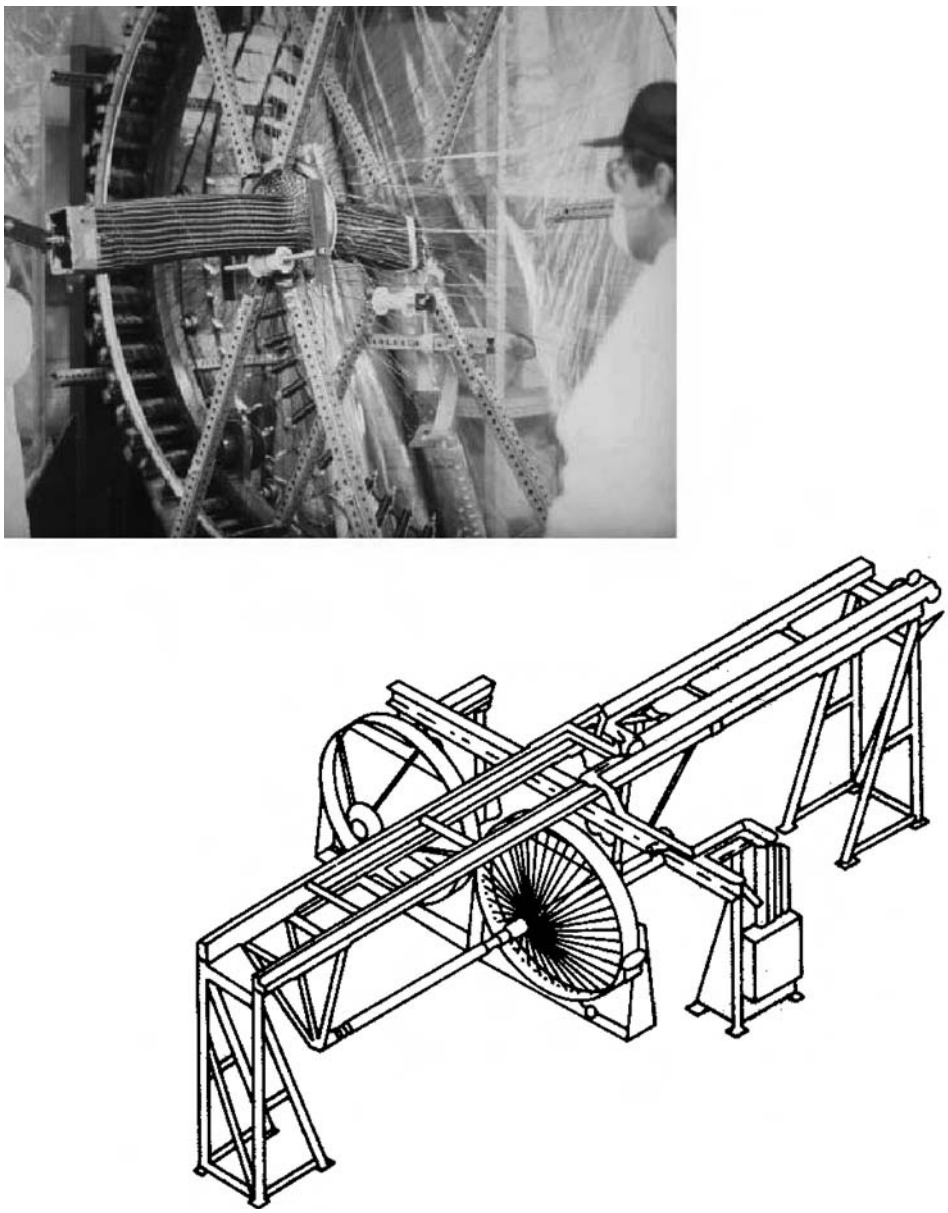


Fig. 5.35 144-carrier horizontal braiding machine. Sources: top: Ref 11; bottom: Ref 12

more difficult it becomes to achieve as high a fiber volume in the cured composite as with unidirectional materials. For example, unidirectional laminates usually contain about 60 volume percent fiber, while many 3-D product forms are in the 50 to 55 volume percent range. This can also lead to large resin pockets that are prone to microcracking on cool-down from cure.

Some of the advantages and disadvantages of the different textile processes used to make preforms are summarized in Table 5.3.

Preform Lay-Up. Since the stiffness and strength of polymeric composites are dominated by the reinforcing fibers, maintaining accurate positioning of the fibers during all steps in the manufacturing process is paramount. Poor handling and processing after preforming can destroy

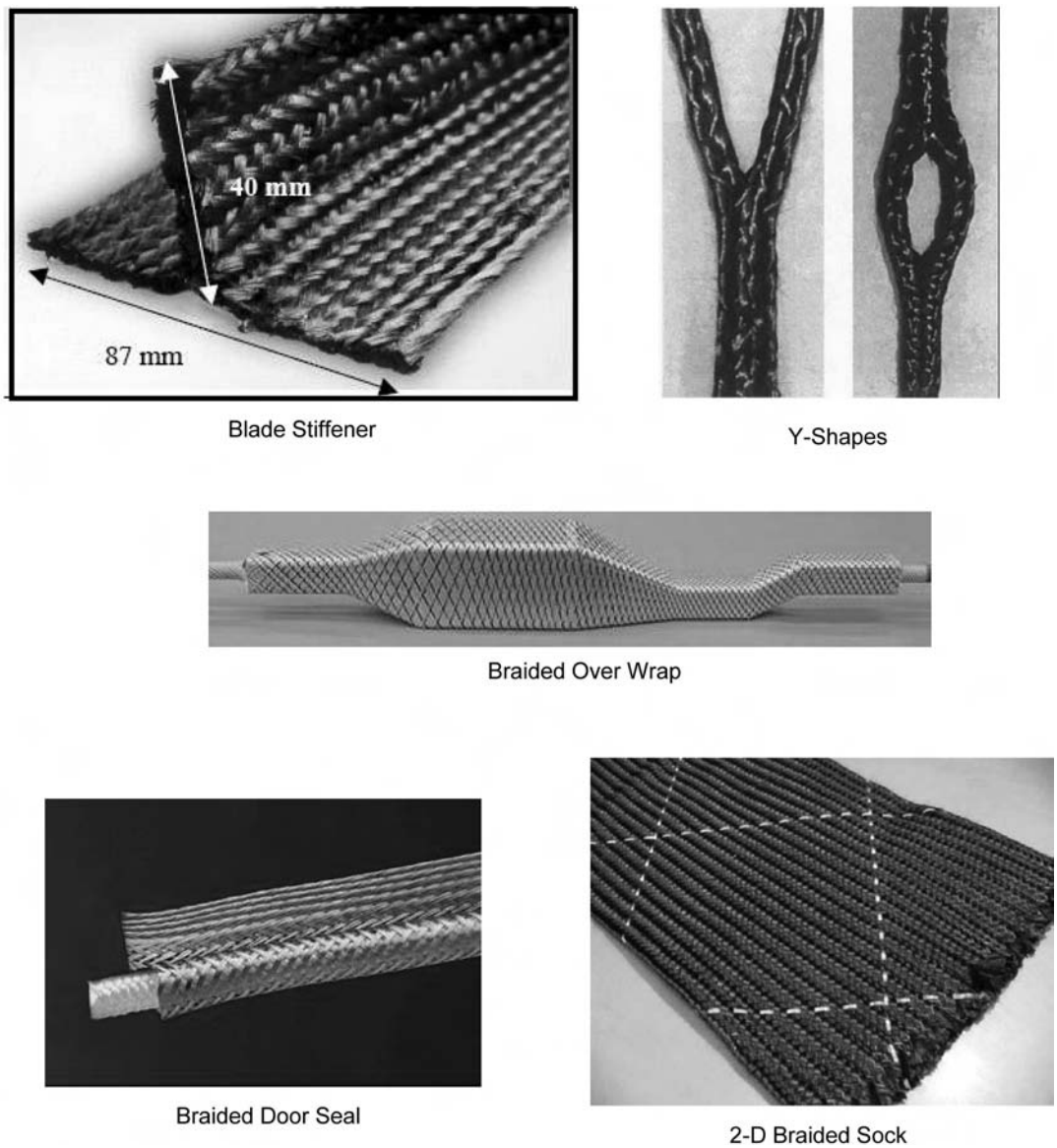


Fig. 5.36 Braided preform examples. 2-D, two-dimensional

fiber uniformity. Uncontrolled material handling, draping the material over curved tools, debulking, and tool closure can spread or distort the fibers. Manufacturing prove-out parts should be examined to establish that the minimum fiber volume fractions have been obtained, with particular attention paid to geometric details such as joints. Maintaining the desired fiber content is most challenging when fabrics are draped. The draping characteristics of a fabric over a singly curved surface are a direct function of the shear flexibility of the weave. Satin weaves have fewer crossover points than plain weaves, as well as lower shear rigidity, and are therefore more easily draped. Draping over a complex compound contour also depends on the in-plane extensibility and compressibility of the fabric. This is difficult for fabrics containing high-volume fractions of more or less straight in-plane fibers, as required for most structural applications. For

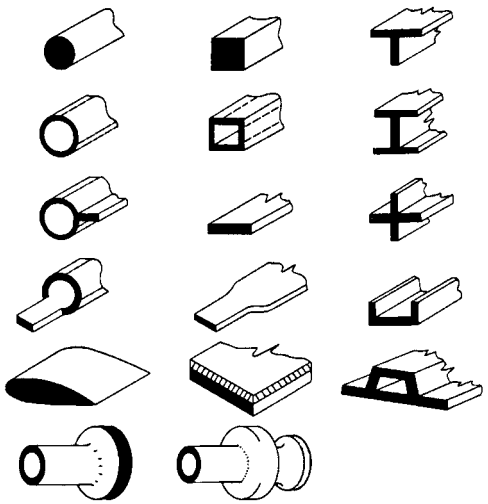


Fig. 5.37 Examples of net shaped three-dimensional braided structures. Source: Ref 13

these products, only mild double curvature can be accommodated by draping without a significant loss of fiber regularity. However, compound contours can be achieved through net shape processes, such as braiding onto a mandrel, thus avoiding the problems of draping.

There are several reasons that preforming is conducted prior to the injection process. First, preforming does not tie up the expensive matched die tool; the tool can be used to cure parts while the preforming operations are done ahead of time and off-line. Second, a well-constructed preform (Fig. 5.38) will be rather stiff and rigid as opposed to laying up loose fabric directly into the mold. Therefore, preforming improves the fiber alignment of the resultant part and reduces part-to-part variability.

Planar fabric preforms can be stitched together or held together with a tackifier. A tackifier is usually an uncatalyzed thermoset resin that is applied as a thin veil, a solvent spray, or a powder. Veils can be placed between adjacent plies of fabric, followed by fusing the ply stacks with heat and pressure to form the preform. Tackifiers can be thinned with a solvent and then sprayed on the fabric plies. A third method is to apply powder to the surface, followed by heating to melt the powder and allowing it to impregnate the fabric. Tackified fabric can be thought of as a low-resin-content prepreg (usually in the range of four to six percent) that can be made into ply kits using conventional automated broadgoods cutting equipment. It is important to keep the tackifier content as low as possible because it reduces the permeability of the preform and makes resin filling more difficult. It is also important that the tackifier and the resin to be injected are chemically compatible, preferably with the same base resin system. Once the tackifier has been applied to the fabric layers, they are formed to the desired shape on a low-cost preforming tool and then heat-set by heating to approximately 200 °F (95 °C) for 30 to 60 seconds.

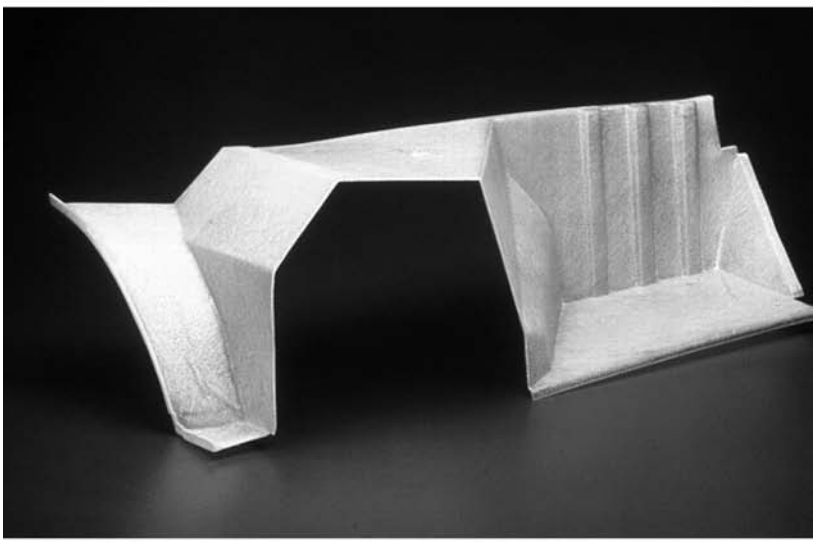
Table 5.3 Relative advantages and disadvantages of various textile processes

Textile process	Advantages	Disadvantages
2-D woven fabric	• Good in-plane properties • Good drapeablility • Highly automated preform fabrication process • Integrally woven shapes possible • Suited for large area coverage • Extensive data base	• Limited tailorability for off-axis properties • Low out-of-plane properties
3-D woven fabric	• Moderate in-plane and out-of-plane properties • Automated preform fabrication processes • Limited woven shapes possible	• Limited tailorability for off-axis properties • Poor drapeablility • Process is slow and expensive
2-D braided preform	• Good balance of off-axis properties • Automated preform fabrication process • Well suited for complex curved parts • Good drapeablility	• Size limitation due to machine availability • Low out-of-plane properties
3-D braided preform	• Good balance of in-plane and out-of-plane properties • Well suited for complex shapes	• Process is slow and expensive • Size limitation due to machine availability
Multiaxial warp knit	• Good tailorability for balanced in-plane properties • Highly automated preform fabrication process • Multilayer high throughput material suited for large area coverage	• Low out-of-plane properties unless stitched • Low design flexibility • Poor drapeability
Stitching	• Good in-plane properties • Highly automated process provides excellent damage tolerance and out-of-plane strength • Excellent assembly aid	• Small reduction in in-plane properties • Poor accessibility to complex curved shapes

2-D, two-dimensional; 3-D, three-dimensional.



Fiberglass Preform



Liquid Molded Part

Fig. 5.38 Example of a preform and a liquid molded part

The compaction behavior of a preform depends on the preform method used, the type of reinforcement, the tackifier used, the compaction pressure, and the compaction temperature. The effects of compaction pressure and temperature are notionally shown in Fig. 5.39. A tackifier can act as a lubricant and increase compaction, but this will also decrease the preform permeability and make injection more difficult. For any preform construction, it is important that the preform be dried prior to resin injection to remove all moisture that may have condensed on the surface from the atmosphere.

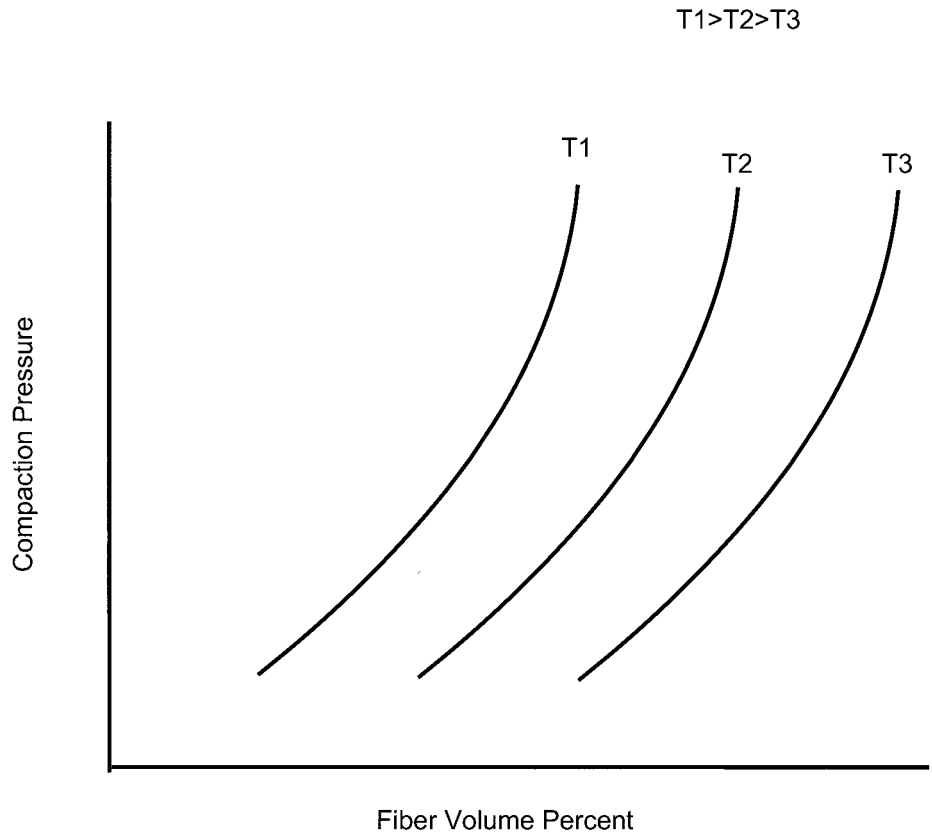


Fig. 5.39 Influence of compaction pressure and temperature on preform fiber volume. Source: Ref 14

5.5.2 Resin Injection

Resin injection follows Darcy's law of flow through a porous medium, which predicts that the flow rate per unit area (Q/A) is proportional to the preform permeability (k) and the pressure gradient ($\Delta P/L$) and inversely proportional to the viscosity (η) of the resin and the flow length (L):

$$\frac{Q}{A} = \frac{k\Delta P}{\eta L} \qquad \text{(Eq 5.2)}$$

Therefore, for a short injection time (high Q/A), one would want a preform with high permeability (k), high pressure (ΔP), low resin viscosity (η), and short flow length (L). This equation can provide useful guidelines for RTM: (1) use resins with low viscosity, (2) use higher pressures for faster injections, and (3) use multiple injection ports and vents for faster injections.

The ideal resin for RTM will have (1) low viscosity to allow flow through the mold and complete impregnation of the fiber preform, (2) a sufficient pot life where the viscosity is low enough to allow complete injection at reasonable pressures, (3) low volatile content to minimize the occurrence of voids and porosity, and (4) a reasonable cure time and temperature to produce a fully cured part. A more complete list of the variables that can affect the RTM process is given in Table 5.4.

Resin viscosity is a major consideration when selecting a resin system for RTM. Low-viscosity resins are desirable, with an ideal range of 100 to 300 centipoise (cps) and about 500 cps as the upper limit. Although resins with higher viscosity have been successfully injected, high injection pressures or temperatures are required, which results in the use of more massive tools to prevent tool deflection. Normally, the resin is mixed and catalyzed before it is injected into the mold; alternatively, if the resin is a solid at room temperature with a latent curing agent, it must be melted by heating. Vacuum degassing in the injection pot (Fig. 5.40) is a good practice to remove entrained air from mixing and low boiling

point volatiles. Both epoxies and bismaleimides are amenable to RTM, and preformulated resins are available from a large number of suppliers. As with prepreg resins, it is important to understand the resin viscosity and cure kinetics of any resin used for RTM.

Table 5.4 Resin transfer molding (RTM) processing variables and their effects

RTM process parameter	Potential effects on processing or structure
Resin viscosity	• 100–1000 cps typical flow processing range • Processing at 10–100 cps at high temperatures also typical • Higher viscosity—preform fails to wet out • Lower viscosity—rapid infusion may leave dry areas and voids
Resin pot life	• Too short—resin fails to fill preform • Too long—process cycle lengthened unnecessarily
Resin injection pressure	• Helps drive resin into mold and preform • Too fast or too high—may move prefom within mold • Too high—may damage mold or tooling • Too high—may 'blow' out seals and cause leakage • Too low—cycle times very long • Too low—resin may gel during fill period
Resin injection vacuum level	• 10–28 in. Hg is typical processing range • Helps pull resin into mold and preform • Aids in reducing void content • Assists in holding mold halves together • Aids in removing moisture and volatiles
Multiple injection ports	• Commonly used to assure complete wet-out • Sometimes used sequentially to fill very long parts
Internal rubber/ elastomeric tooling	• Rubber inserts used to provide very high compaction • High fiber volumes (>65%) achievable • Very low void contents typical • Tooling must be robust to withstand high pressures
Closed mold pressurization	• Pressure increased to 100–200 psig after resin wet out • Desreases microvoids by collapse of bubble cavities
Fiber sizing or coupling agents	• Sizing chemistry must be compatible with resin selection • Sizing level reduces resin flow (lower permeability)
Fiber volume	• Resin flow permeability inversely proportional to volume • High fiber volumes (>60%) require more work to wet out • Commercial market- usually 25–55% by volume • Aerospace market- usually 50–70% by volume
Mold-in inserts and fitting	• Very possible with RTM process • Resin flow around fittings can leave dry areas and voids

Source: Ref 8

Although resin injection pressures can range from vacuum only up to an applied pressure of 400 to 500 psi (2800 to 3400 kPa), applied pressures are normally 100 psi (690 kPa) or lower. Although high pressures are often needed to fully impregnate the preform, the higher the injection pressure, the greater the chance of preform migration; that is, the pressure front can cause the dry preform to migrate and move out of its desired location. Resin transfer molding dies are normally designed either so that they are stiff enough to oppose the injection pressures or they are placed in a platen press under pressure to oppose the injection pressure. As a rule of thumb, the higher the injection pressure, the higher the tooling cost. Heating the resin or tool prior to or during injection can reduce the viscosity, but it will also reduce the working or pot life of the resin. It is normal practice to vacuum degas the resin prior to injection to remove as many volatiles as possible, thereby reducing the chance of voids and porosity in the cured part. A vacuum is also frequently used during the injection process to remove entrapped air from the preform and mold. The vacuum pressure also helps to pull resin into the mold and preform, helps to remove moisture and volatiles, and aids in reducing voids and porosity. It has been reported that the use of a vacuum is a significant variable in improving product quality by reducing the occurrence of voids and porosity.

The time it takes for the resin to fill the mold is a function of the resin viscosity, the permeability of the fiber preform, the injection pressure, the number and location of the injection ports, and the size of the part. The injection strategy usually consists of one of three main types shown in Fig. 5.41: (1) point injection, (2) edge injection, or (3) peripheral injection. Point injection is usually done by injecting at the center of the part and allowing the resin to flow radially into the reinforcement as air is vented along the part's periphery. Edge injection consists of injecting the resin at one end of the part and allowing it to flow unidirectionally down the length as air is vented at the opposite end. Finally, in peripheral injection, the resin is injected into a channel around the part, and the flow is radially inward as air is vented at the center of the part. Peripheral injection is usually the fastest of the three methods, although it is not uncommon to use more than one of them on the same part. Additionally, the locations of the injection and venting ports are important considerations in achieving complete filling without entrapped air

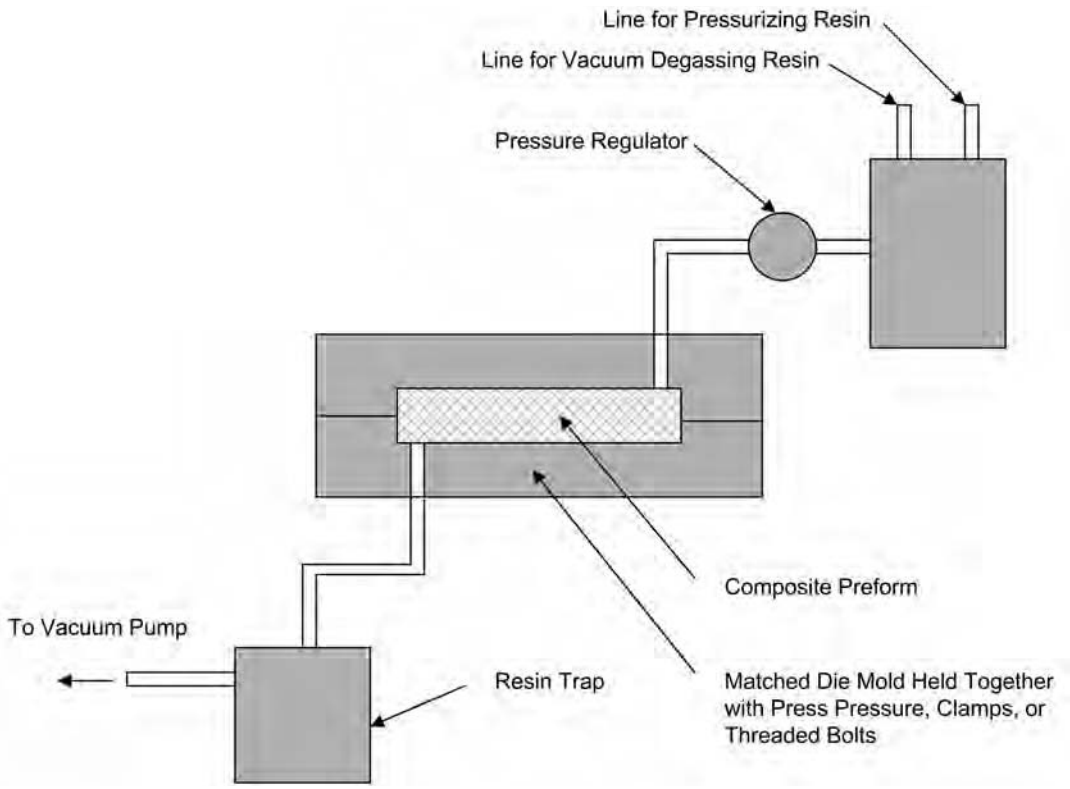


Fig. 5.40 Schematic of a typical resin transfer molding (RTM) process

pockets or unimpregnated dry spots. Although there are several ways to reduce the time needed to fill the mold, such as using lower-viscosity resins or higher injection pressures, the most effective method is to design an injection and porting system that minimizes the distance the resin has to flow. However, in designing an injection and porting system, the most important consideration is to have a system that will minimize any entrapped air pockets, as these will result in dry, unimpregnated areas in the cured part. In peripheral injection, a phenomenon known as *race tracking* can occur in which the resin runs around the peripheral injection channel and then migrates inward but traps air pockets, resulting in dry spots. This can usually be avoided by the judicious selection of the location and number of the porting vents.

Vacuum assistance during injection will usually help to reduce the void content significantly. However, it is important that the mold be vacuum tight (sealed) if vacuum assistance will be used. If the mold leaks, air will be sucked into it, causing a potentially higher void content. In addition to entrapped air in the preform and mold, entrained air, moisture, and volatiles within the resin itself can be sources of voids and porosity. The normal practice is to thoroughly vacuum degas the mixed resin at room or slightly elevated temperature to remove these gases prior to resin injection. During the injection process, when the mold is almost full, resin will start flowing out through the porting system. If there is evidence of bubbles in the exiting resin, the resin should be allowed to continue to bleed out until the bubbles disappear. To further reduce the possibility of voids and porosity, once the injection is complete, the ports can be sealed while the pumping system is allowed to build up hydrostatic resin pressure within the mold.

5.5.3 Priform Process

Even though some preforms used for RTM have 3-D reinforcement to provide greater toughness and damage tolerance, the use of toughened epoxies, rather than brittle unmodified epoxies, would naturally be desirable for RTM parts.

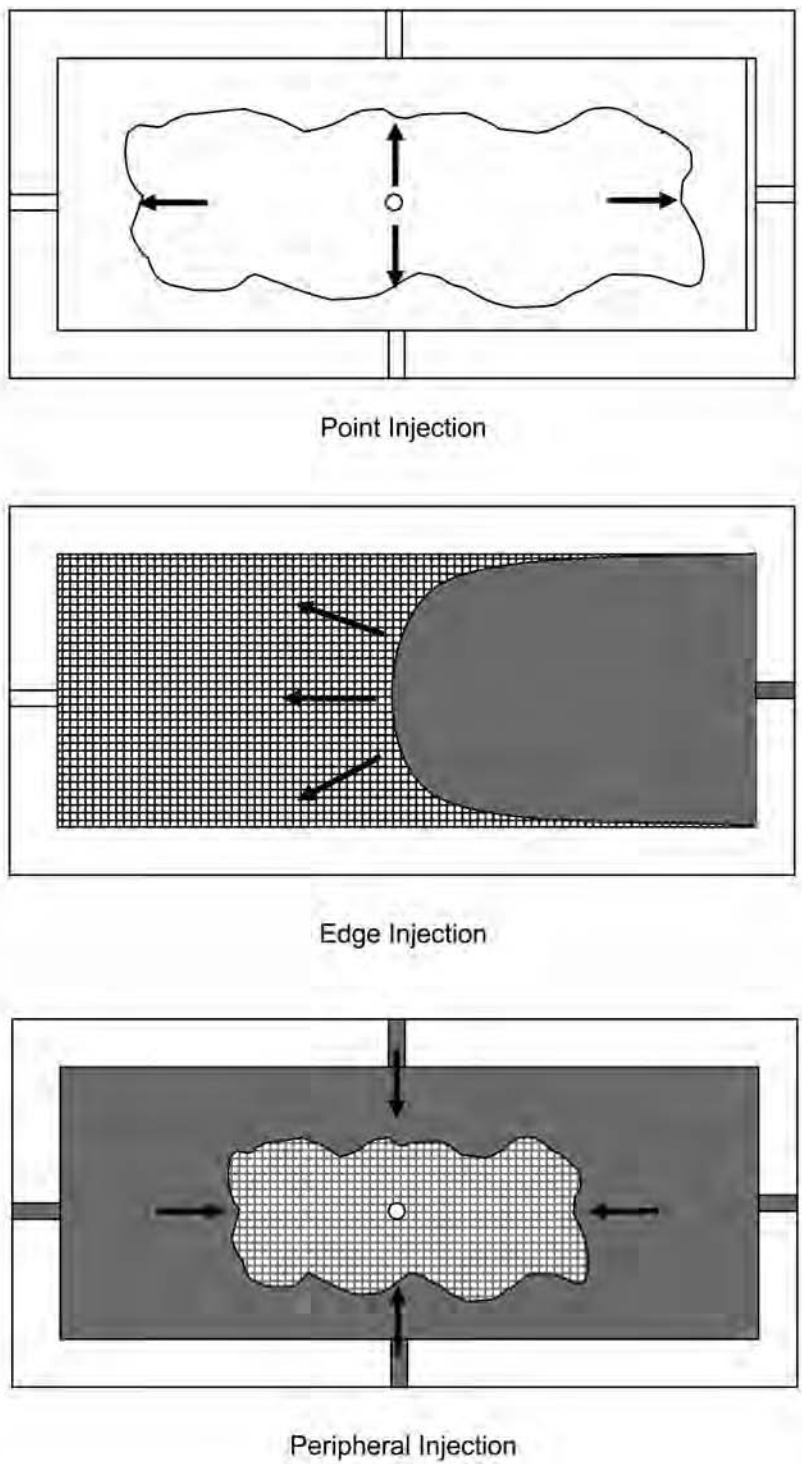


Fig. 5.41 Resin injection strategies

However, as shown in Fig. 5.42, the viscosity of toughened resin systems is too high to obtain complete preform filling during normal injection pressures. In this comparison, 977-2 is a thermoplastic-modified toughened epoxy matrix system that is used as a prepreg resin system. The resin designated as 977-20 is exactly the same resin system except that the thermoplastic toughener has been removed. It falls within the range of viscosities necessary to obtain well-impregnated RTM parts.

To circumvent this viscosity problem with toughened resin, Cytec Engineered Materials removed the thermoplastic toughener from 977-2 and spun it into fibers that were then woven into the carbon cloth preform, a product form and process they supply under the name Priform™. Thus, the much lower-viscosity, untoughened resin is injected into the preform, and when the part is heated for cure, the thermoplastic fibers melt and mix with the resin to form a fully toughened matrix. The time required for dissolution of the thermoplastic fibers, as a function of temperature, is shown in Fig. 5.43. During the heat-up to the 350 °F (175 °C) cure temperature, a hold is incorporated at 250 to 285 °F (120 to 140 °C) to give the thermoplastic fibers adequate time to dissolve and mix with the resin. Obviously, the advantage of this process is that one can obtain an RTM part with a tough, damage-tolerant matrix. The disadvantage is the extra cost of having to spin thermoplastic fibers and then integrally weave them into the preform. A preform and a finished aircraft spoiler hinge made using the Priform process are shown in Fig. 5.44. Since this is a hinge that could experience out-of-plane loadings, the preform was also stitched together to provide *z*-direction reinforcement.

5.5.4 RTM Curing

Curing can be accomplished using several methods:

1. Matched die molds are used with integral heaters—electric, hot water, or hot oil.
2. Matched die molds are placed in an oven.
3. Matched die molds are placed between a heated platen press that provides the heat and reaction pressure on the mold.
4. For liquid molding processes that use vacuum injection only, such as vacuum-assisted resin transfer molding (VARTM), a single-sided tool with only a vacuum bag is used for pressure application. In this case, heat can be provided by integral heaters, ovens, or even heat lamps if a low-temperature curing resin is used.

In comparison to autoclave curing, where the operator can control the variables time, temperature, and pressure, in RTM the pressure variable is often predetermined by the pressure applied to the resin during the injection process; in VARTM it is limited to the pressure that can be developed by a vacuum less than or equal to 14.7 psia (101 kPa). In some match mold applications, the vent ports

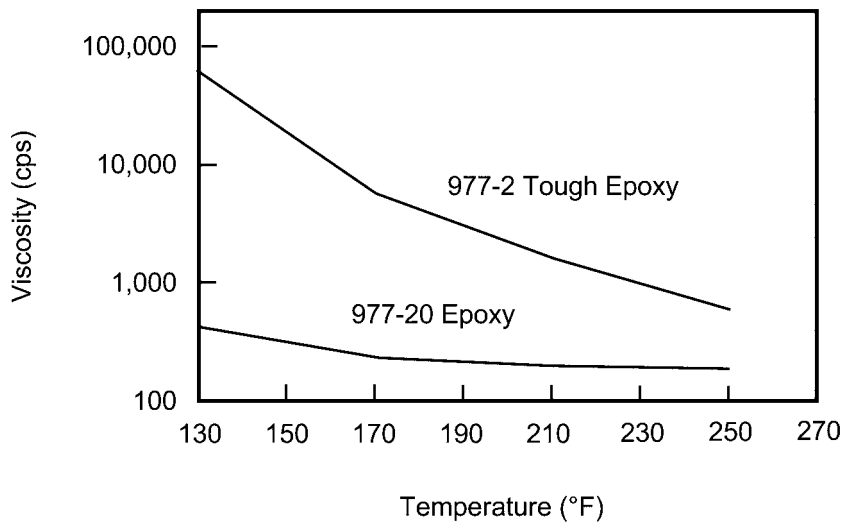


Fig. 5.42 Viscosity comparison: toughened and untoughened epoxy. Source: Cytec Engineered Materials

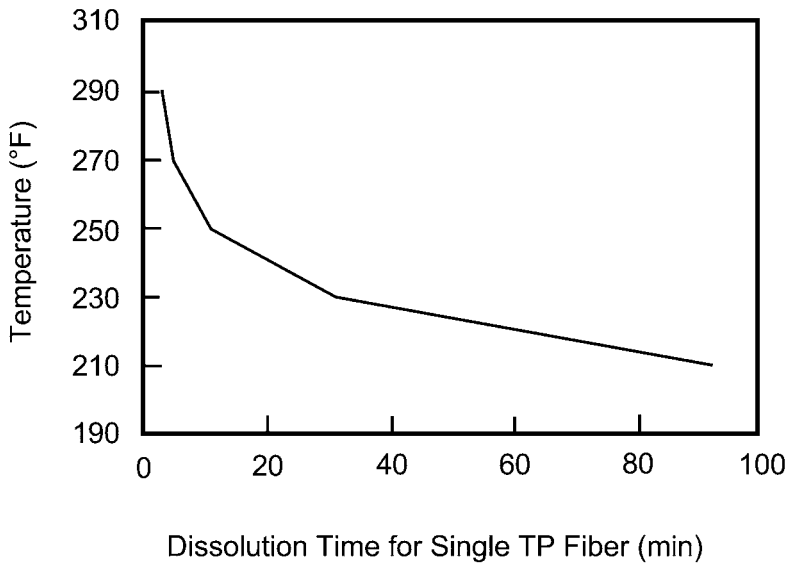
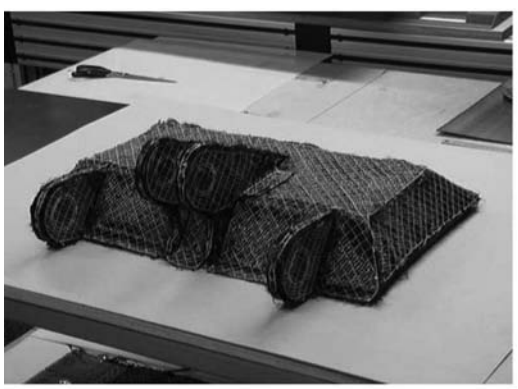
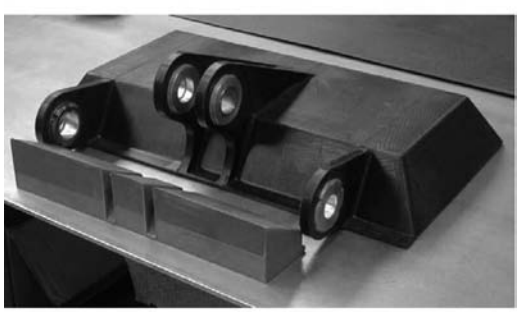


Fig. 5.43 Dissolution time for thermoplastic (TP) fiber. Source: Cytec Engineered Materials



Stitched Preform



Completed Fitting

Fig. 5.44 Spoiler fitting made from Priform. Source: Cytec Engineered Materials

can be sealed off and pressure can continue to be applied by the pump. To improve productivity, RTM parts are frequently cured in their molds, demolded, and then given freestanding postcures in ovens. Several examples of completed RTM composite parts are shown in Fig. 5.45.

5.5.5 RTM Tooling

Tooling is probably the single most important variable in the RTM process. A properly designed and built mold will normally yield a good part, while a poorly designed or fabricated mold will almost certainly produce a deficient part. There are several characteristics that must be considered when designing a tool for RTM:

1. The tool must be stiff enough to not deflect when the preform is initially loaded into the tool, and it must be able to react or oppose the resin injection pressures during molding. If the mold will be used freestanding or not in a platen press, it may be necessary to incorporate external stiffening structure to prevent the mold from deflecting during the injection process.
2. It is extremely important that the tool be capable of being vacuum sealed to prevent air from being sucked into it when vacuum assistance is used during injection. Although several different approaches are used, they



Fig. 5.45 Examples of resin transfer molding (RTM) carbon composite parts. Source: GKN Aerospace Services

usually involve some type of rubber O-ring that fits within a groove placed around the periphery of the tool (Fig. 5.46). If possible, it is best to keep the seal on a single plane since it is more difficult to effectively seal a tool along a curved surface.

3. The mold clamping system must be sufficient to hold the mold together during preform compression and resin injection. Large threaded bolts are frequently used, although hydraulic systems have been used for high-volume applications. Note that injection pressures can exert tremendous separation forces on a tool. For example, an injection pressure of 60 psi (415 kPa) on a mold with an area of 20 ft^2 (2 m^2) will exert a force of 80 tons (73 metric tons) on the mold.
4. The mold must either be integrally heated or placed in an oven or press for curing.
5. The mold must have an injection and porting system that will allow complete preform impregnation and mold filling during injection. The location and number of injection and venting ports is not a science; they are frequently determined by experience and trial and error.

Conventional RTM tooling consists of matched molds, usually machined from tool steel. If the part is complex, even small dies can contain numerous pieces that must all fit together precisely (Fig. 5.47). Steel dies yield long lives for large production runs and are resistant to handling damage. The dies are usually blended and buffed to a fine surface finish that will provide good surface finishes on the RTM part. Many matched metal molds are built with sufficient rigidity that they do not need to be placed in a platen press during injection and cure to oppose the resin injection pressures. Since these molds necessarily become extremely heavy, attachment fittings are built into the mold to provide hoisting capability for cranes. They are held together with a system of heavy bolts and are often designed with internal ports for heating with hot water or oil. Hot water heaters are effective up to about 280 °F (135 °C). Above that temperature, hot oil must be used. Electric heaters can also be placed within the mold, but they are generally less reliable than hot oil because of the problems of replacing burned-out heaters. Resin transfer molds can also be placed in convectively heated ovens, but for large tools the heat-up rates will be extremely slow.

Steel matched metal molds have two disadvantages: (1) they are expensive and (2) the heat-up and cool-down rates are slow. Matched metal molds have been fabricated from Invar 42 to match the coefficient of thermal expansion of carbon composites. They have also been fabricated from aluminum because it is easier to machine (less costly) and has a high coefficient of thermal expansion that can be useful in some applications; however, it is much more

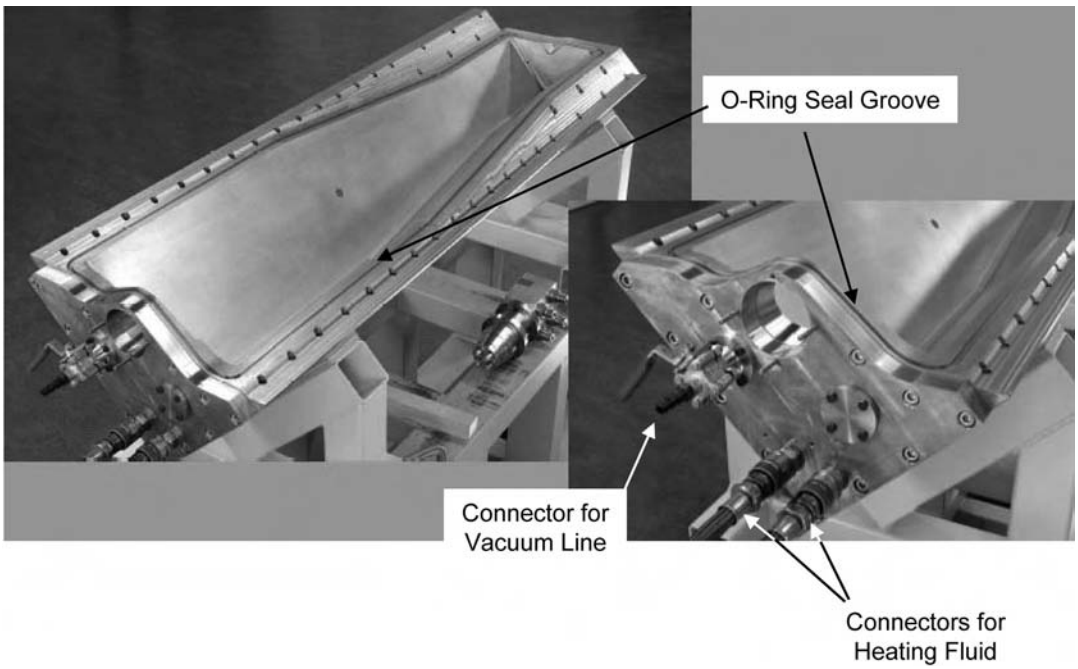


Fig. 5.46 Typical resin transfer molding (RTM) die

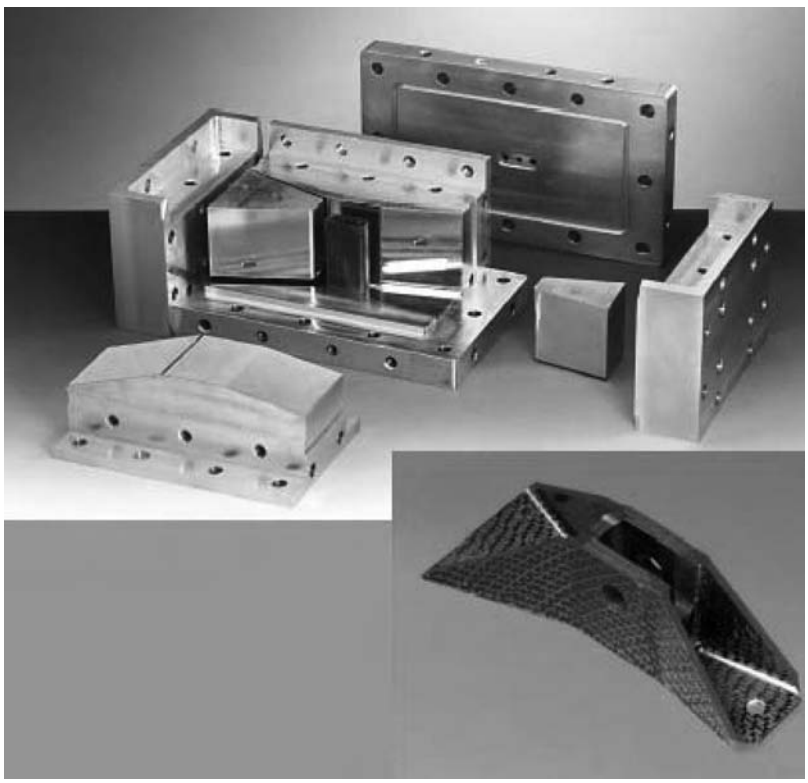


Fig. 5.47 Matched-metal resin transfer molding (RTM) die complexity

prone to wear and damage than steel or Invar. For prototype and short production runs, matched molds can be made of high-temperature resins that are frequently reinforced with glass or carbon fibers. If the injection pressures are not too high, prototype dies can be numerical control (NC) machined directly from mass cast blocks laminated on a master model or laminated first, then finished by NC machining of the surface.

A distinct advantage of processes that use only vacuum pressure during injection and cure, such as VARTM, is that the tooling is much simpler. The lower pressures used in VARTM allow much lighter and thus less expensive tooling. In fact, most of these processes use single-sided hard tooling on one side and a vacuum bag on the other side. For VARTM processes, a porous distribution medium is almost always used on top of the fiber preform to aid in resin filling during injection.

5.5.6 RTM Defects

If the radii in a part are designed too tight, some bridging of the preform in the radius may occur, often resulting in a resin-rich area on the outside of the radius, as illustrated in Fig. 5.48. Since the resin is not reinforced with fiber, it will often craze or break off. If the bridging condition at the radius is extremely severe, ply compaction may be inadequate and delaminated plies may result. As a general rule, the radius should be at least three times larger than the part thickness. There are also other potential problems with radii that are too small: (1) they can restrict resin impregnation; (2) they make it more difficult to fit the preform in the tool; (3) fiber damage can occur when the mold is closed; and (4) if the mold is made of a soft material, such as a composite laminate, the tool itself can be damaged.

During injection, the resin is very fluid and will follow the path of least resistance. If there are gaps between the preform and the tool, or locations in the preform where the permeability is higher than average, the resin can "race" ahead of the flow front and isolate areas in the preform where air pressure cannot escape; dry or unimpregnated spots will result. This "race tracking" phenomenon is shown schematically in Fig. 5.49. It is important that the preform fits tightly around the periphery of the mold. If it does not then extra sealing material may need to be placed between the preform edges and the mold (Fig. 5.50). Proper design of the inlet and venting systems is also important in preventing race tracking. The problem is more prevalent with peripheral injection systems than with point or edge injection designs. A somewhat similar phenomenon can also occur in sandwich construction in which the resin flows faster along one surface than the other, resulting in nonuniform skin thicknesses. The core is actually pushed toward the thinner skin by the advancing flow front. To circumvent some of the infusion problems with foam cores, core manufacturers can supply core with scoured

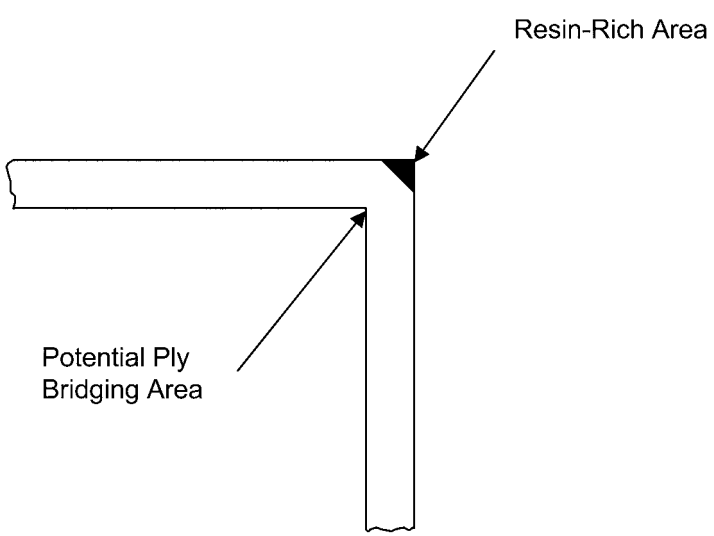


Fig. 5.48 Resin-rich area formed between preform and tool

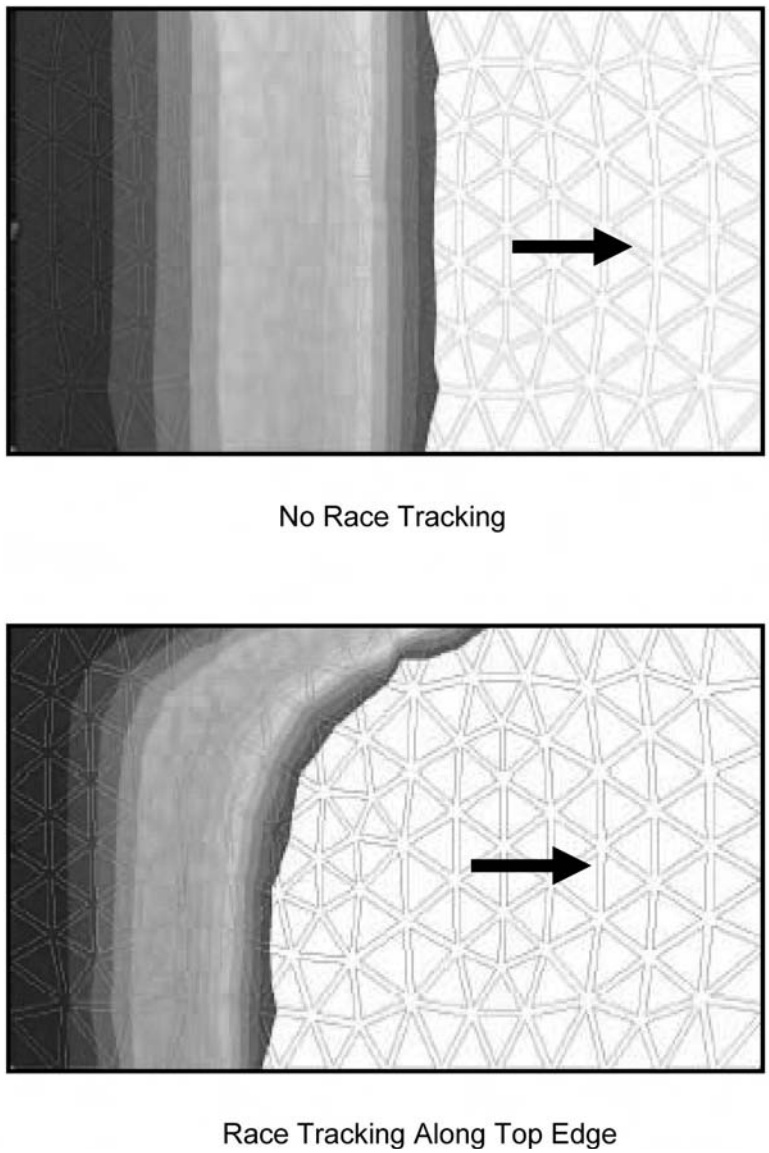


Fig. 5.49 Resin race tracking during injection

intersecting lines on the surface to provide infusion paths, and even holes through the foam that allow the resin to flow through the core and equalize the pressure on both sides. This approach is frequently used with VARTM to reduce infusion time and improve part quality.

If the injection pressure is too high, the advancing flow front can actually displace portions of the perform, resulting in *fiber wash*. This is a more prevalent problem in parts with lower fiber volume percents. With higher fiber volume loadings, there are usually higher compaction pressures from the tool that react with the forces causing fiber wash. However, higher compaction pressures also lower the permeability of the preform and make injection more difficult.

Voids in RTM parts are usually not as much of a problem as in conventional autoclave-cured parts. However, voids can occur if vacuum assistance is used to remove air from the mold during the injection process. This is usually the result of a leak in the mold sealing system that allows the vacuum to pull additional air into the mold. Several steps can be taken to reduce

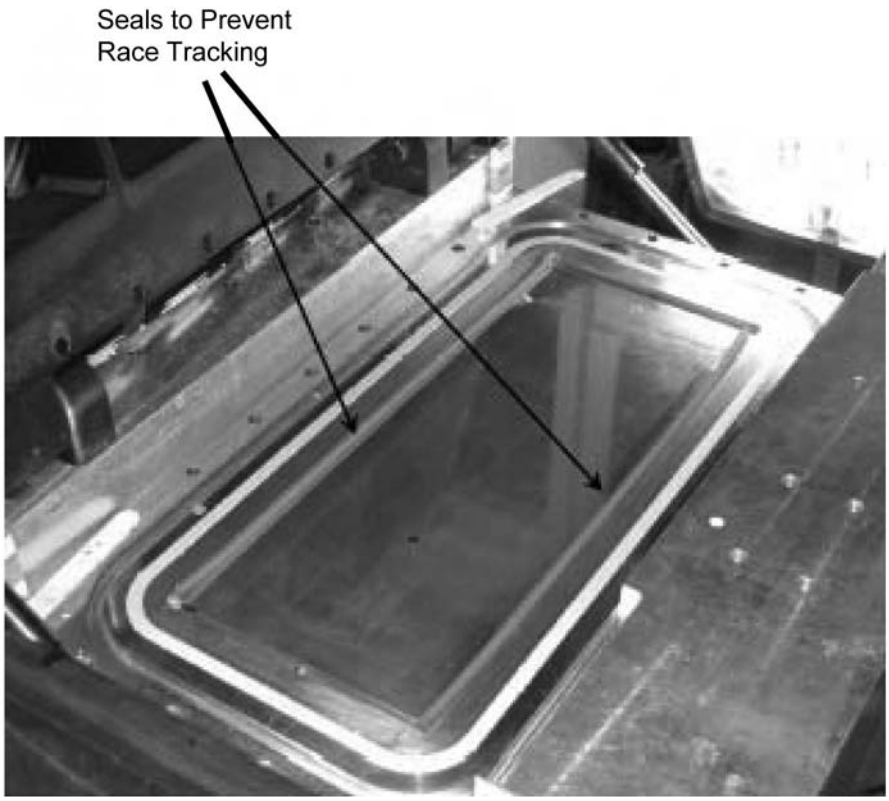


Fig. 5.50 Edge seals to prevent race tracking during injection

voids: (1) make sure that the mold is vacuum tight, particularly if vacuum will be used during the injection process; (2) vacuum degas the resin in the pot to remove volatiles and entrained air just prior to injection; (3) let the resin exiting the vent tubes flow until all air bubbles disappear; and (4) continue to apply pressure after the mold is sealed off to ensure that there is adequate hydrostatic pressure on the resin during the cure cycle.

All liquid molding processes, including RTM, can benefit from mathematical modeling of both the preforming process and the injection process. Using the product geometry, there are finite element models that can be used to predict both fiber movement and distortions during the preforming process, as well as the flow of resin into the tool and preform during injection. The proper use of these advanced models can significantly reduce the time and cost needed to develop a new part configuration. The proper application of these models can also be a significant aid in developing injection and venting strategies for new tool configurations.

5.5.7 Vacuum-Assisted Resin Transfer Molding

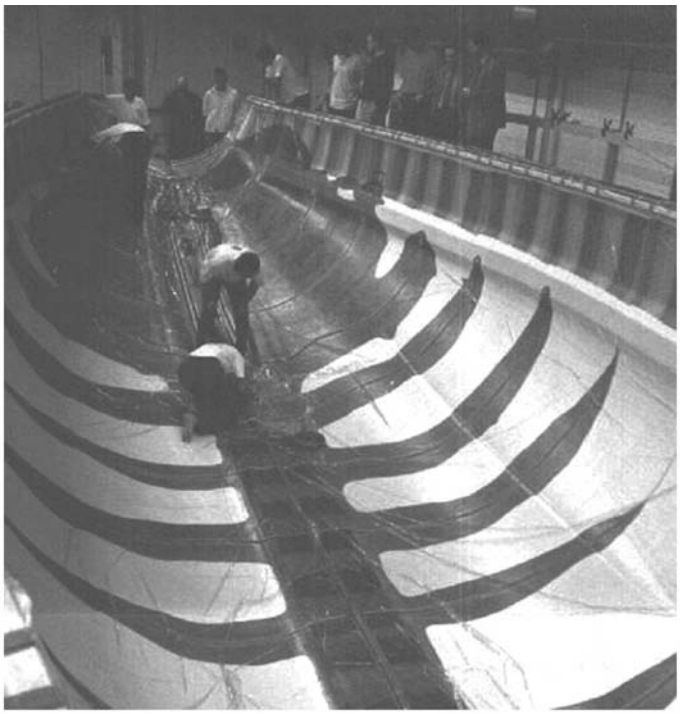
Since VARTM processes use only vacuum pressure for both injection and cure, the single biggest advantage of VARTM is that the tooling is much less expensive and simpler to design than that for conventional RTM processes. In addition, since an autoclave is not required for curing, the potential exists to make very large structures using VARTM processes, such as the large boat hull shown in Fig. 5.51. Also, much lower pressures are used in VARTM processes; thus, lightweight foam cores can easily be incorporated into the lay-ups. VARTM-type processes have been used for many years to build fiberglass boat hulls, but they have only recently attracted the attention of the aerospace industry.

A typical VARTM process, shown in Fig. 5.52, consists of single-sided tooling with a vacuum bag. VARTM processes normally use some type of porous medium on top of the preform to facilitate resin flow across and then saturation through the preform. This porous distribution medium

should be a highly permeable material that allows resin to flow through the material with ease. When a porous distribution medium is used, the resin typically flows through the distribution medium and then migrates down into the preform. Typical distribution media include nylon screens and knitted polypropylene. Since resin infiltration is in the through-the-thickness direction, race tracking and resin leakage around the preform are largely eliminated.

Since the VARTM processes use only vacuum pressure for both injection and cure, autoclaves are not required and parts with very large sizes can be made. Ovens and integrally heated tools are normally used, and because the pressures are low, in this case, less than or equal to 14.7 psia (101.4 kPa), low-cost, lightweight tools can be used. Some manufacturers use double vacuum bags to minimize variations in compaction pressure and to guard against potential vacuum leaks in the primary vacuum bag. A layer of breather between the two bags increases the ability to remove any air from leak locations. Reusable vacuum bags can also be used to reduce the cost of bagging complex shapes. One of the keys to successful VARTM processes is maintaining a very good vacuum (greater than 27 in. (686 mm) of mercury) during the entire process.

The resins used for VARTM processing should have an even lower viscosity than those used for traditional RTM. Resin viscosities less than 100 cps are desirable to give the flow needed to impregnate the preform at only vacuum pressure. Vacuum degassing prior to infusion is often used to help remove entrained air from the mixing operation. Some resin systems may be infused at room temperature, while others require heating. It is desirable to keep the resin source and the vacuum trap away from the heated tool. This makes it easier to control the temperature of the resin at the source and minimizes the chance of an exotherm at the trap. For large part sizes, multiple injection and venting ports are utilized. As a rule of thumb, resin feed lines and vacuum sources should be placed about 18 in. (45 cm) apart. It is more difficult to obtain high fiber volume contents in thick preforms. Since perfect fiber bundle nesting does not occur, there



Note the locations where the resin has wetted the preform, indicating the use of multiple injection ports.

Fig. 5.51 Vacuum-assisted resin transfer molding (VARTM) of a large boat hull

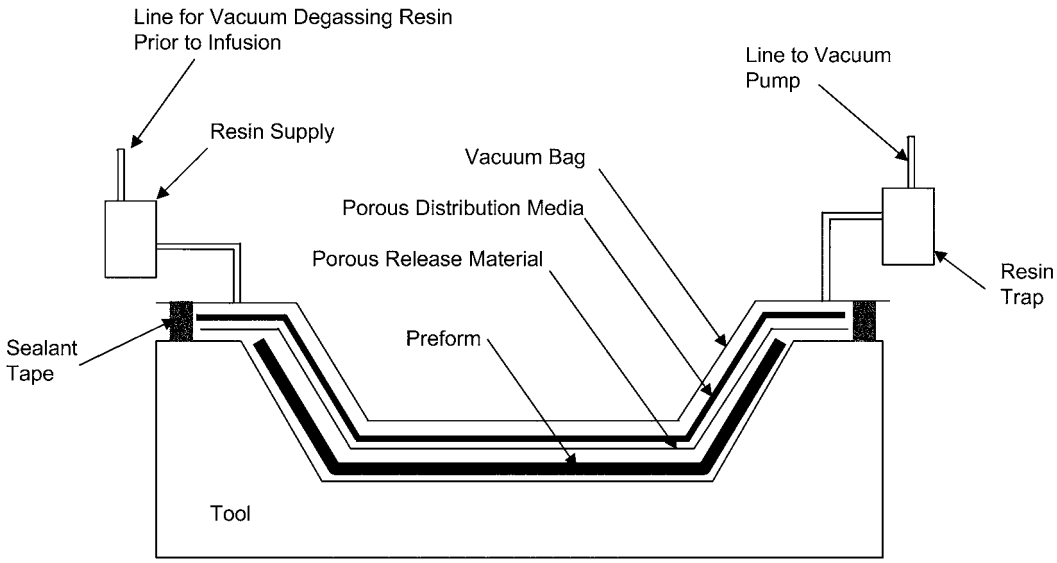


Fig. 5.52 Typical vacuum-assisted resin transfer molding (VARTM) process setup

is an increase in free volume with every additional layer, which results in lower fiber volume contents in thick parts.

Since the pressure is much lower than that normally used in the conventional RTM or autoclave processes, it is more difficult to obtain as high a fiber volume percent as with the higher-pressure processes; however, this process disadvantage is being overcome with near-net preforms. In addition, the VARTM processes cannot hold as tight dimensional tolerances as conventional RTM, and the bag-side surface finish will not be as good as that of a hard-tooled surface. Thickness control is generally a function of the preform lay-up, the number of plies, the fiber volume percent, and the quality of the vacuum applied during the process.

5.6 Resin Film Infusion

Resin film infusion (RFI) is a process originally developed by NASA and the Long Beach division of McDonnell-Douglas (now Boeing). There were two drivers for the development of this process: (1) the desire to have three-dimensional (3-D) reinforcement for a damage-tolerant commercial wing design and (2) the desire to use a qualified prepreg resin system for the matrix resin. The problem with using prepreg resin systems for conventional RTM is that the minimum viscosities (greater than 500 cps) are too high for successful injection and filling of the stitched preform during injection. The process developed by NASA and Boeing, shown schematically in Fig. 5.53, consists of placing a controlled layer of matrix resin (Hexcel's 3501-6), which is a solid at room temperature, in the bottom of the mold. A stitched preform is then loaded into the mold on top of the resin layer. During autoclave cure the resin melts, and vacuum and autoclave pressure are used to draw the liquid resin up through the tool to impregnate the preform. Once the infiltration cycle is complete, the temperature is raised to the cure temperature and the part is cured using autoclave heat and pressure. The key to the RFI process is understanding the compaction and permeability of the preform and the viscosity and kinetics of the resin system. For example, infusing a large preform may require a resin with a viscosity of less than 250 cps at 250 °F (120 °C) for one to two hours. In addition, preform design and placement within the tool, as well as tool design and dimensional control, are critical for this process. A special cure cycle was developed to achieve the correct time-temperature-viscosity profile to ensure complete preform saturation.

Boeing-Long Beach, under the NASA Composite Wing Program, successfully designed, built, assembled, and tested a 42 ft (13 m) long by 8 ft (2.4 m) wide composite wing using the RFI

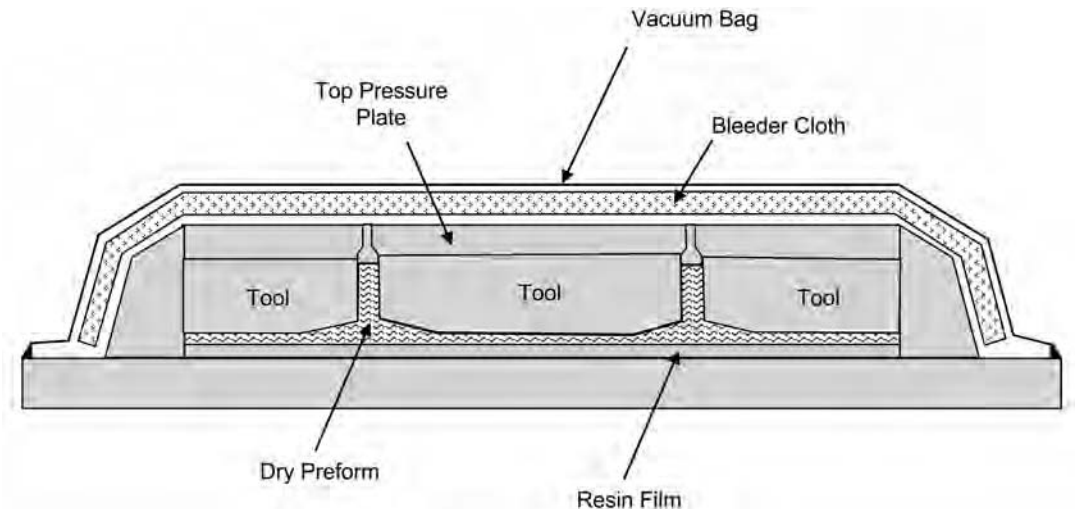


Fig. 5.53 Schematic of the resin film infusion (RFI) process. Source: Ref 15

process. For this program, they used the matrix resin 3501-6 with stitched preforms supplied by the Saertex Company of Germany. A completed stitched, infused, and cured wing cover is shown in Fig. 5.54. The Saertex material was supplied as either seven- or nine-layer-thick material with typical orientations of 0°, ± 45°, and 90°.

A schematic of the stitching processes used is shown in Fig. 5.55. The skin, stringers, and intercostals were individually stitched and then the skin, stringers, and intercostal clips were stitched together. The Saertex stack-ups were stitched together using 1600 denier aramid fiber (in this case, DuPont's Kevlar 29) thread. A typical stitching operation is shown in Fig. 5.56. A modified lock stitch was used to stitch the stack-ups on a 0.20 in. (5.1 mm) wide spacing with a pitch of eight stitches per inch. The large wing covers normally contained five to eleven stacks of the Saertex material with built-up areas as thick as 17 stacks at 0.94 in. (24 mm).

To extend the time at low viscosity, a reduced-catalyst version of 3501-6 was used that maintained a low viscosity (100 to 300 cps) for up to two hours to allow time for the resin to flow up the tool and impregnate the preform. It was important to allow sufficient time during the initial heat-up to 250 °F (120 °C) and to hold at that temperature for the resin to melt and thoroughly infuse the preform. Additionally, the resin was vacuum degassed to reduce voids and surface porosity.

A variant of the RFI process involves using thin layers of resin film between the dry preform layers (Fig. 5.57) instead of putting a large mass of resin in the bottom of the tool. The advantage of this process, sometimes referred to as SP Resin Infusion Technology (SPRINT), is that the resin does not have to flow very far to impregnate each layer, and vacuum bag pressure is often sufficient for full impregnation. However, for thicker laminates, lay-up bulk can be a problem.

5.7 Pultrusion

Pultrusion is a mature process that has been used in commercial applications since the 1950s. In the pultrusion process, continuous fibrous reinforcement is impregnated with a matrix and is then continuously consolidated into a solid composite. While there are several different variations of the pultrusion process, the basic process for thermoset composites is shown in Fig. 5.58. The reinforcement, usually glass rovings, is pulled from packages on a creel stand and gradually brought together and pulled into an open resin bath where the reinforcement is impregnated with liquid resin. After emerging from the resin bath, the reinforcement is first directed through a preform die that aligns the rovings to the part shape and then guides them into a heated constant cross-section die where the part cures as it progresses through the die. Curing takes place from the outside of the part toward the interior. Although the die initially heats the resin, the exotherm resulting from the curing polyester



Fig. 5.54 Integral wing cover panel fabricated by the resin film infusion (RFI) process. Source: Ref 16

resin can also provide a significant amount of the heat required for cure. The temperature peak caused by the exotherm should occur within the confines of the die and allow the composite to shrink away from the die at the exit. The composite part emerges from the die as a fully cured part, which cools as it is being pulled by the puller mechanism. Finally, the part is cut to the required length by a cutoff saw.

While pultrusion has the advantage of being an extremely cost-effective process for making long, constant cross-section composite parts, it is definitely a high-volume process, as the setup time for a production run can be rather costly. In addition, there are limitations in that the part must be of constant cross section, and the flexibility in defining reinforcement orientation is somewhat limited. Pultrusion is capable of making a wide variety of structural shapes, as shown in Fig. 5.59, including hollow sections when a mandrel is used. While glass fiber/polyester materials dominate the market, a considerable amount of work has been done to develop the process for the aerospace industry with higher-performance carbon/epoxy materials. Floor beams in commercial aircraft are a potential application.

The major advantages of the pultrusion process are (1) low production cost due to the continuous nature of the process; (2) low raw material costs and minimal scrap; (3) uncomplicated machinery; and (4) a high degree of automation. However, there are several disadvantages: (1) the process is limited to constant cross-section shapes; (2) setup times and initial process start-up are

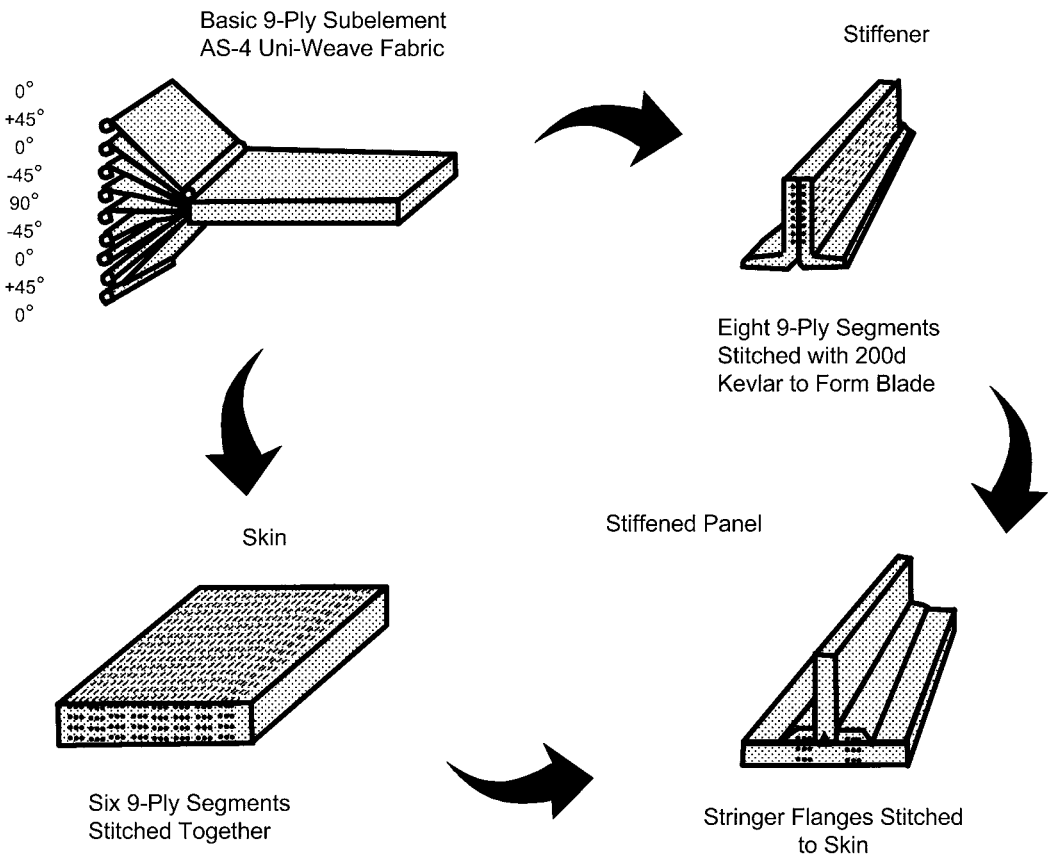


Fig. 5.55 Process flow for stitching a resin film infusion (RFI) wing cover. Source: Ref 11

labor intensive; (3) parts may have higher void contents than allowed for some structural applications; (4) the majority of the reinforcement is oriented in the longitudinal direction; (5) the resin used must have low viscosity and long pot life; and (6) in the case of polyesters, styrene emissions can create worker health concerns. The critical processing variables are die design, resin formulation, material guidance before and after impregnation, and temperature control in the die.

Due to the nature of the pultrusion process, continuous reinforcement must be used, either in the form of rovings or rolls of fabric; however, discontinuous mats and veils can be incorporated. To facilitate setup, creel stands are often placed on wheels so that the majority of the setup can be done off-line, reducing the downtime for the pultruder. A consideration for the preimpregnation guide mechanism is that the reinforcement is usually fragile and, in the case of glass and carbon, abrasive. Dry rovings are often guided by ceramic eyelets to reduce wear on both the fibers and the guidance mechanism. Fabrics, mats, and veils can be guided with plastic or steel sheets with machined slots or holes. Chopped strand mat is often used at an areal weight of 1.5 oz/yd^2 (51 g/m^2) in rolls of up to 300 ft (90 m) with a minimum width of 4 in. (10 cm). Several sets of guidance mechanisms may be required to gradually shape the reinforcements prior to impregnation. In a process called *pull-winding*, moving winding units are used to overwrap the primarily unidirectional reinforcement, thereby providing additional torsional stiffness.

Several different methods can be used for the impregnation process. The first, and most common, is to guide the reinforcements down into an open resin bath. Impregnation results from capillary action and by sets of rods in the bath that the reinforcements pass over and under. This method produces good impregnation and is simple; however, in the case of polyester resins, styrene emissions can be a problem. To reduce

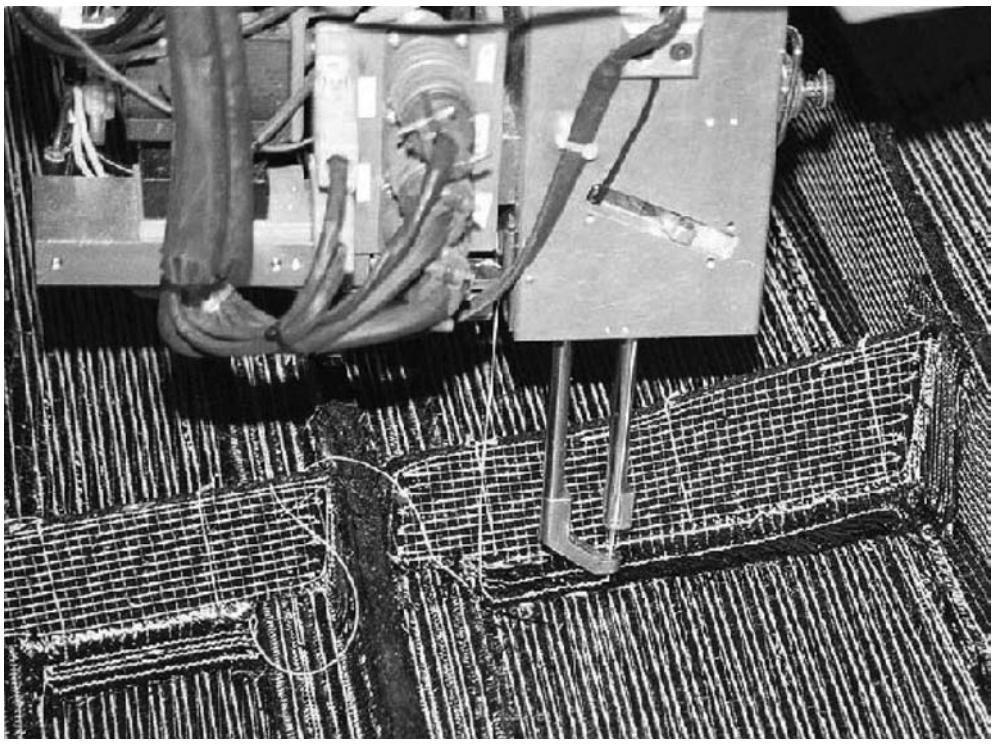


Fig. 5.56 Stitching of the intercostal substructure to the wing cover. Source: Ref 16

this problem, another approach uses an enclosed bath in which the reinforcement travels horizontally and enters and exits the bath through slots cut in the ends of the bath. The main advantage of this method is that the reinforcement is not bent and the styrene emissions are somewhat reduced. Vented hoods are frequently placed over the resin bath to help remove the styrene fumes from the immediate work area. A third method, called *injection* or *reaction injection pultrusion* (Fig. 5.60), injects the resin under pressure after the reinforcement has entered the die. While this method virtually eliminates the styrene emissions problem, the temperature of the die at the injection point must be closely controlled to prevent premature resin gelation. It should also be noted that this method significantly complicates die design. The dies are usually longer, more complex, and more expensive than conventional dies. A fourth method, although rarely used to date, is to use preimpregnated reinforcements. Although more costly than the inline impregnation methods, preimpregnation allows better control of the resin content and fiber areal weight.

For the open bath impregnation process, the resin must have low viscosity (approximately 10 poise) and long pot life so that it will readily impregnate the fibers and not gel in the bath. Resin impregnation baths are usually 3 to 6 ft (0.9 to 1.8 m) long. The resin can be heated to reduce the viscosity, but this will generally shorten the pot life considerably. For the injection pultrusion process, more reactive resins with shorter pot lives can be used. The resin should crosslink throughout the part thickness before it exits the die. The faster it crosslinks—while keeping the exotherm under control so that thermally induced residual stresses are minimized and resin cracking is prevented—the faster and more productive the process. However, for epoxy resins that do not react as quickly as polyesters and vinyl esters, a freestanding postcure in an oven after pultrusion may be required to complete the cure reaction. After the reinforcements have been impregnated, they pass through another set of guidance devices to further shape the reinforcements prior to entering the die cavity. These guidance devices aid in gradually shaping the reinforcements prior to curing.

The pultrusion die itself is usually machined from tool steel and typically has a length of 24 to 60 in. (0.6 to 1.5 m). With the exception of a

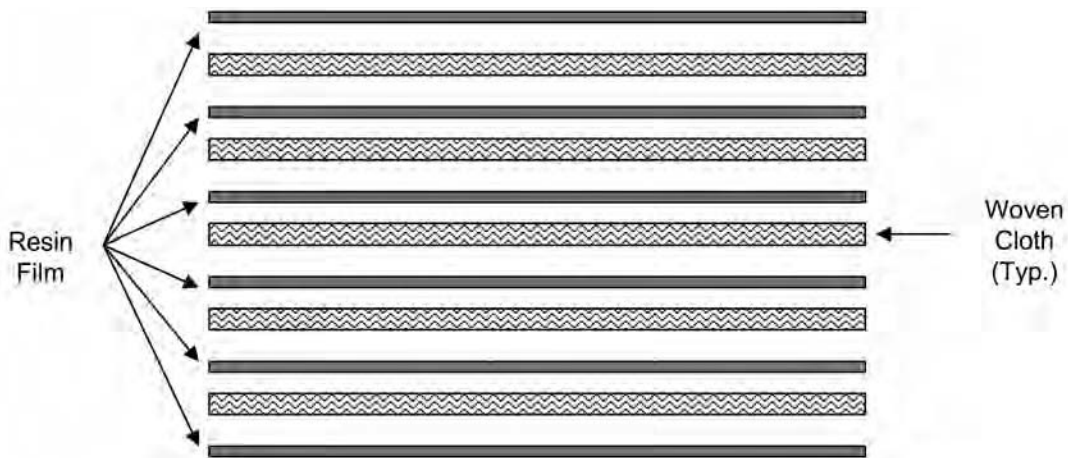


Fig. 5.57 Resin film infusion (RFI) with resin film

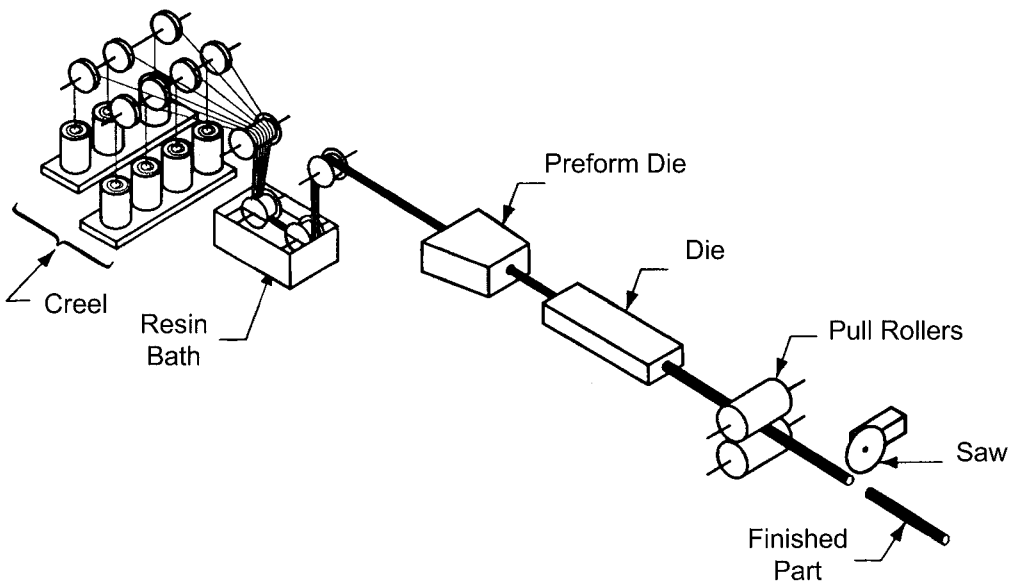


Fig. 5.58 Pultrusion process. Source: Ref 7

gradual taper at the entrance end of the die, the die cross section is usually constant, with extremely smooth surfaces that have been chrome plated for durability and reduced friction. Almost all dies are segmented so that they may be taken apart for inspection and cleaning. Pultrusion dies generally have multiple heating zones that allow the temperature to be varied along the length of the die. For high exothermic resin systems such as polyesters, they may even have cooling zones near the exit to help maintain temperature control.

After the part is cured in the die, it is gripped and pulled over a rather long distance to allow it to cool sufficiently before being cut to length. A number of different puller mechanisms are used in industry. The simplest method is to use a series of rubber wheels that grip the part in pairs and pull it. Although this method is simple and cheap, it is limited to small cross sections where the pulling forces are low. Conventional belt pullers may also be used; frequently, these are caterpillar belt pullers where successive rubber pads are mounted on the belt. The most common

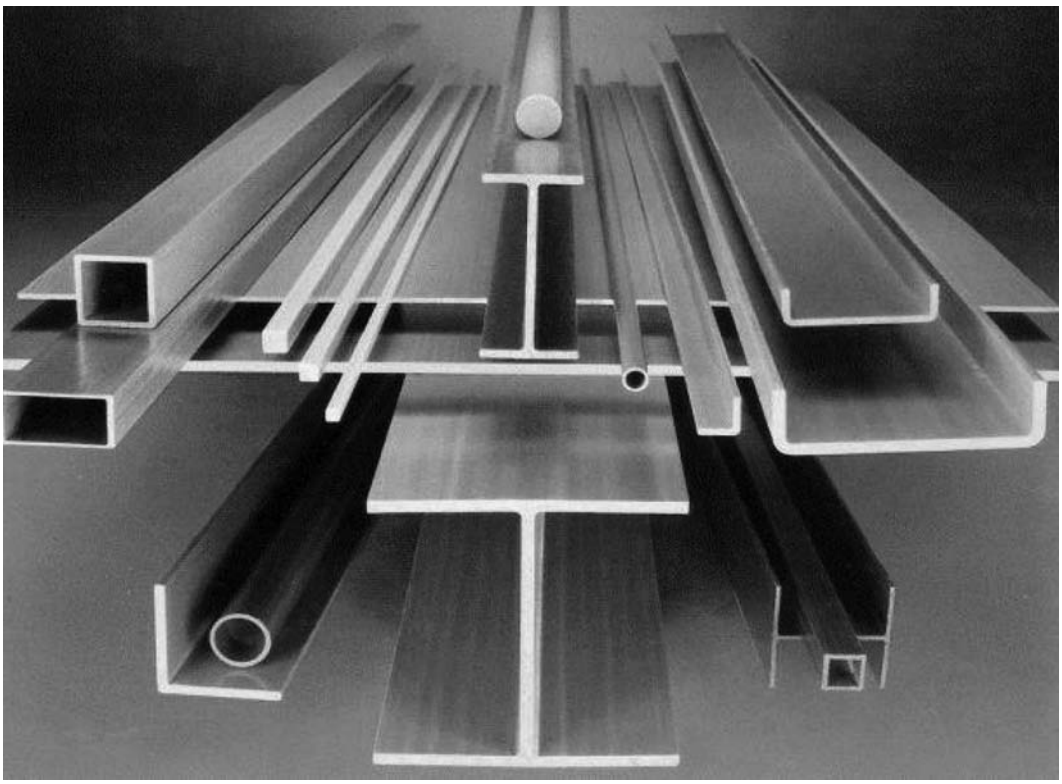


Fig. 5.59 Pultruded parts

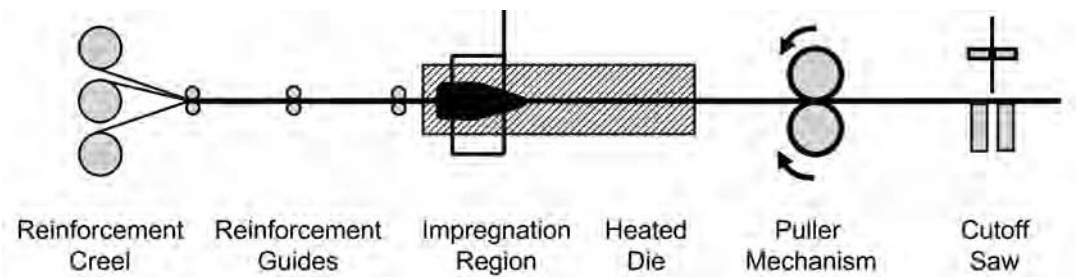


Fig. 5.60 Injection pultrusion die process. Source: Ref 17

pulling method involves hydraulic clamp pullers with rubber pads. The pulling motion may be intermittent or continuous. It should be noted that the rubber pads must be tailored to fit the part geometry; otherwise, excessive lateral pressure may be exerted on the part. A typical puller mechanism may have a pulling capacity of 5 to 10 tons (4.5 to 9.0 metric tons), although larger machines may have a capacity of several hundred tons. A water-cooled abrasive cutoff saw is used to cut the pultruded part to the required length. The saw is mounted to the pultrusion unit and travels with the puller mechanism. Depending on the material to be cut, the cutting may be done dry or with flood coolant. Diamond-impregnated or carbide circular saw blades are normally used to produce a clean cut.

Glass/polyester is the predominant material used for pultruded parts. Other matrices used include vinyl esters, acrylics, phenolics, and epoxies. A processing advantage of polyesters and vinyl esters is the high shrinkage (seven to nine

percent) they undergo during cure. This helps the part to shrink away from the die, reducing the friction and pulling forces required. By contrast, epoxies exhibit much less shrinkage during cure (one to four percent), and the friction and pulling forces are substantially higher. In general, epoxies do not produce as good a surface finish, and the process must be run at higher temperatures and slower speeds. Typical processing speeds for polyesters are 24 to 48 in./min (0.6 to 1.2 m/min); however, under certain circumstances, speeds may approach 200 in./min (5 m/min). As the pulling speed increases, the pulling force increases. Too fast a pulling speed may move the peak exotherm temperature outside of the die and result in defects such as scaly and cracked surfaces, porosity and internal cracks, warpage, and discoloration. Although a longer die may ensure that the peak exotherm temperature remains inside the die, the trade-off is that greater pulling forces will be required. In fact, the pulling force required during pultrusion is often used as an indicator of the health of the process. If the pulling force starts to increase above the normal force required, it might be an indication that the process is going out of control.

Continuous glass rovings are the most prevalent reinforcement, although it is standard practice to interleave chopped or continuous strand mats to improve transverse properties and surfacing mats, veils, and nonwovens to improve the surface finish. For applications that require higher transverse strength or torsional stiffness, fabrics and braids that are stitched together can be used.

REFERENCES

1. Virtek LaserEdge product literature
2. M.N. Grimshaw, Automated Tape Laying, *ASM Handbook*, Vol 21, *Composites*, ASM International, 2001, p 480–485
3. M.N. Grimshaw, C.G. Grant, and J.M.L. Diaz, Advanced Technology Tape Laying for Affordable Manufacturing of Large Composite Structures, *46th International SAMPE Symposium*, May 2001, p 2484–2494
4. D.O. Evans, Fiber Placement, *ASM Handbook*, Vol 21, *Composites*, ASM International, 2001, p 477–479
5. L. Repecka and J. Boyd, "Vacuum-Bag-Only-Curable Prepregs That Produce Void-Free Parts," *SAMPE 2002*, 12–16 May 2002
6. S.C. Mantel and D. Cohen, Filament Winding, *Processing of Composites*, Hanser, 2000
7. M.K. Grover, *Fundamentals of Modern Manufacturing: Materials, Processes, and Systems*, Prentice Hall Inc., 1996
8. S.W. Beckwith and C.R. Hyland, Resin Transfer Molding: A Decade of Technology Advances, *SAMPE J.*, Vol 34 (No. 6), November/December 1998, p 7–19
9. J.B. Ardolino and T.M. Fegelman, Fiber Placement Implementation for the F/A-18 E/F Aircraft, *39th International SAMPE Symposium*, April 1994, p 1602–1616
17. B.T. Astrom, *Manufacturing of Polymer Composites*, Chapman & Hall, 1997
8. S.W. Beckwith and C.R. Hyland, Resin Transfer Molding: A Decade of Technology Advances, *SAMPE J.*, Vol 34 (No. 6), November/December 1998, p 7–19
9. B.N. Cox and G. Flanagan, "Handbook of Analytical Methods for Textile Composites," NASA Contractor Report 4750, March 1997
10. A. Dobrowolski and N. White, "Re-Useable Customized Vacuum Bags," *33rd International SAMPE Technical Conf.*, November 2001
11. M.B. Dow and H.B. Dexter, "Development of Stitched, Braided and Woven Composite Structures in the ACT Program and at Langley Research Center (1985 to 1997), Summary and Bibliography," NASA/TP-97-206234, November 1997
12. F.K. Ko, Braiding, *Engineered Materials Handbook*, Vol 1, *Composites*, ASM International, 1987, p 519–528
13. T.G. Gutowski, Cost, Automation, and Design, *Advanced Composites Manufacturing*, John Wiley & Sons, Inc., 1997
14. C.C. Poe, H.B. Dexter, and L.S. Raju, "A Review of the NASA Textile Composites Research," AIAA, 1997
15. B.R. Gebart and L.A. Strombeck, Principles of Liquid Composite Molding, *Processing of Composites*, Hanser, 2000, p 359–386
16. R. Palmer, "Techno-Economic Requirements for Composite Aircraft Components," *Fiber-Tex 1992 Conference*, NASA Conference Publication 3211, 1992
17. M. Karal, "AST Composite Wing Program—Executive Summary," NASA/CR-2001-210650, March 2001
18. B.T. Astrom, *Manufacturing of Polymer Composites*, Chapman & Hall, 1997

SELECTED REFERENCES

- J.B. Ardolino and T.M. Fegelman, Fiber Placement Implementation for the F/A-18 E/F Aircraft, *39th International SAMPE Symposium*, April 1994, p 1602–1616
- M. Braley and M. Dingeldein, Advancements in Braided Materials Technology, *46th International SAMPE Symposium*, May 2001, p 2445–2454
- L. Dickinson, M. Salama, and D. Stobbe, Design Approach for 3D Woven Composites: Cost vs. Performance, *46th International SAMPE Symposium*, May 2001, p 765–777
- G. Dillon, P. Mallon, and M. Monaghan, The Autoclave Processing of Composites, *Advanced Composites Manufacturing*, John Wiley & Sons, Inc., 1997, p 205–258
- "FRP—An Introduction to Fiberglas-Reinforced Plastics/Composites," Owens/Corning Fiberglas Corporation, 1976
- J.S. Hayward and B. Harris, Effect of Process Variables on the Quality of RTM Mouldings, *SAMPE J.*, Vol 26 (No. 3), May/June 1990, p 35–46
- S. Hinrichs, R. Palmer, and A. Ghumman, Mechanical Property Evaluation of Stitched/RFI Composites, *5th NASA/DoD Advanced Composites Technical Conf.*, NASA CP-3294, Vol 1, 1995, p 697–716
- K. Jackson, Low Temperature Curing Materials: The Next Generation, *43rd International SAMPE Symposium*, May/June 1998, p 1–8
- J.L. Kittleson and S.C. Hackett, Tackifier/Resin Compatibility Is Essential for Aerospace Grade Resin Transfer Molding, *39th International SAMPE Symposium*, April 1994, p 83–96
- F.K. Ko and G.W. Du, Processing of Textile Preforms, *Advanced Composites Manufacturing*, John Wiley & Sons, Inc., 1997
- A.C. Loos, J. Sayre, R. McGrane, and B. Grimsley, VARTM Process Model Development, *46th International SAMPE Symposium*, May 2001, p 1049–1060
- W.C. Mace, Curing Polyimide Composites, *Engineered Materials Handbook*, Vol 1, *Composites*, ASM International, 1987
- P.K. Mallick, *Fiber Reinforced Composites: Materials, Manufacturing and Design*, Marcel Dekker, Inc., 1993
- R. Palmer, Manufacture of Multi-Axial Stitched Bonded Non-Crimp Fabrics, *46th International SAMPE Symposium*, May 2001, p 779–788
- S.T. Peters, W.D. Humphrey, and R.F. Foral, *Filament Winding Composite Structure Fabrication*, 2nd ed., SAMPE, 1995
- T.L. Price, G. Dalley, P.C. McCullough, and L. Choquette, "Handbook: Manufacturing Advanced Composite Components for Airframes," Report DOT/FAA/AR-96/75, Office of Aviation Research, April 1997
- C. Ridgard, Low Temperature Moulding (LTM) Tooling Prepreg with High Temperature Performance Characteristics, *Reinf. Plast.*, March 1990, p 28–33
- C. Ridgard, Affordable Production of Composite Parts Using Low Temperature Curing Prepregs, *42nd International SAMPE Symposium*, May 1997, p 147–161
- C. Ridgard, Advances in Low Temperature Curing Prepregs for Aerospace Structures, *45th International SAMPE Symposium*, May 2000, p 1353–1367
- C. Ridgard, "Composite Tooling—Design and Manufacture: Getting It Right," The Advanced Composites Group
- L.R. Sanders, "Braiding—A Mechanical Means of Composite Fabrication," *8th National SAMPE Conference*, October 1976
- S.B. Shim, K. Ahn, J.C. Seferis, and A.J. Berg, Cracks and Microcracks in Stitched Structural Composites Manufactured with Resin Film Infusion Process, *J. Adv. Mater.*, July 1995, p 48–62
- P. Simacek, J. Lawrence, and S. Advani, Numerical Mold Filling Simulations of Liquid Composite Molding Processes—Applications and Current Issues, *2002 European SAMPE*, p 137–148
- A.B. Strong, *Fundamentals of Composite Manufacturing: Materials, Methods, and Applications*, Society of Manufacturing Engineers, 1985
- A.B. Strong, Manufacturing, *International Encyclopedia of Composites*, Stuart Lee, ed., VCH Publishers, Inc., 1990, p 102–126
- J. Wittig, Robotic Three-Dimensional Stitching Technology, *46th International SAMPE Symposium*, May 2001, p 2433–2444
- G.F. Xu, L. Repecka, and J. Boyd, Cycom X5215—An Epoxy Prepreg That Cures Void Free Out of Autoclave at Low Temperature, *43rd International SAMPE Symposium*, May/June 1998, p 5–15

Copyright © 2010, ASM International®
All rights reserved.
www.asminternational.org

CHAPTER 6

Thermoplastic Composite Fabrication Processes

THERMOPLASTIC COMPOSITE FABRICATION PROCESSES are discussed in this chapter. The three main areas covered are consolidation, thermoforming, and joining. The basics of thermoplastic composite materials were discussed in Chapter 3, "Matrix Resin Systems."

6.1 Thermoplastic Consolidation

Consolidation of melt-fusible thermoplastics consists of heating, consolidation, and cooling, as depicted schematically in Fig. 6.1. As with thermoset composites, the main processing variables are time (t), temperature (T), and pressure (P).

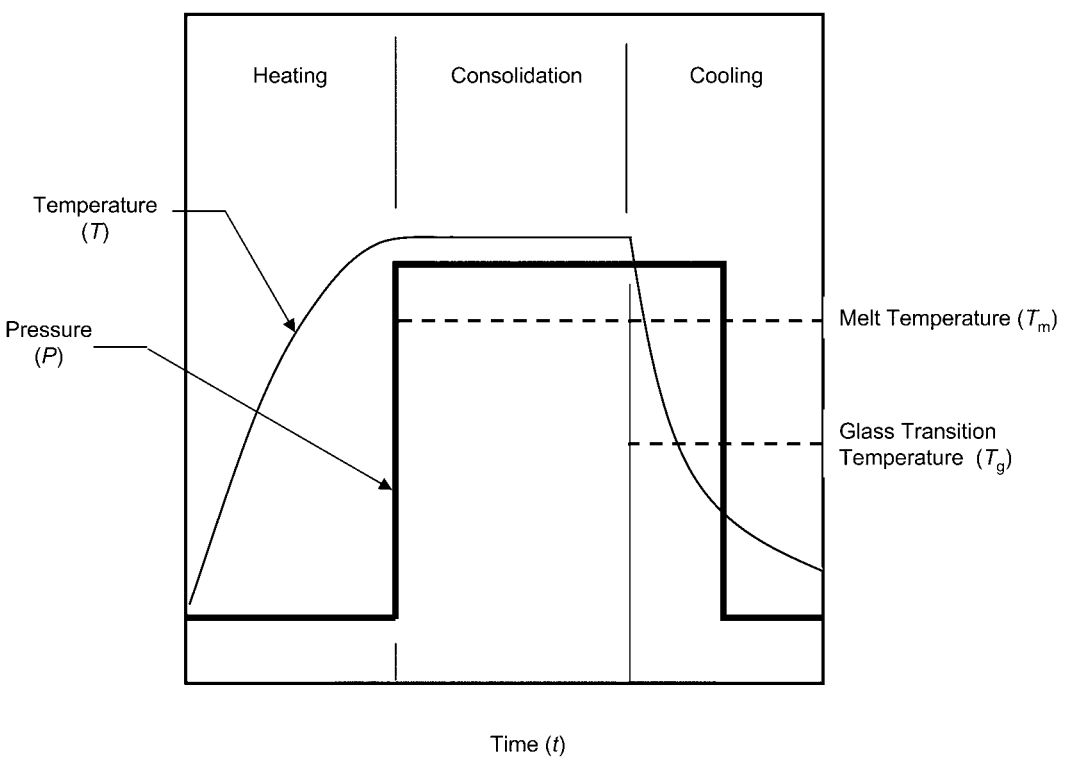


Fig. 6.1 Typical thermoplastic composite process cycle. Source: Ref 1

Heating can be accomplished with infrared heaters, convection ovens, heated platen presses, or autoclaves. Since time for chemical reactions is not requisite, the time required to reach consolidation temperature is a function of the heating method and the mass of the tooling. The consolidation temperature depends on the specific thermoplastic resin, but it should be well above the glass transition temperature T_g for amorphous resins or above the melt temperature T_m for semicrystalline materials.

As a general rule, the processing temperature for an amorphous thermoplastic composite should be 400 °F (205 °C) above its T_g, and for a semicrystalline material it should be 200 °F (95 °C) or less above its T_m. However, heating most thermoplastics above 800 °F (425 °C) will result in degradation. The time at the consolidation temperature is primarily a function of the product form used. For example, well-consolidated hot melt–impregnated tape can be successfully consolidated in very short times (minutes if not seconds), while woven powder coated or comingled prepregs require longer times for the resin to flow and impregnate the fibers. Occasionally, a process called *film stacking* is used, in which alternating layers of thermoplastic film and dry woven cloth are layed up and consolidated. The time for successful consolidation for film stacked lay-ups becomes even longer, since the high-viscosity resin has even longer distances to flow. A typical processing cycle to achieve fiber wet-out and full consolidation for a film stacked laminate might be one hour at 150 psi (1035 kPa) applied pressure. Like the heat-up rate, the cool-down rate from consolidation is a function of the processing method used and the tooling mass. The only caveat concerning cooling is that semicrystalline thermoplastics should not be cooled so quickly or quenched so that they fail to form the desired semicrystalline structure that provides optimal elevated-temperature performance and solvent resistance. During cooling, the pressure should be maintained until the temperature falls well below the T_g. This restricts the nucleation of voids, suppresses the elastic recovery of the fiber bed, and helps to maintain the desired dimensions. Finally, pressure during the process provides the driving force to put the layers in intimate contact, pushes them together, and further helps to impregnate the fiber bed. It should be noted that the properties of solvent-impregnated prepreg, powder-coated, comingled, and film-stacked laminates are not as good as those made from hot melt–impregnated prepreg due to the superior fiber-to-matrix bond formed during the hot melt impregnation process.

Several methods are employed to consolidate thermoplastic composites. Flat sheet stock can be preconsolidated for subsequent forming in a platen press. Two press processes are shown in Fig. 6.2. In the platen press method, precollated ply packs are preheated in an oven and then rapidly shuttled into the pressure application zone for consolidation. If the material requires time for resin flow for full consolidation or crystallinity control, then the press may require heating. If a well-consolidated prepreg is used, then rapid cooling in a cold platen press may suffice. It should be pointed out that this process still requires collation of the ply packs or layers, usually a hand lay-up operation. Since the material contains no tack, soldering irons, heated to 800 to 1200 °F (425 to 650 °C), are frequently used to tack the edges to prevent the material from slipping. Handheld ultrasonic guns have also been used for ply tacking. A continuous consolidation process is the double belt press that contains both pressurized heating and cooling zones. This process is widely used in making glass mat thermoplastic prepreg for the automotive industry, with polypropylene as the resin and glass fiber as the reinforcement.

If the part configuration is complex, an autoclave is certainly an option for part consolidation; however, there are several disadvantages to this technique. First, it may prove difficult to find an autoclave that is capable of attaining the 650 to 750 °F (345 to 400 °C) temperatures and 100 to 200 psi (690 to 1380 kPa) pressures required for some advanced thermoplastics. Second, at these temperatures, the tooling will be expensive and may be massive, dictating slow heat-up and cool-down rates. Third, since high processing temperatures are required, it is very important that the coefficient of thermal expansion of the tool match that of the part. For carbon fiber thermoplastics, monolithic graphite, cast ceramic, steel, and Invar 42 are normally used. Fourth, the bagging materials must be capable of withstanding the high temperatures and pressures. In a typical bagging operation (Fig. 6.3), the materials required include high-temperature polyimide bagging material, glass bleeder cloth, and silicone bag sealant. The polyimide bagging materials (for example, Kapton or Upilex) are more brittle and harder to work with than the nylon materials used for 250 to 350 °F (120 to 175 °C) curing thermosets. In addition, the high-temperature silicone rubber sealants have minimal tack and tend not to

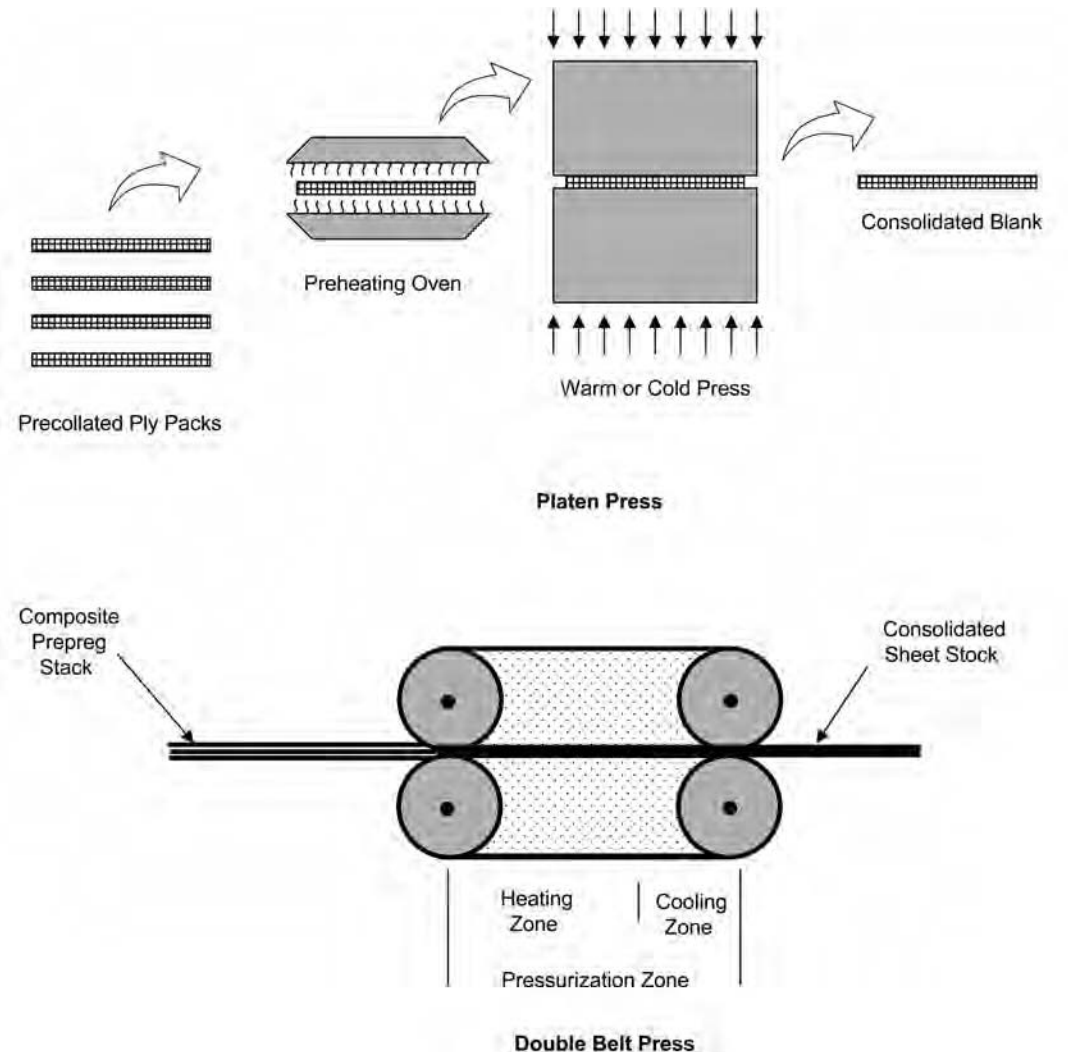


Fig. 6.2 Fabrication methods for sheet stock

seal very effectively at room temperature. Clamp bars are often placed around the periphery to help get the seal to tack at room temperature. As the temperature is increased, the sealant develops tack under pressure and the seal becomes much more effective. A typical autoclave consolidation cycle for carbon/polyetheretherketone (PEEK) prepreg would be 680 to 750 °F (360 to 400 °C) at 50 to 100 psi (345 to 690 kPa) pressure for 5 to 30 minutes; however, the actual cycle time to heat and cool large tools is normally in the range of 5 to 15 hours. In spite of all of these disadvantages, autoclaves have a place in thermoplastic composite part fabrication for parts that are too complex to make by other methods.

Autoconsolidation, or in situ placement of melt-fusible thermoplastics, is a series of processes that includes hot tape laying, filament winding, and fiber placement. In the autoconsolidation process, only the area that is being immediately consolidated is heated above the melt temperature; the remainder of the part is held well below that temperature. Two processes are shown in Fig. 6.4—a hot tape laying process that relies on conduction heating and cooling from hot shoes, and a fiber placement process that uses a focused laser beam at the nip point for heating. Other forms of heating include hot gas torches, quartz lamps, and infrared (IR) heaters. The mere fact that autoconsolidation is possible illustrates

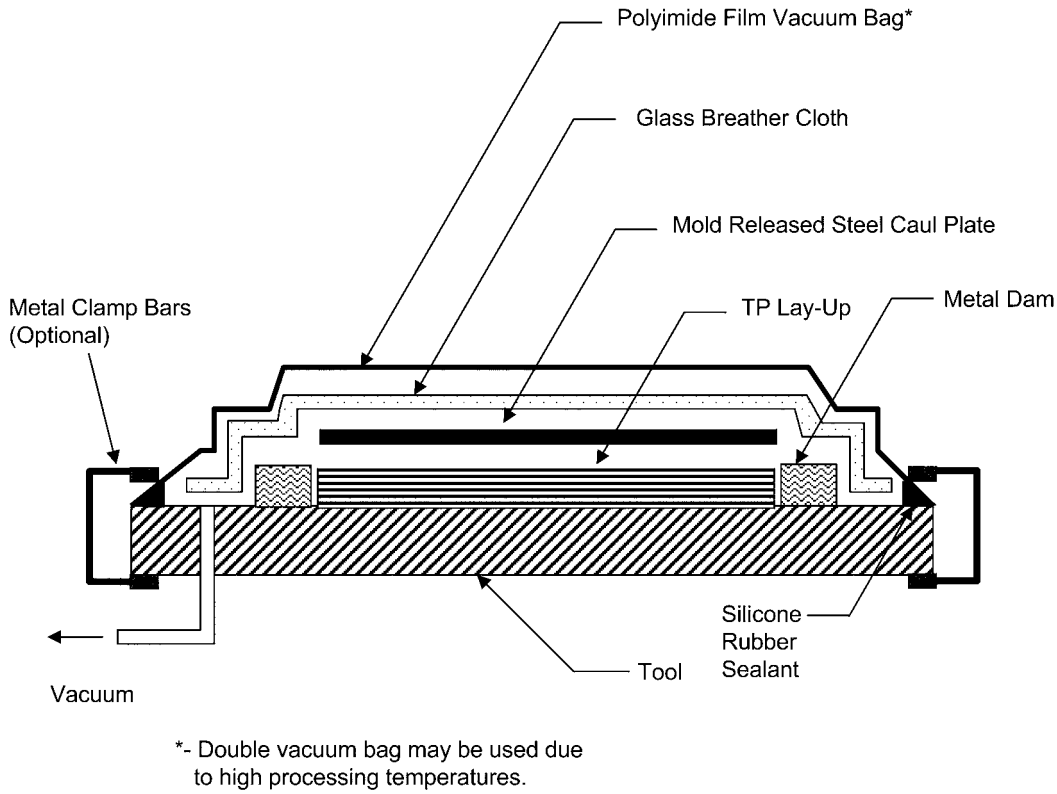


Fig. 6.3 Typical vacuum bag configuration

that the contact times for many thermoplastic polymers at normal processing temperatures can be quite short. Provided that full contact pressure is made at the ply interfaces, autoconsolidation can occur in less than half a second.

A potential problem with autoconsolidation is lack of consolidation due to insufficient diffusion time. If a well-impregnated prepreg is used, then only the ply interfaces need be consolidated. However, if there are intraply voids, then the process time is so short as to be insufficient to heal and consolidate these voids, and a post-consolidation cycle will be required to achieve full consolidation. Previous studies have shown that the interlaminar shear strength of a composite is reduced about seven percent for each one percent of voids up to a maximum of four percent. A reasonable goal is 0.5 percent or less porosity. It has been reported that hot tape laying operations usually result in 80 to 90 percent consolidation, indicating the necessity of secondary processing to obtain full consolidation. However, productivity gains for processes such as hot tape laying of 200 to 300 percent have been cited compared to traditional hand lay-up methods.

6.2 Thermoforming

One of the main advantages of thermoplastic composites is their ability to be rapidly processed into structural shapes by thermoforming. The term *thermoforming* encompasses a broad range of manufacturing methods. However, thermoforming is essentially a process that uses heat and pressure to form a flat sheet or ply stack into a structural shape. A typical thermoforming setup is shown in Fig. 6.5. The first step in thermoforming is to collate the ply pack. The collated ply pack could then be preconsolidated into a flat laminate or the thermoforming operation could be conducted using the unconsolidated ply pack. There is some disagreement as to whether it is better to use preconsolidated blanks or loose, unconsolidated ply packs for thermoforming. Preconsolidated blanks offer the advantage of being well consolidated, with

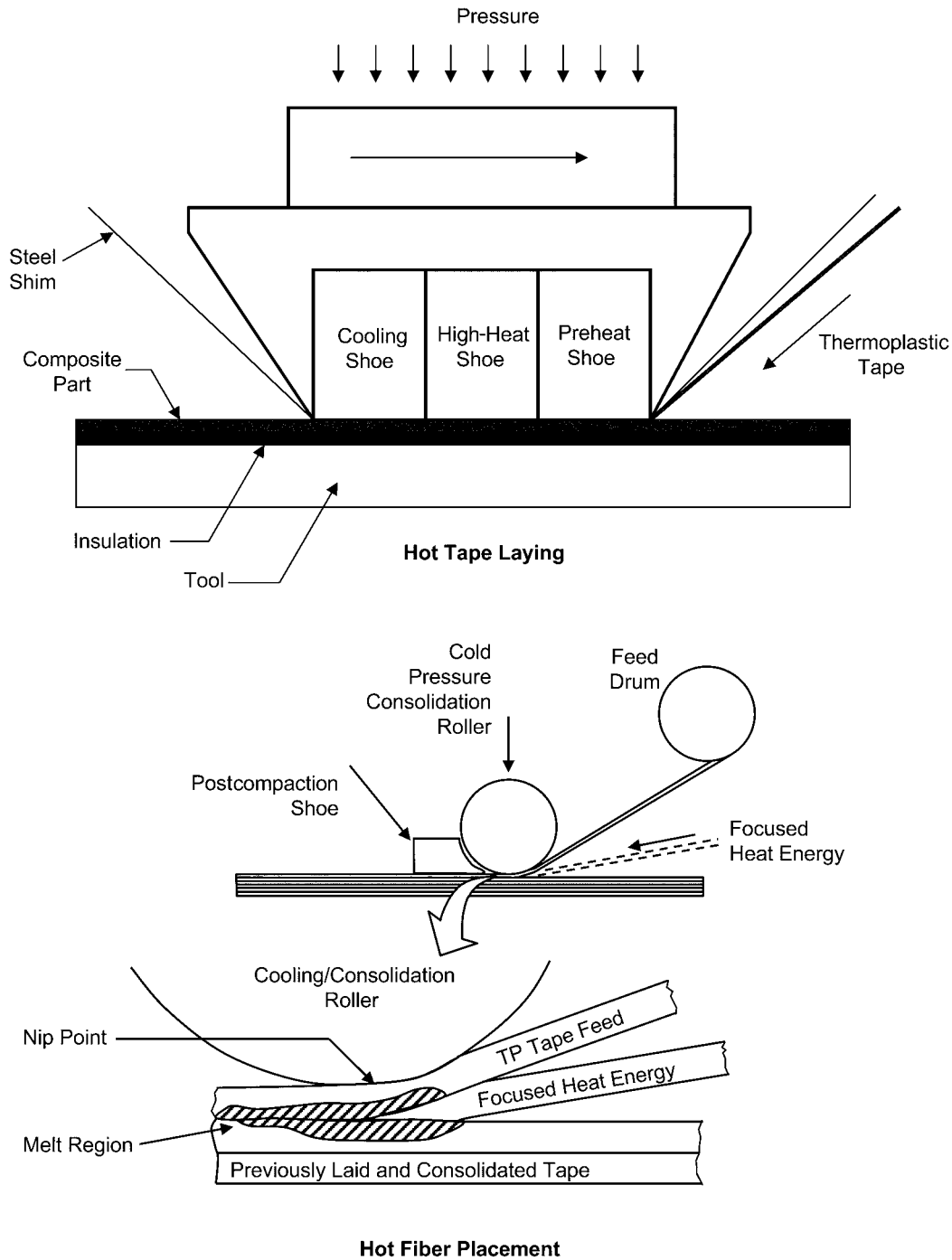


Fig. 6.4 Principle of autoconsolidation

no voids or porosity, but they do not slip as well as loose, unconsolidated ply packs during the forming operation. The laminate or unconsolidated ply pack would then be heated for forming, such as in the IR oven shown in Fig. 6.5. After reaching the forming temperature, it would be rapidly transferred to the thermoforming press and formed. The part must be held under pressure

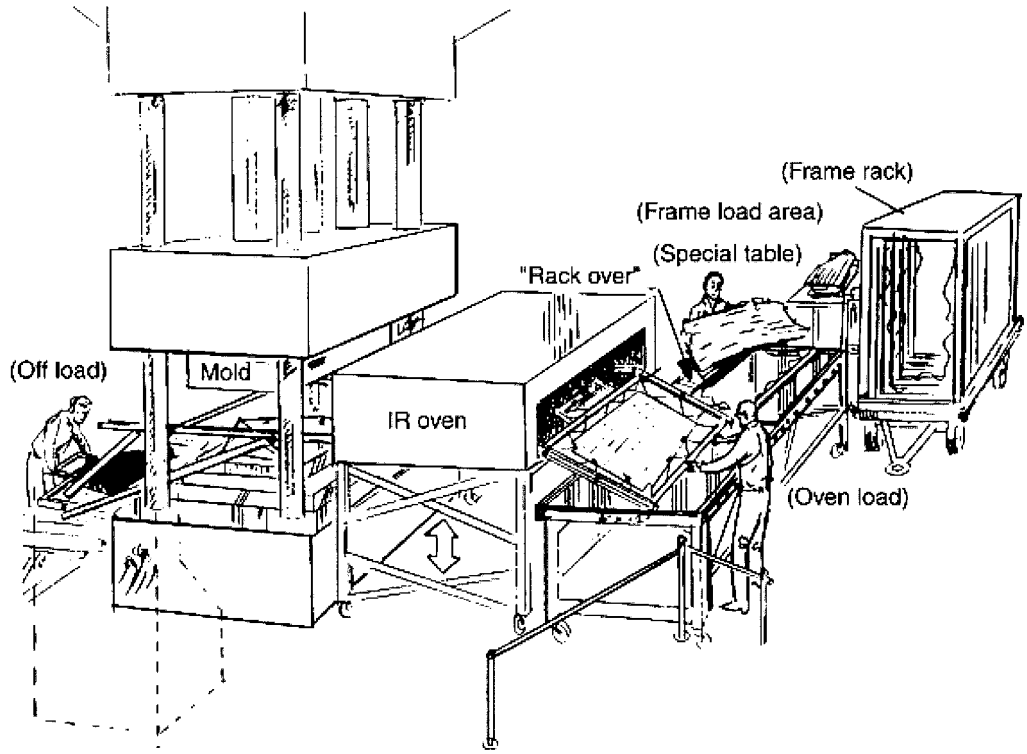


Fig. 6.5 Typical thermoforming setup. Source: Ref 2

until it cools below its T_g to avoid inducing residual stresses and part warpage.

The primary preheating methods used for press thermoforming are IR heater banks, convection ovens, and heated platen presses. In IR heating the heating time is typically short, in this case, one to two minutes, but temperature gradients can form within thick ply packs. Since the surface heats considerably faster than the center, there is a danger of overheating unless the temperature is carefully controlled. In addition, it is difficult to obtain uniform heating of complex contours. Nevertheless, IR heating is a good choice for thin preconsolidated blanks of moderate contour. By contrast, convection heating takes longer, in this case, 5 to 10 minutes but is generally more uniform through the thickness and is the preferred method for unconsolidated blanks and blanks containing high contour. Impingement heating is a variation of convection heating that uses a multitude of high-velocity jets of heated gas that impinge on the surfaces, greatly enhancing the heat flow and reducing the time required to heat the part.

In any thermoforming operation, the transfer time from the heating station to the press is critical. The part must be transferred or shuttled to the press and formed before it cools below its T_g for amorphous resins or below its T_m for semicrystalline resins. This usually dictates a transfer time of 15 seconds or less. For optimum results, presses with fast closing speeds, for example, 200 to 500 in./min (5.1 to 12.7 m/min), that are capable of producing pressures of 200 to 500 psi (1380 to 3445 kPa) are preferred.

Although matched metal dies can be used for thermoforming, they are expensive and unforgiving; that is, if the dies are not precisely made and aligned, there will be high- and low-pressure points that will result in defective parts. The dies can be made with internal heating and/or cooling capability. Facing one of the die halves with a heat-resistant rubber, typically a silicone rubber, can help equalize the pressure. Similarly, one of the die halves can be made entirely from rubber, either as a flat block or one that is cast to the shape of the part (Fig. 6.6). Although the flat block is simpler and cheaper to fabricate, the shaped block provides more uniform pressure distribution and better part definition. Silicone rubber of 60 to 70 Shore A hardness is commonly

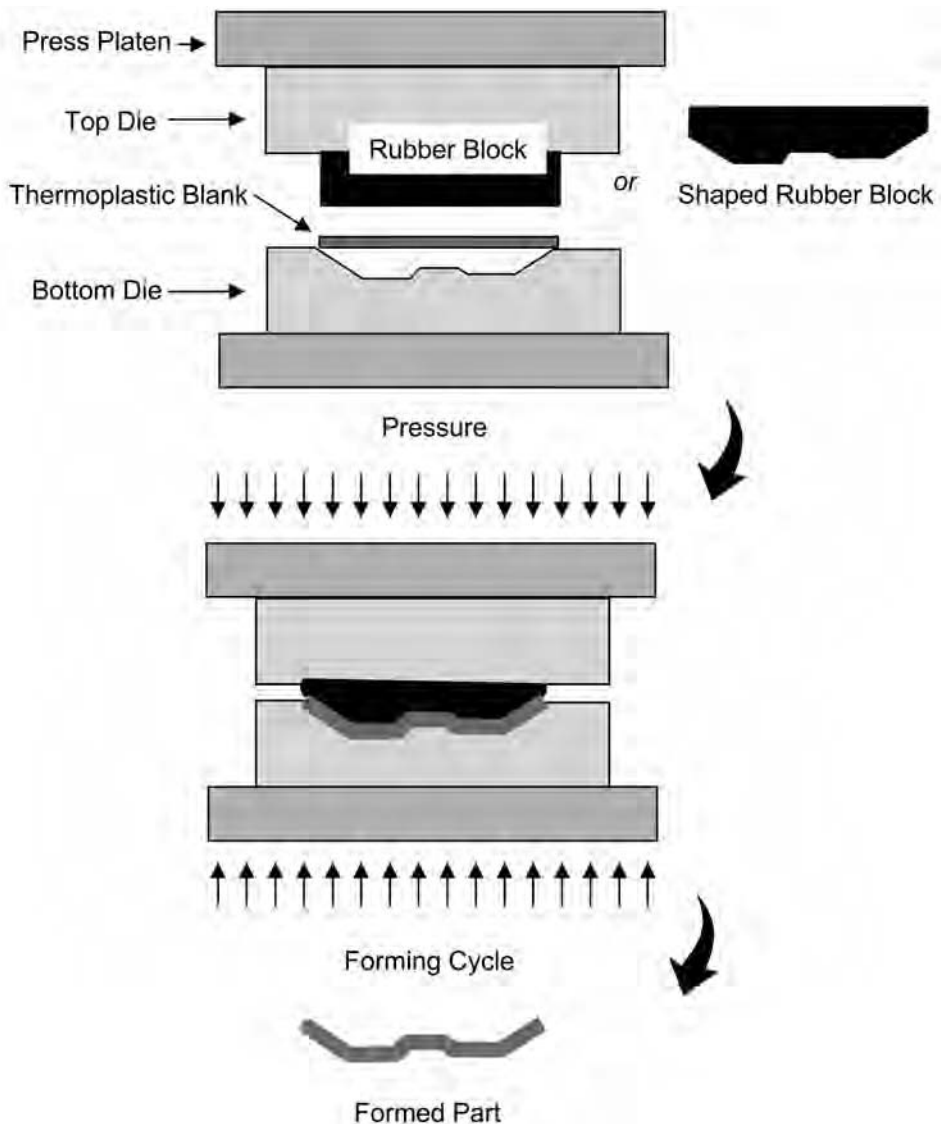


Fig. 6.6 Rubber block forming

used. A press used for thermoforming and several formed parts are shown in Fig. 6.7. Another method of applying pressure during the forming process is hydroforming, in which an elastomeric bladder is forced down around the part and the lower die half using fluid pressure. Typical thermoforming pressures are 100 to 500 psi (690 to 3445 kPa); however, some hydroforming presses are capable of pressures as high as 10,000 psi (68,945 kPa).

While these approaches seem fairly straightforward, they are actually quite complicated because of the inextensibility of the continuous fiber reinforcement. There are four primary resin flow phenomena that must be dealt with when consolidating and forming thermoplastic composite parts (Fig. 6.8): (1) resin percolation, (2) transverse squeeze flow, (3) interply slip, and (4) intraply slip. Resin percolation and transverse squeeze flow normally occur during consolidation but are also factors during forming. Resin percolation is the flow of the viscous polymer through or along the fiber bed that allows the plies to bond together, while transverse squeeze flow eliminates slight variations in prepreg thickness by allowing the prepreg layers to spread



Fig. 6.7 Thermoforming press and composite parts

laterally due to applied pressure. The polymer matrix tends to flow parallel to the fiber axis, while flow through the fiber bed is much more difficult. When flow occurs in a direction off-axis to the fiber orientation, the fibers tend to move with the resin. Interply slip, or slip between the plies at the resin-rich ply interfaces, and intraply slip, or slip within the plies themselves by a combination of transverse and axial shear, are normally encountered in thermoforming. If these slip mechanisms did not occur during forming, the reinforcing fibers would either break or buckle or fail to form the part. Another way of looking at these flow mechanisms is shown in Fig. 6.9. To form a double-contoured part requires all four mechanisms, while a single-curvature part requires only three. Consolidation of flat or mildly contoured skins requires only resin percolation and transverse squeeze flow. Some examples of these mechanisms are shown in Fig. 6.10 and 6.11. In Fig. 6.10, transverse flow of a single-curvature part often results in ply thickening and ply thinning, particularly at or near radii. In Fig. 6.11, interply slip prevents buckling or wrinkling of the plies at the radius.

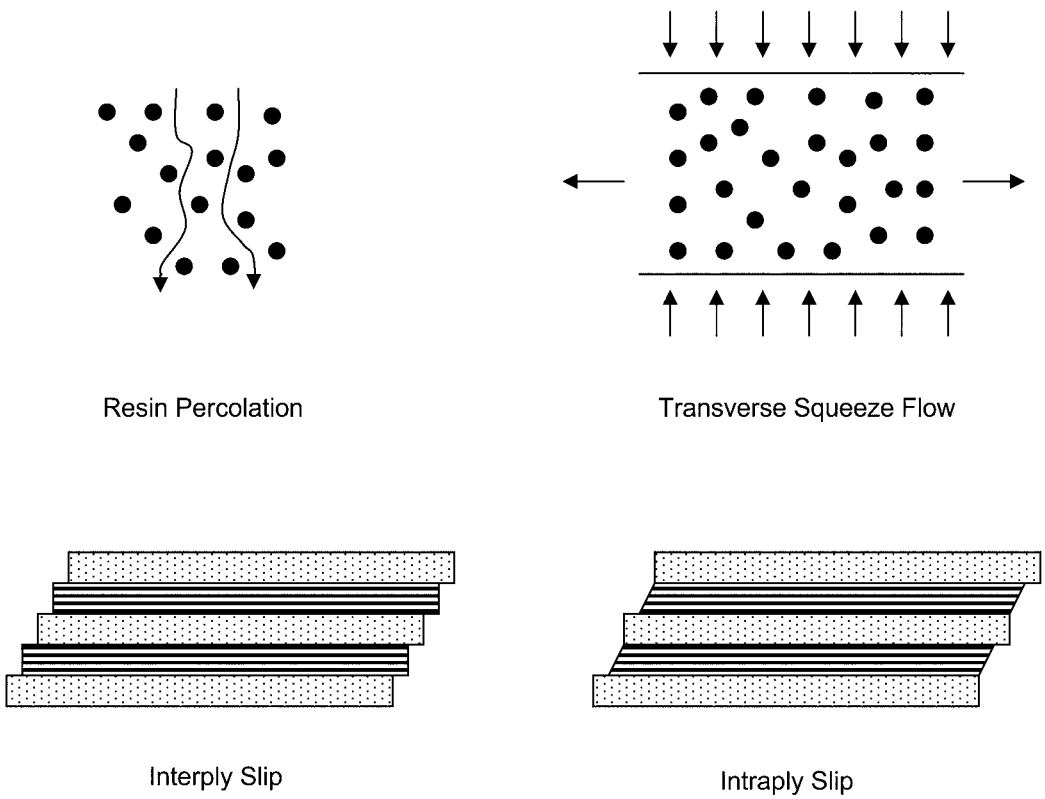


Fig. 6.8 Resin flow patterns during thermoplastic composite processing. Source: Ref 3

Carbon fibers in a viscous, or near-liquid, thermoplastic resin are still extremely strong in tension but will buckle and wrinkle readily when placed in compression. Therefore, either the part shape or the die has to be designed to keep the fibers in tension throughout the forming process, but at the same time allow them to move through slip. If neither the part shape nor the die design is amenable to preventing compression buckling of the fibers, a special holding/clamping fixture can be used during the forming operation. These fixtures (Fig. 6.12) can be as simple as peripheral clamping fixtures for the blank that allow the material to slip as necessary during forming, or they can be sophisticated mechanisms involving springs located at strategic positions to provide variable tension. Properly designed, the springs allow the part to rotate out-of-plane, yielding improved force to fiber directional alignment and allowing greater variations in draw depth. The type of holding fixture, and the location of its springs, are usually determined by previous experience and by considerable trial and error. Slower forming speeds also help to reduce wrinkling and buckling. It has been shown that fiber buckling and waviness reduce part strength by up to 50 percent and that tensioning pressures of 40 to 100 psi (275 to 690 kPa) are often sufficient to suppress fiber buckling.

Diaphragm forming is a unique process that is capable of making a wider range of part configurations, and more severe contours, than can be made by press forming. A typical diaphragm forming cycle for a PEEK thermoplastic part is shown in Fig. 6.13. Diaphragm forming can be done in either a press or an autoclave. In this process, unconsolidated ply packs, to more readily promote ply slippage, rather than preconsolidated blanks, are placed between two flexible diaphragms. A vacuum is drawn between the diaphragms to remove air and provide tension on the lay-up. The part is then placed in a press and heated above the melt temperature. Gas pressure is used to form the pack down over the tool surface. During forming, the plies slide within the diaphragms, creating tensile stresses that reduce the tendency toward wrinkling. The gas pressure both forms and consolidates the part to the tool

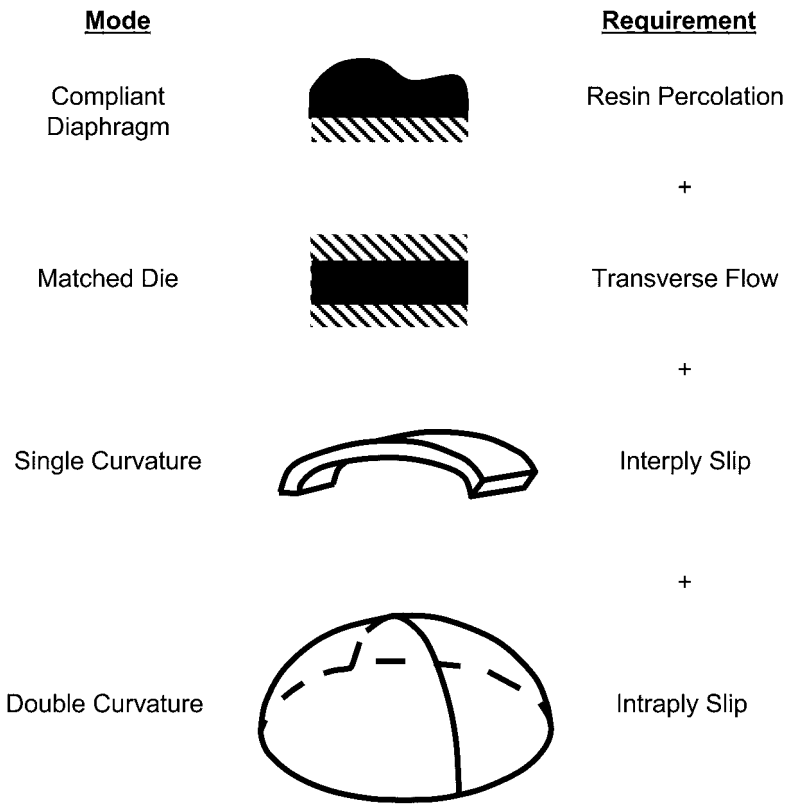


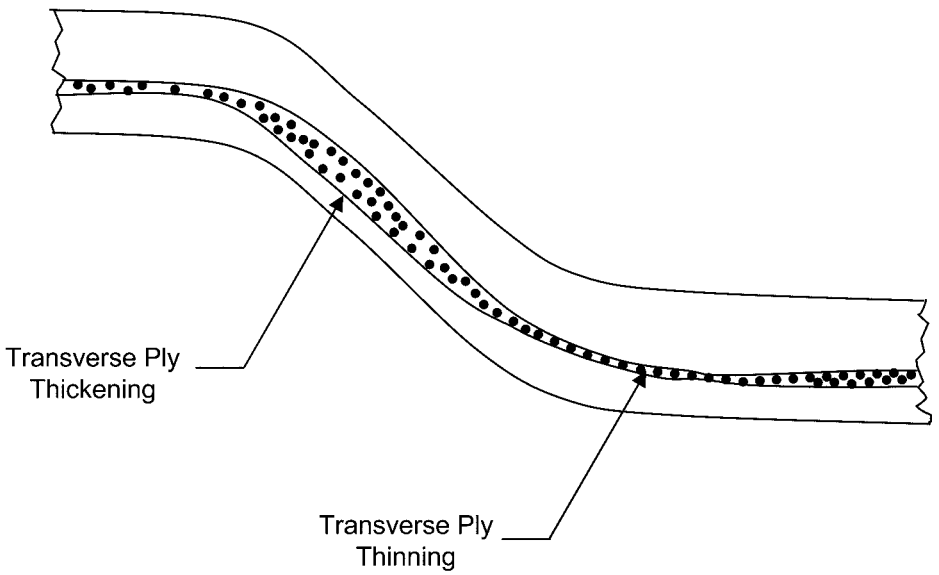
Fig. 6.9 Deformation processes during consolidation and forming. Source: Ref 3

contour. Pressures usually range from 50 to 150 psi (345 to 1035 kPa) with cycle times of 20 to 100 minutes; however, for more massive tools, cycle times of four to six hours are not unusual. Slow pressurization rates are recommended to avoid out-of-plane buckling. Diaphragm materials include Supral superplastic aluminum and high-temperature polyimide films (Upilex-R and Upilex-S). Supral aluminum sheet is more expensive than the polyimide films but is less susceptible to rupturing during the forming cycle. Therefore, polyimide films work well for thin parts with moderate draws, while Supral sheet is preferred for thicker parts with complex geometries. Typical diaphragm-forming temperatures are 750 °F (400 °C) for Supral and 570 to 750 °F (300 to 400 °C) for the polyimide films. One disadvantage of this process is that the materials that can be formed must comply with the forming temperatures of the available diaphragm materials. In addition, the diaphragm materials are expensive (especially Supral) and can be used only once.

Many other processes have been evaluated for fabricating thermoplastic composite structural shapes, including continuous consolidation, roll forming, and pultrusion. A continuous consolidation process is shown in Fig. 6.14 and a roll forming process is shown in Fig. 6.15. The trick with both of these processes is to maintain uniform pressure on all portions of the part throughout heat-up, forming, and cool-down. If uniform pressure is not maintained on the molten portions of the part being formed, deconsolidation will occur due to relaxation of the fiber bed. Thermoplastic composites have also been successfully pultruded, but due to the high melt temperatures and viscosities, the process is much more difficult and expensive than that for thermosets.

6.3 Thermoplastic Joining

Another unique advantage of thermoplastic composites is the many joining options available.



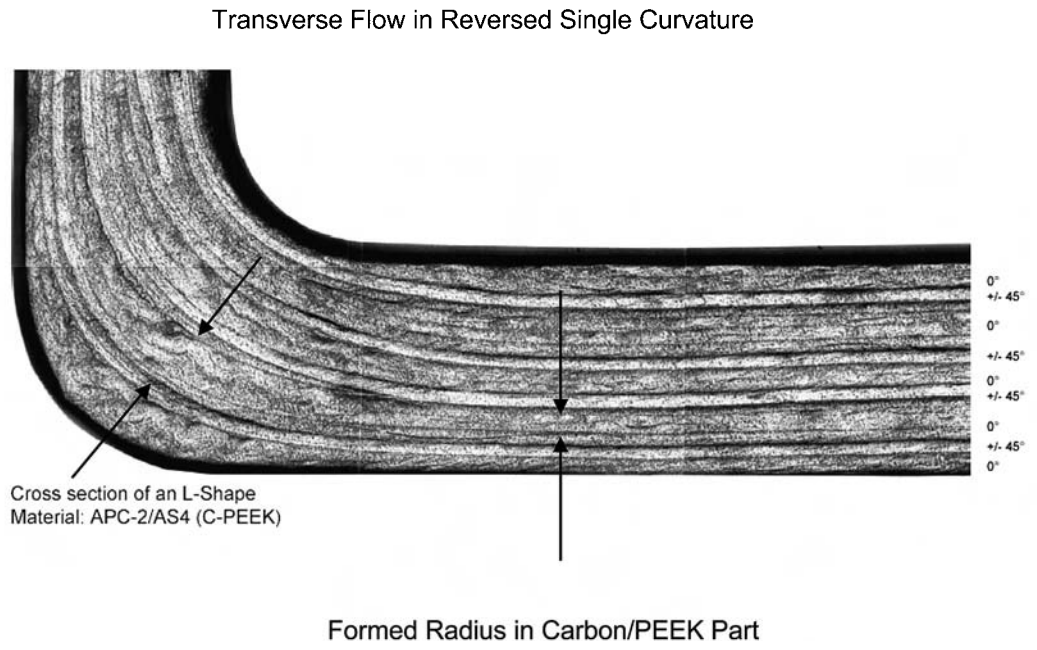


Fig. 6.10 Transverse flow affects ply thickness. Source: Ref 4

While thermosets are restricted to cocuring, adhesive bonding, and mechanical fastening, thermoplastic composites can be joined by melt fusion, dual resin bonding, resistance welding, ultrasonic welding, or induction welding, as well as by conventional adhesive bonding and mechanical fastening.

Adhesive Bonding. In general, structural bonds using thermoset such as epoxy adhesives produce lower bond strengths with thermoplastic

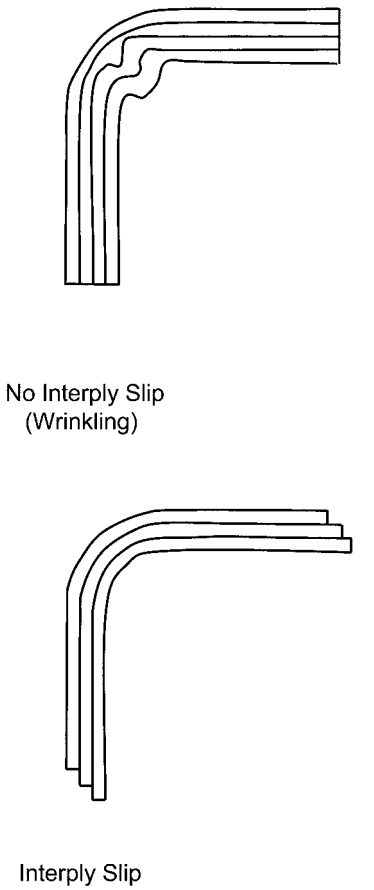


Fig. 6.11 Importance of interply slip during forming

composites than with thermoset composites. This is believed to be due primarily to the differences in surface chemistry between thermosets and thermoplastics. Thermoplastics contain rather inert, nonpolar surfaces that impede the ability of the adhesive to wet the surface. A number of different surface preparations have been evaluated, including sodium hydroxide etching, grit blasting, acid etching, plasma treatments, silane coupling agents, corona discharge, and Kevlar (aramid) peel plies. While a number of these surface preparations, or combinations of them, give acceptable bond strengths, the long-term service durability of thermoplastic adhesively bonded joints has not yet been established.

Mechanical Fastening. Thermoplastic composites can be mechanically fastened in the same manner as thermoset composites. Initially, there was concern that thermoplastics would creep excessively, resulting in a loss of fastener preload and thus lower joint strengths. Extensive testing has shown that this was an unfounded fear and that mechanically fastened thermoplastic composite joints behave very similarly to thermoset composite joints.

Melt Fusion. Since thermoplastics can be processed multiple times by heating above their T_g for amorphous resins or above their T_m for semicrystalline resins with minimal degradation, melt fusion essentially produces joints as strong as those of the parent resin. An extra layer of neat (unreinforced) resin film can be placed in the bondline to fill gaps and to ensure that there is adequate resin to facilitate a good bond. However, if the joint is produced in a local area,

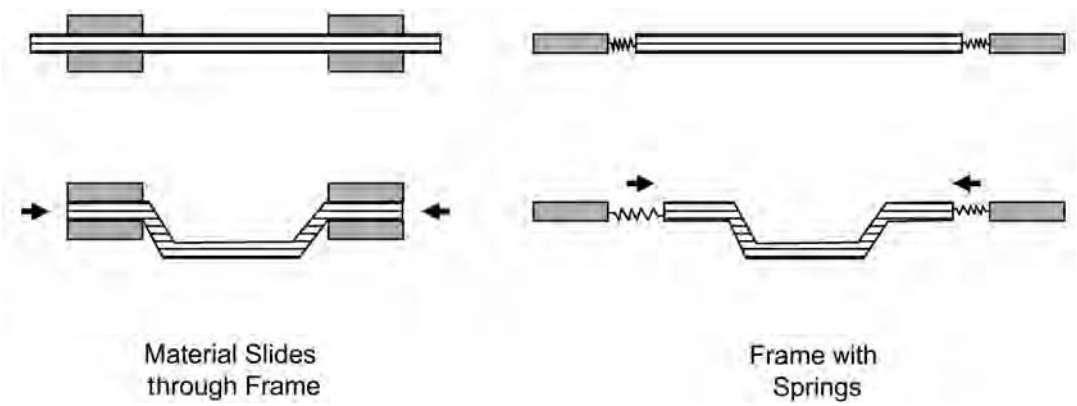


Fig. 6.12 Typical tensioning methods

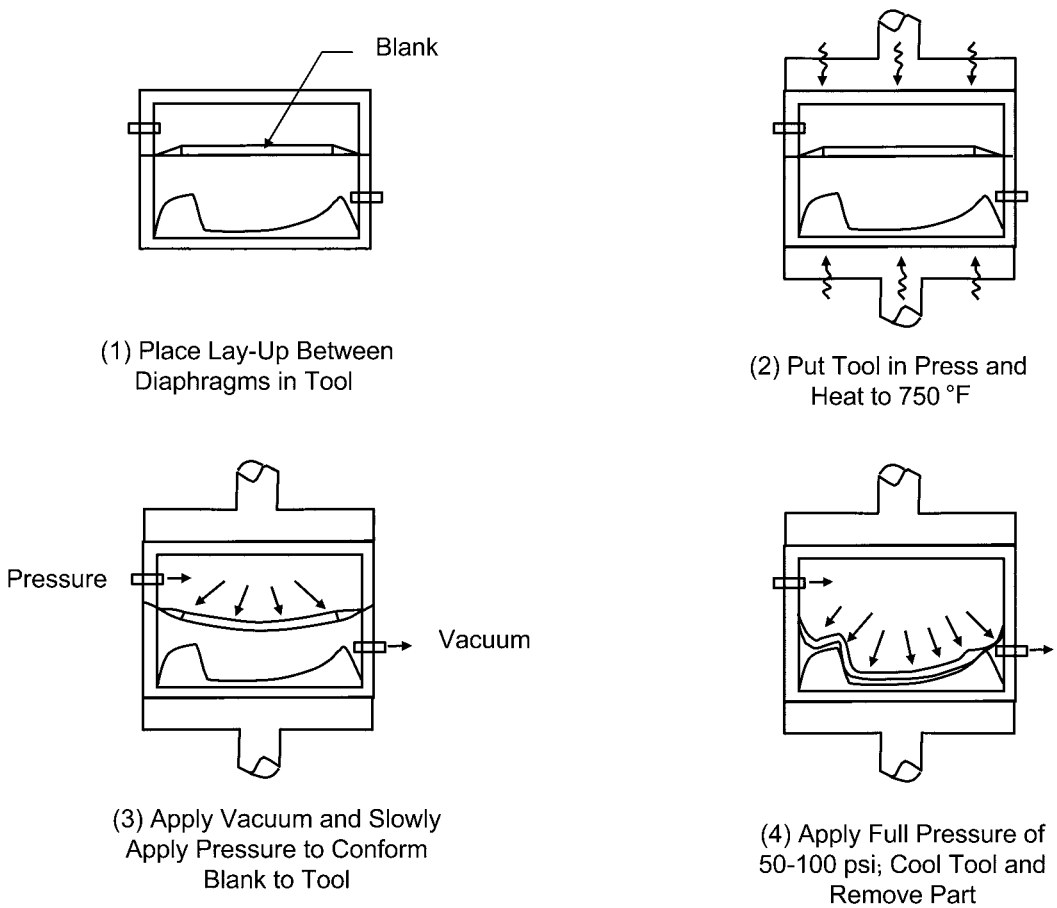


Fig. 6.13 Diaphragm forming method for carbon/PEEK parts

adequate pressure must be provided over the heat-affected zone to prevent the elasticity of the fiber bed from producing delaminations at the ply interfaces.

Dual Resin Bonding. In this method, a lower melting temperature thermoplastic film is placed at the interfaces of the joint to be bonded. As shown in Fig. 6.16, in a process called *amorphous bonding* or the *Thermabond process*, a layer of amorphous polyetherimide (PEI) is used to bond two PEEK composite laminates together. To provide the best bond strengths, a layer of PEI is fused to both PEEK laminate surfaces prior to bonding to enhance resin mixing. In addition, an extra layer of film may be used at the interfaces for gap-filling purposes. Since the processing temperature for PEI is below the melt temperature of the PEEK laminates, the danger of ply delamination within the PEEK substrates is avoided. Like the melt fusion process, dual resin bonding is normally used to join large sections together, such as bonding stringers to skins.

Resistance Welding. In resistance welding, a metallic heating element is embedded in a thermoplastic film and placed in the bondline (Fig. 6.17). This process is used to weld the ribs to the skin for the Airbus A380 wing leading edge. For all fusion welding operations with thermoplastic composites, it is necessary to maintain adequate pressure at all locations that are heated above the melt temperature. If pressure is not maintained at all locations that exceed the melt temperature, deconsolidation due to fiber bed relaxation will likely occur. The pressure should be maintained until the part is cooled below its T_g. Typical processing times for resistance

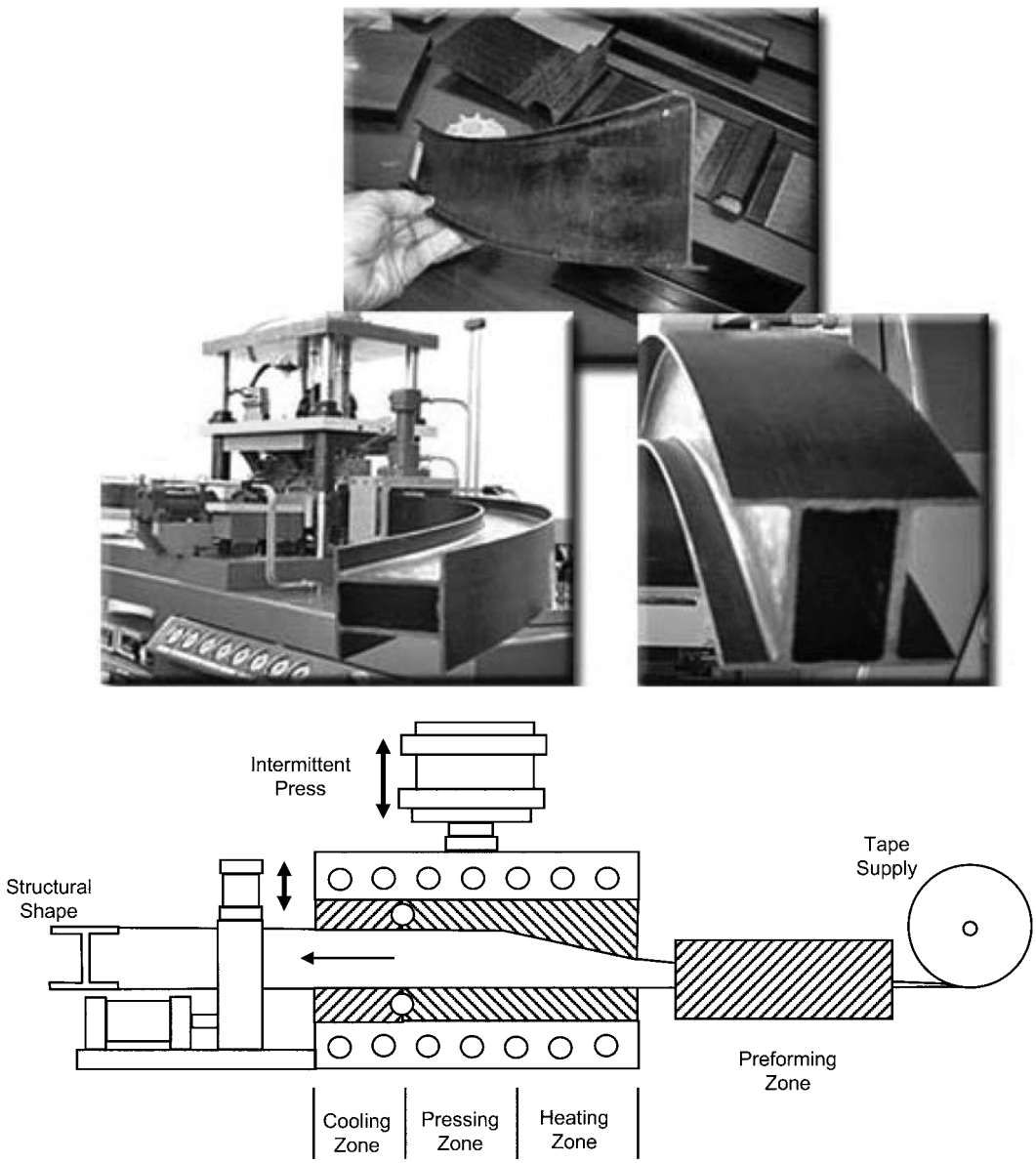


Fig. 6.14 Continuous compression molding

welding are 30 seconds to 5 minutes at 100 to 200 psi (690 to 1380 kPa) pressure.

Ultrasonic Welding. Ultrasonic welding is used extensively in commercial processes to join lower-temperature unreinforced thermoplastics and can also be used for advanced thermoplastic composites. An ultrasonic horn, also known as a *sonotrode*, is used to produce ultrasonic energy at the composite interfaces to convert electrical energy into mechanical energy. The sonotrode is placed in contact with one of the pieces to be joined. The second piece is held stationary while the vibrating piece creates frictional heating at the interface. Ultrasonic frequencies of 20 to 40 kHz are normally used. The process works best if one of the surfaces has small asperities (protrusions) that act as energy directors or intensifiers. The asperities have a high energy per

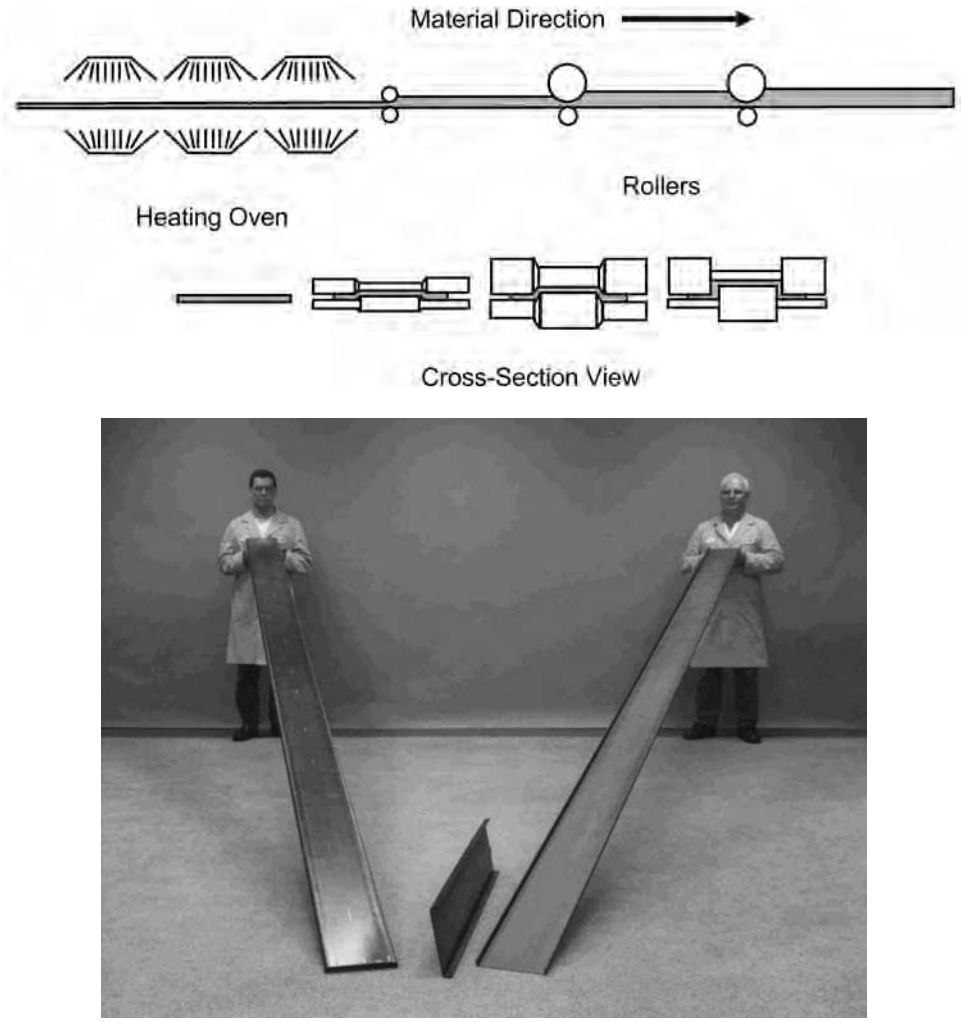


Fig. 6.15 Roll forming of thermoplastic composites

unit volume and melt before the surrounding material. The quality of the bond is increased with increasing time, pressure, and amplitude of the signal. Again, it is common practice to incorporate a thin layer of neat resin film to provide gap filling. Typical weld parameters are less than 10 seconds at 70 to 200 psi (480 to 1380 kPa) pressure. This process is somewhat similar to spot welding of metals.

Induction Welding. Induction welding techniques have been developed in which a metallic susceptor may or may not be placed in the bondline. However, it is generally accepted that the use of a metallic susceptor produces superior joint strengths. A typical induction setup uses an induction coil to generate an electromagnetic field that results in heating due to eddy currents in the conductive susceptor and/or hysteresis losses in the susceptor. Susceptor materials that have been evaluated include iron, nickel, carbon fibers, and copper meshes. Typical welding parameters are 5 to 30 minutes at 50 to 200 psi (345 to 1380 kPa) pressure.

A comparison of single-lap shear strengths produced in thermoplastic composites, using the various techniques described above, is given in Fig. 6.18. Note that adhesive bonding yields lower joint strengths than fusion bonding techniques and is very dependent on the surface preparation method used. Autoclave coconsolidated

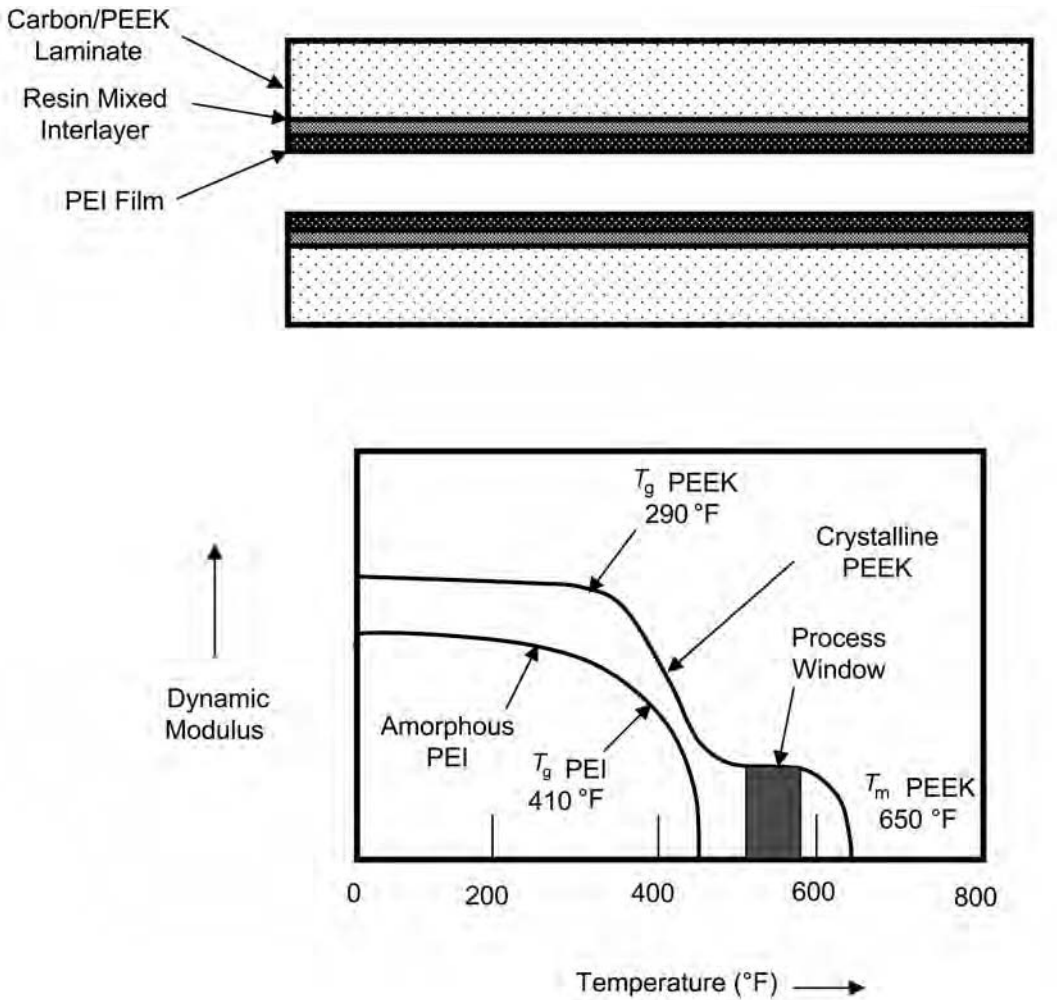


Fig. 6.16 Amorphous or dual-resin bonding. PEEK, polyetheretherketone; PEI, polyetherimide

(melt fusion) joint strengths approach virgin autoclave molded strengths. Typically, resistance and induction welding strengths exhibit similar properties, both of which are superior to those of ultrasonic welding.

REFERENCES

1. J. Muzzy, L. Norpoth, and B. Varughese, Characterization of Thermoplastic Composites for Processing, *SAMPE J.*, Vol 25 (No. 1), Jan/Feb 1989, p 23–29
2. D.A. McCarville and H.A. Schaefer, Processing and Joining of Thermoplastic Composites, *ASM Handbook*, Vol 21, *Composites*, ASM International, 2001, p 633–645
3. F.N. Cogswell, *Thermoplastic Aromatic Polymer Composites*, Butterworth-Heinemann Ltd., 1992
4. D.C. Leach, F.N. Cogswell, and E. Nield, High Temperature Performance of Thermoplastic Aromatic Polymer Composites, *31st National SAMPE Symposium*, 1986, p 434–448

SELECTED REFERENCES

- F.N. Cogswell and D.C. Leach, Processing Science of Continuous Fibre Reinforced

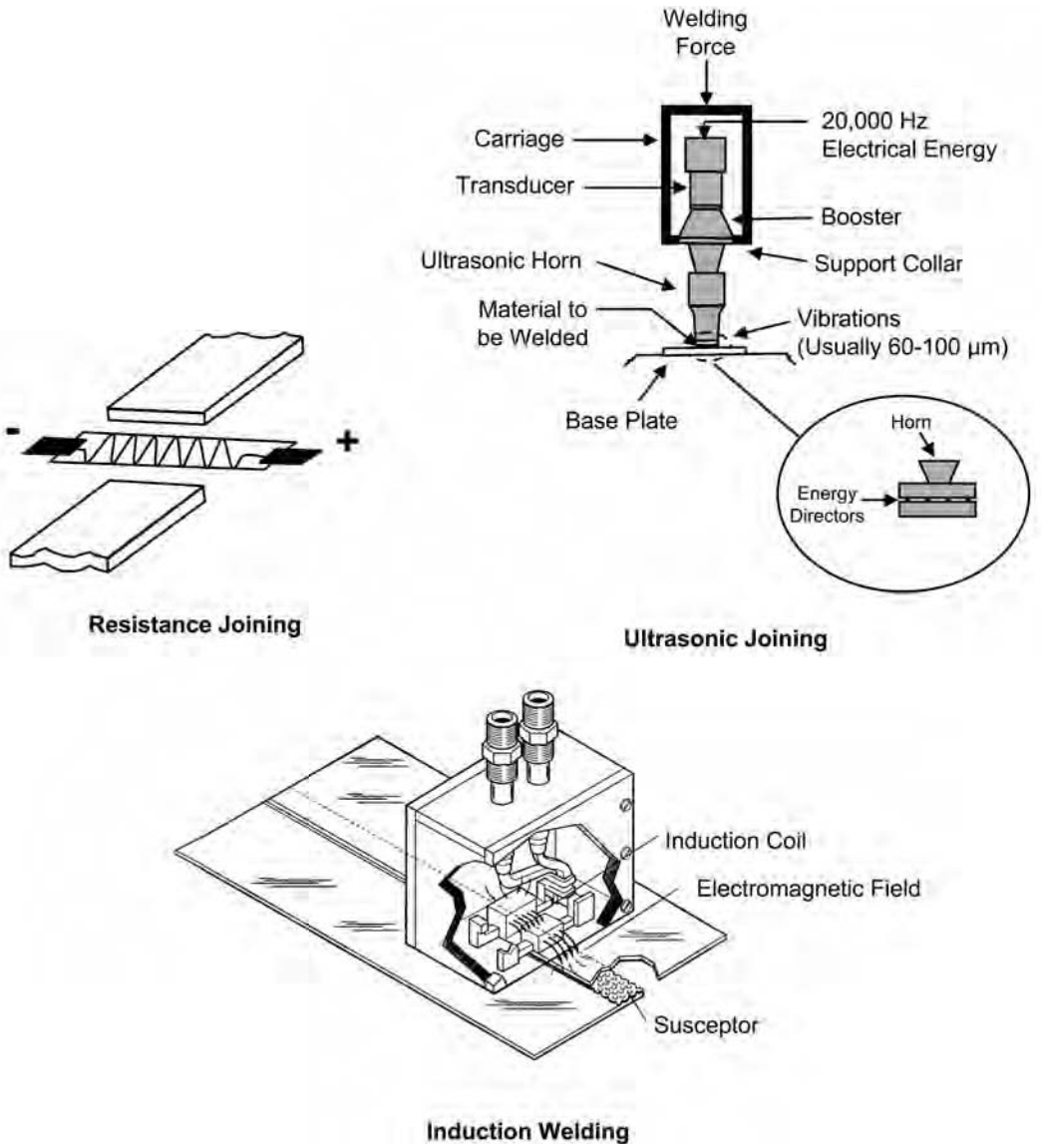


Fig. 6.17 Thermoplastic welding methods. Source: Ref 2

Thermoplastic Composites, *SAMPE J.*, May/June 1988, p 11–14

- R.C. Harper, Thermoforming of Thermoplastic Matrix Composites—Part I, *SAMPE J.*, Vol 28 (No. 2), Mar/Apr 1992, p 9–17
- R.C. Harper, Thermoforming of Thermoplastic Matrix Composites—Part II, *SAMPE J.*, Vol 28 (No. 3), May/June 1992, p 9–17
- A.C. Loos and M.-C. Li, Consolidation During Thermoplastic Composite Processing, *Processing of Composites*, Hanser/Gardner Publications, Inc., 2000
- J.D. Muzzy and J.S. Colton, The Processing Science of Thermoplastic Composites, *Advanced Composites Manufacturing*, John Wiley & Sons, Inc., 1997
- R.K. Okine, Analysis of Forming Parts from Advanced Thermoplastic Sheet Materials, *SAMPE J.*, Vol 25 (No. 3), May/June 1989, p 9–19

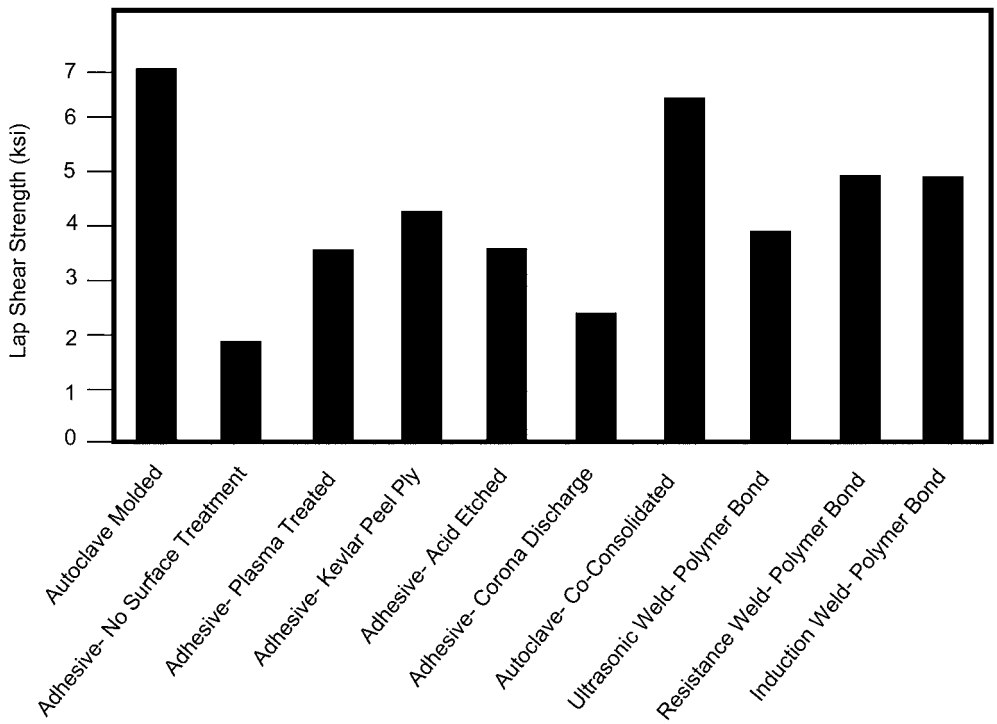


Fig. 6.18 Lap shear strength comparison of different joining methods. Source: Ref 2

- W. Soll and T.G. Gutowski, Forming Thermoplastic Composite Parts, *SAMPE J.*, May/June 1988, p 15–19
- A.B. Strong, *High Performance and Engineering Thermoplastic Composites*, Technomic Publishing Co., Inc., 1993

Copyright © 2010, ASM International®
All rights reserved.
www.asminternational.org

CHAPTER 7

Processing Science of Polymer Matrix Composites

PROCESSES FOR NEW COMPOSITE MATERIALS, during the 1960s and 1970s, were based solely on previous experience and a great deal of empirical testing. In the 1980s, to reduce the amount of testing required and to add some scientific basis to composite processing, the concept of processing science evolved and matured. While an appreciable amount of testing and process development is still required, composite processing science allows one to design and execute more informed process development. In addition, a more in-depth understanding greatly aids in troubleshooting when a process is out of control. Processing science consists of mathematical modeling of the cure process, methods of monitoring the curing reactions during processing, and experiments to validate the models and theories of the processes that occur during composite curing.

A number of mathematical models of the curing process have been developed that can quite accurately predict resin kinetics, resin viscosity, resin flow, heat transfer, void formation, and residual stresses. Like in-process cure monitoring, these models can be invaluable tools for characterizing new materials and for cure cycle development. They can also be used for modeling the heat-up and cool-down rates for candidate tool designs. Models have been developed for processes such as thermoset curing, thermoplastic consolidation, filament winding, pultrusion, and liquid molding. In addition, for many years, models have been successfully developed for injection and compression molding.

A simplified cure model for an addition-curing thermoset composite is shown in Fig. 7.1. The kinetic submodel predicts the amount of conversion, or degree of cure, of the resin during processing. The viscosity submodel predicts the viscosity of the resin as it initially melts, flows, and then gels during cure. The heat transfer submodel predicts the transfer of heat that occurs during cure. The output of the heat transfer submodel drives both the kinetic and viscosity models. The most complicated submodel is the flow submodel, which predicts the resin flow through the fiber bed in both the horizontal and vertical directions during cure. The void submodel predicts how processing conditions can lead to voids and porosity in the final cured part. Finally, the

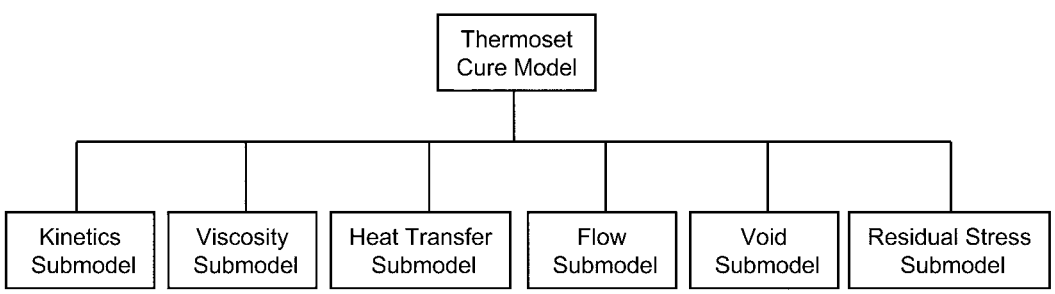


Fig. 7.1 Thermoset cure model framework

residual stress submodel predicts the buildup of residual stresses that occur during cure and cooldown. Although Fig. 7.1 does not indicate it, these models are highly interdependent. For example, the resin flow submodel depends on the viscosity as predicted from the viscosity submodel, which in turn is dependent on the resin kinetics (kinetics submodel), which in turn is dependent on heat (heat transfer submodel). When using any model, it is important to understand (1) the mathematics of the equations that make up the model, (2) all assumptions that were made in the model formulation, (3) the boundary conditions for the model, and (4) the solution method used for the model.

7.1 Kinetics

Commercial resin systems are complex, consisting of several different epoxies and one or more curing agents. In addition, because the reactions do not occur isothermally but occur under dynamic heating conditions, both the kinetic and viscosity submodels are normally developed empirically. In the case of kinetics, differential scanning calorimetry is used to characterize the resin in both the isothermal and dynamic heating modes. Typical isothermal and dynamic scans for an epoxy resin are shown in Fig. 7.2.

The total heat of reaction to complete a curing reaction is equal to the area under the rate of heat generation-time curve obtained in a dynamic heating mode:

$$H_R = \int_0^{t_f} \left(\frac{dQ}{dt}\right)_d dt \qquad \text{(Eq 7.1)}$$

where:
H_R = heat of reaction
$(dQ/dt)_d$ = rate of heat generation in a dynamic test
t_f = time required to complete the reaction

The amount of heat released in time t at a constant curing temperature is determined from isothermal experiments. The area under the rate of heat generation-time cure is expressed as:

$$H = \int_0^{t} \left(\frac{dQ}{dt}\right)_i dt \qquad \text{(Eq 7.2)}$$

where:
H = amount of heat released in time t
$(dQ/dt)_i$ = rate of heat generation in an isothermal test conducted at temperature t

The degree of cure α at any time t can then be expressed as:

$$\alpha = \frac{H}{H_R} \qquad \text{(Eq 7.3)}$$

As shown in Fig. 7.3, the rate of reaction ($d\alpha/dt$) proceeds more rapidly at higher temperatures,

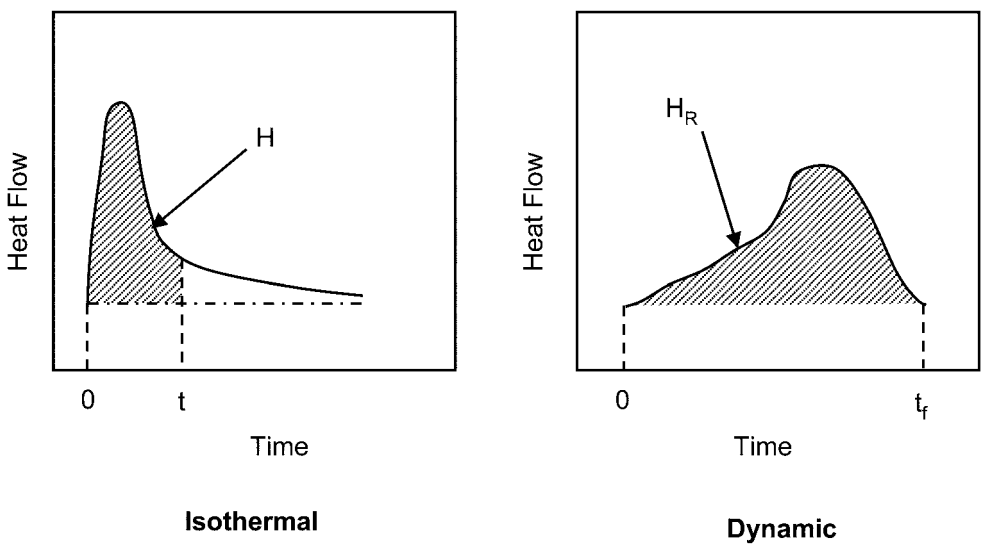


Fig. 7.2 Differential scanning calorimetry curves

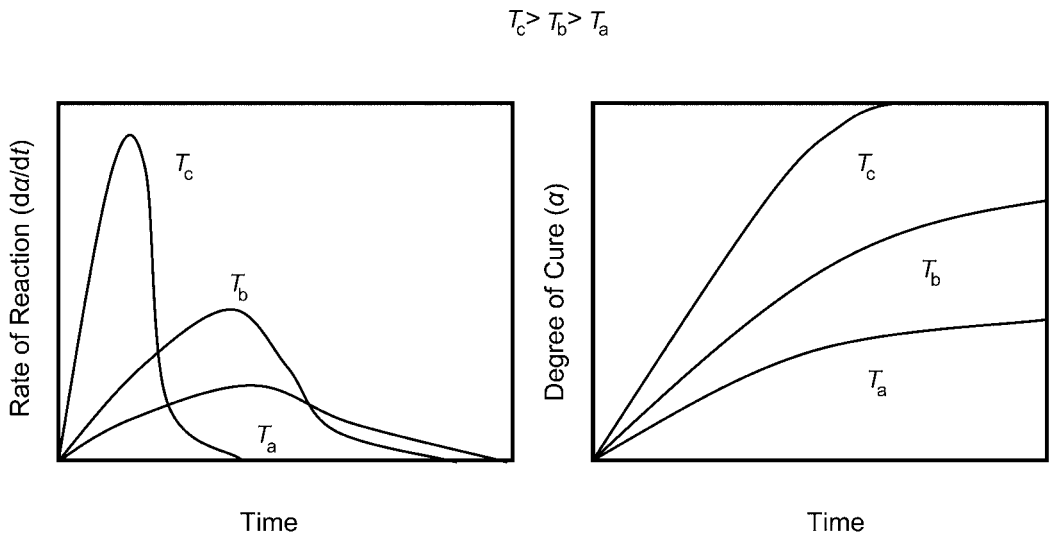


Fig. 7.3 Temperature effects on curing

and sufficiently high temperatures are required to obtain a high degree of cure (α). At the highest temperature T_c, both the rate of reaction and the degree of cure are obtained within reasonable times. However, for the lower temperatures T_a and T_b, the conversion rate is much slower and a high degree of cure will either not be obtained at all or not be obtained within a reasonable cure time.

It is generally recognized that resin flow prior to gellation is a critical variable in processing carbon/epoxy laminates. Too much flow can result in resin-starved laminates, which will often contain excessive porosity, while too little flow can produce resin-rich laminates, which can exceed thickness tolerances and cause assembly fit-up problems. Formulators of epoxy resin systems often use catalysts to control or alter the flow behavior of their base resin systems. Since a catalyst increases the reaction rate, it is normal for a catalyzed resin to exhibit less total flow during processing than an uncatalyzed system. However, the addition of a catalyst will also affect the resin system kinetics. The effect of catalyst additions can be seen in the dynamic differential scanning calorimetry (DSC) curves for three different epoxy resins shown in Fig. 7.4. The chemical compositions of all three are the same except for the amount of boron trifluoride (BF_3) catalyst. The resin with no catalyst exhibits only a single large exothermic peak characteristic of epoxy resins lacking a BF_3 catalyst, such as Hexcel's 3502 and Cytec's 5208. This resin also has a much higher total heat of reaction. Again, this is a function of the absence of the catalyst; since the catalyst reacts rapidly at low temperatures, total heat of reaction is reduced. The epoxy with a 1.1% BF_3 catalyst exhibits two distinct exotherm peaks, typical of Hexcel's 3501-6 resin. The first, or minor peak, is a direct result of the BF_3 catalyst. On the other hand, for the resin with twice the normal catalyst content (2.2% BF_3), the first exothermic peak (usually the minor) is larger than the second peak.

The proposed sequenced of the reactions for an epoxy resin cured with a primary amine is shown in Fig. 7.5. In general, the reaction rate constant K_3 is much smaller than K_1 and K_2, and the reactivities of primary amine and secondary amine are similar for many systems. Since hydroxy groups and other proton donor species in the system act as catalytic sites in the cure reaction, an overall kinetic equation may be written in the terms of epoxide conversion as:

$$\frac{d\alpha}{dt} = (K_1 + K_2\alpha)(1-\alpha)(B-\alpha) \qquad \text{(Eq 7.4)}$$

where K_1 and K_2 are rate constants and B is the initial ratio of diamine equivalents to epoxide equivalents.

In some epoxy systems, especially ones catalyzed by Lewis acids, such as Hexcel's 3501-6, which contains a BF_3 catalyst, an overlapping

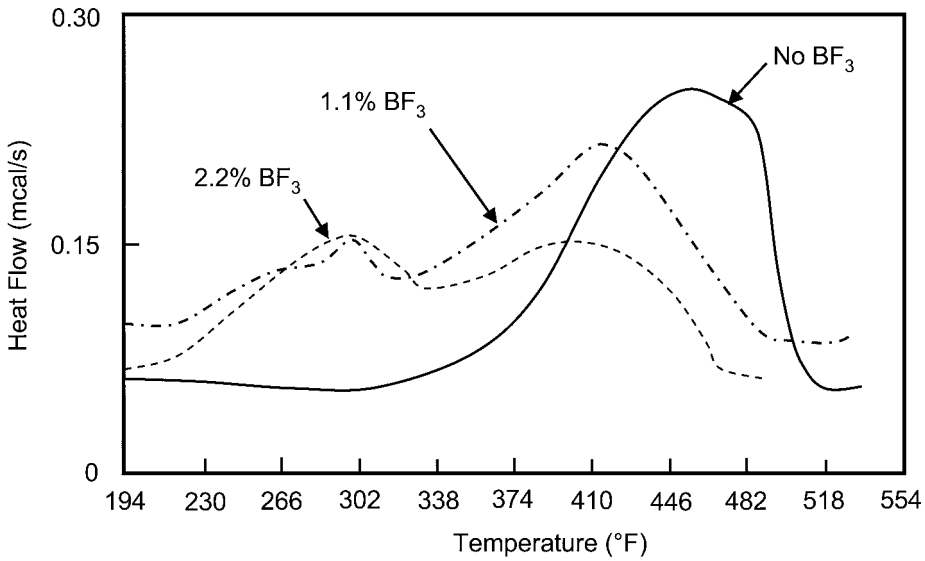
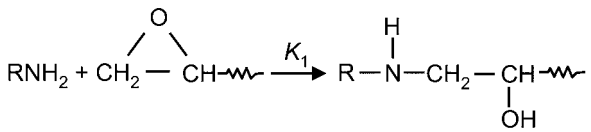
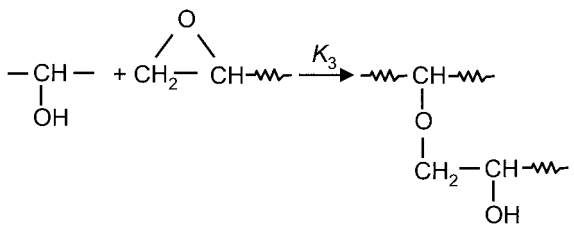


Fig. 7.4 Dynamic DSC scan comparison. Source: Ref 1

1. Reaction of the primary amine with an epoxy group to form a secondary amine:



2. Reaction with another epoxy group to form a tertiary amine:



3. Reaction with an hydoxy formed with an epoxy group (etherification):

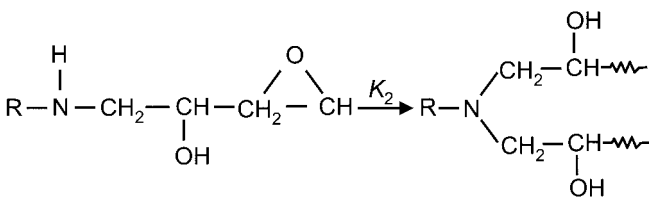


Fig. 7.5 Possible reactions for an epoxy cured with a primary amine. Source: Ref 2

multiple-peak exotherm is observed. The kinetic equations can then be modified as:

$$\frac{d\alpha}{dt} = (K_1 + K_2\alpha)(1-\alpha)(B-\alpha) \text{ for } \alpha \le 0.3 \quad \text{(Eq 7.5)}$$

$$\frac{d\alpha}{dt} = K_3(1-\alpha) \text{ for } \alpha > 0.3 \quad \text{(Eq 7.6)}$$

where K_1, K_2, K_3, and B are determined by segmental curve fitting.

When a thermoset polymer cures, the chemical reactions give off heat and the reaction is exothermic. The concern when curing a composite laminate in an autoclave is that the heat-up rate can be too fast, resulting in a significant rise in temperature in a thick laminate, as shown in Fig. 7.6. This could result in degradation of the laminate by overheating or cause uneven curing through the thickness. In a worst-case scenario, the exotherm could be so great that the laminate and bagging materials would catch fire or at least char.

This condition rarely occurs in production for epoxy resins because (1) thick laminates usually drive thick tools that exhibit very slow heat-up rates and (2) thick laminate parts are often made in matched metal tools. In order to get the lay-up to fit within these tools, the plies, or ply packs, either have to be hot debulked if the material is a net resin content prepreg or prebled to remove resin and compact the lay-up if the material is an excess resin content prepreg. These two factors, namely, large and heavy matched metal dies with slow heat-up rates and compacted net resin content plies that have been advanced during the hot debulking or prebleeding operation, are the main reasons why runaway exothermic reactions are not widely observed in industry. If a part is experiencing an excessive temperature rise due to an exothermic reaction, then it may be necessary to use net resin content prepregs, slow the heat-up rate, and even put in intermediate holds that allow the autoclave and the part to stabilize at the same temperature. If exotherm still remains a problem, it may be necessary to use a resin with a less reactive curing agent. Embedding thermocouples within a test laminate and monitoring their temperatures during cure can measure the potential for an exotherm in thick laminates.

In thermoplastic composites, bonding of the layers occurs by the process of autohesion, as explained in Chapter 6, "Thermoplastic Composite Fabrication Processes." During autohesion, segments of long polymer chains migrate across the

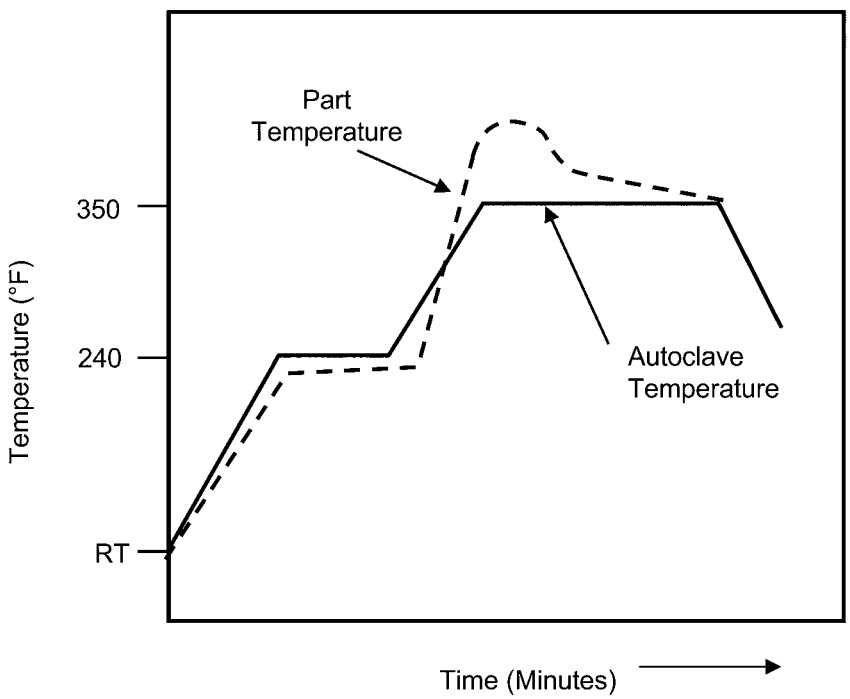


Fig. 7.6 Conceptual exotherm during composite curing

ply interfaces to obtain good ply-to-ply bonding. The movement of polymers in the fibers is modeled by reptation theory for molecular movement, with the degree of autohesion D_{au} defined as:

$$D_{au} = \frac{S}{S_\infty} \quad \text{(Eq 7.7)}$$

where S = bond strength at time t and S_∞ = ultimate bond strength at t_∞. The degree of autohesion is generally assumed to follow the relationships:

$$D_{au} = \chi t_a^{1/4} \quad \text{(Eq 7.8)}$$

and

$$\chi = \chi_0 \exp(-E/RT) \quad \text{(Eq 7.9)}$$

where:
χ = Arrhenius-type temperature-dependent constant
χ_0 = constant
E = activation energy
R = universal gas constant
T = temperature in degrees Kelvin

It has been found that autohesion occurs very rapidly and is not a concern in relatively slow processes such as autoclave or press consolidation. It only comes into play for the very short processing cycles in autoconsolidation processes, such as hot tape laying or hot filament winding.

While thermoplastics do not undergo a cure during processing, control of crystallinity during processing is important for the semicrystalline thermoplastics. Differential scanning calorimetry can be used to determine the crystallinity in a fashion analogous to that of the degree of cure:

$$c_{max} = \frac{H_T}{H_{Ult}} c_r \quad \text{(Eq 7.10)}$$

where:
c_{max} = maximum theoretical crystallinity
H_T = heat of reaction at temperature T
H_{Ult} = theoretical ultimate heat of reaction
c_r = relative crystallinity in polymer in weight percent

Additional information on thermoplastic crystallinity is given in Chapter 3, "Matrix Resin Systems."

7.2 Viscosity

The viscosity of a fluid is a measure of its resistance to flow under shear stress. As shown in Fig. 7.7, when a solid B-staged resin is initially heated, it melts and flows. As it starts to polymerize, the viscosity increases as the reaction progresses. Finally, crosslinking occurs and the resin becomes a solid gel. The resin viscosity prior to gellation affects the resin flow in the laminate and the resultant final resin content and thickness of the cured part. Like kinetics, viscosity is determined empirically for the particular resin system under consideration.

Chemical composition affects the viscosity. The dramatic effect of the BF_3 catalyst is again evident in the viscosity curves shown in Fig. 7.8. In addition to viscosity-versus-time curves, flow number:

$$\text{Flow Number} = \int_{t_0}^{t_{get}} \frac{dt}{\eta} \quad \text{(Eq 7.11)}$$

is calculated from each curve. Flow is the reciprocal of viscosity (η) when integrated as a function of time between the starting time (t_0) and the time to gellation (t_{gel}).

The resin with a high catalyst content (2.2% BF_3) exhibits a flow number approximately one-half that of the resin with a catalyst content of 1.1% BF_3 and an order of magnitude less flow than that of the resin with no catalyst. The minimum viscosity for the resin with no catalyst is much lower than that of the resin with 2.2% BF_3 catalyst. The gel temperature also shows the effect of varying the catalyst content. The resin with a high catalyst content (2.2% BF_3) gells at a lower temperature than the resin with 1.1% BF_3, while the resin with no catalyst gells at a much higher temperature. The temperature at the minimum viscosity is also significantly higher. These results can be explained by the fact that the BF_3 catalyst greatly accelerates the reaction at relatively low temperatures, resulting in higher reaction rates, lower total flow, higher minimum viscosities, and lower gellation temperatures. When the catalyst is absent, higher temperatures are necessary to initiate the chemical reactions, thereby providing more time for total flow and higher gellation temperatures.

The influence of kinetics on resin viscosity is normally described in models such as:

$$\eta = \eta_\infty \exp\left(\frac{E}{RT} + k\alpha\right) \quad \text{(Eq 7.12)}$$

where:
η = viscosity
η_∞ = constant
E = activation energy for viscous flow

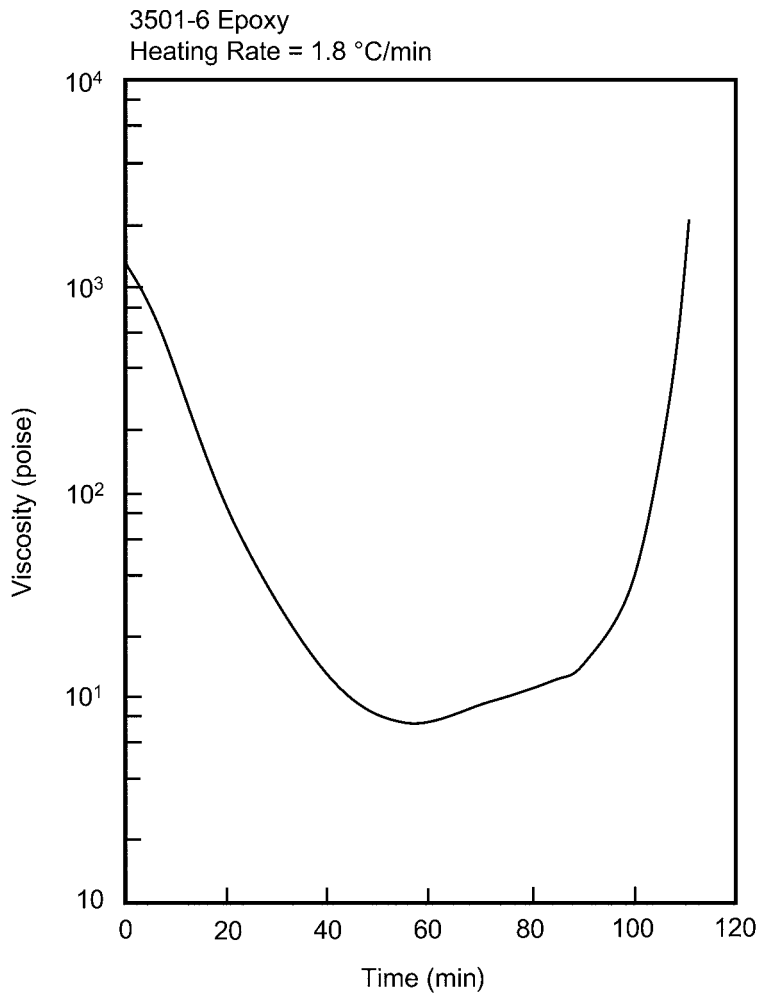


Fig. 7.7 Typical viscosity curve for an epoxy resin

k = temperature-independent constant
R = gas constant
T = temperature in degrees Kelvin

7.3 Heat Transfer

Autoclaves are normally pressurized with inert gas, usually nitrogen or carbon dioxide. Air can be used, but it increases the danger of a fire within the autoclave during the heated cure cycle. A schematic of the gas flow in a typical autoclave is shown in Fig. 7.9. The gas is circulated by a large fan at the rear of the vessel and passes down the walls next to a shroud containing the heater banks, usually electrical heaters, but steam heating is sometimes used. The heated gas strikes the front door and then flows back down the center of the vessel to heat the part. There is considerable turbulence in the gas flow near the door, which produces higher velocities that stabilize as the gas flows toward the rear. The practical effect of this flow field is that higher heating rates are often encountered for parts placed close to the door; however, the flow fields are dependent on the design of the autoclave and its gas flow characteristics. Another problem that may be encountered is blockage, in which large parts can block the flow of gas to smaller parts located behind them. Manufacturers typically use large racks to ensure even heat flow and to maximize the number of parts that can be loaded for cure.

At least three non-tool-related variables are known to affect convective heat transfer in an

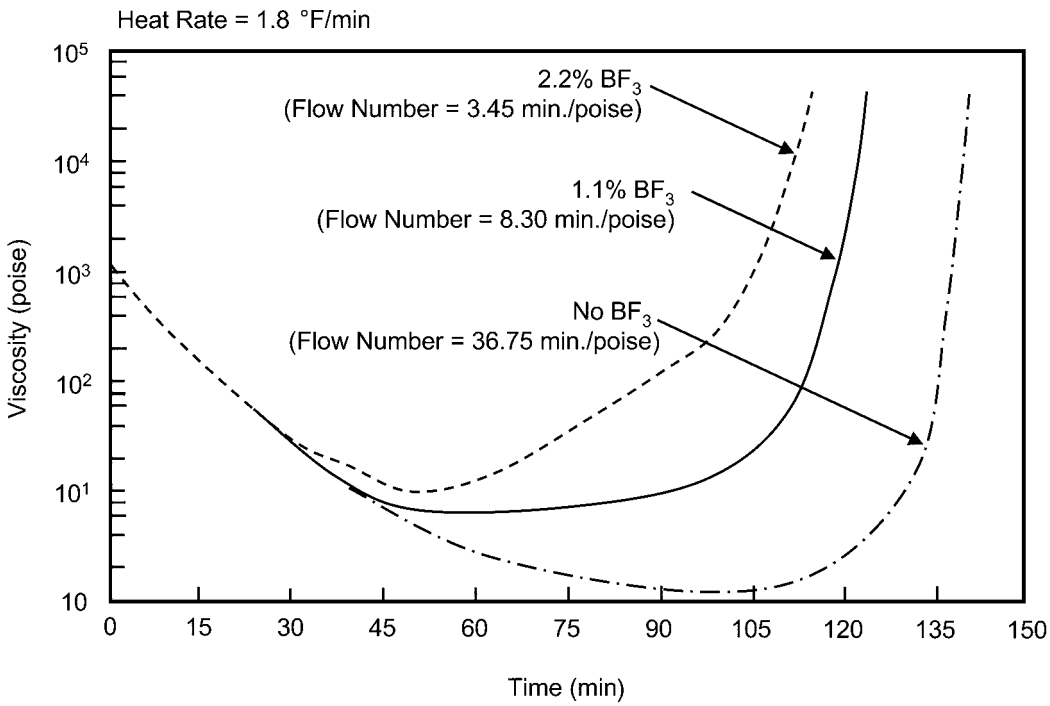


Fig. 7.8 Effect of catalyst content on viscosity. Source: Ref 1

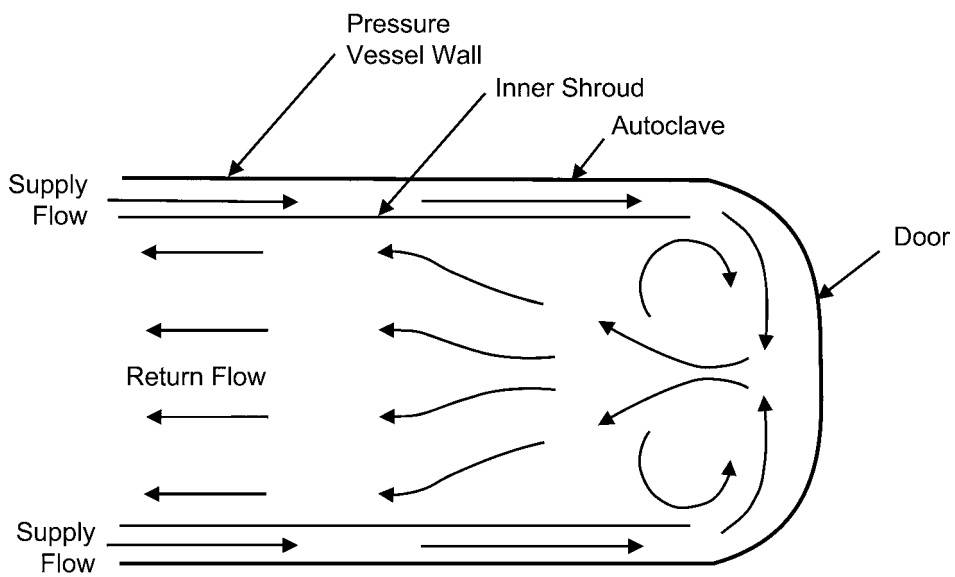


Fig. 7.9 Gas flow velocity turbulence near autoclave door

autoclave: (1) increasing the gas pressure, (2) increasing the gas velocity, and (3) increasing the gas flow turbulence all improve convective heat transfer. In one study, a standard production size autoclave was used that was 40 ft (12.2 m) in length and 12 ft (3.7 m) in diameter, with a heating capability to 650 °F (345 °C) and a maximum pressure of 150 psi (1035 kPa). The autoclave

was pressurized with nitrogen gas circulated by a 600 rpm fan producing a gas flow of 60,000 cfm. The results showed that:

1. the highest velocities occurred near the front and along the centerline of the autoclave. As a result, a low- or zero-velocity region occurred at some outer radial positions. Analysis showed that recirculation occurs in this region. The high-velocity region is caused by the supply flow striking the autoclave door at the edges and moving toward the center to form a rearward-flowing high-velocity plume. As the gas moves rearward, the plume dissipates and the flow becomes slower and more uniform. This velocity drop over the tools in the middle of the autoclave causes their convection coefficient to be lower than for parts located near the door.
2. the velocity was noticeably higher at the top of the autoclave than at the sides.
3. the average axial velocity was between 10 and 16 fps (3 and 5 mps); however, velocities as high as 44 fps (13.4 mps) occurred near the door.
4. the axial variation in velocity started to decrease approximately 13 ft (4 m) from the door (entrance) and became more and more uniform downstream.
5. the turbulence intensity was very high at the door region, typically 13 to 15 percent, dampening out at the same time that the radial velocity distribution became more uniform and kept decreasing toward the rear of the autoclave.

Tool design can also dramatically affect part heat-up rates. Recommendations for the design of an individual tool are fairly obvious and well understood in industry: Thin tools heat faster than thick tools; materials with high thermal conductivity heat faster than those with lower thermal conductivity; and tools with well-designed gas flow paths heat faster than those with restricted flow paths for example, tools with open egg-crate support structures heat faster than those without open support structures). Match die tooling, often used for complex parts and large unitized structures, presents its own special set of problems. Tool dimensions and fit become critical. If the tool is not dimensionally correct, it will not be possible to obtain quality parts. Mismatches and incorrect dimensions will result in high- and low-pressure areas during cure, resulting in excessive thin-out, voids, and porosity.

While convective heat transfer is certainly important, heat transfer is usually modeled as conduction of heat through the thickness of the lay-up:

$$\frac{\partial(\rho C_v T)}{\partial t} = \frac{\partial}{\partial x}\left(K_x \frac{\partial T}{\partial x}\right) + \frac{\partial}{\partial y}\left(K_y \frac{\partial P}{\partial y}\right) + \frac{\partial}{\partial z}\left(K_z \frac{\partial P}{\partial z}\right) + \frac{dH}{dt} \qquad \text{(Eq 7.13)}$$

where ρ and C_v are the density and specific heat of the composite; K_x, K_y, and K_z are the thermal conductivities in the *x*-, *y*-, and *z*-directions; and *T* is the temperature. The rate of heat generation by chemical reaction *dH*/*dt* is defined as:

$$\frac{dH}{dt} = \frac{d\alpha}{dt} H_R \qquad \text{(Eq 7.14)}$$

where H_R is the total heat of reaction and α is the degree of cure as predicted by the kinetic submodel. In addition to supporting kinetic and viscosity submodels, heat transfer submodels are useful during the initial design phases for tooling. They can be used to predict and compare heat-up rates for candidate tool designs.

7.4 Resin Flow

Under the influence of heat and pressure applied during the cure cycle, the prepreg resin flows in both the vertical and horizontal directions (Fig. 7.10). As the top plies lose resin into the bleeder, they move closer together and become compacted. This makes it harder for the plies in the middle and those at the bottom close to the tool to bleed and compact. Note that as resin bleeding occurs and the fiber volume percentage increases in the top plies, the through-the-thickness permeability decreases (Fig. 7.11), making it harder for the plies underneath to effectively bleed. This can often result in laminates containing a resin content and thickness gradient through the thickness, as shown for the resin content results in Fig. 7.12. Here three different laminate thicknesses (10, 25, and 60 plies) were cured at three different pressures of 25, 50, and 100 psi (175, 345, and 690 kPa). The nominal prepreg resin content before curing was 42 percent by weight. Only the thinnest laminate (10 plies) had a fairly uniform resin content through-the-thickness. Both the 25- and 60-ply thick laminates exhibited higher resin contents

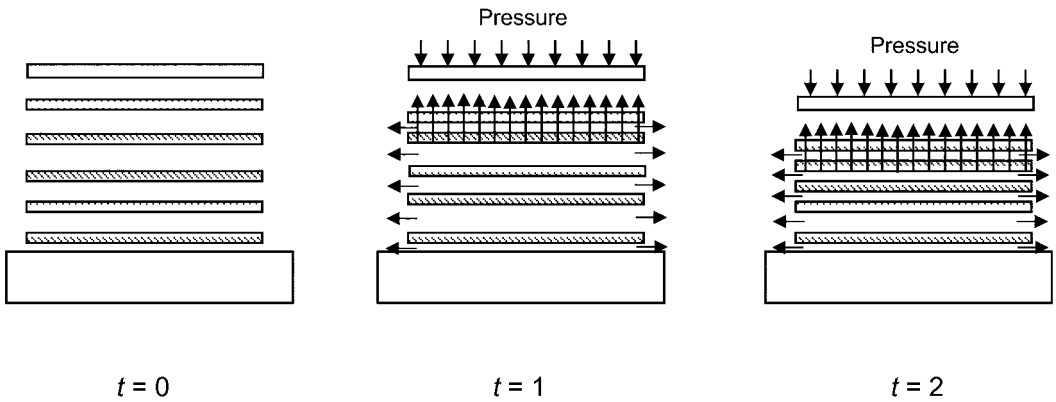


Fig. 7.10 Horizontal and vertical resin flow

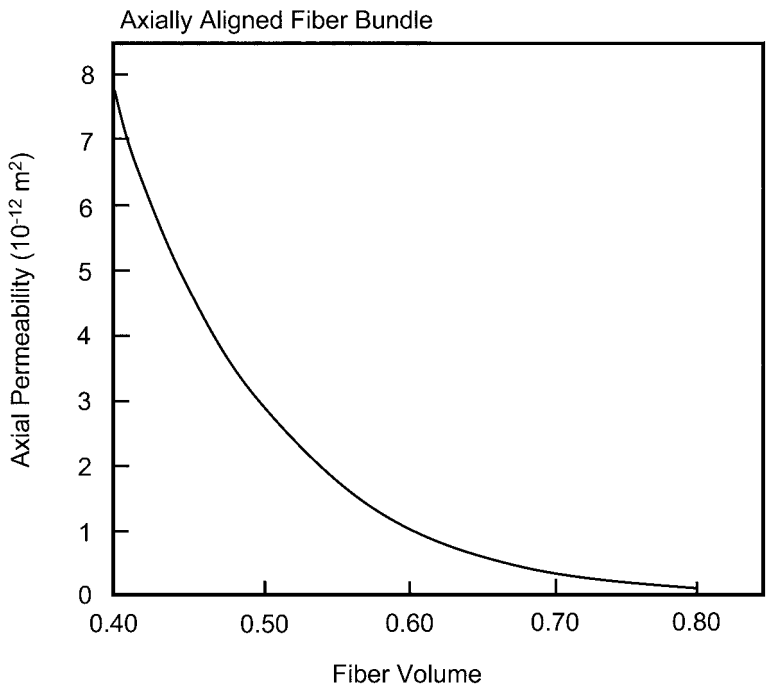


Fig. 7.11 Effect of fiber volume on permeability. Source: Ref 3

at the middle and tool side, indicating that most of the vertical bleeding occurred on the top surface.

However, the current trend in the composites industry is toward net or near-net resin systems (32 to 35 percent resin by weight) that require little or no bleeding, in contrast to the more traditional 40 to 42 percent resin systems. This simplifies the bagging system since the labor and the cost of the bleeder material are eliminated. However, when using this type of material, it is even more important to seal the inner bag system properly to prevent resin loss during cure; otherwise, resin-starved laminates may result. The edges are a particularly critical area since excessive gaps or leaks in the dams can result in excessive resin loss and thinner than desired edges. In addition to eliminating the need for a bleeder pack, net resin content prepregs produce laminates with more uniform thickness and resin content. The problem with the traditional 40 to

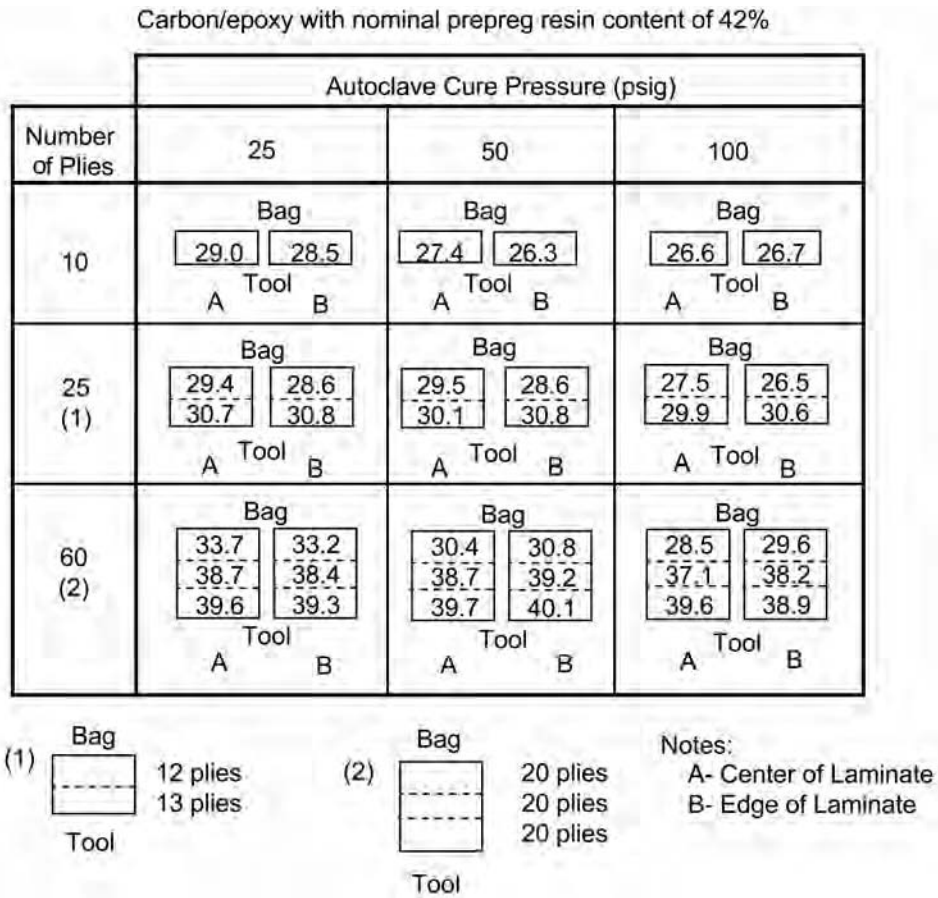


Fig. 7.12 Through-the-thickness resin content measurements

42 percent resin content prepregs is that as the laminate gets thicker in this case, as the number of plies increases), the ability to bleed resin through the thickness decreases. As more and more bleeder is added, the plies closest to the surface become overbled, while those in the middle and on the tool side of the laminate are underbled.

To develop a better understanding of the interactions of the resin flow process, a mechanical analogy is presented in Fig. 7.13. In this analogy, a laminate undergoing cure is simulated as a piston-spring-valve setup. The spring represents the fiber bed and is assumed to have a load-carrying capability. Just like a spring, the fiber bed will support larger and larger loads as it undergoes compression. The liquid contained in the piston represents the ungelled liquid resin. Finally, the valve is the means by which the liquid resin can leave the system; that is, it could be representative of bleeder, a poorly dammed part, or any other system leak.

Each step in this simplified model is described:

Step 1 Initially, there is no load on the system. The liquid hydrostatic pressure and the load carried by the fiber bed are zero.

Step 2 A 100 lb (45 kg) load is applied to the system, but no liquid has escaped (closed valve). The liquid carries the entire load, and the load on the fiber bed is zero. Note that the downward force (in this case 100 lb) is equal to the upward force (again 100 lb). This upward force is the sum of the load carried by the liquid (100 lb) and the spring-like fiber bed (0 lb).

Step 3 The valve is now opened, allowing resin to escape (e.g., resin bleeding). However, at this point the resin still carries the entire 100 lb load.

Step 4 Liquid continues to escape, but at a decreasing rate since a portion of the load is now being carried by the spring

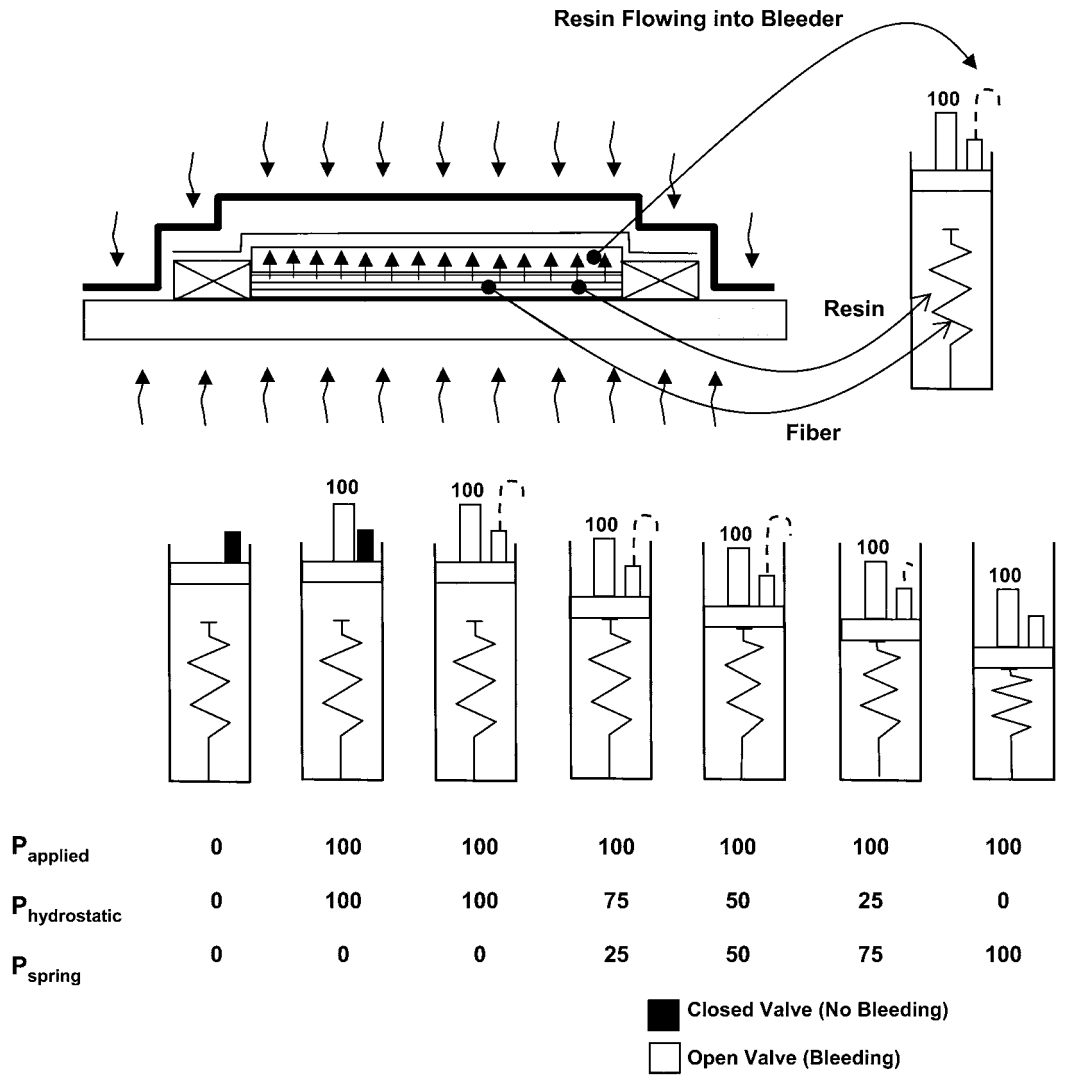


Fig. 7.13 Resin flow analogy. Source: Ref 4

at 25 lb (11.3 kg). This is analogous to bleeding in a laminate occurring rapidly until the fiber bed starts supporting a portion of the applied autoclave pressure.

Steps 5 and 6 Liquid continues to escape, but at an ever-decreasing rate, as a greater portion of the load is being carried by the spring. In an actual laminate, the rate of bleeding would be retarded both by the increasing fiber bed load-carrying capability and by the reduced permeability of the fiber bed as it is compacted.

Step 7 No further bleeding occurs because the pressure on the resin has now dropped to zero, and the entire load (100 lb) is being carried by the spring. If this condition occurs during actual autoclave processing before the resin gels (solidifies), it would be quite easy for dissolved volatiles to vaporize out of solution and form voids.

Although this analogy greatly simplifies the composite flow process, it illustrates several key points. In the early stages of the cure cycle, the hydrostatic resin pressure should be equal to the applied autoclave pressure. As resin flow occurs, resin pressure drops. If a laminate is severely

overbled, the resin pressure could drop to a low enough level to allow void formation; therefore, the hydrostatic resin pressure is directly dependent on the amount of resin bleeding that occurs. As the amount of bleeding increases, the fiber volume increases, resulting in an increase in the load-carrying capability of the fiber bed (Fig. 7.14). It should be noted that resin flow and bleeding can be intentional or unintentional. Intentional bleeding is, of course, caused by the bleeder cloth used to remove excess resin from the prepreg during cure. Examples of unintentional bleeding are excessive gaps between the dams and the laminate, tears in the inner bag that allow resin to flow into the breather material, and mismatched tooling details that allow escape paths for the liquid resin. Therefore, the hydrostatic resin pressure is directly dependent on the amount of resin bleeding that occurs. As resin bleeding increases, fiber volume increases, resulting in an increase in the load-carrying capability of the fiber bed and a decrease in the hydrostatic resin pressure.

Once a laminate is collated, it must be bagged for autoclave curing. The bagging operation includes several variables that can affect part quality, a number of which are illustrated in Fig. 7.15. If too much bleeder is used, overbleeding can occur, which could result in a large drop in the hydrostatic resin pressure, a condition conducive to porosity and void formation. If the resin has low viscosity in this case, high flow, the danger of overbleeding is even greater. Even if the correct amount of bleeder is used, an improperly sealed inner bagging system can allow resin to escape into the breather system. For example, if the caul plate severs the inner bag or the dams are not properly sealed, the resin will escape and the hydrostatic resin pressure could fall below the volatile vapor pressure, leading to voids and porosity. Another variable that occasionally causes a problem is that if the caul plate is misallocated or slips and bridges over the top of a dam, the result can be a localized low-pressure area along the edge of the laminate that will experience voids or possibly even large delaminations. Finally, if the outer vacuum bag (usually nylon film) bridges and ruptures during the autoclave cycle, a partial or total loss of the compaction force can result. If the resin has not already

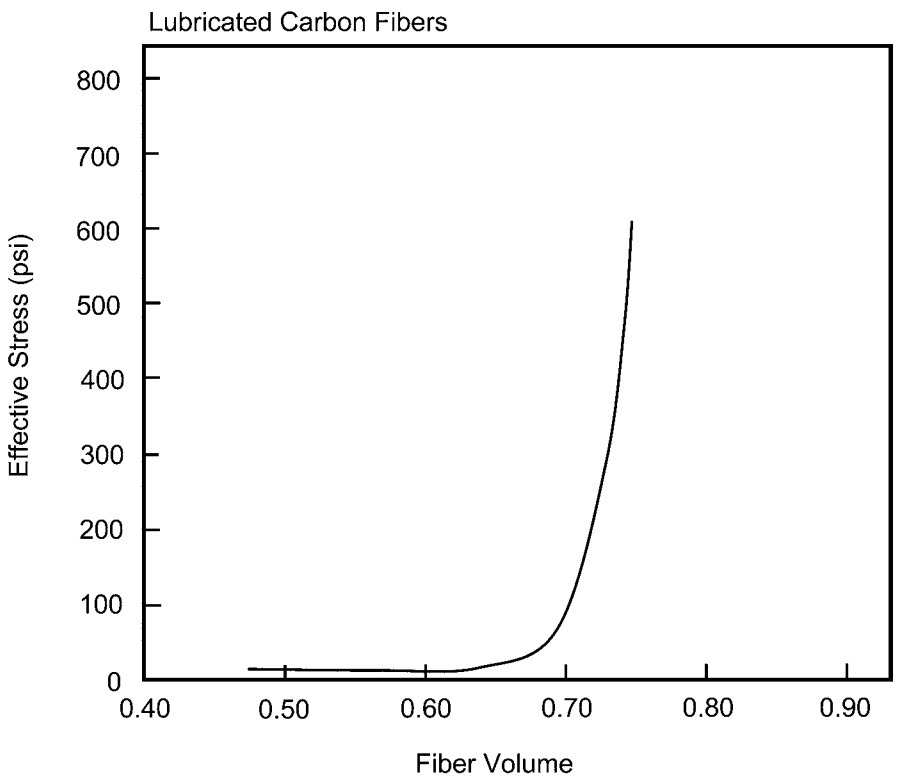


Fig. 7.14 Effect of fiber volume on bulk compressive stress. Source: Ref 3

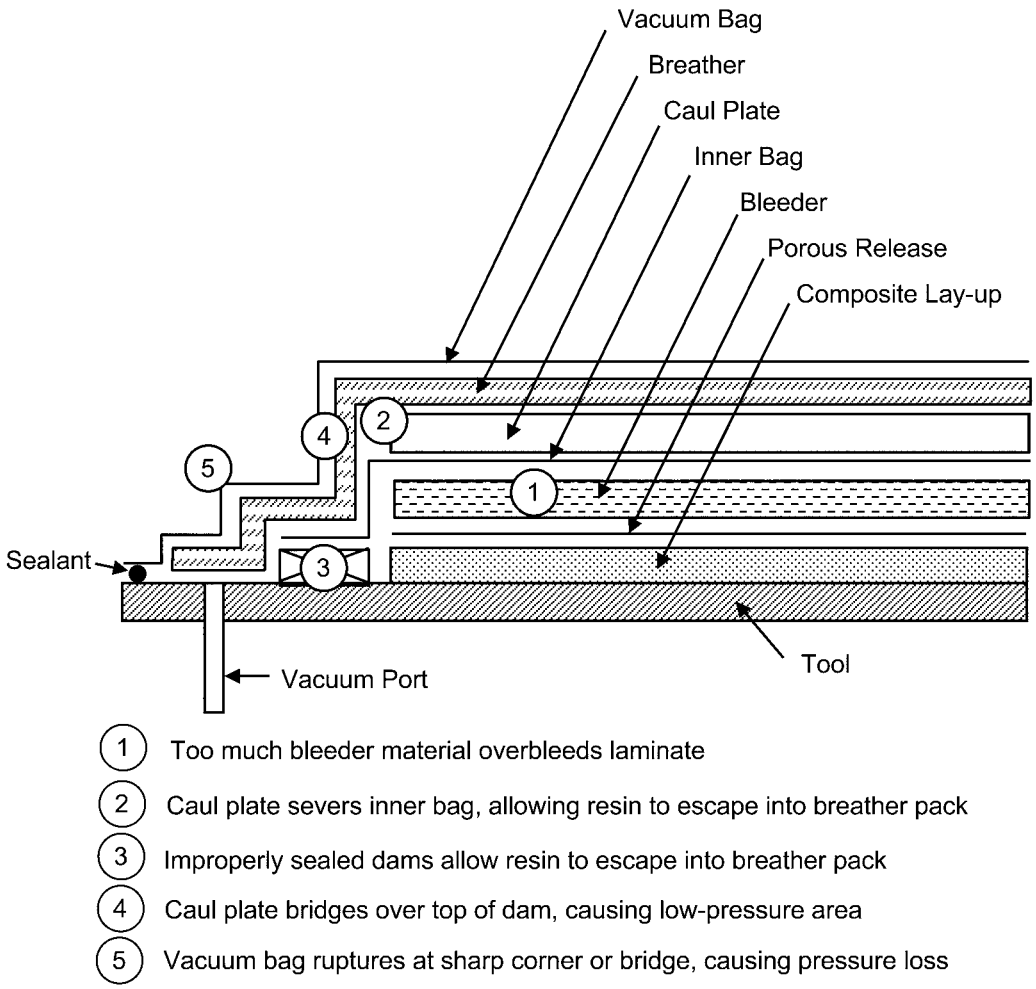


Fig. 7.15 Potential bagging problems

reached the point of gellation in the cure cycle, massive amounts of voids and porosity can form.

7.4.1 Hydrostatic Resin Pressure Studies

The experimental setup in Fig. 7.16 was used to study the flow behavior of real laminates. To measure the hydrostatic resin pressure, a transducer was recessed into the tool surface and filled with an uncatalyzed liquid resin. To ensure that the laminate did not deflect under pressure and contact the transducer, a stiff wire screen was placed over the transducer recess. Two different laminate thicknesses were evaluated; 10 plies and 40 plies thick. In both cases, Hexcel's 3501-6 carbon/epoxy prepreg was used, and the laminates were cross-plied containing 0-, 90-, and ±45-degree plies. A standard cure cycle was used for both tests.

The resin pressure results for a thin (10 plies) and a thick (40 plies) laminate are shown in Fig. 7.17. Note that the resin pressure for the thicker laminate essentially follows the applied autoclave pressure. However, since the resin pressure was measured at the tool surface, it was not known if there was a through-the-thickness pressure gradient in the thicker laminate. The higher resin pressure exhibited for the 40 ply laminate could be due to the inability to bleed thicker laminates. This has been qualitatively observed with materiallographic sections taken from 0.5 in. (12.7 mm) thick laminates in which the surface plies appear to be overbled (i.e., thin per ply thicknesses) and the center and tool side

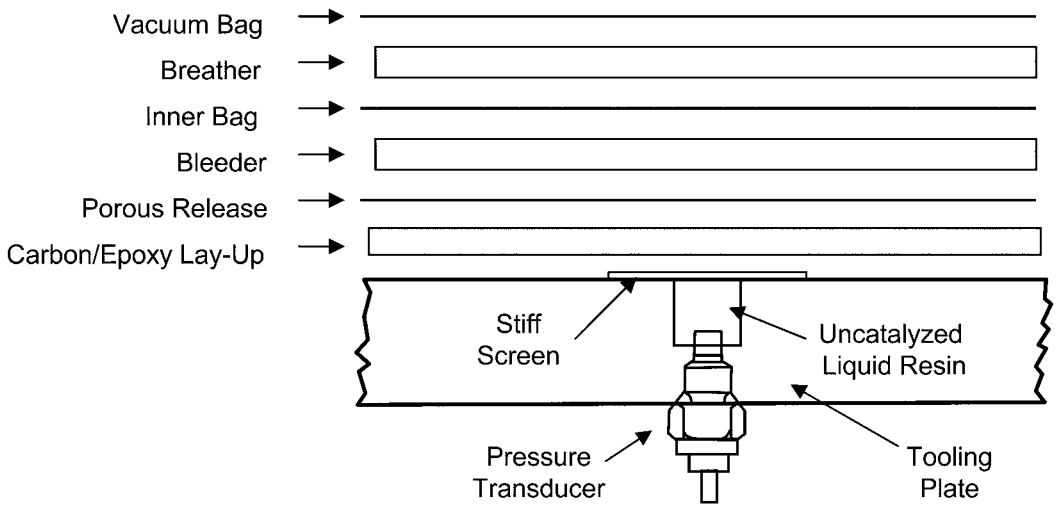


Fig. 7.16 Hydrostatic resin pressure setup. Source: Ref 4

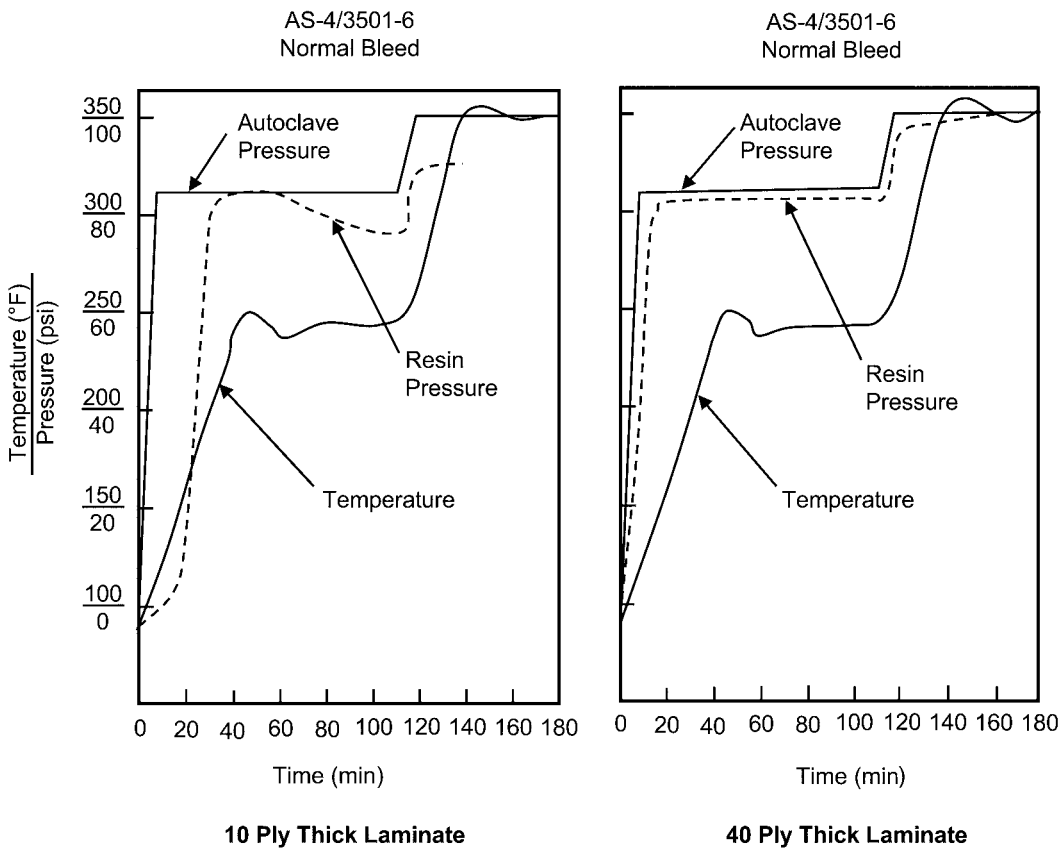


Fig. 7.17 Laminate thickness comparison. Source: Ref 4

plies appear to be underbled in this case, thick per ply thicknesses).

To investigate the potential pressure gradients that can exist within a laminate during curing, miniature pressure transducers capable of measuring the hydrostatic resin pressure were embedded at multiple locations within laminates to study the effects of vertical and horizontal pressure gradients. Because the previous thick laminate test (40 plies) showed almost no pressure drop at the tool surface, a 60-ply laminate was collated with miniature pressure transducers embedded at multiple locations within the laminate and the bleeder. Three tool-mounted transducers were also used to monitor the resin pressure at several locations along the surface of the tool. The pressure curves from this vertical flow test (Fig. 7.18) confirmed that a significant pressure gradient can exist within a laminate. Again, the resin pressure at the tool surface was essentially equal to the applied autoclave pressure. These results also illustrate the vertical compaction process. Initially, the resin pressure within the entire laminate is near the applied autoclave pressure. As resin bleeding occurs, the hydrostatic resin pressure at the top of the laminate drops (Transducer 3). At this point, resin begins to bleed from the middle of the laminate toward the top and the pressure drops here also (Transducer 2), but it remains above the pressure at the top. The opposite process occurs in the bleeder. As resin fills the bleeder, the pressure in the bleeder rises. Resin contents and photomicrographs were taken to confirm the resin pressure results. One resin content specimen was split into three pieces, one each from the top, middle, and bottom 20 plies. The resin content at the top was 24.6 percent, at the middle it was 31.0 percent, and at the bottom it was 33.0 percent, confirming the resin pressure results. The photomicrographs showed the same results; the top plies were compacted considerably more than those at the laminate bottom near the tool surface.

Just as the thick laminate experienced a pressure gradient, it was suspected that a horizontal pressure gradient also existed. Previously, all measurements had been conducted at the center of the laminate. Two laminates were processed to investigate horizontal pressure gradients. The first had cork dams located as close as possible to the laminate edges, while the second had a large 0.5 in. (13 mm) gap between the laminate edges and the dams. Both laminates (Fig. 7.19) contained nonporous release film against the top surface to prevent vertical flow. The pressure curves for both laminates (Fig. 7.20) show the existence of a horizontal pressure gradient and demonstrate that the magnitude of the gradient depends on the amount of horizontal flow; that is, the larger gap distance between the laminate edges and the dams resulted in more horizontal flow. The pressure curves also illustrate the horizontal flow process. Initially, the resin pressure approaches the applied autoclave pressure and then decreases as bleeding occurs. The opposite occurs in the bleeder. Initially, the applied vacuum is measured, and the pressure increases as

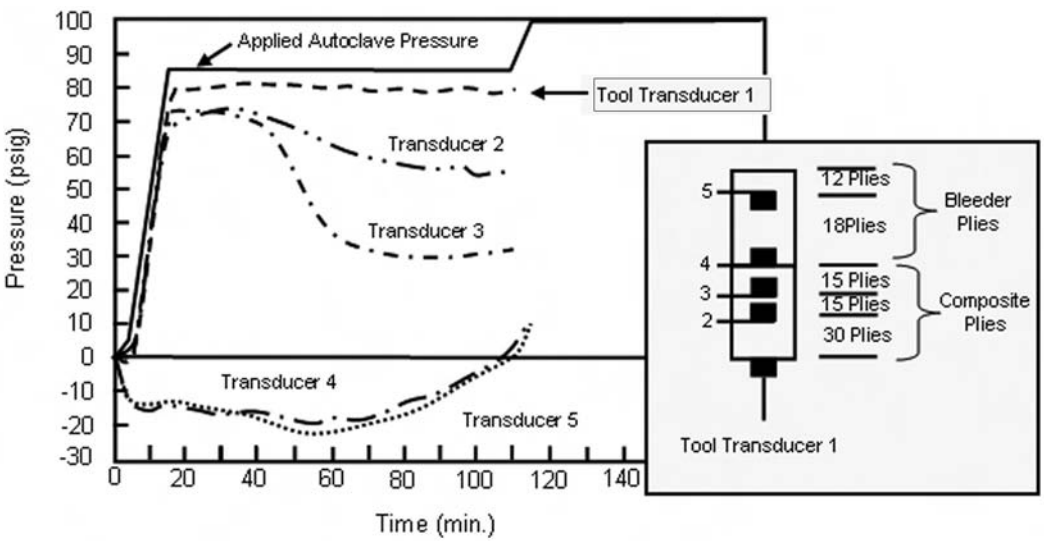


Fig. 7.18 Vertical flow laminate. Source: Ref 4

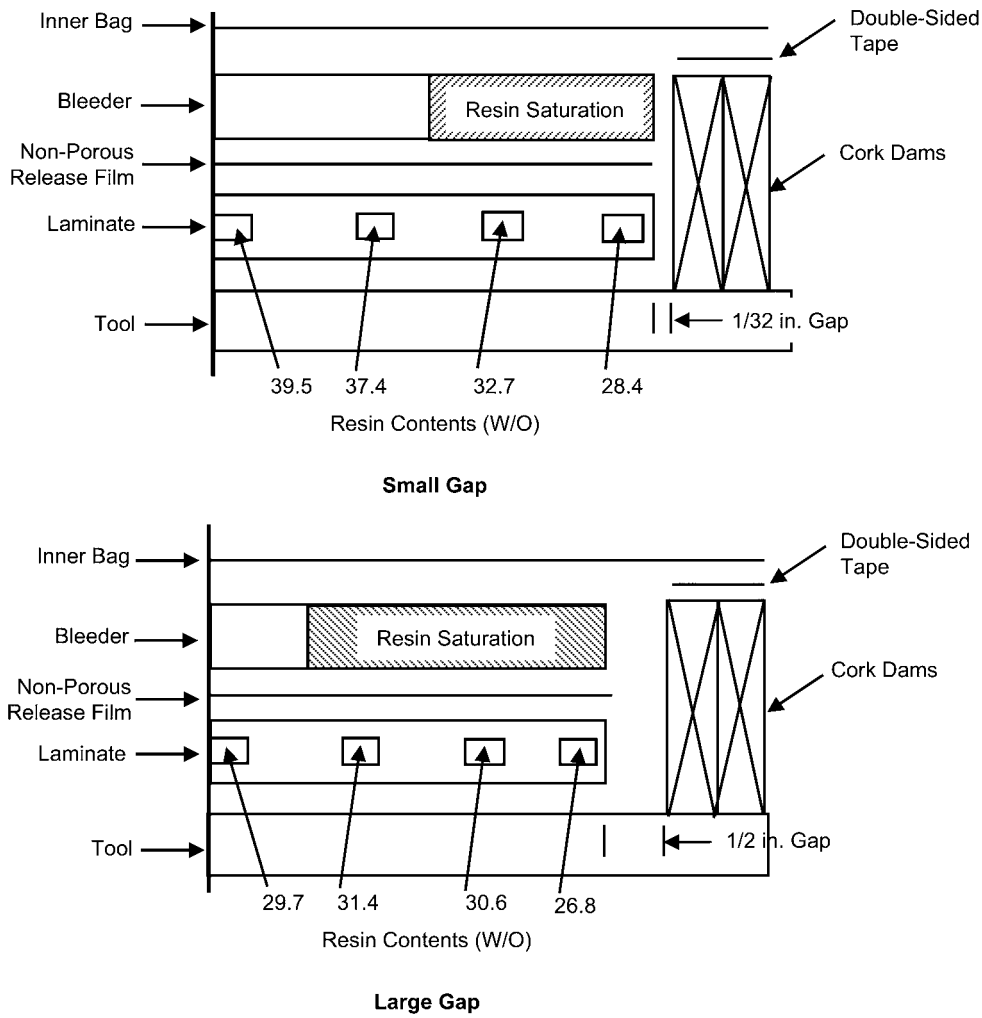


Fig. 7.19 Horizontal flow bagging arrangement showing resultant resin contents. Source: Ref 4

resin begins to fill the bleeder. Note that the horizontal pressure gradient is very small for a majority of the laminate but becomes large near the edges. Resin content results confirmed the resin pressure results, showing that a large resin content gradient (Fig. 7.19) existed at the edge of the laminate. Figure 7.19 also shows that resin bled further into the bleeder when a large gap was used between the laminate edges and the dams.

7.4.2 Resin Flow Modeling

The resin flow in the laminate is usually modeled in terms of Darcy's law for flow in a porous medium, which requires the determination of the permeability k of the fiber bed and the viscosity η of the flowing resin:

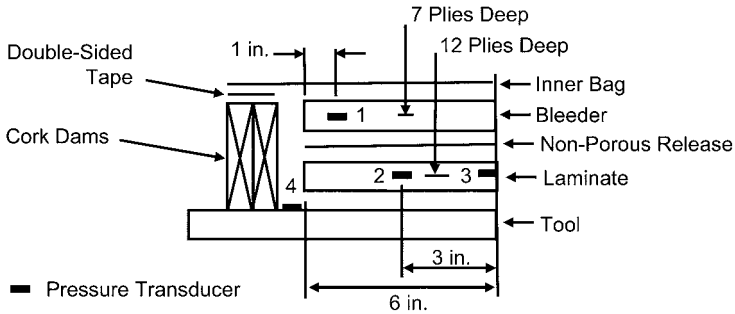
$$q = -\frac{k}{\eta}\frac{dP}{dx} \qquad \text{(Eq 7.15)}$$

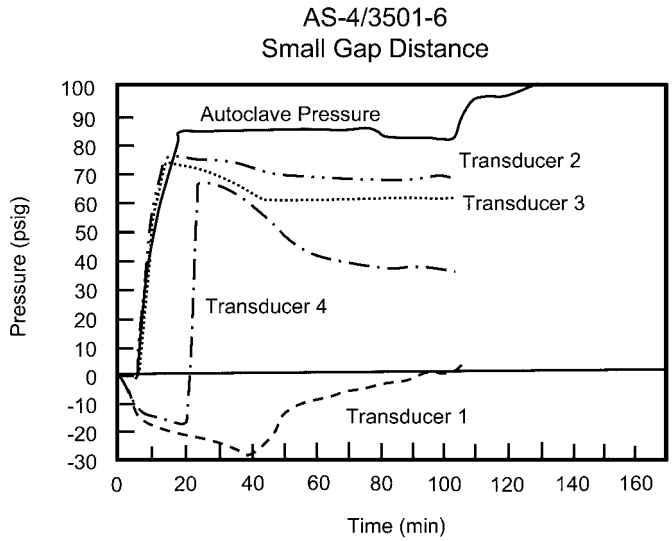
where:

q = volumetric flow rate per unit area in the x-direction
k = permeability
η = viscosity
dP/dx = pressure gradient, which is negative for flow in the x-direction

The permeability is determined by the Kozeny-Carman equation for horizontal flow or flow along the fiber direction:

$$k_x = -\frac{r_f^2}{4k}\frac{(1-V_f)^3}{V_f^2} \qquad \text{(Eq 7.16)}$$





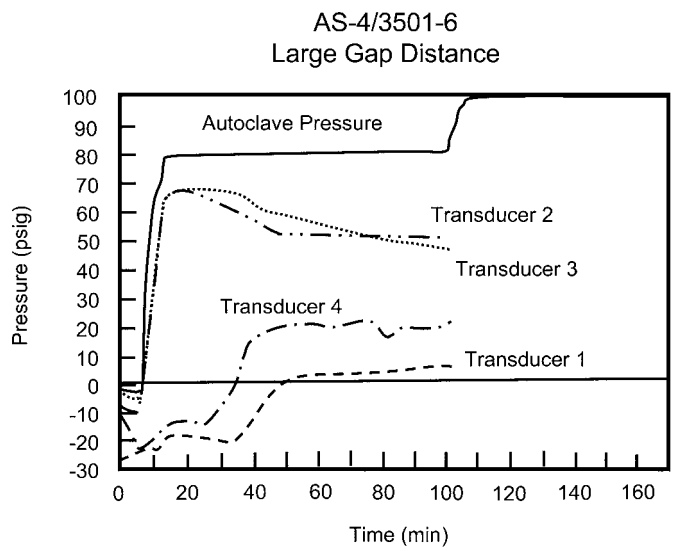


Fig. 7.20 Horizontal flow laminates. Source: Ref 4

where:
r_f = fiber radius
k = Kozeny constant based on the geometric form of the fibrous bed (k_x is the Kozeny constant for horizontal flow)
V_f = fiber volume fraction

For vertical flow or flow transverse to the fibers, Eq 7.16 was modified to account for the decrease of vertical flow as the resin content increases:

$$k_z = -\frac{r_f^2}{4k'} \frac{\left(\sqrt{V_a'/V_f - 1}\right)^3}{\left(V_a'/V_f + 1\right)} \quad \text{(Eq 7.17)}$$

where V_a' is the available fiber volume fraction when vertical flow stops and k_z is the Kozeny constant for vertical flow.

Using these inputs, the equation governing flow is:

$$\frac{\partial P}{\partial t} = \frac{1}{\eta m_v}\left[\frac{\partial}{\partial x}\left(k_x \frac{\partial P}{\partial x}\right) + \frac{\partial}{\partial y}\left(k_y \frac{\partial P}{\partial y}\right) + \frac{\partial}{\partial z}\left(k_z \frac{\partial P}{\partial z}\right)\right] \quad \text{(Eq 7.18)}$$

where:
k_x, k_y, k_z = specific permeabilities in the *x*-, *y*-, and *z*-directions
P = hydrostatic resin pressure
t = time
m_v = coefficient of volume change

7.5 Voids and Porosity

Voids and porosity have been two of the major problems in composite part fabrication. As shown in Fig. 7.21, voids and porosity can occur at either the ply interfaces (interlaminar) or within the individual plies (intralaminar). The terms *voids* and *porosity* are generally interchangeably in industry; however, *void* usually implies one large pore, whereas *porosity* implies a series of small pores. There are two main reasons for voids and porosity in composite laminates: (1) entrapped air during lay-up and (2) insufficient resin hydrostatic pressure to keep any residual moisture or volatiles dissolved in the liquid resin until gellation occurs.

High pressures such as 100 psi (690 kPa) are commonly used during autoclave processing to provide ply compaction and suppress void formation. Autoclave gas pressure is transferred to the laminate due to the pressure differential between the autoclave environment and the vacuum bag interior. Translation of the autoclave pressure to the resin depends on several factors, including the fiber content, laminate configuration, and the amount of bleeder used. Even though a relatively high autoclave pressure such as 100 psi (690 kPa) may be used during the cure cycle, the hydrostatic resin pressure or the actual pressure on the resin can be significantly less.

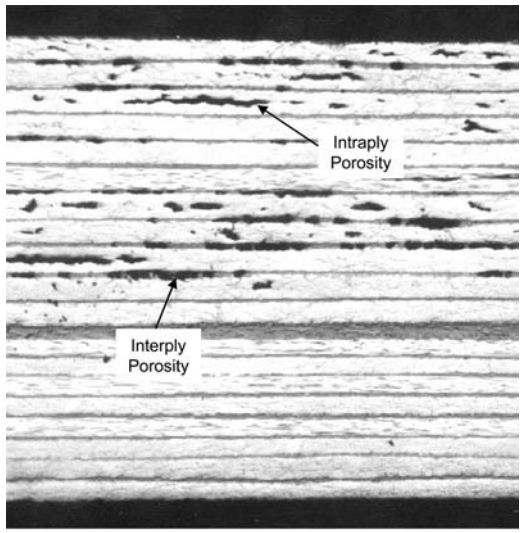


Fig. 7.21 Interply and intraply voids and porosity

During collation or ply lay-up, air can become entrapped between the prepreg plies. The amount of air entrapped depends on many variables: the prepreg tack, the resin viscosity at room temperature, the degree of impregnation of the prepreg and its surface smoothness, the number of intermediate debulk cycles used during collation, and geometrical factors such as ply drop-offs, radii, and so forth. An obvious place where entrapped air pockets form is at the terminations of internal ply drop-offs. In addition, air can be entrained in the resin itself during the mixing and prepregging operations.

It is been found through hard experience that prepreg physical quality can greatly influence final laminate quality (Fig. 7.22). The original carbon/epoxy prepregs supplied to the aerospace industry in the 1970s were made by the original hot melt impregnation process (Section 2.10). They had a rather rough surface due to the predominance of fibers on the prepreg surface—sometimes referred to as a *corduroy texture*—and in general, they made porosity-free parts. Although it was not known at the time, the somewhat rough texture provided evacuation paths

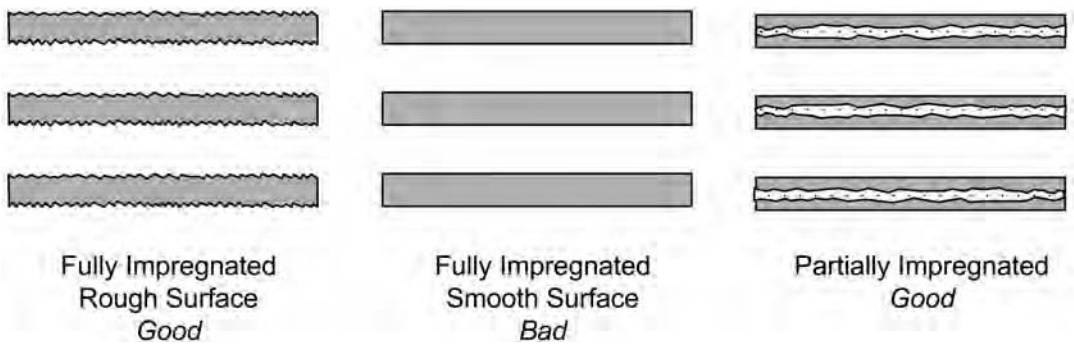


Fig. 7.22 Effects of prepreg physical quality

for air to escape during the initial portions of the cure cycle. Later, when resin filming became the predominant method of prepreg manufacture, the prepreg surfaces were nice and smooth but produced many porous parts. After several years, it was determined that the slick, smooth surfaces mated, sealed off, and did not allow air evacuation; air became trapped in the laminate, resulting in porosity. To circumvent this problem while maintaining the quality advantages of the resin filming process, the manufacturers deliberately began only partially impregnating the prepreg. It should be noted that partially impregnated prepregs have the same resin content and fiber areal weight as fully impregnated material. The only difference is the placement of the resin with respect to the fibers. Since the fibers in the center of the layer are fairly dry, they provide the evacuation paths for air. After the air is evacuated and the resin melts, it flows into the dry fiber areas and impregnates them.

Prepreg tack can also influence final laminate quality. Prepreg tack is a measure of the stickiness, or self-adhesive nature, of the prepreg plies. Often prepregs with a high tack level have resulted in laminates with severe voids and porosity. This could be due to the potential difficulty of removing entrapped air pockets during collation with tacky prepreg. Moisture can be a factor; prepregs with a high moisture content have been found to be inherently tackier than those with a low moisture content. Previous work has indicated a possible correlation between prepreg tack and resin viscosity; that is, prepregs that are extremely tacky also have high initial resin viscosities.

The resin mixing and prepregging operations can also influence the processability of the final prepreg. During normal mixing operations, air can easily be mixed into the resin. This entrained air can later serve as nucleation sites for voids and porosity. However, some mixing vessels are equipped with seals that allow vacuum degassing during the mixing operation, a practice that has been found to be effective in removing entrained air and may be beneficial in producing superior-quality laminates.

Void formation and growth in addition-curing composite laminates can also occur as a result of entrapped volatiles, primarily water absorbed by the prepreg but also residual solvents from the resin mixing or prepregging process. Higher temperatures result in higher volatile pressures. Void growth will potentially occur if the void pressure or the volatile vapor pressure exceeds the actual pressure on the resin in this case the hydrostatic resin pressure, while the resin is a liquid (Fig. 7.23). The prevailing relationship is:

$$\text{If } P_{\text{void}} > P_{\text{hydrostatic}} \rightarrow \text{Then Void Formation and Growth}$$

When the liquid resin viscosity dramatically increases or gellation occurs, the voids are locked into the resin matrix. Note that the applied pressure on the laminate is not necessarily a factor. As we have shown, the hydrostatic resin pressure can be low even though the applied autoclave pressure is high, leading to void formation and growth.

Composite prepregs, like most organic materials, absorb moisture from the atmosphere. The amount of moisture absorbed is dependent on the relative humidity of the surrounding environment, while the rate of moisture absorption is dependent on the ambient temperature. While the carbon fibers themselves absorb minimal moisture, epoxy resins readily absorb moisture. Thus, the final prepreg moisture content is a function

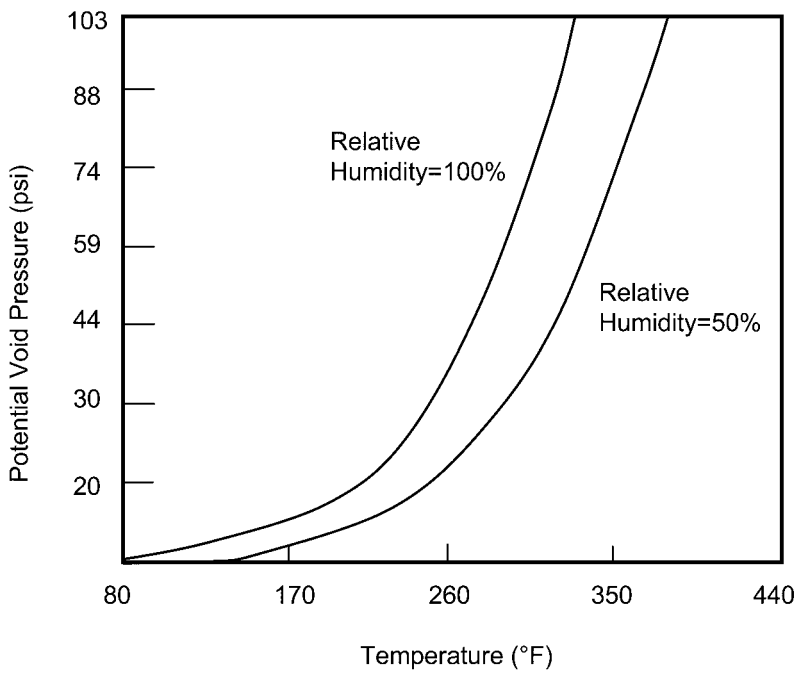


Fig. 7.23 Potential for void formation. Source: Ref 5

of the relative humidity, ambient temperature, and prepreg resin content.

Since moisture is typically the most predominant volatile present in hot melt addition curing prepregs, the amount of absorbed moisture in the prepreg determines the resultant vapor pressure of volatiles generated during the cure cycle. An examination of Fig. 7.23 explains why composite fabricators control the lay-up room environment; that is, higher moisture contents result in higher vapor pressures, increasing the propensity for void formation and growth. Even though relatively small amounts of moisture are involved as much as one percent, they can generate large gas volumes and pressures when heated. It should also be pointed out that other types of volatiles, such as solvents used in a solvent impregnation process or volatiles resulting from condensation-curing reactions, can greatly complicate this problem, leading to much higher vapor pressures and a much greater propensity for void formation. Because of the load-carrying capability of the fiber bed in a composite lay-up, the hydrostatic resin pressure needed to suppress void formation and growth can be only a fraction of the applied autoclave pressure. The hydrostatic resin pressure is critical, because it is this pressure that helps to keep volatiles dissolved in solution. If the resin pressure drops below the volatile vapor pressure, then volatiles will come out of solution and form voids.

Referring to the cure cycle shown in Fig. 7.24, the second ramp portion of this cycle is critical from a void nucleation and growth standpoint. During this ramp portion the resin is still a liquid, the temperature is high, the resin pressure can be near its minimum, and the volatile vapor pressure is high and rising with the temperature. These are the ideal conditions for void formation and growth.

Several more laminates were fabricated to further assess resin pressure using the same test setup shown in Fig. 7.16. These results showed that:

1. A high-flow resin system experiences a larger pressure drop than a low-flow system.

A comparison of the resin pressures for 3501-6 and 3502 (Fig. 7.25) shows that the higher-flow 3502 resin system experiences a larger pressure drop than the lower-flow 3501-6 system. The 3501-6 system is a lower-flow system because it contains a boron trifluoride (BF_3) catalyst that significantly alters the cure behavior, resulting in a lower-flow system that gels at a lower temperature. Since high-flow resin systems are more

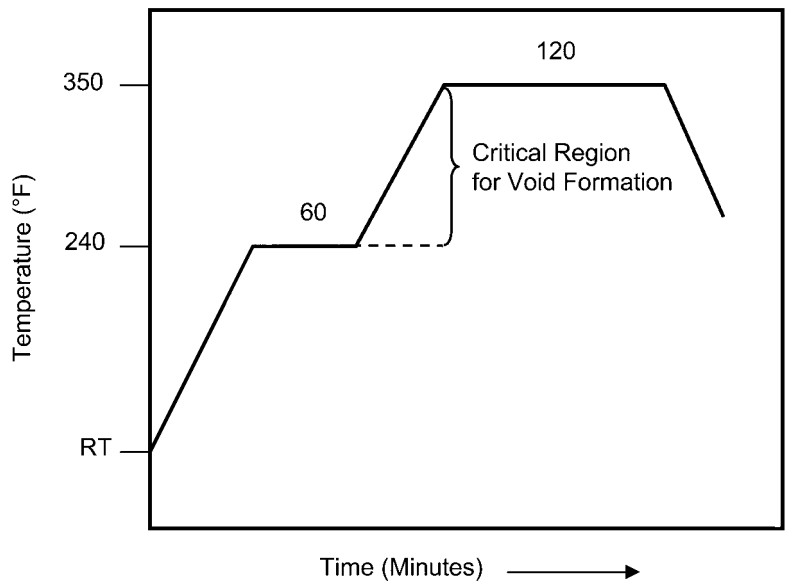


Fig. 7.24 Typical carbon/epoxy cure cycle

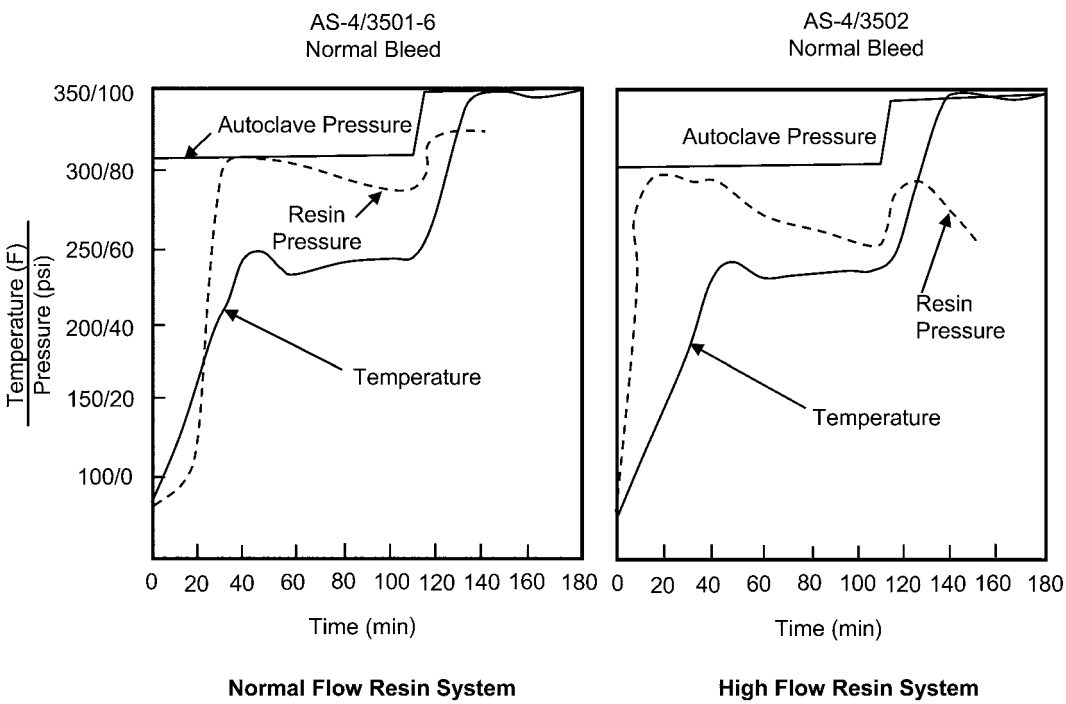


Fig. 7.25 Resin flow comparison. Source: Ref 4

prone to bleeding, additional care must be taken when they are tooled or bagged. High-flow laminates should be tightly bagged and sealed to eliminate leak paths. Since high-flow resin systems also typically have high gel temperatures, additional care must be taken to ensure that the potential void pressure does not exceed the hydrostatic resin pressure prior to resin gellation.

2. Overbleeding a laminate causes a large drop in resin pressure.

A comparison of normal bleeding with overbleeding is shown in Fig. 7.26. Overbleeding was accomplished by using three times the normal amount of glass bleeder and by removing the inner bag to create a free-bleeding condition. While this would normally not be done in composite part fabrication, overbleeding can and does occur because of leaky damming systems or leaky matched die molds. The analysis of these cured laminates included nondestructive testing (NDT), thickness measurements, resin content determinations, and materiallographic cross sections. The resin contents and thickness measurements showed the dramatic effect of overbleeding. The resin contents and thickness values of the overbled laminate were significantly lower than those of standard bled laminate. Since the resin pressure actually dropped to below zero psi due to the vacuum pulled underneath the bag, little resistance to void growth existed. As expected, the ultrasonic NDT results and materiallographic cross sections revealed gross voids and porosity in the overbled laminate.

3. Internal bag pressure can be used to maintain hydrostatic resin pressure and reduce resin flow.

Internally pressurized bag (IPB) curing was originally developed during the Ref 6 program. In this process, two separate pressure sources are used: (1) a normal external applied autoclave pressure that provides the ply compaction and (2) a somewhat smaller internal bag pressure that applies hydrostatic pressure directly to the liquid resin to keep volatiles in solution and thereby prevent void nucleation and growth. An autoclave setup for IPB curing is shown in Fig. 7.27. In the cycle used for this experiment (Fig. 7.28), an external applied autoclave pressure of 100 psi (690 kPa) was used along with an internal bag pressure of 70 psi (480 kPa). This results in a compaction or membrane pressure of 30 psi (205 kPa) (applied autoclave pressure – internal bag pressure = 100 psi – 70 psi) on the plies and a hydrostatic pressure of 70 psi (480 kPa) minimum on the resin. There is nothing magical about these pressure selections. If desired, the compaction pressure could be raised again to 100 psi (690 kPa) by simply increasing the applied autoclave pressure to 170 psi (1170 kPa). The only restriction is that the applied autoclave pressure must be greater than the internal bag pressure to prevent blowing the bag off of the tool. Of course, the internal bag pressure needs to be high enough to keep the volatiles in solution to prevent void nucleation and growth. To test a worst-case condition, the IPB laminate was bagged in the same

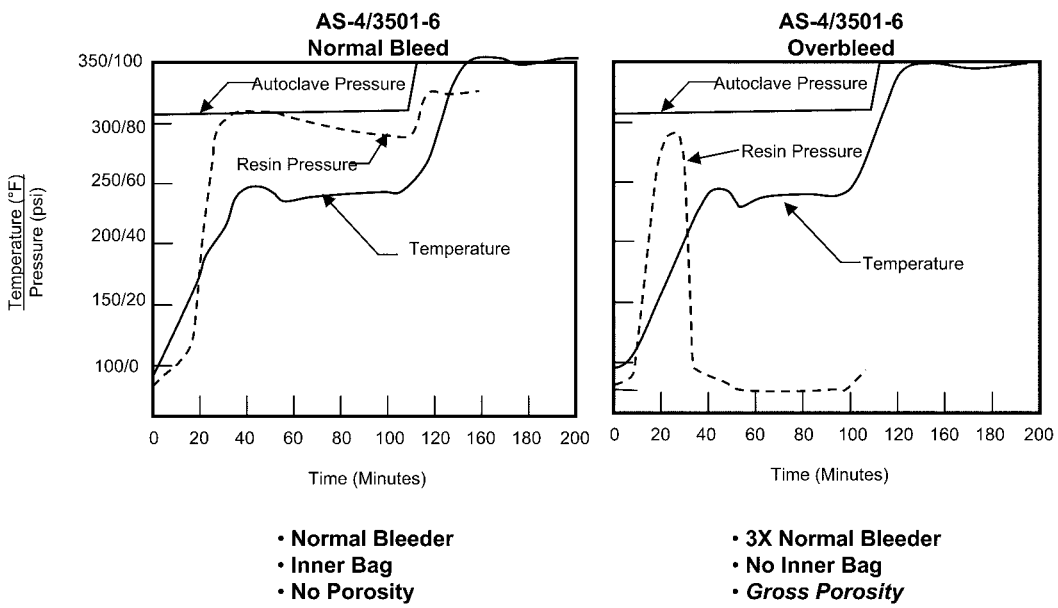


Fig. 7.26 Overbleeding causes pressure loss. Source: Ref 4

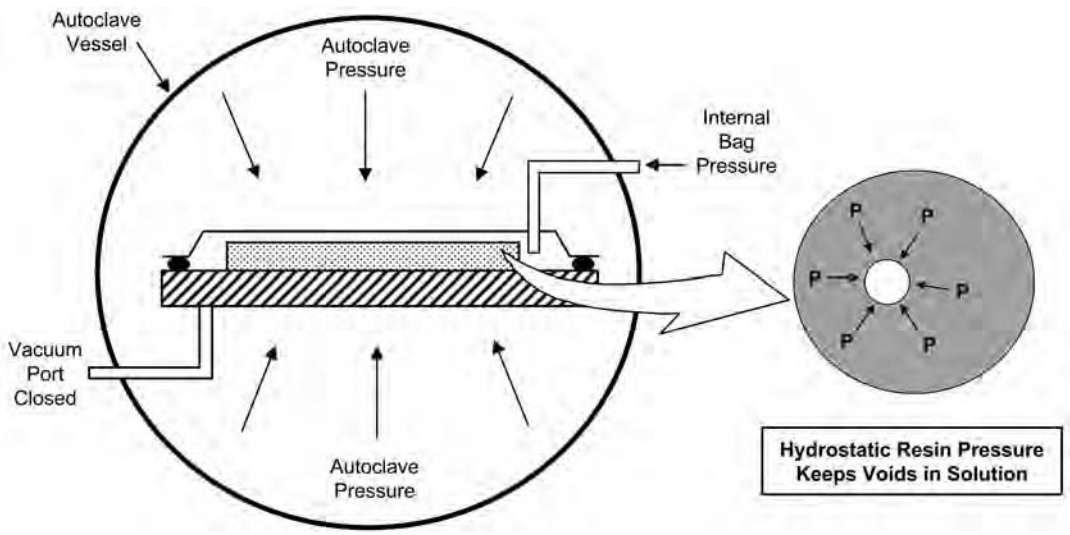


Fig. 7.27 Principle of internal bag pressurization

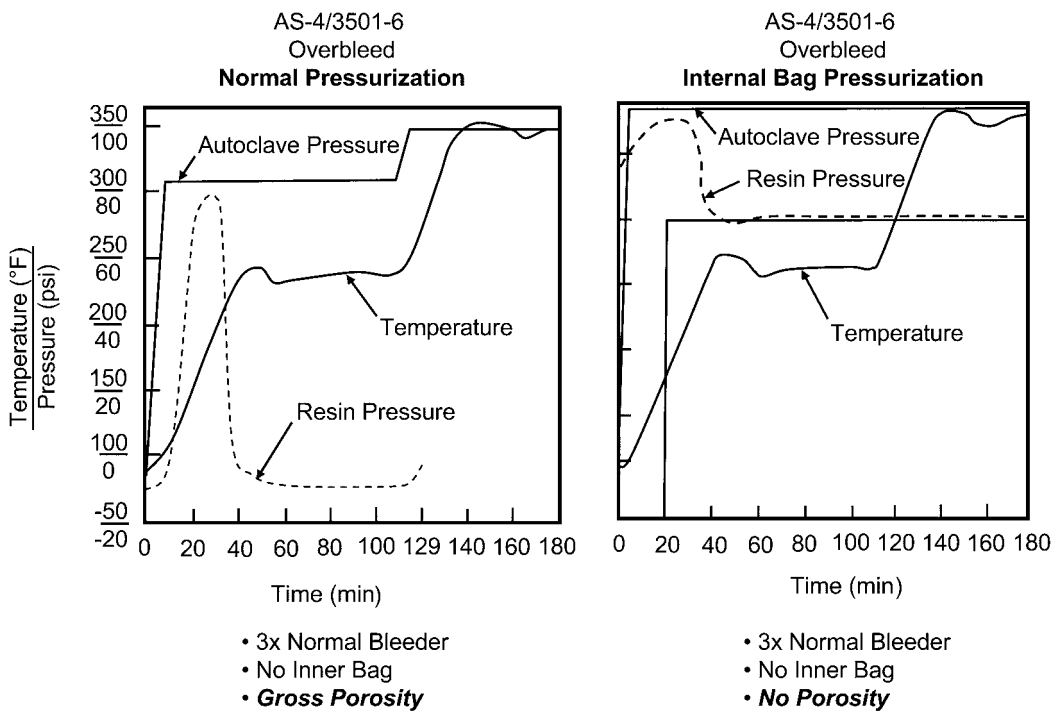


Fig. 7.28 IPB maintains resin pressure. Source: Ref 4

manner as the previous overbled laminate in which the resin pressure had dropped to zero. Even though this bagging procedure resulted in a severely overbled and porous laminate in the previous test, the addition of internal bag pressure prevented both overbleeding and porosity. The absence of overbleeding was a result of the lower membrane pressure (30 psi (205 kPa) for the IPB cure versus 100 psi (690 kPa) for the normal cure).

Internally pressurized bag curing is not normally used because it is not needed if one forms

a proper hydraulic cell with the inner bag. One application in which it proved useful was for the sine wave spars shown in Fig. 7.29. In this instance, the aluminum matched metal tools became worn from repeated use and allowed excessive amounts of resin to escape from the tool during cure, resulting in gross porosity, especially in the relatively thin webs. Three actions were taken to resolve the porosity problem—(1) the cure was switched to an IPB-type cure to reduce the resin loss and keep hydrostatic pressure on the resin; (2) the solvent-impregnated woven cloth was switched to a hot melt–impregnated cloth to remove any problem with residual

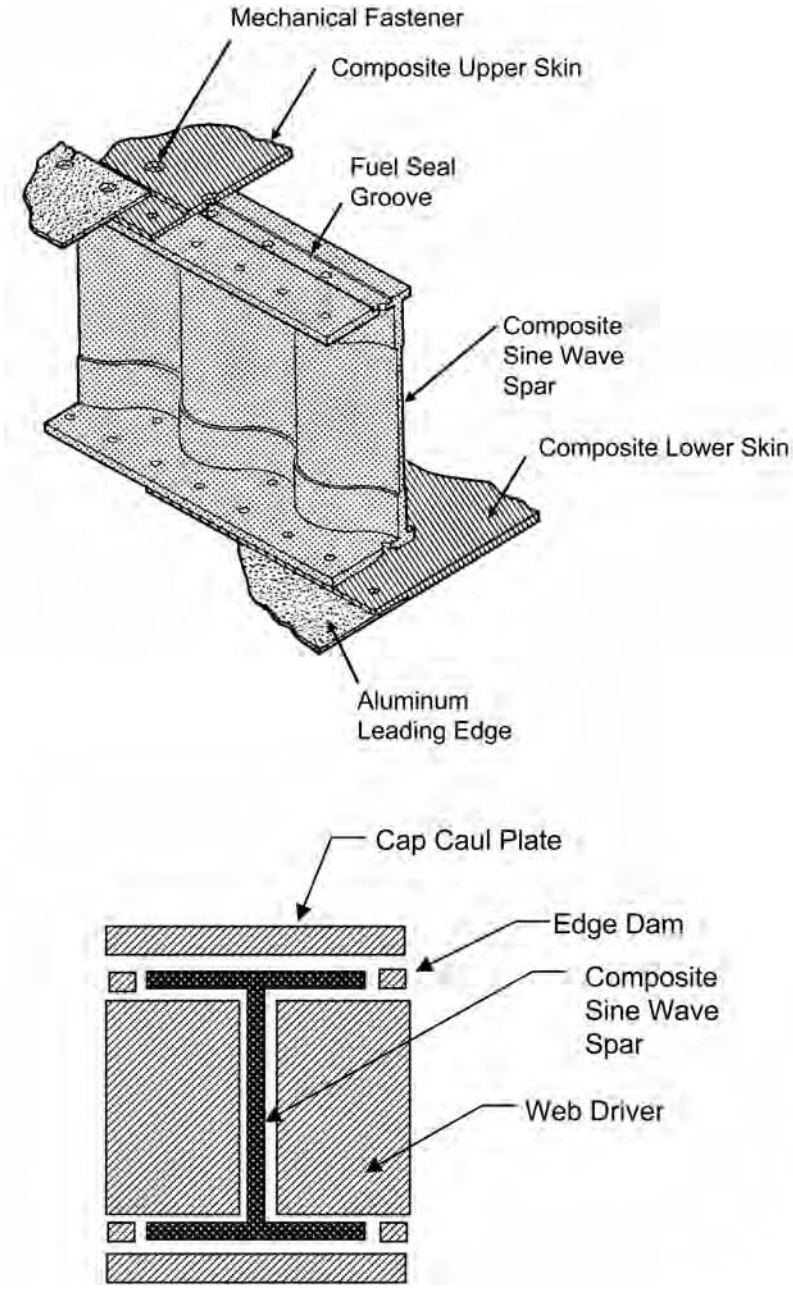


Fig. 7.29 Complex sine wave spar

solvent; and (3) a layer of film adhesive was added to both surfaces of the web to provide more resin and help seal the surfaces.

Changes in chemical composition can also affect processability. A real-world example of the effect of chemical composition on flow was experienced during the early development work for the cocured rib shown in Fig. 7.30. Due to its geometrical complexity, this rib was manufactured in match die tooling. The resin system was a new toughened epoxy that had high viscosity in this case, very little resin flow). The result was that the resin did not flow enough to adequately fill the tool. This yielded unacceptable parts in which the surfaces contained numerous "dry" areas that were resin starved, and the net molded edges were rough and poorly impregnated. Ultrasonic inspection revealed numerous areas of porosity and voids. The solution selected was to have the material supplier reformulate the resin so that it had lower viscosity. Of course, if the viscosity is too low, this can also create problems with excessive resin leaking out of the tool. Since matched die tools normally consist of a number of tooling details that must be fitted together during lay-up, they contain multiple leak paths that can allow a very-low-viscosity resin to escape during the cure cycle. Thus, complex part processing requires not only resin systems amenable to matched die tooling but also well-designed tooling.

7.5.1 Condensation-Curing Systems

Condensation-curing systems, such as polyimides and phenolics, give off water and alcohols as part of their chemical crosslinking reactions. In addition, the reactants are often dissolved in high-temperature boiling point solvents, such as dimethylformamide, dimethylactamide, *N*-methylpyrrolidone (NMP) or dimethylsufoxide, to allow prepregging. Even the addition-curing polyimide PMR-15 uses methanol as a solvent for prepregging. The eventual evolution of these volatiles during cure creates a major volatiles management problem that can result in high void and porosity percentages in the cured part. Unless a heated platen press with extremely high pressures for example, 1000 psi (6900 kPa) is used to keep the volatiles in solution until gellation, they must be removed either before the cure cycle or during cure heat-up. In addition, since these materials boil or condense at different temperatures during heat-up, it is important to know the point(s) during the cycle when the different species will evolve. An example of the complex volatile evolution for the thermoplastic polyimide K-IIIB is shown in Fig. 7.31. Here one has to deal not only with water but also with large amounts of ethanol and NMP volatile evolution. In addition, the volatiles are continually evolving over a major portion of the cure cycle.

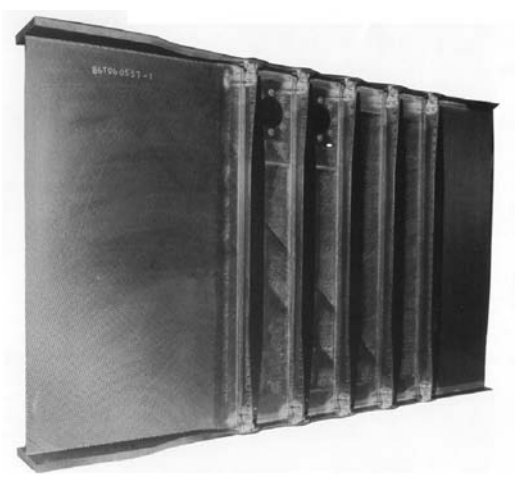


Fig. 7.30 Complex cocured rib

7.6 Residual Curing Stresses

Residual stresses develop during the elevated temperature cure of composite parts. They can result in either physical warpage or distortion of the part (particularly thin parts) or in matrix microcracking either immediately after cure or during service. Distortion and warpage cause problems during assembly and are more troublesome for composite parts than metallic ones. While the distortion in thin sheet metal parts can often be pulled out during assembly, composite parts run the danger of cracking, and even delamination, if they are stressed too much during assembly. Microcracking is known to result in degradation of the mechanical properties of the laminate, including the moduli, Poisson's ratio, and the coefficient of thermal expansion (CTE). Microcracking (Fig. 7.32) can also induce secondary forms of damage, such as delamination, fiber breakage, and the creation of pathways for the ingression of moisture and other fluids. Such damage modes have been known to result in premature laminate failure.

The major cause of residual stresses in composite parts is the thermal mismatch between the

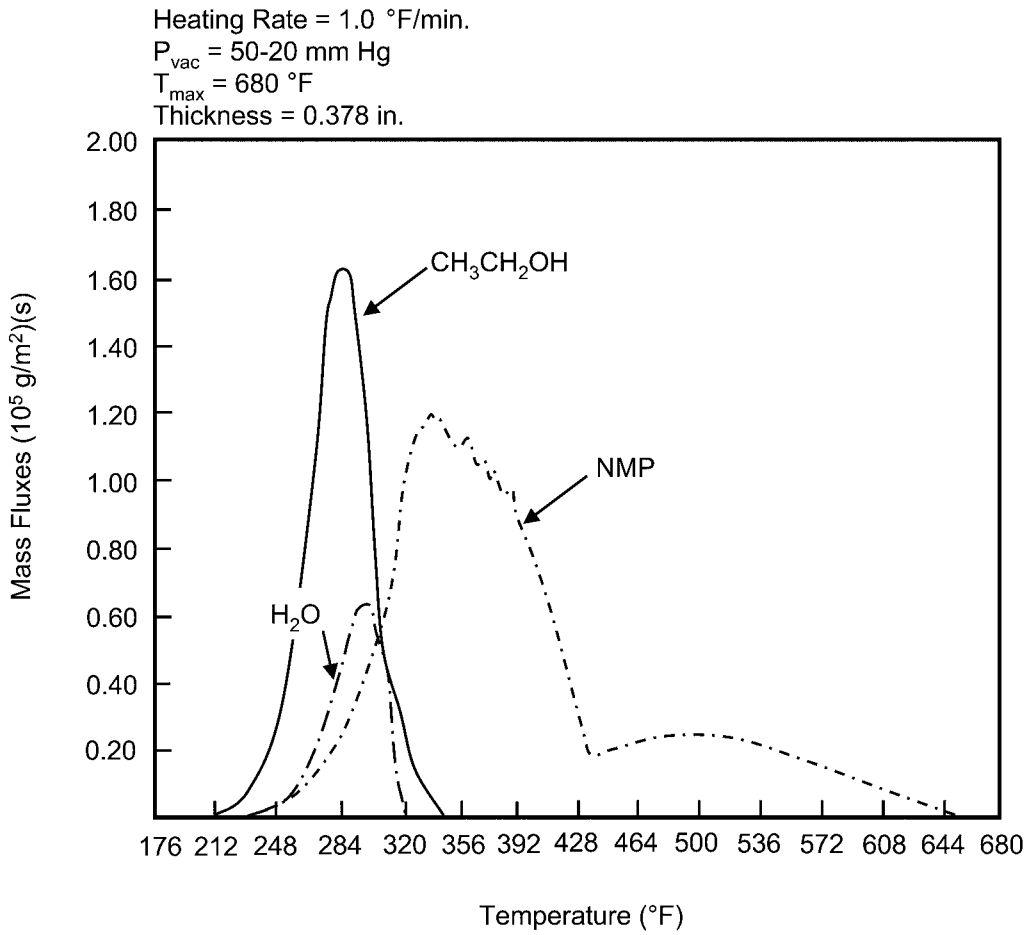


Fig. 7.31 Volatile evolution of K-IIIB prepreg. Source: Ref 5

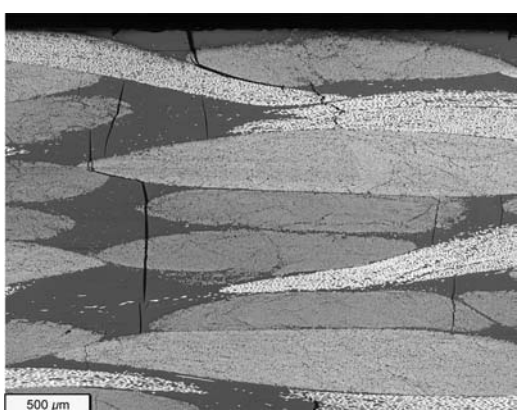


Fig. 7.32 Matrix microcracking

fibers and the resin matrix. Recall that the residual stress on a simple constrained bar is:

$$\sigma = \alpha E \Delta T \qquad \text{(Eq 7.19)}$$

where:
σ = residual stress
α = coefficient of thermal expansion (CTE)
E = modulus of elasticity
ΔT = temperature change

A rather simplified analogy for a composite part is that the CTE difference between the fibers (approximately zero for carbon fiber) and the resin is large (approximately 20 to 35 $\times$ 10^{-6}/°F for thermoset resins). The modulus difference between the fibers (30 to 140 msi) and the resin (0.5 msi) is also large. The temperature difference (ΔT) is the difference from the time when

the resin becomes a solid gel during cure and the use temperature. The so-called stress-free temperature is somewhere between the gel temperature and the final cure temperature as the crosslinking structure develops strength and rigidity. The use temperature for epoxy composites usually ranges anywhere from –67 to 250 °F (–55 to 120 °C).

There are several observations that we can make from this simplified analogy. High-modulus carbon, graphite, and aramid fibers have negative CTEs. Normally, the higher the fiber modulus, the more negative the CTE becomes, which leads to increases in residual stresses and helps to explain why more matrix microcracking is observed with high-modulus graphite fibers than with high-strength carbon fibers. Carbon/epoxy resin systems are usually cured at either 250 or 350 °F (120 or 175 °C). Since ΔT will be smaller for the systems cured at 250 °F (120 °C) (Fig. 7.33), they should experience less microcracking than the systems cured at 350 °F (175 °C). Very-high-temperature polyimides, and many thermoplastics, that are cured or processed at temperatures in the range of 600 to 700 °F (315 to 370 °C) develop very high residual stresses and are susceptible to microcracking. Most thermoplastics are tough enough to resist microcracking; however, the locked-in residual stresses are still high. Since the ΔT differential becomes larger when the use temperature is lowered — for example, when the temperature is –40 to –67 °F (–40 to –55 °C) for a cruising airliner at 30,000 to 40,000 ft (9.1 to 12.2 km) — more microcracking is normally observed after cold exposures than after elevated-temperature exposures. The analogy presented above greatly oversimplifies the residual stress problem in composite structures. In fact, analysis of residual stresses in composites is probably one of the most complex problems analysts have tried to address, and there is quite a bit of conflicting data in the literature on the various causes of residual stresses and the effects of material, lay-up, tooling, and processing variables on residual stresses.

Composites by their very nature are anisotropic materials, and residual stresses result due to differences in ply orientations. For example, as shown in Fig. 7.34, a zero-degree ply expands very little during cure because it has a very low CTE, while a 90-degree ply expands significantly because it is dominated by the thermal expansion of the matrix. Similar types of residual stress are created at all ply interfaces having a different orientation (for example, at +45- and –45-degree ply interfaces). If the laminate is not balanced and symmetric, macrowarpage will certainly occur during cool-down. A balanced laminate is one in which, for every +θ-ply in the lay-up, there is an equivalent –θ-ply in the lay-up. An example of

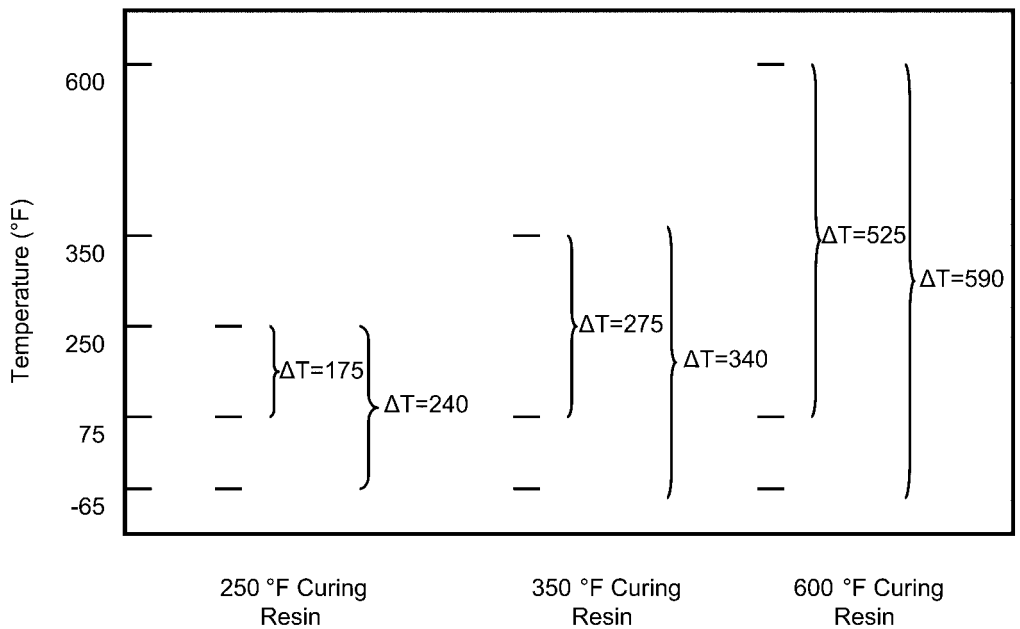


Fig. 7.33 Residual curing stresses increase with increases in cure temperature (°F)

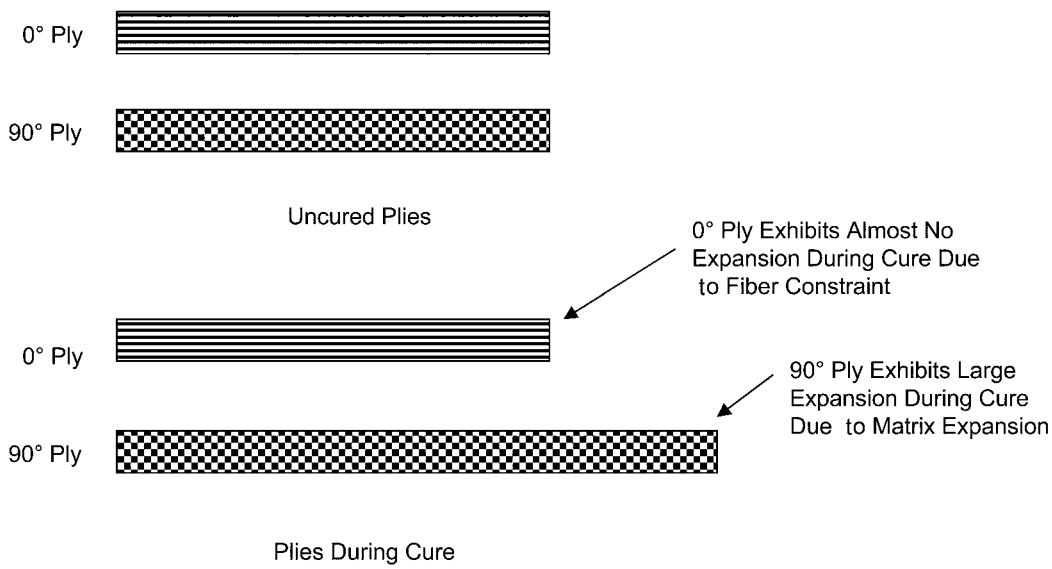


Fig. 7.34 Differential ply expansion during cure. Source: Ref 7

a balanced laminate is 0°, +45°, –45°, 90°, –45°, +45°, 0°, while an unbalanced laminate would be 0°, +45°, –45°, 90°, –45°, +45°, 90°. A symmetric laminate is one that is balanced at its centerline and forms a mirror image on both sides of the centerline. For example, a balanced and symmetric laminate would be 0°, +45°, –45°, –45°, +45°, 0°, while a nonsymmetric laminate would be 0°, +45°, –45°, +45°, –45°, 0°. To complicate the situation even further, small deviations in ply alignment, even a couple of degrees, can produce warpage in thin laminates. While the warpage may not show up in thicker laminates, it still exists as residual stress but is constrained by the thickness of the laminate.

In the simplified analogy presented at the beginning of this section, the concept of ΔT and stress-free temperature was introduced. There is considerable controversy in the literature over whether the gel temperature or the cure temperature should be taken as the stress-free temperature. Actually, a lot depends on the cure cycle employed. For example, it is possible to heat many carbon/epoxy systems to their cure temperatures using fairly aggressive heat-up rates and have the resin not gel until the 350 °F (175 °C) cure temperature is reached. On the other hand, one can use a slow heat-up rate such as 1 to 2 °F/min (0.6 to 1.2 °C) and gel the resin at temperatures as much as 15 to 30 °C (25 to 50 °F) below the final 350 °F (175 °C) cure temperature.

A resin fraction gradient through the thickness of the laminate has been shown to influence the distortion of both flat and complex shaped symmetric parts. Since it is common practice to bleed laminates from the bag side, in a thick laminate the side of the laminate closest to the bag will generally have a lower resin content than the side closest to the tool. The bleeder materials cause the bag side of the laminate to be resin poor, while the center and tool side may have too high a resin content. Fiber volume percentages of 52 and 59 percent have been observed for the bag and tool side, respectively, while the middle had a fiber volume of 57 percent. This produces an asymmetric laminate condition with more shrinkage in the areas with more resin because of the high CTE of the resin and the chemical shrinkage of the resin due to crosslinking. The high resin CTE, together with the chemical shrinkage that occurs during cure, causes the bottom of the laminate to shrink more than the top portion because of the higher resin fraction in the bottom portion, resulting in distortion in a convex-up curvature shape.

In general, the more complex the shape, the more complex the residual stress state becomes. The spring-in that occurs during curing in a simple 90° angled part is shown in Fig. 7.35. This is somewhat analogous to the springback phenomena observed in sheet metal formation, although the causes are totally different. Volumetric shrinkage usually occurs in epoxies

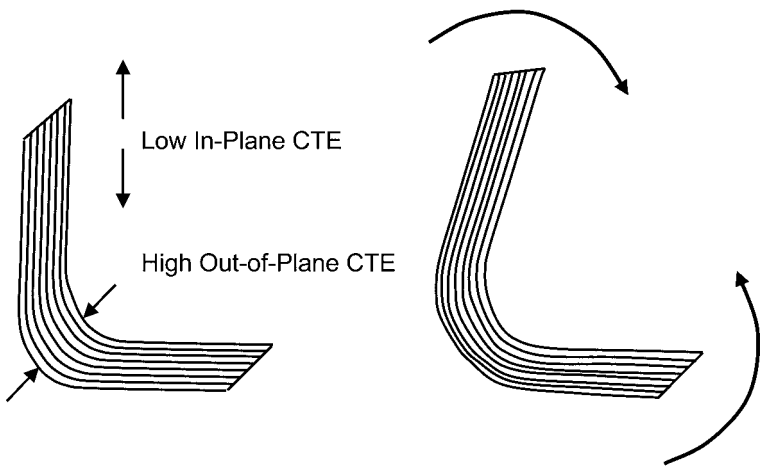


Fig. 7.35 Composite part spring-in

(approximately minus one to four percent) as they cure. While the fiber reinforcement tends to limit this effect in the in-plane direction, shrinkage through the thickness is largely unrestrained. This has little effect on flat symmetric laminates, but it contributes to the spring-in of curved parts. This effect can be illustrated by considering a laminate with a bend that is compressed through its thickness. If the bend angle is constrained during this compression, the inside ply will be stretched while the outside ply is compressed. When the constraint is removed after cure, spring-in results. A further complicating factor is that it is quite common for male corners to thin out at the radius due to pressure intensification, while female corners are often too thick due to lack of pressure (Fig. 7.36). Taking a ply of 0°, 90° woven cloth and draping it over any shape makes it obvious to even the casual observer that the fibers move and adjust to accommodate the shape; the more complex the shape, the more the fibers must move to accommodate it. Tool dimensions must be sized to account for these dimensional changes that occur in both the tool and the part during cure. As was discussed in Chapter 4, "Fabrication Tooling," it is common practice to accommodate spring-in by adjusting the tooling angle outwards by one to three degrees.

Differences in thermal expansion between the tool material and the composite part must also be considered. For example, an aluminum tool that has a very high CTE will require more compensation than a composite tool that has almost the same CTE as the composite part. In addition,

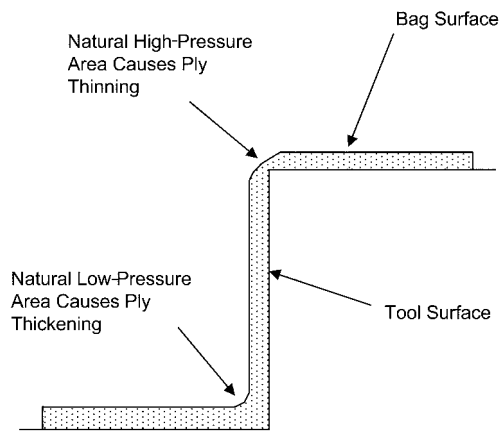


Fig. 7.36 Low- and high-pressure areas during cure

there is the potential for part-tool interaction or mold stretching (Fig. 7.37) due to CTE differences between the tooling and the composite part. It should be noted that while some researchers have found that part-tool interactions are dependent on the type of tooling material, others have failed to find any significant effects. According to part-tool interaction theory, large differences in the CTE of metal tools (such as, aluminum with a CTE of 23.6 με/°C) and carbon/epoxy composite parts with a CTE of approximately zero for a zero-degree ply results in shear stresses in the part surface as the tool heats up. Based on friction between the part and the tool surface, the tool pulls the fibers on the tool surface layer of the composite as it expands. A state

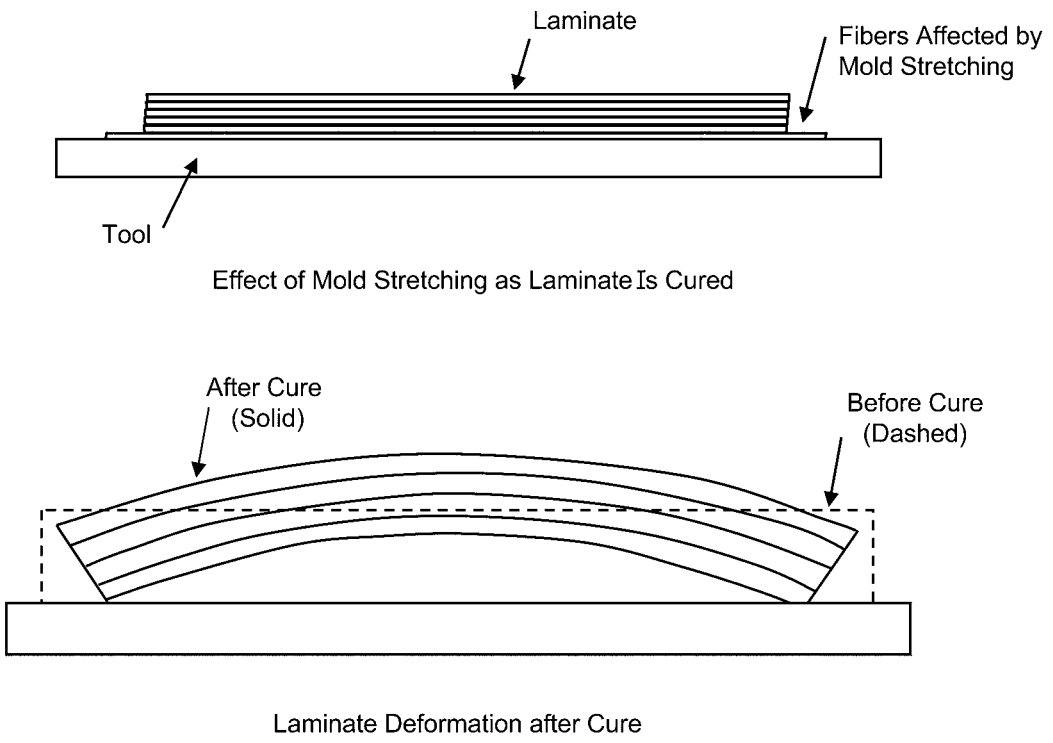


Fig. 7.37 Mold stretching during cure. Source: Ref 8

of residual tensile strain develops in the tool surface plies as the surrounding resin cures at elevated temperature. Upon removal of the autoclave pressure and separation of the part from the tool after cool-down, part curvature results as the tensile strains cause the plies that were adjacent to the tool surface to contract. However, test results have shown that the surface roughness of the tool does not have a strong effect on distortion, while the tooling material does, as shown in Fig. 7.38 for thin and thick laminates cured on aluminum, steel, and glass tooling plates. Note that the thicker laminates displayed less distortion than the thin laminates. However, this does not necessarily mean that the residual stress state was lower for the thick laminates. The fact that they were thicker would help to minimize the visible distortion. In fact, some experimental data suggest that thicker laminates, while not displaying as much distortion, have a greater tendency to microcrack during thermal cycling.

One study that was conducted on the effects of processing temperature and lay-up on T300/976 carbon/epoxy laminates found that spring-in was lower when lower cure temperatures were used and when the degree of cure α was lower. The study proposed a cure cycle in which the part is first cured at a low temperature to develop an α of 0.5 to 0.7 followed by a final elevated-temperature cure. For such a cure cycle, the spring-in was less than when the laminates were cured at a constant elevated temperature. The study also found that the spring-in was somewhat less with a slow cooling rate, although others have found no such effect. Other researchers also found that higher cure temperatures caused the formation of microcracks that were more tortuous and wider than those in laminates cured at lower temperatures. They concluded that larger thermal stresses were generated in laminates cured at higher temperatures and that fracture processes relieved these stresses in the laminates when cycled to cryogenic temperatures (liquid nitrogen), resulting in delaminations, wider microcracks, and higher microcrack densities. A concurrent study found that adding rubber toughening agents to the resin increased the cryogenic microcracking resistance.

While residual stresses in composites are extremely complicated, and while there are considerable conflicting data on the effects of different

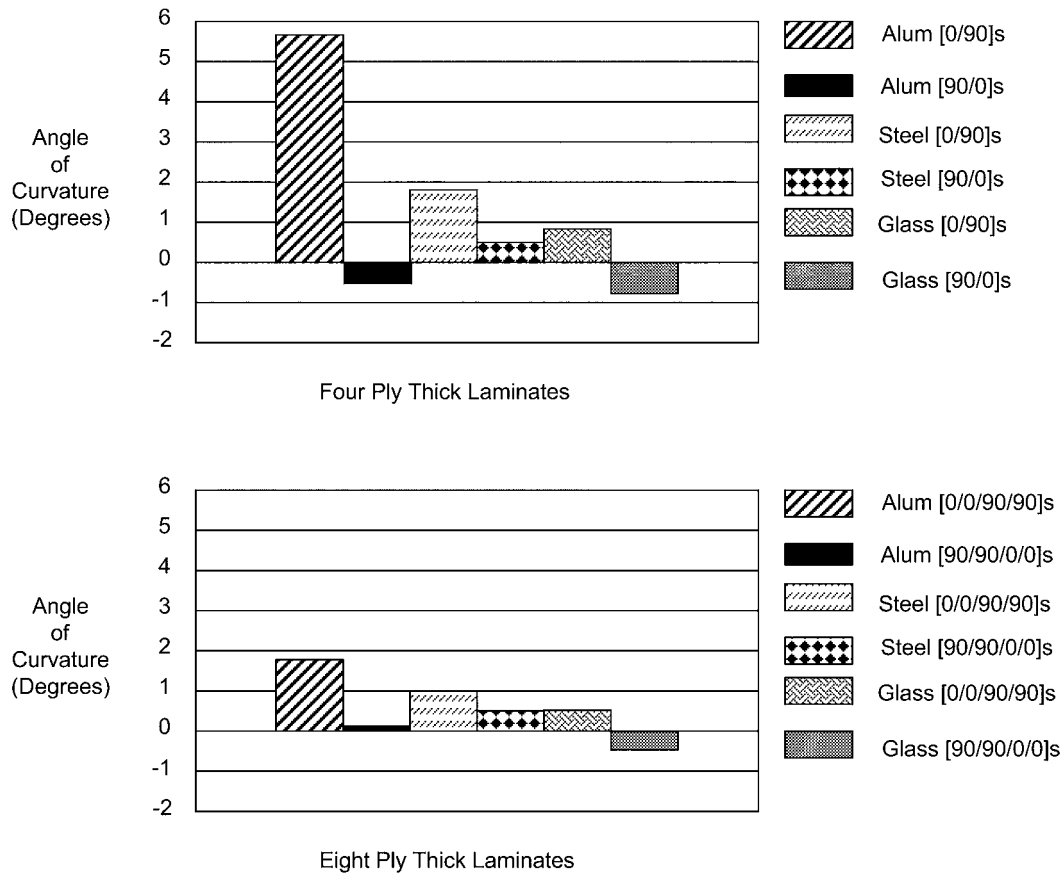


Fig. 7.38 Effects of tool material, orientation, and thickness on laminate distortion. Source: Ref 8

variables, the following guidelines are offered for minimizing their effects:

- Use only balanced and symmetric laminates. Minimize ply lay-up misorientation or distortion whenever possible.
- Design tools with compensation factors to account for thermal growth and angular spring-in. The use of low-CTE tools will probably help to minimize residual stresses when curing carbon fiber composites.
- The use of lower-modulus fibers and tougher resin systems helps to minimize residual stresses and microcracking.
- Slow heat-up rates during cure with intermediate holds and lower curing temperatures are likely to help minimize residual stresses by balancing the rate of chemical resin shrinkage with the rate of thermal expansion. There is also some evidence that slow cool-down rates help to minimize residual stresses.

7.7 Cure Monitoring Techniques

Over the past 35 years, considerable research has been done on in-process curing monitoring. The most thoroughly researched method is dielectrics, in which either a sensor is placed on the laminate or sensors are placed on both surfaces of the laminate. As the resin melts and flows during the initial part of the cure cycle, the molecules fluctuate within the alternating dielectric field and give an indication of the viscosity of the resin. The readings taken by the dielectrometer can then be used to indicate when the resin viscosity starts to rise and full autoclave pressure should be applied. There is also a body of evidence showing that the end of cure can also be detected, so one would know when the cure is complete and when to start cool-down; however, as curing proceeds, molecular activity decreases drastically and the dielectric response becomes weaker. Other methods that have been

researched include acoustic emission, ultrasonics, acousto-ultrasonics, fluorescence techniques, and mechanical impedance analysis. In spite of all of this research, thermocouples, usually attached to the bottom of the tool, remain the industry standard.

In-process cure monitoring is a good tool for resin characterization and cure cycle development, but it has rarely been used in production for two reasons: (1) the incorporation of sensors during lay-up adds to both the collation and bagging costs; and (2) when multiple parts are cured in an autoclave, they may experience different heat-up rates and it becomes difficult to know which part should be the controlling one for pressure application. As stated previously, for addition-curing thermosets, it is usually better to apply the pressure at the start of the cure cycle, thus removing any decision making from the autoclave operator. However, if condensation-curing systems are being used where one needs to delay full pressure application until all the volatiles are removed from the resin, then the use of in-process cure monitoring may be warranted, at least during the early stages of part production.

ACKNOWLEDGMENT

Dr. C.E. Browning, while at the U.S. Air Force Materials Laboratory, initiated the concept of processing science of polymer matrix composites. During the 1980s and 1990s, he funded and championed a number of processing science programs that has greatly expanded our understanding of composite materials.

REFERENCES

1. F.C. Campbell, A.R. Mallow, and J.F. Carpenter, Chemical Composition and Processing of Carbon/Epoxy Composites, *American Society of Composites, Second Technical Conference*, Sept 1987, p 77–96
2. L.J. Lee, Liquid Composite Molding, *Processing of Composites*, Hanser, 1999, p 393–456
3. T. Gutowski et al., Consolidation Experiments for Laminate Composites, *J. Compos. Mater.*, Vol 21, July 1987, p 650–669
4. F.C. Campbell, A.R. Mallow, and C.E. Browning, Porosity in Carbon Fiber Composites: An Overview of Causes, *J. Adv. Mater.*, Vol 26 (No. 4), July 1995, p 18–33
5. J.L. Kardos, Void Growth and Dissolution, *Processing of Composites*, Hanser, 1999, p 182–206
6. R.A Brand, G.G. Brown, and E.L. McKague, "Processing Science of Epoxy Resin Composites," Air Force Contract No. F33615-80-C-5021, Final Report for Aug 1980 to Dec 1983
7. S.W. Tsai, Composites Design—1986, *Think Composites*, 1986, p 15-1–15-21
8. D.A. Darrow and L.V. Smith, Evaluating the Spring-In Phenomena of Polymer Matrix Composites, *33rd International SAMPE Technical Conference*, Nov 2001, p 326–337

SELECTED REFERENCES

- C.E. Browning, F.C. Campbell, and A.R. Mallow, Effect of Precompaction on Carbon/Epoxy Laminate Quality, *AIChE Conference on Emerging Materials*, Aug 1987
- M.T. Cann and D.O. Adams, Effect of Part-Tool Interaction on Cure Distortion of Flat Composite Laminates, *46th International SAMPE Symposium*, May 2001, p 2264–2277
- A.K. Dharia, B.S. Hays, and J.C. Seferis, Evaluation of Microcracking in Aerospace Composites Exposed to Thermal Cycling: Effect of Composite Lay-up, Laminate Thickness and Thermal Ramp Rate, *33rd International SAMPE Technical Conference*, Nov 2001, p 120–128
- J.M. Griffith, F.C. Campbell, and A.R. Mallow, Effect of Tool Design on Autoclave Heat-Up Rates, Society of Manufacturing Engineers, *Composites in Manufacturing 7 Conference and Exposition*, 1987
- J.L. Kardos, The Processing Science of Reactive Polymer Composites, *Advanced Composites Manufacturing*, John Wiley and Sons, Inc., 1997, p 68–77
- R. Karkkainen, M. Madhukar, J. Russell, and K. Nelson, Empirical Modeling of In-Cure Volume Changes of 3501-6 Epoxy, *45th International SAMPE Symposium*, May 2000, p 123–135
- R. Kim, B. Rice, A. Crasto, and J. Russell, Influence of Process Cycle on Residual Stress Development in BMI Composites, *45th International SAMPE Symposium*, May 2000, p 148–155
- M. Nobelen, B.S. Hayes, and J.C. Seferis, Low-Temperature Microcracking of Composites: Effects of Toughness Modifier

Concentration, *33rd International SAMPE Technical Conference,* Nov 2001, p 1619–1628

- H. Sarrazin, B. Kim, S.H. Ahn, and G.E. Springer, Effects of Processing Temperature and Layup on Springback, *J. Compos. Mater.*, Vol 29 (No. 10), 1995, p 1278–1294
- A.M. Sastry, Impregnation and Consolidation Phenomena, *Comprehensive Composite Materials*, Vol 2, *Polymer Matrix Composites*, Elsevier Science Ltd., 2000
- B. Thorfinnson and T.F. Bierrinann, Production of Void Free Composite Parts without Debulking, *31st International SAMPE Symposium and Exposition,* Apr 1986
- B. Thorfinnson and T.F. Bierrinann, Measurement and Control of Prepreg Impregnation for Elimination of Porosity in Composite Parts, *Society of Manufacturing Engineers, Fabricating Composites '88,* Sept 1988
- J.F. Timmerman, B.S. Hayes, and J.C. Seferis, Cryogenic Cycling of Polymeric Composite Materials: Effects of Cure Conditions on Microcracking, *33rd International SAMPE Technical Conference,* Nov 2001, p 1597–1606

Copyright © 2010, ASM International®
All rights reserved.
www.asminternational.org

CHAPTER 8

Adhesive Bonding

ADHESIVE BONDING is a method of joining structures together that eliminates some, or all, of the cost and weight of mechanical fasteners. In adhesive bonding, a polymeric adhesive is used to join two separate pieces—the adherends or substrates. Cured composites or metals are adhesively bonded to other cured composites, honeycomb core, foam core, or metallic pieces. A number of possible adhesive bonding joint configurations are shown in Fig. 8.1. The ability to make large bonded structures can eliminate a significant amount of the assembly costs. In addition to fabricating large bonded components, adhesive bonding is frequently used for repairing damaged structural parts.

Adhesives used for structural bonding are cured at either room or elevated temperatures and must possess adequate strength to transfer the loads through the joint. There are many types of structural adhesives; however, epoxies, bismaleimides, cyanate esters, and polyimides are the most prevalent for composite bonding.

In this chapter, the basics of adhesive bonding will be covered. The *uses* of adhesives in sandwich and integrally cocured structure are covered in Chapter 9, "Sandwich and Integrally Cocured Structure." In addition, some of the design and analysis considerations for adhesively bonded joints are discussed in Chapter 17, "Structural Joints—Bolted and Bonded." Adhesive bonding can also be used to join thermoplastic composites. The specifics of adhesive bonding and other joining methods for thermoplastic composites are covered in Chapter 6, "Thermoplastic Composite Fabrication Processes."

8.1 Theory of Adhesion

Although there are a number of theories on the nature of adhesion during adhesive bonding, there is general agreement about what leads to a good adhesive bond. Surface roughness plays a key role. The rougher the surface, the more surface area is available for the liquid adhesive to penetrate and lock onto. However, for this penetration to be effective, the adhesive must wet the surface, a function of adherend cleanliness, adhesive viscosity, and surface tension. The importance of surface cleanliness cannot be overemphasized; it is one of the cornerstones of successful adhesive bonding.

In metals, coupling effects, as a result of chemical etching/anodizing, or other treatments, can also play a role in adhesion by providing chemical end groups that attach to the metal adherend surface and provide other end groups that are chemically compatible with the adhesive.

Therefore, for the best possible adhesive joint, the following conditions must exist: the surface must be clean, the surface should have maximum area through mechanical roughness, the adhesive must flow and thoroughly wet the surface, and the surface chemistry must be such that there are attractive forces on the adherend surface to bond to the adhesive.

8.2 Surface Preparation

Surface preparation of a material prior to bonding is the basis of the adhesive bond. Extensive field service experience with structural adhesive bonds has repeatedly demonstrated that adhesive durability and longevity depend on the stability and bondability of the adherend surface. The effects of several different surface preparations on aluminum adherends are shown in Fig. 8.2. Phosphoric acid anodize and chromic acid anodize are both considered acceptable surface preparations for

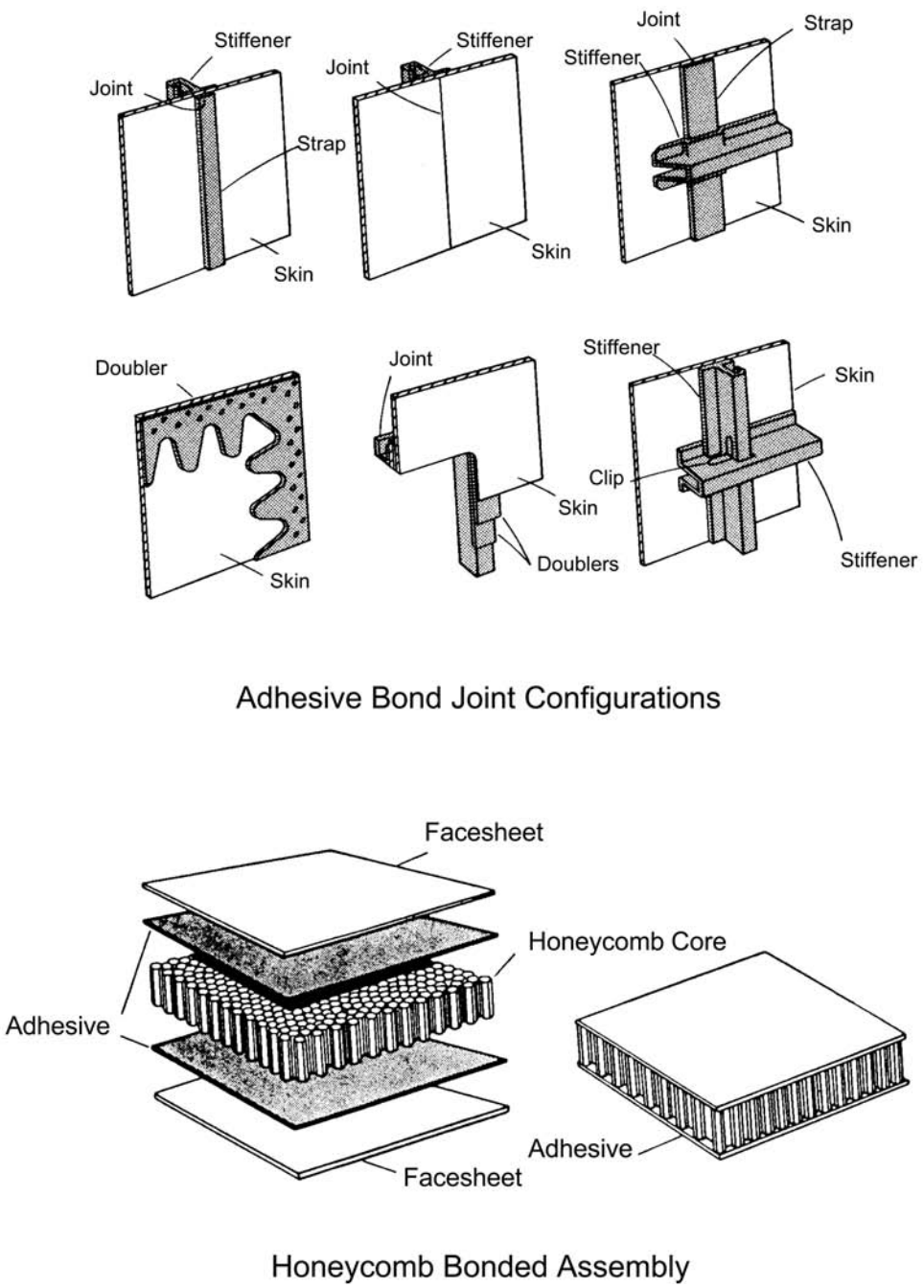


Fig. 8.1 Examples of adhesively bonded joint configurations. Source: Ref 1

aluminum; plain grit blasting and solvent degreasing are not, as they quickly degrade under heat and moisture.

High-performance structural adhesive bonding requires that great care be exercised throughout the bonding process to ensure the quality of the bonded product. Chemical composition control of the adhesive, strict control of surface preparation materials and process parameters, and control of the adhesive lay-up, part fit-up,

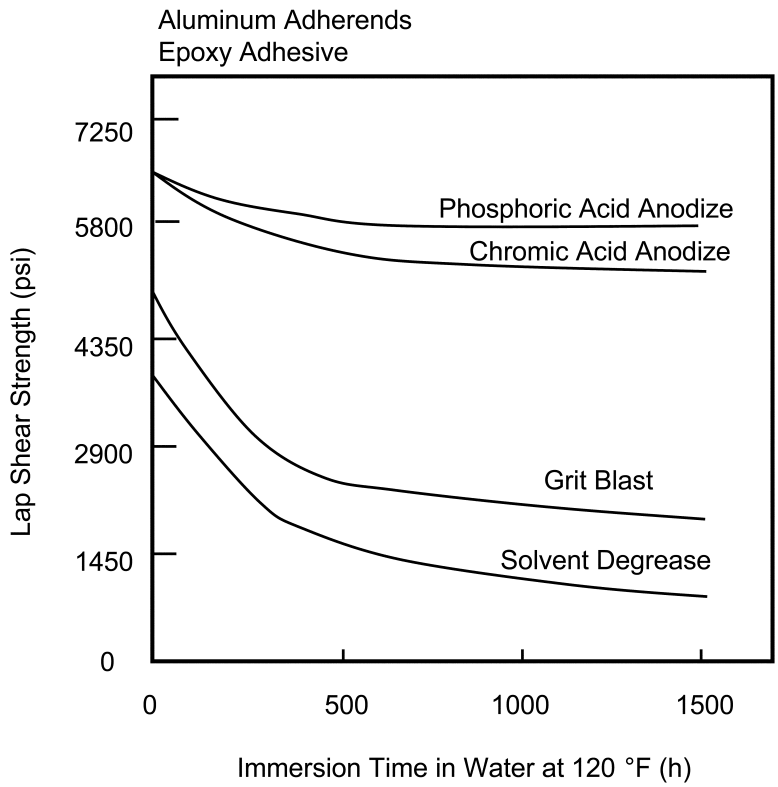


Fig. 8.2 Effect of aluminum surface treatments on bond durability. Source: Ref 2

tooling, and the curing process are all required to produce durable structural assemblies.

8.2.1 Composite Surface Preparation

Moisture absorption of the laminate is the first consideration in preparing a composite part for secondary adhesive bonding. Absorbed laminate moisture can diffuse to the surface of the laminate during elevated-temperature cure cycles, resulting in weak bonds or porosity or voids in the adhesive bondline. In extreme cases, where fast heat-up rates are used, actual delaminations can occur within the composite laminate plies. If honeycomb is used in the structure, moisture can turn to steam, resulting in node bond failures or blown core. The dramatic reduction in the hot-wet strength of adhesively bonded joints caused by as little as 0.25 percent absorbed moisture in composite adherends before bonding is shown in Fig. 8.3. Less than 20 percent of the room-temperature strength was retained.

Relatively thin composite laminates (0.125 in. (3mm) or less in thickness) can be effectively dried in an air circulating oven at 250 °F (120 °C) for four hours minimum. Drying cycles for thicker laminates should be developed empirically using the actual adherend thicknesses. After drying, the surface should be prepared for bonding and then the actual bonding operation conducted as soon as possible. Prebond thermal cycles, such as those using encapsulated film adhesive to check for part fit-up prior to bonding, can also serve as effective drying cycles for thin sections. In addition, storage of dried details in a temperature- and humidity-controlled lay-up room can extend the time between drying and curing.

Numerous surface preparation techniques are currently used prior to the adhesive bonding of composites. The success of any technique depends on establishing comprehensive material, process, and quality control specifications and adhering to them strictly. One method that has gained wide acceptance is the use of a peel ply. In this technique, a closely woven nylon or polyester cloth is used as the outer layer of the composite during lay-up; this ply is torn or peeled away just before bonding or painting. The theory

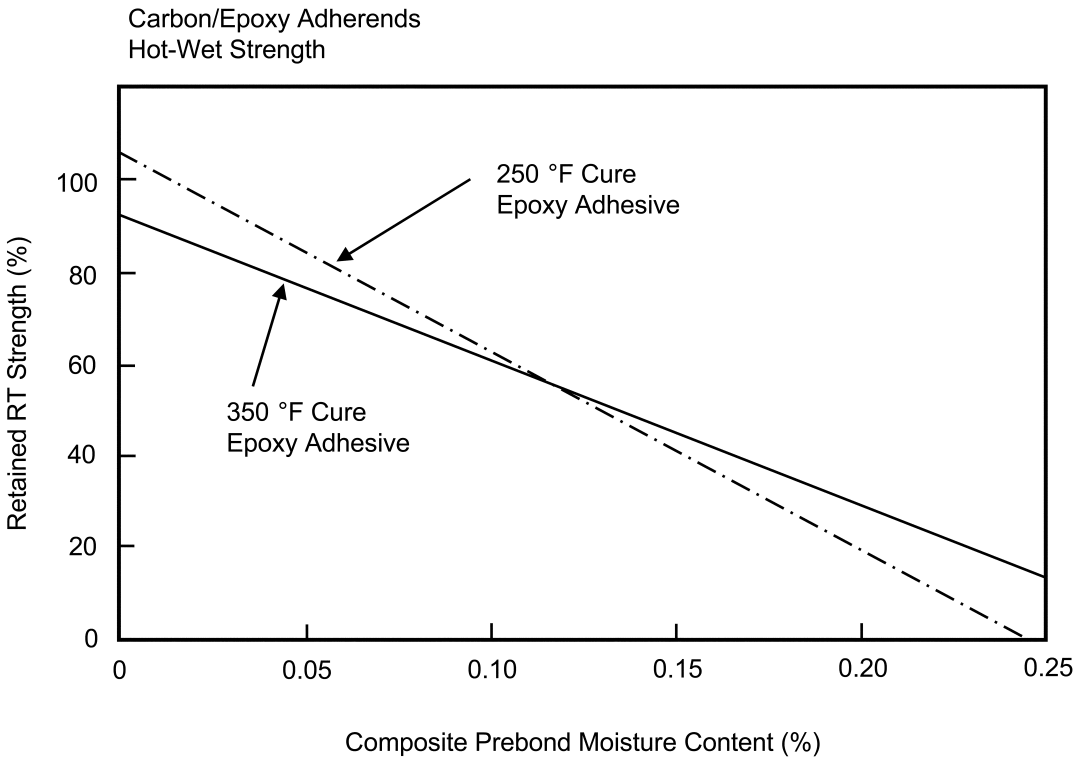


Fig. 8.3 The effect of prebond moisture on bond strength. Source: Ref 3

is that the tearing or peeling process fractures the resin matrix coating and exposes a clean, virgin, roughened surface for the bonding process. The surface roughness attained can, to some extent, be determined by the weave characteristics of the peel ply. Some manufacturers state that this is sufficient, while others maintain that an additional hand sanding or light grit blasting is required to adequately prepare the surface. The abrasion increases the surface area of the surfaces to be bonded and may remove residual contamination, as well as removing fractured resin left behind from the peel ply. However, the abrading operation should be conducted with care to avoid exposing or rupturing the reinforcing fibers near the surface.

The use of peel plies on composite surfaces that will be structurally bonded certainly deserves careful consideration. Factors that need to be considered include the chemical makeup of the peel ply such as, nylon vs. polyester, as well as its compatibility with the composite matrix resin; the surface treatment used on the peel ply because silicone coatings that make the peel ply easier to remove can also leave residues that inhibit structural bonding; and the final surface preparation for example, hand sanding vs. light grit blasting. Overall, peel plies are very effective in preventing gross surface contamination that could occur between laminate fabrication and secondary bonding.

A typical cleaning sequence would be to remove the peel ply and then lightly abrade the surface with a dry grit blast at approximately 20 psi (138 kPa). After grit blasting, any remaining residue on the surface can be removed by dry vacuuming or wiping with a clean dry cheesecloth. Although hand sanding with 120 to 240 grit silicon carbide paper can be substituted for grit blasting, it is not as effective as grit blasting in reaching all of the surface impressions left by the weave of the peel ply. In addition, the potential for removing too much resin and exposing the carbon fibers is higher for hand sanding than it is for grit blasting.

If it is not possible to use a peel ply on a surface requiring adhesive bonding, the surface can be precleaned (prior to surface abrasion) with a solvent such as methyl ethyl ketone to remove any gross organic contaminants. In cases where a peel ply is not used, some type of light abrasion

followed by a dry wipe (or vacuuming) is required to break the glazed finish on the matrix resin surface. The use of solvents to remove residue after hand sanding or grit blasting is discouraged due to the possibility of recontaminating the surface.

All composite surface treatments should have the following principles in common: (1) the surface should be clean prior to abrasion to avoid smearing contamination into the surface; (2) the glaze on the matrix surface should be roughened without damaging the reinforcing fibers or forming subsurface cracks in the resin matrix; (3) all residue should be removed from the abraded surface using a dry process in this case, no solvent; and (4) the prepared surface should be bonded as soon as possible after preparation.

8.2.2 Aluminum Surface Preparation

Although seemingly adequate bond strength can be obtained with simple surface treatments such as, surface abrasion or sanding of aluminum adherends, long-term durable bonds in actual service environments can suffer significantly if the metal adherend has not been processed using the proper chemical surface preparation. The formation of a suitable oxide layer on aluminum adherends is critical for long-term durability. There have been many instances of adhesively bonded aluminum structures failing when placed in service due to improper surface preparation. A successful adhesive bond requires a systematic approach (Fig. 8.4) that includes a suitable oxide on the aluminum surface, a corrosion-resistant primer, and a compatible adhesive layer. The oxide layer must be strong enough to resist stresses, either residual or applied, at the interface between the oxide and the adhesive. In addition, the oxide layer must resist hydration of diffused moisture to protect the aluminum adherends from corrosion. Surface preparation treatments first remove any grease or oil and then remove the existing oxide layer so that it can be replaced with an optimized oxide.

Surface preparation techniques for aluminum adherends consist of either etching or anodizing in acid solutions. These techniques result in microrough adherend morphologies, which have been shown to produce the best bond durability. The three most prevalent commercial processes used for aluminum alloys are chromic/sulfuric acid etch (Forest Products Laboratory, FPL), phosphoric acid anodize (PAA), and chromic acid anodize (CAA).

Forest Products Laboratory etching is a chromic/sulfuric acid etch and is one of the earliest of the modern methods developed for aluminum surface preparation. The FPL oxide morphology (Fig. 8.5) consists of shallow pores and whisker-like protrusions of amorphous Al_2O_3 on top of a thin barrier layer. The microroughness provides a means of mechanical interlocking between the adhesive and the oxide surface that is critical for bond durability.

The PAA process was developed by the Boeing Company in the late 1960s and early 1970s to improve the durability of bonded structures. Bonds formed with PAA-treated adherends exhibit durability during exposure to humid environments that is superior to the durability of bonds formed using the FPL process. In addition, PAA bonds are less sensitive than FPL bonds to process variables, such as rinse water chemistry and time before rinsing. The PAA oxide (Fig. 8.6) has an even greater degree of microroughness than the FPL etch. The oxide consists of a well-developed network of pores on top of a barrier layer. Whiskers

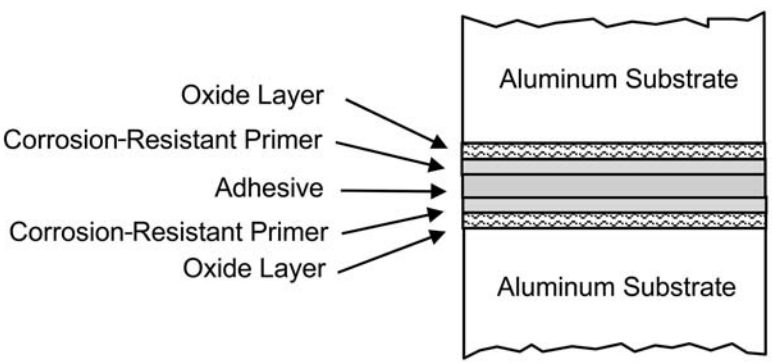


Fig. 8.4 Aluminum adhesive bonded system

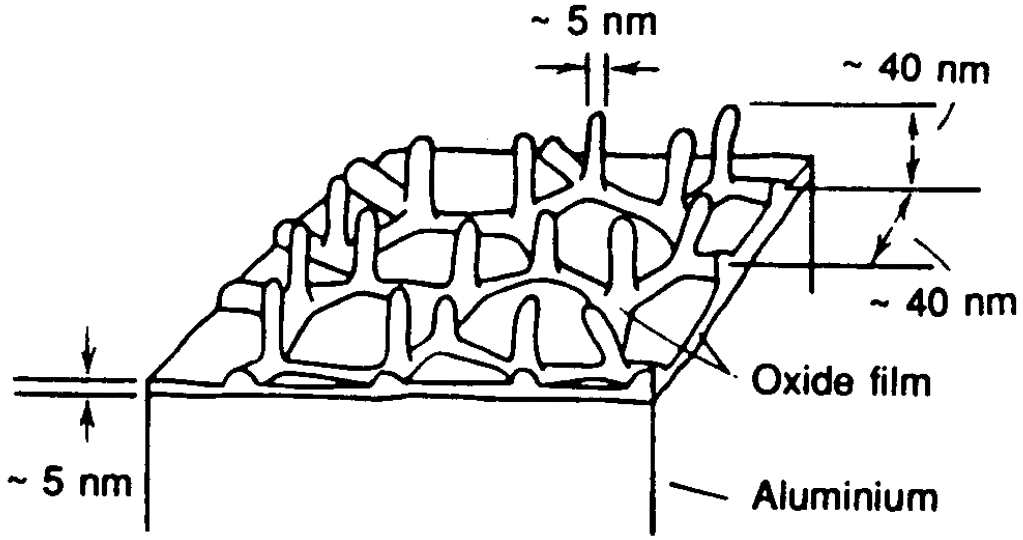


Fig. 8.5 Surface morphology of chromic/sulfuric acid etch (FPL). Source: Ref 4

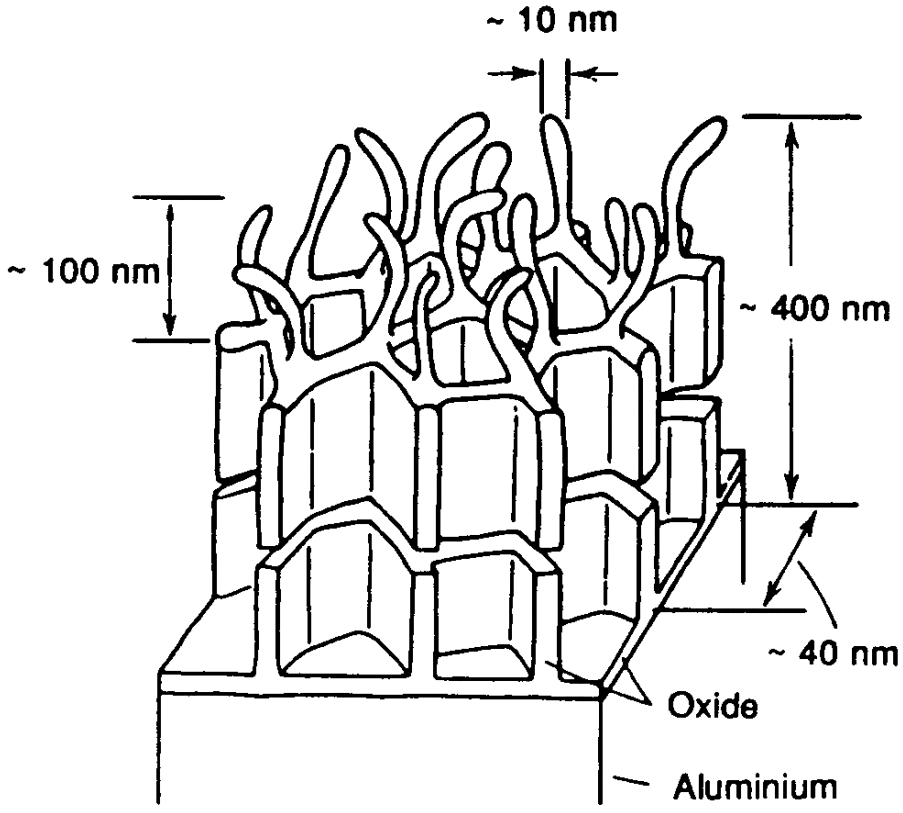


Fig. 8.6 Surface morphology of phosphoric acid anodize (PAA). Source: Ref 4

protrude from the pores away from the alloy adherend. The total oxide thickness is approximately 400 nm. This degree of microroughness can provide more mechanical interlocking than FPL-treated adherends for improved bond strength and durability, but the improvement occurs only if the primer has low enough viscosity to penetrate the oxide. Chemically, the PAA film is amorphous Al_2O_3, with a layer of phosphate incorporated onto the surface.

Although the CAA process is not as popular as the FPL and PAA processes in the United States, it has been extensively developed and is widely used in Europe. In contrast to the PAA process, which is conducted at a constant voltage, the CAA process uses a variable voltage that is gradually increased during processing. The CAA oxide is a dense structure of tall columns (Fig. 8.7). The outer surface can be quite smooth, with fine pores running through most of the oxide layer at the junction of the column walls. The total oxide thickness is 1 to 2 μm, which is much greater than that of the other treatments. The barrier layer at the bottom of the columns is also relatively thick because of the high anodization voltages used. The CAA oxide is also Al_2O_3, the upper portion being amorphous with indications that the lower portion is crystalline. Although it might seem that the denser oxide would have less interlocking potential than the PAA oxide, it has been shown that primers can readily penetrate the pores. Pretreatments prior to conducting the CAA process or varying processing conditions are also used to modify the final surface morphology. One advantage of the CAA process is that the oxide is more robust and not as susceptible to damage.

Nearly all long-term durability failures of aluminum adhesively bonded joints have been initiated by moisture. The wedge-crack propagation test (ASTM D 3672), illustrated in Fig. 8.8, is often used to evaluate surface preparation

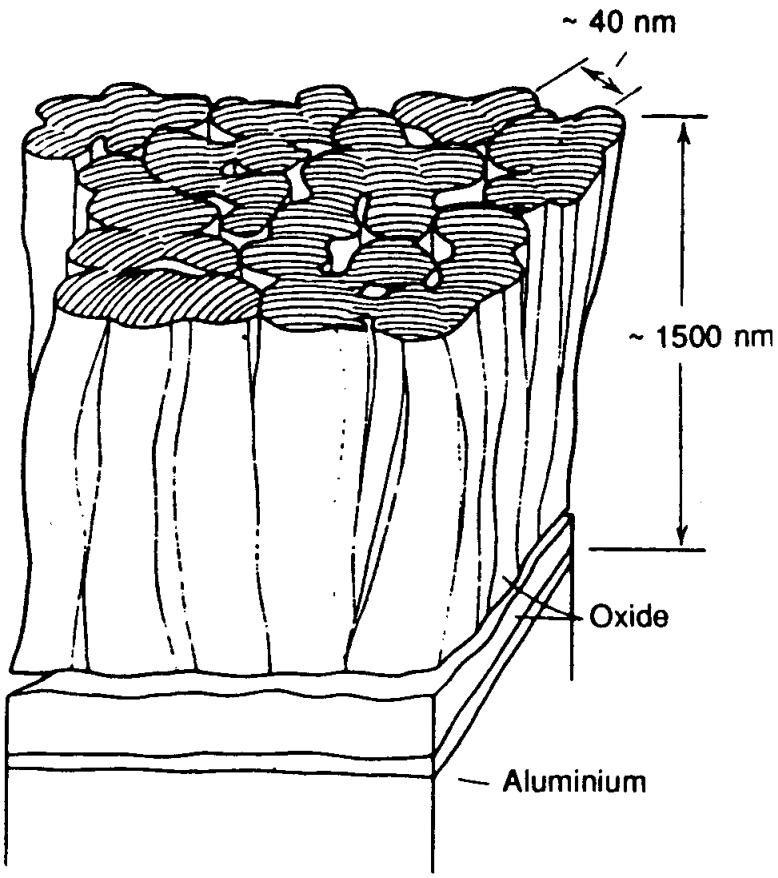


Fig. 8.7 Surface morphology of chromic acid anodize (CAA). Source: Ref 4

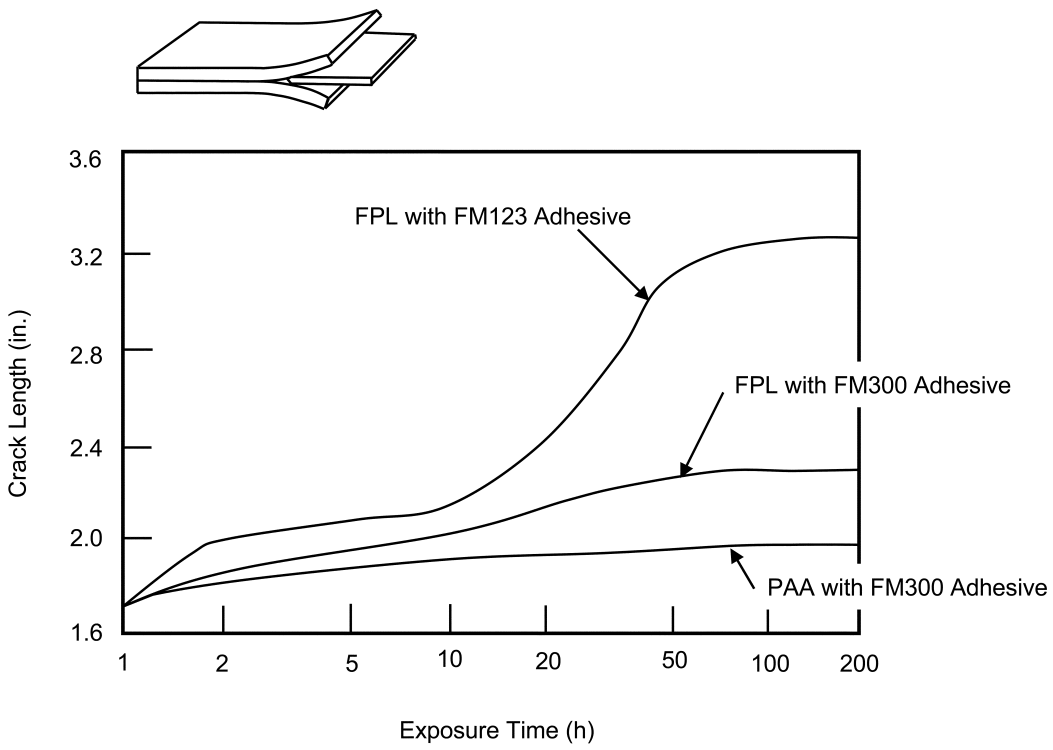


Fig. 8.8 Wedge-crack propagation test results. Source: Ref 1

techniques for long-term durability. A crack is initiated in one end of the test specimen, and its propagation in a wet environment is recorded as a function of time. Failure analysis is then performed to provide insight into the mechanism of crack propagation. Because water is present at the crack tip while it is under stress, the wedge test is more severe than the lap shear test, in which moisture must diffuse into the bondline from the edges of the specimen. When the test specimens are subjected to moisture, the oxide surface adsorbs water from the adhesive and subsequently hydrates. This hydration of the monolayer is believed to be responsible for the bond failure, that is, the disruption of the adhesive-to-oxide bond.

Because crack propagation occurs as a result of hydration, bond durability can be improved by decreasing the rate of water diffusion through the adhesive or along the bondline and/or by increasing the hydration resistance of the oxide. These improvement concepts are shown in Fig. 8.8. The poorest bond durability is the one with the FPL etch with a moisture-wicking adhesive (FM123). When the FPL etch is used with a more moisture-resistant adhesive (FM300), much better bond durability results. The best bond durability is the one with the PAA process used with a corrosion-inhibiting primer (BR127) and the FM300 adhesive. Bonds made with the PAA process exhibit better durability than those with the FPL etch because of the better hydration resistance of the PAA process and the more developed microroughness and interlocking capability of the oxide and adhesive. The CAA oxides, which are somewhat equivalent to the PAA oxides, protect the aluminum surface as a result of their greater thickness.

While it is permissible to bond composite adherends to aluminum honeycomb core, composite adherends should never be bonded to solid aluminum adherends. The coefficients of thermal expansion are so different that if the bond does not fail on cool-down from the cure temperature, it will contain high residual stresses that invariably will cause it to fail when the joint is exposed to low temperatures in service.

8.2.3 Titanium Surface Preparation

Several methods are also used with titanium. Any method developed for titanium surface prep-

aration should undergo a thorough test program prior to production implementation and must be monitored closely during production usage. A typical process used in the aerospace industry involves:

- Solvent wiping to remove all grease and oils
- Liquid honing at 40 to 50 psi (276 to 345 kPa) pressure
- Alkaline cleaning in an air-agitated solution maintained at 200 to 212 °F (90 to 100 °C) for 20 to 30 minutes
- Thorough rinsing in tap water for three to four minutes
- Etching for 15 to 20 minutes in a nitric/hydrofluoric acid solution maintained at a temperature below 100 °F (40 °C)
- Thorough rinsing in tap water for three to four minutes followed by rinsing in deionized water for two to four minutes
- Inspecting for a water break–free surface
- Oven drying at 100 to 170 °F (40 to 80 °C) for 30 minutes minimum
- Adhesive bonding or applying primer within eight hours of cleaning

The combination of liquid honing, alkaline cleaning, and acid etching results in a complex chemically activated surface topography, increasing the surface area that the adhesive can penetrate and adhere to. The adhesive bond strength is a result of both mechanical interlocking and chemical bonding. Other methods, such as dry chromic acid anodizing, are also used.

Because metallic cleaning is such a critical step, dedicated processing lines are normally constructed and chemical controls, as well as periodic lap shear cleaning control specimens, are employed to ensure in-process control. Automated overhead conveyances are used to transport the parts from tank to tank in computer-controlled cycles to ensure the proper processing time in each tank.

8.2.4 Aluminum and Titanium Primers

Due to the rapid formation of surface oxides on both titanium and aluminum, the surfaces should be bonded within eight hours of cleaning or primed with a thin protective coat 0.0001 to 0.0005 in. (2.5 to 13 μm) of epoxy primer. Primer thickness is important. In practice, thinner coatings within this range give better long-term durability than thicker coatings. Color chips are often used in production to determine primer thickness. For parts that will function in a severe service environment, priming is always recommended, because today's primers contain corrosion-inhibiting compounds (strontium chromates) that enhance long-term durability (Fig. 8.9). The two critical variables in corrosion of metal bonds are the

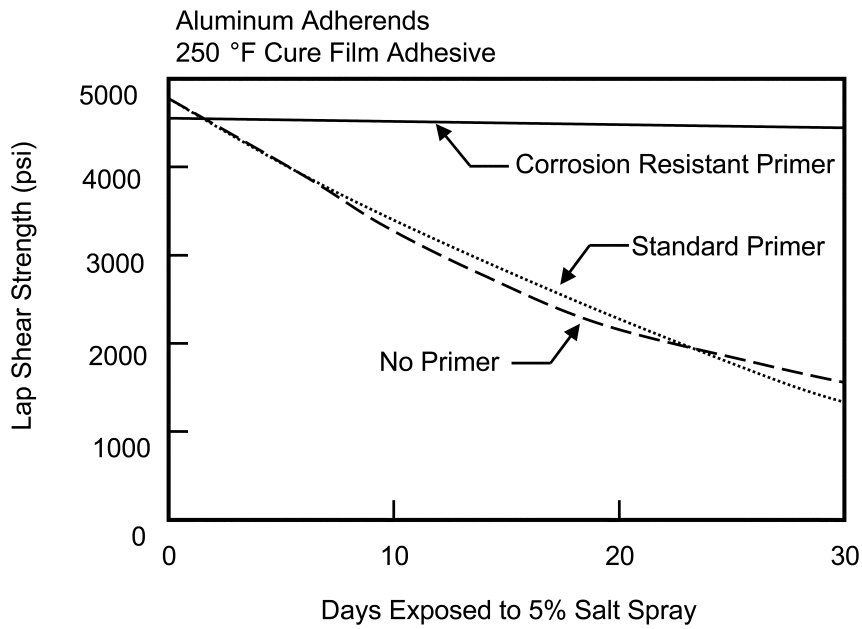


Fig. 8.9 Effect of primers on bond durability. Source: Ref 5

metal surface preparation treatment and the chemistry of the primer. Some primers contain phenolics, which have been found to produce outstanding bond durability. Once the primer has been cured, for instance, at 250 ºF (120 ºC), the parts may be stored in an environmentally controlled clean room for long periods of time, for example, up to 50 days or longer would not be unusual.

All cleaned and primed parts should be carefully protected during handling or storage to prevent surface contamination. Normally, clean white cotton gloves are used during handling, and wax-free kraft paper may be used for wrapping and longer storage. Gloves, which are used to handle cleaned and/or primed adherends, should be tested to ensure that they do not contain silicones or hydrocarbons, which can contaminate the bondline, or sulfur, which can inhibit the cure of the adhesive.

Materials containing silicone should be avoided during all stages of adhesive bonding. Silicone contamination can result in weak kissing bonds that have no strength. In addition, once a part is contaminated with silicone, it is very difficult, if not impossible, to remove it. Wiping with solvent just smears it around the surface. Potential sources of silicone include peel plies (it makes them easier to remove), mold release agents, adhesives on pressure-sensitive tapes, coatings on rubber gloves, and silicone rubber sheet stock used as pressure pads during bonding. All materials that can potentially enter a bond room area should be chemically checked for the presence of silicones.

8.3 Epoxy Adhesives

The selection of an adhesive is often determined by the maximum service temperature. For example, a high-temperature structure fabricated from carbon/bismaleimide will normally warrant the use of a compatible bismaleimide adhesive. Film adhesives for epoxy, bismaleimide, cyanate ester, and polyimide structures are available.

Epoxy-based adhesives are by far the most commonly used materials for bonding or repair of aircraft structures. Epoxy adhesives create high-strength bonds and provide long-term durability in a wide range of temperatures and environments. The ease with which formulations can be modified allows the epoxy adhesive fabricator to employ various materials to control specific performance properties, such as density, toughness, flow, mix ratio, pot life/shelf life, shop handling characteristics, cure time/temperature, and service temperature.

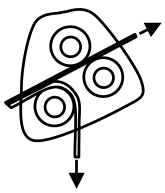
Advantages of epoxy adhesives include excellent adhesion, high strength, low or no volatiles during cure, low shrinkage, and good chemical resistance. Disadvantages include relatively high cost, brittleness unless modified, moisture absorption that adversely affects properties, and relatively long cure times. A wide range of one- and two-part epoxy systems are available. Some systems cure at room temperature, while others require elevated temperatures.

Epoxy resins used as adhesives are generally supplied as liquids or low-melting-temperature solids. The rate of the reaction can be adjusted by adding accelerators to the formulation or by increasing the cure temperature. To improve structural properties, particularly at elevated temperatures, it is common to use cure temperatures close to (or preferably above) the maximum use temperature. Epoxy resin systems are usually modified by a wide range of additives that control particular properties, including accelerators, viscosity modifiers and other flow control additives, fillers and pigments, flexibilizers, and toughening agents. Epoxy-based adhesives are available in two basic cure chemistries: room-temperature and elevated-temperature cure.

The properties of two toughened and two untoughened epoxy film adhesives are shown in Table 8.1. Toughened epoxy adhesive one is cured at 250 °F (120 °C) and has a recommended maximum usage temperature of 180 °F (80 °C). It has a combination of a high single lap shear strength of 6000 psi (41.4 MPa) and peel strength of 70 pli when tested at room temperature. Toughened epoxy adhesive two has a higher usage temperature of 300 °F (150 °C) that results in a somewhat lower single lap shear strength of 5080 psi (35 MPa) and peel strength of 29 pli. The lower strength and lower peel resistance are the results of a trade-off that is made to obtain a higher usage temperature. The two untoughened epoxy adhesives have even lower lap shear strengths of 4200 and 4100 psi (29 and 28.3 MPa) and, since they are not toughened, dramatically lower peel strengths of 3 and 8 pli. Toughening of epoxy adhesives is often accomplished by the addition of liquid rubber compounds (for example, approximately 15 percent of carboxyl terminated butadiene rubber) that precipitate during cure, as was discussed in Chapter 3, "Matrix Resin Systems." The rubber toughener increases the strength and peel resistance but also lowers

Table 8.1 Properties of several epoxy film adhesives

Adhesive type	Toughened epoxy 1	Toughened epoxy 2	Untoughened epoxy 1	Untoughened epoxy 2
Cure temperature (°F)	250	350	350	350
Glass transition temperature (°F)	203	296	345	352
Maximum usage temperature (°F)	180	300	350	420
RT single lap shear (psi)	6000	5080	4200	4100
Metal-to-metal peel (pli)(a)	70	29	3	8
Single lap shear @ service temperature (°F)	4340 @180 °F	2900 @300 °F	3100 @350 °F	1850 @420 °F



(a) Metal-to-metal peel can be measured by the rolling ball method. Results are reported as pounds per linear inch (pli).

the maximum usage temperature, as illustrated by the lower glass transition temperatures for the two toughened epoxy adhesives shown in Table 8.1. The results of thick adherend testing of a number of epoxy film adhesives are given in Fig. 8.10. In this series of tests, three different environmental conditions were evaluated: room temperature dry (RTD), elevated temperature dry (ETD) at 180 °F (80 °C), and elevated temperature wet (ETW) at 180 °F (80 °C) after conditioning at 145 °F (65 °C) and 85 percent relative humidity for 1000 hours (approximately 42 days). Both the strength and the modulus decrease at elevated temperatures, especially when they have been exposed to moisture.

Bismaleimide and polyimide adhesives have even higher service temperatures but are generally not as strong or tough as the lower-temperature epoxy adhesives. However, there are some formulations of both bismaleimide and cyanate ester adhesives that are toughened with thermoplastic additions with only a moderate reduction in upper usage temperature.

The data shown in Table 8.1 are for short-term elevated-temperature exposures. Untoughened adhesive two still has a single lap shear strength of 2900 psi (20 MPa) at 420 °F (220 °C). However, these data are for an extremely short exposure at elevated temperature, and no moisture conditioning was performed. Since moisture lowers the glass transition temperature T_g of adhesives in the same manner as it does for the resin matrices, it is extremely important to test adhesives under the same environmental conditions that the actual structure will experience in service. In fact, the reported dry glass transition temperature of untoughened adhesive 2 of 352 °F (180 °C) is lower than the recommended maximum usage temperature of 420 °F (220 °C). Unless the time at temperature is extremely short, it is never sound practice to use an adhesive or matrix resin system at a temperature that is higher than its T_g.

8.3.1 Two-Part Room-Temperature Curing Epoxy Liquid and Paste Adhesives

Epoxy-based adhesives are most commonly used when a room-temperature cure is desired. They are available as clear liquids or as filled pastes, with a consistency ranging from low-viscosity liquids to heavy-duty putties. Typical cure times at room temperature are five to seven days; however, in most cases, 70 to 75 percent of the ultimate cure can be achieved within 24 h and, if needed, the pressure can usually be released at that point. Under normal bondline thickness conditions at 0.005 to 0.010 in. (0.1 to 0.3 mm), cure can be accelerated with heat without fear of exotherm. A typical elevated temperature cure is one hour at 180 °F (80 °C).

A comparison between two room-temperature-curing epoxy adhesives is shown in Table 8.2. One of these is a low-viscosity resin and the other is a filled thixotropic paste. Both of these are the same resin and curing agent, the only difference being that the paste contains a filler to increase the viscosity. The properties of both are

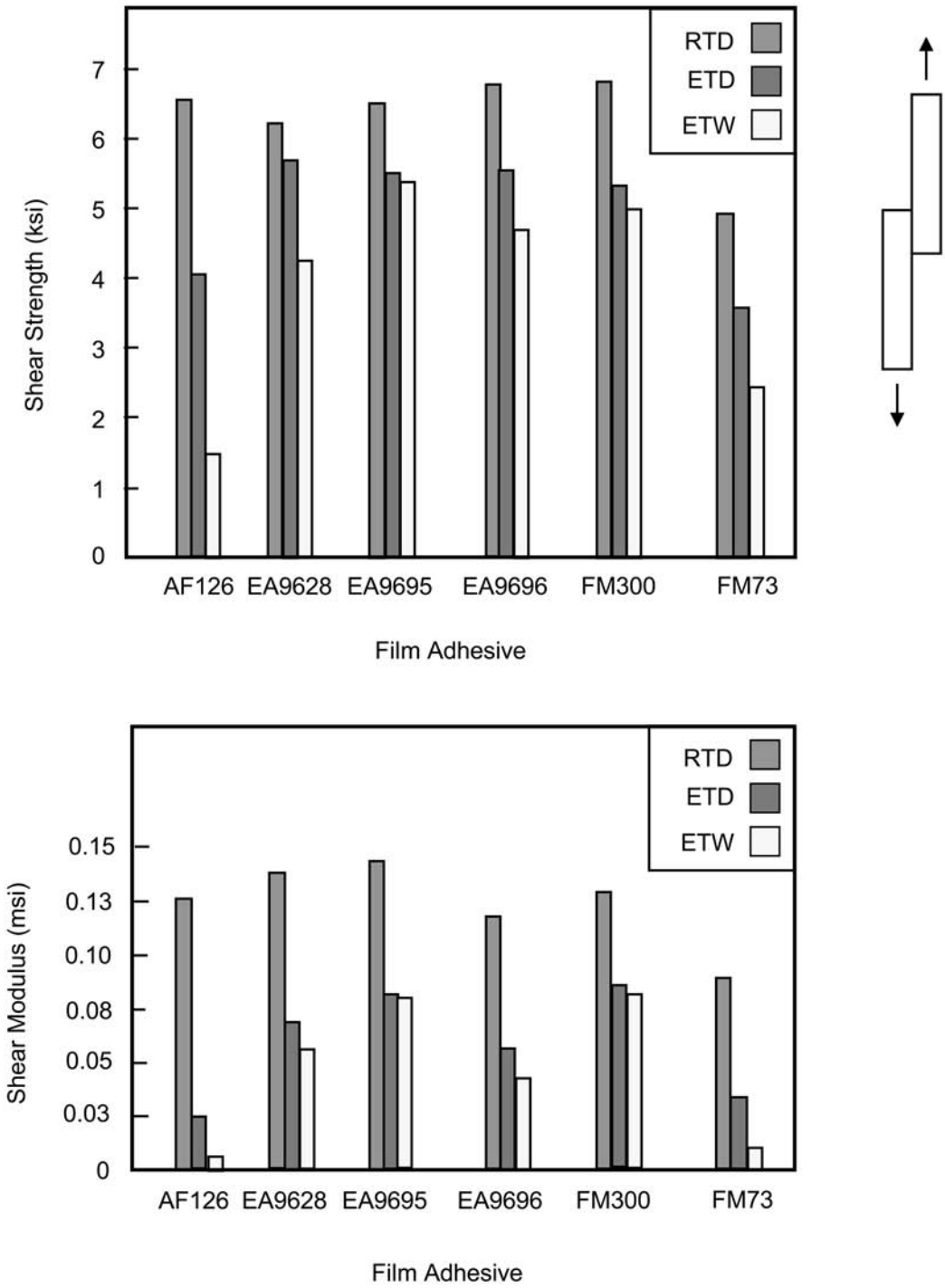


Fig. 8.10 Thick adherend properties of several epoxy adhesives. RTD, room temperature dry; ETD, elevated temperature dry; ETW, elevated temperature wet. Source: Ref 6

Table 8.2 Comparison of low-viscosity and paste epoxy adhesives

Property	Low-viscosity adhesive	Filled paste adhesive
Single lap shear strength (psi)		
−55 °F	3300	3300
77 °F	3500	4200
180 °F	3200	2900
300 °F	1800	1600
350 °F	1250	1200
400 °F	…	600

Note: Epoxy adhesives; 2024-T3 Al adherends.

similar at all test temperatures. Even though these adhesives were cured at room temperature, they have fairly respectable strengths up to around 300 to 350 °F (150 to 180 °C), at least in the dry condition. Since these adhesives cure at room temperature, they generally contain some type of aliphatic curing agent that generates exothermic heat to cure the resin.

Two-part systems require mixing Part A (the resin and filler portion) with Part B (the curing agent portion) in a predetermined stoichiometric ratio. Two-part epoxy adhesives usually require mixing in precise proportions to avoid a significant loss of cured properties and environmental stability. The amount of material to be mixed should be limited to that needed to accomplish the task. In general, the larger the mass, the shorter the pot, or working, life of the material. *Pot life* is defined as the period between the time of mixing the resin and curing agent and the time at which the viscosity has increased to the point where the adhesive can no longer be successfully applied as an adhesive. Attempting to use an adhesive beyond the time of its pot life may result in such a high viscosity that the adhesive does not flow enough to wet the surface properly, resulting in bonds of lower than desired strength.

Two-part resin systems are frequently used to repair damaged aircraft assemblies. Low-viscosity versions can be used to impregnate dry carbon cloth for repair patches or injected into cracked bondlines or delaminations. Thicker pastes are used to bond repairs where more flow control is required. For example, if the material has too low a viscosity and is cured under high pressure, the potential for bondline starvation exists due to excessive flow and squeeze-out. Viscosity control of two-part adhesives is usually done with metallic and/or nonmetallic fillers. Fumed silica is frequently added to provide slump and flow control.

Many adhesives are of the same resin and curing chemistry family. However, different versions are manufactured (nonfilled, metallic or nonmetallic filled, thixotroped, low density, and toughened) for specific performance requirements. For example, a nonmetallic-filled adhesive may be preferred over a metallic-filled adhesive if there is concern about possible galvanic corrosion in the joint. In thin structures where bending or flexing is a concern, a toughened adhesive is usually warranted. In addition to bonding and repair applications, two-part epoxy paste adhesives are used for liquid shim applications during mechanical assembly operations. The ability to tailor flow, cure time, and compressive strength has made these materials ideal for use in areas of poor fit-up.

8.3.2 Epoxy Film Adhesives

Structural adhesives for aerospace applications are generally supplied as thin films supported on a release paper and stored under refrigerated conditions, such as, 0 °F (20 °C). Film adhesives are preferred to liquids and pastes because of their uniformity and reduced void content. In addition, since film adhesives contain latent curing agents that require elevated temperatures to cure, the adhesives are stable at room temperature for as long as 20 to 30 days. Film adhesives are available using high-temperature aromatic amine or catalytic curing agents, with a wide range of flexibilizing and toughening agents. Rubber-toughened epoxy film adhesives are widely used in the aircraft industry. The upper temperature limit of 250 to 350 °F (120 to 180 °C) is usually dictated by the degree of toughening required and by the overall choice of resins and curing agents. In general, toughening an adhesive results in a lower usable service temperature. A comparison of the single lap shear strength of a toughened and an untoughened epoxy film adhesive at different temperatures is shown in Fig. 8.11. It is usually desirable to use the toughest adhesive that will meet the operating temperature requirements, because high-strain adhesives are much more forgiving than unmodified systems. While the two may have similar lap shear strengths, the toughened systems offer a great advantage in joints that may experience some peel.

Film materials are frequently supported by fibers (scrim cloth) that serve to improve handling of the films prior to cure, control adhesive flow during bonding, assist in bondline thickness control, and provide galvanic insulation. Fibers can be incorporated as short fiber mats with random orientation or as a woven cloth. Commonly used

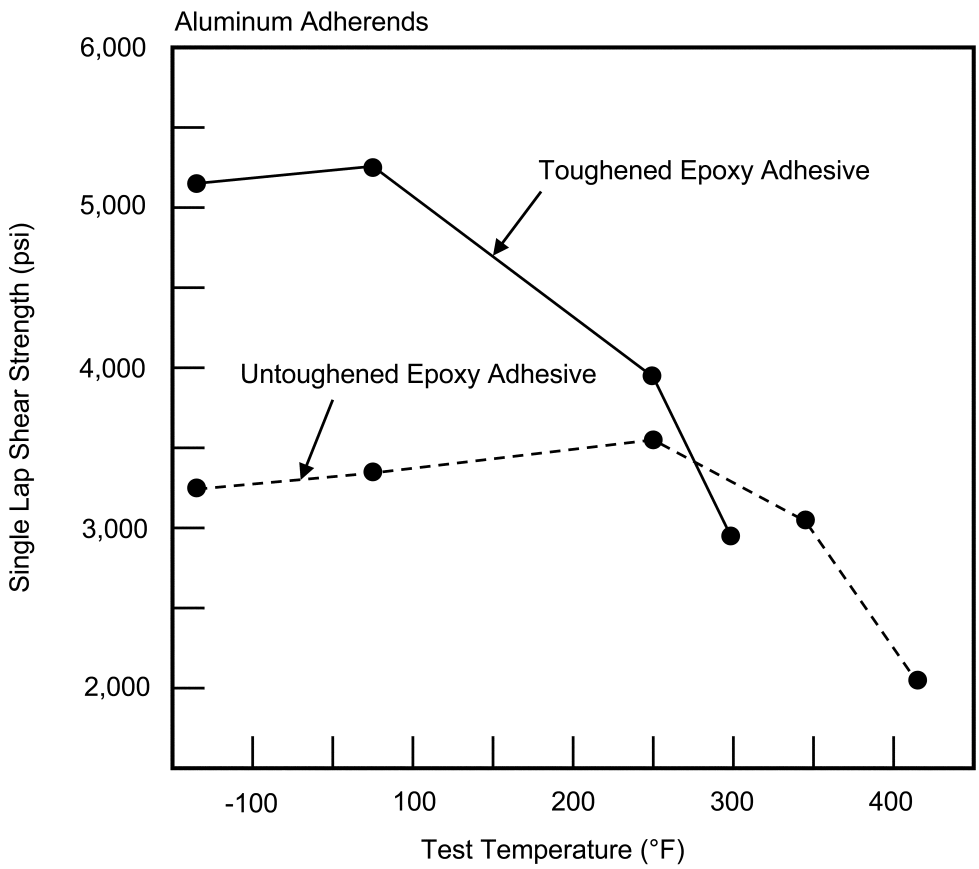


Fig. 8.11 Temperature resistance of two epoxy film adhesives

fibers are polyesters, polyamides (nylon), and glass. Adhesives containing woven cloth may have slightly degraded environmental properties because of wicking of water by the fiber. Random-mat scrim cloth is not as efficient for controlling film thickness as woven cloth, because the unrestricted fibers move during bonding. Spun-bonded nonwoven scrims do not move and are therefore widely used.

The effects of adhesive film weight on the properties of a typical toughened epoxy film adhesive system are shown in Table 8.3. Note that the single lap shear strengths of these materials are quite a bit higher than those of the two-part liquid adhesives shown in Table 8.2. The reason for showing the different film weights relates to honeycomb bonded assemblies. While the metal-to-metal lap shear properties are similar for the different film weights, notice that for honeycomb-bonded assemblies, both the climbing drum peel and flatwise tension strengths are higher for the higher-film-weight materials. Climbing drum peel is a test in which an aluminum facesheet is peeled off a honeycomb core and is measured in torque (in.-lb), usually in 3 in. (7.5 cm) widths. In flatwise tension testing, the facesheet is pulled off a core section in pure tension. The higher-film-weight materials produce more filleting of the honeycomb core and thus higher strengths.

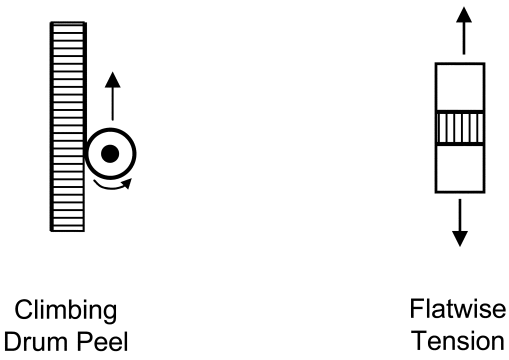
8.4 Bonding Procedures

Some general guidelines for adhesive bonding are summarized in Table 8.4. The basic steps in the adhesive bonding process are:

- Collection of all the parts in the bonded assembly, which are then stored as a kit
- Verification of the fit to bondline tolerances
- Cleaning the parts to promote good adhesion
- Application of the adhesive
- Mating of the parts and adhesive to form the assembly

Table 8.3 Effect of adhesive film weight on properties

Property	Adhesive film weight			
	0.10 psf	0.08 psf	0.05 psf	0.03 psf
Single lap shear strength (psi)				
–67 °F	4300	4500	4300	4000
75 °F	5400	5900	4900	4300
180 °F	5200	5300	5100	4800
250 °F	3800	3700	3800	3600
Honeycomb climbing drum peel (in.-lb/3 in.)(a)				
–67 °F	36	34	15	15
75 °F	50	45	20	17
250 °F	50	45	20	16
Flatwise tension strength (psi)(b)				
–67 °F	1200	1100	950	610
75 °F	1200	1100	900	600
180 °F	1000	950	750	500
250 °F	700	690	500	450



Note: Modified epoxy adhesive; 2024-T3 Al adherends; aluminum honeycomb core. (a) Climbing drum peel test peels skin off the honeycomb core. (b) Flatwise tension test pulls honeycomb core off skin in tension.

Table 8.4 General considerations for adhesive bonding

- When received, the adhesive should be tested for compliance with the material specification. This may include both physical and chemical tests.
- The adhesive should be stored at the recommended temperature.
- Cold adhesive should always be warmed to room temperature in a sealed container.
- Liquid mixes should be degassed, if possible, to remove entrained air.
- Adhesives which evolve volatiles during cure should be avoided.
- The humidity in the lay-up area should be below 40% relative humidity for most formulations. Lay-up room humidity can be absorbed by the adhesive and is released later during heat cure as steam, yielding porous bondlines and possibly interfering with the cure chemistry.
- Surface preparation is absolutely critical and should be conducted carefully.
- The recommended pressure and the proper alignment fixtures should be used. The bonding pressure should be great enough to ensure that the adherends are in intimate contact with each other during cure.
- The use of a vacuum as the method of applying pressure should be avoided whenever possible, since an active vacuum on the adhesive during cure can lead to porosity or voids in the cured bondline.
- Heat curing systems are almost always preferred, because they yield bonds that have a better combination of strength, and resistance to heat and humidity.
- When curing for a second time, such as during repairs, the temperature should be at least 50 °F below the earlier cure temperature. If this is not possible, then a proper and accurate bond form must be used to maintain all parts in proper alignment and under pressure during the second cure cycle.
- Traveler coupons should always be made for testing. These are test coupons that duplicate the adherends to be bonded in material and joint design. The coupon surfaces are prepared by the same method and at the same time as the basic bond. Coupons are also bonded together at the same time with the same adhesive lot used in the basic joint and subjected to the same curing process simultaneously with the basic bond. Ideally, traveler coupons are cut from the basic part, on which extensions have been provided.
- The exposed edges of the bond joint should be protected with an appropriate sealer, such as an elastomeric sealant or paint.

Source: Ref 7

- Application of force concurrent with application of heat to the adhesive to promote cure, if required
- Inspection of the bonded assembly

8.4.1 Prekitting of Adherends

Many adhesives have a limited working life at room temperature, and adherends, especially metals, can become contaminated by exposure to the environment. Thus, it is normal practice to kit the adherends so that application of the adhesive and buildup of the bonded assemblies can proceed without interruption. The kitting sequence is determined by the product and the production rate. Prefitting of the details is also useful in determining locations of potential mismatch such as high and low spots. A prefit check fixture is often used for complex assemblies containing multiple parts. This fixture simulates the bond by locating the various parts in their exact relationship to one another as they will appear in the actual bonded assembly. Prefitting is usually conducted prior to cleaning so that the details can be reworked if necessary.

8.4.2 Prefit Evaluation

For complex assemblies, a prefit evaluation (*verifilm*) is frequently conducted, as depicted in Fig. 8.12. The bondline thickness is simulated by placing a vinyl plastic film, or the actual adhesive encased in plastic film, in the bondlines. The assembly is then subjected to the heat and pressure normally used for curing. The parts are disassembled, and the vinyl film or cured adhesive is then evaluated visually or dimensionally to see what corrections are required. These corrections can include sanding the parts to provide more clearance, reforming metal parts to close

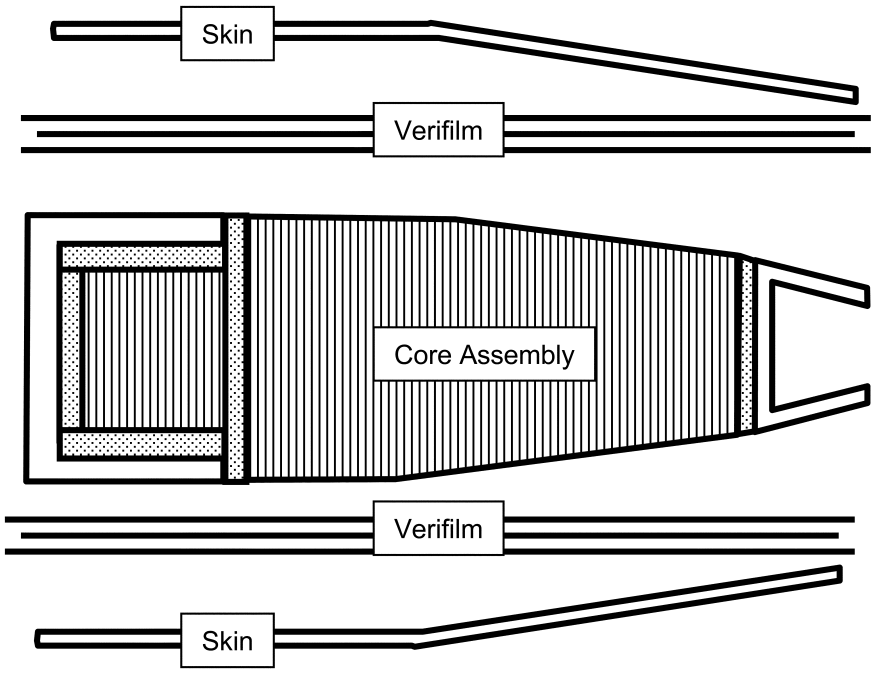


Fig. 8.12 Prefit of details using verifilm

the gaps, or applying additional adhesive (within permissible limits) to particular locations in the bondline. Verification of bondline thickness may not be required for all applications, but the technique can be used to validate the fit of the mating parts prior to the start of production or to determine why large voids are produced in repetitive parts. Once the fit of mating parts has been evaluated, any necessary corrections can be made. For cases in which the component parts can be dimensionally corrected, it is much more efficient to make the correction than to risk having to scrap the bonded assembly or, worse, having it fail in service. Prior to bonding, all substrates made of polymeric materials should be dried to prevent moisture that could either interfere with the curing reaction or cause voids when absorbed moisture boils off during elevated-temperature curing.

8.4.3 Adhesive Application

In general, the adhesive should be stored according to the manufacturer's recommended procedure. Film adhesives normally require storage at 0 °F (–20 °C) or lower. Two-part adhesives are frequently stored at room temperature or refrigerated at around 40 °F (5 °C). The manufacturer's recommended storage conditions should always be followed. When an adhesive is removed from cold storage, it is important to allow it to come to room temperature before opening it; otherwise, moisture condensation may form on the adhesive and perhaps inhibit proper curing or create voids when the moisture boils during elevated-temperature curing. The dramatic loss in fatigue life under slow-cycle testing of bonded aluminum joints, as a function of different levels of moisture in the adhesive film prior to bonding, is shown in Fig. 8.13. Like prepreg, film adhesives should be handled and applied in a temperature- and humidity-controlled clean room.

The most commonly used adhesives are supplied as liquids, pastes, or prefabricated films. The liquid and paste systems may be supplied as one-part or two-part systems. The two-part systems must be mixed before use and thus require scales and a mixer. The amount of material to be mixed should be limited to the amount needed to accomplish the task; the larger the mass, the shorter the pot or working life of the mixed adhesive. To prevent potential exotherm conditions, excess mixed material should be removed from the container and spread out in a thin film. This will prevent the risk of mass-related heat buildup and the possibility of a fire or the release of toxic fumes.

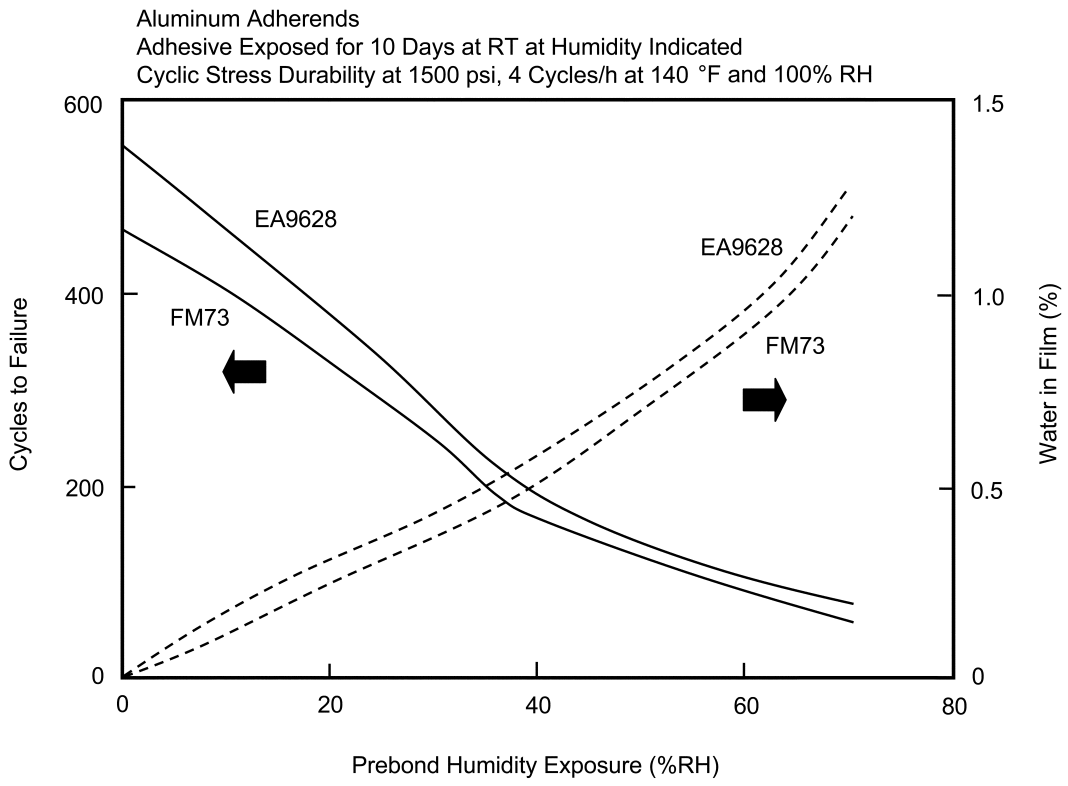


Fig. 8.13 Effects of prebond moisture on fatigue strength. Source: Ref 8

One factor that must be considered in adhesive application is the time interval between adhesive preparation and final assembly of the adherend. This factor, which is referred to as *pot, open, outtime*, or *working life*, must be matched to the production rate. Obviously, materials that are ready to bond quickly are needed for high-rate applications, such as those found in the automotive and appliance industries. Many two-part systems that cure by chemical reaction at room temperature have a limited working life before they become too viscous to apply. Application of liquid adhesives can be accomplished using brushes, rollers, manual sprays, or robotically controlled sprays. Application of paste adhesives can be accomplished by brush, by spreading with a grooved tool, or by extrusion from cartridges or sealed containers using compressed air.

Film adhesives are high quality but costly and thus are used mainly in aircraft applications. They consist of an epoxy, bismaleimide, cyanate ester, or polyimide resin film and a fabric carrier. The fabric guarantees a minimum bondline thickness, because it prevents adherends from contacting each other directly. These adhesives are manually cut to size, usually with knives, and placed in the bondlines. When applying film adhesives, it is important to prevent or eliminate entrapped air pockets between the adherend and the adhesive film by pricking bubbles or "porcupine" rolling over the adhesive prior to application.

8.4.4 Bondline Thickness Control

Controlling the thickness of the adhesive bondline is an important factor in bond strength. This control can be obtained by matching the quantity of available adhesive to the size of the gap between the mating surfaces under actual bonding conditions (heat and pressure). For liquid and paste adhesives, it is common practice to embed nylon or polyester fibers in the adhesive to prevent adhesive-starved bondlines. Applied loads during bonding tend to reduce bondline thickness. A slight overfill is usually desirable to ensure that the gap is totally filled. Conversely, if all of the adhesive is squeezed out of a local

area due to a high spot in one of the adherends, a disbond can result.

For highly loaded bondlines and large structures, film adhesives are used that contain a calendared film with a thin fabric layer. The fabric maintains the bondline thickness by preventing contact between the adherends. In addition, the carrier acts as a corrosion barrier between carbon skins and the aluminum honeycomb core. In the most common case, bondline thickness can vary from 0.002 to 0.010 in. (0.05 to 0.3 mm). Extra adhesive can be used to handle up 0.02 in. (0.5 mm) gaps. Larger gaps must be accommodated by reworking the parts or by producing hard shims to bring the parts within tolerance.

When bonding substrates that contain a large amount of bond area, entrapped air can result in adhesive voids. One method that has been found to be effective in reducing air entrapment is to stage and emboss the adhesive, as shown in Fig. 8.14. This can be done by placing the film adhesive on a flat plate, then covering it with a layer of polytetrafluoroethylene (PTFE) film. A section of honeycomb core is then placed on top of the PTFE film and a vacuum bag is placed over the assembly. The adhesive is then staged at a low temperature in an oven under vacuum bag pressure. This leaves an imprint of the honeycomb cell structure on the adhesive that allows the removal of air before the adhesive melts and flows to fill in the embossed pattern. This process of staging and embossing the adhesive is also used for bonding repair patches.

8.4.5 Bonding

Theoretically, only contact pressure is required so that the adhesive will flow and wet the surface during cure. In reality, somewhat higher pressures are usually required to (1) squeeze out

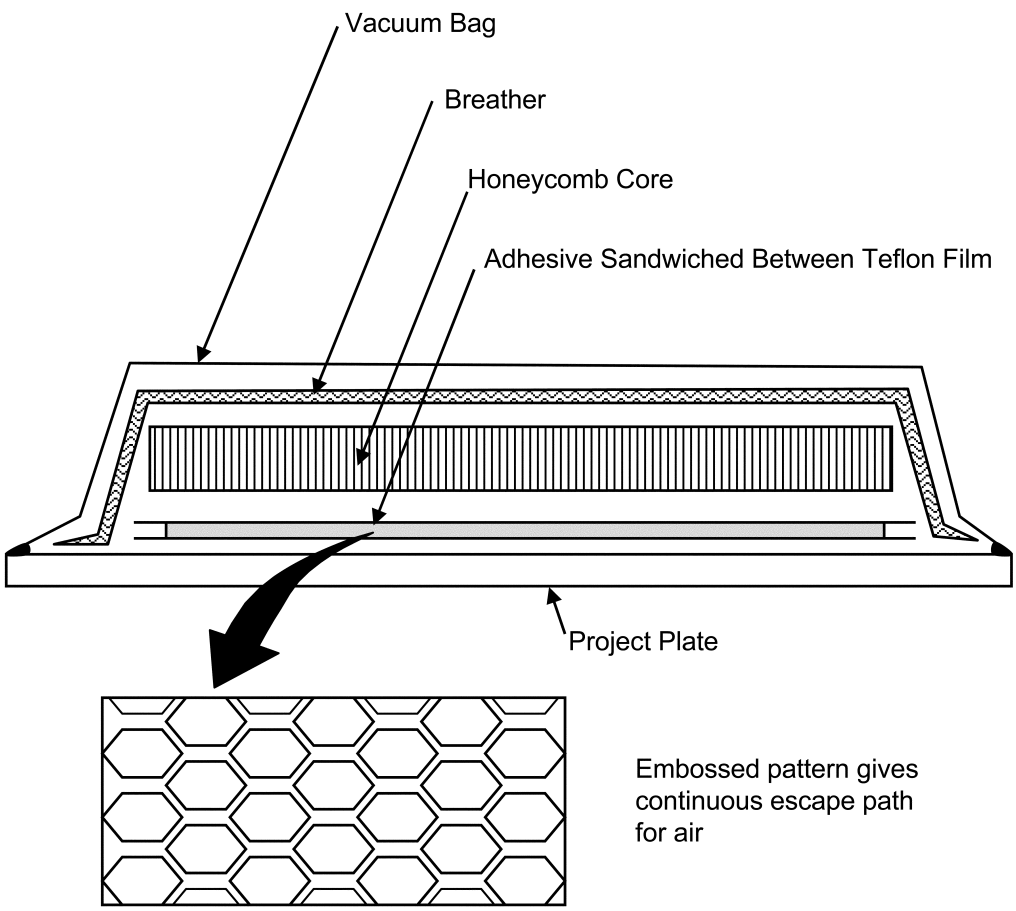


Fig. 8.14 Staging and embossing of adhesive film

excess adhesive to provide the desired bondline thickness and/or (2) provide sufficient force to ensure that all of the interfaces obtain intimate contact during cure.

The position of the adherends must be maintained during cure. Slippage of one of the adherends before the adhesive gels will result in the need for costly reworking or even the scrapping of the entire assembly. When a paste or liquid adhesive is used, it is usually helpful to have a load applied to the joint to deform the adhesive to fill the bondline. C-clamps, spring-loaded clamps, shot bags, and jack screws are frequently used for simple configurations. But if elevated-temperature curing is required, care must be taken to ensure that these pressure devices do not become heat sinks.

Liquid and paste adhesives that are cured at room temperature will normally develop enough strength after 24 hours that the pressure can be removed. For those adhesives that require moderate cure temperatures at 180 ºF (80 ºC), heat lamps or ovens are frequently used. When heat lamps are used, caution is necessary to ensure that the part does not get locally overheated. If the contour is complex, it may be necessary to bag the part and employ the isostatic pressure of an autoclave. Instead of using the positive pressure of a vented bag in an autoclave, a vacuum bag less than 15 psia in an oven is commonly used. The disadvantage of this process is that the vacuum tends to cause many adhesives to release volatiles and form porous and weak bondlines.

When elevated-temperatures ranging 250 to 350 ºF (120 to 180 ºC) curing film adhesives are used, autoclave pressures of 15 to 50 psi (103 to 345 kPa) are normally used to force the adherends together. The majority of these adhesive systems cure in one to two hours at elevated temperature. Autoclave bonded parts are made on bond tools very similar to the ones used for cure tooling. The bagging procedures for autoclave bonding are also very similar to those used for composite curing except that bleeder is not required since there is no attempt to remove any excess resin during cure. Both straight heat-up and ramped (intermediate hold) cure cycles are used. A typical autoclave cure cycle for a 350 ºF (180 ºC) curing epoxy film adhesive is:

- Pull a 20 to 29 in. Hg vacuum on the assembly and check for leaks. If the assembly contains honeycomb core, do not pull more than an 8 to 10 in. Hg vacuum.
- Apply autoclave pressure, usually in the range of 15 to 50 psi (103 to 345 kPa). Vent the bag to atmosphere when the pressure reaches 15 psi (103 kPa).
- Heat to 350 ºF (180 ºC) at a rate of 1 to 5 ºF/min (0.5 to 3 ºC/min). (An optional intermediate hold at 240 ºF (120 ºC) for 30 minutes is sometimes used to allow the liquid resin to flow and thoroughly wet the adherend surfaces.)
- Cure at 350 ± 10 ºF (180 ± 5 ºC) for one to two hours under 15 to 50 psi (103 to 345 kPa).
- Cool to 150 ºF (65 ºC) before releasing autoclave pressure.

During cure, the adhesive flows and forms a fillet or spew at the edge of the bond. It is important not to remove this fillet during cleanup after bonding. Testing has shown that the presence of the fillet significantly improves both the static and fatigue joint strengths.

One of the main disadvantages of adhesive bonding is that there is no reliable method of nondestructively inspecting a bonded assembly to determine the actual strength of the bondlines. Nondestructive testing will determine only whether an interface such as at unbond is present. Therefore, it is common practice to make and destructively test process control or traveler specimens. These tests should be made at the same time and from the same materials as the actual assembly; that is, the actual adhesives are used, the adherends are cleaned and primed along with the assembly adherends, and they are cured at the same time under the same bag. However, as discussed in Chapter 17, "Structural Joints—Bolted and Bonded," the process control specimens will not represent the actual joints since the overlaps are much smaller and the adhesive fails rather than forcing the failure into the adherends, which is the goal of a well-designed joint. Nevertheless, process control specimens, such as single lap shear specimens, are useful in checking that the surface preparation was conducted correctly and that the adhesive was properly cured.

REFERENCES

1. Adhesive Bonding, *ASM Specialty Handbook: Aluminum and Aluminum Alloys*, ASM International, 1993
2. E.M. Petrie, Surfaces and Surface Preparation, *Handbook of Adhesives and Sealants*, McGraw-Hill, 2000
3. B.M. Parker, The Effect of Composite Prebond Moisture on Adhesive-Bonded

CFRP-CFRP Joints, *Composites,* Vol 14, July 1983, p 226–232
4. J.D. Venables, D.K. McNamara, J.M. Chen, T.S. Sun, and R.L. Hopping, "Oxide Morphologies on Aluminum Prepared for Adhesive Bonding," *Appl. Surf. Sci.*, Vol 3, No. 1, 1979, p. 88–98.
5. E.M. Petrie, Primers and Adhesion Promoters, *Handbook of Adhesives and Sealants*, McGraw-Hill, 2000
6. J. Tomblin, W. Seneviratne, P. Escobar, and Y.Yoon-Khian, "Shear Stress-Strain Data for Structural Adhesives," U.S. Department of Transportation, Federal Aviation Administration, DOT/FAA/AR-02/97, Final Report, Nov 2002
7. F.C. Campbell, Secondary Adhesive Bonding of Polymer-Matrix Composites, *ASM Handbook,* Vol 21, *Composites*, ASM International, 2001
8. E.W. Thrall, Prospects for Bonding Primary Aircraft Structures in the 80's, *25th National SAMPE Symposium,* Vol 25, 6–8 May 1980, p 716–727

SELECTED REFERENCES

- D.M. Gleich, M.J. Tooren, and A. Beukers, Structural Adhesive Bonded Joint Review, *45th International SAMPE Symposium,* 21–25 May 2000, p 818–832
- L.J. Hart-Smith, D. Brown, and S. Wong, Surface Preparations for Ensuring That the Glue Will Stick in Bonded Composite Structures, *10th DOD/NASA/FAA Conference on Fibrous Composites in Structural Design*, 1–4 Nov 1993, Hilton Head Island, SC
- L.J. Hart-Smith, G. Redmond, and M.J. Davis, The Curse of the Nylon Peel Ply*, 41st SAMPE International Symposium and Exhibition*, 25–28 Mar 1996, Anaheim, CA
- R.B. Heslehurst and L.J. Hart-Smith, The Science and Art of Structural Adhesive Bonding, *SAMPE J.,* Vol 38 (No. 2), Mar/Apr 2002, p 60–71
- R.J. Hinrichs, Vacuum and Thermal Cycle Modifications to Improve Adhesive Bonding Quality Consistency, *34th International SAMPE Symposium*, 8-11 May 1989, p 2520–2529
- R.B. Krieger, A Chronology of 45 Years of Corrosion in Airframe Structural Bonds, *42nd International SAMPE Symposium*, 4–8 May 1997, p 1236–1242
- "Redux Bonding Technology," Hexcel Composites, Dec 2001
- W.M. Scardino, Adhesive Specifications, *Engineered Materials Handbook,* Vol 1*, Composites*, ASM International, 1987, p 689–701

Copyright © 2010, ASM International®
All rights reserved.
www.asminternational.org

CHAPTER 9

Sandwich and Integral Cocured Structure

SANDWICH AND INTEGRAL cocured structures provide an opportunity to reduce the weight and assembly costs of structures that would otherwise use mechanical fasteners. The term *sandwich structure* normally means a structure that is adhesively bonded with skins on the outside and some type of lightweight core material on the inside. Sandwich structure can be fabricated by first curing the separate composite details and then adhesively bonding them to form a completed assembly. Alternatively, in cocuring, the skins are cured at the same time that they are bonded to the interior sandwich. A third option is a cocured, unitized structure in which all of the details are cured together at the same time without an interior sandwich to produce a one-piece structure. In this option, tooling blocks are used in the interior to define and support the structure. After cure, the tooling blocks are removed.

In this chapter, some of the main methods of fabricating sandwich construction and integral cocured structure will be examined and the advantages and disadvantages of each of these methods will be discussed.

9.1 Sandwich Structure

Sandwich construction is used extensively in both the aerospace and commercial industries, because it is an extremely lightweight type of construction that exhibits high stiffness and high strength-to-weight ratios. The basic concept of a sandwich panel is that the facings carry the bending loads (tension and compression), while the interior sandwich or core carries the shear loads, much like the I-beam comparison shown in Fig. 9.1. As shown in Fig. 9.2, sandwich construction, especially honeycomb core construction, is extremely structurally efficient, particularly in stiffness-critical applications. Doubling the thickness of the core increases the stiffness over seven times with only a three percent weight gain, while quadrupling the core thickness increases stiffness over 37 times with only a six percent weight gain. It is little wonder that structural designers like to use sandwich construction whenever possible. Sandwich panels are typically used for their structural, electrical, insulation, and/or energy absorption characteristics.

Commonly used facesheet materials are aluminum, glass, carbon, and aramid. A typical sandwich structure has relatively thin facing sheets of 0.010 to 0.125 in. (0.25 to 3 mm) with core densities in the range of 1 to 30 pcf (pounds per cubic foot) (16 to 480 kg/m^3). Core materials include metallic and nonmetallic honeycomb core, balsa wood, open and closed cell foams, and syntactics. A cost-performance comparison for core materials is given in Fig. 9.3. Honeycomb cores are more expensive than foam cores but offer superior performance. This explains why many commercial applications use foam cores, which are also easier to work with, while aerospace applications use the higher-performance but more expensive honeycombs. A relative strength-stiffness comparison of different core materials is shown in Fig. 9.4.

9.2 Honeycomb Core Sandwich Structure

The details of a typical honeycomb core panel are shown in Fig. 9.5. Typical facesheets include aluminum, glass, aramid, and carbon**.** Structural

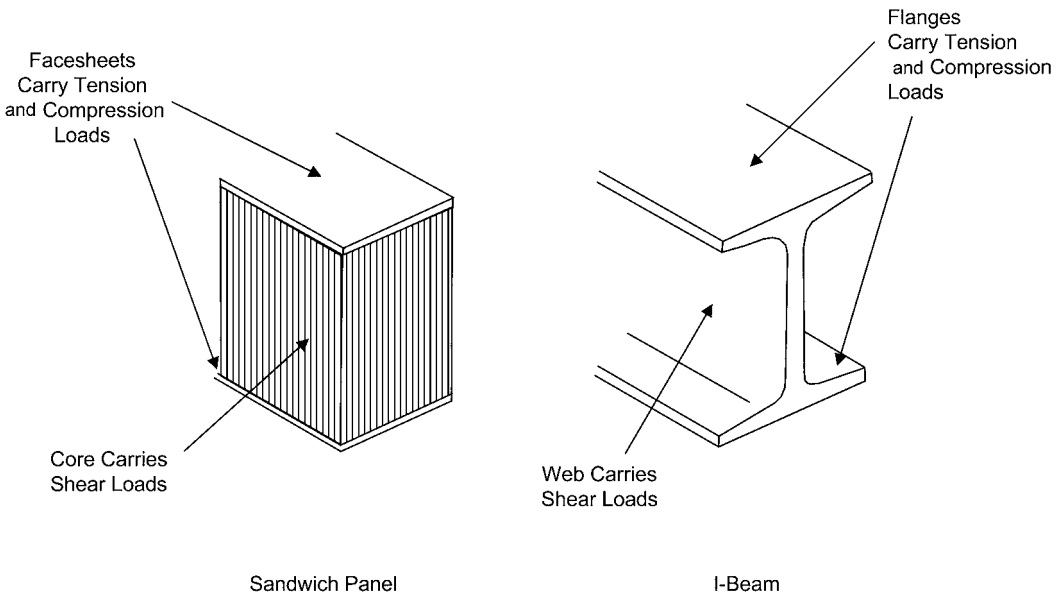


Fig. 9.1 Why sandwich structures are so efficient. Source: Ref 1

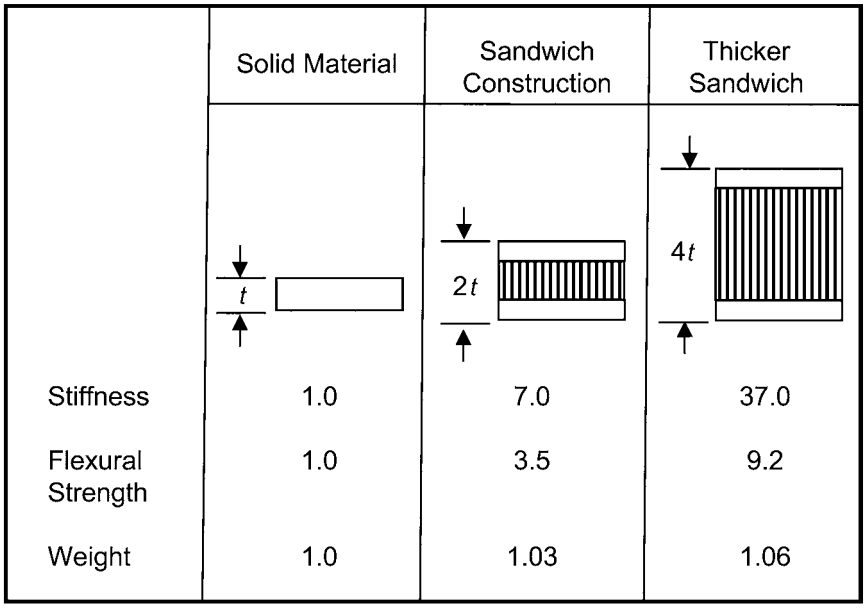


Fig. 9.2 Efficiency of the sandwich structure. Source: Ref 1

film adhesives are normally used to bond the facesheets to the core. It is important that the adhesive provide a good fillet at the core-to-skin interface. Typical honeycomb core terminology is given in Fig. 9.6. The honeycomb itself can be manufactured from aluminum, glass fabric, aramid paper, aramid fabric, or carbon fabric. Honeycomb manufactured for use with organic matrix composites is bonded together with an adhesive, called the *node bond adhesive*. The "*L*" direction is the core ribbon direction and is stronger than the width (node bond) or "*W*" direction.

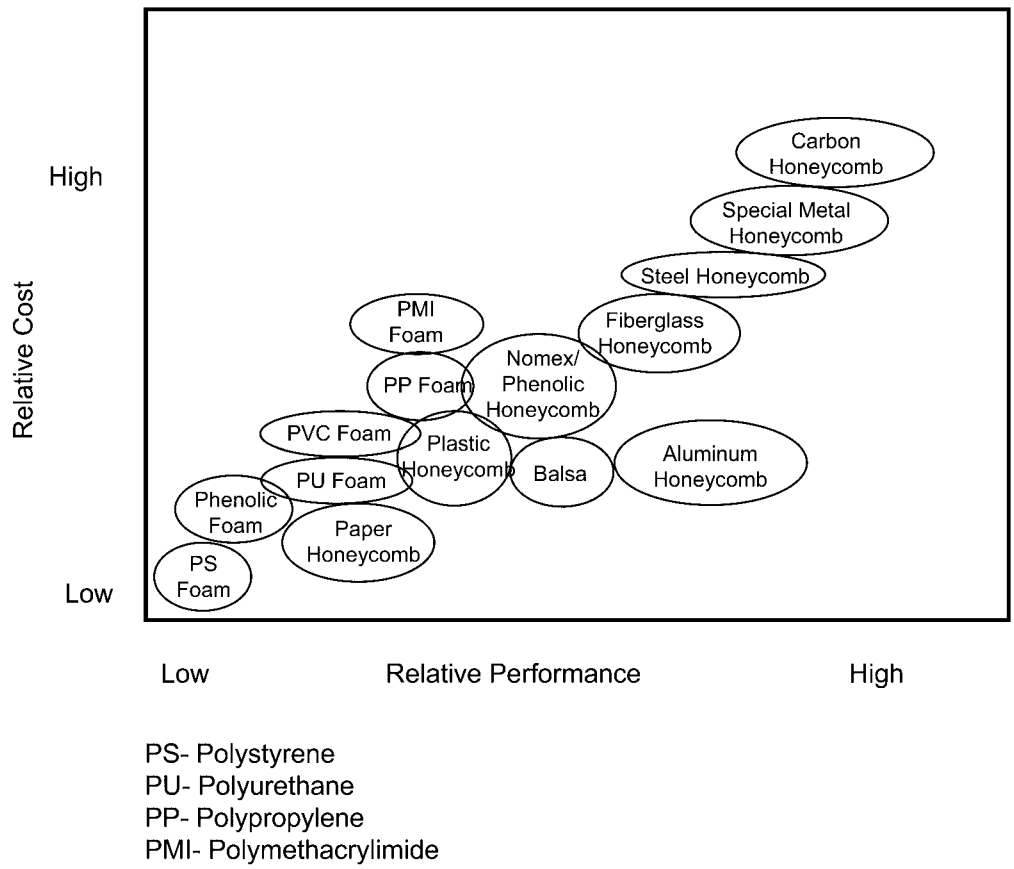


Fig. 9.3 Cost versus performance for core materials. Source: Ref 2

The thickness is denoted by "*t*," and the cell size is the dimension across the cell, as shown in Fig. 9.6.

Although a variety of cell configurations are available, the three most prevalent (Fig. 9.7) are hexagonal core, flexible core, and overexpanded core. Hexagonal core is by far the most commonly used core configuration. It is available in aluminum and all nonmetallic materials. Hexagonal core is structurally very efficient and can even be made stronger by adding longitudinal reinforcement (reinforced hexagonal core) in the "*L*" direction along the nodes in the ribbon direction. The main disadvantage of the hexagonal configuration is its limited formability; aluminum hexagonal core is typically roll-formed to shape, while nonmetallic hexagonal core must be heat-formed. Flexible core was developed to provide much better formability. This configuration provides for exceptional formability on compound contours without cell wall buckling. It can be formed around tight radii in both the "*L*" and "*W*" directions. However, it must be held in place after forming or it will spring back to the flat condition on the release of pressure. Overexpanded core has better formability than hexagonal core, although not as good as that of flexible core. This configuration is hexagonal core that has been overexpanded in the "*W*" direction, providing a rectangular configuration that facilitates forming in the "*L*" direction. The length in the "*W*" direction is about twice that in the "*L*" direction. This configuration, compared to regular hexagonal core, increases the "*W*" shear properties but decreases the "*L*" shear properties.

Honeycomb core is normally made by either the expansion or the corrugation process shown in Fig. 9.8. The expansion process is most prevalent for lower-density ≤10 pcf (≤160 kg/m^3) honeycomb core used for bonded assemblies. The foil is cleaned, corrosion-protected if it is aluminum, printed with layers of adhesive, cut

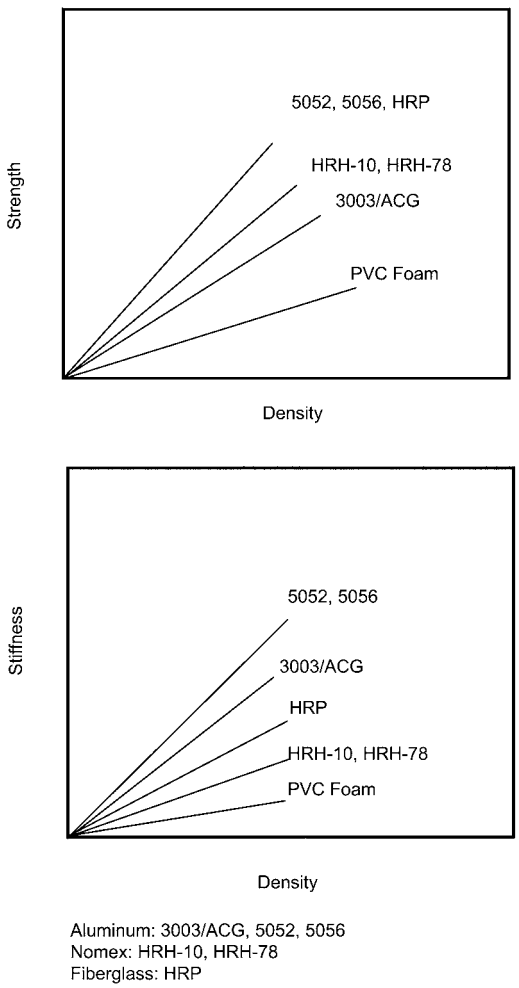


Fig. 9.4 Strength and stiffness of various core materials. Source: Ref 1

to length, stacked, and then placed in a press under heat and pressure to cure the node bond adhesive. After curing, the block, or honeycomb before expansion (called a HOBE) is sliced to the correct thickness and expanded by clamping and then pulling on the edges. Expanded aluminum honeycomb retains its shape at this point due to yielding of the aluminum foil during the expansion process. Nonmetallic cores, such as glass or aramid, must be held in the expanded position and dipped in a liquid resin, which then must be cured before the expansion force can be released. Although epoxy and polyester resin systems are possible, phenolic and to some extent polyimide for higher-temperature applications are by far the most prevalent. Several dip and cure sequences can be required to produce the desired density. Since phenolics and polyimides are high-temperature condensation curing resins, it is important that they are thoroughly cured to drive off all volatiles. If the volatiles are not totally removed during core manufacturing, they can evolve during sandwich curing, creating enough pressure to potentially split the node bonds. Therefore, after the initial cure, it is common practice to postcure the phenolic or polyimide core at higher temperatures to ensure that the reactions are complete. Corrugation is a more expensive process reserved for materials that cannot be made by expansion or for higher-density cores such as ≥10 pcf (≥160 kg/m^3) cores. For example, high-temperature metallic core such as titanium is made by corrugation and then welded together at the nodes to make the completed core sections.

The comparative properties of some commercial honeycomb cores are given in Table 9.1 and typical mechanical properties are shown in Table 9.2. For each material, the first property value listed is for a large-cell honeycomb core with relatively thin cell walls. The second property value listed is for a small-cell honeycomb core with relatively thick cell walls. For example, a large-cell honeycomb core made of thin 5052 aluminum foil has a honeycomb core density of 1.0 pcf. A small-cell honeycomb core made of relatively thick aluminum foil has a honeycomb core density of 12.0 pcf. The strength retentions of a number of honeycomb cores at elevated temperature are shown in Fig. 9.9. Aluminum honeycomb has the best combination of strength and stiffness. The higher-performance aerospace grades are 5052-H39 and 5056-H39, and the commercial grade is 3003 aluminum. Although 2024 aluminum core is available, it is rarely used because it has poor corrosion resistance. Cell sizes range from $^1/_{16}$ to $^3/_8$ in. (1.5 to 9.5 mm) but $^1/_8$ and $^3/_{16}$ in. (3 and 4.8 mm) are the ones most frequently used for aerospace applications. Glass fabric honeycomb can be made from either a normal bidirectional glass cloth or a bias weave (± 45 degrees) cloth. It is usually impregnated with phenolic resin, but for high-temperature applications a polyimide resin is used. The advantage of the bias weave is that it enhances the shear modulus and improves the damage tolerance of the core. Nomex core is made by impregnating aramid paper with either a phenolic or polyimide resin. However, because the resin cannot fully impregnate the paper, excessive moisture absorption can result. Therefore, DuPont has developed an improved aramid paper

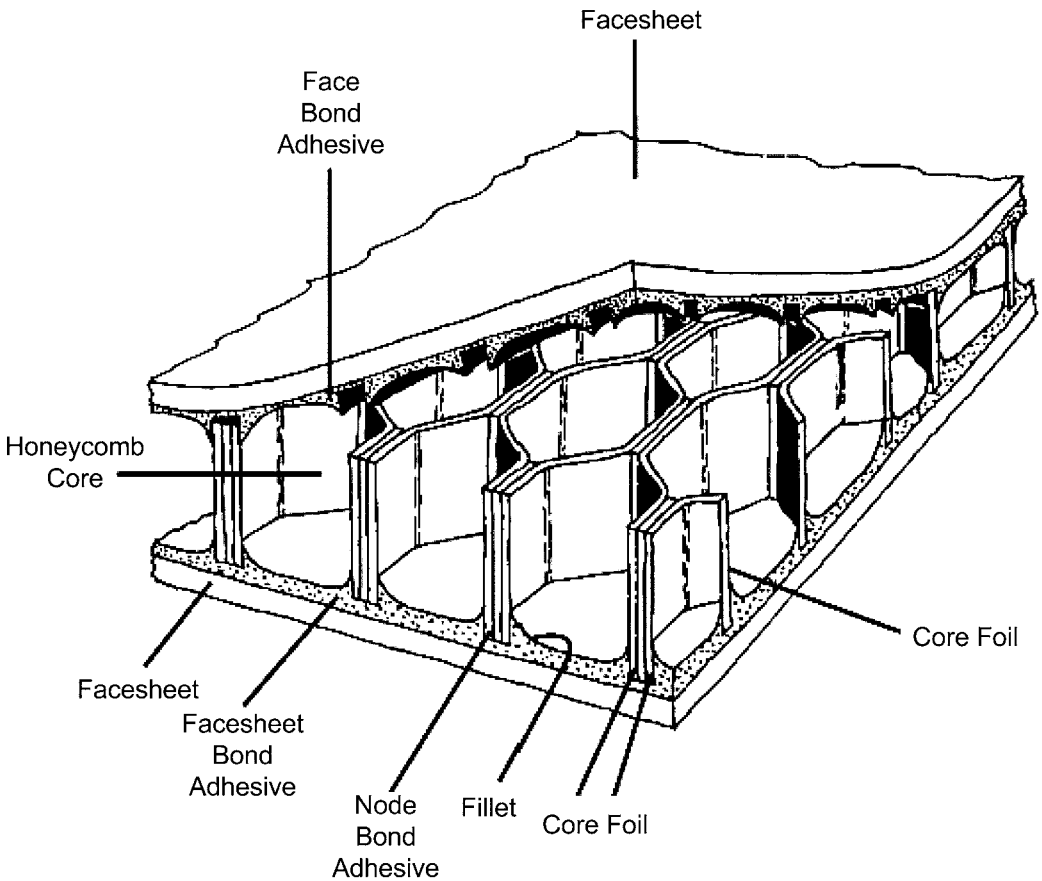


Fig. 9.5 Honeycomb panel construction. Source: Ref 3

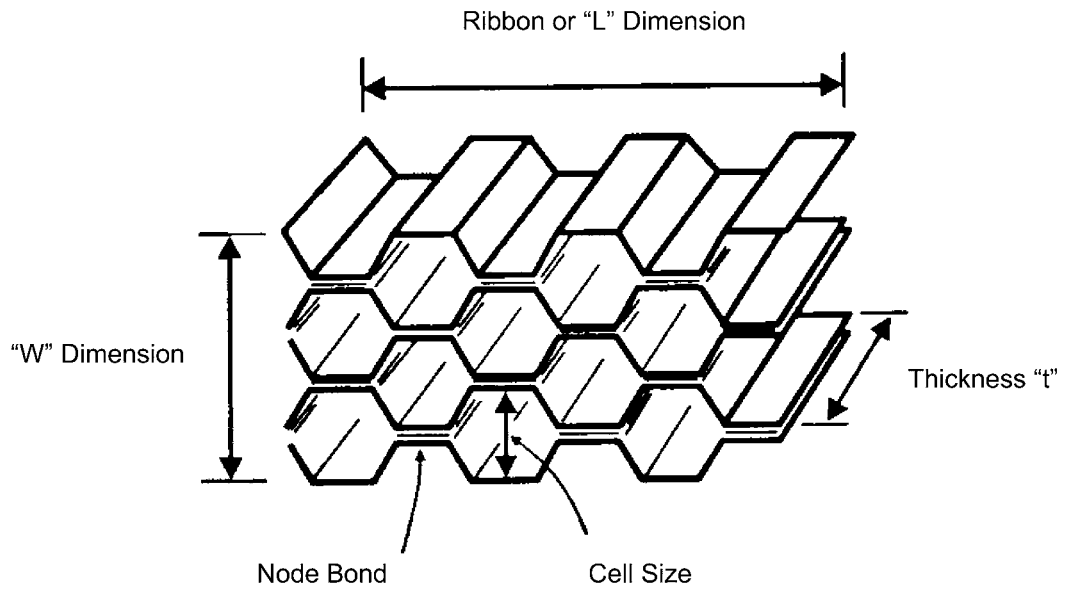


Fig. 9.6 Honeycomb core terminology. Source: Ref 1

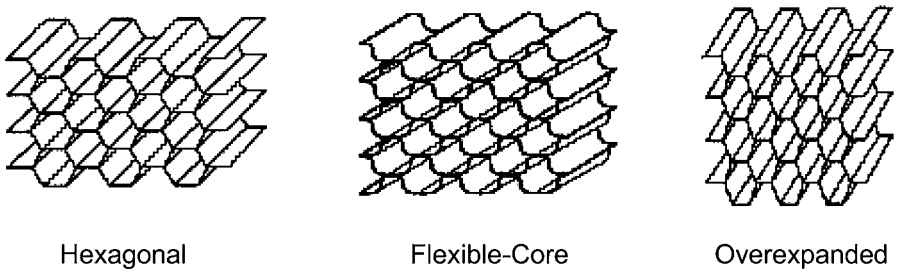


Fig. 9.7 Types of honeycomb core cell configurations. Source: Ref 4

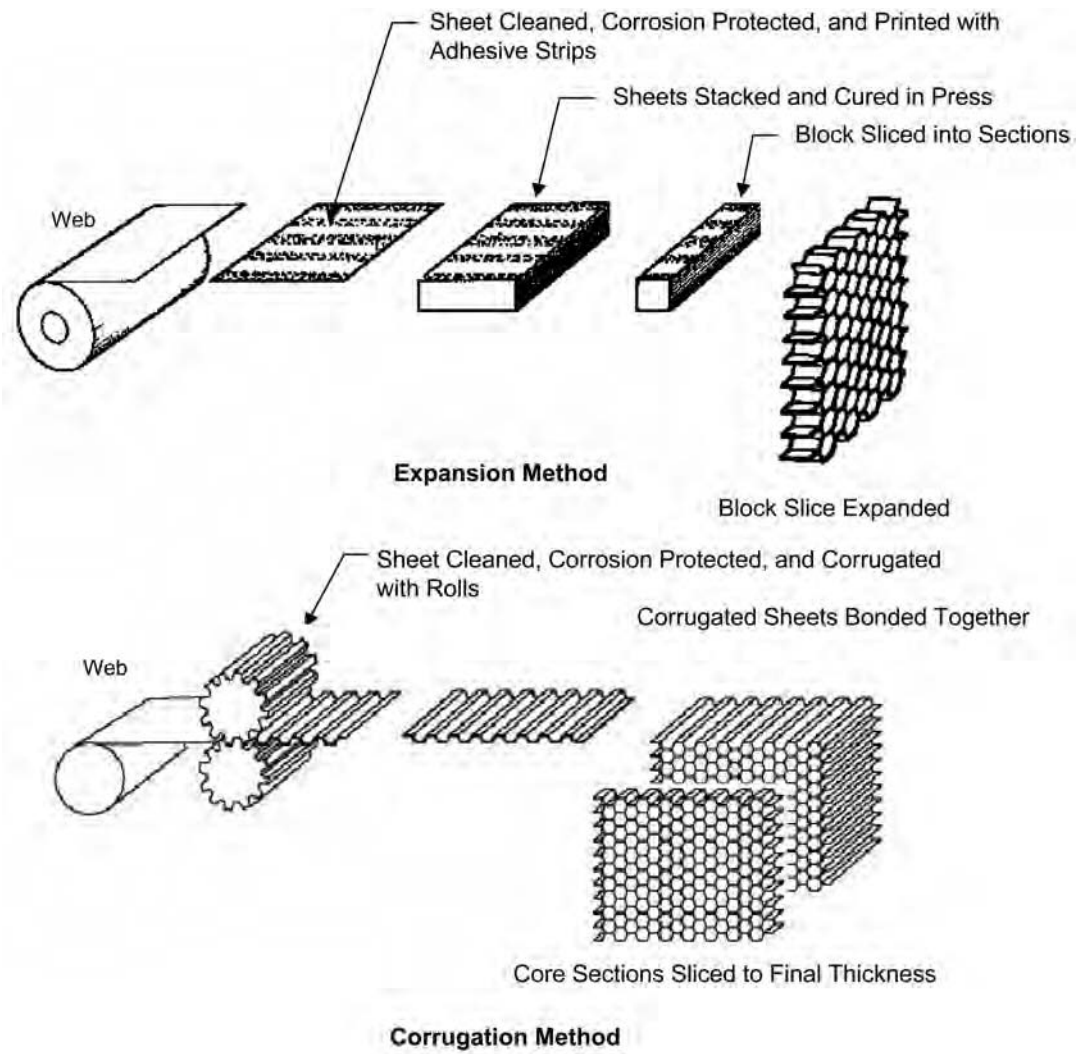


Fig. 9.8 Fabrication methods for the honeycomb core. Source: Ref 4

Table 9.1 Characteristics of typical honeycomb core materials

Name and type of core	Strength/stiffness	Maximum temperature, °F	Typical product forms	Density, pcf
5052-H39 and 5056-H39 Al core	High/high	350	Hexagonal flex-core	1–12 2–8
3003 Al commercial grade hexagonal core	High/high	350	Hexagonal	1.8–7
Glass fabric reinforced phenolic	High/high	350	Hexagonal flex-core OX	2–12 2.5–5.5 3–7
Bias weave glass fabric reinforced phenolic	High/very high	350	Hexagonal OX	2–8 4.3
Bias weave glass fabric reinforced polyimide	High/high	500	Hexagonal	3–8
Aramid paper reinforced phenolic (Nomex)	High/moderate	350	Hexagonal flex-core OX	1.5–9 2.5–5.5 1.8–4
Aramid paper reinforced polyimide (Nomex)	High/moderate	500	Hexagonal OX	1.5–9 1.8–4
High performance aramid Paper reinforced phenolic (N636)	High/high	350	Hexagonal flex-core	2–9 4.5
Aramid fabric reinforced epoxy	High/moderate	350	Hexagonal	2.5
Bias weave carbon fabric reinforced phenolic	High/high	350	Hexagonal	4

Source: Ref 5

Table 9.2 Typical RT mechanical properties of honeycomb core materials

		Compression		Parallel to core ribbon, L shear		Perpendicular to core ribbon, W shear	
Core	Honeycomb core density, pcf	Strength, psi	Modulus, ksi	Strength, psi	Modulus, ksi	Strength, psi	Modulus, ksi
5052	1.0	55	10	45	12	30	7
Aluminum	12.0	2900	900	1940	210	1430	75
5056	1.0	60	15	55	15	35	7
Aluminum	8.1	1900	435	945	143	560	51
2024	2.8	320	40	200	42	120	19
Aluminum	9.5	2500	480	1150	170	650	64
3003	1.3	70	16	55	14	40	7
Aluminum	4.8	630	148	335	63	215	31
0°, 90° fiberglass	2.2	180	13	120	6	60	3
Phenolic	12.0	2520	260	985	48	625	28
± 45° fiberglass	2.0	170	17	115	15	60	5
Phenolic	8.0	1750	129	580	49	340	24
± 45° fiberglass	3.2	310	27	195	19	95	8
Polyimide	8.0	1210	126	700	55	420	22
Nomex	1.5	100	6	75	3	40	2
Phenolic	9.0	2100	90	515	18	300	11
± 45° graphite	5.0	950	85	590	94	350	40
Phenolic	10.0	3060	170	1060	215	760	90

Note: For each material, the first property value listed is for a large-cell honeycomb core with relatively thin cell walls. The second property value listed is for a small-cell honeycomb core with relatively thick cell walls. Source: Ref 4

core, designated N636, that has better moisture resistance. Kevlar honeycomb is made by impregnating Kevlar 49 fabric. Finally, bias weave carbon fabric core is a high-performance but expensive material that was developed for special applications requiring high specific stiffness and thermal stability when bonded with carbon-reinforced facesheets.

Honeycomb core offers superior performance compared to other sandwich cores. A comparison of strength and stiffness for several core types was shown in Fig. 9.4. Aluminum core has the

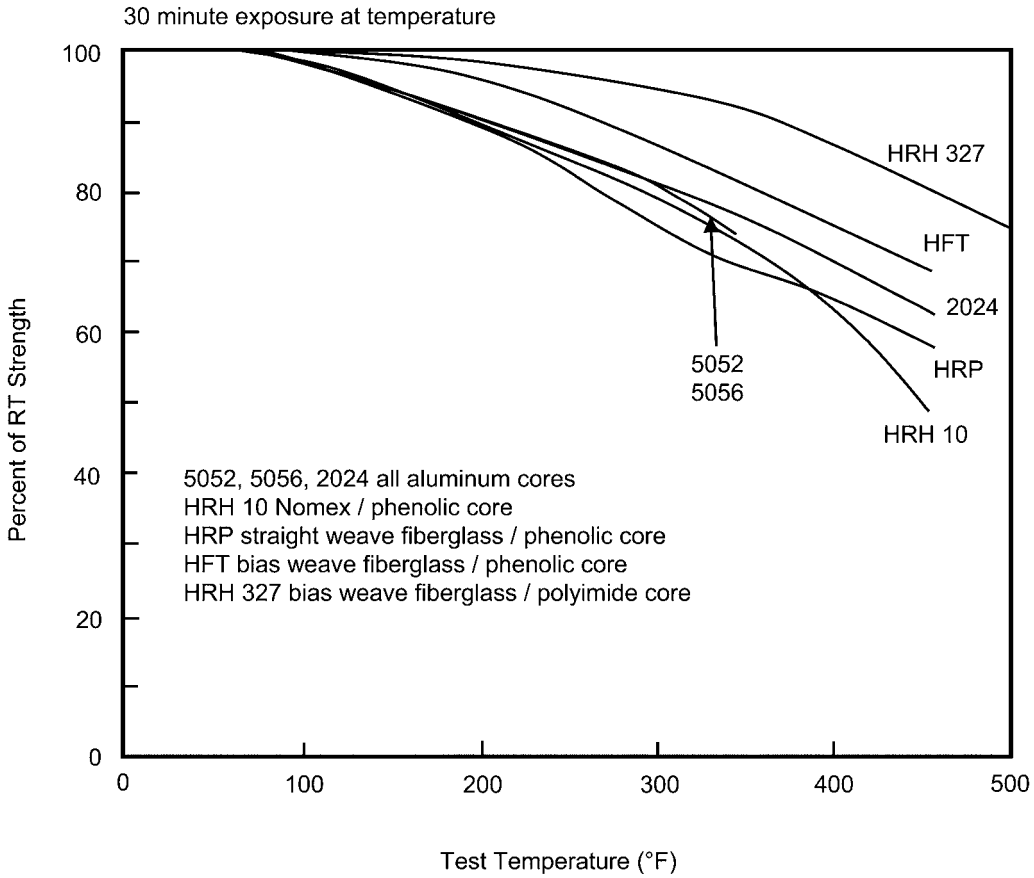


Fig. 9.9 Strength retention at temperature. Source: Ref 4

best combination of strength and stiffness, followed by the nonmetallic honeycombs and then polyvinyl chloride (PVC) foam. Unfortunately honeycomb core is expensive and can be difficult to fabricate into complex assemblies, and the in-service experience, particular with aluminum honeycomb, has not always been good. It can also be difficult to make major repairs to honeycomb assemblies, especially if the assembly has been in service and water is present.

Aluminum honeycomb assemblies have experienced serious in-service durability problems, the most severe being moisture migrating into the assemblies and causing corrosion of the aluminum core cells. An example of severe aluminum honeycomb corrosion is shown in Fig. 9.10. Honeycomb suppliers have responded by producing corrosion-inhibiting coatings that have improved durability. The newest corrosion protection system, called *phosphoric acid anodize* (*PAA*) *core*, is shown in Fig. 9.11. The core foil is first cleaned and phosphoric acid anodized. It is then coated with a corrosion-inhibiting primer before being printed with node bond adhesive. The improved corrosion protection is the result of the very thick primer bonded to the porous PAA oxide layer. However, PAA core costs about 20 percent more than standard conversion-coated aluminum core. Phosphoric acid anodize core has demonstrated an approximate threefold increase in corrosion protection compared to typical (non-PAA) corrosion-resistant aluminum honeycomb. However, even the most rigorous corrosion protection methods will not stop core corrosion but only delay its onset.

If liquid water is present in the honeycomb cells, freeze-thaw cycles encountered during a typical aircraft flight can cause node bond failures. At high altitudes, the standing water in the core freezes, expands, and stresses the cell walls. After landing, the water thaws and the cell walls relax. After a number of these freeze-thaw

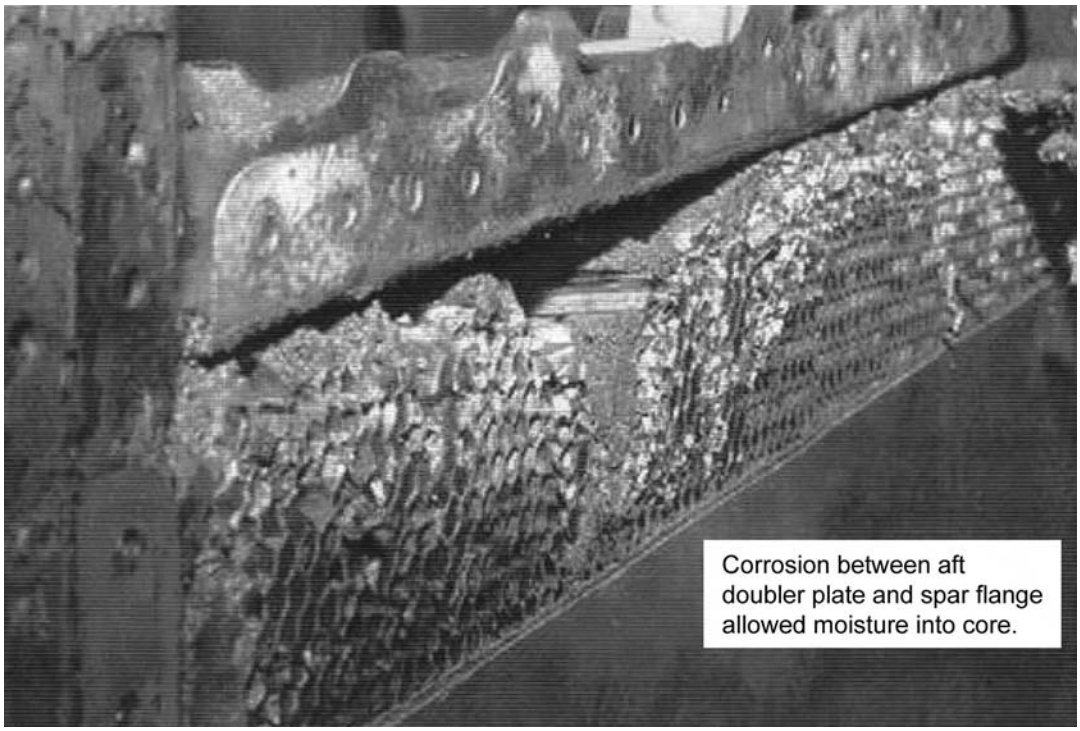


Fig. 9.10 Corroded aluminum honeycomb core

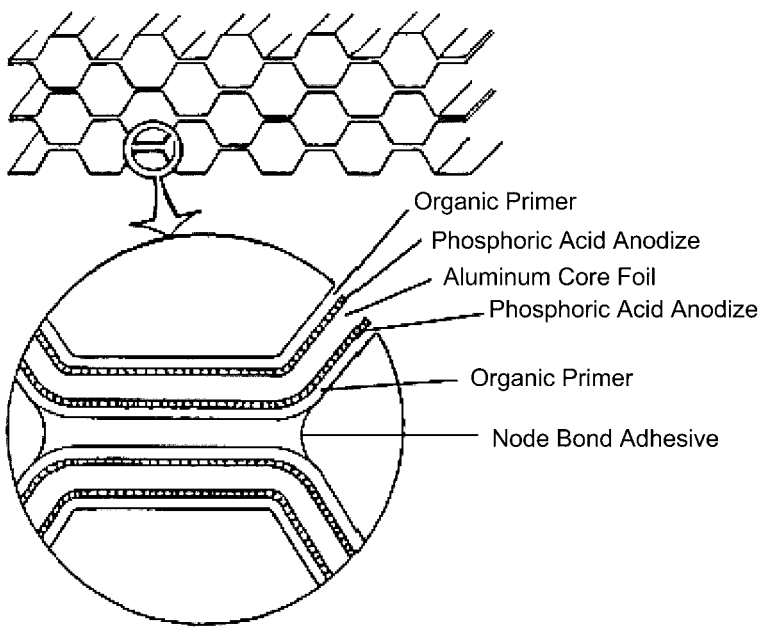


Fig. 9.11 Construction of the phosphoric acid anodize (PAA) honeycomb core. Source: Ref 3

cycles, the node bonds fail and the damage propagates. This freeze-thaw cyclic damage is not confined to aluminum honeycomb but can also occur in nonmetallic cores. Water in the honeycomb can also cause disbonds and delaminate the facesheets, particularly if the temperatures exceeds the boiling point of water 212 ºF (100 ºC), as can happen during operation or repair.

Liquid water normally enters the core through exposed edges, such as panel edges, closeouts, door and window sills, attachment fittings, or almost any location where the skin and core bond terminates. The majority of the damage is typically found at the edges of panels. Adhesive bond degradation will lower the skin-to-core bond strength, the fillet bond strength, and the node bond strength. Node bond degradation can reduce the core shear strength so that the assembly fails prematurely by core failure. In addition, water will enter the assembly through any puncture in the facesheets. Since some honeycomb assemblies contain extremely thin skins, water has been known to pass through the skins and then condense on the cell walls. Interconnected microcracks in thin-skin honeycomb panels can also allow water ingression. Although absorbed moisture affects the properties of any composite assembly, it is the presence of liquid water in the cells that does the majority of the damage. Many field reports blame water ingression on "poor" sealing techniques. Good sealing practices are important, but in most cases it is just a matter of time until water finds its way into the core of most honeycomb designs and initiates the damage process.

9.2.1 Honeycomb Processing

The construction of a typical aircraft control surface is shown in Fig. 9.12. Film adhesive is used to bond the skins to the core and the skins to the closure members (front spar, ribs, and arrowhead). Foaming adhesive is used to bond the core to the closure members. Honeycomb processing before adhesive bonding includes perimeter trimming, mechanical or heat forming, core splicing, core potting, contour machining, and cleaning.

Trimming. The four primary tools used to cut honeycomb to dimensions are a serrated knife, a razor blade knife, a band saw, and a die. The serrated and razor edge knives and the die cutter are used on light-density cores, while heavy-density cores and complex shaped cores are usually cut with a band saw.

Forming. Metallic hexagonal honeycomb can be roll- or brake-formed into curved parts. The brake-forming method crushes the cell walls and densifies the inner radius. Overexpanded honeycomb can be formed to a cylindrical shape on assembly. Flexible core can usually be shaped to compound curvatures on assembly but must be restrained in place. Nonmetallic honeycomb can be heat-formed to obtain curved parts. Usually the core is placed in an oven at high temperature for a short period of time, for example, 550 ºF (290 ºC) for one to two minutes. The heat softens the resin and allows the cell walls to deform more easily. Upon removal from the oven, the core is quickly placed on a shaped tool and held in place until it cools.

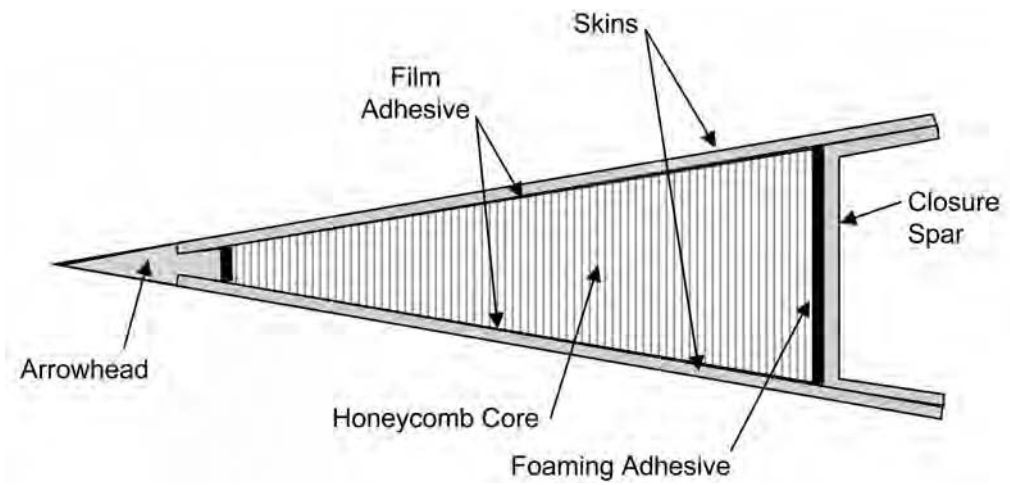


Fig. 9.12 Typical honeycomb control surface

Splicing. When large pieces of core are required or when strength requirements dictate different densities, smaller pieces or different densities of core can be spliced together to form the finished part. This splicing is usually accomplished with a foaming adhesive, as shown in Fig. 9.13. Core splice adhesives normally contain blowing agents that produce gases such as nitrogen during heat-up to provide the expansion necessary to fill the gaps between the core

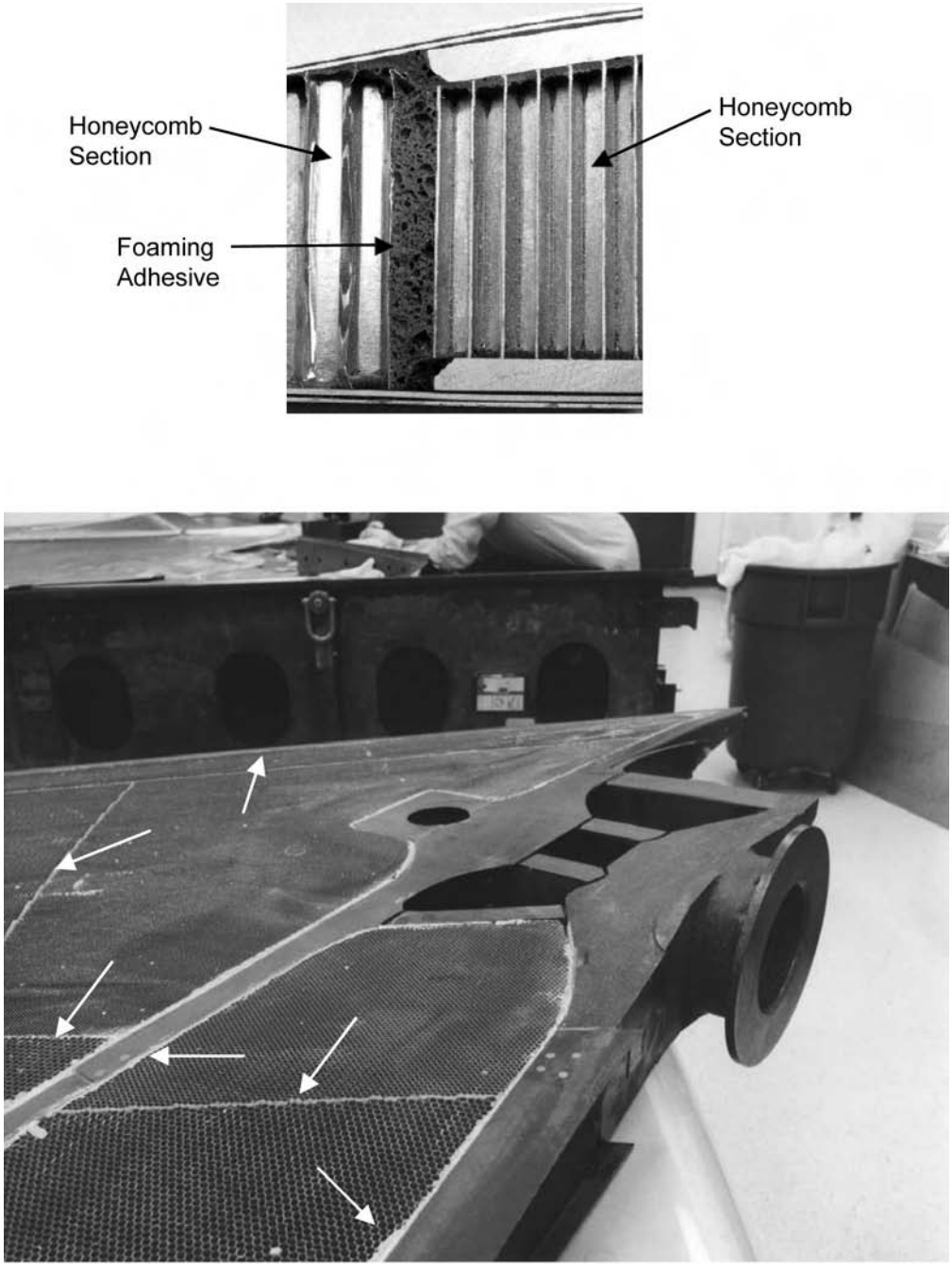


Fig. 9.13 Complex structure with different core densities. (Arrows indicate locations of foam bondlines) Source: The Boeing Company

sections. Foams are one-part epoxy pastes that expand during heating. Foaming film adhesives are thick, unsupported films at 0.04 to 0.06 in. (1 to 1.5 mm) that expand 1.5 to 3 times their original thickness when cured. Although some of these products can damage the core by over-expanding if too much material is used in the joint, most of them just expand to fill the gap and then stop when they meet sufficient resistance. A normal practice is to allow up to three layers of foaming adhesive to fill gaps between core sections. Larger gaps call for rework or replacement of the core section. It is also important not to process some foaming adhesives under a vacuum, or excessive frothing of the foam bondline may occur. Since many foaming core splice adhesives are inherently porous, they can provide a path for water to migrate through the core sections.

Potting. Potting compounds are frequently required for fitting attachments where fasteners must be put through the honeycomb assembly. As shown in Fig. 9.14, the cells are potted with a high-viscosity paste that is cured either during core splicing operations or during final bonding. These compounds usually contain fillers, such as milled glass or aramid fibers, glass or phenolic microballoons, or silica. They can be formulated to cure at room temperature, 250 or 350 ºF (120 or 180 ºC), depending upon the intended use temperature for the structure.

Machining. In most applications, the honeycomb thickness must be machined to some contour. This machining is normally accomplished using valve stem–type cutters on expanded core. Occasionally, before expansion, the solid honeycomb block is machined using milling cutters. Typical machines used for contour machining (carving) are gantry, apex, three-dimensional tracer, and numerically controlled (NC) five-axis machines. With five-axis NC machining, the cutting head is controlled by computer programs, and almost any surface that can be described by *x*-, *y*- and *z*-coordinates can be produced. These machines can carve honeycomb at speeds of up to 3000 in./min (76 m/min) with extreme accuracy. A standard contour tolerance of an NC machine is ± 0.005 in. (± 0.1 mm). Many core suppliers will supply core machined to contour ready for final bonding.

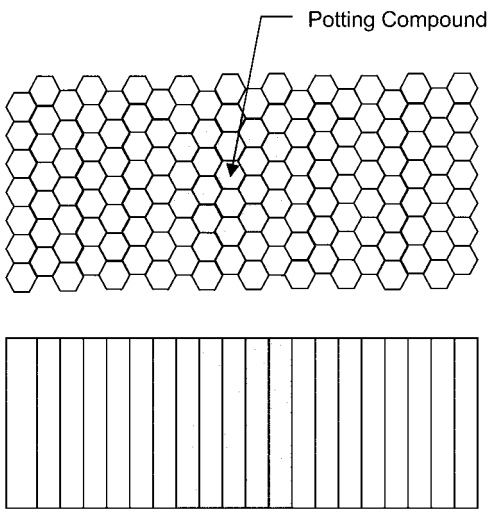


Fig. 9.14 Core potting in the honeycomb core

Cleaning and Drying. It is preferable to keep honeycomb core clean during all manufacturing operations prior to adhesive bonding; however, aluminum honeycomb core can be cleaned effectively by solvent vapor degreasing. Some manufacturers require vapor or aqueous degreasing of all aluminum core prior to bonding, but most part manufacturers accept "Form B" core from the honeycomb suppliers and bond without further cleaning. Nonmetallic core, such as Nomex or N636 (aramid), fiberglass, and graphite core, readily absorbs moisture from the atmosphere. Like composite skins, nonmetallic core sections should be thoroughly dried prior to adhesive bonding. Since the cell walls are relatively thin and have a high surface area, they can reabsorb moisture rapidly after drying; therefore, they should be stored in an environmentally controlled clean room and bonded into assemblies as soon as possible after drying.

Honeycomb Bonding. Honeycomb bonding procedures are similar to regular adhesive bonding, but there are a few special considerations. Unlike many composite assemblies, honeycomb assemblies require special closeouts, several of which are shown in Fig. 9.15. During bonding, these require filler blocks in cavities and ramp areas to prevent edge crushing during the cure cycle. Closeouts are also areas for potential water ingression, so special care is required during both the design and manufacturing processes.

Pressure selection is an important consideration during honeycomb bonding. The pressure should be high enough to push the parts together but not so high that there is danger of crushing or condensing the core. The allowable pressure depends on both the core density and the part geometry. Common bonding pressures range from 15 to 50 psi (100 to 350 kPa) for

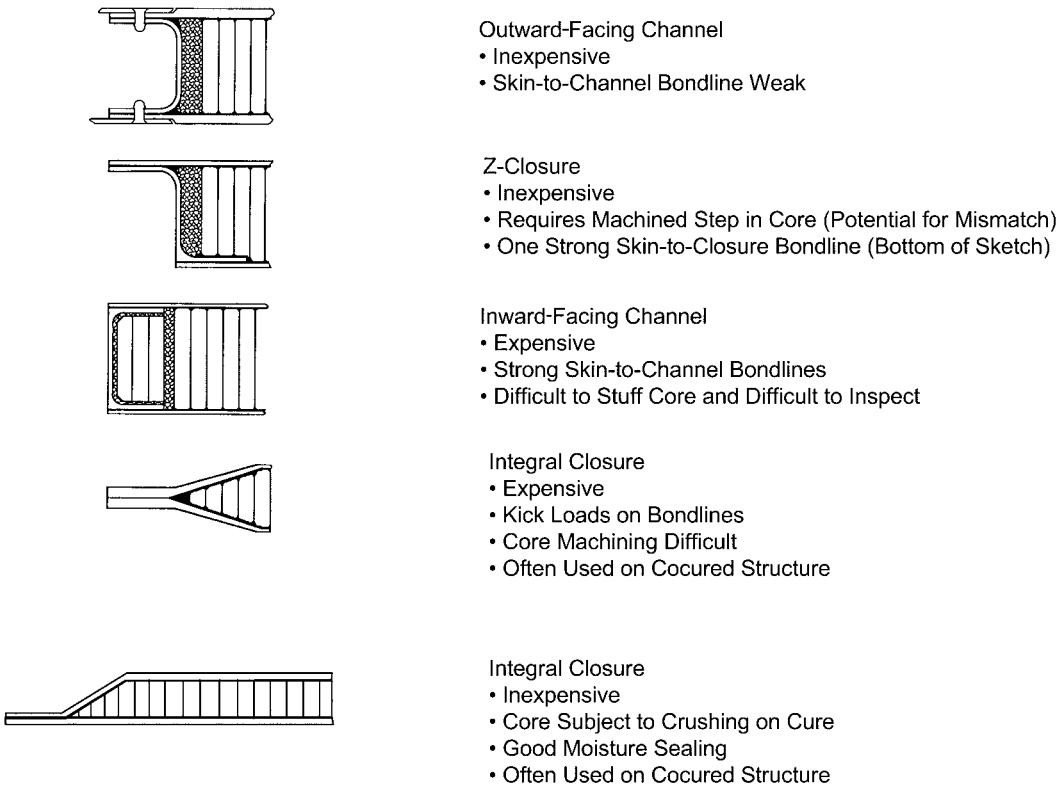


Fig. 9.15 Examples of honeycomb structure closeouts

honeycomb assemblies. The positive pressure of an autoclave, with a vented bag, usually gives quality superior to that of a bond produced in an oven under vacuum bag pressure. The amount of pressure and the adhesive selected are important in forming fillets at the core-to-skin bondlines. The degree of filleting largely determines the strength of the assembly. Therefore, adhesive film weights of at least 0.08 psf (4 Pa) or higher are recommended to provide sufficient filleting.

Pressures applied on the sides of the core can easily condense the cells. Since honeycomb is stronger in the longitudinal (L) direction than in the width (W) direction, the core is more prone to crushing in the "W" direction. Even when the initial vacuum is pulled, vacuum pressure alone has been known to cause core migration and cell crushing. Some manufacturers limit the vacuum level to 8 to 10 in. (27 to 34 kPa) of Hg to help prevent differential pressures within the cells. Autoclave processing of honeycomb assemblies is also more sensitive to bag leaks than regular adhesive bonding. If pressure enters the bag through a leak, it can literally blow the honeycomb apart due to the large differential pressure.

In some applications where weight savings is extremely critical, fabricators will reticulate the adhesive prior to bonding, as shown in Fig. 9.16. In this process, an unsupported film adhesive is placed over the core and a hot-air blast melts the adhesive film so that it coagulates on the cell walls. This allows a lighter film adhesive to be used and eliminates the film weight between the cells. This process is frequently used for lightly loaded panels for space applications. It is also used for engine nacelle assemblies that are designed for the air (noise) to flow through the cells to reduce the noise level.

9.2.2 Cocured Honeycomb Assemblies

Honeycomb assemblies can also be made by cocuring the composite plies onto the core. In this process, the composite skin plies are consolidated and cured at the same time that they are bonded to the core. Although a film adhesive is normally used at the skin-to-core interface,

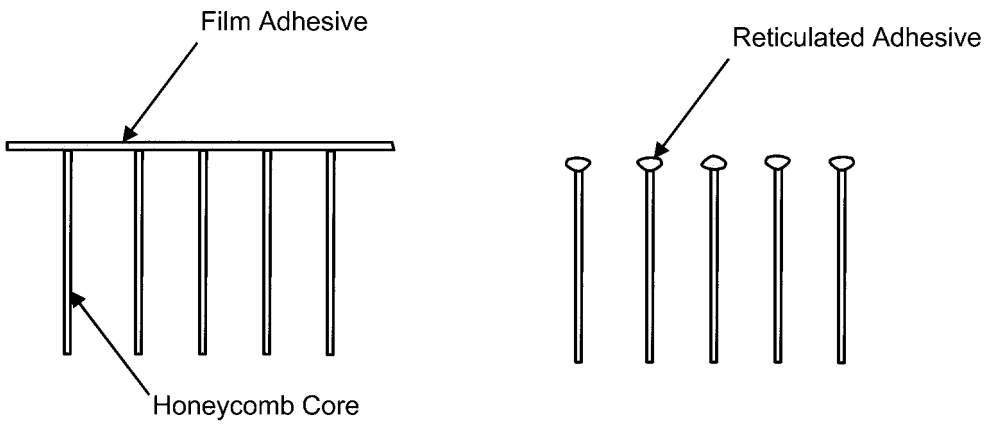


Fig. 9.16 Reticulation of adhesive film

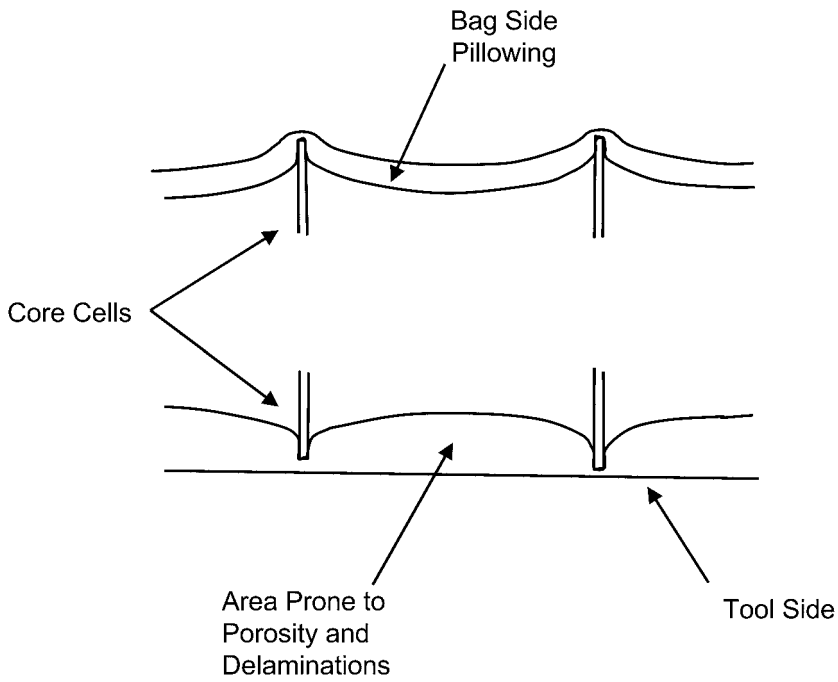
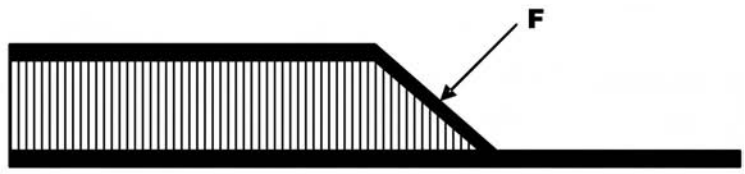


Fig. 9.17 Pillowing effect in composite cocured honeycomb panels

self-adhesive prepreg systems are available that do not require a film adhesive. To prevent core crushing and migration, this process is normally performed at approximately 40 to 50 psi (275 to 345 kPa), as opposed to the normal 100 psi (690 kPa) used for regular laminate processing. This can not only produce skins that are more porous than those processed under higher pressures, but also create pillowing or dimpling in the skins (Fig. 9.17), because the skin is supported only at the cell walls. Although the schematic is somewhat exaggerated in showing the amount of pillowing usually experienced, pillowing does create a serious knockdown in mechanical properties, as much as 30 percent in some cases. The amount of pillowing can be reduced, if not eliminated, by using a smaller cell size such as $^{1}/_{8}$ vs. $^{3}/_{16}$ in. (3 vs. 4.8 mm).

Although core migration and crushing can be problems when bonding precured composite

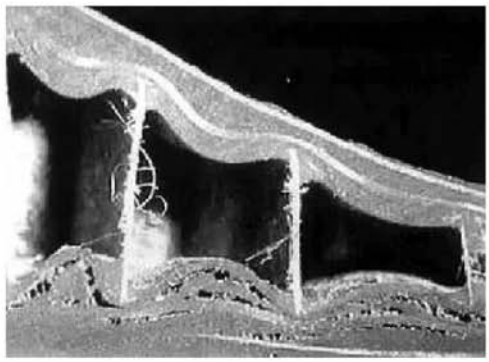
skins, they are even bigger problems with co-cured skins (Fig. 9.18). A considerable amount of work has been done to solve this problem. Potential solutions include: (1) reducing the ramp angle (20 degrees or less is recommended); (2) increasing the core density; (3) using grip, or hold-down, strips to restrain the plies; (4) potting the cells in the ramp area to increase the core rigidity; (5) encapsulating the core with a layer of adhesive prior to cocuring; (6) bonding



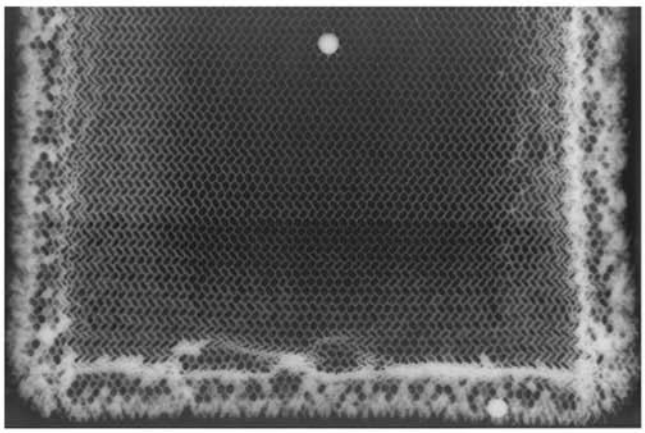
Autoclave pressure vector wants to condense ramps



Top view showing core movement



Section showing distorted plies



X-ray showing condensed cells in ramp

Fig. 9.18 Edge crush in cocured honeycomb panels. **F**, force vector. Source: Ref 23

fiberglass plies into the center of the core (septums) to increase core rigidity; (7) adjusting the temperature and pressure during heat-up; and (8) even using "high-friction" prepregs that minimize ply movement during curing. As the number of these solutions indicates, core migration and crushing are major problems, particularly in cocured assemblies.

There are three basic approaches to producing honeycomb cocured structure. In the first method, both skins are cocured at the same time that they are bonded to the core. Since this process is limited to about 50 psi (345 kPa) autoclave pressure to prevent core crushing, the skins will contain more porosity than skins cured at full autoclave pressure. This process has the shortest cycle time but is the riskiest. The second method consists of precuring one of the skins at full autoclave pressure and then bonding it to the core at the same time that the other skin is cocured. This method takes longer but at least one of the skins should have minimal porosity. In the third method, one skin is precured in an autoclave and then adhesively bonded to the core. Then, in a separate operation, the other skin is cocured and bonded to the core. The main advantage of this third method is that the core is stabilized during the initial bond cycle in which the first precured skin is bonded to the core. This method has been used when core edge migration and crushing are problems. Although this method takes the longest time, it is the least risky approach.

A potential pitfall that can result in unbonds is shown in the data of Fig. 9.19. Although both of

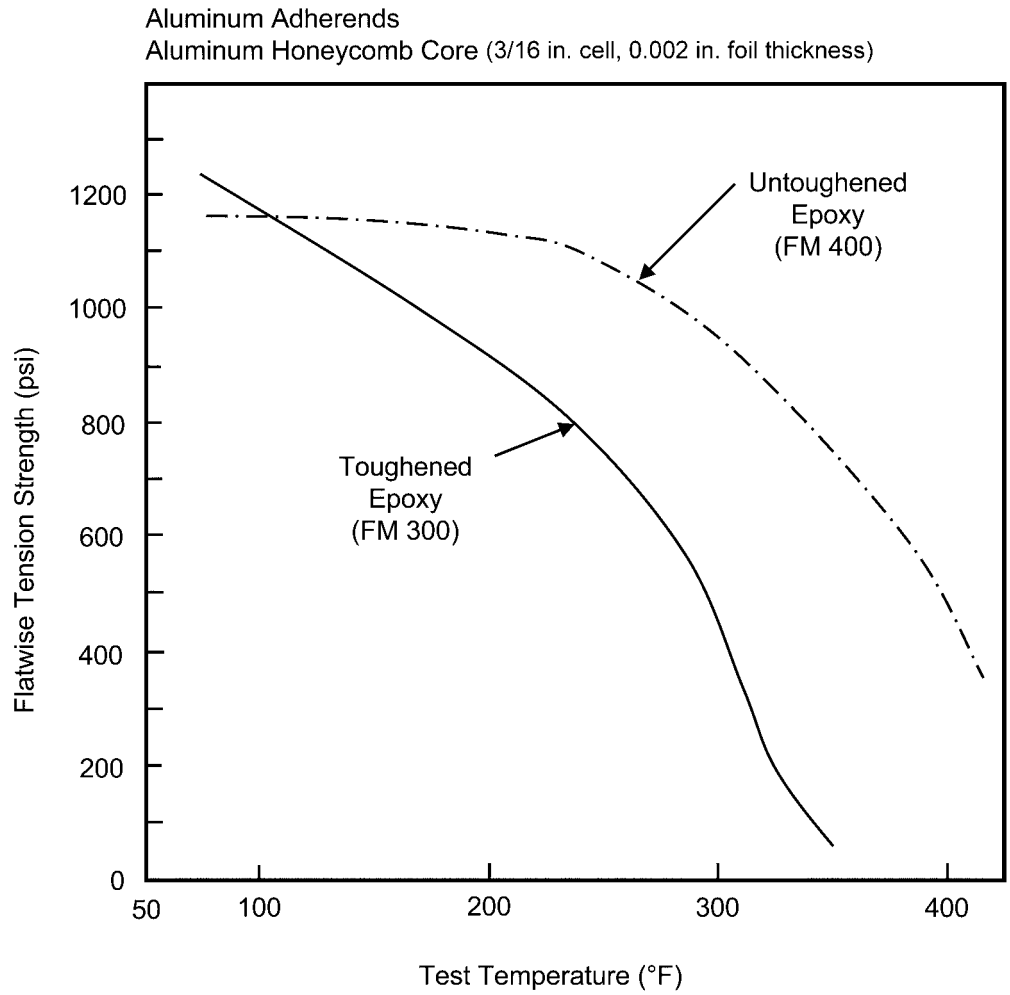


Fig. 9.19 Flatwise tension strength versus test temperature

the adhesives shown are cured at 350 °F (180 °C), the toughened adhesive FM300 has a very low flatwise tension strength at this temperature. If, on completion of the adhesive bond cycle, the pressure is completely vented to facilitate faster autoclave cooling, residual stresses or gas pressure within the cells can push the skins off the core. By comparison, the flatwise tension strength of the untoughened adhesive FM400 is high enough that it will not cause the same problem. In the case of adhesives like FM300, it is wise to keep some pressure on the assembly until it cools down to below 200 °F (90 °C).

Adhesively bonded joints and assemblies are normally nondestructively inspected after all bonding operations are completed. Radiographic and ultrasonic inspection methods are typically used to look for defects in both the bondlines and the honeycomb core portions of the assemblies. In addition, it is common practice to leak-check honeycomb bonded assemblies by immersing the assembly for a short time in a tank of hot water at least 180 °F (80 °C). The hot water heats the residual air inside the honeycomb core, and any leaks can be detected by air bubbles escaping from the assembly.

9.3 Foam Cores

A second type of core material frequently used in adhesively bonded structure is foam core. Although the properties of foam cores are not as good as those of honeycomb core, foam cores are used extensively in such commercial applications as boat building and light aircraft construction. The terms *polymer foam* and *cellular polymer* refer to a class of materials that are two-phase gas-solid systems in which the polymer is continuous and the gaseous cells are dispersed throughout the solid. Polymeric foams can be produced by several methods, including extrusion, compression molding, injection molding, reaction injection molding, and other solid-state methods. Foam cores are made by using a blowing or foaming agent that expands during manufacture to give a porous cellular structure. The cells may be open and interconnected or closed and discrete. Usually, the higher the density, the greater the percentage of closed cells. Almost all foams used for structural applications are classified as closed-cell, meaning that almost all of their cells are discrete. Open-cell foams, while good for sound absorption, are weaker than the higher-density closed-cell foams and also absorb more water. However, water absorption can be problematic in both open- and closed-cell foams. Both uncrosslinked thermoplastic and crosslinked thermoset polymers can be foamed. The thermoplastic foams exhibit better formability, while the thermoset foams exhibit better mechanical properties and higher temperature resistance. Almost any polymer can be made into a foam material by adding an appropriate blowing or foaming agent.

The blowing agents used to manufacture foams are usually classified as either physical or chemical. Physical blowing agents are usually gases, mixed into the resin, that expand as the temperature is increased, while chemical blowing agents are normally powders that decompose on heating to give off gases, usually nitrogen or carbon dioxide. Although there are foams that can be purchased as two-part liquids that expand after mixing for foam-in-place applications, the majority of structural foams are purchased as preexpanded blocks that can be bonded together to form larger sections. Sections may be bonded together using either paste or adhesive film. Sections can also be heat-formed to contour using procedures similar to those used for nonmetallic honeycomb core. Although the uncrosslinked thermoplastic foams are easier to thermoform, many of the thermoset foams are only lightly crosslinked and exhibit some formability. Core densities normally range from about 2 to 40 pcf (32 to 640 kg/m^3). The most widely used structural foams are summarized in Table 9.3. It is important to thoroughly understand the chemical, physical, and mechanical properties of any foam considered for a structural application, particularly with respect to solvent and moisture resistance and long-term durability. Depending on their chemistry, foam core materials can be used in the temperature range 150 to 400 °F (70 to 200 °C).

Polystyrene cores are lightweight, low cost, and easy to sand, but are rarely used in structural applications because of their low mechanical properties. They cannot be used with polyester resins, because the styrene in the resin will dissolve the core; therefore, epoxies are normally employed.

Polyurethane foams are available as either thermoplastics or thermosets, with varying degrees of closed cells. There are polyurethane foams that are available as finished blocks and formulations that can be mixed and foamed in place. Polyurethane foams exhibit only moderate mechanical properties and the resin-to-core

Table 9.3 Characteristics of some foam sandwich materials

Name and type of core	Density, pcf	Maximum temperature, °F	Characteristics
Polystyrene (styrofoam)	1.6–3.5	165	Low-density, low-cost, closed-cell foam capable of being thermoformed. Used for wet or low-temperature lay-ups. Susceptible to attack by solvents.
Polyurethane foam	3–29	250–350	Low- to high-density closed cell foam capable of thermoforming at 425–450 °F. Both thermoplastic and thermoset foams are available. Used for cocured and secondarily bonded sandwich panels with both flat and complex curved geometries.
Polyvinyl chloride foam (Klegecell and Divinycell)	1.8–26	150–275	Low- to high-density foam. Low-density foam can contain some open cells. High-density foam is closed cell. Can be either thermoplastic (better formability) or thermoset (better properties and heat resistance). Used for secondarily bonded or cocured sandwich panels with both flat and complex curved geometries.
Polymethacrylimide foam (Rohacell)	2–18.7	250–400	Expensive high-performance closed-cell foam that can be thermoformed. High-temperature grades (WF) can be autoclaved at 350 °F/100 psi. Used for secondarily bonded or cocured high-performance aerospace structures.

interface bond tends to deteriorate with age, which can lead to skin delaminations. Polyurethane foams can be readily cut and machined to contours, although hot wires should be avoided for cutting since harmful fumes can be released.

Polyvinyl chloride (PVC) foams are among the most widely used core materials for sandwich structures. These foams can be either uncrosslinked (thermoplastic) or crosslinked (thermoset). The uncrosslinked versions are tougher, more damage resistant, and easier to thermoform, while the crosslinked materials have higher mechanical properties, are more resistant to solvents, and have better temperature resistance. However, crosslinked foams are more brittle and more difficult to thermoform than uncrosslinked materials. On the other hand, because they are not highly crosslinked, like normal thermoset adhesives and matrix systems, they can be thermoformed to contours. The crosslinked systems can also be toughened, a process in which some of the mechanical properties of the normal crosslinked systems are traded for some of the toughness of the uncrosslinked materials. The PVC foams are often given a heat stabilization treatment to improve their dimensional stability and reduce the amount of off-gassing during elevated temperature cures. Styrene acrylonitrile foams are also available that have mechanical properties similar to those of crosslinked PVC but have the toughness and elongation of the uncrosslinked PVCs. Patterns of grooves can be scribed in the surfaces of foams to act as infusion aids for resin transfer molding.

Polymethylmethacrylimides are lightly crosslinked closed-cell foams that have excellent mechanical properties and good solvent and heat resistance. They can be thermoformed to contours and are capable of withstanding autoclave curing with prepregs. These foams are expensive and are usually reserved for high-performance aerospace applications.

9.3.1 Syntactic Core

Syntactic core consists of a matrix such as epoxy that is filled with hollow spheres such as glass or ceramic microballoons, as shown in Fig. 9.20. Syntactics can be supplied as pastes for filling honeycomb core or as B-staged formable sheets for core applications. Syntactic cores generally have much higher density than honeycomb, with densities ranging from 30 to 80 pcf (480 to 1300 kg/m^3). The higher the percentage of the microballoon filler, the lighter and weaker the core becomes. Syntactic core sandwiches are used primarily for thin secondary composite structures that would be impractical or too costly to machine honeycomb to thin gages. When cured against precured composite details, syntactics do not require an adhesive. However, if the syntactic core is already cured and requires adhesive bonding, it should be scuff-sanded and then cured with a layer of adhesive.

Glass microballoons are the most prevalent filler used in syntactic core, ranging in diameter from 0.04 to 13.78 mil (1 to 350 μm) but typically from 2 to 4 mil (50 to 100 μm). Glass microballoons have specific gravities 18 times lower than those of fillers like calcium carbonate ($CaCO_3$). Ceramic microballoons have properties similar to those of glass but better elevated-temperature properties, while polymeric microballoons such as phenolic are lower in density than either glass

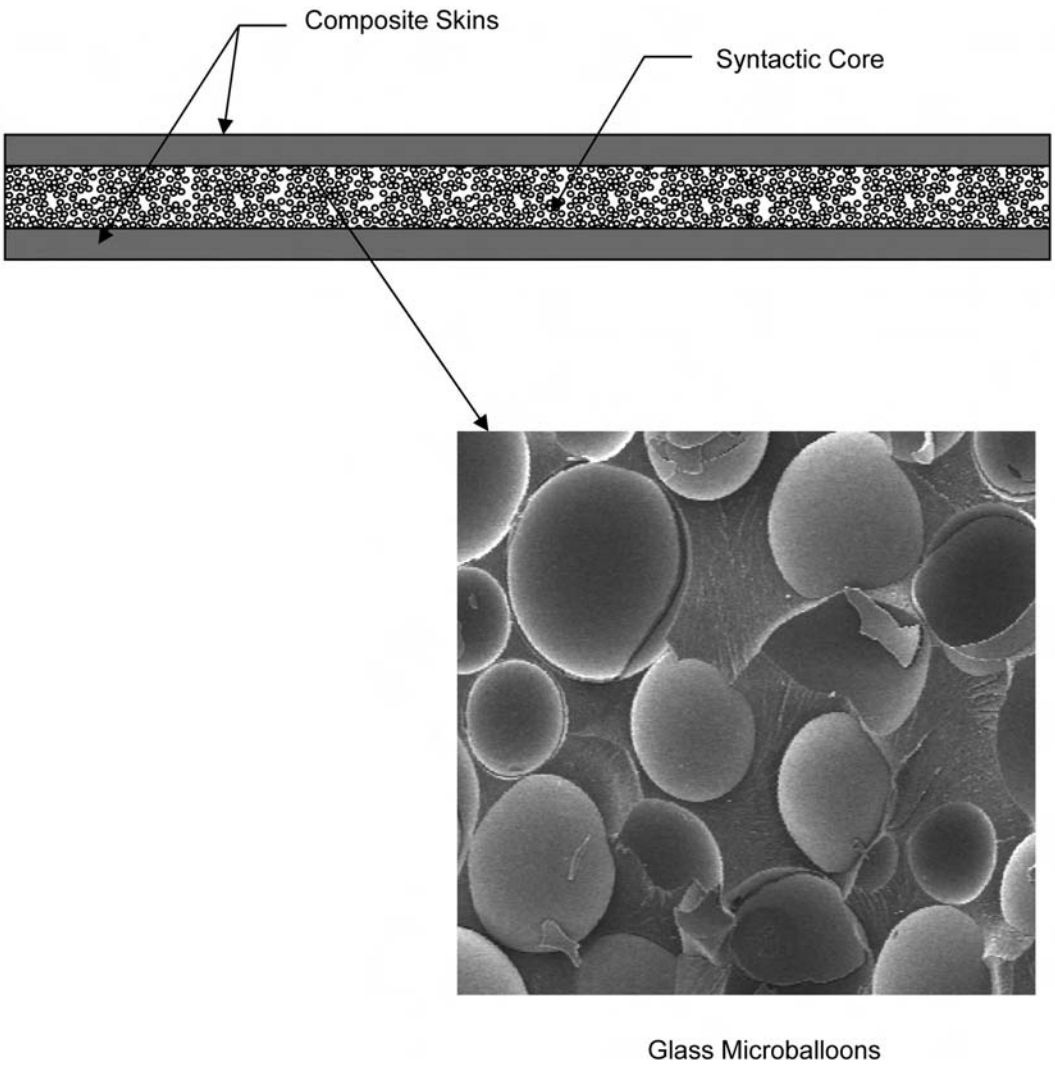


Fig. 9.20 Syntactic core construction

or ceramic but have lower mechanical properties. The properties of the microballoons can be improved by increasing the wall thickness at the expense of higher densities. In most commercial applications, the microballoons have a size distribution to improve the packing density. Packing densities as high as 60 to 80 percent have been achieved.

9.4 Integrally Cocured Unitized Structure

Cocuring is a process in which uncured composite plies are cured and bonded simultaneously during the same cure cycle either to core materials or to other composite parts. Integrally cocured or unitized structure is another manufacturing approach that can greatly reduce the part count and final assembly costs for composite structures. An example of a cocured control surface is shown in Fig. 9.21. In this structure, the ribs were cocured to the lower skin. The upper skin was cured at the same time, but a release film was used so that it could be removed after cure to allow the installation of a metallic hinge fitting.

In cocuring, pressure is provided both by the autoclave and by the expansion of aluminum substructure blocks, as shown in Fig. 9.22.

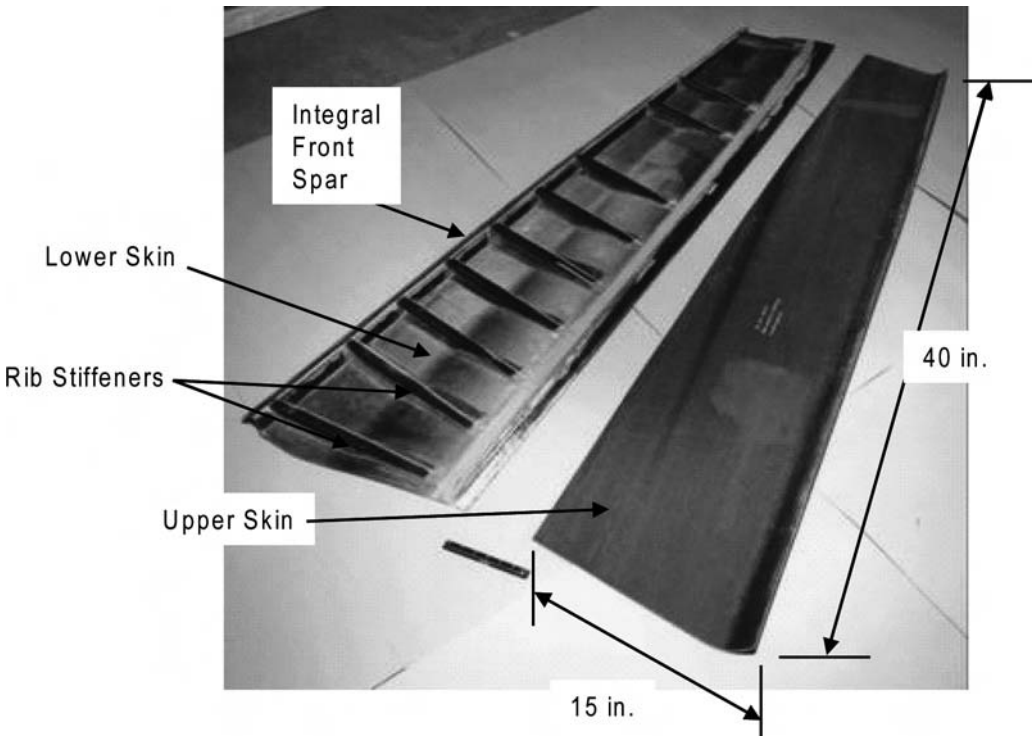


Fig. 9.21 Cocured unitized control surface. Source: The Boeing Company

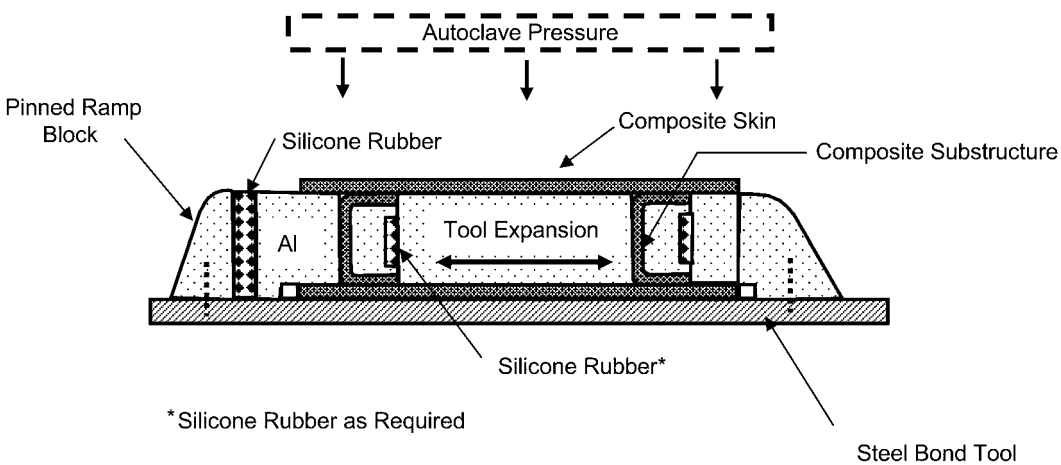


Fig. 9.22 Pressure application for unitized cocured structure

The autoclave applies pressure to the skins and rib caps, while expansion of the aluminum substructure blocks applies pressure to the rib webs. If required, the expansion of the aluminum substructure blocks can be supplemented by the presence of silicone rubber intensifiers.

The advantages of this type of structure are obvious: fewer detail parts, fewer fasteners, and fewer problems with part fit-up on final assembly. The main disadvantages are the cost and accuracy of the tooling required and the complexity of the lay-up, which requires a highly skilled

workforce. To help control tool accuracy, the substructure tooling is usually machined as a single block (Fig. 9.23) and then sectioned into the individual tooling details.

The process flow for this type of structure is shown in Fig. 9.24. The skins, which are unidirectional prepreg, are laid up on separate facility tools and hot debulked. Hot debulking is used to

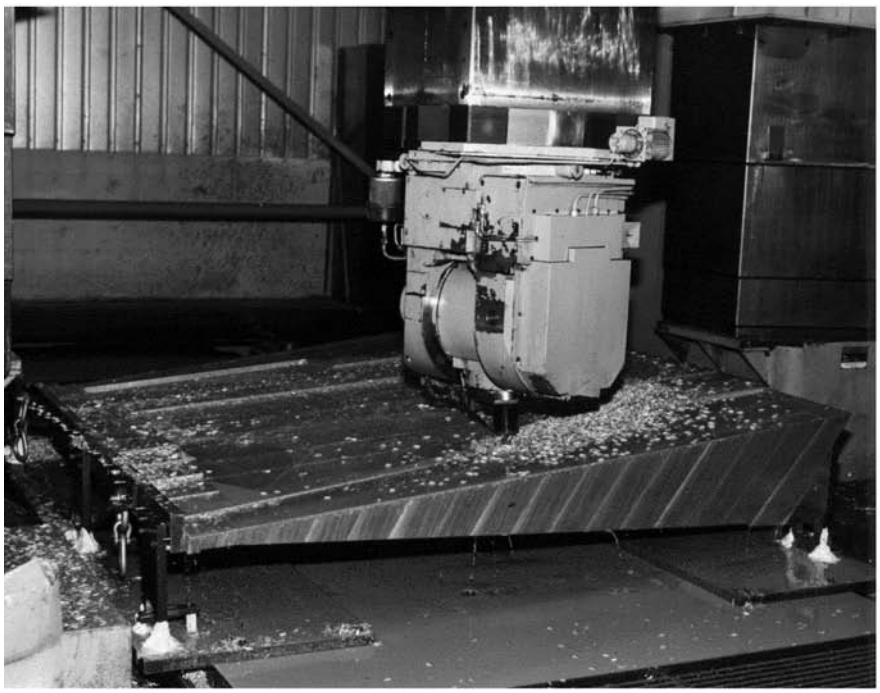


Fig. 9.23 Machining substructure spar mandrels and filler blocks. Photo source: The Boeing Company

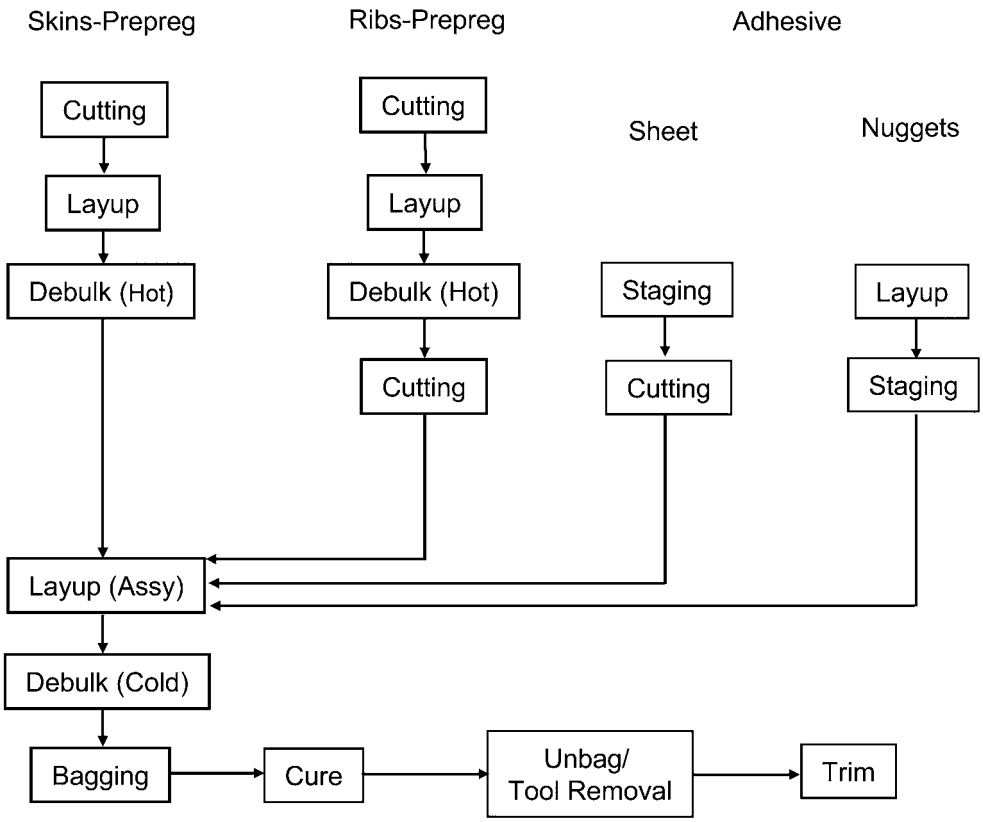


Fig. 9.24 Key processing steps for cocured design

consolidate the lay-up to near-net thickness to aid in tool location. At the same time, the rib plies, made from woven prepreg, are laid up on their individual form blocks and hot debulked. Film adhesive sheet is used between the rib flanges and the lower skin for improved joint strength. It is cut and staged. In addition, twisted film to fill the intersection between the ribs and the lower skin (Fig. 9.25) is cut, twisted, and staged. As shown in the figure, it is important to overstuff the joint at the stiffener-to-skin bond intersection to prevent ply distortion during cure. After all of the components are prepared, the lay-up is assembled (Fig. 9.26) and then autoclave-cured. For larger assemblies where the weight of the tooling becomes an issue, it is possible to use hollow tooling details, as shown in Fig. 9.27.

One potential problem with this type of structure is spring in. As shown in Fig. 9.28, both the spar cap and the web will spring in during cool-down after cure. The web spring in can largely be eliminated by placing a couple of plies on the backside to support the web. However, the spar cap spring in cannot be counteracted by increasing the angle on the tooling block, because that would cause an indentation in the concurrently cured upper skin. It is therefore necessary to shim this joint during final assembly.

Also frequently cocured are skins with cocured hats, such as the one shown during lay-up in Fig. 9.29. Although matched die tooling can be used to make this type of structure, the more common practice is to use localized tooling only at the hat stiffener locations. A typical bagging arrangement, shown in Fig. 9.30, contains an elastomeric mandrel to support the hat during cure, an elastomeric pressure intensifier to ensure that the radii obtain sufficient pressure, and some thin plastic shims to minimize mark-off on the skin from the pressure intensifier. The mandrels are solid elastomer or are an elastomer reinforced with carbon or glass cloth. It is important to keep some autoclave pressure on the assembly during cool-down after curing. If the pressure is dumped immediately after cure, the pressure of

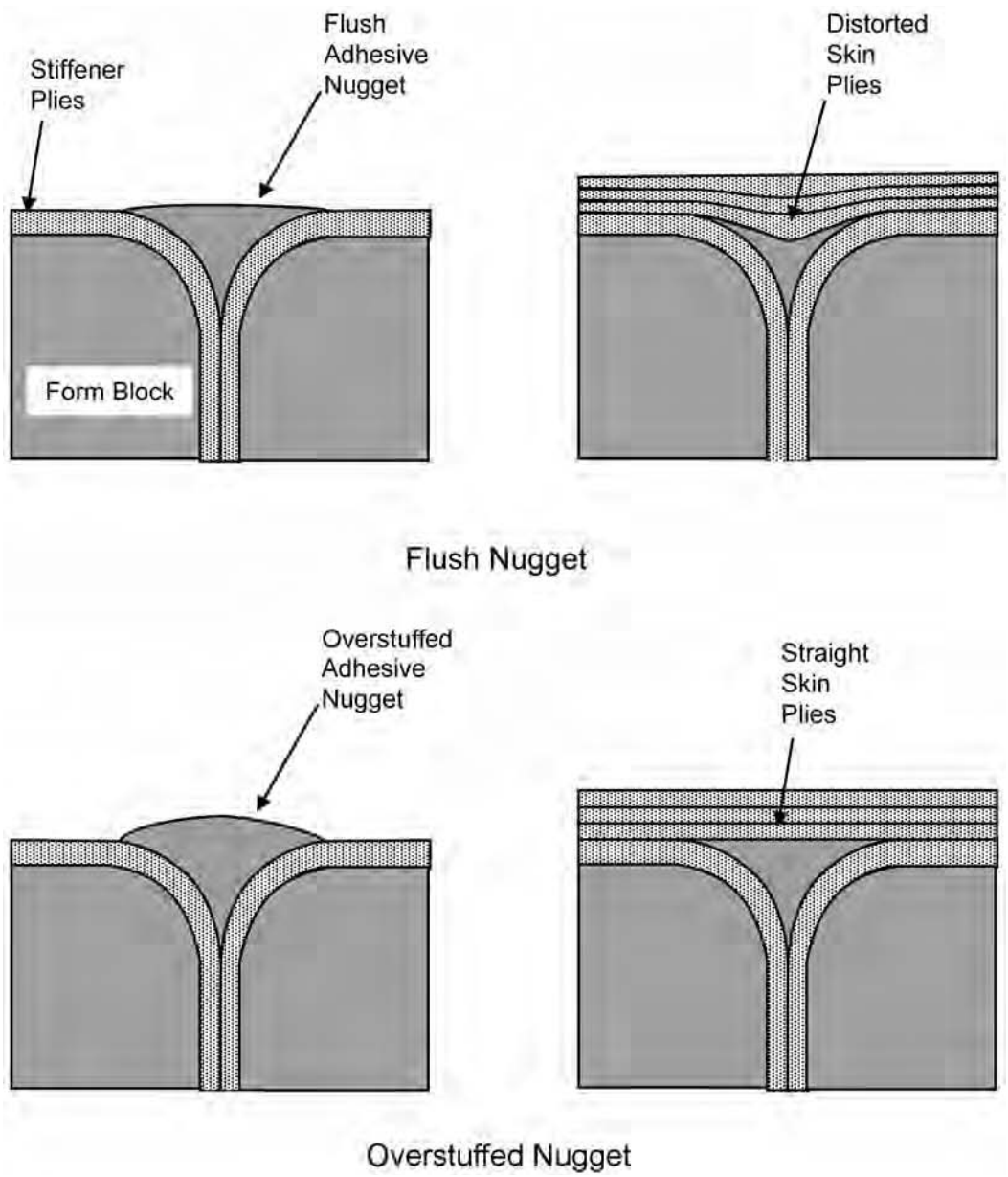


Fig. 9.25 Adhesive nugget application

the elastomeric inset can push the hat section off the skin and create cracks like those shown in Fig. 9.31. If the stiffeners require exact location, it may be necessary to use female cavity tooling similar to that shown in Fig. 9.32.

A key design detail for cocured stiffeners is the stiffener terminations. Since the bond holding the stiffener to the skin is essentially a resin or an adhesive bond, any peel loads induced at the stiffener ends could cause the bondline to "unzip" and fail. The most prevalent method for preventing this involves installing mechanical fasteners near the stiffener terminations. The hat can also be made thicker at the ends and scarfed to further help reduce the tendency for bondline peeling. Other methods include stitching and pinning in the transverse "Z" direction. However, stitching of pregreg lay-ups is expensive and can

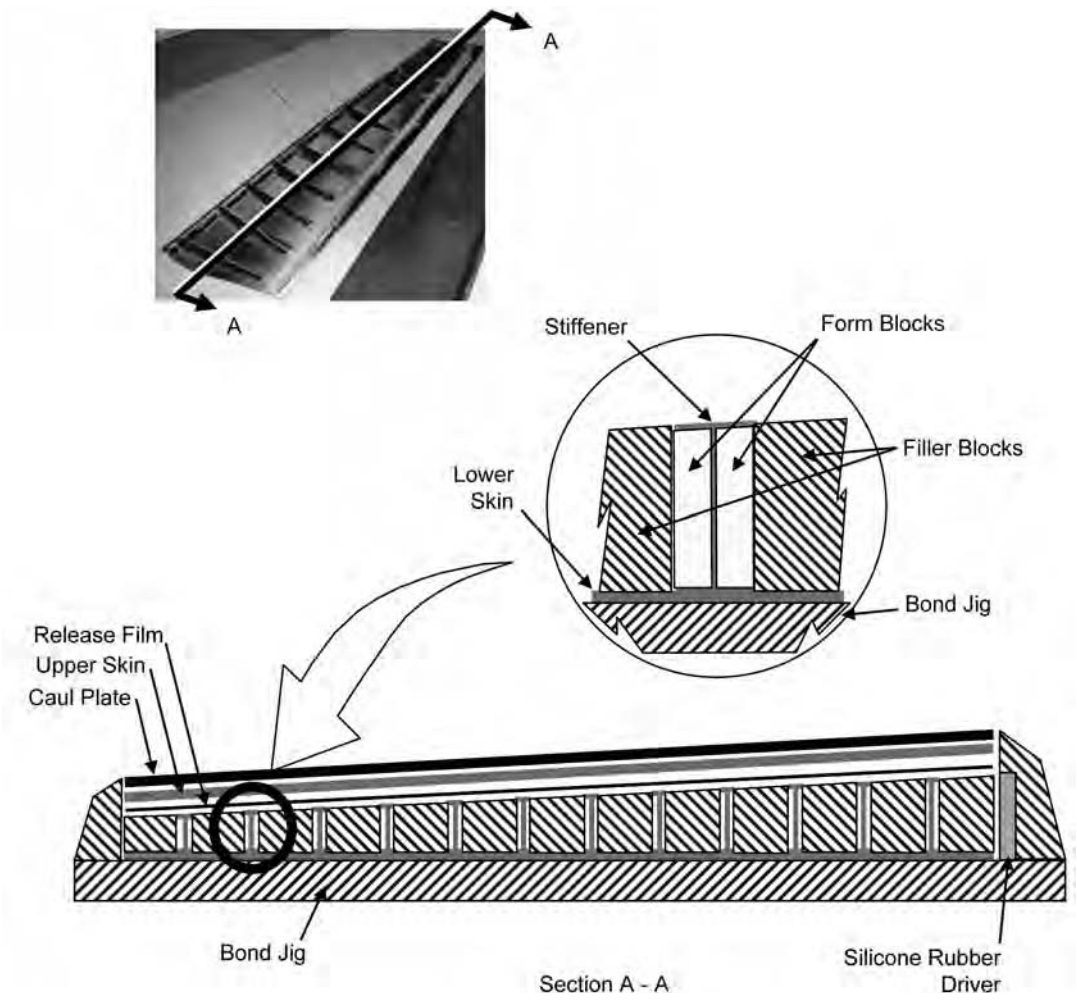


Fig. 9.26 Cocured unitized control surface tooling approach. Photo source: The Boeing Company

damage the fibers. Z-pinning, shown in Fig. 9.33, is a technology in which small-diameter precured carbon pins are driven through the prepreg lay-up before cure with an ultrasonic gun.

Cobonding is a hybrid process combining cocuring and adhesive bonding. As shown in the joint in Fig. 9.34, a series of precured stiffeners are adhesive-bonded to a skin at the same time that the skin is cured. The surfaces of the precured composite parts must, of course, be prepared for adhesive bonding, just as in any other adhesive bonding process. The advantage of this process is that, in certain situations, the amount of tooling required for the curing operation can be reduced.

Cocured unitized structure is a trade-off. The advantages include fewer parts, fewer fasteners, and better fit-up at assembly. These advantages must be weighed against the additional tooling costs and span time required to produce the tooling, the lay-up costs, the personnel requirements for large complex assemblies, and material outtime issues if the lay-up requires a long time.

REFERENCES

1. "HexWeb Honeycomb Sandwich Design Technology," Hexcel Composites, 2000
2. J. Kindinger, Lightweight Structural Cores, *ASM Handbook,* Vol 21, *Composites*, ASM International, 2001
3. F.C. Campbell, Secondary Adhesive Bonding of Polymer-Matrix Composites, *ASM*

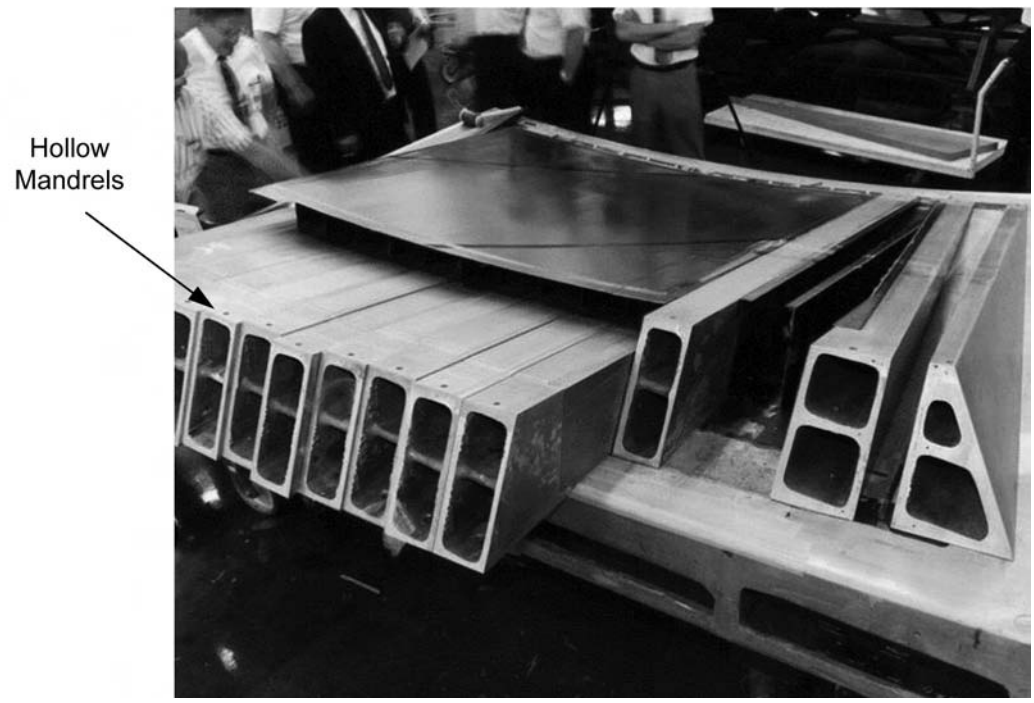


Fig. 9.27 Hollow mandrels to reduce tool mass. Source: The Boeing Company

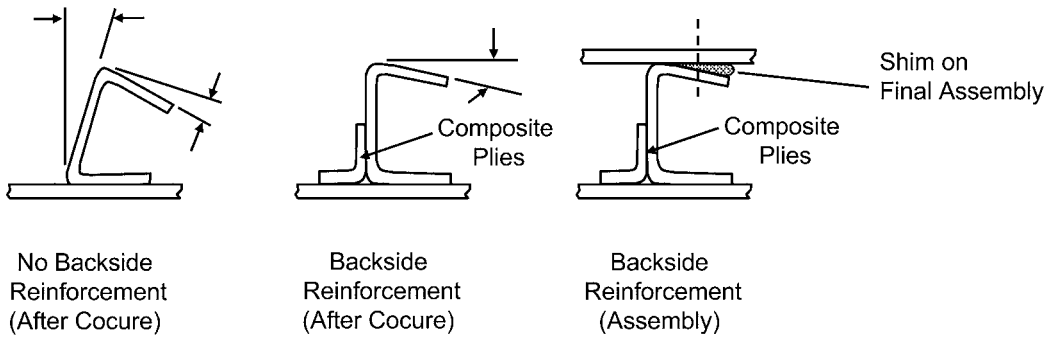


Fig. 9.28 Spring in for cocured joints

Handbook, Vol 21, *Composites*, ASM International, 2001

4. T. Bitzer, *Honeycomb Technology—Materials, Design, Manufacturing: Applications and Testing*, Chapman & Hall, 1997
5. S. Black, Improved Core Materials Lighten Helicopter Airframes, *High-Perform. Compos.*, May 2002, p 56–60
6. S. Zeng, J.C. Seferis, K.J. Ahn, and C.L. Pederson, Model Test Panel for Processing and Characterization Studies of Honeycomb Composite Structures, *J. Adv. Mater.*, January 1994, p 9–21

SELECTED REFERENCES

- T.H. Brayden and D.C. Darrow, Effect of Cure Cycle Parameters on 350 °F Cocured Epoxy Honeycomb Panels, *34th International SAMPE Symposium*, 8–11 May 1989, p 861–874

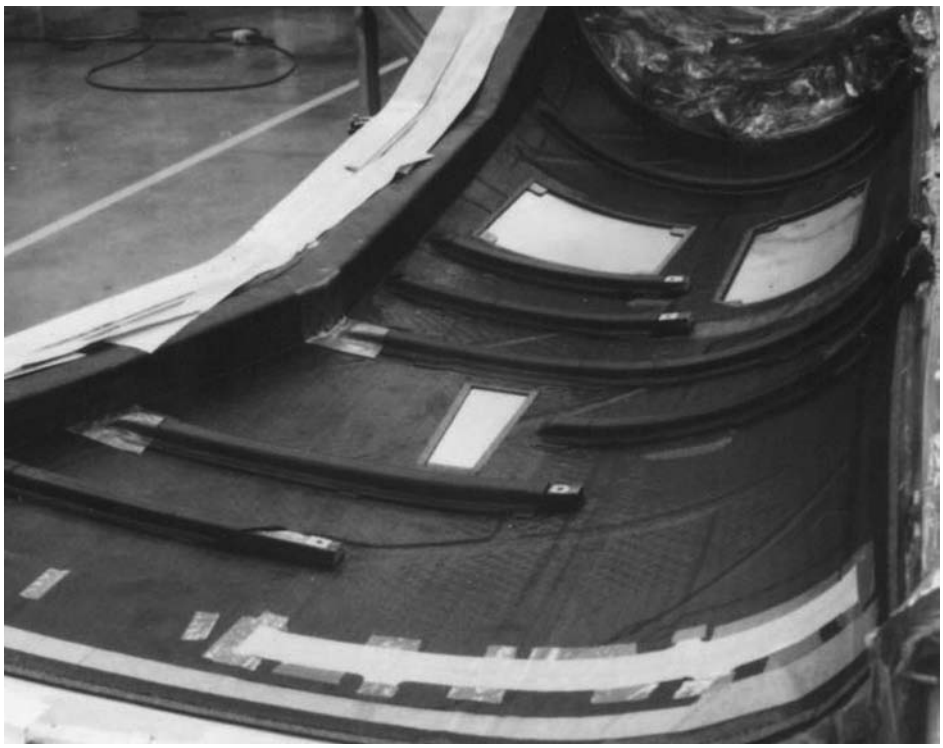


Fig. 9.29 Lay-up of a fuselage panel with cocured hats. Source: The Boeing Company

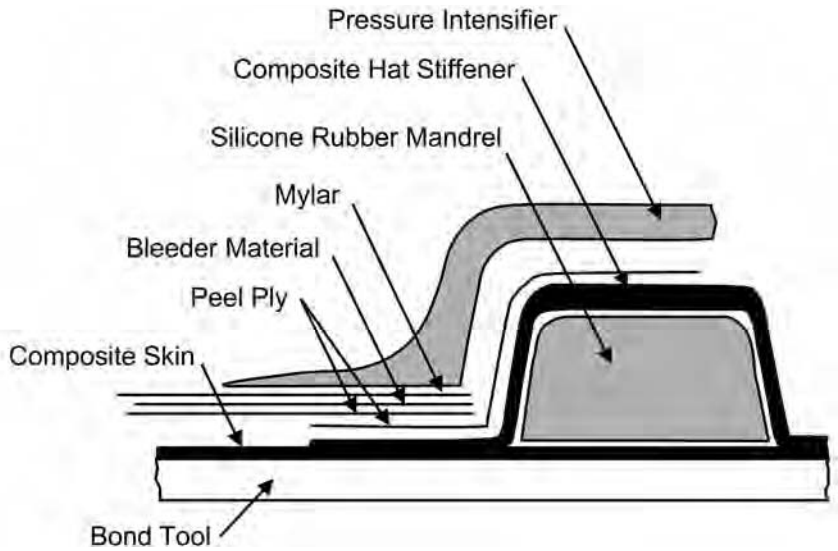


Fig. 9.30 Bagging procedure for a cocured hat section

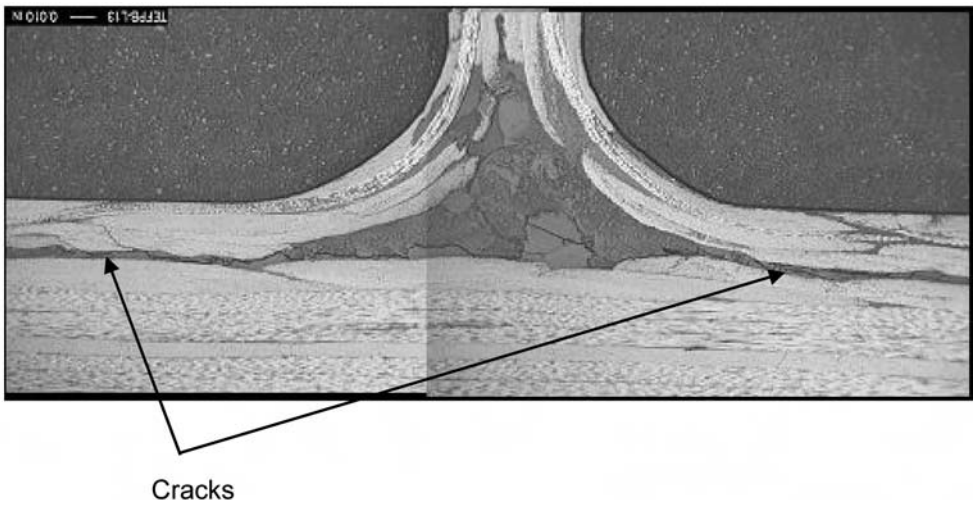


Fig. 9.31 Cracks at a stiffener leg

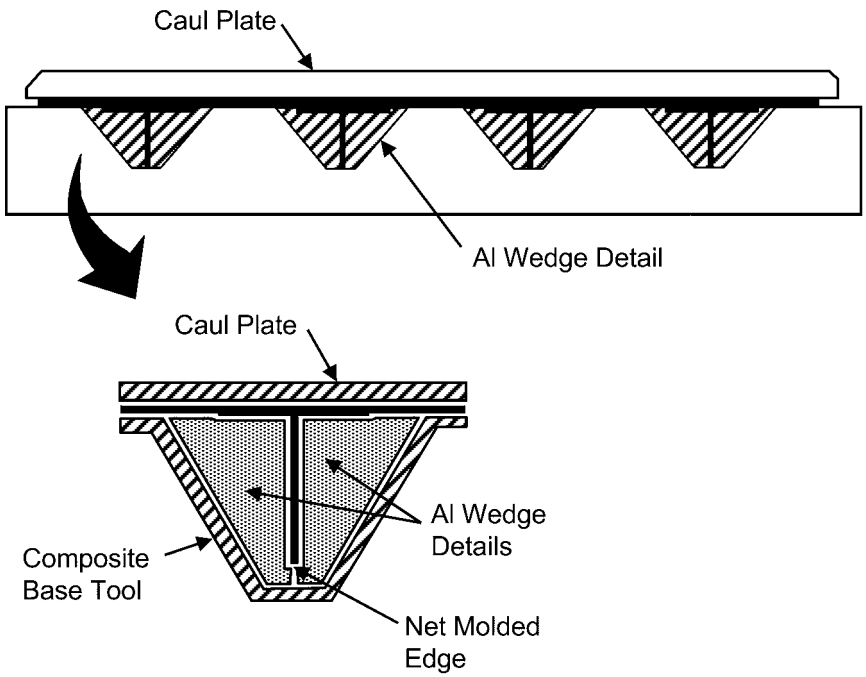


Fig. 9.32 Cavity tool for precise location of substructure. Al, aluminum

- J. Corden, Honeycomb Structures, *ASM Engineered Materials Handbook*, Vol 1, *Composites*, ASM International, 1987
- D. Danver, Advancements in the Manufacture of Honeycomb Cores, *42nd International SAMPE Symposium*, 4–8 May 1997, p 1531–1542
- L. Gintert, M. Singleton, and W. Powell, "Corrosion Control for Aluminum Honeycomb Sandwich Structures," *33rd International SAMPE Technical Conference*, 5–8 Nov 2001
- B. Harmon, J. Boyd, and B. Thai, "Advanced Products Designed to Simplify Co-Cure

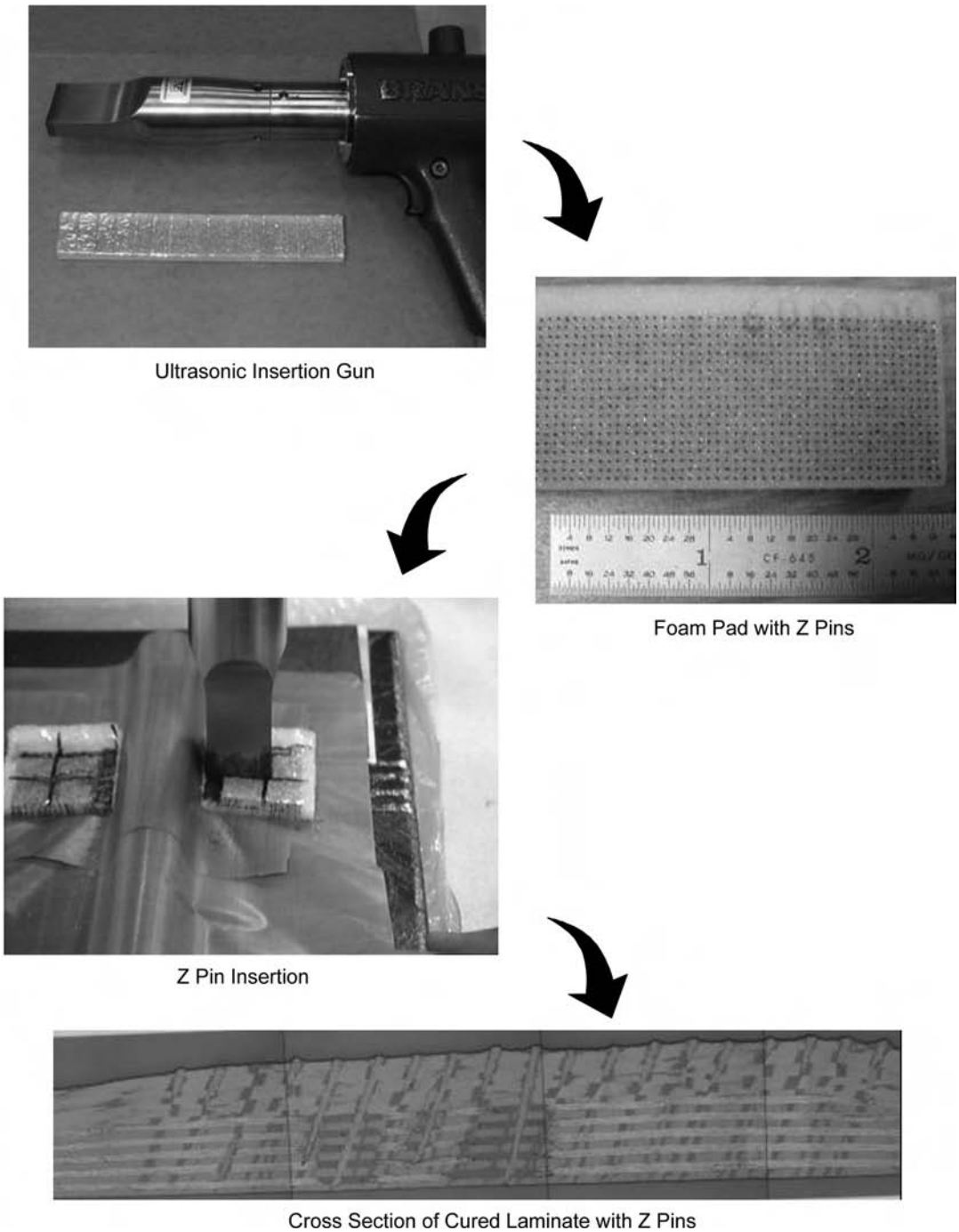
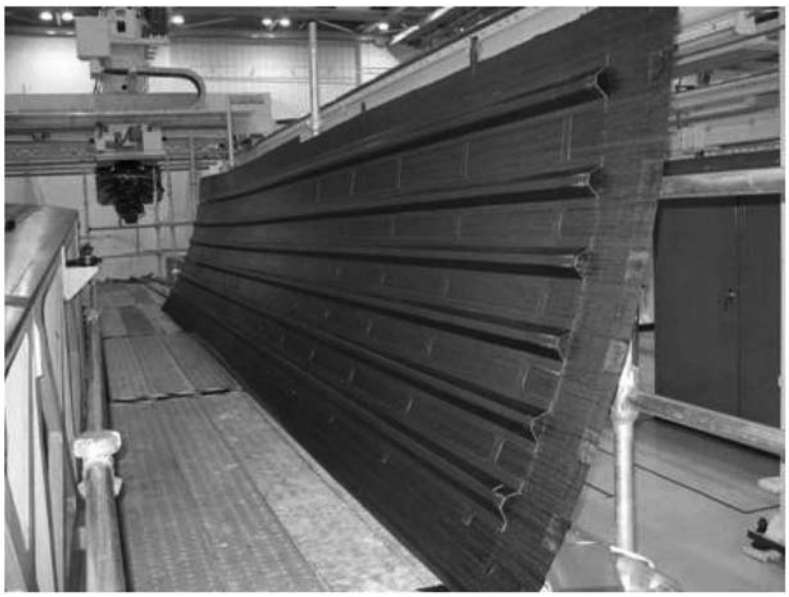


Fig. 9.33 Principle of Z pin reinforcement

Over Honeycomb Core," *33rd International SAMPE Technical Conference*, 5–8 Nov 2001

I.L. Herbeck, M. Kleinberg, and C. Schoppinger, "Foam Cores in RTM Structures: Manufacturing Aid or High-Performance Sandwich?" *23rd International Europe Conference of SAMPE*, 9–11 Apr 2002, p 515–525



Large skins are often better candidates for cobonding rather than cocuring.

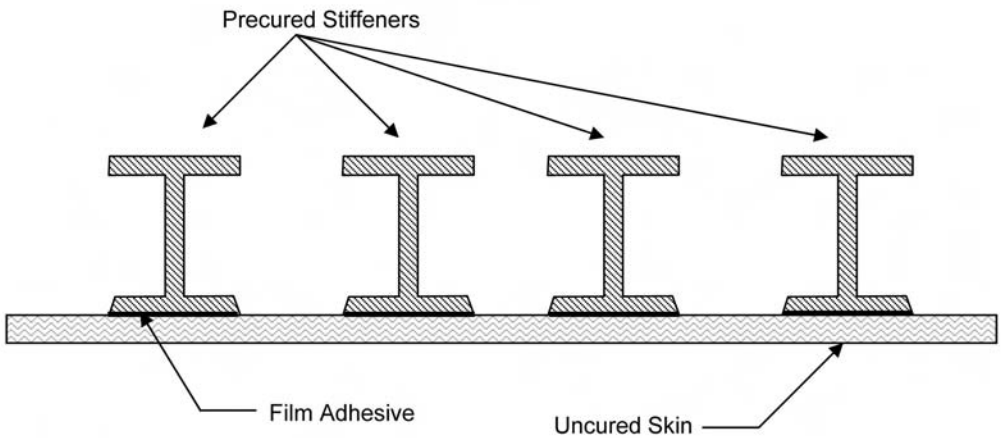


Fig. 9.34 Principle of cobonding. Photo source: The Boeing Company

- "HexWeb Honeycomb Selector Guide," Hexcel Composites, 1999
- H.M. Hsiao, S.M. Lee, R.A. Buyny, and C.J. Martin, "Development of Core Crush Resistant Prepreg for Composite Sandwich Structures," *33rd International SAMPE Technical Conference*, 5–8 Nov 2001
- H.Y. Loken, D.A. Nollen, M.W. Wardle, and G.E. Zahr, "Water Ingression Resistant Thin Faced Honeycomb Cored Composite Systems with Facesheets Reinforced with Kevlar Aramid Fiber and Kevlar with Carbon Fibers," E.I. DuPont de Nemours & Company
- G.F. Moors, A.A. Arseneau, L.W. Ashford, and M.K. Holly, "AV-8B Composite Horizontal Stabilator Development," *5th Conference on Fibrous Composites in Structural Design*, 27–29 Jan 1981
- T.C. Radtke, A. Charon, and R. Vodicka, "Hot/Wet Environmental Degradation of Honeycomb Sandwich Structure Representative of F/A-18: Flatwise Tension Strength," Report

DSTO-TR-0908, Australian Defence Science & Technology Organization (DSTO)

- D.J. Renn, T. Tulleau, J.C. Seferis, R.N. Curran, and K.J. Ahn, Composite Honeycomb Core Crush in Relation to Internal Pressure Measurement, *J. Adv. Mater*., October 1995, p 31–40
- J.E. Shafizadeh and J.C. Seferis, The Cost of Water Ingression on Honeycomb Repair and Utilization, *45th International SAMPE Symposium* 21–25 May 2000, p 3–15
- T.P. Stankunas, D.M. Mazenko, and G.A. Jensen, Cocure Investigation of a Honeycomb Reinforced Spacecraft Structure, *21st International SAMPE Technical Conference*, 25–28 Sept 1989, p 176–188
- J.C. Watson and D.L. Ostrodka, "AV-8B Forward Fuselage Development," *5th Conference on Fibrous Composites in Structural Design*, 27–29 Jan 1981
- E. Weiser, F. Baillif, B.W. Grimsley, and J.M. Marchello, High Temperature Structural Foam, *43rd International SAMPE Symposium*, 31 May–4 June 1998, p 730–740
- S. Whitehead, M. McDonald, and R.A. Bartholomeusz, "Loading, Degradation and Repair of F-111 Bonded Honeycomb Sandwich Panels—A Preliminary Study," Report DSTO-TR-1041, Australian Defence Science & Technology Organization (DSTO)
- S. Zeng, J.C. Seferis, K.J. Ahn, and C.L. Pederson, Model Test Panel for Processing and Characterization Studies of Honeycomb Composite Structures, *J. Adv. Mater.*, January 1994, p 9–21

Copyright © 2010, ASM International®
All rights reserved.
www.asminternational.org

CHAPTER 10

Discontinuous-Fiber Composites

DISCONTINUOUS-FIBER COMPOSITES are used where the higher strength and stiffness of continuous-fiber composites are not required, as they are much less expensive to manufacture. Manufacturing methods such as spray-up, compression and transfer molding, reaction injection molding, and injection molding are much cheaper than the processes used for continuous-fiber composites. Some of these methods are high-volume processes capable of producing millions of parts per year, while others are limited to much smaller quantities.

The two main factors that determine the strength and stiffness of composites are fiber length and orientation. In theory, a discontinuous-fiber composite with a sufficient fiber length that is perfectly oriented will approach the strength and stiffness of a continuous-fiber composite. In reality, it is extremely difficult to control the orientation in discontinuous-fiber composites. During processing, resin flow fronts push the fibers around, causing misorientation. In addition, some processes, such as injection molding, mechanically fracture the fibers, resulting in fiber lengths that are shorter than the starting lengths. Thus, discontinuous or short-fiber composites cannot obtain the strength and stiffness properties of continuous-fiber composites. However, they can be used to improve significantly both the strength and the stiffness of unreinforced polymers, as shown for the epoxy and nylon matrices in Table 10.1.

Table 10.1 Glass-filled epoxy and nylon strength and stiffness

Property	Unfilled epoxy	Glass-filled epoxy, 35%	Unfilled nylon	Glass-filled nylon, 35%	Glass-filled nylon, 60%
Density, g/cc	1.25	1.90	1.15	1.62	1.95
Tensile strength, ksi	10.0	43.5	11.9	29.0	42.0
Tensile modulus, msi	0.50	3.63	0.42	2.10	3.16
Specific tensile strength, σ/ρ	0.055	0.16	0.082	0.16	0.149
Specific tensile modulus, E/ρ	2.8	8.26	2.52	8.26	11.18

10.1 Fiber Length and Orientation

For a single fiber embedded in a matrix, as shown in Fig. 10.1, the stress applied to the matrix is transferred to the fiber by shear across the interface. The matrix and the fiber will experience different tensile strains because their moduli are different. In the region near the fiber ends, the strain in the fiber will be less than that in the matrix. As a result of this strain difference, shear stresses are induced around the fibers in the direction of the fiber axis, and the fiber is stressed in tension. The analytical stress distribution along a fiber aligned parallel to the loading direction of the matrix is shown in Fig. 10.2. The tensile stress is zero at the fiber ends and is maximum at the center of the fiber. By comparison, the shear stress around the fiber is maximum at the fiber ends and, for a sufficiently long fiber, falls to zero at the center. It is the variation of shear stress that causes the buildup of tensile stress in the fiber. To achieve a high degree of reinforcing efficiency, a strong interfacial bond is required. To achieve full stress in the fiber, the fiber length must be at least equal to what is known as the *critical fiber length* l_c. The critical fiber length is the minimum fiber length for a given diameter that will allow tensile failure of the fiber rather than shear failure of the interface

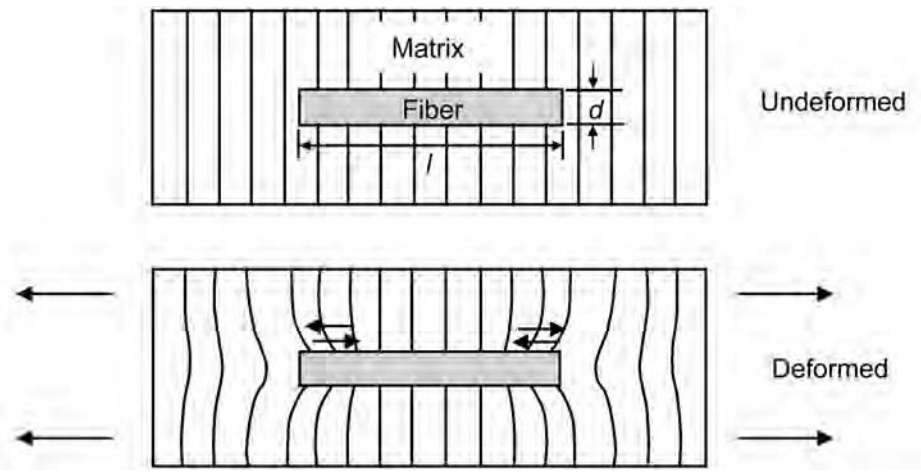


Fig. 10.1 Effect of deformation on strain around a short fiber. Source: Ref 1

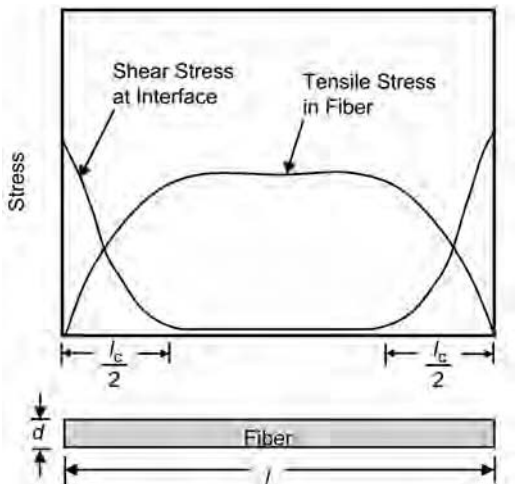


Fig. 10.2 Tensile and shear stresses for short fiber. Source: Ref 1

or matrix. For a fiber with a tensile strength of σ_{tu} and a diameter of d_f, and a fiber-to-matrix interface bond with a shear strength of τ_i, the critical fiber length l_c can be calculated from:

$$l_c = \frac{\sigma_{tu}}{2\tau_i} d_f \qquad \text{(Eq 10.1)}$$

As the interfacial bond strength τ_i increases, the critical fiber length l_c decreases.

The effects of fiber length on failing stress are shown in Fig. 10.3. For $l_f < l_c$, failure will occur either at the fiber-to-matrix interfacial bond or in the matrix before the fiber reaches its ultimate strength. For $l_f > l_c$, the maximum fiber strength will be obtained over much of its length and the fiber will fail before the matrix. However, over a distance $l_c/2$ from each end, the fiber will not obtain its ultimate strength. For effective fiber reinforcement in which the fibers reach their full strength potential, the fiber length l_f needs to be significantly greater than the critical fiber length l_c. While discontinuous-fiber composites are not as strong as continuous-fiber composites, when $l_f > 5\ l_c$, more than 90 percent of strengthening can be achieved with discontinuous fibers, as shown in Fig. 10.4, if the alignment is perfect.

The fiber length and orientation obtained in a discontinuous-fiber composite are dependent on both the material selected and the manufacturing process used to produce the part. For most processes the fiber orientation is random, and it can be hard to predict and control. For example, liquid flow fronts during processing can carry short fibers with them, resulting in either desirable or undesirable orientations. The changes in fiber orientation as a result of shear and elongation flow are shown schematically in Fig. 10.5. Misorientation lowers the strength and stiffness, as shown for the short-fiber reinforced epoxies in Fig. 10.6. In addition, where two flow fronts come together and solidify, they can produce planes of weakness called *knit lines*. Furthermore, processes that contain significant shear forces, such as injection molding, normally fracture the fibers and thus produce fibers shorter than their starting lengths.

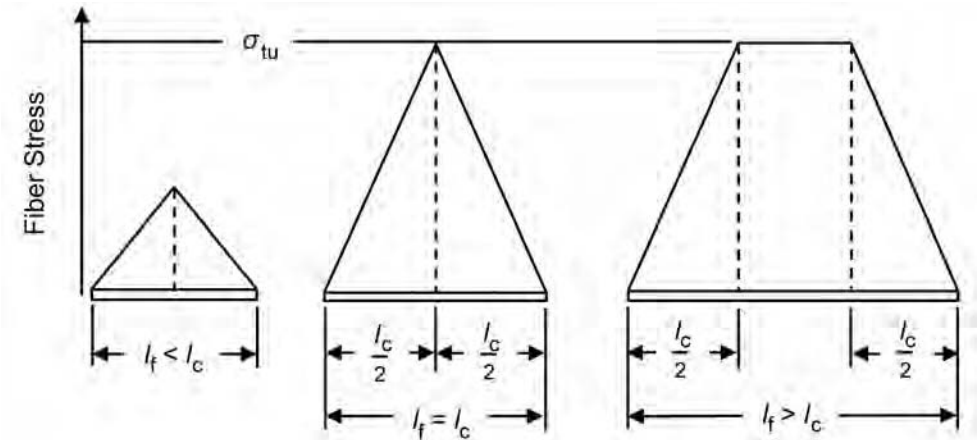


Fig. 10.3 Effect of critical fiber length on stress of discontinuous fiber

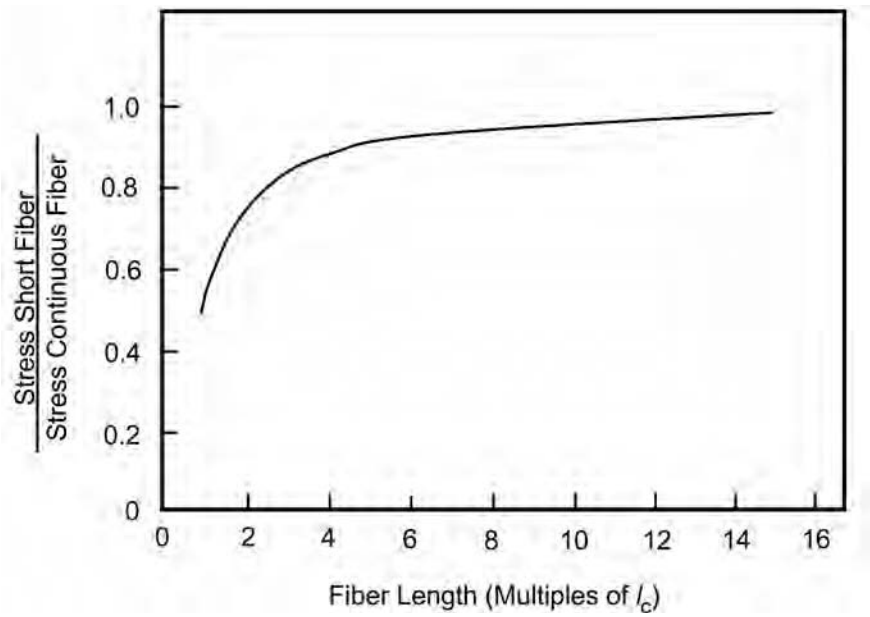


Fig. 10.4 Effect of fiber length on tensile strength. Source: Ref 1

10.2 Discontinuous-Fiber Composite Mechanics

The elastic properties of a unidirectional (zero degrees) discontinuous-fiber lamina or ply (Fig. 10.7a) can be calculated by using the Halpin-Tsai equations:

Longitudinal modulus $$E_{11} = \frac{1 + 2\left(l_f / d_f\right)\eta_L v_f}{1 - \eta_L v_f} E_m \quad \text{(Eq 10.2)}$$

Transverse modulus $$E_{22} = \frac{1 + 2\eta_T v_f}{1 - \eta_T v_f} E_m \quad \text{(Eq 10.3)}$$

Shear modulus $$G_{12} = G_{21} = \frac{1 + \eta_G v_f}{1 - \eta_G v_f} G_m \quad \text{(Eq 10.4)}$$

Poisson's ratio $$\upsilon_{12} = \upsilon_f v_f + \upsilon_m v_m$$
$$\upsilon_{21} = \frac{E_{22}}{E_{11}} \upsilon_{12} \quad \text{(Eq 10.5)}$$

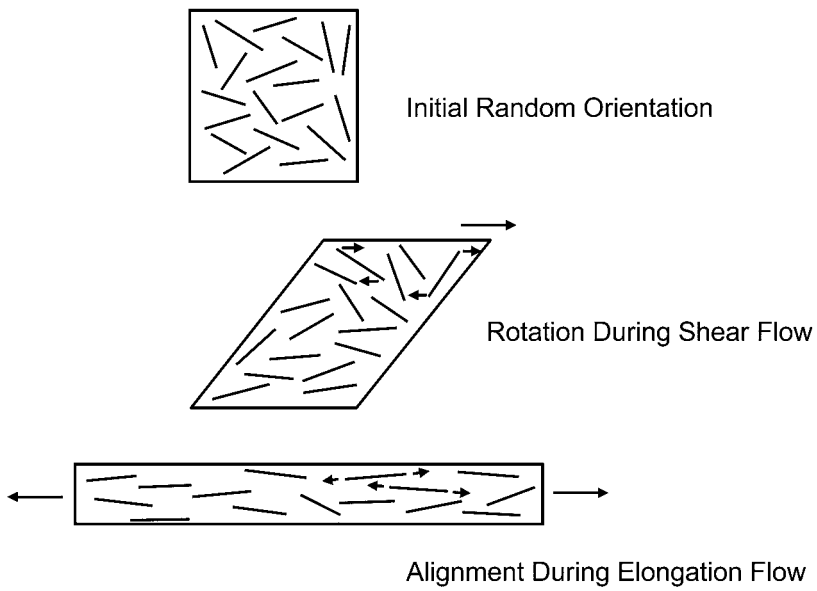


Fig. 10.5 Change in fiber orientation during flow. Source: Ref 2

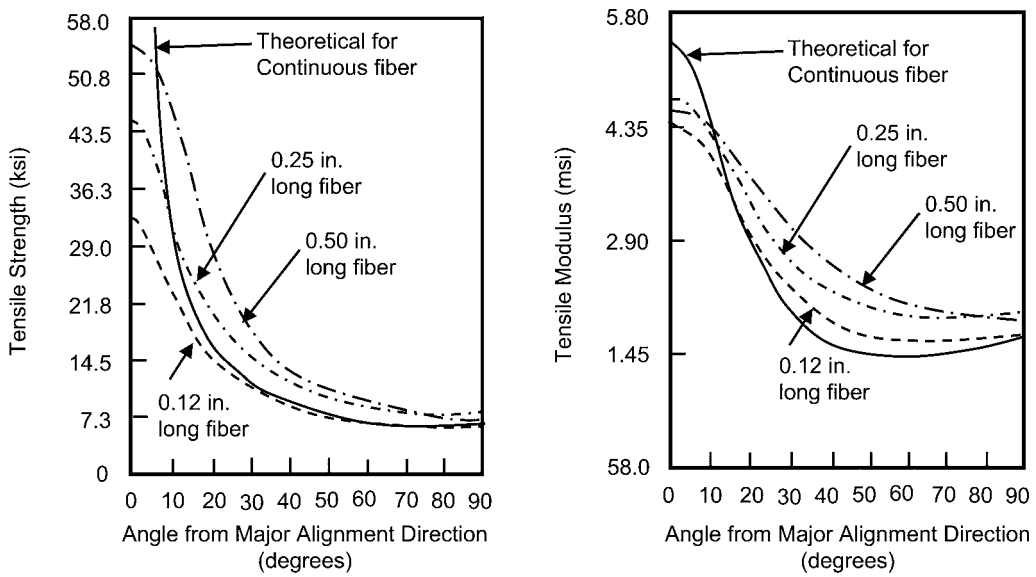


Fig. 10.6 Strength and modulus as functions of load alignment. Source: Ref 3, 4, 5

where:

$$\eta_L = \frac{\left(E_f/E_m\right)-1}{\left(E_f/E_m\right)+2\left(l_f/d_f\right)} \qquad \text{(Eq 10.6)}$$

$$\eta_T = \frac{\left(E_f/E_m\right)-1}{\left(E_f/E_m\right)+2} \qquad \text{(Eq 10.7)}$$

$$\eta_G = \frac{\left(G_f/G_m\right)-1}{\left(G_f/G_m\right)+1} \qquad \text{(Eq 10.8)}$$

If the fiber orientation is random (Fig. 10.7b), then the following equations can be used to estimate the elastic properties:

$$E_{random} = \frac{3}{8}E_{11} + \frac{5}{8}E_{22} \qquad \text{(Eq 10.9)}$$

$$G_{\text{random}} = \frac{1}{8}E_{11} + \frac{1}{4}E_{22} \qquad \text{(Eq 10.10)}$$

$$\upsilon_{\text{random}} = \frac{E_{\text{random}}}{2G_{\text{random}}} - 1 \qquad \text{(Eq 10.11)}$$

10.3 Fabrication Methods

There are a number of important composite fabrication processes that are used more widely in the commercial marketplace than for high-performance aerospace products. In this chapter, four of the most important of these processes will be covered: spray-up, compression molding, reaction injection molding, and injection molding. Some of these processes are capable of producing over a million parts per year, while others are more amenable to low production rates. Some are restricted to thermoset resins, while others can accommodate both thermoset and thermoplastic resins. Although many different types of reinforcement can be used, E-glass fibers are the most predominant because of their relatively low cost, the availability of a large number of product forms, and their overall good combination of physical and mechanical properties.

10.4 Spray-Up

Spray-up is a low- to medium-volume, open-mold method similar to hand lay-up in its suitability for simple medium to large part sizes. However, greater shape complexity is possible with spray-up than with hand lay-up. Continuous-strand glass roving is fed through a combination chopper and spray gun. The gun (Fig. 10.8) simultaneously deposits chopped roving 1 to 3 in. (2.5 to 7.5 cm) long and catalyzed resin onto the tool. The laminate is then densified with rollers or squeegees in order to remove air and work the resin thoroughly into the reinforcing strands.

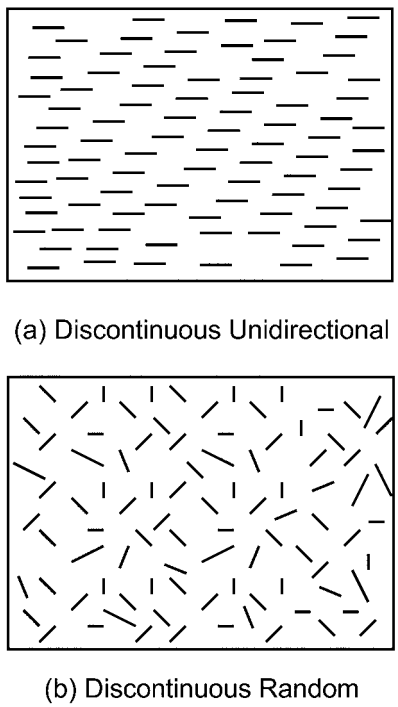


Fig. 10.7 Discontinuous unidirectional and random orientations

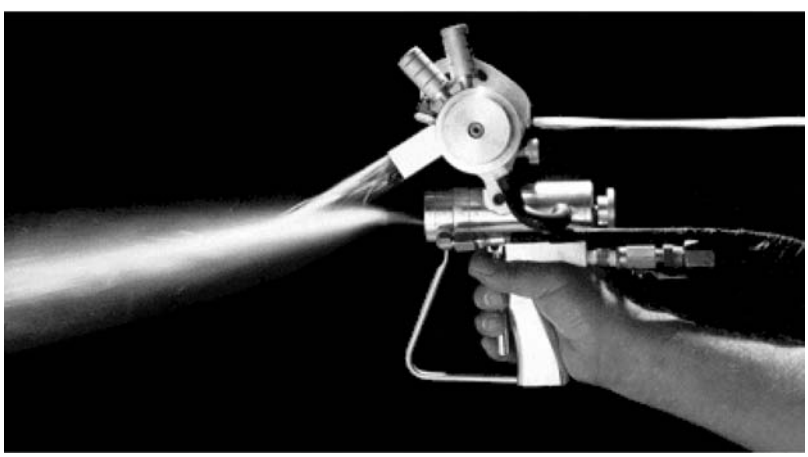


Fig. 10.8 Chopped fiber spray-up gun

Additional layers of chopped roving and resin are added as required for thickness. Cure is usually performed at room temperature but can be accelerated by the moderate application of heat. As with hand lay-up, superior surface finishes can be achieved by spraying a gel coat onto the tool surface prior to spray-up. Woven roving or cloth is occasionally added to the laminate to provide higher strengths in certain locations, and core materials are easily incorporated. General-purpose, room-temperature-curing or low-temperature-curing polyesters are used with single-sided tools. If the part complexity or size requires it, the tool can be assembled in sections and then disassembled when the part is removed. As with the wet lay-up process, the major advantages are low-cost tooling, simple processing, portable equipment that permits on-site fabrication, and virtually unlimited part sizes. An additional advantage of spray-up is that it is very amenable to automation, thereby reducing labor costs and the exposure of workers to potentially hazardous fumes. Sprayed-up glass parts are limited to a maximum of about 30 to 35 weight percent or 15 to 20 volume percent reinforcement. Typical properties are a tensile strength of around 10 ksi (70 MPa), a tensile modulus of 1 msi (7 GPa), and an elongation of 1.8 percent.

10.5 Compression Molding

At the other end of the manufacturing spectrum, compression molding is a high-volume, high-pressure process suitable for molding complex, high-strength, glass fiber-reinforced parts using either thermoset or thermoplastic resins. Compression molding is the single largest primary manufacturing process used for automotive composite applications today. The three main groups of materials that are compression molded are sheet molding compounds for thermosets, glass-fiber-mat-reinforced thermoplastics, and long-fiber-reinforced thermoplastics. Compression molding (Fig. 10.9) is a matched-die process that can produce fairly large parts with excellent overall surface finishes, good dimensional control, and a high degree of complexity. "High volume" means that at least 1000 parts per year, but more typically approximately 100,000 parts per year, would be needed to justify the investment in equipment and tooling. The process is capable of producing parts with surface areas ranging from 1 to 40 ft^2 (0.09 to 3.7 m^2), although less than 10 ft^2 (0.9 m^2) is more typical. Wall sections can be as thin as 0.05 in. (1.3 mm). Molded-in inserts for attachments are common.

10.5.1 Thermoset Compression Molding

Thermoset compression molding begins with a compression molding compound consisting of chopped strands of glass fiber in combination with a resin, in either sheet form (sheet molding compound) or bulk form (bulk molding compound). A "charge" of these compounds is placed in a matched metal mold and cured under heat and pressure. During cure the material flows to

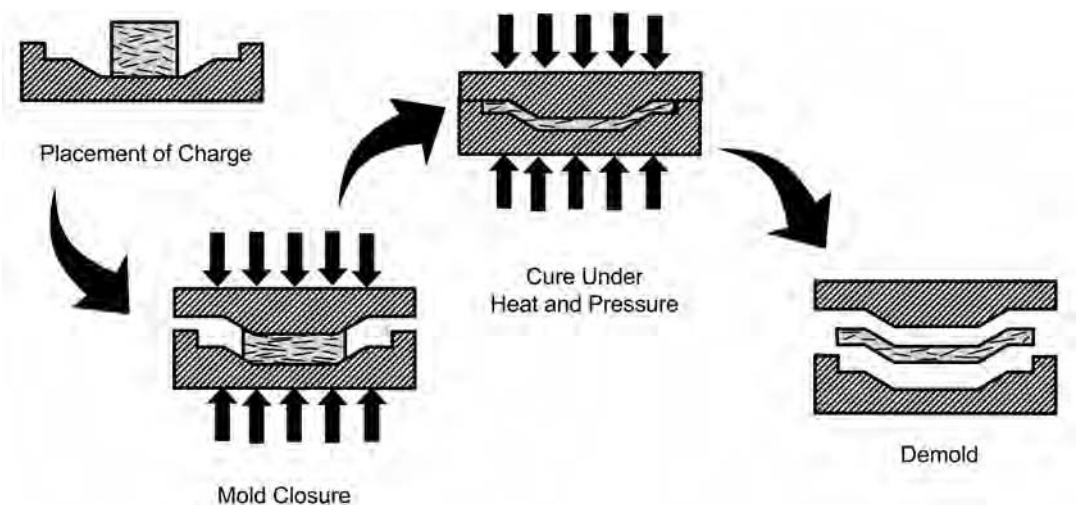


Fig. 10.9 Compression molding of thermosets

fill the mold. For more complex parts, preforms of glass fiber can be fabricated ahead of time and then placed in the tool for cure.

Compression Molding Compounds usually consist of phenolics, but alkyds and epoxies are also available. A typical compound might contain 40 percent glass fibers 0.040 in. (1 mm) in length or shorter. Prior to molding, the compound is palletized into cylinders 0.5 to 2.5 in. (1.5 to 6.5 cm) in diameter by 0.25 to 1 in. (0.5 to 2.5 cm) long. A typical compression molding cycle for phenolics would be 340 to 375 °F (170 to190 °C) and 700 to 3000 psi (5 to 20 MPa) for one to ten minutes. The parts are frequently postcured when elevated-temperature resistance is required.

Sheet Molding Compound (SMC). A typical process schematic for making thermoset sheet molding compound (SMC) is shown in Fig. 10.10. Continuous-strand glass fiber roving is chopped to the desired length of 1 to 2 in. (2.5 to 5 cm) and deposited onto a coat of filled polyester resin paste traveling on a polyethylene film web. After fiber deposition is complete, a second web also carrying resin paste joins the first web, forming a continuous sandwich of glass and resin. This is compacted and rolled under controlled tension onto standard package-sized rolls. Typical SMC is 0.25 in. (0.5 cm) thick and comes in rolls 40 to 80 in. (1 to 2 m) wide. The SMC roll is then aged at 85 to 90 °F (approximately 30 °C) for one to seven days in order to thicken it.

A typical composition consists of 25 percent polyester resin, 25 percent glass fiber, and up to 50 percent filler; however, molding compounds with glass contents as high as 65 percent are also available. Although polyesters dominate the market, vinyl esters, phenolics, ureas, melamines, and epoxies are also commonly used as compression molding compounds. Chopped strand mats are used when higher properties are required, and occasionally longitudinal glass strands are added. The resin can be a standard polyester, a low-shrink formulation, or a low-profile formulation. Standard polyesters are used when the highest mechanical properties are required, but they also shrink the most during molding (0.3 percent). Low-shrinkage formulations shrink less (0.05 to 0.3 percent), while low-profile resins exhibit almost no shrinkage (less than 0.05 percent), resulting in better surface finishes and less tendency for cracking. Fillers, such as calcium carbonate, aluminum trihydrates, or kaolins (clays), reduce cost and shrinkage. Mold release agents, such as zinc or calcium sterates, can be added to the

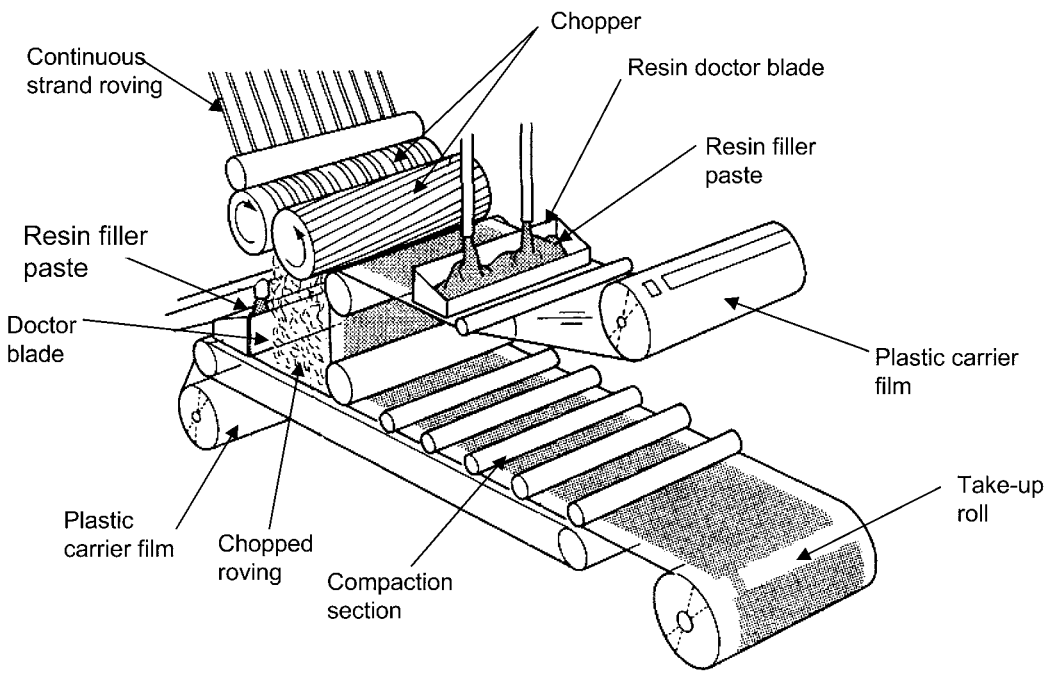


Fig. 10.10 Sheet molding compound machine. Source: Ref 6

formulation to provide self-releasing properties after molding. Thickeners (magnesium oxide (MgO), calcium oxide (CaO), magnesium hydroxide ($Mg(OH)_2$), or calcium hydroxide ($Ca(OH)_2$)) are added to increase viscosity and improve the flow characteristics during molding.

As shown in Fig. 10.11, SMCs can be classified as either SMC-R (random), SMC-CR (continuous/random), or XMC (continuous/random). Random SMC contains 1 to 2 in. (2.5 to 5 cm) long glass fibers oriented in a random order. The influence of fiber content on several mechanical properties of SMC-R containing E-glass fibers in a polyester resin is shown in Fig. 10.12. Continuous/random SMC consists of an oriented array of unidirectional strands covered with a mixture of random fibers. Continuous/random XMC contains continuous strands arranged in an X-pattern where the angle between the interlaced strands is between five and seven degrees. Sheets of XMC are manufactured by a filament winding process in which continuous strand rovings are pulled through a tank of resin paste and wound under tension around a large rotating cylindrical drum. Chopped fibers, usually 1 in. (2.5 cm) long, are deposited on the continuous

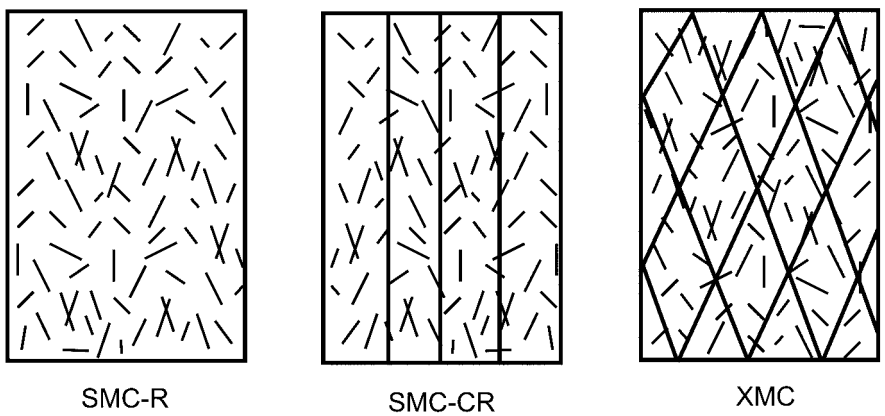


Fig. 10.11 Types of sheet molding compound. Sheet molding compound (random) SMC-R; sheet molding compound (continuous/random) SMC-CR; sheet molding compound (continuous/random with continuous in X-pattern) XMC

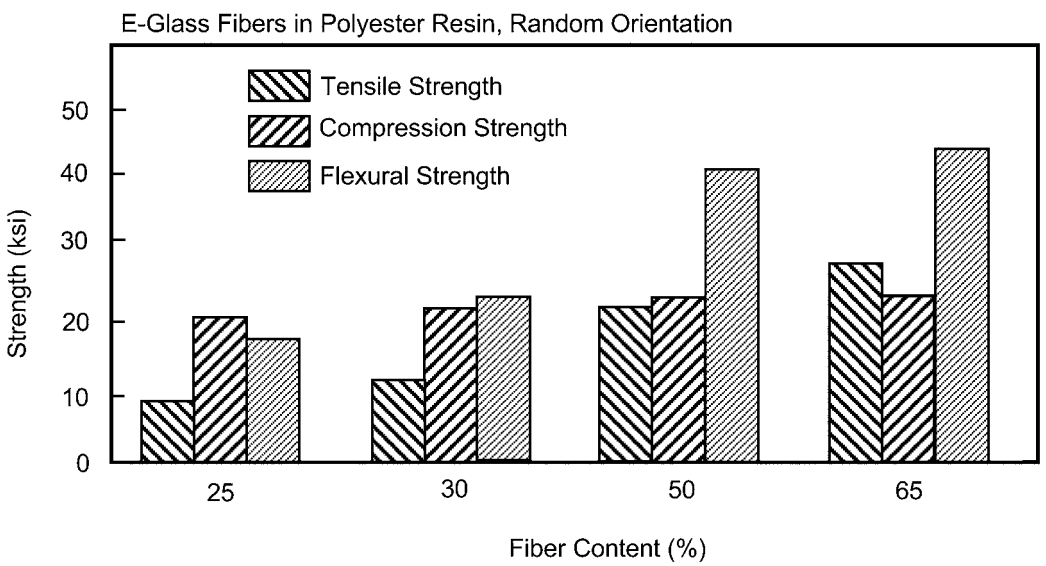


Fig. 10.12 Effect of fiber content on strength of sheet molding compound (SMC). Source: Ref 7

fiber layer during winding. After the desired thickness is obtained, the built-up material is cut off the drum to form a sheet. Due to the unidirectional strands, SMC-CR and XMC are stronger but also harder to mold. Random SMC is used more frequently due to its lower cost, better flow, and moldability. A comparison of these different forms of sheet molding compounds is given in Table 10.2.

Layers of SMC are stacked into "charges" for compression molding. The charge size is typically 40 to 70 percent smaller than the projected mold surface. The weight of the charge is made a bit larger than the weight of the part to be molded in order to ensure mold filling and include some additional material for edge trimming. Different thicknesses of charge can be placed in different portions of the mold to account for thickness or geometry changes in the part. Close control of charge weight and size allows the production of molded parts with very little excess material on the edge that has to be trimmed after cure. Charge placement is critical to minimizing knit lines where two flow fronts merge and create a location of lower strength. The charges are heated in a continuous oven with infrared (IR) or forced-air impingement heaters. They are then placed in heated matched-die molds and press-cured.

Bulk molding compound (BMC) is a mixture of shorter 0.125 to 1.25 in. (0.3 to 3 cm) glass fibers and resin containing filler, catalyst, pigment, and other additives. The fiber reinforcement level is usually 10 to 20 percent. Bulk molding compounds are usually made in an extruder. This premixed material, with the consistency of modeling clay, can be provided in bulk form or can be extruded into rope 1 to 2 in. (2.5 to 5 cm) in diameter or log-like forms for easier handling. As with SMC, the weighed charge of BMC is placed into a heated matched-metal die, the die is closed, and pressure is applied. The completed cured part is removed from the die after an interval of several seconds to a few minutes, depending on part size and thickness. Bulk molding compound is commercially available in various combinations of resin, additives, and glass reinforcements. These provide for a variety of end use requirements in high-volume applications where good finishes, good dimensional stability, part complexity, and good overall mechanical properties are important. The longer fiber lengths obtainable with SMC provide higher mechanical properties compared to parts made with BMC, especially those having relatively thin cross sections. More BMC is used for thermoset injection molding than for the traditional compression molding process.

Preforming. A third approach to the preparation of a ready-to-mold form of preblended glass fiber reinforcement and resin is the preform. This is a mat of chopped glass fiber strands with a binder that allows the preform to hold its shape. The preform is made to the approximate shape of the product to be molded. There are two common methods of producing preforms, the directed-fiber method and the plenum-chamber method. In the directed-fiber method (Fig. 10.13), continuous-strand glass fiber roving is cut into 1 to 2 in. (2.5 to 5 cm) lengths and blown with a binder onto a rotating metal screen that approximates the shape of the final part. Suction is used to hold the fibers in place. After the binder is heat-set in an oven, the preform is ready for the die. The plenum-chamber method is similar but involves the distribution of chopped fibers and binder into an air chamber, where they are sucked onto a rotating preform screen. Preform methods are used for applications requiring medium-sized to large parts having relatively constant cross sections and high concentrations of glass reinforcement. In preform molding, the major

Table 10.2 Mechanical properties of selected sheet molding compounds (SMCs)

Properties	SMC-R25	SMC-R50	SMC-R65	SMC-C20R30	XMC-31
Specific gravity	1.83	1.87	1.82	1.81	1.97
Tensile strength, ksi	12.0	23.8	32.9	41.9 (L), 12.2 (T)	81.4 (L), 10.2 (T)
Tensile modulus, msi	1.91	2.29	2.15	3.05 (L), 1.74 (T)	5.22 (L), 1.74 (T)
Poisson's ratio	0.25	0.31	0.26	0.30 (L), 0.18 (T)	0.31 (L), 0.12 (T)
Strain to failure, %	1.34	1.73	1.63	1.7 (L), 1.6 (T)	1.7 (L), 1.5 (T)
Compressive strength, ksi	26.5	32.6	34.6	44.4 (L), 24.1 (T)	63.9 (L), 22.3 (T)
Compressive modulus, msi	1.70	2.31	2.60	2.90 (L), 1.74 (T)	5.37 (L), 2.03 (T)
Flexural strength, ksi	31.9	32.6	58.5	92.8 (L), 23.2 (T)	141 (L), 20.3 (T)
In-plane shear strength, ksi	11.5	8.99	18.6	12.2	13.2
In-plane shear modulus, msi	0.65	0.86	0.78	0.60	0.65
Interlaminar shear strength, ksi	4.35	4.63	6.53	5.95	7.98

Glass fibers in polyester resin. (L): property values measured in the longitudinal direction (parallel to the continuous fibers); (T): property values measured in the transverse direction (perpendicular to the continuous fibers). Source: Ref 8

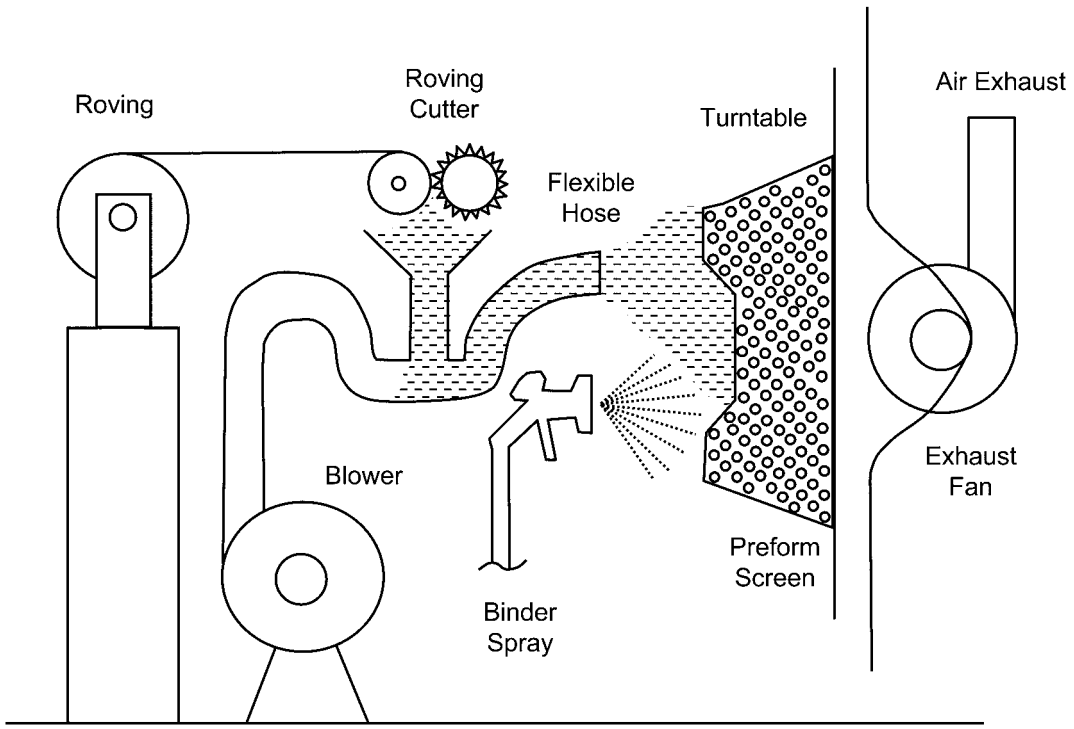


Fig. 10.13 Directed fiber spray-up process for preforms. Source: Ref 9

portion of the resin is added just before molding or after the preform is placed within the mold. Most applications use either SMC or BMC, but for flat sheets and simple shapes, glass mats can be placed directly into the mold, resin poured over the mat, and the mold closed under pressure to consolidate the resin and glass. For complex parts, preforms are normally made before they are placed in the tool.

During compression molding, the matched-die mold is mounted in a hydraulic or modified mechanical molding press such as the one shown in Fig. 10.14. The two halves of the die are closed, and heat and pressure are applied at 225 to 320 °F (105 to 160 °C), 150 to 2000 psi (1 to 14 MPa). Parts with higher glass contents or more complex geometries require higher pressures. Depending on the thickness, size, and shape of the part, cure cycles range from less than one minute to about five minutes. Press closing occurs in two steps: a fast initial step followed by a slower step to allow the material time to flow. Higher molding temperatures and faster curing times require faster closing speeds to prevent premature gellation. If a condensation curing resin, such as a phenolic, is being molded, it is common practice to open the mold momentarily to let the volatiles escape during the curing process. After cure, the mold is opened and the finished part is removed. If hollow parts are required, low-melting eutectic metals can be inserted into the mold and then melted out after molding.

The matched-metal dies usually are made from hardened and chrome-plated steel. They can be single or multiple-cavity molds, usually cored for steam or hot-oil heating. Electrical and hot-water heating systems can also be used. Side cores, provisions for inserts, and other features are often employed. The dies are also equipped with part ejectors that may employ either mechanical pins or air pressure. Mold materials include cast or forged steel, cast iron, and cast aluminum. Compression molding is an ideal process when the volume is high enough to justify the investment in precision matched-metal dies, and with the advent of high-speed machining of aluminum dies, the process is becoming more economical for lower-volume production runs. It is capable of producing extremely uniform parts with superior surface finishes. Inserts and attachments can be molded in, and final trimming and machining operations are minimal.

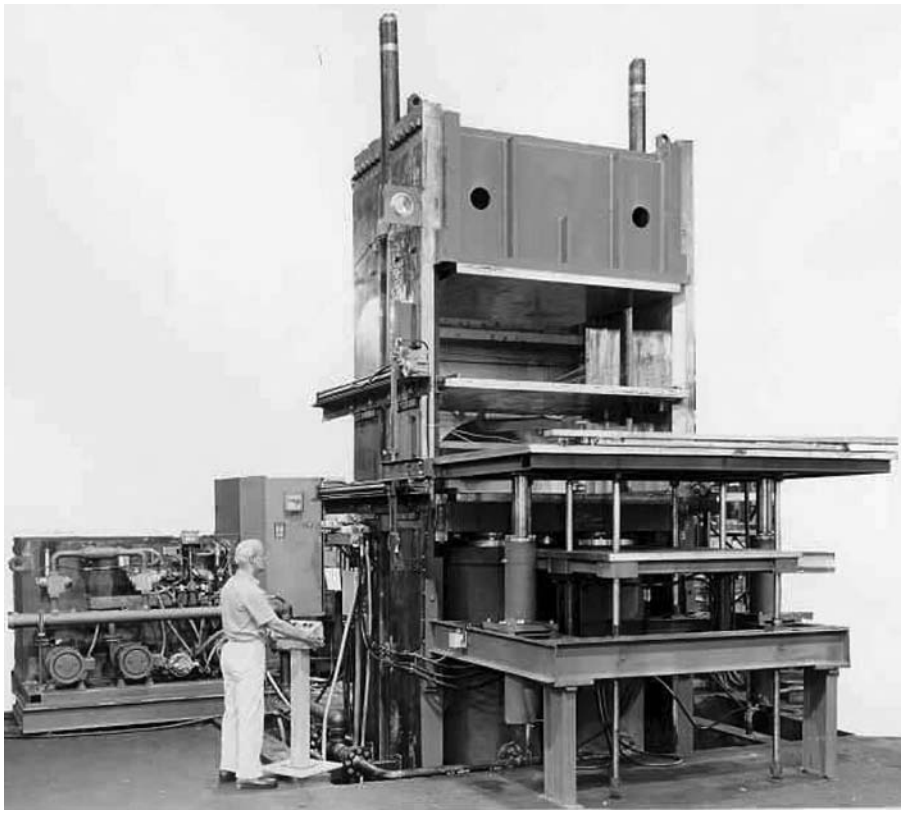


Fig. 10.14 Compression molding machine

Transfer molding (Fig. 10.15) is similar to compression molding, except that the charge of molding compound is heated to 300 to 350 °F (150 to 180 °C) in a separate chamber, then transferred by a ram under heat and pressure into a closed die, where the shape of the part is determined and cure takes place, usually in 45 to 90 seconds. The process is used for small, intricate parts requiring tight dimensional tolerances. Although good resin flow is required, the process is not sensitive to precise charge weight. Typical reinforcement levels are 10 to 35 percent.

10.5.2 Thermoplastic Compression Molding

Glass mat thermoplastic (GMT) consists of glass-reinforced thermoplastic, usually polypropylene, that flows to fill the mold during the compression molding cycle. A typical GMT fabrication line is shown in Fig. 10.16. Several reinforcements are available, including continuous fiber mat, chopped fiber mat, and unidirectional fiber mat, normally at a glass content of 40 volume percent. This process has gained a foothold in the automotive market because of the automation used and the short processing cycles (some as short as 30 seconds, although longer times are sometimes required to obtain the proper amount of crystallinity). Glass mat thermoplastic material is made using the double-belt process described in Chapter 6, "Thermoplastic Composite Fabrication Processes." The material is then reheated in continuous moving furnaces using IR heater banks to 600 °F (320 °C) in two to three minutes. It is then inserted into a high-speed hydraulic press with the mold heated to 275 °F (135 °C) and consolidated under 1000 to 4000 psi (7 to 28 MPa) pressure. A two-stage pressurization cycle is frequently used; the pressure is applied quickly, 200 to 500 in./min (5 to 12 m/min), in the first stage and more slowly in the second stage, 1 to 10 in./min (2 to 25 cm/min), to allow the material time to flow and fill the mold. Such high pressures are needed to move the reinforcement structure throughout the cavity and ensure a high degree of air expulsion and composite consolidation. Sometimes, holding fixtures are required during cooling to minimize distortion

or warping. Most applications contain some reprocessed production waste products, ranging from a few percent up to 50 percent recyclate.

Long Discontinuous Thermoplastic. The long-fiber thermoplastic (LFT) process uses glass reinforcements in a polypropylene matrix. The fibers are normally 0.5, 1.0, or 2.0 in. (12, 25, or 50 mm) long. The LFT process is even more highly automated than the GMT process. The polypropylene is fed into an extruder that heats and melts the material and then adds the glass fiber near the end. This feedstock is then transferred directly to the compression molding press without the need to reheat it, as required in the GMT process, thus further reducing costs. In comparison to the GMT and SMC processes, the individual discontinuous production process steps are eliminated. As in the GMT process, recycled material is frequently included in the LFT process to reduce costs.

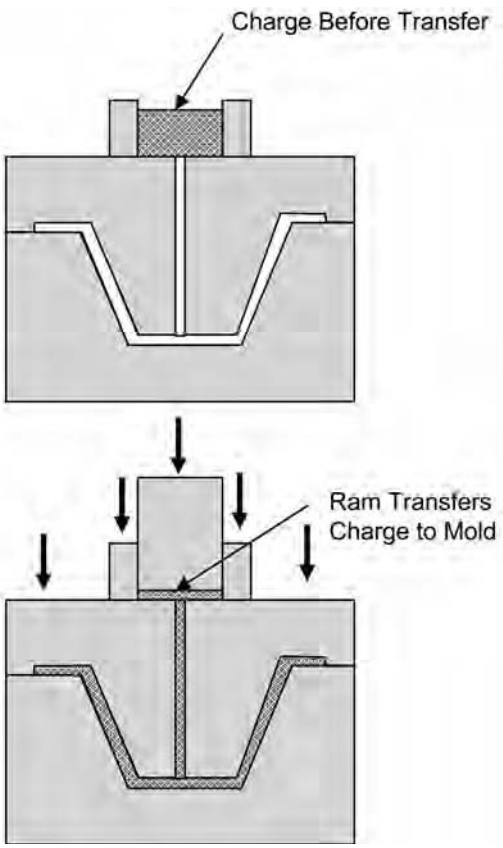


Fig. 10.15 Principle of transfer molding

The advantages of the LFT process are:

1. The process is more cost effective than GMT, not only due to the elimination of single process steps, but also because less manpower is needed for production.
2. In comparison with GMT, cycle times are reduced by 15 percent as a result of better flowability of the plasticized material.
3. The impregnation process for LFT is superior to that for GMT in not being susceptible to surface defects caused by poor impregnation.

Comparative properties of GMT, LFT, and SMC molded test pieces are given in Table 10.3.

10.6 Structural Reaction Injection Molding

Reaction injection molding (RIM), shown in Fig. 10.17, is a process for rapid fabrication of unreinforced thermoset parts. A highly reactive

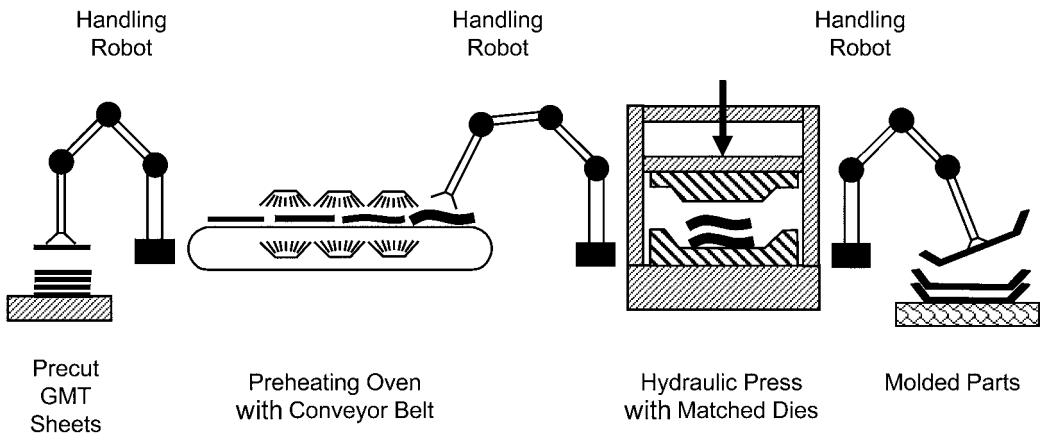


Fig. 10.16 Automated fabrication of glass mat thermoplastic (GMT) parts

two-component resin system is injected into a closed mold, where the resin quickly reacts and cures. Reaction injection molding resins must have low viscosities (500 to 2,000 cps) and fast cure cycles. Polyurethanes are the most prevalent, but nylons, polyureas, acrylics, polyesters, and epoxies have also been used. The two components (isocyanate and polyol in the case of polyurethanes) are kept separate and are constantly recirculated under high pressure. They are mixed in a dynamic mix head under high pressures of 1500 to 3000 psi (10 to 20 MPa) and high speeds of 4000 to 8000 in./s (100 to 200 m/s). The crosslinking reaction is initiated by mixing rather than by heat and gel and can occur in as little time as two to ten seconds. The actual injection pressure is quite low, and the die is heated to about 120 to 150 °F (50 to 70 °C) to accelerate cure and then remove the exothermic heat of reaction during the latter part of cure. Since RIM resin systems have very low viscosities, they can be injected at low pressures less than 100 psi (700 kPa). These low pressures allow the use of inexpensive molds and low-force clamping systems. Typical tooling materials are steel, cast aluminum, electroformed nickel, and composites. Cycle times as short as two minutes for large automotive bumpers have been reported. Since isocyanate vapors are harmful, RIM work cells must be provided with exhaust ventilation.

Reinforced reaction injection molding (RRIM), as shown in Fig. 10.18, is similar to RIM except that short glass fibers are added to one of the resin components. The fibers must be extremely short at least 0.03 in. (0.8 mm) or the resin viscosity will be too great. Short fibers, milled fibers, and flakes are commonly used. Again, polyurethanes are the predominant resin system in RRIM. The addition of the fibers improves the modulus, impact resistance, and dimensional tolerance and lowers the coefficient of thermal expansion.

Structural reaction injection molding (SRIM) is similar to the previous two processes except that a continuous glass preform is placed in the die prior to injection (Fig. 10.19). This process, too, is used almost exclusively with polyurethanes. Because of the highly reactive resins and short cycle times, SRIM cannot produce as large a part size as resin transfer molding see Chapter 5, "Thermoset Composite Fabrication Processes". Also, SRIM parts have lower fiber volumes and generally more porosity than RTM parts.

Table 10.3 Comparative properties of LFT, GMT, and SMC

Property	LFT	GMT	SMC
Glass fiber content, wt%	40	40	30
Recyclate content, wt%	30	…	5
Tensile strength, ksi	8.7	9.4	8.7
Tensile modulus, msi	1.0	0.9	1.4
Flexural strength, ksi	16	16	23
Flexural modulus, msi	0.8	0.6	1.3
Impact strength, kJ/m^2	60	75	70
Density, g/cm^3	1.21	1.21	1.80

LFT—long fiber thermoplastic; GMT—glass mat thermoplastic; SMC—sheet molding compound. Source: Ref 7

10.7 Injection Molding

Injection molding, which is capable of producing more than a million parts per year, is the highest-volume method of any of the processes for fabricating parts of glass-fiber-reinforced

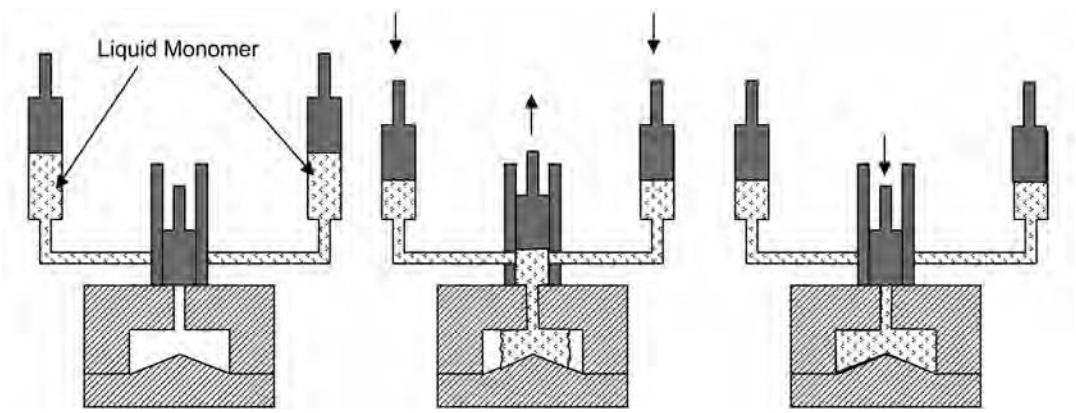


Fig. 10.17 Reaction injection molding (RIM) (no reinforcement)

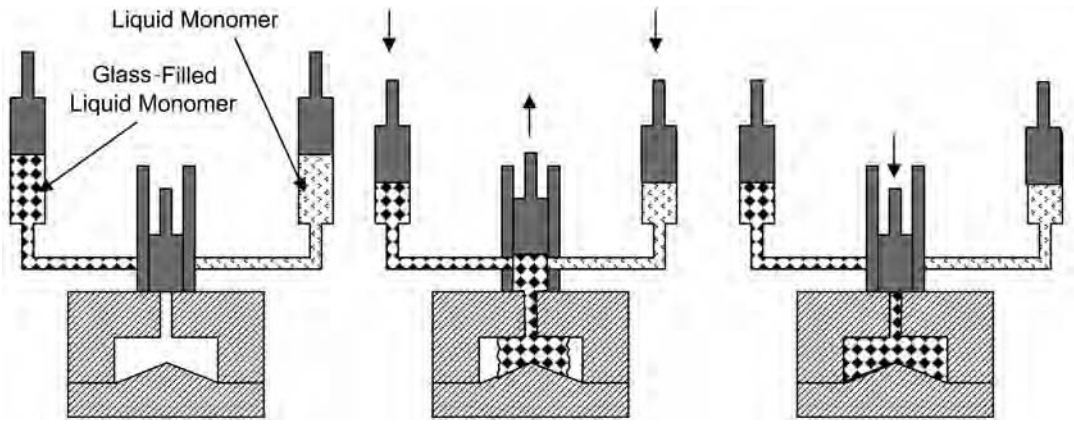


Fig. 10.18 Reinforced reaction injection molding (RRIM) (short-fiber reinforcement)

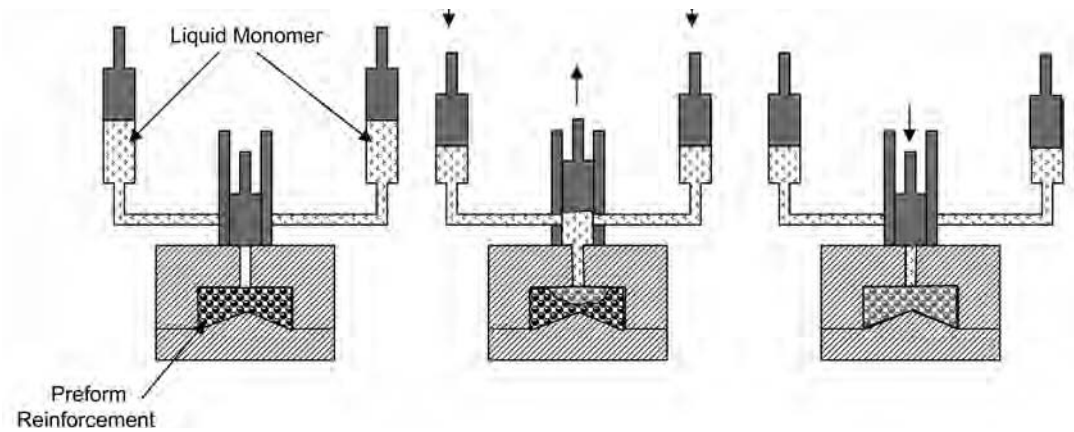


Fig. 10.19 Structural reaction injection molding (SRIM) (long-fiber reinforcement)

materials. Injection molding can be used to fabricate either unreinforced or reinforced parts. Like compression molding, injection molding requires expensive matched-metal dies because of the high processing temperatures and pressures. However, because many complex parts can be molded at high production rates, the cost per part can often be quite low. Although other reinforcements are occasionally used, glass fibers are most common. Since the fibers are short ranging 0.03 to 0.125 in. (0.8 to 3 mm), the volume percentage of fiber is low (typically 30 to 40 percent), and the fiber orientation is random or aligned by flow into the mold, the mechanical properties of injection-molded parts are again much lower than those of continuous-fiber reinforced parts. However, very complex parts with all surfaces closely controlled can be achieved with injection molding. Either single- or multicavity dies are used to produce very large volumes of complex parts at very high production rates, from a wide range of thermoplastic resins and with a variety of resultant properties.

10.7.1 Thermoplastic Injection Molding

Injection-molded glass-fiber-reinforced thermoplastics are used extensively in the automotive and appliance industries. Design flexibility, the ability of glass-fiber-reinforced thermoplastics to form intricate shapes, very high production rates, and low cost per piece account for the extensive application thermoplastic injection molding.

In injection molding, the molding compound, in pellet form, compound concentrate, or dry

blend, is heated in the injection chamber of the molding machine. A typical injection molding cycle is illustrated in Fig. 10.20. As the material progresses down the screw, it is melted by a combination of heat from the barrel and the shearing action of the screw. The material accumulates in the barrel and is then injected under high pressure as a hot fluid into a relatively cold closed die. After the desired *shot size* is accumulated, the screw stops rotating and moves forward at a controlled rate, acting as a ram or plunger and forcing the plastic melt in front of the screw into the mold. The molten material flows through the nozzle into a water-cooled die where it flows through a sprue, a runner system, and finally the gate into the mold cavity. When the mold is completely filled, the screw remains stationary to keep the thermoplastic in the mold under pressure. During this hold or dwell time, additional melt is injected into the mold to compensate for the shrinkage due to cooling. After the gate freezes, the mold becomes isolated from the injection unit. The melt that accumulates at the end of the screw pushes the screw backward; that is, the screw is rotating and moving backward at the same time. The rate at which the plastic melt accumulates in front of the screw for the next shot is controlled by the backpressure, which is the hydraulic pressure exerted on the screw. When a sufficient melt has accumulated in front of the screw, the screw stops rotating while the part in the mold cools and solidifies. After a short cooling cycle, usually 20 to 120 seconds, the part has solidified sufficiently to enable it to be removed from the mold without distortion. The cycle time for the process is usually controlled by the cooling rate, which in turn is usually dependent on the die design, part thickness, and reinforcement content. After cooling, knockout pins eject the part from the mold. The sprue, runners, and gates are separated from the part and are usually recycled by grinding them into powder and mixing them with fresh material.

Virtually all thermoplastics are injection-moldable, including nylon, acetal, vinyl, polycarbonate, polyethylene, polystyrene, polypropylene, polysulfone, modified polyphenylene oxide, fluorocarbons, polyetherimide, acrylonitrile-butadiene-styrene, and styrene-acrylonitrile. For injection molding, chopped strands of glass fiber can be blended with thermoplastic resin molding powders or pellets. Carbon fibers can be used when higher properties are required. These fibers also provide enhanced electrical and thermal conductivity. Carbon fibers are frequently used as electrically conductive fillers in parts requiring electromagnetic interference shielding, antistatic, electrostatic discharge, and other electrical properties.

A lower-cost thermoplastic resin can often be strengthened by the addition of glass fiber reinforcement to the point where it will offer the

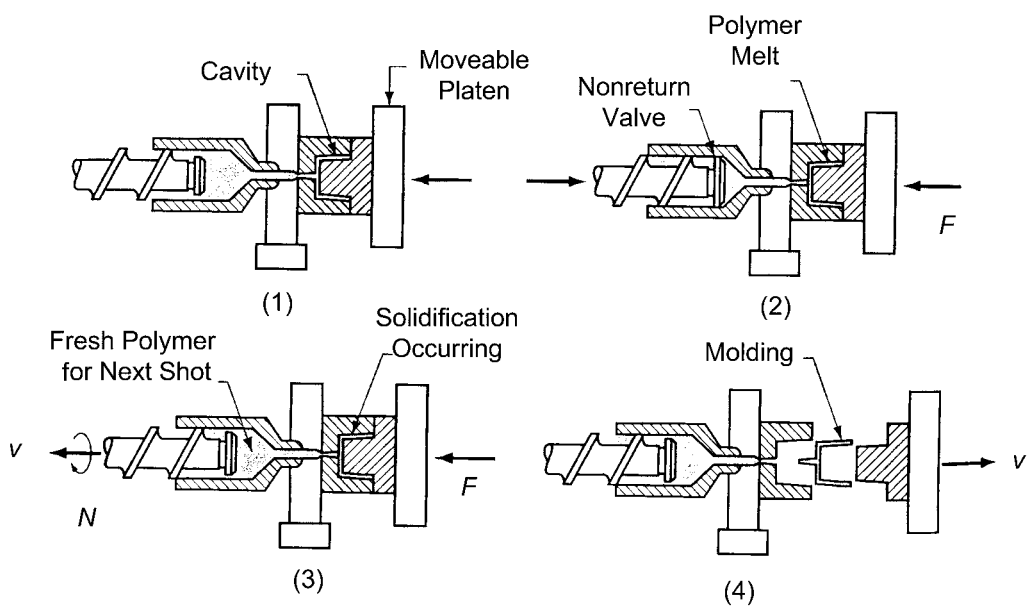


Fig. 10.20 Injection molding machine sequence. Source: Ref 10

superior performance characteristics of a more costly unreinforced resin. The addition of glass fibers also provides sufficient strength and dimensional stability to enable many reinforced thermoplastics to compete effectively with stamped sheet metal and die castings. Thermoplastic molding compounds usually include pigments, fillers, mold release agents, and lubricants, and may occasionally contain other additives for special purposes. Their corrosion resistance and molded-in color also provide design advantages. The list of thermoplastics reinforced with glass fibers for injection molding is long and includes resins offering an extremely broad range of mechanical, chemical, electrical, and thermal properties. Some polymers require both injection speed and injection pressure to vary during the molding cycle. A heat-sensitive polymer, for example, can be degraded if the fill rate is too rapid; forcing the polymer through the small restrictions of the sprue, runner, and gate systems at high speed will increase the internal shear and raise the temperature to the point where polymer degradation occurs. Programming different injection speeds and pressures during the injection process may be required to prevent resin degradation.

Injection molding compounds are usually supplied in a form that can be fed directly into the injection molding machine. They are usually made by mixing short chopped fibers with a powdered or pelletized resin in an extruder. In extrusion processing, fiber breakage is a major problem. To minimize breakage, deep flighted screws or twin screws are used and the fibers are fed into the barrel after the resin has melted. Prepelletized blends are available in controlled ratios of glass fiber reinforcement to resin and with specified additives such as pigments, flame retardants, stabilizers, and lubricants. These pellets are available in nearly all of the common injection-molding thermoplastics. Concentrates are similar to the glass fiber/resin prepelletized blends but have very high percentages of glass to resin, up to 80 percent by weight compared to the 10 to 40 percent customary in pellets. The concentrated pellets are blended with nonreinforced thermoplastic pellets to achieve the desired glass-to-resin ratio in the molded part. With these formulations, the injection molder can select a glass-reinforced compound to satisfy end-use needs with respect to mechanical properties, chemical properties, impact strength, surface finish, and color.

It is important that the material be thoroughly dried prior to injection molding. Drying can be accomplished off-line as a batch drying process or on-line in a hopper dryer on the machine. Some polymers absorb moisture primarily on the surface (nonhydroscopic), while others absorb moisture into the pellets or granules (hygroscopic). Drying of nonhydroscopic materials, such as polypropylene and polyethylene, can be accomplished by simply heating to evaporate the moisture from the surface. Hydroscopic materials, such as nylon and polycarbonate, must be dried using dehumidified hot air to remove the moisture and generally require longer drying cycles. It is common practice to use up to 20 percent regrind for injection-molded parts; however, since the properties of the part will often decrease with increasing regrind content, it is important to test prior to incorporating regrind. The reinforcing effects of glass and carbon fibers decrease with repeated processing because repeated exposure to heat causes breakdown of the fibers and thermal degradation of the resin.

The advantages of glass-reinforced injection-molded parts over unreinforced parts include higher tensile strength and modulus, greater impact resistance, reduced shrinkage, improved dimensional stability, and higher temperature capability. Whereas normal polymers shrink about five percent, fiber-reinforced parts usually shrink one percent or less. A disadvantage of fiber reinforcement is lower ductility. In general, slightly higher injection pressures and barrel temperatures are required for reinforced parts due to their higher viscosities. The mixing and shearing action of the injection molder reduces the fiber length; therefore, the gates and runners should be as large as possible. Injection pressures are usually 10 to 15,000 psi (70 kPa to 100 MPa). Minimal back pressure at 25 to 50 psi (170 to 350 kPa) and low screw speeds (30 to 60 rpm) should be utilized to avoid excessive fiber breakage. Cavities should be filled as rapidly as possible to minimize the degree of fiber orientation and enhance knit-weld-line integrity, especially for thin-walled parts. Higher barrel temperatures at 30 to 60 °F (15 to 30 °C) (than those for unfilled resin) are also used when injection molding reinforced parts; the higher temperature minimizes fiber breakage by melting the polymer rather than allowing it to be melted by the heat generated by the shearing action of the screw. After the cavity is filled, a longer hold time is needed to help maintain the dimensional tolerances. One problem with reinforced parts is that the fiber orientation is largely controlled by the flow forces and the part geometry and can result in parts with variable strengths in different sections of

the part. Also, knit lines form where the flow fronts meet and result in areas of lower strength. This problem is accentuated for parts containing longer fibers and higher fiber contents.

The main parts of an injection molding machine (Fig. 10.21) are the clamping unit and the injection unit (also called a *plasticizing unit*). The clamping unit, which holds the die, contains fixed and moving plates, tie bars, and the mechanisms for opening, closing, and clamping the die. The injection unit melts the thermoplastic and injects it into the mold, and a drive unit provides power for both the injection and clamping units. Screw machines dominate the injection molding industry, but plunger machines are also available. Reciprocating plunger machines are inferior to screw machines, because all of the heat has to be supplied by conduction from the barrel heaters and mixing is not as thorough; the consequences are low plasticizing (melting) rates and thermally nonuniform melts. Screw machines generate heat within the material and provide mixing, thus producing much more uniform melts. Generally, a screw consists of three sections: (1) a feed section, (2) a compression section, and (3) a metering section. The feed section transports pellets from the hopper to the heated section of the barrel. In the feed section, the screw flights are along the same dimension. In the compression section, the polymer is melted by the combined heat generated by the barrel heaters and the shearing action of the screw. In this section, the volume of the screw flights decreases to compensate for changes in the material density. Finally, in the metering section, the flight dimensions are constant as the final melting and mixing of the polymer occur. Screw designs vary with the material being molded. Three screw designs are shown in Fig. 10.22. A design for highly crystalline polymers is shown in Fig. 10.22(a). Since these materials have very sharp melting points, a very short compression section is used. The compression section is longer for semicrystalline thermoplastics (Fig. 10.22b) because they require more time to melt. For an amorphous thermoplastic (Fig. 10.22c) that does not have a true melting point, the screw is designed with a gradually increasing compression over its length. The barrel heaters are divided into zones to provide better control of the heating process.

Injection molding machines are rated in terms of tons of mold clamping capacity and ounces of shot size and can range from laboratory units of 2 tons, 0.25 oz (1800 kg, 7 g) to large industrial units of 3500 tons, 1500 oz (3200 metric tons, 40 kg). A typical laboratory-size injection molding machine is shown in Fig. 10.23. The clamping mechanism must have sufficient locking force to resist the tendency of the molten polymer, in motion and under pressure, to force the mold halves apart. Since reinforced thermoplastics have higher viscosities than unreinforced resins, they are injected at higher pressures; therefore, the clamping mechanism must be even stronger. Mold clamping pressure is usually provided by either a toggle lock or a hydraulic cylinder or a combination of the two. Modern injection molding machines are equipped with automatic feedback control systems that monitor the process parameters to produce consistently high-quality parts. Important processing parameters that need to be controlled include individual control of the injection and holding pressures, ram position and velocity, back pressure, and screw speed. Barrel and nozzle temperature control is important for

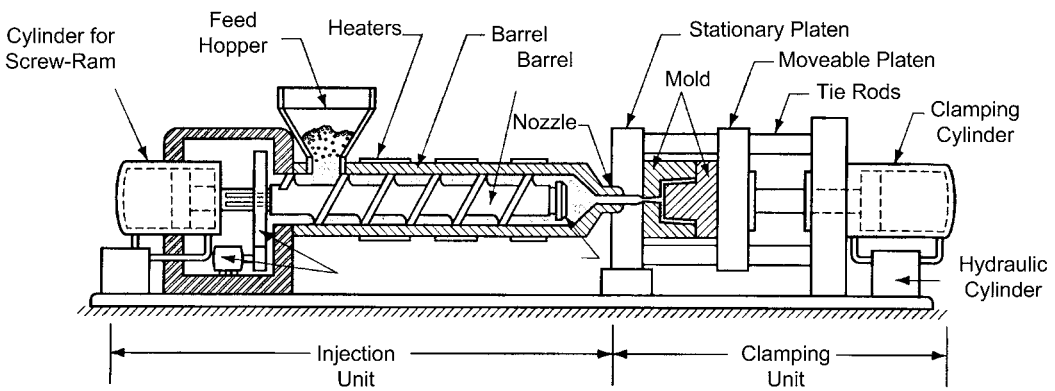


Fig. 10.21 Injection molding machine schematic. Source: Ref 10

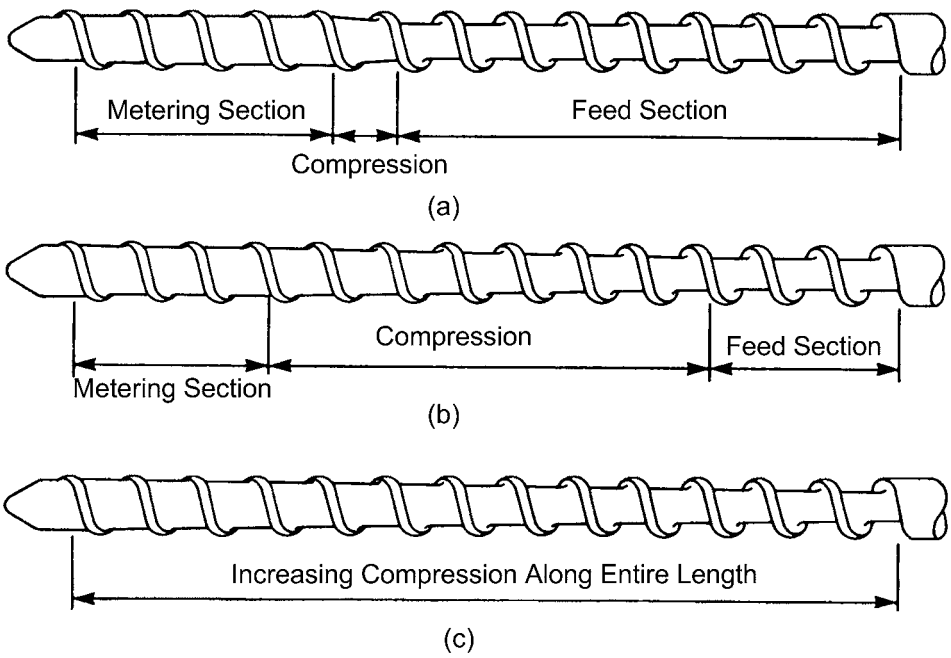


Fig. 10.22 Injection molding screw designs. Source: Ref 11



Fig. 10.23 Injection molding machine

achieving low thermal stresses in the molded part. Lower molding temperatures will promote rapid cooling and higher production rates but produce lower-quality parts. Rapid cooling affects internal stresses, the degree of fiber orientation, postmold shrinkage, and warpage.

Matched-metal dies for thermoplastic production runs are normally made of high-strength tool steels that are often plated for additional abrasion resistance. Typical coatings include nickel phosphorus impregnated with polymers, hard chrome, electroless nickel, titanium nitride, and diamond black (boron carbide thin film with tungsten disulfide). In the two-plate cold-runner configuration (Fig. 10.24a), the material is injected through the sprue bushing, the runner system, and the gates into the die cavities. After cooling, the parts are removed along with the sprue, runner system, and gates. The sprue, runner system, and gates are then removed manually for recycling. In the three-plate cold-runner system shown in the bottom portion of Fig. 10.24(b), the middle plate separates the sprue, runner system, and gates from the parts during the ejection cycle. There are also more expensive three-plate hot-runner systems that keep the sprue, runner

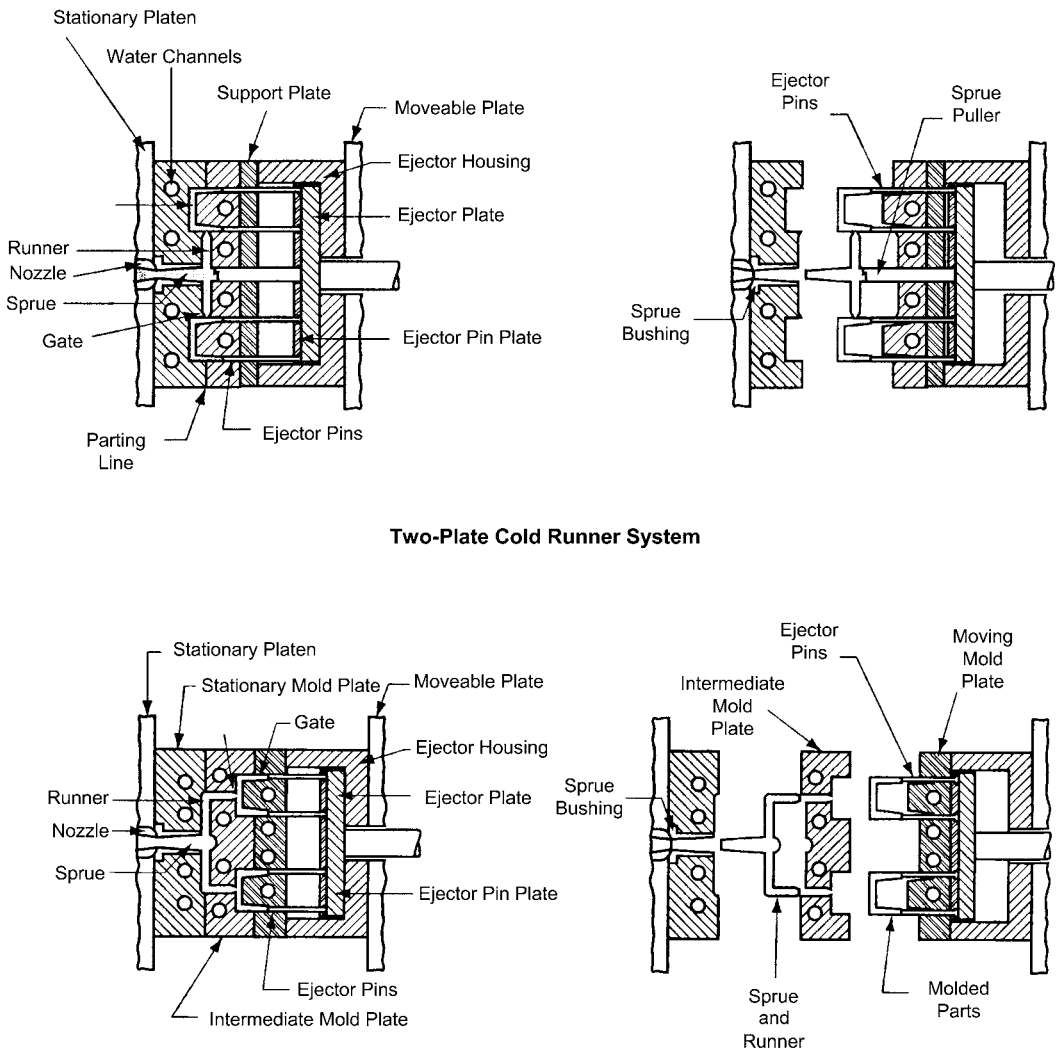


Fig. 10.24 Injection molding runner designs. Source: Ref 10

system, and gates in a molten state throughout the process for more economical recycling since there is no labor or material waste associated with recycling the sprue, runner, and gate system. Injection molding dies normally contain vents to let the air in the die escape as the hot polymer flows into the die cavity. Vents are usually placed in the areas that fill last, near knit lines, and even in the runner system. Sprues and runners should have gentle bends. Runners should be as short as possible to avoid pressure drops. The gates control the fill rate, the amount of material flowing into the cavity, and the rate of material solidification. The gating system should be designed to avoid or minimize weak weld or knit lines. If more than one gate is needed to fill the mold, weld lines will result; these should be located in lower-stressed locations in the part. Since part cooling is often the longest part of the injection molding cycle, dies should be designed with efficient cooling channels. In general, (1) since cooling rate is dependent on thickness, cooling fluid should be located close to the cavity surface; (2) cooling lines should be located exactly where they are needed to cool the part uniformly; (3) turbulent flow of the cooling medium should take place in a manner that provides maximum heat transfer (sharp turns and high speeds promote turbulent flow); and (4) the cooling system should be designed so that cooling is uniform in each mold half.

One of the main challenges in injection molding is producing parts with correct dimensional accuracy and minimal warpage. Warpage occurs when the internal stresses in the part exceed the inherent part stiffness and cause a permanent deformation. Cooling gradients, which lead to differential shrinkage, are the primary cause of part warpage. Shrinkage is dependent on the material, the part design, the mold design, and the processing parameters. Because of their lower inherent shrinkages, amorphous resins are frequently selected over semicrystalline resins when tight tolerances are required. In general, the addition of fibrous fillers increases part warpage because of the anisotropic nature of their flow patterns as the fibers align with the flow. When differential cooling occurs, part designs with nonuniform wall thicknesses tend to warp more than those with uniform wall thicknesses. Stiffeners or gussets are often incorporated during design to reduce or minimize warpage. Gate location and cooling passages are important considerations during die design. Ideally, the mold should be filled uniformly during the injection process and then cool uniformly until it is ready for ejection. If the gates and the cooling system are not properly designed, regions in the part cavity will fill prematurely and start to solidify before the remainder of the mold is filled. Likewise, an improperly designed cooling system will result in thermal gradients during the cooling process. During processing, cavity fill time is important. If the time is too short, high shear rates can cause substantial melt shearing and high residual stresses, which lead in turn to part warpage. If the time is too long, a large melt temperature drop occurs as cavity filling is completed, resulting in thermal gradients leading to part warpage.

Gas-assist molding is used to mold hollow injection-molded parts by the controlled injection of an inert gas (N_2) into the hot polymer melt. The gas forms a continuous channel through the hotter, less viscous, thicker sections of the melt. Gas injection pressures of 400 to 800 psi (2.8 to 5.5 MPa) are commonly used. Injection compression molding is another variant in which the melted polymer is injected into a partially opened mold. The mold closes, compresses the melt, and distributes it throughout the cavity. The injection compression molding process helps to prevent fiber breakage and improve the properties of the molded part. Thin wall injection molding is a process capable of making parts with 0.020 to 0.080 in. (0.5 to 2 mm) walls and a flow length-to-thickness (l/t) ratio of greater than 75. Since thinner walls cool rapidly, equipment capable of extremely high fill pressures of 15 to 35 ksi (100 to 240 MPa) is required along with very short fill times (less than 0.75 seconds) to produce the part. This process usually requires thicker dies to resist deflections with specially designed runner and vent systems. In structural foam molding, chemical blowing agents are used to produce parts with solid skins and foamed cores. This process allows the fabrication of large parts with high strength-to-weight ratios and good dimensional control. Tooling costs can be lower because aluminum dies are acceptable for some part configurations.

10.7.2 Thermoset Injection Molding

Thermoset molding compounds can be injection-molded when the injection screw or plunger and chamber of the molding machine are maintained at low temperatures and the mold itself is heated at 250 to 400 °F (120 to 200 °C). This causes the thermoset material to cure after

several minutes in the mold under heat and pressure. Precise control of temperature and cycle time must be maintained to prevent the resin from gelling in the barrel. The process requires low-viscosity resins that maintain their low viscosity for a period of time but cure quickly after gelation. Particulate fillers, chopped glass fibers, and short milled fibers less than 0.80 in. (2 cm) can be used for reinforcement; however, chopped and milled glass fibers increase the viscosity of the resin more than particulate fillers and are therefore harder to mold. For thermoset injection molding, the screw is usually shorter and has a lower compression ratio. The barrel is set at low temperatures ranging 160 to 212 °F (70 to 100 °C), and cure is conducted with heated molds with injection pressures of 7.5 to 15 ksi (50 to 100 MPa). Adequate venting of volatiles is critical, especially for condensation curing phenolics; venting passages are therefore built into the mold at parting lines, ejector pins, and core pins. The maximum weight of parts made using this process is about 10 lb. Bulk molding compounds (BMCs) are also frequently used for thermoset-injection-molded parts. Polyesters, vinyl esters, and epoxies are used with glass fibers 0.25 to 1 in. (6 to 25 mm) in length. When BMC is used, larger machines are frequently employed to produce larger moldings at lower pressures such as 750 to 1500 psi (5 to 10 MPa) than for conventional thermoset injection molding. Typical cures occur in two to five minutes.

REFERENCES

1. F.L. Mathews and R.D. Rawlings, *Composite Materials: Engineering and Science*, Woodhead Publishing Ltd., 1994
2. D. Hull, *An Introduction to Composite Materials*, Cambridge University Press, 1981
3. L. Kacir, M. Narkis, and O. Ishai, Oriented Short Glass-Fiber Composites, I, Preparation and Statistical Analysis of Aligned Fiber Mats, *Polym. Eng. Sci.*, Vol 15, Society of Plastics Engineers, 1975, p 525–532
4. L. Kacir, M. Narkis, and O. Ishai, Oriented Short Glass-Fiber Composites, III, Structure and Mechanical Properties of Molded Sheets; *Polym. Eng. Sci.*, Vol 17, Society of Plastics Engineers, 1977, p 234–241
5. L. Kacir, M. Narkis, and O. Ishai, Oriented Short Glass-Fiber Composites, IV, Dependence of Mechanical Properties on the Distribution of Fiber Orientations; *Polym. Eng. Sci.*, Vol 18, Society of Plastics Engineers, 1978, p 45–52
6. Molding Compounds, *ASM Handbook*, Vol 21, *Composites*, ASM International, 2001, p 141–149
7. C.W. Peterson, G. Ehnert, K. Liebold, K. Horsting, and R. Kuhfusz, Compression Molding, *ASM Handbook*, Vol 21, *Composites*, ASM International, 2001, p 515–535
8. D.A. Reigner and B.A. Sanders, *Proceedings of National Technical Conference*, Society of Plastics Engineers, 1979
9. B.Z. Zang, *Advanced Polymer Composites: Principles and Applications*, ASM International, 1994
10. M.P. Groover, *Fundamentals of Modern Manufacturing—Materials, Processes, and Systems*, Prentice-Hall, Inc., 1996
11. V. John, *Introduction to Engineering Materials*, Industrial Press Inc., 1992, p 342–343

SELECTED REFERENCES

- B.T. Astrom, *Manufacturing of Polymer Composites*, Chapman & Hall, 1997
- "Injection Molding Processing Guide," LNP Engineering Plastics Inc., 1998
- B.Z. Jang, *Advanced Polymer Composites: Principles and Applications*, ASM International, 1994
- P.K. Mallick, *Fiber-Reinforced Composites: Materials, Manufacturing, and Design*, 2nd ed., Marcel Dekker, 1993
- R.D. Pistole, Compression Molding and Stamping, *ASM Engineered Materials Handbook*, Vol 2, *Engineering Plastics*, ASM International, 1988
- S.L. Rosen, *Fundamental Principles of Polymeric Materials*, John Wiley & Sons, 1982
- A.B. Strong, *High Performance and Engineering Thermoplastics*, Technomic Publishing, 1993
- "User's Guide for Short Carbon Fiber Composites," Zoltek Companies Inc., 2000

"*This page left intentionally blank.*"

Copyright © 2010, ASM International®
All rights reserved.
www.asminternational.org

CHAPTER 11

Machining and Assembly

COMPOSITES ALLOW for the manufacture of large integral structures, thereby reducing the number of parts and mechanical fasteners required to assemble them. Many structures can be either cocured or bonded together to integrate a significant number of detail parts into a single assembly. In spite of these technical advances, assembly still accounts for a significant portion of the total manufacturing cost, representing as much as 50 percent of the total cost of a delivered part. Assembly operations are labor-intensive and involve many steps. For example, a composite wing requires, first, a framing operation in which all of the spars and ribs must be properly located and connected with shear ties. Each skin must then be located on the substructure, and shimmed; holes must be drilled and fasteners installed. During and after skin installation, various sealing operations must be performed. Last, the leading edges, wing tips, and control surfaces of the wing torque box must be assembled. A typical fighter aircraft can have 200,000 to 300,000 mechanical fasteners, whereas a commercial airliner or transport aircraft can have 1,500,000 to 3,000,000, depending on the aircraft size. A hole must be drilled for each fastener, and then the fastener must be installed. This brief description is a gross oversimplification of the complexity involved in assembling a large structural component.

In this chapter, the basic machining and assembly operations are explained, with an emphasis on hole preparation and the types of mechanical fasteners used in composite structures. Some of the design and analysis aspects for mechanical fasteners are covered in Chapter 17, "Structural Joints—Bolted and Bonded."

11.1 Trimming and Machining Operations

Composites are more prone to damage during trimming and machining than conventional metals, as they contain strong and very abrasive fibers held together by a relatively weak, brittle matrix. During machining, they are prone to delaminations, cracking, fiber pull-out, fiber fuzzing (aramid fibers), matrix chipping, and heat damage. It is therefore important to minimize forces and heat generation during machining. During metallic machining, the chips help to remove much of the heat generated during the cutting operation. Because of the much lower thermal conductivity of the fibers (especially glass and aramid), heat buildup can occur rapidly and degrade the matrix, resulting in matrix cracking and even delaminations. When machining composites, high speeds, low feed rates, and small depths of cuts are used to minimize damage.

Although conventional machining methods such as milling are not normally used on composite parts (since they cut through the continuous fibers and reduce the strength), most such parts require peripheral edge trimming after cure. Edge trimming is done either manually with high-speed cutoff saws or automatically with numerically controlled (NC) abrasive water jet machines. Lasers have often been proposed for trimming of cured composites, but the surfaces become charred by the intense heat and are unacceptable for most structural applications.

Carbon fibers are very abrasive and quickly wear out conventional steel cutting blades; therefore, trimming operations should be conducted using either diamond-coated circular saw blades, carbide router bits, or diamond-coated router bits. A typical manual edge-trimming operation,

shown in Fig. 11.1, is conducted with a high-speed air motor at 20,000 rpm using either a carbide router bit or, less commonly, a diamond-impregnated cutoff wheel. Fiberglass laminate trim templates are often clamped to the part to ensure that the true trim path is followed and provide edge support to help prevent delaminations. Typical feed rates are 10 to 14 in./min (25 to 35 cm/min). Hand trimming requires that the operator wear a respirator, have eye and ear protection, and wear heavy-duty gloves. Many facilities have installed ventilated trim booths to help control the noise and fine dust generated by this operation. As trimming is a hand operation, the quality of the cut is strongly dependent on the skill of the operator. Too fast a feed rate can cause excessive heat, which in turn can cause matrix overheating and ply delaminations.

Abrasive water jet trimming has emerged as the preferred method for trimming cured composites; however, the process uses large, expensive NC machine tools (Fig. 11.2). The advantages of abrasive water jet cutting are that consistent delamination-free edges are produced and that tooling requirements are simpler because the cutting path is NC. Abrasive water jet cutting is primarily an erosion process rather than a true cutting process, so very little force is exerted on the part during trimming; therefore, only simple holding fixtures are required to support the part. In addition, no heat is generated during cutting, so there is no risk of matrix degradation. Water pumped at low volumes of 1 to 2 gal/min (4 to 8 L/min) enters the top of the head and is then mixed with garnet grit that is expelled through a 0.040 in. (1 mm) diameter sapphire nozzle at 40 to 45 ksi (280 to 340 MPa). In general, higher grit size numbers (smaller grain diameters) produce better surface finishes, with a typical grit size being #80. Once the abrasive slurry has penetrated the composite laminate, there is a catcher filled with steel balls that spin to dissipate the flow. Other than the expense of these tools, the main disadvantage is the noise generated during the process. It is not unusual for the noise of trimming operations to exceed 100 dB; therefore, ear protection is required, and many units are isolated within their own soundproof rooms. If edge sanding is required, die grinders at speeds of 4000 to 20,000 rpm can be used along with 80-grit aluminum oxide paper for roughing and 240- to 320-grit silicon carbide paper for finishing.

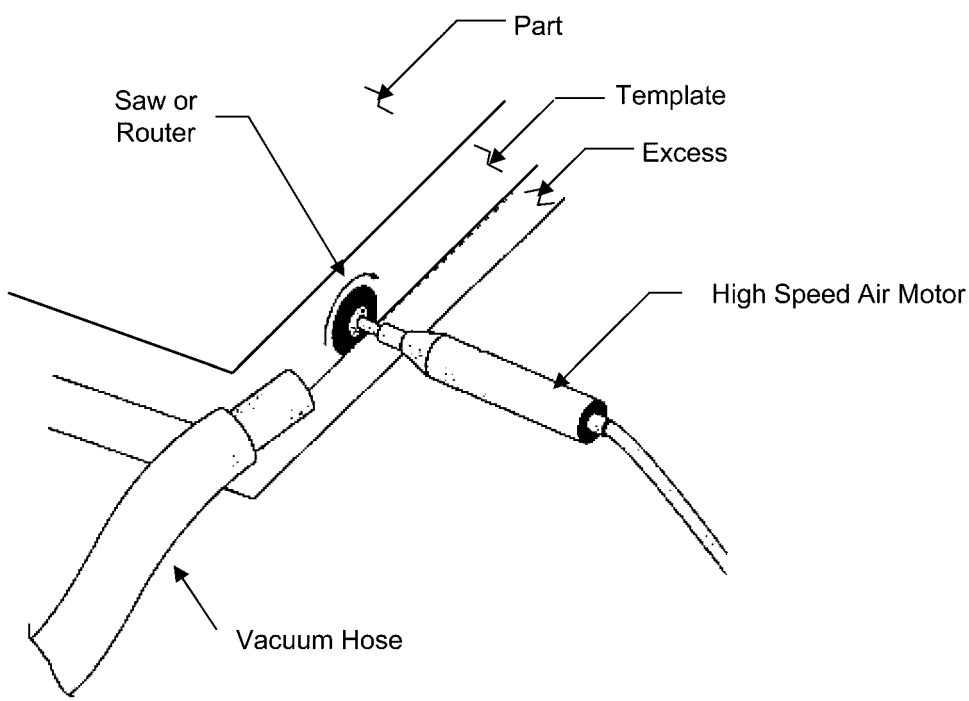


Fig. 11.1 Hand trimming. Source: Ref 1

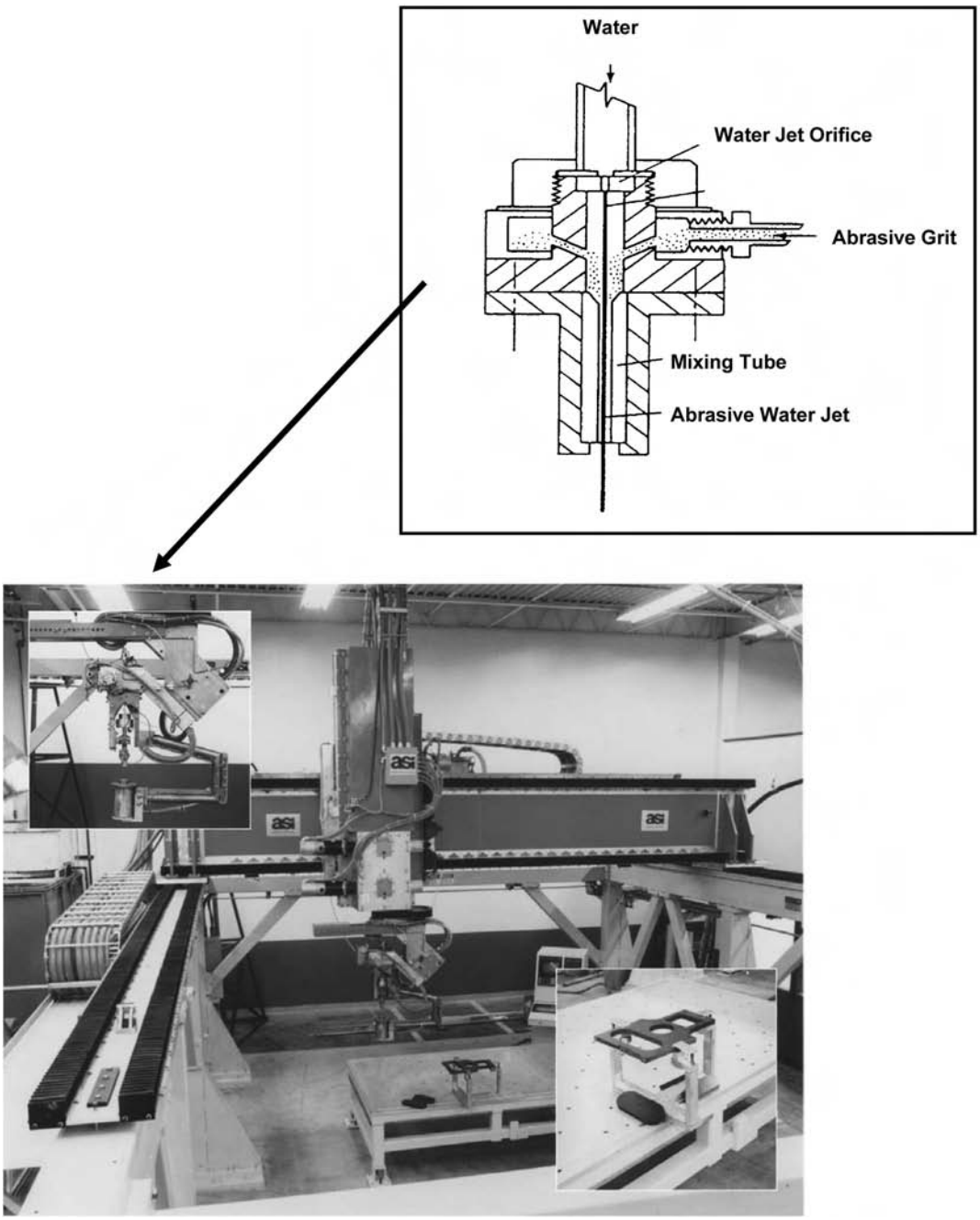


Fig. 11.2 Abrasive water jet trimming machine tool. Source: The Boeing Company

11.2 General Assembly Considerations

Framing operations, in which the substructure is located and fastened in its proper location, have made significant progress in the last 40 years. In the 1960s and 1970s, substructures were manually located (with a few positions located using hard tooling), usually supplemented with large pieces of clear plastic film that's typically biaxially oriented polyethylene terephthalate (boPET, such as DuPont's Mylar) scribed with hole pattern locations. The design, tooling, and fabrication

databases were not necessarily coordinated, so high variability and poorly fitting parts were common. During the 1980s and 1990s, there was less use of boPET and greater reliance on hard tooling to position parts, which increased the nonrecurring investment required at the start of a new program. With the advent of solid modeling and electronic master models in the 1990s, a process called *determinant assembly* emerged. In this process, coordinated undersized fastener holes are drilled in the parts during fabrication. These holes are then used to position the parts during assembly, eliminating the need for hard tooling locators. Another recent development is the use of laser projection units for establishing part and hole location. A typical application for a laser projection system is shown in Fig. 11.3.

It is important to check all joints for gaps before starting to drill holes and install fasteners. Gaps can unnecessarily preload metallic members when fasteners are installed, and such preloading can initiate premature fatigue cracking and even stress corrosion cracking of aluminum. However, gaps in composite structures can cause even more serious problems than in metallic structures. Since composites do not yield and are more brittle and less forgiving than metals, excessive gaps can result in delaminations during fastener installation. The force exerted by the fastener can bend the composite, which may then develop matrix cracks and/or delaminations around the holes. Cracks and delaminations usually occur on multiple layers through-the-thickness and can adversely affect joint strength. Gaps can also trap metal chips and contribute to backside hole splintering. If the skin is composite and the substructure is metal, and if an appreciable gap is present during fastener installation, the composite skin will often crack and delaminate. If both the skin and substructure are composite, cracks can develop in either the skin or the substructure, or both. Substructure cracking often occurs at the radius between the top of the stiffener and the web.

To prevent unnecessary preloading of metallic structure, and the possibility of cracking and delaminations in composite structure, it is important to measure all gaps and then shim any that are greater than 0.005 in. (0.1 mm). Liquid shim, which is a filled thixotropic epoxy paste adhesive, can be used to shim gaps between 0.005 and 0.030 in. (0.1 and 0.8 mm). If the gap exceeds 0.030 in. (0.8 mm), then a solid shim is normally used. Engineering approval is often

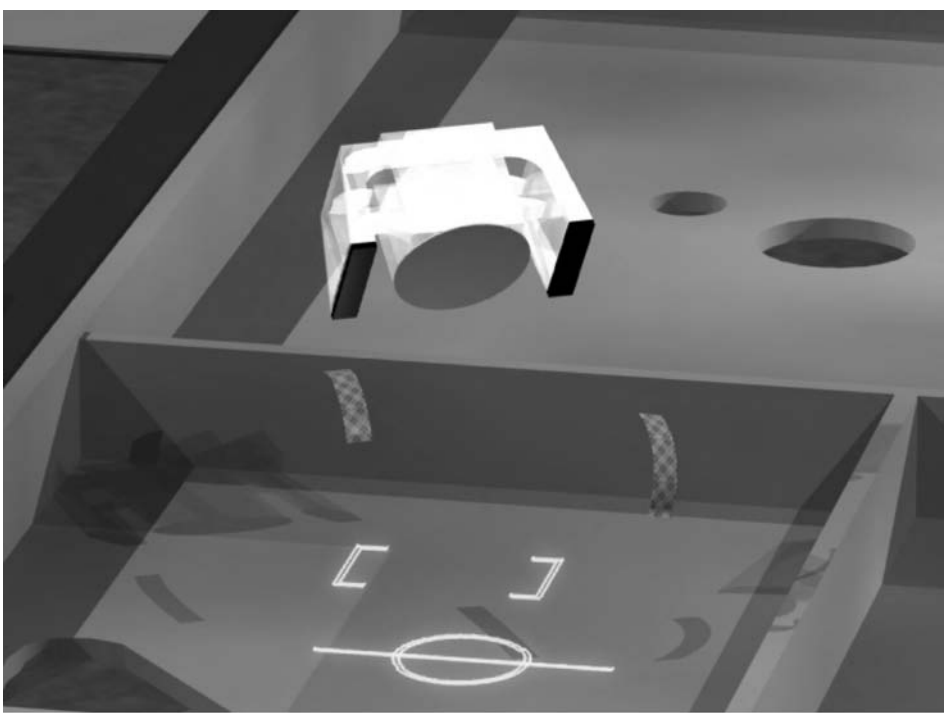


Fig. 11.3 Laser projection location. Source: Laser Projection Technologies, Inc.

required for a gap this large. Solid shims can be made from solid metal, laminated metal that can be peeled to the correct thickness, or composite. When selecting a solid shim material, it is important to make sure that there is no potential for galvanic corrosion within the joint.

Liquid shimming can be accomplished by first drilling a series of undersized holes in the two mating surfaces so that temporary fasteners can be installed to provide a light clamp-up during the shimming process. The liquid shim is usually bonded to one of the two mating surfaces. The surface to be bonded should be clean and dry to provide adequate adhesion. Composite surfaces are scuff-sanded. The other surface is covered with release tape or film. After the liquid shim is mixed, it is buttered onto one surface; the other surface is located and then clamped with mold-released temporary fasteners. The excess or squeeze-out is removed prior to gellation, which usually occurs within one hour of mixing. After the shim material has cured, typically for about 16 hours, the part is disassembled and any voids or holes in the shim are repaired. After the repair has cured, the parts can be assembled.

11.3 Hole Preparation

The differences between fighter aircraft and commercial passenger aircraft create different problems in each. Fighter aircraft designs are highly tailored to performance and loads, and therefore have many thickness variations in the skins and substructure to reduce the weight. As a result, such aircraft incorporate a wide variety of fastener types, grip lengths, and diameters but a limited number of actual fasteners. Because of the smaller size of a fighter airframe, more areas are difficult to access during assembly. By contrast, larger commercial aircraft have much more fastener commonality with regard to type, grip length, and diameter but also, because of their size, many more fasteners. Skins and substructure tend to be more uniform in thickness. Limited access is not as much of a problem, but the large size of the parts makes them difficult to handle. There are many types of drill motors and units that can be used to drill structures, but they can be broadly classified as hand, power feed, and automated drilling units.

11.3.1 Manual Drilling

Manual, or freehand, drilling using handheld drill motors, like the one shown in Fig. 11.4, has



Fig. 11.4 Typical freehand drill motor. Source: Cooper Power Tools

the least chance of making a close-tolerance hole that measures +0.003/–0.000 in. (+0.08 mm/ –0.00 mm). All that really can be controlled is the drill speed (rpm). It is up to the operator to make sure that the drill: (1) is properly located; (2) is perpendicular to the surface; and (3) is fed with enough pressure to generate the hole but not enough to damage it. Although freehand drilling is obviously not the best method, it is frequently used because it requires no investment in tooling such as drill templates, and in many applications in which access is limited, it may be the only viable method. A typical tight-access situation is shown in Fig. 11.5, where a mechanic is installing the collars on Hi-Lok two-part self-locking fasteners. For tight-access areas, right-angle drill motors are available. If freehand drilling is used, the operators should use a drill bushing or a tripod support to ensure normality, and they should be provided with detailed written instructions for hole generation and inspection.

Manual hole drilling during assembly is often done by drilling undersized holes (pilot holes), installing temporary fasteners to hold the parts together, and then bringing the holes up to full size. Pilot holes are usually drilled with small-diameter drill bits measuring 0.09 to 0.125 in. (2 to 3 mm). Hole diameters for aerospace structures nominally range from 0.164 to 0.375 in. (4 to 10 mm) in diameter, with the predominant hole sizes being 0.188 and 0.250 in. (4.8 and 6.4 mm). During drilling, it is important to use a sharp drill bit, which will not wander as easily as a dull one; drilling is faster; and lower forces are required, minimizing the possibility of injury or part damage. When drilling multimaterial stackups, it is important to make sure that they are securely clamped together.

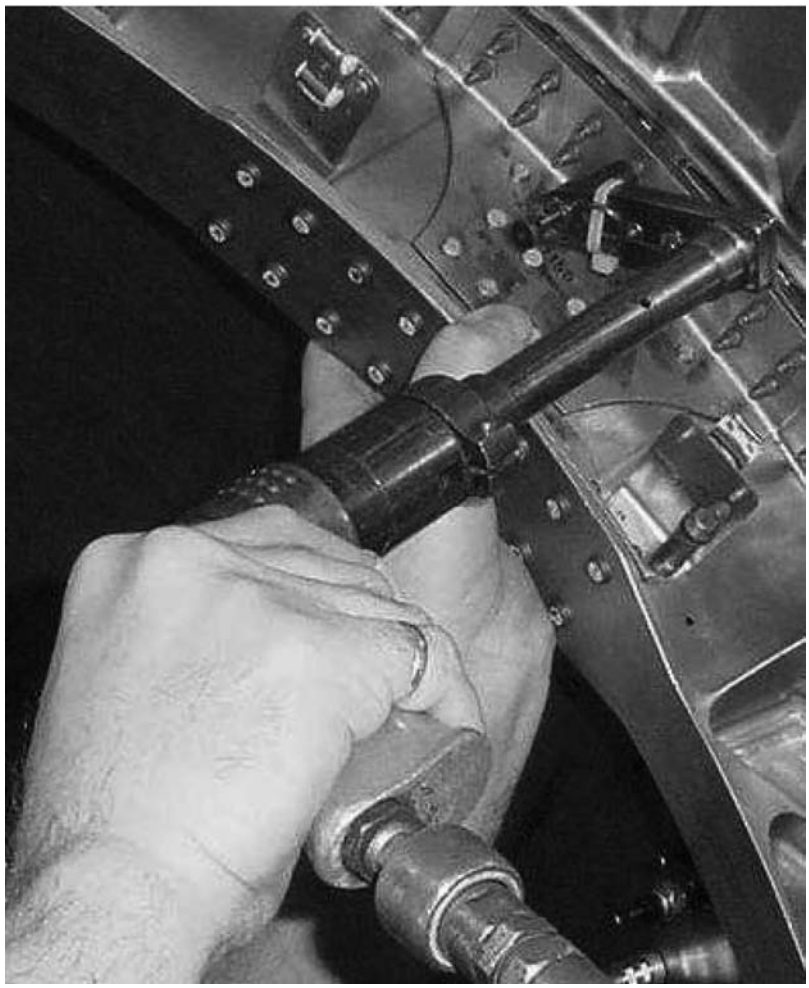


Fig. 11.5 Limited-access fastener installation. Source: The Boeing Company

The speeds used in manual drilling depend on both the materials and their thickness. Drilling holes in composites is more difficult than drilling them in metals because of the tendency of composites to heat damage and their weakness in the through-the-thickness direction. Composites are very susceptible to surface splintering (Fig. 11.6), particularly if unidirectional material is present on the surface. Splintering can occur at either side of the hole. As shown in Fig. 11.7, when the drill enters the top surface, it creates peeling forces on the matrix as it grabs the top plies. When it exits the hole, it induces punching forces that create peel forces on the bottom surface plies. Top-surface splintering is usually a sign that the feed rate is too fast, whereas exit-surface splintering indicates that the feed force is too high. It is common practice to cure a layer of fabric on both surfaces of composite parts. This practice largely eliminates the hole-splintering problem; woven cloth is much less susceptible to splintering than unidirectional material. A backup material such as aluminum or composite, clamped to the backside, will frequently help to prevent backside hole splintering. Coolant is normally not used for carbon/epoxy laminates that are 0.250 in. (6 mm) thick or thinner. When drilling composites dry, operators should be provided with vacuum capability to collect the dust and should always wear both eye protection and a respirator.

Since epoxy matrix composites will start to degrade if heated above 400 °F (200 °C), it is important that heat generation be minimized during drilling. Typical drilling parameters are 2000 to 3000 rpm at feed rates of 0.002 to 0.004 in.

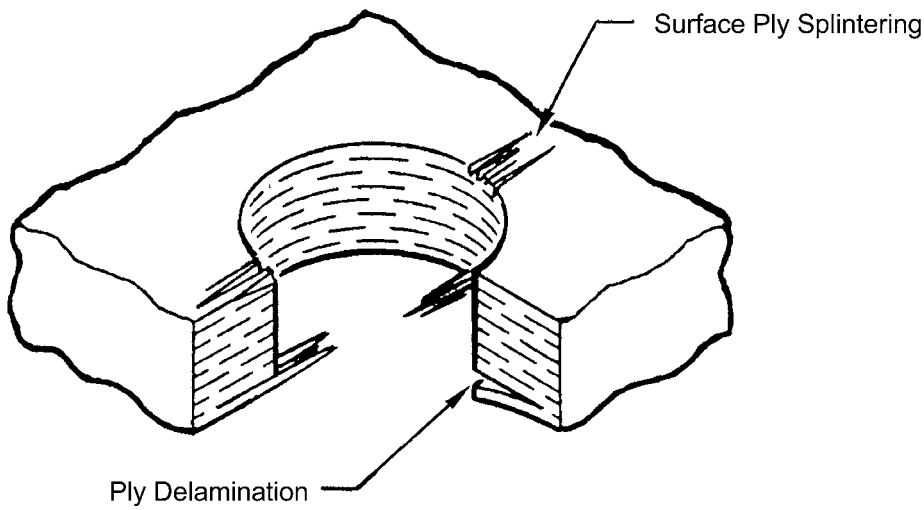


Fig. 11.6 Composite hole splintering

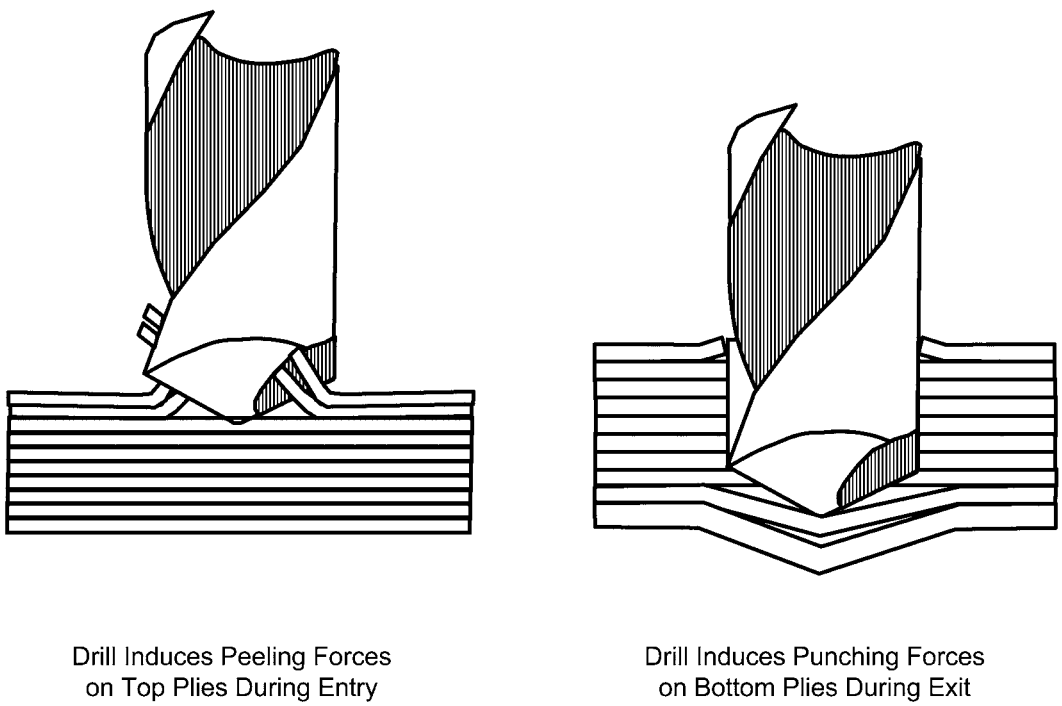


Fig. 11.7 Drilling forces on composite laminate. Source: Ref 2

per revolution (ipr) (0.05 to 0.1 mm/rev), although this will vary, depending on the drill geometry and the type of equipment used. Thermocouples and heat-sensitive paints are often used during drilling parameter development tests to monitor the heat generated. Drilling parameters for composite-to-metal stack-ups are often controlled more by the metal than by the composite. For example, when drilling carbon/epoxy (C/E) to aluminum, a speed of 2000 to 3000 rpm

with a feed rate of 0.001 to 0.002 ipr (0.03 to 0.05 mm/rev) might be used, whereas a stack-up of C/E to titanium would require a slower speed of 300 to 400 rpm and a higher feed rate of 0.004 to 0.005 ipr (0.1 to 0.13 mm/rev). Titanium alloy (Ti-6Al-4V) is also very sensitive to heat buildup (hence the lower speed) and tends to work-harden rapidly if light cuts are used (hence the higher feed rate).

To help to reduce the variability in manual hole drilling, some manufacturers produce detailed written instructions covering specific hole-drilling operations and provide kits that have all of the correct tools needed for a specific operation.

11.3.2 Power Feed Drilling

Power feed drilling is preferable to hand drilling. In this process, the drill unit is locked into a template that establishes hole location and maintains drill normality. In addition, the unit is programmed to drill at a given speed and feed once the drilling operation starts. Some units, such as the one shown in Fig. 11.8, can be programmed for different peck cycles. Peck drilling (Fig. 11.9)



Fig. 11.8 Power feed peck drill. Source: Cooper Power Tools

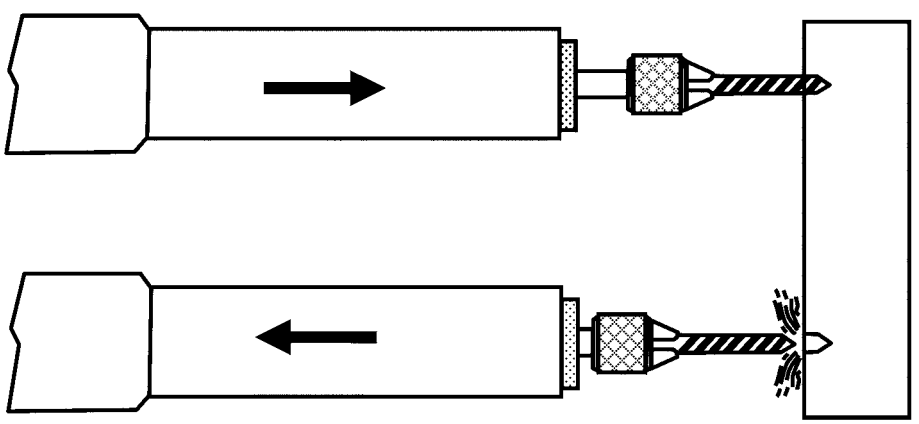


Fig. 11.9 Peck drilling. Source: Ref 3

is a process in which the drill bit is periodically withdrawn to clear the chips from the flutes. It is used almost exclusively when drilling composite-to-titanium stack-ups, because the hard titanium chips have a tendency toward back counterboring (Fig. 11.10). The process also greatly reduces the rapid heat buildup that can occur when drilling titanium.

All of these controls lead to much better and more consistent hole quality, particularly in the drilling of composite-to-metal stack-ups. A typical peck drilling cycle for a 0.188 in. (5 mm) diameter hole through a C/E-to-titanium stack-up comprises a speed of 550 rpm, a feed rate of 0.002 to 0.004 ipr (0.05 to 1 mm/rev), and a peck rate of 30 to 60 pecks per in. (1 to 2 pecks per mm) of thickness.

When drilling into composite-to-metal stack-ups, a phenomenon called *back counterboring* can occur. As shown in Fig. 11.10, as the metal chips of aluminum or titanium travel up the flutes, they tend to erode the softer liquid shim and composite matrix material, causing eroded and oversize holes. Back counterboring can be minimized by: (1) eliminating all gaps; (2) using a drill geometry that produces small chips; (3) changing speeds and feeds; (4) providing better clamp-up; (5) reaming the hole to the final diameter after drilling; or (6) employing peck drilling.

11.3.3 Automated Drilling

For high-volume hole generation, automated drilling equipment can be designed and built for specific applications. Being large, sophisticated machine tools, these units are expensive, so the number of holes drilled and the number of units produced need to be large enough to justify the equipment investment. One of these large units is shown in Fig. 11.11. These machines are extremely rigid and allow for accurate hole location and normality. They are NC, so there is no need for drill templates. They have vision systems that can scan the substructure and software that will then adjust the hole location to match the actual location of the substructure even if it is not exactly where the design says it should be. All drilling parameters are automatically controlled, and it is possible to change speeds and feeds when drilling through different materials. Because of the thick stack-ups that must be drilled in a wing, a water-soluble flood or mist coolant is usually used during the hole-drilling operations. All drilling data are automatically recorded and stored for quality control purposes. The drill holders contain bar codes that the drilling program uses to make sure that the correct drills are used for the correct holes. These machines can also install temporary fasteners to clamp the skins to the substructure during drilling, and they frequently use integral drill-countersink cutters that drill the hole and then continue to countersink it during the same operation.

The current trend in the aerospace industry is to replace these large installations with smaller, more flexible units. An off-the-shelf commercial robot, with some modifications and a special drilling end effector, is used to drill holes in the control surface shown in Fig. 11.12. Another approach is to integrate drilling units into the assembly fixture, using what are called *numerically controlled drill jigs*. An example of such a

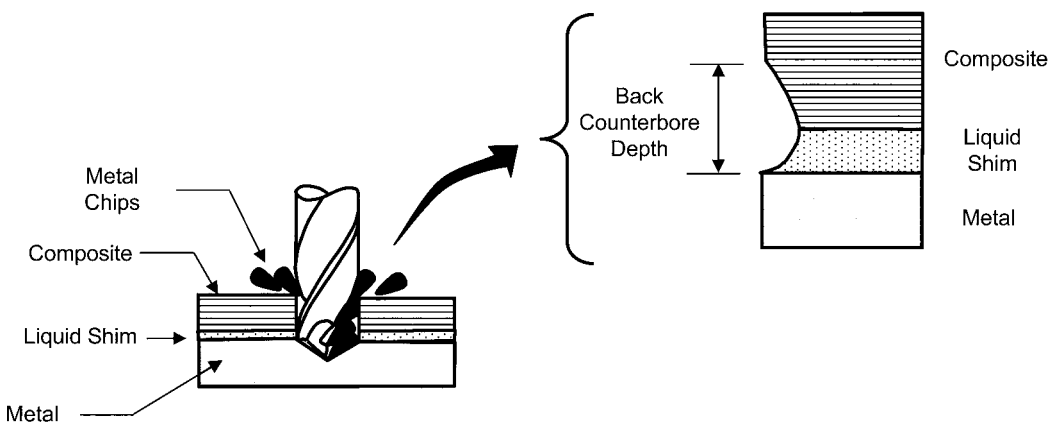
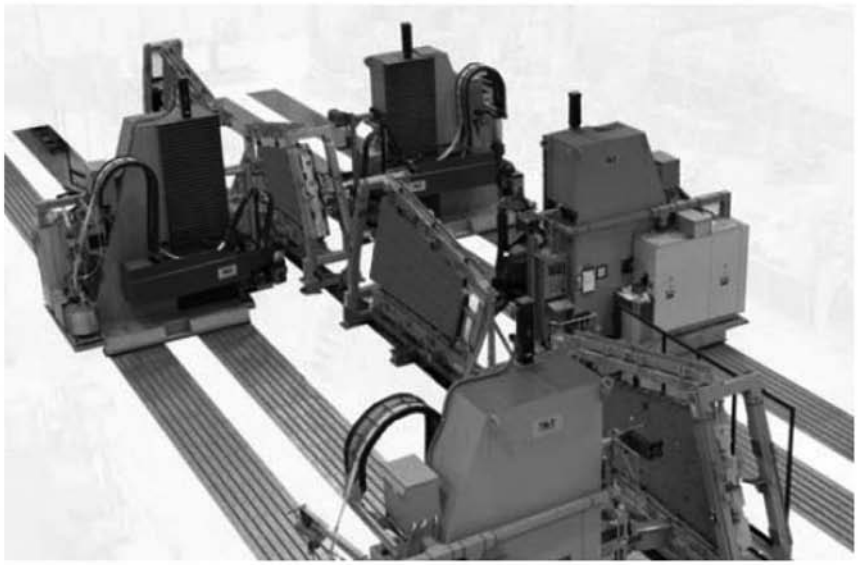


Fig. 11.10 Back counterboring



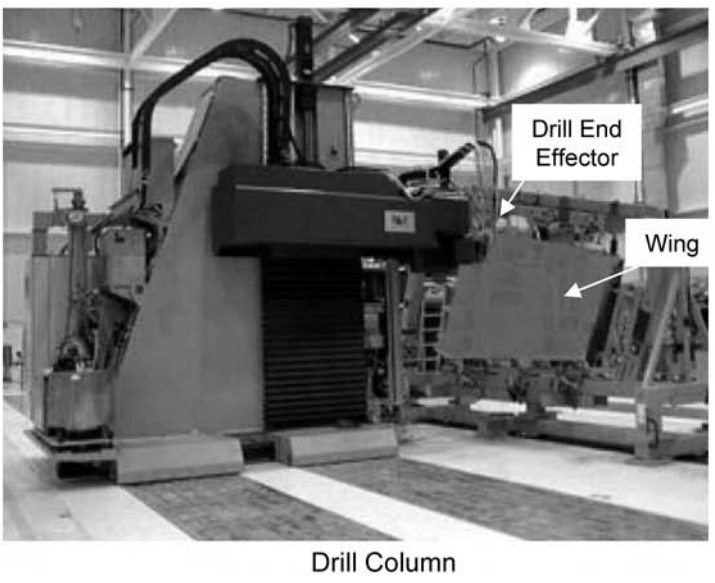


Fig. 11.11 Automated composite wing drilling system. Source: PaR Systems, Inc.

relatively low-cost unit is shown in Fig. 11.13 for a fighter aircraft outer wing.

11.3.4 Drill Bit Geometries

Many variations of twist drills (Fig. 11.14) are used in drilling metallic structures. Since specific drill bit geometries can influence both the quality and the quantity of holes drilled, many geometries are proprietary to the various aerospace manufacturers. Although standard twist drills are used for drilling metallic structures, some unique drill geometries have been developed for composites, several of which are shown in Fig. 11.15. The design of the drill and the drilling procedures are highly depen-

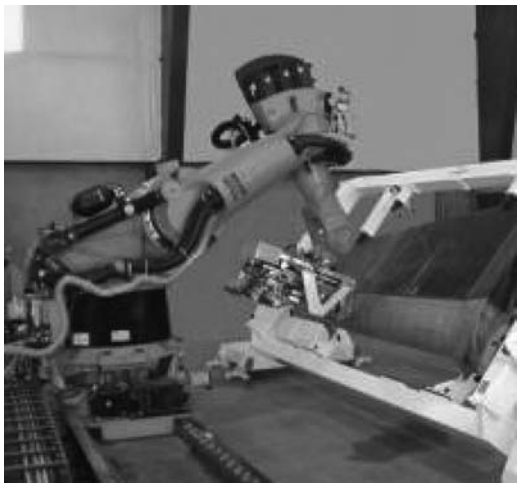


Fig. 11.12 Robotic drilling of composite control surface. Source: The Boeing Company

dent on the materials being drilled. For example, carbon and aramid fibers exhibit different machining behavior and therefore require different drill geometries and procedures. In addition, composite-to-metal stack-ups require different cutters and procedures. The flat two-flute and four-flute dagger drills were developed specifically for drilling stack-ups of C/E. The two-flute variety is normally run at 2000 to 3000 rpm and the four-flute variety at 18,000 to 20,000 rpm. When drilling through composite-to-metal stack-ups, the drill geometry is controlled more by the metal and special twist drill geometries are often used. Due to their low compressive strengths, aramid fibers have a tendency to recede back into the matrix rather than being cleanly cut, resulting in fuzzing and fraying during drilling. Therefore, the aramid drill contains a "C"-type cutting edge that grabs the fibers on the outside of the hole and keeps them in tension during the cutting process. Typical drilling parameters for aramid fiber composites are 5000 rpm and a feed rate of 0.001 ipr (0.03 mm/rev).

Standard high-speed steel (HSS) drills work well in glass and aramid composites, but the extremely abrasive nature of carbon fibers requires that carbide drills be used to obtain an adequate drill life. For example, a HSS drill may be capable of drilling only one or two acceptable holes in C/E, but a carbide drill of the same geometry can easily generate 50 or more acceptable holes. For drilling C/E in rigid automated drilling equipment, polycrystalline diamond (PCD) drills have exhibited outstanding productivity improvements. A PCD drill has a carbide body with a vein of diamond grains sintered into the cutting edge. Although PCD drills are very expensive, the number of holes obtained per drill and the fewer changes required make them cost-effective. However, PCD drills cannot be used with freehand or nonrigid setups; the point will immediately chip and break if any vibration or chatter is present during drilling.

11.3.5 Reaming

Although it is desirable to drill the hole to its final size in one pass, it is often necessary to ream the hole to its final diameter. Reaming is done with carbide reamers at about one-half of the drilling speed at 500 to 1000 rpm. In some composite-to-metal structures, fasteners are installed clearance-fit in the composite and interference-fit in the metallic structure to improve the metallic fatigue life. In this situation, the final hole diameter is drilled in the composite-to-metal stack-up, the composite skin is taken down, and the holes in the composite skin are reamed to provide a clearance fit for the fastener. When the stack-up is reassembled, the fasteners are installed clearance-fit in the composite and interference-fit in the metal.

11.3.6 Countersinking

Countersinking should be used only when protruding-head fasteners will not satisfy design requirements. In general, countersinking reduces static joint strength and fatigue life. During countersinking for flush-head fasteners, it is important not to countersink too deeply and create a knife-edge condition in the countersunk member. A knife edge creates a significant stress riser and also allows the fastener to tilt and rise up on the countersink surface, resulting in low joint yield strength and reduced fatigue life. As a general rule, countersinking should never bring the head of the fastener any closer than 0.025 in. (0.6 mm) to the far side of the sheet or through more than 80 percent of the sheet thickness, as illustrated in Fig. 11.16. Piloted countersinks are helpful in centering the countersink tool in the hole, and microstop cages can be used to control the depth.

Countersinking is performed for composite structures in much the same way as for metals, except that the area where the countersink transitions into the hole must have a radius equal to the fastener's head-to-shank radius. Because of the

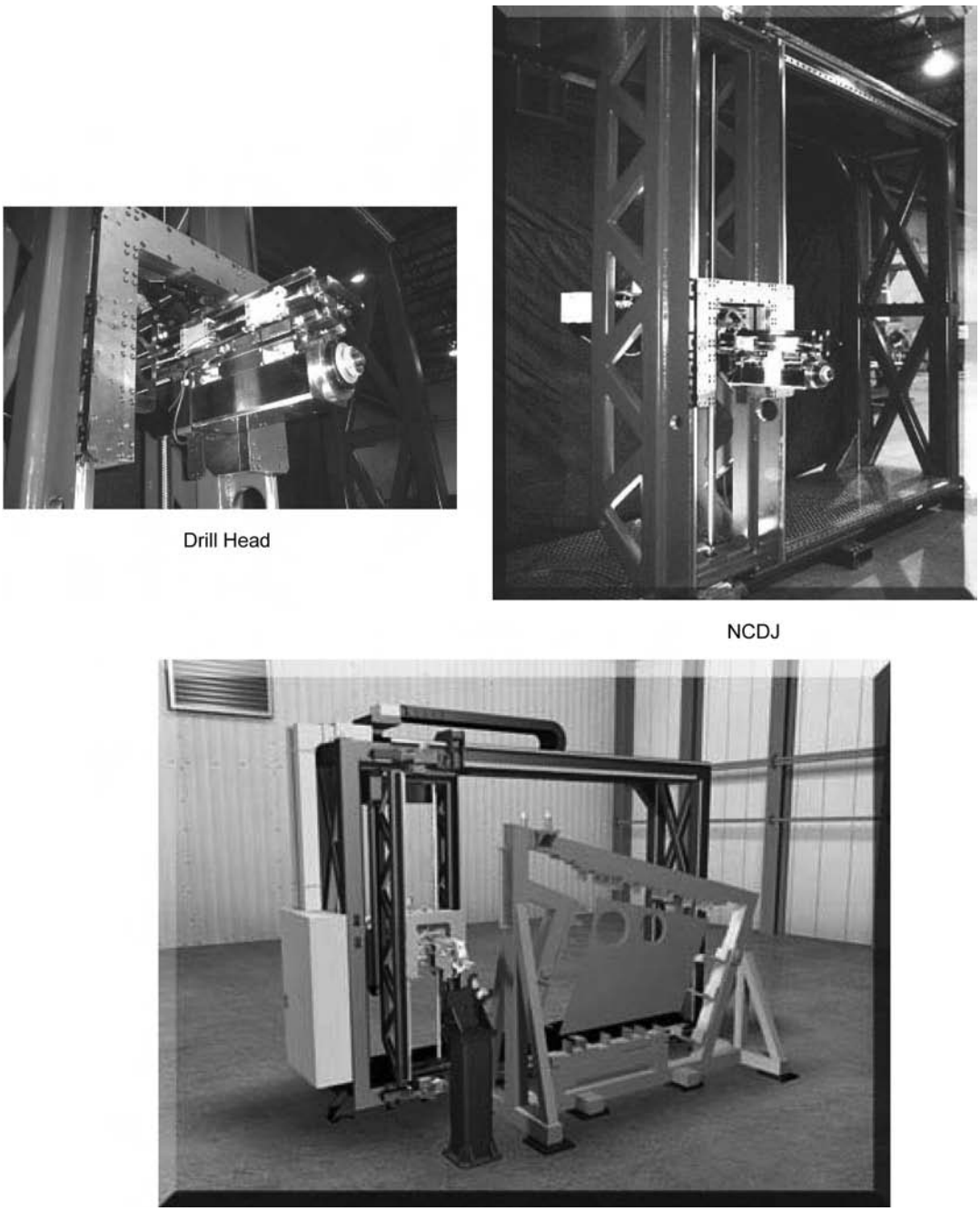


Fig. 11.13 Composite outer wing numerically controlled drill jig (NCDJ) drilling system. Source: The Boeing Company

low interlaminar shear strength of composites, failure to satisfy this condition can result in cracks and delaminations under the force of fastener installation. Countersinking cutters for composites are normally made of solid carbide, steel with carbide inserts, or steel with PCD inserts.

11.4 Fastener Selection and Installation

Many types of fasteners are used in aerospace structural assembly, the most prevalent being solid rivets, pins with collars, bolts with nuts, and blind fasteners. Examples are shown

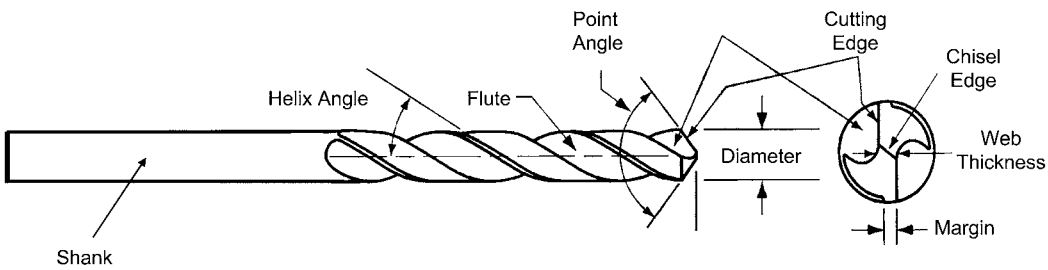


Fig. 11.14 Twist drill geometry

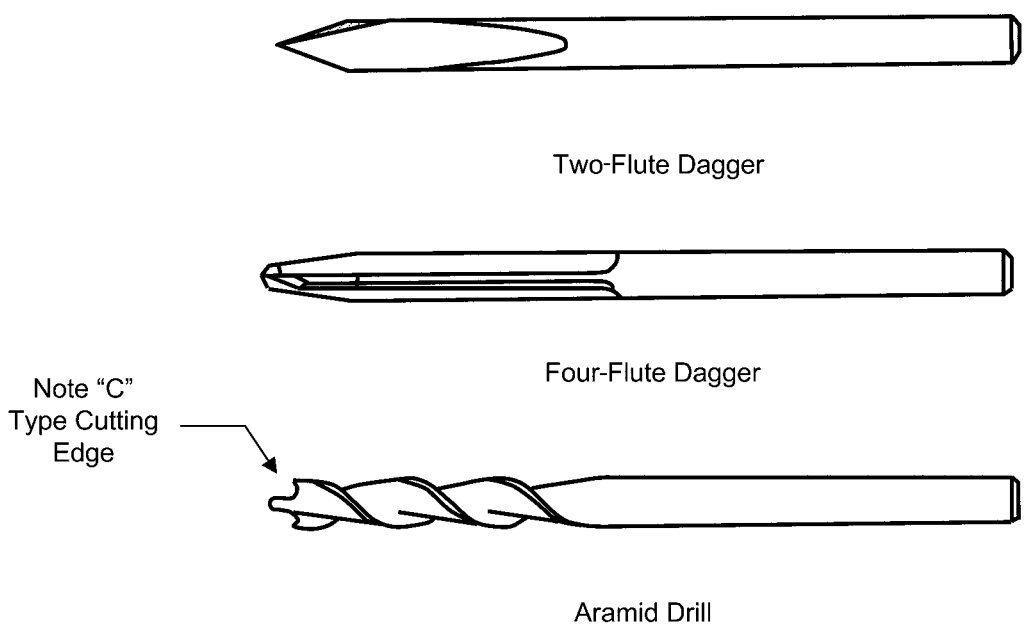


Fig. 11.15 Composite drill configurations

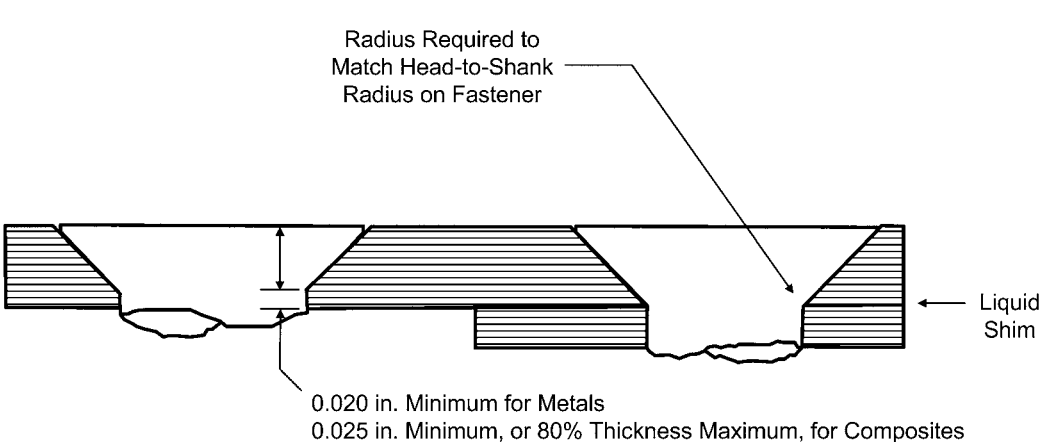


Fig. 11.16 Countersinking

in Fig. 11.17. There are also many other types of fasteners, including quick-release multiple-piece fasteners, latches, straight pins, headed pins, lock pins, cotter pins, threaded inserts, retaining rings, and washers.

Because so many fasteners of so many different types are used in aircraft construction, aerospace companies have developed fastener usage policies that specify, for each program, how fasteners are to be selected and used. Typically, such a policy includes usage limitations, selection criteria, hole size callout information, strength allowables, material compatibility and protection, and lists of approved fasteners. Minimum edge distances and fastener spacing requirements may also be specified in the fastener usage policy if they are not already specified in the individual engineering drawings. For a hole of diameter d, typical edge distances are $2d$ to $3d$ with typical fastener spacings of $4d$ to $6d$.

Mechanical fastener material selection for composites is important in preventing corrosion problems. Aluminum- and cadmium-coated steel fasteners will galvanically corrode in contact with carbon fibers. Titanium alloy (Ti-6Al-4V) is usually the best fastener material for carbon fiber composites because of its high strength-to-weight ratio and corrosion resistance. When higher strength is required, cold-worked A286 iron-nickel or the iron-nickel based alloy Inconel 718 can be used. If extremely high strengths are required for very highly loaded joints, the nickel-cobalt-chromium multiphase alloys MP35N and MP159 are available. Glass and aramid fibers, being nonconductive, do not cause galvanic corrosion of metallic fasteners.

It is important to measure the grip length of a fastener before installing it in a structure. Commercial gauges are available that can be placed through the hole to measure the correct grip length. In determining the fastener grip length for threaded fasteners, it is important that the fastener be long enough that the threads are never loaded in bearing or shear; that is, no threads should be inside the hole. In addition, at least one thread and no more than three threads should be showing when the nut is installed and tightened to the proper torque. Fasteners exposed to the outer moldline of the aircraft are normally installed "wet" by dipping the end of the fastener in polysulfide sealant prior to installation. This practice helps to prevent the intrusion of moisture that can cause corrosion of metallic substructure.

11.4.1 Special Considerations for Composite Joints

When a hole is placed in a composite laminate, it creates a stress concentration and the overall load-bearing capacity of the laminate is severely reduced. Even a properly designed mechanically fastened joint exhibits only 20 to 50 percent of the basic laminate tensile strength. Like hole drilling, fastener installation in composites is more difficult and damage-prone than in metallic structures. Some of the potential problems with fastener installation are shown in Fig. 11.18. As previously discussed, unshimmed gaps can cause cracking of either the composite skin or the composite substructure (or both) as the fastener is being installed. In fuel tanks, channel seal grooves are often used to help prevent fuel leakage. Fasteners with O-ring seals can also be used to further prevent leakage; however, it has been found through experience that fasteners with O-ring seals can result in interlaminar cracking. Although good clamp-up of the fastener is certainly desirable, overtorquing fasteners can also result in cracking. If the countersink radius is too small and does not match that of the fastener head-to-shank radius, the fastener can apply a concentrated point load and cause matrix cracking. Likewise, fastener misalignment, in which the hole and the countersink are not properly aligned, can result in point loading and cracking.

In any mechanically fastened joint, high clamp-up forces are beneficial to both static and fatigue strength. High clamp-up produces friction in the joint, delays fastener cocking, and reduces joint movement or ratcheting during fatigue loading. Most holes eventually fail in bearing as a result of fastener cocking and locally high bearing stresses. To allow the maximum clamp-up in composites without locally crushing the surface, special fasteners have been designed that have large footprints (large heads and nuts that bear against the composite) to help spread the fastener clamp-up loads over as large an area as possible. Washers are also frequently used under the nut or collar to help spread the clamp-up loads. In general, the larger the bearing area, the greater the clamp-up that can be applied to the composite and the higher the resulting joint strength. In addition, tension-head rather than shear-head fasteners are normally used in composites because they are not as susceptible to bolt bending during fatigue and their larger heads help to prevent fastener pull-through during installation in thin structures.

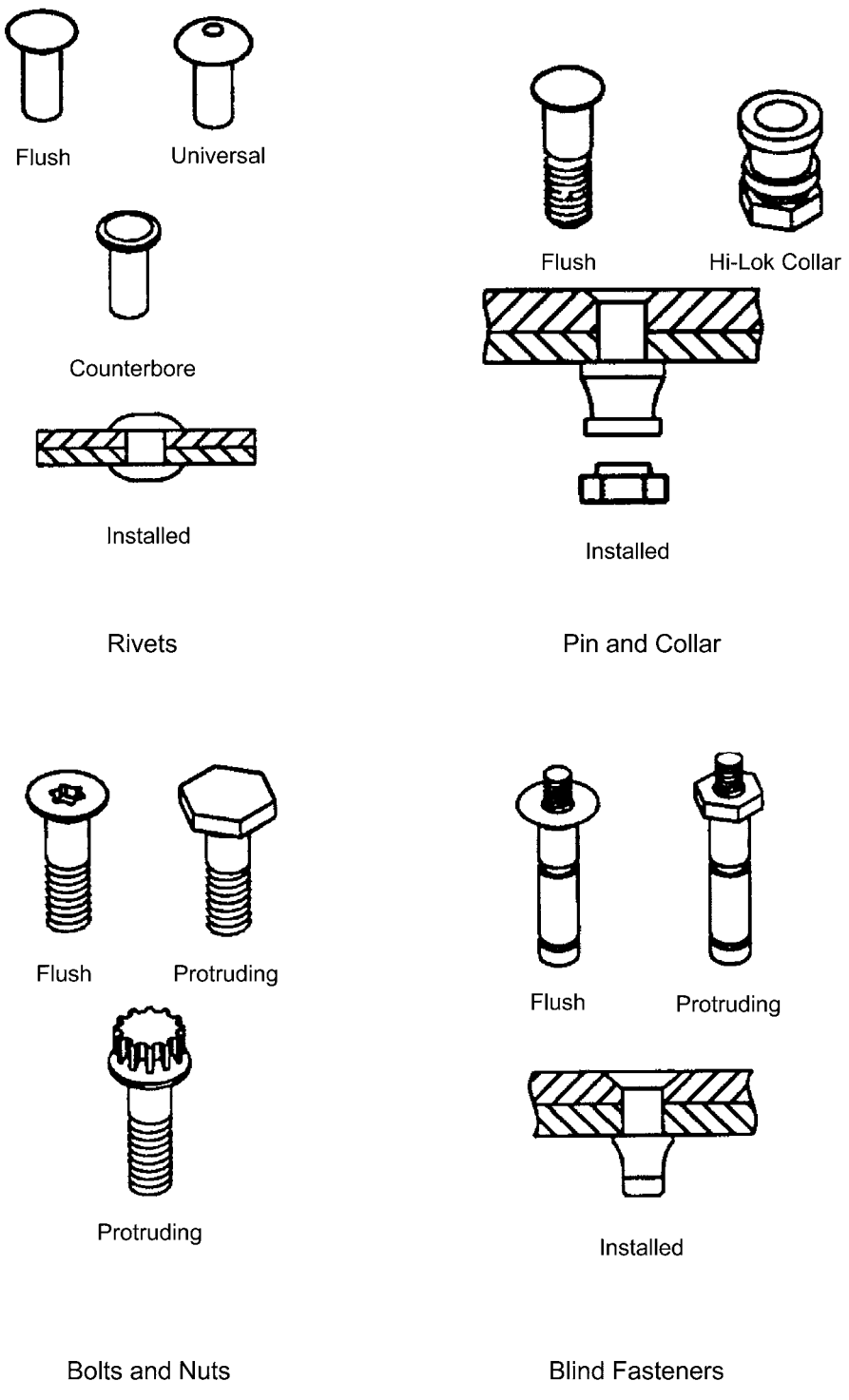


Fig. 11.17 Typical aerospace fastener types

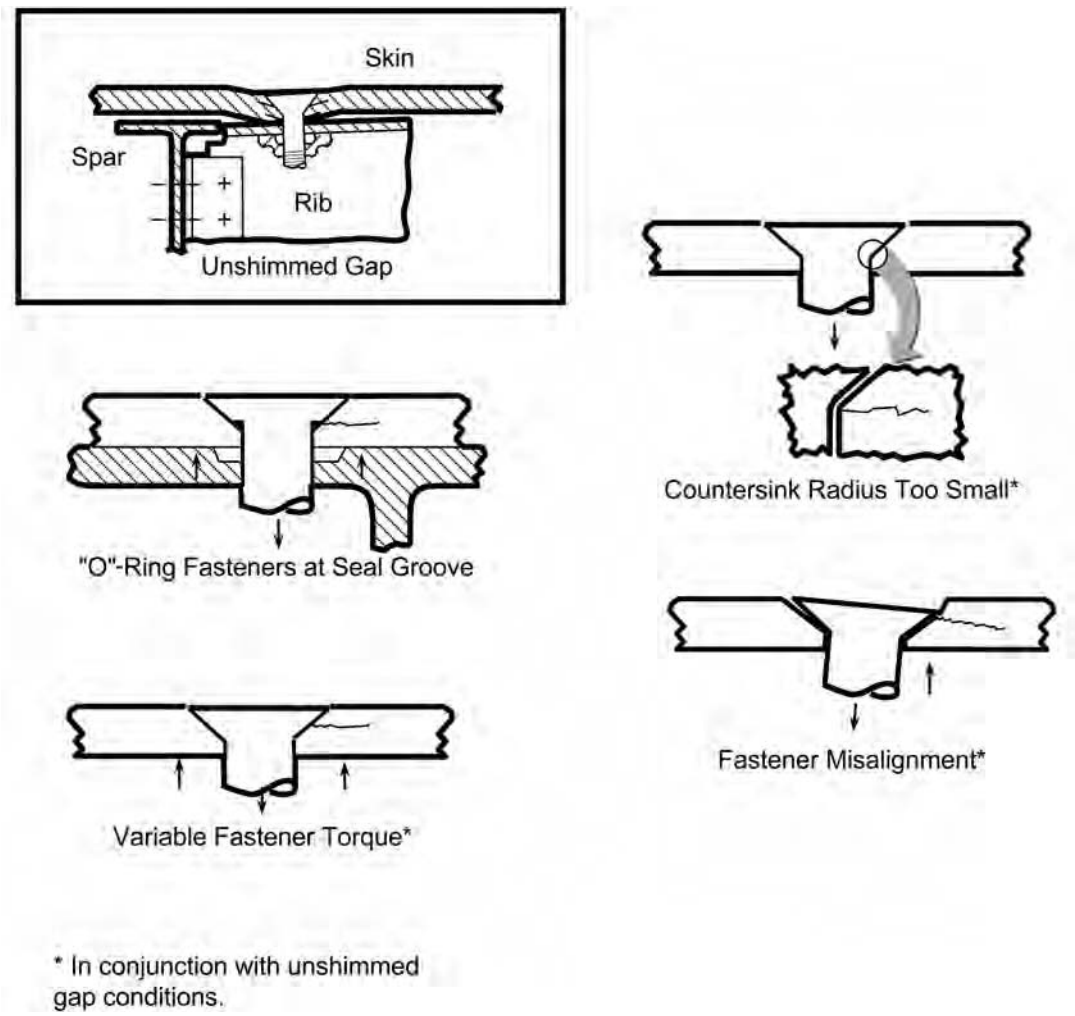


Fig. 11.18 Fastener installation defects

11.4.2 Solid Rivets

Traditionally, riveting has been the most prevalent method of building aerospace structures. As composite and titanium structures replace aluminum structures on newer aircraft, the number of riveted structures will decrease in the future, since rivets are not normally used in titanium or composite structures. However, rivets are, and will remain, an important fastening method for aerospace structures. During rivet installation, several physical changes take place: (1) the rivet expands to fill the hole (thus guaranteeing a tight fit); (2) the hardness of the rivet increases through work hardening; and (3) the manufactured head is formed through plastic deformation.

Rivets are rarely used in composites for two reasons: (1) aluminum rivets galvanically corrode in contact with carbon fibers; and (2) the vibration and expansion of the rivet during the driving process can cause delamination. If rivets are used, the type of rivet selected is usually bimetallic, consisting of a Ti-6Al-4V pin with a softer titanium-niobium tail that is installed by squeezing rather than by vibration driving. In addition, the head that is upset must be against metal rather than composite. There are also hollow-end solid rivets designed to allow flaring of the ends without damaging expansion when used in double-countersunk holes in composites.

11.4.3 Pin and Collar Fasteners

Pin and collar fasteners are the most commonly used fasteners for permanent installations where there is no requirement to remove the fastener later. The pin, similar to a bolt, is used with a self-locking or swaged-on collar that cannot be removed with typical tools without destroying the collar or pin. Pin and collar fasteners are high-strength fasteners made from either Ti-6Al-4V, A286 iron-nickel, or Inconel 718. Typical head designs include the protruding tension head, protruding shear head, 100-degree full countersink, and 100-degree reduced countersink.

A typical pin and collar fastener is the Hi-Lok fastener shown in Fig. 11.19. A Hi-Lok fastener consists of a threaded pin and a collar. The threaded pin is essentially a modified bolt, whereas the collar is basically a nut with a breakaway groove that controls the amount of torque and preload on the pin. Hi-Lok fasteners are available in both flush and protruding heads, and as shear and tension-shear fasteners. Although Hi-Lok fasteners can be installed either clearance-fit or interference-fit, they are normally installed clearance-fit in composite structures. The fastener pin is usually made from Ti-6Al-4V with an A286 nut. Titanium nuts are occasionally used, but these must be coated with an antigalling lubricant; otherwise, the threads tend to gall and long-term clamp-up is adversely affected. A hex key is inserted into the fastener stem to oppose the torque applied to the nut. The nut is tightened down until a predetermined torque level is achieved and the top portion of the nut fractures. Washers can be used under the head to help spread the bearing load on the surface.

The Lockbolt is another common pin and collar fastener that can be installed by either pulling or swaging the collar from the backside. A typical pull-type Lockbolt installation sequence is shown in Fig. 11.20. Lockbolts differ from Hi-Loks in that a Hi-Lok has true threads onto which the nut is threaded, whereas a Lockbolt has a series of annular grooves into which the collar is swaged. Once swaged in place, Lockbolts cannot "back off" (loosen) and they have superior vibration resistance. Lockbolts are available with flush or protruding heads, as shear- or tension-pull types, and as shear-stump types. A Lockbolt is normally lighter and costs less to install than a bolt-nut combinations of the same diameter. Two precautions must be followed when installing Lockbolts in composite structures: (1) Pull-type Lockbolts exert quite a bit of force on composites through the pulling action necessary to swage the collar onto the pin. If the composite is thin, fastener pull-through is possible, and if there are any unshimmed gaps, cracking and delaminations can occur when the fastener pin fractures. (2) If backside Lockbolts (called *stump* Lockbolts) are installed in composites, they should be installed by automated equipment so that the swaging operation can be carefully controlled.

A third type of pin and collar fastener is the Eddie-Bolt shown in Fig. 11.21. As shown in the installation sequence, the collar initially threads onto the pin but then is swaged into flutes on the pin. This swaging provides a positive lock and confers on Eddie-Bolts the advantage of retaining clamp-up loads better than Hi-Loks, which rely on torque only. However, the fasteners and installation tools are expensive, the socket tools are subject to wear, and the installation procedure is difficult. Eddie-Bolts are often specified in inlet duct areas, where it would otherwise be possible for a fastener pin to come loose, fly into the engine blades, and damage the engine.

11.4.4 Bolts and Nuts

Bolts, along with nuts and washers, are used to join highly loaded structural members that may have to be removed to provide service access. They are also used for permanent attachments. Structural bolts are used in fatigue-, shear-, and tension-critical joints. Nuts, which are tightened with wrenches, may be used when there is access to both sides; nut plates and gang channels are used when there is access to only one side. The shank of each structural bolt must be long enough to ensure that there are no threads bearing in the joint. Extra washers may be used to adjust the grip length. However, the use of lock washers is often prohibited because they can damage the protective finish on the structure being joined. A washer should be used under both the bolt head of protruding bolts and the nut to help distribute the load and prevent crushing damage to the composite surface.

There are many head styles, including the protruding tension flange head, protruding shear head, 100-degree full countersink, and 100-degree reduced countersink. For structural bolts, the threads are rolled and the heads are forged for additional strength. Since both of these operations induce residual compressive stresses in the fastener, they also improve the fastener's resistance to stress corrosion cracking. Bolts smaller

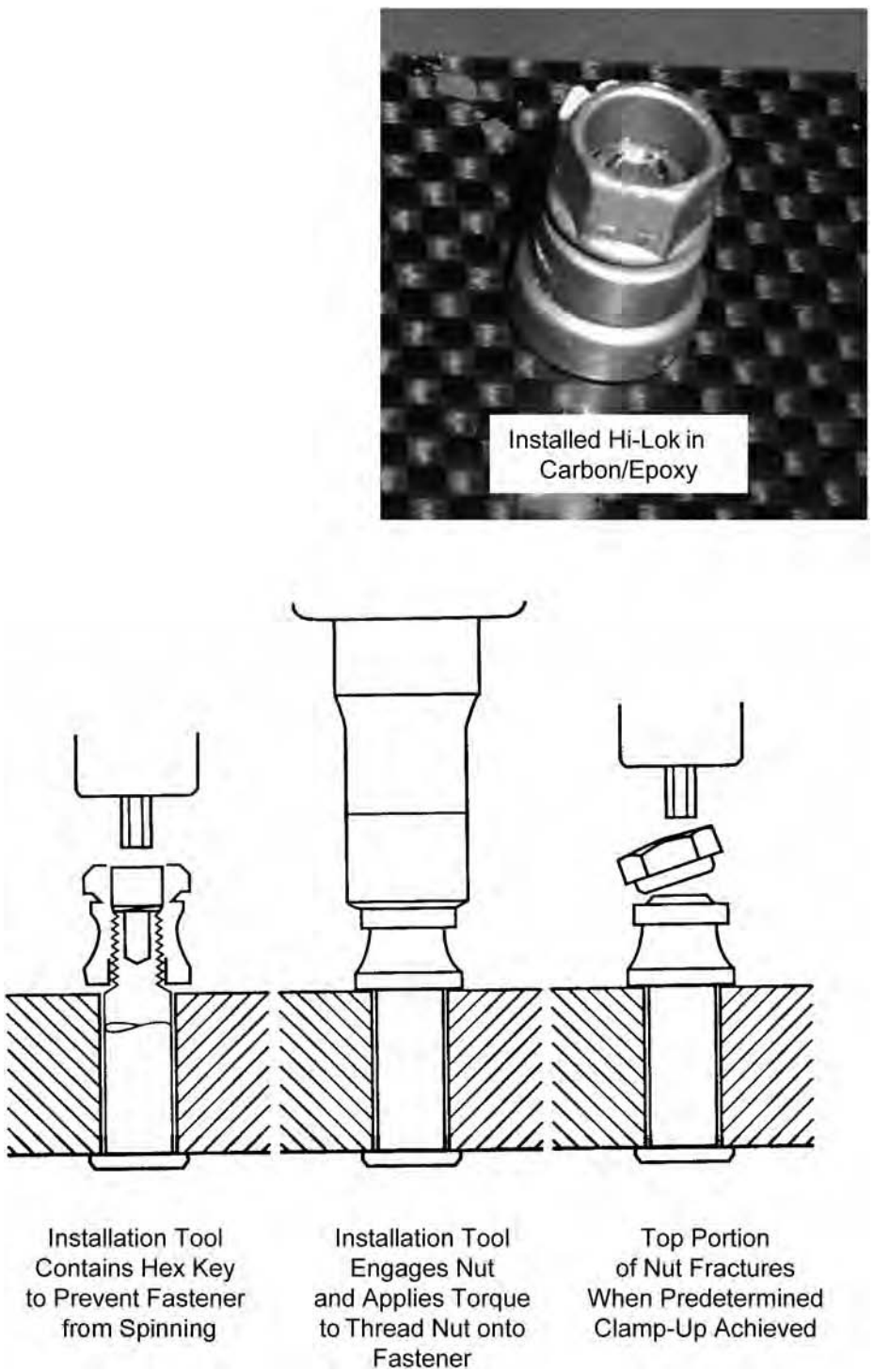


Fig. 11.19 Installation of the Hi-Lok fastener. Source: Ref 4

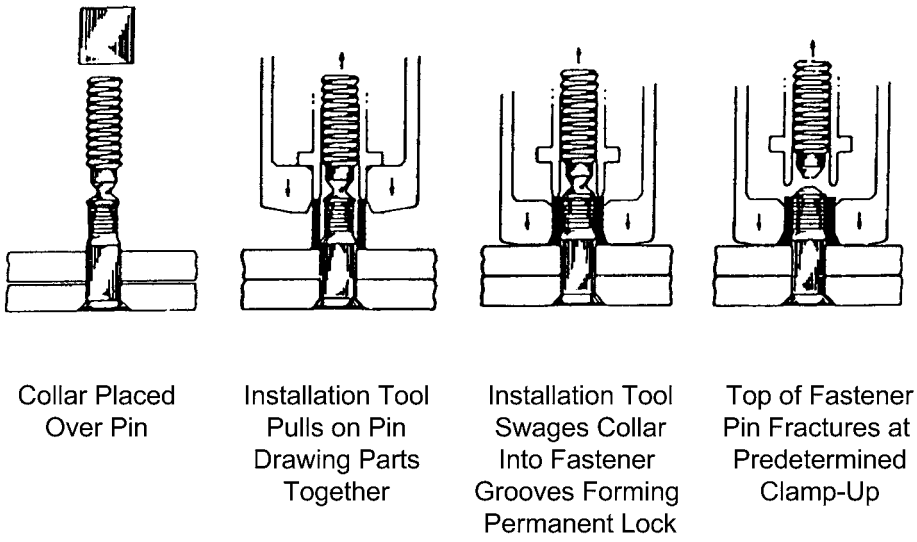


Fig. 11.20 Installation of the pull-type Lockbolt. Source: Ref 4

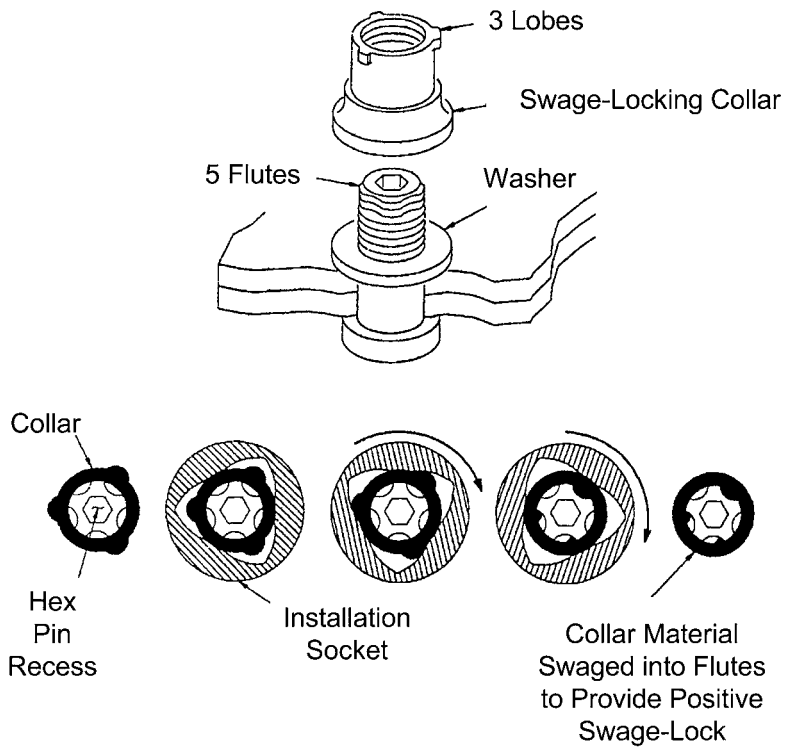


Fig. 11.21 Eddie-bolt positive lock fastener. Source: Refs 4, 5

than 0.190 in. (5 mm) in diameter are considered nonstructural; they are used to attach brackets and other miscellaneous hardware. The threads on nonstructural bolts can be either machined or rolled. Some nuts are self-locking and others are not; cotter pins and safety wire are used to secure those that are not. Self-aligning nuts (up to eight degrees) are also available for situations in

which the structural members are not parallel. There are also nuts designed specifically for tension- or shear-loading applications.

When installing structural bolts, a high preload or high torque helps to prevent fatigue and vibration. However, since a high preload places the bolt under tensile stress, too high a preload can increase the susceptibility of certain fastener materials to stress corrosion cracking. Therefore, bolt preload is usually restricted to about 50 to 60 percent of the bolt's yield strength. It is also important that all of the fasteners in the joint are preloaded to approximately the same torque so that the fasteners share the load equally. If the fasteners are subjected to varying torque, those that are preloaded to higher values will carry a substantially higher portion of the load than those with lower torque. Low bolt preloads can result in joint rotation, misalignment, loosening, and the formation of gaps between mating parts. Low bolt preloads also reduce the fatigue life of the fasteners. For highly loaded bolted joints, torque values are often specified on the engineering drawing.

High-strength bolts or screws, together with nut plates or gang channels, are used for skins that may need to be removed. A typical nut plate and gang channel are shown in Fig. 11.22. Three holes are required for each nut plate: two small holes for rivets to attach the nut plate to the structure, and the main fastener hole, which is threaded to accept the screw. A wide variety of nut plate configurations are available for different installations, including self-aligning nut plates. Because gang channels do not require two rivet holes per fastener, they are frequently used when there are long rows of fasteners to be installed. They are attached at periodic points along the channel, thus saving installation labor. Bolts with nut plates or gang channels do not perform as well as blind fasteners, either in static or fatigue loading, because of increased joint deflection and less stiffness of the fastening system (Fig. 11.23).

11.4.5 Blind Fasteners

Blind fasteners are used in areas where there is limited (or no) access to the backside of the structure. However, the solid pin and collar fasteners previously discussed are usually preferred, because they are stronger, provide better clamp-up, and have better fatigue resistance. Two types of blind fastener are the threaded-core bolt type and the pull type shown in Fig. 11.24. The threaded-core bolt (Fig. 11.25) relies on an internal screw mechanism to deform the head and pull it up tight against the structure, whereas the pull-type blind fastener uses a pure pulling action to form the backside head. Higher clamp-up

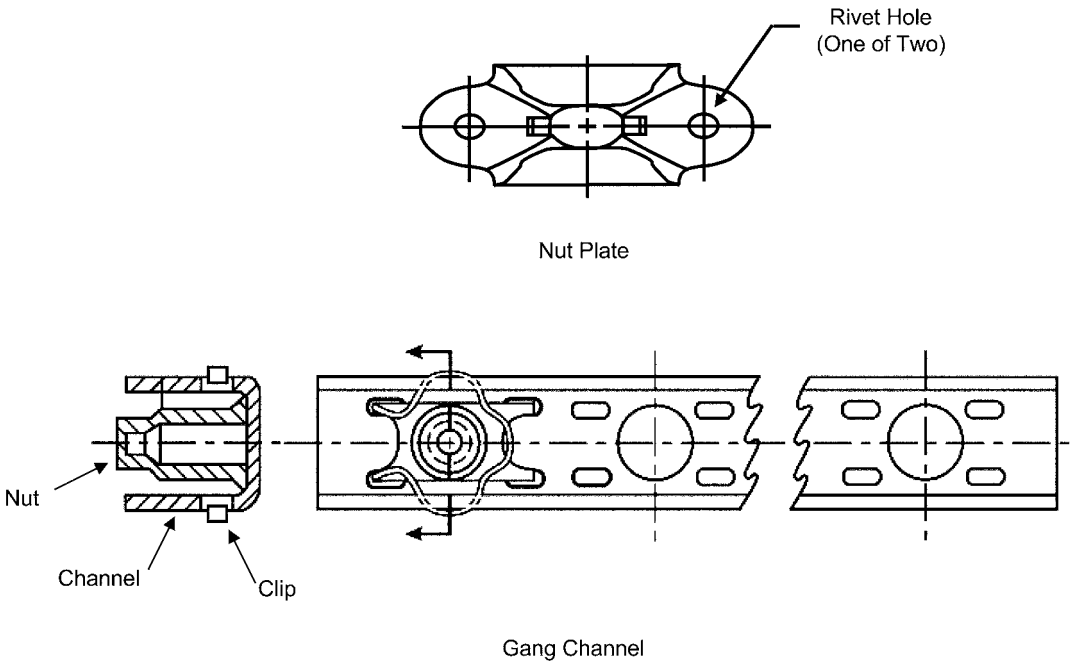


Fig. 11.22 Nut plate and gang channel. Source: Ref 4

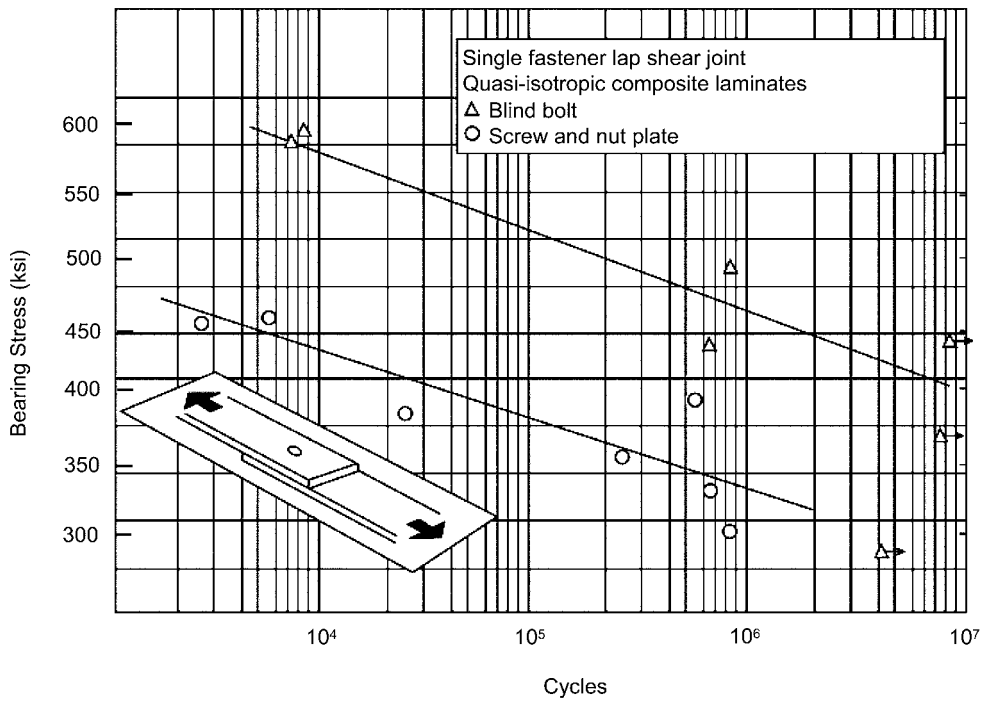


Fig. 11.23 Blind fasteners better in fatigue than screws and nut plates. Source: Ref 4

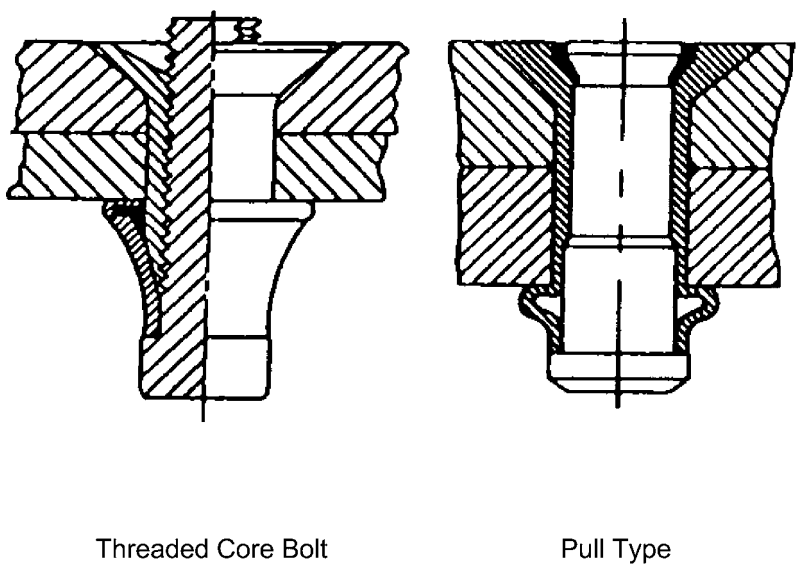


Fig. 11.24 Blind fasteners. Source: Ref 4

forces larger footprints, and therefore longer fatigue life is obtainable with the threaded-core bolt. However, the pull types are installed more quickly, are lighter, and are less expensive. The use of blind fasteners in composite materials is not recommended unless the upset portion of the fastener bears against metal. However, there are some special blind fasteners with large footprints that can be placed directly against composite surfaces.

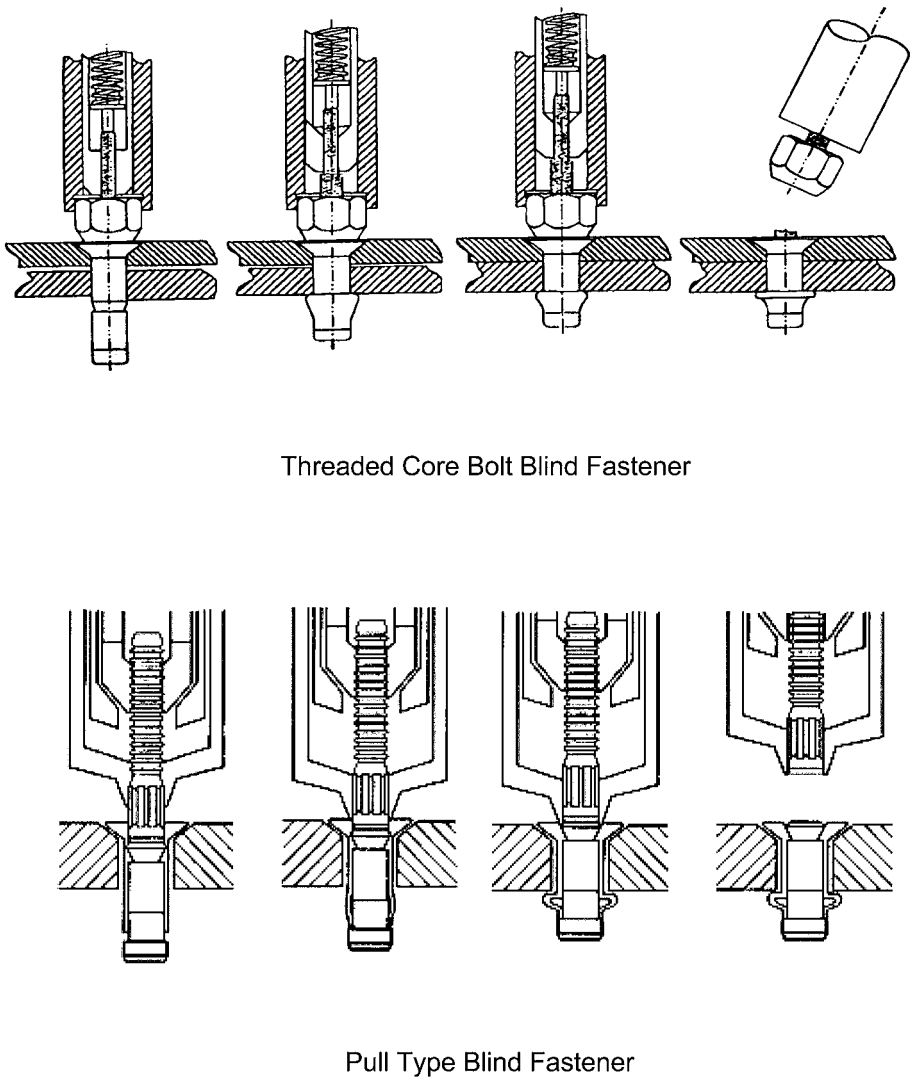


Fig. 11.25 Installation of blind fasteners. Source: Ref 4

11.4.6 Interference-Fit Fasteners

Interference-fit fasteners are also frequently used in metallic structures to improve fatigue life. When the interference-fit fastener is installed in metal, it plastically deforms a small zone around the hole, setting up a compressive stress field, which is beneficial when fatigue loading is primarily in tension. The amount of interference can vary, depending on structural requirements, but it is usually in the range of 0.003 to 0.004 in. (0.08 to 0.1 mm). In some highly loaded holes, both cold working and interference-fit fasteners are used. Although both have been shown to improve the fatigue resistance of metallic structures, each increases assembly costs and should be specified only when it is really needed.

In composite-to-metal assemblies, it is possible to have interference-fit in the metallic structure and clearance-fit in the composite. This is normally accomplished by drilling the hole through the stack-up. The composite skin is removed and opened to a larger diameter with a reamer; the composite skin is then reassembled to the metallic structure, and the fastener is installed clearance-fit through the composite skin

but interference-fit in the metallic substructure. Even then, it is important to be careful when installing the interference-fit fastener; excessive vibration from a rivet gun can produce delaminations around the composite hole even though it is a clearance-fit.

Since composites do not plastically deform, the fatigue life of a composite structure is not improved by interference-fit fasteners. However, they do help to "lock up" the structure and prevent any movement at the joint (called *ratcheting*) during fatigue loading. Installing standard interference-fit fasteners in composites, with as little as 0.0007 in. (0.02 mm) of interference, can lead to cracking and interlaminar delaminations. To eliminate this problem, special sleeve-type interference-fit fasteners (Fig. 11.26) have been designed with sleeves that spread the load evenly during installation, thus preventing delaminations. With these fasteners, interferences as high as 0.006 in. (0.15 mm) have been obtained without damaging the composite. Both pin-and-collar (Lockbolt) fasteners and threaded-core blind bolt fasteners (Fig. 11.27) are available with sleeves. There are several advantages to using interference-fit fasteners in composite structures: lower joint deflection, reduction of fastener cocking (and therefore of high localized bearing stresses), locking up of structure (which prevents ratcheting during fatigue), and reduction of assembly costs when interference fits are required in metallic structures (because no disassembly and ream operation is required for the composite).

11.5 Sealing and Painting

Many structures require sealing to protect against corrosion, keep water out of the structure, or keep fuel in the structure. The typical

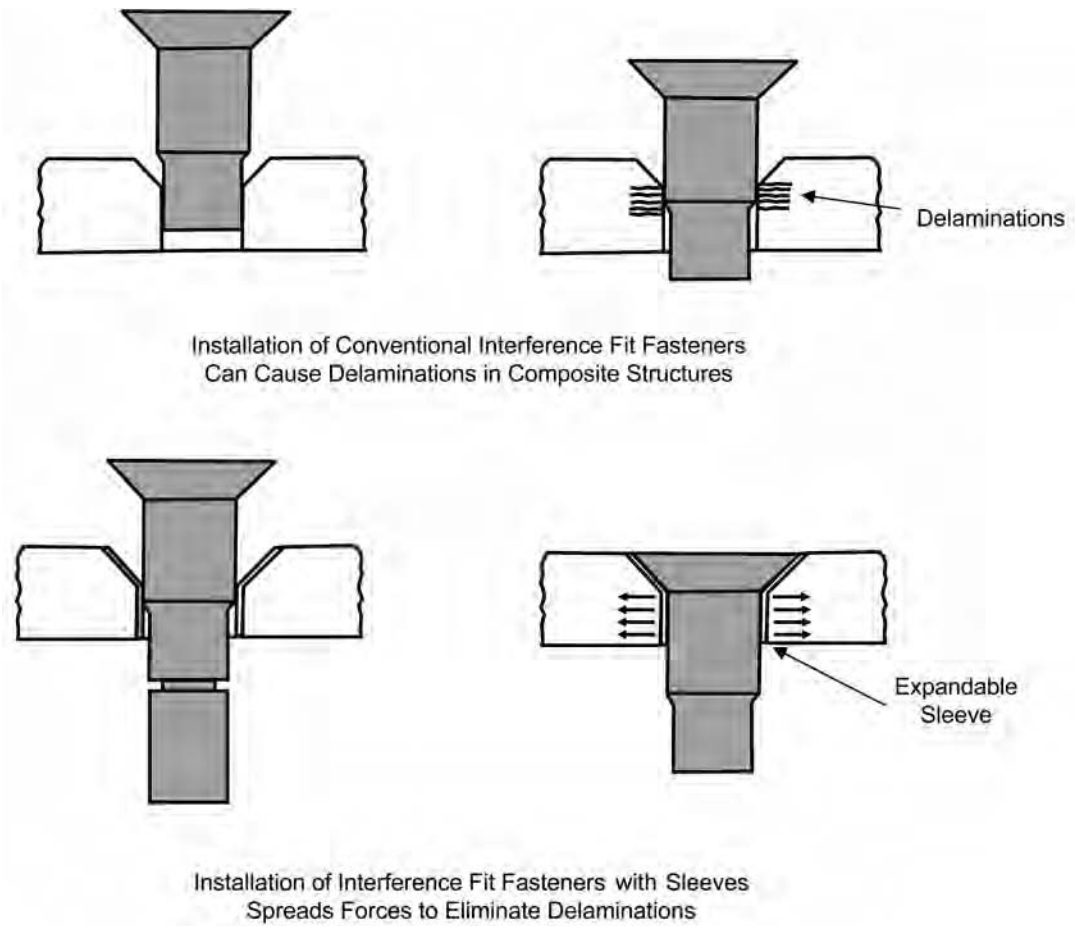
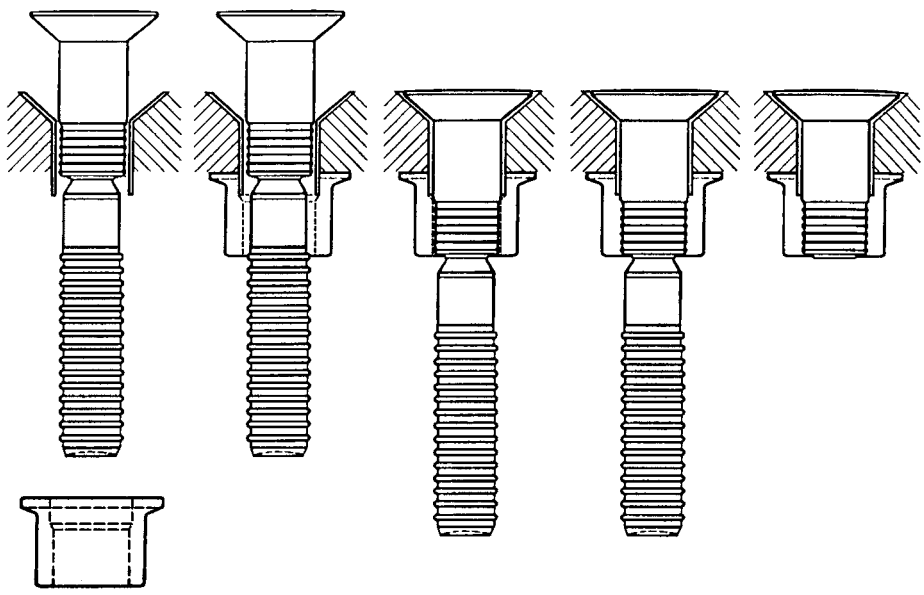
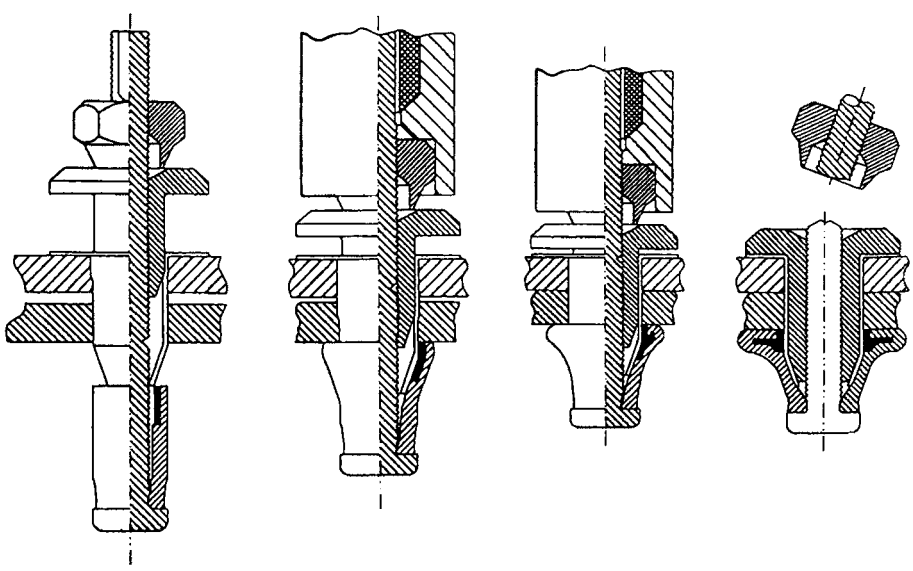


Fig. 11.26 Interference fit fasteners in composites. Source: Ref 4



Interference Fit Sleeve Type Lockbolt



Interference Fit Threaded Corebolt Blind Fastener

Fig. 11.27 Installation of sleeve-type interference fit fasteners. Source: Ref 4

aircraft wing fuel tank configuration shown in Fig. 11.28 illustrates the various sealing and corrosion-protection methods. For joints between carbon/epoxy (C/E) and aluminum parts, it is common practice to cocure or bond a thin layer of glass cloth to the surface of the C/E part to act as an electrical isolation barrier to prevent galvanic corrosion of the aluminum.

A good sealant must have good adhesion properties, high elongation, and high resistance to both temperature and chemicals. Sealing is usually accomplished with polysulfide sealants, which are available in a variety of product forms with a range of viscosities and cure times. Polysulfide sealants are usable in the temperature range of –65 to 250 °F (–50 to 120 °C), and they can withstand temperatures of up to 350 °F (180 °C) for short periods of time. They contain leachable corrosion-resistant compounds that help keep the aluminum substructure from corroding. If higher temperatures are required, it is possible to use silicone sealants that can withstand temperatures as high as 500 °F (260 °C). Moldline fasteners are usually installed "wet" by applying sealant to the fastener before installation. The nuts are often overcoated after installation. During assembly, the faying surfaces are sealed and then fillet seals are placed around the periphery. The fay surface seal cannot be considered the primary seal because it is extremely thin and may be broken by structural deflections; the fillet seal is the primary seal. All potential leak paths must be fillet-sealed. Fillet beads must be dressed with a filleting tool to work out air bubbles and voids and provide the finished fillet shape. Adequate fillet size is important in preventing leakage. Selecting the right sealant working life is important: If too short a working life is selected, the sealant may set before the job is completed; if the working life is too long, the cure may take so long that the production schedule is affected.

A fuel tank often has a channel groove that is packed with a fluorosilicone sealant containing about 10 percent of small microspheres graduated from 0.002 to 0.030 in. (0.05 to 0.8 mm) in diameter for more effective gap filling. These microspheres assist in keeping the compound in the groove and in sealing gaps up to 0.010 in. (0.3 mm) wide. The sealant swells upon contact with fuel, thus helping to seal the structure further. Normally, the channel is prepacked with sealant

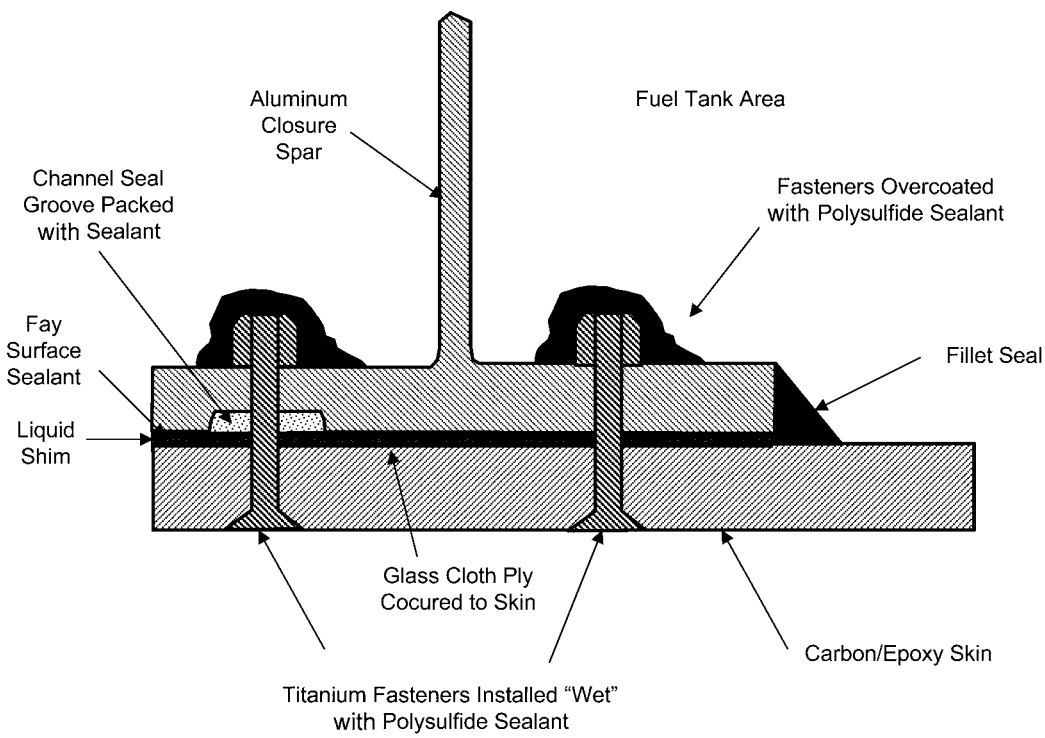


Fig. 11.28 Typical wing fuel tank sealing

and then injected under pressure up to 4000 psi (28 MPa) after assembly. Injection points, usually spaced 4 to 6 in. (10 to 15 cm) apart, can be at fastener holes or through specially designed fasteners that contain internal injection ports.

Making paint adhere to composite structures is not as difficult as it is with metallic structures. The surface should be clean of all dirt and grease. If the part contains a peel ply, it should be removed. The surface can be prepared either by scuff sanding with 150- to 180-grit sandpaper or by lightly grit blasting. For aerospace applications, the standard finishing system is an epoxy primer followed by a polyurethane topcoat. Epoxy primers are addition-curing polyamides that contain the following: (1) strontium chromate, which is an exceptional corrosion inhibitor for aluminum; (2) titanium dioxide, which enhances durability and chemical resistance; and (3) fillers such as silica, which control viscosity and reduce cost. The part should be primed within 36 hours after sanding. The primer is applied to a dry film thickness of 0.0008 to 0.0014 in. (0.02 to 0.04 mm) and then cured for a minimum of six hours. Polyurethane topcoats are aliphatic ester-based polyurethanes that exhibit good weathering resistance, chemical resistance, durability, and flexibility. They are applied to a dry film thickness of about 0.002 in. (0.05 mm) with an initial cure within two to eight hours and a full cure within six to 14 days. More environmentally friendly paint systems are being developed that are free of or low in solvents; these are called *low–volatile organic compound coatings*. Toxic heavy metals such as chromium are being replaced with self-priming topcoats consisting of nonchromated high-solids polyurethane; these replace both the epoxy primer and the traditional polyurethane topcoat.

REFERENCES

1. T.L. Price, G. Dalley, P.C. McCullough, and L. Choquette, "Handbook: Manufacturing Advanced Composite Components for Airframes," Report DOT/FAA/AR-96/75, Office of Aviation Research, Apr 1997
2. B.T. Astrom, *Manufacturing of Polymer Composites*, Chapman & Hall, 1997
3. M.J. Paleen and J.J. Kilwin, Hole Drilling in Polymer-Matrix Composites, *ASM Handbook*, Vol 21, *Composites*, ASM International, 2001
4. R.T. Parker, Mechanical Fastener Selection, *ASM Handbook*, Vol 21, *Composites*, ASM International, 2001
5. K.B. Armstrong and R.T. Barrett, *Care and Repair of Advanced Composites*, SAE International, 1998

SELECTED REFERENCES

- *Aerospace Manufacturing Technology Conference*, 10–14 Sept 2001
- E.L. Bohanan, F/A-18 Composite Wing Automated Drilling System, *30th National SAMPE Symposium*, 19–21 Mar 1985, p 579–585
- J.A. Bolt and J.P. Chanani, Solid Tool Machining and Drilling, *Engineered Materials Handbook*, Vol I, *Composites*, ASM International, 1987
- G.C. Born, "Single-Pass Drilling of Composite/Metallic Stacks," *2001 Aerospace Congress, SAE Aerospace Manufacturing Technology Conference*, 10–14 Sept 2001
- C.A. Fraccihia and R.E. Bohlmann, The Effects of Assembly Induced Delaminations at Fastener Holes on the Mechanical Behavior of Advanced Composite Materials, 39th *International SAMPE Symposium*, 11–14 Apr 1994, p 2665–2678
- J. Jones and M. Buhr, "F/A-18 E/F Outer Wing Lean Production System," *2001 Aerospace Congress, SAE Aerospace Manufacturing Technology Conference*, 10–14 Sept 2001
- J.D. McGahey, A.J. Schaut, E. Chalupa, P. Thompson, and G. Williams, "An Investigation into the Use of Small, Flexible, Machine Tools to Support the Lean Manufacturing Environment," *2001 Aerospace Congress, SAE Aerospace Manufacturing Technology Conference*, 10–14 Sept 2001
- M.C.Y. Niu, *Composite Airframe Structures: Practical Design Information and Data*, Conmilit Press, 1992
- M. Ramulu, M. Hashish, S. Kunaporn, and P. Posinasetti, "Abrasive Waterjet Machining of Aerospace Materials," *33rd International SAMPE Technical Conference*, 5–8 Nov 2001
- A.B. Strong, *Fundamentals of Composites Manufacturing: Materials, Methods, and Applications*, SME, 1989

Copyright © 2010, ASM International®
All rights reserved.
www.asminternational.org

CHAPTER 12

Nondestructive Inspection

FLAWS CAN OCCUR, unfortunately, at almost any stage of the composite manufacturing process or during service. A summary of some potential flaws and damage is shown in Fig. 12.1. During ply collation, foreign objects are the most serious issue. These include the backing paper or plastic liner on the prepreg, lay-up materials such as release films and tapes, and tools such as knife blades. Since these can cause serious delaminations during curing, they normally result in either the need for a repair or scrapping of the part if the foreign object is large enough or located in a highly stressed area. The cure process can also result in defects, the most serious being porosity and voids. If an adhesive bonding operation is involved, adhesive unbonds are some of the most serious flaws, followed closely by a large number of potential honeycomb core defects. Delaminations are the most serious type of defect encountered during machining and assembly, resulting from improper trimming operations, part handling, or hole drilling or from installing fasteners with unshimmed gaps. During service, delaminations are again the most prevalent type of damage. Runway debris hitting control surfaces, hailstones from storms, tools dropped by maintenance mechanics, and collisions with ground handling equipment such as forklifts can all cause varying degrees of damage. It is important to be able to reliably find these types of flaws and damage and repair them if warranted.

Nondestructive inspection (NDI) methods are normally used to inspect completed parts and bonded assemblies to make sure that any flaws are not large enough or located in critical areas that could cause the part to fail in service. Once a part is placed in service, NDI methods are used to locate and evaluate the extent of damage. Based on the severity of the damage, a repair may or may not be required.

Nondestructive inspection is an engineering discipline in its own right. All large aerospace companies and many part manufacturers have NDI groups that work full time at developing new and improved methods of inspecting parts. The literature on NDI is extensive; therefore, in this chapter only the basics, and how NDI can be used to detect flaws in composite parts, will be covered. Nondestructive inspection methods range from simple visual inspections to very sophisticated automated systems with extensive data-handling capabilities. It should be noted that composites are generally more difficult to inspect than metals due to their nonhomogeneous nature; that is, they are laminated structures containing multiple ply orientations with numerous ply drop-offs. In addition, it is important that technicians conducting NDI be trained and certified in the method they are using.

12.1 Visual Inspection

Visual inspection is a very valuable yet limited method for inspecting composite parts. Since only surface or edge defects are visible, visual inspection reveals nothing about the internal integrity of the part. Nevertheless, all parts should be periodically inspected for surface cracks, blisters, porosity, depressions or waviness, edge delaminations, or paint discoloration. Proper lighting and low-power magnifiers (five to ten times) can help with visual inspection. Borescopes and mirrors are often used if the area to be inspected is hidden from direct view. Edge delaminations and tight surface cracks can be enhanced by taking a clean cotton cloth, dampening it with a solvent such as acetone, wiping the suspected area, and

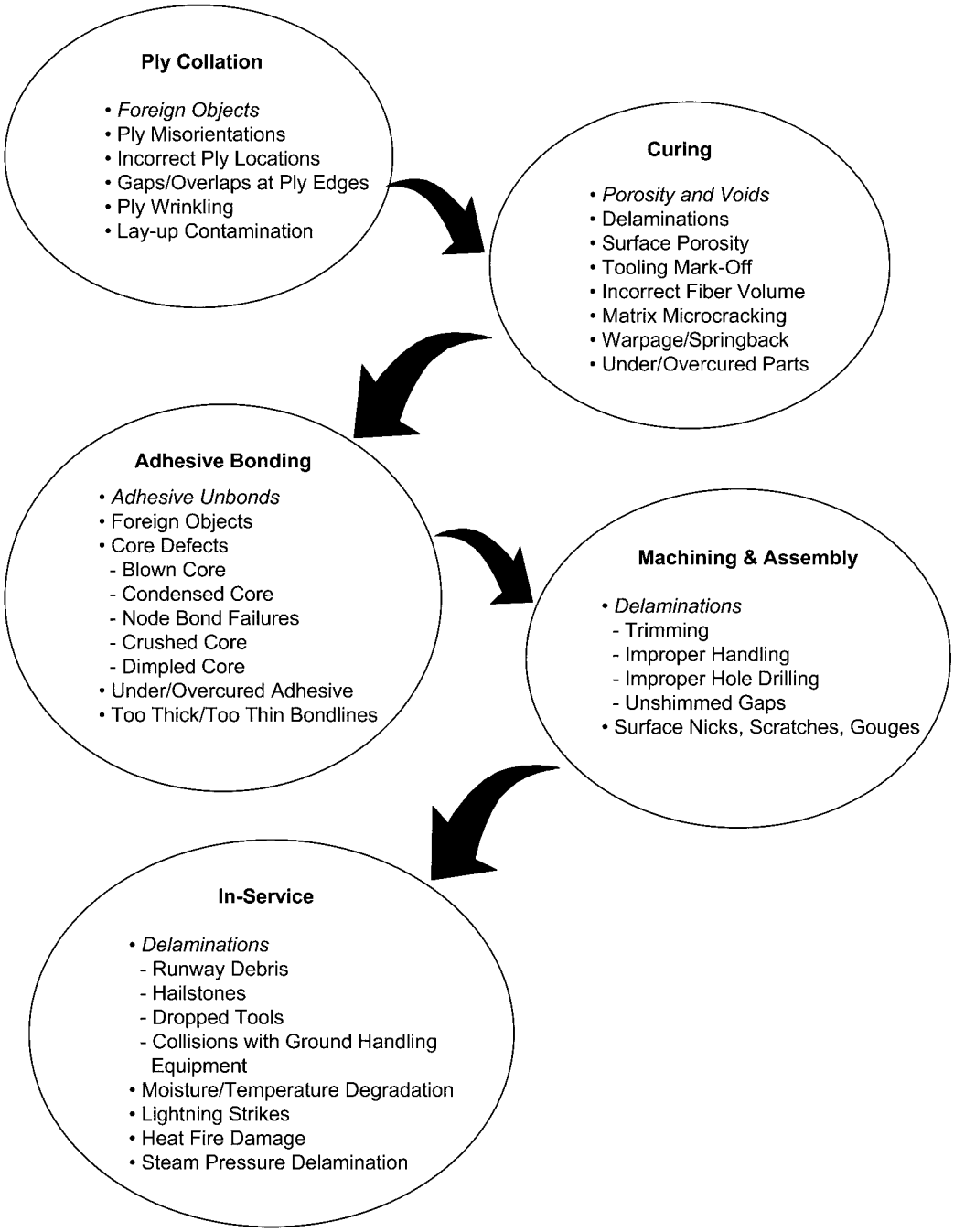


Fig. 12.1 Potential for damage in composite parts

then watching the solvent evaporate. If a crack or delamination is present, some residual solvent will continue to bleed out, revealing the flaw's location and size. However, normal dye penetrants should never be used, because they can contaminate the internal surfaces of the delamination, making subsequent repair more difficult or impossible.

Although tap testing is normally classified as a sonic test method, actually a low-frequency

vibration method, it will be discussed here since it is frequently used during visual inspection. In tap testing, a heavy coin, washer, or small hammer is used to *lightly* tap the surface. If a good region is tapped, the reflected sound will contain more high-frequency vibrations and produce a ringing sound, while if a bad region such as, an unbond is tapped, the reflected sound will contain fewer high-frequency vibrations and the sound will be much duller. Tap testing can do a credible job of finding unbonds or delaminations in honeycomb assemblies containing relatively thin skins less than 0.040 in. (1.0 mm) or thinner. For composite laminates, the tap test may be capable of detecting delaminations in the first few surface plies but it cannot detect deeper defects. About the smallest defect that can be detected is ½ in. (12.7 mm) in diameter at a depth up to about ¼ in. (6.4 mm). Electronic tap testing equipment is available that will provide a more accurate test. Although tap testing can be used as a preliminary screening method, it is strongly recommended that instrumented ultrasonic equipment be used to make the final determination of defect size. For example, an impact delamination may result in only a small indication on the surface at the point of impact; however, the delamination often radiates from the impact point, resulting in an extensive network of internal matrix cracks and delaminations.

12.2 Ultrasonic Inspection

Ultrasonic inspection is the most valuable technique for inspection of composite parts. The two most prevalent fabrication defects in solid laminates are porosity and foreign objects. Porosity is detectable because it contains solid-air interfaces that transmit very little and reflect large amounts of sound. Inclusions, or foreign objects, are detectable if the acoustic impedance of the foreign object is sufficiently different than that of the composite material.

Ultrasonics operates on the principle of transmitted and reflected sound waves. An ultrasonic wave traveling through a composite laminate that encounters a defect such as porosity will reflect some of the energy at the interface while the remainder of the energy passes through the porosity. The more severe the porosity, the greater the amount of reflected energy and the less energy that is transmitted through the defect. Ultrasonic waves are produced when an electrical signal generator sends a burst of electrical energy to a piezoelectric crystal in the transducer, causing the crystal to vibrate and convert the electrical pulses into mechanical vibrations (sound waves). The piezoelectric crystal will also convert the returning sound waves back into electrical energy when the sound is received from the part. A single crystal can be pulsed to send and receive sound waves or two crystals can be used, with one sending and the other receiving the pulse. Flaws are detectable because they alter the amount of sound returned to the receiver.

Ultrasonic inspection is defined as inspection conducted in the frequency range of 1 to 30 MHz, although most composite structure is usually tested at 1 to 5 MHz. Higher frequencies (short wavelengths) are more sensitive to small defects, while lower frequencies (long wavelengths) can penetrate to greater depths. As the ultrasonic beam passes through the composite, it is attenuated or lost due to scattering, absorption, and beam spreading. This loss or attenuation is usually expressed in decibels (dB). Thicker laminates will attenuate more sound than thinner laminates.

Through transmission ultrasonics is one of the two most common methods used to inspect fabricated composite laminates and assemblies. In the through transmission method, shown in Fig. 12.2, a transmitting transducer generates a longitudinal ultrasonic wave that travels through the laminate and is received by a receiving transducer placed on the opposite side of the part. If the part contains a defect, such as porosity or a delamination, some (or all) of the sound will be either absorbed or scattered, so that some (or all) of the sound is not received by the receiving transducer. Through transmission is excellent at detecting porosity, unbonds, delaminations, and some types of inclusions. However, this method cannot detect all types of foreign objects, and it cannot determine the depth of the defects. Mylar film and nylon tapes are particularly difficult to detect with through transmission. Through transmission is usually conducted in a water tank or by using a water squirter method.

Since through transmission is not capable of detecting all types of foreign objects or the depth of defects, pulse echo ultrasonic inspection is frequently used in conjunction with through transmission ultrasonics to inspect parts. In the pulse echo method (Fig. 12.3), the sound is transmitted and received by the same transducer. Thus, it is an excellent method when there is access to only one side of the part. The amplitude of the echo received from the back surface is reduced

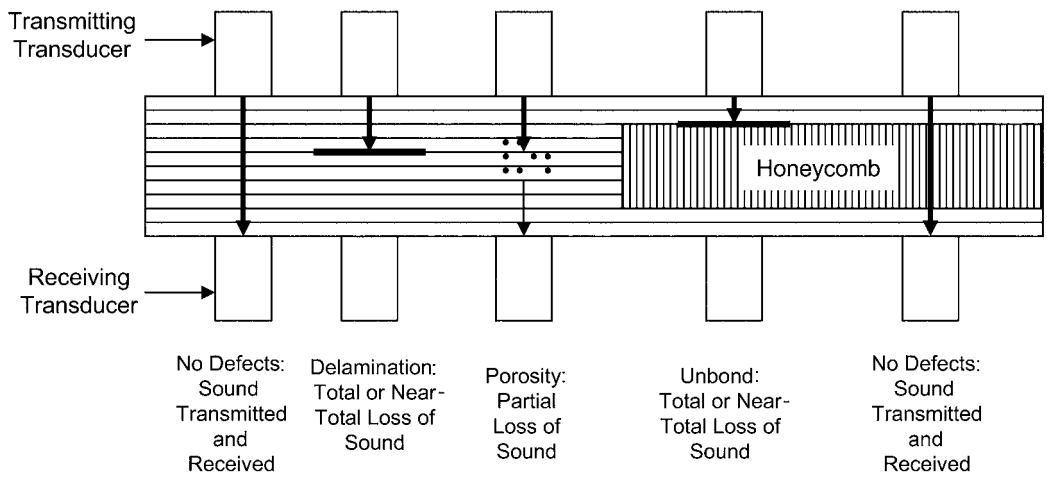


Fig. 12.2 Through transmission ultrasonics

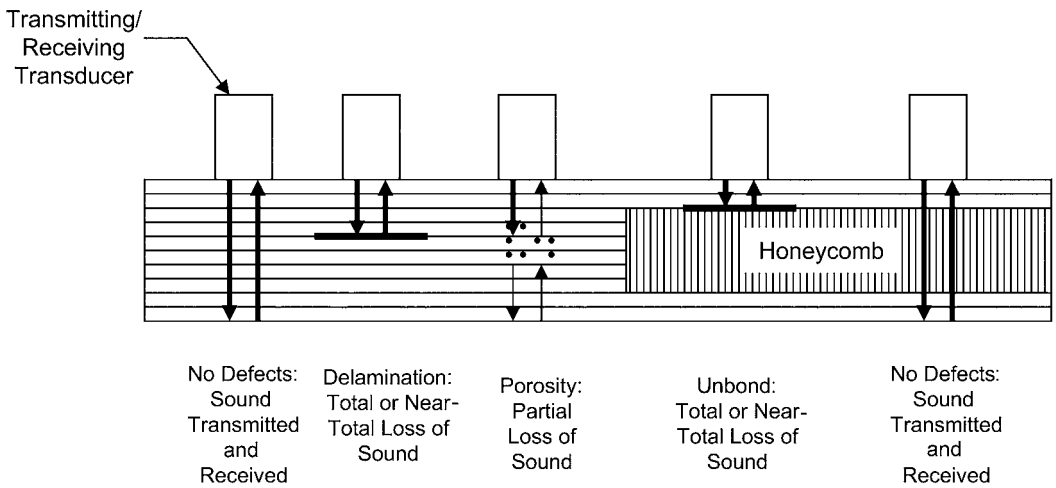


Fig. 12.3 Pulse echo ultrasonics

by the presence of defects in the structure. Attenuation of the ultrasound is affected by internal defects, and the time delay of the pulse is related to the depth of the defect. Pulse echo ultrasonics detects almost all types of foreign objects, but it cannot determine porosity levels as thoroughly as through transmission. If appropriate reference standards are available, pulse echo can be used to measure laminate thickness and the depth of defects. Pulse echo is more sensitive to transducer alignment than through transmission. For pulse echo inspection, the transducer needs to be within about two degrees of normal to the surface, while through transmission can tolerate misalignments up to about ten degrees.

Since there is a large impedance mismatch between air and a solid interface, ultrasound does not propagate well through air; therefore, a couplant is used to transmit the sound more effectively from the transducer to the part. For hand inspection, glycerin compounds are frequently used, while all automated systems use water. As shown in Fig. 12.4, automated systems can either be squirter systems or submerged reflector plate systems. Squirter systems, the most frequently used in production, are usually large gantry systems (Fig. 12.5) that are computer controlled to track the contour of the part and keep the transducers normal to the surface. They also index at the end of each scan pass. The ultrasonic

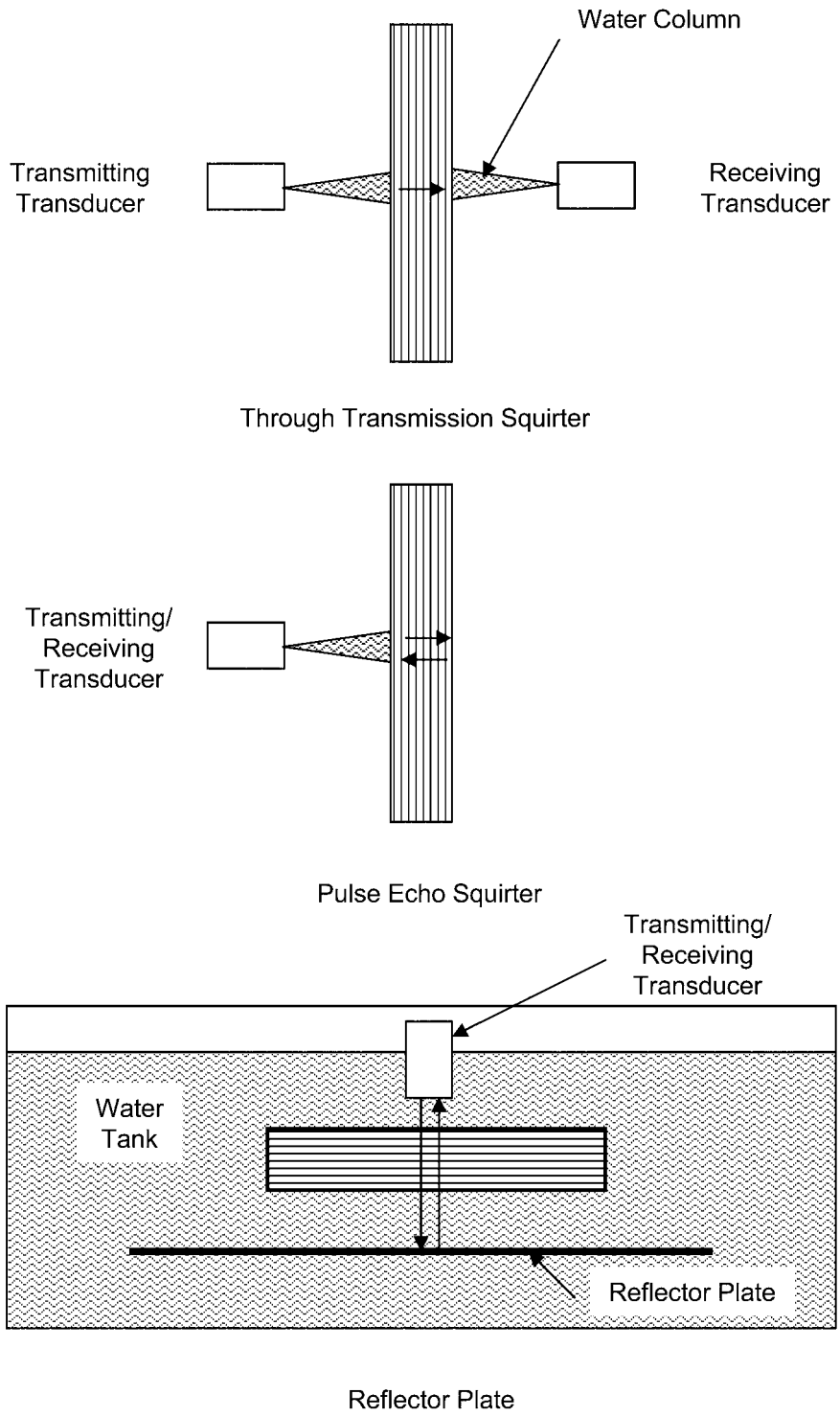


Fig. 12.4 Automated ultrasonic scanning units

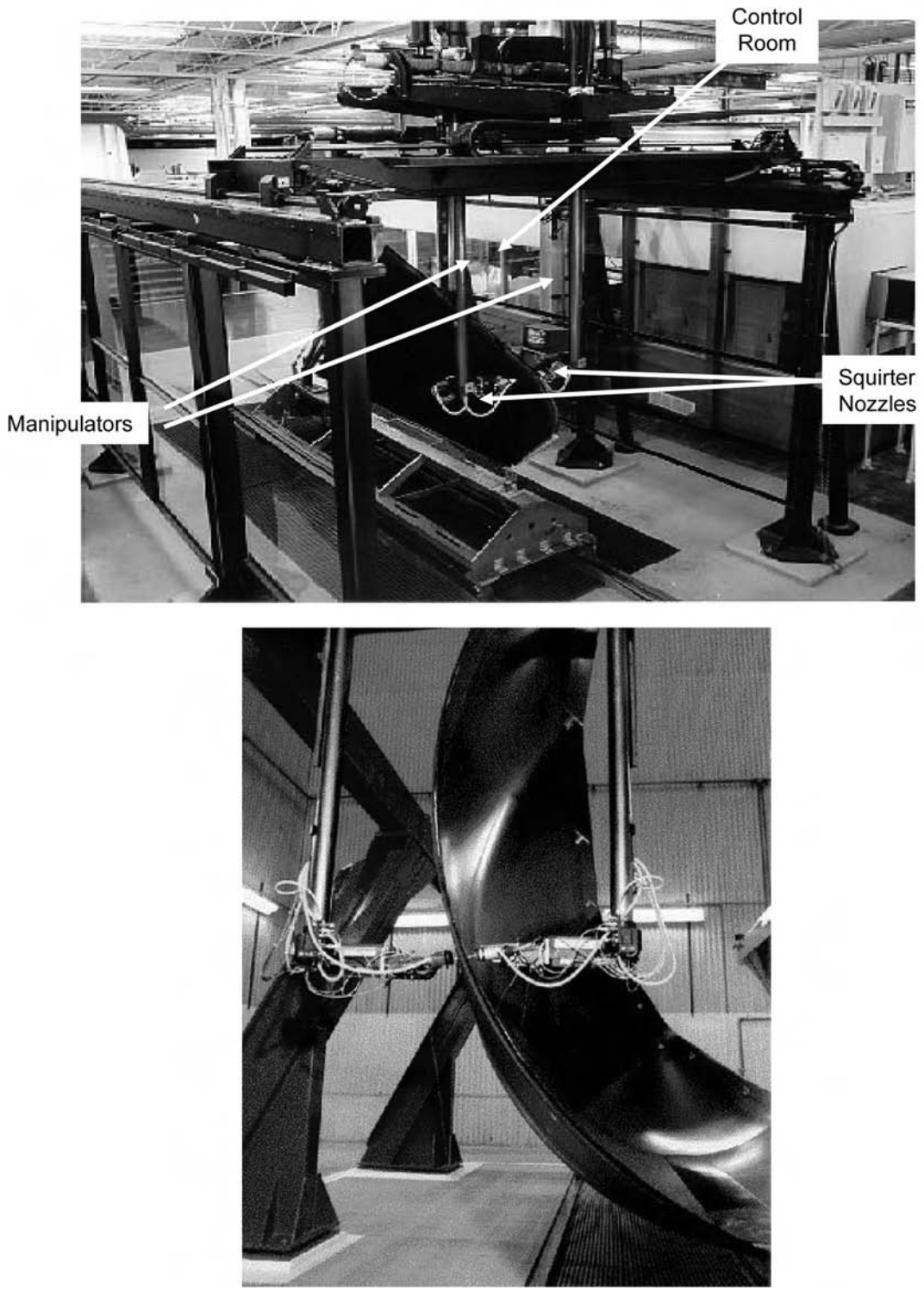


Fig. 12.5 Modern ultrasonic scanning squirter unit. Source: The Boeing Company

energy is converted to digital data and stored in a file. Imaging software allows C-scan displays in either shades of gray or color. Modern units are capable of scan speeds of up to 40 in./s (1.0 m/s), and some units can record through transmission and pulse echo data simultaneously, eliminating the need to scan the part twice. There are also special units for cylindrical parts that contain turntables that rotate the part during the scanning operation.

The output from these automated units is displayed as a C-scan, which is a planar map of the part, where light (white) areas indicate less sound attenuation and are of higher quality than dark (gray to black) areas that indicate more sound attenuation and are of lower quality. Through transmission C-scans of both a good part and one with rejectable porosity are shown in Fig. 12.6. Lead reference standards are placed on the part so that the actual part location can be correlated

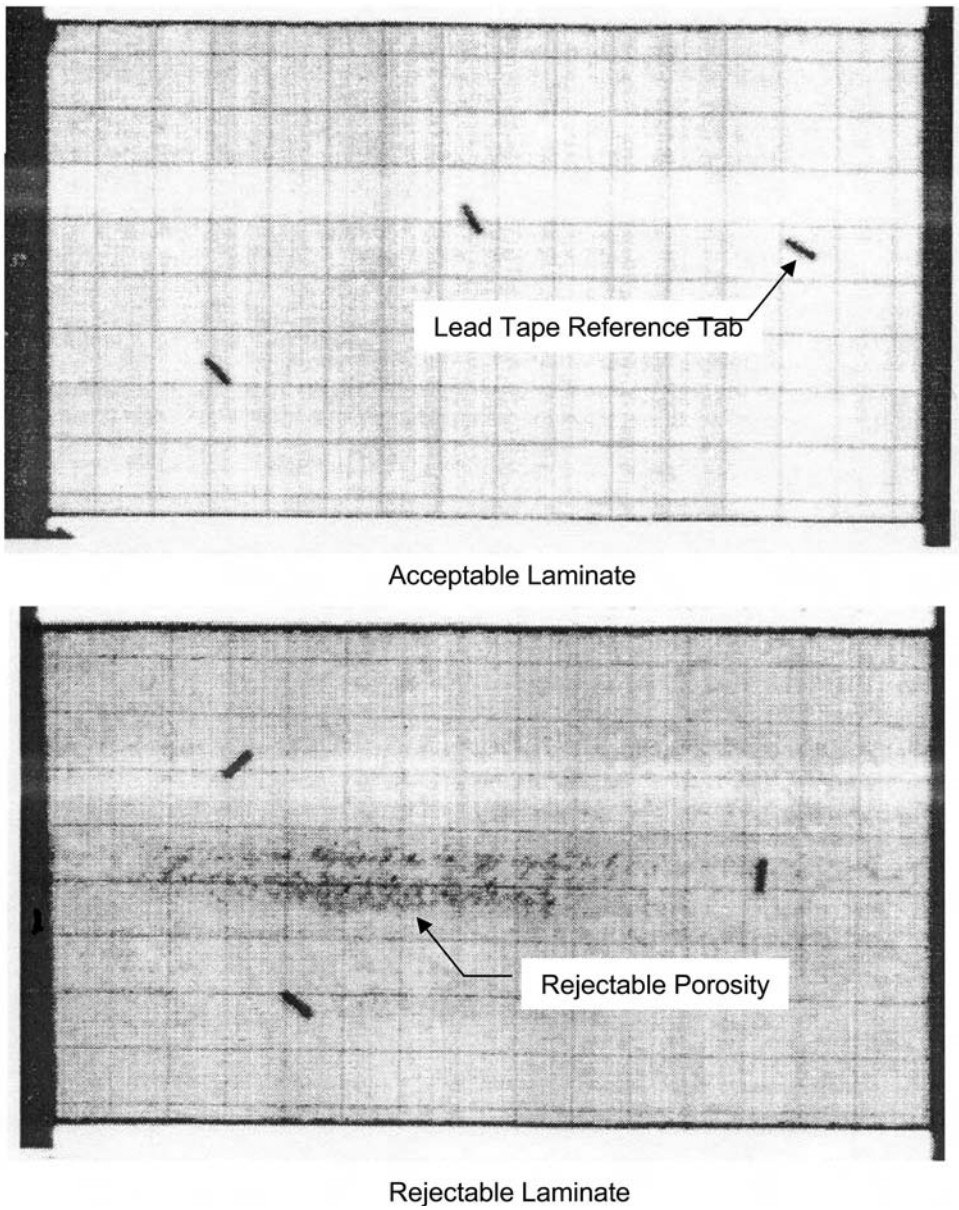


Fig. 12.6 Ultrasonic C-scans of composite laminates

with the C-scan printout. As depicted in Fig. 12.7, the darker the area, the more severe the sound attenuation and the poorer the quality of the part. It should be noted that while through transmission is good at detecting porosity, it cannot tell the difference between scattered porosity (Fig. 12.8) and planar voids if the defect densities are similar. In addition, other defects, such as ply wrinkling, can often appear to be porosity.

C-scan units can be programmed to print out the changes in sound levels as varying shades of gray or can be set in a go-no go mode where only rejectable areas are printed. Part manufacturers usually establish a baseline attenuation in dB for each part. When the attenuation level exceeds the baseline by a predetermined dB, that area of the part is rejected. For example, if the baseline for a good laminate of a given thickness is 25 dB and the rejection threshold is 18 dB, then any indication over 43 dB (25 + 18 dB) would be rejected. Baselines and thresholds are determined by conducting effects-of-defects test programs in which known good laminates are compared with laminates of varying porosity

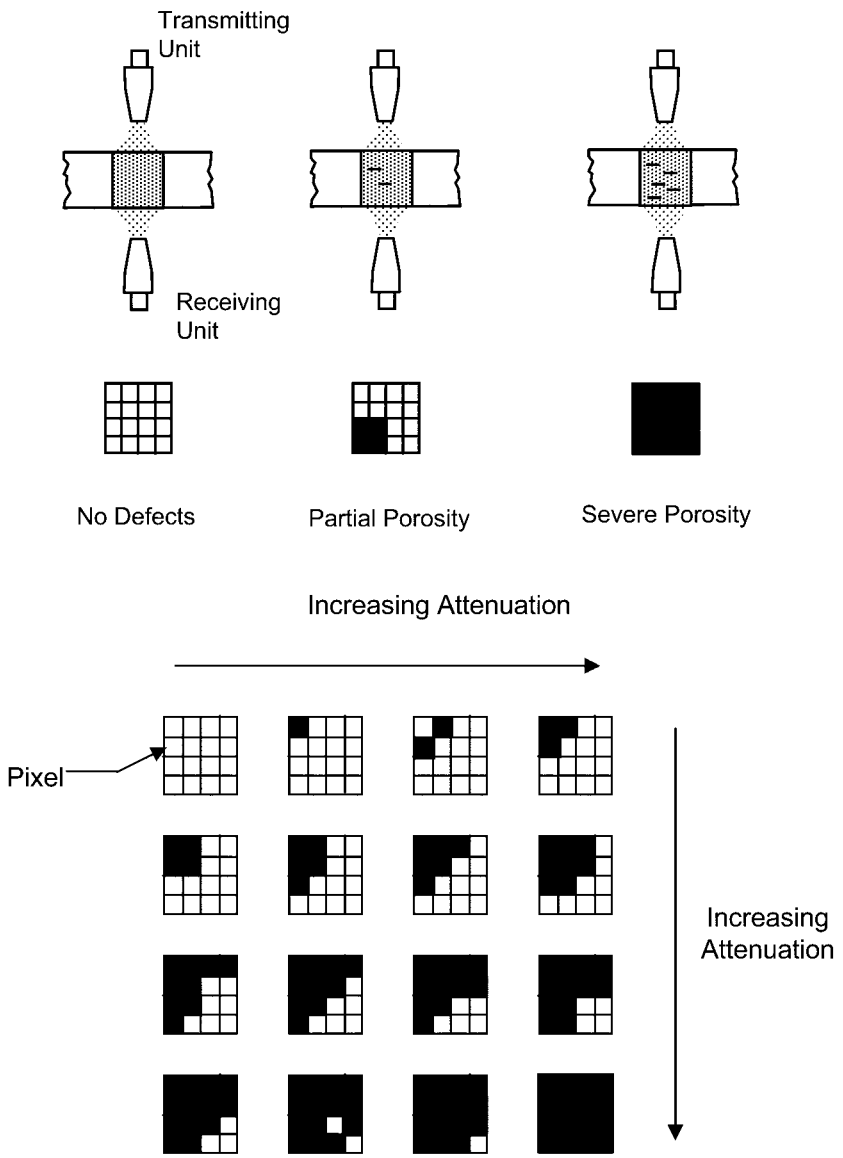


Fig. 12.7 Relationship between attenuation and display

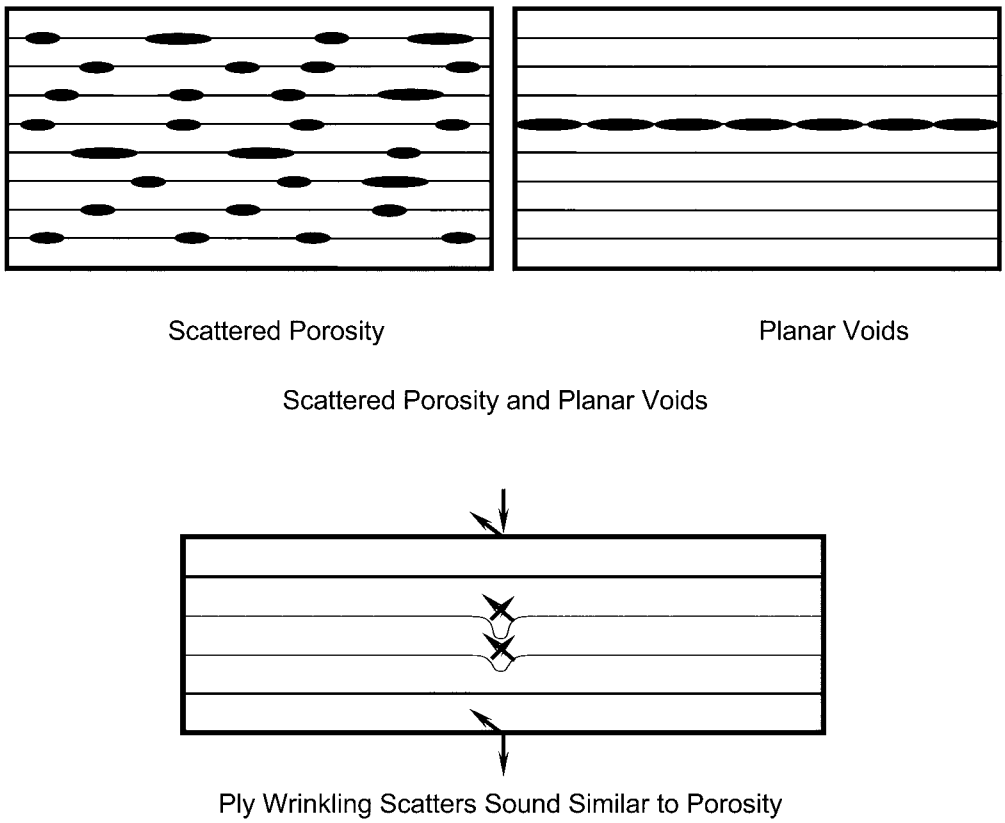


Fig. 12.8 Ultrasonic indications

levels. Both photomicrographs and mechanical property testing are used to establish the threshold levels. Part zoning can also be used to reduce cost. Areas that are highly stressed would be zoned to lower threshold values than noncritical lower-stressed areas.

Carbon/epoxy laminates are usually scanned at around 5 MHz, while honeycomb assemblies require lower frequencies (1 or 2.25 MHz) to penetrate thicker structures. Foam-filled structures require even lower frequencies, with 250 kHz, 500 kHz, or 1 MHz being typical. Since the ability to detect defects is reduced at lower frequencies, parts are generally scanned with the highest frequency that can penetrate the part. Nevertheless, air-coupled ultrasonics are occasionally used for materials with low acoustic impedance (i.e., lower-density materials) such as honeycomb assemblies. Air coupling has been used to inspect honeycomb materials up to 8 in. (20 cm) thick. The transducers are placed close to the part surface within 1 in. (2.5 cm), and frequencies of 50 kHz to 5 MHz are employed.

12.3 Portable Equipment

Both pulse echo and through transmission equipment are available for field inspections. A typical setup, shown in Fig. 12.9, consists of a transducer connected to a console. Again, 1 to 5 MHz frequencies are normally used. Glycerin pastes are frequently used as couplants rather than water. Pulse echo is the most frequently used method, because it requires only one transducer and it can conduct inspections where access to the backside is not available. Note that the display is normally in the A-scan format, in which the height of the amplitude signal is an indication of the severity of the defect, and its location between the front and back surfaces is an indication of its depth.

There are also a fairly large number of *bond testers* that generally operate below 1 MHz, some as low as the audio or near-audio range (12 to 20 kHz). At the low end of the frequency range, a couplant is generally not required. A summary of some of these units is given in Table 12.1.

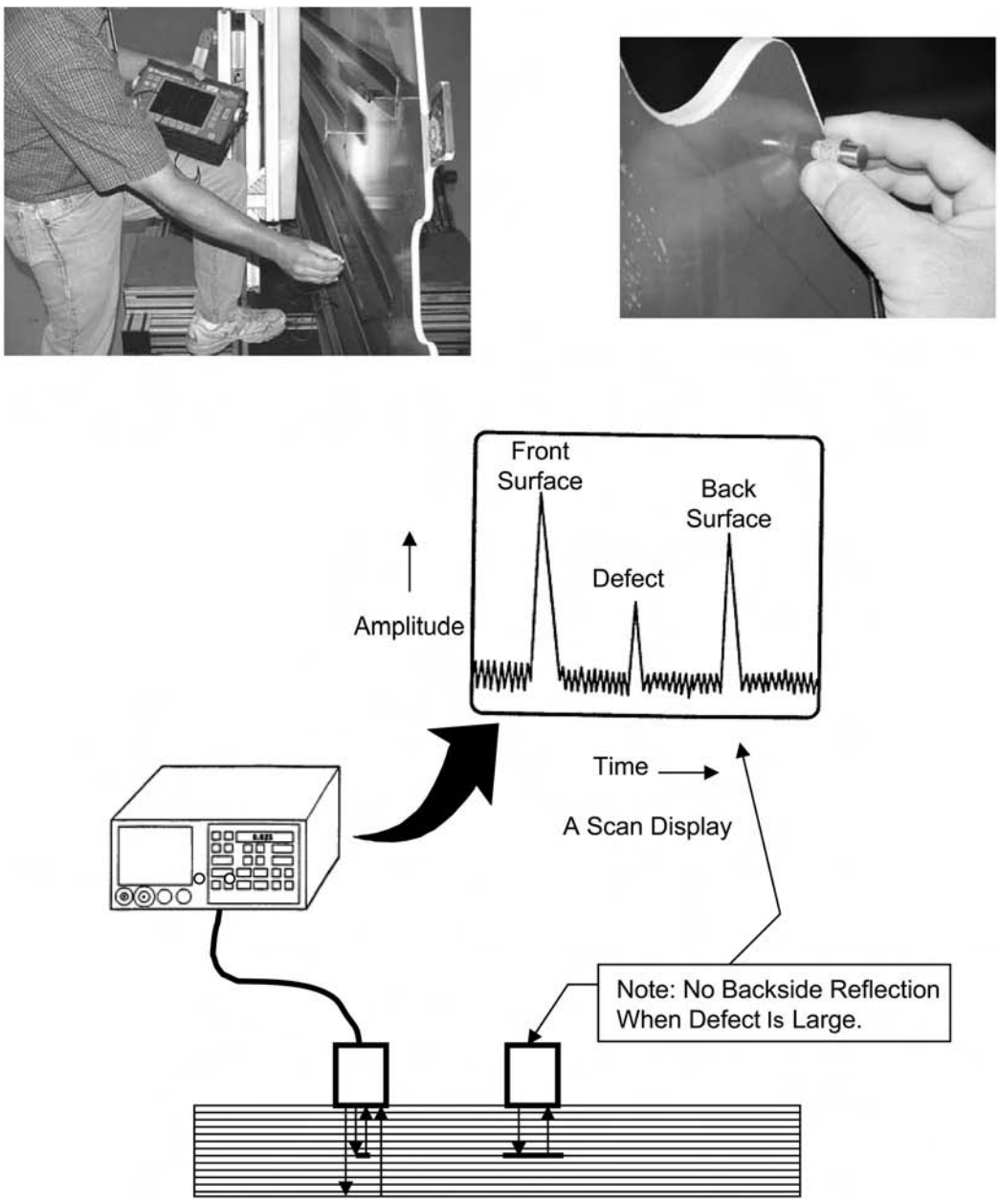


Fig. 12.9 Portable pulse echo unit

Advanced portable units, such as the Mobile Automated Ultrasonic Scanning (MAUS) system shown in Fig. 12.10, can conduct multiple types of inspection, including ultrasonics (through transmission, pulse echo, shear wave), bond tests (resonance, pitch/catch, mechanical impedance) and eddy current (single and dual frequency).

12.4 Radiographic Inspection

Radiographic inspection is normally used to look for microcracks in solid composite laminates and is used extensively to detect defects in honeycomb assemblies. Radiographic inspection is not normally used to inspect composite laminates unless they contain radii that are sus-

Table 12.1 Summary of bond testing techniques

Resonance method	Transducer is driven at the resonance frequency (25–500 kHz), causing electrical impedance changes to detect unbonds or delaminations. Test requires a couplant and a variety of different transducer designs. Capable of detecting unbonds 0.050 in. or larger. Maximum thickness of 0.5 in. Delaminations in the bottom one or two plies are difficult to detect due to small change in material impedance detected by probe.
Pitch/catch sweep method	Dual-element transducer method in which one element transmits sound and the other element receives sound. Sound waves are transmitted across the part in a plate wave mode. Unbonds and deeper defects are detected as the sound loss. Transducer is swept in a circular manner to detect flaws. Sweep frequencies of 20–40 or 30–50 kHz are normally used. No couplant is required.
Pitch/catch impulse method	Dual-element transducer method in which one element transmits sound and the other element receives sound. Low-frequency probes of 5–25 kHz used. Sound waves are transmitted in bursts into the part. Unbonds are detected by differences in wave amplitude and/or phase changes. No couplant is required.
Eddy current sonic tester	Transducer contains an eddy current driver coll surrounding the sonic receiver. Pulsed eddy currents cause unbonds to resonate at the frequency detected by the sonic receiver. Operates at around 14 kHz and requires no couplant. Capable of detecting near and far side unbonds. Frequently used on aluminum honeycomb assemblies. Also known as a *harmonic bond tester*. Capable of detecting crushed and fractured core.
Mechanical impedance method	Dual-element transducer in which the transmitter element generates audible sound waves and the receiver detects the effect of bond variations due to local stiffness changes in the part. The transmitter is swept through 2.5 to 10 kHz during setup to establish the test frequency. This method is capable of detecting unbonds, crushed core, and defects in composite laminates. No couplant is required. Changes in surface contour will influence the response.

pected to contain cracks. Typical honeycomb defects detected include crushed core, core migration, blown core, dimpled core, node bond failures, and the presence of water in the cells.

As depicted in Fig. 12.11, the part is exposed to x-ray radiation that penetrates the part and produces an image on the film located under the part. Images produced on the film are a result of differential absorption of the x-rays due to changes in material makeup or construction. Since composites are nearly transparent to x-rays, low-energy x-rays are used with lower frequencies and longer wavelengths than high-energy x-rays. The sensitivity (radiographic contrast) to feature changes is improved by using x-rays with lower energy, usually less than 50 kV. Higher-energy x-rays are required to penetrate thicker or higher-density materials. An internal void or gap will decrease the amount of solid material through which the radiation passes, increasing the intensity of radiation reaching the film and creating a darker area on the film. By contrast, a metallic inclusion or metallic honeycomb core will increase the amount of solid material that the radiation passes through and decrease the intensity of radiation reaching the film, creating a lighter area on the film.

Variations in density, thickness, and part construction all cause variations in the radiographic image. Changes in density can be caused by changes in part thickness, cracks, porosity, crushed core, or liquid water in honeycomb cells. The film used is a high-contrast film with a small grain size. The source-to-film distance should be as great as possible for the best resolution. As with ultrasonic inspection, reference standards are normally used. Reference standards can be fabricated, such as those shown in Fig. 12.12, but some of the best ones are pieces of scrapped assemblies that are cut up for dissection since they contain the same materials and thicknesses as the part being inspected. Flaw orientation is critical for detection reliability. The major dimension of the flaw should be parallel to the beam direction for maximum sensitivity. Some depth resolution can be obtained by tilting either the x-ray source or the part.

Several forms of radiography are normally employed to inspect composite assemblies. Static x-ray units, like the one depicted in Fig. 12.11, do not move. The part is manually indexed under the x-ray source, and multiple shots are taken to provide complete part coverage. Static x-ray units can be stationary or portable for on-aircraft inspection. Both methods require proper shielding of personnel. In a method called *in-motion x-ray*, there are two robots (a source robot and a media robot) that are mounted on a gantry. The system is computer controlled to synchronize the movement of the two robots along the part as it is being x-rayed. Being computer controlled, the system can be programmed to vary the x-ray parameters along the length of the structure.

A summary of some of the defects detected by x-ray in honeycomb bonded assemblies is shown in Fig. 12.13. Blown core is usually caused by a vacuum bag leak during bonding. Small leaks can result in small areas of blown core, while large leaks, for example, total loss of the vacuum bag, can result in massive areas of blown core to the extent that the part will be unrepairable and



Mobile Automated Scanning System



Vacuum Attachment to Underside of Aircraft

Fig. 12.10 Mobile automated scanning system. Source: The Boeing Company

will have to be scrapped. Condensed core, or lateral compression of the cell walls, is usually a result of the core slipping or migrating before the adhesive gels during the bond cycle. It is more prevalent at edges of parts or at core ramp areas. Node bond failures, in which the foil ribbons are separated at their connecting points or nodes, are usually defects that occur during the core manufacturing process, but they can also result from gas pressure differentials in the cells

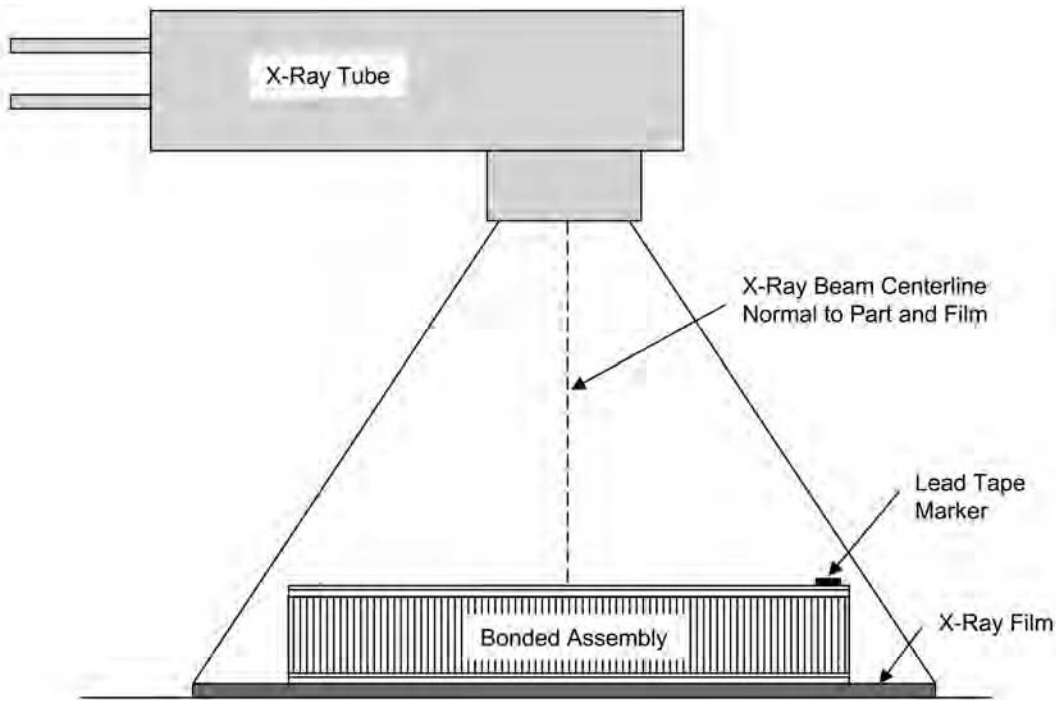


Fig. 12.11 Radiographic inspection. Source: Ref 1

during bonding. Crushed core is usually associated with a dent in the skin or excessive pressure on thick sections of low-density core. Core dimpling, or waviness in the cell walls, is similar to crushed core but does not usually warrant repair. Both crushed core and dimpled core often require x-rays to be taken at a shallow angle for detection.

Water in the core (Fig. 12.14) is a serious problem with honeycomb assemblies. It can lead to corrosion of aluminum core, node bond failures and skin-to-core unbonds due to freeze-thaw cycles, and skin unbonds if the structure is heated above the boiling point of water. For water to be detectable in honeycomb core, ten percent or more of the cell must be filled with liquid water. For thicker composite or aluminum skins, a larger volume of water is required for detection. Since water appears as dark gray areas in discrete cells or groups of cells, this can pose a problem if the part is in service, because water in cells appears very similar to resin in cells, and it is difficult to distinguish between the two without the original radiograph that was taken when the part was manufactured.

Foaming adhesive bondlines can form voids (Fig. 12.15) during bonding that can be difficult to detect. If the foaming adhesive void is less than one-half of the height of the foam bond, detection is questionable. If a void is suspected at a closure member, then pulse echo or a bond test method may be warranted.

Skin-to-core unbonds in sandwich structures (Fig. 12.16) are usually more detectable with ultrasonic methods than with radiography. These adhesive unbonds can be a result of mismatches between detail parts (skins, core, closure members), lack of locally applied pressure due to bridging, entrapped volatiles (air, water, residual solvents), or contaminated skins or core. Although adhesive unbonds are detectable, there are no NDI methods currently available that will determine the strength of an adhesive bond. For example, a high-strength bond with a 5000 psi (34.5 MPa) shear strength will appear the same as a low-strength bond with a 500 psi (3.4 MPa) shear strength. Therefore, mechanical property process control specimens are fabricated along with the production unit using the same surface preparation procedures and adhesives.

12.5 Thermographic Inspection

Although not as widely used as ultrasonics or x-ray, thermographic inspection is a relatively

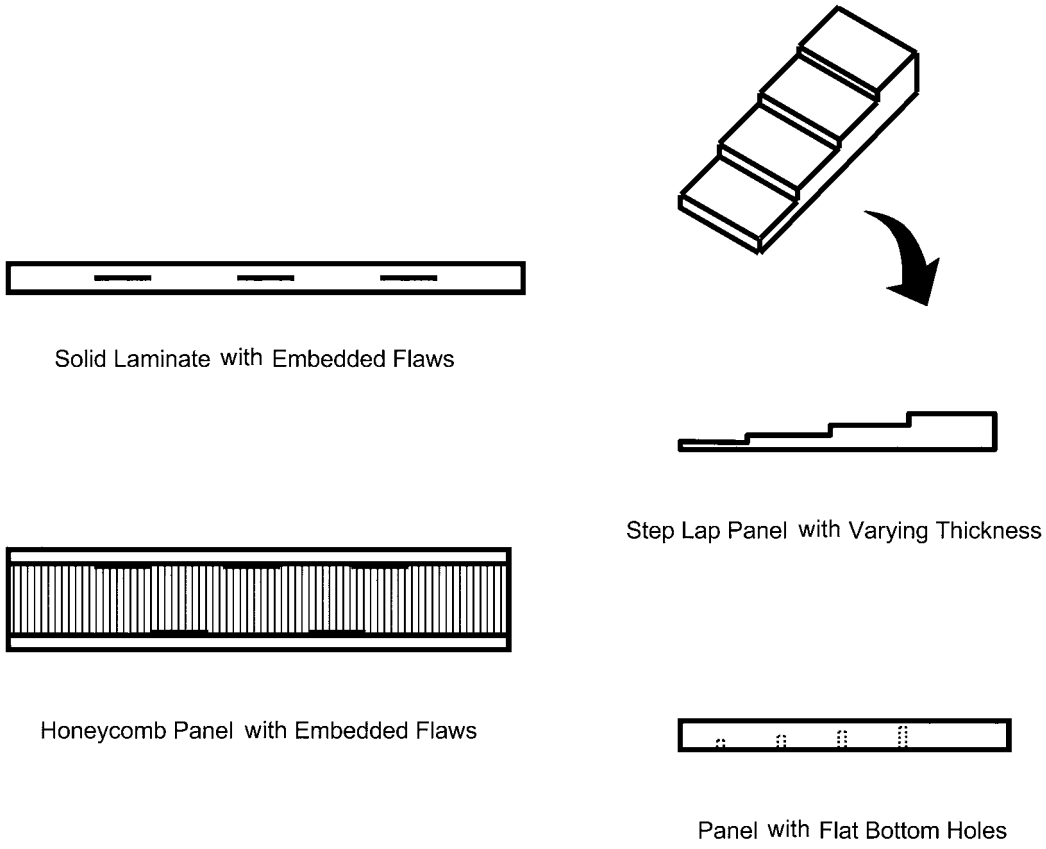
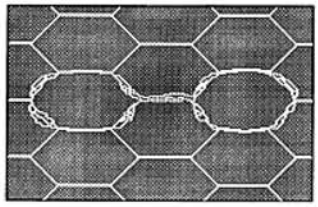


Fig. 12.12 Typical nondestructive inspection (NDI) reference standards

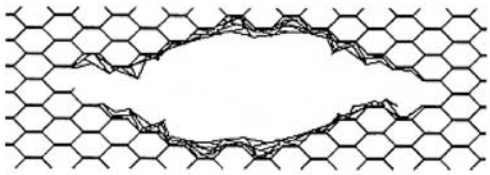
fast, noncontact, single-sided process that has a wide coverage area. It can be used to detect delaminations, impact damage, water ingression into honeycomb, inclusions, and density variations. In thermography (Fig. 12.17), it is first necessary to heat the surface uniformly. This is normally accomplished by flash lamps that pulse for a few milliseconds to provide heat to the surface. High-wattage tungsten halide lamps are frequently used that raise the surface temperature by 12 to 30 °F (7 to 18 °C). As heat is conducted into the part, the surface temperature falls. Since defects cause differences in heat conduction, the surface temperature cools at a different rate above a defect than in a defect-free area. The surface of the part is monitored with an infrared camera that collects the radiation from the surface. Imaging software is then used to examine the radiation received pixel by pixel and provide a map of the surface showing the defects. The output is often a colored map depicting temperature variations as contrasting colors. Airlines often use thermographic inspection to check honeycomb bonded assemblies for the presence of liquid water. This inspection is done immediately after the aircraft lands and before the ice trapped in the cone melts and heats up to ambient temperature. An example of a honeycomb assembly with water ingression is shown in Fig. 12.18.

REFERENCES

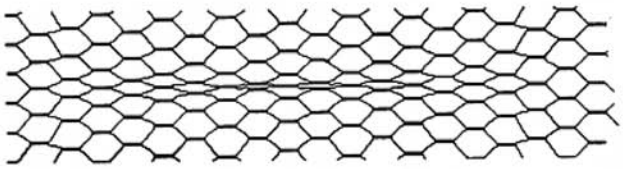
1. T.L. Price, G. Dalley, P.C. McCullough, and L. Choquette, "Handbook: Manufacturing Advanced Composite Components for Airframes," Report DOT/FAA/AR-96/75, Office of Aviation Research, Apr 1997
2. Nondestructive Testing, *ASM Handbook*, Vol 21, *Composites*, ASM International, 2001, p 699–725



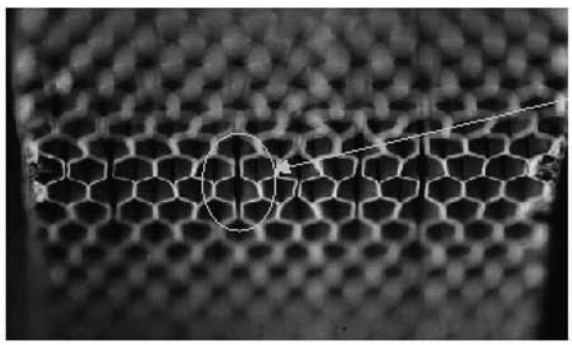
Small Area of Blown Core



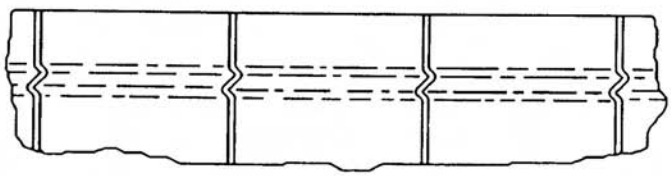
Severe Area of Blown Core



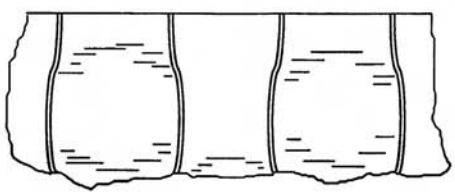
Condensed Core



Node Bond Failures



Crushed Core



Dimpled Core

Fig. 12.13 Common core defects detected by radiography

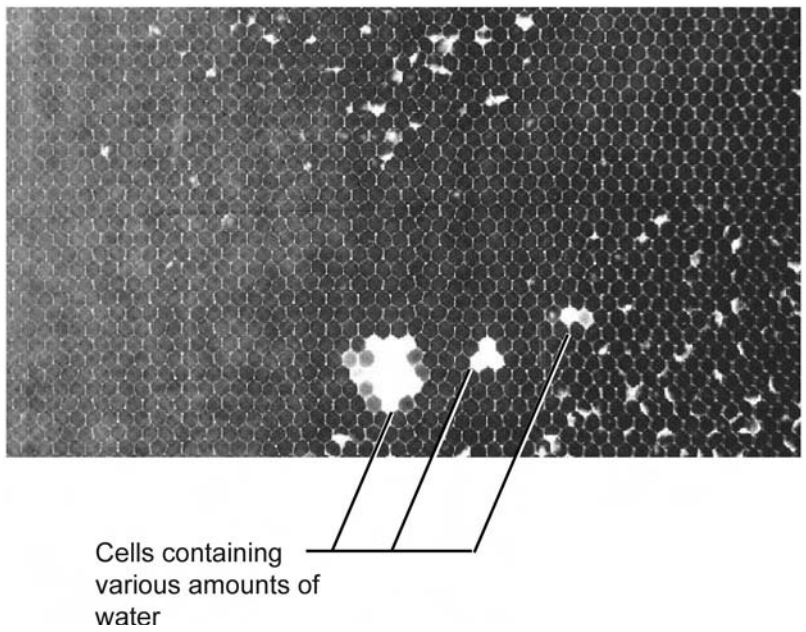


Fig. 12.14 Water in the core detected by radiography

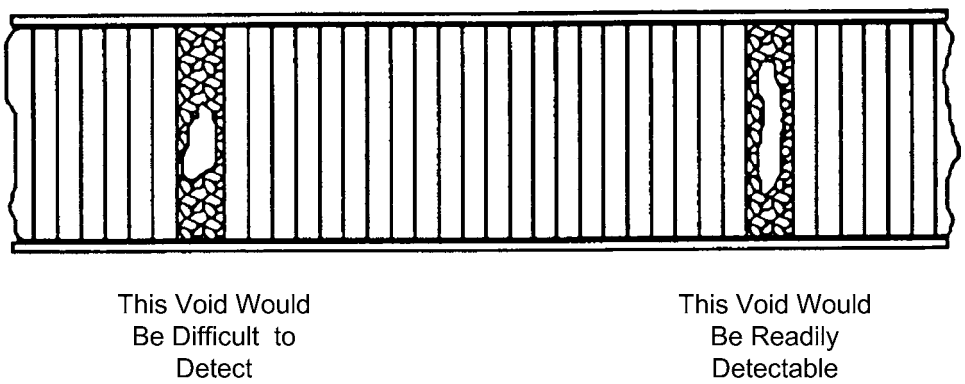


Fig. 12.15 Voids in foaming adhesive

SELECTED REFERENCES

- K.B. Armstrong and R.T. Barrett, *Care and Repair of Advanced Composites*, Society of Automotive Engineers, Inc., 1998
- *ASM Handbook*, Vol 17, *Nondestructive Evaluation and Quality Control*, ASM International, 1989
- R. Bohlmann, M. Renieri, G. Renieri, and Miller, "Advanced Materials and Design for Integrated Topside Structures," training course given to Thales in the Netherlands, 12–19 Apr 2002
- D.J. Hagemaier, Adhesive-Bonded Joints, *ASM Handbook*, Vol 17, *Nondestructive Evaluation and Quality Control*, ASM International, 1989, p 612–640

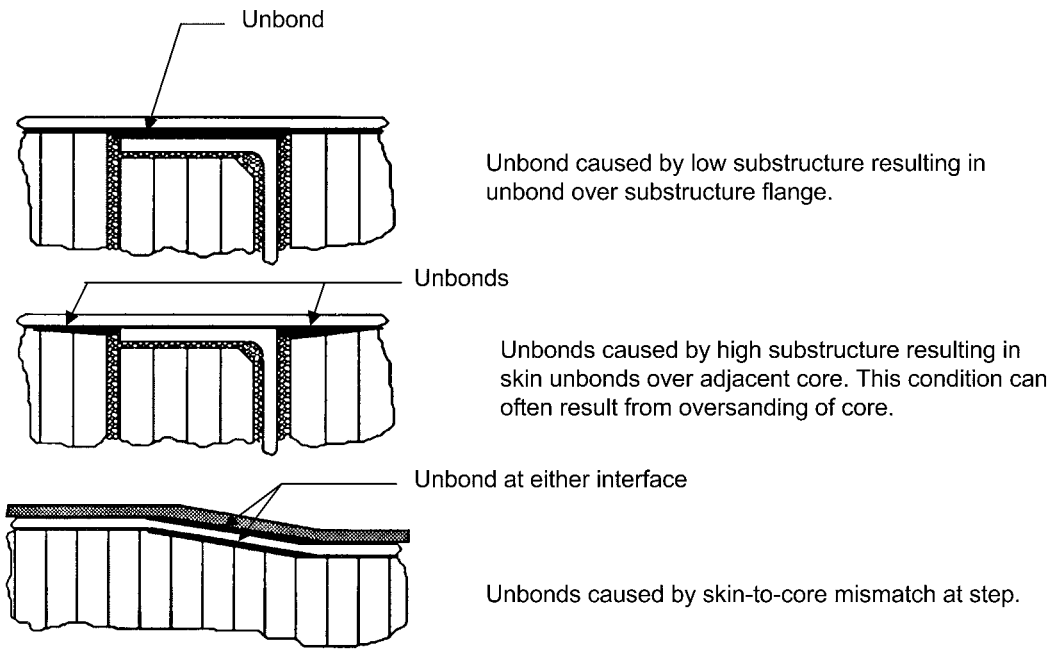


Fig. 12.16 Typical skin-to-core unbonds

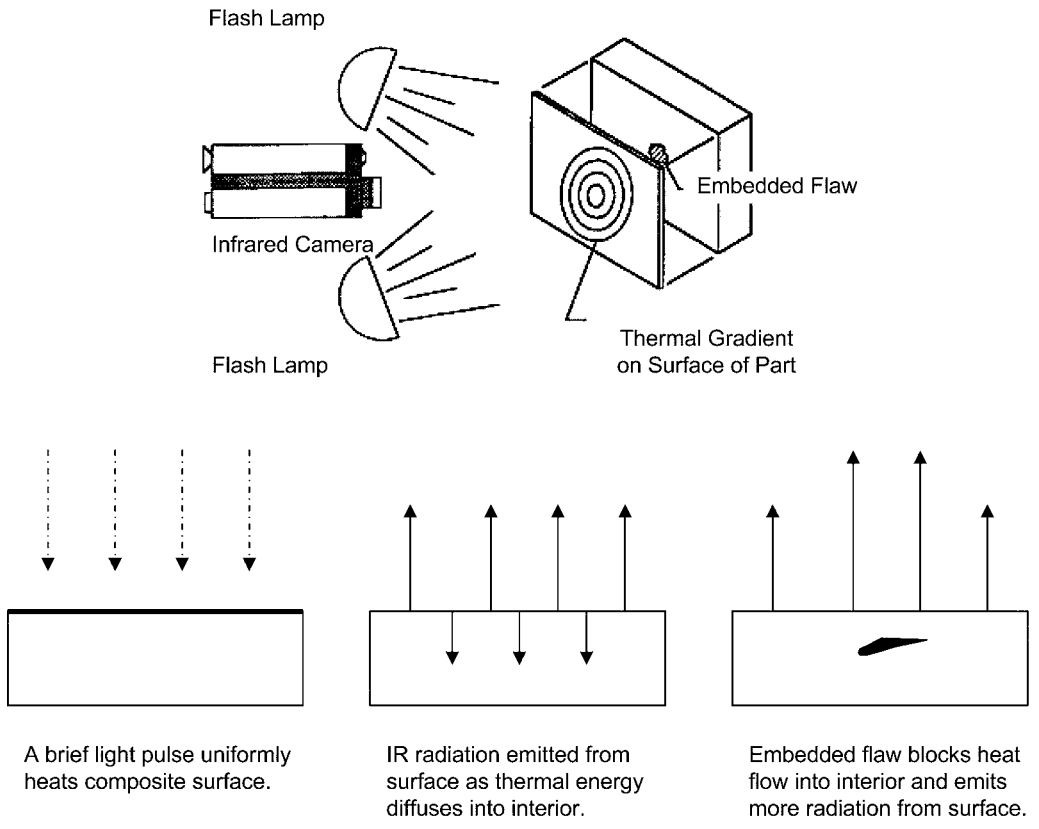


Fig. 12.17 Infrared thermography. IR, infrared. Source: Ref 2

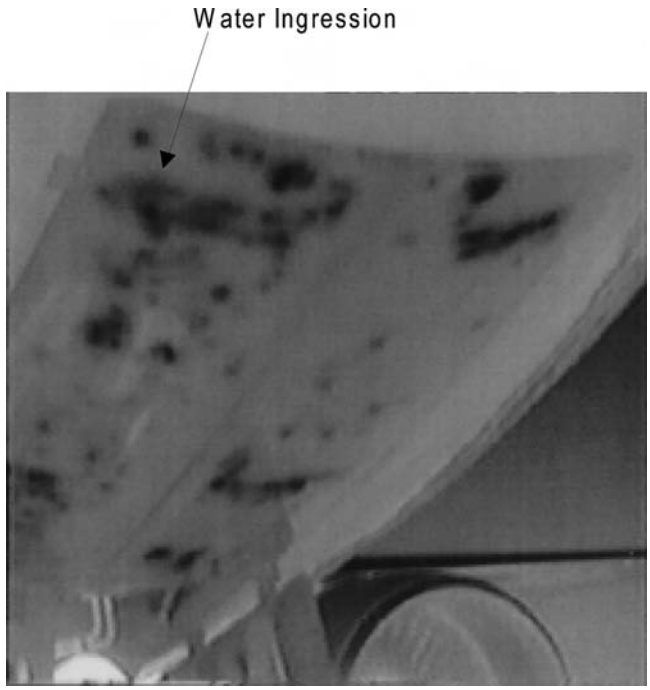


Fig. 12.18 Infrared detection of water in a honeycomb assembly

- J. Krautkramer and H. Krautkramer, *Ultrasonic Testing of Materials*, 4th ed., Springer-Verlag, 1990
- X.P.V. Maldague, *Nondestructive Evaluation of Materials by Infrared Thermography*, Springer-Verlag, 1993
- *Nondestructive Testing Handbook*, 2nd ed., American Society of Nondestructive Testing, 1991
- "Supportability," MIL-HDBK-17-1F, *Volume 3, Materials Usage, Design, and Analysis*, U.S. Department of Defense, 12 Dec 2001, p 8-1–8-60

Copyright © 2010, ASM International®
All rights reserved.
www.asminternational.org

CHAPTER 13

Mechanical Property Test Methods

WHEN HIGH-STRENGTH composites were first developed in the 1960s, the same test methods for homogeneous and isotropic metals were initially used; however, since composite materials are nonhomogeneous (layered) and anistropic (orthotropic), it was necessary to develop specialized test methods. In addition, since early composite development was limited to aerospace companies, each company developed its own procedures. Eventually, standards for testing composites were developed. The two most widely recognized test standards are those of the American Society for Testing Materials (ASTM) and Suppliers of Advanced Composites Manufacturers Association (SACMA). Although SACMA is no longer in existence, many of its standards are still used and are being incorporated as ASTM standards. These standards had to account for: (1) the materials' orthotropy, which required more properties to be determined than for isotropic materials; (2) their laminated construction; (3) the fact that unidirectional composites are extremely strong and stiff in one principal direction and weak and flexible in the other; and (4) the sensitivity they exhibit to temperature and moisture.

Testing is used for many purposes, such as characterization of new materials and processes, development of design allowables, qualification of materials for specific applications, and quality control of production processes. Prior to conducting a large, expensive test program, a preliminary smaller, less expensive test program is usually warranted. A typical procedure would be to characterize the basic lamina properties first. Then, using classical lamination theory, the lamina properties are used to predict laminate properties and behavior. Limited laminate tests are then performed to verify these theoretical predictions. More specialized tests, such as bolt bearing and impact tests, can then be performed. Typical composite test procedures include tension, compression, shear, flexure, open hole tension, open hole compression, bolt bearing, impact and compression after impact, and sometimes fracture toughness. Adhesive bonding test procedures include measurement of adhesive shear strength, measurement of peel strength, and tests to assess the quality of bonding to sandwich cores.

In this chapter, only a brief introduction to test methods for composites and adhesives will be given. Reference 1 gives much more information on composite test methods, and Ref 2 gives a fairly comprehensive list of adhesive test specifications. MIL-HNBK-17-1F (Ref 3) offers an exhaustive source on all aspects of composite testing. The relevant ASTM and SACMA standards explain these methods in great detail.

13.1 Specimen Preparation

Specimen preparation is critical for composite test specimens. Great care is needed at all stages of the preparation process for meaningful results to be obtained. Laminate fabrication procedures should reflect the actual procedures used for production parts. After fabrication, the laminates should be inspected ultrasonically to ensure that they are of high quality. Diamond-coated cutoff wheels with flood coolant are recommended for all trimming operations. Compression specimens usually require flat and parallel ends, which are best achieved using a setup on a surface grinder. All holes must be drilled with carbide drills using the parameters given in Chapter 11, "Machining and Assembly." The adhesive used for applying end tabs must be of sufficient strength to transfer the loads from the grips through shear to the test specimen without failing.

Mechanical properties are usually reported in terms of the volume fraction of fibers or fiber volume percent. However, it is much easier to determine weights using laboratory analysis techniques. For example, a cured sample is first weighed and the matrix is then dissolved in acid. The remaining fibers are dried and weighed. Using these values, the weight percents of the fibers and matrix can be calculated. Using the densities of the fibers (ρ_f) and the matrix (ρ_m), the volume fraction of the fibers (V_f) can be calculated:

$$V_f = \frac{\rho_m W_f}{\rho_m W_f + \rho_m W_f} \qquad \text{(Eq 13.1)}$$

where W_f is the weight of the fibers and W_m is the weight of the matrix, and it is assumed that the void content of the composite is negligible. A comparison of the volume fraction of fibers and the weight fraction of fibers is shown in Fig. 13.1. The densities of carbon, aramid, and glass fibers are all different; therefore, conversions will all be different. In other words, a given weight fraction of fiber will yield a different volume fraction of fiber for carbon, aramid, and glass. Cured resin content is usually expressed as weight percent, the value for a 60 fiber volume percent carbon/epoxy composite means a resin content of around 30 percent by weight and a 70 percent fiber content by weight.

13.2 Flexure Testing

Although the data cannot be used for design purposes, flexure testing is one of the simplest and most straightforward methods for initial screening of new materials for comparison purposes. The flexure test, shown in Fig. 13.2, is essentially a beam in bending, with the bottom surface in tension and the top surface in compression. The maximum shear stress occurs at the center of the cross section. Since the stress varies through the cross section, failure can occur in tension, compression, shear, or some combination of these conditions. Although the three-point test requires less material, the four-point test has the advantage that uniform tensile or compressive stresses are produced over the area between the loading points, not just under the center loading point, as in the three-point bending test.

Flexure testing is covered in ASTM D 790 (three-point loading) and ASTM D 6272 (four-point loading). The specimen length is dependent on the thickness. A span-to-thickness ratio of 16 to 1 is recommended if the ratio of tensile strength to shear strength is less than eight to one. The span-to-thickness must be increased if

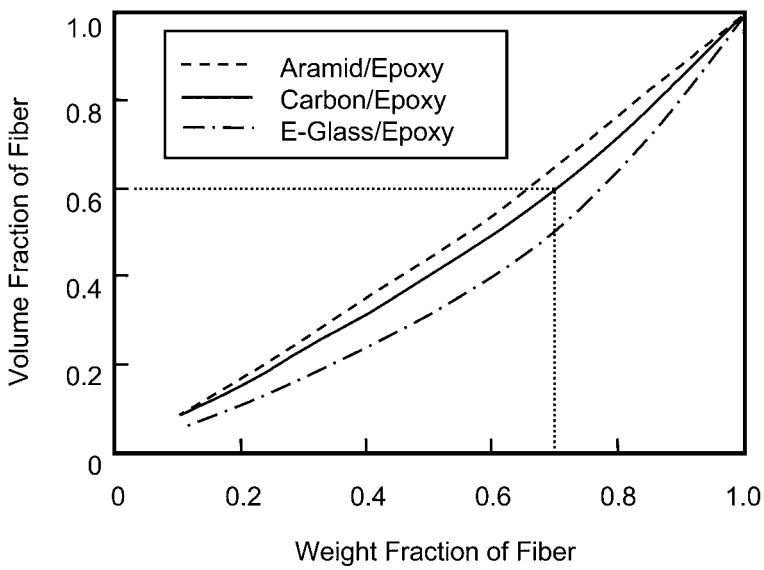


Fig. 13.1 Comparison of fiber volume fraction to fiber weight fraction

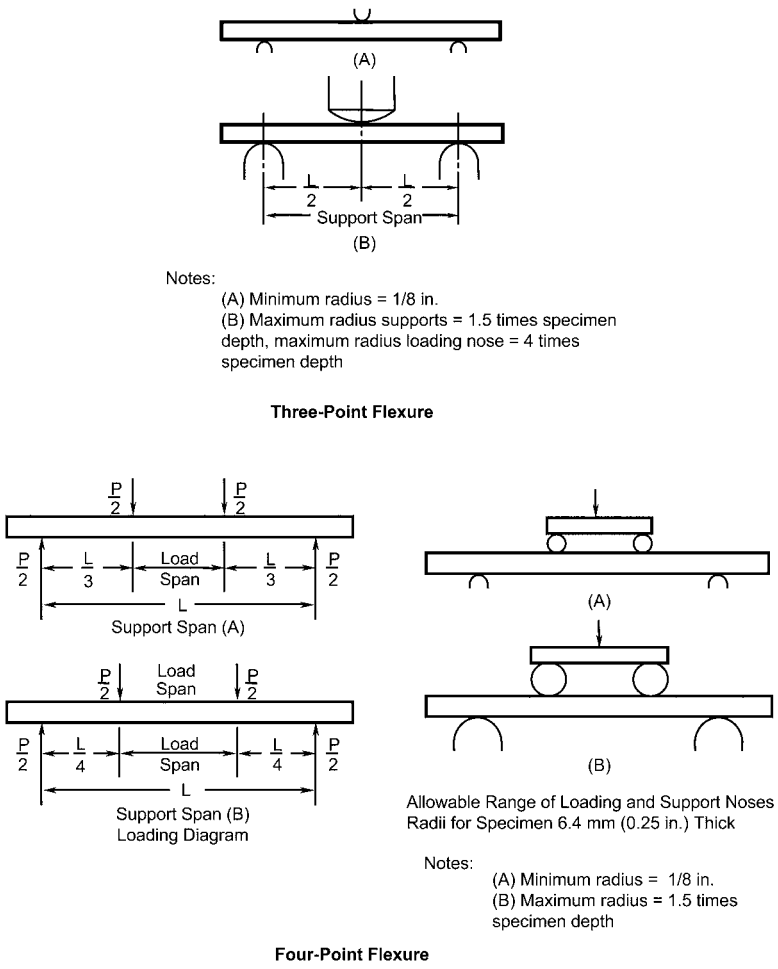


Fig. 13.2 Three- and four-point flexure tests

tensile strength to shear strength is greater than eight to one. Although essentially any orientation can be tested, the normal practice is to test either a zero-degree or 90-degree lamina. A deflectometer can be used to determine the midspan deflection and allows the calculation of a modulus value. Again, this test method is very useful for quality control testing, process verification testing, specification purposes, and comparative testing of different materials. However, the results of flexure testing are not normally used for design purposes.

13.3 Tension Testing

Axial tension testing of unidirectional (zero-degree) composites is a challenge; it is difficult to transmit load from the testing machine to the composite because the composite interlaminar shear strength is much lower than the uniaxial tensile strength. Longitudinal tensile tests are extremely sensitive to fiber alignment; even a deviation of several degrees will result in artificially low values. If a standard metallic dogbone test configuration is used, shear failure in the gripping region is a common problem. Therefore, straight-sided specimens (Fig. 13.3) are used along with fiberglass/epoxy tabs bonded to both ends. The tabs distribute the gripping forces and protect the composite from surface damage. Since the forces are transferred by shear, a large bond area and a strong adhesive are used to prevent the tabs from shearing off under load. A successful test must cause failure within the gage region. Failure at the tab edge (or gripped

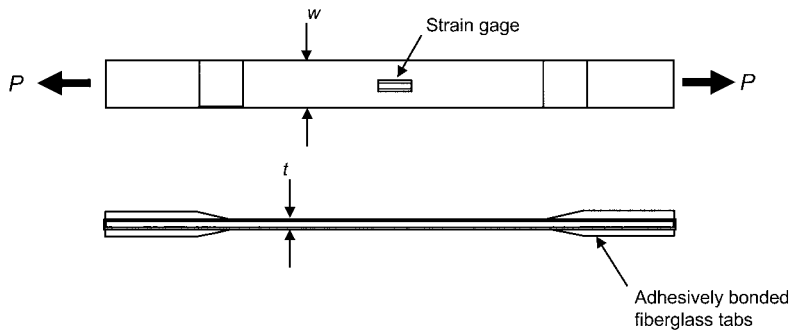


Fig. 13.3 Straight-sided tension test

edge) or within the tab is unacceptable. For longitudinal (zero-degree) specimen tests, thin specimens are preferred to minimize the shear stresses in the adhesive. Since unidirectional composites are rather weak in the transverse or 90-degree direction, transverse testing is much easier, and tabs are not usually required for 90-degree specimens. However, thicker specimens are recommended since thin specimens can be easily damaged during handling.

Tensile testing procedures are covered by ASTM D 3039 and SACMA SRM-13. The most common geometry is a 9 in. (23 cm) long by 1.0 in. (2.5 cm) wide specimen. Different orientations can be tested, such as unidirectional, off-axis, cross-ply, and quasi-isotropic. Mechanical or hydraulic wedge-type grips are used. Either an extensometer or bonded strain gages are used to monitor strain. If Poisson's ratio is desired, then biaxial strain gages are needed.

13.4 Compression Testing

Compression testing is even more difficult than tension testing. Several problems arise in compression testing: Longitudinal compression strength is very sensitive to fiber alignment; end crushing of the composite can occur before true compression strength is attained; and the test setup must be designed to prevent global buckling. Generally, compression failure occurs through buckling, ranging from classical column buckling of the entire specimen cross section to local microbuckling of fibers, which often leads to failure through the process of kink band formation. Therefore, the greater resistance to buckling the test fixture provides to the specimen, the higher the value of compressive strength that is obtained. While many test methods have been developed, the most prevalent are the Modified ASTM D 695, ASTM D 3410, and ASTM D 6641.

Modified ASTM D 695. The Modified ASTM D 695 test method (Fig. 13.4), also covered by SACMA SRM-1, uses two test coupons, one for strength and one for modulus. The method has the advantage that only a small specimen is required but two specimens must be used if both strength and modulus are to be measured. Thickness can range from 0.040 to 0.12 in. (1.0 to 3.0 mm). Since this method introduces the loads by end loading, the ends must be ground flat and parallel. Loading tabs are required for the strength coupon but not for the modulus coupon. This test can be used for unidirectional (zero- and 90-degree) laminae and laminates. The Modified ASTM D 695 compression test fixture is required, but it is a rather small and lightweight fixture. This test is sensitive to the amount the screws in the fixture are tightened; if they are tightened too much, the fixture will pick up some of the load due to friction. Torque values just above finger tight are recommended. Back-to-back strain gages are used for the modulus coupon but no gages are required for the strength coupon. Since two separate coupons are required, a full stress-strain curve cannot be measured.

ASTM D 3410. The Illinois Institute of Technology Research Institute (IITRI) method (Fig. 13.5) is specified in ASTM D 3410. The specimen is 6 in. (15 cm) long by 1.5 in. (3.8 cm) wide with a thickness ranging from 0.12 (3.0 mm) to 0.25 in. (6.4 mm). Any orientation can be tested. Uniaxial back-to-back strain gages are used to monitor potential bending. Biaxial gages

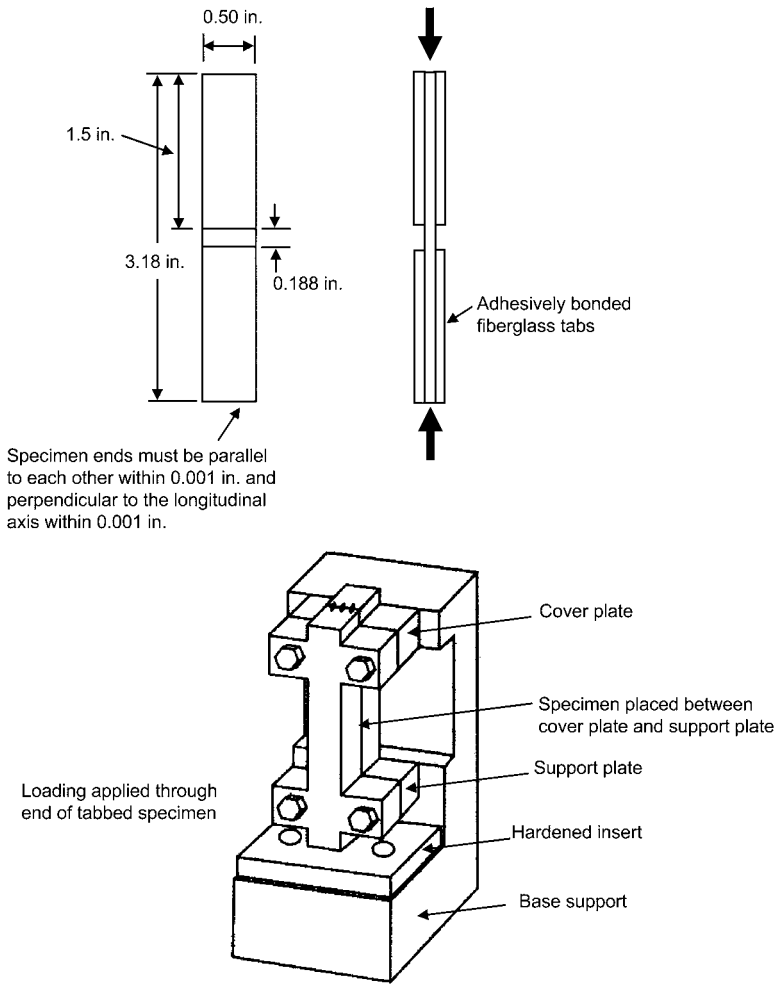


Fig. 13.4 Modified ASTM D 695 compression test

may be used to measure Poisson's ratio. The IITRI method is very sensitive to thickness variations across the width. Since this method introduces the load through shear at the grips, end tabs are not strictly required. However, end tabs are usually used for two reasons: (1) the grips are knurled and tend to bite into the specimen surface; and (2) since the test is sensitive to thickness variations, end tabs are ground flat and parallel across the thickness. If a thin laminate or a laminate with a relatively low modulus is going to be tested, an analytical buckling check is required using the procedure given in ASTM D 3410.

ASTM D 6641. The most recent test procedure is the combined loading compression (CLC) test (Fig. 13.6), which is covered in ASTM D 6641. It is called a *combined loading* test since part of the load is introduced in shear and part through end loading. Since part of the load is introduced at the ends, the ends must be ground flat and parallel. The specimen is 5.5 in. (14.0 cm) long by 0.50 in. (1.3 cm) wide, with a gage length of 0.50 in. (1.3 cm). This test is used for all laminate configurations other than unidirectional zero degrees. A special CLC test fixture is required, but it has the advantage that it is somewhat simpler and lighter than the IITRI fixture. Back-to-back strain gages are recommended to monitor potential bending during the test. If Poisson's ratio is required, then biaxial strain gages are used.

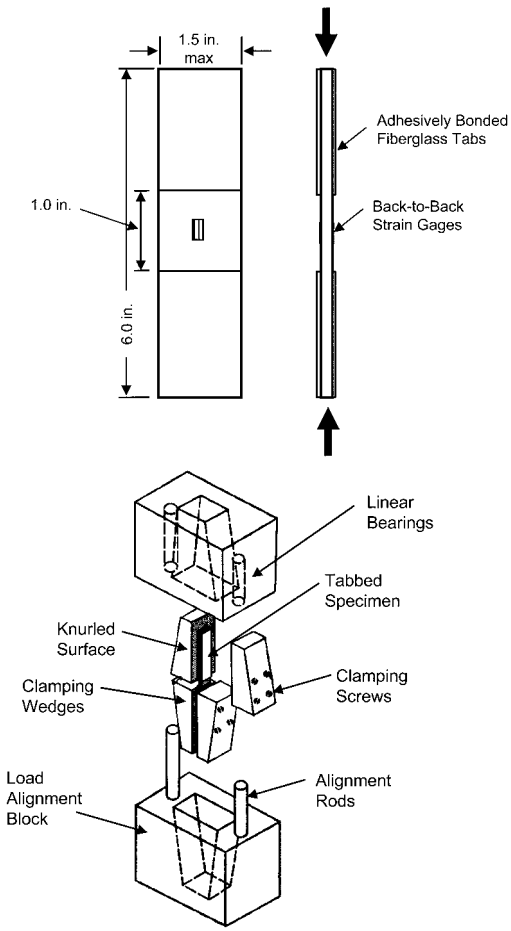


Fig. 13.5 IITRI compression test

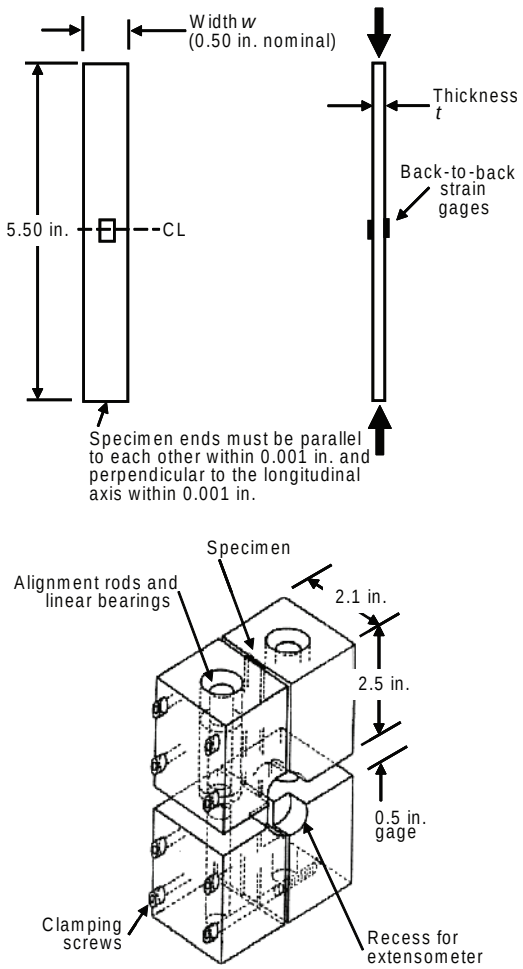


Fig. 13.6 Combined loading compression (CLC) test

13.5 Shear Testing

There are a number of different methods for determining the shear properties of composites, including the ± 45-degree tensile coupon, the rail shear test, the Iosipescu shear test, and the interlaminar or short beam shear test. The ideal test for shear is torsion of a thin-walled tube, which provides a pure shear stress state, yet this method is not often used. The specimens are relatively expensive, fragile, and difficult to hold and align correctly, and the technique requires a torsion testing machine of sufficient capacity.

± 45-degree tensile test (Fig. 13.7) is covered by ASTM D 3518 and SACMA SRM-7. The test is essentially a tensile test of a laminate that has a ± 45-degree lay-up. This test is very similar to standard tensile testing except that biaxial strain gages are used to obtain the necessary data to calculate the shear strength, modulus, and strain-to-failure. This test method yields only the in-plane lamina shear properties. Other methods must be used to obtain data for laminates. Since this test is essentially a ± 45-degree tension test, the ± 45-degree tensile strength and modulus can also be measured.

Rail Shear Test. The rail shear test (Fig. 13.8) is covered in ASTM D 4255. Both two-rail and three-rail shear methods are used. The specimen for the two-rail shear test is 6 by 3 in. (15 by 7.5 cm), while the one for the three-rail test is 6 by 5.375 in. (15 by 13.7 cm). Rosette strain gages are required if shear modulus and shear strains are desired. While this test method has

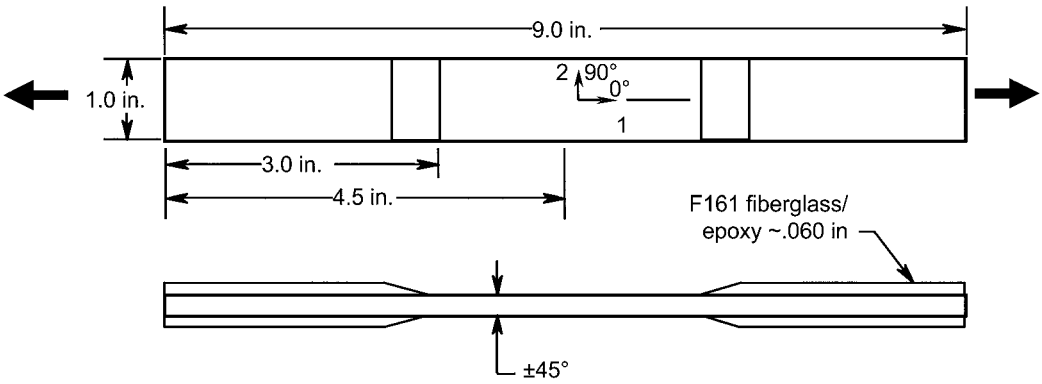


Fig. 13.7 ± 45° Tensile shear test

been used for many years, it requires a large amount of material, the metal rails must be bonded to the specimen, holes for fixture attachment must be drilled in test specimens, and stress concentrations may develop at bolt holes during the test.

Iosipescu Shear Test. The Iosipescu shear test (Fig. 13.9), covered by ASTM D 5379, is a more recent test procedure that can be used to obtain both lamina and laminate in-plane shear properties. The specimen is 3 in. (7.5 cm) long by 0.75 in. (1.9 cm) wide, with a 90-degree notch that is 20 to 22 percent deep and has a root radius of 0.050 in. (0.1 cm). Tabs are recommended to eliminate bearing failures. An Iosipescu fixture is required, and essentially any orientation can be tested. A biaxial or a rosette strain gage is required for modulus and shear strain. An advantage of this test is that it can be used to measure shear properties in any orientation. Thus, the Iosipescu method can be used to provide interlaminar shear properties by machining the specimen so that the interlaminar plane is parallel to the plane of the gage area.

Interlaminar shear test (Fig. 13.10), also commonly referred to as *short beam shear*, is covered in ASTM D 2344 and SACMA SRM-8. The geometry depends on the thickness, with a span-to-thickness ratio of four to one recommended. The width is a minimum of 0.25 in. (0.6 cm). Although any fiber orientation except a 90-degree lamina can be used, the normal practice is to use a zero-degree lamina. No special instrumentation is required; the load-versus-machine crosshead travel is typically recorded. As with the flexure test specimens, failure can occur by tension, compression shear, or mixed mode. Only shear failures yield legitimate results. Shear strength determined by this method cannot be used for design data; however, this test method is relatively inexpensive and is very useful for quality control testing, process verification testing, specification purposes, and comparative type testing of different materials.

13.6 Open-Hole Tension and Compression

The open-hole tension test is very similar to the standard tensile test method; however, end tabs are not generally required. A 0.25 in. (0.6 cm) hole diameter in a 1.50 in. (3.8 cm) wide specimen (Fig. 13.11) is normally used. This test is generally performed on lay-ups representative of actual structure. Gross failure stress and strain are generally reported for comparison with specimens without holes. The open-hole tension test is specified in ASTM D 5766 and SACMA SRM-5. The most common geometry is a specimen 12 in. (30.5 cm) long by 1.5 in. (3.8 cm) wide, with a 0.25 in. (0.6 cm) diameter hole located at the center. It is used to test quasi-isotropic or other lay-ups representative of actual structure. A uniaxial strain gage is required if failure strain is desired. Since this specimen should fail at the hole, end tabs are not typically used.

Open-hole compression testing is covered in ASTM D 6484 and SACMA SRM-3. The specimen is very similar to the open-hole tension specimen; it is normally 12 in. (30.5 cm) long by

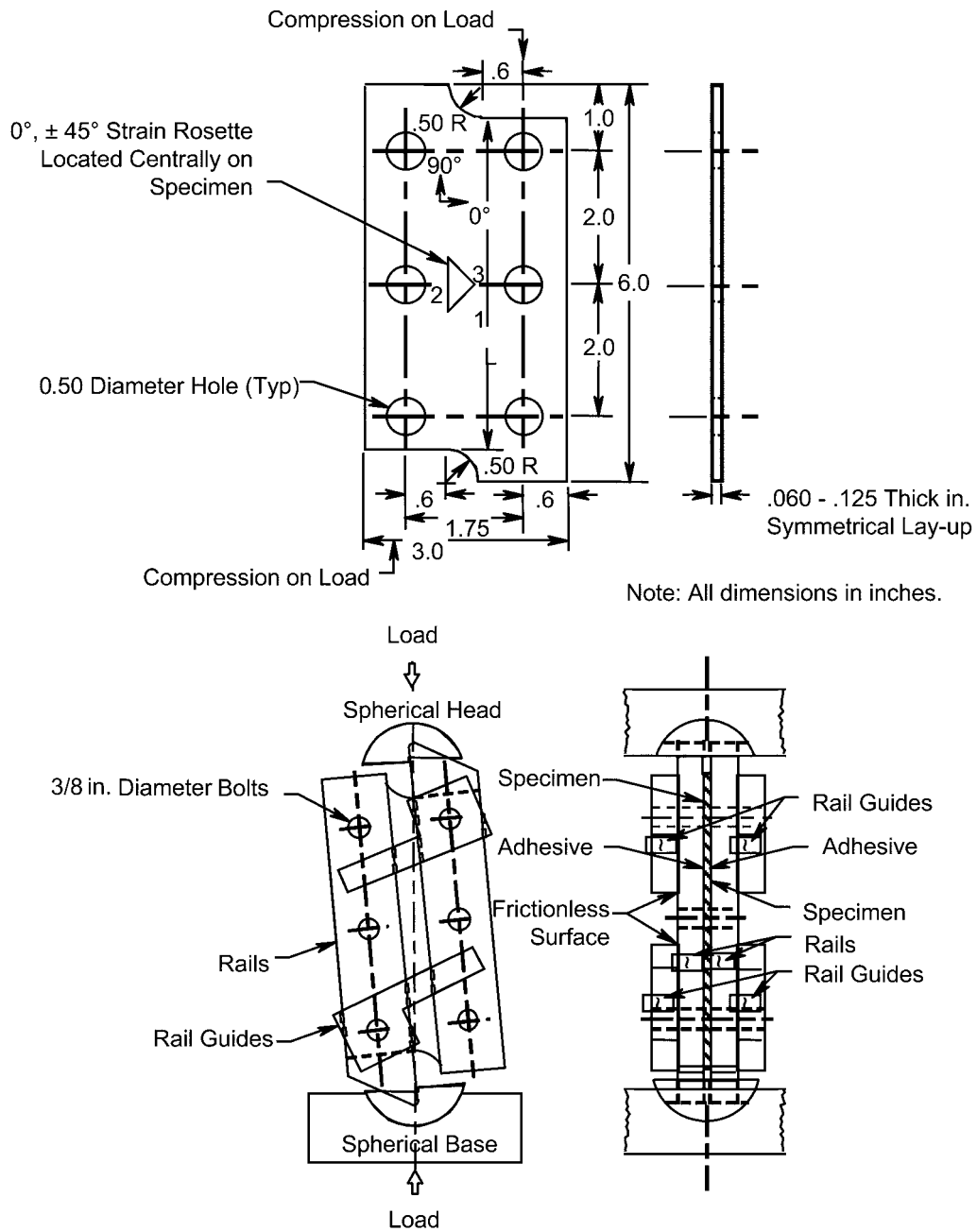


Fig. 13.8 Two-rail shear test

1.5 in. (3.8 cm) wide, with a 0.25 in. (0.6 cm) diameter hole. As in the open-hole tension test, quasi-isotropic or other lay-ups representative of actual structure are tested. Back-to-back uniaxial strain gages are normally used.

13.7 Bolt Bearing Strength

The two most common tests are double shear (pin bearing) and single shear. Many different specimen configurations are used. Often they

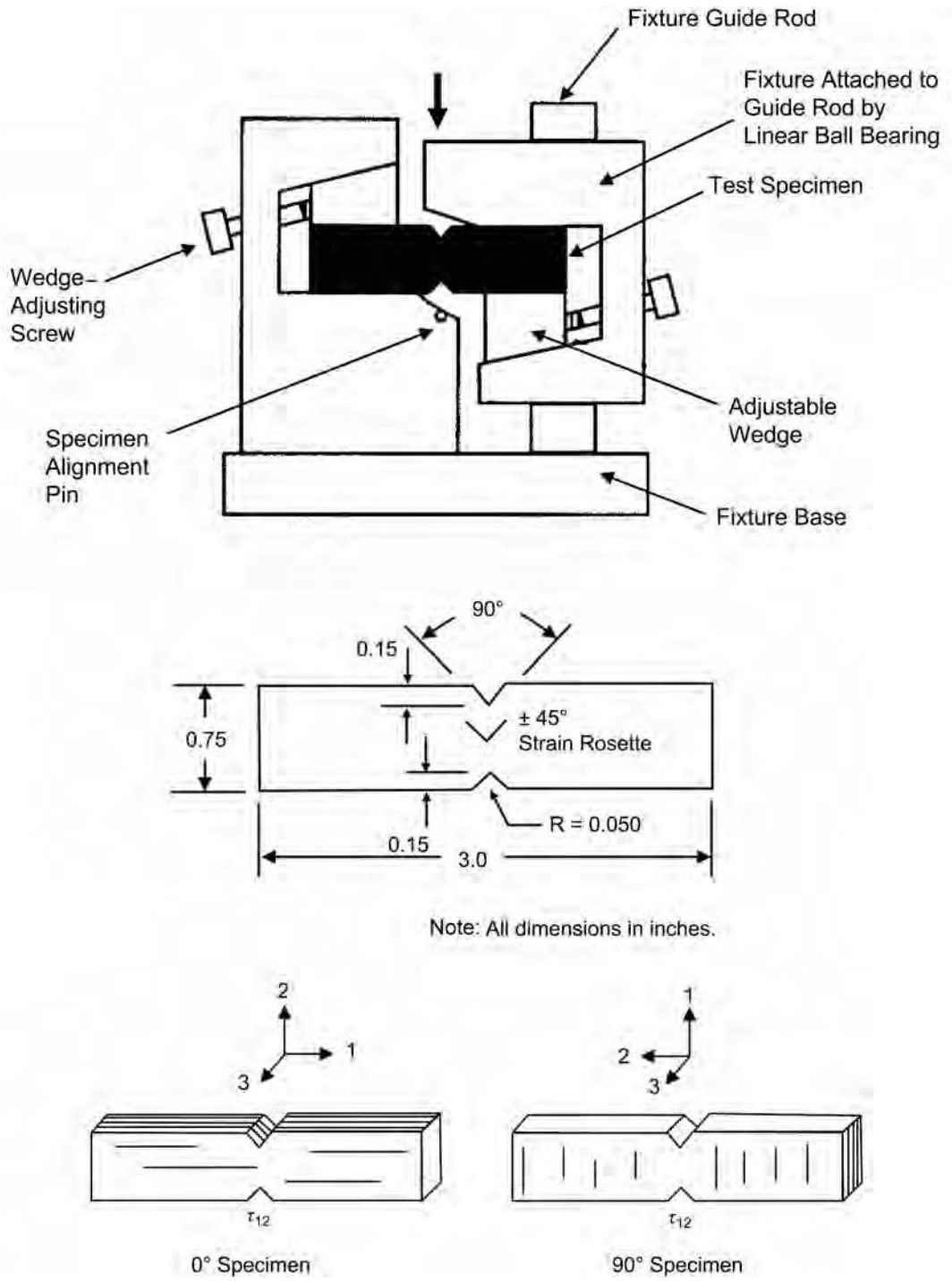
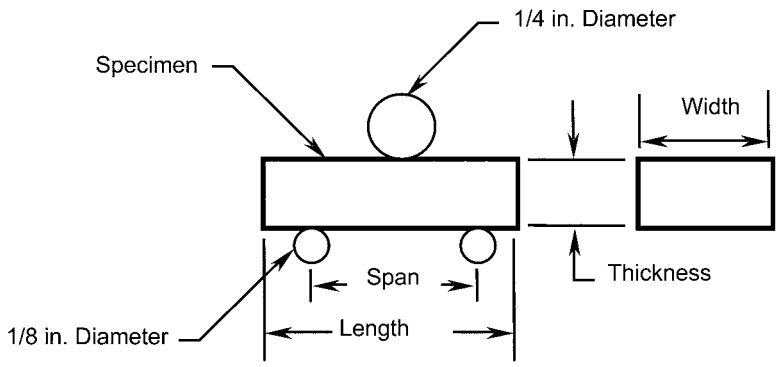


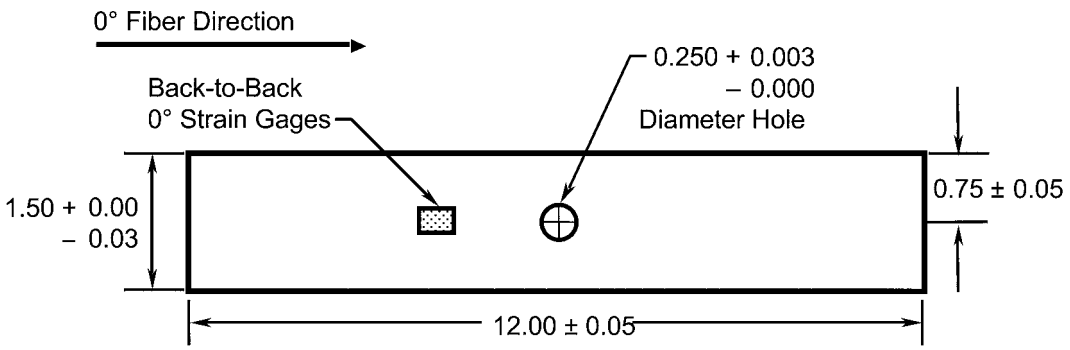
Fig. 13.9 Iosipescu shear test



Recommended Dimensions:

Span = 4 x Thickness
Length = 6 x Thickness
Width = 0.25 in. Minimum
= 2 x Thickness, t > 0.125 in.

Fig. 13.10 Interlaminar shear test

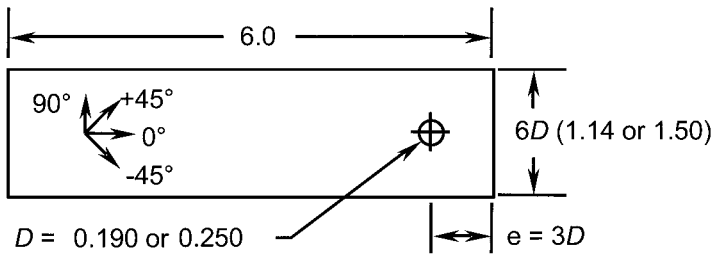


Note: All dimensions in inches.

Fig. 13.11 Typical notched tension/compression test

are representative of actual joint configurations. A typical specimen is 6 in. (15 cm) long by a width six times that of the bolt diameter. A 0.25 in. (0.6 cm) diameter hole is the most common size. Quasi-isotropic or other lay-ups representative of actual structure are tested. The load-versus-head deflection is typically recorded.

Double Shear. The dimensions shown in Fig. 13.12 are for reference only. Other widths, edge distances, and hole diameters can be used to represent actual joint geometries. The thickness should be representative of actual joints. Normally, the fastener torque is only finger tight. Loading results in pure bearing stress in the hole and double shear on the fastener.



Specimen Configuration

$$F_{BR} = \frac{P}{Dt}$$

Where:
P = Failing Load (lb)
D = Bolt Diameter (in.)
t = Specimen Thickness (in.)
F_{BR} = Bearing Stress (psi)

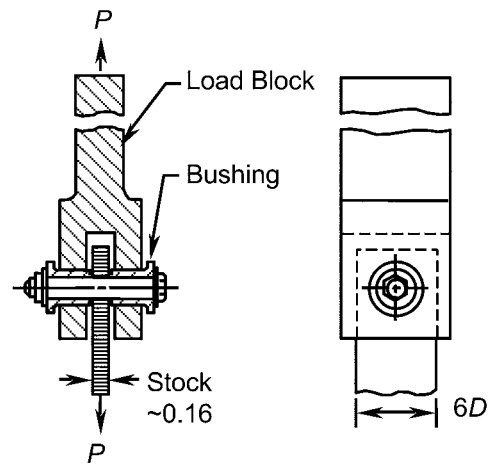


Fig. 13.12 Double shear bolt bearing test

Single Shear. The configuration of the single shear specimen (Fig. 13.13) is very similar to that of the double shear specimen. Single shear specimens usually have a countersunk hole. Their dimensions are usually the same as those of the double shear specimen. Although eccentricities cause bending moments and the fastener tends to rotate and dig into the composite, this configuration is representative of many actual joint geometries. As a result of these eccentricities, this test does not give the true bearing strength.

13.8 Flatwise Tension Test

Flatwise tension testing of composite laminates is covered in ASTM D 7291. Either a 1 or 2 in. (2.5 or 5 cm) diameter disk is adhesively bonded to metal loading blocks, as shown in Fig. 13.14. Although any laminate orientation can be used, a quasi-isotropic orientation is the most common. No instrumentation is used, and only the flatwise tension strength is reported. Photographs of the failed surfaces are recommended to document the failure mode.

13.9 Compression Strength After Impact

After impacting in accordance with ASTM D 7136, the compression strength after impact can be determined using ASTM D 7137. The specimen (Fig. 13.15) is 6 in. (15 cm) long by 4 in. (10 cm) wide, with a quasi-isotropic or lay-up representative of the actual structure. A "picture frame" impact test fixture is used for the impact, and then the specimen is loaded to failure in compression. Ultrasonic inspection is normally

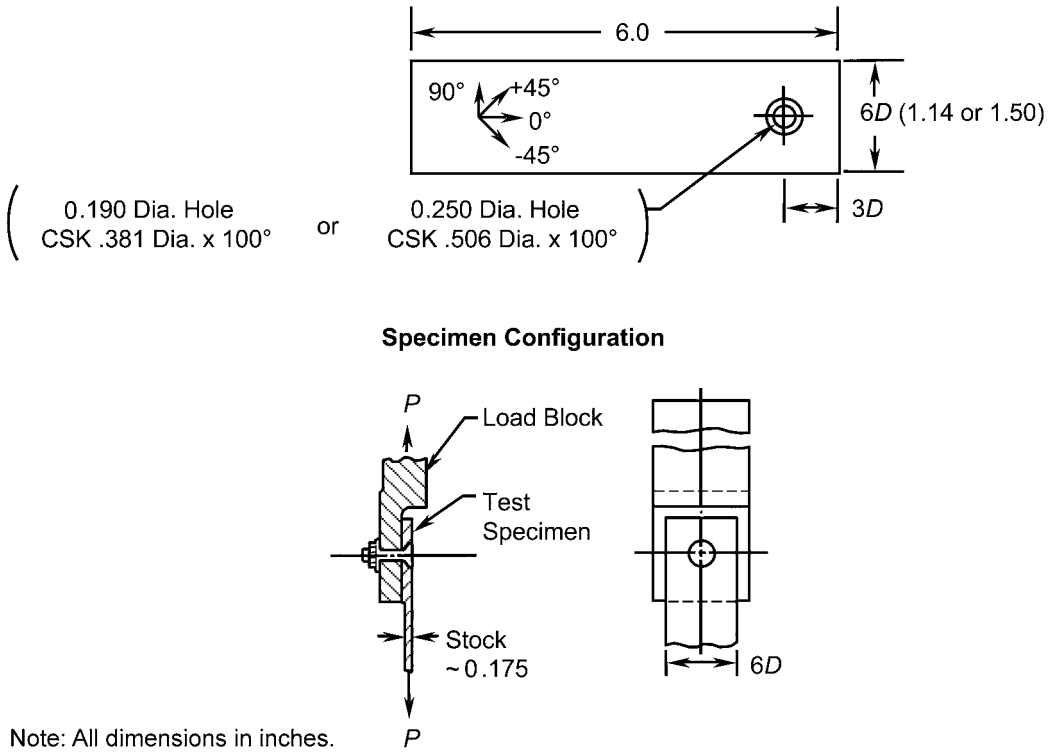


Fig. 13.13 Single shear bearing test

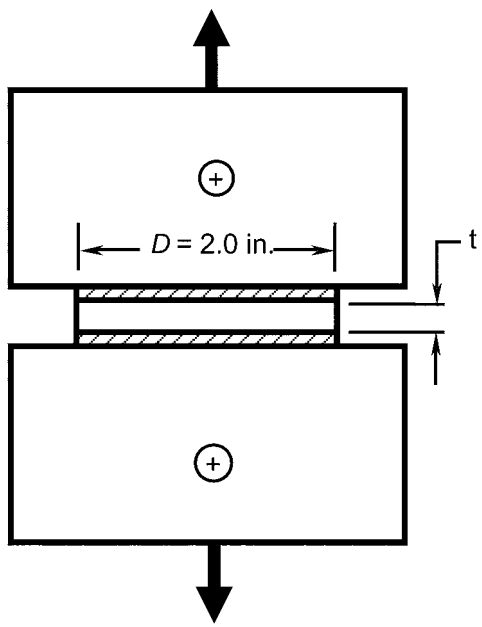
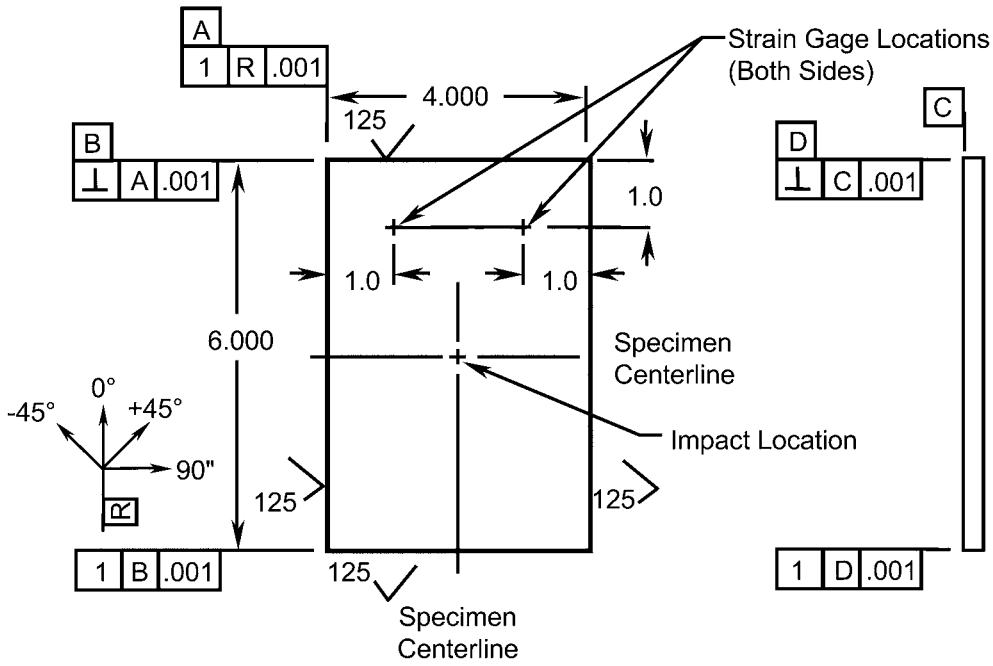


Fig. 13.14 Laminate flatwise tension test

used to determine the extent of damage after impact but before compression testing. Four uniaxial strain gages are used during the compression test. Different energy levels can be tested; 1500 in.-lb/in. is often used. The compression strength and modulus for impacted specimens are compared with those for control (no impact damage) specimens.

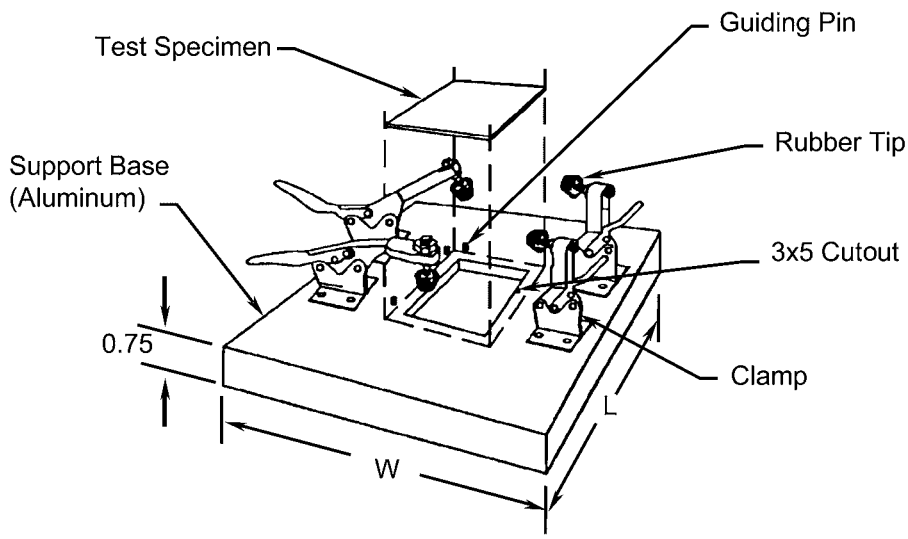
13.10 Fracture Toughness Testing

Fracture toughness testing originated with metals, where it is widely used to determine the life of metallic structures. The application of fracture mechanics to composite materials is much less widely used. The three modes of failure are Mode I (opening mode), Mode II (shear mode), and Mode III (tearing mode), as shown in Fig. 13.16. Fracture toughness tests (Fig. 13.17) for composites include the double cantilever beam per ASTM D 5528, end notched flexure, cracked lap shear, and edge delamination tests. The most prevalent test is the double



Notes:

1. Unless otherwise specified, dimensional tolerances are ± 0.005 in.
2. All dimensions in inches.



Note: All dimensions in inches.

Fig. 13.15 Compression after impact test

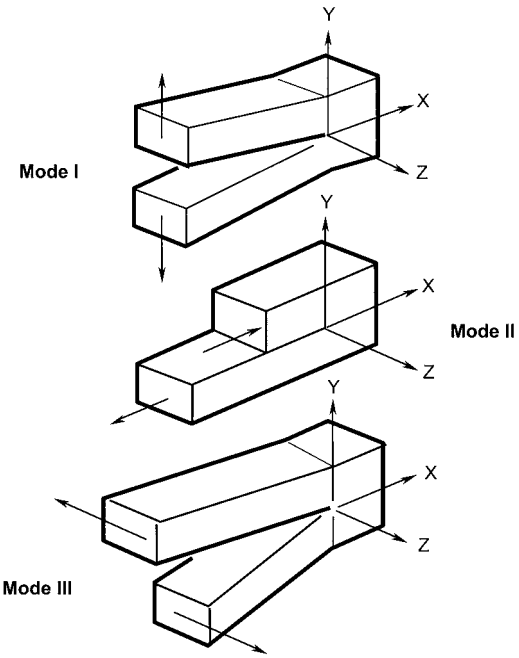


Fig. 13.16 Modes of crack opening displacement

cantilever beam test, which measures the Mode I or opening mode of failure. This test is often used to compare the matrix toughness of different resin systems. Reference 1 describes the various fracture toughness tests used for composites.

13.11 Adhesive Shear Testing

The three most prevalent shear tests for adhesives (Fig. 13.18) are the single lap shear test, the double lap shear test, and thick adherend testing. When testing adhesives, it is important to examine the failure mode. Failure of the adhesive itself (cohesive failure) is the desired failure mode. If the adhesive pulls off of the adherend (adhesive failure), it is not a valid test and is usually indicative of improper surface preparation. Surface preparation methods for aluminum, titanium, and composite adherends are covered in Chapter 8, "Adhesive Bonding."

Single lap shear test (ASTM D 1002) is the simplest but least efficient test due to the presence of eccentric loading, as shown in Fig. 13.19. Due to the eccentric load path, the adherends try to bend with increasing load, inducing peel loads at the ends of the bondlines. While metal adherends (aluminum more so than titanium) will bend to try to compensate, composite adherends, being brittle, will often fail in interlaminar peel. In addition, the bondline is not long enough, typically the overlap is 0.5 in. (1.3 cm), to be representative of actual bonded joints. In spite of these shortcomings, the single lap shear test is used extensively for process control testing of adhesively bonded structures. It is useful for verifying surface preparation and the cure of the adhesive. Although either zero-degree laminae or oriented laminates can be tested, it is more common to test the adhesive shear strength using either aluminum or titanium adherends. No instrumentation is used, and only the lap shear strength is reported.

The double lap shear test (Fig. 13.20), per ASTM D 3528, is the recommended configuration for adhesive screening tests and for the determination of typical shear stress values. Since the load path is essentially straight, it does not suffer from the eccentric problem, as does the single lap shear configuration. This test is frequently used with composites, as well as with metal adherends. It can be used to determine the shear stress of both secondarily bonded and cocured composite joints. Again, no instrumentation is used and only the lap shear strength is reported.

The thick adherend test (Fig. 13.21), specified in ASTM D 5656, is used to determine the design properties of an adhesive system. Although it is a single lap shear configuration, the adherends are so thick that bending does not occur. Two KGR-1 extensometers are used to accurately monitor very small deflections approximately 0.000001 in. (0.025 4 μm). The true shear stress, shear modulus, and shear strain can be measured in this test, as shown in the example shear stress-strain curve in Fig. 13.22. The significance and use of these properties are covered in Chapter 17, "Structural Joints—Bolted and Bonded."

13.12 Adhesive Peel Testing

Although it is never desired to intentionally load an adhesive bondline in peel, it is important to understand the peel strength of any adhesive

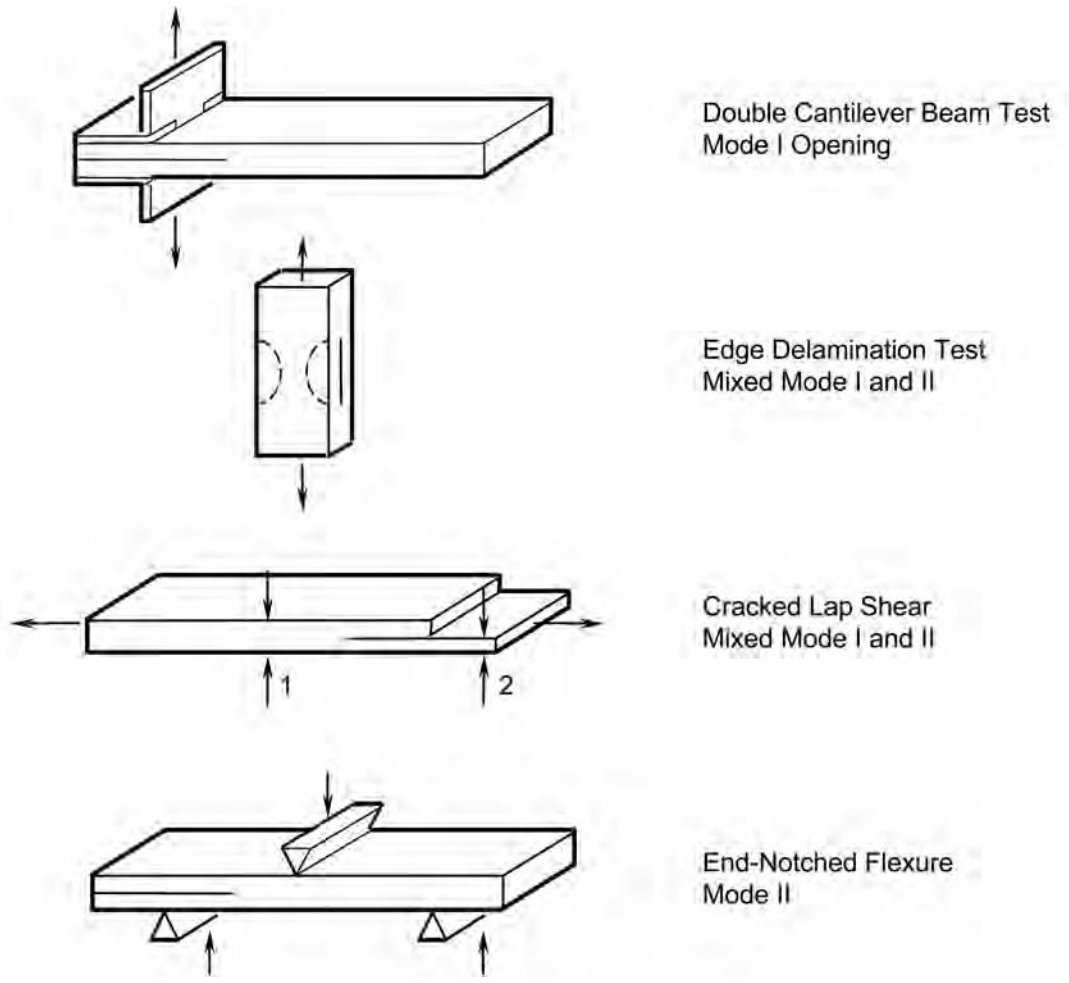


Fig. 13.17 Typical composite materials fracture toughness tests

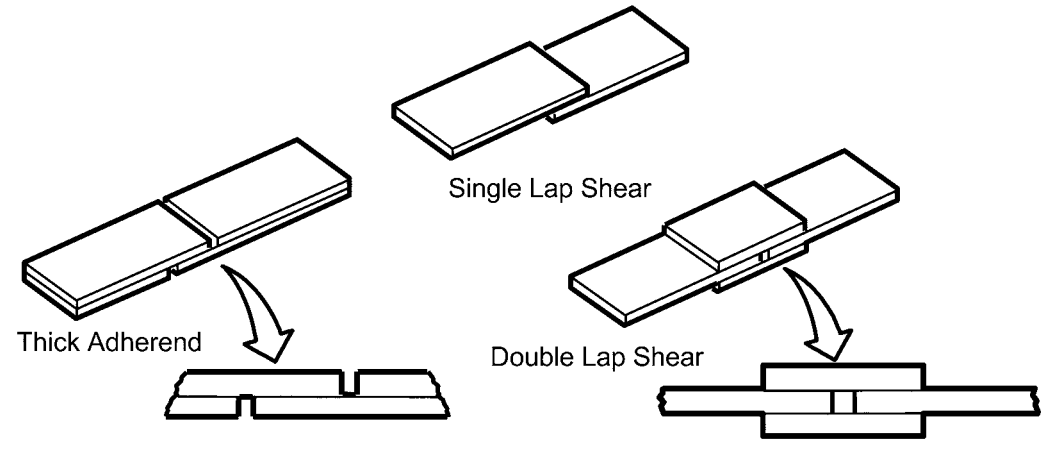
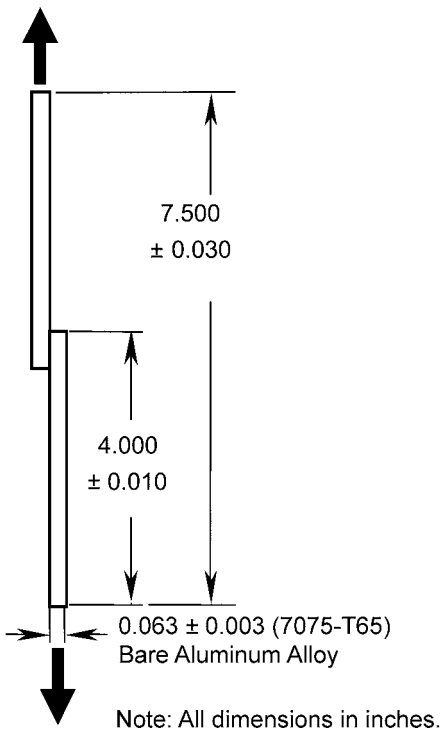
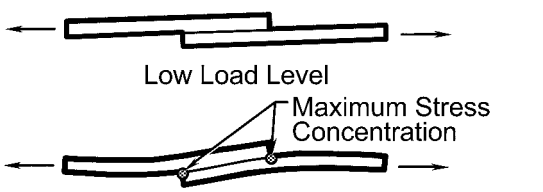


Fig. 13.18 Adhesive shear tests



Typical Single Lap Shear Specimen



Deformation of Adherends Under Moderate Load

Brittle Adherend



"Interlaminar" Failure of Filamentary
Composite Adherends

Yielding Adherend



High Load Level (Metal Adherends)



Permanently Deformed (Metal)
Adherends After Failure of Adhesive

Failure Modes

Fig. 13.19 Single lap shear test

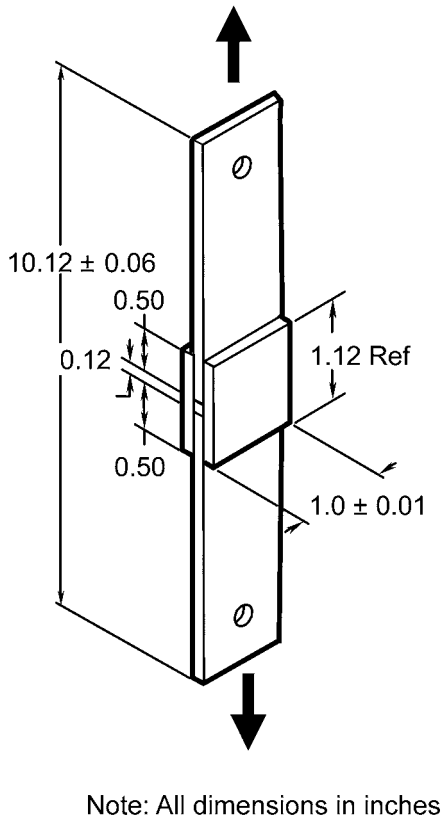


Fig. 13.20 Typical double lap shear test

used. The two most widely used peel tests are the roller bell peel test and the climbing drum peel test. Since both of these tests involve peeling an adherend off of another adherend or from the honeycomb core, a flexible adherend is required; therefore, aluminum is used rather than composite. The floating roller bell peel test (ASTM D 3167), shown in Fig. 13.23, is used for testing metal-to-metal adhesive bonds, while the climbing drum peel test (Fig. 13.24) tests the peel strength of the adhesive on the honeycomb core. The climbing drum peel test (ASTM D 1781) checks both the filleting and peel strength characteristics of a film adhesive. During testing, one of the aluminum adherends is progressively peeled off of the honeycomb core. Both strength and failure mode are important. In a proper failure mode, most of the adhesive will be present on the peeled adherend but there will still be a significant amount of adhesive adhering to the cells of the honeycomb core, indicating good filleting.

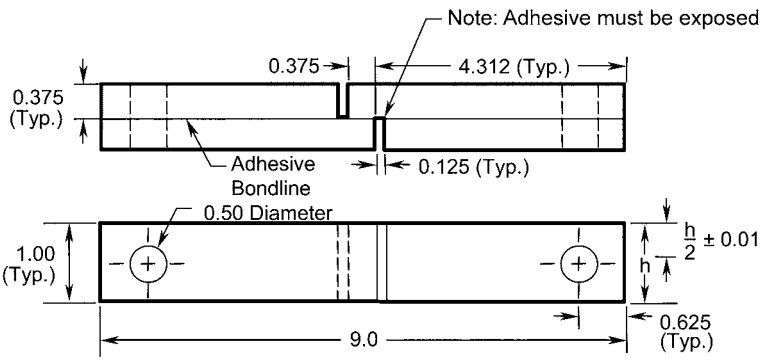
13.13 Honeycomb Flatwise Tension

Flatwise tension testing (Fig. 13.25), specified in ASTM C297, checks filleting and the flatwise tension strength of film adhesives. The specimen can be round or square, and both metal and composite facesheets can be used. A sandwich panel is fabricated and then tested in tension, pulling the adhesively bonded skins off of the core. Both strength and failure mode are important. Failure should occur either within the adhesive or within the core (core tearing). If failure occurs within the adhesive, there should be a significant amount of adhesive residue adhering to the honeycomb cell walls. The strength measured in this test is strongly dependent on the density of the honeycomb core. Higher values will be found for higher-density cores that have smaller cell sizes and thicker cell walls.

13.14 Environmental Conditioning

Since composite materials are sensitive to the ravages of the environment, it is common practice to environmentally condition specimens prior to testing. Tests on composites are usually conducted at the lowest usage temperature, for example, –67 °F (–53 °C), room temperature, and the highest usage temperature, for example, 250 °F (120 °C) for epoxies. In addition, matrix-dependent test specimens, such as compression, 90-degree tension, and shear specimens, are moisture conditioned prior to testing. Elevated temperatures combined with moisture result in the largest degradations. Typically, moisture conditioning is conducted using elevated temperatures in a humidity cabinet to drive the moisture into the laminate. The use of elevated temperatures is a valid approach provided that the mode of diffusion remains unchanged and no matrix damage is introduced. MIL-HDBK-17 recommends conditioning at a level of up to 170 °F (75 °C) for 350 °F (175 °C) curing composites and 150 °F (65 °C) for 250 °F (120 °C) curing composites. Although boiling water is sometimes used to accelerate moisture uptake, there is the danger that it will cause matrix cracking and the test results will then be suspect. However, water boil testing is often used as a screening test because it is fast and cheap.

A higher initial humidity level can be used to force moisture more rapidly into the sample



Note: All dimensions in inches. Material 7075-T651 Bare.

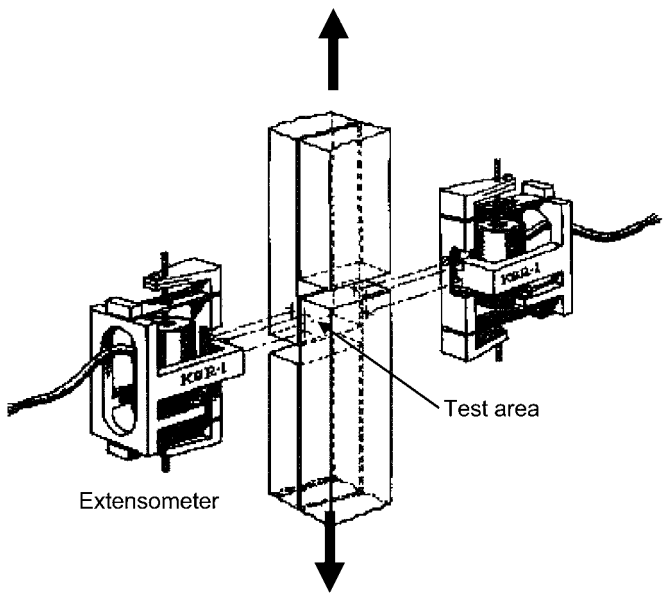


Fig. 13.21 Thick adherend test method. Source: Ref 4

center before equilibrium is achieved at the target humidity level. MIL-HDBK-17 states that this practice is acceptable provided that the humidity level does not exceed 95 percent relative humidity (RH). A typical procedure is shown in Fig. 13.26. Here an exposure of 160 °F (70 °C) and 95 percent RH was used to accelerate the initial moisture intake. The humidity was then reduced to 70 percent RH to obtain the desired moisture content within 90 days. Note that the specimen exposed to a constant 70 percent RH and 160 °F (70 °C) did not absorb the desired moisture content even after 180 days. Testing should be conducted immediately after humidity testing, and soaks at elevated temperature must be minimized to prevent the specimens from desorbing moisture.

Typically, most thermosets and semicrystalline thermoplastics are resistant to most common solvents and hydraulic fluids, but some amorphous thermoplastics are very sensitive to solvents, especially paint strippers that con-

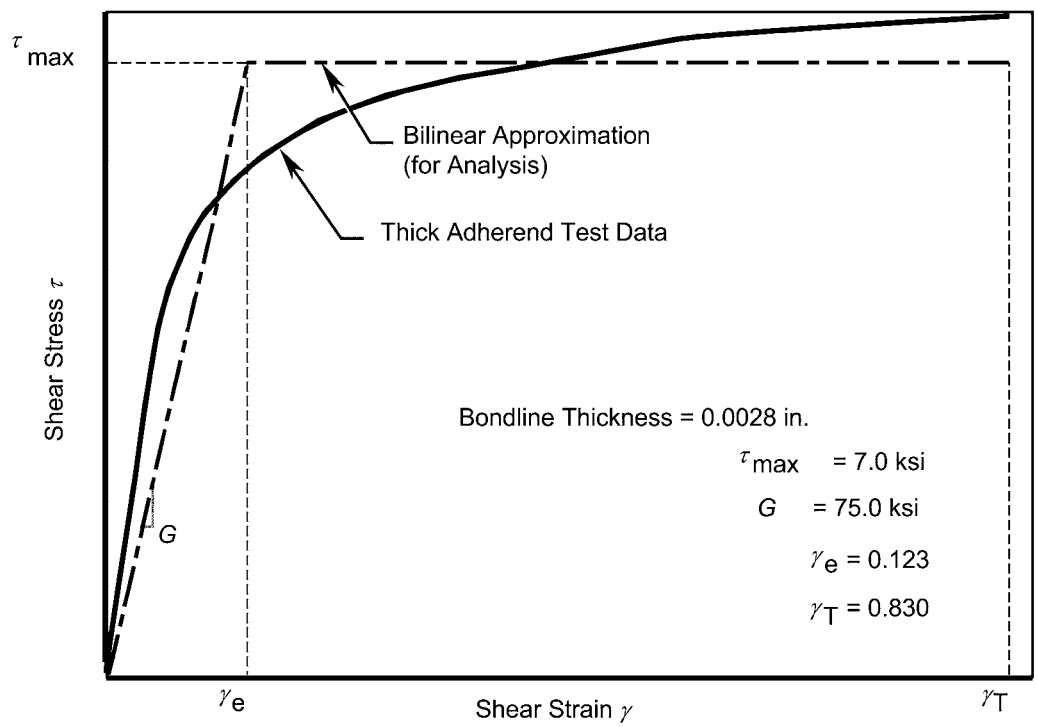


Fig. 13.22 Thick adherend adhesive shear stress-strain curve

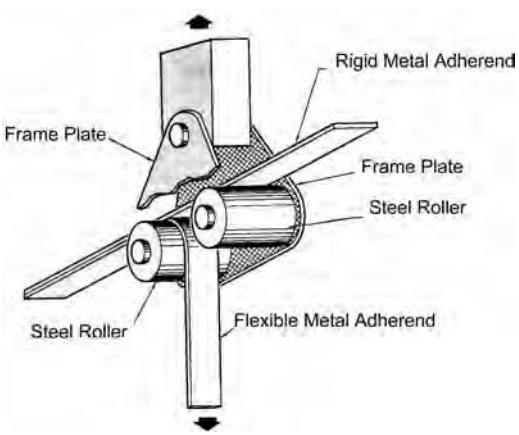


Fig. 13.23 Metal-to-metal floating roller bell peel test

tain methylene chloride. Testing should be conducted after exposure to the various fluids that the composite can be exposed to in service.

13.15 Data Analysis

Design allowables for composite materials usually assume a normal distribution, although other types of statistical distributions are available and are used. Three types of design allowables are considered: A-basis, B-basis, and S-basis. A-basis and B-basis allowables are calculated using the following formulas:

$$\sigma_A = \bar{\sigma} - K_A s \quad \text{(Eq 13.2)}$$

$$\sigma_B = \bar{\sigma} - K_B s \quad \text{(Eq 13.3)}$$

where:
σ_A = A-basis design allowable
σ_B = B-basis design allowable
σ = mean or average strength
s = standard deviation
K_A = one-sided tolerance factor corresponding to a proportion at least 0.99 of a normal distribution with a confidence coefficient of 0.95

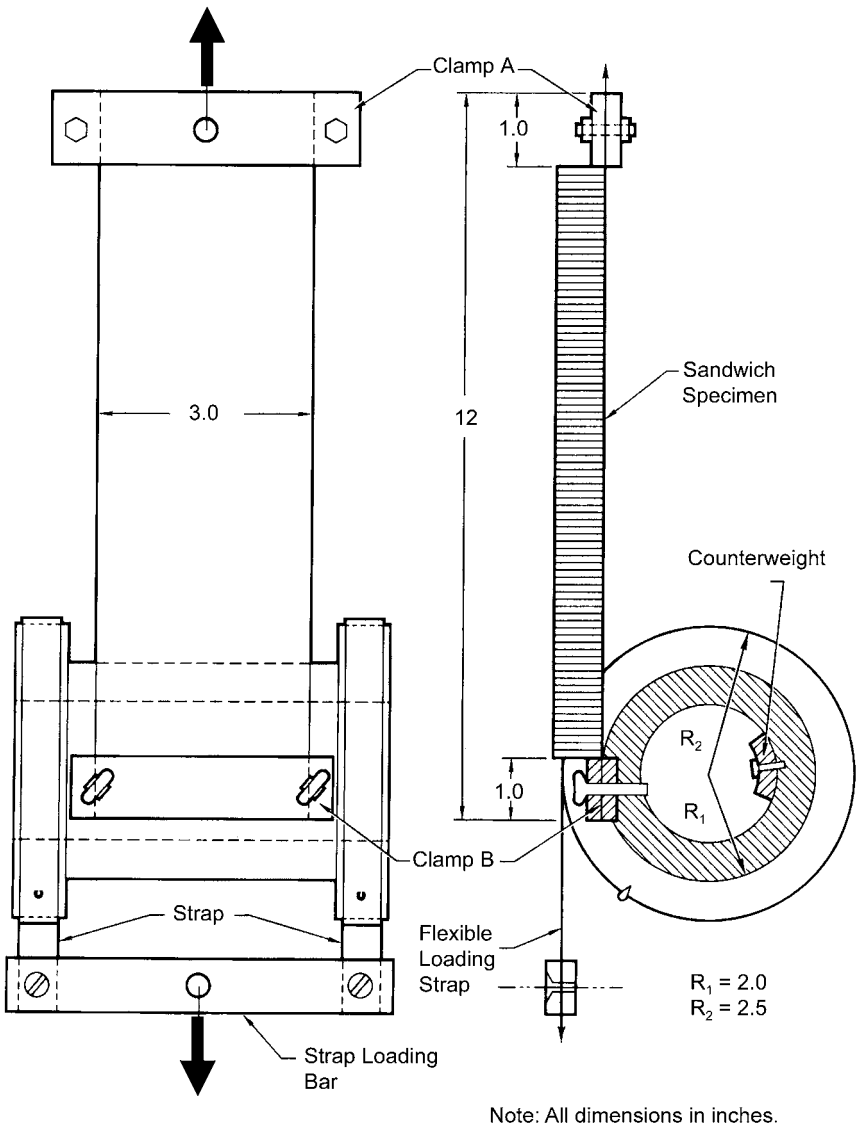


Fig. 13.24 Honeycomb sandwich climbing drum peel test

K_B = one-sided tolerance factor corresponding to a proportion at least 0.90 of a normal distribution with a confidence coefficient of 0.95

Therefore, if we test 100 specimens, 99 of them will have a value that is greater than the A-basis allowable. Likewise, if we test 100 specimens, 90 of them will be higher than the B-basis allowable. Our confidence level that this will happen is 95 percent. Therefore, A-basis allowables are more conservative than B-basis allowables. However, the more common practice in industry is to use B-basis allowables. A list of K_B factors is given in Table 13.1. Sometimes S-basis allowables are quoted; however, S-basis allowables are just swags and have absolutely no statistical basis.

A- and B-basis allowables are very dependent on the number of specimens tested. For example, if the sample size is 10 specimens with an average value of 125 ksi and a standard deviation of 15 ksi, the B-basis allowable will be 90 ksi. If the sample size is increased to 30 specimens and the

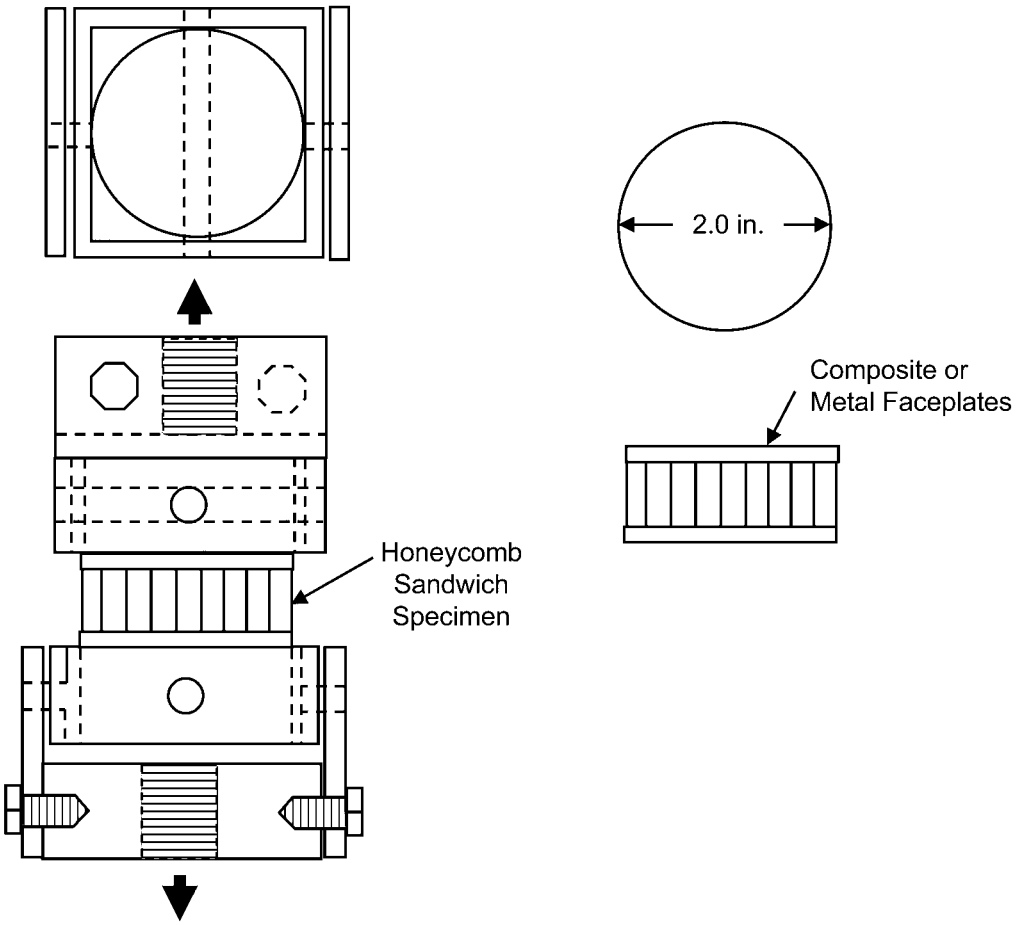


Fig. 13.25 Honeycomb sandwich flatwise tension test

Table 13.1 B-basis factors for normal distribution

n	K_B	*n*	K_B
1	…	21	1.905
2	20.581	22	1.886
3	6.155	23	1.869
4	4.162	24	1.853
5	3.407	25	1.838
6	3.006	26	1.824
7	2.755	27	1.811
8	2.582	28	1.799
9	2.454	29	1.788
10	2.355	30	1.777
11	2.275	35	1.732
12	2.210	40	1.697
13	2.155	45	1.669
14	2.109	50	1.646
15	2.068	55	1.626
16	2.033	60	1.690
17	2.002	70	1.581
18	1.974	80	1.559
19	1.949	90	1.542
20	1.926	100	1.527

same average and standard deviation are obtained, the B-basis allowable increases to 98 ksi. A standard procedure for design allowables generation is to require five separate batches of materials with six specimens tested from each batch to give a total sample size of 30.

Distributions other than a normal distribution are also used. One of the most popular alternative distributions is the two-parameter Weibull distribution.

REFERENCES

1. D.F. Adams, L.A. Carlsson, and R.B. Pipes. *Experimental Characterization of Advanced Composite Materials*, 3rd ed., CRC Press, 2003

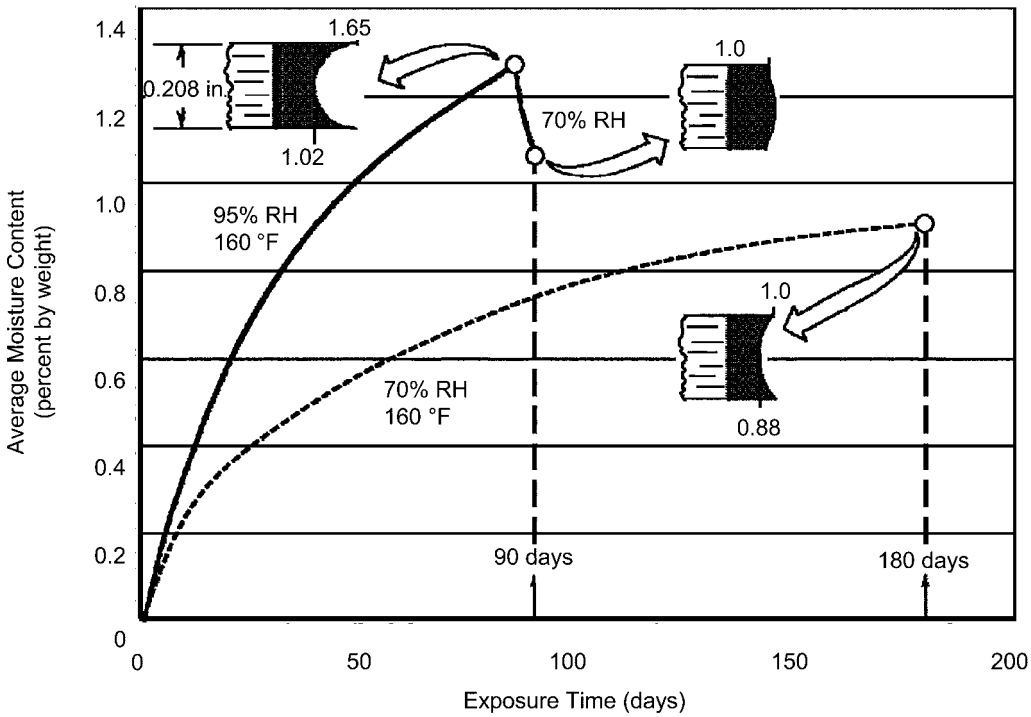


Fig. 13.26 Accelerated moisture absorption procedure

2. W.M. Scardino, Adhesive Specifications, *ASM Engineered Materials Handbook*, Vol 1, *Composites*, ASM International, 1987, p 689–701
3. MIL-HNBK-17-1F, *Polymer Matrix Composites*, Vol I, *Guidelines for Characterization of Structural Materials*, U.S. Department of Defense, 2001
4. R.B. Krieger, Analyzing Joint Stresses Using an Extensometer, *Adhes. Age*, Vol 28 (No. 11), Oct 1985, p 26–28

Copyright © 2010, ASM International®
All rights reserved.
www.asminternational.org

CHAPTER 14

Composite Mechanical Properties

THE MECHANICAL PROPERTIES of a composite material depend on many factors, including whether or not the fibers are continuous or discontinuous; the strength and stiffness of the fibers themselves; whether or not the fibers are in an orderly arrangement or are randomly oriented; the amount or volume percentage of the fiber reinforcement; the strength and stiffness of the matrix; whether the loading is static or fluctuating; and the specific operating temperature and environment.

Some comparative mechanical properties for unidirectional composites made from E-glass/epoxy, aramid/epoxy, high-strength carbon/epoxy, and intermediate modulus carbon/epoxy are summarized in Table 14.1. With regard to this table, there are two words of caution: (1) the properties shown are for unidirectional composites, which are useful for comparing material systems but not for determining overall structural performance since purely unidirectional composites are almost never used in real applications; they must be cross-plied to accept loads in several directions; and (2) mechanical properties are very dependent on the specific fiber and resin system and also on the fabrication method used. The reader is cautioned to view all composites data available from vendors and the literature with great skepticism. Design allowables should always be based on the actual material systems to be used, and all specimens should be fabricated using the same conditions that will be used for the actual parts. In addition, obtaining reliable test data from composite materials is generally trickier than for isotropic metals, and a lot of conflicting data are reported. Even in this chapter, the careful reader will note discrepancies in the results reported, a result of obtaining data from multiple sources. Test methods for determining the mechanical properties of composite materials are discussed in Chapter 13, "Mechanical Property Test Methods."

The largest publicly accessible database for composite materials is the MIL-HNBK-17 series (Ref 1 to 5). Volume 2 contains databases on polymer matrix systems, and Volumes 4 and 5 contain information on metal and ceramic matrix composites, respectively. However, even here the reader is cautioned. The data sets in these volumes, although rigorously controlled, are from many different sources fabricated under widely differing conditions. The bottom line is that there is no substitute for one's own fabrication and testing.

Table 14.1 Typical properties of unidirectional composite materials

Property	E glass/epoxy	Aramid/epoxy	High-strength carbon/epoxy	Intermediate-modulus carbon/epoxy
Specific gravity	2.1	1.38	1.58	1.64
0° tensile strength, ksi	170	190	290	348
0° tensile modulus, msi	7.60	12.0	18.9	24.7
90° tensile strength, ksi	5.08	5.08	11.6	11.6
90° tensile modulus, msi	1.16	1.16	1.31	1.31
0° compression strength, ksi	131	36.3	189	232
0° compression modulus, msi	6.09	10.9	16.7	21.8
In-plane shear strength, ksi	8.70	6.53	13.4	13.8
In-plane shear modulus, msi	0.580	0.304	0.638	0.638
Interlaminar shear strength, ksi	10.9	8.70	13.4	13.1
Poisson's ratio	0.28	0.34	0.25	0.27

In this chapter the static, fatigue, and damage tolerance properties of glass, aramid, and carbon fiber systems will be examined. In addition, the effects of some important types of defects will be discussed. The details of environmental degradation on properties are further discussed in Chapter 15, "Environmental Degradation."

14.1 Glass Fiber Composites

Due to their low material costs compared to aramid and carbon fibers, glass fiber composites are the most widely used composite material. They are available in the widest variety of product forms, ranging from short chopped fibers that are randomly oriented within the matrix to unidirectional continuous fiber composites. The biggest advantage of glass fiber composites, especially those with E-glass, is fairly good tensile strength at a low material cost. The biggest disadvantage of glass is its relatively low modulus compared with aramid and especially carbon. In addition, glass fiber composites have somewhat higher densities than aramid and carbon fiber composites. Another problem with glass fiber composites is that they are more sensitive to fatigue loading than aramid or carbon fiber composites.

One of the largest markets for glass-reinforced composites is injection molding. While both thermosets and thermoplastic materials can be injection molded, by far the greatest number are molded using thermoplastics. Since the fibers are short and randomly oriented, the amount of strength and stiffness improvement is only nominal, as shown for the properties of E-glass/nylon in Table 14.2. However, the improvement is substantial compared to the unreinforced polymer.

Longer glass fibers, usually 1 to 2 in. (2.5 to 5 cm), are used extensively in sheet molding compounds (SMCs), which are compression molded in matched metal dies into structural parts. Although the reinforcements can be either random or continuous, random reinforcements are more prevalent. Normally, polyester resins are used that contain fillers such as calcium carbonate. Some typical properties of several SMCs are shown in Table 14.3. The SMC-R material contains randomly oriented short glass fibers and has somewhat isotropic properties in the two planes of the molded sheet. The designations SMC-R25 and SMC-R50 indicate that the fibers are random and the glass contents are 25 and 50 percent, respectively. The SMC-C20/R-30 material contains 20 percent continuous fibers and 30 percent random fibers, giving a total glass content of 50 percent. Naturally, the strength is higher in the direction of the continuous fibers. The last material shown, XMC, contains continuous fibers in a ± 7.5-degree X-pattern with a high glass fiber content of 75 percent. The materials with random fibers, SMC-R, are the most widely used because they flow better in the mold and are thus capable of making more complex part shapes than the materials containing continuous glass fibers.

Reaction injection molding (RIM) is another process conducted in a matched die mold. Here, rapidly polymerizing polymers, frequently polyurethanes, are injected into a mold where cure times are less than one minute. Glass fibers can be added to these polymers for additional strength and stiffness, as shown in Table 14.4. When milled or chopped glass fibers are added to the

Table 14.2 Typical properties of injected molded E-glass/nylon

Property	Unreinforced	30% glass fibers
Specific gravity	1.14	1.39
Tensile strength, ksi	12.0	24.9
Tensile modulus, msi	0.42	1.31
Elongation, %	60	4
Flexural strength, ksi	17.3	36.0
Flexural modulus, msi	0.40	1.31
Notched izod impact, j/m	53	107
Heat deflection temperature, °F	194	486

Table 14.3 Typical sheet molding compound (SMC) properties

Material	Specific gravity	Glass, wt%	Tensile strength, ksi	Elongation, %	Flexural modulus, msi
SMC-R25	1.83	25	12.0	1.34	1.70
SMC-R50	1.87	50	23.8	1.73	2.30
SMC-C20/R30	1.81	50	…	…	…
Longitudinal	…	…	41.9	1.73	3.73
Transverse	…	…	12.2	1.58	0.86
XMC-3 ± 7.5°X-pattern	1.97	75	…	…	…
Longitudinal	…	…	81.4	1.66	4.95
Transverse	…	…	10.1	1.54	0.99

Source: Ref 6

process, it is referred to as *reinforced reaction injection molding* (RRIM). In milled glass fiber, with lengths of $^1/_{32}$ to $^1/_8$ in. (0.8 to 3.2 mm), reinforced parts tend to develop directional properties due to the fiber orientation that occurs during the injection process; chopped glass fibers can be added to the formulation to reduce the directionality. The properties of RRIM parts tend to be somewhat lower than those produced with compression-molded SMCs. Strength and stiffness more comparable to those of SMC parts can be produced by placing preforms containing continuous glass fibers in the mold before injection. The material is then referred to as *structural reaction injection molding* (SRIM).

Manual wet lay-up and spray-up of glass fiber composites are used to make low- to medium-volume applications. The mechanical properties of a number of these types of materials impregnated with polyester resin are shown in Table 14.5. Spray-up, in which chopped glass fibers are mixed with resin and then sprayed onto the mold, produces more or less randomly oriented fibers 1 to 2 in. (2.5 to 5 cm) long. Since the fiber content is only moderate (30 to 35 percent), the properties are normally fairly low. Chopped strand mat (CSM) is also a randomly oriented product form in which glass fibers are either chopped and sprayed to produce a mat or are swirled into a mat product. Depending on the fiber content, the properties are again only low to moderate. Higher strength and stiffness can be obtained by combining CSM with continuous fiber woven roving, as shown in Table 14.6. In this table, CSM properties are compared with those of roving woven combi, which is a combination of CSM and woven cloth; a biaxial 0°/90° woven cloth; and a unidirectional woven cloth that has a high percentage of reinforcement in the zero-degree direction. Both the strength and stiffness are improved as the amount of continuous reinforcement is increased.

Higher-strength glass fiber parts are also fabricated by processes such as filament winding and pultrusion. The properties of filament-wound and pultruded parts are compared in Table 14.7. In filament winding, rovings of continuous glass fibers are impregnated with a liquid resin, wound around a mandrel, and then cured; in pultrusion, the reinforcement is impregnated with a resin,

Table 14.4 Typical reinforced reaction injection molding (RRIM) properties

Material	Specific gravity	Glass, wt%	Tensile strength, ksi	Elongation, %	Flexural modulus, msi
RRIM-milled glass/polyurethane	1.08	15	…	…	…
longitudinal	…	…	2.80	110	0.078
transverse	…	…	2.80	140	0.048
RRIM-chopped glass/polyurethane	1.15	20	…	…	…
longitudinal	…	…	3.50	25	0.194
transverse	…	…	3.65	35	0.180
RRIM-chopped glass/polyurea	1.18	20	…	…	…
longitudinal	…	…	4.83	31	0.244
transverse	…	…	4.43	31	0.250
SRIM glass/polyurethane	1.5	37	24.9	4.2	1.80

Source: Ref 6

Table 14.5 Typical properties of glass chopped strand mat (CSM) composites

Property	Spray roving	Chopped strand mat	Chopped strand mat	Chopped strand mat	Chopped strand mat/ woven roving
Glass content, wt%	30–35	25–30	30–35	35–40	45–50
Glass content, vol%	16–20	14–16	16–20	20–24	28–32
Density, g/cm^3	1.45	1.40	1.45	1.50	1.68
Tensile strength, ksi	10	10	13	16	26
Tensile elongation, %	1.0	1.8	1.8	1.8	2.0
Tensile modulus, msi	1.0	0.9	1.1	1.3	1.8
Flexural strength, ksi	20	20	22.5	25	35
Flexural modulus, msi	0.9	0.8	0.95	1.2	1.5
Compressive strength, ksi	16	14.5	17.4	20	22
Compressive modulus, msi	1.1	0.95	1.2	1.4	1.8

Source: Ref 7

normally a polyester, and then pulled through a die, where it is simultaneously formed into a shape and cured. Although most of the reinforcement is normally aligned axially along the length of the part, glass mat and woven cloth can be incorporated to improve the off-axis properties.

Glass fibers are also available as both unidirectional and fabric prepreg that can be vacuum bag or autoclave molded. Again, E-glass, being fairly low in cost, is the most prevalent product form. For demanding aerospace applications, the higher-cost S-2 glass can be used. As shown in Table 14.8, S-2 glass provides both higher strengths and stiffnesses, but at a higher cost.

In addition to having a lower modulus and thus less stiffness than carbon fiber composites, glass fiber composites have fatigue properties that are not as good as those of carbon or aramid fiber composites (Fig.14.1). In general, stiffer fibers such as carbon, and to some extent aramid, strain the matrix less during fatigue cycling and are thus more fatigue resistant. In addition, glass fiber composites are subject to static fatigue or stress rupture. Static fatigue is the time-dependent fracture of a material under a constant load, as opposed to the cyclic load employed in a conventional fatigue test. This phenomenon is illustrated in Fig. 14.2. When glass fiber–reinforced composites are exposed to moist or other aggressive environments, they are also prone to degradation caused by weakening of the fiber-to-matrix interfacial bond. This generally occurs by chemical attack at the fiber surface. The degree of weakening depends on the matrix, the fiber coating, and the type of fiber. Weakening of the interface will result in significant loss in matrix-dominated mechanical properties such as transverse tension, shear, and compression strength. Thus, environmental degradation is a significant concern for structural applications in which the ability to carry high loads is required and particularly in applications under long-sustained loading.

Table 14.6 Typical properties of glass chopped strand mat (CSM)/woven composites

Property	Chopped strand mat	Woven roving combi	Biaxial 0/90	Biaxial unidirectional
Fiber content, wt%	35	50	58	60
Fiber content, vol%	20	32	41	42
Density, g/cm^3	1.50	1.60	1.70	1.75
Tensile strength, ksi	18.1	29.7	50.7	87.0
Tensile elongation, %	1.9	1.9	2.5	2.4
Tensile modulus, msi	1.1	2.3	2.9	4.1
Compressive strength, ksi	21.7	36.2	40.6	78.3
Compressive modulus, msi	1.1	2.4	3.0	4.2

Source: Ref 7

14.2 Aramid Fiber Composites

Aramid composites, introduced in the 1970s, originally had tensile properties somewhat similar to those of the carbon fiber composites produced at that time. However, the properties of carbon fibers have improved dramatically over the past 35 years to the point where aramid is not as competitive with carbon as it once was. Aramid fiber composites offer good tensile properties at a lower density than glass fiber composites but at a higher cost. However, their compressive properties are extremely poor, which limits them to tension-dominated designs. The unidirectional composites shown in Fig. 14.3 exhibit the poor compressive strength of aramid composites. In addition, due to the relatively poor fiber-to-matrix bond strength, the matrix-dominated properties, such as in-plane and interlaminar shear and trans-

Table 14.7 Typical properties of filament-wound and pultruded glass fiber composites

		Property			
Processing method	Material	Tensile strength, ksi	Tensile modulus, msi	Flexural strength, ksi	Compression strength, ksi
Filament winding	30–80 wt% glass roving-epoxy resin, variable angle	40–80	3.0–6.0	40–80	45–70
Pultrusion rod and bar	60–80 wt% glass roving only	60–100	4.5–6.0	50–80	40–60
Pultrusion profile	40–55 wt% glass roving/ continuous strand mat	12–30	1.0–2.5	15–35	15–30
Pultrusion profile	50–65 wt% glass roving/ continuous strand mat/ fabric	30–45	3.9–4.5	20–50	14–55

Source: Ref 8

Table 14.8 Unidirectional E- and S-glass/epoxy properties

Property	E-glass/epoxy	S-glass/epoxy
Density, lb/in.^{3}	0.072	0.072
0° tensile strength, ksi	170	235
0° tensile modulus, msi	7.60	8.60
90° tensile strength, ksi	5.80	5.80
90° tensile modulus, msi	1.74	2.32
0° compression strength, ksi	90	100
In-plane shear strength, ksi	10.1	11.6
In-plane shear modulus, msi	0.798	1.10
Interlaminar shear strength, ksi	10.2	11.6
Poisson's ratio	0.28	0.28

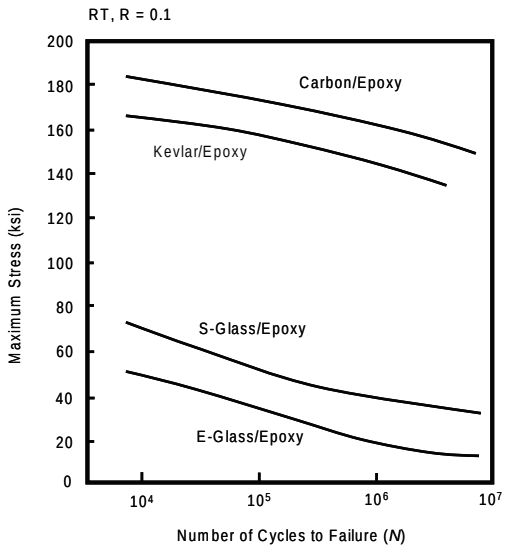


Fig. 14.1 Fatigue behavior of unidirectional composites

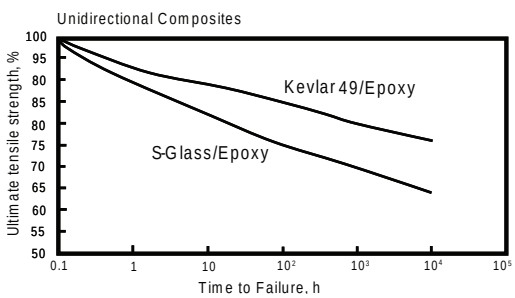


Fig. 14.2 Stress rupture properties of Kevlar 49 and S-glass epoxies. Source: Ref 9

verse tension, are somewhat lower than those of glass and carbon fiber composites. Even if a surface treatment is used to increase the fiber-to-matrix bond strength, the fibers themselves will then tend to fail through defibrillation, and no increase in properties is observed.

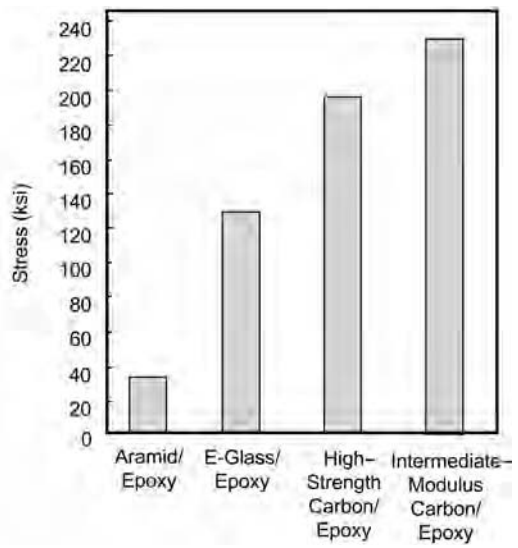


Fig. 14.3 Relative compression strengths of unidirectional composites

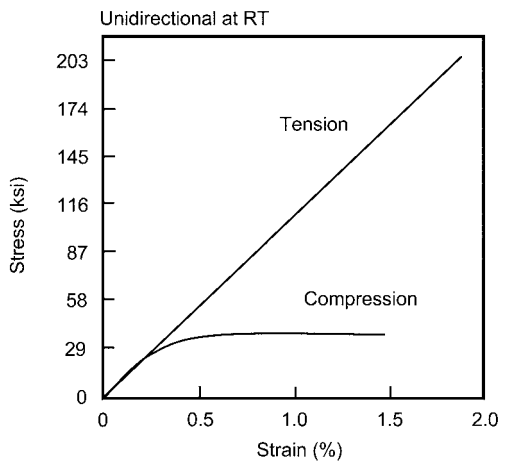


Fig. 14.4 Typical tension and compression behavior of aramid composite. Source: Ref 9

Although unidirectional aramid composites respond elastically when loaded in tension, they exhibit nonlinear ductile behavior under compression. At a compression strain of only 0.3 to 0.5 percent, a yield is observed (Fig. 14.4). This corresponds to the formation of structural defects known as *kink bands*, which are related to compressive buckling of the aramid fiber molecules. As a result of this compression behavior, the use of aramid composites in applications that are subject to high-strain compressive or flexural loads is limited. However, the compressive

buckling characteristics have led to the development of crashworthy structures that rely on the fail-safe behavior of aramid composites under sustained high compressive loads.

Although not as good as carbon fiber composites (Fig. 14.1), aramid composites perform very well in fatigue. For aramids, tension-tension fatigue generally is not of significant concern in applications where an adequate static safety factor has been used. Aramid composites have been found to be superior to glass fiber composites in both tensile-tensile and flexural fatigue loading. For the same number of cycles to failure, Kevlar 49/epoxy composites can operate at a significantly larger percentage of their static strength than glass fiber composites.

Fiber-dominated laminates of aramid composites exhibit very little creep. In general, creep strain increases with increasing temperature, increasing stress, and decreasing fiber modulus. However, under long-term loading, aramid composites, like glass fiber composites, are subject to stress rupture, that is, failure of the fiber under sustained loading with little or no accompanying creep. The stress rupture performance of Kevlar 49 compared to that of S-glass is shown in Fig. 14.2. Although aramids perform better than glass fiber composites, the phenomenon of stress rupture must be considered in any design where long-term loading is anticipated.

Aramid fibers are noted for their toughness and damage tolerance. The same microstructural characteristics that lead to the weakness of aramid fibers in buckling also make them very tough. During failure, the widespread bending, buckling, and other internal damage to the fibers absorb a great deal of energy. The fibrillar structure and compressive behavior of aramid fibers contribute to composites that are less notch sensitive and that fail in a ductile, nonbrittle, or noncatastrophic manner, as opposed to carbon fiber composites. In addition, the strength of aramid fibers is not very strain rate sensitive; an increase in strain rate of more than four orders of magnitude decreases the tensile strength by only about 15 percent. The good energy-absorbing properties of aramid fibers make them useful for ballistics, tires, ropes, cables, asbestos replacement, and protective apparel.

Because aramid yarns and rovings are relatively flexible and nonbrittle, they can be processed in most conventional textile operations, such as twisting, weaving, knitting, carding, and felting. Yarns and rovings are used in filament-winding, prepreg tape, and pultrusion processes. Applications include missile cases, pressure vessels, sporting goods, cables, and tension members. Although continuous-filament forms dominate composite applications, discontinuous- or short-fiber forms are also used, because the inherent toughness and fibrillar nature of aramid allow the creation of fiber forms not readily available with other fibers.

As a result of their high tensile strengths and superior damage tolerance, aramid composites are often used for lightweight pressure vessels, usually fabricated by filament winding. A comparison of Kevlar 49/epoxy and S-glass/epoxy pressure vessels is presented in Table 14.9. The density is lower and the strength and modulus of the Kevlar pressure vessel are higher than those of the S-glass vessel. In pressure vessels, the relative performance is often measured by the parameter PV/W, that is, the burst pressure P times the volume V divided by the vessel weight W. The PV/W index is higher for the Kevlar vessel. In addition, the fatigue performance is superior for the Kevlar vessel, an important parameter if the vessel will be subjected to multiple pressurization/depressurization cycles.

Being an organic fiber, aramid absorbs moisture. Aramid composites exhibit a linear decrease in both tensile strength and modulus when tested at elevated temperatures in air. The effects of temperature and moisture on a Kevlar 49/epoxy woven cloth are shown in Fig. 14.5. Aramid fiber has an equilibrium moisture content that is determined by the relative humidity (RH). At 60 percent RH, the equilibrium moisture of Kevlar 49 fiber is about four percent. The gain of moisture is completely reversible and, once removed, produces no permanent property changes. At cryogenic temperatures, the modulus increases slightly and the strength is not degraded.

Ultraviolet radiation also can degrade bare aramid fibers. However, in composite form, they are protected by the matrix, which is normally painted before being placed in service. In aramid

Table 14.9 Mechanical properties of filament-wound Kevlar 49/epoxy

Property	Kevlar 49/epoxy	S-glass/epoxy
Density, lb/in^{-3}	0.044	0.069
Fiber volume, %	65	65
Tensile strength, ksi	223	197
Tensile modulus, msi	13.2	8.8
PV/W, 10^6	4.1	3.0
Relative fatigue performance at 90% of ultimate strength	10	1

Source: Ref 9

composite laminates, in-service strength loss has not been observed. Because aramid is an organic fiber that is susceptible to oxidation, aramid composites are generally not used for long times at temperatures above 300 °F (150 °C). In the transverse direction, aramid fibers are like most other materials in that they expand with increasing temperature. However, in the longitudinal direction, the fibers contract somewhat as temperature increases. The negative thermal expansion coefficient of aramid fibers can be used to advantage in designing composites with a tailored or zero thermal expansion coefficient.

The poor off-axis and compressive properties of aramid fibers must be considered in any design. However, because of their high strength in axial tension and their toughness, aramid fiber composites are often used in applications such as pressure vessels, where the loading is almost totally in longitudinal tension. Although composites with carbon fibers have now supplanted aramid composites as having the highest specific strengths, aramids still offer combinations of properties not available with any other fiber. For example, aramids offer high specific strength, toughness, and creep resistance combined with moderate cost. However, the applications of aramid composites continue to be limited by their poor compressive and off-axis properties and, in some applications, by their tendency to absorb water. Nonetheless, aramids will continue to be a fiber of choice when outstanding impact resistance is critical.

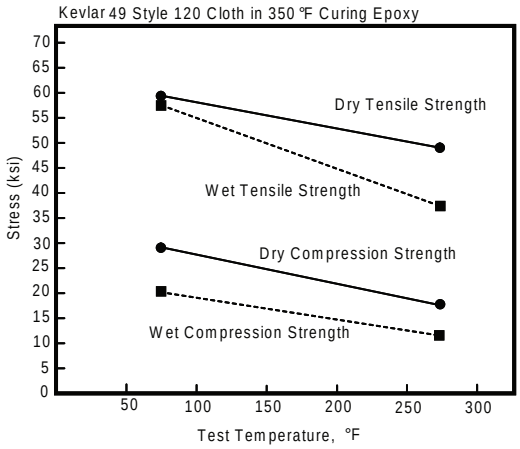


Fig. 14.5 Effect of temperature and moisture on Kevlar/epoxy strength

14.3 Carbon Fiber Composites

The mechanical properties of a typical second-generation toughened epoxy (Cycom 977-3) with an intermediate modulus carbon fiber (IM-7) are summarized in Table 14.10. This material system cures at 350 °F (175 °C) and has an acceptable usage up to 300 °F (150 °C), although it is often restricted in usage to 250 °F (120 °C). It is generally accepted that the critical environmental conditions for carbon fiber composites are cold-dry tension and hot-wet compression. The cold-dry condition normally produces less of a problem than the hot-wet condition. Note that the cold-dry condition of –75 °F (–60 °C) produces only a moderate reduction in 0° tensile strength, while the 0° wet compression strength progressively decreases with increasing temperatures up to 300 °F (150 °C) (Fig. 14.6). Part of this

Table 14.10 Properties of intermediate modulus carbon/toughened epoxy

			220 °F		250 °F		270 °F		300 °F	
Property	**–75 °F**	**RT**	**-Dry**	**-Wet**	**Dry**	**Wet**	**Dry**	**Wet**	**Dry**	**Wet**
0° tensile strength, ksi	353	364	…	…	…	…	…	…	…	…
0° tensile modulus, msi	22.9	23.5	…	…	…	…	…	…	…	…
90° tensile strength, ksi	…	9.3	…	…	…	…	…	…	…	…
90° tensile modulus, msi	…	1.21	…	…	…	…	…	…	…	…
0° compression strength, ksi	…	244	…	221(a)		195(a)	…	180(a)		160(a)
0° compression modulus, msi	…	22.3	21.4	21.2(a)	20.4	21.2(a)	20.2	22.6(a)	21.5	21.7(a)
0° flexural strength, ksi	…	256	246	173(a)	221	162(a)	218	140(a)	206	125(a)
0° flexural modulus, msi	…	21.7	22.4	20.1(a)	20.8	21.2(a)	21.0	19.6(a)	21.0	18.9(a)
90° flexural strength, ksi	…	19.0	…	…	…	…	…	…	…	…
90° flexural modulus, msi	…	1.19	…	…	…	…	…	…	…	…
In-plane shear modulus, msi	…	0.72	…	0.61(c)	…	0.58(c)	…	0.50(c)	…	0.34(c)
Interlaminar shear strength, ksi	…	18.5	13.6	12.9(a)	13.3	11.4(a)	12.4	10.1(a)	11.4	9.0(a)
Open-hole comp. strength, ksi	…	46.7	…	37.0(b)	…	35.0(b)	…	…	…	…
Compression after impact, ksi	…	28.0	…	…	…	…	…	…	…	…

Fiber dominated properties normalized to 0.60 fiber volume. (a) Wet = 1 week immersion in 160 °F water. (b) Wet = 2 week immersion in 160 °F water. (c) Wet = 150 °F/85% RH to equilibrium, approximately 1.1% weight gain. Source: Ref 10

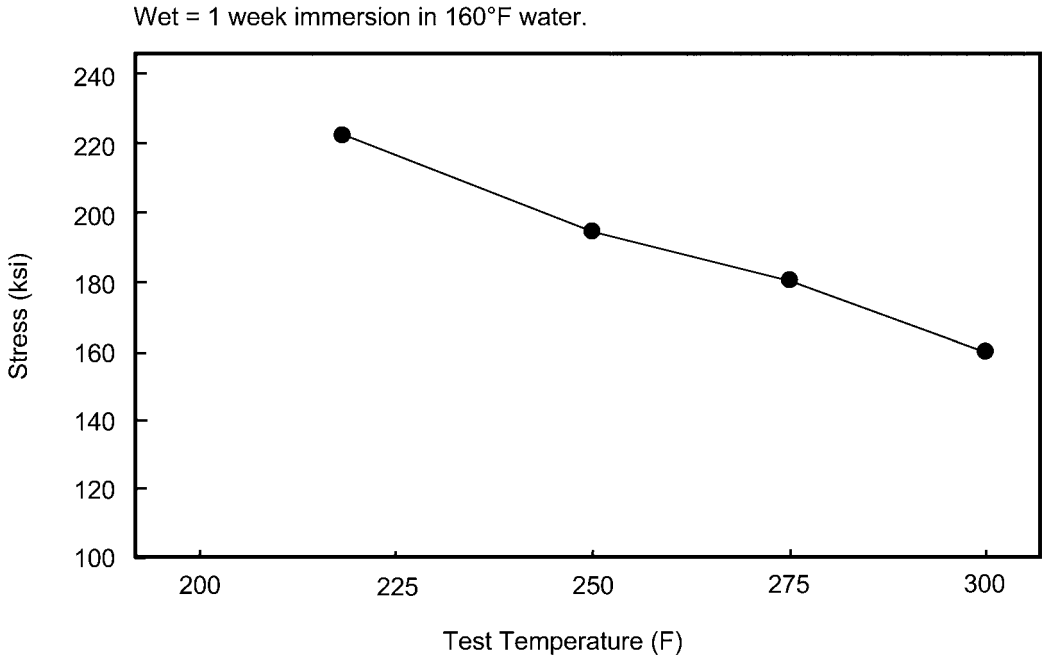


Fig. 14.6 Hot-wet compression strength of an intermediate-modulus carbon-toughened epoxy

reduction in compression strength is due to a simple temperature increase and part is due to the absorbed moisture. The plot of interlaminar shear strength versus temperature for both dry and wet specimens in Fig. 14.7 illustrates the reduction due to both temperature and moisture. Other matrix-dependent properties affected by temperature and humidity include 90-degree tension and compression, the shear properties (in-plane and interlaminar), the flexural properties, and open-hole compression strength. While one might logically think that zero-degree compression and zero-degree flexural properties are fiber-dependent properties, the compression strength depends on the matrix to stabilize the fiber against microbuckling.

For a longitudinal (zero-degree) specimen loaded in axial compression, microbuckling of the fibers can occur either by what is known as the *extensional mode* or by the shear mode, as illustrated in Fig. 14.8. In the extensional mode, adjacent fibers buckle in opposite directions. This mode derives its name from the fact that the major deformation of the matrix is an extension of the matrix material in a direction perpendicular to the fibers. In the shear mode, the fibers buckle in the same wavelength and in phase with one another so that the matrix material between the adjacent fibers deforms primarily by a shear. The shear mode occurs in composites with a higher volume fraction of fibers and is therefore the predominant failure mode in high-strength carbon fiber composites. The main reason aramid fiber composites have such low compression strengths is that the fibers themselves form kink bands (see Fig. 2.9) at rather low stresses. Tests have shown that the modulus of elasticity of the matrix is also important, with stiffer matrices providing better support to the fibers and thus higher compression strengths.

To date, most high-performance carbon/epoxy structures have been fabricated using prepreg that is autoclave cured at either 250° or 350 °F (120° or 175 °C). In the early 1990s, work began on the development of lower-temperature curing prepregs at less than 200 °F (95 °C) that could be cured under only vacuum bag pressure. The driver for this development was the need to be able to produce small numbers of parts without large expenditures for expensive autoclave-hardened tooling. Initially, the same prepregs that were being used to produce carbon/epoxy tools were used, but later developments resulted in nonautoclave low-temperature/vacuum bag (LTVB) materials that have the same properties as autoclave-cured prepregs, at least for reason-

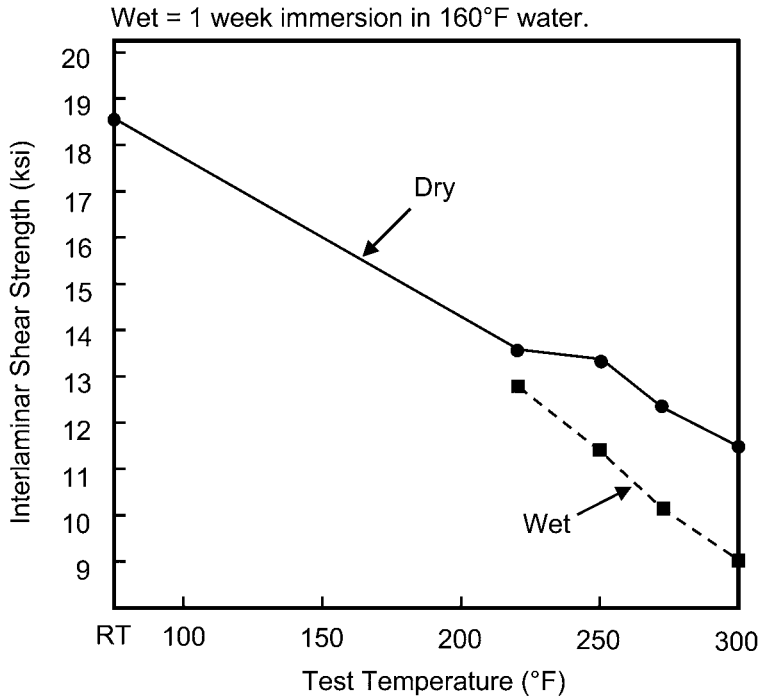


Fig. 14.7 Effect of temperature and moisture on interlaminar shear strength

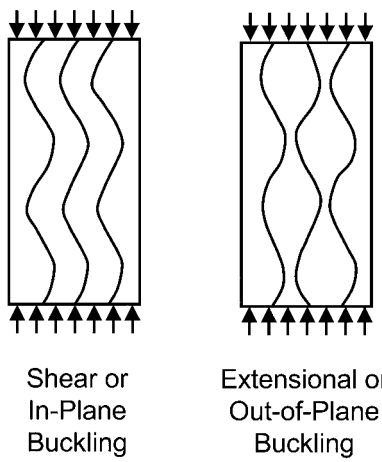


Fig. 14.8 Compression buckling modes for unidirectional composites

ably sized parts. The properties of one of these materials, Cycom 5215, are compared with those of a standard autoclave-cured carbon/epoxy in Table 14.11. The standard carbon/epoxy material was cured at 350 °F (175 °C) for two hours under 85 psi (586 kPa) autoclave pressure. The low-temperature/vacuum bag 5215 material was initially cured for 14 hours at 150 °F (65 °C) under vacuum bag pressure and then removed from the tool and given a freestanding postcure at 350 °F (175 °C) for two hours. The properties of both materials in unidirectional and woven cloth form are essentially equivalent. However, two points need to be made concerning these materials. First, since there is no autoclave pressure to suppress void formation and since the removal of entrapped air is critical, it may be more difficult to produce consistent void-free parts, especially for larger and thicker parts where the air evacuation paths are longer. The second point is that currently these materials have compression strengths after impact (CAI) somewhat equivalent to those of the first-generation brittle epoxies. However, this toughness limitation is only temporary; a toughened version of this material (Cycom 5320) has recently been introduced.

High-modulus pitch-based carbon/epoxy is used in spacecraft applications where extremely lightweight, stiff, and dimensionally stable structures are required. However, as shown in Table 14.12, all of the properties except the longitudinal modulus are lower for high-modulus material compared to the standard high-strength material. High-modulus materials are also considerably

Table 14.11 Comparative properties of Cycom 5215 carbon/epoxy

Property	Unidirectional tape		6k 5 harness satin woven cloth	
	G30-500 carbon/ 1st generation epoxy	G30-500 carbon/ 5215 epoxy	G30-500 carbon/ 1st generation epoxy	G30-500 carbon/ 5215 epoxy
RT dry 0° tensile strength, ksi	200	297	75.0	95.0
RT dry 0° compression strength, ksi	205	210	67.5	105
250 °F dry 0° compression strength, ksi	145	175	45.0	76.9
RT dry interlaminar shear strength, ksi	15.0	15.5	8.5	8.0
250 °F dry interlaminar shear strength, ksi	9.0	10.0	6.5	7.1
250 °F wet(a) interlaminar shear strength, ksi	7.5	8.7	2.5	4.4
Compression after impact, ksi	17.5	16.0	25.0	23.7
Dry glass transition temperature T_g, °F	350	378	350	366
Wet(b) glass transition temperature T_g, °F	250	331	250	328

(a) Wet = 24 h water boil. (b) Wet = 48 h water boil. Source: Ref 10

Table 14.12 Comparative properties of high-strength and high-modulus composites

Property	AS-4/3501-6 carbon/epoxy	GY-70/934 carbon/epoxy
Specific gravity	1.58	1.59
Fiber volume, %	63	57
0° tensile strength, ksi	331	85.3
0° tensile modulus, msi	20.6	42.6
0° tension strain, %	0.015	0.002
90° tensile strength, ksi	8.27	4.26
90° tensile modulus, msi	1.48	0.93
90° tensile strain, %	0.006	0.005
0° compression strength, ksi	209	71.2
In-plane shear strength, ksi	10.3	8.58
In-plane shear modulus, msi	1.04	0.71
Poisson's ratio μ_{12}	0.27	0.23

Table 14.13 Comparative properties of unidirectional carbon/PEEK and carbon/PEKK

Property	AS-4/ PEEK	AS-4/ PEKK	IM-7/ PEEK	IM-7/ PEKK
0° tensile strength, ksi	341	340	421	400
0° tensile modulus, msi	20.0	19.7	24.9	24.4
0° compression strength, ksi	197	234	190	177
0° compression modulus, msi	18.0	17.8	22.0	21.8
In-plane shear strength, ksi	27.0	21.2	26.0	18.9
In-plane shear modulus, msi	0.826	0.812	0.797	0.711
Interlaminar shear strength, ksi	15.2	14.2	…	…
Open-hole tens. strength, ksi	61.8	56.4	69.0	74.6
Open-hole comp. strength, ksi	47.0	48.6	47.0	45.7
Compression after impact, ksi	51.1	36.4	53.1	44.5

Fiber dominated properties normalized to 0.60 fiber volume. Source: Ref 11

more expensive than the standard modulus materials. In addition, more expensive cynate ester resins are often specified because they absorb less moisture and are thus more dimensionally stable and less prone to outgassing in the near-vacuum atmosphere of space. Therefore, high-modulus carbon and graphite fiber composites are somewhat restricted for usage in specialized applications.

Although much work has been done on thermoplastic composites, very few applications have resulted for the reasons discussed in Chapter 6, "Thermoplastic Composite Fabrication Processes." One of the main attractions of thermoplastics is their improved damage tolerance compared to brittle epoxies. The majority of the development work has been conducted using polyetheretherketone (PEEK). More recently, the emphasis has shifted to polyetherketoneketone (PEKK) for two reasons: (1) the basic PEKK polymer is inherently less expensive to produce than the PEEK polymer, and (2) PEKK composites can be processed at lower temperatures at 645 °F (340 °C) than PEEK composites at 735 °F (390 °C). The properties of the two materials are compared in Table 14.13 and appear to be fairly equivalent when both high-strength and intermediate-modulus carbon fibers are used, although the CAI strength of the PEKK composites, at least for this data set, appears to be a little lower than that of the PEEK composites. The tensile and flexural properties for several other thermoplastic composites are shown in Table 14.14. Polyetherimide is an amorphous thermoplastic with good high-temperature resistance up to 250 °F (120 °C). Polyphenylene sulfide is a semicrystalline thermoplastic with a lower usage temperature at less than 200 °F (95 °C) than PEEK and PEKK at 250 °F (120 °C). Finally, polypropylene is a semicrystalline thermoplastic that is limited to low usage temperatures at less than 150 °F (65 °C).

Epoxy matrix composites are generally limited to service temperatures of around 250 °F (120 °C). For higher usage temperatures, bismaleimides, cyanate esters, and polyimides are

Table 14.14 Comparative properties of unidirectional thermoplastic composites

Property	AS-4/PEI	AS-4/PPS	E-Glass/PP
Fiber volume fraction, %	59	59	60
0° tensile strength, ksi	278	297	108
0° tensile modulus, msi	18.8	18.5	4.1
90° tensile strength, ksi	11.0	7.2	…
90° tensile modulus, msi	1.3	1.3	…
0° flexural strength, ksi	269	243	85
0° flexural modulus, msi	17.8	16.3	3.8

PEI, polyetherimide; PP, polypropylene; PPS, polyphenylene sulfide. Source: Ref 12

available. Bismaleimide and cyanate ester composites are useful at temperatures up to around 350 to 400 °F (175 to 205 °C) For higher temperatures, up to 500 to 600 °F (260 to 315 °C), polyimides must be used. While cyanate esters and bismaleimides process in a similar manner to epoxies, polyimides are generally condensation curing systems that require high processing temperatures and pressures. Since the condensation reaction gives off either water or alcohols, polyimides are very prone to developing voids and porosity. In addition, they are brittle systems that are subject to microcracking. The relative temperature performance of a number of these material systems is shown in the plot of interlaminar shear strength versus temperature in Fig. 14.9.

14.4 Fatigue

Fatigue failures occur due to the application of fluctuating stresses that are much lower than the stress required to cause failure during a single application of stress. Three basic factors are necessary to cause fatigue: (1) a maximum stress of sufficiently high value, usually a tensile stress, (2) a large enough variation or fluctuation in the applied stress, and (3) a sufficiently large number of cycles of the applied stress. There are many types of fluctuating stresses. Several of the more common types encountered are shown in Fig. 14.10. A completely reversed stress cycle is commonly used in testing where the maximum and minimum stresses are equal. Another common stress cycle is the repeated stress cycle, in which a mean stress (σ_m) is applied on top of the maximum and minimum stresses. Figure 14.10 shows the condition in which both stresses are tensile in nature, but one could also test with both stresses in compression. In addition, the maximum and minimum stresses do not necessarily have to be equal. The last type shown is the random or spectrum (irregular) stress cycle, in which the part is subjected to random loads during service, often referred to as *spectrum loading*.

A fluctuating stress is made up of two components, a mean or steady stress σ_m and an alternating or variable stress σ_a. The stress range σ_r is the difference between the maximum and minimum stress in a cycle:

$$\sigma_r = \sigma_{max} - \sigma_{min} \quad \text{(Eq 14.1)}$$

The alternating stress is one-half of the stress range:

$$\sigma_a = \frac{\sigma_r}{2} = \frac{\sigma_{max} - \sigma_{min}}{2} \quad \text{(Eq 14.2)}$$

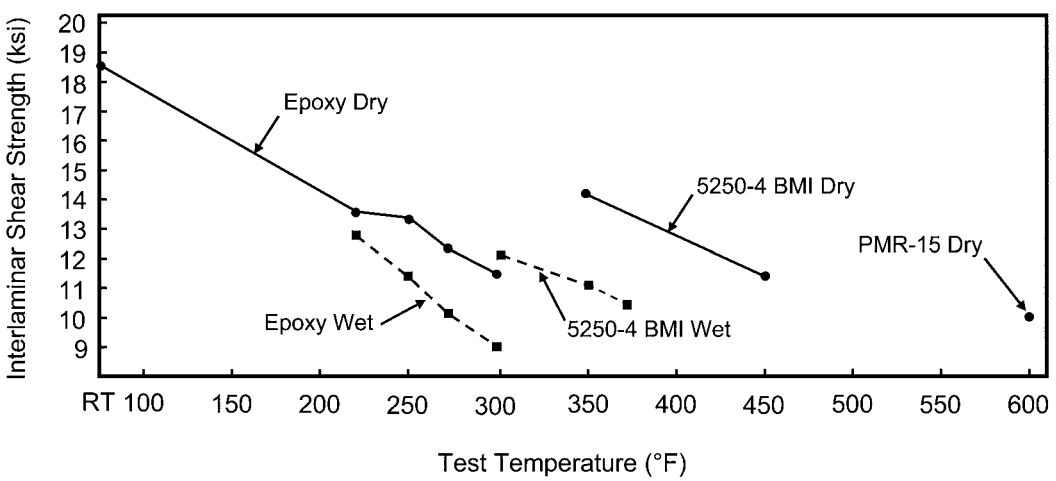
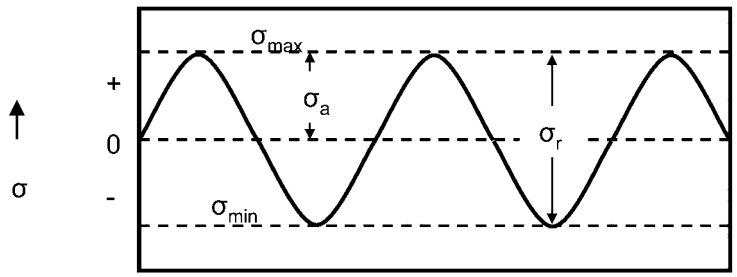
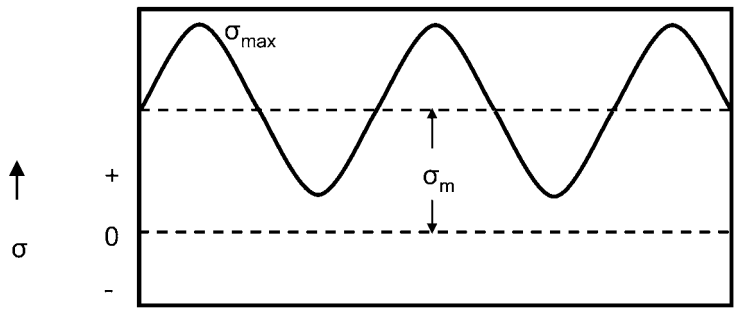


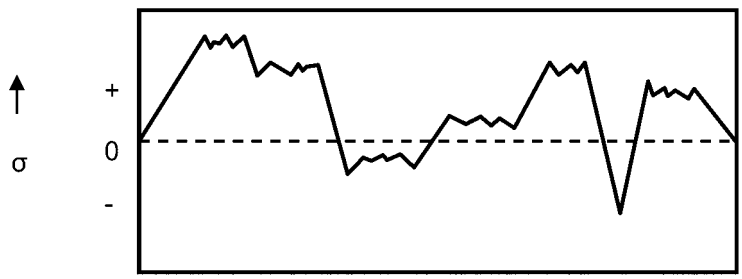
Fig. 14.9 Elevated-temperature interlaminar shear strength. BMI, bismaleimide



Fully Reversed Loading



Tension-Tension with Applied Stress



Random or Spectrum Loading

Cyclic Stress Range: $\sigma_r = \sigma_{max} - \sigma_{min}$

Cyclic Stress Amplitude: $\sigma_a = \dfrac{\sigma_{max} - \sigma_{min}}{2}$

Mean Stress: $\sigma_m = \dfrac{\sigma_{max} + \sigma_{min}}{2}$

Stress Ratio: $R = \dfrac{\sigma_{min}}{\sigma_{max}}$

Fig. 14.10 Typical fatigue loading cycles

The mean stress is the algebraic average of the maximum and minimum stress in the cycle:

$$\sigma_m = \frac{\sigma_{max} + \sigma_{min}}{2} \quad \text{(Eq 14.3)}$$

Two ratios frequently used in presenting fatigue data are:

Stress Ratio: $$R = \frac{\sigma_{min}}{\sigma_{max}} \quad \text{(Eq 14.4)}$$

Amplitude Ratio: $$A = \frac{\sigma_a}{\sigma_m} = \frac{1-R}{1+R} \quad \text{(Eq 14.5)}$$

Fatigue data inherently have more scatter than static test results, and since composites display more scatter than metals in static testing, it stands to reason that fatigue data for composites will have considerable scatter in the results. Therefore, to obtain meaningful data, a number of specimens should be tested at each stress level.

Compared to metals, carbon fiber composites exhibit superior fatigue performance. A comparison of the fatigue performance of a carbon/epoxy laminate with that of several aerospace-grade metals is shown in Fig. 14.11. In comparison with metals, advanced composites exhibit superior fatigue performance due to their high fatigue limit and resistance to corrosion. Compared to metals, in which fatigue life is a major design parameter, for a well-designed carbon fiber composite structure, static load capability rather than fatigue life is normally the critical design parameter. This is probably a result of two

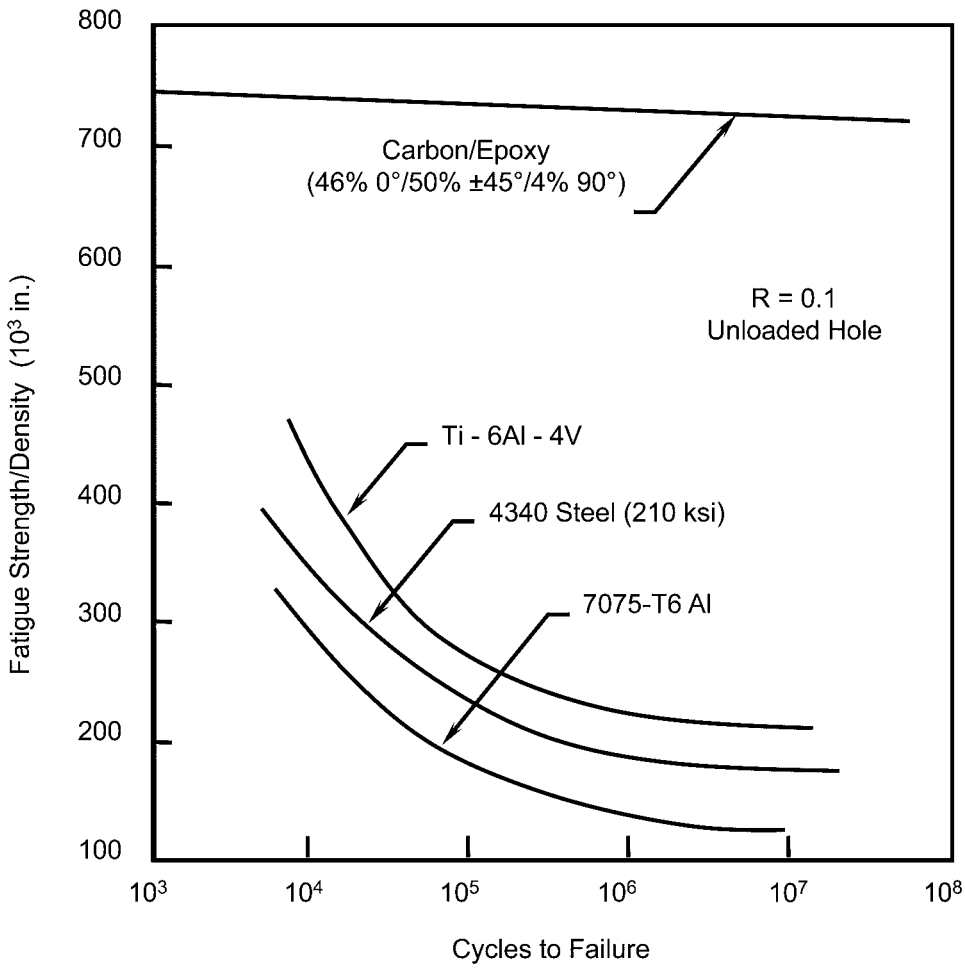


Fig. 14.11 Fatigue properties of aerospace materials. Source: Ref 13

factors: (1) carbon fiber composites have inherently superior fatigue properties; and (2) since high-performance composites are still a rather new class of material, the structures designed to date have used rather conservative design strains. In the future, as designers try to squeeze more and more performance out of composite materials, fatigue can be expected to become a bigger problem. Currently, the main concerns for carbon fiber designs are impact damage, delaminations, stability under compression loading, the low bearing strength of joints, and environmental degradation.

The fatigue failure mechanisms in metals and composites are vastly different. Fatigue failure in metals normally results from a single crack that slowly propagates through the section until it becomes so long that the remaining section can no longer support the load and failure occurs. Fatigue of composites is considerably different. Instead of one discrete crack, many different kinds of damage occur at different locations and eventually link up to cause failure. There are five major damage mechanisms: matrix cracking, fiber fracture, crack coupling, delamination initiation, and delamination growth and fracture.

The damage state versus percent of life in a quasi-isotropic subjected to tension-compression fatigue loading during the three phases of damage progression is illustrated in Fig. 14.12.

Phase I: Matrix Cracking. During the first phase, matrix cracks develop due to tension loads in the off-axis plies, initially in the 90-degree plies and then in the 45-degree plies. More and more matrix cracks develop until they reach a steady state or saturation level that is a function of ply thickness and material properties. The damage during this phase is relatively small and occurs during the first 10 to 25 percent of life. Although the strength loss is negligible and the stiffness loss is less than 10 percent, matrix cracks are the precursors for future damage events. In addition, if the matrix cracks are open to the surface (and they almost always are), they can provide paths for moisture ingression, which can accelerate the failure process.

Phase II: Fiber Fracture, Crack Coupling, and Delamination Initiation. As the matrix

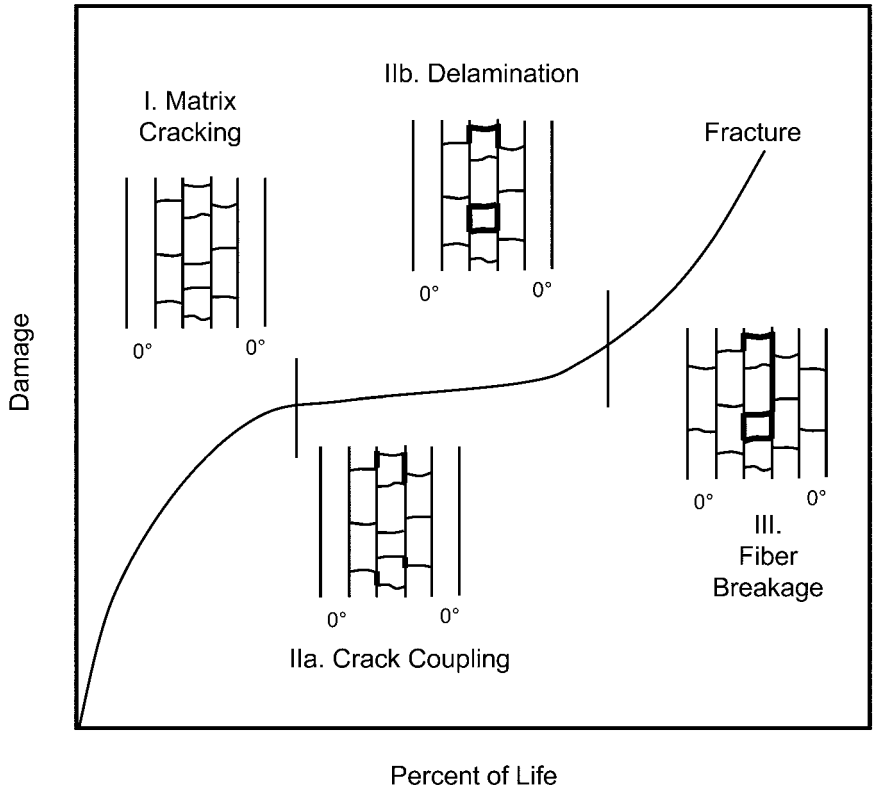


Fig. 14.12 Progressive fatigue damage. Source: Ref 14

cracks grow in the off-axis plies, they eventually intersect the main load-bearing zero-degree plies. The zero-degree plies blunt the crack growth, but this results in stress concentrations that initiate fiber fracture in the adjacent plies and induce longitudinal cracks running parallel to the zero-degree fibers and perpendicular to the matrix cracks. This combination of longitudinal and matrix cracking is called *crack coupling*. During the latter stages of Phase II, as a result of extensive crack coupling, large interlaminar stresses develop at the intersection of the matrix cracks and the longitudinal cracks, leading to the initiation of delaminations. Phase II damage occurs at a slower rate than Phase I damage and accounts for the next 70 to 80 percent of life.

Phase III: Delamination Growth and Fracture. The final phase is dominated by delamination growth and the eventual failure of the zero-degree plies. The delaminations initiated during Phase II start growing between the ply interfaces, eventually isolating the zero-degree plies. When the delaminations become large enough, the laminate section is essentially divided into a number of sublaminates, resulting in a large reduction in stiffness. The presence of compression loads during Phase III is especially detrimental, since the compression loads cause the sublaminates to start buckling. Eventually, the strength and stiffness become so reduced that gross section failure occurs.

As the percentage of zero-degree plies in a laminate increases, the fatigue life increases because a larger percentage of the load is carried by the axially aligned fibers, as shown in the *S-N* curves in Fig. 14.13 for T-300/934 carbon/epoxy laminates under tension-compression loading. The lower fatigue lives for the laminates with more off-axis plies are an effect of higher loads in the matrix resulting in the acceleration of damage associated with off-axis matrix cracking, crack coupling, and delamination formation and growth. Compared with metals, the curves of the composite have a relatively high fatigue threshold, and the slope is relatively low due to the insensitivity of carbon fibers to fatigue. For practical laminates, the slope of the *S-N* curve tends to increase, becoming less negative, as the percentage of off-axis plies increases.

The effect of loading variations can be determined by constructing *S-N* curves for different stress ratios (R), such as tension-tension, compression-compression, and tension-compression loading. Tension-compression loading is the most severe, followed by compression-compression and tension-tension loading. In tension-compression

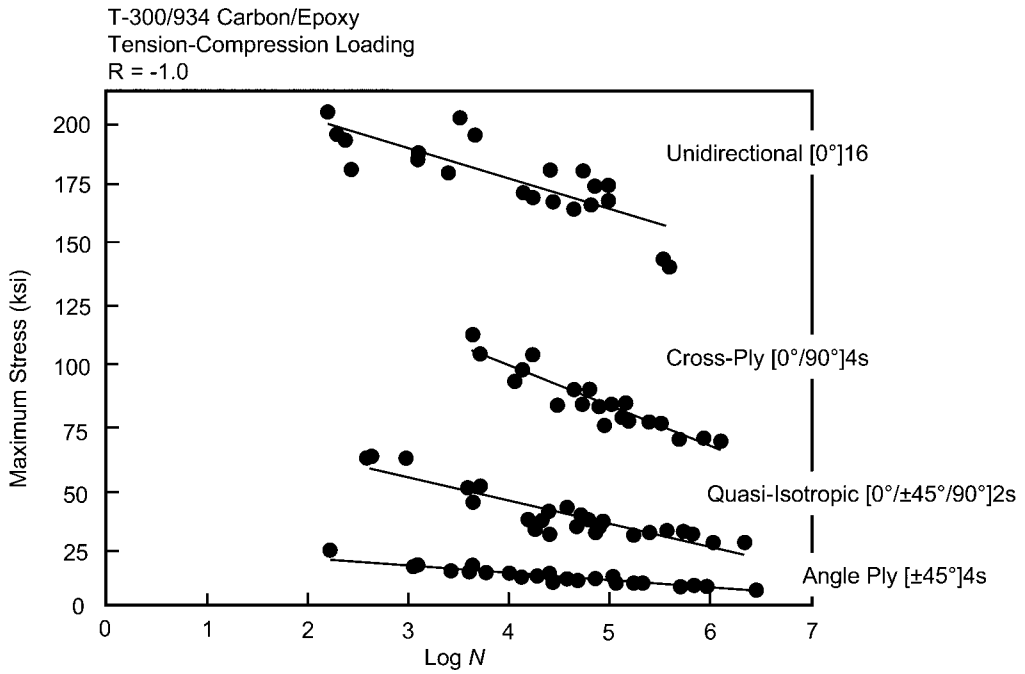


Fig. 14.13 *S/N* fatigue curves for carbon/epoxy laminates. Source: Ref 15

loading, the tension cycles initiate matrix cracking leading to small delaminations and the formation of sublaminates, which are then subject to buckling during the compression cycles.

A primary concern in the fatigue of composites is delamination. However, *S-N* data representing in-plane axial loading provide little information in characterizing interlaminar failure. Thus, it is necessary to develop *S-N* relationships between interlaminar stresses and interlaminar failure. Experience has shown that three- or four-point short beam shear testing can be used to correlate cyclic interlaminar shear stress with delamination. The axial tension-tension and short beam shear *S-N* curves for unidirectional carbon/epoxy laminates are shown in Fig. 14.14.

When cyclic tests are conducted at ambient temperatures, experience has shown that, within reasonable limits, results are relatively insensitive to the cyclic rate. For example, test results from panels tested at 5 Hz have correlated well with results from panels tested at 25 cycles per minute (0.5 Hz). The latter simulates a loading rate that might be applied to spectrum cycling of a large full-scale test component. The 5 Hz rate is considered a maximum rate for composite small coupon cyclic load testing.

14.5 Delaminations and Impact Resistance

Delaminations can occur during manufacturing operations or later when the part is placed in service. Manufacturing-induced delaminations can occur during part fabrication or assembly. Examples of fabrication delaminations are those caused by foreign objects left in the lay-up (such as release paper) or by insufficient pressure during cure due to vacuum bag rupture or poorly fitting tool details. During assembly, improper hole drilling can cause surface splintering of the plies; even more serious are delaminations caused by unshimmed gaps during fastener installation. The clamping force that is applied as the fastener is torqued can cause matrix cracking and delaminations at gap locations. When

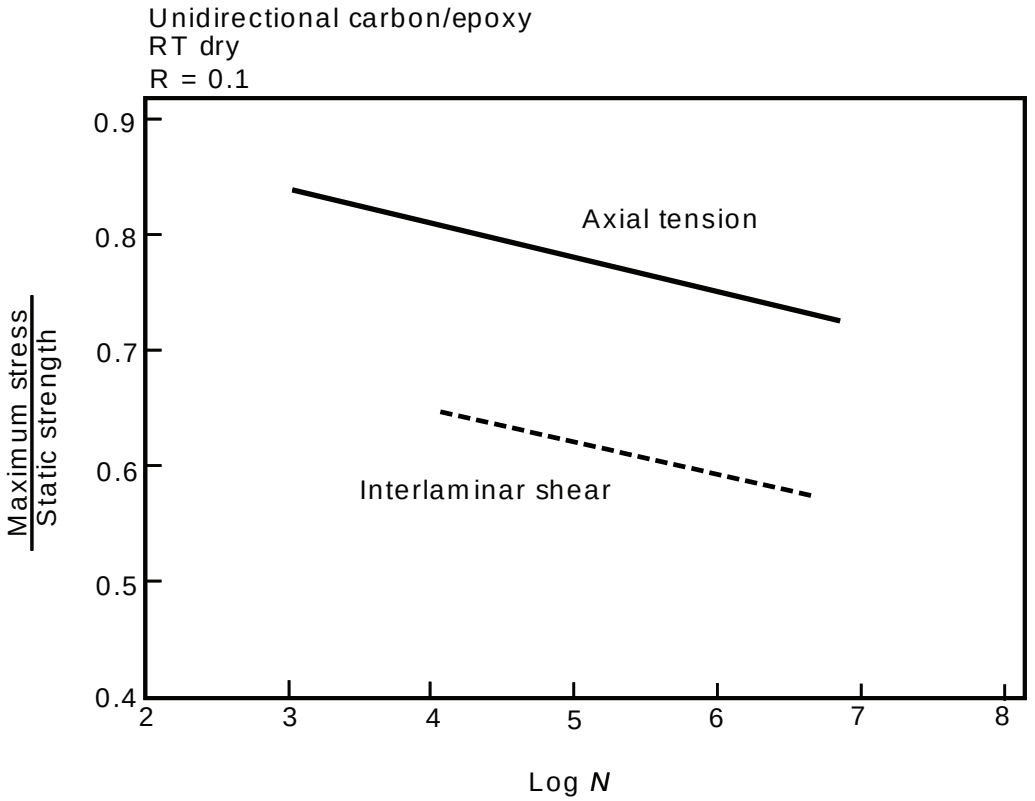


Fig. 14.14 *S/N* fatigue curves for axial tension and interlaminar shear. Source: Ref 16

the part is placed in service, delaminations can occur from runway debris, hail storms, bird impacts, or dropped tools or other unintended maintenance impacts.

When a delamination occurs, the main concern is in compression loading. Since a delamination splits the single laminate into two or more sublaminates, the section at the delamination is more susceptible to buckling during compression loading. Another key issue is whether or not the delamination will grow and get bigger under fatigue loading, compression loading again being the prime concern.

Low-velocity impacts are an important concern because they not only create delaminations, but also result in a network of matrix cracking and some crushing of fibers, depending on the energy level of the impact. The delaminations normally occur at the ply interfaces, as shown in the impact-damaged carbon/epoxy laminate in Fig. 14.15. Extensive diagonal shear cracks occur in the matrix between the transverse-oriented fibers, that is, the fibers oriented normal to the plane. Extensive delamination has also taken place in the matrix between the plies. In most instances of low-velocity impact, the damage is confined to the matrix and little fiber damage occurs. Therefore, the in-plane tension strength of the laminate may not be seriously degraded. However, even with impact levels that leave little indication of damage on the surface, the matrix damage may be significant; therefore, the ability of the matrix to stabilize the fibers in compression may be seriously degraded. For this reason, tolerance to impact damage is often the critical design consideration, and compression is the critical loading mode.

Take another look at Fig. 14.15. Note that there is very little evidence of damage on the surface impacted. This damage could be difficult to detect visually. It spreads out like a pine tree at the point of impact, with most of the damage being internal and with higher energy impacts producing broken fibers on the exit side. Thus, one of the main concerns is that the structure could sustain a low-velocity impact that no one is aware of, which could then grow under either static or fatigue loading, eventually leading to failure. This concern has led to the concept of *barely visible impact damage*. This is a somewhat arbitrary term since the ability to detect an impact is dependent on lighting conditions, the type of surface finish on the part, the observer's distance from the impact, and differing capabilities of the human eye. Nevertheless, a lot of work has been conducted to correlate impacts with differing energy levels and with the visual ability to detect them.

A comparison of the compressive static and fatigue degradation for delaminations and impact damage of carbon/epoxy laminates is shown in Figs. 14.16 and 14.17, respectively. The degradation due to a single-layer delamination is less than that of an impact, since the damage is confined to a single layer. In addition, since delaminations usually occur during manufacturing, they are more likely to be detected during routine

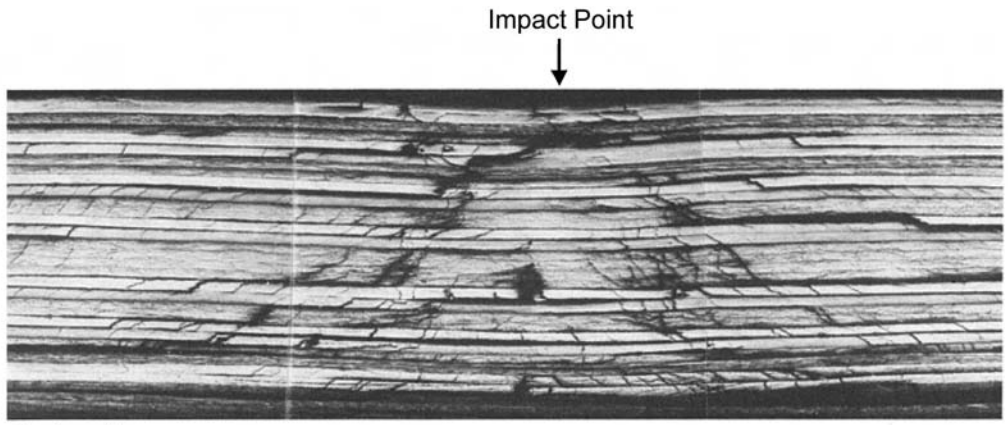


Fig. 14.15 Impact damage in carbon/epoxy laminate

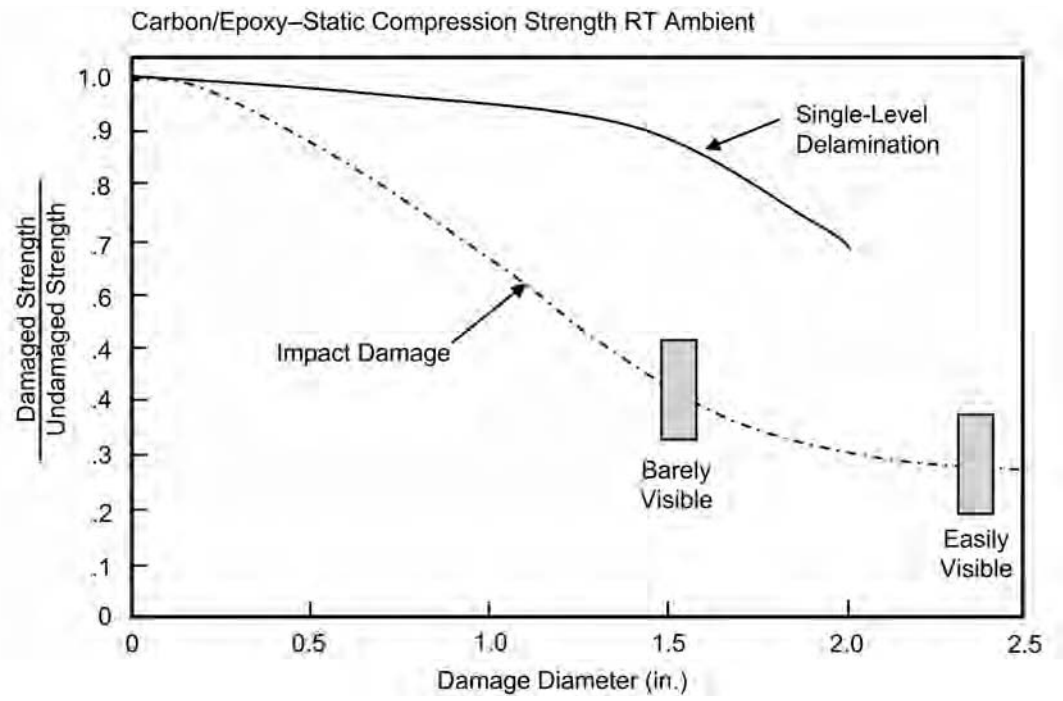


Fig. 14.16 Static strength loss due to impact damage

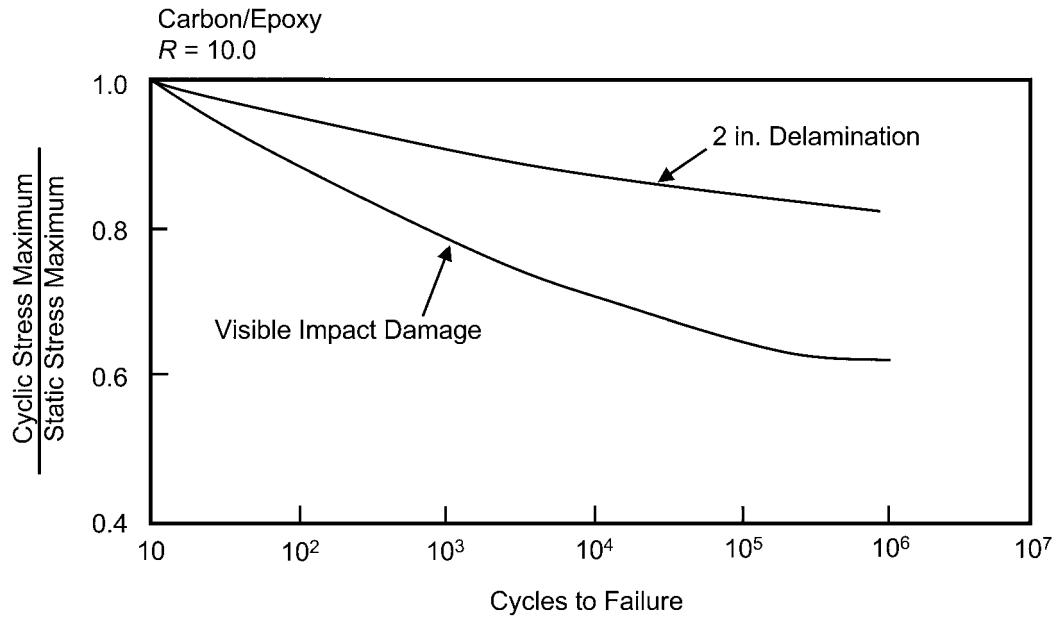


Fig. 14.17 Relative severity of defects on compression fatigue strength

nondestructive testing. Although impacts can also occur during manufacturing, they are more likely to occur in service, where, unless they are visible on an inspectable surface, they can remain undetected for a long time or even for the life of the structure. The concern with impact damage is apparent in Fig. 14.16, where a laminate can lose 60 to 65 percent of its undamaged static compression strength during an impact event that is essentially invisible. The loss of cyclic load-carrying capability is also greatest when an impact occurs. Thus, while fatigue and corrosion are the Achilles heels of metals, delaminations and impact resistance are the weak points of carbon fiber composites.

The type of fiber, the matrix, and the material product form can all affect the impact performance of composite laminates. The impact resistance of glass, in particular S-glass, and of aramid composites is quite good (Fig. 14.18). S-glass/epoxy composites are about seven times more impact resistant than high-strength carbon/epoxy and about 35 times more resistant than high-modulus carbon/epoxy. Glass/epoxy and Kevlar/epoxy composites are even more impact resistant than 4330 steel and 7075-T6 aluminum, a common aircraft grade of aluminum. Both glass/epoxy and aramid fiber composites are used when high resistance to impact damage is required, such as in gas pressure vessels subject to rough handling. The ballistic performance of S-glass and aramid fiber composites is similar, as measured by the V50 parameter. The V50 parameter is the velocity at which there is a 50 percent probability that a projectile will penetrate the target. This type of evaluation shows that both S-glass and aramid fiber composites provide a similar level of protection, and both are superior to E-glass and aluminum.

The early epoxy systems used from the 1970s through the mid-1980s, now referred to as *first-generation epoxies*, were highly crosslinked systems that were fairly brittle. A comparison of the compression strength after impact (CAI) of these systems and of some of the newer toughened epoxies and thermoplastics is shown in Fig. 14.19. Several points are noteworthy here. First, even for the first-generation epoxies, the impact resistance of woven cloth is somewhat better than that of tape material. Second, the newer thermoplastic-toughened epoxies have much higher CAI values, some of which approach those of

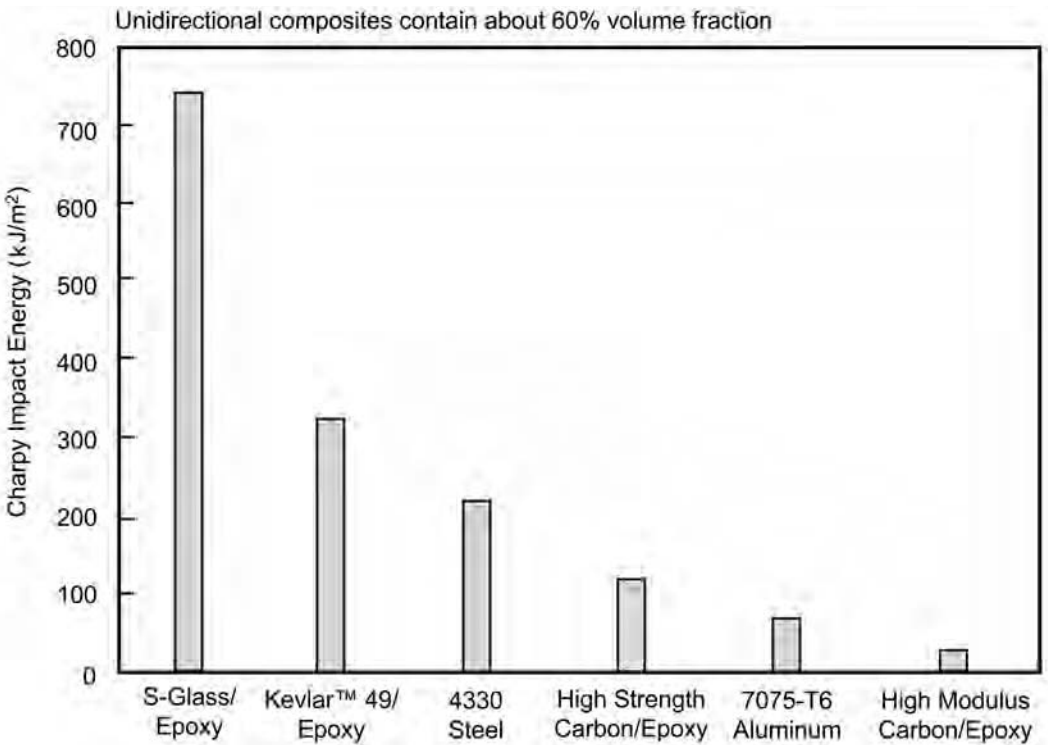


Fig. 14.18 Impact properties of various engineering materials. Source: Ref 17

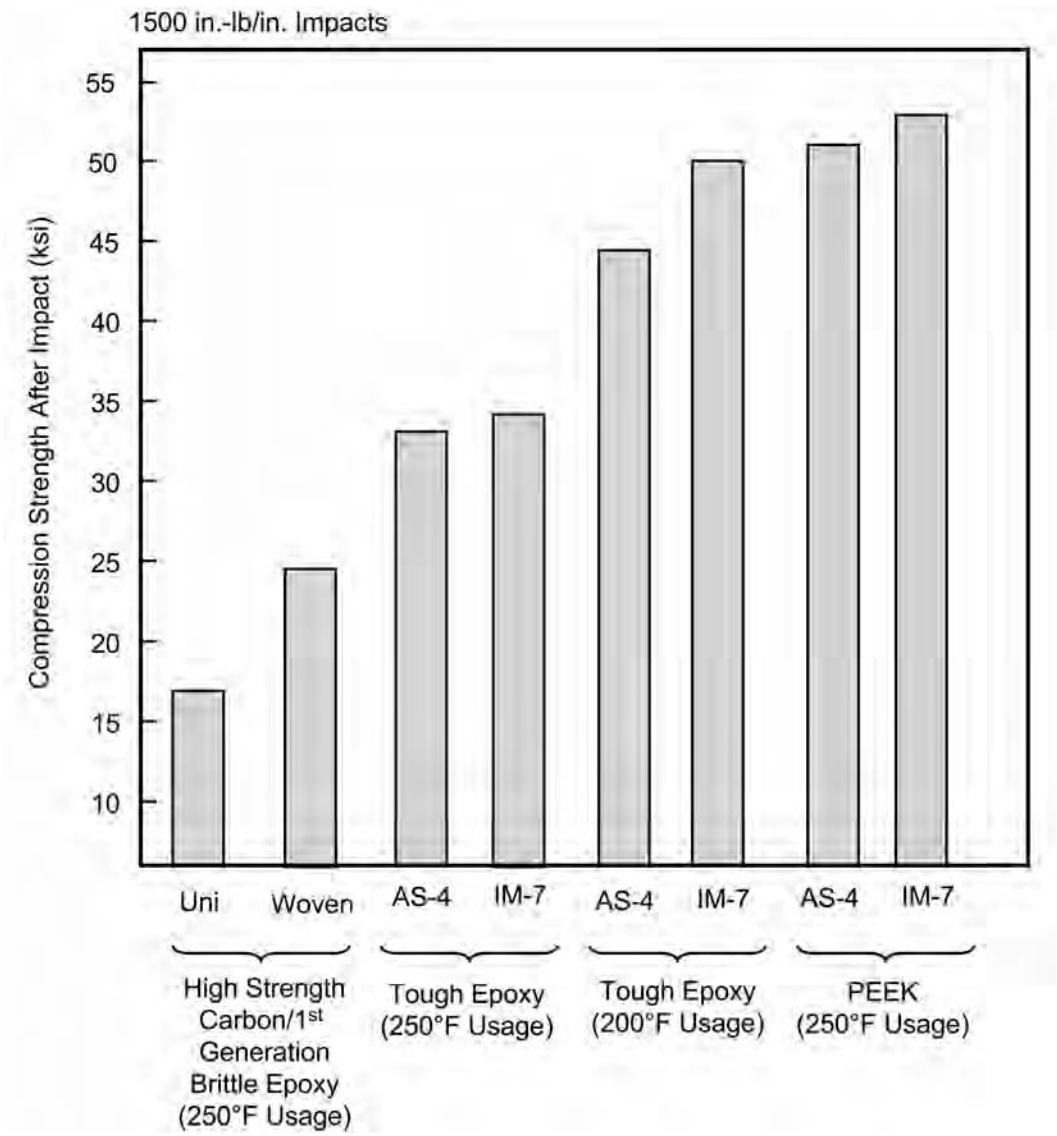


Fig. 14.19 Relative CAI strengths of carbon-reinforced composite systems

thermoplastics. Third, the CAI performance of the 200 °F (95 °C) system is higher than that of the 250 °F (120 °C) system. In other words, greater toughness can be obtained for systems with lower operating temperatures. Fourth, the impact performance is somewhat improved with the newer intermediate-modulus carbon fibers, although other design factors will determine whether a high-strength or intermediate-modulus fiber is selected.

A third method of improving damage tolerance is product form selection. Through-the-thickness reinforcement has been shown to improve the delamination resistance and impact performance of composites. Various methods have been developed including stitching, three-dimensional weaving, and three-dimensional braiding, usually in conjunction with liquid molding techniques, as described in Chapter 5, "Thermoset Composite Fabrication Processes." An example of the improvement due to through-the-thickness stitching is shown in Fig. 14.20. However, through-the-thickness reinforcement usually results in a reduction of the in-plane properties.

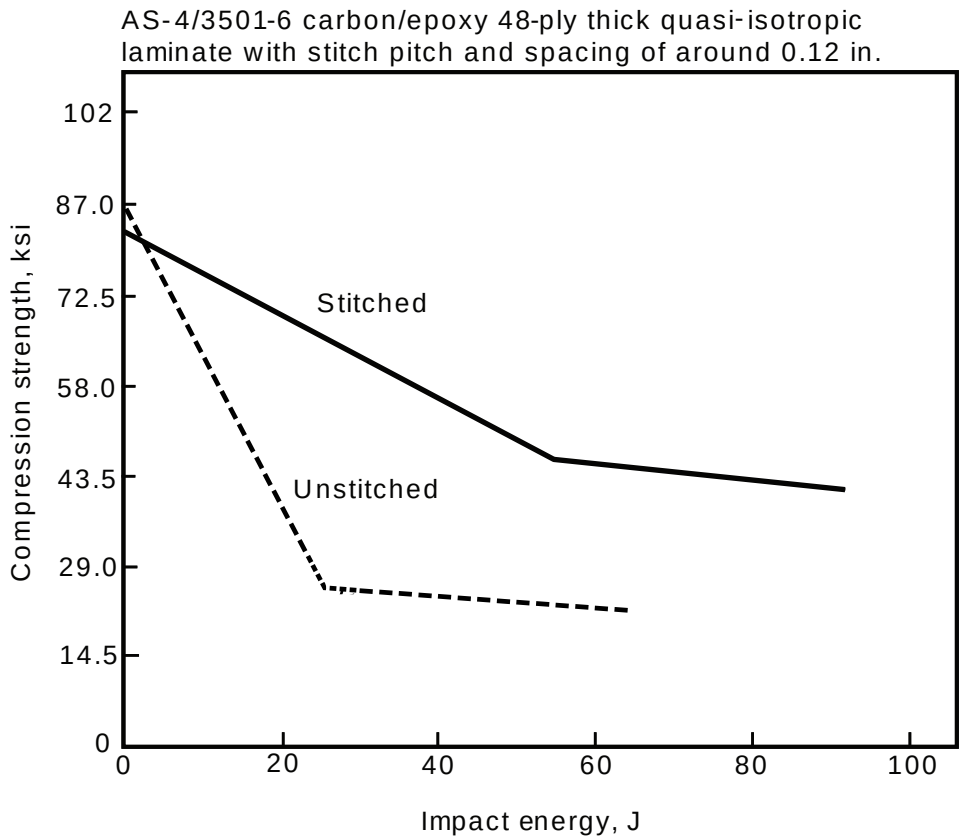


Fig. 14.20 Use of stitching to improve damage tolerance. Source: Ref 18

14.6 Effects of Defects

Besides delaminations and impact-induced damage, other types of defects can degrade the performance of composite parts. Again, the major effect is on the compression properties. Three types of manufacturing-related defects are discussed in this section: voids and porosity, fiber distortion, and fastener hole defects.

14.6.1 Voids and Porosity

Voids and porosity are one of the most detrimental manufacturing defects that can occur during manufacturing. While porosity control is discussed in some detail in Chapter 7, "Processing Science of Polymer Matrix Composites," the two main reasons for porosity in continuous fiber polymer matrix composites that are autoclave processed are (1) air that becomes trapped between the plies during lay-up and cannot be successfully evacuated later during the initial part of the cure cycle and (2) dissolved water or other entrapped volatiles that come out of solution as the cure temperature increases and are then locked in place when the matrix solidifies or gels. Porosity can form either at the ply interfaces (interply porosity) or within the individual plies (intraply porosity), as shown in Fig. 14.21. It can form in isolated areas or it can be pervasive throughout the part. Although the terms *voids* and *porosity* are generally used interchangeably, porosity is usually smaller and more extensive, while voids are usually larger and fairly discrete.

Porosity adversely affects almost all of the matrix-dependent mechanical properties. The curves in Figs. 14.22 and 14.23 illustrate the reduction in interlaminar shear and compression strength due to porosity. Note that as little as two percent porosity causes a significant reduction in properties. A properly processed autoclave-cured laminate should contain one percent or less porosity. Fiber-dominated longitudinal tensile strength is minimally affected, but the

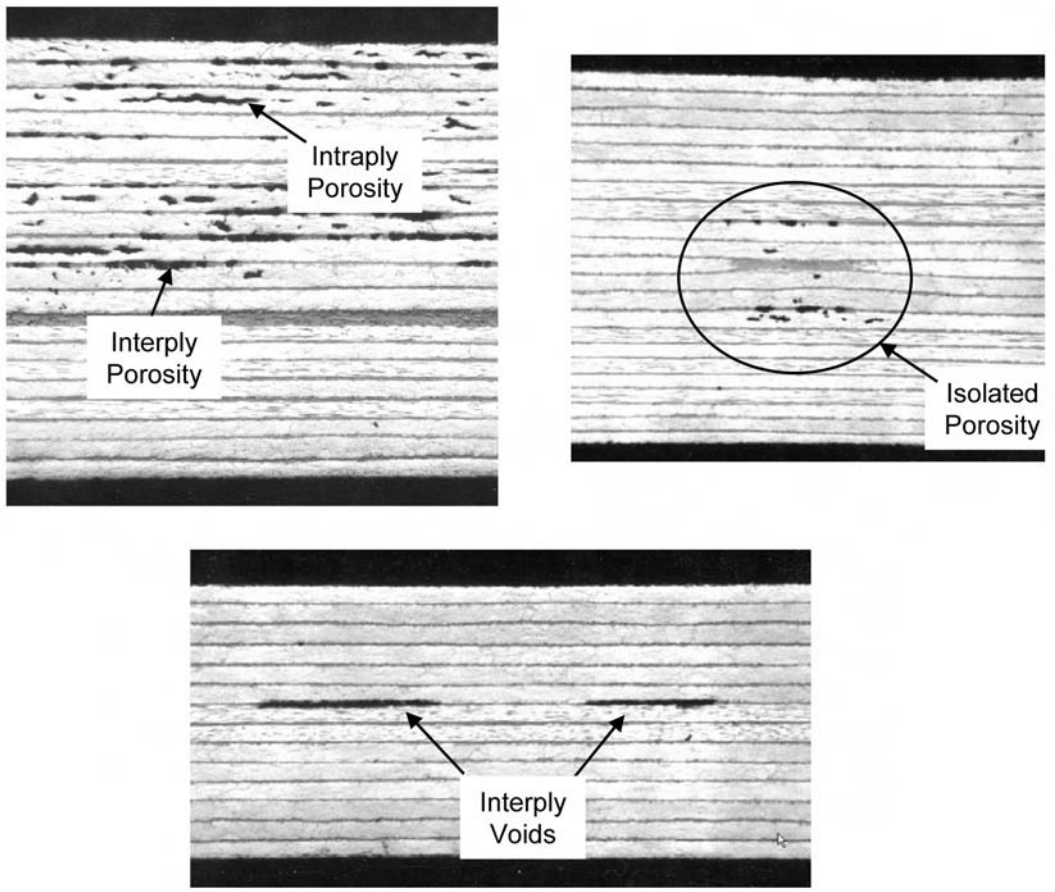


Fig. 14.21 Various forms of voids and porosity

matrix-dependent properties, such as flexural strength, interlaminar shear strength, and compression strength, degrade with increasing percentages of porosity.

To study the interaction of matrix-dependent properties, a combined compression-interlaminar shear strength test was performed using the test setup shown in Fig. 14.24. In this test, both compression and shear loading can be individually controlled but can also be applied at the same time. The results of this test method are shown in Fig. 14.25 for a series of carbon/epoxy laminates with negligible porosity and those containing two percent porosity. As shown, porosity adversely affects both static and fatigue strength.

One of the problems in studying the effects of porosity is accurately determining the porosity level and its extent. One method is to use acid digestion to dissolve the matrix and then use the constituent weights and densities to calculate the porosity. However, this method depends on an assumed fiber and resin density. Due to inaccuracies in these assumptions, even negative porosity levels are sometimes reported! In addition, while this method gives a gross porosity level, it tells nothing about how the porosity is distributed. Another method involves a materiallographic examination, such as the photomicrographs shown in Fig. 14.21. The problem with this method is that only a small area is examined. A third method is the use of ultrasonic inspection. Ultrasonic inspection is discussed in more detail in Chapter 12, "Nondestructive Inspection," but the method used to quantify porosity is the ultrasonic attenuation method; that is, the more porous the laminate, the more sound is attenuated (lost because of absorption and scattering) due to the presence of porosity. If one knows what the sound attenuation is for a porosity-free laminate, then it is assumed that attenuation above that level is due to porosity, and the greater the attenuation, the greater the

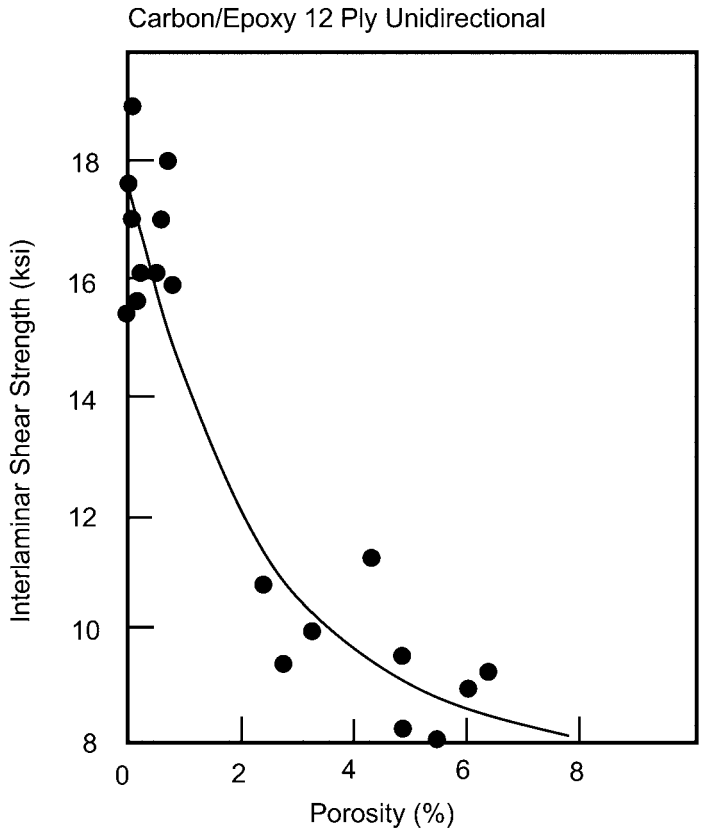


Fig. 14.22 Effect of porosity on interlaminar shear strength of carbon/epoxy. Source: Ref 19

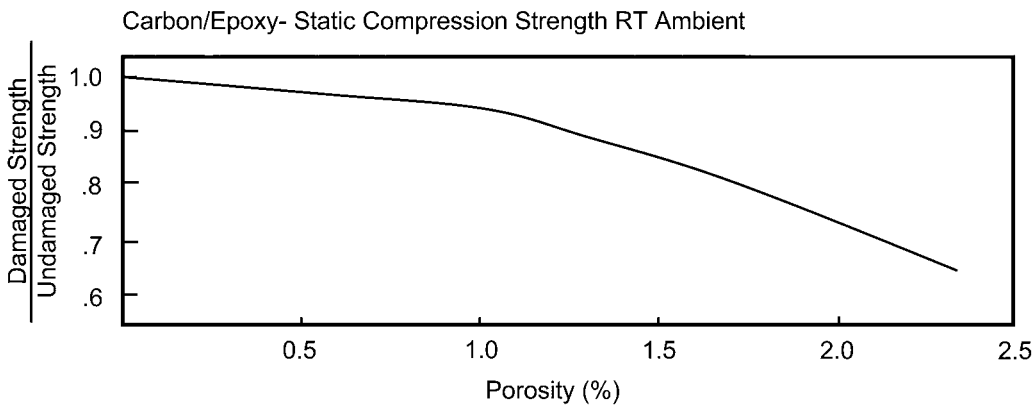


Fig. 14.23 Strength loss due to porosity

amount of porosity. For example, if a porosity-free laminate attenuates sound to a level of 20 dB and a similar laminate with porosity attenuates at 36 dB, it can be assumed that the extra attenuation (Δ16 dB) is due to porosity and that a similar laminate that attenuates at 56 dB is worse than the one at 36 dB. To confirm that these assumptions are correct, extensive cross sections are taken from areas with different attenuation levels and examined for porosity. In what is

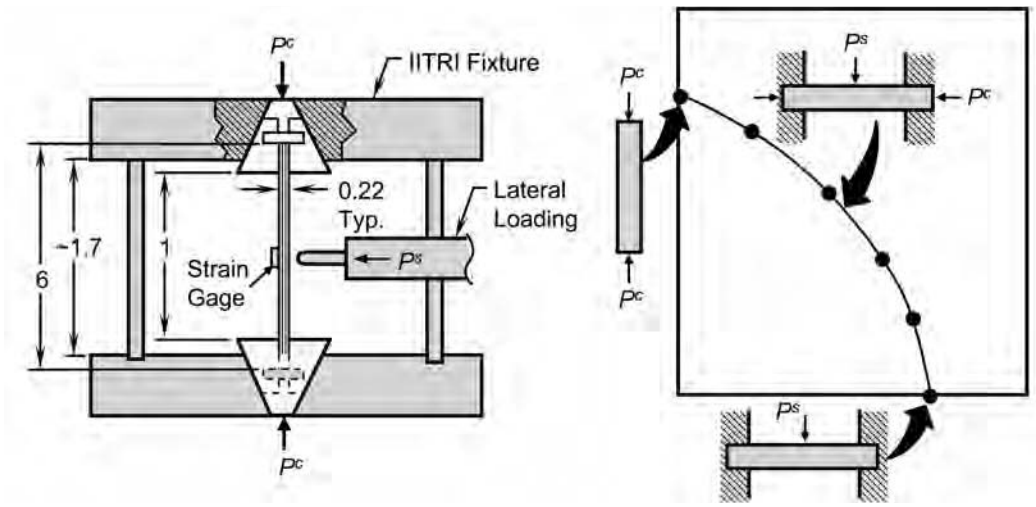


Fig. 14.24 Combined compression shear test method. ITTRI, Illinois Institute of Technology Research Institute

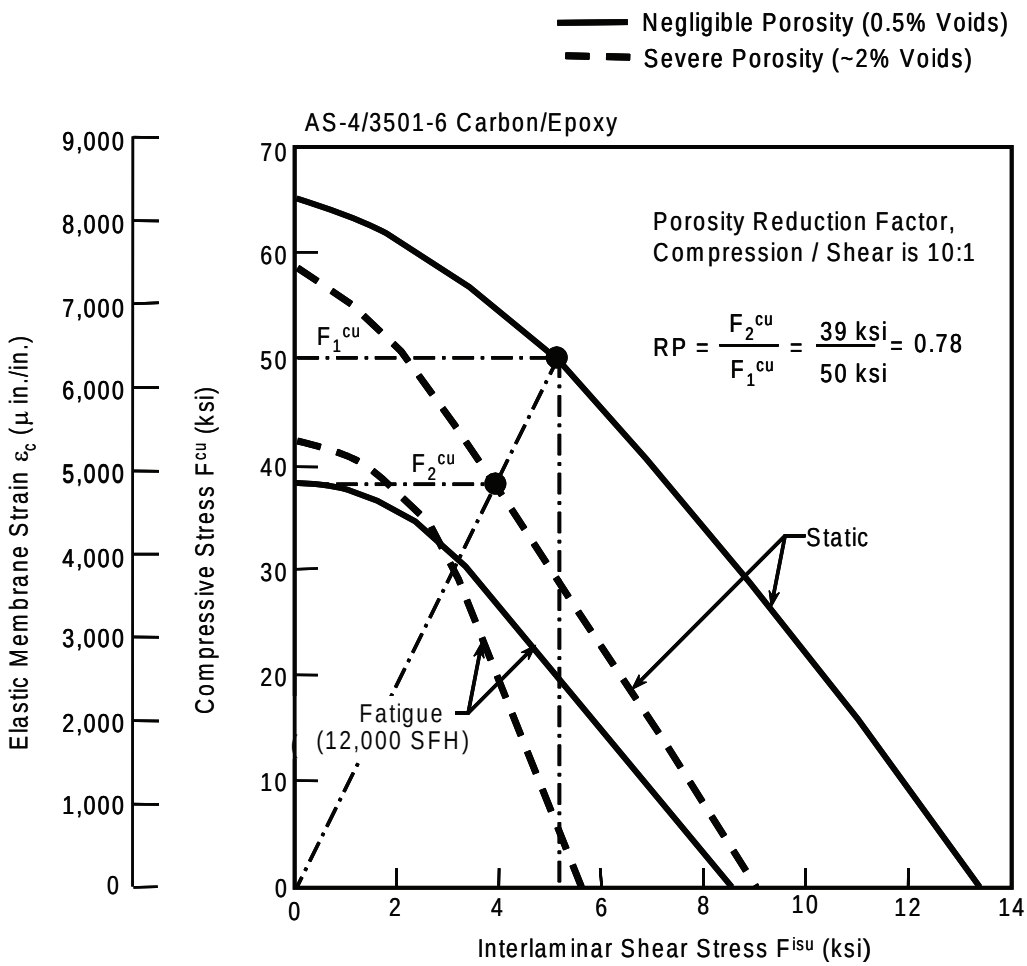


Fig. 14.25 Effects of porosity on combined compression-interlaminar shear properties

called an *effect of defects* test program, matrix-dependent mechanical properties are measured on both porosity-free laminates and those containing various degrees of porosity. Once this work is completed, it provides a way of determining the severity of porosity in production parts. A curve showing the reduction in interlaminar shear strength of carbon/epoxy with increasing ΔdB levels is shown in Fig. 14.26. In this example, if a 0.15-inch thick laminate had an attenuation of 40 dB over the baseline for this thickness of laminate, the interlaminar shear strength would be reduced to about 80 percent of that of a nonporous laminate.

14.6.2 Fiber Distortion

While fibers used in high-performance composites are strong and stiff in tension, they also have very small diameters that make them rather weak in compression when they are not supported by a fully cured matrix. Thus, during curing, when the matrix is a fairly low-viscosity fluid, the fibers can be subjected to movement and rearrangement due to the hydraulic pressures caused by the flowing resin. In addition, mismatches in tooling details can result in fiber wrinkling and distortion, also known as *fiber marcelling*. A number of examples of fiber distortion caused by tool mark-off are shown in Fig. 14.27. Mark-off that is caused by a vacuum bag wrinkle will usually have some resin buildup on the surface. These resin lumps can make the mark-off appear deeper than it really is. Therefore, the resin buildups can be removed by lightly sanding to obtain a true mark-off depth.

While wrinkled fibers will reduce almost all of the mechanical properties to some extent, it is the compression strength that is most adversely affected, as shown for the carbon/epoxy laminate in Fig. 14.28. Since the wrinkled carbon fibers are already prebuckled, it should not be surprising that the compression strength is adversely affected. Note that in the example shown in Fig. 14.28, the compression strength was reduced by almost 80 percent for a 40 percent indentation. It is obvious that when this type of defect is detected, it needs to be fully characterized and corrective action immediately taken. Unfortunately, ply wrinkling can be difficult to detect. During ultrasonic inspection, since the

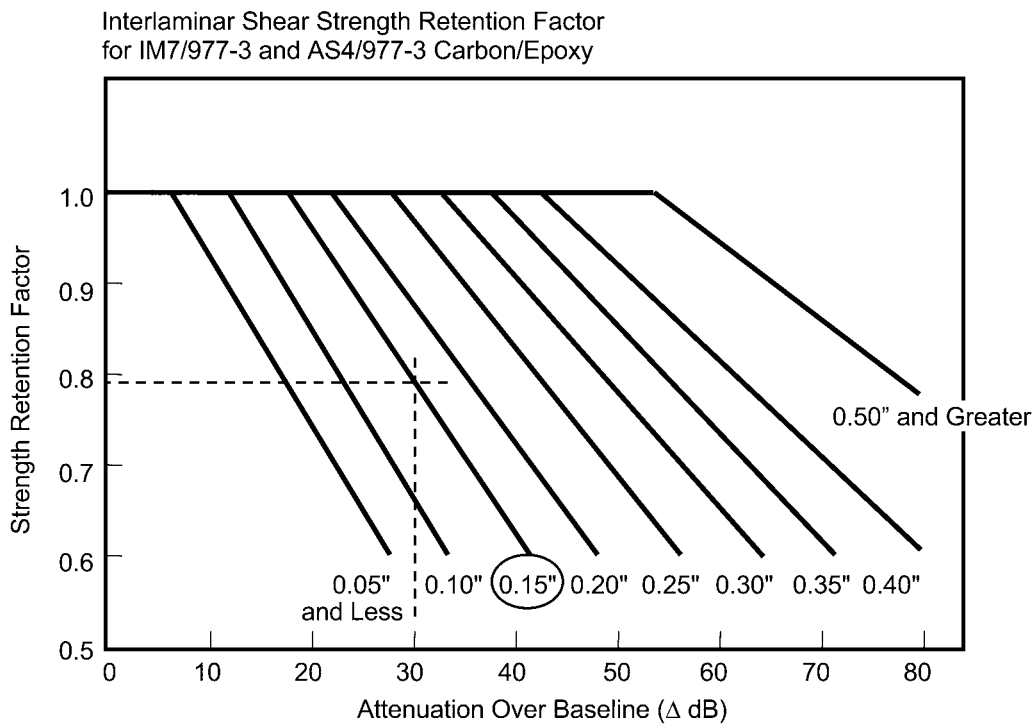


Fig. 14.26 Ultrasonic attenuation for porosity characterization

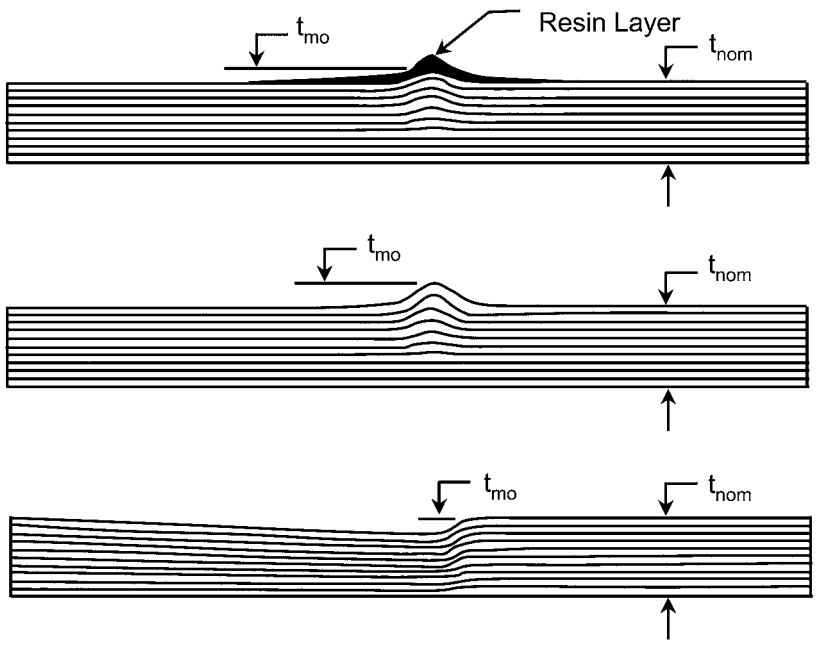


Fig. 14.27 Examples of tool mark-off causing ply distortion

wrinkled plies scatter sound in a manner similar to that of porosity, wrinkled plies will often be mistaken for porosity.

14.6.3 Fastener Hole Defects

Fastener hole preparation and fastener installation in composites are more error prone than for metals. As discussed in more detail in Chapter 11, "Machining and Assembly," composites are subject to delaminations on both the entrance and exit sides of holes; they can be damaged by excessive heat generated during machining or drilling; and fasteners that are not installed in properly prepared holes can further induce delaminations. While interference fit fasteners are often used in metallic structures to improve fatigue life, normal interference fit fasteners installed in composite structures have often resulted in matrix crushing and delaminations. The effects of a number of these defects on the tension and compression strength of carbon/epoxy are shown in Table 14.15. Two of the most severe defects are improper fastener seating depth and tilted countersinks. These are detrimental because they tend to cause delaminations in the plies adjacent to the holes when placed under load. Severe porosity around the hole is especially detrimental in elevated-temperature compression loading.

REFERENCES

1. MIL-HNBK-17-1F, *Polymer Matrix Composites*, Vol 1, *Guidelines for Characterization of Structural Materials*, U.S. Department of Defense, 2001
2. MIL-HNBK-17-2F, *Polymer Matrix Composites*, Vol 2, *Polymer Matrix Composites Materials Properties*, U.S. Department of Defense, 2001
3. MIL-HNBK-17-3F, *Polymer Matrix Composites*, Vol 3, *Materials Usage, Design, and Analysis*, U.S. Department of Defense, 2001
4. MIL-HNBK-17-4A, *Composites Materials Handbook*, Vol 4, *Metal Matrix Composites*, U.S. Department of Defense, 2002
5. MIL-HNBK-17-5, *Composites Materials Handbook*, Vol 5, *Ceramic Matrix Composites*, U.S. Department of Defense, 2002
6. J.C. Reindl, Commercial and Automotive Applications, *Engineered Materials Handbook*, Vol 1, *Composites*, ASM International, 1987

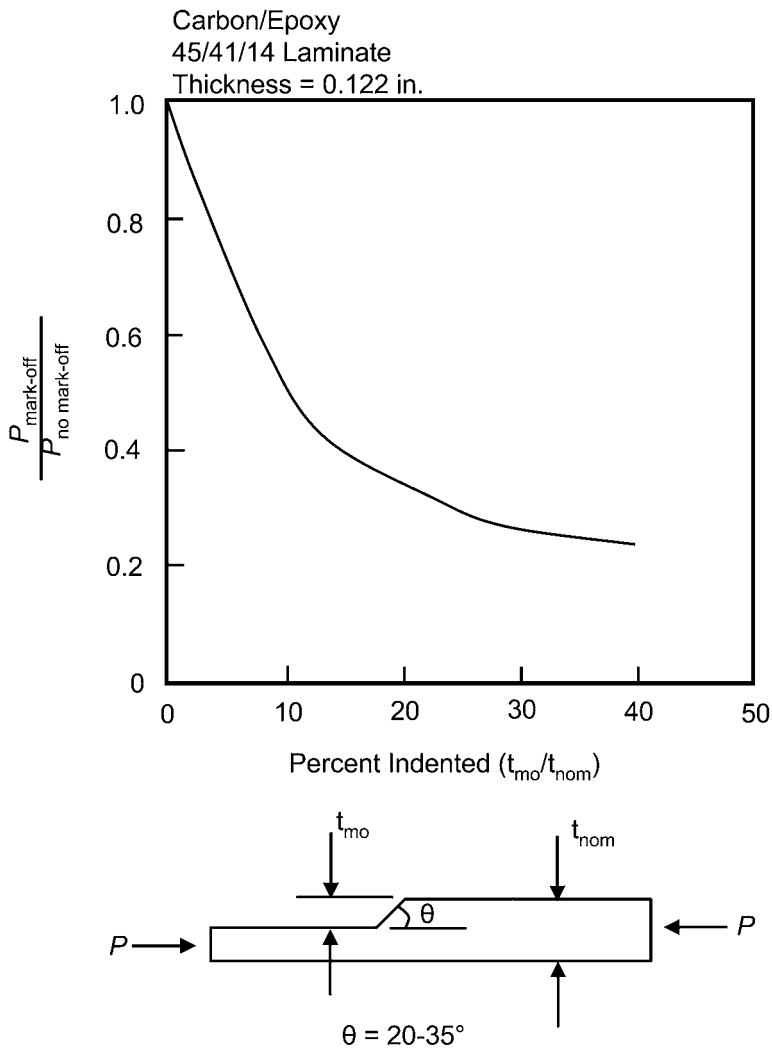


Fig. 14.28 Effect of tool mark-off on compression strength of carbon/epoxy

7. F.R. Andresen, Open-Molding: Hand Lay-Up and Spray-Up, *ASM Handbook*, Vol 21, *Composites,*ASM International, 2001
8. J.E. Sumerak and J.D. Martin, Pultrusion, *ASM Handbook*, Vol 21, *Composites*, ASM International, 2001
9. M.W. Wardle, Aramid Fiber Reinforced Plastics—Properties, *Comprehensive Composite Materials*, Vol 2, *Polymer Matrix Composites*, Elsevier Science Ltd., 2000
10. "Cycom 977-3 Toughened Epoxy Resin," Cytec Engineered Materials data sheet, 1995
11. J-M. Bai and D. Leach, High Performance Thermoplastic Polymers and Composites, presented at a *SAMPE* conference, Long Beach, CA, 1–5 May, 2005
12. TenCate Advanced Composites Data Sheet, "CETEX Thermo-Lite Thermoplastic Composites for Automated Fiber Placement & Rapid Lamination Processes," 2008
13. R. Bohlmann, M. Renieri, G. Renieri, and R. Miller, Training course notes given to Thales in The Netherlands entitled "Advanced Materials and Design for Integrated Topside Structures," 14–19 April 2002
14. R.L. Reifsnider, *Composite Materials Series: Fatigue of Composite Materials*, Vol 4, Elsevier Science Publishing Company, 1991

Table 14.15 Strength degradation due to fastener hole defects

		Compression	
	RTD Tension	RT(a)	250° F(a)
Out-of-round holes			
50/40/10 laminate	(b)	…	…
30/60/10 laminate	–4.8	…	…
Broken fibers exit side of hole			
Severe	–7.3	–8.4	–9.2
Moderate	–1.4	–3.2	–4.2
Porosity around hole			
Severe	(b)	–10.3	–30.8
Severe with freeze/thaw	…	–11.6	…
Moderate	…	–7.1	–13.3
Moderate with freeze/thaw	…	–8.4	…
Improper fastener seating depth			
80% thickness	–16.4	…	…
100% thickness	–34.3	…	…
Tilted countersinks			
Away from bearing surface	(b)	…	–16.7
Toward bearing surface	–21.4	…	–16.7
Interference fit tolerances, in.			
50/40/10 @ 0.003	(b)	…	+9.1(c)
@ 0.008	(b)	…	+9.1(c)
30/60/10 @ 0.003	(b)	…	(b, c)
@ 0.008	(b)	…	(b, c)
Fastener removal and reinstallation			
100 cycles	(b)	…	–8.3

Notes: Elipses indicates no test. (a) Moisture content = 0.86%. (b) Less than 2% change. (c) Tensile loading.

15. A. Rotem and H.G. Nelson, Residual Strength of Composite Laminates Subjected to Tensile-Compressive Fatigue Loading, *J. Compos. Technol. Res.*, Vol 12 (No. 2), 1990, p 76–84
16. J.R. Schaff, Fatigue and Life Prediction, *ASM Handbook*, Vol 21, *Composites*, ASM International, 2001
17. S.K. Mazumdar, *Composites Manufacturing: Materials, Product, and Process Engineering*, CRC Press, 2002
18. C.C. Poe, H.B. Dexter, and I.S. Raju, Review of NASA Textile Composites Research, *J. Aircr.*, Vol 36 (No. 5), 1999, p 876–884
19. M.J. Yokota, In-Process Controlled Curing of Resin Matrix Composites, *SAMPE J.*, Vol 11, 1978

SELECTED REFERENCES

- A. Baker, S. Dutton, and D. Kelly, *Composite Materials for Aircraft Structures*, 2nd ed., American Institute of Aeronautics and Astronautics, Inc., 2004
- L.L. Clements, Organic Fibers, *Handbook of Composites*, Chapman & Hall, 1982
- "Cycom 5215 Modified Epoxy Resin," Cytec Engineered Materials data sheet
- R.E. Horton and J.E. McCarty, Damage Tolerance of Composites, *Engineered Materials Handbook*, Vol 1, *Composites*, ASM International, 1987
- J.R. Schaff and A. Dobyns, "Fatigue Analysis of Helicopter Tail Rotor Spar," AIAA Report 98-1738, *American Institute of Aeronautics and Astronautics—ASM Symposium*, Long Beach, CA, 1998
- G.D. Sims and W.R. Broughton, Glass Fiber Reinforced Plastics—Properties, *Comprehensive Composite Materials*, Vol 2, *Polymer Matrix Composites*, Elsevier Science Ltd., 2000

Copyright © 2010, ASM International®
All rights reserved.
www.asminternational.org

CHAPTER 15

Environmental Degradation

EXPOSURE OF COMPOSITES to various environmental conditions may or may not cause degradation, depending on the specific material system and the specific environment. When environmental degradation does occur, it is usually, but not always, the matrix that is affected. In this chapter, a number of potential environments that can cause varying degrees of loss of performance will be covered. Since water is pervasive, moisture absorption in polymeric matrix composites is a primary concern. Other potential degradation conditions covered include fluids, ultraviolet radiation, erosion, lightning strikes, thermo-oxidative stability of high-temperature polymeric composites, heat damage, and flammability.

15.1 Moisture Absorption

When a composite absorbs moisture, the properties of the matrix are affected in several ways (Fig. 15.1):

1. Since moisture attacks the matrix, it is the elevated-temperature matrix-dependent properties (the hot-wet condition) that are most affected. Since real laminates that are used in structures normally have 40 to 50 percent off-axis plies, almost all laminates are affected to some degree.
2. If liquid water is trapped in microcracks or delaminations, since water expands when it freezes, it can form larger macrocracks or delaminations when the composite is subjected to freeze-thaw cycles.
3. Absorbed moisture can cause the composite to swell, producing strains in the through-the-thickness direction, which can lead to warpage.
4. In adhesives, especially untoughened adhesives, the plasticizing effect of moisture can actually be beneficial in that the adhesive becomes more ductile and forgiving.
5. Absorbed moisture can be a detriment when conducting elevated-temperature repairs. The moisture can inhibit proper cure of the repair patch or adhesive or, if present in sufficient quantities during elevated-temperature cures, can result in steam pressure delamination. Therefore, parts to be repaired by bonding at elevated temperature should always be thoroughly dried before being heated.
6. Thermal spiking, or rapidly heating to elevated temperatures, can cause matrix cracking and greater amounts of moisture absorption.
7. Finally, if liquid water is present in either a honeycomb assembly or within a laminate, heating it to high temperatures can turn the trapped water into steam, resulting in steam pressure delamination.

When a polymer matrix absorbs moisture from the atmosphere, it reduces the glass transition temperature T_g in the manner shown for the carbon/epoxy and carbon/bismaleimide composites in Fig. 15.2. As moisture is absorbed, the temperature at which the matrix changes from a glassy solid to a softer, more viscous state decreases. Thus, the elevated-temperature strength properties decrease with increasing moisture. Since the glass transition temperature is reduced, the maximum usage temperature of the composite must be reduced.

Epoxy resins are the most widely used matrix systems, and they have multiple sites for hydrogen bonding for water molecules, such as hydroxyl groups, phenol groups, amine groups, and sulfone groups. Water molecules become attached to the main molecular chains and also form secondary crosslinking in the manner shown in Fig. 15.3. The crosslinking mechanism shown contributes

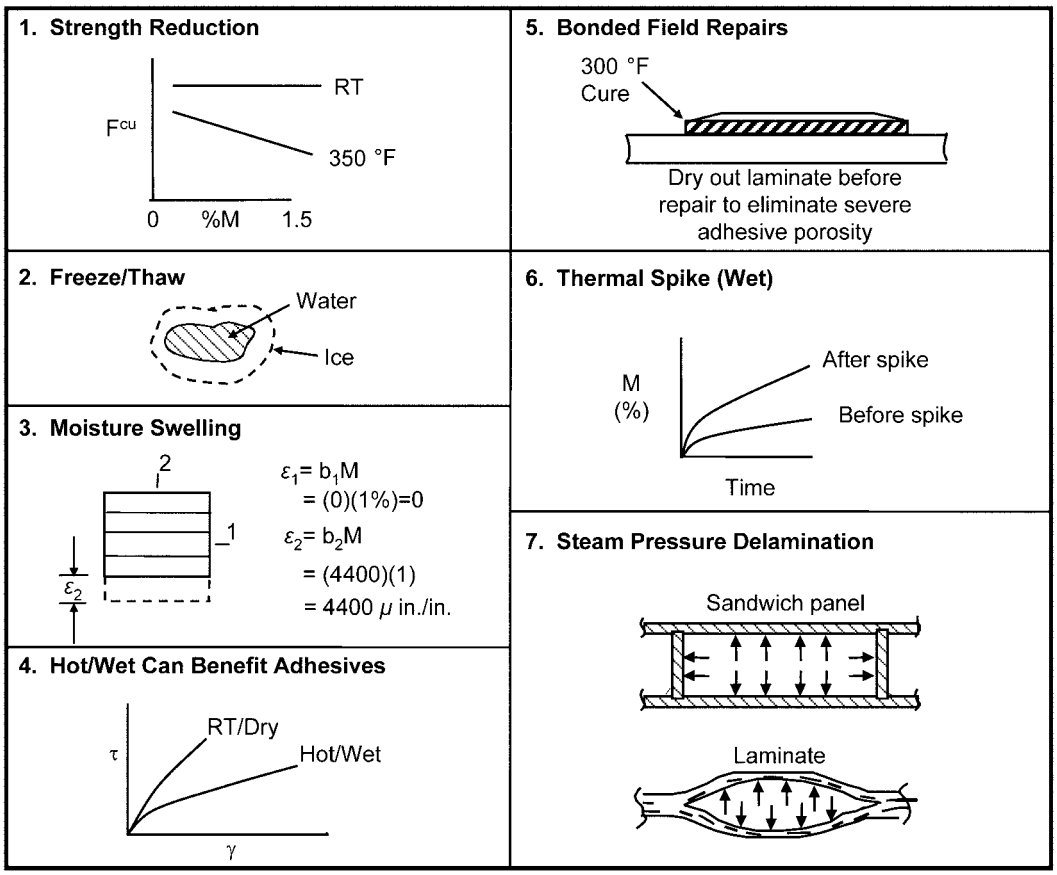


Fig. 15.1 Potential moisture effects

to matrix swelling that occurs during moisture absorption. However, provided that there is no damage such as microcracking or delaminations, this process is reversible. When the moisture content of the composite is decreased, the glass transition temperature increases and the original strength properties return.

The effects of absorbed moisture on the tensile and compressive strengths of carbon/epoxy are shown in Fig. 15.4. While moisture does not appreciably affect the fiber-dominated longitudinal tensile strength, it severely impairs the hot-wet compression strength. The most severe degradation is at the highest temperature of 350 °F (175 °C); however, epoxies are usually limited to lower usage temperature ranging 225 to 250 °F (105 to 120 °C), where the degradation is more modest but still large enough to be of concern. All matrix-dependent properties are affected. Examples of transverse tensile strength and interlaminar shear strength are shown in Fig. 15.5. Again, the degradation is more modest at the lower temperatures. In these plots, the term *wet* indicates that the material is fully saturated. This condition corresponds to a state of equilibrium with the environment at which the relative humidity (RH) is nearly 100 percent. The equilibrium moisture content at full saturation for typical epoxy composite systems ranges from about 1.0 to 2.5 percent weight gain. However, as we shall see, full saturation usually does not occur in service.

When a material is subjected to a moist environment, depending on the environment and the material, it may absorb or lose moisture. The percent moisture content or percent weight gain M is calculated by:

$$M = \frac{\text{Weight of Moist Material} - \text{Weight of Dry Material}}{\text{Weight of Dry Material}} \times 100 \qquad \text{(Eq 15.1)}$$

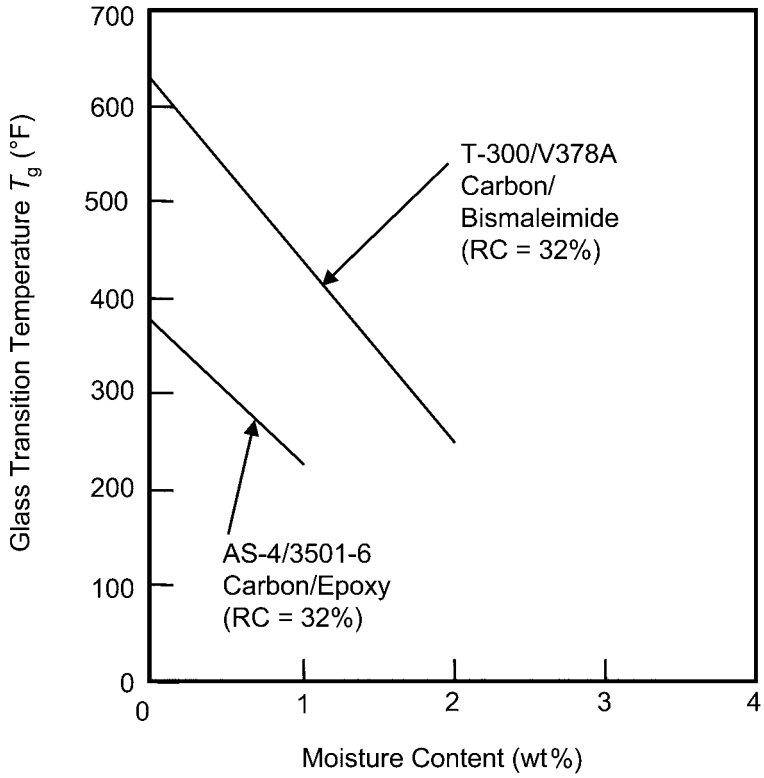


Fig. 15.2 Effect of moisture on glass transition temperature

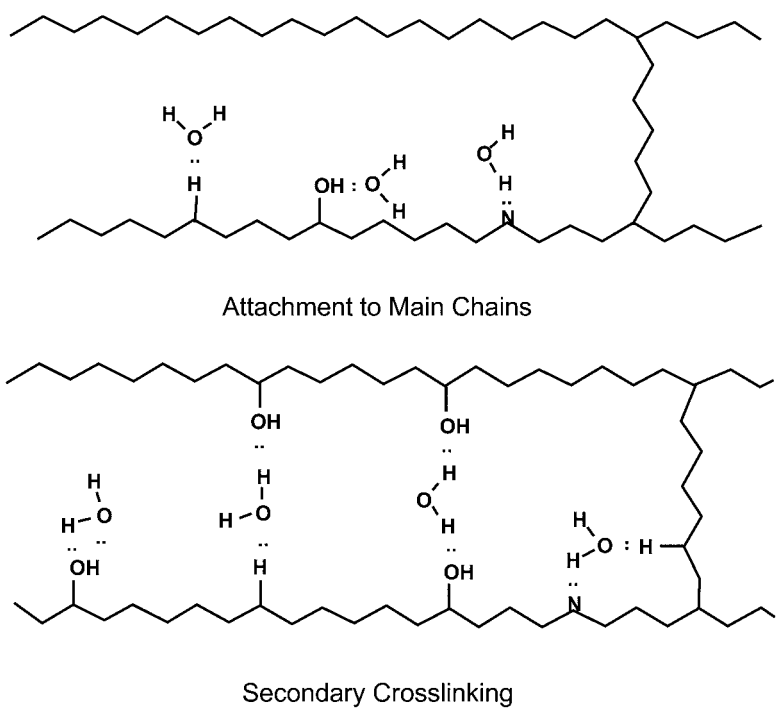


Fig. 15.3 Water attachment to molecular structure. Source: Ref 1

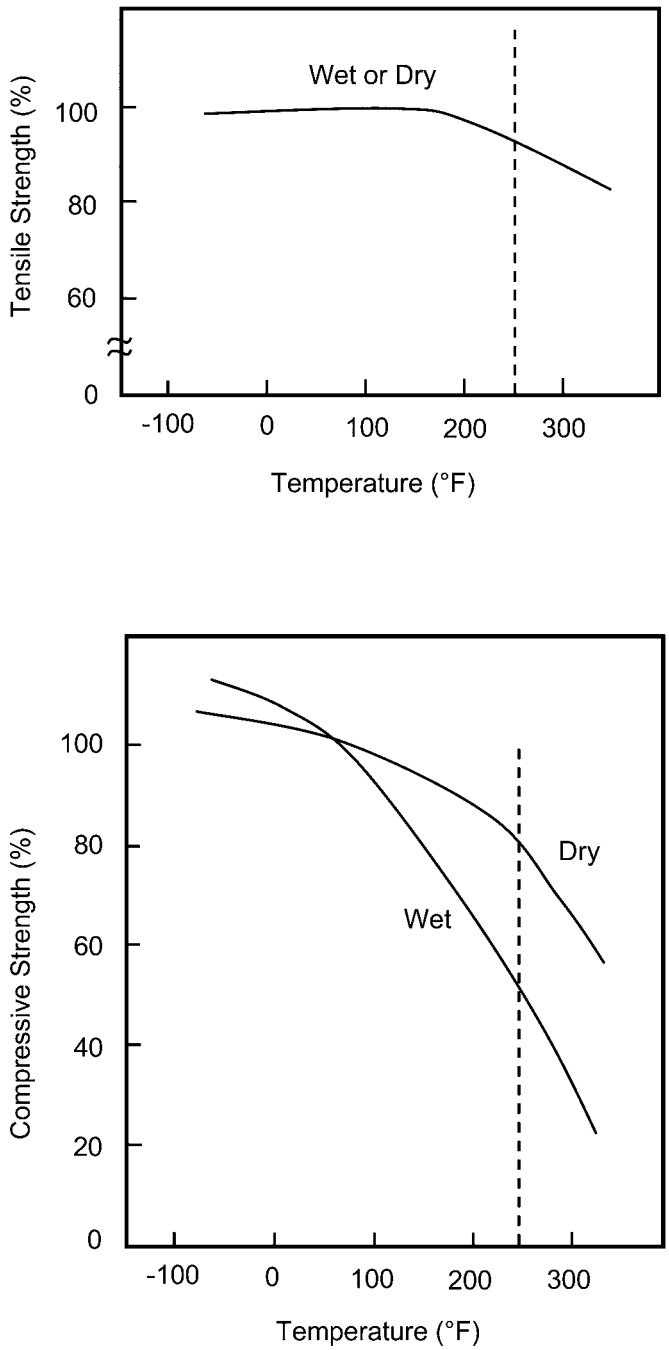


Fig. 15.4 Effects of moisture on tension and compression strength of carbon/epoxy. Source: Ref 2

Moisture can be absorbed through humid air or by immersion in liquid water. In either case, the actual absorption is controlled by diffusion. Moisture diffusion can occur in either a Fickian or non-Fickian manner. Fortunately, the diffusion behavior of most composite matrix systems is Fickian. In this type of diffusion, the moisture uptake reaches an asymptotic value as it approaches saturation or equilibrium M_{eq} (Fig. 15.6). If the weight gain of a sample exposed to constant

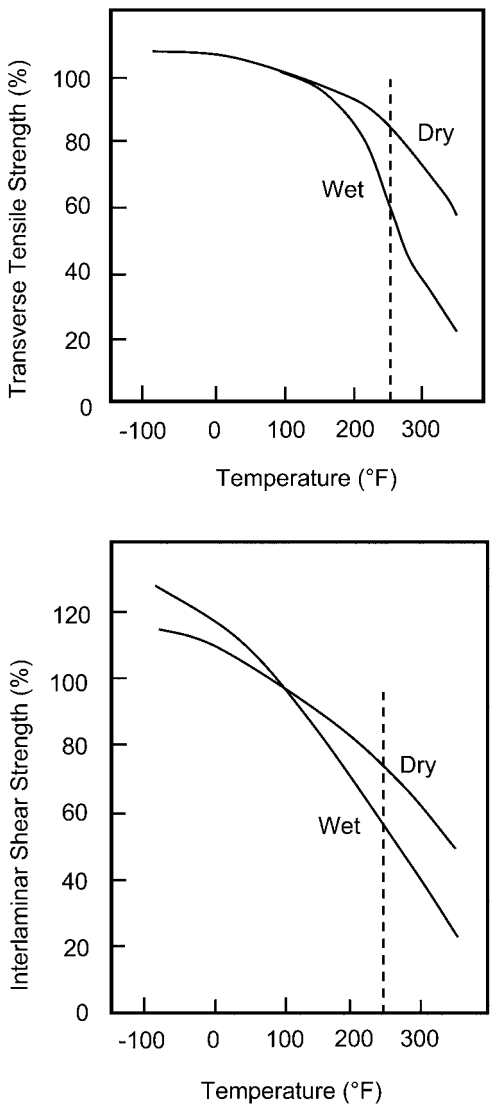


Fig. 15.5 Effects of moisture on matrix-dominated properties of carbon/epoxy. Source: Ref 2

humidity and temperature is plotted against the square root of time, there will be a linear region up to about 60 percent of the maximum moisture uptake followed by a gradual approach to a constant or asymptotic saturation level. Since composite structures are generally thin, with large surface areas and small amounts of edge, Fick's first law of diffusion states that the flux of moisture in the through-the-thickness direction x will be dependent only on the moisture concentration through the sample in that direction.

$$\text{Moisture Flux} = -D_x \frac{\partial c}{\partial x} \qquad \text{(Eq 15.2)}$$

where D_x is the diffusivity or diffusion constant and c is the concentration of moisture.

Fick's second law defines the differential equation for the diffusion process if the diffusivity D_x is independent of x:

$$\frac{\partial c}{\partial t} = D_x \frac{\partial^2 c}{\partial x^2} \qquad \text{(Eq 15.3)}$$

The diffusion constant D_x is independent of time and is assumed to be constant through the sample thickness; however, it varies exponentially with temperature according to the Arrhenius equation:

$$D_x = D_0 \exp\left(-E_d / RT\right) \qquad \text{(Eq 15.4)}$$

where D_0 is a preexponential constant, E_d is the activation energy, R is the universal gas constant, and T is the absolute temperature. An 18 °F (10 °C) increase in temperature typically doubles the diffusion rate.

Solutions to this time-dependent problem (Eq 15.3) are readily available, and considerable work has been performed in the area of moisture absorption. The most interesting feature of the solutions to Eq 15.3 relates to the magnitude of the coefficient D_x, which is a measure of the speed of moisture diffusion. In typical epoxy matrix systems, D_x is on the order of 645×10^{-8} mm^2/s (1×10^{-8} in.^{2}/s) to 645×10^{-10} mm^2/s (1×10^{-10} in.^{2}/s). Thus, the diffusion coefficient is sufficiently small that full saturation of a resin matrix composite may require months or even years, even when subjected to 100 percent RH. Equation 15.3 is usually solved using a computer program, such as the one found in Ref 3.

The maximum moisture content of many composite materials is related to the RH by:

$$\text{Maximum Moisture Uptake} = \text{k}\left(RH\right)^n \qquad (15.5)$$

where k is a constant, usually around 0.017 to 0.019, and n is between 1.4 and 1.8 for many composite materials. For a typical carbon/epoxy material with a 60 percent volume fraction, the maximum moisture uptake for exposure at 100 percent RH is around two percent.

Moisture absorption is a function of RH (Fig. 15.7). As the RH increases, the amount of absorbed moisture increases. The effect of increasing temperature on moisture absorption is illustrated in Fig. 15.8. Increasing the temperature increases the rate of moisture absorption since the diffusion constant increases with increasing

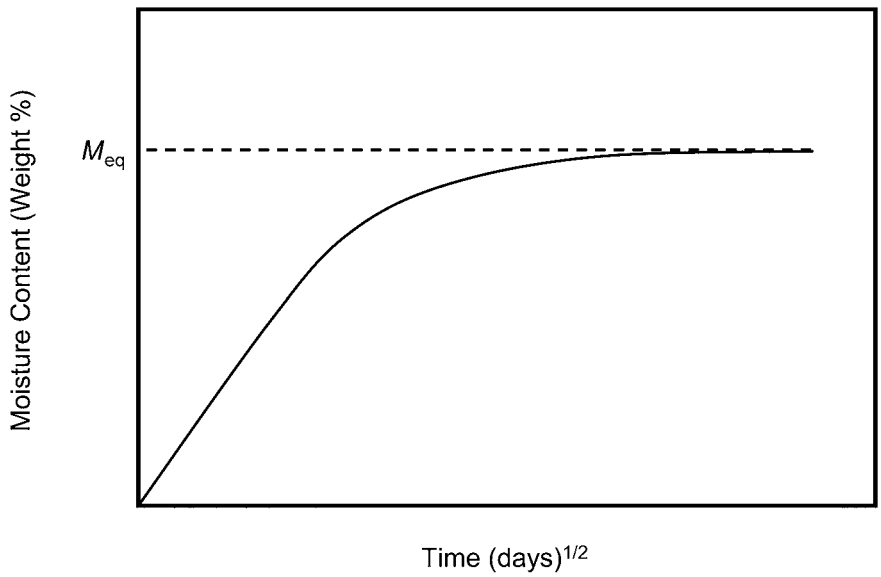


Fig. 15.6 Typical moisture absorption behavior

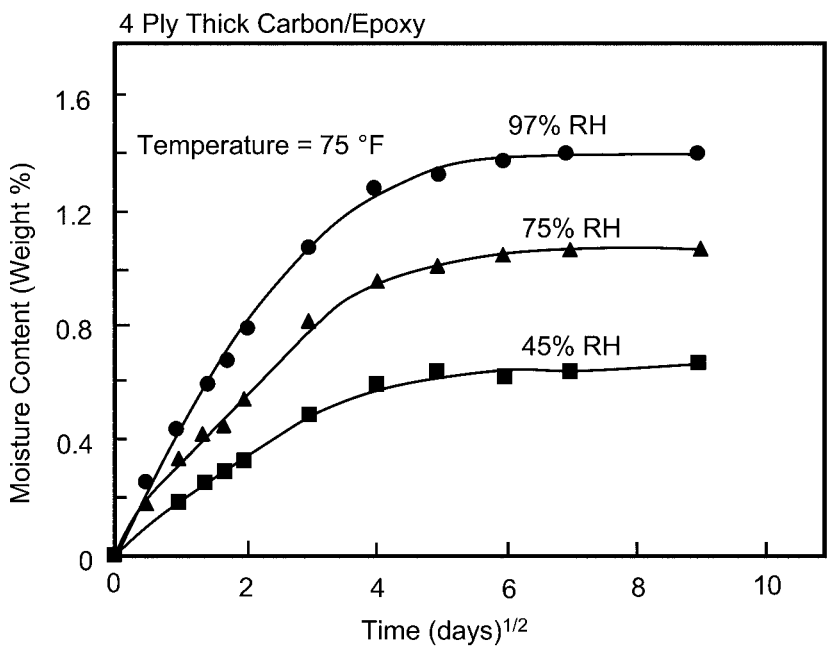


Fig. 15.7 Moisture absorption as a function of humidity. Source: Ref 4

temperature. However, while increasing the temperature accelerates the rate of moisture absorption, it does not increase the final or equilibrium moisture content (M_{eq}). In other words, the M_{eq} of the samples exposed at the two lower temperatures 73 °F and 110 °F (20 °C and 45 °C), if exposed long enough, would be the same as that of the sample exposed at 170 °F (75° C) at about 1.7 percent.

When a sample is exposed to moisture, since moisture is a diffusion-driven process, the surface plies saturate first, while the center of the

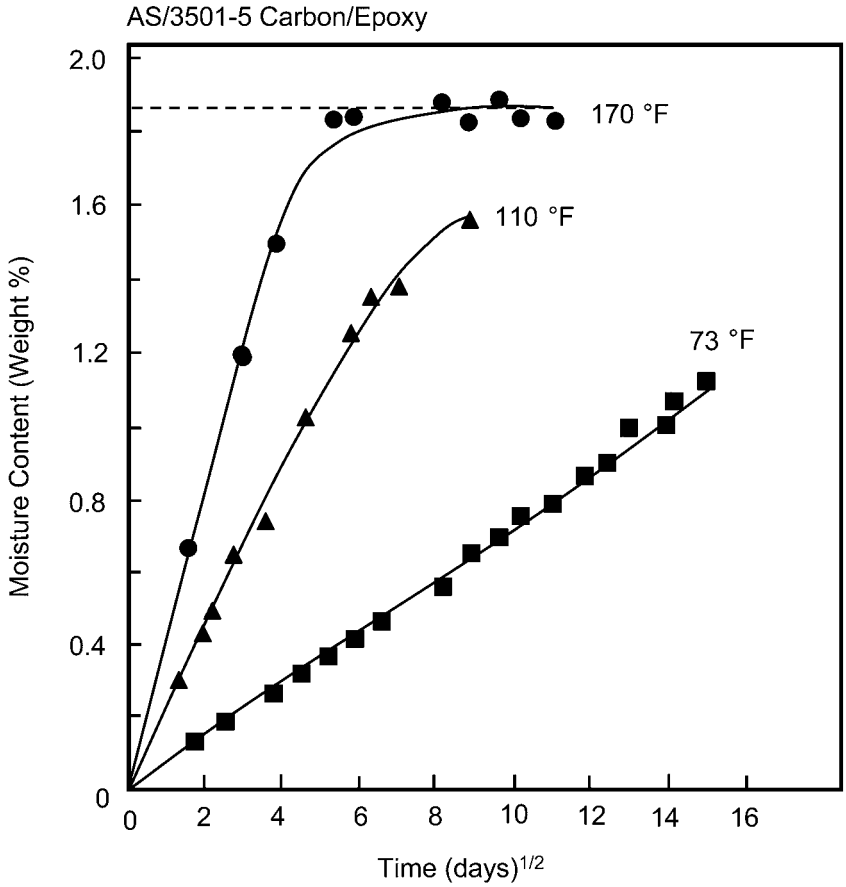


Fig. 15.8 Moisture absorption as a function of temperature

sample is still dry. The effects of sample thickness on moisture absorption are shown in Fig. 15.9. These data illustrate that as sample thickness increases, it takes longer to reach an equilibrium moisture content through the entire thickness. As shown, for a sample thickness of only 0.080 in. (2.0 mm), full saturation will not have occurred after two years of exposure, and for thicker laminates at 0.24 in. (6.1 mm), even after 50 years the specimen will not have reached equilibrium. Therefore, most thick structures will contain moisture gradients through their thickness.

To complicate the situation even further, real structures are exposed to environments in which both the temperature and humidity fluctuate. The samples in Fig. 15.10 were moisturized at 140 °F (60 °C) and 68 percent RH, and then they were demoisturized by lowering the humidity level at 140 °F (60 °C) to eight percent RH. If no structural damage is associated with the moisturization cycle, then the original dry properties will to a large extent be reestablished. However, composites exposed to multiple absorption-desorption cycles will often display more rapid moisturization than the original material.

The results of long-term outdoor environmental exposure in Malaysia are shown in Fig. 15.11. Three different types of specimens were tested. Specimens classed as “exposed” were fully exposed to solar radiation during the day, “protected” specimens were fully protected from direct incident radiation by a stainless steel plate, and “shaded” specimens were placed beneath a piece of aluminum honeycomb that restricted direct exposure to radiation to only a few hours at midday. The protected coupons had the highest moisture content, as they were not subject to direct sunlight, which dries out the composite. Also, note that decreases in weight occurred due to loss of epoxy material from the exposed surface layer caused by ultraviolet degradation. Thus, even though carbon/epoxy can absorb upward of

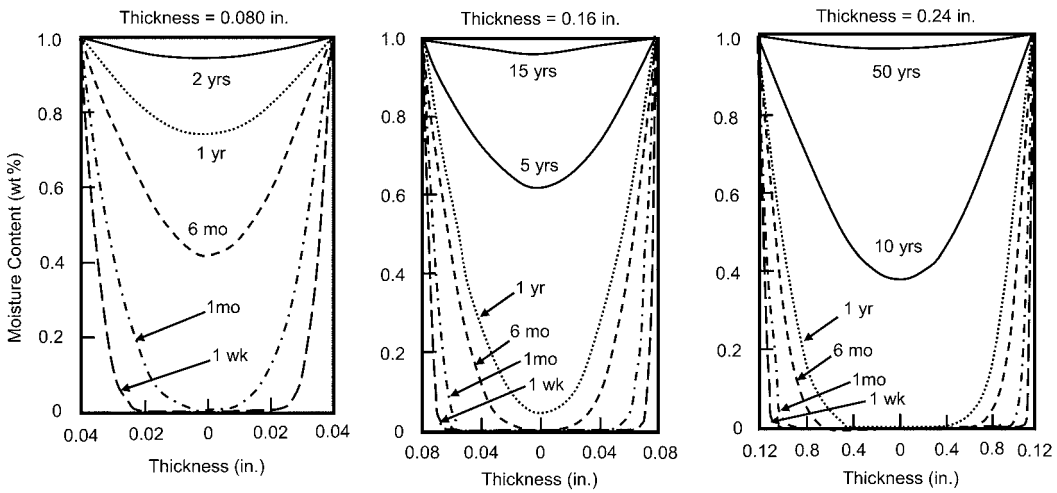


Fig. 15.9 Moisture absorption profiles as a function of thickness. Source: Ref 1

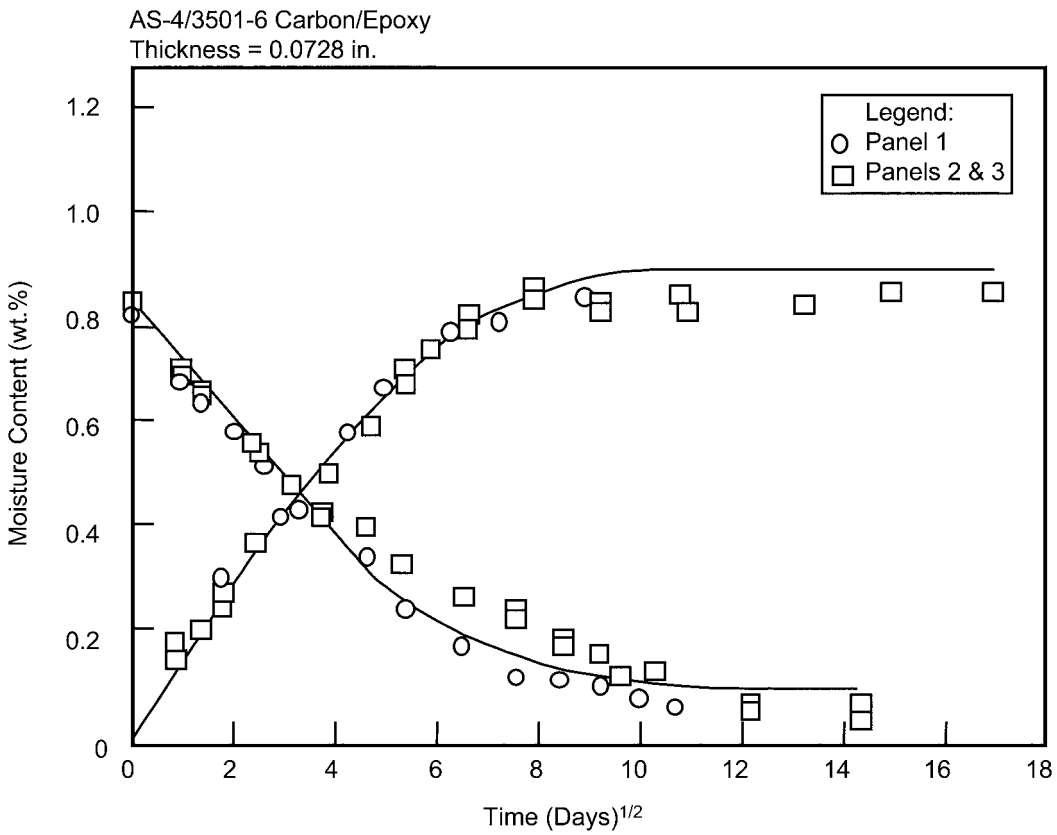


Fig. 15.10 Moisture absorption and desorption for carbon/epoxy

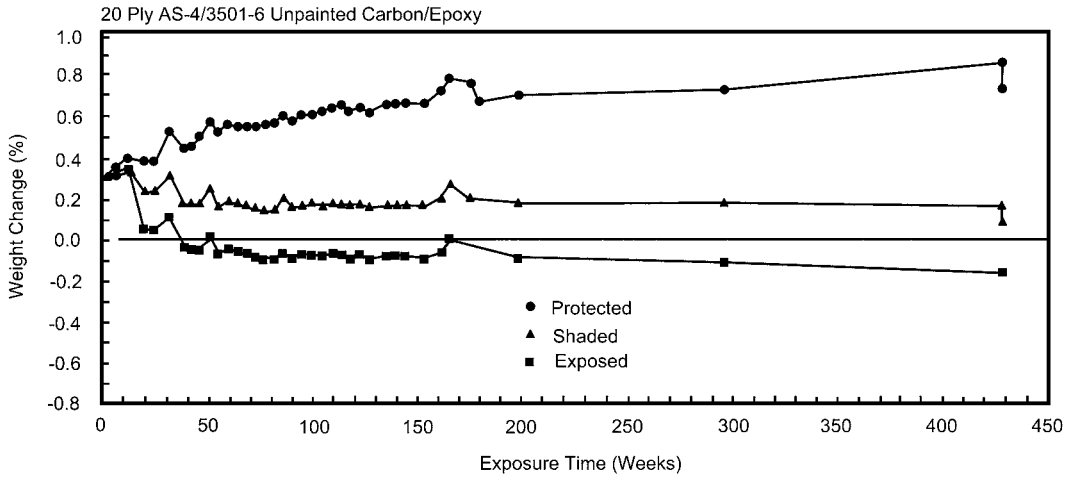


Fig. 15.11 Environmental exposure of carbon/epoxy in Malaysia. Source: Ref 5

two percent under constant-exposure humidity cabinet conditions, a real-world environment usually produces moisture absorption levels of around 1.0 percent. The absorption and desorption of moisture will occur on a continual basis for the life of a component in service as it is exposed to a changing environment.

Moisture absorption causes the matrix to swell and exert through-the-thickness strain. The coefficient of moisture expansion defines the way a volume changes during moisture absorption.

The volume change in a composite due to swelling can be approximated by the empirical relation:

$$\frac{\Delta V}{V_0} = 0.01\left[c + \frac{\Delta M}{M_0}\right]d \qquad \text{(Eq 15.6)}$$

where V_0 and M_0 represent initial volume and mass and c and d are swelling constants. For a typical epoxy resin (3501-6), the swelling constants are $c = -0.61$ and $d = 0.87$.

The type of reinforcement can substantially change the moisture absorption behavior. Carbon fibers are generally unaffected by most moisture conditions, and the interface between the fiber and resin is usually relatively stable. While glass fibers themselves are largely unaffected by moisture, surface effects can be substantial. Adhesion of the resin to the glass fiber is critical and is affected by the sizes, finishes, and binders applied. Moisture can migrate along the fiber-to-matrix interface, affecting the adhesion. The surface of the fiber can also be attacked. Aramid fibers are unusual in that they can absorb a higher weight percentage of moisture than the matrix.

One of the potential advantages of thermoplastic composite materials is that they inherently absorb less moisture than thermosets. The moisture absorption characteristics of several thermosets and thermoplastic composites are shown in Fig. 15.12. The lowest moisture levels are attained with the semicrystalline thermoplastic polyetheretherketone. The amorphous thermoplastic, high temperature amorphous (HTA), absorbs more moisture but is still better than the two thermosets. Note that while the final moisture contents of the two thermosets are similar, the bismaleimide material absorbs moisture faster than the epoxy.

The moisture absorption discussed so far has been well-behaved Fickian diffusion. However, non-Fickian behavior can occasionally occur, which can cause unusual-looking moisture absorption-desorption curves. An example is shown in Fig. 15.13. Here an anhydride curing agent was used to cure an epoxy. When the epoxy was exposed to a humid environment at 105 °F (40 °C), excess anhydride curing agent combined with the water to produce an acid that resulted in progressive degradation of the matrix. On drying, severe weight loss resulted.

Another potential moisture problem can occur if thermal spiking is experienced. Thermal spiking is the effect of exposing a composite to rapid

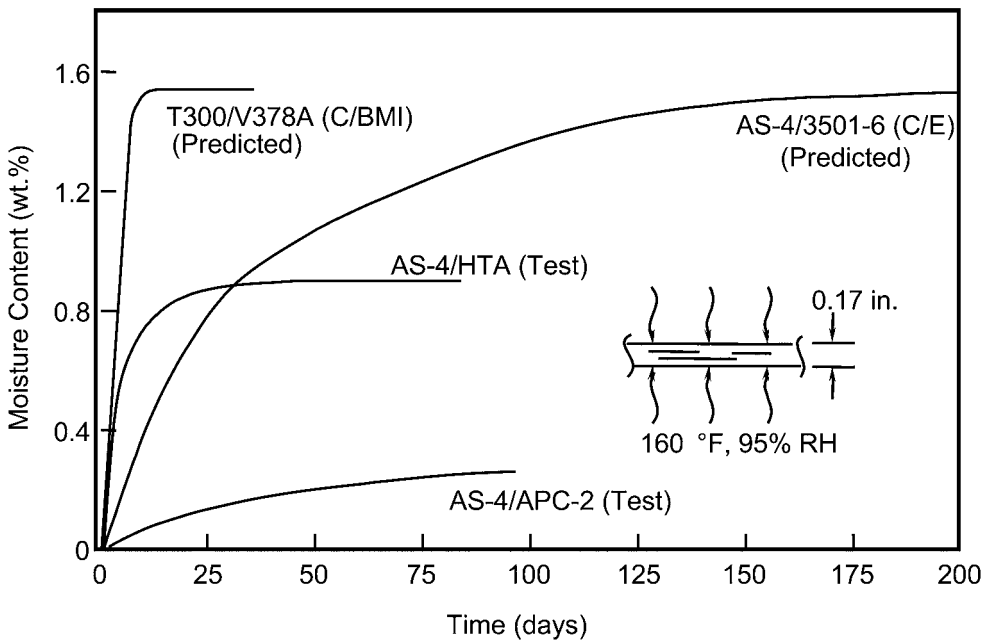


Fig. 15.12 Moisture absorption for thermosets and thermoplastics. C/BMI, carbon/bismaleimide; C/E, carbon/epoxy

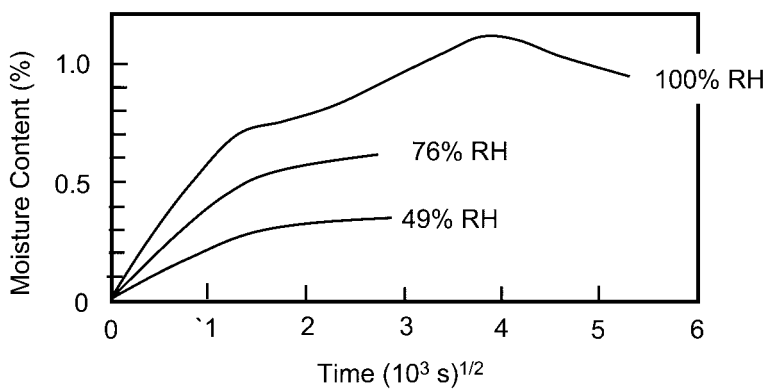


Fig. 15.13 Example of non-Fickian diffusion. Source: Ref 1

increases in temperature. Microcracks can form during rapid thermal cycles, which result in higher equilibrium moisture contents and can even result in delaminations if the temperature increases are sufficient. As shown in Fig. 15.14, the surfaces are the most vulnerable. A steam pressure delamination curve for a carbon/BMI material is shown in Fig. 15.15. When the internal pressure due to the formation of steam exceeds the flatwise or through-the-thickness tensile strength, panel delamination can occur. Thermal spikes on dry composite laminates are normally not detrimental.

Low temperatures can also have an impact on composite properties. Water trapped in cracks or delaminations can freeze when exposed to cold temperatures. Since water expands 8.3 percent in volume on freezing and has a bulk modulus three to four times greater than that of the epoxy matrix, it will create pressure within the cracks or delaminations, making them grow in size and allowing even greater amounts of moisture absorption.

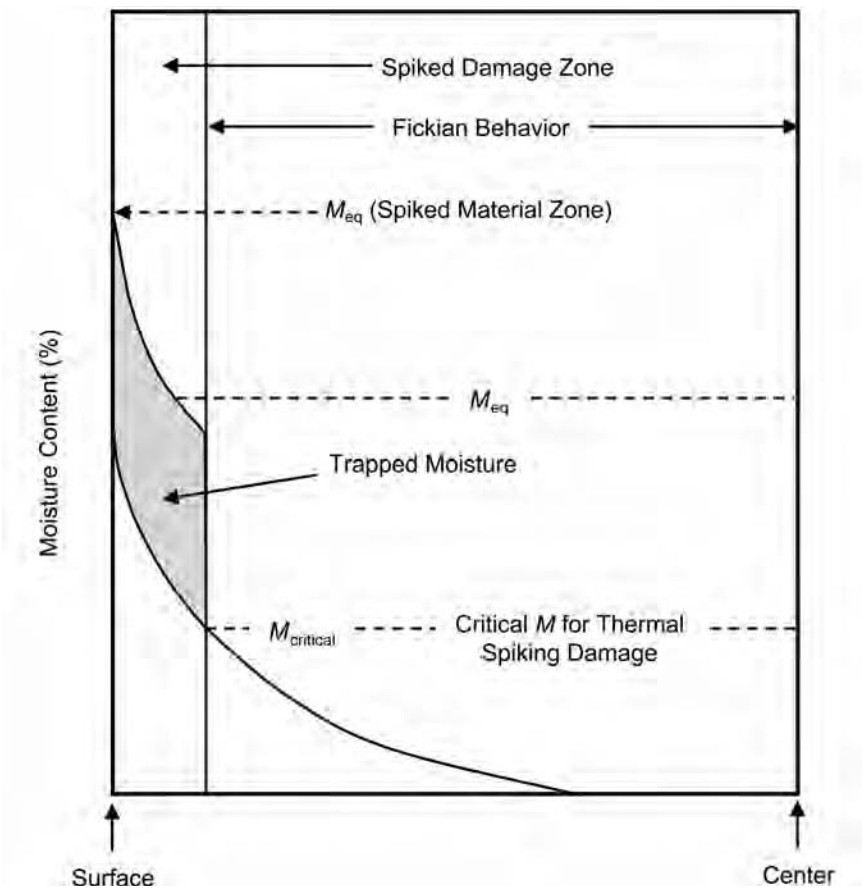


Fig. 15.14 Effects of thermal spiking on moisture absorption of carbon/epoxy. Source: Ref 6

15.2 Fluids

The resistance of thermoset and semicrystalline matrices to most aircraft fluids is good. However, amorphous thermoplastics are susceptible to a number of solvents. For example, methylene chloride, which is used in many paint strippers, will dissolve most amorphous thermoplastics. The maximum moisture contents of two thermoset composites in several aircraft fluids are shown in Table 15.1, and the maximum moisture contents of several polyester and vinyl ester E-glass composites are given in Table 15.2. Note the severe effects of antifreeze and gasoline on the sheet molding compounds. The important point to remember is that any composite should be tested for fluid resistance using the fluids that it will, or by accident can, encounter in service. Interlaminar shear testing at room and elevated temperatures is often used as a test method in fluids screening.

15.3 Ultraviolet Radiation and Erosion

Since all polymers absorb moisture to varying degrees, protective coatings such as paints provide little protection against moisture absorption. However, paint systems are useful in protecting composite structures from ultraviolet (UV) radiation. Ultraviolet radiation is the band of light from 300 to about 4000 Å. It can cause degradation through molecular weight change and crosslinking in the resin system. However, this damage is generally limited to darkening of the resin at the surface layer. Aramid fiber, in particular, is subject to UV degradation. In general, polyester resins are more resistant to UV radiation than epoxies. Standard marine paint, pigmented gel coatings, and polyurethanes have been used to prevent UV damage and weathering erosion of marine composites. Paint systems, and more robust and thicker polyurethane coatings, are useful in minimizing damage due to rain erosion, snow, and ice impact.

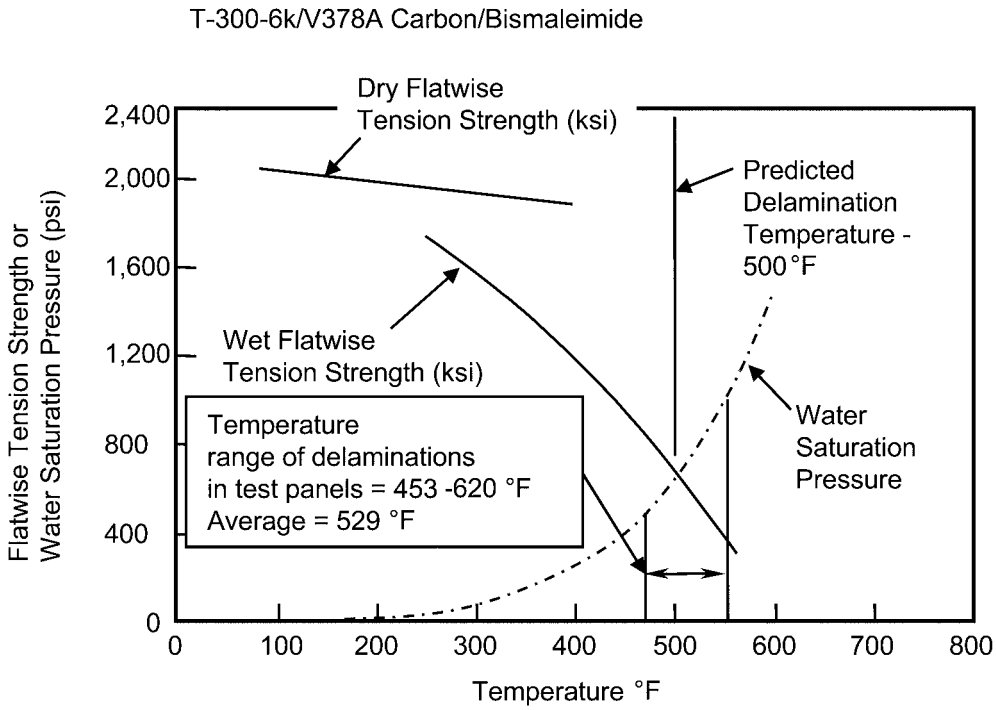


Fig. 15.15 Steam pressure delamination curve for carbon/bismaleimide

Table 15.1 Maximum absorption in carbon/epoxy immersed in aircraft fluids

	Maximum absorption, %	
Fluid	AS/3501-5 carbon/epoxy	T-300/5208 carbon/epoxy
Distilled water	1.90	1.50
Saturated salt water	1.40	1.12
No. 2 diesel fuel	0.55	0.45
Jet A fuel	0.52	0.40
Aviation oil	0.65	0.60

Source: Ref 3

15.4 Lightning Strikes

Aircraft extremities, such as the nose, tail cone, wing tips, and engine nacelles, are the most vulnerable areas for lightning attachment. Surfaces aft of the attachment points may be susceptible to swept strokes in which the lightning attaches to the structure as it sweeps over the surface. The lightning strike zones for a commercial airliner are shown in Fig. 15.16. Zone 1 areas are subject to direct lightning attachment, while Zone 2 is subject to swept attachment as a result of the direct strike. Attachments in Zone 3 areas are referred to as *indirect effects* in which voltage and/or currents induced by lightning in electrical wiring can upset or damage electrical and electronic systems. Zone 1 and 2 attachments can produce physical damage to the aircraft structure and electrical systems by burning and vaporizing aircraft surfaces. These lightning attachment mechanisms for a wing are shown in Fig. 15.17. Note that the currents are quite high, as much as 200 kA for a direct attachment. Traditional aluminum airframes conduct electrical currents readily and are able to dissipate the energy experienced during a lightning strike. However, composites either do not conduct electrical energy at all or, in the case of carbon fiber composites, conduct electricity but not nearly as well as aluminum does.

When carbon fiber thermoset composites experience a lightning strike, the temperature rises instantaneously and the resin matrix begins to break down, typically as a result of burning or pyrolysis. If the gases that the burning resins give off are trapped in the laminate, an explosive release may occur, with attendant damage to the structure (Fig. 15.18). The damage may be great enough to result in a puncture. The principal risk is structural damage, although this is normally

Table 15.2 Maximum absorption in sheet molding compounds exposed to different environments

Substance	Temperature, °F	Maximum absorption, %		
		Polyester SMC-R25	Vinyl ester SMC-R50	Polyester SMC-R50
50% RH humid air	73	0.17	0.13	0.10
	200	0.10	0.10	0.22
100% RH humid air	73	1.00	0.63	1.35
	200	0.30	0.40	0.56
Distilled water	73	3.60	–	–
	122	3.50	–	–
Salt water	73	0.85	0.50	1.25
	200	2.90	0.75	1.20
No. 2 diesel fuel	73	0.29	0.19	0.45
	200	2.80	0.45	1.00
Lubricating oil	73	0.25	0.20	0.30
	200	0.60	0.10	0.25
Antifreeze	73	0.45	0.30	0.65
	200	4.25	3.50	2.25
Gasoline	73	3.50	0.25	0.60
	200	4.50	5.00	4.25

Source: Ref 3

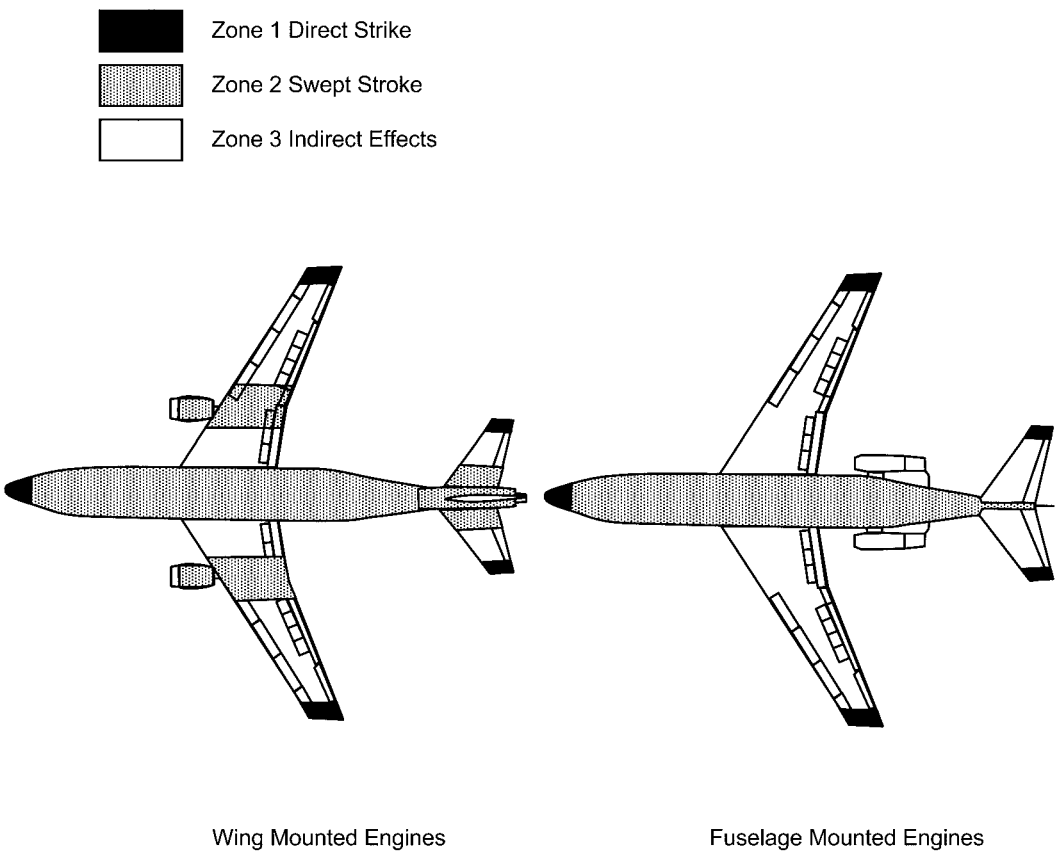


Fig. 15.16 Lightning strike zones on commercial airliners. Source: Ref 7

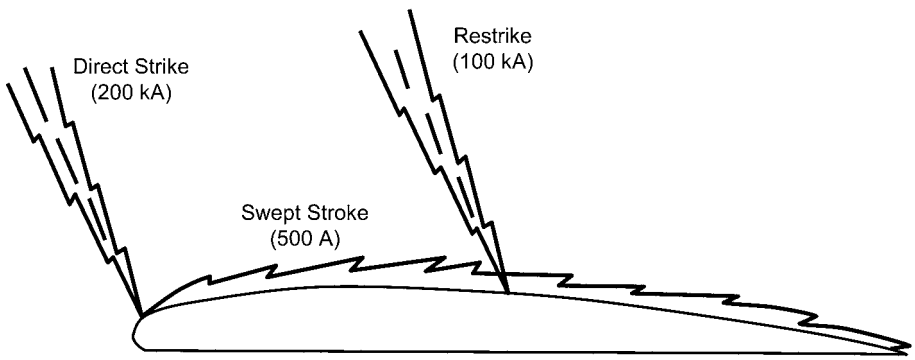


Fig. 15.17 Lightning strike on wing. Source: Ref 7

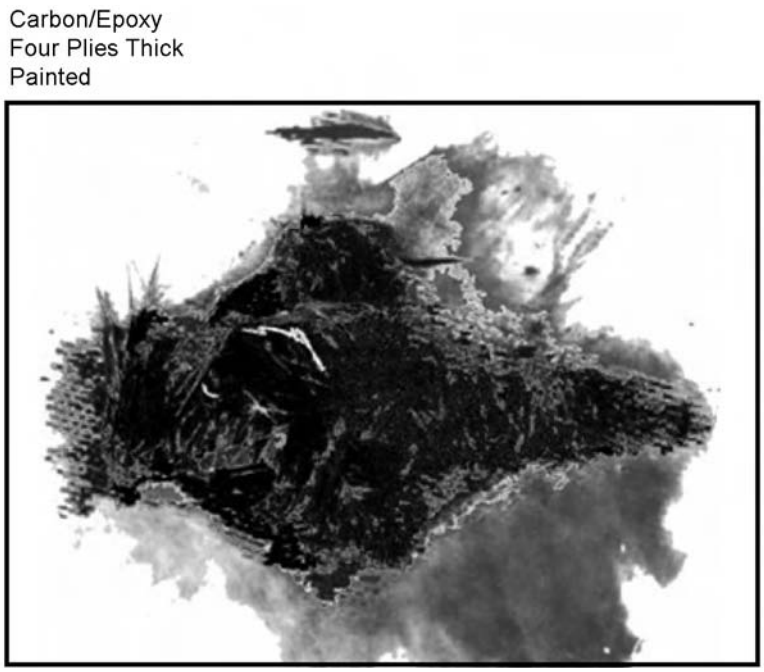


Fig. 15.18 Lightning strike damage of carbon/epoxy laminate

local to the puncture, especially if the punctured skin is comprised of cloth plies. Unidirectional tape ply laminates may allow damage to propagate further, at least on the surface ply.

A conductive coating can be applied to the exterior surfaces of composites to prevent electric field penetration and puncturing and to conduct lightning currents. Protective materials include arc or flame-sprayed metals, woven wire fabrics, expanded metal foils, aluminized fiberglass, nickel-plated aramid fiber, and metal-loaded paints. All of these coatings are applied to the exterior surface of a composite skin, and there should be only one layer of protective material. When applying lightning protection materials to carbon fiber composites, one has to make sure that the carbon fibers will not cause galvanic corrosion to the metal protection material.

Some weight penalty is always associated with lightning protection materials. The interwoven wires in carbon/epoxy have the least impact, while the weights of other materials are dependant on thicknesses and adhesion methods. Wire fabric alone weighs about 2 lb/100 sq ft

(0.1 kg/m^2) and, when cocured, the total weight is about 3 lb/100 sq ft (0.15 kg/m^2). Secondary bonding with additional adhesive can increase the weight to 5 lb/100 sq ft (0.25 kg/m^2). A summary of typical weight penalties that may be expected is given in Table 15.3.

15.5 Thermo-Oxidative Stability

One of the advantages of polyimides like PMR-15 is that they are capable of operating at about twice the temperature of epoxy-based composites, in the range of 500 to 600 °F (260 to 315 °C). However, with extended aging at these temperatures, their thermo-oxidative stability (TOS) becomes an issue. Thermal-oxidative aging can result in embrittlement, changes in the glass transition temperature, and microcracking ultimately leading to reductions in stiffness, strength, and fracture toughness, as shown for compression strength in Fig. 15.19. Matrix degradation is usually measured in terms of weight loss. A primary measure of the TOS of PMR-15 and other high-temperature composite materials is the percentage weight loss as a function of aging time and temperature (Fig. 15.20).

Table 15.3 Weights of lightning protection systems

Coating material	Weight, lb/100 ft^2
Interwoven wire (aluminum)	0.024
Expanded aluminum foil	1.6–6 (2.9 typical)
Woven wire mesh	2.5–5
Wire fabric	3–5
Thermal spray (aluminum)	5.75–8
Aluminum foil (solid)	8.5
Conductive paint (silver)	8

Both the fiber and the resin matrix can be affected. The early polyacrylonitrile-based carbon fibers contained significant alkali content and exhibited poor TOS. The sodium and potassium on the fiber surfaces catalyzed air oxidation of the fibers at elevated temperatures. More recently produced carbon fibers have much lower sodium contents and greatly improved TOS.

The dominant degradation mechanism for the carbon/polyimides is oxidation of the matrix at the laminate edges. Photomicrographic examination reveals that the degradation occurs as a

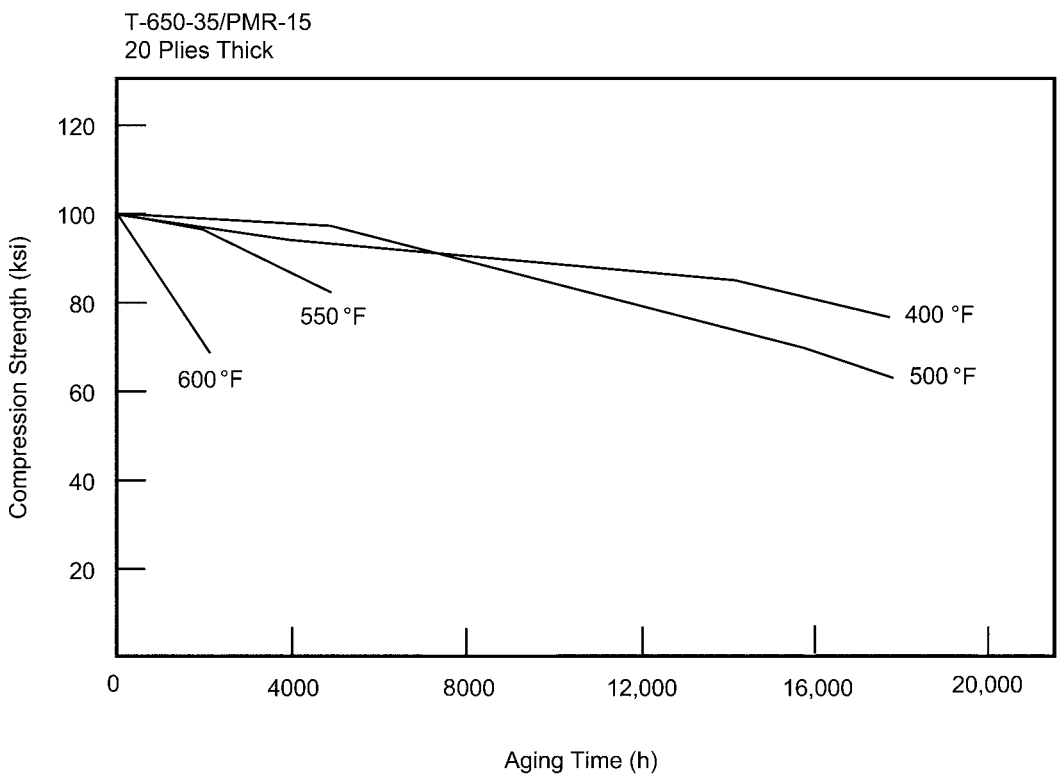


Fig. 15.19 Compression strength versus aging time for PMR-15. Source: Ref 8

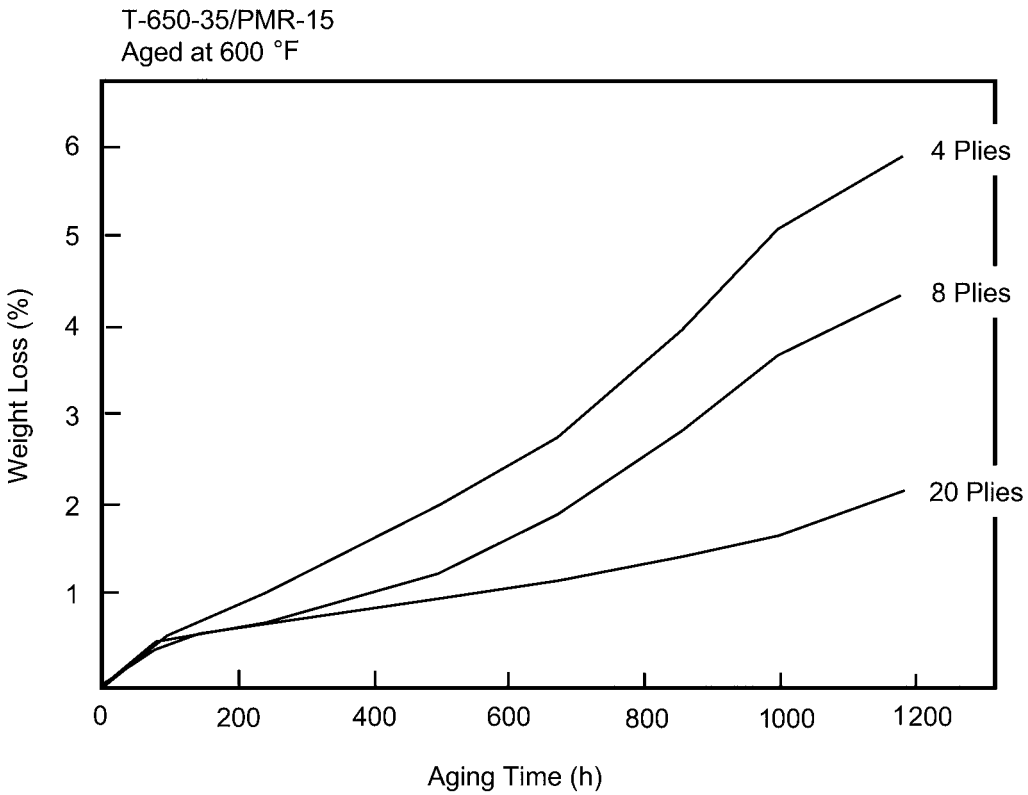


Fig. 15.20 Weight loss versus aging time for PMR-15 at 600 °F. Source: Ref 8

thin surface layer that develops near the specimen edges and grows inward with thermal aging. The surface layer develops matrix microcracking and voids and has a chemical composition that is somewhat different from that of the inner bulk matrix. The major mechanism associated with the weight loss is believed to be the release of a reaction volatile component (cyclopentadiene), followed by oxidation resulting in the formation of the surface layer. As a result of the composition differences between the surface layer and the bulk matrix, surface tensile stresses develop that result in matrix cracking. Machined edges are the most susceptible to attack; in particular, those that have the fibers perpendicular to the cut edges allow the cracks to grow inward in the composite and expose more resin and fiber surfaces to degradation. For cut surfaces with the fibers parallel to the cut surfaces, the fibers act as a protective barrier for the matrix resin.

Embrittlement of the surface layer induced by thermal oxidation leads to density increase and weight loss; both processes contribute to shrinkage of the oxidized layer, which generates tensile stresses and possibly spontaneous cracks. The crack faces provide additional diffusion surfaces and accelerate the material degradation and growth of the oxidation layer. Severe surface oxidation degradation results in the formation of fiber-matrix disbonds coalescing into transverse surface cracks (Fig. 15.21). These cracks not only reduce strength but also create enhanced pathways for oxygen to penetrate deeper into the composite. Microcracking can also accelerate moisture absorption and desorption, and can make the laminate subject to steam pressure delamination if thermal spiking occurs.

15.6 Heat Damage

The material system AS-4/3501-6 carbon/epoxy is normally used in the temperature range of 225 to 250 °F (105 to 120 °C). However, it can be exposed to higher temperatures in service, for example, due to hot gas blasts from engine exhausts. The effects of elevated temperatures on the unidirectional and cross-plied interlaminar shear

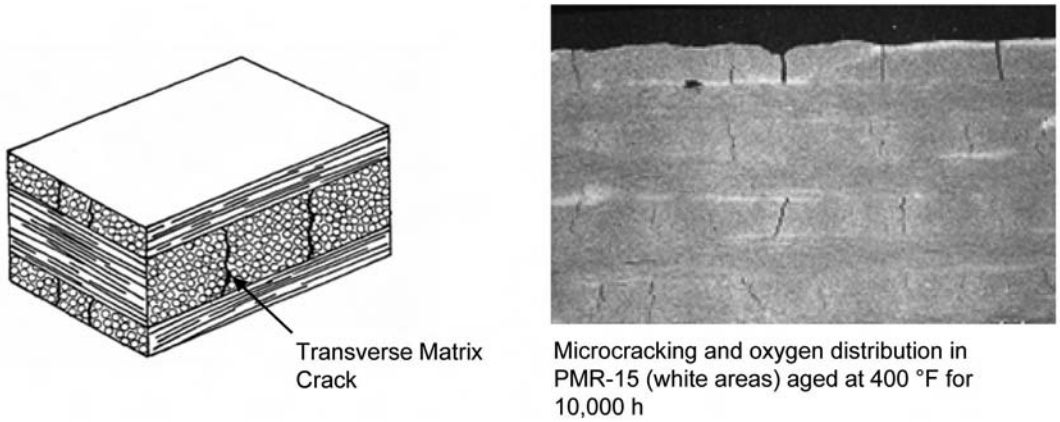


Fig. 15.21 Matrix microcracking and oxidation. Source: Ref 9

strengths are shown in Fig. 15.22. This particular material is fairly stable for up to one hour at 500 °F (260 °C) and then starts to degrade rapidly in the 500 to 600 °F (260 to 315 °C) range, with longer times causing greater strength loss. The effects of exposure to 550 °F (285 °C) on tensile and compression strengths are shown in Fig. 15.23.

15.7 Flammability

Composite structures contain two components, the fibers and the resin, which behave differently in a fire, depending on their respective thermal stabilities. All the fibers used for composites except ultrahigh molecular weight polyethylene are relatively nonflammable; however, at high temperatures they soften, char, or melt, and their mechanical strength is reduced. Composite laminates tend to burn in layers. When heated, the resin in the first layer degrades, and any combustible products formed are ignited. The heat penetrates the adjacent fiber layer and then penetrates further, reaching the underlying resin, causing it to degrade; any products formed will then move to the burning zone through the fibrous char. A laminate will burn in distinct stages as the heat penetrates subsequent layers and degradation products move to the burning zone through the fibrous layers. In general, the thickness of a structure can affect the surface flammability characteristics, depending on the external heat flux. At lower heat fluxes, thicker laminates burn more slowly, but at higher heat fluxes, thick and thin laminates burn at about the same rate.

Studies indicate that ranking of fire resistance of thermoset resins is:

Phenolic > Polyimide > Bismaleimide > Epoxy > Vinyl Esters > Polyesters

Cured phenolic resins do not ignite easily because of their high thermal stability and high charring tendency on decomposition. The inherent fire-retardant behavior of the phenolics is due to the char-forming tendency of their crosslinked chemical structure. Since they contain a large proportion of aromatic structures, phenolic resins carbonize in a fire and self-extinguish once the source of fire is removed. Indeed, as a result of their charring characteristics, phenolic composites are used for ablative exhaust nozzles for rockets and as a starting material in the production of carbon-carbon composites. They basically encapsulate themselves in char and therefore do not produce much smoke. The principal volatile decomposition products are methane, acetone, carbon monoxide, propanol, and propane. Polyimides are also characterized by high char formation on pyrolysis, low flammability, and low smoke production.

Epoxy and unsaturated polyesters, on the other hand, carbonize less than phenolics and continue to burn in a fire, and structures based on these aromatic compounds produce more smoke. Crosslinked epoxy resins are combustible, and their burning is self-supporting. Because of their structure, polyesters flame readily, sometimes vigorously after ignition. Unsaturated polyesters, crosslinked with styrene, burn with heavy

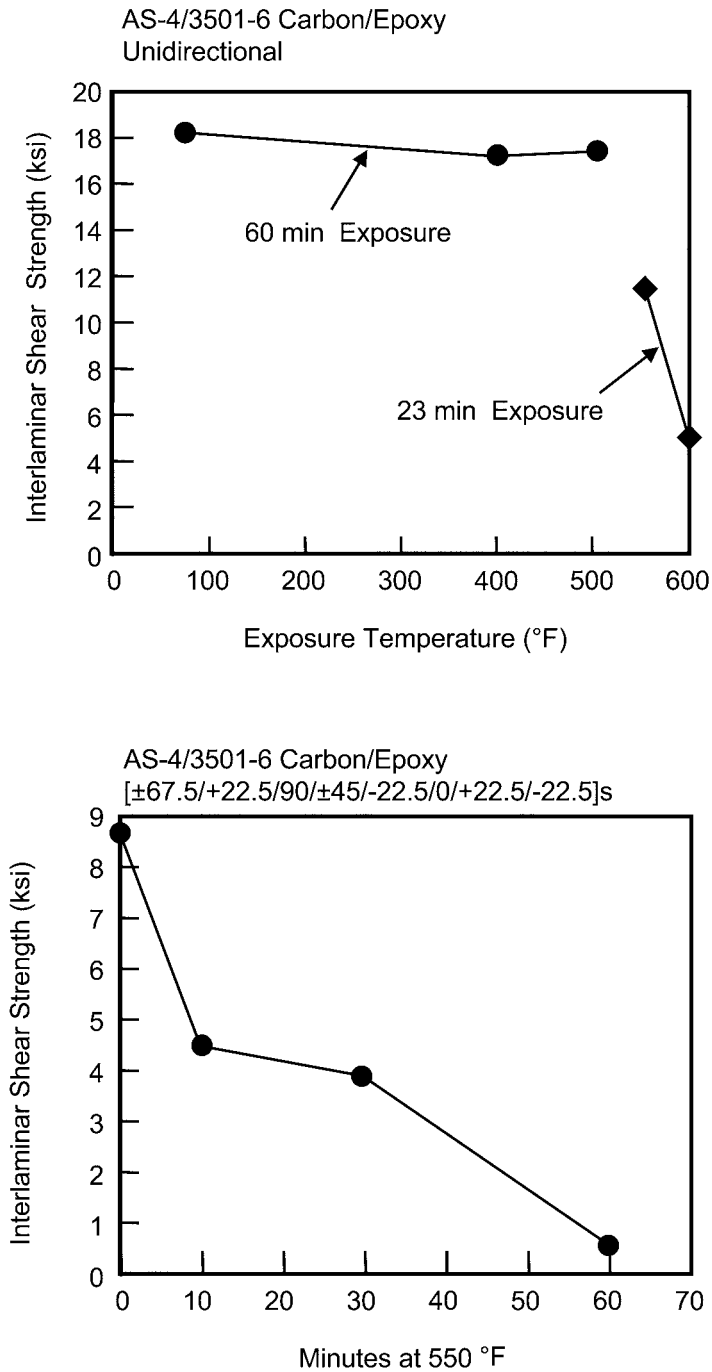


Fig. 15.22 RT interlaminar shear strength after exposure to elevated temperature

sooting. The burning behavior of vinyl esters falls between that of polyester and epoxy resins.

For a flame-retarding thermoset matrix, reactive additive agents are generally used. If flame-retardant chemicals, which are compatible with both fibers and resin matrix, are selected, the effect can be synergistic. Char-forming agents seem to be the best choice, and there are commercially available resins that improve the flame-retardance properties. The flame resistance of

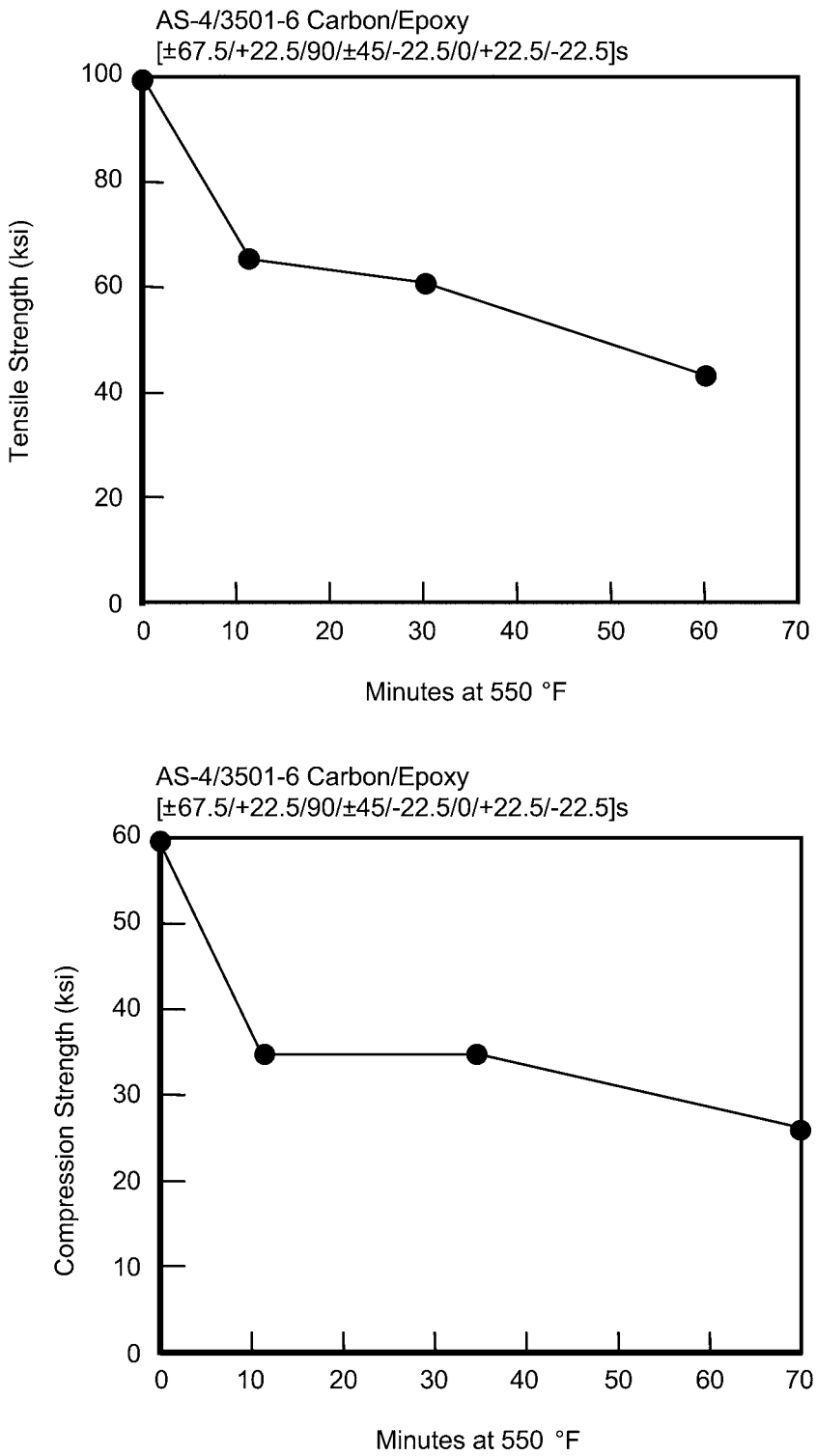


Fig. 15.23 RT tension and compression strength after exposure to 550 °F

epoxy and other thermoset polymers, such as polyesters, can be improved by using flame retardants such as aluminum oxide trihydrate, halogenated compounds in combination with antimony oxide, and phosphorus and phosphorus-halogen compounds.

Thermoplastics soften when heated. In a fire, such materials can soften enough to flow under their own weight and drip or run. The extent of dripping depends on such factors as the thermal environment, the polymer structure, the molecular weight, and the presence of additives and fillers. Dripping can increase or decrease the fire hazard, depending on the fire situation. With small ignition sources, removal of heat and flame by the dripping away of burning polymer can protect the rest of the material from the spreading flame. In other situations, the flaming molten polymer might flow and ignite other materials.

REFERENCES

1. A.R. Bunsell and J. Renard, *Fundamentals of Fibre Reinforced Composite Materials*, Institute of Physics Publishing, 2005
2. Macromechanics Analysis of Laminate Properties, *ASM Handbook*, Vol 21, *Composites*, ASM International, 2001
3. G.S. Springer, *Environmental Effects on Composite Materials*, Vol I, Technomic Press, 1981
4. C.H. Shen and G.S. Springer, Moisture Absorption and Desorption of Composite Materials, *J. Compos. Mater.*, Vol 10 (No. 2), 1976
5. R. Vodicka, B. Nelson, J. van den Berg, and R. Chester, "Long-Term Environmental Durability of F/A-18 Composite Material," DSTO-TR-0826, Defense Science and Technology Organisation, 1999
6. G. Clark, D.S. Saunders, T.J. van Blaricum, and M. Richmond, Moisture Absorption in Graphite/Epoxy Laminates, *Compos. Sci. Technol.*, Vol 39 (No. 355), 1990
7. M.C.Y. Niu, *Composite Airframe Structures*, 2nd ed., Hong Kong Conmilit Press Limited, 2000
8. K.J. Bowles, "Thermal and Mechanical Durability of Graphite-Fiber-Reinforced PMR-15 Composites," Technical Memorandum 113116/Rev 1, National Aeronautics and Space Administration, July 1998
9. K.J. Bowles, L. McCorkle, and L. Ingrahm, "Comparison of Graphite Fabric Reinforced PMR-15 and Avimid N Composites After Long Term Isothermal Aging at Various Temperatures", NASA/TM-1998-107529, National Aeronautics and Space Administration, Feb 1998

SELECTED REFERENCES

- A. Baker, S. Dutton, and D. Kelly, *Composite Materials for Aircraft Structures*, 2nd ed., American Institute of Aeronautics and Astronautics, 2004
- B.K. Kandola and A.R. Horrocks, Composites, *Fire Retardant Materials*, CRC Press, 2000
- D.R. Ruffner, Hygrothermal Behavior, *ASM Handbook*, Vol 21, *Composites*, ASM International, 2001
- G.A. Schoeppner, G.P. Tandon, and E.R. Ripberger, Anistropic Oxidation and Weight Loss in PMR-15 Composites, *Composites Part A, Applied Science and Manufacturing*, Vol 38, 2007, p 890–904
- G.P. Tandon, K.V. Pochiraju, and G.A. Schoeppner, Modeling of Oxidative Development in PMR-15 Resin, *Polym. Degradation Stab.*, Vol 91, 2006, p 1861–1869
- A.F. Whitaker, M.M. Finckenor, H.W. Dursch, R.C. Tennyson, and P.R. Young, Environmental Effects on Composites, *Handbook of Composites*, Chapman & Hall, 1982

Copyright © 2010, ASM International®
All rights reserved.
www.asminternational.org

CHAPTER 16

Structural Analysis

STRUCTURAL ANALYSIS deals with stresses, strains, and deformations in engineering structures subjected to mechanical and thermal loads. The analysis of composite structures is more complicated than that of conventional metallic structures. While metallic structures can usually be treated as isotropic materials in which the properties do not depend on orientation, composite materials are not homogeneous and are anistropic in nature. In this chapter, we will give a brief introduction to lamina and laminate analysis. Lamina or ply analysis will be addressed first, initially for a unidirectional ply and then for plies oriented an angle to the loading axis. Once the properties of the plies are determined, classical lamination theory can then be used to determine the response of a laminate to external loads and moments. The calculations for ply and laminate analysis are tedious, time-consuming, and prone to human error. Computer programs are therefore generally used to conduct calculations, so only a cursory introduction is given here. Much more extensive treatment of composite structural analysis can be found in the references listed at the end of this chapter. Since composite laminates are normally thin compared to their length and width and are loaded in plane stress conditions, the emphasis will be on in-plane loading.

16.1 Lamina or Ply Fundamentals

Consider the single ply shown in Fig. 16.1. Two right-hand coordinate systems are shown. The 1-2-3 system is known as the *principal material axes system*, with the 1-direction parallel or longitudinal to the fiber direction (zero-degree) and the two-direction perpendicular or transverse to the fiber direction (90-degree). The second system, represented by *x*-*y*-*z*, is the structural loading direction or the direction in which loads are applied to the ply. The angle θ between the *x*-axis and the 1-axis is called the *fiber orientation angle*. By convention, the sign of the angle depends on the right-hand coordinate system that is specified. If the 1- and *z*-axes point vertically upward from the ply plane, then θ is positive when measured in a counterclockwise direction from the positive *x*-axis. However, if the *z*-axis is oriented downward from the ply plane, then θ is measured clockwise from the positive *x*-axis. For a zero-degree ply, the principal material axis 1 is parallel to the loading axis *x*, while for a 90-degree ply, the principal material axis 1 is at a 90-degree angle to the structural axis. Composite plies and laminates possess three mutually orthogonal planes of symmetry and are known as *orthotropic*. Under plane-stress conditions, the stresses in the material axes are denoted as σ_{11}, σ_{22}, and τ_{12}, with the associated strains denoted as ε_{11}, ε_{22}, and γ_{12}.

Such ply properties as tensile modulus, shear modulus, and Poisson's ratio are denoted by two subscripts, as illustrated in Fig. 16.2. The first subscript represents the direction of the outward normal to the plane in which the stress component acts, while the second subscript represents the direction of the stress component. For example, the shear stress component τ_{xy} operates in the *y*-direction and the *x* denotes the outward normal to the *xy* plane. Composite laminates constructed of unidirectional plies are almost always loaded in plane stress conditions, that is, in the 1-2 plane. Loading in the 3- or *z*-direction can be catastrophic, as there are no fibers parallel to this direction to carry the load, only the relatively weak matrix.

Since the mechanical behavior of an isotropic material is independent of the direction of shear stresses, the sign convention for shear stresses

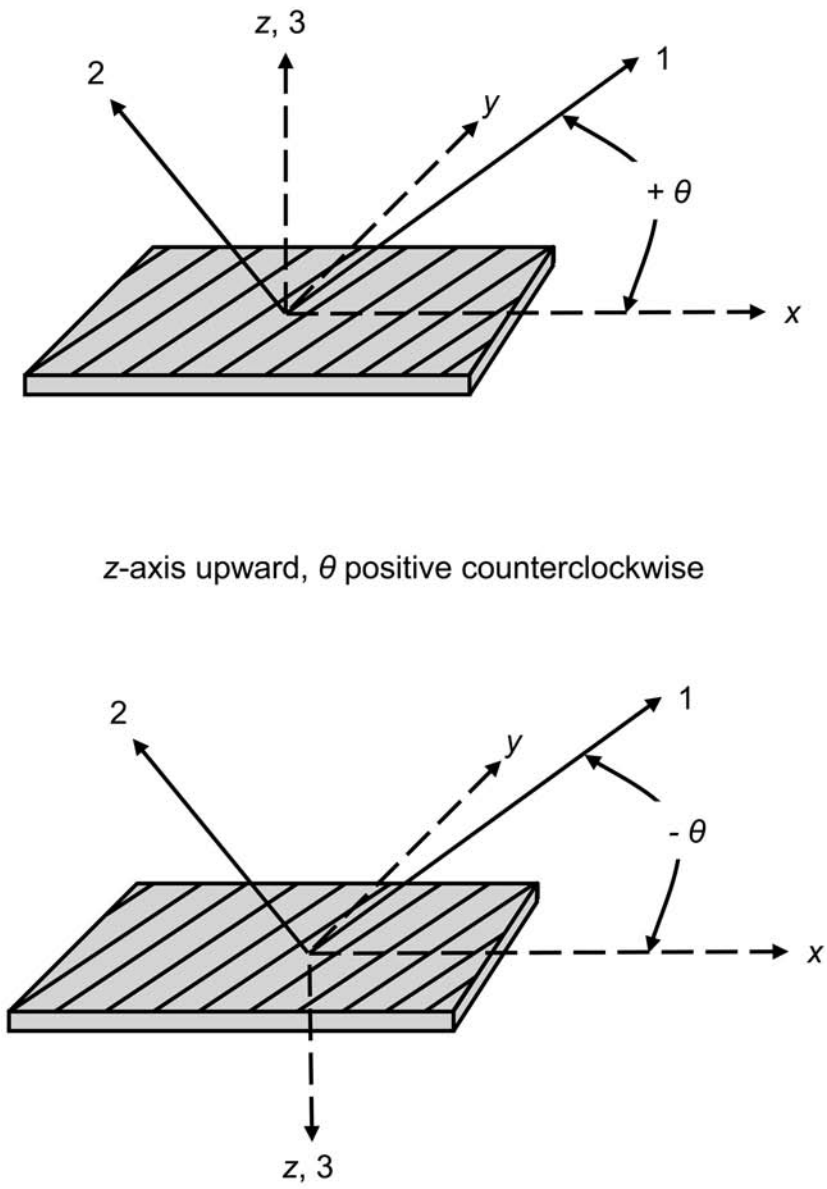


Fig. 16.1 Material and structural coordinate systems

and strains does not matter for an isotropic material. This is not the case for an orthotropic composite material. As shown in Fig. 16.3, for a positive shear stress, the maximum tensile stress is parallel to the fiber direction and is supported by the strong fibers. However, if the shear stress is negative, the maximum tensile stress is perpendicular to the fiber direction and the much

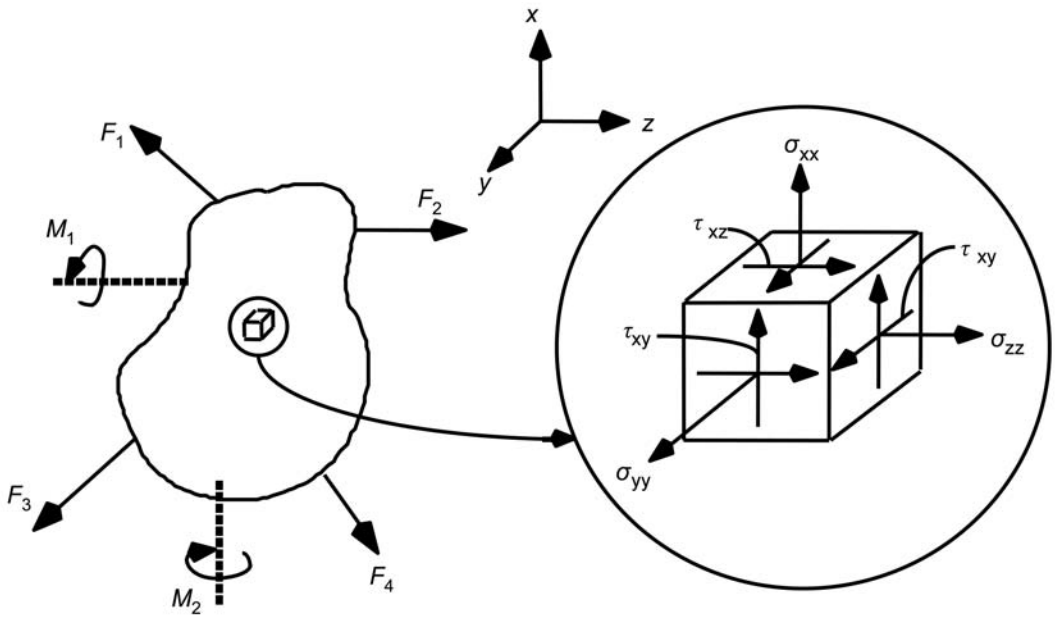


Fig. 16.2 Stress-strain notation

weaker matrix must support the load. Thus, a positive shear stress leads to a higher load-carrying capability than a negative shear stress.

Since real laminates are composed of many plies oriented at different angles, it is important to be able to calculate the stress-strain relationships of the off-axis ply. Once the elastic constants of both the on-axis and off-axis plies are obtained, they may be used to predict the overall laminate response using classical lamination theory. As shown in Fig. 16.1, angle θ is measured from the *x*-axis to the 1-axis. The stresses in the structural axes (σ_{xx}, σ_{yy}, and τ_{xy}) can be obtained from those in the material axes (σ_{11}, σ_{22}, and τ_{12}) by:

$$\begin{Bmatrix}\sigma_{xx}\\ \sigma_{yy}\\ \tau_{xy}\end{Bmatrix}=\begin{bmatrix}m^2 & n^2 & -2mn\\ n^2 & m^2 & 2mn\\ mn & -mn & m^2-n^2\end{bmatrix}\begin{Bmatrix}\sigma_{11}\\ \sigma_{22}\\ \tau_{12}\end{Bmatrix} \qquad \text{(Eq 16.1)}$$

where $m = \cos\theta$ and $n = \sin\theta$.

It is also possible to transform the stress from the structural axes (σ_{xx}, σ_{yy}, and τ_{xy}) to the material axes (σ_{11}, σ_{22}, and τ_{12}). This can be accomplished as follows:

$$\begin{Bmatrix}\sigma_{11}\\ \sigma_{22}\\ \tau_{12}\end{Bmatrix}=\begin{bmatrix}m^2 & n^2 & 2mn\\ n^2 & m^2 & -2mn\\ -mn & mn & m^2-n^2\end{bmatrix}\begin{Bmatrix}\sigma_{xx}\\ \sigma_{yy}\\ \tau_{xy}\end{Bmatrix} \qquad \text{(Eq 16.2)}$$

The strains in the material axes (ε_{11}, ε_{22}, and γ_{12}) can be obtained from those in the structural axes (ε_{xx}, ε_{yy}, and γ_{xy}) as follows:

$$\begin{Bmatrix}\varepsilon_{11}\\ \varepsilon_{22}\\ \gamma_{12}\end{Bmatrix}=\begin{bmatrix}m^2 & n^2 & mn\\ n^2 & m^2 & -mn\\ -2mn & 2mn & m^2-n^2\end{bmatrix}\begin{Bmatrix}\varepsilon_{xx}\\ \varepsilon_{yy}\\ \gamma_{xy}\end{Bmatrix} \qquad \text{(Eq 16.3)}$$

In like manner, the strains from the structural axes (ε_{xx}, ε_{yy}, and γ_{xy}) can be transformed to the material axes (ε_{11}, ε_{22}, and γ_{12}) as follows:

$$\begin{Bmatrix}\varepsilon_{11}\\ \varepsilon_{22}\\ \gamma_{12}\end{Bmatrix}=\begin{bmatrix}m^2 & n^2 & 2mn\\ n^2 & m^2 & -2mn\\ -2mn & 2mn & m^2-n^2\end{bmatrix}\begin{Bmatrix}\varepsilon_{xx}\\ \varepsilon_{yy}\\ \gamma_{xy}\end{Bmatrix} \qquad \text{(Eq 16.4)}$$

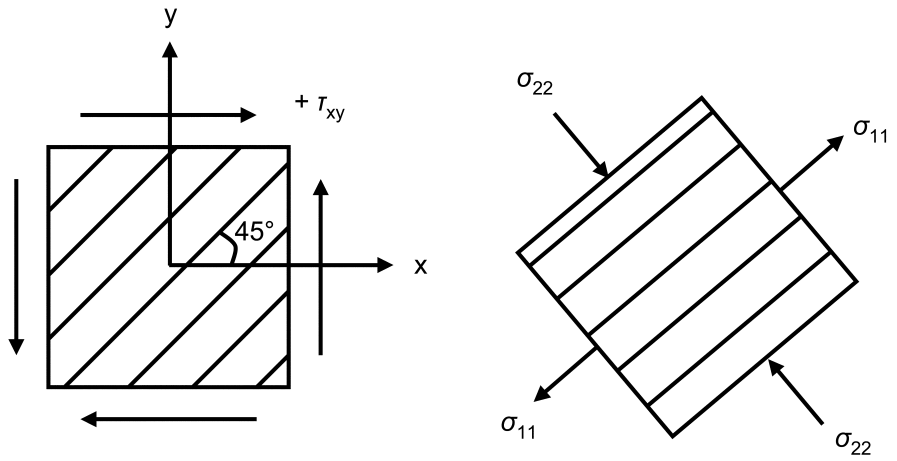
For a thin isotropic material in plane stress loading (Fig. 16.4a), the stress-strain relationships within the elastic range are:

$$\varepsilon_{xx}=\frac{\sigma_{xx}}{E}-\nu\frac{\sigma_{yy}}{E}$$

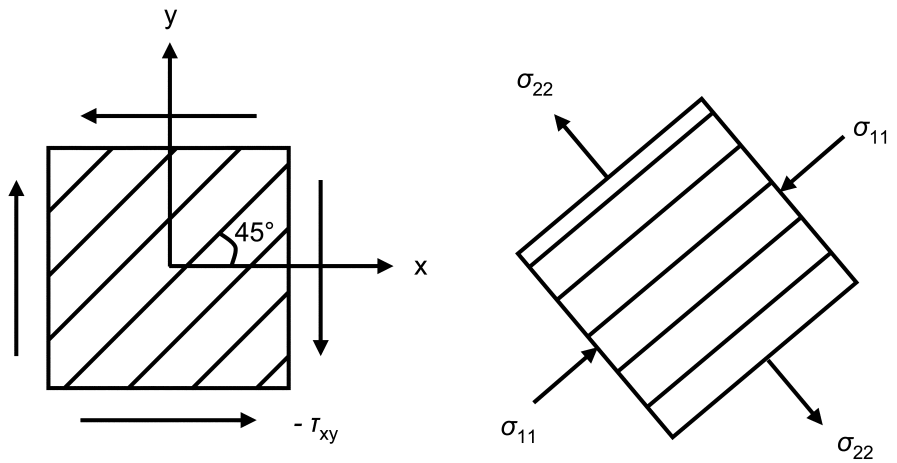
$$\varepsilon_{yy}=-\nu\frac{\sigma_{xx}}{E}+\frac{\sigma_{yy}}{E}$$

$$\gamma_{xy}=\frac{\tau_{xy}}{G} \qquad \text{(Eq 16.5)}$$

where E, G, and ν are the modulus of elasticity, the shear modulus, and Poisson's ratio, respectively.



Positive Shear Stress



Negative Shear Stress

Fig. 16.3 Shear stress state on 45° lamina

The stress-strain relationships for a thin orthotropic laminate in plane stress (Fig. 16.4b) within the elastic region are similar:

$$\varepsilon_{xx} = \frac{\sigma_{xx}}{E_{xx}} - \nu_{yx}\frac{\sigma_{yy}}{E_{yy}} - m_x\tau_{xy}$$

$$\varepsilon_{yy} = -\nu_{xy}\frac{\sigma_{xx}}{E_{xx}} + \frac{\sigma_{yy}}{E_{yy}} - m_y\tau_{xy}$$

$$\gamma_{xy} = -m_x\sigma_{xx} - m_y\sigma_{yy} + \frac{\tau_{xy}}{G_{xy}} \qquad \text{(Eq 16.6)}$$

The additional elastic constants, m_x and m_y, are called the *coefficients of mutual influence*. They result from the extension-shear coupling that occurs when a ply is loaded in tension, as discussed in Chapter 1, "Introduction to Composite Materials." The coefficients m_x and m_y are given by:

$$m_x = (\sin 2\theta)\left[\frac{\nu_{12}}{E_{11}} + \frac{1}{E_{22}} - \frac{1}{2G_{12}} - (\cos^2\theta)\left(\frac{1}{E_{11}} + \frac{2\nu_{12}}{E_{11}} + \frac{1}{E_{22}} - \frac{1}{G_{12}}\right)\right]$$

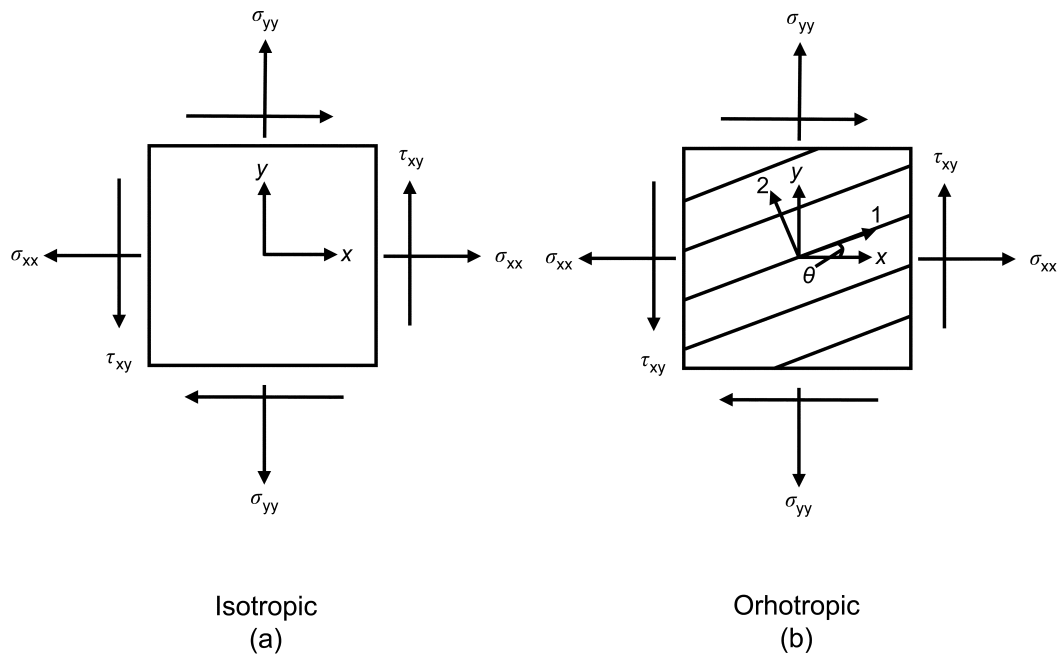


Fig. 16.4 Plane stress conditions

$$m_y = (\sin 2\theta)\left[\frac{\nu_{12}}{E_{11}} + \frac{1}{E_{22}} - \frac{1}{2G_{12}} - (\sin^2\theta)\left(\frac{1}{E_{11}} + \frac{2\nu_{12}}{E_{11}} + \frac{1}{E_{22}} - \frac{1}{G_{12}}\right)\right] \quad \text{(Eq 16.7)}$$

For a ply in which the fibers have either a zero-degree or 90-degree orientation, no extension-shear coupling exists and m_x and m_y are both equal to zero. When this is the case and the principal material axes 1 and 2 coincide with the loading axes x and y, the ply is known as a *specially orthotropic ply* and the stress-strain relationships simplify as follows:

$$\varepsilon_{xx} = \varepsilon_{11} = \frac{\sigma_{xx}}{E_{11}} - \nu_{21}\frac{\sigma_{yy}}{E_{22}} \quad \text{(Eq 16.8)}$$

$$\varepsilon_{yy} = \varepsilon_{22} = -\nu_{12}\frac{\sigma_{xx}}{E_{11}} + \frac{\sigma_{yy}}{E_{22}} \quad \text{(Eq 16.9)}$$

$$\gamma_{xy} = \gamma_{yx} = \gamma_{12} = \gamma_{21} = \frac{\tau_{xy}}{G_{12}} \quad \text{(Eq 16.10)}$$

The coefficients of mutual influence m_x and m_y are functions of the fiber orientation angle θ and exhibit maximum values at an intermediate angle between θ = 0° and 90°, as shown in Fig. 16.5.

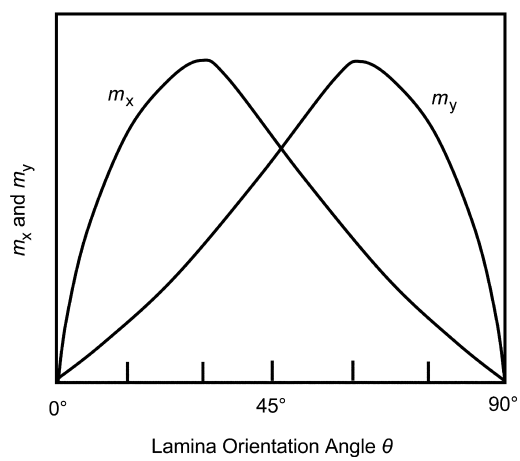


Fig. 16.5 Coefficients of mutual influence as a function of ply angle

16.2 Stress-Strain Relationships for a Single Ply Loaded Parallel to the Material Axes (θ = 0° or 90°)

In the structural analysis of composite materials, it is convenient to express the elastic constants in terms of the reduced stiffness coefficients and to represent the stress-strain relationships in matrix form. As previously mentioned, a specially

orthotropic ply is one in which the ply is oriented at either a zero-degree or 90-degree direction. The stress-strain relationship for a specially orthotropic material under in-plane stress loading with the load applied parallel with the material axes ($\theta = 0°$ or 90°) is as follows:

$$\{\varepsilon\} = [S]\{\sigma\}$$

$$\begin{Bmatrix} \varepsilon_{xx} \\ \varepsilon_{yy} \\ \gamma_{xy} \end{Bmatrix} = \begin{bmatrix} S_{11} & S_{12} & 0 \\ S_{21}(=S_{12}) & S_{22} & 0 \\ 0 & 0 & S_{66} \end{bmatrix} \begin{Bmatrix} \sigma_{xx} \\ \sigma_{yy} \\ \tau_{xy} \end{Bmatrix} \quad \text{(Eq 16.11)}$$

where:

$$S_{11} = 1/E_{11}$$
$$S_{12} = S_{21} = -\nu_{12}/E_{11} = -\nu_{21}/E_{22}$$
$$S_{22} = 1/E_{22}$$
$$S_{66} = 1/G_{12}$$

where E_{11} and E_{22} are the moduli of elasticity in the 1- and 2-directions, respectively, ν_{12} is the major Poisson's ratio specifying the contraction in the 2-direction for a tension load in the 1-direction, ν_{21} is the minor Poisson's ratio for a contraction in the 1-direction for a tension load in the 2-direction, and G_{12} is the in-plane shear modulus. By symmetry:

$$\frac{\nu_{12}}{E_{11}} = \frac{\nu_{21}}{E_{22}} \quad \text{(Eq 16.12)}$$

Therefore, there are only four independent material constants required for analysis (E_{11}, E_{22}, ν_{12}, and G_{12}).

Example 16.1: Determine the strains induced in a unidirectional carbon/epoxy composite specially orthotropic ply subjected to in-plane stresses where the magnitude of each stress component is:

$$\sigma_{xx} = \sigma_{11} = 30{,}000 \text{ psi}$$
$$\sigma_{yy} = \sigma_{22} = 5{,}000 \text{ psi}$$
$$\tau_{xy} = \tau_{12} = 2{,}000 \text{ psi}$$

Use the following material properties:

$$E_1 = 18.2 \times 10^6 \text{ psi}$$
$$E_2 = 1.82 \times 10^6 \text{ psi}$$
$$\nu_{12} = 0.30$$
$$G_{12} = 1.0 \times 10^6 \text{ psi}$$
$$\nu_{21} = (\nu_{12}/E_{11})\, E_{22} = (0.30/18.2 \times 10^6)\, 1.82 \times 10^6 = 0.03$$

Solution: Each term within the reduced compliance matrix can be calculated using Eq 16.11:

$$\begin{Bmatrix} \varepsilon_{xx} \\ \varepsilon_{yy} \\ \gamma_{xy} \end{Bmatrix} = \begin{bmatrix} 1/E_1 & -\nu_{21}/E_2 & 0 \\ -\nu_{12}/E_1 & 1/E_2 & 0 \\ 0 & 0 & 1/G_{12} \end{bmatrix} \begin{Bmatrix} \sigma_{xx} \\ \sigma_{yy} \\ \tau_{xy} \end{Bmatrix}$$

Substituting in the values gives:

$$\begin{Bmatrix} \varepsilon_{xx} \\ \varepsilon_{yy} \\ \gamma_{xy} \end{Bmatrix} = \begin{bmatrix} 5.49 \times 10^{-8} & -1.65 \times 10^{-8} & 0 \\ -1.65 \times 10^{-8} & 5.49 \times 10^{-7} & 0 \\ 0 & 0 & 1.00 \times 10^{-6} \end{bmatrix} \times \begin{Bmatrix} 33{,}000 \\ 5{,}000 \\ 2{,}000 \end{Bmatrix}$$

Completing the matrix multiplication gives:

$$\varepsilon_{xx} = \left(5.49 \times 10^{-8}\right)(33{,}000) + \left(-1.65 \times 10^{-8}\right)(5000)$$
$$= 1570 \times 10^6 \text{ in./in.}$$

$$\varepsilon_{yy} = \left(-1.65 \times 10^{-8}\right)(33{,}000) + \left(5.49 \times 10^{-7}\right)(5000)$$
$$= 2260 \times 10^6 \text{ in./in.}$$

$$\gamma_{xy} = \left(1.00 \times 10^{-6}\right)(2000) = 2000 \times 10^6 \text{ in./in.}$$

If a specially orthotropic ply is loaded parallel to the material's natural axes, the resulting stresses can be related to the accompanying strains by the reduced stiffness [Q] matrix:

$$\{\sigma\} = [Q]\{\varepsilon\}$$

$$\begin{Bmatrix} \sigma_{xx} \\ \sigma_{yy} \\ \tau_{xy} \end{Bmatrix} = \begin{bmatrix} Q_{11} & Q_{12} & 0 \\ Q_{12} & Q_{22} & 0 \\ 0 & 0 & Q_{66} \end{bmatrix} \begin{Bmatrix} \varepsilon_{xx} \\ \varepsilon_{yy} \\ \gamma_{xy} \end{Bmatrix} \quad \text{(Eq 16.13)}$$

where the reduced stiffness coefficients Q_{ij} are given by:

$$Q_{11} = E_1/(1 - \nu_{12}\nu_{21})$$
$$Q_{12} = \nu_{21}E_1/(1 - \nu_{12}\nu_{21})$$
$$Q_{22} = E_2/(1 - \nu_{12}\nu_{21})$$
$$Q_{66} = G_{12}$$

Equations 16.11 through 16.13 are applicable not only to a single ply but also to a unidirectional laminate in which the fiber direction

(zero-degree or 90–degree) is the same in all of the plies.

16.3 Stress-Strain Relationships for a Single Ply Loaded Off-Axis to the Material Axes ($\theta \neq 0°$ or 90°)

The elastic constants for an angle ply or off-axis ply can be calculated by using the following equations:

$$E_{xx} = \left[\cos^4\theta / E_{11} + \left(1/G_{12} - 2\nu_{12}/E_{11} \right) \sin^2\theta \cos^2\theta + \sin^4\theta / E_{22} \right]^{-1} \quad \text{(Eq 16.14)}$$

$$E_{yy} = \left[\sin^4\theta / E_{11} + \left(1/G_{12} - 2\nu_{12}/E_{11} \right) \sin^2\theta \cos^2\theta + \cos^4\theta / E_{22} \right]^{-1} \quad \text{(Eq 16.15)}$$

$$G_{xy} = \left[2\left(2/E_{11} + 2/E_{22} + 4\nu_{12}/E_{11} - 1/G_{12} \right) \sin^2\theta \cos^2\theta / E_{11} + \left(\sin^4\theta + \cos^4\theta / G_{12} \right) \right]^{-1} \quad \text{(Eq 16.16)}$$

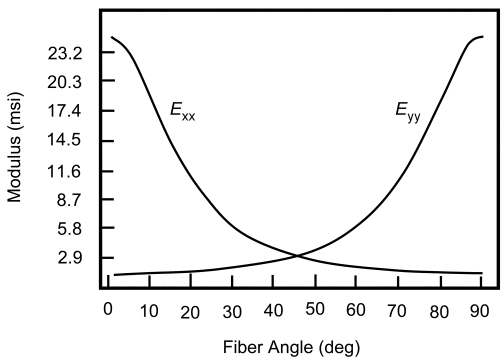
$$\nu_{xy} = E_{xx} \left[\nu_{12} \left(\sin^4\theta + \cos^4\theta \right) / E_{11} - \left(1/E_{11} + 1/E_{22} - 1/G_{12} \right) \sin^2\theta \cos^2\theta \right] \quad \text{(Eq 16.17)}$$

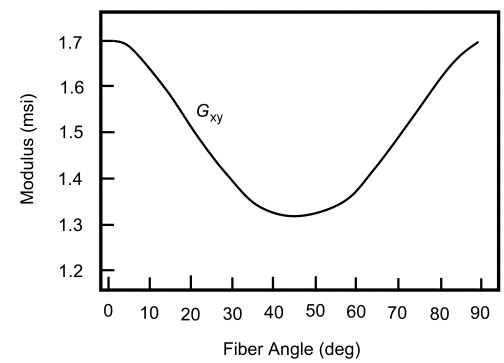
$$\nu_{yx} = \nu_{xy} \frac{E_{yy}}{E_{xx}} \quad \text{(Eq 16.18)}$$

The variations of elastic constants with fiber orientation are shown in Fig. 16.6. At $\theta = 0°$, $E_{xx} = E_{11}$ and at $\theta = 90°$, $E_{xx} = E_{22}$. The shear modulus G_{xy} reaches a maximum value at $\theta = 45°$, and ν_{xy} and ν_{yx} are the same as $\theta = 45°$.

The stress-strain relationships for a general orthotropic ply ($\theta \neq 0°$ or 90°) are given below, where $[\bar{S}]$ represents the compliance matrix:

$$\begin{Bmatrix} \varepsilon_{xx} \\ \varepsilon_{yy} \\ \gamma_{xy} \end{Bmatrix} = \left[\bar{S} \right] \begin{Bmatrix} \sigma_{xx} \\ \sigma_{yy} \\ \tau_{xy} \end{Bmatrix}$$





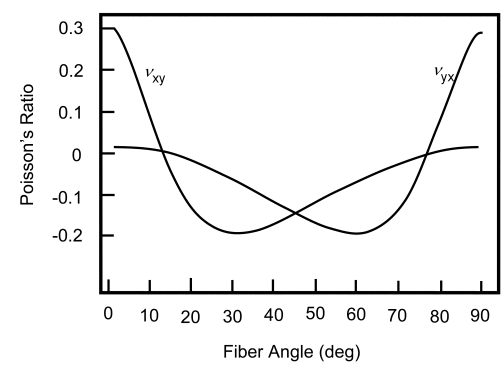


Fig. 16-6 Variation of elastic constants with fiber orientation

$$\begin{Bmatrix} \varepsilon_{xx} \\ \varepsilon_{yy} \\ \gamma_{xy} \end{Bmatrix} = \begin{bmatrix} \bar{S}_{11} & \bar{S}_{12} & \bar{S}_{16} \\ \bar{S}_{12} & \bar{S}_{22} & \bar{S}_{26} \\ \bar{S}_{16} & \bar{S}_{26} & \bar{S}_{66} \end{bmatrix} \begin{Bmatrix} \sigma_{xx} \\ \sigma_{yy} \\ \tau_{xy} \end{Bmatrix} \quad \text{(Eq 16.19)}$$

where:

$$\bar{S}_{11} = S_{11}\cos^4\theta + \left(2S_{12} + S_{66} \right) \sin^2\theta \cos^2\theta + S_{22}\sin^4\theta$$

$$\bar{S}_{12} = S_{12}\left(\sin^4\theta + \cos^4\theta\right) + \left(S_{11} + S_{22} - S_{66}\right)\sin^2\theta\cos^2\theta$$

$$\bar{S}_{16} = \left(2S_{11} - 2S_{12} - S_{66}\right)\sin\theta\cos^3\theta - \left(2S_{22} - 2S_{12} - S_{66}\right)\sin^3\theta\cos\theta$$

$$\bar{S}_{22} = S_{11}\sin^4\theta + \left(2S_{12} + S_{66}\right)\sin^2\theta\cos^2\theta + S_{22}\sin^4\theta$$

$$\bar{S}_{26} = \left(2S_{11} - 2S_{12} - S_{66}\right)\sin\theta^3\cos\theta - \left(2S_{22} - 2S_{12} - S_{66}\right)\sin\theta\cos^3\theta$$

$$\bar{S}_{66} = 2\left(2S_{11} + 2S_{22} - 4S_{12} - S_{66}\right)\sin^2\theta\cos^2\theta + S_{66}\left(\sin^4\theta + \cos^4\theta\right)$$

Inverting Eq 16.19 allows the stiffness matrix $[\bar{Q}]$ to be written:

$$\begin{Bmatrix}\sigma_{xx}\\ \sigma_{yy}\\ \tau_{xy}\end{Bmatrix} = \left[\bar{Q}\right]\begin{Bmatrix}\varepsilon_{xx}\\ \varepsilon_{yy}\\ \gamma_{xy}\end{Bmatrix}$$

$$\begin{Bmatrix}\sigma_{xx}\\ \sigma_{yy}\\ \tau_{xy}\end{Bmatrix} = \begin{bmatrix}\bar{Q}_{11} & \bar{Q}_{12} & \bar{Q}_{16}\\ \bar{Q}_{12} & \bar{Q}_{22} & \bar{Q}_{26}\\ \bar{Q}_{16} & \bar{Q}_{26} & \bar{Q}_{66}\end{bmatrix}\begin{Bmatrix}\varepsilon_{xx}\\ \varepsilon_{yy}\\ \gamma_{xy}\end{Bmatrix} \quad \text{(Eq 16.20)}$$

where:

$$\bar{Q}_{11} = Q_{11}\cos^4\theta + 2\left(Q_{12} + 2Q_{66}\right)\sin^2\theta\cos^2\theta + Q_{22}\sin^4\theta$$

$$\bar{Q}_{12} = Q_{12}\left(\sin^4\theta + \cos^4\theta\right) + \left(Q_{11} + Q_{22} - 4Q_{66}\right)\sin^2\theta\cos^2\theta$$

$$\bar{Q}_{16} = \left(Q_{11} - Q_{12} - 2Q_{66}\right)\sin\theta\cos^3\theta + \left(Q_{12} - Q_{22} + 2Q_{66}\right)\sin^3\theta\cos\theta$$

$$\bar{Q}_{22} = Q_{11}\sin^4\theta + 2\left(Q_{12} + 2Q_{66}\right)\sin^2\theta\cos^2\theta + Q_{22}\cos^4\theta$$

$$\bar{Q}_{26} = \left(Q_{11} + Q_{12} - 2Q_{66}\right)\sin^3\theta\cos\theta + \left(Q_{12} - Q_{22} + 2Q_{66}\right)\sin\theta\cos^3\theta$$

$$\bar{Q}_{66} = \left(Q_{11} + Q_{22} - 2Q_{12} - 2Q_{66}\right)\sin^2\theta\cos^2\theta + Q_{66}\left(\sin^4\theta + \cos^4\theta\right)$$

Trigonometric identities can be used to write the elements of the $[\bar{Q}]$ matrix as:

$$\begin{aligned}
\bar{Q}_{11} &= U_1 + U_2\cos 2\theta + U_3\cos 4\theta\\
\bar{Q}_{12} &= \bar{Q}_{21} = U_4 - U_3\cos 4\theta\\
\bar{Q}_{16} &= 1/2\,U_2\sin 2\theta + U_3\sin 4\theta\\
\bar{Q}_{22} &= U_1 - U_2\cos 2\theta + U_3\cos 4\theta\\
\bar{Q}_{26} &= 1/2\,U_2\sin 2\theta - U_3\sin 4\theta\\
\bar{Q}_{66} &= U_5 - U_3\cos 4\theta
\end{aligned} \quad \text{(Eq 16.21)}$$

where U_1 through U_5 are equal to:

$$\begin{aligned}
U_1 &= 1/8\left(3Q_{11} + 3Q_{22} + 2Q_{12} + 4Q_{66}\right)\\
U_2 &= 1/2\left(Q_{11} - Q_{22}\right)\\
U_3 &= 1/8\left(Q_{11} + Q_{22} + 2Q_{12} - 4Q_{66}\right)\\
U_4 &= 1/8\left(Q_{11} + Q_{22} + 6Q_{12} - 4Q_{66}\right)\\
U_5 &= 1/2\left(U_1 - U_4\right)
\end{aligned}$$

Similar expressions for the elements of the $[\bar{S}]$ matrix are:

$$\begin{aligned}
\bar{S}_{11} &= V_1 + V_2\cos 2\theta + V_3\cos 4\theta\\
\bar{S}_{12} &= \bar{S}_{21} = V_4 - V_3\cos 4\theta\\
\bar{S}_{16} &= V_2\sin 2\theta + 2V_3\sin 4\theta\\
\bar{S}_{22} &= V_1 - V_2\cos 2\theta + V_3\cos 4\theta\\
\bar{S}_{26} &= V_2\sin 2\theta - 2V_3\sin 4\theta\\
\bar{S}_{66} &= V_5 - 4V_3\cos 4\theta
\end{aligned} \quad \text{(Eq 16.22)}$$

where:

$$\begin{aligned}
V_1 &= 1/8\left(3S_{11} + 3S_{22} + 2S_{12} + S_{66}\right)\\
V_2 &= 1/2\left(S_{11} - S_{22}\right)\\
V_3 &= 1/8\left(S_{11} + S_{22} - 2S_{12} - S_{66}\right)\\
V_4 &= 1/8\left(S_{11} + S_{22} - 6S_{12} - S_{66}\right)\\
V_5 &= 2\left(V_1 - V_4\right)
\end{aligned}$$

These trigonometric identities are useful if manual calculations are required.

Example 16.2: Determine the elements of the stiffness matrix for an angle-ply of carbon/epoxy. Consider fiber orientations of both +45° and –45°. Use the following ply values:

$$E_{11} = 18.2 \times 10^6 \text{ psi}$$
$$E_{22} = 1.82 \times 10^6 \text{ psi}$$

$$G_{12} = 1.00 \times 10^6 \text{ psi}$$
$$\upsilon_{12} = 0.30$$
$$\upsilon_{21} = 0.03 \text{ since } \upsilon_{21} = \upsilon_{12}(E_{22}/E_{11})$$

Solution: The first step is to calculate the values Q_{11}, Q_{22}, $Q_{12,}$ Q_{21}, and Q_{66}.

$$Q_{11} = \frac{E_{11}}{1 - \upsilon_{12}\upsilon_{21}} = \frac{18.2 \times 10^6}{1 - (0.30)(0.03)} = 18.37 \times 10^6 \text{ psi}$$

$$Q_{22} = \frac{E_{22}}{1 - \upsilon_{12}\upsilon_{21}} = \frac{1.82 \times 10^6}{1 - (0.30)(0.03)} = 1.84 \times 10^6 \text{ psi}$$

$$Q_{12} = Q_{21} = \frac{\upsilon_{12}E_{22}}{1 - \upsilon_{12}\upsilon_{21}} = \frac{(0.30)1.82 \times 10^6}{1 - (0.30)(0.03)}$$
$$= 0.551 \times 10^6 \text{ psi}$$

$$Q_{66} = G_{12} = 1.00 \times 10^6 \text{ psi}$$

Next, calculate the angle-invariant stiffness properties U_1, U_2, U_3, U_4, and U_5.

$$U_1 = 1/8(3Q_{11} + 3Q_{22} + 2Q_{12} + 4Q_{66})$$
$$= 1/8\left[(3)(18.37 \times 10^6) + (3)(1.84 \times 10^6) + (2)(0.551 \times 10^6) + (4)(1.00 \times 10^6)\right]$$
$$= 8.22 \times 10^6 \text{ psi}$$

$$U_2 = 1/2(Q_{11} - Q_{22})$$
$$U_2 = 1/2\left[18.37 \times 10^6 - 1.84 \times 10^6\right] = 8.27 \times 10^6 \text{ psi}$$

$$U_3 = 1/8(Q_{11} + Q_{22} - 2Q_{12} - 4Q_{66})$$
$$U_3 = 1/8 = \left[18.37 \times 10^6 + 1.84 \times 10^6 - (2)(0.551 \times 10^6) - (4)(1.0 \times 10^6)\right] 1.89 \times 10^6 \text{ psi}$$

$$U_4 = 1/8(Q_{11} + Q_{22} + 6Q_{12} - 4Q_{66})$$
$$U_4 = 1/8\left[18.37 \times 10^6 + 1.84 \times 10^6 + (6)(0.551 \times 10^6) - (4)(1.0 \times 10^6)\right] = 2.44 \times 10^6 \text{ psi}$$

$$U_5 = 1/2(U_1 - U_4)$$
$$U_5 = 1/2\left[8.22 \times 10^6 - 2.44 \times 10^6\right] = 2.89 \times 10^6 \text{ psi}$$

Finally, calculate the elements of the stiffness matrix $\bar{Q}_{11}$, $\bar{Q}_{12}$, $\bar{Q}_{22}$, $\bar{Q}_{16}$, $\bar{Q}_{26}$, and $\bar{Q}_{66}$, for the ply orientation of $\theta = +45°$.

$$\bar{Q}_{11} = U_1 + U_2\cos 2\theta + U_3\cos 4\theta$$
$$\bar{Q}_{11} = 8.22 \times 10^6 + 8.27 \times 10^6(\cos 90°) + 1.89 \times 10^6(\cos 180°) = 6.33 \times 10^6 \text{ psi}$$

$$\bar{Q}_{12} = Q_{21} = U_4 - U_3\cos 4\theta$$
$$\bar{Q}_{12} = 2.44 \times 10^6 - 1.89 \times 10^6(\cos 180°)$$
$$= 4.33 \times 10^6 \text{ psi}$$

$$\bar{Q}_{22} = U_1 - U_2\cos 2\theta + U_3\cos 4\theta$$
$$\bar{Q}_{22} = 8.22 \times 10^6 - 8.27 \times 10^6(\cos 90°) + 1.89 \times 10^6(\cos 180°) = 6.33 \times 10^6 \text{ psi}$$

$$\bar{Q}_{16} = 1/2\,U_2\sin 2\theta + U_3\sin 4\theta$$
$$\bar{Q}_{16} = 1/2(8.27 \times 10^6)(\sin 90°) + 1.89 \times 10^6(\sin 180°)$$
$$= 4.14 \times 10^6 \text{ psi}$$

$$\bar{Q}_{26} = 1/2\,U_2\sin 2\theta - U_3\sin 4\theta$$
$$\bar{Q}_{26} = 1/2(8.27 \times 10^6)(\sin 90°) - 1.89 \times 10^6(\sin 180°)$$
$$= 4.14 \times 10^6 \text{ psi}$$

$$\bar{Q}_{66} = U_5 - U_3\cos 4\theta$$
$$\bar{Q}_{66} = 2.89 \times 10^6 - 1.89 \times 10^6(\cos 180°)$$
$$= 4.78 \times 10^6 \text{ psi}$$

In a similar manner, the values for the stiffness matrix for a ply with an orientation of $\theta = -45°$ are:

$$\bar{Q}_{11} = 6.33 \times 10^6 \text{ psi}$$
$$\bar{Q}_{12} = 4.33 \times 10^6 \text{ psi}$$
$$\bar{Q}_{22} = 6.38 \times 10^6 \text{ psi}$$
$$\bar{Q}_{16} = -4.14 \times 10^6 \text{ psi}$$
$$\bar{Q}_{26} = -4.14 \times 10^6 \text{ psi}$$
$$\bar{Q}_{66} = 4.78 \times 10^6 \text{ psi}$$

Note that the values for the +45° and –45° plies are the same except that the signs are negative for $\bar{Q}_{16}$ and $\bar{Q}_{26}$ for the –45° orientation.

16.4 Laminates and Laminate Notations

Laminae or plies are stacked together at various angles and cured together to form laminates.

There are a number of standard laminate types and notations that are important:

Unidirectional Laminates. In a unidirectional laminate, all of the plies are oriented in the zero-degree or 90-degree direction. An example is the four-ply thick zero-degree laminate [0°, 0°, 0°, 0°]. Note that this is the same as a single ply or lamina, only thicker, as a result of multiple layers.

Angle-Ply Laminates. In an angle-ply laminate, all of the plies follow a sequence of +θ/–θ. An example is a $[30°/–30°]_4$ laminate with a stacking sequence of [30°, –30°, 30°, –30°, 30°, –30°, 30°, –30°]. The subscript 4 indicates that the pattern is repeated four times.

Cross-Ply Laminates. In a cross-ply laminate, the plies are stacked in alternating layers of zero-degree and 90-degree. An example is $[0°, 90°]_2$, where the subscript 2 indicates that the pattern repeats twice [0°, 90°, 0°, 90°].

Symmetric Laminates. In a symmetric laminate, the ply fiber orientation is symmetrical about the centerline of the laminate. For each ply above the centerline, there is an identical ply of the same material and thickness at an equal distance below the centerline. An example of a symmetric laminate is $[0°, 45°, –45°, 90°]_s$, where the subscript s indicates the laminate is symmetric and only the first half of the stacking sequence is shown. The full form is [0°, 45°, –45°, 90°, 90°, –45°, 45°, 0°].

Balanced Laminates. In a balanced laminate, for every ply of + θ orientation, there is an identical ply of the same material and thickness of –θ orientation. An example of a balanced laminate is [0°, 30°, –30°, 30°, –30°, 0°]. This laminate is balanced but is not symmetric. However, it could be made symmetric by reordering the stacking order to [0°, 30°, –30°, –30°, 30°, 0°].

Quasi-Isotropic Laminates. A quasi-isotropic laminate is made up of three or more plies of identical materials and thicknesses with equal angles between each ply and the next. If the total number of plies is n, the angle between plies is π/n. Quasi-isotropic laminates usually exhibit isotropic elastic behavior in the xy plane. An example of a balanced and symmetric quasi-isotropic laminate is [0°, 90°, 45°, –45°, –45°, 45°, 90°, 0°]. This laminate has two 0° plies, two 90° plies, two 45° plies, and two –45° plies.

Hybrid Laminates. Hybrid laminates consist of a mixture of different materials, such as carbon and glass. A possible designation of a carbon-glass hybrid laminate would be $[0^\circ_c, \pm45^\circ_g, \overline{90}^\circ_c]_s$ where c stands for carbon and g stands for glass. The bar over the 90° ply indicates that the centerline of symmetry passes midway through the 90° ply. In the expanded form, this laminate would be represented as $[0^\circ_c, 45^\circ_g, –45^\circ_g, 90^\circ_c, –45^\circ_g, 45^\circ_g, 0^\circ_c]$.

Some other laminate notations are as follows:

The designation $\mp45°$ indicates that the –45° ply comes before the +45° ply.

The designation 0°_3 in the balanced and symmetric laminate $[0^\circ_3, \pm45°, 90°]_s$ indicates that there are three 0° plies lumped together; i.e., [0°, 0°, 0°, 45°, –45°, 90°, 90°, –45°, 45°, 0°, 0°, 0°].

The designation $[\pm45°]_{2s}$ indicates that the ±45° grouping repeats twice on either side of the center of symmetry, that is, [45°, –45°, 45°, –45°, –45°, 45°, –45°, 45°].

The designation [50, 40, 10] is a shorthand notation used in the aerospace industry and indicates that the laminate contains 50% 0°, 40% ± 45°, and 10% 90° plies but tells nothing about their specific orientations.

16.5 Laminate Analysis—Classical Lamination Theory

Lamination theory is used to calculate the stresses, strains, and curvature in each ply of a thin laminate under loading, as well as the overall elastic constants of the laminate. The main assumptions in classical plate lamination theory are these:

1. The thickness of the plate is much smaller than the in-plane direction.
2. The strains in the deformed plate are small compared to unity.
3. Normals to the undeformed plate surface remain normal to the deformed plate surface.
4. Vertical deflection does not vary through the thickness.
5. Stress normal to the plate is negligible.

A coordinate system is established such that the midplane of the laminate contains the x- and y-axes with the z-axis normal to the midplane. As shown in Fig. 16.7, a laminate with a total thickness of t is constructed from N plies. The individual thicknesses of each ply are t_1, t_2, t_3, and so on.

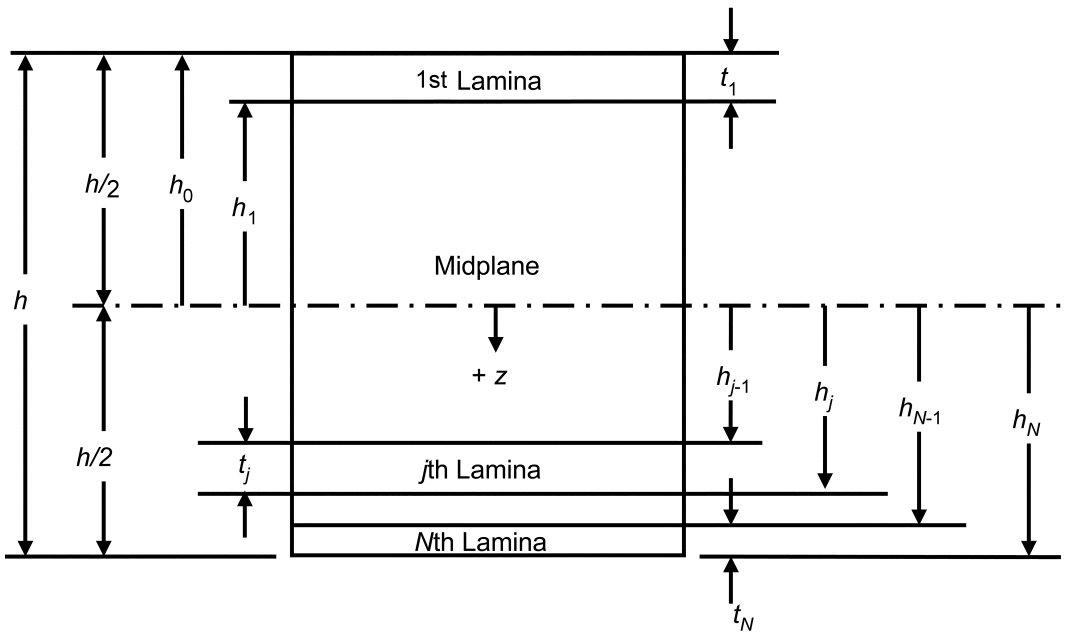


Fig. 16.7 Laminate stacking sequence notation

The sequence of steps in a typical calculation is as follows:

1. Calculate the stiffness matrices for the laminate from the ply stiffness matrices $[Q_{ij}]$ and $[\bar{Q}_{ij}]$.
2. Calculate the midplane strains and curvatures for the laminate as a result of a given set of forces and moments.
3. Calculate the in-plane strains ε_{xx}, ε_{yy}, and γ_{xy} for each ply.
4. Calculate the in-plane stresses σ_{xx}, σ_{yy}, and τ_{xy} in each ply.
5. Calculate the explicit elastic constants E_{xx}, E_{yy}, ν_{xy}, ν_{yx}, and G_{xy} of the laminate.
6. Estimate the laminate strength by using a suitable failure criterion.

On the basis of the assumptions listed above, it can be shown that the in-plane displacements consist of a midsurface displacement, designated by the superscript 0, plus a linear displacement through the thickness, as indicated by:

$$\varepsilon_{xx} = \varepsilon^{\circ}_{xx} + zk_{xx}$$
$$\varepsilon_{yy} = \varepsilon^{\circ}_{yy} + zk_{yy}$$
$$\gamma_{zz} = \varepsilon^{\circ}_{zz} + zk_{zz} \qquad \text{(Eq 16.23)}$$

where:
ε°_{xx}, ε°_{yy} = midplane normal strains in the laminate
ε°_{zz} = midplane shear strain in the laminate
k_{xx}, k_{yy} = bending curvatures in the laminate
k_{zz} = twisting curvature in the laminate
z = distance from the midplane in the thickness direction

The in-plane, bending, and twisting loads experienced by a laminate are shown in Fig. 16.8. It can be shown that the applied force and moment resultants are related to the midplane strains and curvatures by:

$$N_{xx} = A_{11}\varepsilon^{\circ}_{xx} + A_{12}\varepsilon^{\circ}_{yy} + A_{16}\gamma^{\circ}_{xy} + B_{11}k_{xx} + B_{12}k_{yy} + B_{16}k_{xy}$$
$$N_{yy} = A_{12}\varepsilon^{\circ}_{xx} + A_{22}\varepsilon^{\circ}_{yy} + A_{26}\gamma^{\circ}_{xy} + B_{12}k_{xx} + B_{22}k_{yy} + B_{26}k_{xy}$$
$$N_{xy} = A_{16}\varepsilon^{\circ}_{xx} + A_{26}\varepsilon^{\circ}_{yy} + A_{66}\gamma^{\circ}_{xy} + B_{16}k_{xx} + B_{26}k_{yy} + B_{66}k_{xy}$$
$$M_{xx} = B_{11}\varepsilon^{\circ}_{xx} + B_{12}\varepsilon^{\circ}_{yy} + B_{16}\gamma^{\circ}_{xy} + D_{11}k_{xx} + D_{12}k_{yy} + D_{16}k_{xy}$$
$$M_{yy} = B_{12}\varepsilon^{\circ}_{xx} + B_{22}\varepsilon^{\circ}_{yy} + B_{26}\gamma^{\circ}_{xy} + D_{12}k_{xx} + D_{22}k_{yy} + D_{26}k_{xy}$$
$$M_{xy} = B_{16}\varepsilon^{\circ}_{xx} + B_{26}\varepsilon^{\circ}_{yy} + B_{66}\gamma^{\circ}_{xy} + D_{16}k_{xx} + D_{26}k_{yy} + D_{66}k_{xy} \qquad \text{(Eq 16.24)}$$

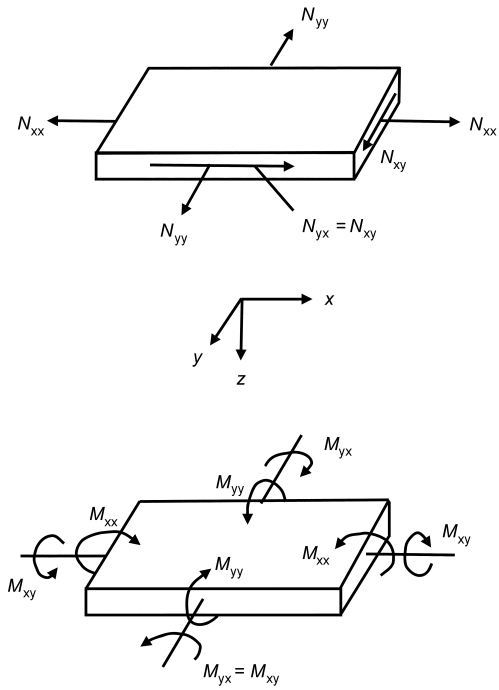


Fig. 16.8 In-plane, bending, and twisting loads applied to a laminate

where:
N_{xx}, N_{yy} = normal force resultants in the x- and y-directions per unit width
N_{xy} = shear force resultant per unit width
M_{xx}, M_{yy} = bending moment resultants in the yz and xz planes per unit width
M_{xy} = twisting moment resultant per unit width

In matrix form:

$$\begin{bmatrix} N_{xx} \\ N_{yy} \\ N_{xy} \end{bmatrix} = [A] \begin{bmatrix} \varepsilon^{\circ}_{xx} \\ \varepsilon^{\circ}_{yy} \\ \gamma^{\circ}_{xy} \end{bmatrix} + [B] \begin{bmatrix} k_{xx} \\ k_{yy} \\ k_{xy} \end{bmatrix} \quad \text{(Eq 16.25)}$$

and

$$\begin{bmatrix} M_{xx} \\ M_{yy} \\ M_{xy} \end{bmatrix} = [B] \begin{bmatrix} \varepsilon^{\circ}_{xx} \\ \varepsilon^{\circ}_{yy} \\ \gamma^{\circ}_{xy} \end{bmatrix} + [D] \begin{bmatrix} k_{xx} \\ k_{yy} \\ k_{xy} \end{bmatrix} \quad \text{(Eq 16.26)}$$

The extensional stiffness matrix [A] in lb/in. for the laminate is:

$$[A] = \begin{bmatrix} A_{11} & A_{12} & A_{16} \\ A_{12} & A_{22} & A_{26} \\ A_{16} & A_{26} & A_{66} \end{bmatrix} \quad \text{(Eq 16.27)}$$

The coupling stiffness matrix [B] in lb for the laminate is:

$$[B] = \begin{bmatrix} B_{11} & B_{12} & B_{16} \\ B_{12} & B_{22} & B_{26} \\ B_{16} & B_{26} & B_{66} \end{bmatrix} \quad \text{(Eq 16.28)}$$

The bending stiffness matrix [D] in lb-in. for the laminate is:

$$[D] = \begin{bmatrix} D_{11} & D_{12} & D_{16} \\ D_{12} & D_{22} & D_{26} \\ D_{16} & D_{26} & D_{66} \end{bmatrix} \quad \text{(Eq 16.29)}$$

The elements of the stiffness matrices [A], [B], and [D] are calculated from:

$$A_{mn} = \sum_{j=1}^{N} \left(\bar{Q}_{mn}\right)_j \left(h_j - h_{j-1}\right) \quad \text{(Eq 16.30)}$$

$$B_{mn} = \frac{1}{2} \sum_{j=1}^{N} \left(\bar{Q}_{mn}\right)_j \left(h_j^2 - h_{j-1}^2\right) \quad \text{(Eq 16.31)}$$

$$D_{mn} = \frac{1}{3} \sum_{j=1}^{N} \left(\bar{Q}_{mn}\right)_j \left(h_j^3 - h_{j-1}^3\right) \quad \text{(Eq 16.32)}$$

where, referring to Fig. 16.7:

N = total number of plies in the laminate
$[\bar{Q}_{mn}]_j$ = element of the $[\bar{Q}]$ matrix of the jth ply
h_{j-1} = distance from midplane to the top of the jth ply
h_j = distance from the midplane to the bottom of the jth ply

where h is taken to be positive below the midplane and negative above the midplane.

The important characteristics of the [A], [B], and [D] matrices are as follows:

- The elements of the [A], [B], and [D] matrices that cause coupling effects are shown in Fig. 16.9. The terms A_{16} and A_{26} bring in tension-shear coupling, while the terms B_{16} and B_{26} represent tension-twisting coupling. The terms D_{16} and D_{26} represent flexure-twisting coupling when a moment is applied.
- The [A] matrix represents extensional stiffness. The terms A_{11}, A_{12}, A_{22}, and A_{66} are never negative. For a balanced laminate, $A_{16} = A_{26} = 0$, and no normal stress-shear coupling exists. The [A] matrix is not affected by stacking sequence.

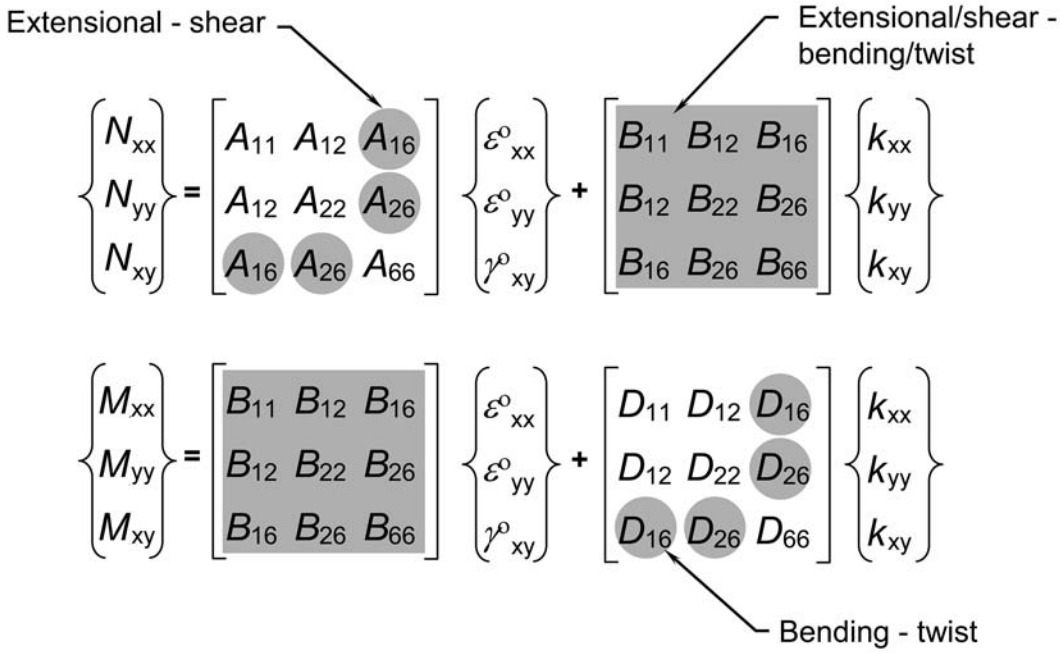


Fig. 16.9 Characteristics of the *ABD* matrices

- The [*B*] matrix represents coupling stiffness. In a symmetric laminate, the [*B*] matrix = 0 and no extension-bending occurs. In laminates where the [*B*] matrix is nonzero, a normal force such as N_{xx} or a bending moment such as M_{xx} will produce extensional and shear deformations as well as bending-twisting curvatures. In other words, if the [*B*] matrix is nonzero, these laminates will warp under a load or a moment. For a laminate that is both balanced and symmetric, $[B] = A_{16} = A_{26} = 0$.
- The [*D*] matrix represents bending stiffness. The terms D_{11}, D_{12}, D_{22}, and D_{66} are always positive. The [*D*] matrix is most affected by stacking sequence. The terms D_{16} and D_{26} are zero for all plies with a 0° or 90° orientation. The terms D_{16} and D_{26} will also be zero if, for each ply oriented at +θ and at a given distance above the midplane, there is an identical ply oriented at –θ at the same distance below the midplane. However, such a laminate will not be symmetric and $[B] \neq 0$. The terms D_{16} and D_{26} will not be zero for any midplane symmetric laminate except for a unidirectional laminate (zero-degree or 90-degree) or a cross-ply laminate (zero-degree, 90-degree). However, D_{16} and D_{26} become small when a large number of plies are stacked at ±θ. Generally, D_{16} and D_{26} become insignificant for thicknesses of more than 16 plies.
- Laminates that are not balanced and symmetric tend to bend, twist, and/or warp under applied loads and moments. In fact, due to thermal contraction, they tend to warp and twist on cooling down from elevated-temperature cure cycles. They should be avoided if at all possible; balanced and symmetric laminates should always be used.

Example 16.3: Determine the [*A*], [*B*], and [*D*] matrices for (a) a [+45°, –45°] angle ply laminate and (b) a $[+45°, –45°]_s$ symmetric laminate.

Solution: Part (a). From Example 16.2, we have already calculated the $[\bar{Q}]_{45°}$ and $[\bar{Q}]_{45°}$ matrices.

$$[\bar{Q}]_{45°} = \begin{bmatrix} 6.33 & 4.33 & 4.14 \\ 4.33 & 6.33 & 4.14 \\ 4.14 & 4.14 & 4.78 \end{bmatrix} 10^6 \text{psi}$$

$$[\bar{Q}]_{-45°} = \begin{bmatrix} 6.33 & 4.33 & -4.14 \\ 4.33 & 6.33 & -4.14 \\ -4.14 & -4.14 & 4.78 \end{bmatrix} 10^6 \text{psi}$$

For part (a), shown in Fig. 16.10, $h_0 = -0.005$ in., $h_1 = 0$, and $h_2 = +0.005$ in.

The first term of the [A] matrix, A_{11}, can be calculated using Eq 16.30:

$$A_{mn} = \sum_{j=1}^{N} \left(\bar{Q}_{mn}\right)_j \left(h_j - h_{j-1}\right)$$

where:

$$\left(\bar{Q}_{mn}\right)_1 = \left(\bar{Q}_{mn}\right)_{45^\circ}$$
$$\left(\bar{Q}_{mn}\right)_2 = \left(\bar{Q}_{mn}\right)_{-45^\circ}$$

$$A_{11} = \left(\bar{Q}_{11}\right)_{45^\circ}\left(h_1 - h_0\right) + \left(\bar{Q}_{11}\right)_{-45^\circ}\left(h_2 - h_1\right)$$
$$A_{11} = [6.33]\left[(0) - (-0.005)\right] + [6.33]\left[(0.005) - (0)\right]$$
$$= 6.33 \times 10^4 \text{ lb/in.}$$

The remainder of the [A] matrix is calculated in a similar manner.

$$[A] = \begin{bmatrix} 6.33 & 4.33 & 0 \\ 4.33 & 6.33 & 0 \\ 0 & 0 & 4.78 \end{bmatrix} 10^4 \text{ lb/in.}$$

The first term of the [B] matrix, B_{11}, can be calculated using Eq 16.31:

$$B_{mn} = \frac{1}{2}\sum_{j=1}^{N} \left(\bar{Q}_{mn}\right)_j \left(h_j^2 - h_{j-1}^2\right)$$

$$B_{mn} = \frac{1}{2}\left[\left(\bar{Q}_{mn}\right)_{45^\circ}\left(h_1^2 - h_0^2\right) + \left(\bar{Q}_{mn}\right)_{-45^\circ}\left(h_2^2 - h_1^2\right)\right]$$
$$B_{11} = \frac{1}{2}\left[\left(\bar{Q}_{11}\right)_{45^\circ}\left(h_1^2 - h_0^2\right) + \left(\bar{Q}_{11}\right)_{-45^\circ}\left(h_2^2 - h_1^2\right)\right]$$
$$B_{11} = \frac{1}{2}\left\{[6.33]\left[(0)^2 - (-0.005)^2\right] + [6.33]\left[(0.005)^2 - (0)^2\right]\right\} = 0 \text{ lb}$$

The remainder of the [B] matrix is calculated in a similar manner.

$$[B] = \begin{bmatrix} 0 & 0 & -1.04 \\ 0 & 0 & -1.04 \\ -1.04 & -1.04 & 0 \end{bmatrix} 10^2 \text{ lb}$$

The first term of the [D] matrix, D_{11}, can be calculated using Eq 16.32.

$$D_{mn} = \frac{1}{3}\sum_{j=1}^{N} \left(\bar{Q}_{mn}\right)_j \left(h_j^3 - h_{j-1}^3\right)$$

$$D_{mn} = \frac{1}{3}\left[\left(\bar{Q}_{mn}\right)_{45^\circ}\left(h_1^3 - h_0^3\right) + \left(\bar{Q}_{mn}\right)_{-45^\circ}\left(h_2^3 - h_1^3\right)\right]$$
$$D_{11} = \frac{1}{3}\left[\left(\bar{Q}_{11}\right)_{45^\circ}\left(h_1^3 - h_0^3\right) + \left(\bar{Q}_{11}\right)_{-45^\circ}\left(h_2^3 - h_1^3\right)\right]$$
$$D_{11} = \frac{1}{3}\left\{[6.33]\left[(0)^3 - (-0.005)^3\right] + [6.33]\left[(0.005)^3 - (0)^3\right]\right\} = 0.510 \text{ l}$$

The remainder of the [D] matrix is calculated in a similar manner.

$$[D] = \begin{bmatrix} 0.510 & 0.378 & 0 \\ 0.378 & 0.510 & 0 \\ 0 & 0 & 0.416 \end{bmatrix} \text{lb-in.}$$

Solution: Part (b). To solve part (b), see Fig. 16.11, where:
$h_0 = -0.010$ in.
$h_1 = -0.005$ in.
$h_2 = 0$ in.
$h_3 = 0.005$ in.
$h_4 = 0.010$ in.

Then the first term of the [A] matrix, A_{11}, can be calculated using Eq 16.30:

$$A_{mn} = \sum_{j=1}^{N} \left(\bar{Q}_{mn}\right)_j \left(h_j - h_{j-1}\right)$$



Fig. 16.10 Example 16-3a ply diagram

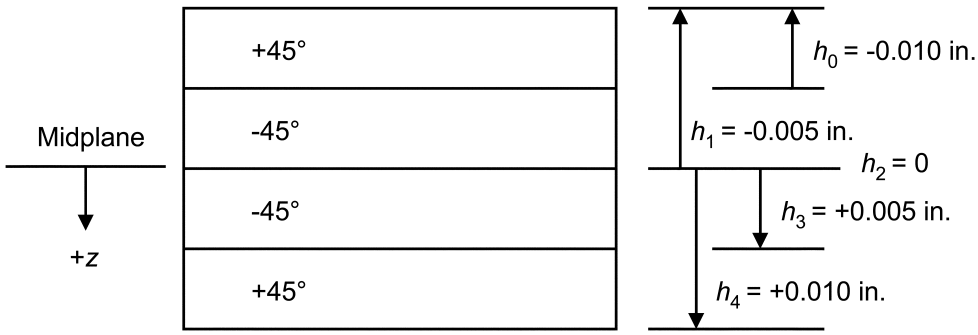


Fig. 16.11 Example 16, 3b ply diagram

where:

$$\left(\bar{Q}_{mn}\right)_1 = \left(\bar{Q}_{mn}\right)_4 = \left(\bar{Q}_{mn}\right)_{45^\circ}$$
$$\left(\bar{Q}_{mn}\right)_2 = \left(\bar{Q}_{mn}\right)_3 = \left(\bar{Q}_{mn}\right)_{-45^\circ}$$

$$A_{mn} = \left[\left(\bar{Q}_{mn}\right)_{45^\circ}\left(h_1 - h_0\right) + \left(\bar{Q}_{mn}\right)_{-45^\circ}\left(h_2 - h_1\right) + \left(\bar{Q}_{mn}\right)_{-45^\circ}\left(h_3 - h_2\right) + \left(\bar{Q}_{mn}\right)_{45^\circ}\left(h_4 - h_3\right)\right]$$

$$A_{11} = \left(\bar{Q}_{11}\right)_{45^\circ}\left(h_1 - h_0 + h_4 - h_3\right) + \left(\bar{Q}_{11}\right)_{-45^\circ}\left(h_2 - h_1 + h_3 - h_2\right)$$

$$A_{11} = [6.33]\left[(-0.005) - (-0.010) + (0.010) - (0.005)\right] + [6.33]\left[(0) - (-.005) + (0.010) - (0)\right]$$
$$= 12.7 \times 10^4 \text{ lb/in.}$$

The remainder of the [*A*] matrix and the [*B*] and [*D*] matrices are calculated in a similar manner.

$$[A] = \begin{bmatrix} 12.7 & 8.65 & 0 \\ 8.65 & 12.7 & 0 \\ 0 & 0 & 9.55 \end{bmatrix} 10^4 \text{ lb/in.}$$

$$[B] = 0$$

$$[D] = \begin{bmatrix} 4.22 & 2.88 & 2.07 \\ 2.88 & 4.22 & 2.07 \\ 2.07 & 2.07 & 3.18 \end{bmatrix} \text{lb-in.}$$

Since this a symmetric laminate, [*B*] = 0 and $A_{16} = A_{26} = 0$.

This step calculated the stiffness matrices for the laminate.

Once the applied loads and moments are known, the midplane strains and curvatures can be calculated. This is accomplished by inverting Eq 16.25 and 16.26 to give:

$$\begin{bmatrix} \varepsilon^\circ_{xx} \\ \varepsilon^\circ_{yy} \\ \gamma^\circ_{xy} \end{bmatrix} = [a]\begin{bmatrix} N_{xx} \\ N_{yy} \\ N_{xy} \end{bmatrix} + [b]\begin{bmatrix} M_{xx} \\ M_{yy} \\ M_{xy} \end{bmatrix} \quad \text{(Eq 16.33)}$$

and

$$\begin{bmatrix} k_{xx} \\ k_{yy} \\ k_{xy} \end{bmatrix} = [c]\begin{bmatrix} N_{xx} \\ N_{yy} \\ N_{xy} \end{bmatrix} + [d]\begin{bmatrix} M_{xx} \\ M_{yy} \\ M_{xy} \end{bmatrix} \quad \text{(Eq 16.34)}$$

where:

$$[a] = \left[A^{-1}\right] + \left[A^{-1}\right][B]\left[\left(D^*\right)^{-1}\right][B]\left[A^{-1}\right]$$
$$[b] = -\left[A^{-1}\right][B]\left[\left(D^*\right)^{-1}\right]$$
$$[c] = -\left[\left(D^*\right)^{-1}\right][B]\left[A^{-1}\right]$$
$$[d] = \left[\left(D^*\right)^{-1}\right]$$
$$\left[D^*\right] = [D] - [B]\left[A^{-1}\right][B]$$

(Eq 16.35)

While these matrix transformations seem quite daunting, in practice they are usually performed by a computer program. In addition, the situation is much simpler for a symmetric laminate. For a symmetric laminate, [*B*] = 0 and therefore [a] = [A^{-1}], [*b*] = [*c*] = 0, and [*d*] = [D^{-1}]. In this case, the equations for midplane strains and curvatures become:

$$\begin{bmatrix} \varepsilon^\circ_{xx} \\ \varepsilon^\circ_{yy} \\ \gamma^\circ_{xy} \end{bmatrix} = \left[A^{-1}\right]\begin{bmatrix} N_{xx} \\ N_{yy} \\ N_{xy} \end{bmatrix} \quad \text{(Eq 16.36)}$$

and

$$\begin{bmatrix} k_{xx} \\ k_{yy} \\ k_{xy} \end{bmatrix} = \left[D^{-1} \right] \begin{bmatrix} M_{xx} \\ M_{yy} \\ M_{xy} \end{bmatrix} \quad \text{(Eq 16.37)}$$

Equations 16.36 and 16.37 show that for symmetric laminates, in-plane forces produce in-plane strains with no curvatures, and bending and twisting moments produce curvatures with no in-plane strains.

The values of the midplane strains and curvatures can be used to calculate the strains in the individual plies. As a result of the linear relationship of strain in the thickness direction, we have:

$$\begin{bmatrix} \varepsilon_{xx} \\ \varepsilon_{yy} \\ \gamma_{xy} \end{bmatrix} = \begin{bmatrix} \varepsilon^{\circ}_{xx} \\ \varepsilon^{\circ}_{yy} \\ \gamma^{\circ}_{xy} \end{bmatrix} + z_j \begin{bmatrix} k_{xx} \\ k_{yy} \\ k_{xy} \end{bmatrix} \quad \text{(Eq 16.38)}$$

where z_j is the distance from the laminate midplane to the midplane of the jth ply. The stresses in the jth ply can be calculated by using its stiffness matrix.

$$\begin{bmatrix} \sigma_{xx} \\ \sigma_{yy} \\ \tau_{xy} \end{bmatrix}_j = \left[\bar{Q}_{mn} \right]_j \begin{bmatrix} \varepsilon_{xx} \\ \varepsilon_{yy} \\ \gamma_{xy} \end{bmatrix}_j$$

$$= \left[\bar{Q}_{mn} \right]_j \begin{bmatrix} \varepsilon^{\circ}_{xx} \\ \varepsilon^{\circ}_{yy} \\ \gamma^{\circ}_{xy} \end{bmatrix} + z_j \left[\bar{Q}_{mn} \right]_j \begin{bmatrix} k_{xx} \\ k_{yy} \\ k_{xy} \end{bmatrix} \quad \text{(Eq 16.39)}$$

For a balanced symmetric laminate, where $[B] = 0$ and $A_{16} = A_{26} = 0$, the extensional stiffness matrix $[A]$ simplifies to:

$$[A] = \begin{bmatrix} A_{11} & A_{12} & 0 \\ A_{12} & A_{22} & 0 \\ 0 & 0 & A_{66} \end{bmatrix} \quad \text{(Eq 16.40)}$$

The inverse of the $[A]$ matrix is:

$$\left[A^{-1} \right] = \frac{1}{A_{11}A_{22} - A_{12}^2} \begin{bmatrix} A_{22} & -A_{12} & 0 \\ -A_{12} & A_{11} & 0 \\ 0 & 0 & \dfrac{\left(A_{11}A_{22} - A_{12}^2 \right)}{A_{66}} \end{bmatrix} \quad \text{(Eq 16.41)}$$

Therefore, Eq 16.36 gives:

$$\begin{bmatrix} \varepsilon^{\circ}_{xx} \\ \varepsilon^{\circ}_{yy} \\ \gamma^{\circ}_{xy} \end{bmatrix} = \frac{1}{A_{11}A_{22} - A_{12}^2} \begin{bmatrix} A_{22} & -A_{12} & 0 \\ -A_{12} & A_{11} & 0 \\ 0 & 0 & \dfrac{\left(A_{11}A_{22} - A_{12}^2 \right)}{A_{66}} \end{bmatrix} \begin{bmatrix} N_{xx} \\ N_{yy} \\ N_{xy} \end{bmatrix} \quad \text{(Eq 16.42)}$$

For the case of a uniaxial tensile load applied in the x-direction with $N_{xx} = h\sigma_{xx}$ and $N_{yy} = N_{xy} = 0$, we have:

$$\varepsilon^{\circ}_{xx} = \frac{A_{22}}{A_{11}A_{22} - A_{12}^2} h\sigma_{xx}$$

$$\varepsilon^{\circ}_{yy} = \frac{A_{12}}{A_{11}A_{22} - A_{12}^2} h\sigma_{xx}$$

$$\gamma^{\circ}_{xy} = 0$$

which gives:

$$E_{xx} = \frac{\sigma_{xx}}{\varepsilon^{\circ}_{xx}} = \frac{A_{11}A_{22} - A_{12}^2}{hA_{22}} \quad \text{(Eq 16.43)}$$

$$\nu_{xy} = \frac{\varepsilon^{\circ}_{yy}}{\varepsilon^{\circ}_{xx}} = \frac{A_{12}}{A_{22}} \quad \text{(Eq 16.44)}$$

In turn, applying N_{xx} and N_{xy} separately, it can be determined that:

$$E_{xy} = \frac{A_{11}A_{22} - A_{12}^2}{hA_{11}} \quad \text{(Eq 16.45)}$$

$$\nu_{yx} = \frac{A_{12}}{A_{11}} \quad \text{(Eq 16.46)}$$

$$G_{xy} = \frac{A_{66}}{h} \quad \text{(Eq 16.47)}$$

The bending behavior of a balanced symmetric laminate beam where $[B] = 0$ can be analyzed as follows. First, the $[D]$ matrix:

$$[D] = \begin{bmatrix} D_{11} & D_{12} & D_{16} \\ D_{12} & D_{22} & D_{26} \\ D_{16} & D_{26} & D_{66} \end{bmatrix}$$

is inverted to give:

$$\left[D^{-1} \right] = \frac{1}{D_0} \begin{bmatrix} D^{\circ}_{11} & D^{\circ}_{12} & D^{\circ}_{16} \\ D^{\circ}_{12} & D^{\circ}_{21} & D^{\circ}_{26} \\ D^{\circ}_{16} & D^{\circ}_{26} & D^{\circ}_{66} \end{bmatrix} \quad \text{(Eq 16.48)}$$

where the elements of the $[D^{-1}]$ matrix are:

$$D_0 = D_{11}\left(D_{22}D_{66} - D_{26}^2\right) - D_{12}\left(D_{12}D_{66} - D_{16}D_{26}\right) + D_{16}\left(D_{12}D_{26} - D_{22}D_{16}\right)$$

$$D_{11}^\circ = D_{11}\left(D_{22}D_{66} - D_{26}^2\right)$$

$$D_{12}^\circ = -D_{12}\left(D_{12}D_{66} - D_{16}D_{26}\right)$$

$$D_{16}^\circ = D_{16}\left(D_{12}D_{26} - D_{22}D_{16}\right)$$

$$D_{22}^\circ = D_{22}\left(D_{11}D_{66} - D_{16}^2\right)$$

$$D_{26}^\circ = -D_{26}\left(D_{11}D_{26} - D_{12}D_{16}\right)$$

$$D_{66}^\circ = D_{66}\left(D_{11}D_{22} - D_{12}^2\right) \qquad \text{(Eq 16.49)}$$

If a bending moment is applied in the *yz*-plane to produce M_{xx}, and M_{yy} and M_{xy} are both zero, the specimen curvatures can be obtained from Eq 16.37:

$$k_{xx} = \frac{D_{11}^\circ}{D_\circ} M_{xx}$$

$$k_{yy} = \frac{D_{12}^\circ}{D_\circ} M_{xx}$$

$$k_{xy} = \frac{D_{16}^\circ}{D_\circ} M_{xx} \qquad \text{(Eq 16.50)}$$

Even though no twisting moment is applied, the laminate would tend to twist, owing to the presence of k_{xy}, unless $D_{16}^\circ = D_{16}$ $(D_{12}D_{26} - D_{22}D_{16}) = 0$. This is possible only if a balanced symmetric laminate contains plies in the 0° and 90° directions.

Example 16.4: For the $[0°, 45°, –45°, 90°]_s$ symmetric laminate, calculate the ply stresses at the midplane of each ply generated by an applied load of $N_{xx} = 100$ lb/in. The material properties for the carbon/epoxy material are:

$$E_{11} = 25.0 \times 10^6 \text{ psi}$$
$$E_{22} = 1.70 \times 10^6 \text{ psi}$$
$$\upsilon_{12} = 0.30$$
$$\upsilon_{21} = 0.020 \text{ since } \upsilon_{21} = \upsilon_{12}(E_{22}/E_{11})$$

Solution: The first step is to calculate the values Q_{11}, Q_{22}, Q_{12}, Q_{21}, and Q_{66} using Eq 16.13:

$$Q_{11} = 25.15 \times 10^6 \text{ psi}$$
$$Q_{22} = 1.71 \times 10^6 \text{ psi}$$
$$Q_{12} = Q_{21} = 5.13 \times 10^6 \text{ psi}$$
$$Q_{66} = 6.50 \times 10^6 \text{ psi}$$

The $\bar{Q}$ matrices are then determined for the 0°, 45°, –45°, and 90° plies in the same manner as illustrated in Example 16.3.

For the 0° plies:

$$\left[\bar{Q}\right]_{0^\circ} = \begin{bmatrix} 251.5 & 5.13 & 0 \\ 5.13 & 17.1 & 0 \\ 0 & 0 & 6.50 \end{bmatrix} 10^5 \text{ psi}$$

For the +45° plies:

$$\left[\bar{Q}\right]_{45^\circ} = \begin{bmatrix} 7.62 & 6.32 & 5.86 \\ 6.32 & 7.62 & 5.86 \\ 5.86 & 5.86 & 6.45 \end{bmatrix} 10^6 \text{ psi}$$

For the –45° plies:

$$\left[\bar{Q}\right]_{-45^\circ} = \begin{bmatrix} 7.62 & 6.32 & -5.86 \\ 6.32 & 7.62 & -5.86 \\ -5.86 & -5.86 & 6.45 \end{bmatrix} 10^6 \text{ psi}$$

For the 90° plies:

$$\left[\bar{Q}\right]_{90^\circ} = \begin{bmatrix} 17.1 & 5.13 & 0 \\ 5.13 & 251.5 & 0 \\ 0 & 0 & 6.50 \end{bmatrix} 10^5 \text{ psi}$$

The $[A]$, $[B]$, and $[D]$ matrices can now be determined in a manner similar to that of Example 16.3. Since this is a symmetric laminate, $[B] = 0$. The $[A]$ matrix for this laminate is:

$$[A] = \begin{bmatrix} A_{11} & A_{12} & 0 \\ A_{12} & A_{22} & 0 \\ 0 & 0 & A_{66} \end{bmatrix} = \begin{bmatrix} 4.38 & 1.42 & 0 \\ 1.42 & 4.38 & 0 \\ 0 & 0 & 1.48 \end{bmatrix} 10^5 \text{ in./lb}$$

The effective laminate constants can now be determined from Eq 16.43 through 16.47:

$$E_{xx} = \frac{A_{11}A_{22} - A_{12}^2}{hA_{22}}$$

$$= \frac{\left(4.38 \times 10^6\right)\left(4.38 \times 10^6\right) - \left(1.42 \times 10^6\right)^2}{\left(0.0416\right)\left(4.38 \times 10^6\right)}$$

$$= 9.42 \times 10^6 \text{ psi}$$

$$E_{xy} = \frac{A_{11}A_{22} - A_{12}^2}{hA_{11}} = 9.42 \times 10^6 \text{ psi}$$

$$G_{xy} = \frac{A_{66}}{h} = 3.55 \times 10^6 \text{ psi}$$

$$\nu_{xy} = \frac{A_{12}}{A_{22}} = 0.325$$

$$\nu_{yx} = \frac{A_{12}}{A_{11}} = 0.325$$

Since this is a quasi-isotropic laminate, E_{xx} and E_{yy} are the same.

The inverse of the [A] matrix can be found by using Eq 16.41:

$$\left[A^{-1}\right] = \frac{1}{A_{11}A_{22} - A_{12}^2} \begin{bmatrix} A_{22} & -A_{12} & 0 \\ -A_{12} & A_{11} & 0 \\ 0 & 0 & \dfrac{\left(A_{11}A_{22} - A_{12}^2\right)}{A_{66}} \end{bmatrix}$$

The first term is calculated as follows:

$$A^{-1}{}_{11} = \frac{1}{A_{11}A_{22} - A_{12}^2}\left(A_{22}\right)$$

$$= \frac{1}{\left(4.38 \times 10^5\right)\left(4.38 \times 10^5\right) - \left(1.42 \times 10^5\right)^2}\left(4.38 \times 10^5\right)$$

$$= 2.55 \times 10^{-6} \text{ in./lb}$$

The remainder of the [A^{-1}] matrix is:

$$\left[A^{-1}\right] = \begin{bmatrix} 2.55 & -0.829 & 0 \\ -0.829 & 2.55 & 0 \\ 0 & 0 & 6.76 \end{bmatrix} 10^{-6} \text{ in./lb}$$

Using Eq 16.36 and 16.37, the [$\varepsilon°$] and [k] matrices can now be calculated. First, the [$\varepsilon°$] matrix is calculated as follows:

$$\begin{bmatrix} \varepsilon_{xx}^{\circ} \\ \varepsilon_{yy}^{\circ} \\ \gamma_{xy}^{\circ} \end{bmatrix} = \left[A^{-1}\right] \begin{bmatrix} N_{xx} \\ N_{yy} \\ N_{xy} \end{bmatrix}$$

$$= \begin{bmatrix} 2.55 & -0.829 & 0 \\ -0.829 & 2.55 & 0 \\ 0 & 0 & 6.76 \end{bmatrix} 10^{-6} \text{ in./lb} \begin{bmatrix} 100 \\ 0 \\ 0 \end{bmatrix} \text{lb/in.}$$

which yields:

$$\varepsilon_{xx}^{\circ} = 2{,}550 \times 10^{-6} \text{ in./in.}$$
$$\varepsilon_{yy}^{\circ} = -829 \times 10^{-6} \text{ in./in.}$$
$$\gamma_{xy}^{\circ} = 0$$

Since this is a balanced and symmetric laminate, the [A] and [B] matrices are uncoupled, [B] = 0, and there are no applied moments, it can be inferred that the curvature matrix [k] is zero, and the strains in each ply in the laminate coordinate system are identical to the midplane strains. In pure uniaxial tension of a symmetric and balanced laminate, the strains will be constant through the thickness but the stresses may vary, as shown in Fig. 16.12. The 0° plies carry the most stress and the 90° plies carry the least. For flexural loading, the strains vary linearly through the thickness and the stresses vary with the loading condition and their stress-carrying capability.

Now, using Eq 16.39, σ_{xx}, σ_{yy}, and τ_{xy} are calculated at the midplane of the 0°, +45°, –45° and 90° plies.

For the 0° plies:

$$\begin{bmatrix} \sigma_{xx} \\ \sigma_{yy} \\ \tau_{xy} \end{bmatrix}_{0^\circ} = \left[\bar{Q}_{mn}\right]_{0^\circ} \begin{bmatrix} \varepsilon_{xx} \\ \varepsilon_{yy} \\ \gamma_{xy} \end{bmatrix}_{0^\circ}$$

$$= \begin{bmatrix} 251.5 & 5.13 & 0 \\ 5.13 & 17.1 & 0 \\ 0 & 0 & 6.50 \end{bmatrix} 10^5 \text{ psi} \begin{bmatrix} 2550 \\ -829.0 \\ 0 \end{bmatrix} 10^{-6} \text{ in./in.}$$

$$= \begin{bmatrix} 6370 \\ -11.0 \\ 0 \end{bmatrix} \text{psi}$$

For the +45° plies:

$$\begin{bmatrix} \sigma_{xx} \\ \sigma_{yy} \\ \tau_{xy} \end{bmatrix}_{+45^\circ} = \left[\bar{Q}_{mn}\right]_{+45^\circ} \begin{bmatrix} \varepsilon_{xx} \\ \varepsilon_{yy} \\ \gamma_{xy} \end{bmatrix}_{+45^\circ}$$

$$= \begin{bmatrix} 7.62 & 6.32 & 5.86 \\ 6.32 & 7.62 & 5.86 \\ 5.86 & 5.86 & 6.45 \end{bmatrix} 10^6 \text{ psi} \begin{bmatrix} 2550 \\ -829.0 \\ 0 \end{bmatrix} 10^{-6} \text{ in./in.}$$

$$= \begin{bmatrix} 1420 \\ 980.0 \\ 1010 \end{bmatrix} \text{psi}$$

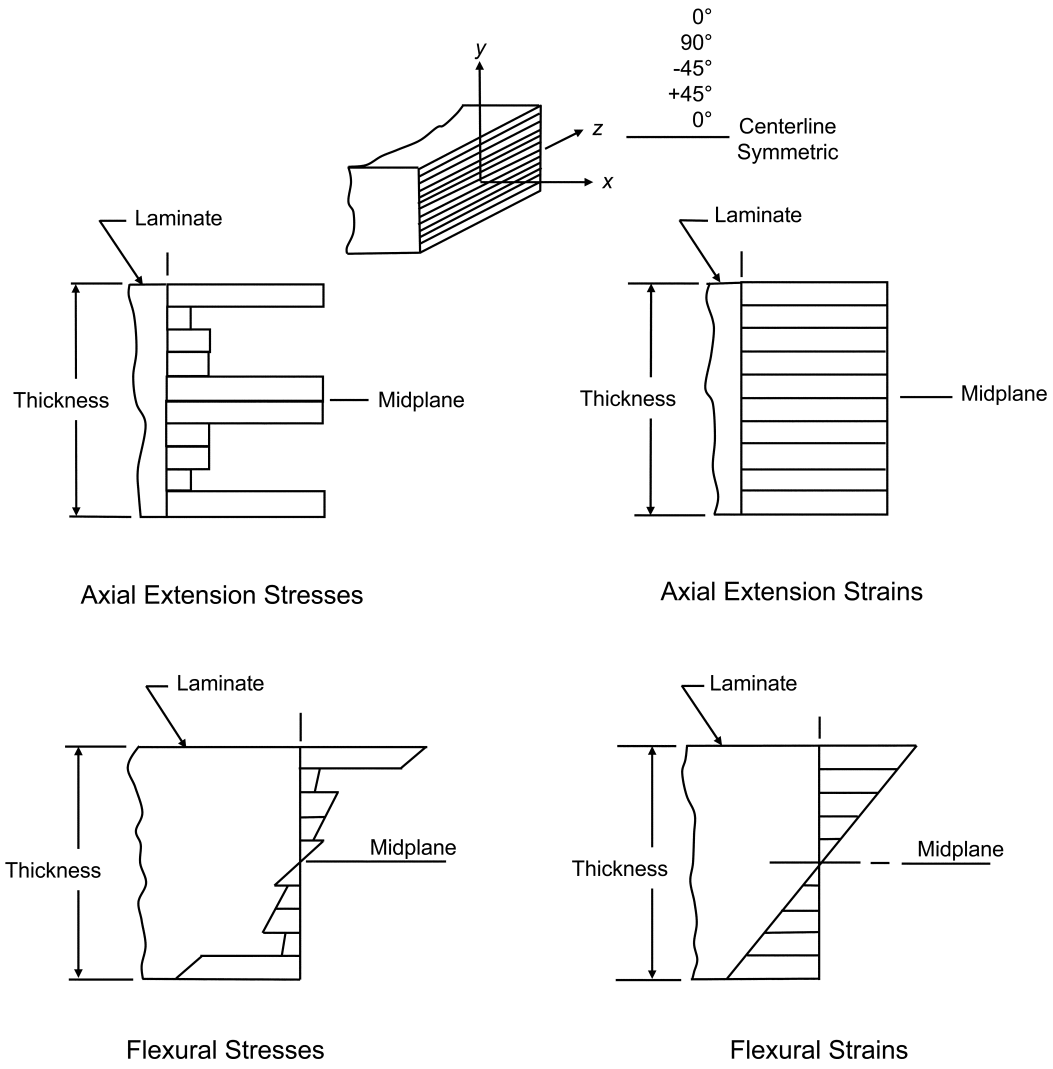


Fig. 16.12 Variation of ply stresses and strains through the laminate thickness

For the –45° plies:

$$\begin{bmatrix}\sigma_{xx}\\ \sigma_{yy}\\ \tau_{xy}\end{bmatrix}_{-45^\circ} = \left[\bar{Q}_{mn}\right]_{-45^\circ}\begin{bmatrix}\varepsilon_{xx}\\ \varepsilon_{yy}\\ \gamma_{xy}\end{bmatrix}_{-45^\circ} = \begin{bmatrix}1420\\ 980.0\\ -1010\end{bmatrix}\text{psi}$$

For the 90° plies:

$$\begin{bmatrix}\sigma_{xx}\\ \sigma_{yy}\\ \tau_{xy}\end{bmatrix}_{90^\circ} = \left[\bar{Q}_{mn}\right]_{90^\circ}\begin{bmatrix}\varepsilon_{xx}\\ \varepsilon_{yy}\\ \gamma_{xy}\end{bmatrix}_{90^\circ} = \begin{bmatrix}394.0\\ -1954\\ 0\end{bmatrix}\text{psi}$$

Although the strains are the same through the thickness, the stresses in the plies are a function of the ply orientation, with the 0° plies carrying the highest stresses. If desired, these stresses can be converted to the 1-2 coordinate system by using the stress transformation equation (Eq 16.2).

16.6 Interlaminar Free-Edge Stresses

Provided that the laminate is sufficiently wide, lamination theory estimates laminate behavior fairly accurately in the interior of the laminate. However, within about one laminate thickness

of free edges, lamination theory breaks down and fails to predict the large interlaminar stresses that can develop. At the free edges, delamination under in-plane loading can occur. Large interlaminar stresses can develop, leading to delamination of plies or matrix cracking at the edges.

Edge effects arise as a result of the requirement for strain compatibility between the plies in the laminate. Interlaminar shear and through-the-thickness peel stresses develop near the free edges of the laminate. The principal reason for the development of these interlaminar stresses is the mismatch of Poisson's ratios ν_{xy} and the coefficients of mutual influence m_x and m_y between adjacent plies. The result is the production of normal stresses σ_{xy} in each ply and interlaminar shear stress τ_{yz} at the ply interfaces. Consider a laminate consisting of alternating 0° and 90° plies under tensile loading parallel to the zero-degree plies. The difference in Poisson's ratios leads to different transverse contractions, as shown in Fig. 16.13. However, since the plies are bonded together, they have the same transverse strain. This leads to interlaminar shear stresses between the plies, forcing the zero-degree ply to expand in the transverse direction and the 90-degree ply to contract. The shear force is confined to the edge because once the required tension σ_{yy} is established in the zero-degree ply, compatibility will be ensured across the middle of the laminate. At the free edge, the tension stress must drop to zero if there is no applied edge stress. Since the shear stress shown in Fig. 16.13 is offset from the axis of the resultant the stress σ_{yy}, a turning moment is produced. To balance this moment, peel stresses σ_{zz} develop in the laminate with the distribution indicated in the figure. These peel stresses can cause delaminations at the edge. Interlaminar shear stresses also occur in angle-ply laminates as the plies distort differently under applied loads.

The magnitude of free-edge stresses is a function of laminate lay-up, stacking sequence, properties of the constituent materials, and stress state. As an example of laminate lay-up, a cross-plied $[0°, 90°]_s$ laminate experiences less severe interlaminar stress components than a $[\pm 30°, 90°]_s$ laminate. Thus, the $[\pm 30°, 90°]_s$ laminate is more prone to free-edge delamination. The stacking sequence can determine whether an interlaminar normal stress will be tensile or compressive at the free edges and determine the magnitude of the interlaminar stress components. Under the same uniaxial tensile loading condition, $[\pm 45°, 0°, 90°]_s$ and $[90°, 45°, 0°, -45°]_s$ laminates produce large tensile and compressive σ_{zz} stresses at the midsurface, respectively. Therefore, the latter laminate is not as prone to delamination under tensile loading as the former laminate. Interspersing the ±45° plies to produce an alternating positive and negative stress state has been found to reduce σ_{zz} and thus also the tendency to delaminate.

Any free edge, including a hole, can introduce interlaminar stresses. The consequences of these stresses need to be evaluated for structural applications, particularly when fatigue loading is present. It becomes extremely complex to develop quantitative analytical solutions for free-edge stresses in all but the simplest geometric shapes. The magnitude and effects of free-edge stresses are usually evaluated by finite difference or finite element methods. In most cases, the possibility of delaminations as a result of free-edge stresses is determined through testing rather than by computation.

16.7 Failure Theories

Failure prediction for metallic structures is normally performed by comparing stresses or strains caused by applied loads with the allowable strength or strain capacity of the material. For isotropic materials that exhibit yielding, either the Tresca maximum shear stress theory or the von Mises distortional energy theory is commonly used. However, composites are not isotropic and they do not yield. Failure modes in composites are generally noncatastrophic and may involve localized damage via such mechanisms as fiber breakage, matrix cracking, debonding, and fiber pull-out. These can progress simultaneously and interactively, making failure prediction for composites complex.

There are five independent strength constants that are important for a single ply:

- S_{Lt} or ε_{Lt}—longitudinal tensile strength or strain
- S_{Tt} or ε_{Tt}—transverse tensile strength or strain
- S_{Lc} or ε_{Lc}—longitudinal compressive strength or strain
- S_{Tc} or ε_{Tc}—transverse compressive strength or strain
- S_s or γ_s—in-plane shear strength or strain

Maximum Stress Criterion. According to this theory, failure occurs when any stress in the principal material directions is equal to or greater

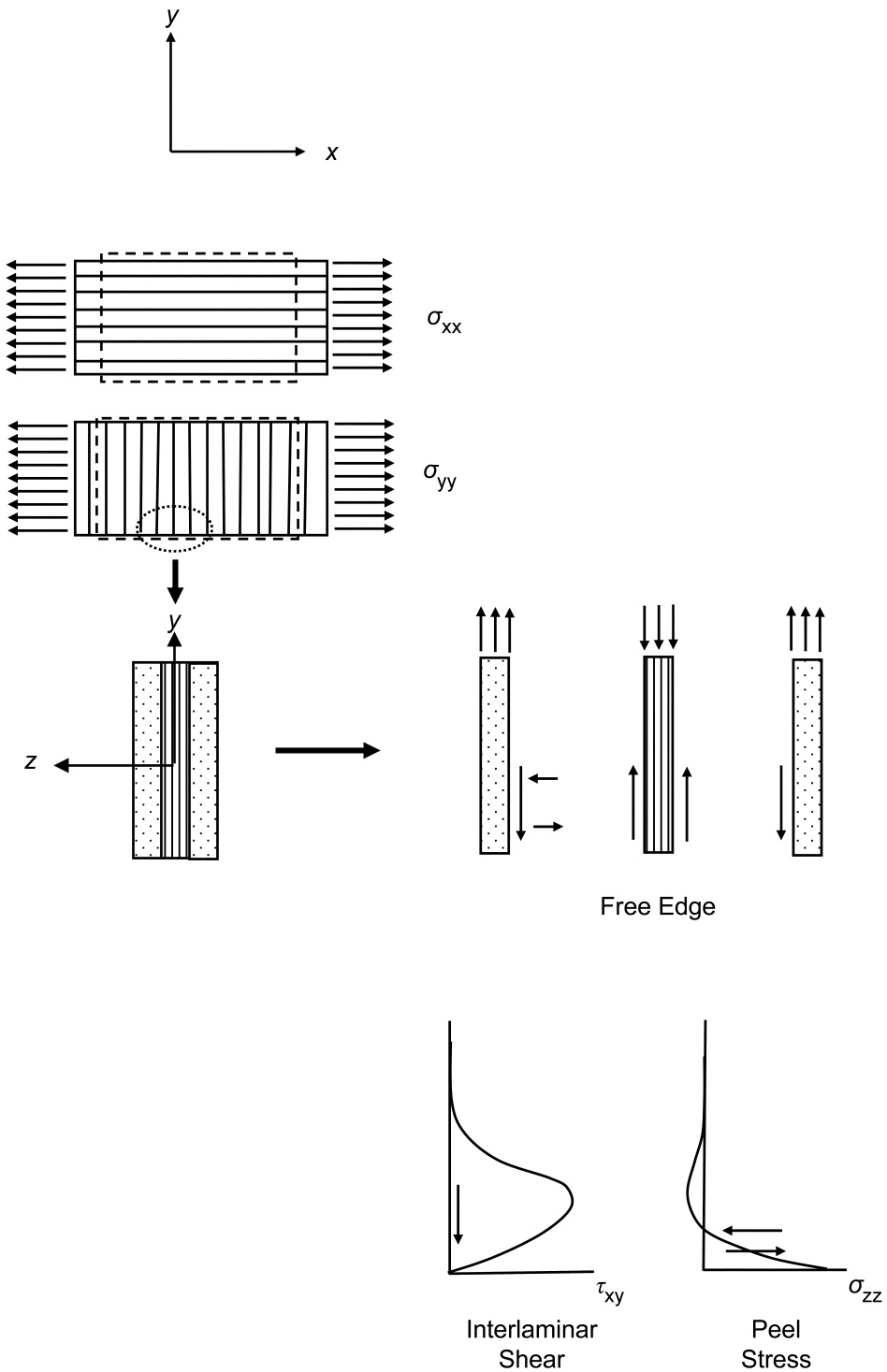


Fig. 16.13 Interlaminar shear and peel stresses in a 0°, 90° laminate. Source: Ref 1

than the corresponding allowable strength. To avoid failure, one must have:

$$\begin{aligned} -S_{Lc} < \sigma_{11} < S_{Lt} \\ -S_{Tc} < \sigma_{22} < S_{Tt} \\ -S_s < \tau_{12} < S_s \end{aligned} \qquad \text{(Eq 16.51)}$$

For the case of simple tension where σ_{xx} is present and $\sigma_{yy} = \sigma_{xy} = 0$, depending on the angle θ, three failure modes are considered:

1. Failure parallel to the fiber direction dominated by fiber fracture:

$$\sigma_{xx} = \frac{S_{Lt}}{\cos^2\theta} \qquad \text{(Eq 16.52)}$$

2. Failure transverse to the fiber direction dominated by matrix failure or fiber-matrix interface failure:

$$\sigma_{xx} = \frac{S_{Tt}}{\sin^2\theta} \qquad \text{(Eq 16.53)}$$

3. Failure by shear of the matrix or fiber-matrix interface, or both:

$$\sigma_{xx} = \frac{S_s}{\sin\theta\cos\theta} \qquad \text{(Eq 16.54)}$$

The disadvantage of this theory is that it does not account for the interaction of stresses and the occurrence of mixed-mode failures.

Maximum Strain Theory. The maximum strain theory is very similar to the maximum stress theory except that strains are used instead of stresses. According to this theory, failure will occur if any strain in the principal material axes is equal to or greater than the corresponding allowable strain. To avoid failure, one must have:

$$\begin{aligned} -\varepsilon_{Lc} < \varepsilon_{11} < \varepsilon_{Lt} \\ -\varepsilon_{Tc} < \varepsilon_{22} < \varepsilon_{Tt} \\ -\gamma_s < \gamma_{12} < \gamma_s \end{aligned} \qquad \text{(Eq 16.55)}$$

For an orthotropic ply subjected to a simple tension stress σ_{xx}, it can be shown that in the principal material directions the following hold:

$$\begin{aligned} \varepsilon_{11} &= \frac{\sigma_{11}}{E_{11}} - \nu_{21}\frac{\sigma_{22}}{E_{22}} = \frac{1}{E_{11}}\left(\cos^2\theta - \nu_{12}\sin^2\theta\right)\sigma_{xx} \\ \varepsilon_{22} &= \frac{\sigma_{22}}{E_{22}} - \nu_{12}\frac{\sigma_{11}}{E_{11}} = \frac{1}{E_{22}}\left(\sin^2\theta - \nu_{21}\cos^2\theta\right)\sigma_{xx} \\ \gamma_{12} &= \frac{\tau_{12}}{G_{12}} = \frac{1}{G_{12}}\left(\sin\theta\cos\theta\right)\sigma_{xx} \end{aligned} \qquad \text{(Eq 16.56)}$$

Failure occurs when:

$$\begin{aligned} \varepsilon_{11} > \varepsilon_{Lt} \\ \varepsilon_{22} > \varepsilon_{Lt} \text{ or} \\ \gamma_{12} > \gamma_s \end{aligned}$$

On the assumption that the material is linearly elastic up to the failure strain, failure of the ply occurs if the applied stress σ_{xx} exceeds the smallest of these values:

$$\begin{aligned} \frac{E_{11}\varepsilon_{Lt}}{\cos^2\theta - \nu_{12}\sin^2\theta} &= \frac{S_{Lt}}{\cos^2\theta - \nu_{12}\sin^2\theta} \quad \text{or} \\ \frac{E_{22}\varepsilon_{Tt}}{\sin^2\theta - \nu_{21}\cos^2\theta} &= \frac{S_{Tt}}{\sin^2\theta - \nu_{21}\cos^2\theta} \quad \text{or} \\ \frac{G_{12}\gamma_s}{\sin\theta\cos\theta} &= \frac{S_s}{\sin\theta\cos\theta} \end{aligned} \qquad \text{(Eq 16.57)}$$

The maximum stress theory and the maximum strain theory give similar results. Again, there is no interaction between strengths in different directions.

Azzi-Tsai-Hill Maximum Work Theory. The maximum work theory states that for plane stress, failure initiates when the following inequality is violated:

$$\frac{\sigma_{11}^2}{S_{Lt}^2} - \frac{\sigma_{11}\sigma_{22}}{S_{Lt}^2} + \frac{\sigma_{22}^2}{S_{Tt}^2} + \frac{\tau_{12}^2}{S_s^2} < 1 \qquad \text{(Eq 16.58)}$$

where σ_{11} and σ_{22} are both tensile stresses. When the state of stress is compression rather than tension, the compressive stresses σ_{11} and σ_{22} are used in Eq 16.58. In uniaxial tension, failure is predicted if:

$$\sigma_{xx} \geq \frac{1}{\left[\dfrac{\cos^4\theta}{S_{Lt}^2} - \dfrac{\sin^2\theta\cos^2\theta}{S_{Lt}^2} - \dfrac{\sin^4\theta}{S_{Tt}^2} - \dfrac{\sin^2\theta\cos^2\theta}{S_s^2}\right]^{\frac{1}{2}}} \qquad \text{(Eq 16.59)}$$

A failure envelope for the Azai-Tsai-Hill failure criterion for plane stress conditions is shown in Fig. 16.14. The failure envelope is a graphic representation of the safe and unsafe conditions for loading. It can be separated into quadrants.

In the first quadrant, where σ_{11} and $\sigma_{22} > 0$:

$$\frac{\sigma_{11}^2}{S_{Lt}^2} - \frac{\sigma_{11}\sigma_{22}}{S_{Lt}^2} + \frac{\sigma_{22}^2}{S_{Tt}^2} = 1 - \frac{\tau_{12}^2}{S_s^2}$$

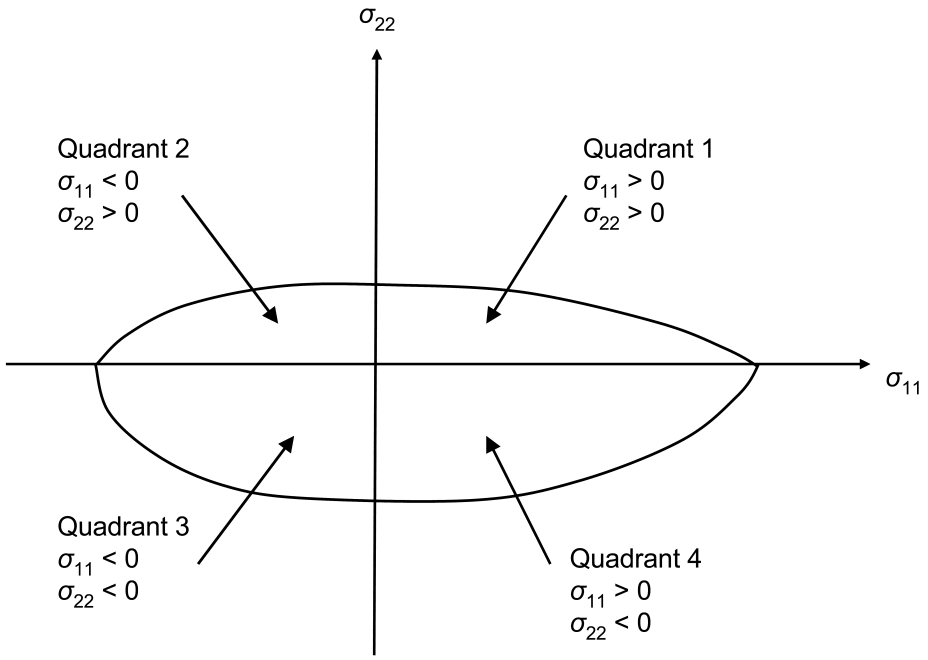


Fig. 16.14 Failure envelope for the Azai-Tasi-Hill failure criterion

In the second quadrant, where $\sigma_{11} < 0$ and $\sigma_{22} > 0$:

$$\frac{\sigma_{11}^2}{S_{Lc}^2} + \frac{\sigma_{11}\sigma_{22}}{S_{Lc}^2} + \frac{\sigma_{22}^2}{S_{Tt}^2} = 1 - \frac{\tau_{12}^2}{S_s^2}$$

In the third quadrant, where σ_{11} and $\sigma_{22} < 0$:

$$\frac{\sigma_{11}^2}{S_{Lc}^2} - \frac{\sigma_{11}\sigma_{22}}{S_{Lc}^2} + \frac{\sigma_{22}^2}{S_{Tc}^2} = 1 - \frac{\tau_{12}^2}{S_s^2}$$

In the fourth quadrant, where $\sigma_{11} > 0$ and $\sigma_{22} < 0$:

$$\frac{\sigma_{11}^2}{S_{Lt}^2} + \frac{\sigma_{11}\sigma_{22}}{S_{Lt}^2} + \frac{\sigma_{22}^2}{S_{Tc}^2} = 1 - \frac{\tau_{12}^2}{S_s^2}$$

The advantage of the Azai-Tsai-Hill criterion is that the interaction between strengths and failure modes is taken into account. As shown in the comparison with the maximum stress and maximum strain theories (Fig. 16.15), the Azai-Tsai-Hill criterion gives a better fit to the experimental data.

Tsai-Wu Failure Criterion. In the Tsai-Wu criterion, a composite ply subject to plane stress conditions will fail when the following condition is satisfied:

$$F_{11}\sigma_{11} + F_2\sigma_{22} + F_6\tau_{12} + F_{11}\sigma_{11}^2 + F_{22}\sigma_{22}^2 + F_{66}\tau_{12}^2 + 2F_{12}\sigma_{11}\sigma_{22} = 1 \qquad \text{(Eq 16.60)}$$

where the strength coefficients are defined as:

$$F_1 = \frac{1}{S_{Lt}} - \frac{1}{S_{Lc}}$$

$$F_2 = \frac{1}{S_{Tt}} - \frac{1}{S_{Tc}}$$

$$F_6 = 0$$

$$F_{11} = \frac{1}{S_{Lt}S_{Lc}}$$

$$F_{22} = \frac{1}{S_{Tt}S_{Tc}}$$

$$F_{66} = \frac{1}{S_s^2}$$

Although the strength coefficients F_1, F_2, F_{11}, F_{22}, and F_{66} can be calculated using the tensile, compressive, and shear strength properties in the principal material directions, F_{12} must be determined by a biaxial tensile test. Under a biaxial stress state with $\tau_{12} = 0$ and σ_{11} and $\sigma_{22} = \sigma$ at failure, Eq 16.60 reduces to:

$$(F_1 + F_2)\sigma + (F_{11} + F_{22} + 2F_{12})\sigma^2 = 1 \qquad \text{(Eq 16.61)}$$

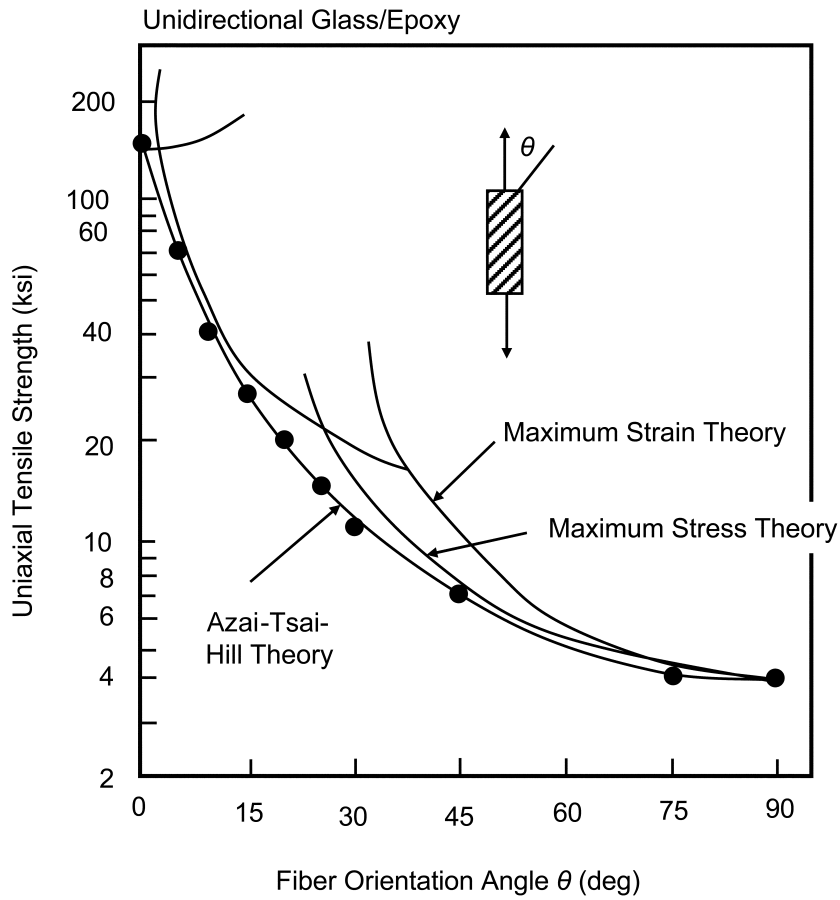


Fig. 16.15 Comparison of maximum stress, maximum strain, and the Azai-Tsai-Hill failure criterion. Source: Ref 2 and 3

which can be rearranged to give:

$$F_{12} = \frac{1}{2\sigma^2}\left[1 - \left(\frac{1}{S_{Lt}} - \frac{1}{S_{Lc}} + \frac{1}{S_{Tt}} - \frac{1}{S_{Tc}}\right)\sigma - \left(\frac{1}{S_{Lt}S_{Lc}} + \frac{1}{S_{Tt}S_{Tc}}\right)\sigma^2\right]$$

since a biaxial tensile test is difficult to conduct, an approximate value for F_{12} is given by:

$$-\frac{1}{2}\left(F_{11}F_{22}\right)^{1/2} \le F_{12} \le 0$$

The Tsai-Wu criterion is generally believed to give the best fit to experimental test data. Representative failure envelopes for the maximum strain, Azai-Tsai-Hill, and Tsai-Wu failure criteria are shown in Fig. 16.16. It should also be noted that these are not the only failure criteria; a number of others are available.

Once a failure criterion is selected, the procedure to predict laminate failure is as follows:

1. Calculate the stresses or strains in each ply using lamination theory.
2. Transform the individual stresses or strains in the loading direction into stresses or strains in the principal material directions.
3. Using one of the failure criteria, determine whether a ply has failed. After a ply fails, the stresses and strains in the remainder of the laminate increase and the laminate stiffness is reduced.
4. Since the failed ply may not carry its share of the load in all directions, several methods can be used to account for the failed ply and subsequent laminate behavior:

Total discount method. In this method, zero strength and stiffness are assigned to the failed ply in all directions.

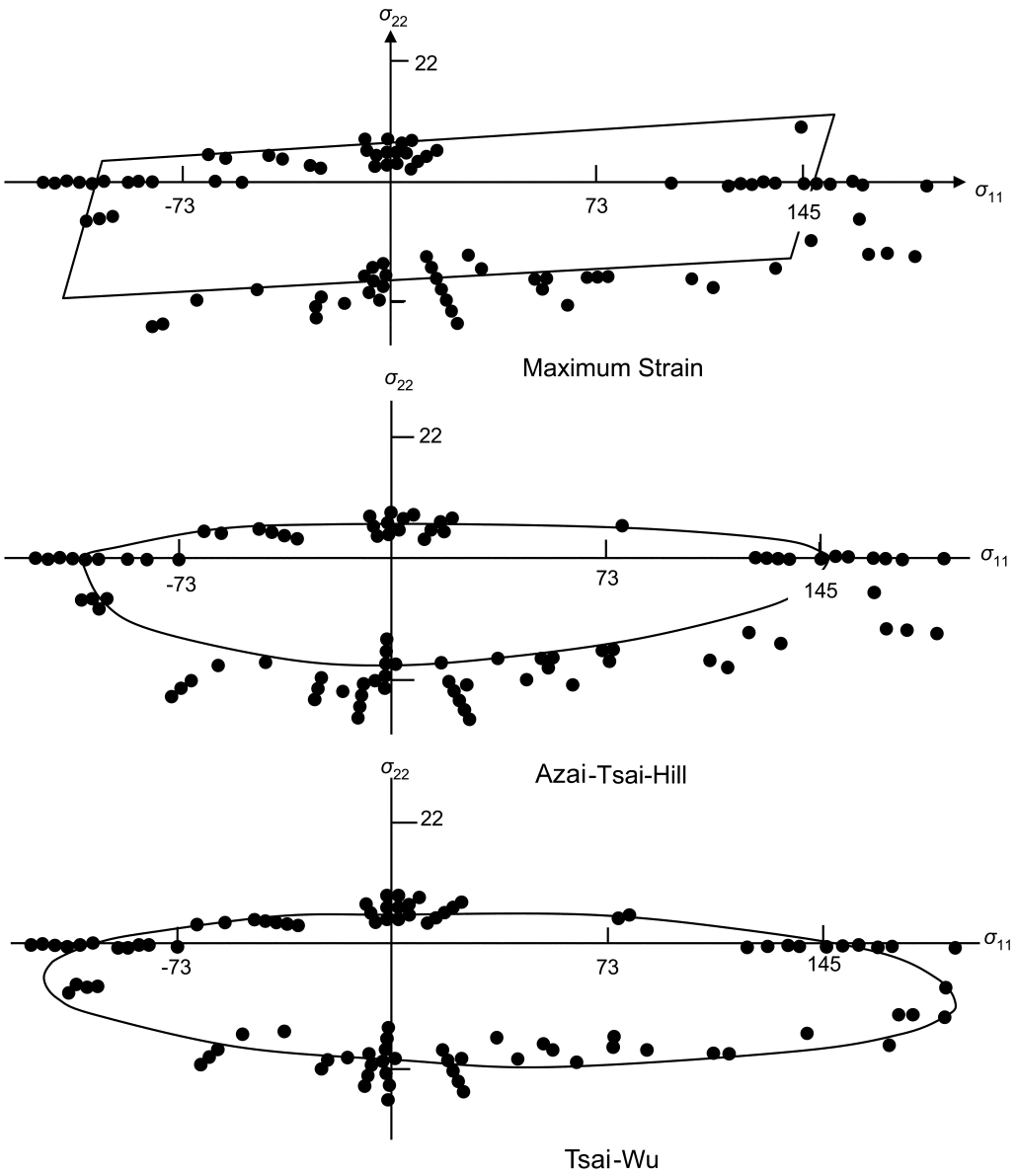


Fig. 16.16 Failure envelopes for maximum strain, Azai-Tsai-Hill, and Tsai-Wu criteria. Source: Ref 4

Limited discount method. If the ply failure occurs in the matrix, then zero strength and stiffness are assigned to the failed ply for the transverse and shear modes. If the ply fails by fiber rupture, then the total discount method is used.

Residual property method. In this method, residual strength and stiffness are assigned to the failed ply.

When a laminate is loaded to failure, not all plies fail at the same time. The progressive ply failures in a $[0°/45°/90°/–45°]_s$ laminate are shown in Fig. 16.17. Plies will fail successively in increasing order of strength in the loading direction. Because the transverse strength of unidirectional plies is lower than the longitudinal strength, the transverse plies will fail first. Failure of the 90-degree plies is generally followed by failure of other off-angle plies such as ±45°, and finally of the much stronger zero-degree pl The occurrence of first ply failure, although a

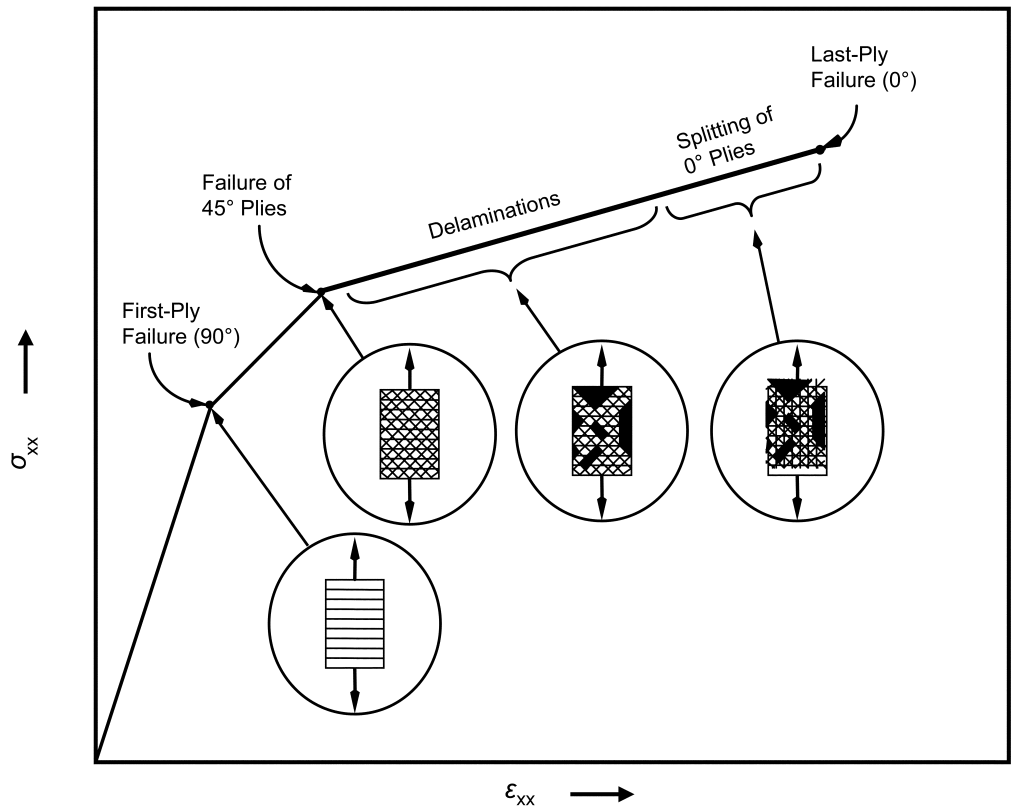


Fig. 16.17 Progressive ply failure for a $[0°/45°/90°/-45°]_s$ laminate

relatively conservative design criterion, is often used in the aerospace industry to indicate laminate failure.

16.8 Concluding Remarks

This chapter gives only a brief introduction to composite structural analysis. Actual analysis of composite structures requires a much deeper understanding of the available analysis methods. Again, the reader is referred to more detailed texts for a more rigorous treatment. Lamination theory can also be expanded to account for thermal stresses that result from curing at elevated temperatures and the effects of moisture absorption. Any respectable computerized laminate code is capable of handling these extensions.

REFERENCES

1. A. Baker, S. Dutton, and D. Kelly, *Composite Materials for Aircraft Structures*, 2nd ed., American Institute of Aeronautics and Astronautics, 2004
2. V.D. Azai and S.W. Tsai, *Exp. Mech.*, Vol 5 (No. 283), 1965
3. R.M. Jones, *Mechanics of Composite Materials*, 2nd ed., Hemisphere Publications, 1998
4. S.W. Tsai and H.T. Hahn, *Inelastic Behavior of Composite Materials*, American Society of Mechanical Engineers, 1975

SELECTED REFERENCES

- B.D. Agarwal and L.J. Broutman, *Analysis and Performance of Fiber Composites*, John Wiley and Sons, Inc., 1980
- V.K.S. Choo, *Fundamentals of Composite Materials*, Knowen Academic Press, 1990
- R.M. Christensen, *Mechanics of Composite Materials*, Dover Publications, 2005
- I.M. Daniel and O. Ishai, *Engineering Mechanics of Composite Materials*, 2nd ed., Oxford University Press, 2005

- D. Gay, S.W. Hoa, and S.W. Tsai, *Composite Materials Design and Applications*, CRC Press, 2003
- Z. Hahin, B.W. Rosen, E.A. Humphreys, C. Newton, and S. Chaterjee, *Fiber Composite Analysis and Design: Composite Materials and Laminates,* Vol I, U.S. Department of Transportation, Federal Aviation Administration, DOT/FAA/AR-95/29, I, Final Report, Oct 1997
- L.P. Kollar and G.S. Springer, *Mechanics of Composite Structures*, Cambridge University Press, 2002
- M. Piggott, *Load Bearing Fibre Composites*, 2nd ed., Kluwer Academic Publishers, 2002
- G.H. Stabb, *Laminar Composites*, Butterworth-Heinemann, 1999
- S.W. Tsai and H.T. Hahn, *Introduction to Composite Materials*, Technomic Publishing, 1980
- M.E. Tuttle, *Structural Analysis of Polymeric Composite Materials*, Marcel Dekker, Inc., 2004
- V.V. Vasiliev and E.V. Morozov, *Mechanics and Analysis of Composite Materials*, Elsevier Science Ltd., 2001
- J.R. Vinson and R.L. Sierakowski, *The Behavior of Structures Composed of Composite Materials*, 2nd ed., Kluwer Academic Publishers, 2004

"*This page left intentionally blank.*"

Copyright © 2010, ASM International®
All rights reserved.
www.asminternational.org

CHAPTER 17

Structural Joints—Bolted and Bonded

ANALYTICAL CONSIDERATIONS, as discussed in the previous chapter, includes much discussion of unnotched laminates. However, for practical purposes, the joints in a composite structure should be designed first and then the space between them filled in with appropriate laminate orientations. Optimization of the basic structure first can often compromise the design of the joints, resulting in lower overall structural efficiency and possibly producing a structure that is more difficult to repair.

Two primary methods of joining are used for polymer matrix composites: mechanical fastening and adhesive bonding. Since fastener holes cut through the fibers and destroy the load path, much more efficient load transfer can be obtained with adhesively bonded joints. A well-designed adhesively bonded joint will actually be stronger than the base laminate. On the other hand, even a well-designed mechanically fastened joint will be only about 40 to 50 percent as strong as the base laminate. In spite of this advantage, adhesively bonded joints are not always practical. Bonded joints are preferred if thin composite sections are to be joined where bearing stresses in bolted joints would be unacceptably high or when the weight penalty for mechanical fasteners is too high. In general, thin structures with well-defined load paths are good candidates for adhesive bonding, whereas thicker structures with complex load paths are good candidates for mechanical fastening.

The low efficiency of mechanically fastened joints in composites is a direct consequence of their inherent brittleness. When a metallic structure is highly loaded, the metal will yield locally in the vicinity of the bolt hole to reduce the elastic stress concentration. However, since composites are relatively brittle, they do not yield and the stress concentration remains high. The stress concentration is reduced somewhat due to localized delaminations around the fastener hole, but the reduction is small compared to the gross yielding that occurs in metallic alloys. In addition, nearly quasi-isotropic laminates with 0°, ± 45°, 90° orientations are required to develop sufficient joint strengths, which lowers the basic laminate strength from a more highly orthotropic (0° dominated) laminate orientation.

This chapter discusses mechanically fastened joints and adhesively bonded joints. Like the Chapter 16, "Structural Analysis," this chapter is primarily an overview of analytic considerations for joints. Much more extensive treatments can be found in some of the references listed at the end of this chapter. The details of hole preparation and fastener installation are found in Chapter 11, "Machining and Assembly," and adhesive bonding procedures are covered in Chapter 8, "Adhesive Bonding."

17.1 Mechanically Fastened Joints

Compared to adhesive bonding, mechanically fastened joints have both advantages and disadvantages. The advantages of mechanical fastening include the following:

- Mechanical fastening is a much more straightforward and less risky joining process. Whereas adhesive bonding requires stringent surface preparations and the quality of the bond is dependent on the cure of polymerizable materials, mechanical fastening does not require much surface preparation and is much less affected by environmental exposure.
- Compared to adhesive bonding, mechanical fastening provides better through-the-thickness

reinforcement and is not as sensitive to peel stresses or residual-stress effects.
- Unlike adhesively bonded joints, mechanically fastened joints do not normally require nondestructive testing.
- Many mechanically fastened joints allow disassembly or panel removal. Depending on the specific fastener selected, some are designed for permanent installation and others allow easy removal.
- Mechanically fastened joints are much more amenable to field repairs because cleanliness, perishable materials, and elevated-temperature cures are not concerns.

The disadvantages of mechanical fastening include the following:

- Much lower joint efficiencies are obtained with mechanically fastened joints. Composites are notch sensitive, and even the best mechanically fastened joints can only attain about 40 to 50 percent of the base laminate strength.
- Composites have low bearing strengths compared to metals and can experience hole elongation due to in-service fatigue, which degrades joint strength.
- Improper hole preparation procedures and poor shimming practices can induce delaminations during assembly. Unshimmed gaps are a major problem and can result in delaminations in both composite skins and substructure.
- Composite-to-metal joints are subject to fretting and corrosion of the metal in service. Fatigue cracking of metal components can also be a problem.

17.2 Mechanically Fastened Joint Analysis

A simple single-fastener single-lap shear joint is shown in Fig. 17.1. The key dimensions are these:

d—fastener diameter
t—thickness of the joint elements
w—width of the plate
e—edge distance
P—load
dt—bearing area loaded in compression
2et—total shear-out area loaded in shear
(*w*-*d*)/*t*—net section loaded in tension
wt—gross section loaded in tension

The average stresses in the joint are as follows:

Average bearing stress $\sigma_b = P/dt$ (Eq 17.1)

Average shear-out stress $\sigma_{so} = P/2et$ (Eq 17.2)

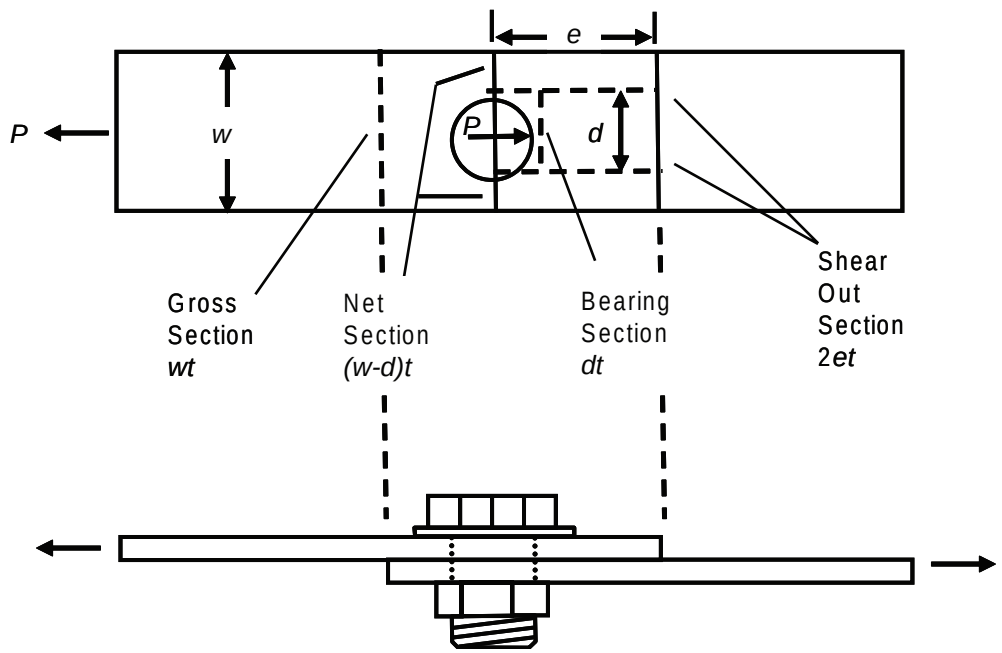


Fig. 17.1 Single-shear joint. Source: Ref 1

Average net section stress $\sigma_n = P/(w\text{-}d)t$ (Eq 17.3)

Average gross section stress $\sigma_g = P/wt$ (Eq 17.4)

In traditional joint analysis, it is necessary to calculate the failing stress for each of these conditions. Failure will occur at the condition with the lowest joint strength. However, since bolted joints are always weaker than the base laminate, gross section failures will not occur unless the joint area has been thickened considerably. In addition, the selection of a nearly quasi-isotropic laminate is necessary in order for the bolt loads to be carried effectively and shear-out failures to be thereby eliminated. Therefore, the emphasis of the following discussion will be on bearing and net tension failures.

The various failure modes for composite joints are shown in Fig. 17.2. Potential causes include:

1. *Bearing*: Bearing failures are characterized by localized damage, such as delaminations and matrix crazing around the hole. Localized compression loading caused by the

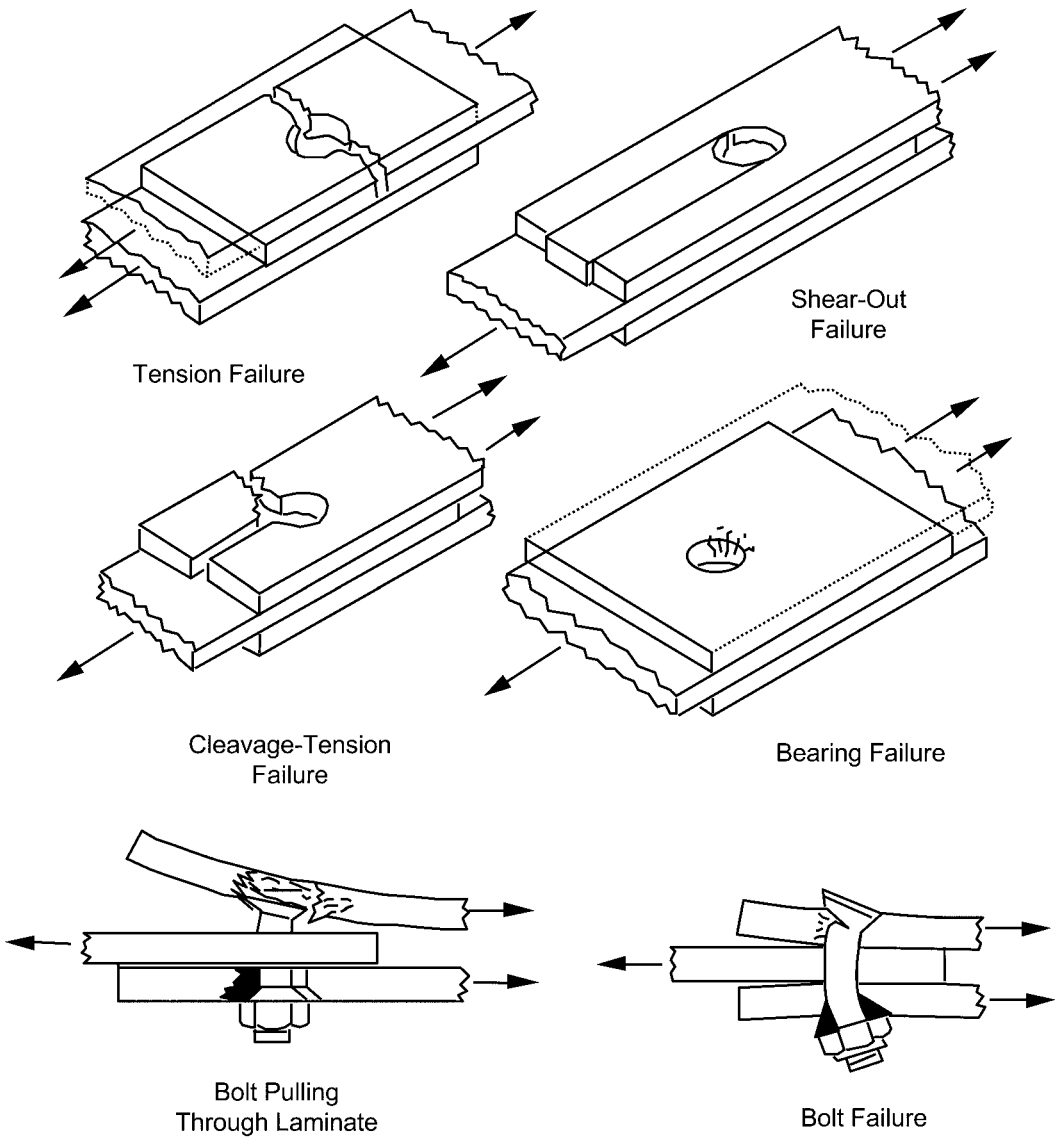


Fig. 17.2 Mechanically fastened composite joint failure modes

fastener leads to buckling and kinking of the fibers followed by crushing of the matrix.
2. *Shear-out*: Shear-out failures result from insufficient edge distance or from having too many plies oriented in the load direction, for example 0°.
3. *Tension*: Tension failures are caused by insufficient width or by having too few plies oriented in the load direction, for example 0°.
4. *Cleavage-tension*: Cleavage-tension failures occur due to insufficient edge distance and width or an insufficient number of cross-plies, for example ± 45º and 90º.
5. *Fastener pull-through*: Fastener pull-through can occur when the countersink is too deep or when a shear head fastener is used.
6. *Fastener failure*: The fastener itself can fail if it is too small for the laminate thickness, if there are unshimmed gaps or excessive shimmed gaps in the joint, or if there is insufficient fastener clamp-up.

If a high-strength, highly orthotropic laminate has a large portion of 0° plies, the joint strength will be low because of the likelihood of fastener shear-out. Using an insufficient number of 0° plies in a laminate will result in tension failure at a lower than desired load. Therefore, a more balanced laminate is required, that is, a laminate that is close to quasi-isotropic consisting of 0°, ± 45°, 90° ply orientations. The 0° fibers carry the bearing and tension loads, and the ± 45° and 90° fibers carry the load around the hole to prevent shear-out or cleavage-type failures. The addition of 0° plies improves bearing strength up to about 60 percent. However, above about 60 percent, failure occurs by splitting because the transverse tensile strength becomes insufficient to prevent shear-out failures. The optimum bearing strength for a 0°, ± 45° laminate occurs with fiber orientations of about 50 percent, 0°; and 50 percent ± 45° plies. Because interplay stresses are reduced as the laminate becomes more homogeneous, bearing strength can further be improved by thoroughly dispersing the 0° and ± 45° plies throughout the lay-up. Some designers consider bearing failures to be the only acceptable failure mode because they are not catastrophic, whereas through-the-thickness tension failures are abrupt and catastrophic. However, designing in accordance with this criterion will result in less than optimum joint strengths. Tension failure modes are associated with far higher bolted composite joint strengths; it is all but impossible to design a multirow bolted joint that will fail by bearing.

The failure mode is also dependent on the ratios of the edge distance to the diameter of the fastener (*e*/*d*) and the width of the joint to the diameter of the fastener hole (*w*/*d*), as illustrated for a quasi-isotropic laminate in Fig. 17.3. For large values of *e*/*d* and *w*/*d*, the joint fails in bearing with the failing load being independent of *e*/*d* or *w*/*d*. If the edge distance *e* is reduced, then a shear-out failure occurs with the joint strength approaching zero at *e*/*d* = 0.5. If the width *w* is

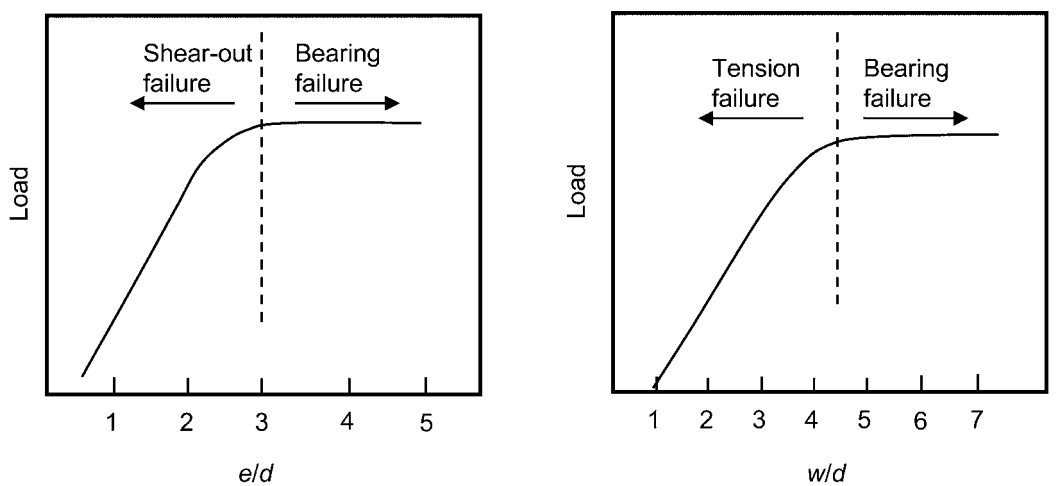


Fig. 17.3 Effects of edge distance and width on mechanically fastened failure modes. Source: Ref 2

reduced, then a net tension failure will occur with the joint strength approaching zero at $w/d = 1$.

The preferred fiber orientation design envelope for mechanically fastened joints is shown in Fig. 17.4. Shear-out does not occur within the recommended design envelope of laminate patterns shown here. However, outside the recommended design envelope, shear-out with through-the-thickness cracks parallel to the 0° plies is likely to result in premature failures. Shear-out cannot be corrected by adding more edge distance e to a highly orthotropic laminate. Even an increase in thickness, without changing to a more quasi-isotropic laminate pattern, is not very effective. Therefore, the joint can never be loaded to the levels predicted by lamination theory for unnotched laminates. The strength of composite structures with both loaded and unloaded holes depends only slightly on the fiber pattern for nearly quasi-isotropic laminates; the stress concentration factor increases almost as rapidly as the unnotched strength for slightly orthotropic patterns. Therefore, throughout the range of fiber patterns surrounding the quasi-isotropic lay-up, the bearing strengths and gross-section strengths are almost constant.

Since we are dealing with holes, which are notches, stress concentration factors K must be

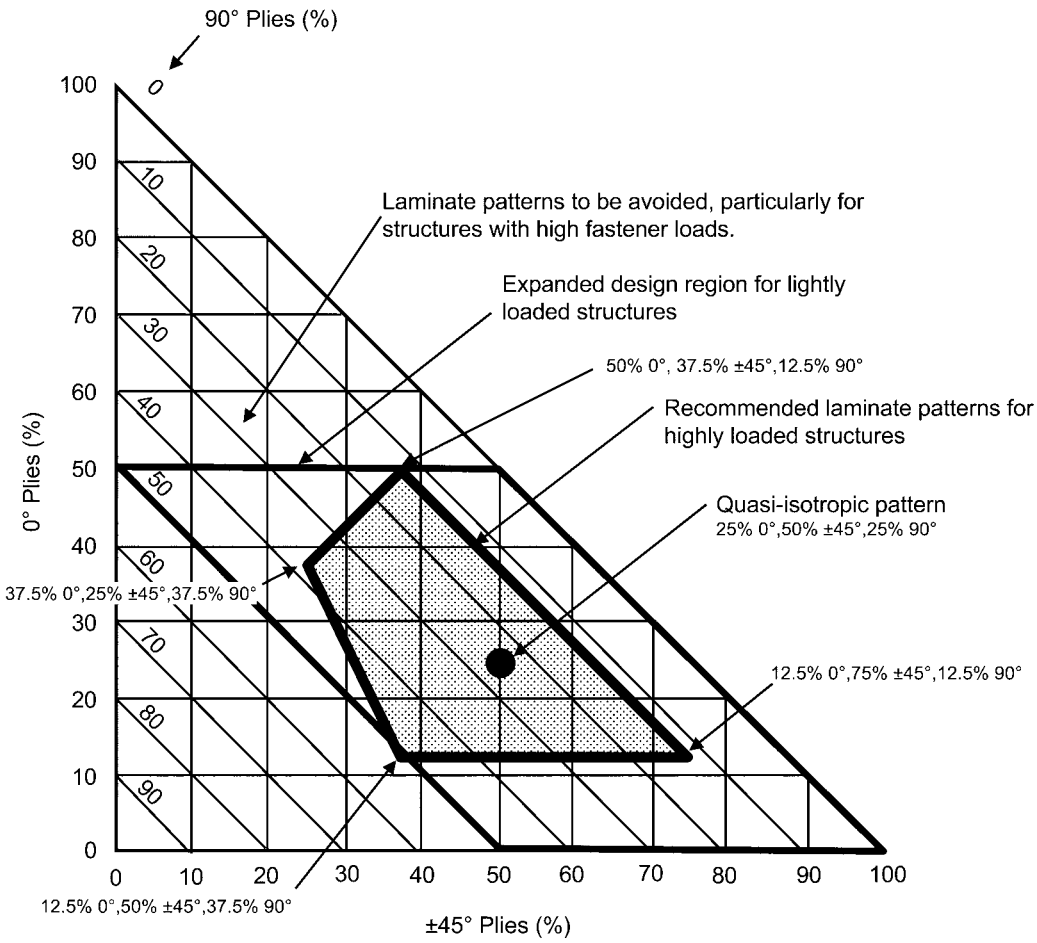


Fig. 17.4 Recommended design envelope for mechanically fastened composites. Source: after Ref 3

used. They account for the increase in stress σ_{max} over the nominally applied stress σ_{nom}. In other words:

$$\sigma_{max} = K\sigma_{nom} \quad \text{(Eq 17.5)}$$

The stress concentration factor varies with the severity of the notch; sharper notches produce higher stress concentration factors and thus increase the applied nominal stresses. For an isotropic metal with a round hole, the stress concentration factor is usually taken as 3.0 within the elastic region.

In a composite laminate, the degree of stress concentration effect depends on the laminate pattern. Analysis has shown that the theoretical elastic stress concentration K_{te} at the edge of a hole at 90° to an applied tension stress is given by the following equation:

$$K_{te} = 1 + \sqrt{\left\{2\left[\sqrt{\left(\frac{E_{xx}}{E_{yy}}\right)} - \nu_{xy}\right] + \frac{E_{xx}}{G_{xy}}\right\}} \quad \text{(Eq 17.6)}$$

According to this equation, K_{te} varies from 7.5 for a 100 percent 0° laminate down to about 1.8 for a 100 percent ± 45° laminate. Since the laminate tensile strength falls with an increase in the percentage of ± 45° plies, the optimum ply configuration is again on the order of 50 percent ± 45° plies. The peak stress level does not necessarily occur at 90° to the applied load; in the case of an all ± 45° laminate, the peak stress occurs at 45° to the loading direction.

When a mechanically fastened composite joint is loaded, microcracks and delaminations around the hole cause internal load redistributions that are not accounted for in elastic design. Thus, there is substantial nonlinear behavior associated with the normal fastener sizes used in composite structures. While these softened zones (Fig. 17.5) are not the same as yielding zones in metallic structures, they produce somewhat similar effects. For example, any increase in the softened zone around fasteners in composites causes an increase in the static tensile strength, and the gentle fatiguing of bolted composite structures can increase the static tensile strength toward the unnotched net section strength. The corresponding increase in compressive strength will not be as large, because (1) it is dominated

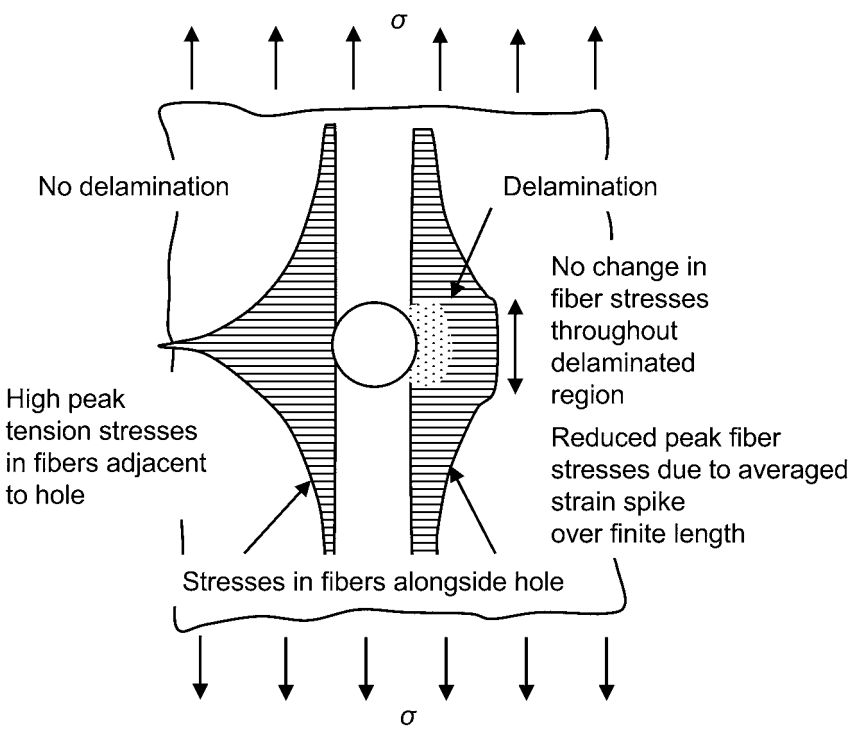


Fig. 17.5 Stress concentration reduction in composite laminates. Source: Ref 3

more by bearing stresses than by net section stresses and (2) the localized damage area destabilizes axially compressed fibers. As shown in Fig. 17.6, at the elastic level the peak tension stress alongside the loaded bolt hole in an isotropic panel is of the same order of magnitude as the average bearing stress (P/dt). Keeping the bearing stress low is a key to structurally efficient bolted composite joints, particularly multirow joints. Since the peak hoop tension stress is of the same order of magnitude as the average bearing stress, the bolts should be placed close together to minimize the peak hoop tension stresses.

Because of the nonlinear material behavior of composites around both loaded and unloaded holes, empirically established correlation factors are required. Using this method, it is necessary to assume that the amount of stress concentration relief is proportional to the intensity of the original elastic stress concentration. With a correlation factor determined from single-hole test specimens as a starting point, the strength of highly loaded multirow bolted composite joints can be effectively predicted. Corrections both for the nonlinear behavior around a fastener and for orthotropy can be combined into a single correlation coefficient C (as discussed below), provided that the mode and location of failure do not change. Separate analyses are needed for bearing failures and for tension through-the-hole failure modes. Compression strengths tend to be higher and not as sensitive to stress concentrations, because some of the load can be transmitted through the fastener rather than around it.

Two other semiempirical criteria are currently used for analyzing the tensile stress state around a hole in a plate of finite width: the *average stress* and *point stress* criteria. Under the average stress criterion, failure is considered to occur when the average value of the tensile stress over some characteristic length a_0 from the hole reaches the unnotched ultimate tensile strength of the laminate. Under the point stress criterion, failure is considered to occur when the local value of the stress at some characteristic distance d_0 from the hole reaches the unnotched ultimate tensile strength. The values a_0 and d_0, which are considered to be material properties, are determined from plots of strength reduction versus hole size to give the best fit to the experimental results. The two criteria are related through the relationship $a_0 = 4d_0$. However, in the following discussion, we will use the correlation coefficient C.

17.3 Single-Hole Bolted Composite Joints

The relationships between the strengths of bolted joints in ductile metals, composites, and brittle materials are shown in Fig. 17.7. For

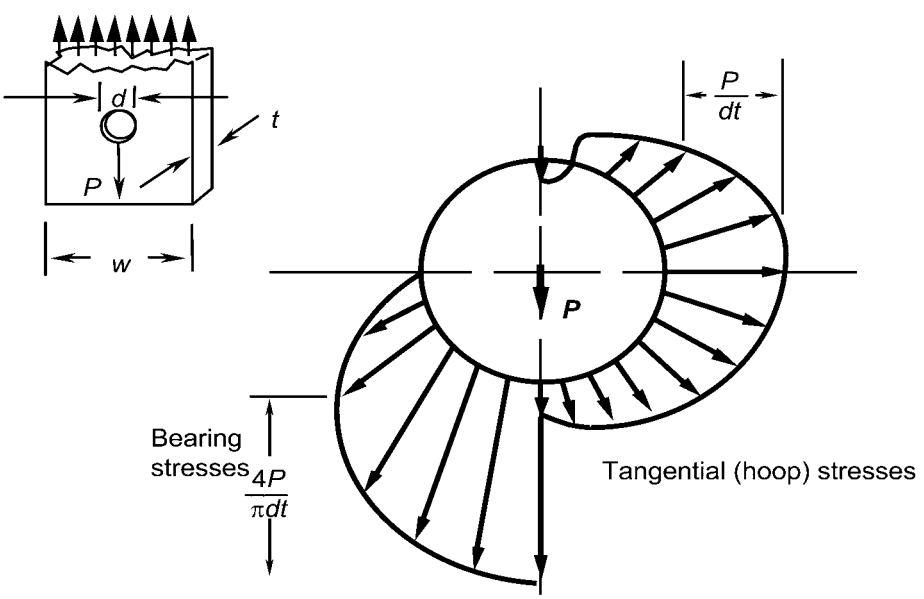


Fig. 17.6 Bearing and hoop stresses at the bolt hole. Source: Ref 3

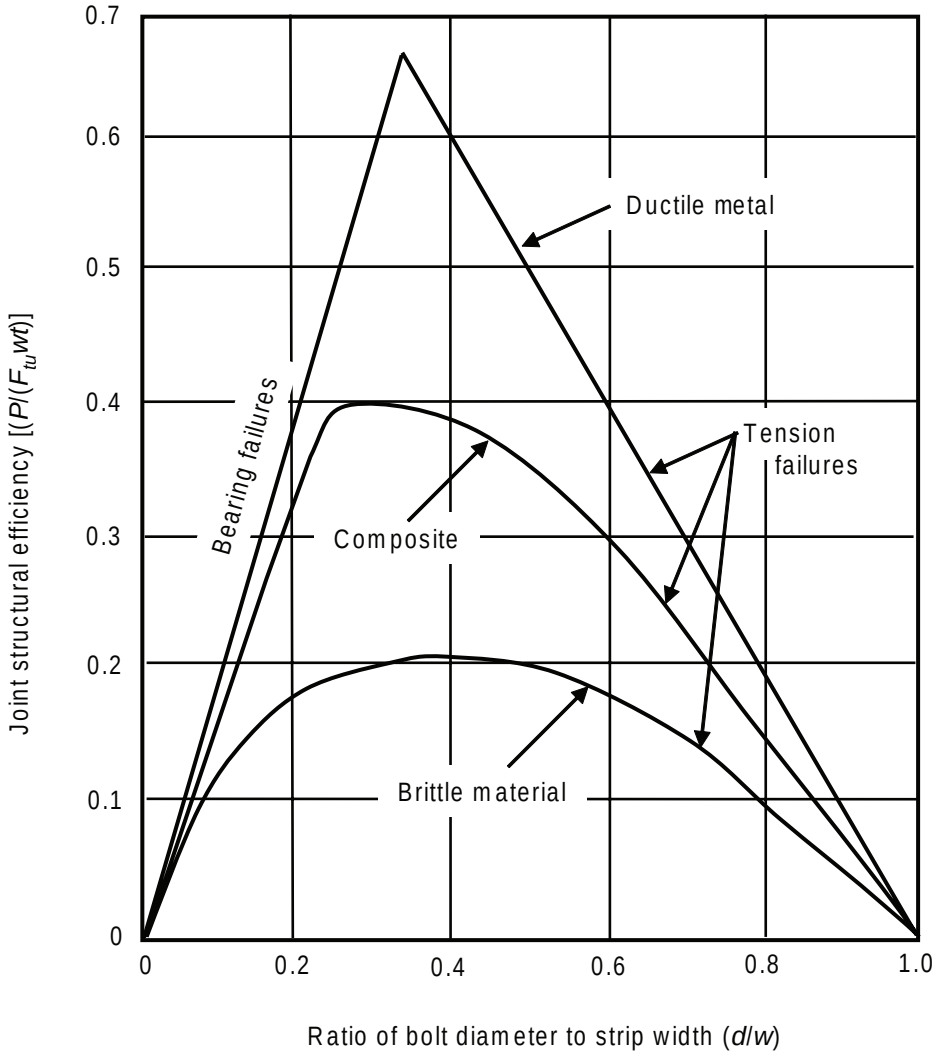


Fig. 17.7 Joint efficiency versus *d*/*w* for ductile metals, composites, and brittle materials. Source: Ref 3

metals under high stresses, localized yielding reduces the effective stress concentration factor from 3.0 to around 1; therefore, failure is simply dependent on the net cross-section area. However, for a purely brittle material, since no yielding occurs, the effective stress concentration factor remains high. For composites, as a result of the localized damage adjacent to the hole, there is some stress concentration relief, but not as much as for gross localized yielding in metals. The maximum attainable joint efficiencies are 65 percent for metal, 40 percent for composite, and 21 percent for a perfectly brittle material. For both metal and composite, a change in failure mode from net tension to bearing is predicted to occur at a *d*/*w* of approximately 0.3. Also, the strength increase shown in Fig. 17.7 for roughly 0.25 in. (6.5 mm) diameter bolts in carbon/epoxy composites decreases asymptotically as the fastener diameter increases, and, for very large bolt holes or cutouts, the linearly elastic predictions would be expected to apply.

As can be derived from Eq 17.3, the maximum tensile stress σ_{max} at the edges of a loaded hole in a joint under a load P is given by the following equation:

$$\sigma_{max} = K_{tc}\left(\text{average net section stress}\right) = \frac{K_{tc}P}{t\left(w-d\right)} \quad \text{(Eq 17.7)}$$

where K_{tc} is the effective stress concentration factor based on the net section. Note that K_{tc} is lower than the theoretical stress concentration factor K_{te} owing to the localized damage mechanisms adjacent to the hole, which produce a softening effect (Fig. 17.5). The relationship between K_{tc} and K_{te} is determined experimentally from strength tests on joints. A summary of some of the important stress concentration factors for various geometries is given in Table 17.1. An approximate linear relationship exists and can be expressed as follows:

$$K_{tc} = 1 + C(K_{te} + 1) \qquad \text{(Eq 17.8)}$$

where C is the correlation coefficient for the particular laminate pattern, joint geometry, and environmental conditions. For a perfectly plastic material, the value of C is 0, and for a purely brittle material, the value of C is 1.0. The value of C is close to 0.25 for 0.25 in. (6.5 mm) bolts in quasi-isotropic carbon/epoxy laminates. The value of C will increase for more orthotropic laminates. For 0.25 in. (6.5 mm) diameter fasteners in laminates within the shaded area in Fig. 17.4:

$$C \approx \frac{\%\,0^\circ \text{ Plies}}{100} \qquad \text{(Eq 17.9)}$$

This linear relationship between C and the percentage of 0° plies is shown in Fig. 17.8.

Table 17.1 Theoretical stress concentration factors K_{te} for composites

Stress concentration factor for an unloaded hole of diameter d in a finite strip of width w	$k_{te} = 2 + \left(1 - \frac{d}{w}\right)^3$
Stress concentration factor for an infinite plate with a row of unloaded holes at a pitch p	$k_{te} = 1 + 2\left(1 - \frac{d}{w}\right)^{1.5}$
Stress concentration factor for a loaded hole in a finite-width strip with the center of the hole a distance e from the edge of the laminate	$k_{te} = \frac{w}{d} + \frac{d}{w} + 0.5\left(1 - \frac{d}{w}\right)\Theta, \approx \frac{w}{d} + \frac{d}{w}$ where: $\Theta = \left(\frac{w}{e} - 1\right)$ for $e/w \le 1$ $\Theta = 0$ for $e/w \ge 1$
Stress concentration for a row of loaded holes in an infinite panel at a pitch of p	$k_{te} = \frac{p}{d} + 0.5\left(1 - \frac{d}{p}\right)\Theta, \approx \frac{p}{d}$ where: $\Theta = \left(\frac{p}{e} - 1\right)$ for $e/p \le 1$ $\Theta = 0$ for $e/p \ge 1$

The use of a single value for C is applicable only when the failure mode does not change. For small d/w (or large w/d) ratios, the laminates will fail at a lower load in bearing under the bolt rather than by tension through the hole. Therefore, a lower-bound cutoff is needed to cover this failure mode. This is shown on the left of the middle curve in Fig. 17.7. Bearing failures also occur for ductile metal alloys, as shown to the left of the top curve in Fig. 17.7. However, this approach becomes invalid for most of the fiber patterns outside the shaded area shown in Fig. 17.4 because of a predominance of shear-out failures.

When allowance is made for the nonlinear behavior of the composite around the bolt holes, the optimal w/d ratio is approximately three to one for 0.25 in. (6.5 mm) diameter bolts, being slightly higher for smaller bolts and lower for larger ones. This optimal ratio applies to single-row joints in which all of the load is transferred through a single row of fasteners; different values are required for multi-row composite joints. Also, whereas the maximum strength for ductile metals occurs at the intersection of the bearing and tension strengths, the maximum efficiency for single-row bolted composite joints is developed by tensile failures of the net section, at a bearing stress that is typically only about three-fourths of the bearing stress the composite material could withstand at wider bolt spacings.

The bearing strength of composite laminates is strongly influenced by the amount of through-the-thickness clamp-up, as shown in Fig. 17.9. There is a nearly two to one difference between the pin-loaded case, in which there is no clamp-up at all, and the finger-tight case, in which the bolt head and nut prevent any initially damaged composite material from unloading itself by deflecting sideways. Because all of the material is confined with the finger-tight condition, the joint can carry higher loads. This improvement in strength is customarily accounted for in design. However, the even greater strengths that can be achieved by torquing the bolts down tightly should not be relied on for design purposes, because it would be very difficult to detect a single undertorqued fastener that would substantially reduce the static strength of the joint. In contrast, the loss of clamp-up in metal joints would merely reduce the fatigue life, with no associated reduction in static strength. In any case, the improvement in bearing strength of composites because of additional bolt torque is often not realized, because tension through-the-hole

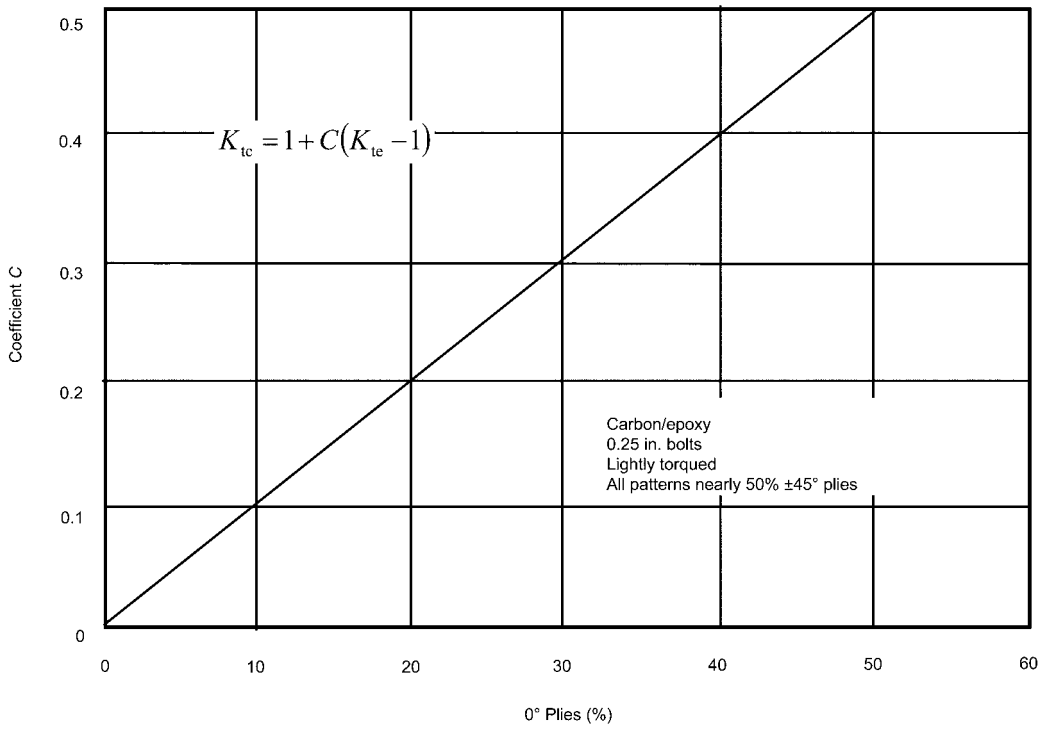


Fig. 17.8 Stress concentration relief at bolt holes in composite laminates. Source: Ref 3

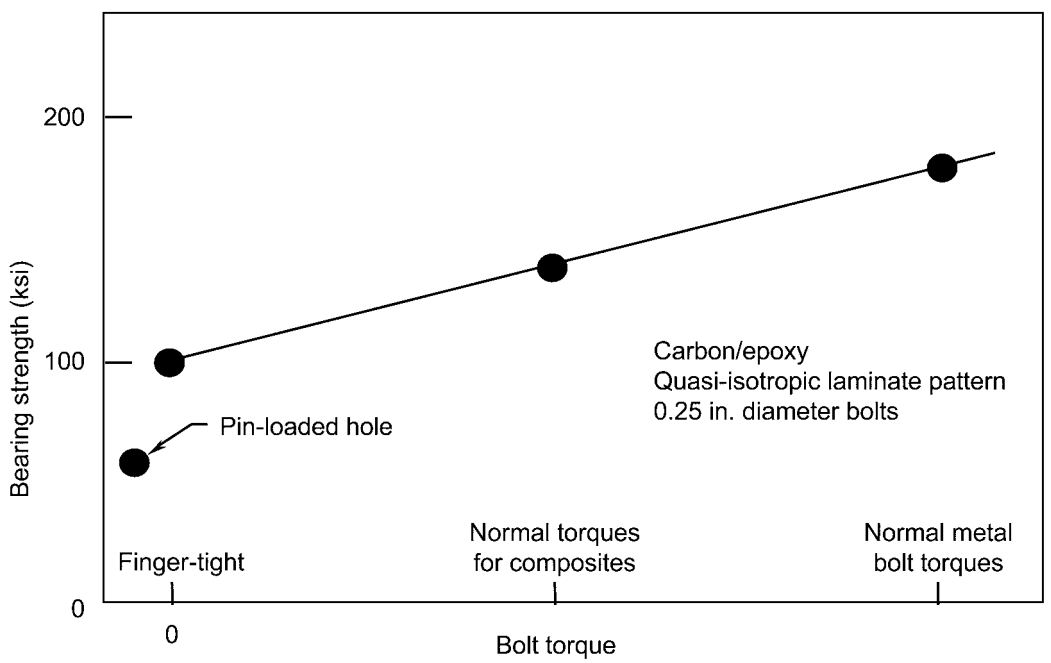


Fig. 17.9 Effect of bolt torque on bearing strength. Source: Ref 3

strength may govern the design, particularly for large fasteners.

Because bearing strength depends to a large degree on the strength of the matrix and elevated temperatures decrease matrix strength and stiffness, the effects of elevated temperature on the bearing strength of two 350 °F (180 °C) cured carbon/epoxy material systems are shown in Fig. 17.10. At the recommended maximum usage temperature of around 250 °F (120 °C), the bearing strengths are still fairly respectable.

The use of countersunk fasteners, particularly in single shear joints, causes problems because of the eccentric load path, which makes fasteners rotate (Fig. 17.11). Fastener cocking during loading can result in point loading and lead to progressive damage during fatigue cycling. Therefore, double shear joints are preferable when possible. Some propose that in the analysis of countersunk fasteners, the head should be totally discounted. Such an approach means restricting the depth of the countersink. The countersink depth has to be closely controlled to prevent a knife edge in thin structure; the recommended countersink depth is no more than 50 to 70 percent of the thickness of the countersunk member.

17.4 Multirow Bolted Composite Joints

Single-row fastened joints in composite structures are not weight-competitive with well-designed aluminum structures; multi-row fastener patterns must be used. The nomenclature for a multi-row joint is shown in Fig. 17.12. The use of softening strips such as fiberglass plies adjacent to the holes or local pad-ups at the holes allows for higher operating strains and thus higher structural efficiency. However, such a structure may be irreparable in areas adjacent to the holes as a direct consequence of the higher operating strains. As shown in Fig. 17.13, in a

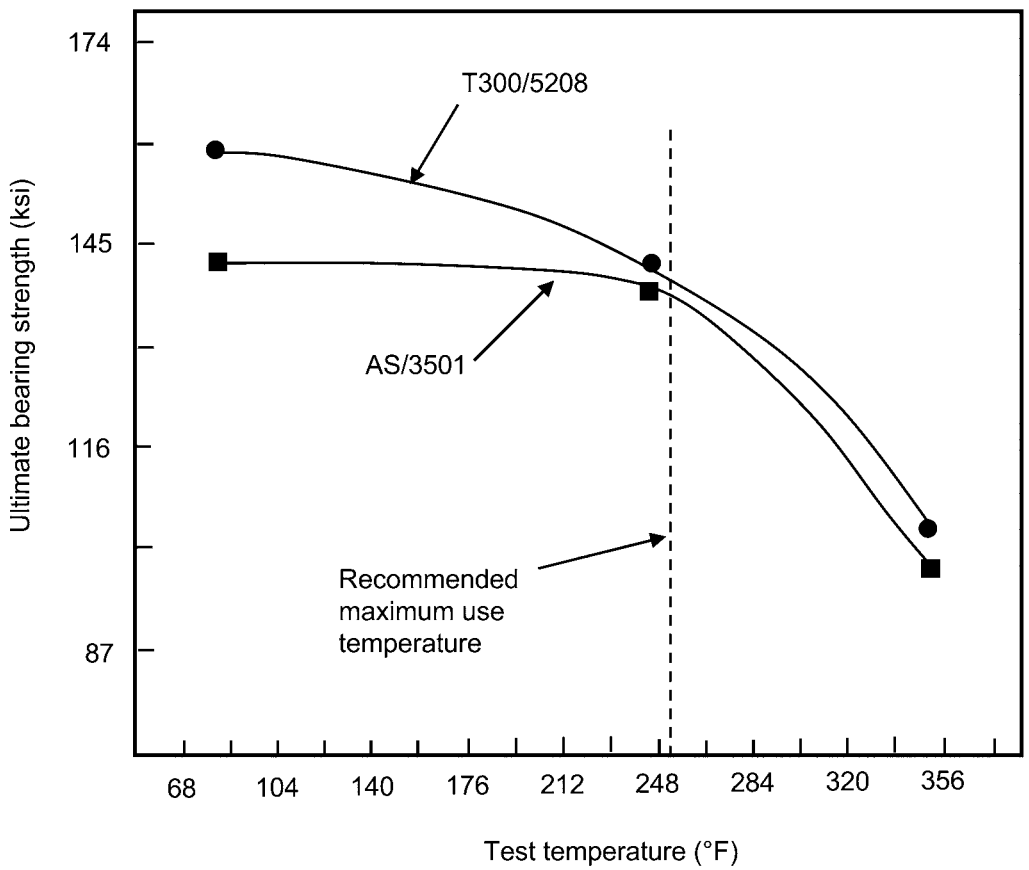


Fig. 17.10 Effect of temperature on bearing strength. Source: Ref 4

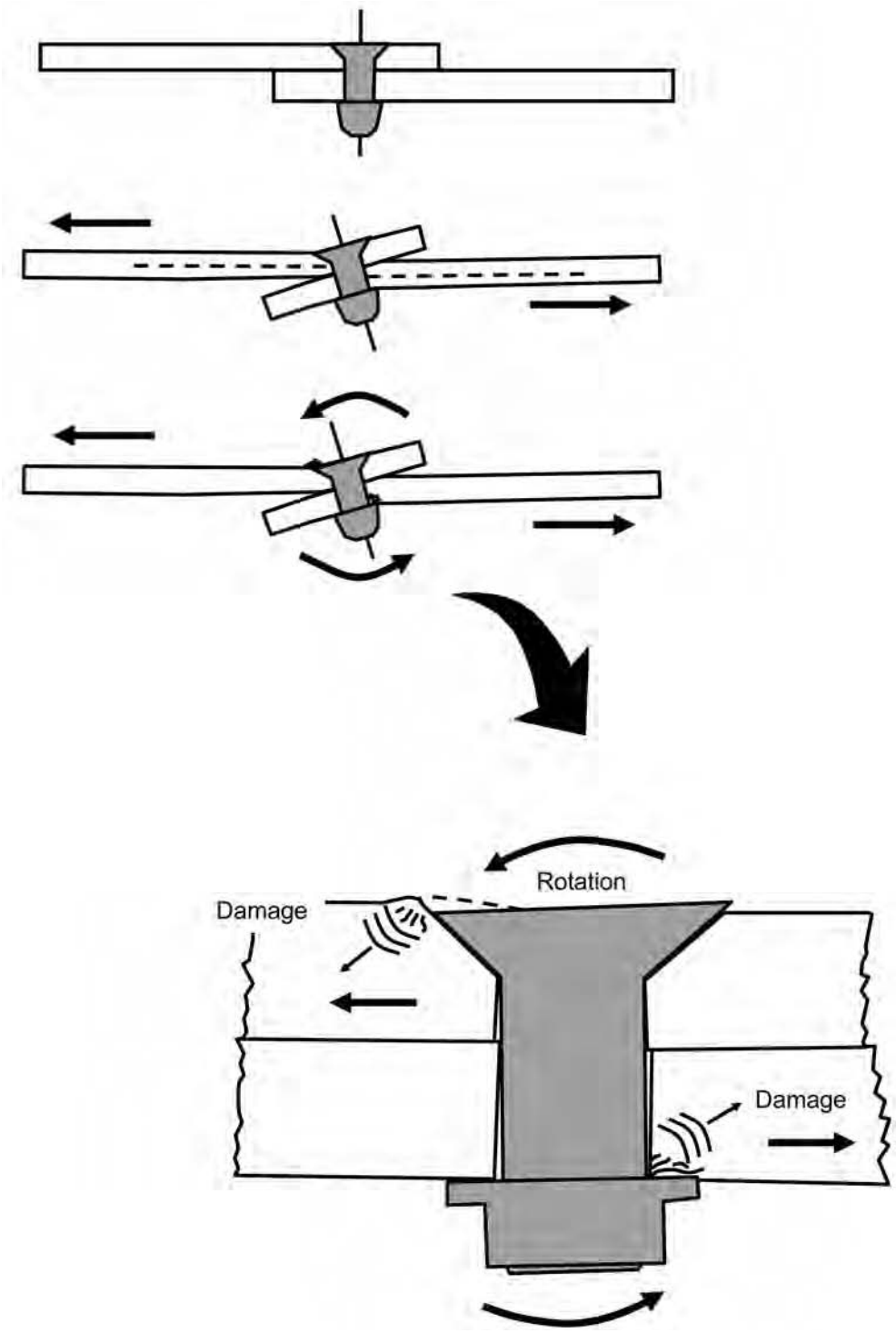


Fig. 17.11 Fastener cocking in single lap shear. Source: Ref 5

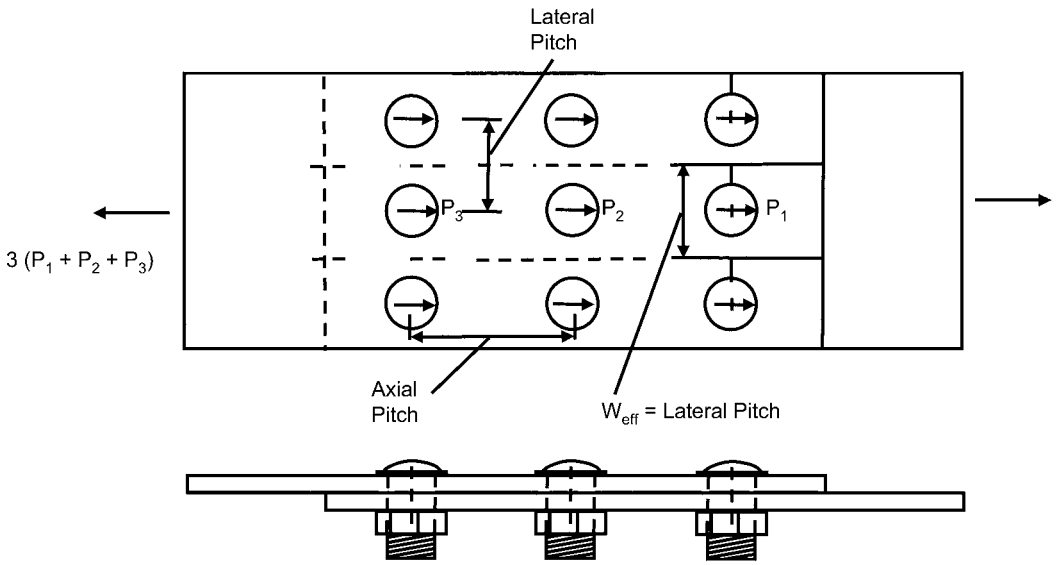


Fig. 17.12 Multifastener joint. Source: Ref 1

metallic joint, the elements yield under load to even out load transfer among the fasteners. Since composites are brittle and do not yield, the load transfer is not uniform. Therefore, for the high structural efficiency of bolted composite joints to be attained, each fastener must accept its correct share of the load. Normally, computer programs are required to predict the correct pattern of load sharing among the fasteners. Because composites fail at a very low strain level, proper load sharing is incompatible with loose-fit holes. Therefore, close tolerance +0.003/ –0.000 in. (+0.08 mm/–0.000) is normally specified. If the joint has been properly designed to reduce bearing loads, the joint will fail in net tension under tension loading. For multirow joints, two loads must be considered: (1) the bearing load that is opposed or reacted by the fastener and (2) the bypass load that passes by the fastener and is opposed or reacted by other parts of the joint. This interaction for tensile loads is shown in Fig. 17.14. The situation for compression loading is somewhat more complex, as shown in Fig. 17.15.

When the bearing load is high enough, there is a bearing stress cutoff for sufficiently wide fastener spacings, but for closer spacings, the failure will be in the net section whether the load is all taken out on that fastener (pure bearing) or all picked up by other fasteners in the joint (pure bypass). As shown in Fig. 17.14, there is a linear interaction between bearing and bypass loads whenever the joint fails in tension through the hole; that is:

$$\sigma_{net} K_{tc} + \sigma_{brg} K_{tb} \leq F_{tu} \text{ and } \sigma_{brg} \leq F_{brg} \qquad \text{(Eq 17.10)}$$

where K_{tb} is the bearing stress concentration factor and F_{brg} is the ultimate bearing strength.

Joint efficiency charts like the one shown in Fig. 17.16 can be constructed to cover all the intermediate cases for single-row joints between a pure bypass load along the upper envelope and a pure bearing load on the lowest curve. The only way to improve the joint efficiency of an optimized single-row joint is to move the fasteners in the most critical row farther apart and simultaneously decrease the bearing stress on the same row of fasteners. The last row of a multi-row joint in each member, where there is no bypass load left and a reduced total load, can be designed using the geometry for an optimized single-row joint.

Analyses of multi-row bolted composite joints have shown that if the basic structure is to be reparable, the optimal splices must contain uniformly thick skins with tapered splice plates, as shown in Fig. 17.17. The diameters of the fasteners vary throughout the joint. The innermost bolts, adjacent to where the skins butt together, are largest, at about a *w*/*d* ratio of three to one. The splice plate is thickest at this location. The next two rows of fasteners are sized at a *w*/*d* ratio of four to one, because some bypass load is

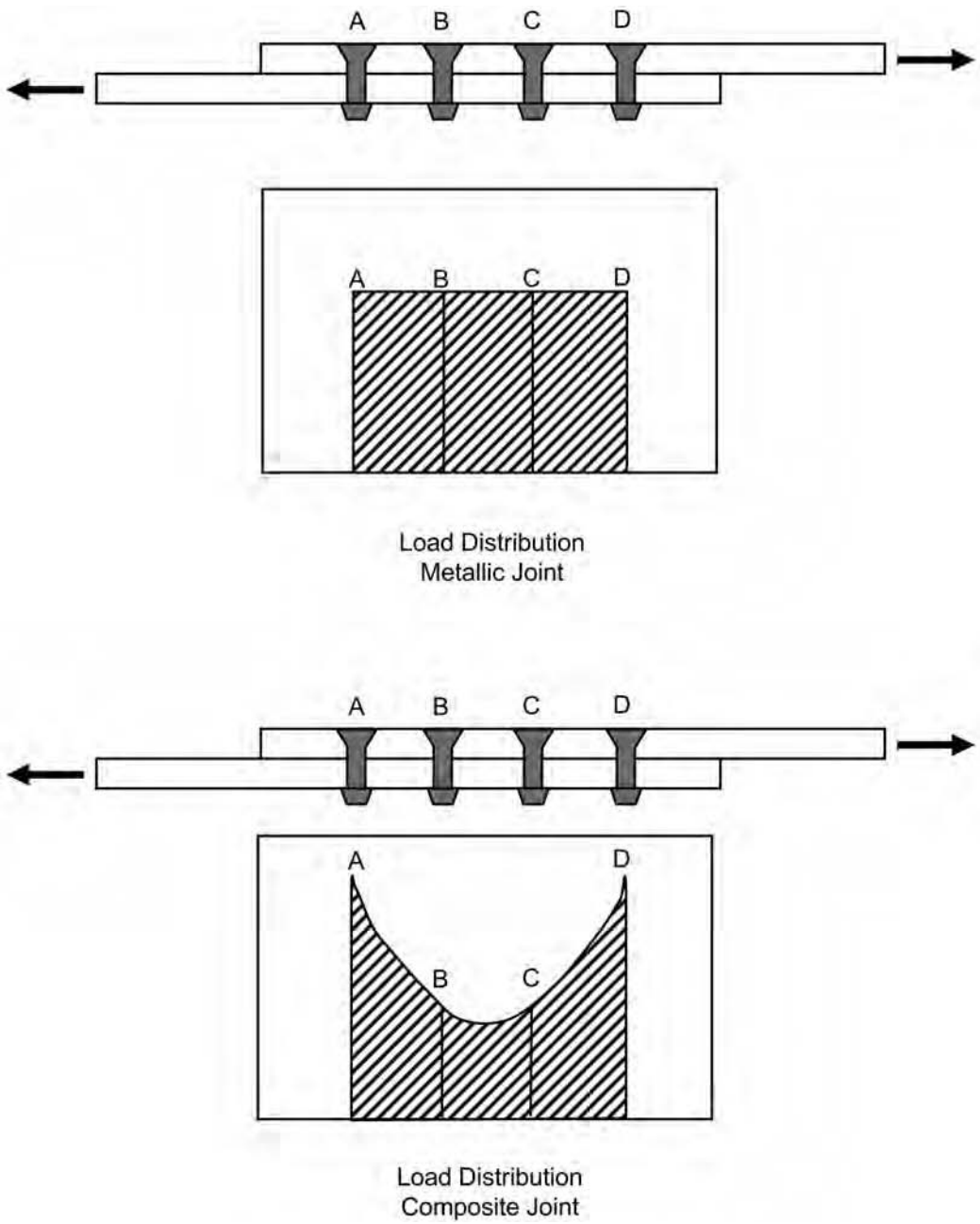


Fig. 17.13 Metal versus composite joint load transfer comparison. Source: Ref 2

present in all members. The critical fastener row is the outermost one, near the tip of the splice plate. The smallest, most flexible fasteners are used there ($w/d = 5$), and the tip thickness of the splice plate is limited to prevent those bolts from picking up too much load. It has been found that the bearing stress in the skin on that critical row of fasteners can be kept below 25 percent of the ultimate bearing strength. The resulting high structural efficiency, at a gross-section strain of 5000 μ in./in. (50 μm/cm), is much higher than can be obtained with either optimized single-row bolted composite joints or nonoptimized multi-row bolted composite joints.

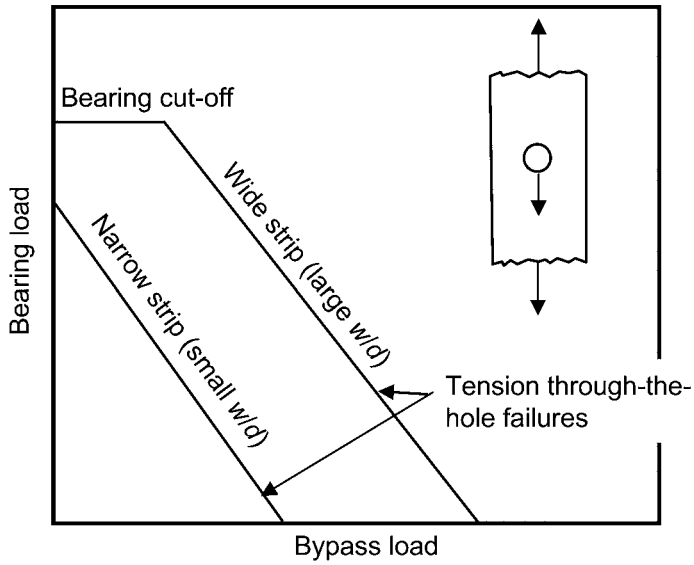


Fig. 17.14 Tension bearing-bypass load interaction. Source: Ref 6

Considerable simplification of the design process for mechanically fastened composite structures is afforded by the use of diagrams like those shown in Fig. 17.18. These charts can safely cover all of the relatively lightly loaded fasteners, such as skin-to-spar and skin-to-rib joints on wings, leaving only the few major load transfer splices requiring more detailed analysis. Some general design guidelines for mechanically fastened joints are given in Table 17.2.

17.5 Adhesive Bonding

Adhesive bonding offers much more efficient load transfer than mechanically fastened joints. However, the technical and quality-control requirements for adhesive bonding are much more stringent. The advantages of adhesive bonding include the following:

- Bonding provides a more uniform stress distribution than mechanical fasteners by eliminating the individual stress concentration peaks caused by mechanical fasteners. As shown in Fig. 17.19, the stress distribution across the joint is much more uniform for the adhesively bonded joint than for the mechanical joint, leading to better fatigue life than for the mechanically fastened joint. Bonded joints also provide superior vibration and damping capability.
- Because no mechanical fasteners are used, bonded joints are usually lighter than mechanically fastened joints and are less expensive in some applications.
- Bonded joints enable the design of smooth external surfaces and integrally sealed joints with minimum sensitivity to fatigue crack propagation. Dissimilar materials can be assembled with adhesive bonding without galvanic corrosion of metallic adherends because the joints are electrically insulating.
- Bonded joints provide a stiffening effect in comparison to mechanically fastened joints. Whereas mechanical fasteners provide local point stiffening, bonded joints provide stiffening over the entire bonded area. The significance of this effect is shown in Fig. 17.19, where bonded joints may increase the buckling strength of the structure by 30 to 100 percent.

The disadvantages of adhesive bonding include the following:

- Bonded joints should be considered permanent joints. Disassembly is not easy and often results in damage to the adherends and surrounding structure.
- Adhesive bonding is much more sensitive to surface preparation than mechanical fastening. Proper surface preparation is absolutely

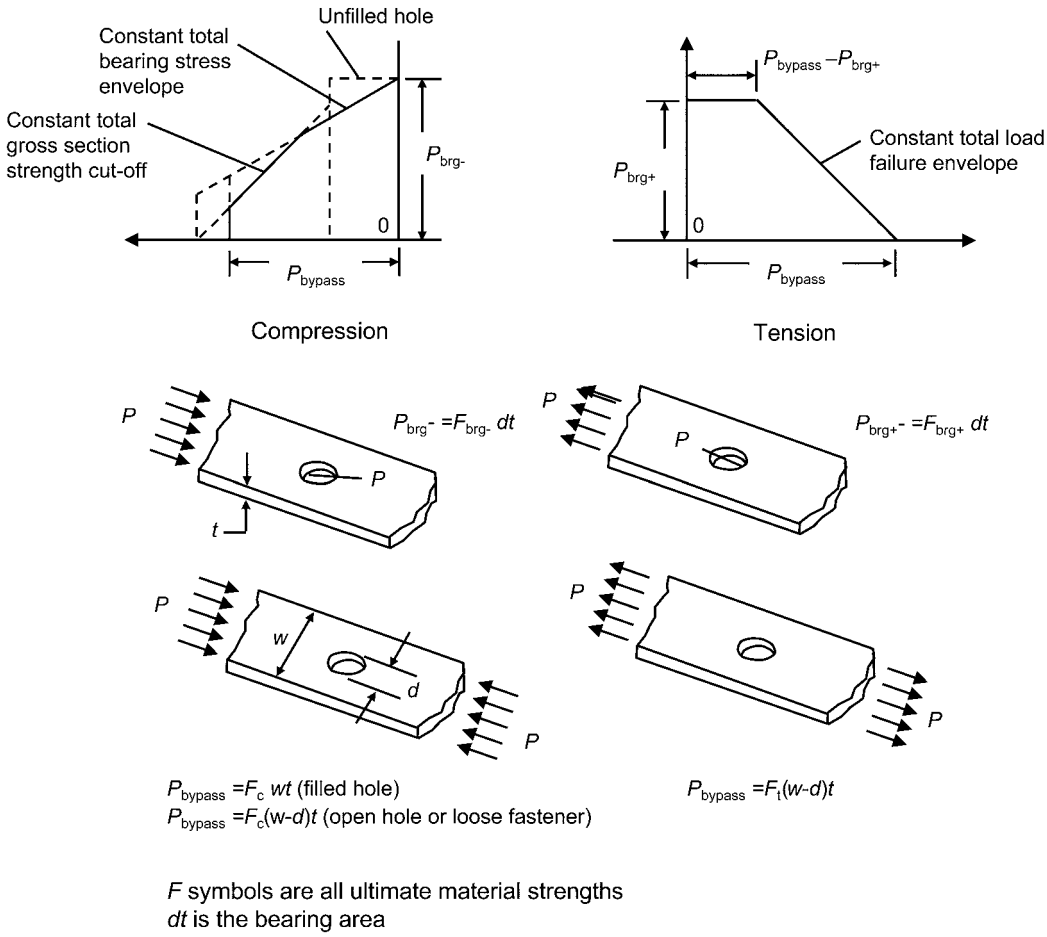


Fig. 17.15 Outer envelope of bearing-bypass load interactions. Source: Ref 6

essential for a strong, durable bond. For field repair applications, proper surface preparation can be extremely difficult. For original manufacturing, adhesive bonding requires clean rooms with temperature and humidity control.

- Although bonded joints can be nondestructively tested for the presence of voids and unbonds, at this time there is no reliable nondestructive method for determining the strength of a bonded joint. Therefore, traveler or process-control test specimens must be fabricated and destructively tested using the same surface preparation, adhesive, and bond cycle as the actual structure.
- Adhesive materials are perishable. They must be stored according to the manufacturer's recommended procedures (which often include refrigeration). Once mixed or removed from the freezer, they must be assembled and cured within a specified time.
- Adhesives are susceptible to environmental degradation. Most will absorb moisture and exhibit reduced strength and durability at elevated temperature. Some are degraded by such chemicals as paint strippers and other solvents.

17.6 Bonded Joint Design

In a structural adhesive joint, the load in one component is transferred through the adhesive layer to another component. The load transfer efficiency depends on the joint design, the adhesive characteristics, and the adhesive/substrate interface. To transfer loads through the adhesive effectively, the substrates (or adherends) are

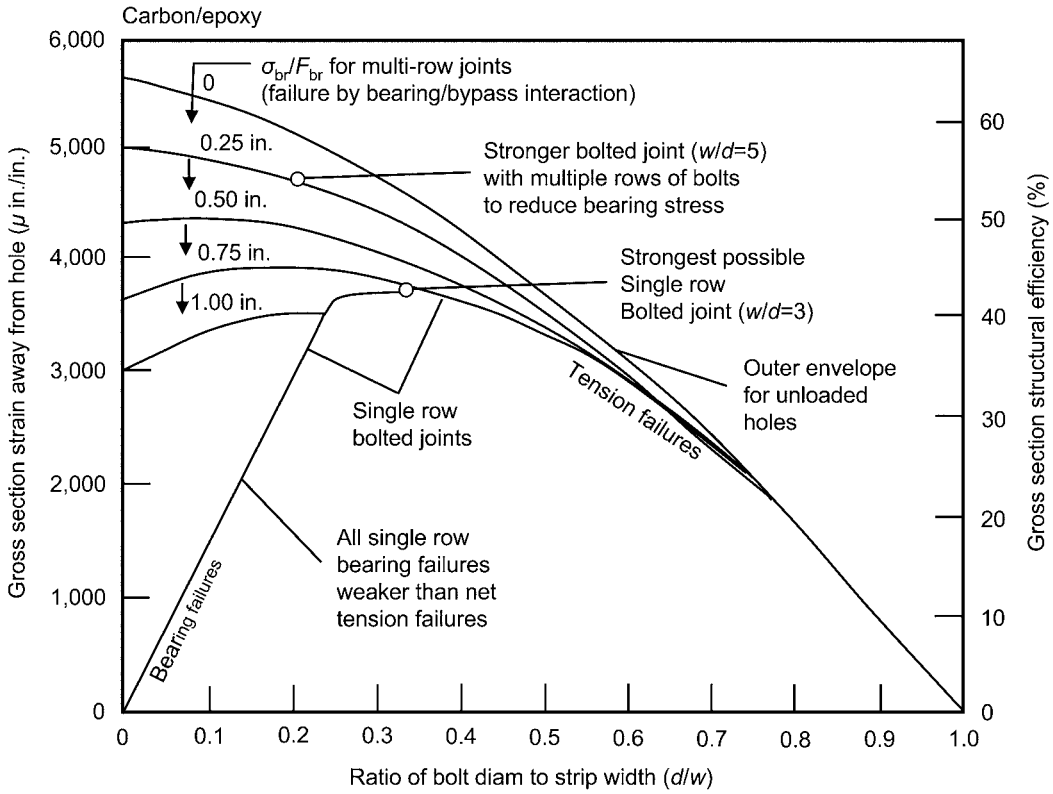


Fig. 17.16 Influence of bolted joint design on structural efficiency. Source: Ref 3

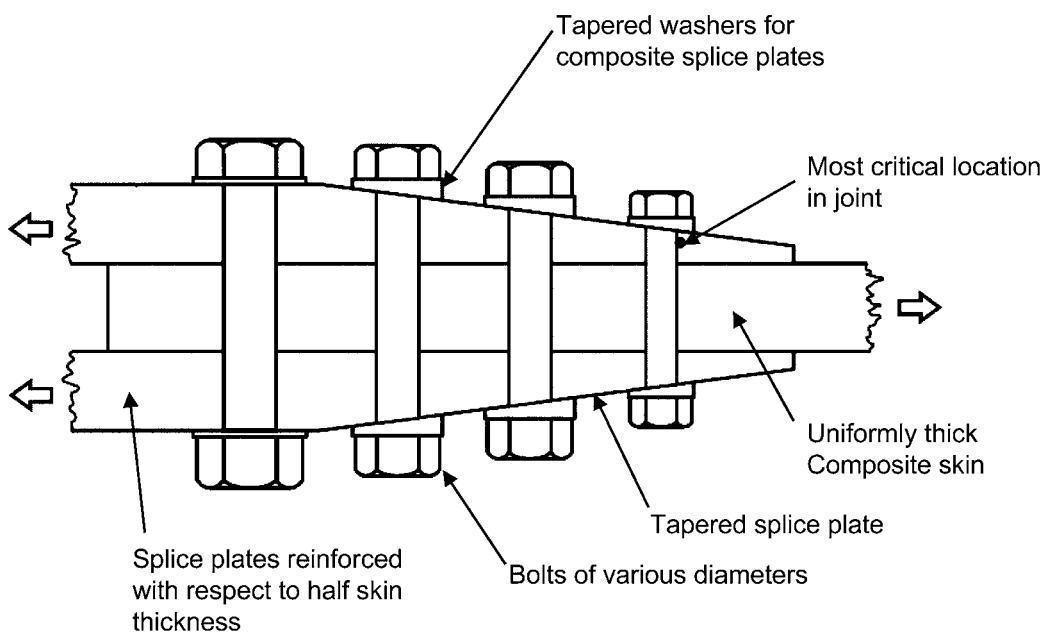


Fig. 17.17 Example of optimized multirow bolted composite joint. Source: Ref 3

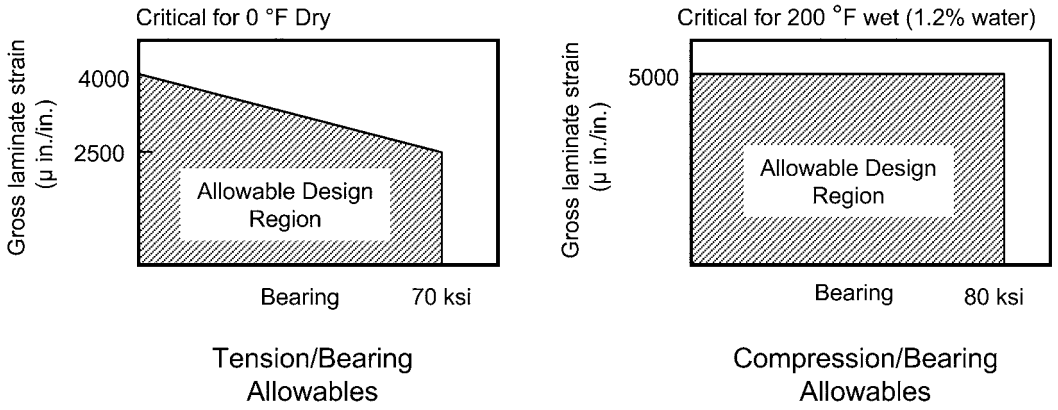


Fig. 17.18 Bearing-bypass interaction diagrams

overlapped so that the adhesive is loaded in shear. Typical joint designs are shown in Fig. 17.20. There is a limit to the thickness of the adherends that can be loaded by a single bondline. As the applied loads increase, the thickness of the adherends increases; eventually, one must move from the single-lap to the double-lap joint and finally to the double-cocured scarf or stepped-lap joint. The effect of joint design with increasing loads is shown in Fig. 17.21. The increase in joint complexity is necessary to ensure that the bond strength is higher than the strength of the increasing adherend thickness.

The load path for a single-lap shear joint is highly eccentric, producing large secondary bending moments and thereby resulting in severe peel stresses. Therefore, this type of joint should be used only for very lightly loaded structures or skins that are supported by such underlying structures as internal frames or stiffeners. Normally, single-lap joints should not be considered for joints thicker than about 0.07 in. (1.8 mm) for quasi-isotropic composite laminates. Although the double-lap joint has no primary bending moment because the resultant load is collinear, peel stresses arise as a result of the moment produced by the unbalanced shear stresses at the ends of the outer adherend. The resulting peel stresses are much smaller than those in single-lap joints; however, they do limit the thickness of the material that can be joined. As shown in Fig. 17.21, tapering the ends of the joint significantly increases the load capability of the double-lap joint. Because the scarf and stepped-lap joints develop negligible peel stresses, they can be used to join thicker composite laminates. However, the scarf joint requires a shallow taper angle to transfer the load effectively and its use can therefore result in a very long joint in a thick composite laminate. Therefore, it is rarely used as a primary joining technique, although it is frequently used for repairing thin skins in honeycomb structures. Although the stepped-lap joint configuration is difficult to fabricate, it does contain discrete steps that can be used for ply location during fabrication. Because of these difficulties associated with scarf and stepped-lap joints, mechanical fastening is probably a more viable option for laminates thicker than about 0.125 in. (3 mm).

The analysis and design of adhesively bonded joints are conducted using an elastic-plastic adhesive model. Detailed analyses of single-lap, double-lap, scarf and stepped-lap bonded joints can be found in Ref 9 to 11, respectively. In addition, the A4E series of computer programs is available for joints of various geometries. The design and analysis of stepped-lap joints are somewhat more complex and are based on nonlinear continuum mechanics.

17.7 Adhesive Shear Stress-Strain

Adhesive bond strength is usually measured by the simple single-lap shear test shown in Fig. 17.22. The lap shear strength is reported as the failing stress in the adhesive, which is calculated by dividing the failing load by the bond area. Because the stress distribution in the adhesive is not uniform over the bond area (it peaks at the edges of the joint), the reported shear stress is lower than the true ultimate strength of the adhesive. While this test specimen is relatively

Table 17.2 Guidelines for mechanically fastened joints

Guidelines		Remarks
1.	Design the joint first and fill in the gaps afterward; optimizing the basic structure first compromises the joint design and results in low overall structural efficiency.	
2.	The best bolted joint design can barely exceed half of the strength of unnotched laminates.	
3.	Laminate percentages for efficient load transfer: 0° = 30–50%; 45°/135° = 40–60% 90° = minimum of 10%	>50% 0° results in in-plane shear failure and no load redistribution.
4.	Maximize ply dispersion throughout the laminate. Keep the laminate as symmetric and balanced as possible.	Ply concentrations of the same angle do not allow load shearing between plies.
5.	Composite joints should be designed to fail in either bearing or tension.	Shear-out failures result in low joint strengths.
6.	Minimum fastener edge distance (E/D) should be 2.6D.	E/D less than 2.6 can result in a shear failure (eliminates load redistribution).
7.	Minimum fastener pitch (W/D) should be 4.	
8.	Many bolted composite joints contain too few bolts, spaced too far apart, and the diameters are too small to permit maximizing the strength of the laminate.	Use $d/t \sim 1$ d = bolt diameter t = laminate thickness
9.	Rated shear strength of selected fastener should be conservative.	Allows redistribution of loading without concern that fastener will fall in shear.
10.	Peak hoop tension stress around bolt holes is roughly equal to the average bearing stress.	
11.	Bolt-bearing strength is sensitive to through-the-thickness clamp-up of laminates.	Higher clamp-up results in higher bearing strength.
12.	Bolt bending is much more significant for composites than for metals, because composite members are thicker (for a given load).	$d/t \sim 1$ generally provides sufficient bolt bending strength.
13.	Countersink depth should not exceed two-thirds of the total sheet thickness.	Leaves one-third of total sheet thickness to carry most of the bearing load.
14.	The preferred fastener material for use with carbon composites is titanium.	Best coefficient of thermal expansion match and minimum corrosion problem.
15.	Do not use interference fit-type fasteners that require driving the fasteners into the hole.	May cause hold damage, which will degrade bearing strength.
16.	Use a CRES washer on all bolt/nut systems.	Minimize corrosion.
17.	Do not buck rivets in composite structure.	Shank expansion will damage holes.
18.	Squeeze rivets can be used if a washer is provided on the tail side.	Washer will spread out the bearing stress from installation.
19.	Do not overtorque flush countersunk fasteners	May cause bearing failure under the head of the fastener.
20.	Avoid the use of 3/16 in. diameter fasteners for through-the-thickness tension loading.	Small-diameter fasteners can be easily overtorqued and fail during installation. Use 1/4 in. minimum.
21.	Consider fastener fatigue effects of end fasteners in a multirow joint since they have the highest load.	
22.	There are no fastener threads in bearing.	Threads could initiate a delamination and reduce fatigue life.
23.	Use only titanium or A286, PH13-8MO, or PH17-4 stainless steel fasteners with carbon/epoxy.	To prevent corrosion of fasteners. Titanium is preferred; steel is acceptable only in a low-corrosion environment.
24.	Do not use aluminum, cadmium-plated steel, or aluminum-coated fasteners with graphite/epoxy.	These materials are very susceptible to corrosion.
25.	Steel fasteners in contact with carbon should be permanent and installed with sealant.	To prevent corrosion of fasteners.
26.	Use a layer of fiberglass or Kevlar (0.005 in. minimum) on faying surfaces of graphite/epoxy panels adjacent to aluminum.	To prevent corrosion.
27.	Use tension head fasteners for all applications. Shear head fasteners may be used in special applications with stress approval only.	Potentially high bearing stress under fasteners head; may cause laminate bearing failure.
28.	For blind attachments to composite substructure, use big-foot-type titanium blind fasteners or equivalent recommended.	To prevent damage to composite substructure.
29.	Use close tolerance fit.	Improved load distribution in a multifastener joint.

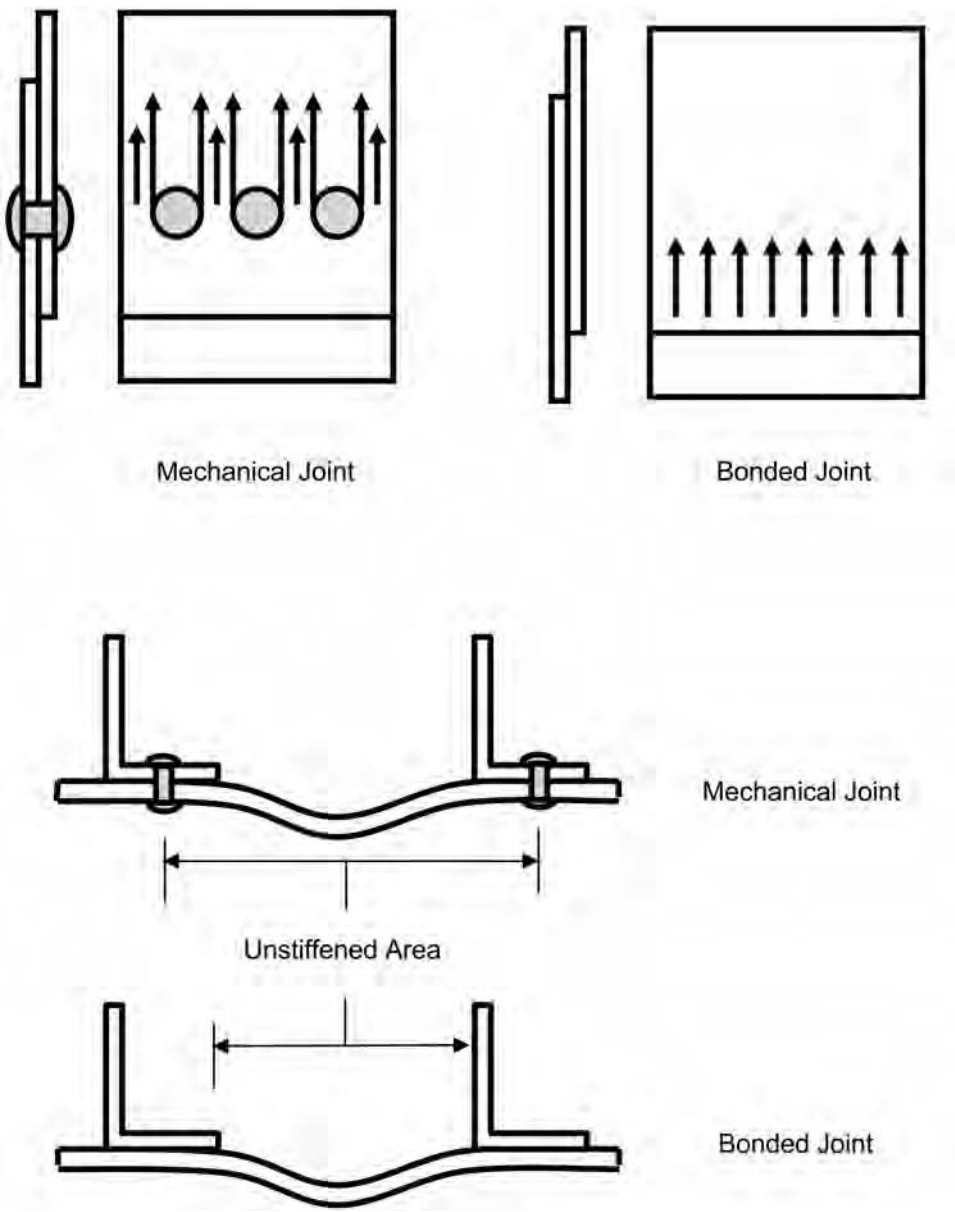


Fig. 17.19 Load distribution comparison for mechanically fastened and bonded joints. Source: Ref 7

easy to fabricate and test, it does not give a true measure of the shear strength because of adherend bending and induced peel loads. In addition, there is no method of measuring the shear strain and thus calculating the adhesive shear modulus that is required for structural analysis. Even in a balanced double-lap shear joint, the load transfer is not uniform along the bondline but peaks at the ends of the overlap in the manner shown in Fig. 17.23. This nonuniform load transfer results from the compatibility of deformations associated with the variation of direct stress within the adherends from one end of the bonded joint to the other.

The design of adhesively bonded structures is based on stress-strain curves generated by the thick adherend test, as previously discussed in Section 13.11. To measure the adhesive shear stress-strain properties, an instrumented thick-adherend test can be conducted where the adherends are so thick that the bending forces are neg-

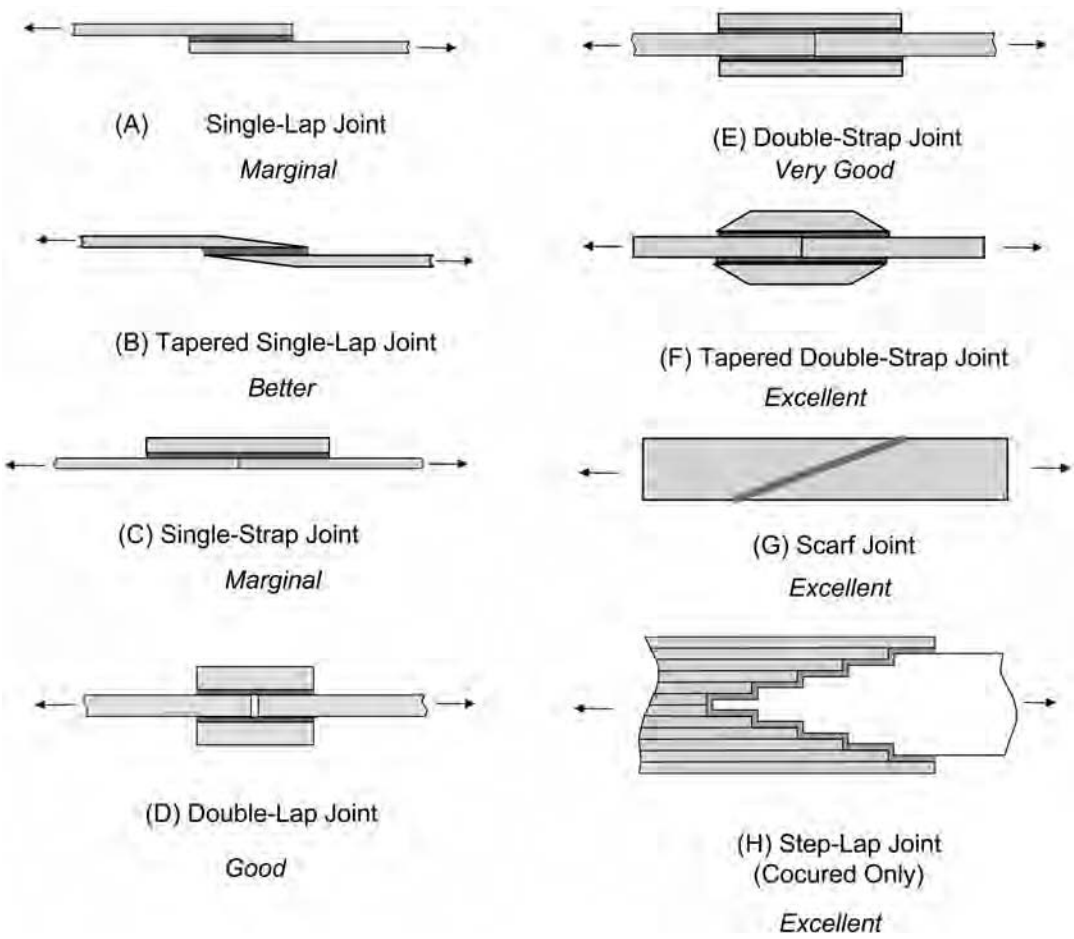


Fig. 17.20 Typical adhesively bonded joint configurations

ligible (Fig. 17.24). A properly instrumented thick-adherend test will allow the calculation of shear stress (τ), shear modulus (G), and shear strain (γ). However, the single-lap shear test is an effective screening and process-control test for evaluating adhesives and surface preparations as well as for in-process control.

The room-temperature shear stress/shear strain behavior of a lower-strength, lower-modulus ductile adhesive and a higher-strength, higher-modulus brittle adhesive are shown in Fig. 17.25. The ductile epoxy-based film adhesives used today for service temperatures up to 250 °F (120 °C) are toughened by the addition of rubber, nylon, or vinyl. Because the addition of these tougheners lowers the glass transition temperature T_g, epoxy adhesives intended for higher usage temperatures are generally untoughened. As a result, their elevated-temperature resistance is increased but their room-temperature peel resistance is reduced. Although the brittle adhesive has the highest strength, the tough ductile adhesive, which has a much larger area under the shear stress-strain curve, would be a much more forgiving adhesive, particularly in structural joints that may be subject to peel and bending loads. However, even the brittle adhesives exhibit substantial ductility when tested at elevated temperatures approaching their upper use-service temperatures.

The elastic-plastic model used for bondline design is shown in Fig. 17.26 along with an actual stress-strain curve. The model at ultimate load has the same peak shear stress and strain as the actual stress-strain curve and the same strain energy (area under the curve). As indicated in the figure, the effective shear modulus and shear yield stress used in the model will vary with the

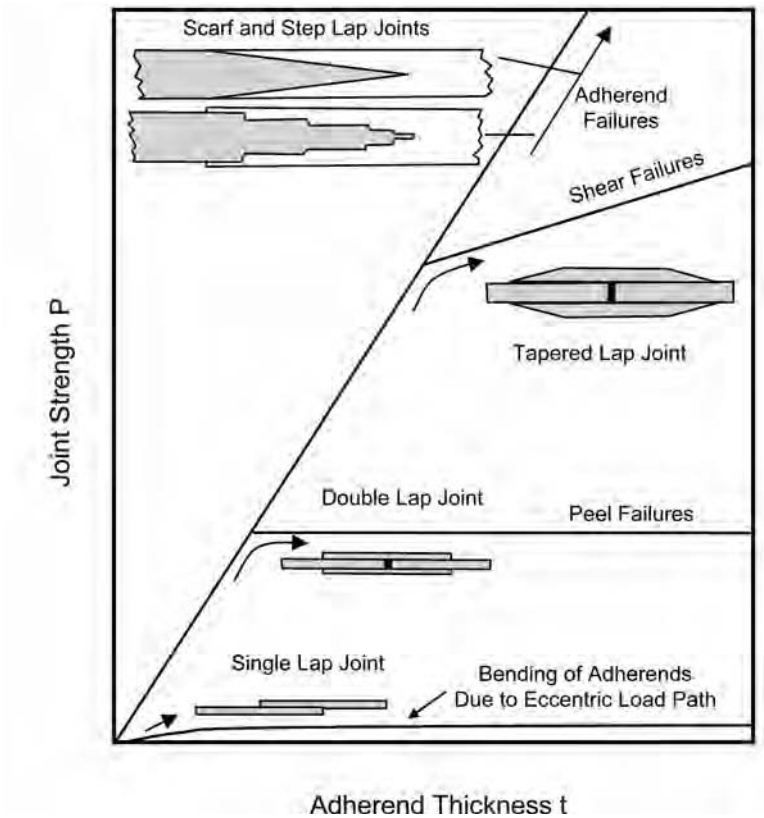


Fig. 17.21 Effect of adherend thickness on failure modes of adhesively bonded joints. Ref 8

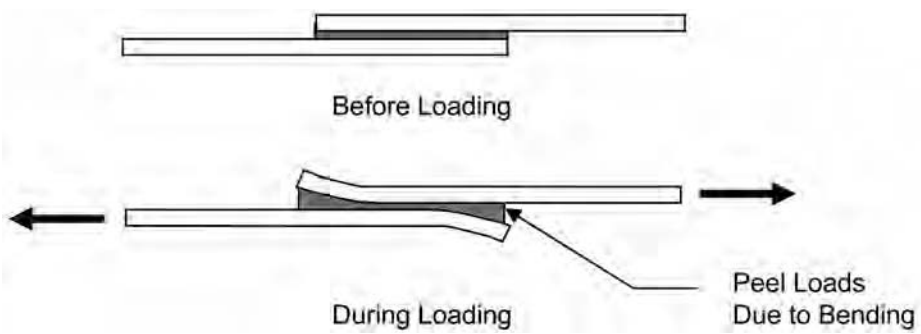


Fig. 17.22 Typical single-lap shear test specimen

strain level. Two analyses are normally required: (1) an elastic analysis using the actual adhesive shear modulus to make sure that the adhesive will not deform plastically at limit load and (2) an elastic-plastic analysis to predict the actual joint strength. The elastic-plastic analysis is inappropriate for the lower-load-level case, because the initial shear modulus is too low and the elastic strain energy is too high. It is important to understand that the simple elastic-plastic model is a mathematical approximation. On unloading, while there is some hysteresis, there is almost complete recovery of the strain; however, it is far from a straight-line load reduction.

The adhesive shear stress-strain curves for a ductile adhesive vary with the operating envi-

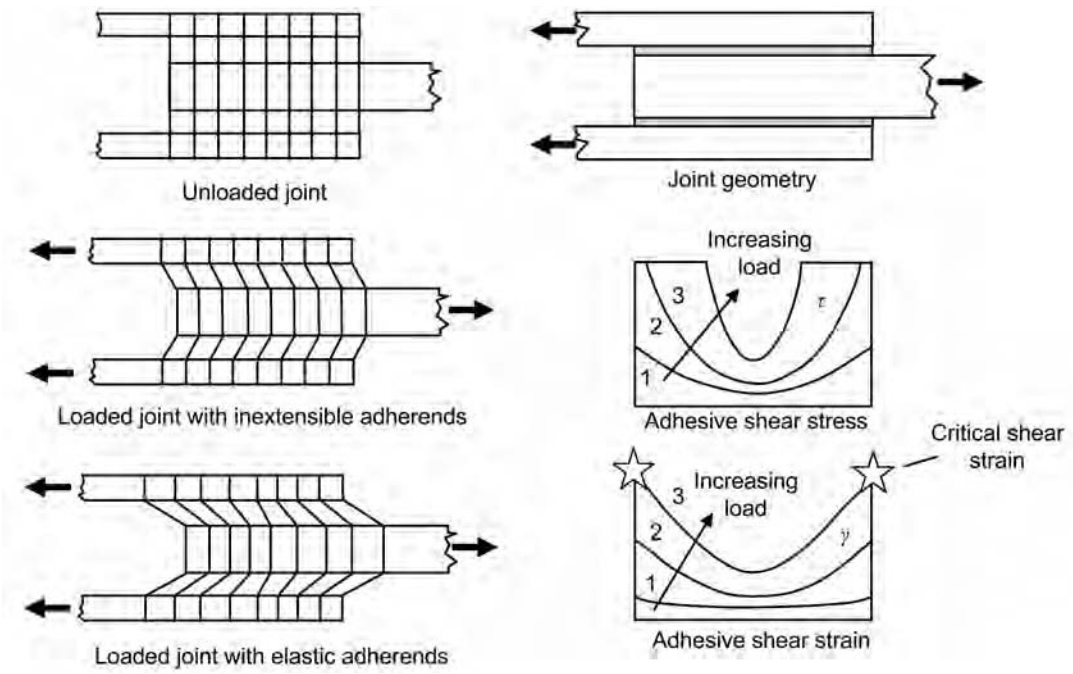


Fig. 17.23 Shear of adhesive in balanced joints. Source: Ref 12

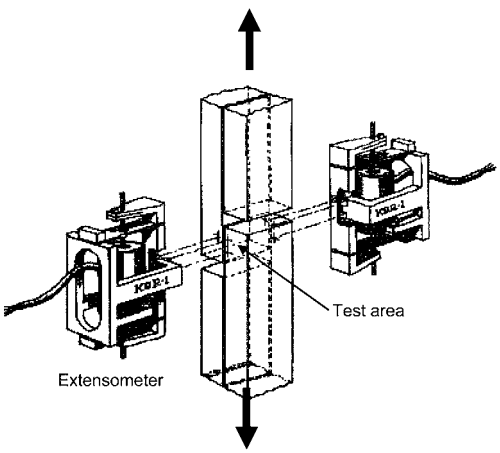


Fig. 17.24 Thick adherend test method. Source: Ref 13

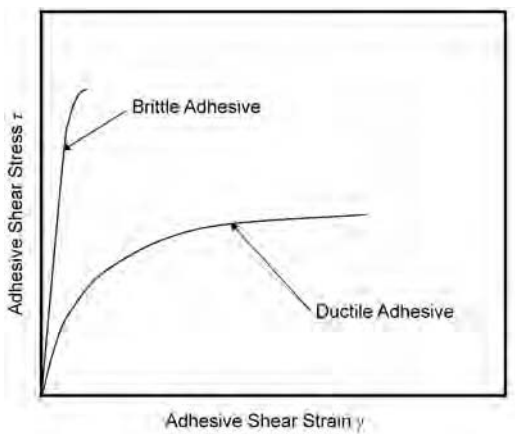


Fig. 17.25 Typical stress-strain behavior for brittle and ductile adhesives. Source: Ref 8

ronment, as illustrated in Fig. 17.27 for a typical example. While the individual properties, such as peak shear strength and strain-to-failure, vary greatly with temperature, the areas under all three curves are quite similar. The ultimate strength of a long-overlap bonded joint between uniform adherends is shown by analysis to be defined by the strain energy of the adhesive layer in shear, not by any individual properties, such as peak shear stress. The strain energy is proportional to the area under each of these curves. Consequently, the strength of a realistically configured bonded joint is not very sensitive to its operating environment, provided that its temperature is kept below the adhesive's glass transition temperature.

There are several important points that should be considered when testing or characterizing adhesive materials: (1) All test conditions must

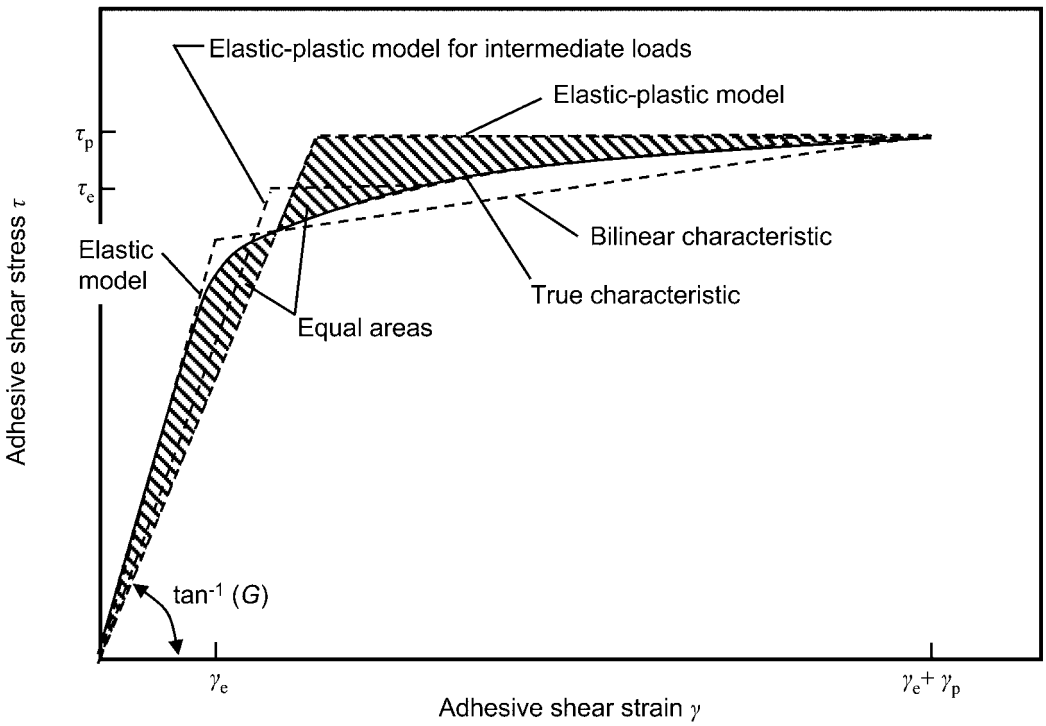


Fig. 17.26 Elastic-plastic model. Source: Ref 12

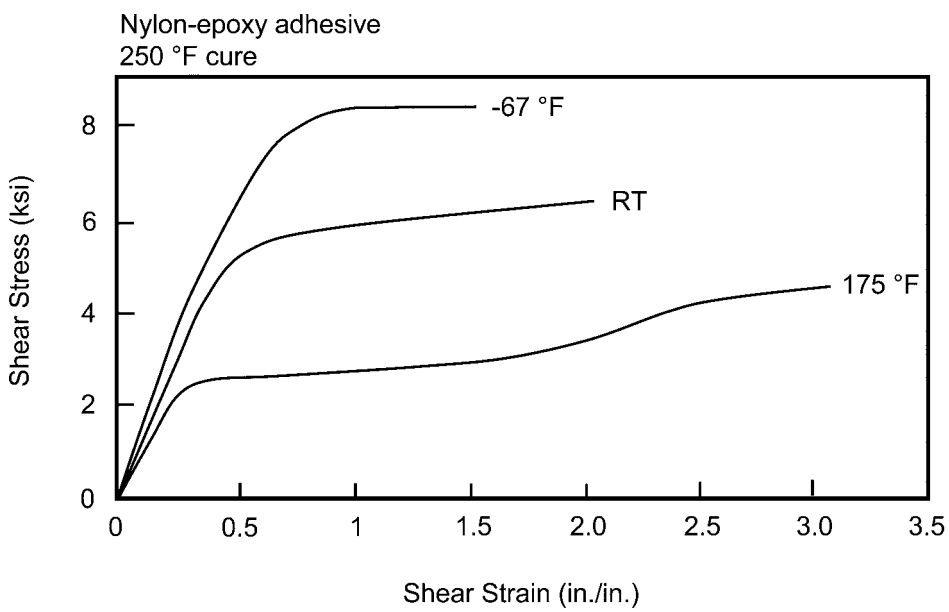


Fig. 17.27 Effect of temperature on adhesive shear stress-strain. RT, room temperature; Source: Ref 12

be carefully controlled, including the surface preparation, the adhesive, and the bonding cycle. (2) Tests should be run on the actual joint(s) that will be used in production. (3) A thorough evaluation of the in-service conditions must be made, including temperature, moisture, and any solvents or fluids to which the adhesive will be exposed during its service life. The failure modes for all test specimens should be examined. Some acceptable and unacceptable failure modes are shown in Fig. 17.28. For example, if the specimen exhibits an adhesive failure at the adherend-to-adhesive interface, rather than a cohesive failure within the adhesive, this may be an indication of a surface preparation problem that will result in decreased joint durability. The desired failure mode is a 100 percent cohesive failure of the adhesive bondline (Fig. 17.29).

Bonding to composites rather than metals introduces significant differences in criteria for adhesive selection for two reasons: (1) composites have lower interlaminar shear stiffness than

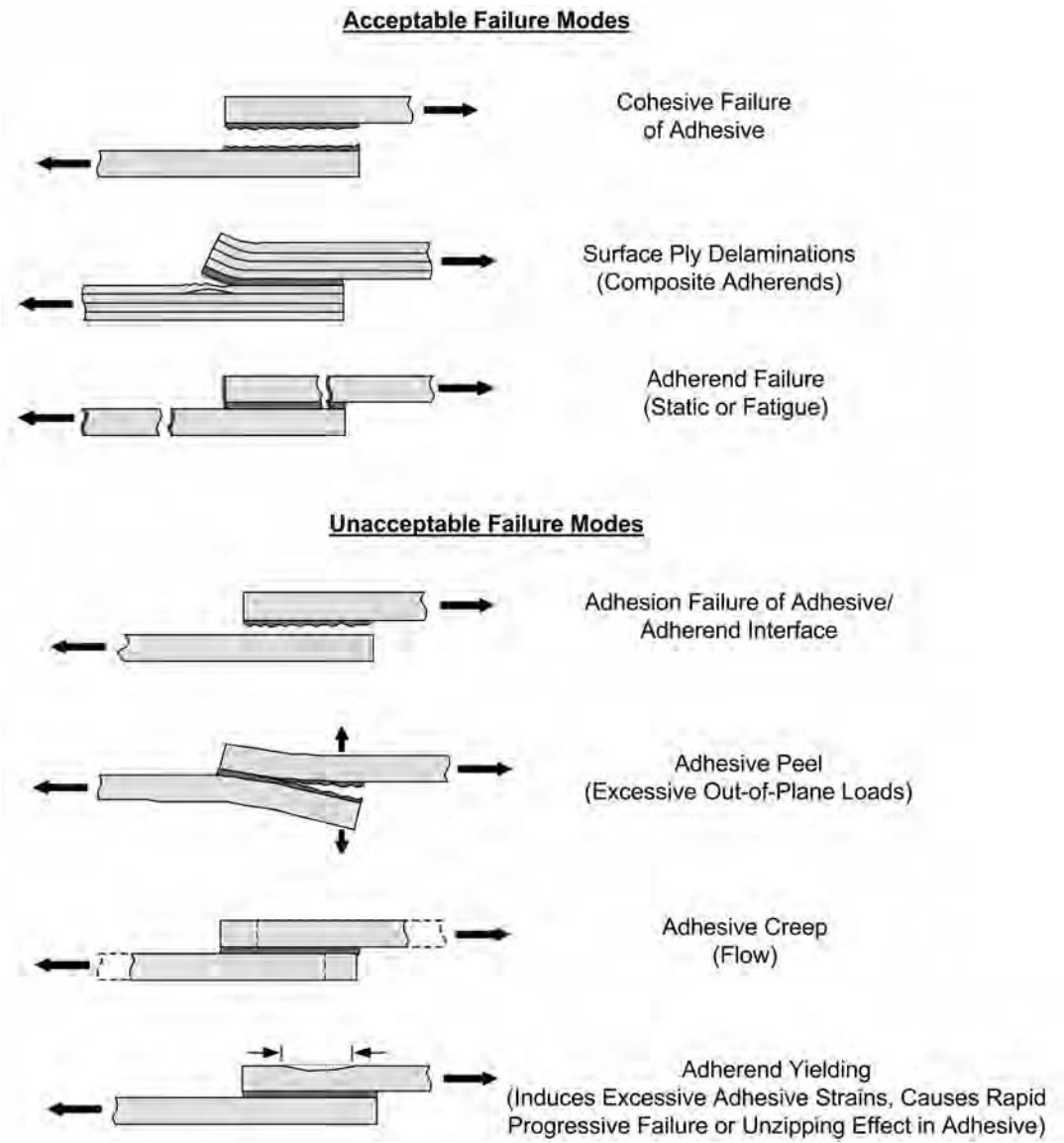


Fig. 17.28 Typical failure modes of bonded joints

metals and (2) composites have much lower shear strengths than metals. (Interlaminar shear stiffness and strength depend on the properties of the matrix, not of the fibers.) The exaggerated deformations in a composite laminate bonded to a metal adherend under tension loading are shown in Fig. 17.30. The composite laminate tends to shear like a deck of cards. The adhesive passes the load from the metal into the composite until, at some distance *L*, the strains in each material are equal. In the composite, the matrix resin acts as an adhesive to pass load from one fiber ply to the next. Because the matrix shear stiffness is low, the composite plies deform unequally in tension. Failure tends to initiate in the composite ply next to the adhesive near the beginning of the joint or in the adhesive in the same neighborhood. A typical first ply failure in a composite-to-composite joint is shown in Fig. 17.31. The highest failure loads are achieved by an adhesive with a low shear modulus and high strain-to-failure.

Basic design practice for adhesively bonded composite joints should ensure that the surface fibers in a joint are parallel to the load direction (0°) to minimize interlaminar shear, or failure, of the bonded adherend or substrate layer. A design in which joint areas have been machined to a stepped-lap configuration may have a joint interface composed of fibers at an orientation other than the optimal 0° orientation to the load direction. This orientation tends to induce substrate failure more readily than would otherwise occur.

Aluminum and titanium are often bonded into composite assemblies. Solid aluminum adherends should never be hot bonded directly to carbon/epoxy because the large differences in the coefficients of thermal expansion will result

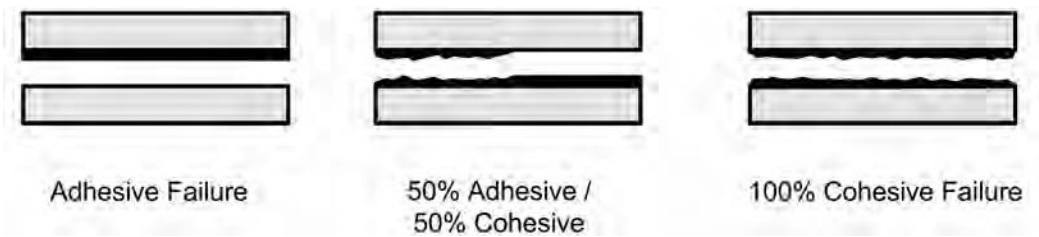


Fig. 17.29 Difference between cohesive and adhesive failure modes

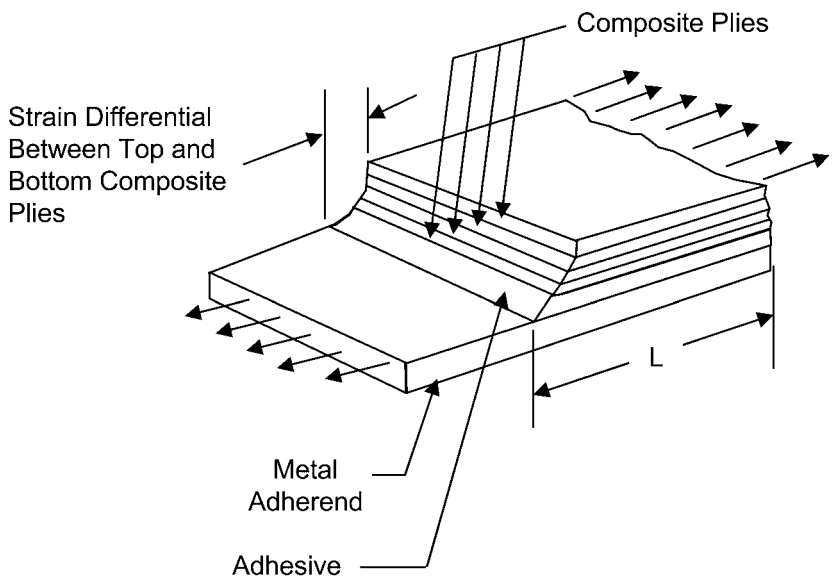


Fig. 17.30 Uneven strain distribution in composite plies. Source: Ref 14

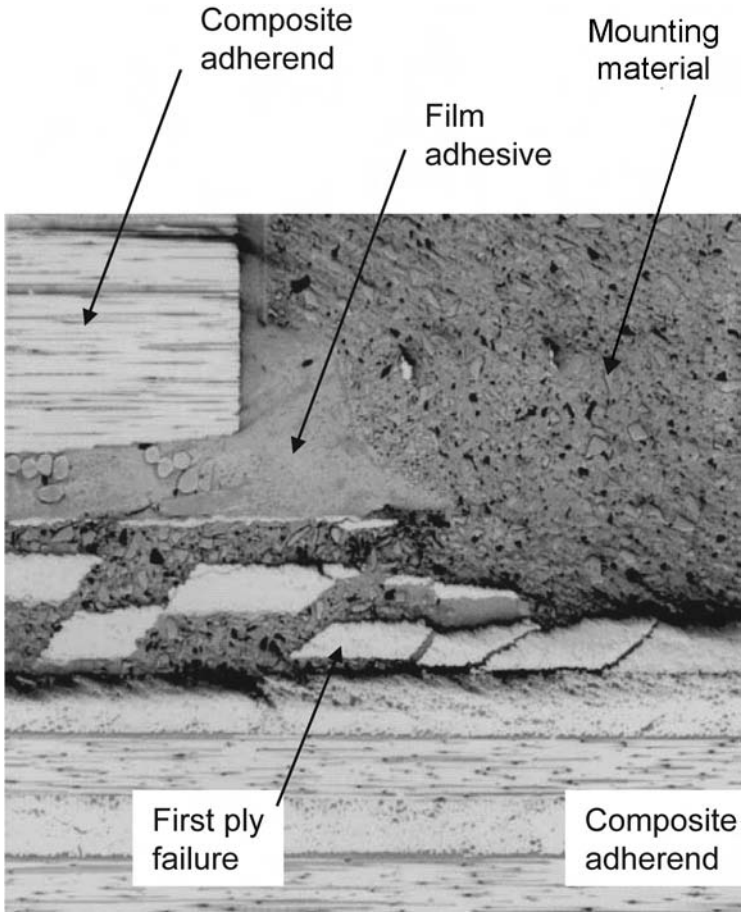


Fig. 17.31 First ply failure in a composite-to-composite joint

in significant residual stresses, and because carbon fiber in contact with aluminum will form a galvanic cell that will corrode the aluminum. Total destruction of a bond between carbon/epoxy and aluminum has been observed. A test article was fabricated in which aluminum hinges were cocured to a carbon/epoxy control surface. Even though a high strain toughened epoxy film adhesive was used, the bondline totally split apart (100 percent cohesive failure) on cooling down from the 350 °F (180 °C) cure cycle due to the residual stresses that developed as a result of the large differences in coefficients of thermal expansion between the two. Even if the bond had survived cool-down to room temperature, it would have had little chance of survival if the operating environment subjected it to cold temperatures, for example, –55 °F (–50 °C), in which the residual stresses would have been even greater.

17.8 Bonded Joint Design Considerations

The first rule of adhesively bonded joint design is that in no case should the strength of the joint be less than that of the surrounding structure; otherwise, the bonded joint will have little damage tolerance and can act as a weak link. The strong ductile adhesives typically used by the aerospace industry produce a bond that is inevitably stronger than the adherends for properly designed joints between thin members. For thicker structures, the bond can always be made stronger than the structure by using enough steps in a stepped-lap joint. Because adhesively bonded joints can be strong in shear but are inevitably weak in peel, the second rule of adhesively bonded joint design is to make sure that the adhesive is loaded in shear while minimizing any

direct or induced peel stresses. Tension, cleavage, and peel loading (Fig. 17.32) should all be avoided when using adhesives. In practice, tension loading is acceptable for nonstructural bonds as long as there is appreciable surface area, but certainly not in the butt joint shown.

It is important that bonded joint strengths exceed the strengths of the adherends by at least 50 percent to allow for minor manufacturing flaws or imperfections. The loss of bond strength that is sometimes associated with bondline flaws or damage to the bond is shown in Fig. 17.33. Even with such degradation, the bond will be stronger than the adherends. If the adherend thickness is greater than that for which the bond and member strengths are equal, there is absolutely no tolerance with respect to flaws, porosity, or damage. The slightest imperfection would lead to catastrophic unzipping of the entire bond area if sufficient load were applied.

There are two factors that affect the long-term durability of adhesively bonded joints: (1) surface preparation and (2) adhesive creep. The importance of proper surface preparation is covered in Chapter 8, "Adhesive Bonding." Creep is restricted by selecting a long enough overlap to produce a low-stress trough, as shown in Fig. 17.34. If a short overlap is used, the minimum adhesive

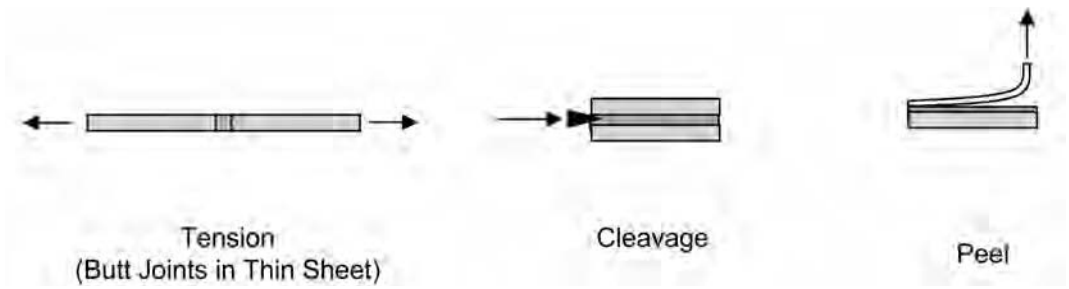


Fig. 17.32 Load paths to avoid in bonded structure. Source: Ref 14

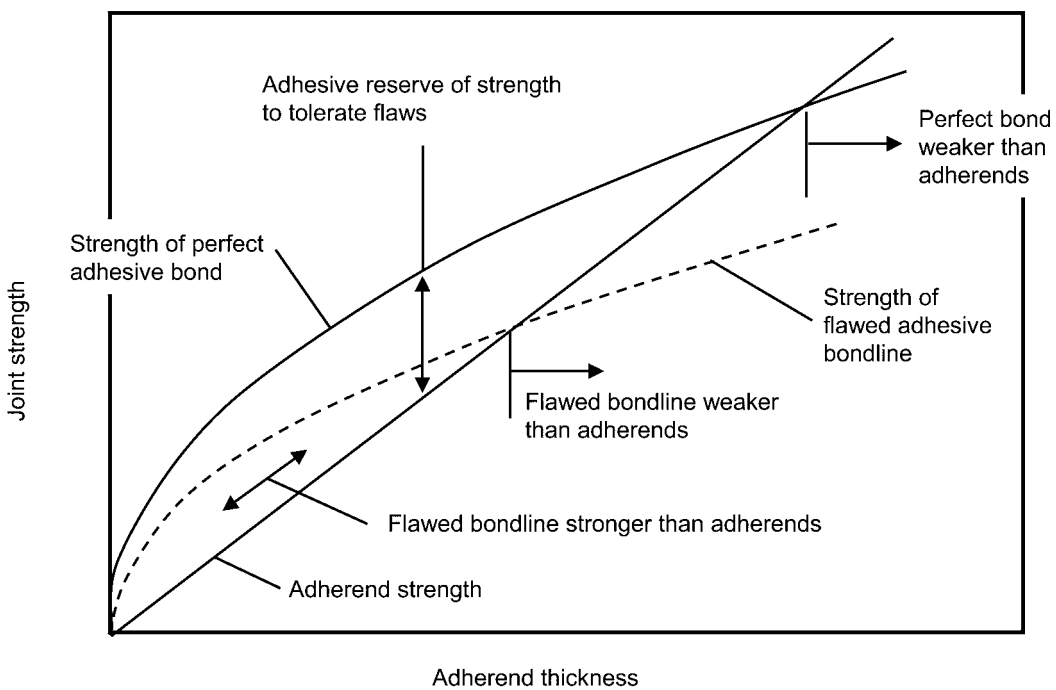


Fig. 17.33 Relative strength of adhesive and adherends as affected by bond flaws. Source: Ref 6

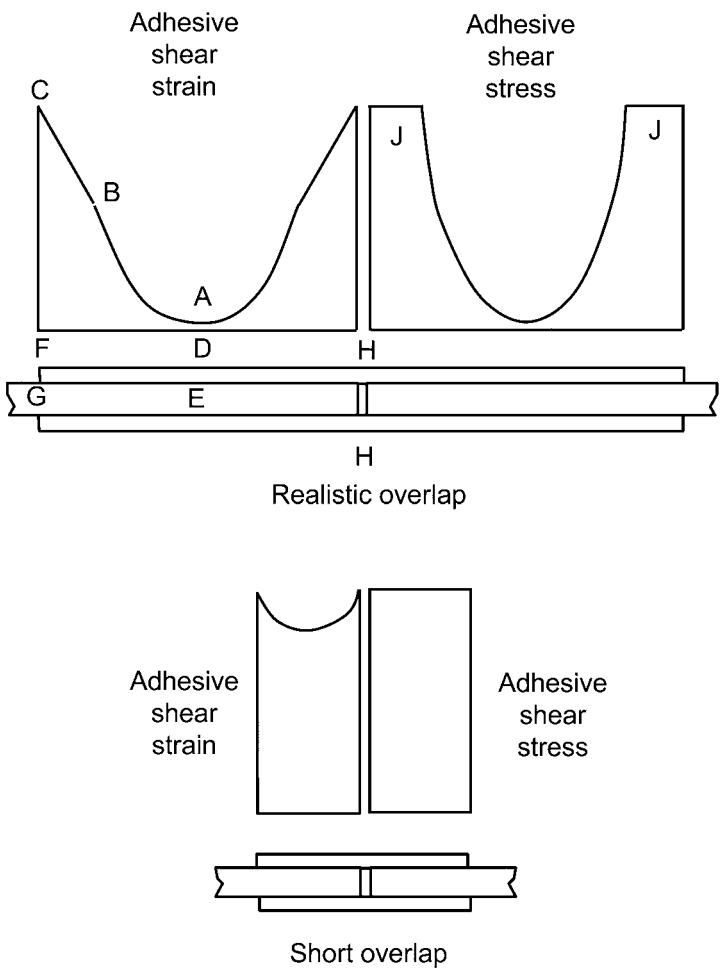


Fig. 17.34 Nonuniform stresses and strains in bonded joints. Source: Ref 6

shear stress and strain are nearly as high as the peak values at the ends. Because adhesive creep can accumulate under both static and cyclic loads, there is no mechanism for the adhesive to recover to its original state when the load is removed. A joint with short overlap is susceptible to creep failure, but the adhesive shear stress and strain can be made as low as desired by using a sufficiently long overlap. Although there is creep in the adhesive at the ends of the long overlap, between points *F* and *G*, where the stress at point *J* is high, there is none in the middle, between points *D* and *E*, if the stress at point *A* is low enough. Consequently, the creep that does occur cannot accumulate, because the stiff adherends push the adhesive back to its original position whenever the joint is unloaded. This recovery in part of the adhesive prevents gross creep and is a key to a durable bonded structure. Without it, there can be no successfully bonded structure.

For structural aluminum alloys, an overlap of approximately 30 times the central adherend thickness is used in a double-lap joint. In addition, because the modulus of nearly quasi-isotropic carbon/epoxy laminates is of the same order of magnitude as for aluminum alloys, a similar overlap-to-thickness ratio would also be satisfactory for such laminates. The static strength of bonded joints between uniform adherends is quite insensitive to the precise length of a sufficiently long overlap, as shown in Fig. 17.35. Any longer overlap beyond point *C* would be superfluous. For all overlaps longer than the abrupt drop in the adhesive shear strain shown in the upper diagram, the maximum strain in the

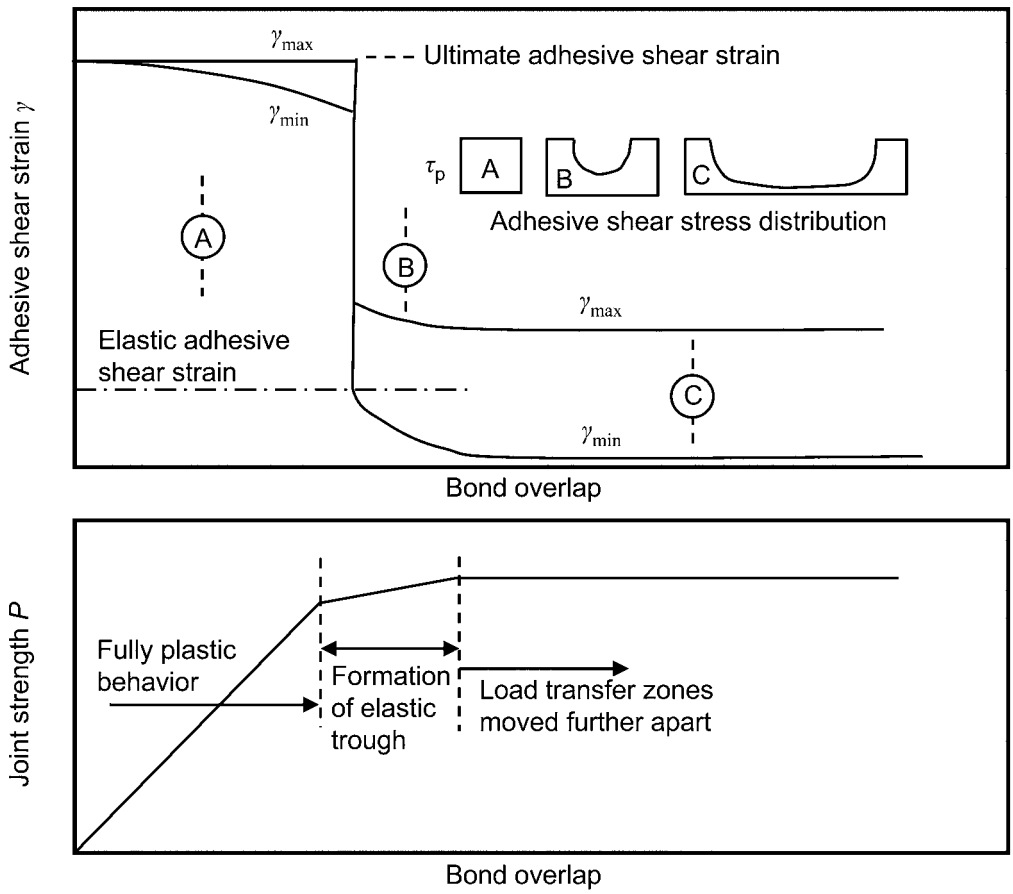


Fig. 17.35 Influence of overlap on adhesive shear strains. Source: Ref 6

adhesive is limited by the adherend strength to a value below that which would be needed to make the adhesive fail. No such protection is afforded for short overlaps or thick adherends. If the adherends are too thick, the limit on the peak shear strain shown in Fig. 17.35 disappears. Therefore, a more complex stepped-lap joint is appropriate for adherends thicker than about 0.125 in. (3 mm). The limiting strength of the joint is usually set by the lowest service temperature, whereas the design overlap is set by the highest service temperature, at which the adhesive is the softest.

Another consideration in the design of bonded joints is the need to restrict the maximum shear strain developed in the adhesive at the ends of the bonded overlap. Once the knee in the stress-strain curve has been exceeded, progressively more damage occurs in the adhesive as a result of the tensile stress associated with the shear deformations. It is therefore necessary to ensure that the design limit load does not strain the adhesive beyond the knee in the stress-strain curve. Because the shear strength of the bonded joint is proportional to the square root of the adhesive strain energy in shear, a design ultimate load 50 percent higher than the limit load would be associated with an ultimate shear strain almost twice that at the knee, as shown in Fig. 17.36. The remainder of the stress-strain curve for ductile adhesives is reserved for damage tolerance and the redistribution of loads around local damage. For brittle adhesives, the limits on joint strength would be established by equating the design ultimate load to the end of the stress-strain curve, which would not contain any distinct knee.

After the overlap length is determined, the elimination of peel stress needs to be addressed. Peel stresses occur for single-lap joints due the eccentricity in the load path, as previously shown in Fig. 17.22. Although not immediately

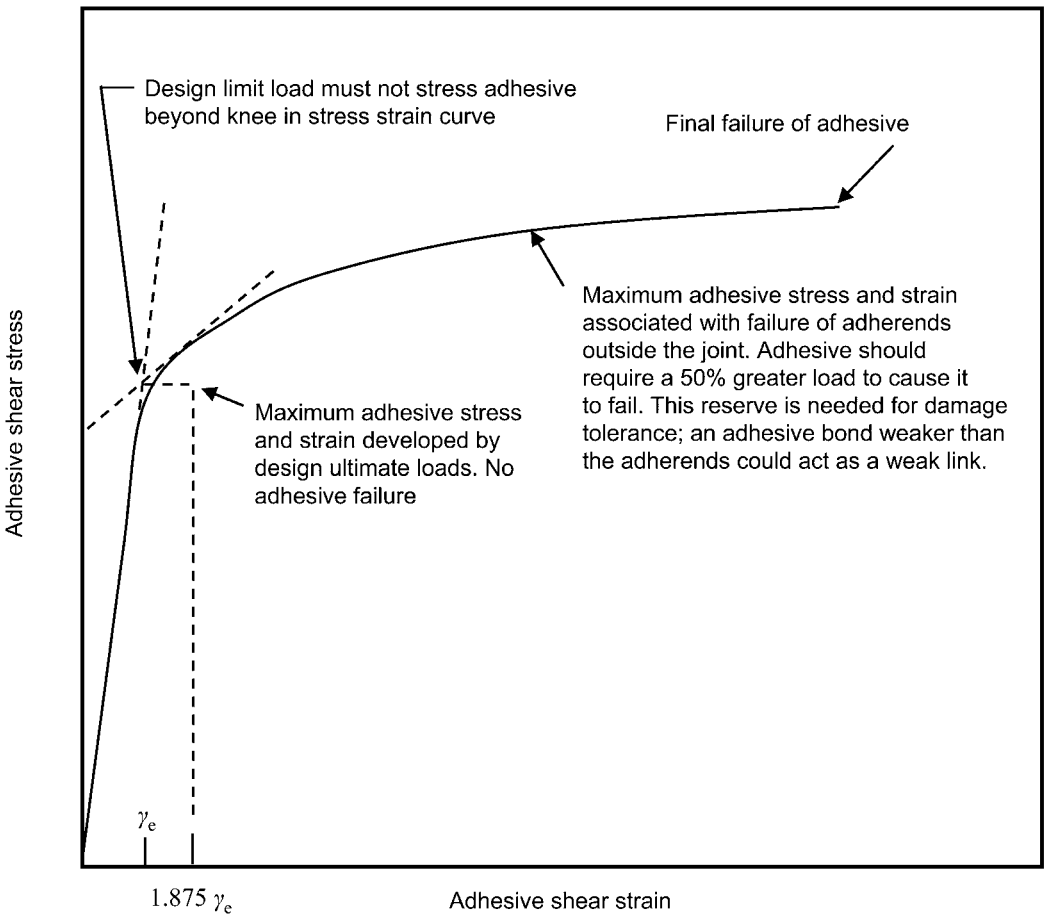


Fig. 17.36 Modeling of adhesives for design of shear loads. Source: Ref 12

apparent, peel stresses also occur in seemingly balanced double-lap joints, as shown for the thick composite adherends in Fig. 17.37. The elimination of peel stresses is accomplished by slightly modifying the joint geometry, as shown in Fig. 17.38, in which the tips of the adherends are made thin and flexible so that only negligible peel stresses can develop. Local thickening of the adhesive at the tips is beneficial. However, such local thickening of the adhesive layer must be used cautiously with high-flow elevated-temperature-curing adhesives to prevent the creation of voids by capillary action. The use of additional adhesive or scrim fillers can help to prevent any such problems. The exact proportions in tapering the adherend or thickening the adhesive layer are not critical. If the overlap is long enough, it is impossible to overdo the peel stress relief. In addition, the natural fillet, or spew, that occurs when the adhesive flows during cure should never be removed. Testing has shown that it improves both the static and fatigue properties of the joint.

17.9 Stepped-Lap Adhesively Bonded Joints

Composite laminates that are too thick (and hence too strong) to be joined by simple uniform lap shear-bonded joints can be successfully bonded together using stepped-lap joints of the type shown in Fig. 17.39. Scarf joints are not attractive because the scarf slope needs to be very shallow (no more than about 0.02), so very long joints would be required for thick laminates. Each step of the stepped-lap bonded joint is governed by the same differential equation that governs double-lap joints. Consequently, there

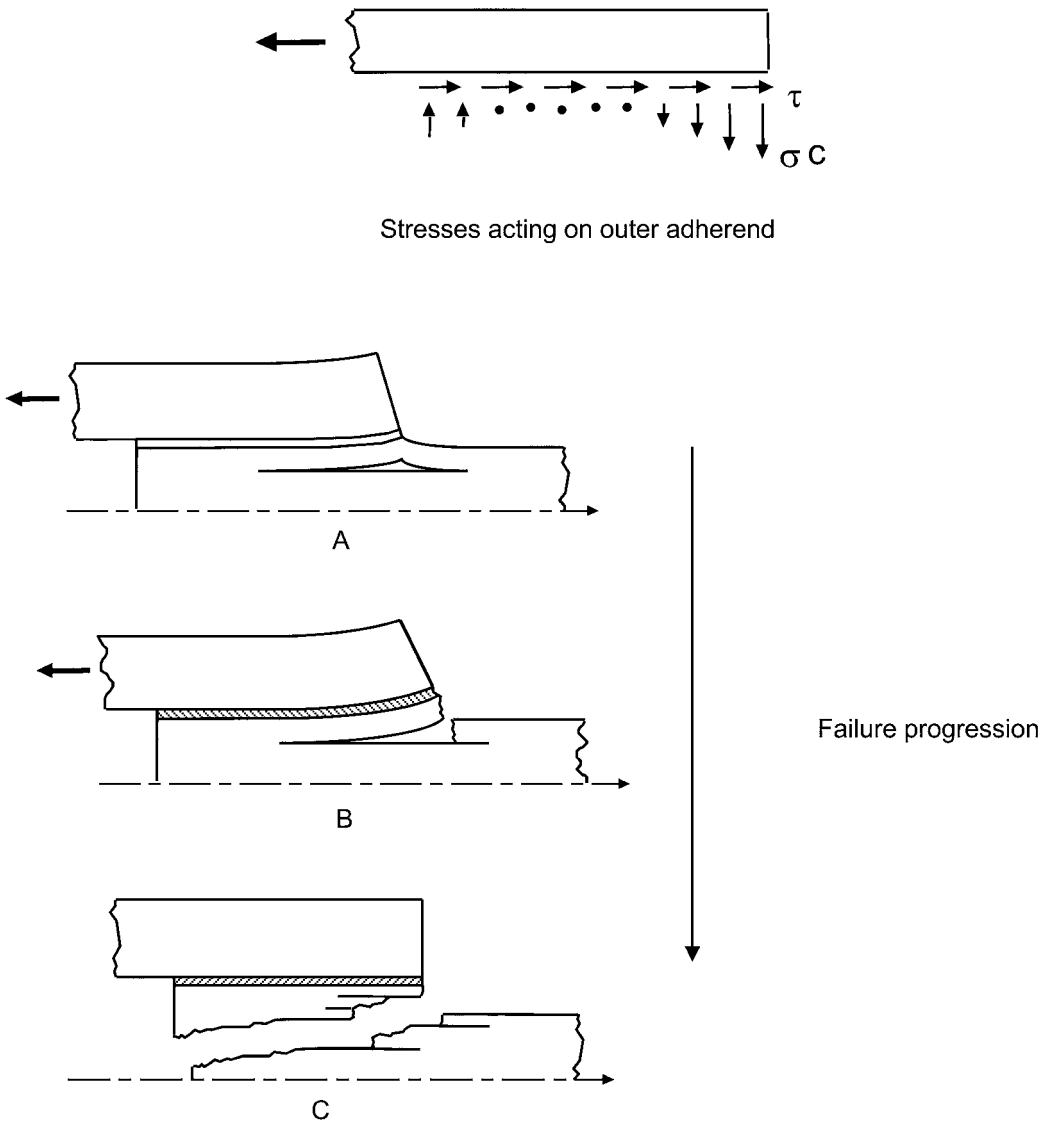


Fig. 17.37 Peel stress failure of thick composite joints. Source: after Ref 12

is a highly nonuniform shear stress distribution in the adhesive, with the load transfer concentrated at the ends of each step, as shown in Fig. 17.40.

The design and analysis of stepped-lap bonded joints are conducted using computer programs based on an elastic-plastic shear model. Some rules of thumb for initial design are as follows. The end steps must be neither too thick nor too long; 0.030 in. (0.8 mm) thick titanium with a step length of 0.375 in. (10 mm) is typical to prevent fatigue failures. Most of the other steps are usually 0.50 to 0.75 in. (13 to 19 mm) long, with step thicknesses no greater than 0.02 in. (0.5 mm) and preferably much less on either side of the joint, with one longer step near the middle of the overlap to provide creep resistance. Once the proportions have been adjusted properly, the most powerful variable with which to increase the joint strength is the number of steps; merely increasing the bond area for the same number of steps is not effective. The strength continues to increase as the number of steps is increased to one per ply, and the number should always be sufficient to ensure that the bond strength exceeds the adherend strengths by at least 50 percent.

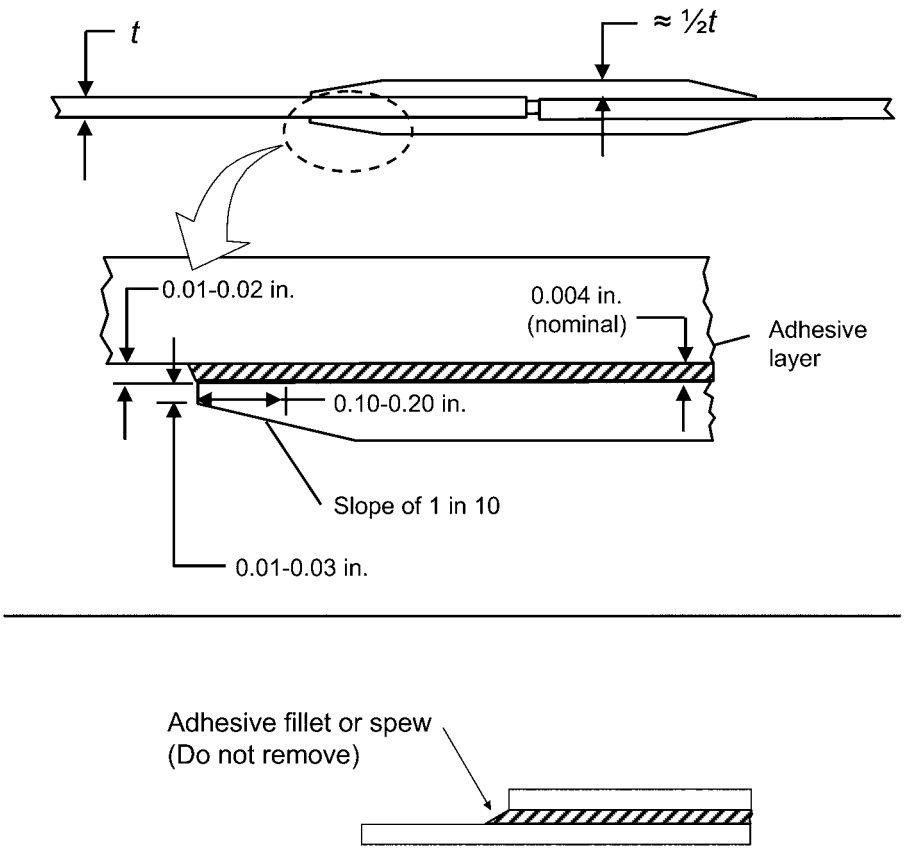


Fig. 17.38 Tapering edges to reduce peel stresses. Source: after Ref 12

While cocured stepped-lap joints can be used to produce weight-efficient joints in thick composites, they are difficult to manufacture and inspect. A cocured stepped-lap joint is used on the F/A-18 fighter aircraft at the wing root fitting, as shown in Fig. 17.41. A distinct advantage of this joint is that it allows the entire wing to be removed and replaced if necessary, as per contractual requirements. Manufacturing consists of laying up the bottom half of the plies using templates to locate the plies correctly for mating with the bottom half of the splice plate. The titanium splice plate is covered with a layer of film adhesive that is staged at elevated temperature in an oven; staging increases the adhesive viscosity and makes the step locations on the splice plate more easily visible. The staged splice plate is then placed on the bottom half of the lay-up, and the top halves of the plies are laid up to the steps. However, during cure, because the resin becomes liquid, hydraulic pressure tends to push the plies off the steps, creating gaps. These gaps produce wrinkling of the continuous plies that bridge over the steps, as shown schematically in Fig. 17.42. While these wrinkles only moderately degrade the tension properties, large gaps (wrinkles) can seriously degrade the compression properties because the load-bearing fibers are already prebuckled. Also, inspection and detection of gaps must be done using special radiographic inspection techniques, and interpretation of the radiographs is difficult. Although this joint has performed flawlessly in service, in practice it probably makes more sense to use mechanically fastened joints for thick composite structures.

17.10 Bonded-Bolted Joints

Analysis has shown that in a joint that is both bonded and mechanically fastened, the mechanical fasteners carry only about one percent of the load. In other words, the adhesive carries almost

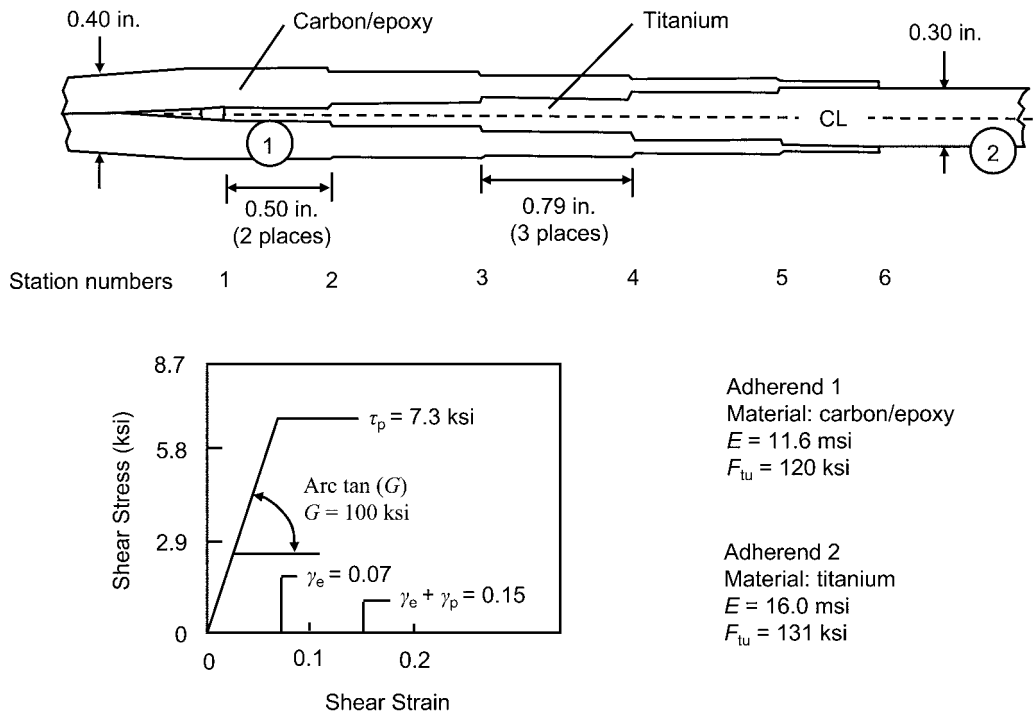


Fig. 17.39 Typical cocured stepped-lap joint. Source: Ref 6

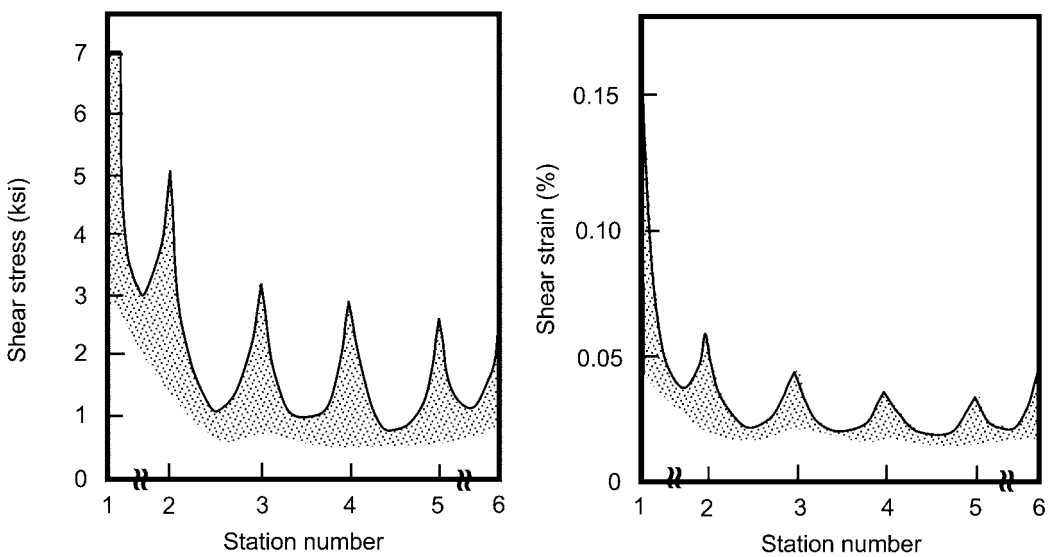


Fig. 17.40 Shear stress and strain distribution in a stepped-lap joint. Source: Ref 6

all of the load until it fails, and then the fasteners pick up the load. Therefore, unless a redundant joint is needed, the fasteners just add cost and weight. On the other hand, fasteners are often used to prevent peel stresses in certain instances, such as at the ends of cocured stiffeners, as shown in Fig. 17.43. Here, three different peel prevention concepts are used: (1) antipeel fasteners are used at the end of the hat to prevent delaminations from propagating down the length

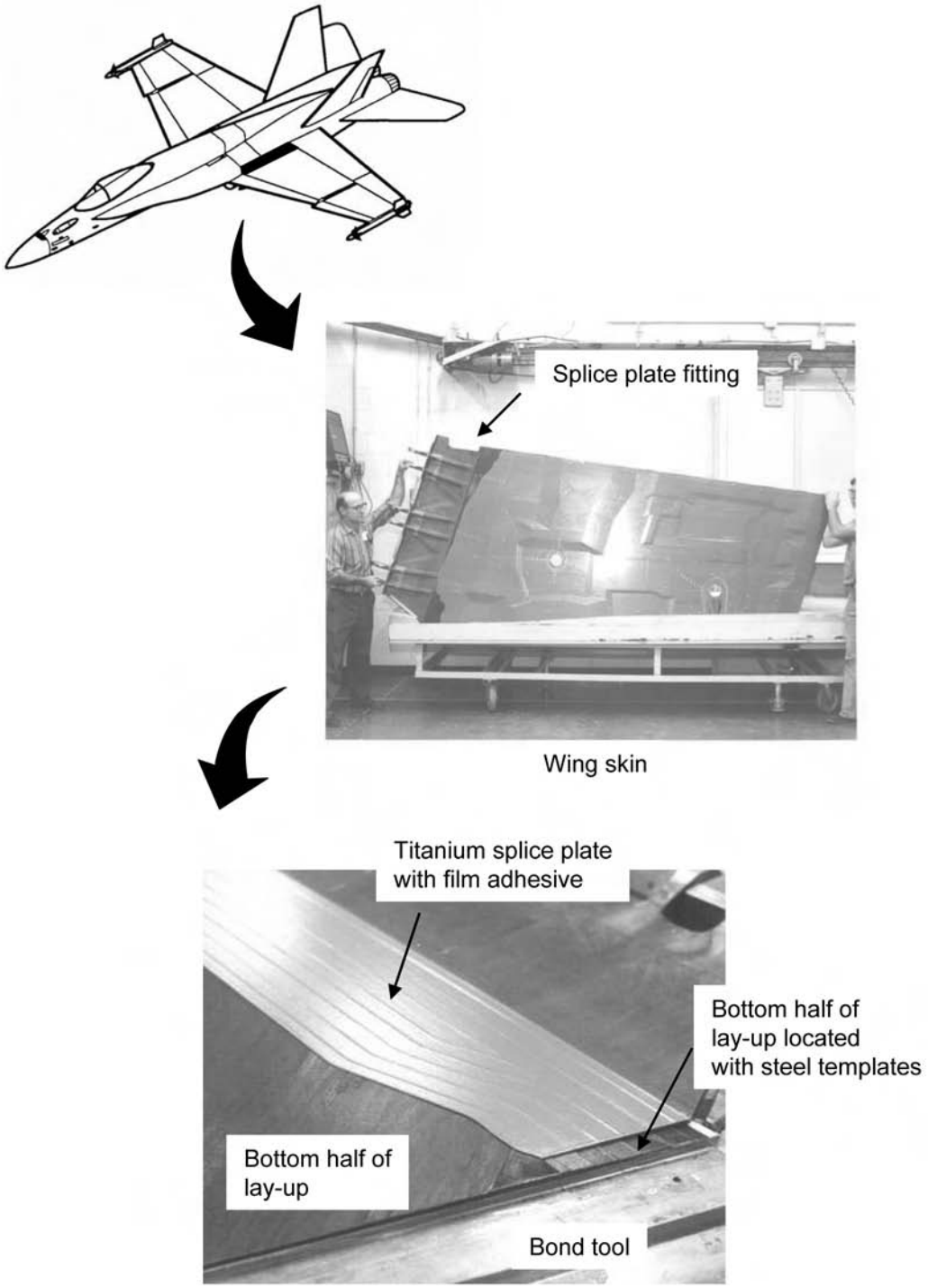


Fig. 17.41 Wing root splice fabrication. Source: The Boeing Company

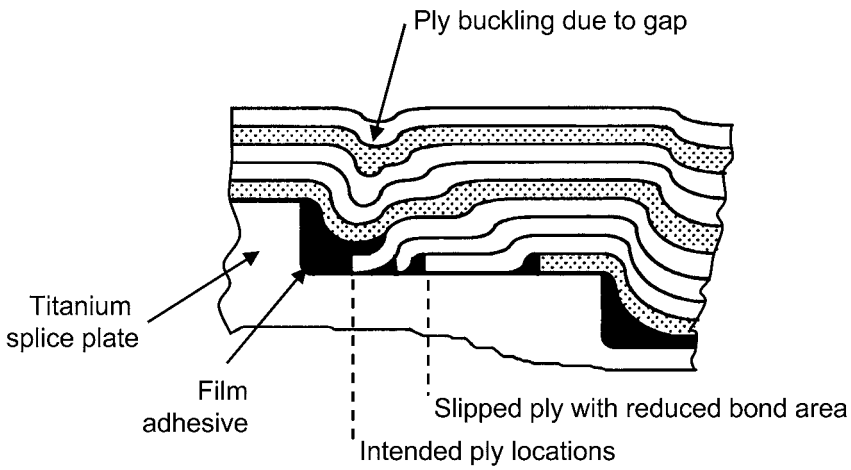


Fig. 17.42 Gaps on a splice plate

This design actually illustrates three methods of reducing peel stresses at the termination of the cocured hat stiffener:

(1) Antipeel fasteners
(2) Scarfing at the end of the hat
(3) Thickening at the end of the hat

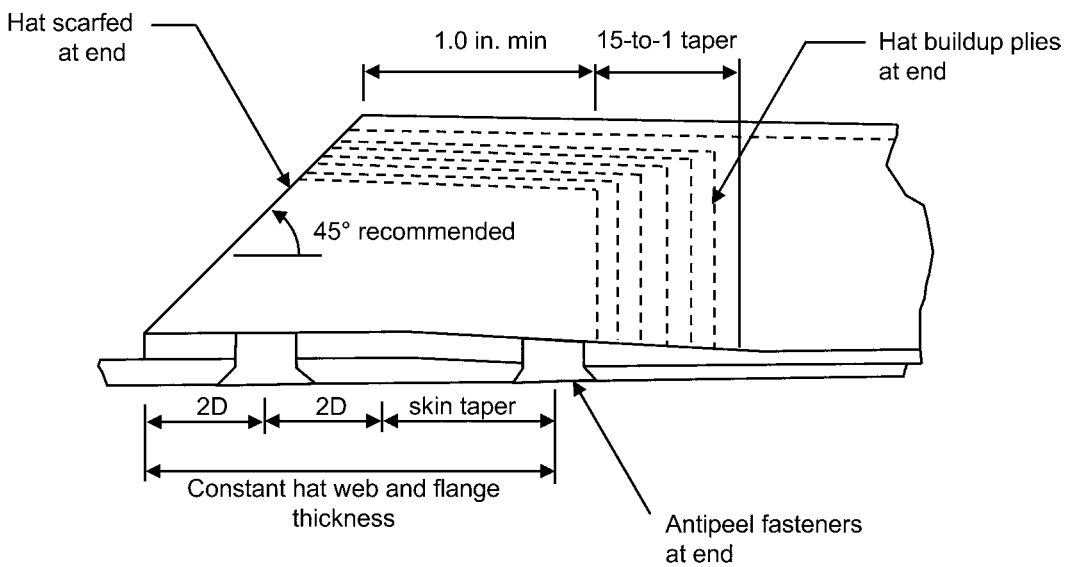


Fig. 17.43 Bonded-bolted joint to prevent peel failures

Table 17.3 Guidelines for adhesively bonded joints

Guidelines	Remarks
1. Never design for an adhesive bond to be the weak link in a structure. The bonds should always be stronger than the members being joined.	Bonded joints must always be designed to be stronger than the adjacent structure; otherwise, the bond can act as a weak-link fuse and unzip catastrophically from a local defect.
2. Use secondary adhesive bonding extensively for thin, lightly loaded composite structures, restricting the use of mechanical fastening mainly to thicker, more heavily loaded structures.	Thick bonded joints can fail prematurely in peel. Bonding works best for thin structures.
3. Proper joint design should be used, avoiding tension, peel, or cleavage loading whenever possible. If peel forces cannot be avoided, a lower modulus (nonbrittle) adhesive having a high peel strength should be used.	Adhesives work best in shear and are poor in peel. Composites are even weaker in interlaminar tension.
4. Ensure that the bonded joint configuration is 100% inspectable.	…
5. Proper surface preparation is critical. Beware of cleaning solvents and peel plies. Mechanical abrasion is more reliable.	Surface gloss must be removed. Some peel plies use silicone.
6. Bonded joint strength is usually less in a cold environment, where adhesive is brittle.	…
7. Balanced adherend stiffnesses improve joint strength.	…
8. Minimize joint eccentricities.	Eccentricities cause bending and peel stresses in adhesive.
9. Use adherends with similar coefficients of thermal expansion.	…
10. Use ductile adhesives rather than brittle ones.	Ductile adhesives are far more forgiving than brittle adhesives.
11. Use film adhesives rather than pastes.	Film adhesives have higher strength and controlled bondline thickness.
12. Adhesives are well characterized by a thick-adherend test coupon, generating a complete nonlinear stress-strain curve in shear.	…
13. Be aware of the need to dry laminates before doing bonded repairs.	Desorbing moisture during cure can blow out adhesive.
14. Care is needed to taper the ends of bonded overlaps—down to 0.020 in. thick with a 1-in-10 slope—to minimize induced peel stresses that would cause premature failures.	…
15. Design of simple, uniformly thick (for nearly quasi-isotropic carbon/epoxy) bonded splices is very simple—about 30t overlap in double shear, 80t overlap for single-lap joints, and a 1-in-30 slope for scarf joints.	…
16. For highly loaded bonded joints, cocured, multiple-step, double-sided lap joints are preferred.	…
17. Thick bonded structures need complex stepped-lap joints to develop adequate efficiency.	…
18. Design of stepped-lap joints for thick structure needs a nonlinear analysis program.	…
19. Thick bonded structures are very difficult to repair; so, except for one-shot and throwaway structures, original designs should be bolted together to permit bolted repairs.	…
20. The fillet or spew at the end of the exposed joint should not be removed.	Fillet improves static and fatigue properties.
21. Selection tests for structural adhesives should include durability testing for heat, humidity (and/or fluids), and stress simultaneously.	Prevents unexpected long-term durability problems.
Composite-to-metal splice joints	
22. Bonded step joints preferred to scarf joints.	More consistent results.
23. Where possible, 0° plies (primary load direction) should be placed adjacent at the bondline; 45° plies are also acceptable; 90° plies should never be placed adjacent to the bondline unless it is also the primary load direction.	To maximize lap shear.
24. For a stepped joint, the metal thickness at the end step should be 0.020 in. minimum.	To prevent metal failure

(continued)

Table 17.3 (continued)

Guidelines	Remarks
25. If possible, have ± 45° plies end on the first and last steps of bonded step joints.	…
26 If possible, do not end more than two 0° plies (not more than 0.014 maximum thickness) on any one step surface.	…
27. Tension and peel stresses should be avoided in adhesive bonded joints.	Good design practice.
Composite-to-metal continuous joints	
28. Bonding composites to titanium (preferred) and steel (acceptable).	Material compatibility and best match of expansion coefficients.
29. Thermal expansion of dissimilar materials must be considered. Due to the large thermal expansion difference between carbon composite and aluminum, adhesively bonded joints between these two materials have been known to fail during cool-down from elevated-temperature cures as a result of the thermal stresses induced by their differential expansion coefficients.	To minimize interlaminar shear stress due to the large difference in the coefficient of thermal expansion between carbon composites and aluminum.

of the bondline, (2) the end of the hat is scarfed to allow a more gradual transition of the loads, and (3) the skin itself is thickened under the hat end to make the joint stiffer.

Some general design guidelines for adhesively bonded joints are given in Table 17.3.

ACKNOWLEDGMENT

Dr. John Hart-Smith, while working for the Douglas Aircraft Company, a part of McDonnell-Douglas Corporation and now Boeing, is the acknowledged world leader in developing analysis methods for both mechanically fastened and adhesively bonded joints. He developed almost all of the concepts covered in this chapter.

REFERENCES

1. D.W. Oplinger, Mechanical Fastening and Adhesive Bonding, *Handbook of Composites*, Chapman & Hall, 1982
2. A. Baker, S. Dutton, and D. Kelly, *Composite Materials for Aircraft Structures*, 2nd ed., American Institute of Aeronautics and Astronautics, Inc., 2004
3. L.J. Hart-Smith, "Bolted Joint Analysis for Fibrous Composite Structures—Current Empirical Methods and Future Scientific Prospects," ASTM STP 1455, *Joining and Repair of Composite Structures*, American Society for Testing and Materials, 2004
4. J.A. Baile, M.F. Duggan, N.C. Bradshaw, and T.G. McKenzie, "Design Data for Carbon Cloth Epoxy Bolted Joints at Temperatures up to 450K," ASTM STP 749, *Joining of Composite Materials*, American Society for Testing and Materials, 1981
5. R.T. Parker, Mechanical Fastener Selection, *ASM Handbook*, Vol 21, *Composites*, ASM International, 2001, p 651–658
6. L.J. Hart-Smith, Bolted and Bonded Joints, *ASM Handbook*, Vol 21, *Composites*, ASM International, 2001
7. "Redux Bonding Technology," Hexcel Composites, December 2001
8. R.B. Heslehurst and L.J. Hart-Smith, The Science and Art of Structural Adhesive Bonding, *SAMPE J.*, Vol 38 (No. 2), Mar/Apr 2002, p 60–71
9. L.J. Hart-Smith, "Adhesive-Bonded Single-Lap Joints," NASA Contract Report NASA CR 112236, 1973
10. L.J. Hart-Smith, "Adhesive-Bonded Double-Lap Joints," NASA Contract Report NASA CR 112235, 1973
11. L.J. Hart-Smith, "Adhesive-Bonded Scarf and Stepped-Lap Joints," NASA Contract Report NASA CR 112237, 1973
12. L.J. Hart-Smith, The Design of Adhesively Bonded Joints, *Adhesion Science and Engineering*, Vol 1, *The Mechanics of Adhesion*, Elsevier Science, 2002
13. R.B. Krieger, Analyzing Joint Stresses Using an Extensometer, *Adhes. Age*, Vol 28 (No. 11), Oct 1985, p 26–28
14. F.C. Campbell, Secondary Adhesive Bonding of Polymer-Matrix Composites, *ASM Handbook*, Vol 21, *Composites*, ASM Handbook 21, ASM International, 2001

SELECTED REFERENCES

- L.J. Hart-Smith, "Design Methodology for Bonded-Bolted Composite Joints," AFWAL-TR-81-3154, 1982
- L.J. Hart-Smith, Design and Analysis of Bolted and Riveted Joints in Fibrous Composite Structures, *Recent Advances in Structural Joints and Repairs for Composite Materials*, Kluwer Academic Publishers, 2003
- L.J. Hart-Smith, Adhesively Bonded Joints for Fibrous Composite Structures, *Recent Advances in Structural Joints and Repairs for Composite Materials*, Kluwer Academic Publishers, 2003

"*This page left intentionally blank.*"

Copyright © 2010, ASM International®
All rights reserved.
www.asminternational.org

CHAPTER 18

Design and Certification Considerations

THE AUTHOR WORKED on his first aircraft program in the mid-1970s when there were no computers or workstations. Designers made drawings on large plastic sheets with ink pens. The strength engineer specified the laminate orientations and number of plies needed to meet strength and stiffness requirements; the designer took overall responsibility for the design, consulting with the proper engineering group when there was a technical question.

Today's design environment is totally different. Designs are now created by concurrent engineering or integrated product definition (IPD) teams that consist of engineering, tooling, manufacturing, quality, and supportability personnel. Even the customers participate in preliminary, critical, and final design reviews. Design tools have also greatly improved. Computerized laminate analysis codes and finite element modeling tools are available for detailed composite designs. Modern design is done on workstations with advanced computer-aided design (CAD)/computer-aided manufacturing (CAM) packages.

Integrated product definition teams have more freedom with composite construction than they do when using traditional metals, because with composites they are free to select different reinforcements, combine them with a choice of different matrices, and then fabricate them using a variety of processes. The design team is free to determine the amount and distribution of the constituents. A composite laminate can be built to any thickness, and the fibers may be oriented to achieve the desired strength and stiffness. Although this design freedom increases the number of choices, it also makes the process more complex.

This chapter will cover, to a very limited extent, the activities of the IPD team during the design process. Topics covered include material selection, manufacturing process selection, initial trade studies to select the material and design concept, the building block approach to testing and certification used in the aerospace industry, design allowables, and some guidelines for detailed design. In addition, a number of considerations important in composites design are covered, including damage tolerance and environmental sensitivity. Although these activities are discussed serially in this chapter, they are actually conducted in an iterative manner, especially in the early stages of the design process. Once the design is finalized, it is expensive to have to go back and change it. It has been postulated that as much as 90 to 95 percent of the final product cost is determined by the decisions made during the first five percent of the design process. Therefore, it is important to do the upfront work carefully before the detailed design starts.

18.1 Material Selection

In the materials selection process, a broad choice can be made between the use of composite construction, metals, unreinforced polymers, and natural materials. As a general guideline, if a part can easily be fabricated from a traditional material like aluminum, steel, wood, or plastic, this choice may represent the lowest-cost solution. However, composite construction has many advantages, including reduced weight, higher stiffness, and better corrosion resistance.

18.2 Fiber Selection

Since the fibers provide the strength and stiffness, it is appropriate to consider fiber selection first. Glass fibers are the most widely used reinforcement because of their good balance of mechanical properties and low cost. E-glass is the most common glass fiber and is used extensively in commercial composite products. E-glass is a low-cost, high-density, low-modulus fiber that has good corrosion resistance and good handling characteristics. S-2 glass was developed in response to the need for a higher-strength fiber for filament-wound pressure vessels and solid rocket motor casings. Although more expensive than E-glass, it has a density, performance and cost between those of E-glass and carbon. Quartz fiber is used in many electrical applications because of its low dielectric constant; however, it is very expensive.

Aramid fiber (such as Kevlar) is an organic fiber that has a low density and is extremely tough, exhibiting excellent damage tolerance. It has a high tensile strength but performs poorly in compression. It is also sensitive to ultraviolet light and should be used for long-term service only at temperatures less than 300 °F (150 °C). Another organic fiber is made from ultra-high molecular weight polyethylene (UHMWPE), such as Spectra. It has a low density with excellent radar transparency and a low dielectric constant. Because of its low density, it exhibits very high specific strength and modulus at room temperature. However, being polyethylene, it cannot withstand temperatures higher than 200 °F (90 °C). Like aramid and S-2 glass, UHMWPE has excellent impact resistance; however, like aramid, it often exhibits poor adhesion to its matrix.

Carbon fiber offers the best combination of properties but is also more expensive than either glass or aramid. Carbon fiber has a low density and a low coefficient of thermal expansion (CTE), and it is conductive. It is structurally very efficient and exhibits excellent fatigue resistance. It is also brittle (strain-to-failure less than two percent) and exhibits low impact resistance. Being conductive, it causes galvanic corrosion if placed in direct contact with more anodic metals (such as aluminum). Carbon and graphite fibers are available in a wide range of strength and stiffness, with strengths of 300 to1000 ksi (2000 to 7000 MPa) and moduli of 30 to 145 msi (4 to 21 GPa). With this wide range of properties, carbon fiber is frequently classified as either (1) high strength, (2) intermediate modulus, or (3) high modulus. Both carbon and graphite fibers are produced as untwisted bundles called *tows*. Common tow sizes are 1k, 3k, 6k, 12k, and 24k, where k = 1000 fibers. Immediately after fabrication, carbon and graphite fibers are normally surface-treated to improve their adhesion to the polymeric matrix.

Several other fibers are occasionally used for polymeric composites. Boron fiber was the original high-performance fiber before carbon was developed. It is a large-diameter fiber that is made by pulling a fine tungsten wire through a long, slender reactor in which boron is applied by chemical vapor deposition. Since it is made one fiber at a time rather than thousands of fibers at a time, it is very expensive. Owing to its large diameter and high modulus, it exhibits outstanding compression properties. On the negative side, it does not conform well to complicated shapes and is very difficult to machine. Other high-temperature ceramic fibers, such as silicon carbide (Nicalon), aluminum oxide, and alumina boria silica (Nextel), are frequently used in ceramic-based composites but rarely in polymeric composites.

The following factors should be considered when choosing among glass, aramid, and carbon fibers:

- *Tensile strength.* If tensile strength is the primary design parameter, E-glass may be the best selection because of its low cost.
- *Tensile modulus.* When designing for tensile modulus, carbon has a distinct advantage over both glass and aramid.
- *Compression strength.* If compression strength is the primary requirement, carbon has a distinct advantage over glass and aramid. Because of its poor compression strength, aramid should be avoided.
- *Compression modulus.* Carbon fiber is the best choice, E-glass the worst.
- *Density.* Aramid fibers have the lowest density, followed by carbon and then S-2 and E-glass.
- *Coefficient of thermal expansion.* Aramid and carbon fibers have a CTE that is slightly negative, whereas the CTEs of S-2 and E-glass are positive.
- *Impact strength.* Aramid and S-2 fibers have excellent impact resistance, but carbon is brittle and should be avoided. However, it should be noted that matrix selection also has a significant influence on impact strength.
- *Environmental resistance.* Matrix selection has the biggest impact on composite environ-

mental resistance. However, (1) aramid fibers are degraded by ultraviolet light, and the long-term service temperature should be kept below 300 °F (150 °C); (2) carbon fibers are subject to oxidation at temperatures exceeding 700 °F (370 °C), although long-term 1000 hours of thermal oxidation stability tests in polyimides have shown strength decreases in the 500 to 600°F (260 to 315 °C) range; and (3) glass sizings tend to be hydrophilic and absorb moisture.

Cost. E-glass is the least expensive fiber and carbon is the most expensive. In carbon, the smaller the tow size, the more expensive the fiber. Larger tow sizes help reduce labor costs because more material is deposited with each ply. However, large tow sizes in woven cloth can increase the chances of voids and matrix microcracking caused by larger resin pockets.

18.3 Product Form Selection

A multitude of material product forms are used in composite structures, some of which are illustrated in Fig. 18.1. The fibers can be continuous or discontinuous. They can be oriented or disoriented (random). They can be furnished as dry fibers or preimpregnated with resin (prepreg).

Not all fiber or matrix combinations are available in a particular material form, since the market drives availability. In general, the more operations required by the supplier, the higher the cost. For example, prepreg cloth is more expensive than dry woven cloth. While complex dry

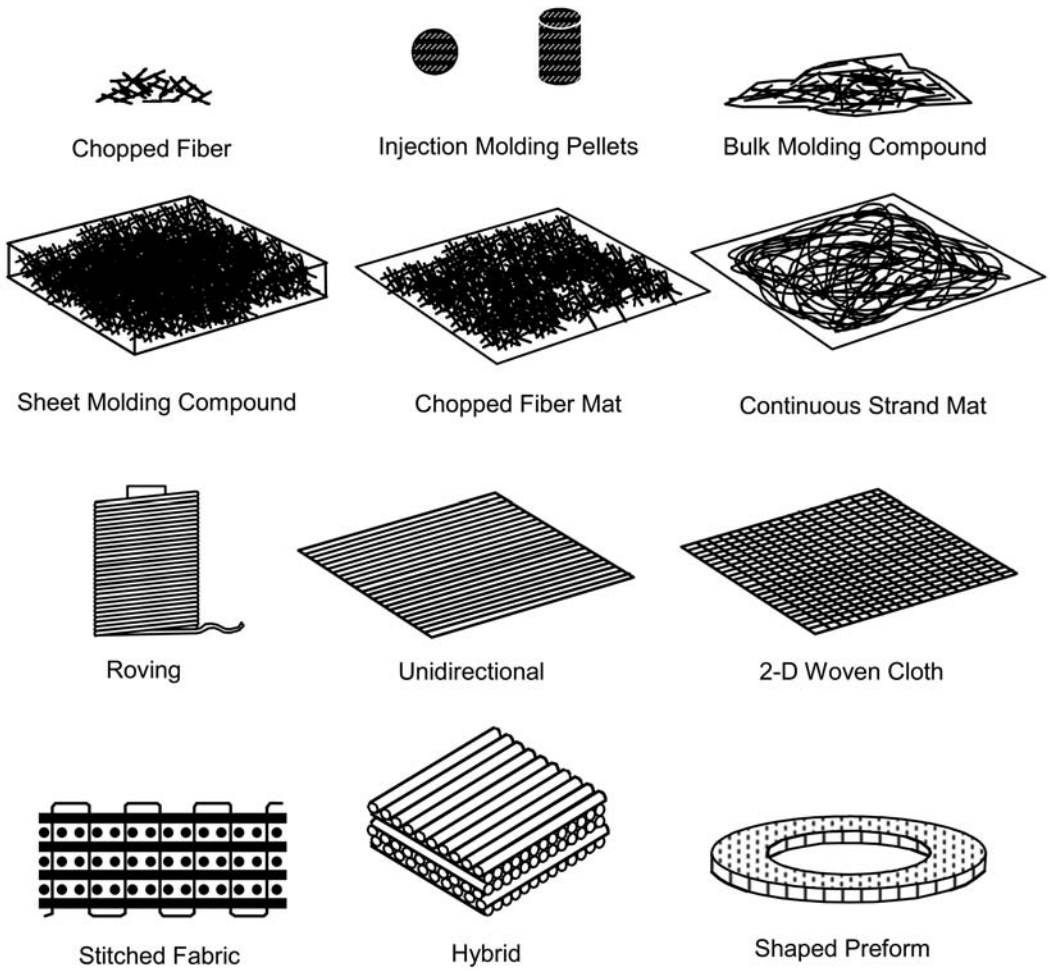


Fig. 18.1 Product forms used in composites

preforms may be expensive, using them can lower fabrication costs overall by reducing or eliminating hand lay-up costs. If structural efficiency and weight are important design parameters, continuous-reinforced product forms are normally used because discontinuous fibers yield lower mechanical properties. Some common trade-offs when selecting composite materials are given in Table 18.1, and a comparison of between dry fiber/neat resin and prepreg is presented in Table 18.2.

18.3.1 Discontinuous-Fiber Product Forms

Chopped fiber is made by mechanically chopping rovings, yarns, or tows into short lengths, typically $^1/_4$ to 2 in. (6 to 50 mm) long. It is important that the chopped fibers be no shorter than this to ensure maximum reinforcement efficiency. Milled fibers, typically $^1/_{32}$ to $^1/_4$ in. (0.8 to 6 mm) long, have low aspect ratios (length/diameter) that provide minimal strength and therefore should not be considered for structural applications. The strength of the composite is greatly improved with increased fiber length, although stiffness is much less affected. Chopped glass fibers are often embedded in thermoplastic or thermoset resins in the form of pellets for injection molding.

Chopped fibers or entangled continuous strands are combined with a binder to form mat or veil materials. A *veil* is a thin mat that is used to improve the surface finish of a molded composite. This material form is used extensively for automotive, industrial, recreational, and marine applications, where high-quality Class A exterior surface finishes are required. These are very inexpensive product forms in which E-glass is the fiber most commonly used. Other fibers may be available in mat form, but they are generally expensive due to the specialty nature of the product. At the time of this writing, carbon mats are uncommon because of low demand. Some carbon veils for electromagnetic interference protection are available (though expensive). Historically, the aerospace industry has not been interested in this product form because of its low structural inefficiency and the weight penalty associated with its discontinuous reinforcement. The automotive industry has not been interested in it either; although the industry uses mats extensively, it has not been willing to pay the cost penalty for carbon-fiber material.

Sheet molding compound (SMC) consists of flat sheets of chopped, randomly oriented fibers, typically 1 to 2 in. (25 to 50 mm) in length, with a B-staged resin matrix, usually consisting of E-glass fiber in either a polyester or vinyl ester resin. The material is available either as rolls or as precut sheets. Bulk molding compounds (BMCs) are also short, randomly oriented preimpregnated materials; however, the fibers are normally only $^1/_8$ to $1^1/_4$ in. (3 to 6 mm) long, and the reinforcement percentage is lower. As a result, the mechanical properties of BMC composites are lower than those of SMC composites.

Table 18.1 Common trade-offs when selecting composite materials

Design decision	Common trade-offs	Typically lowest cost	Typically highest performance
Fiber type	Cost, strength, stiffness, density (weight), impact strength, electrical conductivity, environmental stability, corrosion, thermal expansion	E-glass	Carbon
Tow size (if carbon is selected)	Cost, fiber volume, improved fiber wet-out, structural efficiency (minimize ply thickness), surface finish	12K tow	3K tow
Fiber modulus (if carbon is selected)	Cost stiffness, weight, brittleness	Lowest-modulus carbon	Highest-modulus carbon
Fiber form (continuous vs. discontinuous)	Cost, strength, stiffness, weight, fiber volume, design complexity	Random/discontinuous	Oriented and continuous
Matrix	Cost, service temperature, compressive strength, interlaminar shear, environmental performance (fluid resistance, UV stability, moisture absorption), damage tolerance, shelf life, processability, thermal expansion	Vinyl ester and polyester	High-temperature—polyimide(a) Low-moderate temperature—epoxy Toughness—toughened epoxy
Composite material forms	Cost (material and labor), process compatibility, fiber volume control, material handling, fiber wet-out, material scrap	Base form—neat resin/Rovings	Prepreg(b)

(a) Depends on how "highest performance" is defined—high temperature, toughness, and superior mechanical properties. (b) Material form is not driven by performance, but is typically defined by the manufacturing process.

Table 18.2 Relative comparison of dry fiber/neat resin and prepreg

	Dry fiber/neat resin	Prepreg
Cost	Lower	Higher
Shelf life	Better	Worse
Storage	Better	Worse
Material handling		
• Drapability	Better	Worse
• Tack	Worse	Better
Resin control	Worse	Better
Fiber volume control	Worse	Better
Part quality	Worse	Better

Bulk molding compounds are available in dough-like bulk form or are extruded into logs for easier handling. Vinyl esters, polyesters, and phenolics are the most common matrices used for BMCs. Sometimes, for convenience of terminology, chopped prepreg, used for compression molding, is referred to as BMC.

18.3.2 Continuous-Fiber Product Forms

Rovings, tows, and yarns are collections of continuous fiber. This is the basic material form; it can be chopped, woven, stitched, or prepregged into other product forms. It is the least expensive product form, and it is available for all fiber types. Rovings and tows are supplied with no twist; yarns have a slight twist, which improves their handleability at the expense of fiber strength. Some processes, such as wet filament winding and pultrusion, use rovings as their primary product forms.

Continuous-thermoset prepreg materials are available in many fiber and matrix combinations. A prepreg is a fiber form that has a predetermined amount of uncured resin impregnated in the fiber by the material supplier. Prepreg rovings and tapes are usually used in automated processes (for example, filament winding and automated tape laying); unidirectional tape and prepreg fabrics are used for hand lay-up. Unidirectional prepreg tapes offer improved structural properties compared to woven prepregs because there is no fiber crimp and because designs can be tailored more easily. However, the increased drapability of woven prepregs makes them attractive for complex substructure parts. With the exception of predominantly unidirectional designs, unidirectional tapes require placement of more individual plies during lay-up. For example, with cloth, for every 0° ply in the lay-up, a 90° reinforcement is also included. With unidirectional tape, a 0° ply and a separate 90° ply must be placed on the tool.

Prepregs are supplied with either a net resin (prepreg resin content ≈ final part resin content) or excess resin (prepreg resin content > final part resin content). The excess resin approach relies on the matrix flowing through the plies, removing entrapped air, while the extra resin is removed by impregnating bleeder plies on top of the lay-up. The amount of bleeder used in the lay-up dictates the final fiber and resin content; however, as the laminate gets thicker, it becomes more difficult to remove the excess resin. Accurate calculations of the number and areal weight of bleeder plies for a specific prepreg are required to ensure the correct final physical properties. Since the net resin approach contains the final resin content weight in the prepreg, no resin removal is necessary and the fiber and resin volumes can therefore be easily controlled. Thermoset prepreg properties include volatile content, resin content, resin flow, gel time, tack, drape, shelf life, and out-time. Careful testing, evaluation, and control of these characteristics are necessary to ensure that the prepreg materials' handling characteristics are optimal and final part structural performance is obtained.

Woven fabric is the most common continuous dry material form. A woven fabric consists of interlaced warp and fill yarns. The warp is in the 0° direction as the fabric comes off the roll, and the fill (or weft) is the 90° fiber. Typically, woven fabrics are more drapable than stitched materials; however, the specific weave pattern will affect their drapability. The weave pattern will also affect the handleability and structural properties of the woven fabric. Many weave patterns are available. All weaves have advantages and disadvantages, and consideration of the part configuration is necessary during fabric selection. Most fibers are available in woven fabric form. However, it can be very difficult to weave some high-modulus fibers due to their inherent brittleness. Advantages of woven fabric include drapability, ability to achieve high fiber volumes, structural efficiency, and market availability. A disadvantage of woven fabric is the crimp that is introduced in the fibers during weaving, which adversely affects the strength properties. Finishes or sizings are typically put on the fibers to aid in the weaving process and minimize fiber damage. It is important to ensure that the finish is compatible with the matrix selection when specifying a fabric.

A stitched fabric consists of unidirectional fibers oriented in specified directions and then stitched together. A common stitched design

includes 0°, +45°, 90°, and −45° plies in one multidirectional fabric. Advantages include the following: (1) Off-axis orientations can be incorporated as the fabric is removed from the roll. Off-axis cutting is not needed for a multidirectional stitched fabric and can reduce scrap rates (up to 25 percent) compared to conventional woven materials. (2) Labor costs are also reduced when multi-ply stitched materials are used because fewer plies need to be cut or handled during fabrication of a part. (3) Ply orientation remains intact during handling because of the z-axis stitch threads. Disadvantages include the following: (1) Only specific stitched ply set designs are available without customization. Typically, tailoring to the requirements of a customer will necessitate a special order. (2) Not as many companies stitch as weave. (3) Drapability is reduced (which, however, can be an advantage for parts with large, simple curvature). Careful selection of the stitching thread is necessary to ensure compatibility with the matrix and process temperatures.

Hybrids are material forms that make use of two or more fiber types. Common hybrids include glass/carbon, glass/aramid, and aramid/carbon fibers. Hybrids are used to take advantage of properties or features of each reinforcement type. In a sense, a hybrid is a trade-off reinforcement that allows increased design flexibility. Hybrids can be interply (two alternating layers), intraply (both in one layer), or hybridized only in selected areas. Hybridization with carbon in selected areas is usually performed to increase the local strength or stiffness of a part, whereas hybridization with glass in carbon laminates is performed to make the laminate locally softer. Carbon/aramid hybrids have low thermal stresses compared to other hybrids (because the two materials have similar CTEs), increased modulus and compressive strength compared to an all-aramid design, and increased toughness compared to an all-carbon design. Carbon/E-glass hybrids have increased properties compared to an all-E-glass design but lower cost than an all-carbon design. The CTE of each fiber type in a hybrid needs careful evaluation to ensure that no high internal stresses are introduced to the laminate during cure, especially at higher cure temperatures. The use of hybrids normally increases the amount of material that must be stocked and can increase the lay-up costs.

A preform is a preshaped fibrous reinforcement that has been formed on a mandrel or in a tool before it is placed into a mold. The shape of the preform closely resembles the final part configuration; a simple multi-ply stitched fabric is not a preform unless it is shaped to approximately its final configuration. The preform is the most expensive dry, continuous, oriented fiber form; however, using preforms can reduce fabrication labor. A preform can be made using rovings, chopped, woven, stitched, or unidirectional material forms. These reinforcements are formed and held in place by stitching, braiding, or three-dimensional weaving, or with organic binders or tackifiers. Advantages include reduced labor costs, minimal material scrap, reduced fiber fraying of woven or stitched materials, improved damage tolerance for three-dimensional stitched or woven preforms, and the fact that desired fiber orientations are locked in place. Disadvantages include high preform costs, fiber wettability concerns for thick, complex shapes, possible incompatibility between the tackifier or binder and the matrix, and limited flexibility if design changes are required. A common defect is that the preform is out of tolerance and therefore hard to place in the tool, and it may have to be trimmed. The use of preforms is not appropriate for all applications. All issues must be carefully considered before a preform is baselined. If the component is not a very complex configuration, the money saved in labor reduction may not offset the cost of the preform. Each application should be evaluated individually to determine whether the preform approach offers cost and quality advantages.

8.4 Matrix Selection

The matrix holds the fibers in their proper position, protects the fibers from abrasion, transfers loads between fibers, and provides the matrix-dependent mechanical properties. A properly chosen matrix also provides resistance to heat, chemicals, and moisture; has a high strain-to-failure; cures at as low a temperature as possible and yet has a long pot or out-time life; and is nontoxic. Matrices for polymeric composites can be either thermosets or thermoplastics. The most prevalent thermoset resins used for composite matrices are polyesters, vinyl esters, epoxies, bismaleimides, cynate esters, polyimides, and phenolics. A comparison of the major thermoset resin systems is given in Table 18.3.

The first consideration in selecting a resin system is the service temperature required for the part. The glass transition temperature T_g is a good indicator of the temperature capability of

Table 18.3 Comparison of thermoset matrix systems

Attribute	Polyester	Vinyl ester	Epoxy	Phenolic	Bismaleimide	Cynate ester
Applications						
Typical applications	Marine, general	Marine, general	Aerospace, general	Fire, smoke, and toxicity apps.	Aerospace, electrical	Aerospace
Performance						
Structural	Fair	Good	Good	Good, brittle	Good	Good
Corrosion and chemical resistance	Poor	Excellent	Good	Excellent	Good	Excellent
Moisture absorption	Poor	Excellent	Fair to good	Excellent	Fair to good	Excellent
Glass transition temperature (T_g)(°F)(a)	160	160–325 with post cure	200–350 with post cure	160–250+ with post cure	300–425 with post cure	350–450 with post cure
Fire, smoke, and toxicity	…	Requires additives	Reqs. adds.	Excellent	Good	Good

(a) Actual *T*g varies with each system and cure method. Source: Ref 1

the matrix. The T_g of a polymeric material is the temperature at which it changes from a rigid, glassy solid to a softer, semiflexible material. At this point, the polymer structure is still intact but the crosslinks are no longer locked in position. A resin should never be used above its T_g unless the service life is very short (for example, a missile body). A good rule of thumb is to select a resin in which the T_g is 50 °F (28 °C) higher than the maximum service temperature. Since most polymeric resins absorb moisture, thereby lowering the T_g, it is not unusual to require that the T_g be as much as 100 °F (56 °C) higher than the service temperature. Therefore:

$$\text{Maximum Usage Temperature} = \text{Wet } T_g - 50\ ^\circ\text{F} \quad \text{(Eq 18.1)}$$

Different resins absorb moisture at different rates, and the saturation levels can be different as well; therefore, each specific resin candidate must be evaluated for environmental performance. In general, thermoplastics absorb less moisture than thermosets. However, some thermoplastics, in particular amorphous thermoplastics, have poor solvent resistance. Most thermoset resins are fairly resistant to solvents and chemicals.

In general, the higher the temperature performance required, the more brittle and less damage-tolerant the matrix. Toughened thermoset resins are available, but they are more expensive and their T_gs are typically lower. High-temperature resins are also more costly and more difficult to process. Temperature performance is difficult to quantify because it is dependent on time at temperature, but it is important to have a thorough understanding of the environment in which the matrix is expected to perform.

Higher-T_g resins also require higher cure temperatures and longer times. Epoxies generally have cure times of two to six hours at elevated temperatures. A postcure may not be required for some epoxies, polyesters, and vinyl esters; therefore, elimination of postcure requirements should be evaluated as a possible way to decrease processing costs if the service temperature is low enough. Higher-T_g resins (such as bismaleimides and polyimides) require longer cure cycles and postcures. Postcuring further develops higher-temperature mechanical properties and improves the T_g of the matrix for some epoxies, bismaleimides, and polyimides. Very short cure times are desired for some processes (such as compression molding and pultrusion). Cure temperatures can range from 250 to 350 °F (120 to 180 °C) for epoxies. Bismaleimide cure temperatures typically range from 350 to 475 °F (177 to 246 °C), including postcure. Polyimide cure and postcure temperatures range from 600 to 700 °F (315 to 370 °C).

Polyesters, vinyl esters, epoxies, cynate esters, and bismaleimides are all addition-curing systems, whereas phenolics and polyimides cure by condensation reactions that evolve water or alcohols. Since the evolution of volatiles increases the propensity for voids and porosity, condensation-curing materials are more difficult to process. However, phenolics are often processed by compression molding processes, in which high pressures can be applied to suppress void formation. In addition, phenolic matrix composites are often used for interior furnishings for commercial aircraft because they tend to char instead of burn. Since these are only lightly loaded structures, the void content is not very important. Since polyimide matrix composites are more difficult to process than addition-curing systems, their usage should be restricted to high-temperature applications where they are really required.

Although fiber selection usually dominates the mechanical properties of the composite, matrix selection can also influence performance. Some resins wet out and adhere to fibers better than others, forming a chemical and/or mechanical bond that affects the fiber-to-matrix load transfer capability. The matrix can also microcrack during cure or in service. Resin-rich pockets and brittle resin systems are susceptible to microcracking, especially when the processing temperatures are high and the use temperatures are low, for example −65 °F (−36 °C), since this condition creates a very large difference in thermal expansion between the fibers and the matrix. Again, toughened resins help prevent microcracking but often at the expense of elevated-temperature performance.

18.5 Fabrication Process Selection

Once the fiber, product form, and matrix are selected, the fabrication process selection is narrowed to those used to make discontinuous-fiber composites and those used to make the higher-strength and -stiffness continuous-fiber composites. Often the material product form will be a major determining factor in the process selected, as shown in the examples in Table 18.4.

18.5.1 Discontinuous-Fiber Processes

Injection molding is a high-volume process used to make small to medium-sized parts. The reinforcement is usually chopped glass fibers with either a thermoplastic or thermoset resin; the majority of applications use thermoplastics because these process faster and have greater toughness. In the injection molding process, pellets containing embedded fibers or chopped fibers and resin are fed into a hopper. They are heated to their melting temperature and then injected under high pressure into a matched metal die. After the thermoplastic part cools or the thermoset part cures, they are ejected and the next cycle is started. Since expensive matched die molds are required, the number of parts to be produced must be large enough that the tooling cost can be recovered. Labor costs are minimal, as most injection molding facilities are highly automated and have only a minimal number of operators.

Spray-up is a more cost-effective process than wet lay-up, but the mechanical properties are greatly reduced by the use of randomly oriented chopped fibers. Continuous glass roving is fed into a special gun that chops the fibers into short lengths and simultaneously mixes them with either a polyester or a vinyl ester resin that is then sprayed onto the tool. Manual compaction with rollers is used to compact the lay-up. Vacuum bag cures can be used to improve part quality, but this is not common practice. Since the fibers are short and the orientation is random, this process is not used to make structural load-bearing parts.

Compression molding is another matched-die process that uses either discontinuous, randomly oriented SMC or BMC. A charge of predetermined weight is placed between the two dies, and then heat and pressure are applied. The molding compound flows to fill the die and then cures in one to five minutes, depending on the type of polyester or vinyl ester used. Thermoplastic composites, usually consisting of glass fiber and polypropylene for the automotive industry, are compression molded using highly automated production lines.

Reaction injection molding (RIM) is a process for rapidly making unreinforced thermoset parts.

Table 18.4 Typical material product forms versus process

	Process					
Material form	**Pultrusion**	**RTM**	**Compression molding**	**Filament winding**	**Hand lay-up**	**Auto tape laying**
Discontinuous						
Sheet molding compound	…	…	●	…	…	…
Bulk molding compound	…	…	●	…	…	…
Random continuous						
Swirl mat/neat resin	●	●	●	●	●	…
Oriented continuous						
Unidirectional tape	…	…	●	…	●	●
Woven prepreg	…	…	●	…	●	…
Woven fabric/neat resin	●	●	…	●	●	…
Stitched material/neat resin	…	●	…	…	…	…
Prepreg roving	…	…	…	●	…	…
Roving/neat resin	●	…	…	●	●	…
Preform/neat resin	…	●	…	…	…	…

A two-component highly reactive resin system is injected into a closed mold, where the resin quickly reacts and cures. Polyurethanes are the most prevalent, but nylons, polyureas, acrylics, polyesters, and epoxies have also been used. The RIM resin systems have very low viscosities and can be injected at low pressures less than 100 psi (700 kPa) so that inexpensive molds and low-force clamping systems can be used. Typical tooling materials include steel, cast aluminum, electroformed nickel, and composites. Cycle times as short as two minutes for large automotive bumpers are typical. Reinforced reaction injection molding (RRIM) is similar to RIM except that short glass fibers are added to one of the resin components. The fibers must be extremely short, for example 0.03 in. (0.8 mm), or the resin viscosity will be too great. Short fibers, milled fibers, and flakes are commonly used. Again, polyurethanes are the predominant resin system. The addition of the fibers improves modulus, impact resistance, and dimensional tolerance and lowers the CTE. Structural reaction injection molding (SRIM) is similar to the previous two processes except that a continuous glass preform is placed in the die prior to injection. Again, this process is used almost exclusively with polyurethanes. Owing to the highly reactive resins and short cycle times, SRIM cannot produce as large a part size as resin transfer molding (RTM). Also, SRIM parts have lower fiber volumes and are more porous than RTM parts.

18.5.2 Continuous-Fiber Processes

Wet lay-up in open molds is the least expensive process for a relatively small number of units. This is a common process for large production marine manufacturing, where thick, heavy, woven fiberglass mat and randomly oriented chopped fiber mat are hand or spray impregnated with polyester resin and cured at room temperature. After the ply is placed on the lay-up, hand rollers are used to remove excess resin and air and compact the plies. After lay-up, cure can be done at room or elevated temperature. Cure is frequently performed without a vacuum bag, but vacuum pressure helps to improve laminate quality. Since cure is usually performed at room or low temperatures, very inexpensive tooling (such as wood or fiberglass) can be used to minimize the cost. Although the process is conducive to large and inexpensive production, it does not generally optimize fiber properties and often fails to minimize weight, and the level of precision is very operator-dependent.

Prepreg materials often offer the best mechanical properties. Prepreg provides a consistent product with a uniform distribution of reinforcement and resin, with high fiber volume fractions possible. Since laminated structures typically require much hand labor and autoclave processing, the manufacturing costs are relatively high. Prepreg lay-up is a process in which individual layers of prepreg are laid up on a tool, in the required directions and to the correct thickness. A vacuum bag is then placed over the lay-up, and the air is evacuated to draw out air between the plies. The bagged part is placed in an oven or an autoclave and cured under specified time, temperature, and pressure conditions. If oven curing is used, atmospheric pressure at 14.7 psi or less (100 kPa or less) is the maximum that can be obtained. An autoclave offers the advantage that much higher pressures, for example 100 psi (700 kPa), can be used with the result that better compaction, higher fiber volume percentages, fewer voids, and less porosity are achieved. Presses can also be used for this process, but they have several disadvantages: (1) the size of the part is limited by the press platen size, (2) the platens may produce high- and low-pressure spots if the platens are not flat and parallel, and (3) complex shapes are difficult to produce. The combination of automated ply cutting, manual ply collation or lay-up, and autoclave curing is the most widely used process for high-performance composites in the aerospace industry. Although manual ply collation is expensive, this process is capable of making high-quality, complex parts.

To reduce the costs of expensive autoclave hardened tooling, low-temperature/vacuum bag prepregs were developed. These materials are capable of producing autoclave quality parts by initially curing the part at low temperatures on less expensive tooling under vacuum bag pressure. The part is then removed from the tool and given a freestanding postcure in an oven to increase its temperature resistance. However, even with these materials, the potential for voids and porosity exists, especially for larger parts, from which it may be more difficult to remove the entrapped air during the evacuation portion of the cure cycle.

The term *liquid molding* covers a fairly extensive set of processes. In resin transfer molding, a dry preform or lay-up is placed in a matched metal die and a low-viscosity resin is injected

under pressure to fill the die. Since this is a matched-die process, it is capable of holding very tight dimensional tolerances. The die can contain internal heaters or be placed in a heated platen press for cure. Other variations of this process include vacuum-assisted resin transfer molding (VARTM), in which a single-sided tool is used along with a vacuum bag. Instead of injecting the resin under pressure, a vacuum pulls the resin through a flow medium that helps to impregnate the preform. The biggest disadvantage of RTM is the typical expense of large, complicated matched-die tools. Since VARTM uses single-sided tools and the pressures are lower, it is inherently less expensive than RTM.

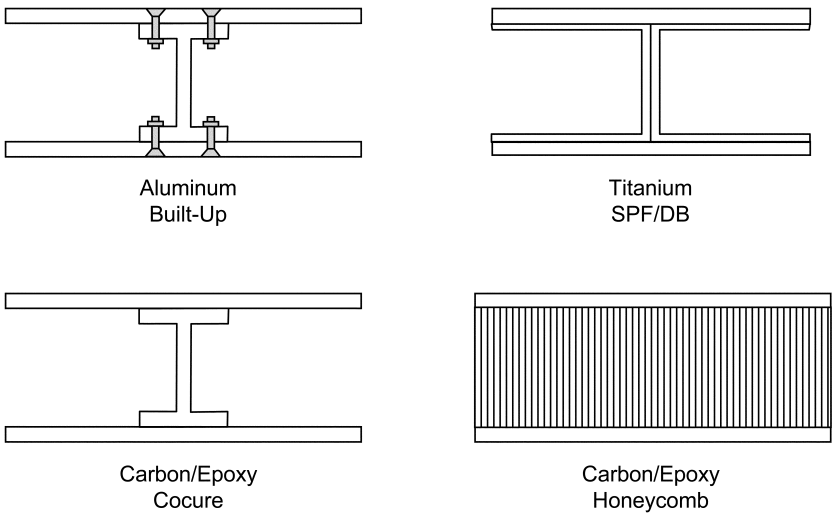
Filament winding is a process that has been used for many years to build highly efficient structures that are, or are nearly, bodies of revolution. Wet winding, in which dry fiber rovings are pulled through a resin bath prior to winding on the mandrel, is the most prevalent process, but prepregged roving or tows can also be filament wound. Wet filament winding is the primary manufacturing method for cylindrical or spherical pressure vessels, because continuous fibers can be easily placed in the hoop direction. Low-cost constant-cross-section components can be made using a filament winder with two degrees of freedom: the rotation of the mandrel and the translation of the payout eye. Additional payout eyes can increase the speed of the process. Increasing the number of degrees of freedom increases the complexity both of the process and of the parts that can be created. Hoop (circumferential) winding involves laying fibers at nearly 90° with respect to the longitudinal axis of the mandrel. This process results in a cylinder with high hoop strength. However, helical (off-axis) or polar (axial, near-longitudinal) windings provide reinforcement along the length of the structure. As these fibers are wound, they have a tendency to slip. One exception is a geodesic path, which is a straight line on the flattened equivalent surface. As the part is formed, its thickness increases, thus changing the geometry of the process. Curing is usually conducted in an oven with or without a vacuum bag.

Pultrusion is a specialized composite fabrication process that is capable of making long, constant-thickness parts. Dry E-glass rovings are normally pulled through a wet resin bath and then preformed to a desired shape before entering a heated die. Mats and veils are frequently incorporated into the part. Cure occurs inside the die, and the cured part is pulled to the desired length and cut off. Quick-curing polyesters and vinyl esters are the predominant resin systems. Design limitations include the need for a large proportion of reinforcement in the longitudinal (axial) direction.

18.6 Trade Studies

Trade studies are conducted early in the design process to determine the best material, process, and structural configuration for a given part. The first task of the integrated product definition (IPD) team is to determine the requirements or important attributes of the part, such as stiffness, weight, fatigue resistance, nonrecurring and recurring costs, and damage tolerance/repairability. Once the attributes are determined, they are assigned relative weighting factors based on their importance. The team then identifies candidate structural configurations along with their respective materials and processes. Once the candidate configurations have been identified, the team assigns relative scores to each of the important part attributes. The scores are then tabulated to identify the winning concept.

The results of a notional trade study for an aircraft control surface are shown in Fig. 18.2. In this study, four candidate designs were considered. The first design, an aluminum built-up structure, consists of machined aluminum skins and substructure that is assembled with mechanical fasteners. This structure scored low in stiffness, weight, and fatigue resistance but high in cost and damage tolerance/repairability. The second design is a titanium structure fabricated using superplastic forming/diffusion bonding. Its stiffness is better than that of the aluminum structure, but it is heavier and the nonrecurring tooling cost is high. However, it has outstanding damage tolerance. The third design, which is the first composite structure, cocured carbon/epoxy, scored high marks where one would expect: in stiffness, weight, and fatigue resistance. However, the nonrecurring tooling costs are high, and the damage tolerance and repairability of the structure are lower than for the metallic structures. Even though the fourth design, the carbon/epoxy honeycomb, also scored low in damage tolerance and repairability, this structure was the one selected, primarily because of its outstanding stiffness, weight, and fatigue resistance. Although a detailed structural analysis is not required at this point, rough order sizing is needed to obtain comparative weights, properties, and costs.



Candidate Designs	Attributes						Total Score
	Stiffness .2	Weight .2	Fatigue Resistance .2	Nonrecurring Cost .05	Recurring Cost .2	Damage Tolerance/ Repairability .15	
Aluminum Built-Up	20	40	30	80	85	80	51.00
Titanium SPF/DB	35	20	50	35	60	90	48.25
Carbon/Epoxy Cocured	50	50	60	40	70	70	58.50
Carbon/Epoxy Honeycomb	60	70	70	65	75	30	62.75

Total score is determined by multiplying each weighting factor by the raw attribute score and then adding the totals. For example, the score for the aluminum built-up concept is: 0.2(20) + 0.2(40) + 0.2(30) + 0.05(80) + 0.2(85) + 0.15(80) = 51.00.

Fig. 18.2 Trade study example. SPF/DB, super plastic forming/diffusion bonding

Although a quantified trade study like the one in Fig. 18.2 is not entirely objective, it is hoped that the widely differing knowledge, experience, and beliefs of the members of the IPD team will result in an overall objective choice.

18.7 Building Block Approach

The building block approach to testing and certification is used extensively in the aerospace industry. It starts with large numbers of simple coupon tests and, at each succeeding level, builds on the level below with fewer but more complicated tests. The pyramid in Fig. 18.3 illustrates the building block concept. At the lowest levels, the basic materials properties are determined using large quantities of small test specimens from multiple batches (usually five or six) of material. At each succeeding level, progressively more complicated specimens and structures are built and tested, and the failure modes and loads are predicted by analysis based on the lower-level data. When more data are obtained,

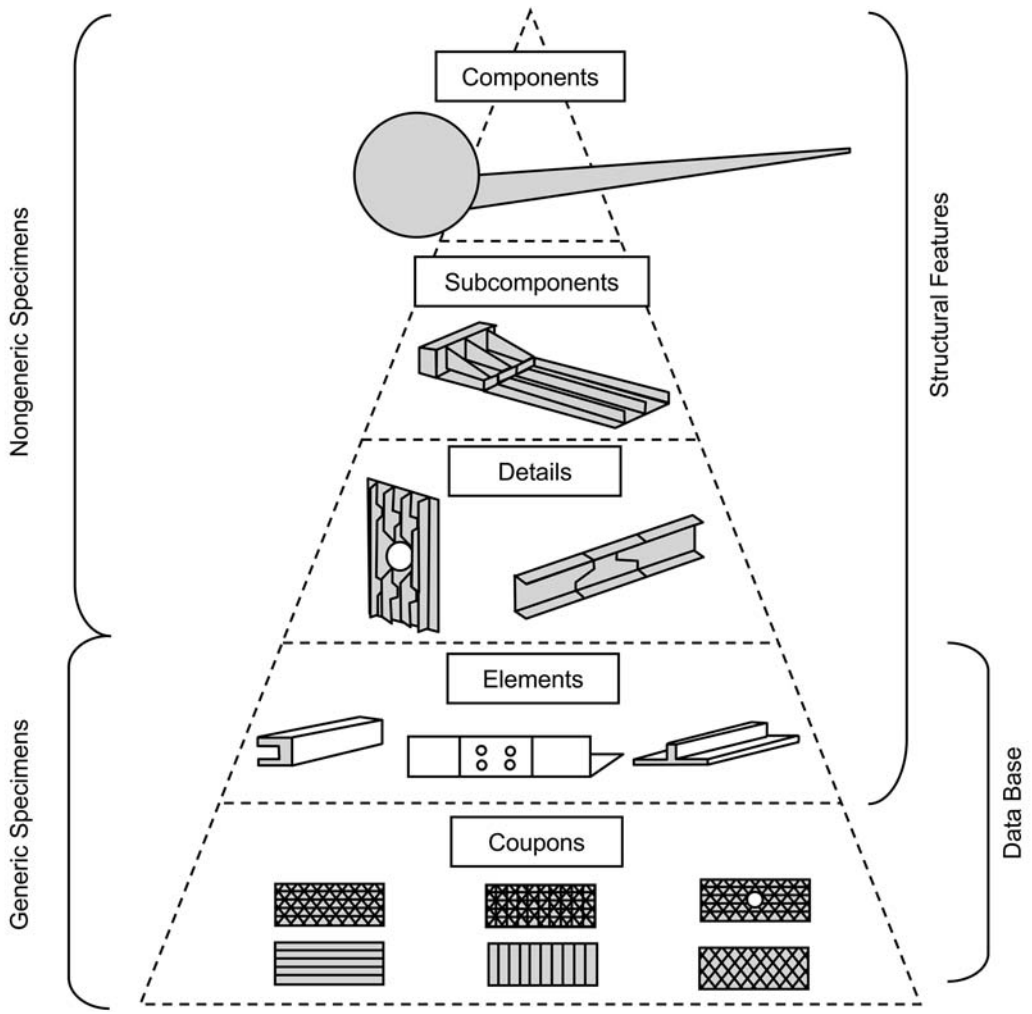


Fig. 18.3 Aircraft industry building block approach. Source: Ref 2

the structural analysis models are refined as needed to agree with the test results. As the test structures become more complex, the number of replicate specimens of the same type and environment and the number of environments are reduced. The culmination of the building block pyramid is often a single confirming test of a full-scale component or a full-scale structural assembly.

Large full-scale tests are not normally performed in the worst-case design environment; it would be extremely difficult, for example, to expose to the environment a large structure like an entire airframe and then conduct the test at an elevated temperature. Data from the lower levels of the building block test program are used to establish environmental compensation values that are applied to the loads of higher-level room-temperature tests. Similarly, lower-level fatigue tests are used to determine truncation approaches for fatigue spectra and compensation for fatigue scatter at the full-scale level.

The building block approach consists of the following steps:

- Order materials to a specification that includes controls on the chemical and physical properties of the fibers, resins, and prepregs. Normally, five or six separate batches are required using fibers from different lots and resins from different batches of raw ingredients.

- Perform coupon testing at the lamina and laminate levels on each batch of prepreg. Calculate preliminary design allowables using statistical analysis. Perform lamina testing to establish allowables that can be used along with classical lamination theory to predict laminate properties. Perform laminate testing to confirm those predictions. The laminate orientations tested should be the major ones to be used in the final structure.
- Based on analysis of the structure, select critical areas and design features for subsequent verification tests. For each critical design feature, determine the load–environment combination that is expected to produce a given failure mode with the lowest margin. Special attention should be given to matrix-sensitive failure modes, such as compression, shear, bondlines, and potential "hot spots" caused by out-of-plane loads.
- Design and test a series of test specimens, each of which simulates a single selected failure mode and a load–environment condition. Compare the test results to previous analytical predictions and adjust analysis models or design properties as necessary.
- Conduct increasingly complicated tests that evaluate more complex loading situations with the possibility of failure from several different potential failure modes. Compare the test results to previous analytical predictions and adjust analysis models as necessary.
- Conduct, as required, full-scale component or assembly static and fatigue testing for final validation of internal loads and structural integrity. Compare the results to the analysis. In the aircraft industry, this means conducting a full-scale static test and a full-scale fatigue test of two separate airframes.

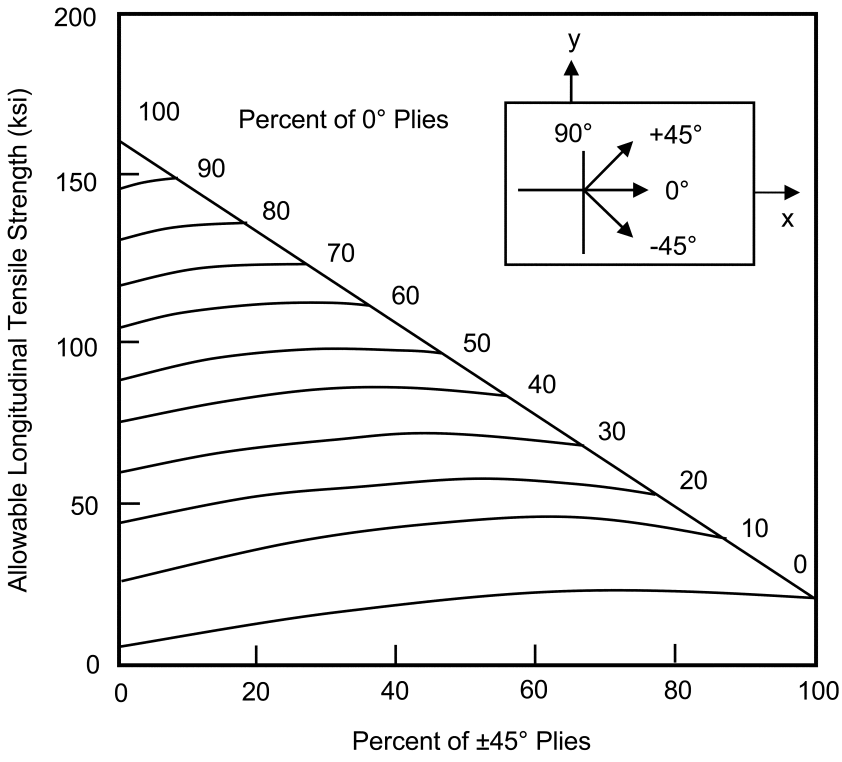
The building block approach is more than just a test program. During all levels of increasing complexity, manufacturing has the opportunity to develop and refine tooling and processing approaches that will later be used during production. Since this is an expensive and lengthy process, small-scale testing should be conducted on candidate materials prior to full-scale qualification. Although this is a very expensive approach involving thousands of tests, it has been used successfully to design and build sophisticated systems such as aircraft systems, where safety is paramount. Such an extensive test program should not be required for many applications in which unexpected product failure would not result in injury or death.

18.8 Design Allowables

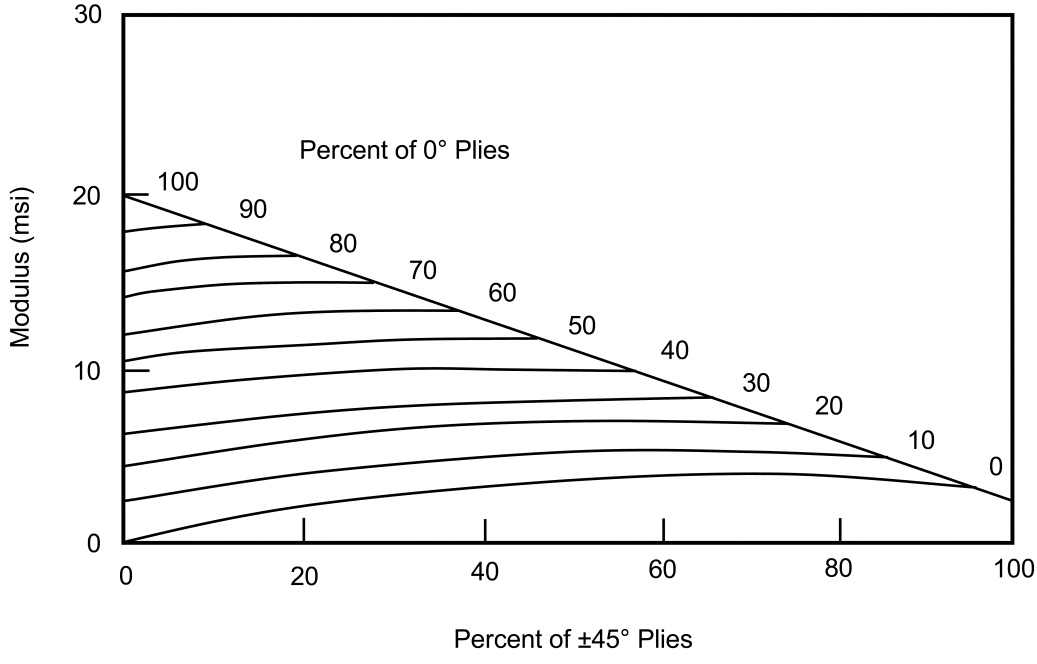
Design allowables are statistically determined material property values derived from test data generated during the building block approach. They are the limits of stress, strain, or stiffness that are allowed for a specific material, configuration, application, and environmental condition. Design allowables must account for all materials property variability that can reasonably be expected in the manufacture and assembly of a composite component. They must also account for manufacturing process variations and acceptable anomalies as well as for limitations of structural analysis. The selection of appropriate design allowables for structures composed of composite materials is essential for the safe and efficient use of these materials.

Values for design allowables are chosen to ensure that failure will not occur. Statistics are applied to select an acceptable likelihood of failure. Typical statistical values are termed *A-basis* and *B-basis*. Methods for calculating A- and B-basis allowables are given in Section 13.15. For A-basis, 99 percent of the test results should exceed the allowable value with 95 percent assurance. For B-basis, 90 percent of the test results should exceed the allowable value 95 percent of the time. A-basis allowables are more conservative and are used on single-load-path structures, in which failure of the part will result in failure of the structure. B-basis values are typically higher than A-basis values and are used where multiple load paths exist and failure of one part will not ordinarily result in failure of the entire structure. Allowables must also account for the environmental spectrum to which the structure will be exposed during its service life. For this purpose, mechanical testing is performed with coupons conditioned at room temperature, at the minimum and maximum temperatures of the expected exposure range, and at critical temperatures after environmental exposure.

Given specific angle orientations as constraints and the assumption of a uniaxial load, laminate data can be represented by carpet plots, which are maps of a laminate property versus the percentage of one of the lamina orientations. Typical carpet plots for the strength and modulus of carbon/epoxy tape are shown in Fig. 18.4. The carpet



Tensile Strength



Modulus

Fig. 18.4 Typical carpet plots for carbon/epoxy tape

plot is for a given design temperature and for a certain design strength criterion, such as B-basis for the ultimate properties.

The strength that a structure must possess is based on the ultimate combination of loads that will be applied under the most severe environmental conditions for the structure. However, to ensure that the structure will not fail at this ultimate load condition, a safety factor is applied. A typical safety factor for aircraft structures is 1.5. Therefore, if the design limit load (DLL) is the maximum load anticipated for a structure, then the design ultimate load (DUL) at which no failure or unacceptable deformations would occur would be:

$$\text{DUL} = 1.5 \times \text{DLL} \qquad \text{(Eq 18.2)}$$

This means that a structure designed to withstand a load of 10,000 lb (4500 kg) will actually be designed to withstand 15,000 lb (6800 kg) ($10{,}000 \times 1.5 = 15{,}000$).

For non-aerospace engineering applications where a weight penalty is not an issue, safety factors as high as 6 to 10 may be applied. The safety factor is often mandated by industry regulations. A safety factor is intended to account for engineering miscalculations, material and process flaws, or assembly defects.

A margin of safety is another method for designing extra strength into a structure. For composite structures, once the safety factor has been applied to the design load and a laminate has been designed to withstand the loading condition, any additional load-carrying capability of the laminate is considered a margin of safety. The ability of a laminate to meet and exceed the required design strength or other criteria is identified by its having a positive margin of safety.

18.9 Design Guidelines

Since the choice of materials, processes, and structural configurations is so extensive, offering detailed design guidelines for composites is an overwhelming and problematic task. However, during the last 40 years of use of high-performance composites in the aerospace industry, many lists of design guidelines and lessons learned have been compiled. The ones listed in MIL-HNBK-17 (Ref 3) are reproduced in Table 18.5. This list, though certainly not comprehensive, was compiled by a team of composite experts representing both government agencies and industry.

Perhaps the most important guideline for the detailed design of composites is to use balanced and symmetric laminates to prevent warpage and distortion on cool-down from elevated-temperature cures (Table 18.6). Laminates cured at room temperature using typical wet lay-up or VARTM do not exhibit the same degree of distortion since they are subjected to much smaller thermal stresses. The residual stresses that result from using unbalanced and/or asymmetric laminates make subsequent assembly operations very difficult, as the laminate will have to be forced back into shape during assembly. Since composites have low out-of-plane properties, the result will be high stresses that can cause matrix cracking and/or delaminations.

As discussed in Chapter 17, "Structural Joints—Bolted and Bonded," the joints are the critical areas. They should be designed first and then the space between them should be filled in with appropriate laminates. Since most composite structures have some type of mechanically attached joints, the use of quasi-isotropic or near-quasi-isotropic laminates is required for the structure to carry the fastener bearing loads. While a quasi-isotropic has equal properties in the 0°, ±45°, and 90° directions, a near-quasi-isotropic laminate may have a few more plies in the main load-carrying direction (e.g., the 0° direction) to provide additional strength and stiffness while maintaining adequate bearing strength.

Along with the joints and basic skin laminate thicknesses and orientations, skin-stiffening approaches need to be considered. Several stiffening methods commonly used with composite structures are shown in Fig. 18.5. Blade stiffeners are simple to fabricate and easy to attach to frames and ribs, but since they do not have a top flange, they are structurally inefficient in bending and provide only marginal torsional stability. J-sections are more difficult to fabricate than blades and have improved bending efficiency but are still somewhat unstable in torsion. I-beams are more difficult to fabricate than either blades or J-sections but are very structurally efficient in both bending and torsion. However, tying them into frames and ribs is somewhat more complicated. Hat sections are also structurally efficient, providing bending and torsional stiffness, but are very difficult to tie in to frames and ribs. In addition, if drain paths are not provided, they can trap water. Finally, honeycomb sandwich

Table 18.5 Guidelines for composite design

Guidelines	Remarks
1. Concurrent Engineering or Integrated Product Design is the preferred design approach. A new product or system is developed jointly and concurrently by a team composed of designers, stress analysts, materials and processes, manufacturing, quality control, and support engineers, (reliability, maintainability, survivability), as well as cost estimators.	To improve the quality and performance and reduce the development and production costs of complex systems.
2. In general, design large cocured assemblies. Large assemblies must include consideration for handling and repair.	Lower cost due to reduced part count and assembly time. If the assembly requires overly complex tooling, the potential cost savings can be negated.
3. Structural designs and the associated tooling should be able to accommodate design changes associated with the inevitable increases in design loads.	To avoid scab-on reinforcements and similar last minute disruptions.
4. Not all parts are suited to composite construction. Material selection should be based on a thorough analysis that includes consideration of performance, cost, schedule, and risk.	The type of material greatly influences performance characteristics as well as producibility factors.
5. Uniwoven and bi-directional woven fabric should be used only when justified by trade studies (reduced fabrication costs). If justified, woven fabric may be used for 45° or 0°/90° plies.	Fabric has reduced strength and stiffness properties and the prepreg material costs more than tape. Fabric may be necessary for complex shapes and some applications may require the use of fabric for its drapeability.
6. Whenever possible, mating surfaces should be tool surfaces to help maintain dimensional control. If this is not possible, either liquid shims or, if the gap is large, a combination of precured and liquid shims should be used.	To avoid excessive out-of-plane loads that can be imposed if adjoining surfaces are forced into place. Large gaps may require testing.
7. Part thickness tolerance varies directly with part thickness; thick parts require larger tolerance.	Thickness tolerance is a function of the number of plies and the associated per ply thickness variation.
8. Carbon fibers must be isolated from aluminum or steel by using an adhesive layer and/or a thin glass fiber ply at faying surfaces.	Galvanic interaction between carbon and aluminum or steel will cause corrosion of the metal.
9. The inspectability of structures, both during production and in-service, must be considered in the design. Large defects or damage sizes must be assumed to exist when designing composite structures if reliable inspection procedures are not available.	There is a much better chance that problems will be found if a structure is easily inspected.
10. In Finite Element Analysis (FEA) a fine mesh must be used in regions of high stress gradients, such as around cut-outs and at ply and stiffener drop-offs.	Improper definition or management of the stresses around discontinuities can cause premature failures.
11. Eliminate or reduce stress risers whenever possible.	Composite (fiber-dominated) laminates are generally linear to failure. The material will not yield locally and redistribute stresses. Thus, stress risers reduce the static strength of the laminate.
12. Avoid or minimize conditions which cause peel stresses such as excessive abrupt laminate terminations or cocured structures with significantly different flexural stiffnesses (i.e., $EI_1 >> EI_2$).	Peel stresses are out-of-plane to the laminate and hence, in its weakest direction.
13. Buckling or wrinkling is permissible in thin composite laminates provided all other potential failure modes are properly accounted for. In general, avoid instability in thick laminates.	Significant weight savings are possible with postbuckled design.
14. Locating 90° and ±45° plies toward the exterior surfaces improves the buckling allowables in many cases. Locate 45° plies toward the exterior surface of the laminate where local buckling is critical.	Increases the load carrying capability of the structure.
15. When adding plies, maintain balance and symmetry. Add between continuous plies in the same direction. Exterior surface plies should be continuous.	Minimizes warping and interlaminar shear. Develops strength of plies. Continuous surface plies minimize damage to edge of ply and help to prevent delamination.
16. Never terminate plies in fastener patterns.	Reduces profiling requirements on substructure. Prevents delamination caused by hold drilling. Improves bearing strength.
17. Stacking order of plies should be balanced and symmetrical about the laminate midplane. Any unavoidable unsymmetric or unbalanced plies should be placed near the laminate midplane.	Prevents warpage after cure. Reduces residual stresses. Eliminates “coupling” stresses.
18. Use fiber dominated laminate wherever possible. The [0°/±45°/90°] orientation is recommended for major load carrying structures. A minimum of 10% of the fibers should be oriented in each direction.	Fibers carry the load; the resin is relatively weak. This will minimize matrix and stiffness degradation.
19. When there are multiple load conditions, do not optimize the laminate for only the most severe load case.	Optimizing for a single load case can produce excessive resin or matrix stresses for the other load cases.
20. If the structure is mechanically fastened, an excess of 40% of the fibers oriented in any one direction is inadvisable.	Bearing strength of laminate is adversely affected.

(continued)

Table 18.5 (continued)

Guidelines	Remarks
21. Whenever possible maintain a dispersed stacking sequence and avoid grouping similar plies. If plies must be grouped, avoid grouping more than 4 plies of the same orientation together.	Increases strength and minimizes the tendency to delaminate. Creates a more homogeneous laminate. Minimizes interlaminar stresses. Minimizes matrix microcracking during and after service.
22. If possible, avoid grouping 90° plies. Separate 90° plies by a 0° or ±45° plies where 0° is direction of critical load.	Minimizes interlaminar shear and normal stresses. Minimizes multiple transverse fracture. Minimizes grouping of matrix critical plies.
23. Two conflicting requirements are involved in the pairing or separating of ±θ° plies (such as ±45°) in a laminate. Laminate architecture should minimize interlaminar shear between plies and reduce bending/twisting coupling.	Separating ±θ° plies reduces interlaminar shear stresses between plies. Grouping ±θ° plies together in the laminate reduces bending/twisting coupling.
24. Locate at least one pair of ±45° plies at each laminate surface. A single ply of fabric will suffice.	Minimizes splintering when drilling. Protects basic load carrying plies.
25. Avoid abrupt ply terminations. Try not to exceed dropping more than 2 plies per increment. The plies that are dropped should not be adjacent to each other in the laminate.	Ply drops create stress concentrations and load path eccentricities. Thickness transitions can cause wrinkling of fibers and possible delaminations under load. Dropping non-adjacent plies minimizes the joggle of other plies.
26. Ply drop-offs should not exceed 0.010 in. thick per drop with a minimum spacing of 0.20 in. in the major load direction. If possible, ply drop-offs should be symmetric about the laminate midplane with the shortest length ply nearest the exterior faces of the laminate. Shop tolerance for drop-offs should be 0.04 in.	Minimizes load introduction into the ply drop-off creating interlaminar shear stresses. Promotes a smooth contour. Minimizes stress concentration.
27. Skin ply drop-offs should not occur across the width of spars, rib, or frame flange.	Provides a better load path and fit-up between parts.
28. In areas of load introduction there should be equal numbers of +45° and –45° plies on each side of the mid-plane.	Balanced and symmetric pairs of ±45° plies are strongest for in-plane shear loads which are common at load introduction points.
29. A continuous ply should not be butt-spliced transverse to the load direction.	Introduces a weak spot in the load path.
30. A continuous ply may be butt-spliced parallel to the load direction if coincident splices are separated by at least four plies of any orientation.	Eliminates the possibility of a weak spot where plies are butted together.
31. The butt joint of plies of the same orientation separated by less than four plies of any direction must be staggered by at least 0.6 in.	Minimizes the weak spot where plies are butted together.
32. Overlaps of plies are not permitted. Gaps shall not exceed 0.08 in.	Plies will bridge a gap, but must joggle over an overlap.

Source: Ref 3

Table 18.6 The importance of using balanced and symmetric laminates

Type	Example orientations	Comments
Symmetrical, balanced	(+45, –45, 0, 0, –45, +45)	Flat, constant midplane stress
Nonsymmetrical, balanced	(90, +45, 0, 90,–45, 0)	Induces curvature
Symmetrical, Nonbalanced	(–45, 0, 0, –45)	Induces twist
Nonsymmetrical, nonbalanced	(90, –45, 0, 90, –45, 0)	Induces twist and curvature

Source: Ref 1

acts much like an I-beam, with the upper and lower skins carrying the bending loads and the core reacting to the shear loads. Although thin-skinned honeycomb assemblies are very structurally efficient, they have poor damage tolerance to impacts and can trap moisture in the cells, degrading both the skin bondlines and the core properties. Each of these methods except honeycomb assemblies requires one or more filler nuggets formed at the radii. For small radii, a twisted rope of a toughened adhesive film can be used. It is important that the adhesive be toughened to prevent microcracking of the nugget. For larger radii, composite plies should be laid up and placed in the void areas.

Any of several fabrication and assembly methods can be selected; four of them are shown in Fig. 18.6. In mechanical fastening, all of the composite parts are cured on their individual tools and then assembled with mechanical fasteners. This method is normally used for such highly loaded structures as wings, in which the loads are too high for bonded structure. The disadvantages of this method are the weight and cost of the mechanical fasteners. In addition, any mismatches in the parts or assembly will have to be properly shimmed. In secondary bonding, the

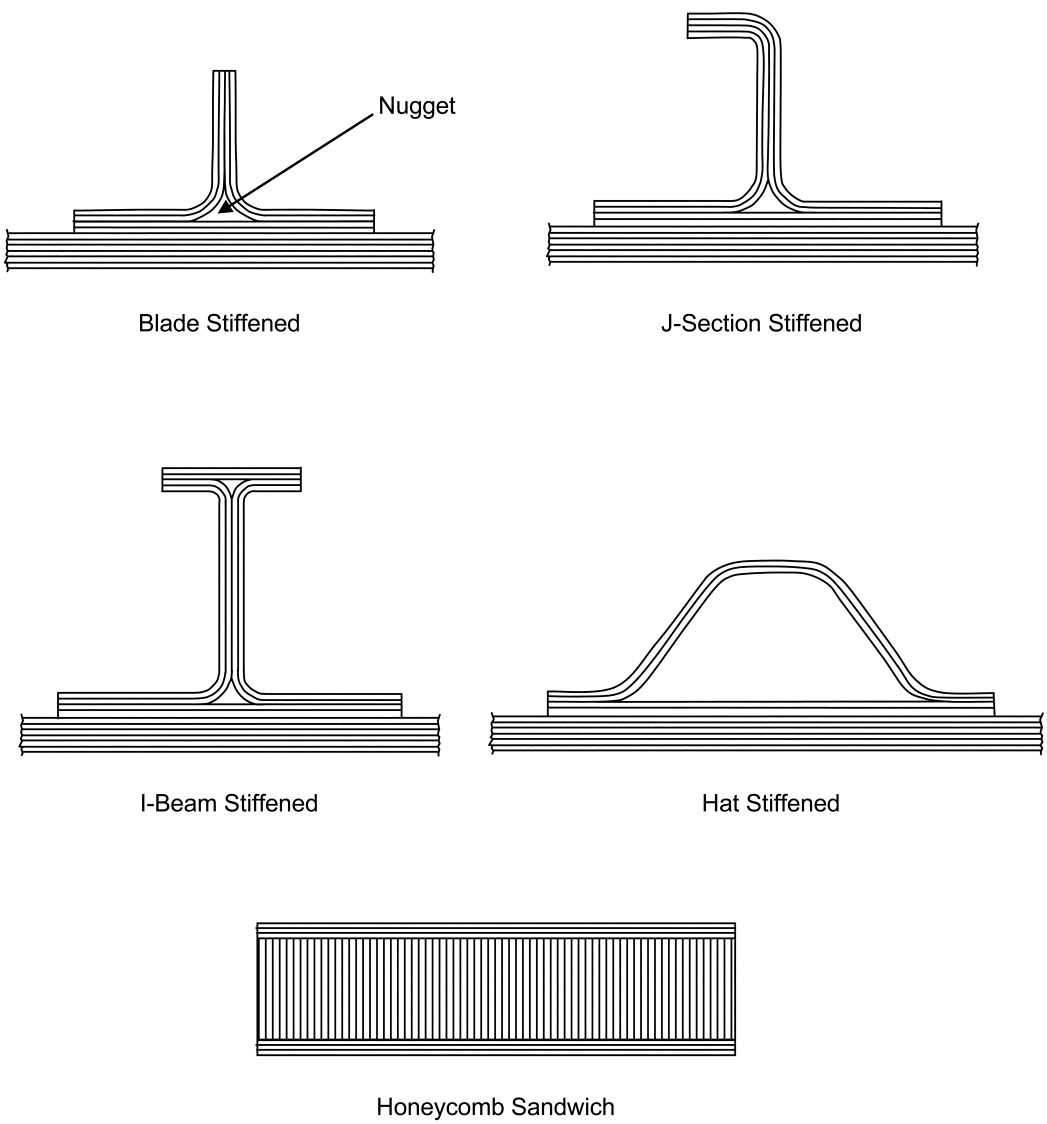


Fig. 18.5 Common composite stiffening approaches

detailed parts are again precured on their individual tools, but instead of using mechanical fasteners, the parts are assembled by adhesive bonding. To reduce the number of cure cycles required, cobonding and cocuring can be considered. In cobonding, the stiffeners are precured on their individual tools and then adhesively bonded to the skin at the same time that the skin is cured. In cocuring, all of the details are layed up on individual tooling details and then assembled; everything is cured and bonded together in one cure cycle. Cobonding is often used for large parts for which the mass of the tooling required for cocuring would be excessive. Both cobonding and cocuring can reduce the number of bond cycles required, but in each the tooling must be precise and a highly skilled workforce is required.

The design of substructure-to-skin joints needs to be performed carefully to prevent peel forces from causing separations or delaminations at the bondlines. As shown in Fig. 18.7, stiffener delamination can occur if the stiffener is not supported to prevent it. Even moderately low side loads on the stiffener web can cause failure at the stiffener-to-skin joint. Stiffener terminations are

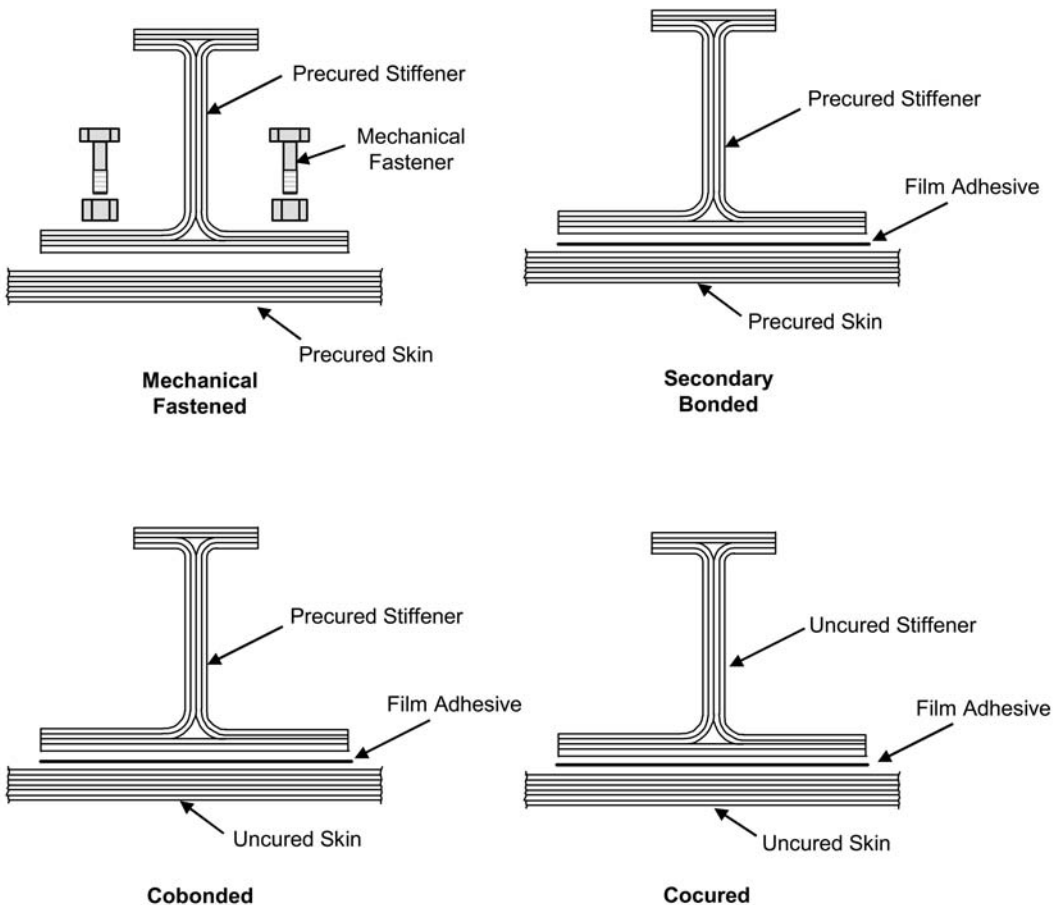


Fig. 18.6 Fabrication and assembly options

another location where peel stresses can cause delaminations. In the hat stiffener design shown in Fig. 18.8, antipeel fasteners are used at the stiffener run-outs, the loads are gradually transitioned by tapering or scarfing the ends of the stiffener, and the skin itself is locally stiffened to minimize peel stresses. The radii used in stiffeners or other members need to be considered with regard to the ability to manufacture different radii, as shown for the male and female radii in Fig. 18.9.

As pointed out earlier, sandwich structures, in particular honeycomb assemblies, are very structurally efficient. However, they should be used with great caution. Thin-skinned honeycomb assemblies have poor resistance to impact damage and are sometimes troubled by moisture ingression. These concerns are emphasized in the MIL-HNBK-17 guidelines listed in Table 18.7.

In thin-skinned assemblies, even minor impacts can penetrate the skin and cause internal core damage that, if not immediately repaired, provides a path for water ingression. Since thin-skinned assemblies do not have sufficient skin thickness to carry fastener-bearing loads, repair of honeycomb assemblies usually requires some type of bonded repair. Thin-skinned aircraft honeycomb assemblies will often have the words "No Step" painted on the exterior skin as a warning to maintenance personnel that their weight could crush the underlying core. However, the author has seen a number of aircraft returned from the field that had visible footprints right on top of the "No Step" warning.

Water ingression in honeycomb assemblies is always a danger and can occur through multiple paths, including cracked-edge potting, cracked paint, failed/cracked sealant, through fasteners, porosity in the skins of cloth or thin unidirectional skins, porous adhesive in lap joints, wicking through aramid fibers, and wicking along

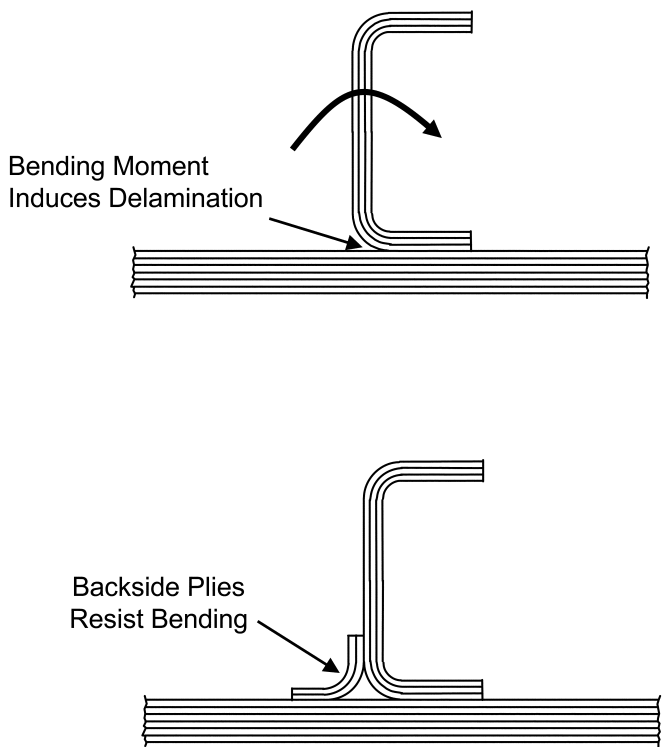


Fig. 18.7 Preventing stiffener delamination

foaming adhesive and along metallic doublers. Once inside the sandwich, the water causes failures through various mechanisms. Water absorbed in the polymer matrix or adhesive lowers its glass transition temperature and significantly degrades its mechanical properties. Water also degrades the honeycomb cell walls, increasing the ease of water migration. Eventually, when a honeycomb cell contains sufficient water, the expansion during freezing can be strong enough to cause the skin to delaminate from the core. If aluminum honeycomb is used, stagnant water within the cells will cause corrosion and the eventual destruction of the core.

During repairs, water must be removed for epoxy repairs to cure and bond properly, even at room temperature. Drying of water adds time to repairs. If water is not detected and sufficiently dried, the subsequent elevated-temperature cure generates steam that often causes delaminations, both in sandwich structures and in solid laminates. If enough water enters the assembly, it can also affect the weight and balance properties of the assembly. During the overhaul of 250 Boeing 757 spoilers conducted by United Airlines, the average weight of water per spoiler was determined to be 3.5 lb (1.6 kg).

18.10 Damage Tolerance Considerations

Damage tolerance is the ability of a structure to sustain a certain level of damage, or to have a preexisting defect of a certain size, and still be able to perform successfully for the duration of its life. The structure must have adequate residual strength and stiffness to continue in service safely until the damage can be detected during a scheduled maintenance inspection or, if the damage is never detected, for the remainder of the structural life. Therefore, safety is the primary goal of damage tolerance. Both static load and durability-related damage tolerance must be determined experimentally because there are few, if any, accurate analytical methods. The normal design approach to ensuring that these requirements can be met is to keep normal operating stresses and strains in the structure low enough that if damage does occur, the structure

This design actually illustrates three methods of reducing peel stresses at the termination of the cocured hat stiffener:
(1) Antipeel fasteners
(2) Scarfing at the end of the hat
(3) Thickening at the end of the hat

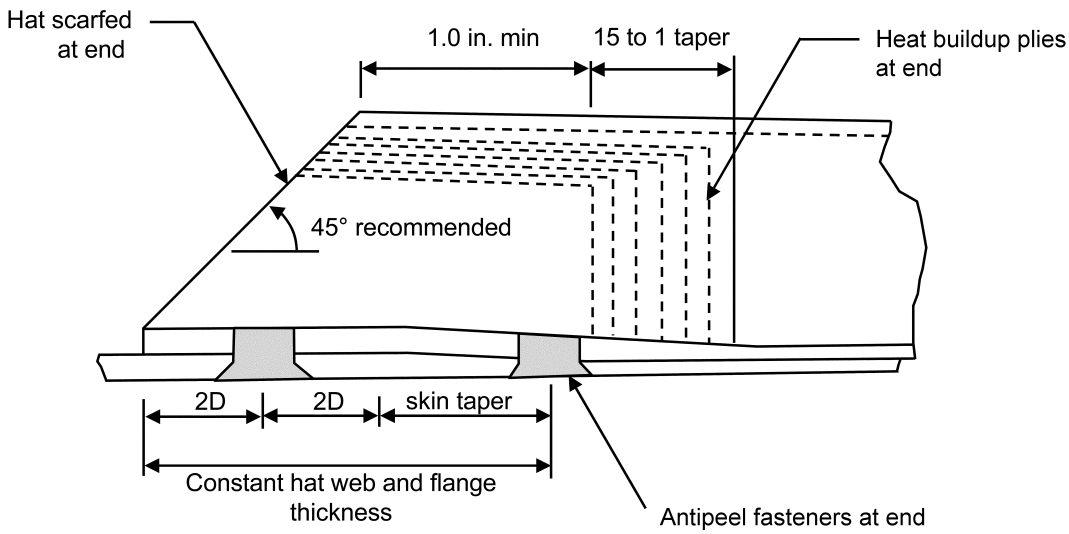


Fig. 18.8 Bonded-bolted joint to prevent peel failures

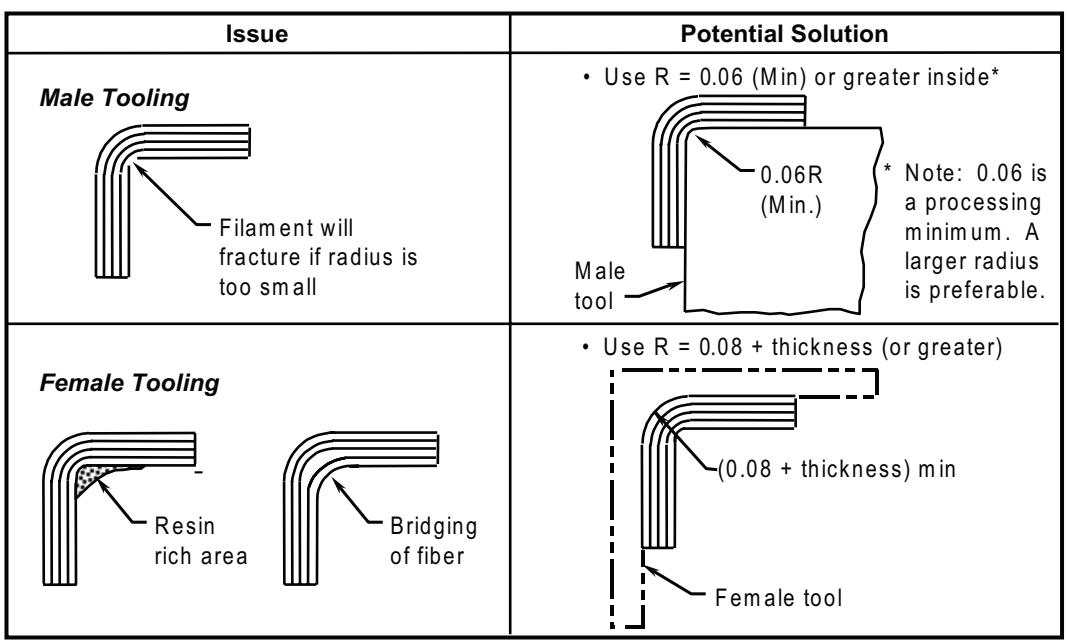
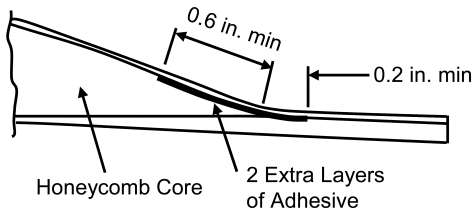


Fig. 18.9 Fabrication limits on radii

Table 18.7 Guidelines for design of sandwich structures

Guidelines	Remarks
1. Facesheets should be designed to minimize people induced damage during handling or maintenance of component.	Thin skin honeycomb structure is very susceptible to damage by harsh handling.
2. When possible avoid laminate buildup on the core side of the laminate.	Minimizes machining of the core.
3. Core edge chamfers should not exceed 20° (from the horizontal plane). Larger angles may require core stabilization. Flex core is more sensitive than rigid core.	Prevents core collapse during cure cycle.
4. Use only non-metallic or corrosion resistant metal honeycomb core in composite sandwich assemblies.	Prevents core corrosion.
5. Choice of honeycomb core density should satisfy strength requirements for resisting the curing temperature and pressure during bonding or cocuring involving the core. 3.1 pcf is a minimum for non-walking surfaces.	Prevents crushing of the core.
6. For sandwich structure used as a walking surface, a core density of 6.1 pcf is recommended.	3.1 pcf core density will result in heel damage to the walking surface.
7. Do not use honeycomb core cell size greater than 3/16 inch for cocuring sandwich assemblies (1/8 in. cell size preferred).	Prevents dimpling of face sheets.
8. When core is required to be filled around bolt holes, etc., this should be done using an approved filler to a minimum of 2D from the bolt center.	Prevents core crushing and possible laminate damage when bolt is installed.
9. Two extra layers of adhesive should be applied to the inner moldline at the core run out (edge chamfer). This should be applied a minimum of 0.6 in. from the intersection of the inner skin and edge band up the ramp and a minimum of 0.2 in. from that point into the edge band.	Curing pressures tend to cause the inner skin to "bridge" in this area creating a void in the adhesive (skin to core bond). 
10. The use of honeycomb sandwich construction must be carefully evaluated in terms of its intended use, environment, inspectability, repairability, and customer acceptance.	Thin skin honeycomb is susceptible to impact damage, water intrusion due to freeze/thaw cycles, and is difficult to repair.

Source: Ref 3

will still have sufficient residual strength to resist failure.

There are basically two types of damage: (1) defects that occur during the manufacturing process and (2) damage that the part suffers when placed in service. While large defects that occur during the manufacturing process should be detected during normal nondestructive testing, some "escapes" beyond acceptable limits may not be detected. Consequently, their occurrence must be assumed during the design process and subsequent static and fatigue testing performed to verify structural integrity.

In-service damage can originate from a variety of sources, including runway debris that hits control surfaces, hailstones from storms, tools dropped by maintenance mechanics, and collisions with ground handling equipment (e.g., forklifts). The major damage tolerance concern for composites is delamination caused by low-velocity impact damage (LVID). When an impact contains sufficient energy, it can cause internal delaminations and extensive matrix cracking that, depending on the energy level and laminate construction, may or may not be visible on the surface of the composite part. Since damage areas can be sizable without being clearly visible, the part must be designed to perform its function when it contains nonvisible damage. Low-velocity impact damage tests are usually performed with 0.5 in. (12 mm) diameter impactors, which tend to limit fiber breakage and maximize delamination damage. A full range of laminate thickness and stacking sequences should be tested at various impact energies to establish the true relationships among panel attributes, impact energy, dent depth, and visibility.

Most criteria define undesirable damage as that which is clearly visible to a trained observer at a set distance, for example 5 ft (1.5 m). A criterion

incorporating this definition allows composite surfaces to be visually inspected during routine walk-around inspections. Although visibility is somewhat subjective, based on the viewing conditions and surface finish, often a dent-depth criterion can be established and matched to a visibility requirement. An upper limit on impact energy is usually established based on an analysis of threats found in the operating environment (Fig. 18.10). In the aircraft industry, once a level of nondetectable damage is established, fatigue testing verifies that it will not endanger the normal operation of the aircraft structure for two lifetimes. After the fatigue tests are completed, the structure is statically loaded to failure.

Other properties of composites affect their damage tolerance characteristics. One factor is ply orientation. Impacted laminates with stiff ply orientations—that is, a higher percentage of plies oriented parallel to the loading direction—typically fail at lower strains than those with softer orientations (Fig. 18.11). However, structural weight is more significantly related to stress capability than to strain. Thus, a laminate with a higher modulus may be able to operate to a higher stress even though its strain capability may be less. Each specific case must be carefully examined. The potential advantage of using a soft laminate, especially in damage-prone areas or in areas where there are stress concentrations, should be considered. For example, a soft laminate might be used effectively for an outer skin, whereas the interior stiffeners, which are exposed to less damage, might advantageously use a stiffer and hence a more weight-efficient but less damage-tolerant lay-up.

Single-layer delaminations are also important; however, unless they are very large (more than 2 in. (5 cm) in diameter), they are only a concern for thin laminates. The effects of such manufacturing defects as porosity and flawed fastener holes that are slightly in excess of the maximum allowable are usually less severe. They are generally accounted for by the use of design allowable properties that have been obtained by testing specimens with stress concentrations, such as open- and filled-hole tension and compression tests. These specimens normally have a 0.25 in. (6 mm) diameter hole located at the center of the specimen, which is left open (no fastener) or filled (fastener installed). Since open holes are more critical than filled holes in compression loading, open-hole specimens are typically used for compression tests. For tension

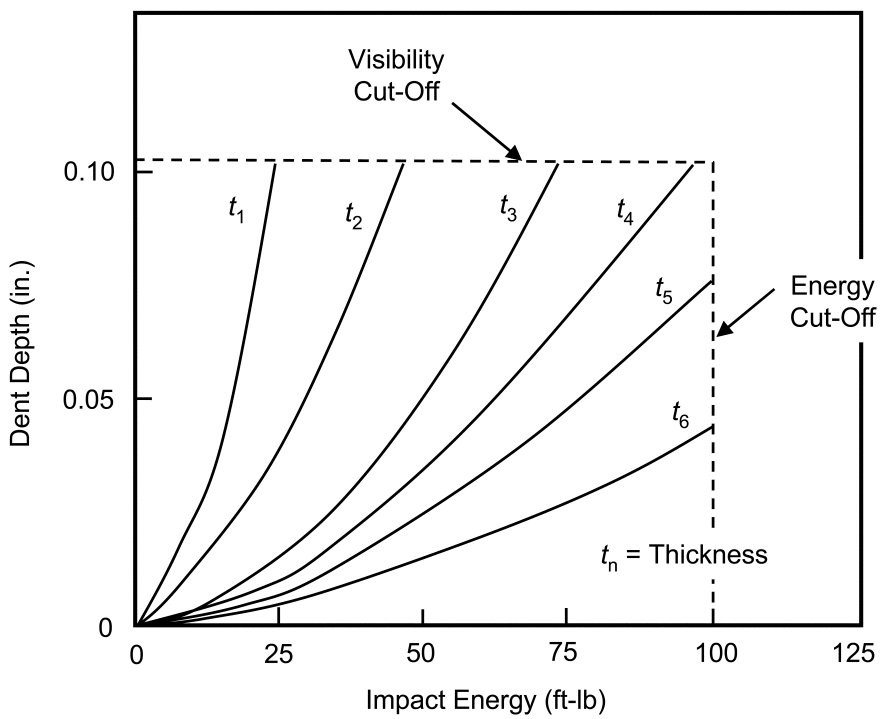


Fig. 18.10 Impact energy cutoff diagram. Source: Ref 4

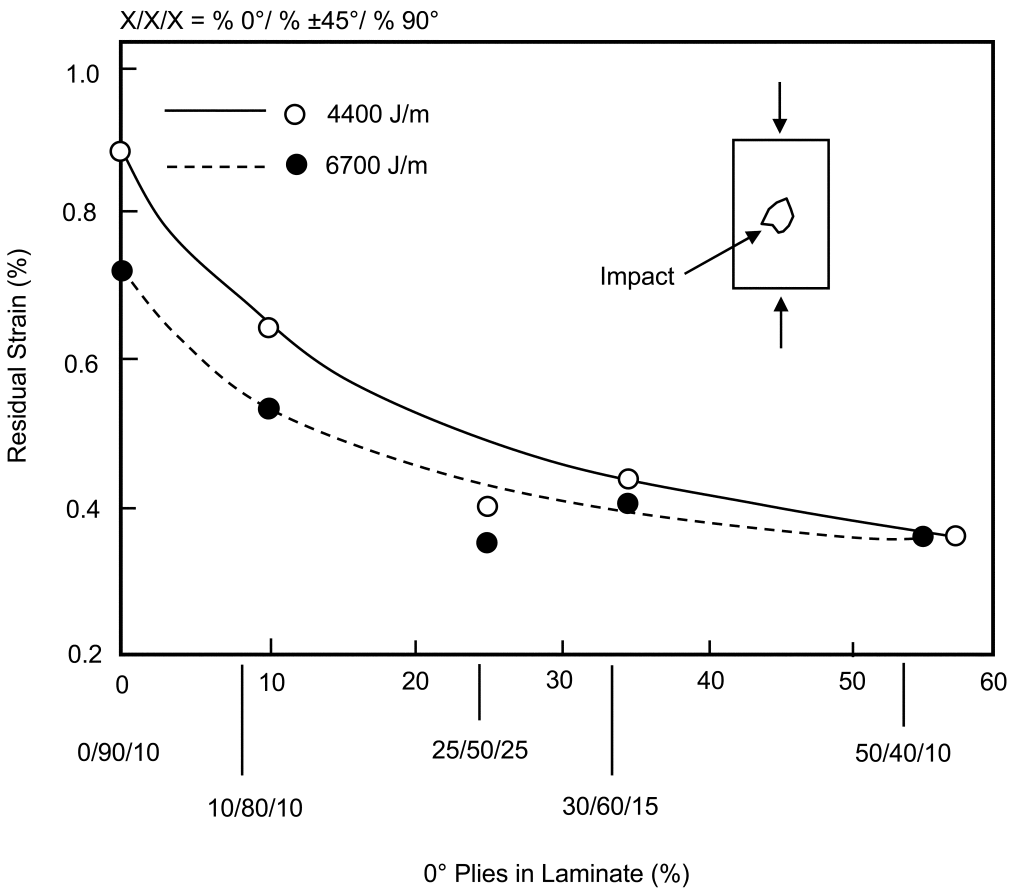


Fig. 18.11 Effect of laminate orientation on residual compression strain after impact. Source: Ref 5

loading, filled holes may be more critical, especially for laminates with ply orientations with a majority of plies oriented in the loading direction. Therefore, the design allowables generated with these tests can be used to account for a nominal design stress concentration caused by an installed or missing fastener, at least to a 0.25 in. (6 mm) diameter.

18.11 Environmental Sensitivity Considerations

As discussed in Chapter 15, "Environmental Degradation," when a polymer matrix composite is exposed to the environment, the matrix absorbs moisture, resulting in a reduction in the glass transition temperature: As moisture is absorbed, the temperature at which the matrix changes from a rigid glassy state to a softer viscous state decreases. Thus, the matrix-dependent strength properties decrease with increasing moisture content when tested at elevated temperatures in what is commonly called the *hot-wet condition*.

When a polymer matrix composite is exposed to a moist environment for a sufficiently long time, the moisture concentration will eventually reach equilibrium and become uniform or achieve saturation. A typical saturation moisture content for severe humidity exposure of epoxy matrix composites is around 1.1 to 1.3 percent weight gain. The approach for design purposes often assumes a worst-case condition. Material allowables can be developed for specimens that are fully saturated and then tested at the maximum use temperature. The reduction of the allowable design strain due to moisture is illustrated in Fig. 18.12. This is a conservative approach, since typical service environments do not generate

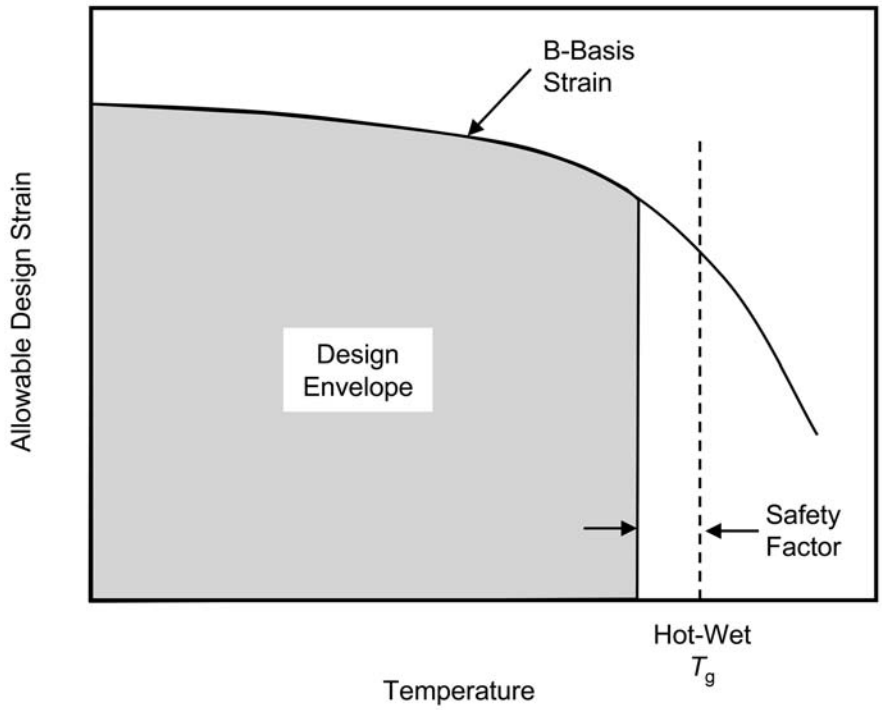


Fig. 18.12 Hot-wet allowable design envelope

full saturation for most real structures. Once the diffusivity of a composite material is known, the moisture content and through-the-thickness distribution can be accurately predicted by moisture diffusion programs.

With metals, corrosion protection is a major design consideration. Polymer matrix composites, by contrast, do not corrode and are immune to varying degrees to most chemical substances. However, if carbon fiber composites are placed in contact with active metals, the metals themselves can corrode. Carbon fiber is cathodic (noble), and aluminum and steel are anodic (least noble), as shown in the galvanic series in seawater in Table 18.8. Thus, carbon fibers in contact with aluminum or steel promote galvanic action that results in corrosion of the metal. Corrosion barriers, made of such materials as fiberglass and sealants, are placed at interfaces between composites and metals to prevent metal corrosion (Fig. 18.13).

Although thermoset polymers are fairly resistant to most chemical compounds, chemical paint strippers are very powerful and can attack the matrix; strippers containing methylene chloride can actually dissolve some amorphous ther-

Table 18.8 Galvanic series in seawater

Cathodic (protected)	Platinum
	Gold
	Graphite
	Titanium
	Silver
	Stainless steels (passive)
	Nickel-based alloys (passive)
	Cu-35% Zn brass
	Nickel-based alloys (active)
	Manganese bronze
	Cu-40% Zn
	Tin
	Lead
	316 stainless steel (active)
	50% Pb-50% Sn solder
	410 stainless steel (active)
	Cast iron
	Low-carbon steel
	2024 aluminum
	2017 aluminum
	Cadmium
	Alclad
	6053 aluminum
	1100 aluminum
	3003 aluminum
	5052 aluminum
	Galvanized steel
	Zinc
Anodic (corrodes)	Magnesium alloys
	Magnesium

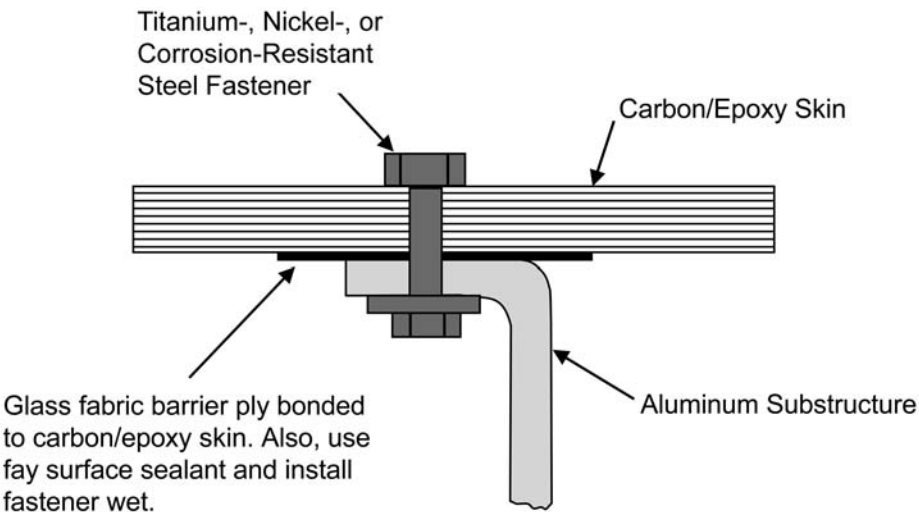


Fig. 18.13 Electrical isolation of carbon/epoxy and aluminum

moplastics. Thus, chemical paint stripping is forbidden on composite structures. Mechanical media blasting is often used on composite structures to remove paint.

Other environmental effects include the effect of long-term exposure to radiation. Ultraviolet rays from the sun can degrade epoxy resins. However, a good paint system will effectively protect the composite. Another factor is erosion or pitting caused by high-speed impact of rain or dust particles. This is likely to occur on the unprotected leading edges of aircraft. Special surface finishes such as thick rain erosion coatings and paints are available to prevent surface wear. Lightning is also a danger to composites; a direct strike can cause considerable damage to a laminate. To prevent it, conductive surfaces are applied to lightning strike susceptible surfaces. In cases in which the substructure is also a composite, the inside end of attachment bolts may need to be connected electrically with each other and grounded by a conducting wire. One important consideration when selecting a lightning strike system is the potential for galvanic corrosion between carbon fibers and the conductive lightning strike material, often aluminum or copper.

Resins are the environmental weak link in a polymer matrix composite. Small impacts, heat, and ultraviolet rays can erode away the resin on the surface of a laminate and leave the fiber reinforcement unsupported. Maintaining a proper surface finish, controlling service temperature, and keeping trimmed edges and fastener holes sealed all help to mitigate the adverse effects of environmental degradation.

REFERENCES

1. J. Bottle, F. Burzesi, and L. Fiorini, Design Guidelines, *ASM Handbook,* Vol 21, *Composites,* ASM International, 2001
2. R.E. Fields, Overview of Testing and Certification*, ASM Handbook,* Vol 21, *Composites,* ASM International, 2001
3. MIL-HNBK-17-3F, *Polymer Matrix Composites,* Vol 3*, Materials Usage, Design, and Analysis*, U.S. Department of Defense, 2001
4. "General Specification for Aircraft Structures," MIL-A-872221, U.S. Air Force, Feb 1985
5. R.E. Horton and J.E. McCarty, Damage Tolerance of Composites, *Engineered Materials Handbook,* Vol 1*, Composites,* ASM International, 1987

SELECTED REFERENCES

- C. Boshers, Design Allowables, *ASM Handbook,* Vol 21*, Composites*, ASM International, 2001
- E. Chesmar, Product Reliability, In-Service Experience, and Lessons Learned, *ASM*

Handbook, Vol 21*, Composites*, ASM International, 2001

- W.F. Cole and M.S. Forte, Maintainability Issues, *ASM Handbook,* Vol 21, *Composites,* ASM International, 2001
- L.J. Hart-Smith and R.B. Heslehurst, Designing for Repairability, *ASM Handbook,* Vol 21*, Composites,* ASM International, 2001
- M.C.Y. Niu, *Composite Airframe Structures*, 2nd ed., Hong Kong Conmilit Press Limited, 2000.
- A.J. Vizzini, Design, Tooling, and Manufacturing Interaction, *ASM Handbook,* Vol 21*, Composites,* ASM International, 2001
- M.R. Woodward and R. Stover, Damage Tolerance, *ASM Handbook,* Vol 21, *Composites,* ASM International, 2001

"*This page left intentionally blank.*"

Copyright © 2010, ASM International®
All rights reserved.
www.asminternational.org

CHAPTER 19

Repair

REPAIRS CAN BE CATEGORIZED as fill, injection, bolted, or bonded, as shown in Fig. 19.1. Simple fill repairs are conducted with paste adhesives to repair such nonstructural damage as minor scratches, gouges, nicks, and dings. Injection repairs use low-viscosity adhesives that are injected into composite delaminations or adhesive unbonds. Bolted repairs are usually done on thick, highly loaded composite laminates, whereas bonded repairs are often required for thin-skin honeycomb assemblies.

All repairs of composite or bonded aircraft assemblies should be conducted according to the specific instructions outlined in the structural repair manual or technical order for the aircraft. Each such manual is prepared by the aircraft manufacturer and approved by the appropriate governing agency, such as the Federal Aviation Agency for commercial aircraft or the Air Force/Navy/Army agency for military aircraft. If the damage exceeds the limits specified in the manual, it is imperative that a qualified stress engineer approve the repair procedure. All personnel conducting structural repairs should be trained and certified in the repair procedure. The instructions in the repair manual must be followed to the letter. A repair that is done incorrectly can often result in a second, more extensive and complicated repair.

Information on the design of bolted repairs is given in Ref 2, while Ref 3 covers bonded repair designs. Detailed procedures for many composite repairs can be found in Ref 4.

19.1 Fill Repairs

Fill repairs are nonstructural and therefore should be confined to minor damage. Two-part high-viscosity thixotropic epoxy adhesives are normally used for these types of repairs. The surface to be repaired should be dry and free of any contamination that would prevent the filler from adhering. Prior to filling, the surface should be lightly sanded with 180- to 240-grit silicon carbide paper. Once the adhesive is mixed and applied to the surface, most epoxy adhesives will cure sufficiently within 24 hours at room temperature so that they can be sanded flush with the surface. It normally takes five to seven days at room temperature for them to develop their full strength. Heat lamps are often used to accelerate the cure by heating the adhesive to 180 °F (80 °C) for one hour. There are also special fillers, called *aerodynamic smoothing compounds*, which are rubber-toughened epoxy resins with high resistance to crazing and cracking in service. It is advisable not to heat these types of repairs to over 200 °F (95 °C), as moisture in the laminate could cause a steam pressure delamination problem that would require a much more extensive repair.

19.2 Injection Repairs

Injection repairs are somewhat controversial and can produce mixed results. If the repair is for an adhesive unbond or a delamination during cure, the internal surfaces of the unbond or delamination will normally contain a glossy oxidized surface to which the injected adhesive may not adhere. On the other hand, if the delamination occurred because of an impact that broke the layers apart, the surfaces will be amenable to bonding with the injected adhesives. However, delaminations caused by impacts are often in multiple layers and connected with tight microcracks that are difficult or impossible to fill.

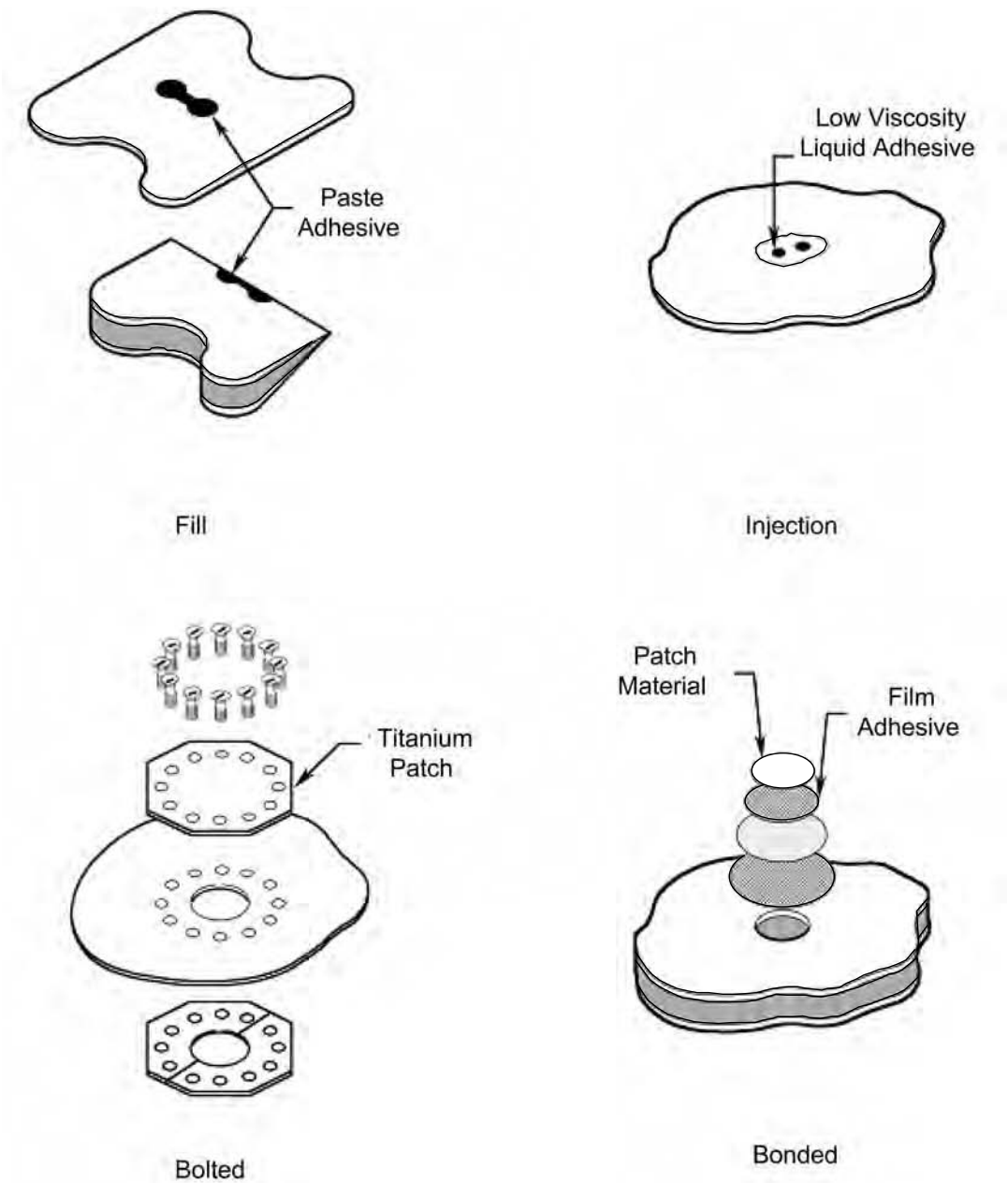


Fig. 19.1 Typical composite repairs. Source: Ref 1

Low-viscosity two-part epoxy adhesives are injected under low or moderate pressure, as shown in the two examples in Fig. 19.2. If the delamination does not extend to an edge, small-diameter, flat-bottom holes 0.050 in. (1.3 mm) in diameter are drilled to a depth usually determined by pulse echo ultrasonics. Two or more holes are generally required, one for injection and one for venting. To help the resin flow into a tight delamination, it is helpful to preheat the delaminated area to 120 to 140 °F (50 to 60 °C). Preheating reduces the resin's viscosity and helps it flow into the delamination. For tight delaminations, pressures as high as 40 psi (280 kPa) can be used if necessary. (If the delamination is successfully filled at lower pressure, adhesive will

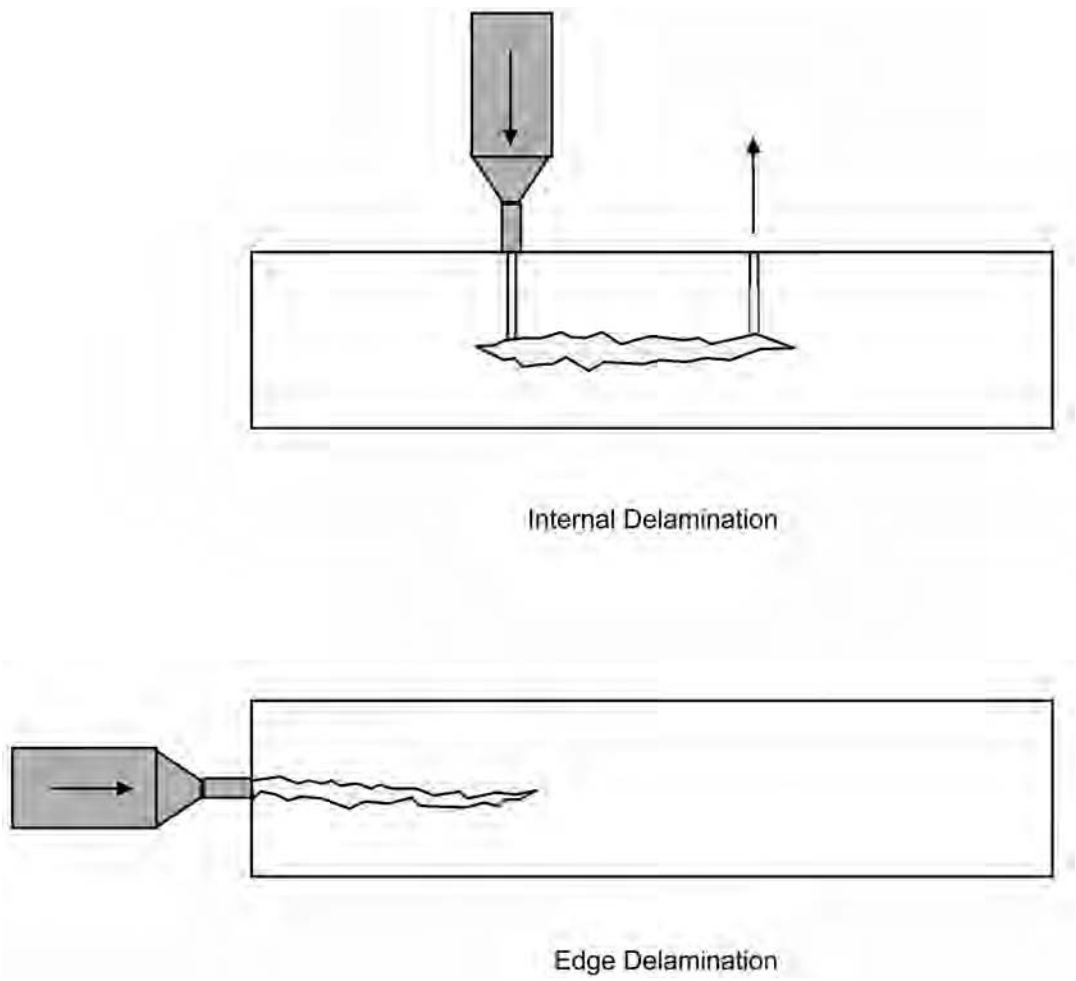


Fig. 19.2 Filling delaminations with low-viscosity resins

flow out of the vent hole.) If honeycomb core will be exposed to the pressure, it should be limited to 20 psi (140 kPa) to prevent the core from blowing. Flow can be verified by injecting air into one hole and monitoring air flow out of the other hole. A useful way to monitor this flow is to seal a piece of rubber hose over the vent hole and immerse the other end in a cup of water; air flow is indicated by the presence of bubbles. Edge delaminations are somewhat easier to fill and do not normally require vent holes. In addition, after filling an edge delamination, C-clamps can be applied to provide pressure to spread the adhesive and push the plies back together.

The multiple-layer nature of a delamination around a fastener hole caused by torquing a fastener down over an unshimmed gap is shown in Fig. 19.3. A photomicrograph of a section through the hole (Fig. 19.4) reveals a complex network of delaminations and matrix cracks on multiple layers through the laminate; some of the delaminations do not even extend to the edge of the hole. An injection scheme for this type of delamination (Fig. 19.5) involves a series of small injection and venting holes. To provide pressure during cure, a temporary mold-released fastener with oversize washers can be placed in the hole and tightened. Ultrasonic pulse echo can be used to map the boundaries and depths of the delaminations.

Although injection repairs may not restore the original strength, they do help to stabilize the sublaminates that occur during delamination, which is particularly important when compression loading is present. As shown in the compression test results for specimens that had delaminations around fastener holes in Fig. 19.6, the specimens

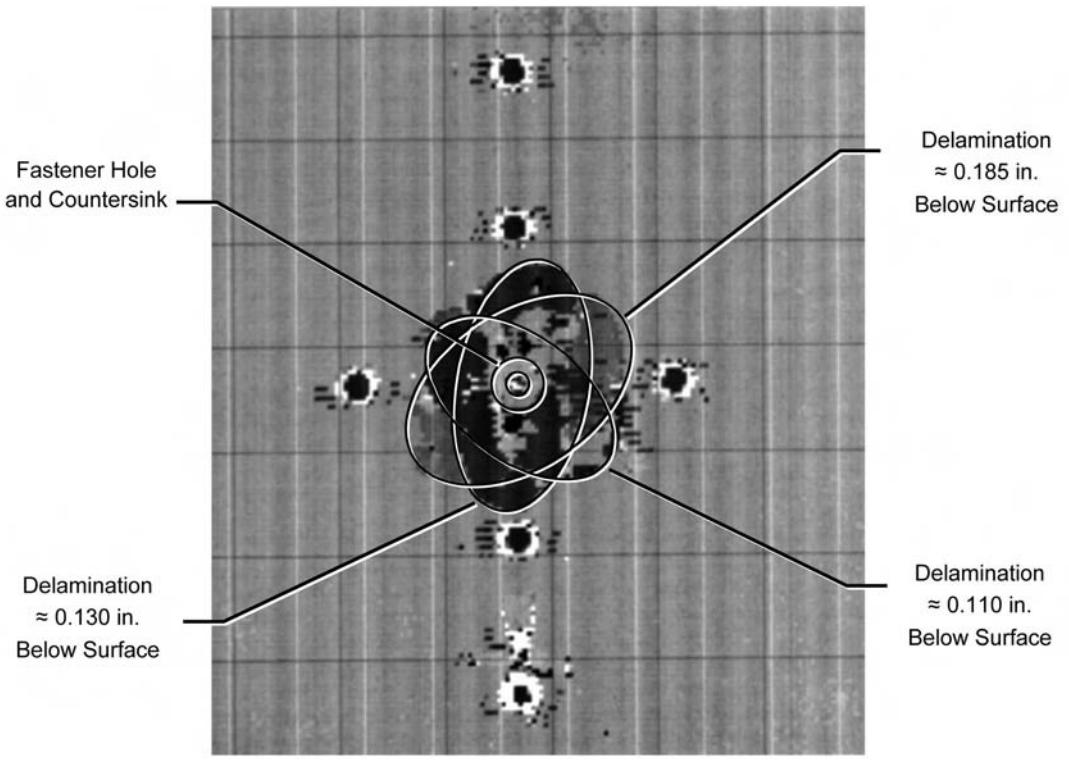


Fig. 19.3 Multiple levels of delamination around the fastener hole. Source: Ref 1

that were repaired by injection had higher compression strengths than the unrepaired specimens.

If a skin-to-core adhesive unbond needs to be injected, the honeycomb assembly should be inverted so that the unbond is on the bottom surface. Using this orientation will prevent the low-viscosity resin from running down the cell walls.

19.3 Bolted Repairs

Bolted repairs are usually preferred over bonded repairs because they are simpler and less prone to errors. A guide to help decide when to use bolted or bonded repairs is given in Table 19.1. The advantages of bolted repairs are obvious; however, the initial design of the structure must be able to accommodate the fastener bearing loads. In other words, the original design strains of the structure must be low enough that a bolted repair can be designed to carry ultimate design loads with a positive margin of safety.

Bolted repair patches (Fig. 19.7) can be applied to the external surface, the internal surface, or both. The load transfer efficiency with single-shear fasteners, as shown for the single external and internal patches, is limited because the fasteners tend to rotate under load, causing edge bearing failure in the composite skin. The double external/internal patch shown has much better load transfer capability because the fasteners are loaded in double shear.

A typical bolted repair (Fig. 19.8) consists of an external titanium patch, a center plug in the damaged area, and a two-piece internal patch. The internal patch is split into two pieces so that it can be inserted inside the skin. Normal composite drilling and fastener installation procedures are used. Both protruding patches (Fig. 19.9) and flush patches (Fig. 19.10) can be designed, although protruding patches are easier to install.

The procedure for installing a one-sided patch is as follows. The area to be repaired is routed to form a circle or oval with no sharp edges or other stress concentrations. Undersize pilot holes are predrilled in the patch. To locate the patch, the skin is marked with intersecting lines establishing the 0° and 90° directions. The patch is then placed on the skin, and two opposing end hole locations are marked. The patch is removed,

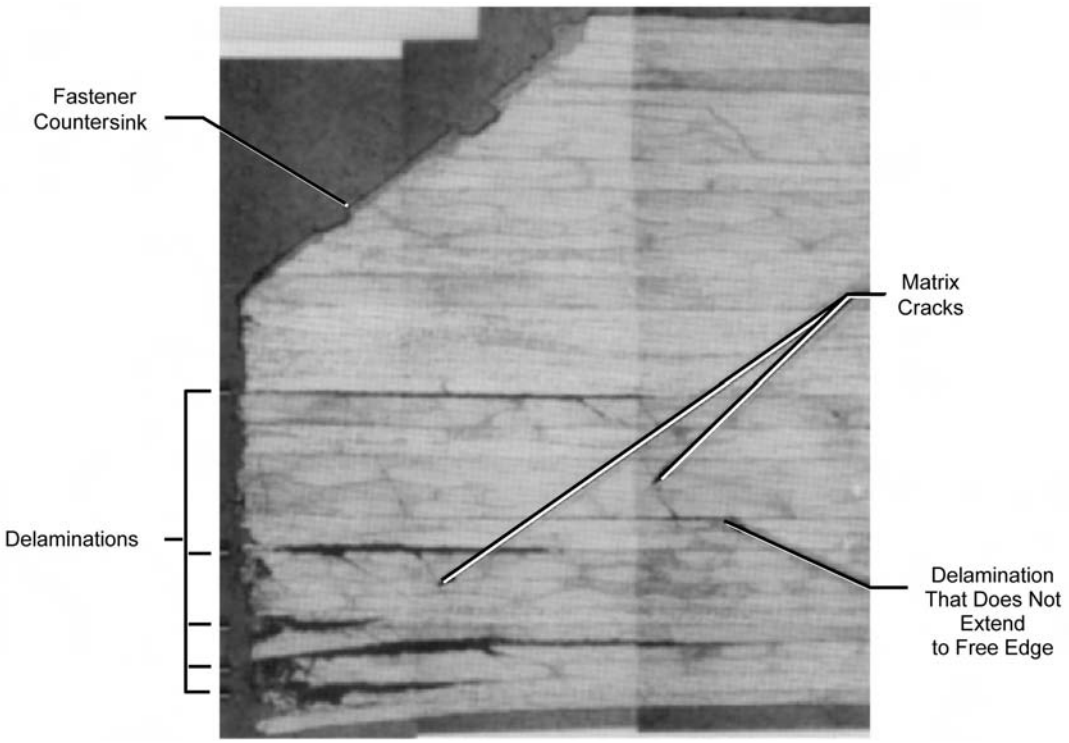


Fig. 19.4 Photomicrograph of delaminations and matrix cracks. Source: Ref 1

and two pilot holes are drilled in the skin. The patch is then repositioned on the skin and held in place by temporary fasteners. A number of other pilot holes are then transferred from the patch to the skin. Additional temporary fasteners are installed as the pilot holes are drilled to provide clamp-up between the patch and skin. After all pilot holes are drilled and clamped in place, they can be enlarged to their final diameter by first drilling and then reaming, usually with a tolerance of +0.003/–0.000 in. (+0.08/–0.00 mm). Again, temporary fasteners are used to provide clamp-up between the patch and fastener. After all of the holes have been drilled and reamed to their final sizes, the patch is removed and deburred. A layer of woven glass cloth is impregnated with sealant to provide both sealing and corrosion protection. The full-size holes in the patch are countersunk, and the patch is installed with either one-sided blind fasteners (if there is access to only one side) or pin and collar fasteners (if there is access to two sides). All fasteners should be installed wet with sealant, and the edges of the patch should be fillet-sealed. Although one-sided patches are easier to install, they provide only single shear and asymmetry in the load path.

Two-sided patches provide double shear and more balanced load paths but are more difficult to install, particularly if only single-sided access is possible. Pilot holes, at least one through each piece, should be mate-drilled through the outside and inside patch pieces before starting installation. The interior patch pieces are often split so that they can be slipped through the hole in the skin. Again, the outer patch is used to establish pilot holes in the skin. The interior and exterior patches are located and held in place with temporary fasteners inserted through the pilot holes located at either end. Using the existing pilot holes in the exterior patch and skin, pilot holes are drilled through the interior patch sections. Temporary fasteners are installed in the pilot holes as they are drilled. After all pilot holes have been drilled, they are brought up to full size by first drilling and then reaming to final size. The patch sections are then removed, countersunk on the exterior surface, deburred, fay-surface-sealed, and reinstalled with temporary fasteners. Full-size fasteners are then

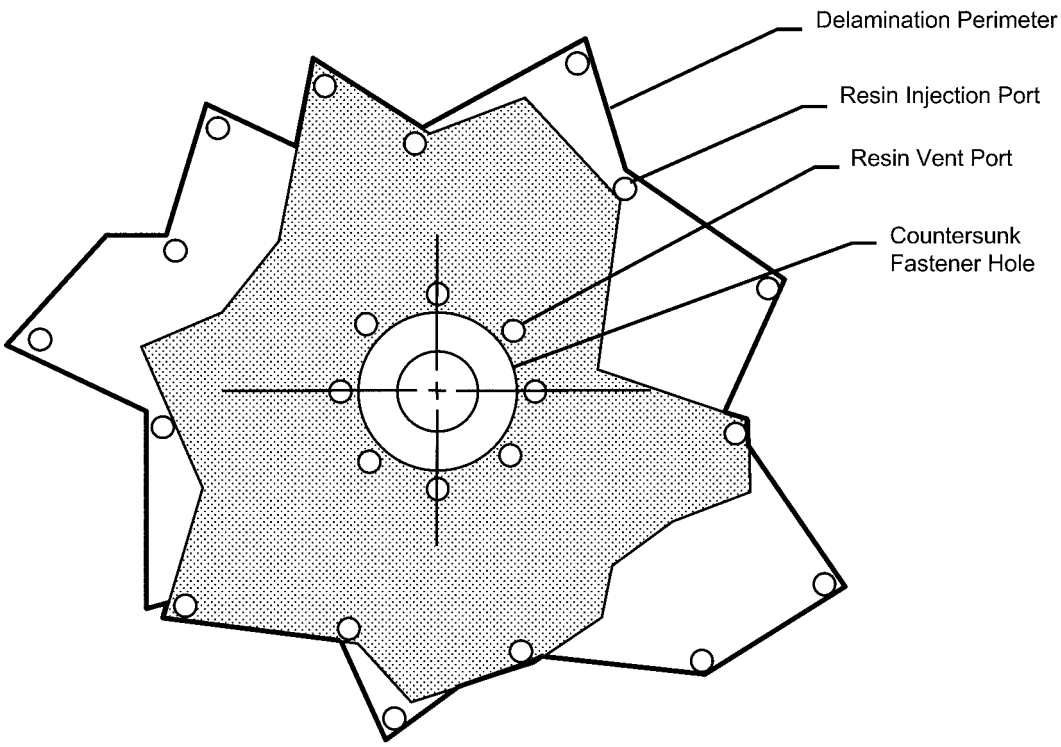


Fig. 19.5 Injection scheme for delaminated fastener hole. Source: Ref 1

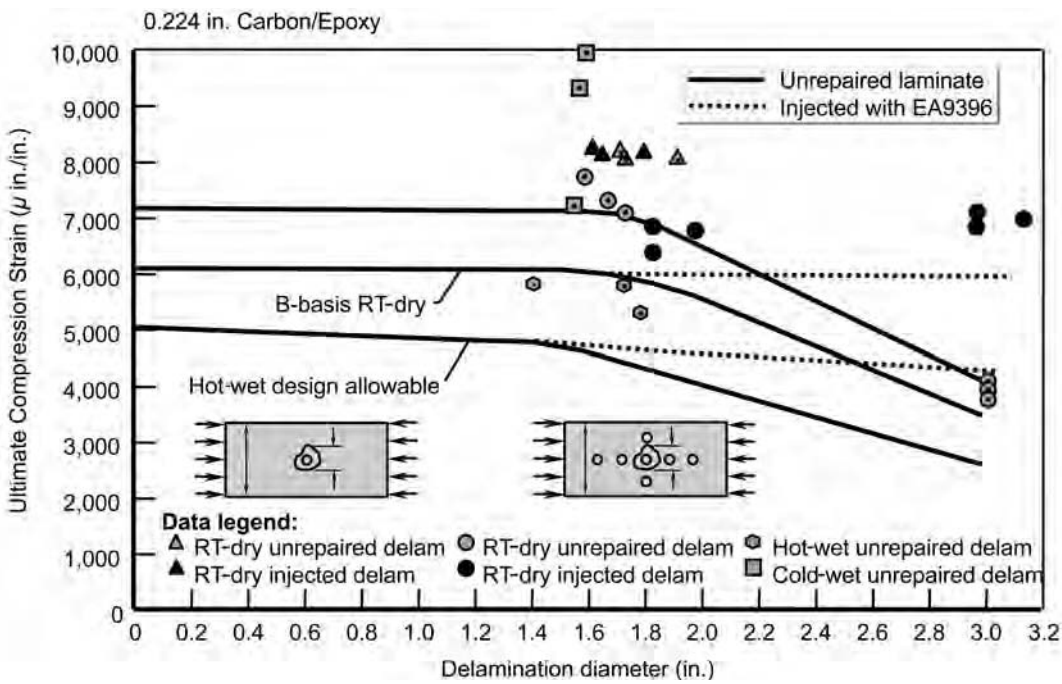


Fig. 19.6 Compression tests on repaired and unrepaired delaminated fastener holes

Table 19.1 Considerations when selecting the structural repair method

Condition		Recommended: Bolting	Recommended: Bonding
Lightly loaded, thin (~<.10 in.)		X	X
Highly loaded, thick (~>.10 in.)		X	…
Peeling stresses high		X	…
High reliability required		X	…
Repairing honeycomb structure		…	X
Adherend surfaces	Dry	X	X
	Wet	X	…
	Clean	X	X
	Contaminated	X	…
Sealing required		X	X
Disassembly required		X	…
Restore "no-hole" strength		…	X

Source: Ref 1

installed. If access to only one side is possible, then either blind fasteners can be used or nut plates can be installed on the interior patch sections for removable screws. Pin and collar fasteners can be used if access to both sides is available.

19.4 Bonded Repairs

Bonded repairs are the most difficult and error-prone repairs. There are many variations of this type of repair, and only a few examples will be given. Three typical bonded repairs (Fig. 19.11) are the bonded patch, the scarf repair, and the stepped-lap repair. The bonded patch repair can be accomplished using prepreg, wet lay-up, or thin titanium sheets bonded together with layers of adhesive. For structures requiring higher load-bearing capability, the scarf or stepped-lap repair is normally required; however, both of these methods require precise machining operations for effective load transfer. Bonded scarf repairs also require significant areas of material to be removed (Fig. 19.12) to prevent high peeling forces on the adhesive.

A typical hot-bonded field repair procedure consists of the following steps:

1. The damaged area is mapped out with pulse echo ultrasonics to determine whether the repair falls within the limits of the structural repair manual. (If it does not, then a strength engineer should be consulted for an alternative course of action.)
2. The damaged plies are carefully removed using high-speed routers with depth control. If the stepped-lap configuration is required, this will probably end up being a tedious job of hand cutting the steps ply by ply.
3. If the repair is to be cured at a temperature of 200 °F (90 °C) or higher, the repair area is dried at 200 °F for a minimum of four hours.
4. The repair area is bagged with a heat blanket (as shown in Fig. 19.13), subjected to full vacuum (22 in. (559 mm) of Hg vacuum minimum), slowly heated to the cure temperature, for example, 250 or 350 °F (120 or 180 °C), and held under vacuum at that temperature for the required period of time, for example, two to four hours. Vacuum pressure is maintained on the cured patch until it cools down to 150 °F (65 °C).
5. The cured patch is unbagged and the area cleaned up. The quality of the repair is inspected with pulse echo ultrasonics. The repaired area is refinished to match the rest of the structure.

For field repairs, there are commercial units (Fig. 19.14) that provide electrical power, thermocouple readouts, and vacuum sources and can be programmed to provide uniform heat-up, hold, and cool-down temperatures.

Bonded repair patches are usually made of prepreg, wet lay-ups, precured composites, or thin titanium sheets adhesively bonded together. Since field repairs are conducted with only vacuum bag pressure (≤14.7 psia or less), the quality of the repair is not as high as that of the original laminate, which was cured in an autoclave at 100 psi (700 kPa). Prepreg patches produce higher-quality patches than wet lay-up patches. However, prepreg must be stored in a 0 °F (–18 °C) freezer and has a shelf life of one year or less. Some resins used for wet lay-up patches can be stored at room temperature for six to 12 months. An additional concern with wet lay-up patches is that it may be difficult or impossible to match the strength and stiffness of the original structure if the structure is thin and made from unidirectional tape, since the wet lay-up material will be woven cloth. Both prepreg and wet lay-up patches have the advantage that they can be easily formed to the contour required for the repair.

Precured patches and patches constructed by adhesively bonding multiple layers of 0.019 to 0.020 in. (0.48 to 0.5 mm) thick titanium sheets together can produce repairs with few or no voids. The bagging operations are also simplified since no bleeder is required. Often a series of small holes is drilled in precured patches to allow air removal at the adhesive bondline. The biggest disadvantage of these patches is that

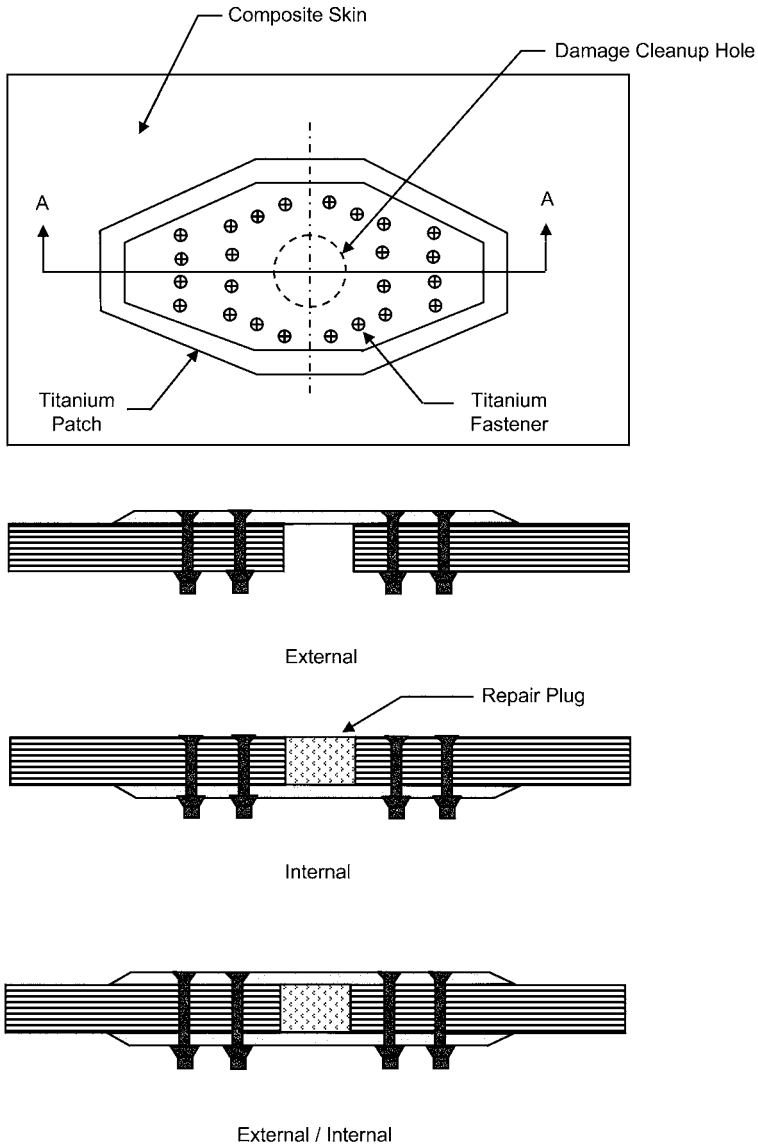


Fig. 19.7 Basic bolted repair joints

they have very limited formability to contour. They are normally used if a number of units require the same repair and the patches can be prepared ahead of time. If titanium patch material is used, it must be precleaned, primed, and stored in moistureproof bags.

All damaged material should be removed and the hole or bottom of the repair should be round or oval, with no sharp edges. Machining of a scarf or stepped-lap repair is an operation that requires a great deal of care and skill. Templates and depth-control fixtures should be used with high-speed sanders or routers. In stepped-lap repairs, it is important not to damage the plies under the step during the machining operation.

It is important that the area to be repaired is thoroughly dry, particularly if the repair area is going to be heated to above 200 °F (90 °C). Absorbed moisture in skins or liquid water in honeycomb can turn to steam and cause delaminations and blistering, and water in core can blow skins or cause additional core damage by blowing core cells. To help prevent moisture damage, the entire repair area should be thoroughly

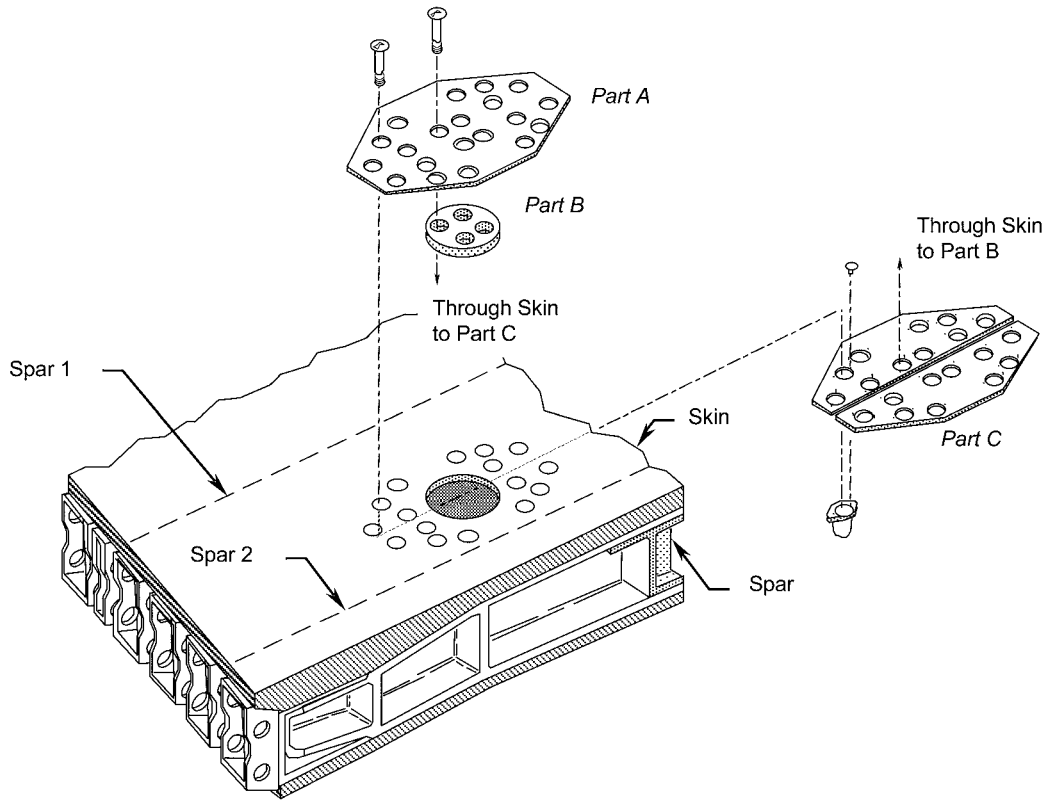


Fig. 19.8 Bolted repair concept. Source: Ref 1

dried by slowly heating, for example, 1 °F/min (0.6 °C/min) to 200 °F (90 °C) and holding for a period of time (typically four hours for thin skins). Thick skins may take a considerably longer time, and it may be necessary to use moisture absorption/desorption computer programs to determine the appropriate drying time. The drying operation can often be combined with a trial run of the repair process by substituting dry glass cloth for the prepreg plies and bagging in the same manner as for the actual patch cure. This trial run will also reveal potential hot or cold spots in the repair area that can be corrected before committing to the actual repair cure cycle. Extra insulation or multiple heat blankets with zone control may be required to obtain uniform temperatures.

The type of resin and adhesive selected for the repair is also important. For example, if the original structure was bonded using a 250 °F (120 °C) curing adhesive, then it would certainly not be appropriate to use a 350 °F (180 °C) curing adhesive for a repair. In general, the lower the cure temperature for the composite patch plies and adhesive, the better the chances for a successful repair that does not result in additional damage to the structure. If the repair is done by the original equipment manufacturer (OEM) or at a depot with an autoclave, then the repair can be performed using the same materials used for the original part manufacture, since the part can be bagged and the repair cured at the same temperature and pressure used during the original fabrication. For example, if 350 °F (180 °C) curing systems were originally used, then the autoclave pressure will hold everything together during a repair performed at 350 °F (180 °C). On the other hand, if only a local vacuum bag is used and the part is heated to 350 °F (180 °C), the part might delaminate or unbond as the adhesive bondlines can become extremely weak at the 350 °F (180 °C) curing temperature. In addition, any moisture in either the laminate or the honeycomb will reach much higher vapor pressures at 350 °F (180 °C) than at lower temperatures, such as 250 °F (120 °C) or less.

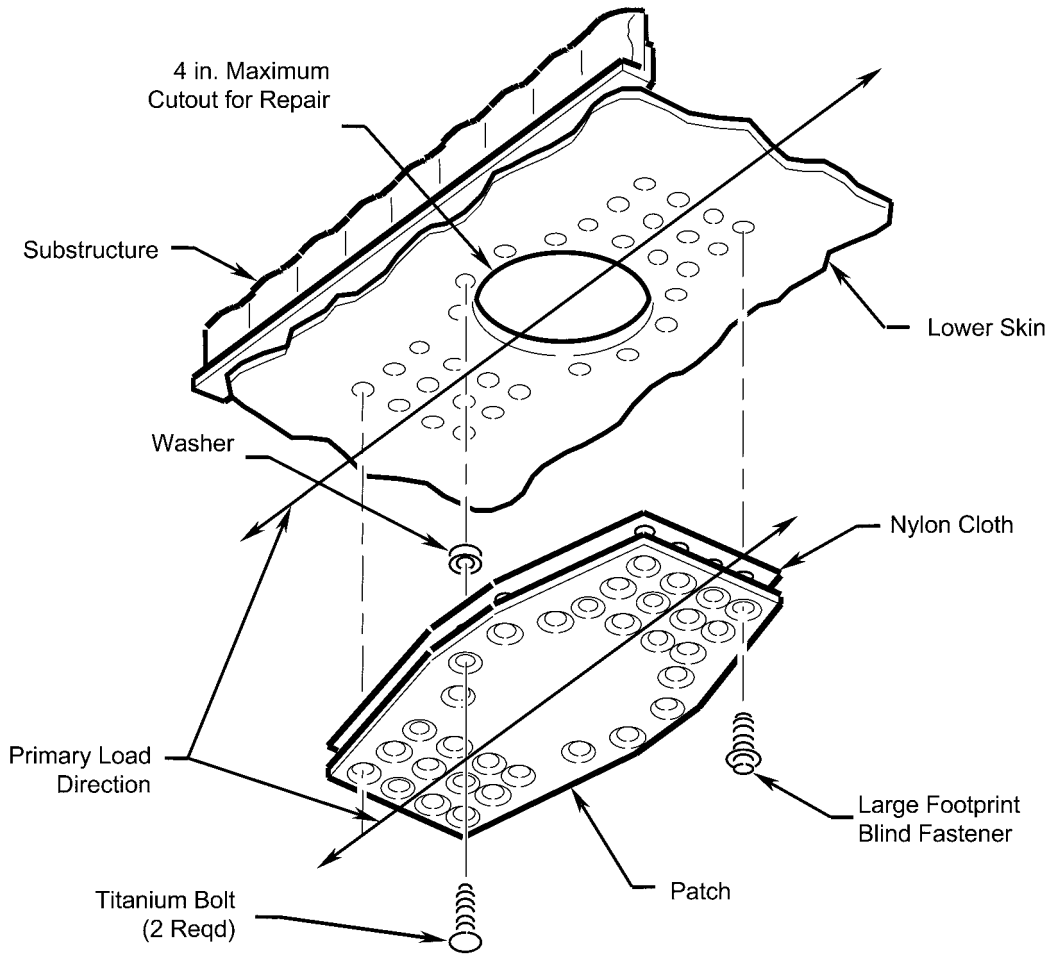


Fig. 19.9 Bolted protruding patch repair. Source: Ref 1

The author once observed the aftermath of a disastrous repair of a large, expensive composite skinned honeycomb assembly. The assembly contained precured carbon/epoxy skins adhesively bonded to full-depth honeycomb core. The adhesive used cured at 350° F (180 °C) but was limited in use to 250 °F (120 °C). A repair was required as a result of a small puncture in one of the skins. The repair seemed straightforward and consisted of adhesive bonding a small titanium patch over the puncture. Rather than placing the assembly back on its tool and vacuum bagging the entire assembly, the repair team placed a small local vacuum bag over the repair area and put the entire assembly in an oven for the 350 °F (180 °C) repair cure. The original adhesive bondlines became so weak at 350 °F (180 °C), with no pressure to hold them together, that residual stresses in the assembly allowed the bondlines to fail. Both skins popped off of the core, and as a result the assembly was scrapped.

For field repairs, where only vacuum pressure is normally available, it is important to use repair materials that cure at temperatures significantly lower (50 to 100 °F (10 to 40 °C)) than the original cure temperatures. Again, it is important to make sure that the entire assembly is dry if it is placed in an autoclave, or that at least the repair area is dry if a vacuum bag is used for a field repair. In general, complicated repairs involving precision machining and complex lay-ups, such as bonded scarf and stepped-lap repairs, should be conducted at either the OEM or a depot where more extensive tooling and autoclaves are available.

Epoxy film adhesives and prepregs are available that cure at 250 to 350 °F (120 to 180 °C)

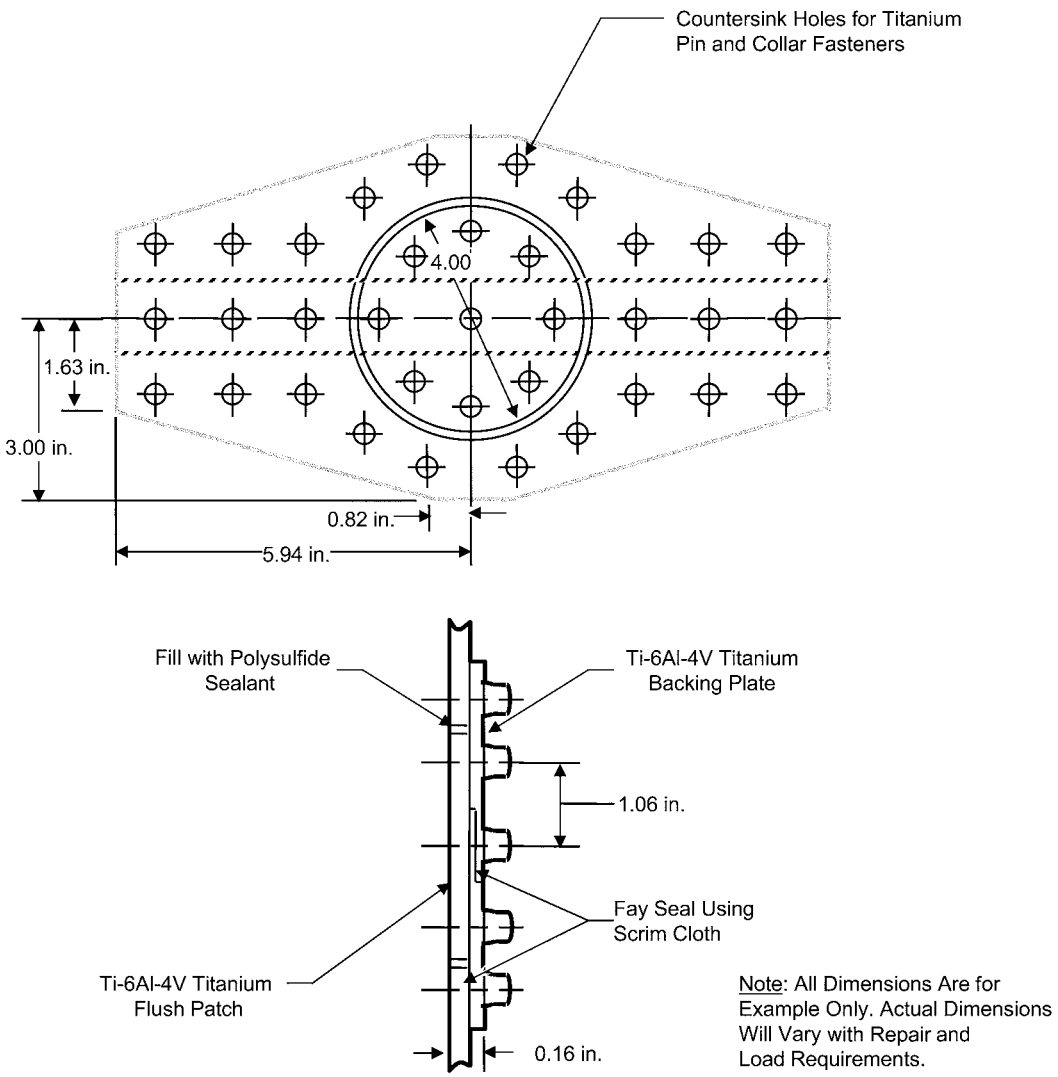


Fig. 19.10 Bolted flush patch repair. Source: Ref 1

for one to four hours. Wet-lay resins and adhesives will generally cure at room temperature in five to seven days; alternatively, they can be heat-cured at 160 to 180 °F (70 to 80 °C) in one to two hours. Although these materials require five to seven days to obtain full strength, they generally cure sufficiently at room temperature in 24 hours so that the pressure can be removed and cleanup such as hand sanding or refinishing can be performed.

Although materials that cure at lower temperatures are beneficial in repairs, the benefit is not unlimited: The lower the cure temperature, the lower the glass transition temperature (T_g) and the ultimate service temperature. If a wet lay-up or precured composite patch is cured with a liquid or paste adhesive, then a lightweight layer of glass cloth should be embedded in the bondline to provide bondline thickness control and corrosion protection if a carbon patch is cured against aluminum honeycomb core.

Pressure for repair cures can be provided by an autoclave, mechanically, for example, with C-clamps, or with a vacuum bag. An autoclave is preferable because it can provide full pressure, for example, 100 psi (700 kPa), and the pressure application is isostatic; however, it does require drying of the entire assembly, usually in

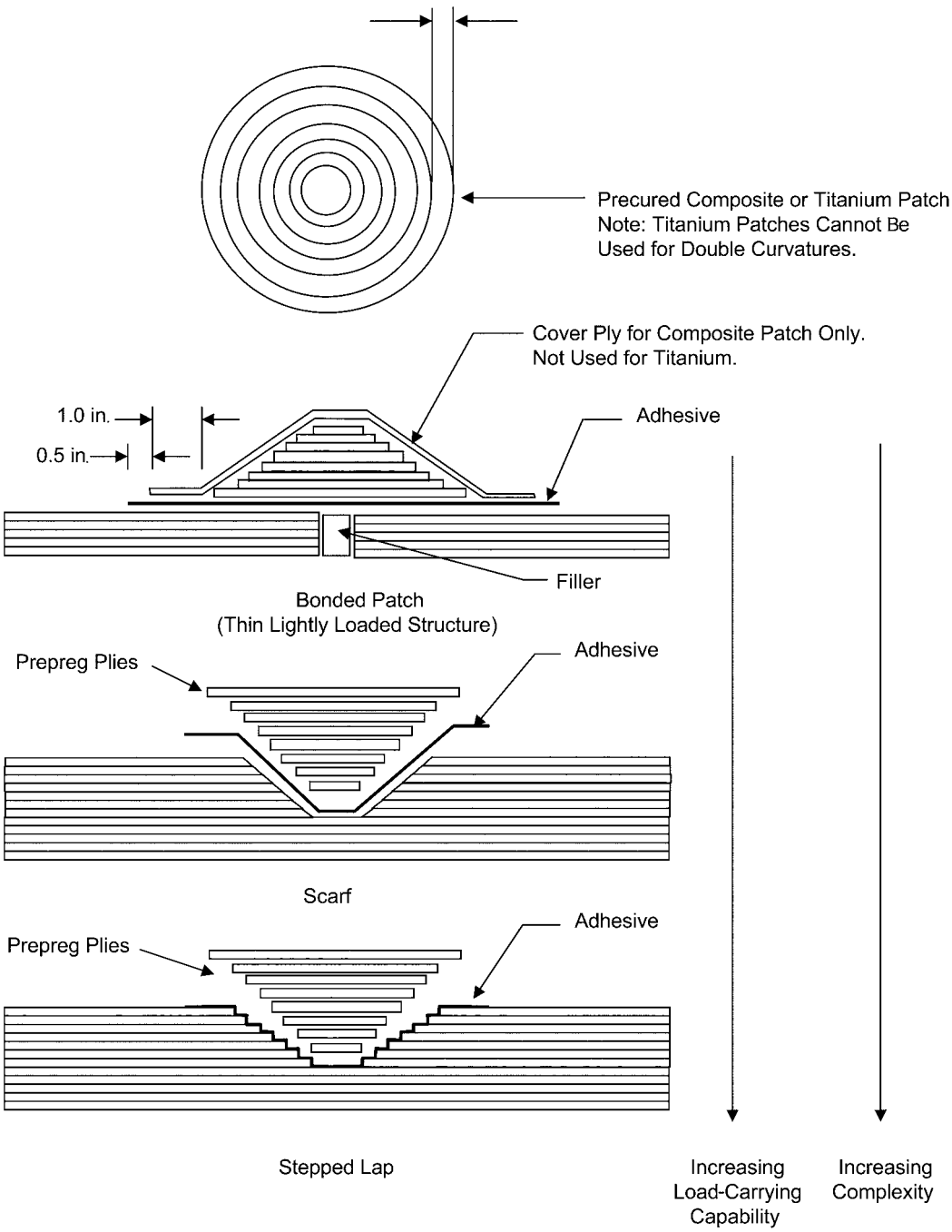


Fig. 19.11 Composite laminate bonded repair approaches

an oven, and either envelope bagging the assembly or placing it on the original tool and vacuum bagging it. Mechanical pressure can be very effective if the repair area is small and located in an area accessible to clamps. Two concerns with clamps, though, are that (1) it is possible to apply too much pressure and locally crush the part and that (2) clamps can act as heat sinks and make it difficult to obtain uniform heating. If clamps are used, pads should be used to spread

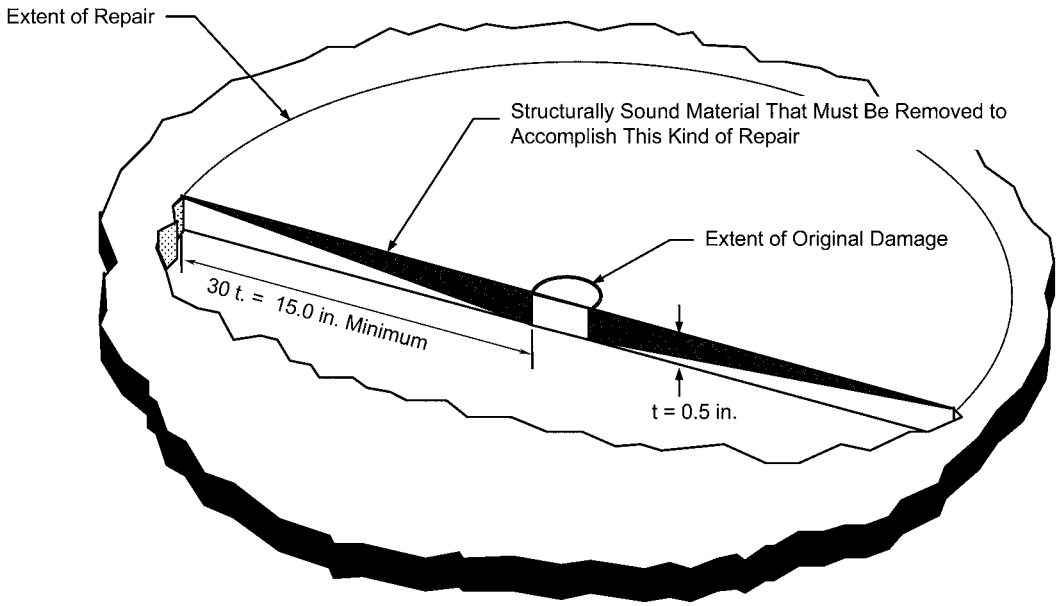


Fig. 19.12 Taper angle required for effective load transfer for bonded repair. Source: Ref 1

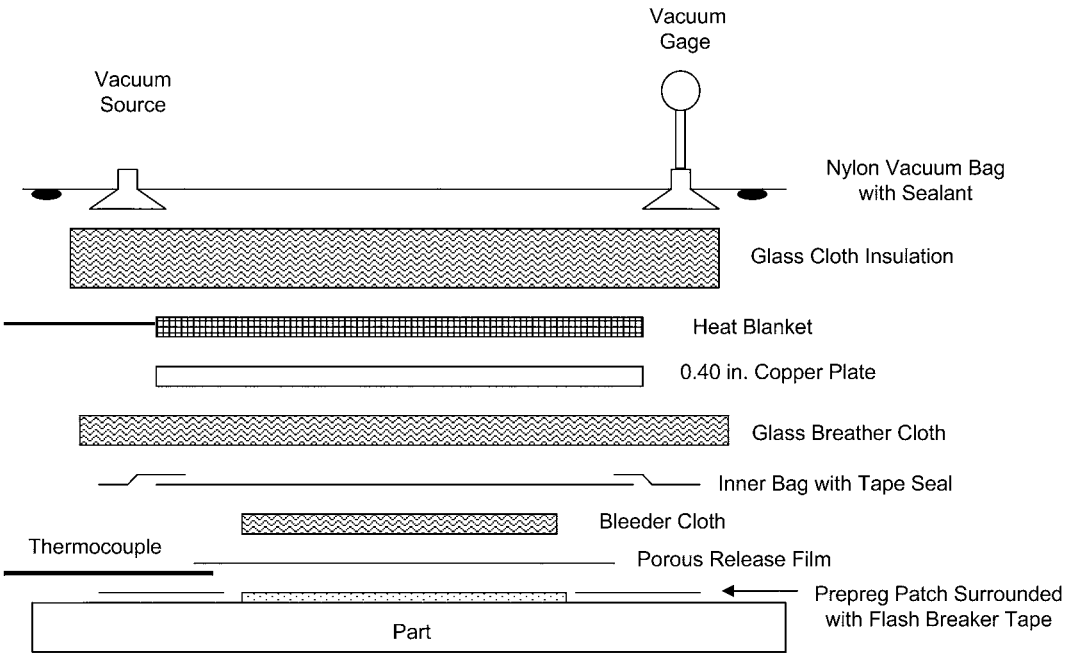


Fig. 19.13 Typical bagging sequence for field repair

the localized clamp loading across the surface. Vacuum bags are frequently used for field repairs because, with them, the repair can often be performed without having to remove the part from the aircraft. There are several disadvantages to vacuum bags: (1) the maximum pressure obtainable is 8 to 15 psi, (55 to 100 kPa); (2) the pressure is applied only at the repair area, and adjacent areas are left without pressure if they get hot during heating; and (3) curing under

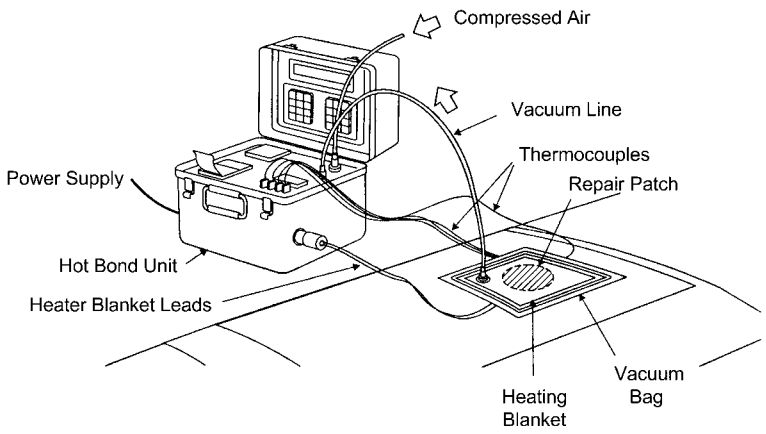


Fig. 19.14 Setup for bonded field repairs

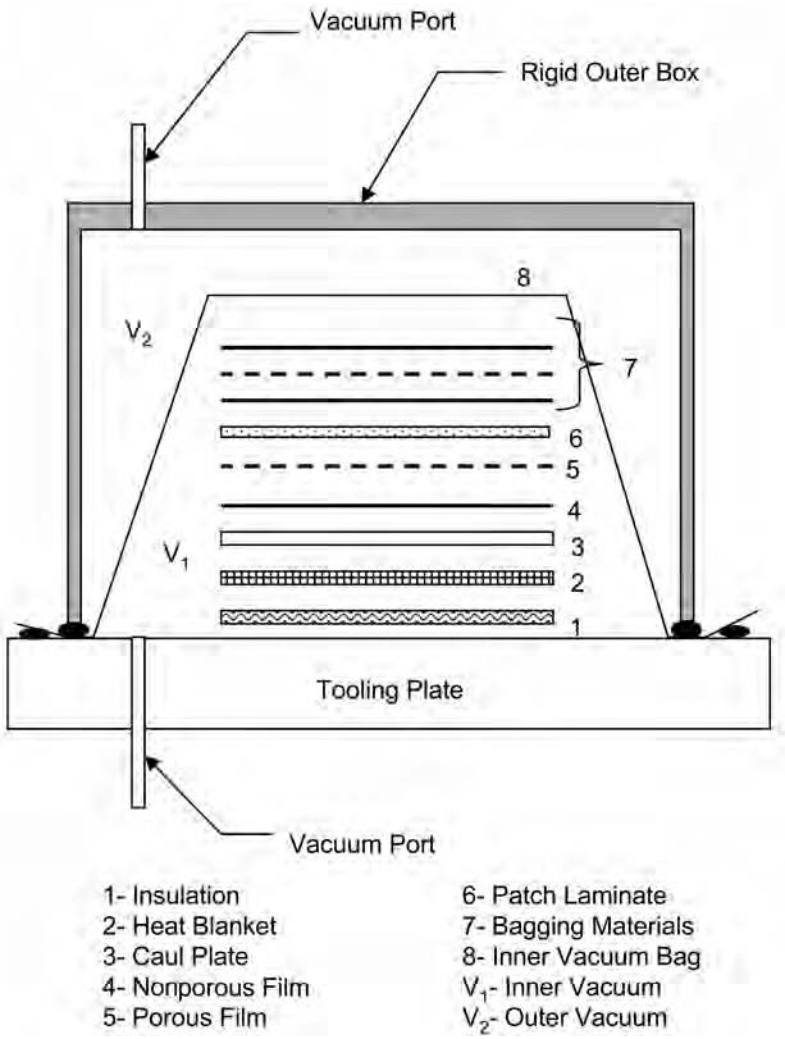


Fig. 19.15 Double-bag method for debulking prepreg and wet lay-up patches

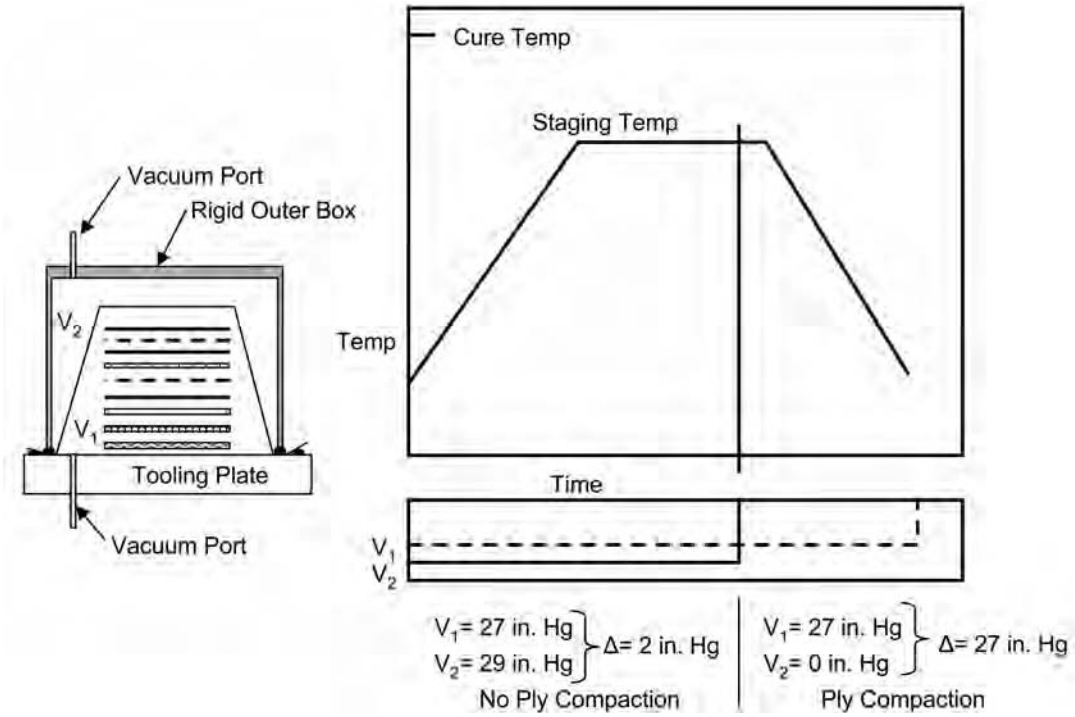


Fig. 19.16 Double-bag staging cycle

vacuum tends to draw volatiles out of the matrix and adhesive during heating and thereby cause voids, porosity, and frothy bondlines.

To improve the quality of vacuum bag cures, the patch (prepreg or wet lay-up) can be staged prior to cure using the double-bag technique shown in Fig. 19.15. A typical double-bag staging cycle is shown in Fig. 19.16. In this procedure, two vacuum bags are used. The inner vacuum is applied by a conventional nylon vacuum bag and the outer vacuum is applied to a hardback chamber. Since the vacuum levels are nearly equal, the outer vacuum applied in the hardback keeps the nylon inner vacuum from consolidating the plies—but at the same time, the inner-bag vacuum atmosphere allows the evacuation of any air and volatiles from the lay-up. The patch is then heated to the staging temperature to remove any volatiles that evolve at higher temperatures. The staging temperature depends on the resin system used, but it should be (1) high enough to allow volatiles to escape from between the plies (since there is no pressure pushing them together), yet (2) low enough that the resin does not gel. For example, the staging temperature for a 350 ºF (180 ºC) curing adhesive might be 240 to 260 ºF (115 to 130 ºC) for 30 minutes. After the staging cycle is completed, the outer vacuum on the hardback is released and the inner vacuum bag is thereby allowed to consolidate the plies. The patch is then cooled to below 150 ºF (70 ºC) before the pressure is released. After staging, the patch can be formed to the required contour by reheating with a hot air gun to soften the resin. The patch is then cured in the normal manner using a vacuum bag. This procedure greatly helps to reduce porosity and voids in cured patches. In addition, staging and embossing the film adhesive, as discussed in Chapter 8, "Adhesive Bonding," is useful in helping to remove entrapped air.

Heat for curing may be supplied by an autoclave, an oven, heat blankets, or heat lamps, depending on where and how the repair is performed. Autoclaves and ovens provide the best temperature control. As previously discussed, if a heat blanket is used, it is advisable to conduct a trial run to make sure that there is sufficient power and to identify any hot or cold spots. Heat blankets are available in a large range of sizes and coil designs that allow multiple blankets to be used if necessary to obtain uniform heating. Heat lamps are often used for simple repairs such as fill repairs or for preheating localized

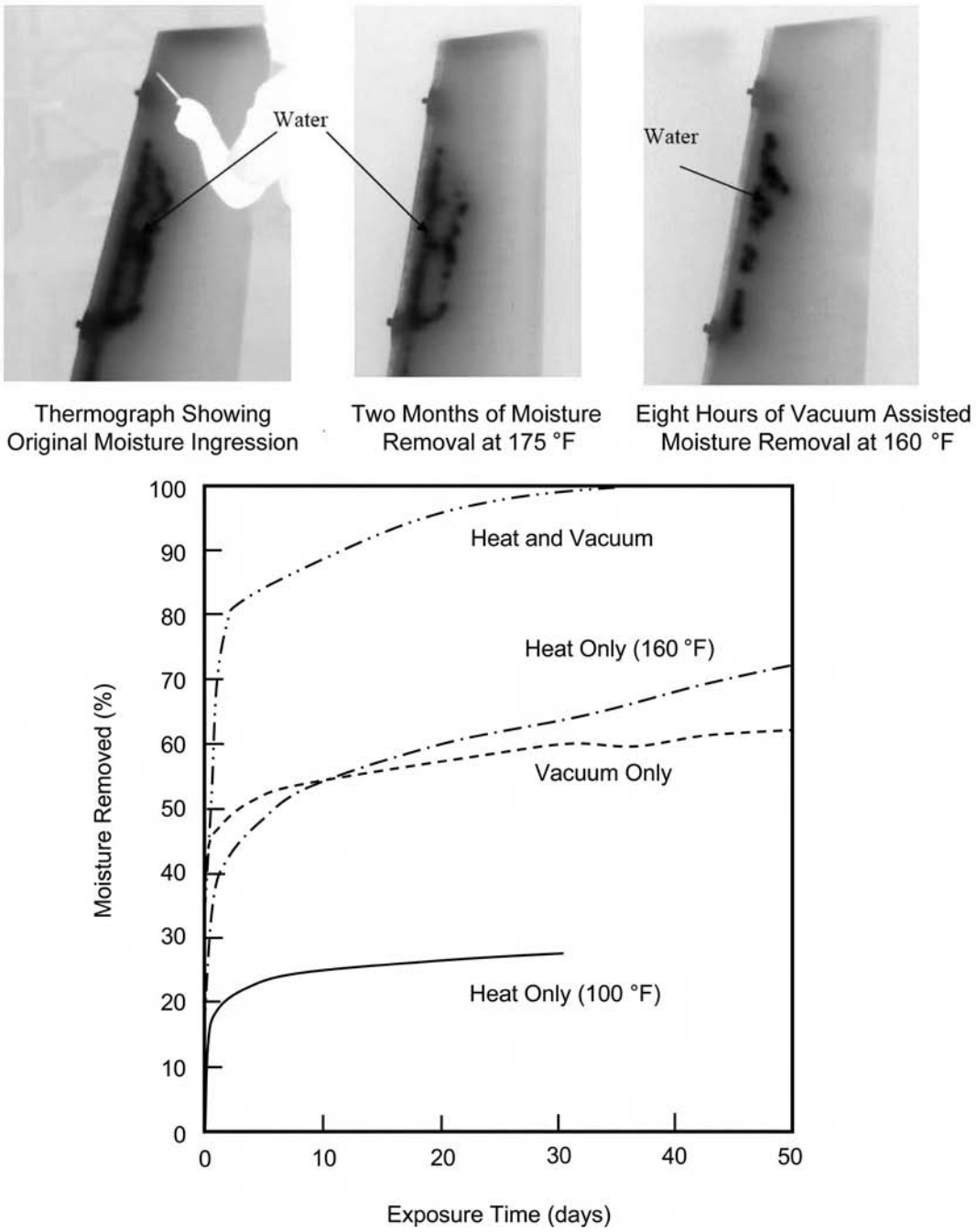


Fig. 19.17 Difficulty of removing moisture from honeycomb assemblies. Source: Ref 5

areas for injection repairs. In all cases, an ample number of thermocouples should be strategically placed so that the hottest and coldest areas are monitored. The cure temperature should be governed by the hottest thermocouple, and the cure time should be governed by the lagging or coldest thermocouple.

After the patch has been allowed to cure below 150 °F (70 °C) under pressure, it can be unbagged, cleaned up, inspected, sealed, and refin-

ished. Cleanup consists of removing all resin flash and sanding the patch area smooth. Flash-breaker release tape may be placed around the patch area before cure to minimize cleanup, but it should not be located so close to the top patch ply that it prevents filleting between the patch and the skin. During lay-up the adhesive film can be allowed to extend beyond the composite patch plies to ensure a good fillet. All bonded repair patches should be inspected after curing, using ultrasonic pulse echo to determine patch quality. If necessary, the patch can be sealed by painting it with a low-viscosity resin and then sanded when cured. The original finish system (primer and top coat) can then be applied.

Repairs of bonded honeycomb assemblies are similar to laminate repairs except that the honeycomb itself is often damaged and has to be replaced. Drying honeycomb assemblies is problematic. The drying cycle recommended for thin laminates at 200 ºF (90 ºC) for four hours may not be sufficient for honeycomb assemblies if there is water in the core. In fact, removing water from honeycomb assemblies is very difficult, as shown in Fig. 19.17. Even with both heat and vacuum, it took 30 days to remove the moisture from this particular assembly. Two points are important: (1) honeycomb assemblies should not be heated above 200 °F (90 ºC) during drying cycles because of the danger of steam pressure delamination, and (2) while vacuum will help remove liquid water from honeycomb assemblies, it will not help remove absorbed moisture from monolithic laminates since moisture removal from them depends on diffusion. The use of x-ray inspection can be helpful in looking for water, but it is difficult to detect small amounts. Moisture is one of the main reasons that many bonded repairs are unsuccessful.

A simple repair on a small area (Fig. 19.18) can often be accomplished by removing the damaged section of core and replacing it with a mixture of paste adhesive and milled glass fibers. After the filler cures, the surface should be scuff-sanded and a repair patch then bonded. If the damaged section is larger, it is necessary to remove the damaged core and replace it with an undamaged piece of the same density. Typical single- and double-sided repairs are shown in Fig. 19.19. Core can often be removed by slicing the cell walls with a sharpened putty knife and pulling pieces out with needle-nose pliers. The remainder can then be ground down to the film adhesive on the undamaged skin. Replacement core is usually bonded into the main core body

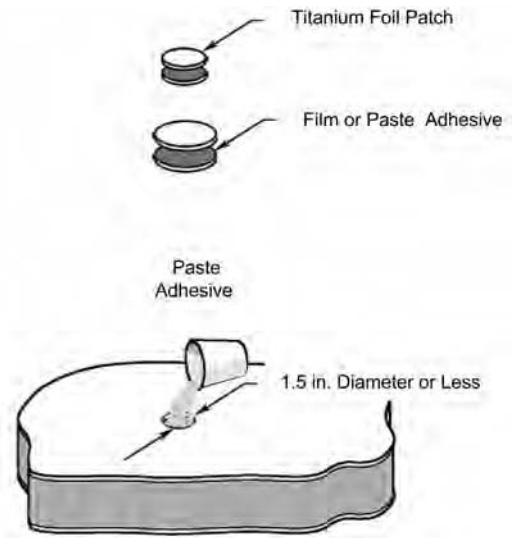


Fig. 19.18 Composite honeycomb minor repair. Source: Ref 1

with either a foaming or a paste adhesive. Foaming adhesives are normally used at the OEM and depot level, where ovens are available, because foaming adhesives froth excessively under vacuum; paste adhesives are usually used for field repairs. The core ribbon direction for the replacement section should match that of the remainder of the structure.

19.5 Metallic Details and Metal-Bonded Assemblies

If metallic details or metallic assemblies are being repaired by adhesive bonding, then all of the details must be chemically cleaned and primed using procedures like those outlined in Chapter 8, "Adhesive Bonding." However, there are procedures and materials that can be used for chemical cleaning for field repairs. While not generally as reliable as the production tank procedures, they are far superior to simple hand sanding or abrading.

A carbon/epoxy repair patch must never be hot-bonded to an aluminum assembly. The coefficients of thermal expansion are so different that the bonded patch will contain extremely high residual stresses, so high that it may even fail on cool-down from the cure temperature. For repairing aluminum assemblies, boron/epoxy prepreg has been used with good success.

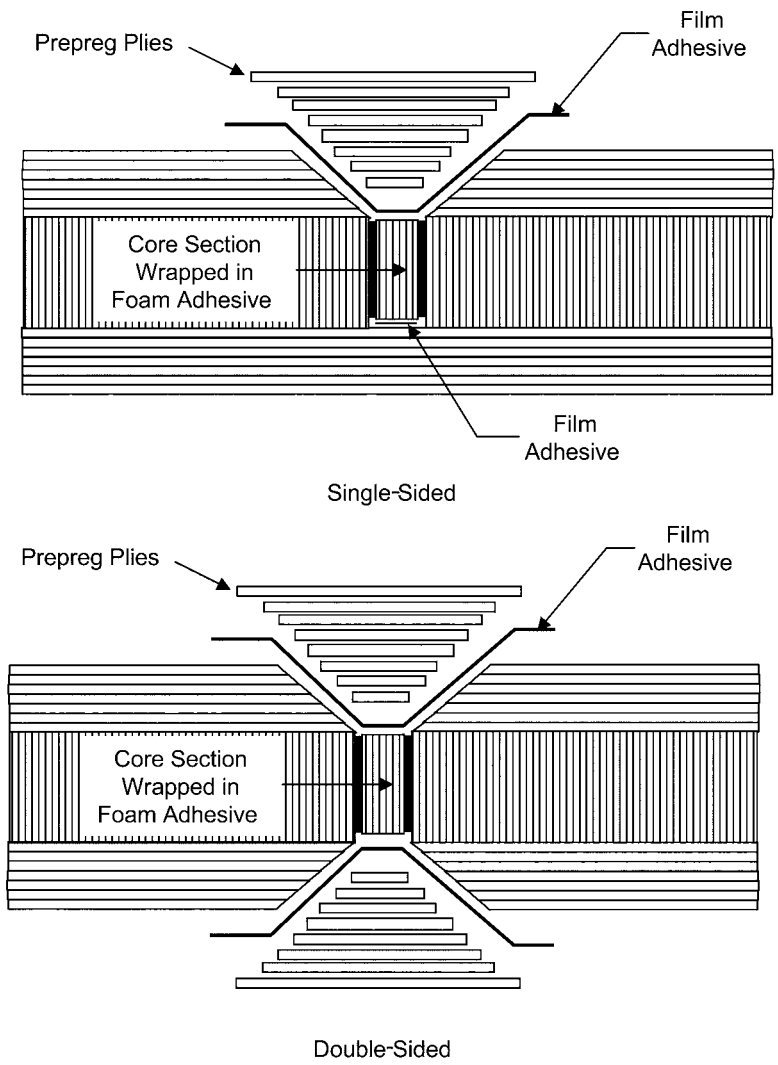


Fig. 19.19 Composite honeycomb bonded repairs

REFERENCES

1. R. Bohlmann, M. Renieri, G. Renieri, and Miller, "Advanced Materials and Design for Integrated Topside Structures," training course given to Thales in the Netherlands, 15–19 Apr 2002
2. R.E. Bohlmann, G.D. Renieri, and M. Libeskind, Bolted Field Repair of Carbon/Epoxy Wing Skin Laminates, *Joining of Composite Materials*, K.T. Kedward, Ed., STP 749, American Society for Materials, 1981, p 97–116
3. C.N. Duong and C.H. Wang, *Composite Repair—Theory and Design*, Elsevier, 2007
4. R.F. Wegman and T.R. Tullos, *Handbook of Adhesive Bonded Repair*, Noyes Publications, 1992
5. C. Li, R. Ueno, and V. Lefebvre, "Investigation of an Accelerated Moisture Removal Approach of a Composite Aircraft Control Surface," Society for the Advancement of Material and Process Engineering, 2006

SELECTED REFERENCES

- S.H. Ahn and G.S. Springer, "Repair of Composite Laminates," DOT/FAA/AR-00/46,

U.S. Department of Transportation/Federal Aviation Administration, 2000

- K.B. Armstrong and R.T. Barrett, *Care and Repair of Advanced Composites*, Society of Automotive Engineers, Inc., 1998
- Baker, F. Rose, and R. Jones, *Advances in the Bonded Repair of Metallic Aircraft Structure*, Vols 1 and 2, Elsevier Science Ltd., 2002
- "Composite Repair," Hexcel Composites, April 1998
- A.L. Seidl, Repair Aspects of Composite and Adhesively Bonded Aircraft Structures, *Handbook of Composites*, Chapman & Hall, 1998
- J.S. Tomblin, L. Salah, J.M. Welch, and M.D. Borgman, "Bonded Repair of Aircraft Composite Sandwich Structures," DOT/FAA/AR-03/74, U.S. Department of Transportation/Federal Aviation Administration, 2004

"*This page left intentionally blank.*"

Copyright © 2010, ASM International®
All rights reserved.
www.asminternational.org

CHAPTER 20

Metal Matrix Composites

METAL MATRIX COMPOSITES (MMCs) offer a number of advantages compared to their base metals, such as higher specific strengths and moduli, higher elevated-temperature resistance, lower coefficients of thermal expansion, and, in some cases, better wear resistance. However, due to their high cost, commercial applications for MMCs are few. There are some limited uses for discontinuously reinforced MMCs but almost no current applications for continuously reinforced MMCs.

In an MMC, the matrix phase is a monolithic alloy, usually a low-density nonferrous alloy, and the reinforcement consists of high-performance carbon, metallic, or ceramic additions. Metal matrix composites can be subdivided according to the type of reinforcement shown in Fig. 20.1. The reinforcement can be particulates (particles that are approximately equiaxed), high-strength single-crystal whiskers, short fibers that are usually random but can contain some degree of alignment, or long aligned multifilament or monofilament fibers.

Discontinuous reinforcements consist mainly of silicon carbide (SiC) in whisker (w) form; particulate (p) types of SiC, alumina (Al_2O_3), and titanium diboride (TiB_2); and short or chopped fibers (c) of Al_2O_3 or graphite. Particulate reinforced composites (Fig. 20.2), primarily SiC or Al_2O_3 ceramic particles in an aluminum matrix, are known as *discontinuously reinforced aluminum* (DRA). They exhibit high stiffness, low density, high hardness, and adequate toughness at volume percentages less than 25 percent, and are relatively low in cost. Normal volume percentages are 15 to 25 percent, with SiC_p particle diameters of 0.19 to 1.2 mil (3 to 30 μm). Discontinuously reinforced aluminum is usually manufactured by melt incorporation during casting or by powder blending and consolidation. The microstructure of a typical SiC_p DRA is shown in Fig. 20.3.

Metal matrix composites can also be reinforced with single-crystal SiC_w whiskers (Fig. 20.4) made by vapor deposition processes or from rice hulls. They have better mechanical properties than particulate-reinforced MMCs, but whiskers are more expensive than particles, they are more difficult to distribute uniformly in the matrix, and they raise health hazard concerns.

Short fibers are also used to reinforce MMCs; for example, Saffil short alumina fibers are used in aluminum matrices. Short fiber reinforced MMCs can also be produced by melt infiltration, squeeze casting, or powder blending/consolidation. Typical fiber lengths are a few micrometers to several hundred micrometers but are broken up during processing so that their aspect ratios (length/diameter) range from three to about 100.

Continuous-fiber reinforcements include graphite, SiC, boron, aluminum oxide (Al_2O_3), and refractory metal wires. Continuous reinforcements usually consist of small multifilaments or much larger monofilaments. Small multifilaments, typically less than 0.79 mil (20 μm) in diameter, usually consist of tows or bundles with thousands of fibers and are derived from textile materials, while monofilaments are much larger, ranging from 3.9 to 5.5 mil (100 to 140 μm) in diameter, and are made one filament at a time by chemical vapor deposition on a small substrate, normally tungsten wire or carbon fiber.

Large, stiff boron and silicon carbide monofilament fibers (Fig. 20.5) have been evaluated for high-value aerospace applications. Early work was conducted in the 1970s with boron or Borsic (a silicon carbide-coated boron fiber) reinforced aluminum for aircraft/spacecraft applications. Later work in the 1990s concentrated on SiC monofilaments in titanium (Fig. 20.6) for the

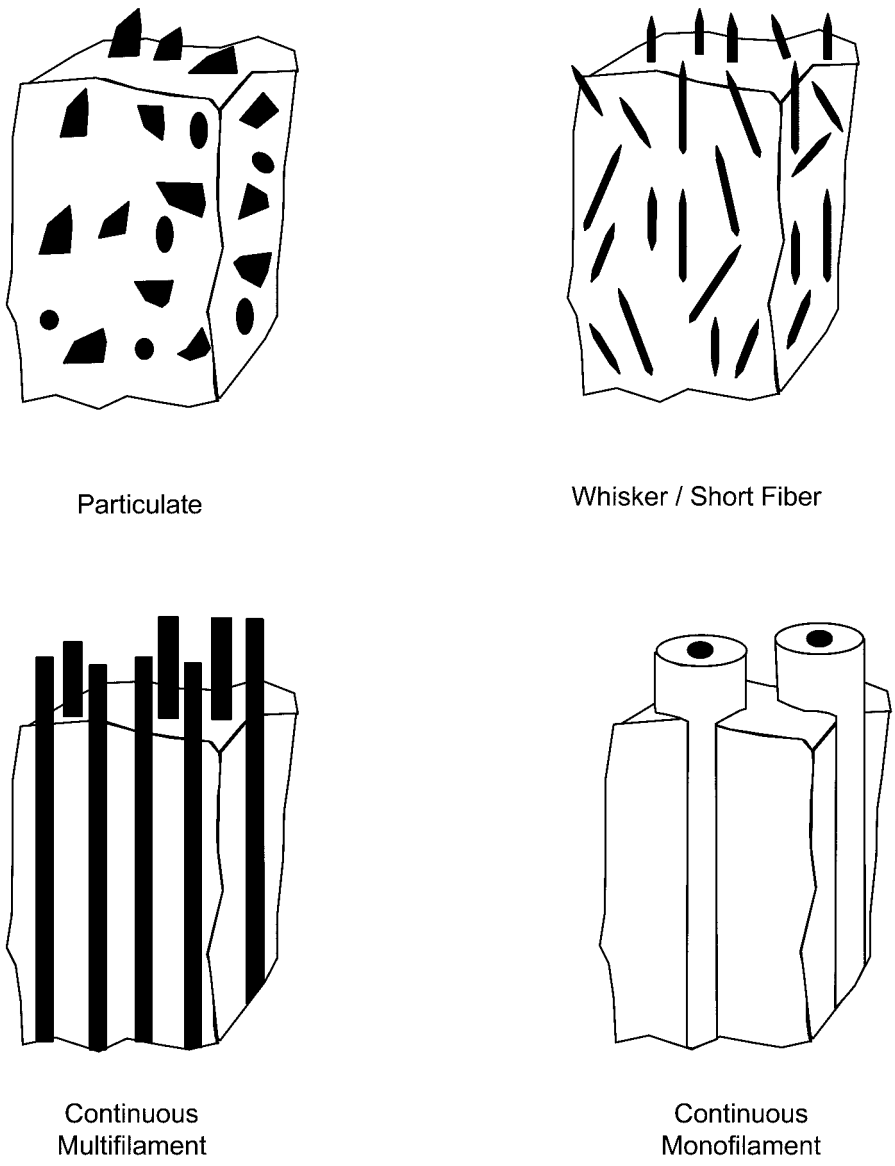


Fig. 20.1 Metal matrix composite reinforcements. Source: Ref 1

National Aerospace Plane. Potential applications are extremely high-temperature airframes and engine components. Multifilament fibers, such as carbon and the ceramic fibers Nextel (alumina based) and Nicalon (silicon carbide), have also been used in aluminum and magnesium matrices; however, the smaller and more numerous multifilament tows are difficult to impregnate using solid state processing techniques, such as diffusion bonding, because of their small size and the tightness of their tow construction. In addition, carbon fiber reacts readily with aluminum and magnesium during processing and can cause these matrices to corrode galvanically during service.

The primary MMC fabrication processes are often classified as either liquid phase or solid state. Liquid phase processing is generally considerably less expensive than solid state processing. Characteristics of liquid phase processed discontinuous MMCs include low-cost reinforcements such as silicon carbide particles, low-temperature melting matrices such as aluminum and magnesium, and near-net-shaped

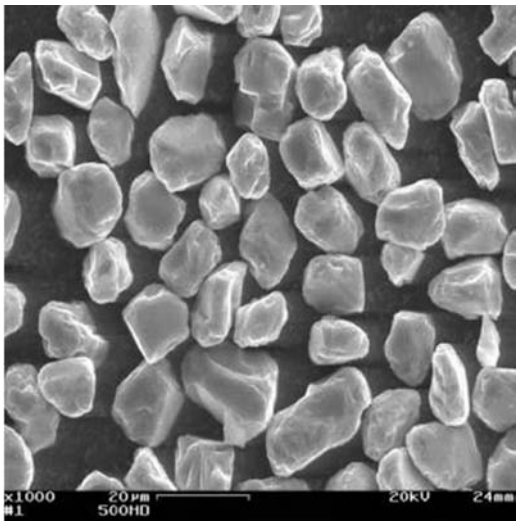


Fig. 20.2 Silicon carbide particulate

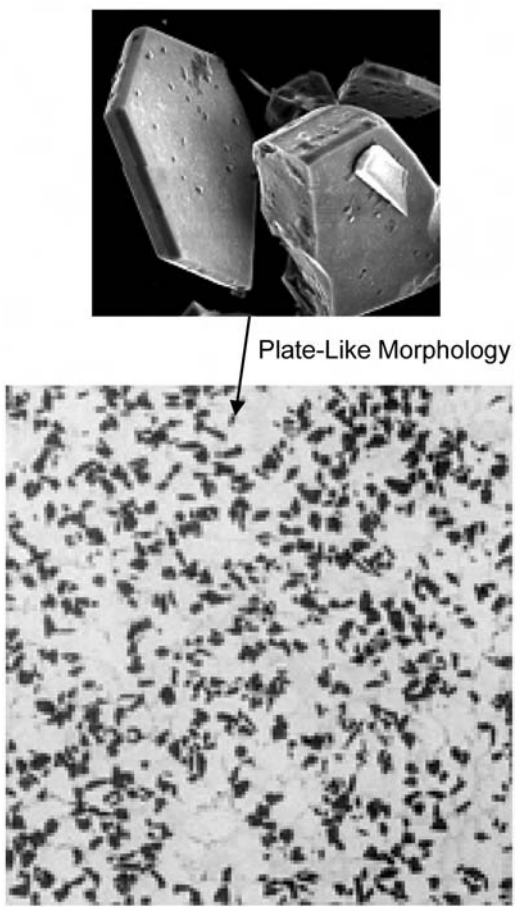


Fig. 20.3 Microstructure of 20 volume percent silicon carbide particulate discontinuously reinforced aluminum. Source: Ref 2,3

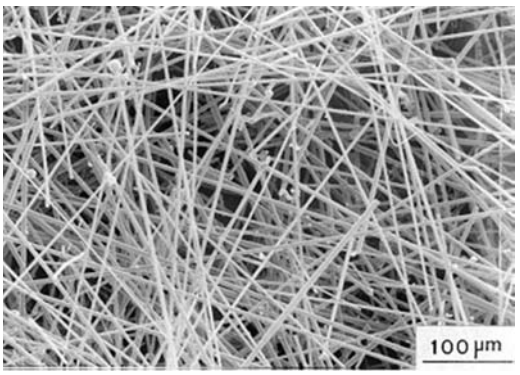


Fig. 20.4 Silicon carbide whiskers

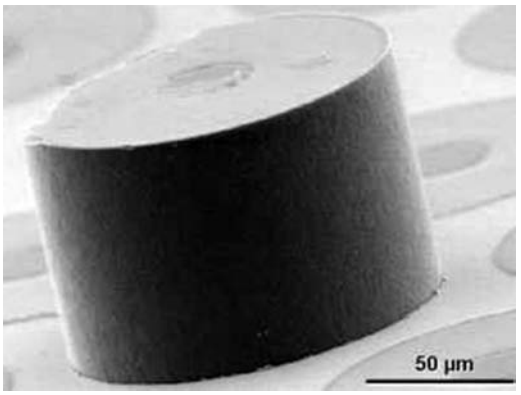


Fig. 20.5 Silicon carbide monofilament

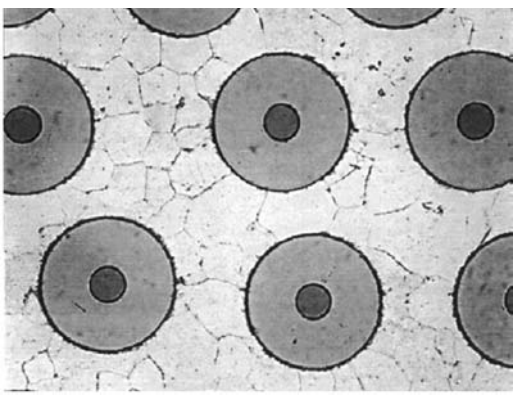


Fig. 20.6 Silicon carbide monofilament/titanium matrix composite

parts. Liquid phase processing results in intimate interfacial contact and strong reinforcement-to-matrix bonds, but can also result in the formation of brittle interfacial layers due to interactions with the high-temperature liquid matrix. Liquid

phase processes include various casting processes, liquid metal infiltration, and spray deposition. However, since continuous aligned fiber reinforcement is normally not used in liquid state processes, the strengths and stiffness are lower.

Solid state processes, in which no liquid phase is present, are usually associated with some type of diffusion bonding to produce final consolidation, whether the matrix is in a thin sheet or powder form. Although the processing temperatures are lower for solid state diffusion bonding, they are often high enough to cause significant reinforcement degradation. In addition, the pressures are almost always higher for the solid state processes. The choice of a fabrication process for any MMC is dictated by many factors, the most important being preservation of reinforcement strength; preservation of reinforcement spacing and orientation; promotion of wetting and bonding between the matrix and reinforcement; and minimization of reinforcement damage, due primarily to chemical reactions between the matrix and reinforcement.

20.1 Aluminum Matrix Composites

Most of the commercial work on MMCs has focused on aluminum as the matrix metal. Aluminum's combination of light weight, environmental resistance, and useful mechanical properties is attractive. The melting point is high enough to meet many applications, yet low enough to allow reasonable processing temperatures. In addition, aluminum can accommodate a variety of reinforcing agents. Although much of the early work on aluminum MMCs concentrated on continuous fibers, most of the present work is focused on discontinuously reinforced (particulate) aluminum MMCs because of their greater ease of manufacture, lower production costs, and relatively isotropic properties. The most common reinforcement materials in discontinuously reinforced aluminum composites are SiC and Al_2O_3, although silicon nitride (Si_3N_4), TiB_2, graphite, and others have also been used in some specialized applications. For example, graphite/aluminum MMCs have been developed for tribological applications due to their excellent antifriction properties, wear resistance, and antiseizure characteristics. Typical fiber volumes of discontinuous DRAs are usually limited to 15 to 25 percent because higher volumes result in low ductility and fracture toughness. The properties of common reinforcements for DRA composites are given in Table 20.1.

The influence of hard particle reinforcement (such as SiC) on the relevant mechanical and physical properties of DRAs can be summarized as follows:

- Both the ultimate tensile strength and yield strength increase with an increase in reinforcement fraction.
- The fracture toughness, ductility, percent elongation, and strain-to-failure decrease with an increase in reinforcement volume fraction.
- The modulus of elasticity increases with an increase in reinforcement volume fraction.
- The thermal and electrical conductivities and the coefficient of thermal expansion decrease with increasing reinforcement volume fraction.

A number of physical and mechanical properties of SiC_p DRA composites, as a function of reinforcement volume percent, are shown in Fig. 20.7. Note that the strength and stiffness increase with increasing volume percent, while the elongation and fracture toughness decrease. The thermal and electrical conductivity and the coefficient of thermal expansion all decrease with increasing percentages of reinforcement. Due to their reinforcement, DRA composites also retain a greater percentage of their strength and stiff-

Table 20.1 Common reinforcements for discontinuous aluminum composites

	Reinforcement				
Property	**SiC_p**	**Al_2O_{3p}**	**TiB_{2p}**	**Al_2O_{3c}(a)**	**SiC_w(b)**
Density, g/cm^3	3.21	3.97	4.5	3.3	3.19
Diameter, *u*m	. . .	. . .	. . .	3–4	0.1–1.0
Coefficient of thermal expansion, $10^{-6} \cdot K^{-1}$	4.3–5.6	7.2–8.6	8.1	9	4.8
Tensile strength, ksi	14.5–116(c)	10–145(c)	101.5–145(c)	>290	435–2030
Young's modulus, msi	29–70	55	75–83	43.5	58–101.5
Elongation, %	. . .	. . .	. . .	0.67	1.23

(a) Saffil (96%Al_2O_3–4%SiO_2) (b) >98% SiC (c) Transverse rupture strength of bulk material. Source: Ref 2

ness at elevated temperatures compared to their base metals (Fig. 20.8).

Because more aluminum MMCs are produced than all other MMCs combined, the Aluminum Association developed a standard designation system for aluminum MMCs that has since been adopted by the American National Standards Institute. ANSI 35.5-1992 uses the following format:

matrix/reinforcement/volume percent form

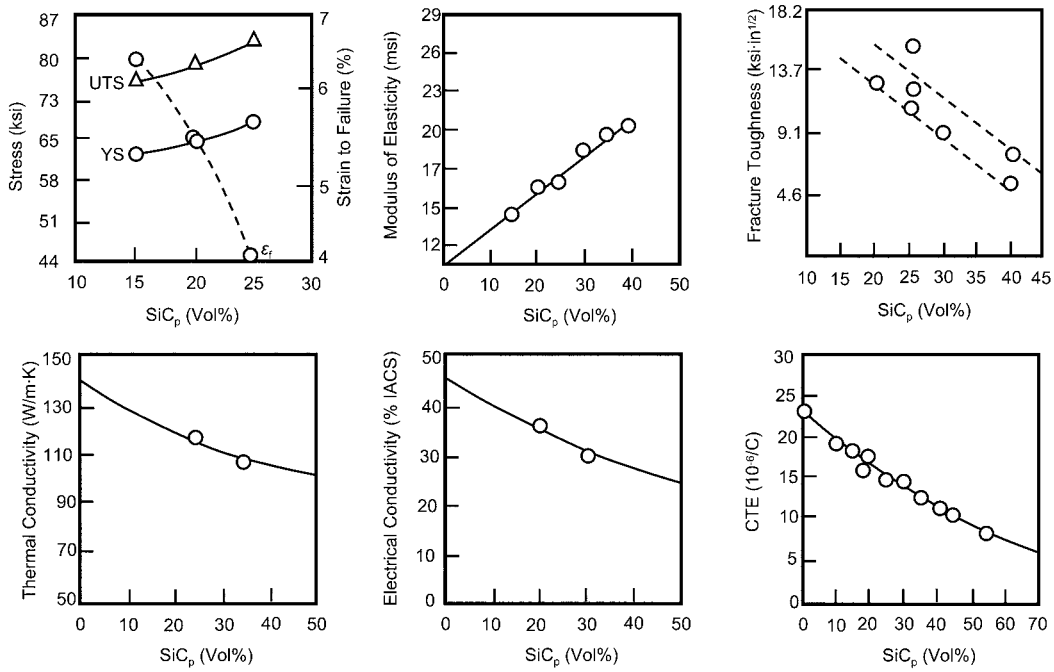


Fig. 20.7 Properties of silicon carbide particulate (SiC_p) discontinuously reinforced aluminum composites. CTE, coefficient of thermal expansion; International Annealed Copper Standard (IACS). Source: Ref 2

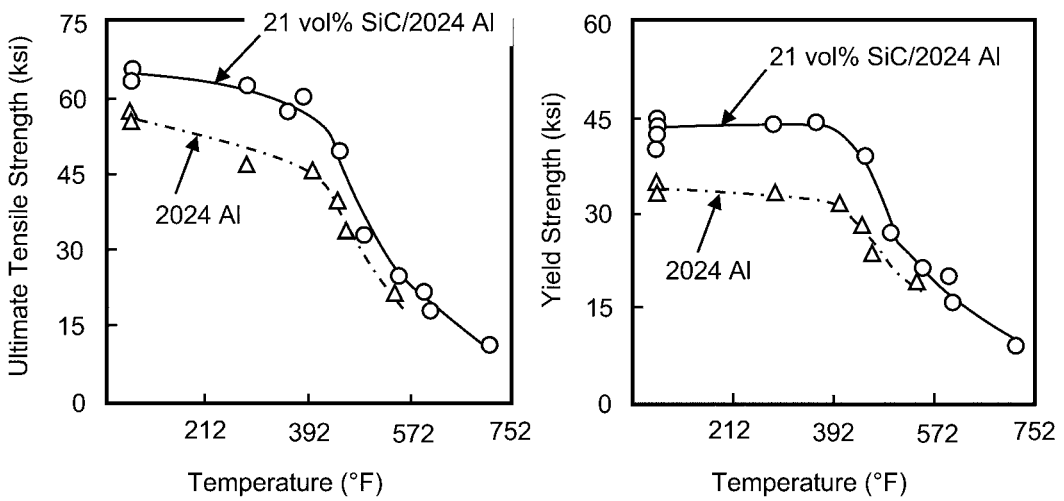


Fig. 20.8 Elevated-temperature properties of silicon carbide (SiC) particulate discontinuously reinforced aluminum (Al) composites. Source: Ref 4

For example, 2124/SiC/25w describes alloy 2124 reinforced with 25 volume percent of silicon carbide whiskers; 7075/Al_2O_3/10p is the alloy 7075 reinforced with 10 volume percent of alumina particles; 6061/SiC/47f is the alloy 6061 reinforced with 47 volume percent of continuous SiC fibers; and A356/C/05c is the casting alloy A356 reinforced with 5 volume percent of chopped graphite fibers.

20.2 Discontinuous Composite Processing Methods

A relative comparison of composite performance with materials and process technologies for a number of MMCs is shown in Fig. 20.9. Continuous fiber MMCs offer the highest performance but also the highest cost, while discontinuous MMCs, in particular those made by casting processes, have lower properties but also much lower costs. Processing methods for discontinuous MMC composites include various casting processes, liquid metal infiltration, spray deposition, and powder metallurgy. A wide range of conventional as well as specialized aluminum casting processes has been explored for DRAs. Casting is currently the least expensive method of producing MMCs and lends itself to the production of large ingots, which can be further worked by extrusion, hot rolling, or forging. In any casting process, reinforcement wetting and distribution are important processing parameters. In addition, any mechanical process, such as blending or stirring, which severely abrades short fibers, will tend to break them up and reduce their aspect ratios.

20.3 Stir Casting

In casting of metal matrix composites, the reinforcement is incorporated into the molten metal matrix as loose particles or whiskers. Because most metal reinforced systems exhibit poor wetting, the mechanical force produced by stirring is required to combine the phases. In stir casting, shown schematically in Fig. 20.10, the particulate/whisker/short-fiber reinforcement is mechanically mixed into a molten metal bath. A

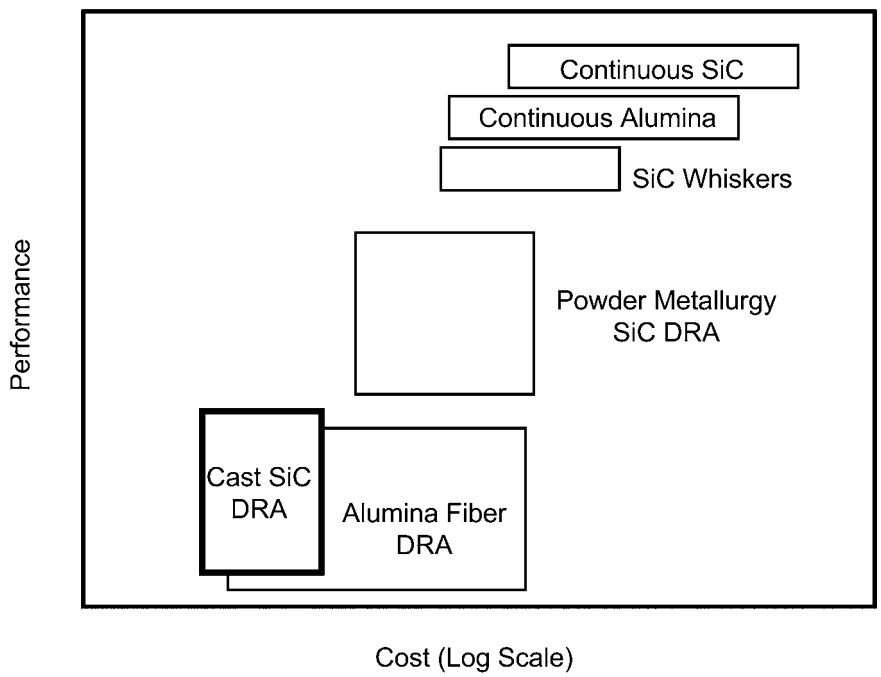


Fig. 20.9 Performance/cost trade-offs for metal matrix composites. DRA, discontinuously reinforced aluminum; SiC, silicon carbide. Source: Ref 4

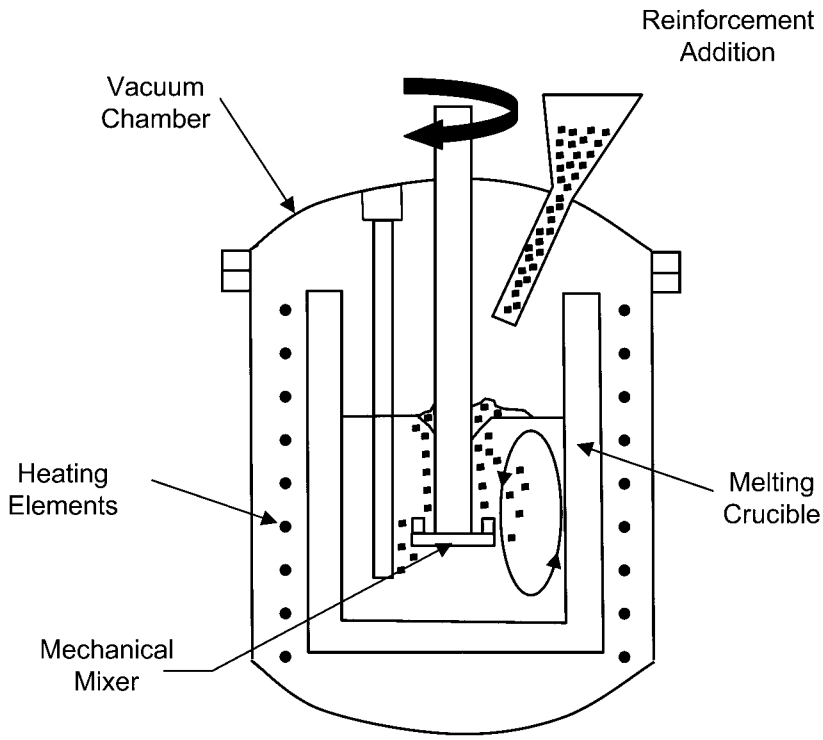


Fig. 20.10 Stir casting. Source: Ref 5

heated crucible is used to maintain the molten matrix at the desired temperature, while a motor drives a mixing impeller that is submerged in the molten matrix. The reinforcement is slowly poured into the molten matrix at a controlled rate to ensure a smooth, continuous feed. As the impeller rotates, it generates a vortex that draws the reinforcement particles into the melt from the surface. The impeller is designed to create high shear to strip adsorbed gases from the reinforcement surfaces. Shearing also helps to cover the reinforcement with molten matrix, promoting reinforcement wetting. Proper mixing techniques and impeller design are required to produce adequate melt circulation and a homogeneous reinforcement distribution. The use of an inert atmosphere or a vacuum is essential to avoid the entrapment of gases. A vacuum prevents the uptake of gases, eliminates the gas boundary layer at the melt surface, and eases the conditions for particle entry into the melt. Difficulties can include segregation/settling of the secondary phases in the matrix, particle agglomeration, particle fracture during stirring, and excessive interfacial reactions.

Good particle wetting is important. Adding particles, especially fibers, to the melt increases the viscosity. In general, ceramic particles are not wetted by the metallic matrix. Wetting can be enhanced by coating the reinforcement with a wettable metal that serves three purposes: (1) protects the reinforcement during handling, (2) improves wetting, and (3) reduces particle agglomeration. For example, the addition of magnesium to molten aluminum has been used to improve the wettability of alumina, and silicon carbide particles have been coated with graphite to improve their wettability in A356 aluminum. Effective wetting also becomes more difficult as the particle size decreases due to increases in surface energy, greater difficulty in dispersing due to increased surface area, and a greater tendency to agglomerate.

Microstructural inhomogeneities can occur due to particle agglomeration and sedimentation in the melt. Redistribution, as a result of the

reinforcements being pushed by an advancing solidification front, can also cause segregation. After mixing, reinforcement segregation can occur due to both gravity effects and solidification effects. The reinforcement, when it encounters a moving liquid/solid interface, may either be engulfed in the metal or it may be pushed by the interface into areas that solidify last, such as interdendritic regions. Because stir casting usually involves prolonged liquid-reinforcement contact, substantial interfacial reactions can result that degrade the composite properties and also increase the viscosity of the melt, making casting more difficult. In SiC_p/Al, the formation of Al_4C_3 and silicon can be extensive. The rate of reaction can be reduced—and even become zero—if the melt is silicon rich, either by prior alloying or as a result of the reaction. Therefore, stir casting of SiC_p/Al is well suited for high-silicon-content aluminum casting alloys but not for most wrought alloys.

Unreinforced liquid metals generally have viscosities in the range of 0.1 to 1.0 poise. Adding particles to a liquid metal increases the apparent viscosity because the particles interact with the liquid metal and with each other, resulting in more resistance to shear. Typical values are in the range of 10 to 20 poise for aluminum reinforced with 15 volume percent SiC_p. Because viscosity is a function of reinforcement percentage, shape, and size, an increase in volume fraction or a decrease in size will increase the viscosity of the slurry, often limiting the reinforcement level to about 30 volume percent.

Porosity in cast parts usually results from gas entrapment during mixing, hydrogen evolution, and/or shrinkage during solidification. Preheating the reinforcement before mixing can help remove moisture and trapped air between the particles. During casting, porosity can be reduced by (1) casting in a vacuum, (2) bubbling inert gas through the melt, (3) casting under pressure, and (4) deformation processing after casting to close the porosity. It has been observed that porosity in cast composites increases almost linearly with particle content.

Matrix alloys include aluminum-silicon casting compositions specially designed for MMC processing. Reinforcements include 0.39 to 0.79 mil (10 to 20 μm) SiC or Al_2O_3 particles with volume fractions ranging from 10 to 20 percent. The automotive industry is the main proponent of cast DRAs. Current or potential applications include brake rotors and drums, brake calipers, brake pad backing plates, and cylinder liners.

20.4 Slurry Casting—Compocasting

When a liquid metal is vigorously stirred during solidification, it forms a slurry of fine spherical solids floating in the liquid. Stirring at high speeds creates a high shear rate that tends to reduce the viscosity of the slurry, even at solid fractions as high as 50 to 60 percent volume. The process of casting a slurry, in which the liquid metal is held between the liquidus and solidus temperatures, is called *rheocasting*. The slurry can also be mixed with particulates, whiskers, or short fibers before casting. This modified form of rheocasting to produce near-net-shaped MMC parts is called *compocasting*. The particulate reinforcement becomes trapped in the slurry, helping to minimize segregation. Continued stirring then reduces the viscosity, resulting in a mutual interaction between the matrix melt and the reinforcement, which enhances wetting and bonding between the two.

Because their densities differ from that of the melt, reinforcements have a tendency to either float to the top or segregate near the bottom of the melt; the advantages of this process are the increase in apparent viscosity of the slurry and the prevention of settling by the buoyant action of the liquid metal. Continuous stirring of the slurry helps create intimate contact between the reinforcement and the matrix. Good bonding is achieved by reducing the slurry viscosity, as well as by increasing the mixing time. The slurry viscosity can be reduced by increasing the shear rate and by increasing the slurry temperature. Compocasting can be performed at temperatures lower than those conventionally employed in foundry practice during pouring, resulting in reduced thermo-chemical degradation of the reinforcement surface. The slurry can be transferred directly to a shaped mold prior to complete solidification, or it can be allowed to solidify in a billet or rod shape so that it can be reheated into a slurry for further processing by techniques such as die casting.

The melt reinforced slurry can be cast by gravity, die, centrifugal, or squeeze casting. A careful choice of casting technique, as well as the mold configuration, is important in obtaining a uniform distribution of reinforcements in compocast MMCs. Particles and discontinuous fibers of SiC, Al_2O_3, TiC, Si_3N_4, graphite, mica, glass, slag, magnesium oxide and boron carbide have been incorporated into vigorously agitated, partially solidified aluminum alloy slurries by compocasting.

20.5 Liquid Metal Infiltration

Liquid metal infiltration techniques normally consist of infiltrating a discontinuous-fiber preform with a liquid metal. A Saffil Al_2O_3 preform is shown in Fig. 20.11. Binders are frequently required to maintain preform integrity for handling. Binders (5 to 10 weight percent) can either be fugitive ones that are burned off during casting or high-temperature silica or Al_2O_3 compounds that require firing before casting.

20.5.1 Squeeze Casting

Squeeze casting is a metal-forming process in which solidification is accomplished under high pressure (Fig. 20.12) to help eliminate shrinkage porosity and reduce porosity by keeping gases dissolved in solution. Squeeze cast parts are usually fine-grained, with excellent surface finishes and almost no porosity. To produce MMCs, porous preforms of reinforcement material are infiltrated by molten metal under pressure. Reinforcement forms can be continuous fibers, discontinuous fibers, or particulates with aluminum or magnesium alloys. The volume fraction of reinforcement in the MMC can vary from 10 to 70 volume percent, depending on the particular application for the material.

Pressure is applied to the solidifying system by a hydraulically actuated ram. This process is similar to conventional die casting, except that the ram continues to apply pressure during solidification and the pressures are higher (usually in the range of 1.5 to 15 ksi) and applied slowly. High pressure helps to increase processing speed, producing finer matrix microstructures, and producing sounder castings by minimizing solidification shrinkage. To help minimize solidification shrinkage, the pressure is maintained until solidification is complete. If cold dies and reinforcements are used along with high pressures, chemical reactions between the liquid metal and reinforcement can be minimized due to the shorter processing cycles.

Squeeze casting is one of the most economical processes for fabricating MMCs and allows relatively large parts to be made. Squeeze casting is attractive because it minimizes material and energy usage, produces net shape components, and offers the capability for selective reinforcement. Both discontinuous and continuous aluminum-copper, aluminum-silicon, and aluminum-magnesium casting alloys reinforced with up to 45 volume percent SiC have been produced.

20.5.2 Pressure Infiltration Casting

Pressure infiltration casting (PIC) is similar to squeeze infiltration except that gas, rather than mechanical pressure, is used to promote consolidation. In PIC, an evacuated particulate or fiber preform with molten metal is subjected to

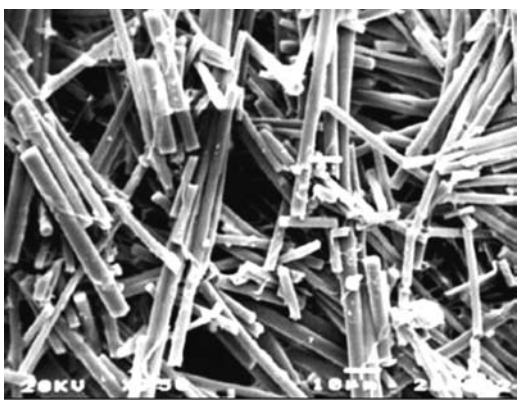


Fig. 20.11 Saffil alumina fiber preform

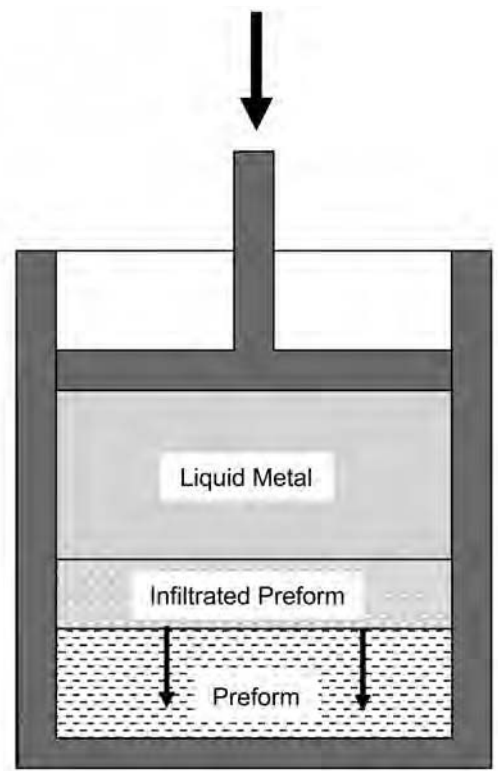


Fig. 20.12 Squeeze casting. Source: Ref 6

isostatically applied gas pressure, usually an inert gas such as argon, in the range of 150 to 1500 psi. The most common composite fabricated using the PIC process is discontinuously reinforced aluminum (DRA). Although there are several variations on the PIC process, all involve the infiltration of molten aluminum into a freestanding evacuated preform by an externally applied isostatic inert gas. Both the mold and the preform are evacuated, generally by placing the entire mold assembly in a vacuum/pressure vessel and evacuating both the mold and the vacuum/pressure chamber. After the mold is preheated and the aluminum melt has reached the desired superheat temperature, inert gas pressure in the range of 150 to 1500 psi is applied. As liquid aluminum infiltrates the preform, the pressure acting on the mold quickly approaches the isostatic state; therefore, the mold supports the pressure difference for only a very short period of time, so that large, expensive, and cumbersome molds are not needed. To minimize porosity, the mold is cooled directionally, and pressure is maintained until the entire casting is solidified.

Discontinuously reinforced aluminum fabricated using a preform provides a uniform reinforcement distribution with no segregation of the reinforcement during solidification. In PIC, the preform acts as a nucleation site for solidification and inhibits grain growth during solidification and cool-down, resulting in a very fine cast microstructure. In addition, because the preform is evacuated and the mold is directionally cooled, properly designed and processed components can be produced without porosity. Preforms have been fabricated and pressure infiltration cast in a range of reinforcement levels varying from 30 percent to greater than 70 percent. Current technology does not allow for lower reinforcement volume fractions, because the preform must have sufficient reinforcement content to produce a stable geometry. Pressure infiltration casting is used to make DRA electronic packages for integrated circuits and multichip modules. The benefits of DRA for this application include a controlled coefficient of thermal expansion that closely matches that of the integrated circuits and high thermal conductivity, which aids in the removal of the heat generated by the electronics.

20.5.3 Pressureless Infiltration

A pressureless metal infiltration process, called the *Primex process*, allows an aluminum alloy to infiltrate a reinforcement preform without the application of pressure or vacuum. The reinforcement level can be controlled by the starting density of the preform being infiltrated. As long as interconnected porosity and appropriate infiltration conditions exist, the liquid aluminum will spontaneously infiltrate the preform. Key process characteristics include an aluminum alloy, the presence of magnesium, and a nitrogen atmosphere. During heating to the infiltration temperature of 1380 °F (750 °C), magnesium reacts with the nitrogen atmosphere to form magnesium nitride (Mg_3N_2). Magnesium nitride is the infiltration enhancer that allows the aluminum alloy to infiltrate the reinforcing phase without the need of applied pressure or vacuum. During infiltration, Mg_3N_2 is reduced by the aluminum to form a small amount of aluminum nitride (AlN). The AlN forms small precipitates and a thin film on the surface of the reinforcing phase. Reinforcement loading can be as high as 75 volume percent, given the right combination of particle shape and size. The most widely used cast composite produced by liquid metal infiltration is an Al-10Si-1Mg alloy reinforced with 30 volume percent SiC_p. The only restriction in the selection of an aluminum alloy is the presence of magnesium to allow the formation of the Mg_3N_2. For SiC_p- containing systems, silicon must also be present in sufficient quantity to suppress the formation of Al_4C_3.

20.6 Spray Deposition

Spray atomization and deposition is a process in which a stream of molten metal is atomized into fine droplets of 11.8 mil (300 μm) or less using a high-velocity inert gas, usually argon or nitrogen, which is then deposited on a mold or substrate. When the particles impact the substrate, they flatten and weld together to form a high-density preform that can be subsequently forged to form a fully dense product. The production of MMCs by spray deposition can be accomplished by introducing particulates into the metal spray, leading to codeposition with the atomized metal onto the substrate. The process is a rapid solidification process because the metal experiences a rapid transition through the liquidus to the solidus, followed by slower cooling from the solidus to room temperature. Inherent in spray processes are composites with minimal reinforcement degradation, little segregation, and fine-grained matrices. The critical process parameters are the

initial temperature, size distribution, and velocity of the metal droplets; the velocity, temperature, and feed rate of the reinforcement; and the temperature of the substrate. In general, spray deposition methods are characterized by significant porosity levels. Careful control of the atomizing and particulate feeding conditions are required to ensure that a uniform distribution of particulates is produced within a typically 90 to 98 percent dense aluminum matrix.

Spray deposition was developed commercially by Osprey, Ltd., as a method of building up bulk material by atomizing a molten stream of metal with jets of cold gas. It has been adapted to particulate MMC production by injection of ceramic powder into the spray. The four stages in the Osprey method, shown in Fig. 20.13, are (1) melting and dispensing, (2) gas atomization, (3) deposition, and (4) collector manipulation. Induction heating is used to produce the melt that flows into a gas atomizer. Melting and dispensing is carried out in a vacuum chamber. The atomized stream of metal is collected on a substrate placed in the line of flight. Overspray is separated by a cyclone and collected. Among the notable microstructural features of Osprey MMC material are strong interfacial bonds, few or no interfacial reaction layers, and very low oxide contents. A major attraction of the process is its high rate of metal deposition.

The advantages of spray deposition processes include fine grain sizes and minimal reinforcement degradation. Disadvantages include high porosity levels and the resulting need to process these materials further to achieve full consolidation. In general, spray processes are more expensive than casting due to the longer processing times, the high costs of the gases used, and the large amount of waste powder that results from spraying.

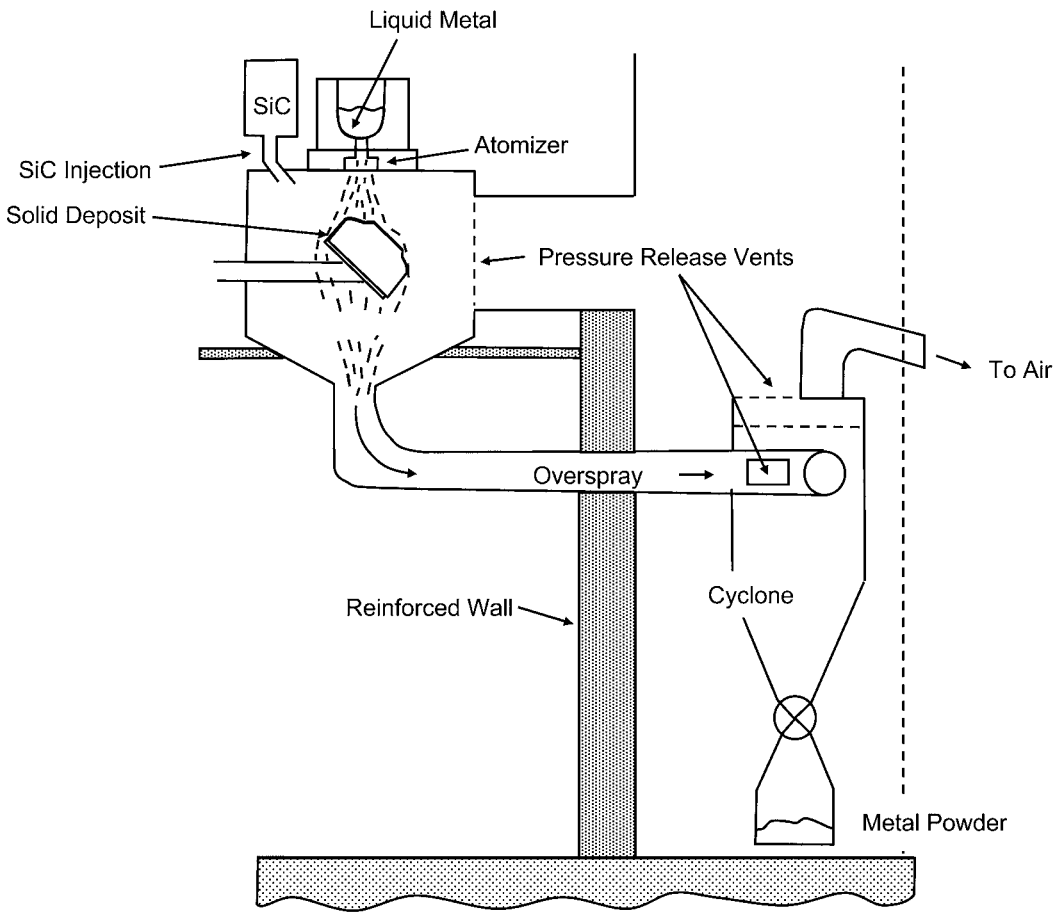


Fig. 20.13 Osprey spray process. Source: Ref 1

A number of aluminum alloys containing SiC particulates have been produced by spray deposition. These include aluminum-silicon casting alloys and wrought alloys of the 2xxx, 6xxx, 7xxx, and the aluminum-lithium alloys of the 8xxx series. Significant increases in specific moduli can be obtained with SiC-reinforced 8090 alloy. Products that have been produced by spray deposition include solid and hollow extrusions, forgings, sheet, and remelted pressure die castings.

20.7 Powder Metallurgy Methods

When higher-strength discontinuous MMCs are required, powder metallurgy (PM) processes are often used because segregation, brittle reaction products, and high residual stresses from solidification shrinkage can be minimized. In addition, with the advent of rapid solidification and mechanical alloying technology, the matrix alloy can be produced as a prealloyed powder rather than starting with elemental blends. Powder metallurgy processing can be used to make aluminum MMCs with both SiC particulates and whiskers, although Al_2O_3 particles and Si_3N_4 whiskers have also been employed. Processing, as shown in Fig. 20.14, involves (1) blending the gas-atomized matrix alloy and reinforcement in powder form; (2) compacting (cold pressing) the homogeneous blend to roughly 75 to 80 percent density; (3) degassing the preform (which has an open interconnected pore structure) to remove volatile contaminants (lubricants and mixing and blending additives), water vapor, and gases; and (4) consolidation by vacuum hot pressing or hot isostatic pressing. Then the consolidated billets are normally extruded, rolled, or forged.

The matrix and reinforcement powders are blended to produce a homogeneous distribution. Prealloyed atomized matrix alloy powder is mixed with the particulate or whisker reinforcement and thoroughly blended. Since the metal powder is usually 1.0 to 1.2 mil (25 to 30 μm) and the ceramic particulates are often much

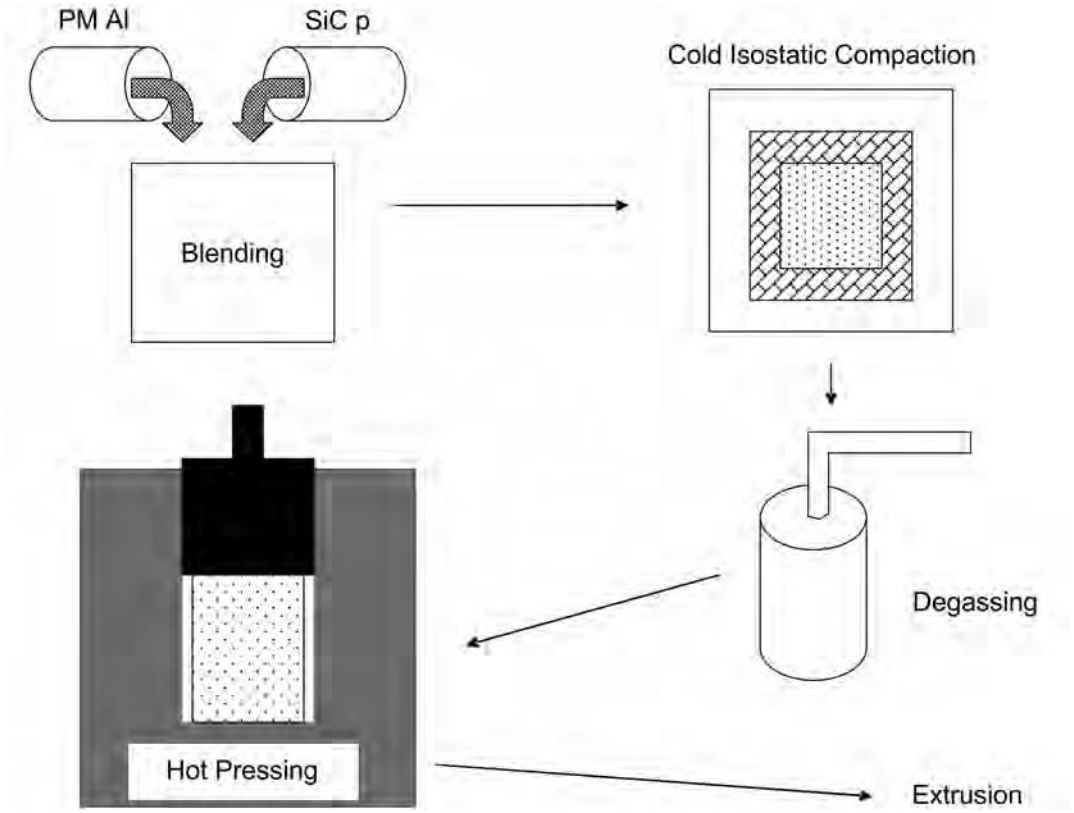


Fig. 20.14 Powder metallurgy processing. PM Al, powder metallurgy aluminum; SiC_p, silicon carbide particulate

smaller 0.04 to 0.20 mil (1 to 5 μm), the large size difference creates agglomeration of the particulates in the blend. Ultrasonic agitation can be used to break up the agglomerations. Dry blending is normally conducted in an inert environment. The blending stage is followed by cold pressing to produce what is called a *green body*, which is about 75 to 80 percent dense and can be easily handled.

The next step is hot pressing, either uniaxial or isostatic, to produce a fully dense billet. The hot pressing temperature can be either below or above that of the matrix alloy solidus. The powder blend is loaded into a metal can and evacuated at 750 to 930 °F (400 to 500 °C) to remove all air and volatiles. Evacuation times are long; times as long as 10 to 30 hours are not unusual. Outgassing removes adsorbed water from the reinforcement and matrix powder, chemically combined water, and other volatile species. After outgassing, the can is sealed. If a vacuum hot press is used, the canning and sealing processes are not necessary and the powder can be loaded directly into the press. Hot pressing or hot isostatic pressing (HIP) is normally conducted at as high a temperature as possible so that the matrix will be in its softest condition. Although liquid-phase sintering is normally not used due to grain boundary segregation and reinforcement degradation, a small amount of liquid phase allows the use of lower pressures. Another method is to consolidate the blend in a can to about 95 percent density by hot pressing, and then removing the can, and HIP to produce full density. Consolidation occurs by creep of the matrix material into the interstices between the reinforcement particles. When all the interconnected porosity is closed at about 90 percent density, diffusion closes the remaining porosity at triple points and grain boundaries. Powder metallurgy-processed billets are then normally extruded, forged, and/or hot rolled to produce useful shapes.

The PM technique generally produces properties superior to those obtained by casting and liquid metal infiltration (squeeze casting) techniques. Because no melting or casting is involved, the PM process offers several advantages. Conventional wrought alloys such as 2xxx, 6xxx, and 7xxx can be processed. A lower temperature can be used compared to that required for casting. This results in less interaction between the matrix and the reinforcement, minimizing undesirable interfacial reactions, which leads to improved mechanical properties. The distribution of particulate or whiskers is usually better when the PM method rather than casting is used. It is popular because it is reliable compared with alternative methods, but it also has some disadvantages. The blending step is a time-consuming, expensive, and potentially dangerous operation. In addition, it is difficult to achieve an even distribution of particulate throughout the product, and the use of powders requires a high level of cleanliness; otherwise, inclusions will be incorporated into the product, with a deleterious effect on fracture toughness and fatigue life.

20.8 Secondary Processing of Discontinuous MMCs

After full consolidation, many discontinuous reinforced MMCs are subjected to additional deformation processes to improve their mechanical properties and produce part shapes. Secondary deformation processing of discontinuously reinforced MMCs helps to break up reinforcement agglomerates, reduce or eliminate porosity, and improve the reinforcement-to-matrix bond.

Extrusion can generate fiber alignment parallel to the extrusion axis, but often at the expense of progressive fiber fragmentation. Due to the presence of 15 to 25 percent hard, nondeformable particulates or whiskers, fracture during extrusion can occur with conventional extrusion dies. Therefore, streamlined dies that gradually neck down are used to help minimize fracture. The degree of fiber fracture decreases with increasing temperature and decreasing local strain rate. Particulate segregation, in which particulate clusters occur next to regions containing little or no reinforcement, can also be a problem. For whisker-reinforced composites, whisker rotation and alignment with the metal flow direction can occur. In addition, the aspect ratio of whiskers is generally reduced due to the shearing action. To prevent extrusion-related defects, it is important that the material remain in compression during the extrusion process. Another microstructural feature of extruded MMCs is the formation of ceramic-enriched bands parallel to the extrusion axis. The mechanism of band formation is still unclear, but it appears to involve the concentration of shear strain in regions where ceramic particles or fibers accumulate. However, extrusion of consolidated MMCs, such as castings, can reduce the level of clustering and inhomogeneities in the material.

Hot rolling is used after extrusion to produce sheet and plate products. Because the compressive

stresses are lower in rolling than in extrusion, edge cracking can occur during rolling. To minimize edge cracking, discontinuous composites are rolled at temperatures around $0.5T_m$, where T_m is the absolute melting temperature, using relatively slow speeds. Isothermal rolling using light reductions and large-diameter rolls can also reduce cracking. Isothermal rolling is often conducted as a pack rolling operation in which the MMC is encapsulated by a stronger metal. During rolling, the outside of the pack cools while the interior containing the MMC remains at a fairly constant hot temperature. When the rolling temperature is low, light reductions and intermediate anneals may be required. As with extrusion, rolling further breaks up the particulate agglomerates. In heavily rolled sheet that has undergone about a 90 percent reduction in thickness, the particulate clusters are completely broken up and the matrix has flowed between the individual particles.

Processes such as rolling and forging, which involve the application of high strains, quickly can cause damage such as cavitation, particle fracture, and macroscopic cracking, particularly at low temperatures. In addition, very high temperatures increase the chance of matrix liquation, resulting in hot tearing or hot shortness. In contrast, HIP generates uniform stresses and therefore is unlikely to give rise to either microstructural or macroscopic defects. It is an attractive method for removing residual porosity. However, it can be very difficult to remove residual porosity in regions of very high ceramic content, such as within particle clusters, and the absence of any macroscopic shear stresses means that such clusters are not readily dispersed during HIP.

Machining discontinuous MMCs can be accomplished using circular saws and router bits. For straight cuts, diamond grit-impregnated saws with flood coolant produce good edges. For contour cuts, solid carbide router bits with a diamond-shaped chisel cut geometry or diamond-coated router bits can be used with good results. Due to the hard reinforcement particles, speeds and feeds for all machining operations must be adjusted. In general, the speed is reduced to minimize tool wear, while the feed is increased to obtain productivity before the tools wear. The higher the reinforcement content, the greater the tool wear, with wear generally being a bigger problem than excessive heat generation. Polycrystalline diamond cutting tools exhibit longer lives than either solid or diamond-coated carbide tools but are also more expensive. They also require a rigid setup to prevent edge chipping. Other methods, such as abrasive water jet cutting and wire electrical discharge machining, can also be used to produce acceptable cuts.

20.9 Continuous-Fiber Aluminum MMCs

As previously shown in Fig. 20.9, aluminum metal matrix composites (MMCs) reinforced with continuous fibers provide the highest strength and stiffness. Some mechanical properties of several aluminum matrix continuous-fiber MMCs are given in Table 20.2. In these data, only unidirectional properties are shown, which is a little misleading since cross-plied constructions are normally required for real-life applications. Of the reinforcements shown, boron and silicon carbide (SCS-2) are monofilaments and graphite and Nextel 610 are multifilaments. The smaller and more numerous multifilament tows are difficult to impregnate using solid state processing techniques, such as diffusion bonding, because of their small size and the tightness of their tow construction. One of the main advantages of both continuous-fiber aluminum and titanium matrix composites is their ability to be used at higher temperatures than their base metals (Fig. 20.15). However, because of their high cost, most applications have been limited, even in the aerospace industry.

Boron/aluminum (B/Al) was one of the first systems evaluated. Applications include the tubular truss members in the mid-fuselage structure of the Space Shuttle orbiter and cold plates in electronic microchip carrier boards. Boron was developed in the early 1960s and was initially

Table 20.2 Properties of continuous-fiber aluminum matrix composites

Property	B/6061 Al	SCS-2/ 6061 Al(a)	P100 Gr/ 6061 Al	Nextel 610/Al(b)
Fiber content, vol%	48	47	43.5	60
Longitudinal modulus, msi	31	29.6	43.6	35
Transverse modulus, msi	. . .	17.1	7.0	23.2
Longitudinal strength, ksi	220	212	79	232
Transverse strength, ksi	. . .	12.5	2	17.4

(a) SCS-2 is a silicon carbide fiber. (b) Nextel 610 is an alumina fiber. Source: Ref 2

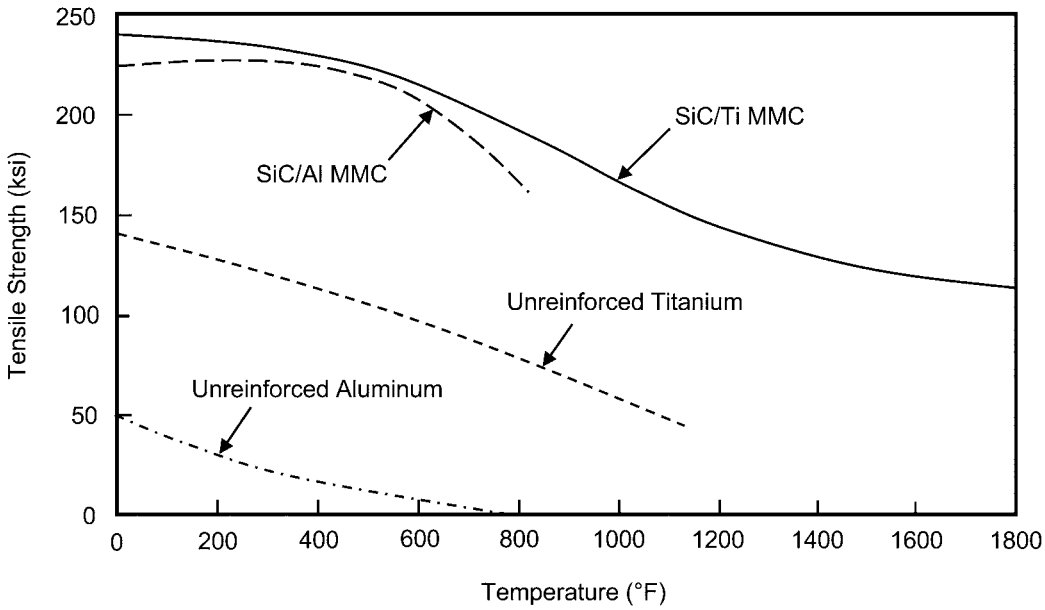


Fig. 20.15 Strength retention at elevated temperature for continuous fiber silicon carbide/aluminum (SiC/Al) and silicon carbide/titanium (SiC/Ti). MMC, metal matrix composite. Source: Ref 7

used successfully in an epoxy matrix on the F-14 and F-15 aircraft. Boron is made as a single monofilament using chemical vapor deposition, as shown schematically in Fig. 20.16. A 12.7 μm tungsten wire is drawn through a long glass reactor where boron trichloride (BCl_3) gas is chemically reduced to deposit boron on the tungsten core. Since this process produces a single 4 mil (101.6 μm) monofilament per reactor, many reactors (Fig. 20.17) are needed to produce production quantities. The process is inherently more expensive than those used for multifilament fiber forms, such as carbon fibers, in which as many as 12,000 fibers are made with a single pass through a reactor. Due to the high cost of continuous-fiber aluminum matrix composites and their limited temperature capabilities, the emphasis has shifted to continuous-fiber titanium matrix composites that have potential payoffs in hypersonic airframes and jet engine components. However, since many of the processing procedures originally developed for aluminum MMCs have been transitioned to titanium, a brief review of these methods will be given.

Early work with boron monofilament/aluminum matrix composites in the 1970s used primarily diffusion bonding. Several methods, shown in Fig. 20.18, were developed for producing single-layer B/Al sheets called *monotapes* that were provided by material suppliers. The original single-ply monotapes were generally made by winding the boron fiber on a drum, applying aluminum foil over the wound fibers, and then securing the fibers with an organic binder. The material supplier then diffusion bonded each monotape layer in a vacuum hot press. These diffusion-bonded monotapes were supplied to the user, who layed up multilayer laminates and diffusion bonded them together. A typical diffusion bonding cycle for B/Al is 950 to 1000 °F (510 to 535 °C) at 1000 to 3000 psi (7 to 21 MPa) for 60 minutes, and a typical microstructure is shown in Fig. 20.19. However, it was soon recognized that the boron fiber could react with aluminum during processing, forming brittle intermetallic compounds at the fiber interface, which degraded the fiber strength properties. Strong interfacial bonding led to reduced longitudinal tensile strengths but higher transverse strengths, while weaker interfacial bonding resulted in higher longitudinal but lower transverse strengths.

Other methods of making monotape included placing a layer of aluminum foil on a mandrel, followed by filament winding the boron fiber over the foil in a collimated manner. An organic fugitive binder, such as an acrylic adhesive, was used to maintain the fiber spacing and alignment once the preform was cut from the mandrel. In this method, often called the *green tape* method (Fig. 20.20), the fibers were normally wound

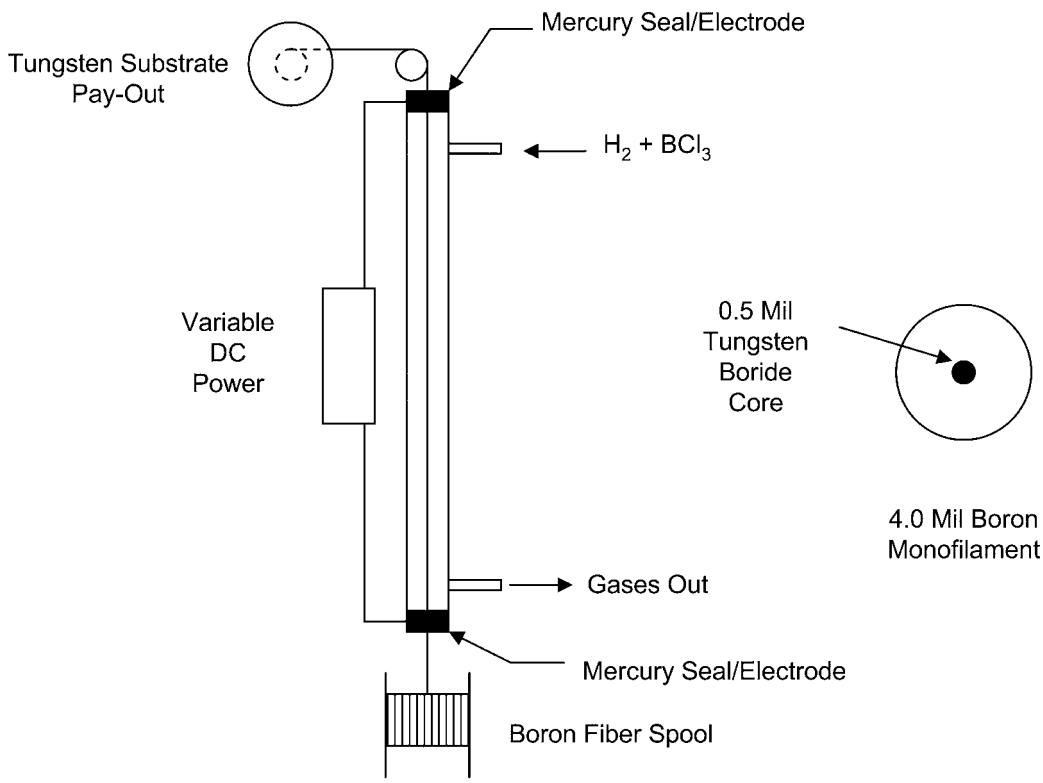


Fig. 20.16 Boron monofilament manufacture. BCl_3, boron trichloride

onto a foil-covered rotating drum and oversprayed with resin, followed by cutting the layer from the drum to provide a flat sheet of monotape. Since this product form contains a fugitive organic binder, it must be removed by outgassing before diffusion bonding. A typical process would be to place the vacuum pack between the platens of a hot press, apply a small load to hold the fibers in place, heat under vacuum to an intermediate level, and hold at that temperature until the binder is outgassed.

Plasma spraying was another method developed for B/Al monotapes. In this process, a mandrel was again covered with a thin layer of aluminum and fibers were wound onto the drum. The fibers were then plasma sprayed with the aluminum matrix material to produce a somewhat porous monotape. The spraying operation was carried out in a controlled atmosphere to minimize matrix oxidation. The advantages of this process were that no organic binders were required that could potentially lead to contamination problems, and no diffusion bond cycle was required to produce the monotape, which lessened the potential for fiber degradation.

With the advent of boron fiber coated with a thin layer of SiC (Borsic) to minimize fiber degradation during processing, a variant of the plasma-sprayed material was offered in which the thin aluminum foil next to the drum surface was replaced with a thin layer of 713 aluminum alloy braze foil. Although the processing temperatures required for braze bonding were somewhat higher than those for diffusion bonding, the pressures were far less. A typical consolidation cycle was 1080 °F (580 °C) for 15 minutes at less than 300 psi (2 MPa). A disadvantage of both plasma-sprayed product forms was that the monotape was extremely stiff and had a tendency to curl due to the residual stresses introduced during plasma spraying, and therefore required vacuum annealing prior to forming structural shapes.

In the 1980s, continuous SiC monofilaments largely replaced boron because they have similar properties and are not degraded by hot aluminum during processing. The SCS-2 SiC monofilament, which was tailored specifically for aluminum matrices, has a 0.04 mil (1 μm) thick carbon-rich coating that increases in silicon



Fig. 20.17 Boron monofilament reactor banks. Source: Specialty Materials Inc.

content toward its outer surface. Hot molding was a low-pressure, hot pressing process designed to fabricate SiC/Al parts at significantly lower cost than was possible with solid state diffusion bonding. Because the SCS-2 fibers can withstand molten aluminum for long periods, the molding temperature could be raised into the liquid-plus-solid region of the alloy to ensure aluminum flow and consolidation at low pressure, thereby eliminating the need for high-pressure die molding equipment. A plasma-sprayed aluminum preform was laid into the mold, heated to near molten aluminum temperature, and pressure consolidated in an autoclave by a metallic vacuum bag. SiC/Al MMCs exhibit increased strength and stiffness compared to unreinforced aluminum, with no weight penalty. In contrast to the base metal, the composite retains its tensile strength at temperatures up to around 500 °F (260 °C).

Graphite/aluminum (Gr/Al) MMCs were developed primarily for space applications where high-modulus carbon or graphite multifilaments could be used to produce structures with high stiffness, low weight, and little or no thermal expansion over large temperature swings. Unidirectional high-modulus graphite P100 Gr/6061 aluminum tubes exhibit an elastic modulus in the fiber direction significantly greater than that of steel, with a density approximately one-third that of steel. In addition, carbon and graphite fibers quickly became less expensive than either boron or SiC monofilaments. However, Gr/Al composites are difficult to process: (1) the carbon fiber reacts with the aluminum matrix during processing, forming Al_4C_3, which acts as a crack nucleation site leading to premature fiber failure; (2) molten aluminum does not effectively wet the fiber; and (3) the carbon fiber oxidizes during processing. In addition, Gr/Al parts can be subject to severe galvanic corrosion if they are used in a moist environment. Two processes have been used for making Gr/Al MMCs: liquid metal infiltration of the matrix on spread

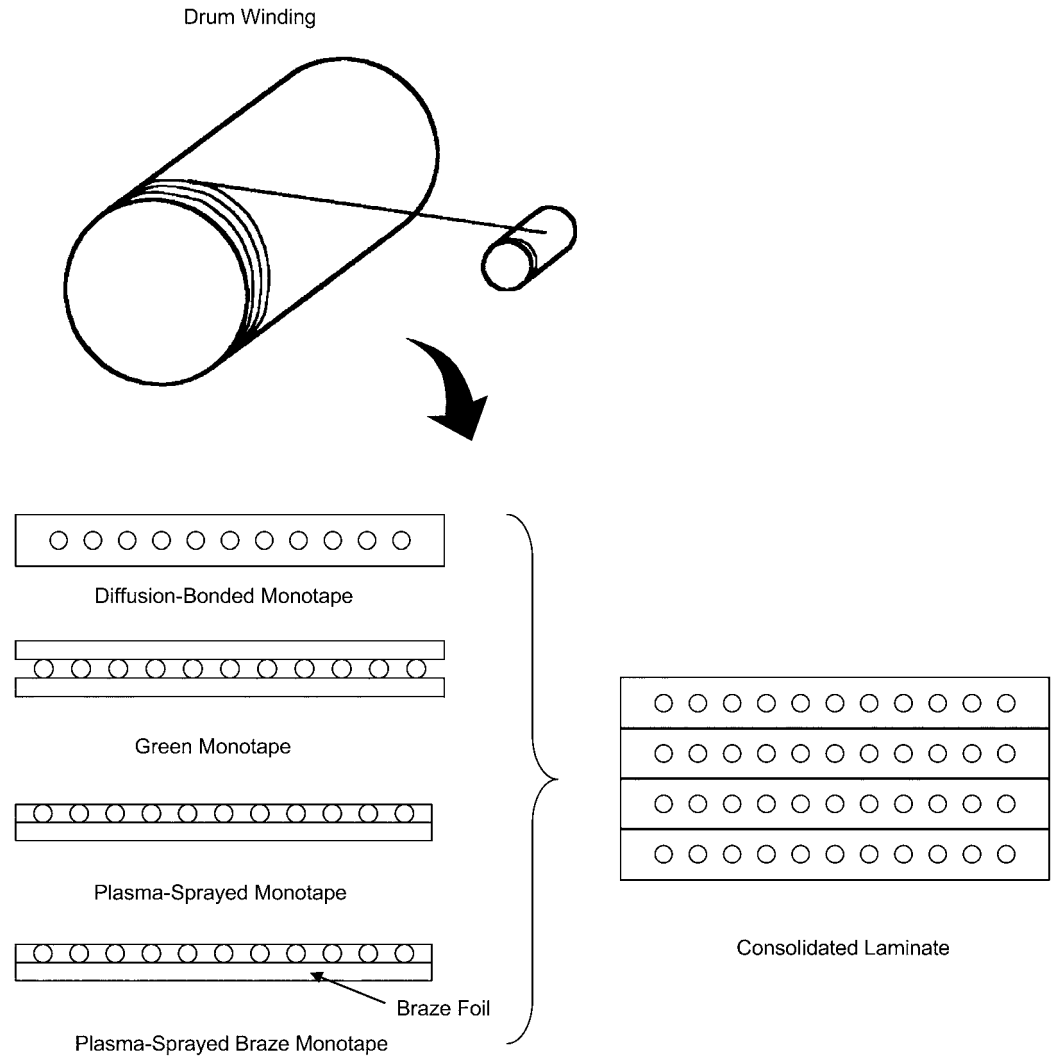


Fig. 20.18 Metal matrix composite monotape product forms

tows and hot press bonding of spread tows sandwiched between thin sheets of aluminum.

Alumina (Al_2O_3)/aluminum MMCs have been fabricated by a number of methods, but liquid or semisolid state processing techniques are commonly used. The 3M Company produces a material by infiltrating Nextel 610 Al_2O_3 fibers with an aluminum matrix at a fiber volume fraction of 60 percent. A fiber-reinforced aluminum MMC is used in pushrods for high-performance racing engines. Hollow pushrods of several diameters are produced; the fibers are axially aligned along the pushrod length. Hardened steel end caps are then bonded to the ends of the MMC tubes.

20.10 Continuous-Fiber Reinforced Titanium Matrix Composites

Continuous monofilament titanium matrix composites (TMCs) offer the potential for strong, stiff, lightweight materials at usage temperatures as high as about 1500 °F (815 °C) (Fig. 20.15). The principal applications for this class of materials are for hot structures, such as hypersonic airframe structures, and for replacing superalloys in some portions of jet engines. However, the use of TMCs has been restricted by the high cost of the materials, fabrication, and assembly procedures.

Specialty Materials' SCS-6 SiC fiber is the fiber most often used in continuous reinforced TMCs. SCS-6 is made in a manner very similar to that of boron fiber. A small-diameter carbon substrate of 1.3 mil (33 μm) in diameter is resistively heated as it passes through a long glass reactor, and SiC is chemically vapor deposited. A gradated carbon-rich SiC protective coating is then applied to help slow the interaction between the fiber and the titanium matrix, both during processing and later during elevated-temperature service. If the metal matrix and the fiber surface interact extensively during processing or elevated-temperature usage, the fiber surfaces can develop brittle intermetallic compounds, and even surface notches, which drastically lower the fiber tensile strength. A photomicrograph of a consolidated SCS-6 TMC laminate is shown in Fig. 20.21. In the insert, the protective carbon coating on the fiber is visible along with a small reaction layer. Typical properties of 5.6 mil (142 μm) diameter SCS-6 fiber include a tensile strength of 550 ksi (4 GPa), a modulus of 58 msi (400 GPa), and a density of 0.11 lb/in.^{3} (3 g/cm^3). Some typical properties of a SCS-6/Ti-6Al-4V composite with unidirectional fiber orientation are listed in Table 20.3.

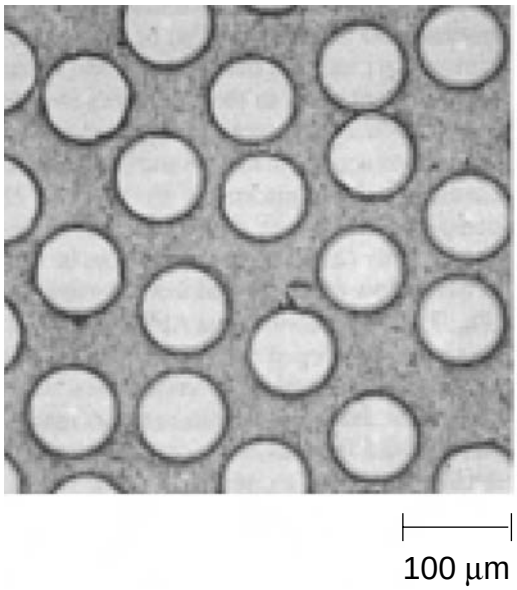


Fig. 20.19 Monofilament boron/aluminum composite. Source: Ref 4

Two other small-diameter SiC fibers, SCS-9 and Sigma, have also been evaluated as reinforcements for TMCs. The SCS-9 fiber, also made by Specialty Materials, is basically the

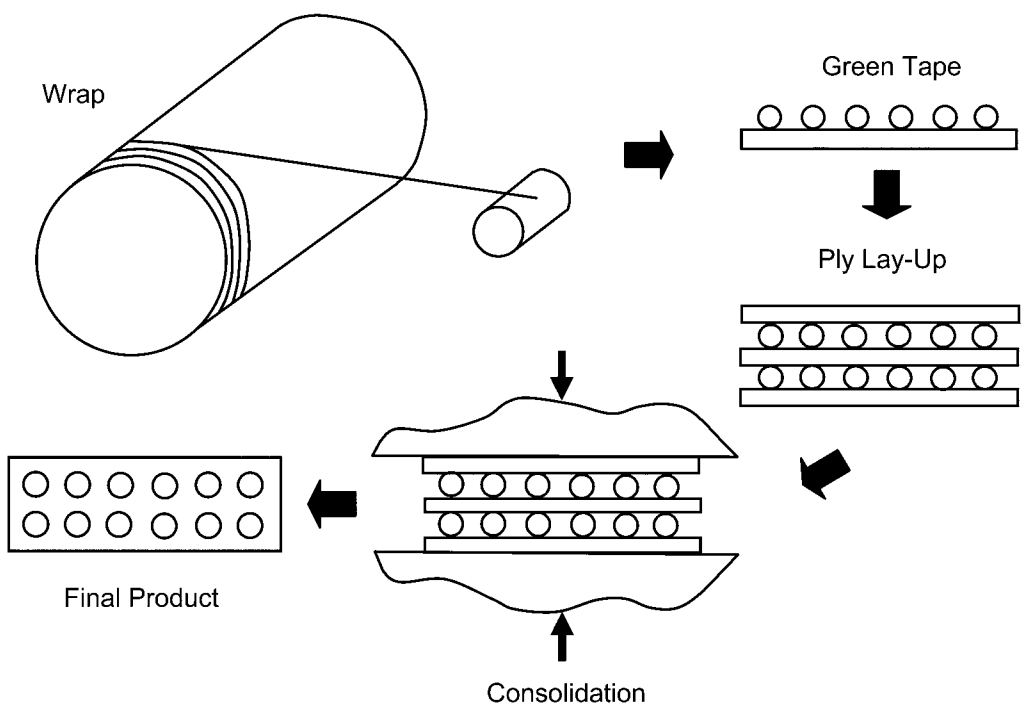


Fig. 20.20 Green tape method for MMC fabrication

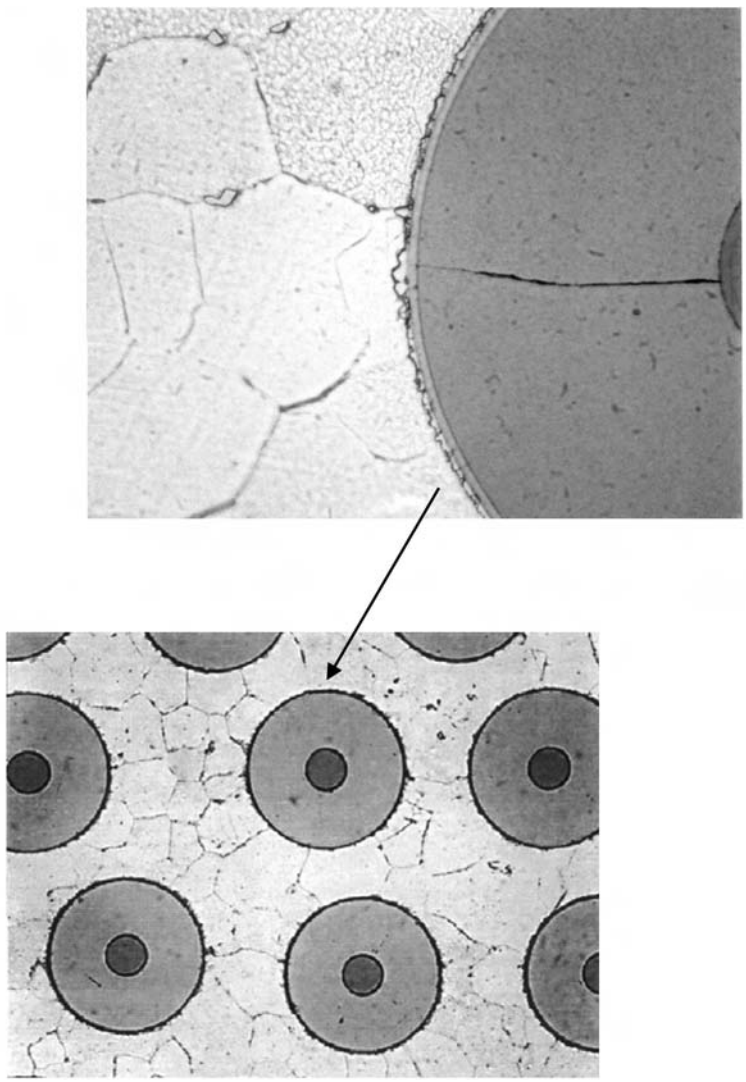


Fig. 20.21 Silicon carbide monofilament/titanium matrix composite

Table 20.3 Properties of unidirectional silicon carbide/titanium metal matrix composite

Property	SCS-6/Ti-6Al-4V
Fiber content, vol%	37
Longitudinal modulus, 10^6 psi	32
Transverse modulus, 10^6 psi	24
Longitudinal strength, ksi	210
Transverse strength, ksi	60

Source: Ref 2

same as SCS-6 except for its smaller diameter of 3.2 mil (8 μm). It is also deposited on a 1.3 mil (33 μm) carbon core. By comparison, the core comprises about 16 percent of the SCS-9 cross section but only about 5 percent of the SCS-6 cross section, so the SCS-9 has lower mechanical properties (a tensile strength of 500 ksi (3.5 GPa) and a modulus of 47 msi (324 GPa) but, being smaller in diameter, has better formability and lower density (0.09 lb/in.^{3}). Sigma is a 4 mil (100 μm) diameter fiber currently produced by the Defence Evaluation and Research Agency in the United Kingdom. Unlike the SCS fibers, Sigma is deposited on a tungsten core rather than on carbon. Sigma has a tensile strength of 500 ksi, a modulus of 60 msi (414 GPa), and a density of 0.1 lb/in.^{3} (2.8 g/cm^3). Sigma SM1240, which contains a 0.04 mil

(1 μm) coating of TiB_2 over a 0.04 mil (1 μm) inner coating of carbon, was developed for titanium aluminide matrices, while SM1140+, which contains a thicker 0.2 mil (4.5 μm) coating of only carbon, was developed originally for beta titanium alloys. Cross sections of an SCS-6 fiber and a Sigma fiber are compared in Fig. 20.22.

Ti-6Al-4V, the most prevalent titanium alloy used in the aerospace industry, was one of the first alloys to be evaluated as a matrix for TMC composites. However, Ti-6Al-4V, being a lean alpha-beta alloy, has at least two serious shortcomings: (1) it has only moderate strength at elevated temperature and (2) it is not very amenable to cold rolling into thin foil for foil-fiber-foil lay-ups or for cold forming into structural shapes. To overcome the forming problem, a considerable amount of work was conducted with the beta alloy Ti-15V-3Cr-3Sn-3Al (Ti-15-3-3-3). Testing showed that the Ti-15-3-3-3 alloy performs well in all respects but one; its oxidation resistance at temperatures approaching 1300 to 1500 °F (705 to 815 °C) is poor. The need for a matrix alloy with the good forming characteristics of Ti-15-3-3-3 but with improved oxidation resistance led Titanium Metals Corporation (Timet) to initiate a program to develop an alloy with improved oxidation resistance. The Ti-15Mo-2.8Nb-3Al-0.2Si alloy was selected as the most promising. This alloy, subsequently designated Beta 21S, was found to be far superior not only to Ti-15-3-3-3 but also to alloys such as Commercially Pure and Ti-6Al-4V from the standpoint of oxidation resistance. It should be noted that the addition of alloying elements such as vanadium, molybdenum, and aluminum has been found to reduce the tendency of the titanium matrix to degrade the fiber. Titanium aluminide matrices offer the potential of even higher temperature usage. However, the aluminides are both difficult to process and very expensive, so their use may be prohibitive from a cost standpoint except where they are required to meet the most stringent high-temperature requirements.

20.11 Continuous-Fiber TMC Processing Methods

Processing techniques for continuous-fiber TMCs include foil-fiber-foil processing, tape casting, plasma spraying, PM, and electron beam deposition of the titanium matrix directly onto the fibers. Of these, the foil-fiber-foil method is probably the most widely studied.

The most prevalent method used to fabricate continuous SiC fiber titanium matrix composites is the foil-fiber-foil method shown in Fig. 20.23. The fabric is a uniweave system in which the relatively large-diameter SiC monofilaments are straight and parallel and held together by a crossweave of molybdenum, titanium, or titanium-niobium wire or ribbon. The titanium foil is normally cold rolled down to a thickness of 4.5 mil (0.11 mm). The foil surfaces must be cleaned prior to lay-up to remove all volatile contaminants. The thin foils should also be uniform in thickness to avoid uneven matrix flow during

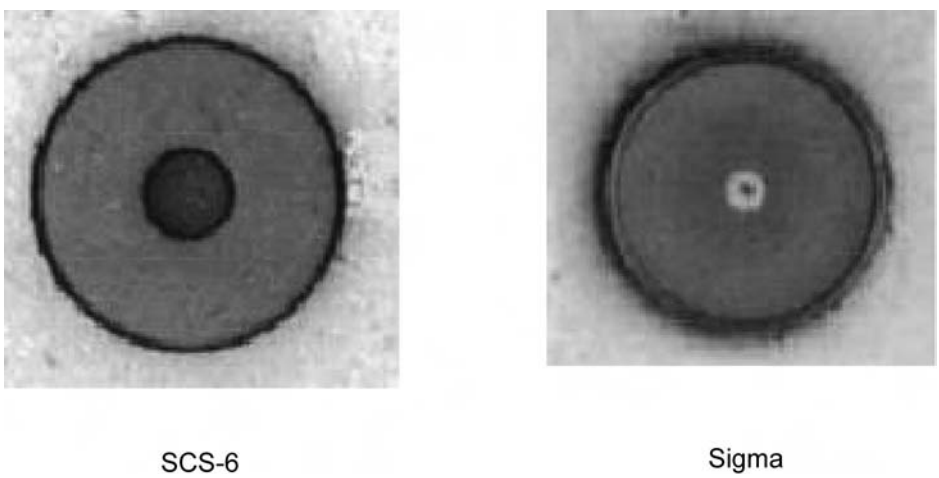


Fig. 20.22 Silicon carbide monofilaments

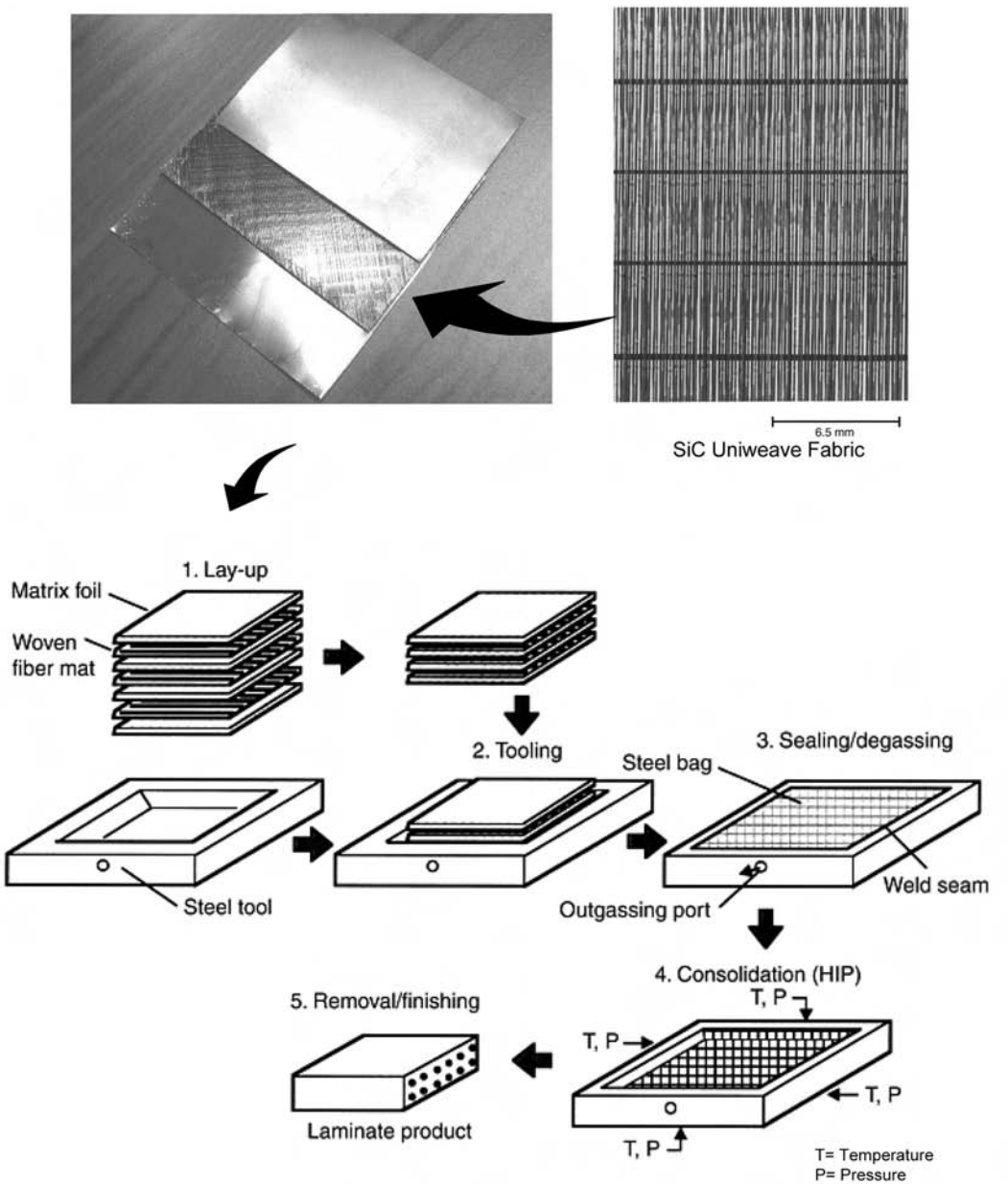


Fig. 20.23 Foil-fiber-foil fabrication process. HIP, hot isostatic pressing; Sic, silicon carbide

diffusion bonding. A fine grain size in the foil will enhance diffusion bonding by facilitating creep and possibly superplastic deformation. Because extremely thin foils with good surface finishes are required, the final rolling condition is cold rolling. For TMC, this dictates the use of beta titanium alloys that can be cold rolled to thin gauges. The plies are cut, layed up on a consolidation tool and then consolidated by either vacuum hot pressing or HIP. A disadvantage the foil-fiber-foil process is the rather poor fiber distribution with some fibers touching, which has a detrimental effect on mechanical properties, especially fatigue crack nucleation.

The green tape method, previously discussed for continuous-fiber aluminum matrix composites (Fig. 20.20), has also been used for continuous-fiber TMCs. The same uniweave fabric used

in the foil-fiber-foil process can be used in a process called *tape casting*. Here a slurry of titanium powder held together by a fugitive organic binder is cast into thin sheets of titanium matrix. These sheets are then combined with uniweave mats to produce the laminate stack-up. As with the green tape method, the fugitive organic binder must be removed prior to final consolidation.

Plasma spraying has also been evaluated for SiC/Ti composites. In vacuum plasma spraying, metallic powders of 0.79 to 3.93 mil (20 to 100 μm) are fed continuously into a plasma, where they are melted and propelled at high velocity onto a single layer of fibers, which have been wound onto a drum. One potential disadvantage of plasma spraying is that titanium, being an extremely reactive metal, can pick up oxygen from the atmosphere, potentially leading to embrittlement problems. This method has been evaluated primarily for titanium aluminide matrix composites due to the extreme difficulty of rolling these materials into thin foil.

Another method for fabricating TMCs is to apply the matrix directly to the SiC fibers using physical vapor deposition (PVD). A single PVD matrix-coated SiC fiber is shown in Fig. 20.24. An evaporation process involves passing the fiber through a region with a high vapor pressure of the metal to be deposited, where condensation takes place to produce a coating. The vapor is produced by directing a high-power of an approximately10 kW electron beam onto the end of a solid bar feedstock. Typical deposition rates are approximately 0.2 to 0.4 mil/min (5 to 10 μm/min). Alloy composition can be tailored, because differences in evaporation rates between different solutes are compensated for by changes in composition of the molten pool formed on the end of the bar until a steady state is reached wherein the alloy content of the deposit is the same as that of the feedstock. Electron beam evaporation from a single source is possible if the vapor pressures of the elements in the alloy are relatively close to each other; otherwise, multiple-source evaporation can be used if low-vapor-pressure elements, such as niobium or zirconium, are present in the alloy.

Composite fabrication is completed by assembling the coated fibers into a bundle and consolidating by vacuum hot pressing or HIP. Very uniform fiber distributions can be produced in this way, with fiber contents of up to about 80 percent, as shown in the Fig. 20.25 photomicrograph. The fiber volume fraction can be accurately controlled by the thickness of the deposited coatings, and the fiber distribution is always very homogeneous. The main advantages of this process are that (1) the fiber distribution and volume

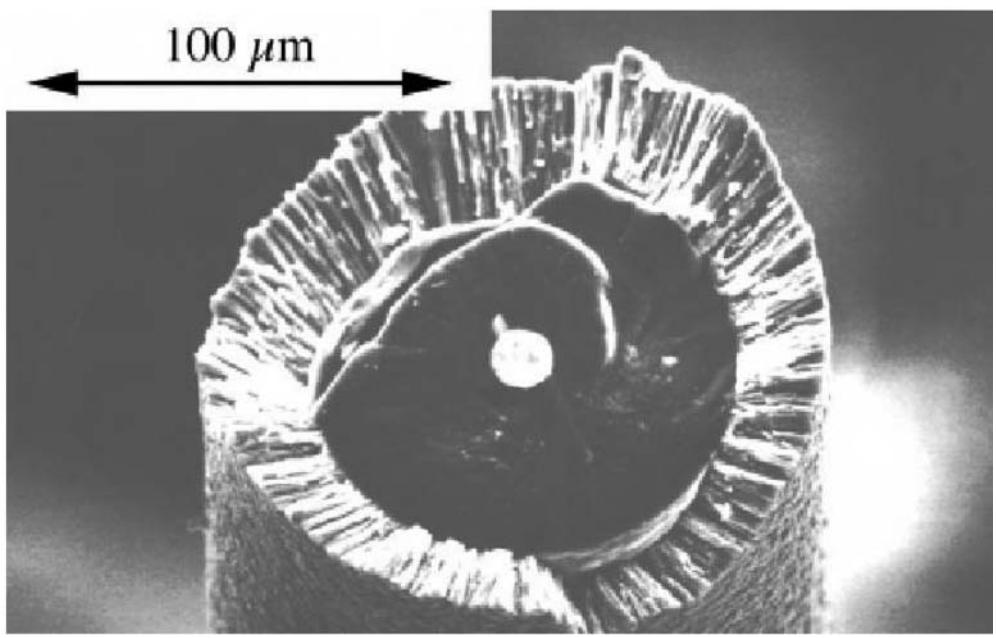


Fig. 20.24 Physical vapor deposition coated silicon carbide monofilament. Source: Ref 8

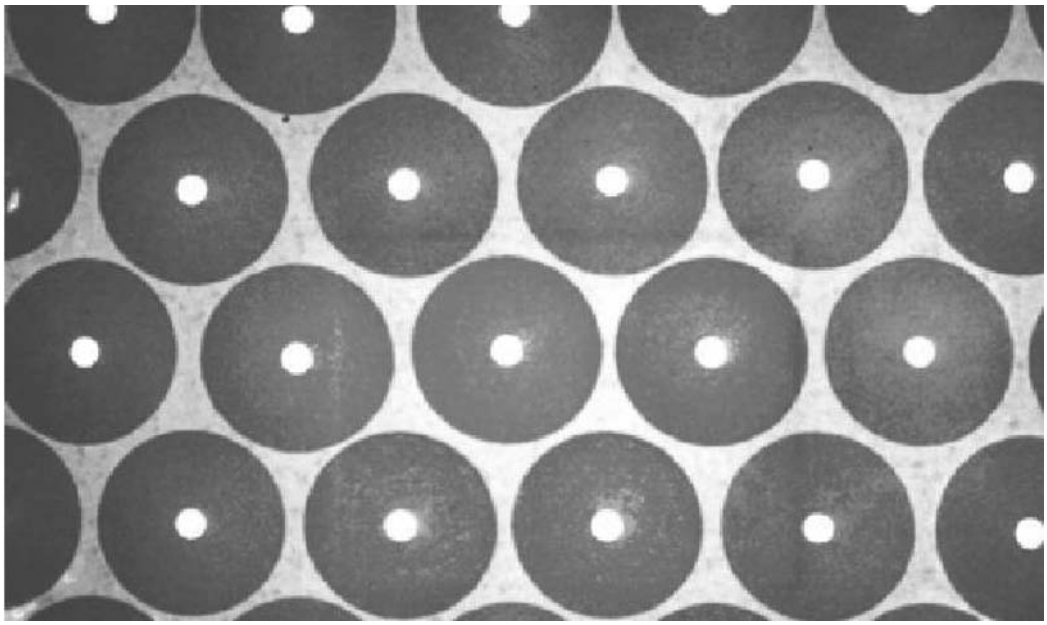


Fig. 20.25 Physical vapor deposition coated silicon carbide/titanium composite. Source: Ref 8

percentage are readily controllable, (2) the time required for diffusion bonding is shorter, and (3) the coated fiber is relatively flexible and can be wound into complex part shapes.

20.12 TMC Consolidation Procedures

The two primary consolidation procedures for continuous-fiber TMCs are vacuum hot pressing (VHP) and HIP. Diffusion bonding is attractive for titanium because the metal dissolves its own oxide at temperatures above about 1300 °F (705 °C) and exhibits extensive plastic flow at diffusion bonding temperatures. Typical fiber contents for continuous-fiber TMC laminates range from 30 to 40 volume percent.

In the VHP technique, the lay-up is sealed in a stainless steel envelope and placed in a vacuum hot press. After evacuation, a small positive pressure is applied by the press platens. This pressure acts to hold the filaments in place during the initial 800 to 1000 °F (425 to 535 °C) soak used to decompose any volatile organics and remove them under the action of a dynamic vacuum. The temperature is then gradually increased to a level where the titanium flows around the fibers under full pressure and the foil interfaces are diffusion bonded together. A typical VHP cycle is 1650 to 1750 °F (900 to 955 °C) at 6 to 10 ksi pressure for 60 to 90 minutes.

Hot isostatic pressing has largely replaced VHP as the consolidation technique of choice. The primary advantages of HIP consolidation are that (1) the gas pressure is applied isostatically, alleviating the concern about uneven platen pressure, and (2) the HIP process is much more amenable to making complex structural shapes. Typically, the part to receive HIP is canned (or a steel bag is welded to a tool), evacuated, and then placed in the HIP chamber. A typical HIP facility is shown in Fig. 20.26. For TMC, typical HIP parameters are 1600 to 1700 °F (870 to 925 °C) at 15 ksi gas pressure for two to four hours. Since HIP processing is a fairly expensive batch processing procedure, it is normal practice to load a number of parts into the HIP chamber for a single run. The vertical HIP units can have large thermal gradients from top to bottom. The temperature is slowly ramped up and held until all points on the tool are at a uniform temperature. The gas pressure is then increased after the tool has reached this uniform temperature. The pressure then deforms the steel bag and plastically consolidates the laminate when everything is soft. The hold time must be sufficient to ensure complete diffusion bonding and consolidation.

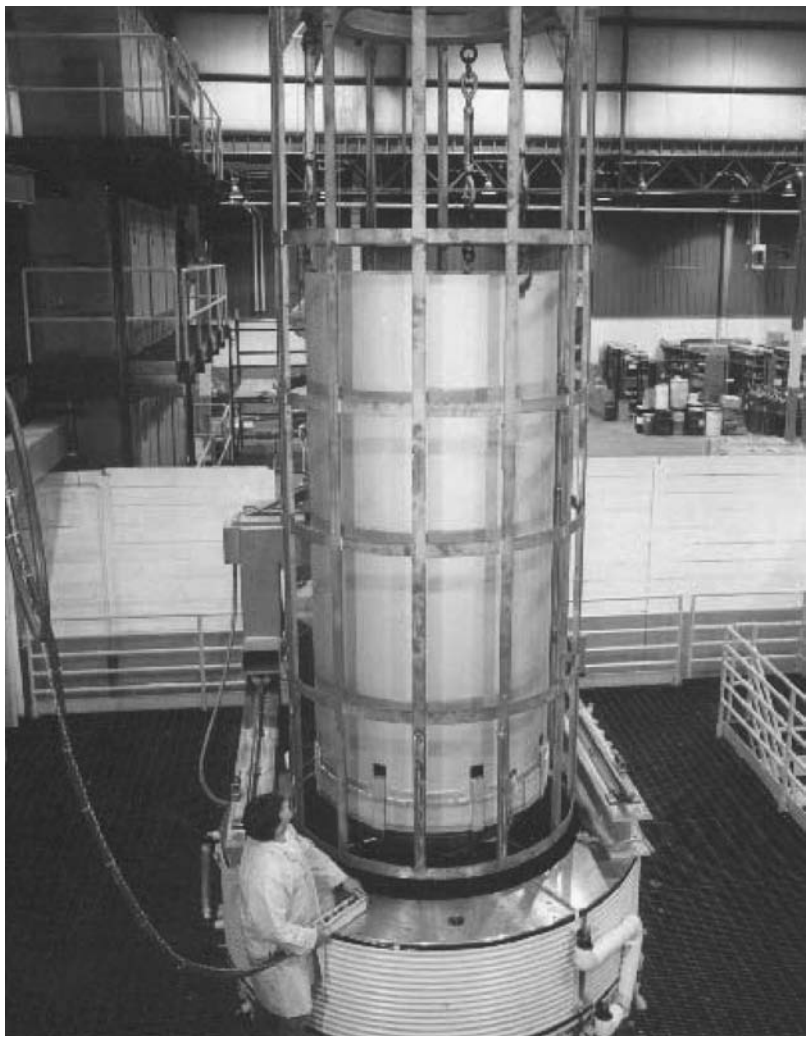


Fig. 20.26 Loading a large hot isostatic pressing furnace

Diffusion bonding consists of creep flow of the matrix between the fibers to make metal-to-metal contact and then diffusion across the interfaces to complete the consolidation process. In the foil-fiber-foil method, obtaining complete flow in the interstices between the fiber midplanes and the foil segments on either side is difficult (Fig. 20.27). Fine-grained foil materials and high temperatures where the matrix is either very soft or superplastic can help. However, high processing temperatures can create fiber-to-matrix reactions that cause degradation of the fiber strength. Thermal expansion mismatches between the fiber and matrix can also cause high residual stresses, resulting in matrix cracking during cool-down.

The selection of diffusion bonding parameters can have an effect on the occurrence of structural defects such as fiber breakage, matrix cracking, and interfacial reactions. For example, reducing the levels of fiber breakage and matrix cracking would dictate high processing temperatures and low pressures, while minimizing interfacial reactions would dictate exactly the opposite: low processing temperatures and high pressures. High consolidation temperatures promote creep and diffusion processes that contribute to void closure but at the same time can result in excessive interfacial reactions and grain growth in the matrix. Low consolidation temperatures lead to long processing times and require higher pressures, which can result in fiber cracking.

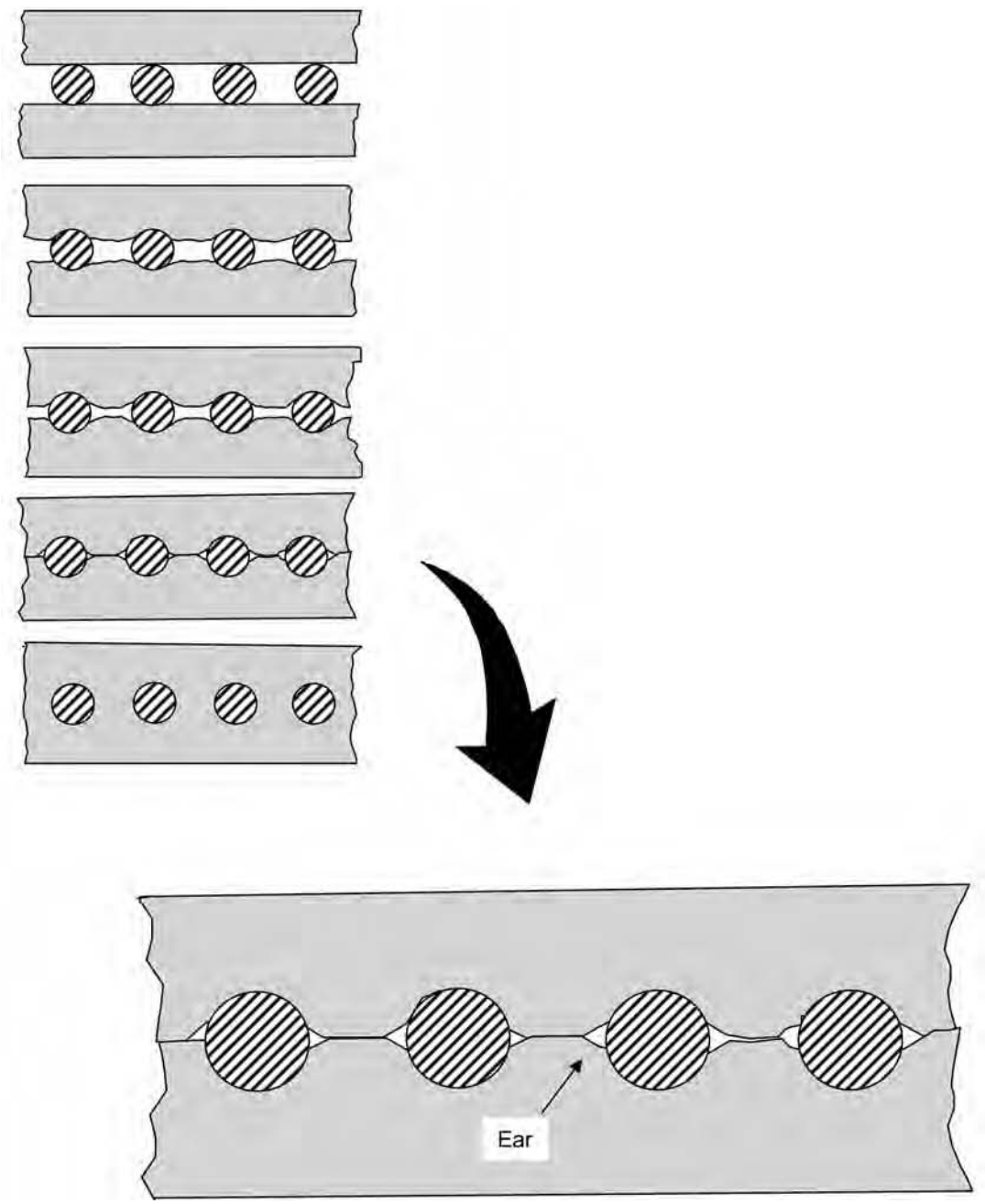


Fig. 20.27 Diffusion bonding progression. Source: Ref 9

20.13 Secondary Fabrication of TMCs

Successful joining of TMC components by diffusion bonding can be accomplished at pressures and temperatures lower than those for normal HIP runs. To process preconsolidated C-channels into spars, as shown in Fig. 20.28, they can be joined together in a back-to-back fashion. For secondary diffusion bonding in a HIP chamber, the parts are assembled and encapsulated in a leak-free steel envelope or bag. Because the bag is subjected to the same high

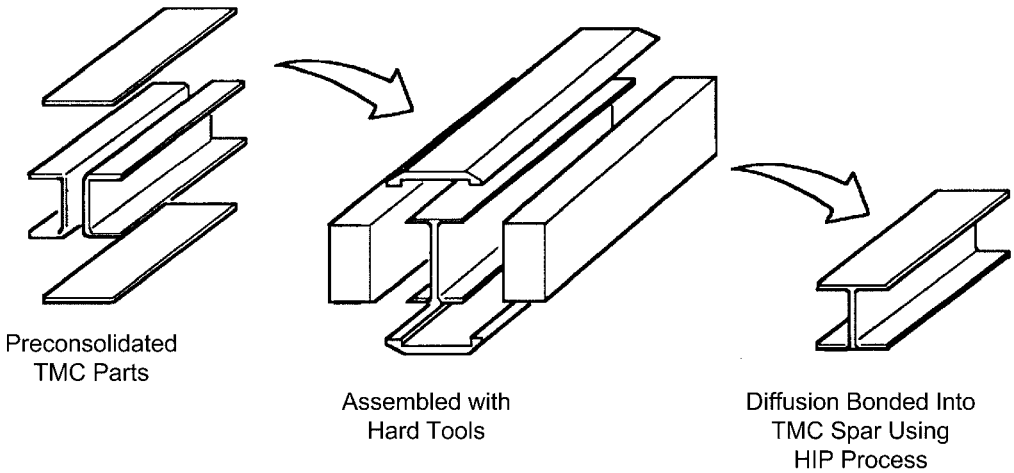


Fig. 20.28 Secondary diffusion bonding of titanium matrix composite (TMC) spars. HIP, hot isostatic pressing

pressure and temperature as the parts, the ability of the bag to withstand the HIP forces is critical for success. If the bag develops a leak, the isostatic pressure is lost and so is the bonding pressure. To minimize the risk associated with the extreme pressures and temperatures required for initial consolidation, lower temperatures and pressures can be used for secondary diffusion bonding. Lower temperatures and pressures reduce the risk of bag failures during the secondary HIP bonding cycle. However, since TMC is inherently stiffer than conventional sheet metal components, it generally requires higher pressures to achieve secondary diffusion bonding. A machined filler is placed in the corner to fill the void created by the C-channels. By not pinning the TMC components together and allowing them to slide a little in relation to one another, complete bonding is achieved. Incomplete bonding or damage can occur if movement is not permitted. Successful bonding can be achieved with HIP pressures as low as 5 ksi at 1600 °F (870 °C) for two hours.

Superplastic forming and diffusion bonding (SPF/DB) can be used to take advantage of elevated-temperature characteristics inherent in certain titanium alloys. Structural shapes, which combine superplastic forming and bonding of the parent metal, can be fabricated from thin titanium alloy sheets to achieve high levels of structural efficiency. Components fabricated from TMC do not lend themselves to superplastic forming. However, since they retain the diffusion bonding capability of the matrix alloy, TMC components can be readily bonded with superplastically formed sheet metal substructures. A TMC-reinforced SPF/DB structural panel retains the structural efficiency of TMC while possessing the fabrication simplicity of a superplastically formed part. Two potential methods of fabricating TMC stiffened SPF/DB panels are shown in Fig. 20.29. The core pack, which forms the substructure, can be fabricated from a higher-temperature titanium alloy, such as Ti-6Al-2Sn-4Zr-2Mo, rather than Ti-6Al-4V, which is normally used in SPF/DB parts. Ti-6Al-2Sn-4Zr-2Mo has good superplastic forming characteristics at a moderate processing temperature of 1650 °F (900 °C). The final shape and size of the substructure are determined by the resistance seam welding pattern of the core pack prior to the SPF/DB cycle, which is inflated during the SPF/DB cycle with argon gas to form the substructure.

Conventional nondestructive testing techniques, including both through transmission and pulse echo ultrasonics, can be used for the detection of manufacturing defects. Conventional ultrasonic and x-ray techniques have the ability to find many TMC processing defects, including lack of consolidation, delaminations, fiber swimming, and fiber breakage. Ultrasonics can find defects as small as $^{3}/_{64}$ in. (1.2 mm) in diameter, with through transmission giving the best resolution. Normal radiographic X-ray inspection can also be used to examine TMC components.

Titanium matrix composite is extremely difficult to machine. The material is highly abrasive, and tool costs can be high. Improper cutting not only damages tools but can damage the part as well. Abrasive waterjet cutting, illustrated in Fig. 20.30, has been found to work well on

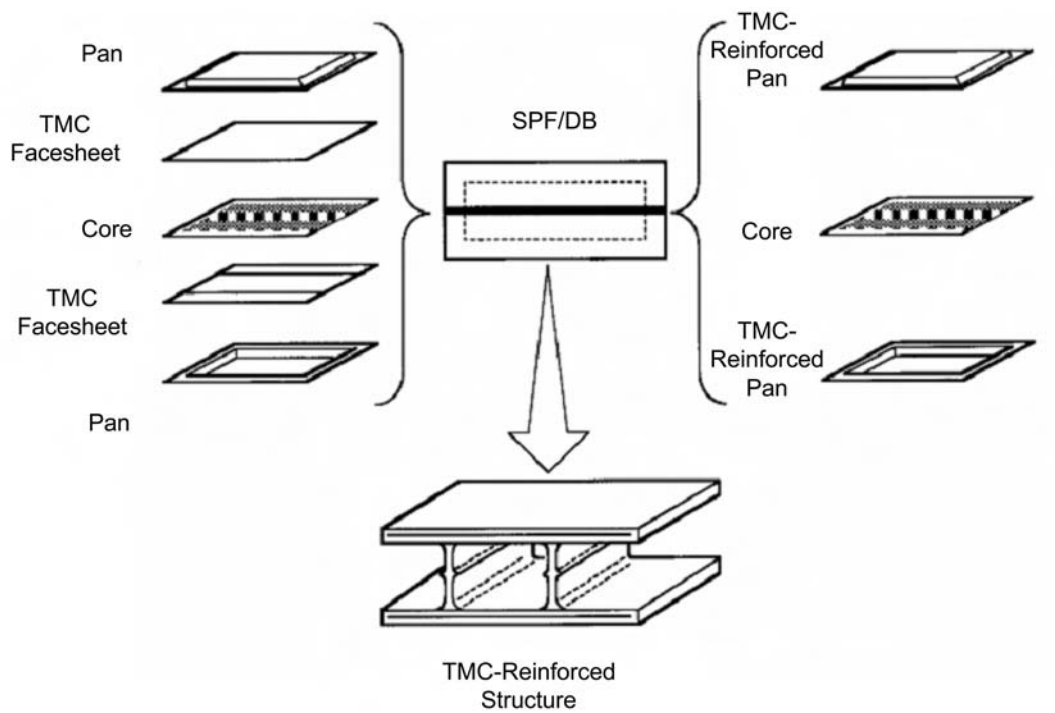


Fig. 20.29 Methods for making superplastic forming and diffusion bonding (SPF/DB) titanium matrix composite (TMC) reinforced parts

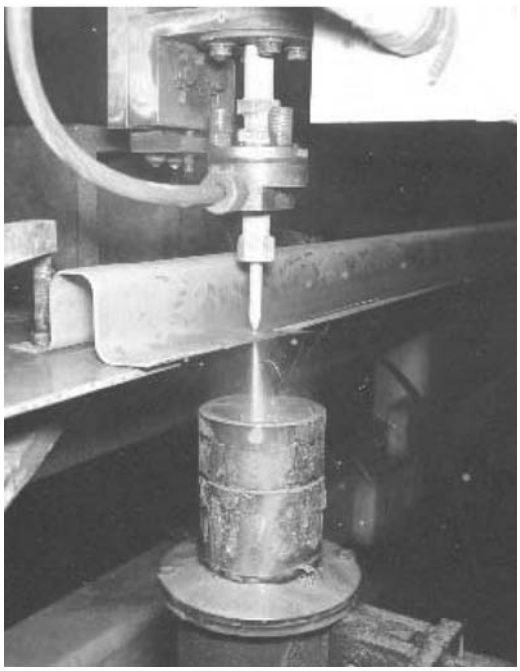


Fig. 20.30 Abrasive waterjet cutting of titanium matrix composite. Source: The Boeing Company

TMC. Typical machining parameters are 45,000 psi water pressure, dynamically mixed with #80 garnet grit, at a feed rate of 0.5 to 1.2 in. per minute. The waterjet cutter has multi-axis capability and can make uninterrupted straight and curved cuts. A diamond cut-off wheel also produces excellent cuts. However, this method is limited to straight cuts and is rather slow. The diamond cut-off wheel is mounted on a horizontal mill, and cutting is done with a flood coolant using controlled speeds and feeds. Because this method is basically a grinding operation, cutting rates are typically slow; however, the quality of the cut edge is excellent.

Wire electrical discharge machining (EDM) is also a flexible method of cutting TMC. It is a noncontact cutting method that removes material through melting or vaporization by high-frequency electric sparks. Brass wire that is 0.010 in. (0.25 mm) in diameter can be used at a feed rate of 0.020 to 0.050 ipm. The EDM unit is self-contained, with its own coolant and power system. Electrical discharge machining has the advantage of being able to make small-diameter cuts, such as small scallops and tight radii. Like waterjet cutting, the EDM method is program-

mable and can make uninterrupted straight or curved cuts.

Several methods can be used to generate holes in TMC. For thin components, such as three plies, with only a few holes; the cobalt grades of high-speed steel , for example M42, twist drills can be used with power feed equipment; however, tool wear is so rapid that several drills may be required to drill a single hole. Punching has also been used successfully on thin TMC laminates. Using conventional dies, punching is fast and clean, with no coolant required. Punching results in appreciable fiber damage and metal smearing, but most of the disturbed metal can be removed and the hole cleaned up by reaming. However, some holes may require several passes, and several reamers, to sufficiently clean up the hole. In some instances, the diameter of the reamer is actually reduced, due to wear of the reamer cutting edges, rather than increasing the diameter of the hole. Punching is not used extensively because of the large number of fastener holes required in the internal portion of structures. In addition, load-bearing sections are normally too thick for punching.

Neither conventional twist drills nor punching will consistently produce high-quality holes in TMC, especially in thicker material. The use of diamond core drills has greatly improved hole drilling quality in thick TMC components. High-quality holes can be produced consistently with diamond core drills. The core drills are tubular, with a diamond matrix buildup on one end. This construction is similar to that of some grinding wheels. A typical core drill and coolant chuck is shown in Fig. 20.31. The important parameters

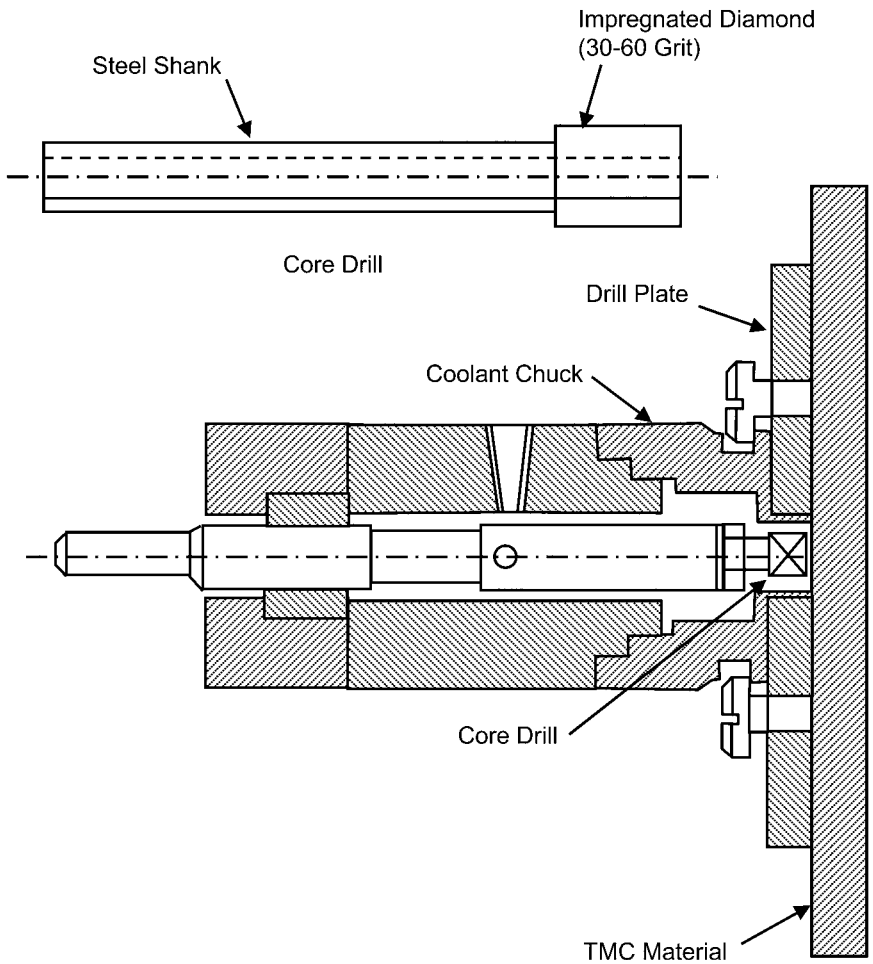


Fig. 20.31 Diamond-impregnated core drill and coolant chuck. TMC, titanium matrix composite

for successful diamond core drilling are drill design, coolant delivery system, drill plate design, type of power feed drilling equipment used, and the speeds and feeds used during drilling. During drilling, the core drill abrasively grinds a cylindrical core plug from the material. Some fabricators even mix an abrasive grit with the water coolant to improve the material removal rate. Multiple drill setups on a TMC structure are shown in Fig. 20.32. The drill plate can hold several drill motors, which allows the operator to operate more than one at a time. The drill plates must be stiff enough to produce a rigid setup. A properly drilled hole can hold quite good tolerances, depending on the thickness of the TMC: ± 0.0021 in. (0.05 mm) in 4 plies, ± 0.0030 in. (0.08 mm) in 15 plies, and ± 0.0055 in. (0.1 mm) in 32 plies.

Another method for joining thin TMC components into structures is resistance spot welding. Conventional 50 kW resistance welding equipment (Fig. 20.33), with water-cooled copper electrodes, has been successfully used to spot weld thin TMC. Fabricators often use conventional titanium, such as Ti-6Al-4V, to set the initial welding parameters. As with any spot welding operation, it is important to thoroughly clean the surfaces before welding. Initial welding parameters should be verified by metallography and lap shear testing.

20.14 Particle-Reinforced TMCs

Particle reinforced-TMCs are processed by PM methods. Although a variety of materials have been studied, the most common combination is Ti-6Al-4V reinforced with 10 to 20 weight percent TiC. These composites offer increased hardness and wear resistance compared to conventional titanium alloys. The properties of unreinforced and reinforced Ti-6Al-4V are compared in Table 20.4.

As opposed to adding reinforcements as distinct and separate constituents, there are some systems in which the reinforcement can be formed within the metallic matrix during solidification, referred to as *in situ composites*. Directional solidification of certain eutectic systems can produce fibers or rod-like structures, as shown for the niobium-niobium carbide system in Fig. 20.34. While these structures can be produced, the growth rates are slow, approximately 0.4 to 2.0 in./h (1 to 5 cm/h), due to the need to maintain a stable growth front, which requires a large temperature gradient. In addition, all of the

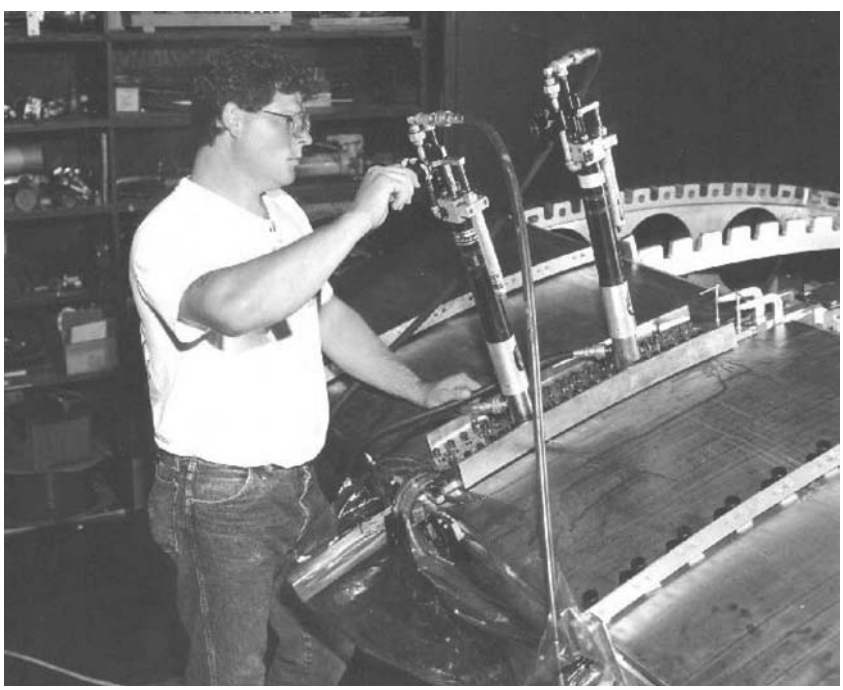


Fig. 20.32 Diamond core drilling of a titanium matrix composite component. Source: The Boeing Company



Fig. 20.33 Spot welding titanium matrix composite hat stiffeners. Source: The Boeing Company

Table 20.4 Mechanical properties of discontinuous titanium carbide particle/ titanium matrix composites

Property	Ti-6Al-4V	10 wt% TiC/ Ti-6Al-4V	20 wt% TiC/ Ti-6Al-4V
Density, lb/in.^{3}	0.160	0.16	0.16
Tensile strength, ksi at:			
RT	130	145	153
1000 °F	65	80	90
Modulus, msi at:			
RT	16.5	19.3	21
1000 °F	13	15.3	16
Fatigue limit, 10^6 cycles, ksi	75	40	. . .
Fracture toughness, ksi · in.$^{1/2}$	50	40	29
Hardness (HRC)	34	40	44

HRC, ; RT, room temperature. Source: Ref 2

reinforcement is aligned in the growth or solidification direction. There are also limitations on the nature and volume fraction of the reinforcement.

Another in situ method, the exothermic dispersion process, utilizes exothermic reactions between two reactants to produce a third compound. Generally, a master alloy is produced that contains a high volume fraction of a ceramic reinforcing phase. The master alloy is then mixed and remelted with a base alloy to produce the desired amount of particle reinforcement. For example, if a mixture of aluminum, titanium, and boron is heated sufficiently, an exothermic reaction takes place between the aluminum and titanium, which produces a mixture of TiB_2 ceramic particles distributed in a titanium aluminide matrix. Strength levels of greater than 100 ksi (690 MPa) were measured at room temperature and at 1470 °F (800 °C) for a gamma titanium aluminide (Ti-45 at % Al) alloy reinforced with TiB_2 ceramic particulates. Compared to the conventional metal matrix composites (MMCs), in situ MMCs offer several possible advantages: (1) the in situ formed reinforcements are thermodynamically stable, leading to less degradation at elevated temperature; (2) the reinforcement-to-matrix interfaces are clean, resulting in a strong interfacial bonding; and (3) the in situ formed reinforcements are finer in size and their distribution in the matrix is more uniform.

20.15 Fiber Metal Laminates

Fiber metal laminates are laminated materials consisting of thin layers of metal sheet and unidirectional fiber layers embedded in an adhesive

system. GLARE (Glass Laminate Aluminum Reinforced) is a type of aluminum fiber metal laminate in which unidirectional S-2 glass fibers are embedded in FM-34 epoxy structural film adhesive. A typical construction is shown in Fig. 20.35. The S-2 glass is bonded to the aluminum sheets with the film adhesive. The aluminum metal layers are chemically cleaned (chromic acid anodized or phosphoric acid anodized) and primed with BR-127 corrosion-inhibiting primer. The adhesion between the FM-34 adhesive and the treated metal surface, and between FM-34 and S-2 glass fibers, is so high that these bondlines often remain intact until cohesive adhesive failure occurs.

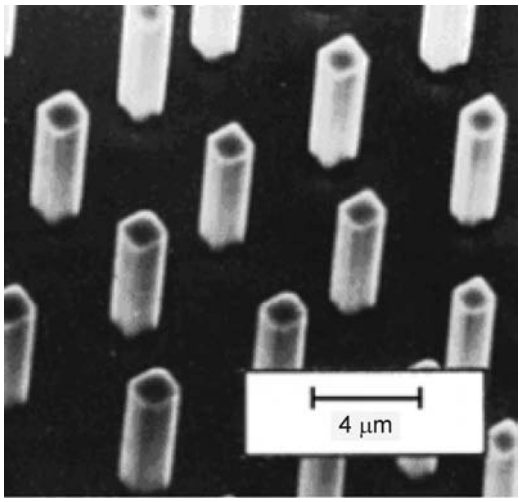


Fig. 20.34 Rod-reinforced niobium carbide/niobium eutectic. Source: Ref 7

GLARE is normally available in six different standard grades, as outlined in Table 20.5. They are all based on unidirectional S-2 glass fibers embedded with FM-34 adhesive, resulting in a 0.005 in. (0.13 mm) thick prepreg with a nominal fiber volume fraction of 59 percent. The prepreg is layed up in different orientations between the aluminum alloy sheets. From 1990 to 1995, GLARE laminates were produced only as flat sheets. It was believed that the aircraft manufacturer would use these sheets to manufacture fuselage panels by applying the curvature, thickness steps, and joints using conventional methods developed for metal structures (forming, bonding, riveting, etc.). Several studies showed the benefits in performance and weight of these GLARE shells, but they also indicated the high cost of these parts in comparison with conventional aluminum structures.

To reduce manufacturing costs, a self-forming technique (SFT) was developed (Fig. 20.36) in which autoclave pressure is used to form the laminate over external and internal doublers,

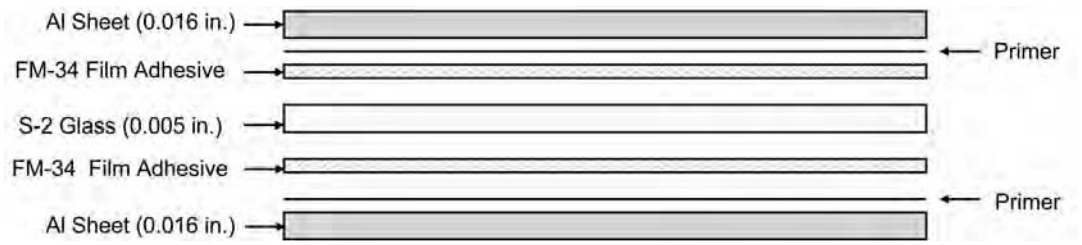


Fig. 20.35 Typical GLARE ply construction. Al, aluminum

Table 20.5 Commercial GLARE grades

Glare grade	Sub grade	Material sheet thickness, in., alloy	Prepreg orientation in each layer	Principal benefits
Glare 1	. . .	0.020–0.016, 7475-T761	0/0	Fatigue, strength, yield strength
Glare 2	Glare 2A	0.0008–0.020, 2024-T3	0/0	Fatigue, strength
	Glare 2B	0.0008–0.020, 2024-T3	90/90	Fatigue, strength
Glare 3	. . .	0.0008–0.020, 2024-T3	0/90	Fatigue, impact
Glare 4	Glare 4A	0.0008–0.020, 2024-T3	0/90/0	Fatigue, strength in 0° direction
	Glare 4B	0.0008–0.020, 2024-T3	90/0/90	Fatigue, strength in 90° direction
Glare 5	. . .	0.0008–0.020, 2024-T3	0/90/90/0	Impact
Glare 6	Glare 6A	0.0008–0.020, 2024-T3	+45/–45	Shear, off-axis properties
	Glare 6B	0.0008–0.020, 2024-T3	–45/+45	Shear, off-axis properties

Source: Ref 10

because the stiffness of the package of thin aluminum layers and still uncured adhesive and fiber layers is low. Additional adhesive, of the same type as that used to impregnate the glass fibers in the prepreg, is also added at certain locations to adhere interrupted metal sheets to each other, to adhere thin aluminum internal or external doublers to the aluminum layers of the laminate, and to fill gaps in the laminate that would otherwise remain unfilled. Splices used during the SFT, shown in Fig. 20.37, are not critical during static or fatigue loading. In other words, the splice is not the weakest link in the panel strength.

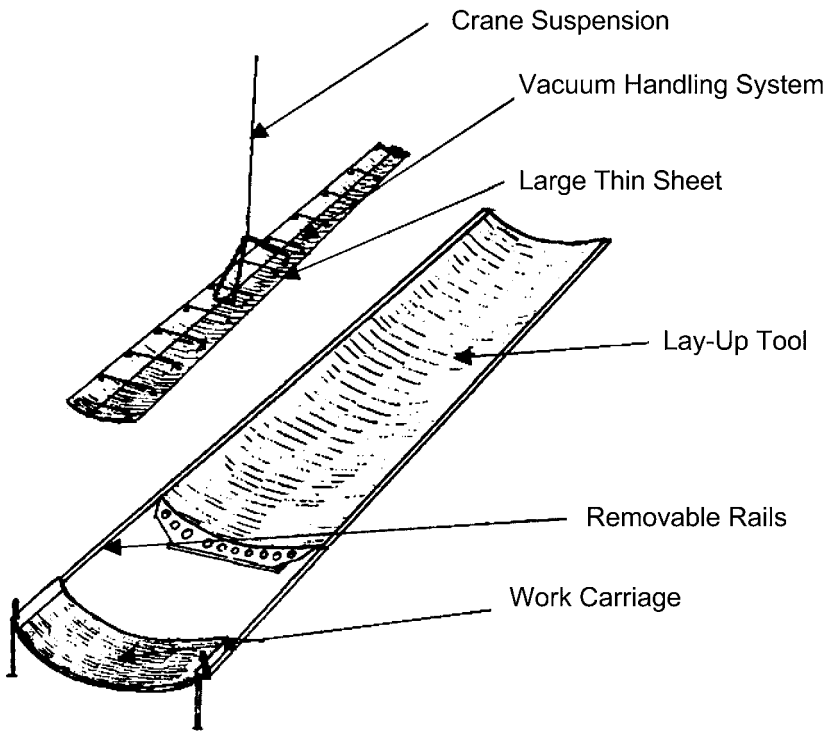


Fig. 20.36 GLARE self-forming technique. Source: Ref 10

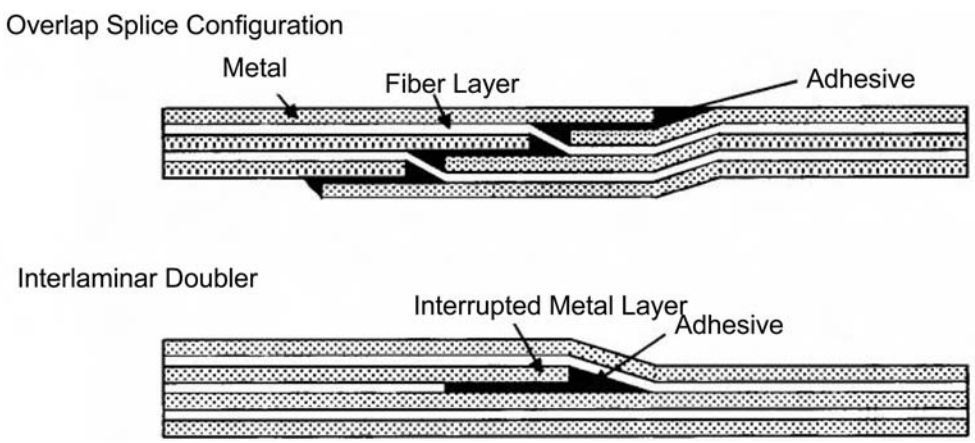


Fig. 20.37 GLARE splice concepts. Source: Ref 10

The primary advantages of GLARE are better fatigue crack propagation resistance than aluminum, superior damage tolerance compared to aluminum, higher bearing strengths than carbon/epoxy, 10 percent lighter weight than aluminum, and lower cost than carbon/fiber composite but higher cost than aluminum. In addition to GLARE, the introduction of titanium foils in carbon/epoxy laminates (TiGr) has been evaluated, primarily for improved bearing strengths.

REFERENCES

1. T.W. Clyne and P.J. Withers, *An Introduction to Metal Matrix Composites*, Cambridge University Press, 1993
2. Metal-Matrix Composites, *Metals Handbook Desk Edition*, 2nd ed., ASM International, 1998
3. C.A. Smith, Discontinuous Reinforcements for Metal-Matrix Composites, *ASM Handbook*, Vol 21, *Composites*, ASM International, 2001
4. Processing of Metal-Matrix Composites, *ASM Handbook*, Vol 21, *Composites*, ASM International, 2001, p 579–588
5. D.R. Herling, G.J. Grant, and W. Hunt, Low-Cost Aluminum Metal Matrix Composites, *Adv. Mater.Process.*, 2001, p 37–40
6. V.J. Michaud, Liquid State Processing, *Fundamentals of Metal-Matrix Composites*, Butterworth-Heinemann, 1993, p 3–22
7. J.V. Foltz and C.M. Blackmon, Metal-Matrix Composites, *ASM Handbook*, Vol 2, *Properties and Selection: Nonferrous Alloys and Special-Purpose Materials*, ASM International, 1990
8. C.M. Ward-Close and P.G. Partridge, A Fibre Coating Process for Advanced Metal Matrix Composites, *J. Mater. Sci.*, Vol 25, 1990, p 4315–4323
9. A.K. Ghosh, Solid State Processing, *Fundamentals of Metal-Matrix Composites*, Butterworth-Heinemann, 1993, p 2-32–2-41
10. A. Vlot and J.W. Gunnick, *Fibre Metal Laminates: An Introduction*, Kluwer Academic Publishers, 2001

SELECTED REFERENCES

- G.B. Bilow and F.C. Campbell, "Low Pressure Fabrication of Borsic/Aluminum Composites," *6th Symposium of Composite Materials in Engineering Design*, May 1972
- J.U. Ejiofor and R.G. Reddy, Developments in the Processing and Properties of Particulate Al-Si Composites, *J. Met.*, Vol 49 (No. 11), 1997, p 31–37
- M.R. Ghomashchi and A. Vikhrov, Squeeze Casting: An Overview, *J. Mater. Process. Technol.*, Vol 101, 2000, p 1–9
- Z.X. Guo and B. Derby, Solid-State Fabrication and Interfaces of Fibre Reinforced Metal Matrix Composites, *Prog. Mater. Sci.*, Vol 39, 1995, p 411–495
- J. Hashim, L. Looney, and M.S.J. Hashmi, Metal Matrix Composites: Production by the Stir Casting Method, *J. Mater. Process. Technol.*, Vol 92–93, 1999, p 1–7
- J. Hashim, L. Looney, and M.S.J. Hashmi, The Wettability of SiC Particles by Molten Aluminum Alloy, *J. Mater. Process. Technol.*, Vol 119, 2001, p 324–328
- J.W. Kaczmar, K. Pietrzak, and W. Wlosinski, The Production and Application of Metal Matrix Composites, *J. Mater. Process. Technol.*, Vol 106, 2000, p 58–67
- V.K. Lindroos and M.J. Talvitie, Recent Advances in Metal Matrix Composites, *J. Mater. Process. Technol.*, Vol 53, 1995, p 273–284
- J.A. McElman, Continuous Silicon Carbide Fiber MMCs, *Engineered Materials Handbook*, Vol 1, *Composites*, ASM International, 1987
- M.A. Mittnick, Continuous SiC Fiber Reinforced Materials, *21st International SAMPE Technical Conference*, Sept 1989, p 647–658
- S.V. Nair, J.K. Tien, and R.C. Bates, SiC-Reinforced Aluminum Metal Matrix Composites, *Int. Met. Rev.*, Vol 30 (No. 275), 1985
- R.A. Shatwell, Fibre-Matrix Interfaces in Titanium Matrix Composites Made with Sigma Monofilament, *Mater. Sci. Eng.*, Vol A259, 1999, p 162–170
- T.S. Srivatsan, T.S. Sudarshan, and E.J. Lavernia, Processing of Discontinuously-Reinforced Metal Matrix Composites by Rapid Solidification, *Prog. Mater. Sci.*, Vol 39, 1995, p 317–409
- D.M. Stefanescu and R. Ruxanda, Fundamentals of Solidification, *ASM Handbook*, Vol 9, *Metallography and Microstructures*, ASM International, 2004

- S. Sullivan, "Machining, Trimming and Drilling Metal Matrix Composites for Structural Applications," ASM International Materials Week 92, Chicago, 2–5 Nov 1992
- Vassel, Continuous Fibre Reinforced Titanium and Aluminum Composites: A Comparison, *Mater. Sci. Eng.*, Vol A263, 1999, p 305–313
- C.M. Ward-Close and P.G. Partridge, A Fibre Coating Process for Advanced Metal Matrix Composites, *J. Mater. Sci.*, Vol 25, 1990, p 4315–4323
- C.M. Ward-Close et al., Advances in the Fabrication of Titanium Matrix Composite, *Mater. Sci. Eng.* Vol A263, 1999, p 314–318

"*This page left intentionally blank.*"

Copyright © 2010, ASM International®
All rights reserved.
www.asminternational.org

CHAPTER 21

Ceramic Matrix Composites

MONOLITHIC CERAMIC MATERIALS have many desirable properties, such as high moduli, high compression strengths, high temperature capability, high hardness and wear resistance, low thermal conductivity, and chemical inertness. As shown in Fig. 21.1, the high-temperature capability of ceramics makes them very attractive materials for extremely high-temperature environments. However, due to their very low fracture toughness, ceramics are limited in structural applications. While metals deform plastically due to the high mobility of dislocations, that is slip, ceramics do not exhibit plastic deformation at room temperature and are prone to catastrophic failure under mechanical or thermal loading. They have very low tolerance to crack-like defects, which can occur either during fabrication or in service. Even a very small crack can quickly grow to critical size, leading to sudden failure.

While reinforcements such as fibers, whiskers, or particles are used to strengthen polymer and metal matrix composites, reinforcements in ceramic matrix composites are used primarily to increase toughness. Some differences between polymer matrix and ceramic matrix composites are illustrated in Fig. 21.2. The toughness

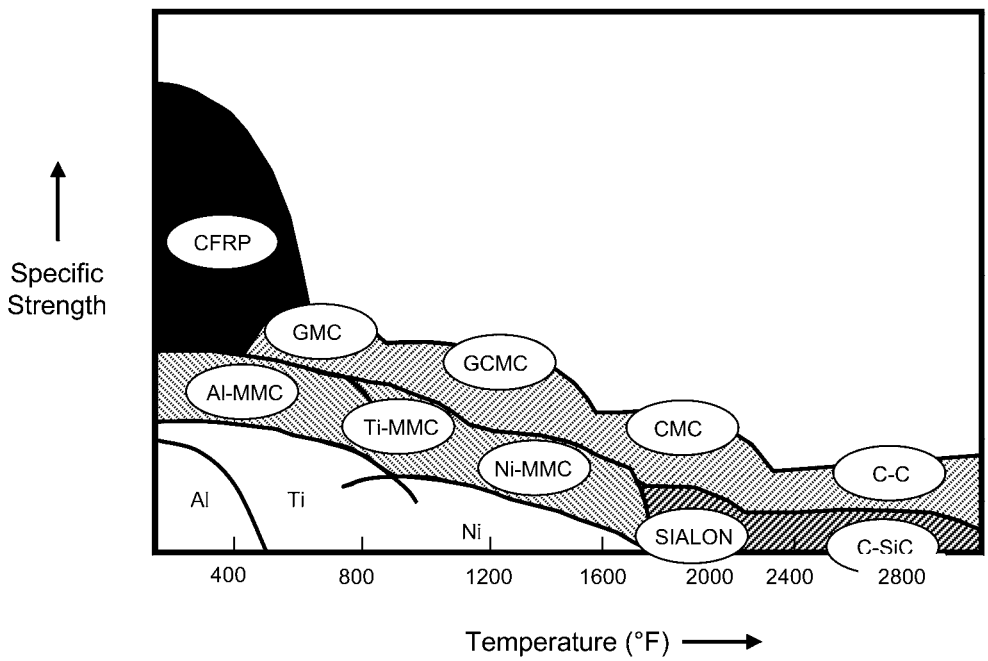


Fig. 21.1 Relative material temperature limits. Carbon-carbon (C-C), carbon fiber reinforced plastic (CFRP), ceramic matrix composite (CMC), carbon-silicon carbide (C-SiC), glass-ceramic matrix composite (GCMC), metal matrix composite (MMC), silicon-aluminum-oxygen-nitrogen (SIALON)

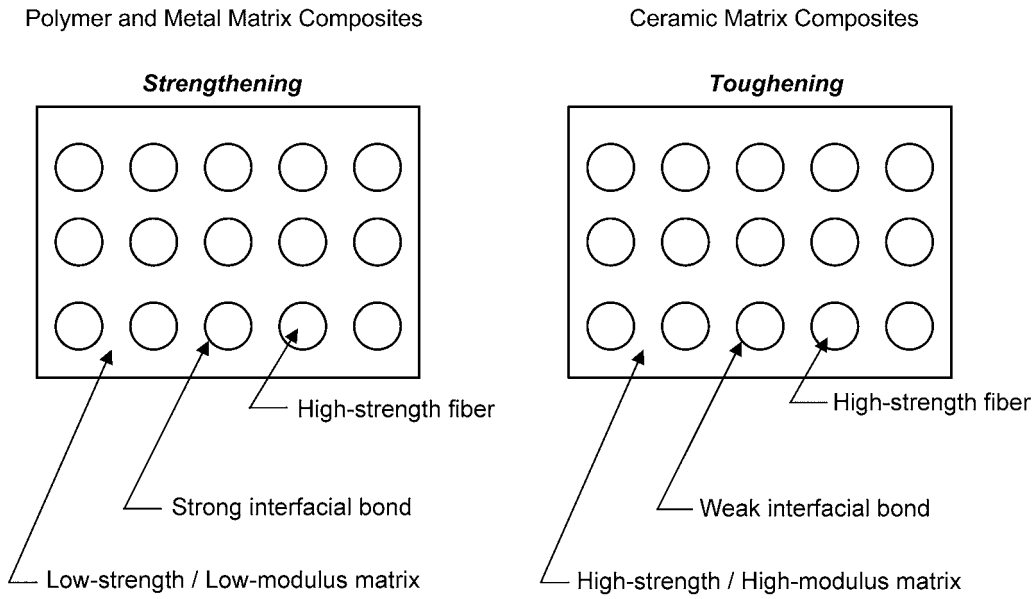


Fig. 21.2 Comparison of polymer and metal with ceramic matrix composites

increases afforded by ceramic matrix composites are due to energy-dissipating mechanisms such as fiber-to-matrix debonding, crack deflection, fiber bridging, and fiber pull-out. A notional stress-strain curve for a monolithic ceramic and a ceramic matrix composite is shown in Fig. 21.3. Since the area under the stress-strain curve is often considered an indication of toughness, the large increase in toughness for the ceramic matrix composite is evident. The mechanisms of debonding and fiber pull-out are shown in Fig. 21.4. For these mechanisms to be effective, there must be a relatively weak bond at the fiber-to-matrix interface. If there is a strong bond, the crack will propagate straight through the fibers, resulting in little or no energy absorption. Therefore, proper control of the interface is critical. Coatings are often applied to protect the fibers during processing and to provide a weak fiber-to-matrix bond.

Carbon-carbon (C-C) composites are the oldest and most mature of the ceramic matrix composites. They were developed in the 1950s by the aerospace industry for use as rocket motor casings, heat shields, leading edges, and thermal protection. It should be noted that C-C composites are often treated as a separate material class from other ceramic matrix composites, but their usage and fabrication procedures are similar and overlap other ceramic matrix composites. A relative comparison of C-C with other ceramic matrix composites is given in Table 21.1. For high-temperature applications, C-C composites offer exceptional thermal stability at greater than 4000 °F (2205 °C) in nonoxidizing atmospheres, along with low densities of 0.054 to 0.072 lb/in.^{3} (1.49 to 1.99 g/cm^3). Their low thermal expansion and range of thermal conductivities provide high thermal shock resistance. In vacuum and inert gas atmospheres, carbon is an extremely stable material, capable of use to temperatures exceeding 4000 °F (2205 °C). However, in oxidizing atmospheres, it starts oxidizing at temperatures as low as 950 °F (510 °C). Therefore, C-C composites for elevated-temperature applications must be protected with oxidation-resistant coating systems, such as silicon carbide that is overcoated with glass. The silicon carbide coating provides the basic protection, while the glass overcoat melts and flows into coating cracks at elevated temperature. Oxidation inhibitors, such as boron, are often added to the matrix to provide additional protection.

Ceramic matrix materials include carbon, glass, glass-ceramics, oxides such as alumina (Al_2O_3) and nonoxides such as silicon carbide (SiC). The majority of ceramic materials are crystalline with predominantly ionic bonding, along with some covalent bonding. These bonds, in particular the strongly directional covalent bond, provide high resistance to dislocation motion and go a long way toward explaining the brittle nature of ceramics. Since ceramics and C-C composites require

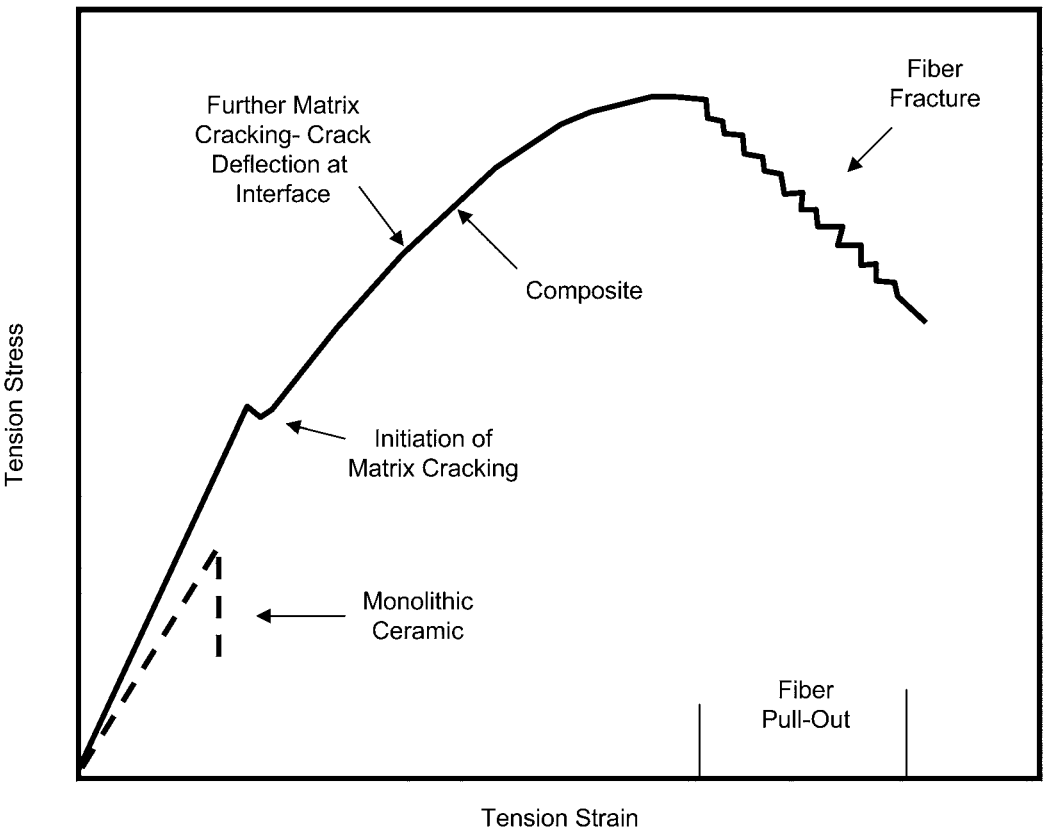


Fig. 21.3 Stress-strain for monolithic and ceramic matrix composites

extremely high processing temperatures compared to polymer or even metal matrix composites, ceramic matrix composites are difficult and expensive to fabricate.

Reinforcements for ceramic matrix composites are usually carbon, oxide, or nonoxide ceramic fibers, whiskers, or particulates. Carbon fiber is used in C-C composites; while oxide fibers such as alumina, or nonoxide fibers such as silicon carbide, are used in glass, glass-ceramic, and crystalline ceramic matrices. Most high-performance oxide and nonoxide continuous fibers are expensive, further increasing the high cost of ceramic matrix composites. The cost and great difficulty of consistently fabricating high-quality ceramic matrix composites have greatly limited their applications to date.

21.1 Reinforcements

Fibers used in ceramic matrix composites, classified according to their diameters and aspect ratios, fall into three general categories: whiskers, monofilaments, and textile multifilament fibers. Reinforcements in the form of particulates and platelets are also used. A summary of a number of oxide and nonoxide continuous ceramic fibers is given in Table 21.2.

Whiskers are nearly perfect single crystals with strengths approaching the theoretical strength of the material. They are usually 0.04 mil (1 μm) in diameter or less and up to 7.9 mil (200 μm) long. Because they are reinforcements, it is their size and aspect ratio (length/diameter) that determine their strengthening effect. Silicon carbide, silicon nitride (Si_3N_4), and alumina are the most commonly used whiskers for ceramic matrix composites.

Monofilament silicon carbide fibers are produced by chemical vapor deposition of silicon carbide on a 1.3 mil (33.0 μm) diameter amorphous carbon substrate, resulting in a large 5.5 mil (139.7 μm) diameter fiber. A carbon substrate is preferred to a tungsten substrate because, above 1500 °F (815 °C), silicon carbide reacts with tungsten, resulting in fiber strength degradation.

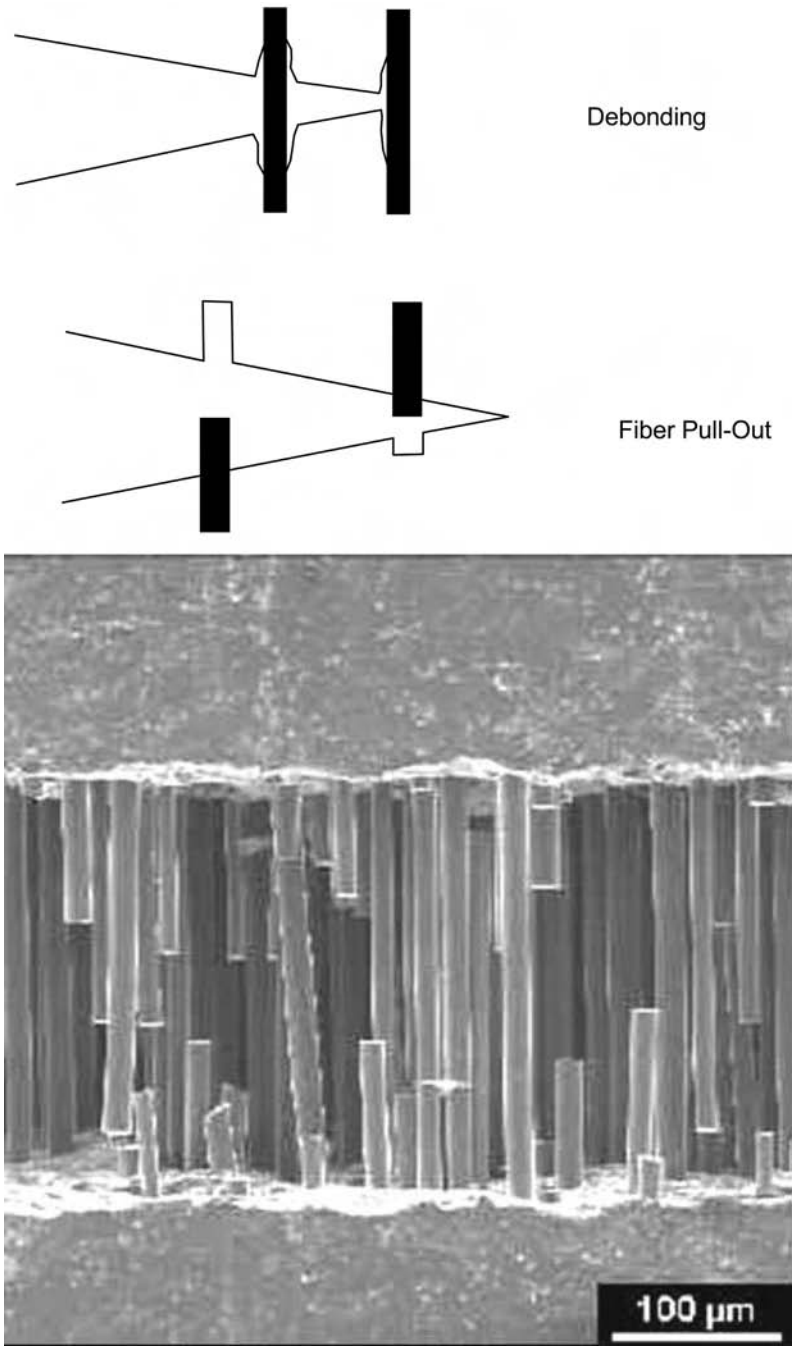


Fig. 21.4 Crack dissipation mechanisms

During manufacture, a 0.04 mil (1 µm) thick layer of pyrolytic graphite is deposited on a resistance-heated carbon substrate to provide a smooth surface and control its electrical conductivity. The coated substrate is then chemically vapor deposited using a mixture of silane and hydrogen gases. When the substrate exits the reactor, a thin layer of carbon and silicon carbide is applied to provide improved handleability, act as a diffusion barrier for reducing the reaction

between the fiber and the matrix, and heal surface flaws for improved fiber strength. Since these monofilaments are large, they can tolerate some surface reaction with the matrix without significant loss of strength. Their use in complex structures is inhibited due to their large diameter and high stiffness, which limits their ability to be formed over tight radii.

Ceramic textile multifilament fibers, in tow sizes ranging from 500 to 1000 fibers, are available that combine high-temperature properties with small diameters of 0.4 to 0.8 mil (10.2 to 20.3 μm), allowing them to be used for a wide range of manufacturing options, such as filament winding, weaving, and braiding. A useful measure of the ability of a fiber to be formed into complex part shapes is the critical bend radius ρ_{cr}, which is the smallest radius that the fibers can be bent before they fracture. The critical bend radius can be calculated by multiplying the fiber failure strain by the fiber radius. High strength, low modulus, and small diameters all contribute to fibers that can be processed using conventional textile technology. For example, while silicon carbide monofilaments have a critical bend radius of only 275.6 mil (7 mm), many ceramic textile multifilament fibers are less than 1 mm (39.4 mil).

Table 21.1 Carbon-carbon and ceramic composite comparison

Carbon-carbon	Continuous CMCs	Discontinuous CMCs
Exceptionally high-temperature mechanical properties	Excellent high-temperature mechanical properties	Excellent high-temperature mechanical properties
High specific strength and stiffness	High specific strength and stiffness	Lower specific strength and stiffness
Low to moderate toughness	Low to moderate toughness	
Dimensional stability	Dimensional stability	Fracture toughness good but lower than that of continuous CMCs
Low thermal expansion	Low thermal expansion	
High thermal shock resistance	Good thermal shock resistance	Thermal shock resistance lower than that of continuous CMCs
Graceful failure modes	Graceful failure modes	
Tailorable properties	Oxidation resistance	Amenable to lower-cost, conventional processes
Machinability	Machining more difficult	
Poor oxidation resistance	Processing more complicated and expensive	Machining expensive

Both oxide and nonoxide fibers are used for ceramic matrix composites. Oxide-based fibers, such as alumina, exhibit good resistance to oxidizing atmospheres; however, due to grain growth, their strength retention and creep resistance at high temperatures are poor. Oxide fibers can have creep rates of up to two orders of magnitude greater than those of nonoxide fibers. Nonoxide fibers, such as carbon and silicon carbide, have lower densities, much better high-temperature strength, and creep retention than oxide fibers, but they have oxidation problems at high temperatures.

Ceramic oxide fibers are composed of oxide compounds, such as alumina (Al_2O_3) and mullite ($3Al_2O_3$-$2SiO_2$). Unless specifically identified as single-crystal fibers, oxide fibers are polycrystalline. 3M's Nextel family of fibers is by far the most prevalent. Nextel is produced by a sol-gel process in which a sol-gel solution is

Table 21.2 Properties of selected continuous ceramic fibers

Fiber	Composition	Tensile strength, ksi	Tensile modulus, msi	Density, g/cm^3	Diameter, mils	Critical bend radii, mm
SCS-6	SiC on C monofilament	620	62	3.00	5.5	7.0
Nextel 312	$62Al_2O_3$-$14B_2O_3$-$15SiO_2$	250	22	2.7	0.4	0.48
Nextel 440	$70Al_2O_3$-$2B_2O_3$-$28SiO_2$	300	27	3.05	0.4–0.5	…
Nextel 480	$70Al_2O_3$-$2B_2O_3$-$28SiO_2$	330	32	3.05	0.4–0.5	…
Nextel 550	$73Al_2O_3$-$27SiO_2$	290	28	3.03	0.4–0.5	0.48
Nextel 610	99 α-Al_2O_3	425	54	3.88	0.6	…
Nextel 720	$85Al_2O_3$-$15SiO_2$	300	38	3.4	0.4–0.5	…
Almax	99 α-Al_2O_3	260	30	3.60	0.4	…
Altex	85 Al_2O_3-$15SiO_2$	290	28	3.20	0.6	0.53
Nicalon NL200	57Si-31C-12O	435	32	2.55	0.6	0.36
Hi-Nicalon	62Si-32C-0.5O	400	39	2.74	0.6	…
Hi-Nicalon-S	68.9Si-30.9C-0.2O	375	61	3.10	0.5	…
Tyranno LOX M	55.4Si-32.4C-10.2O-2Ti	480	27	2.48	0.4	0.27
Tyranno ZM	55.3Si-33.9C-9.8O-1Zr	480	28	2.48	0.4	…
Sylramic	66.6Si-28.5C-2.3B-2.1Ti-0.8O-0.4N	465	55	3.00	0.4	…
Tonen Si_3N_{44}	58Si-37N-4O	360	36	2.50	0.4	0.80

dry spun into fibers, dried, and then fired at 1800 to 2550 °F (980 to 1400 °C). Nextel 312, 440, and 550 were designed primarily as thermal insulation fibers. Both Nextel 312 and 440 are aluminosilicate fibers containing 14 percent boria (B_2O_3) and two percent boria, respectively, which means that both of these fibers contain both crystalline and glassy phases. Although boria helps to retain short-time high-temperature strength, the glassy phase also limits its creep strength at high temperatures. Since Nextel 550 does not contain boria, it does not contain a glassy phase and exhibits better high-temperature creep resistance but lower short-time high-temperature strength. For composite applications, Nextel 610 and 720 do not contain a glassy phase and have more refined α-Al_2O_3 structures, which allows them to retain a greater percentage of their strength at elevated temperatures. Nextel 610 has the highest room-temperature strength due to its fine-grained single-phase composition of α-Al_2O_3, while Nextel 720 has better creep resistance due to the addition of SiO_2 that forms α-$Al_2O_3/3AO_2O_3$-$2SiO_2$, which reduces grain boundary sliding. As a class, oxide fibers are poor thermal and electrical conductors, have higher coefficients of thermal expansion (CTE), and are denser than nonoxide fibers. Due to the presence of glass phases between the grain boundaries, and as a result of grain growth, oxide fibers rapidly lose strength in the 2200 to 2400 °F (1205 to 1315 °C) range.

Ceramic nonoxide fibers are dominated by silicon carbide–based compositions. All of the fibers in this category contain some oxygen, which limits their upper usage temperatures. Nippon's Nicalon series of SiC fibers are the most prevalent. Nicalon fibers are produced by a polymer pyrolysis process that results in a structure of ultrafine ß-SiC particles approximately 1 to 2 nm dispersed in a matrix of amorphous silicon oxide and free carbon. Fiber manufacture consists of synthesizing a spinnable polymer, spinning the polymer into a precursor fiber, curing the fiber to crosslink it so that it will not melt during pyrolysis, and then pyrolyzing the cured precursor fiber into a ceramic fiber. Nicalon's high oxygen content (12 percent) causes instability above 2200 °F (1205 °C) by producing gaseous carbon monoxide. Therefore, a low oxygen content (0.5 percent) variety, called Hi-Nicalon, was developed that has improved thermal stability and creep resistance. The oxygen content is reduced by radiation curing using an electron beam in a helium atmosphere. Their latest fiber, Hi-Nicalon-S, has an even lower oxygen content (0.2 percent) and a larger grain size (21 to 200 nm) for enhanced creep resistance.

Another SiC-type fiber with titanium carbide (TiC) in its structure is Tyranno, produced by Ube Industries. It contains two weight percent titanium to help inhibit grain growth at elevated temperatures. In the Tyranno ZM fiber, zirconium is used instead of titanium to enhance creep strength and improve the resistance to salt corrosion. A new silicon carbide fiber, Sylramic-iBN, contains excess boron in the fiber, which diffuses to the surface, where it reacts with nitrogen to form an in situ boron nitride coating on the fiber surface. The removal of boron from the fiber bulk allows the fiber to retain its high tensile strength while significantly improving its creep resistance and electrical conductivity.

Although the creep strengths of the stoichiometric fibers, such as Hi-Nicalon-S, Tyranno SA, and Sylramic, are better than those of the earlier nonstoichiometric silicon carbide fibers, their moduli are 50 percent higher and their strain-to-failures are one-third lower, which reduces their ability to toughen ceramic matrices. However, of the commercial fibers currently available, the advanced Nicalon and Tyranno fibers are the best in terms of as-produced strength, diameter, and cost of ceramic matrix composites for service temperatures up to approximately 2000 °F (1095 °C).

The oxide-based fibers are typically more strength limited at high temperatures than the nonoxide fibers; however, oxide fibers have a distinct advantage in having greater compositional stability in high-temperature oxidizing environments. While fiber creep can be a problem with both oxide and nonoxide fibers, it is generally a bigger problem with oxide fibers. Fiber grain size is a compromise; small grains contribute to higher strength, while large grains contribute to better creep resistance.

21.2 Matrix Materials

The selection of a ceramic matrix material is usually governed by thermal stability and processing considerations. The melting point is a good first indication of high-temperature stability. However, the higher the melting point, the more difficult the matrix is to process. Mechanical and chemical compatibility of the matrix with the reinforcement determines whether or not a useful composite can be fabricated. For some whisker-reinforced ceramics, even moderate re-

Table 21.3 Select ceramic matrix materials

Matrix	Modulus of rupture, ksi	Modulus of elasticity, msi	Fracture toughness, ksi-in.$^{1/2}$	Density, g/cm^3	Thermal expansion, 20^{-6}/°C	Melting point, °F
Pyrex glass	8	7	0.07	2.23	3.24	2285
LAS glass-ceramic	20	17	2.20	2.61	5.76	…
Al_2O_3	70	50	3.21	3.97	8.64	3720
Mullite	27	21	2.00	3.30	5.76	3360
SiC	56–70	48–67	4.50	3.21	4.32	3600
Si_3Ni_4	72–120	45	5.10	3.19	3.06	3400
Zr_2O_3	36–94	30	2.50–7.70	5.56–5.75	7.92–13.5	5000

Note: Values depend on exact composition and processing.

actions with the matrix during processing can consume the entire reinforcement. Likewise, large differences in thermal expansion between the fibers and matrix can result in large residual stresses and matrix cracking. Several important matrix materials are listed in Table 21.3.

Carbon is an exceptionally stable material in the absence of oxygen, capable of surviving temperatures greater than 4000 °F (2205 °C) in vacuum and inert atmospheres. In addition, carbon is lightweight, with a density of approximately 0.072 lb/in.^{3} (1.99 g/cm^3). However monolithic graphite is brittle, low in strength, and cannot be easily formed into large, complex shapes. To overcome these limitations, C-C composites were developed, in which high-strength carbon fibers are incorporated into a carbon matrix. For high-temperature applications, C-C composites offer exceptional thermal stability greater than 4000 °F (2205 °C) in nonoxidizing atmospheres along with low densities of 0.054 to 0.072 lb/in.^{3} (1.49 to 1.99 g/cm^3). Carbon-carbon composites are used in rocket nozzles, nose cones for reentry vehicles, leading edges, cowlings, heat shields, aircraft brakes, brakes for racing vehicles, and high-temperature furnace setters and insulation. These applications utilize the following nominal properties of C-C composites (which depend on fiber type, fiber architecture, and matrix density):

Ultimate tensile strength greater than 40 ksi (275 MPa)
Modulus of elasticity greater than 10 msi (69 GPa)
Thermal conductivity 0.9 to 19 Btu-in./(s-ft^2-°F)
Thermal expansion 1.1 ppm/K
Density less than 0.072 lb/in.^{3} (1.99 g/cm^3)

The low thermal expansion and range of thermal conductivities give C-C composites high thermal shock resistance. As previously mentioned, the one major shortcoming of C-C composites is their oxidation susceptibility. At temperatures above 950 °F (510 °C), both the matrix and the fiber are vulnerable to oxidation if they are not protected from oxygen exposure. The two primary oxidation protection methods are external coatings and internal oxidation inhibitors. Surface coatings, such as silicon carbide, provide an external barrier to oxygen penetration. The addition of internal oxidation inhibitors acts either as an internal barrier to oxygen ingress or as an oxygen sink (forming a protective barrier). In high-temperature oxidizing environments, the time-temperature cyclic capabilities of these oxidation barriers are the primary limit to the temperature capabilities of current C-C composites.

Because they can be consolidated at lower temperatures and pressures than polycrystalline ceramic materials, glass-ceramics are potentially attractive matrix materials. Since all glass-ceramics contain some residual glass after ceraming, the upper use temperature is controlled by the softening point of the residual glass; however, silica-based glass-ceramics can be used for moderate temperature applications. The most common glass-ceramic systems are LAS, MAS, MLAS, CAS, and BMAS, where L = lithium oxide (Li_2O), A = alumina (Al_2O_3), S = silica (SiO_2), M = magnesium oxide (MgO), C = calcium oxide (CaO), and B = barium oxide (BaO). Glass-ceramics have the advantage, that being glasses, they can be melted to relatively low viscosities during hot pressing to impregnate the fiber bundle, and the processing temperatures are lower than for traditional crystalline ceramics, thereby reducing fiber degradation. After hot pressing, they are converted to a glass-ceramic by a heat treatment, in this case ceraming. The amount of crystalline phase can be as high as 95 to 98 percent. However, the presence of the residual glassy phase limits their elevated temperature creep resistance.

Nonoxide matrices include carbon, silicon carbide, and silicon nitride (Si_3N_4). Carbon is extremely refractory and has a low density; however, for elevated-temperature applications, it must be

protected from oxidation. Silicon carbide has a high melting point and excellent mechanical properties at elevated temperatures. It is a little less refractory than carbon and has a slightly higher density, with oxidation resulting in the formation of silica; however, it can be used up to 2700 °F (1480 °C) in air. Silicon nitride matrices have properties similar to those of silicon carbide, except that they are less thermally stable and exhibit lower conductivities.

Oxide matrices include alumina (Al_2O_3), mullite ($3Al_2O_3$-$2SiO_2$), cordierite ($2MgO$-$2Al_2O_3$-$5SiO_2$), and zirconia (ZrO_2). Oxide matrices are relatively low in cost, rapidly sinter at moderate temperatures, and exhibit high-temperature oxidation resistance. Limitations include poor thermal expansion matches with many fibers, intermediate strength, and low high-temperature properties. Alumina is the most prevalent oxide matrix and contains the best balance of properties. Mullite has lower thermal expansion than alumina, processes well with sol-gel methods and exhibits good toughness. Cordierite has very low thermal expansion and is often used in conjunction with other oxides, such as mullite for matrices. Ziconia, which has excellent toughness when partially stabilized, loses much of its toughness at elevated temperatures.

In selecting a fiber-matrix combination for a ceramic matrix composite, several factors need to be considered. First, the constituents need to be compatible from the standpoint of CTE. If the CTE of the matrix is greater than the radial CTE of the fiber, the matrix, on cooling from the processing temperature, will clamp the fibers, resulting in a strong fiber-to-matrix bond and exhibiting brittle failures in service. On the other hand, if the CTE of the matrix is less than the radial CTE of the fibers, the fibers may debond from the matrix on cooling. Chemical compatibility of the constituents is also an important factor. Due to the high processing temperatures for ceramic matrix composites, reactions between the fiber and matrix resulting in reduced fiber strengths are a constant concern. For example, silicon carbide fibers react with silica-based glass-ceramics, so the fibers must be coated with a protective interfacial coating.

For temperatures exceeding 1800 °F (980 °F), candidate matrices are carbon, silicon carbide, silicon nitride, and alumina. Although these compositions are possible, the performance requirement that the matrix material have a CTE very close to that of the commercially available carbon-, silicon carbide– and alumina-based fibers effectively eliminates silicon nitride and alumina as matrix choices for the silicon carbide fibers and silicon carbide and silicon nitride as matrix choices for the alumina-based fibers. The lack of high thermal conductivity and the availability of oxide-based fibers that are creep resistant for long times above 1800 °F (980 °F) are two factors currently limiting the commercial viability of oxide/oxide ceramic matrix composites.

21.3 Interfacial Coatings

Interfacial, or interphase, coatings are often required to (1) protect the fibers from degradation during high-temperature processing, (2) aid in slowing oxidation during service, and (3) provide the weak fiber-to-matrix bond required for toughness. The coatings (Fig. 21.5), ranging in thickness from 0.004 to 0.04 mil (0.1 to 1.0 μm), are applied directly to the fibers prior to processing, usually by chemical vapor deposition. Chemical vapor deposition produces coatings of relatively uniform thickness, composition, and structure, even with preforms of complex fiber architecture. Carbon and boron nitride (BN) are typical coatings, used either alone or in combination with each other. Frequently, in addition to the interfacial coatings, an overcoating is also applied, such as a thin layer approximately 0.02 mil (0.5 μm) of silicon carbide that becomes part of the matrix during processing. The silicon carbide overcoating helps to protect the interfacial coating from reaction with the matrix during processing. Since carbon and BN interfacial coatings will degrade in an ambient environment due to moisture absorption, the overcoating is usually applied immediately after the interfacial coating. During service, the overcoating also acts to protect the fibers and interfacial coatings from aggressive environments such as oxygen and water vapor. The interfacial coating and overcoating are sometimes repeated as multilayer coatings to provide environmental protection layers in the presence of in-service-generated matrix cracks.

21.4 Fiber Architectures

Fiber architecture is similar to that used for polymer matrix composites. Either unidirectional or woven cloth can be prepregged, or textile techniques such as weaving or braiding can

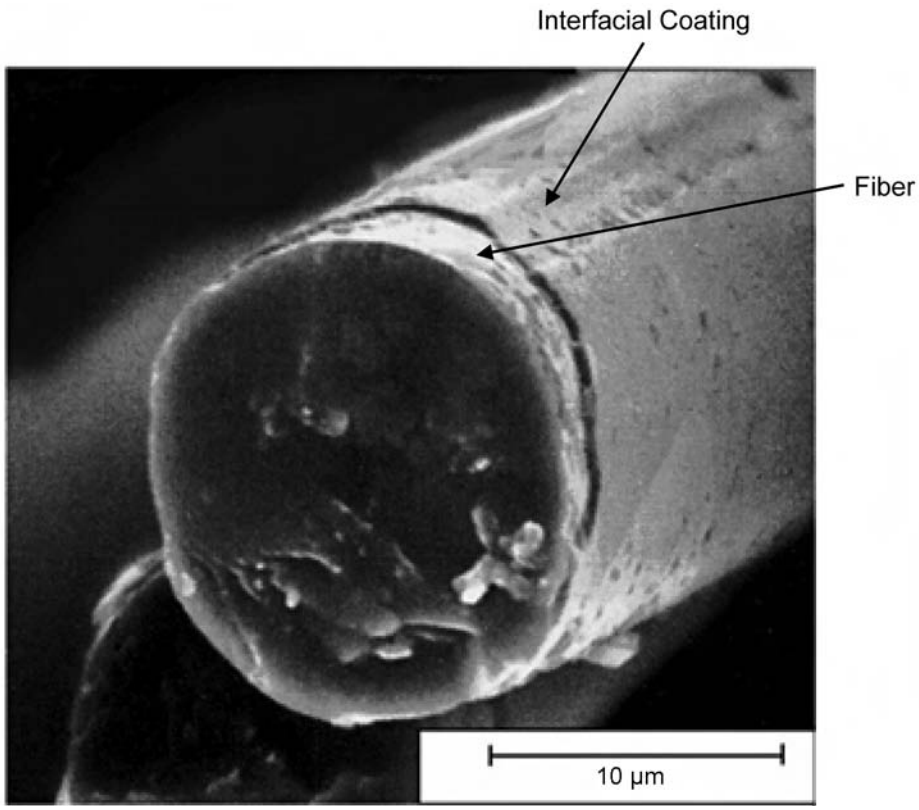


Fig. 21.5 Interfacial coating

be used to form a near-net preform. To form unidirectional prepreg, tows are precoated with the interfacial protection system and filament wound on a drum, which can be prepregged with the ceramic matrix precursor material or held together with a fugitive binder. The sheets are then cut from the drum and layed up in the desired orientation. For fabric constructions, the tows are usually woven prior to applying the interfacial coatings to minimize damage to the coatings. These prepregging approaches are illustrated in Fig. 21.6. Near-net-shaped preforms can also be constructed using textile technologies such as weaving, stitching, and braiding. Again, to avoid coating damage, the interfacial coating system is normally applied after the textile-forming operations are complete.

21.5 Fabrication Methods

Fabrication of ceramic matrix composites can be performed using solid, liquid, or gas phase processing to infiltrate the matrix onto the reinforcement. In any process, the objectives are to achieve minimum porosity, obtain uniform dispersion of reinforcement, and control the fiber-to-matrix bonding. Although many fabrication methods have been explored, the most prevalent fabrication approaches for ceramic matrix composites include:

- Powder processing for discontinuous matrix composites
- Slurry infiltration and consolidation for glass and glass-ceramic composites
- Polymer infiltration and pyrolysis
- Chemical vapor infiltration
- Directed metal oxidation
- Liquid silicon infiltration

21.6 Powder Processing

In a manner similar to that used for monolithic ceramic materials, powder processing can be used to fabricate discontinuously reinforced ceramic matrix composites. While this process works well

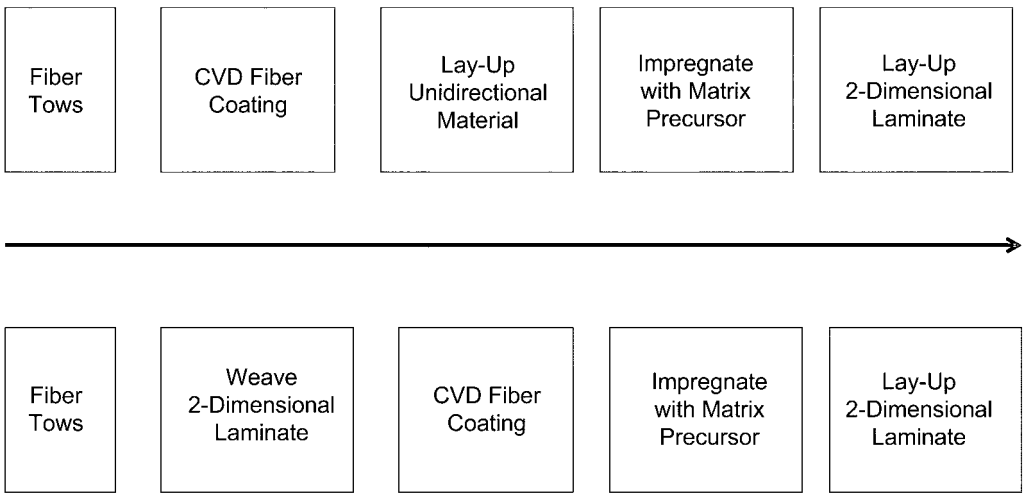


Fig. 21.6 Ceramic prepreg fabrication. Chemical vapor deposition (CVD)

for very small reinforcements such as whiskers and particulates, longer discontinuous fibers are broken into shorter fibers during the mixing and consolidation processes. The basic processing steps are:

- Powder mixing (matrix and reinforcement)
- Green body fabrication
- Machining if required
- Binder removal
- Consolidation and densification
- Inspection

The process flow for the powder method is shown in Fig. 21.7. A uniform, fine dispersion of the reinforcement and matrix powder helps minimize voids in the consolidated composite. When the constituents are not effectively packed, densification becomes more difficult, requiring higher pressures and longer times. Optimum packing occurs when the particle size distribution contains about 30 percent by volume of small particles and 70 percent by volume of large particles. Constituent mixing is often accomplished by ball milling.

Short fibers or whiskers are often mixed with a ceramic powder slurry, dried, and hot pressed. Short fibers and whiskers often undergo some orienting during hot pressing. Whisker agglomeration in the green body is a major problem. Mechanical stirring and adjustment of the pH level of the suspension (whiskers and matrix powder in water) can help. Addition of whiskers to a slurry can result in unacceptable increases in viscosity. Also, whiskers with a large aspect ratio greater than 50 tend to form bundles and clumps. Obtaining well-separated and deagglomerated whiskers is important for a uniform composite. Organic dispersants and techniques such as agitation mixing assisted by ultrasonics can be used along with deflocculation by proper pH control.

Organic binders are usually mixed with the reinforcement and matrix so that near-net-shaped parts can be produced by cold forming processes such as uniaxial pressing, cold isostatic pressing, tape casting, extrusion, and injection molding. After cold consolidation, the green body can be handled and even machined without damage. All organic binders must be burned out either before or during the consolidation process.

While sintering without pressure is often used to fabricate monolithic ceramics, the presence of reinforcements significantly hinders the sintering process. Although SiC whisker-reinforced alumina with whisker contents less than 10 percent by volume can be pressureless sintered to greater than 95 percent theoretical densities, higher volume fractions will result in unacceptable porosity levels. To improve consolidation and provide acceptable levels of porosity, very fine ceramic particle sizes are used as well as pressure applied by hot pressing or hot isostatic pressing (HIP). Both hot pressing and HIP have limitations. Hot pressing is restricted by press size and tonnage and is not practical for complex shapes, while HIP can be expensive and difficult if the part must be "canned" with a metal bag for parts containing porosity open to the surface. Hot pressing is used to make cutting tools, such as

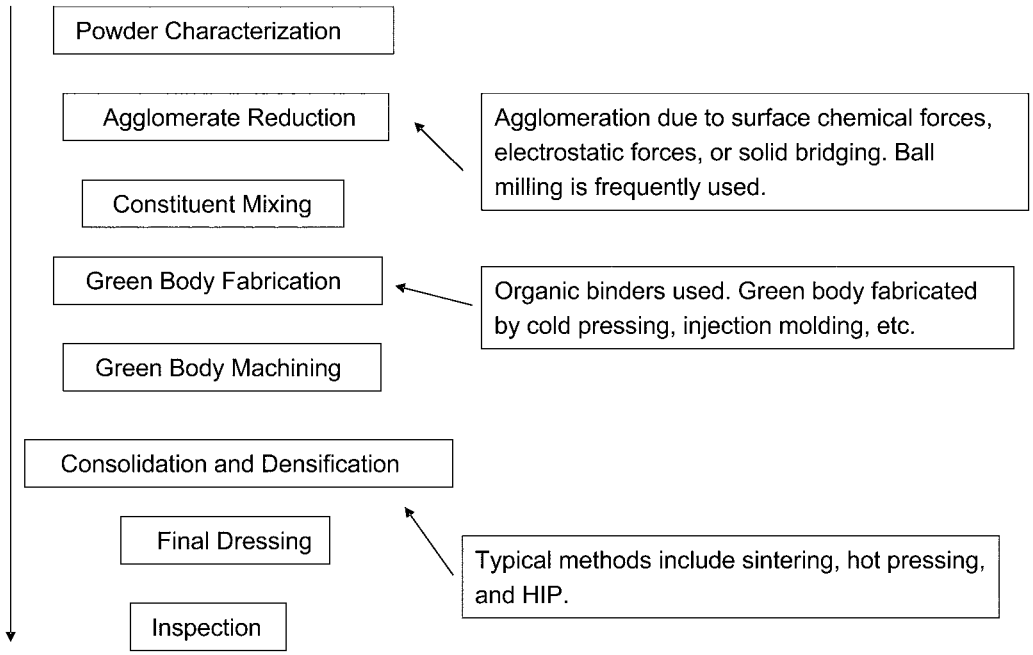


Fig. 21.7 Fabrication sequence for powder processing. Hot isostatic processing (HIP)

those shown in Fig. 21.8, that are used to machine metals that are difficult to machine, such as nickel based superalloys. The SiC_w/Al_2O_3 composites can be hot pressed at 2700 to 3450 °F (1480 to 1900 °C) at pressures of 3 to 6 ksi (20 to 40 MPa).

21.7 Slurry Infiltration and Consolidation

Slurry infiltration and consolidation is the process most often used to make glass and glass-ceramic composites, mainly because the processing temperatures used for glass and glass-ceramics are lower than those used for crystalline ceramics. The melting point of crystalline ceramics is so high that even fibers with interfacial coatings can either be dissolved or severely degraded. Another problem is the large temperature difference between the extremely high processing temperatures and room temperature, which can result in shrinkage and matrix cracking. In addition, crystalline ceramics heated past their melting points have such high viscosities that the infiltration of preforms is very difficult, if not impossible.

Glass-ceramics start as amorphous glasses that can be formed into a shape and transformed into crystalline ceramics by a high-temperature heat treatment (devitrification). During heat treatment, small crystallites approximately 1 nm, nucleate and grow until they impinge on adjacent crystallites. On further heating, very fine, less than 0.04 mil (1 μm), angular crystallites form. The resulting glass-ceramic is a microcrystalline material in a glassy matrix with a crystalline content as high as 95 to 98 percent.

It should be noted that not all glass compositions are capable of forming glass-ceramics. Most commercial glass-ceramics are made from Li_2O-Al_2O_3-SiO_2 (LAS) compositions. LAS glass with small amounts of titanium dioxide (TiO_2) added as a nucleating agent will crystallize into β-spodumene (Li_2O-Al_2O_3-$4SiO_2$) or β-quartz (SiO_2), depending on the initial glass composition. When the LAS glass is heated to 1400 °F (760 °C) for 1.5 hours, titanium dioxide precipitates nucleate in the glass matrix. When the temperature is raised to 1750 °F (955 °C), crystallization initiates at the TiO_2 nuclei.

In slurry infiltration, fiber tows or a preform are impregnated in a tank containing the liquid slurry matrix, as shown in Fig. 21.9. The slurry consists of the matrix powder, an organic binder, and a liquid carrier such as water or alcohol. The slurry composition is very important. Variables

such as the powder content, particle size distribution, and type and amount of binder, as well as the carrier medium, have a significant impact on part quality. For example, using a matrix powder that is smaller than the fiber diameter will facilitate thorough impregnation, thereby reducing porosity. Wetting agents can also be used to help infiltration into the fiber tows or preform.

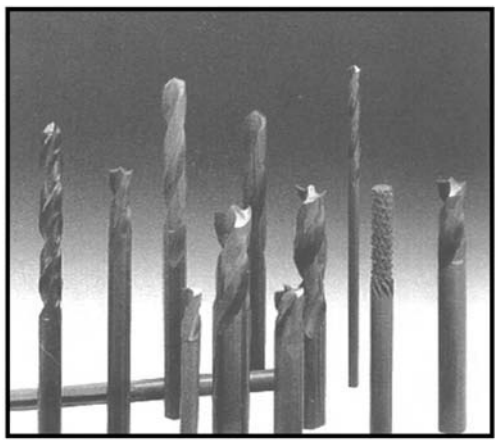


Fig. 21.8 SiC_w/Al_2O_3 composite cutting tools. Source: Greenleaf Corporation

After infiltration, the liquid carrier is allowed to evaporate. The resulting prepreg can then be layed up on a tool for consolidation. Prior to consolidation, the organic binder must be burned out. Consolidation is normally accomplished in a hot press; however, HIP is an option if complex shapes are required. Consolidation parameters (time, temperature, and pressure) also affect part quality. While high temperatures, long times, and high pressures may help to reduce porosity, fiber damage can result from either high pressures (mechanical damage) or high temperatures and long times (interfacial reactions).

The slurry infiltration process generally yields a composite with a fairly uniform fiber distribution and low porosity. The main disadvantage is that it is restricted to relatively low melting or low softening point matrix materials.

21.8 Polymer Infiltration and Pyrolysis (PIP)

The PIP process is very similar to the processes used to make polymer matrix composites. Either a fiber-reinforced prepreg is made with a matrix

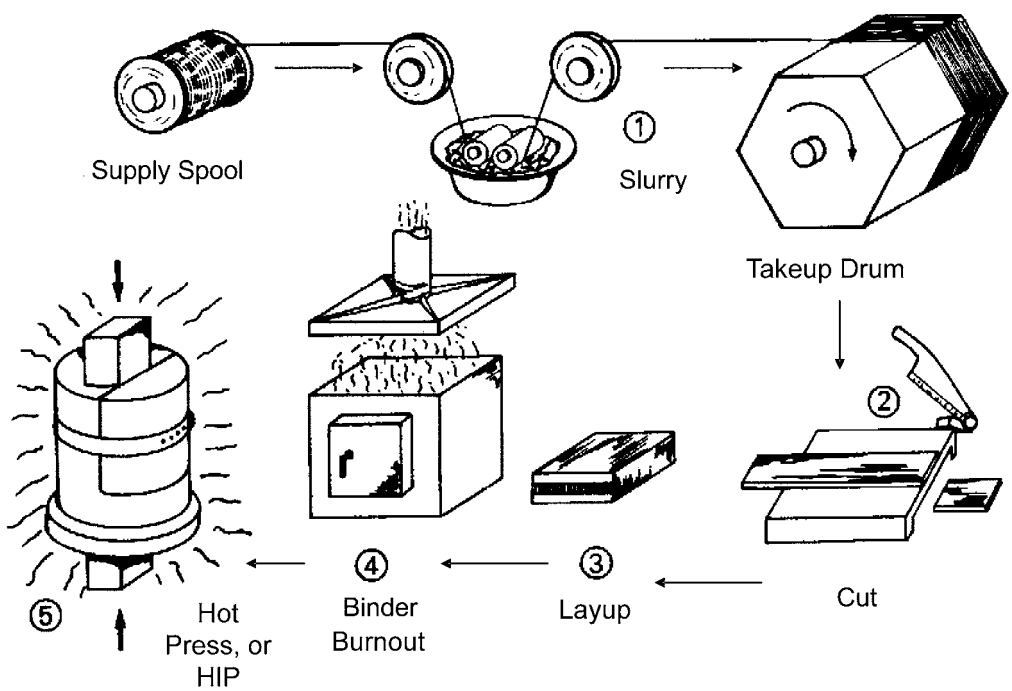


Fig. 21.9 Slurry infiltration and consolidation

material that can be converted to a ceramic upon heat treatment (pyrolysis) or a dry preform is infiltrated multiple times with a liquid organic precursor that can be converted by pyrolysis to a ceramic. In the case of prepreg, after the initial conversion to a ceramic, subsequent infiltrations are performed with a liquid precursor material. Instead of a conventional thermoset resin such as epoxy, an organometallic polymer is used. The PIP process, shown schematically in Fig. 21.10, consists of:

- Infiltration of the preform with the polymer
- Consolidation of the impregnated preform
- Cure of the polymer matrix to prevent melting during subsequent processing
- Pyrolysis of the cured polymer to convert it to a ceramic matrix
- Repetition of the infiltration and pyrolysis process *N* times to produce the desired density

This section covers three types of PIP processes: the Space Shuttle C-C process, the conventional PIP process, and the sol-gel infiltration and pyrolysis process.

21.8.1 Space Shuttle C-C Process

The fabrication process for the C-C Space Shuttle nose cap and wing leading edge components (Fig. 21.11) is a multistep process typical of the infiltration and pyrolysis technology used to produce C-C composites. As shown in Fig. 21.12, initial material lay-up is similar to that used for thermoset composite parts. Plain weave carbon fabric, impregnated with phenolic resin, is layed up on a fiberglass/epoxy tool. Laminate thickness varies from 19 plies in the external skin and web areas up to 38 plies at the attachment locations. The part is vacuum bagged and autoclave cured at 300 °F (150 °C) for eight hours. The cured part is rough trimmed, x-rayed, and ultrasonically inspected. The part is then postcured by placing it in a graphite restraining fixture, loading it into a furnace, and heating it to 500 °F (260 °C) very slowly to avoid distortion and delamination. The postcure cycle alone can take up to seven days.

The next step is initial pyrolysis. The part is loaded into a graphite restraining fixture and placed in a steel retort, which is packed with calcined coke. The part is slowly heated to 1500 °F

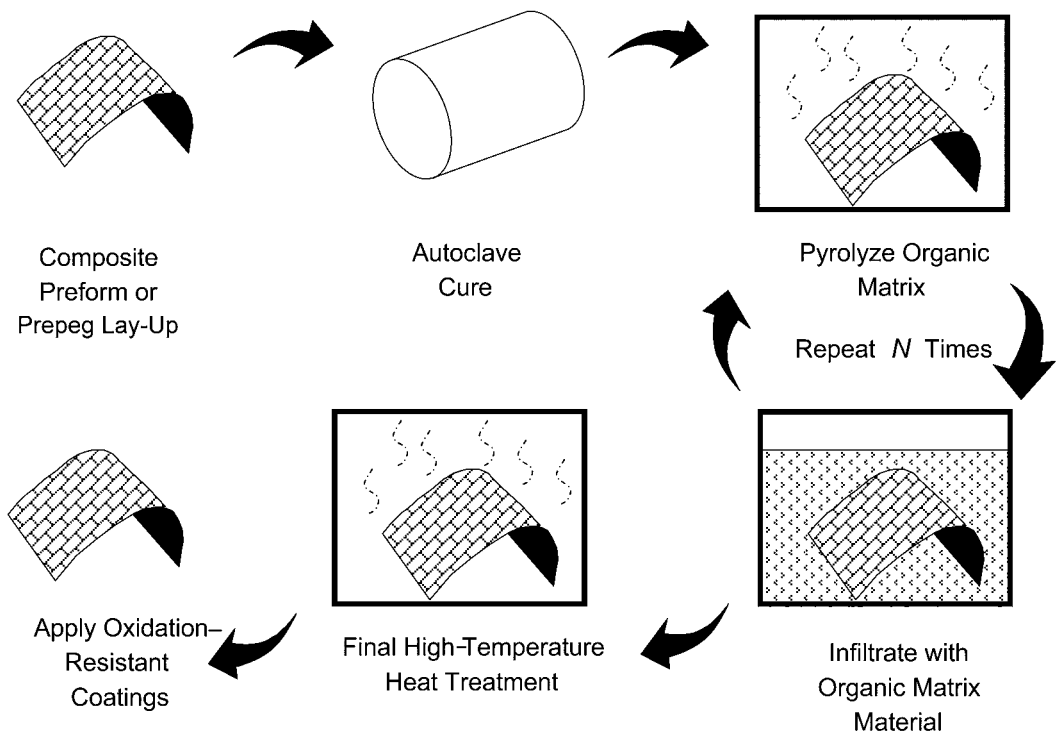


Fig. 21.10 Polymer impregnation and pyrolysis process



Fig. 21.11 Space shuttle carbon-carbon applications.

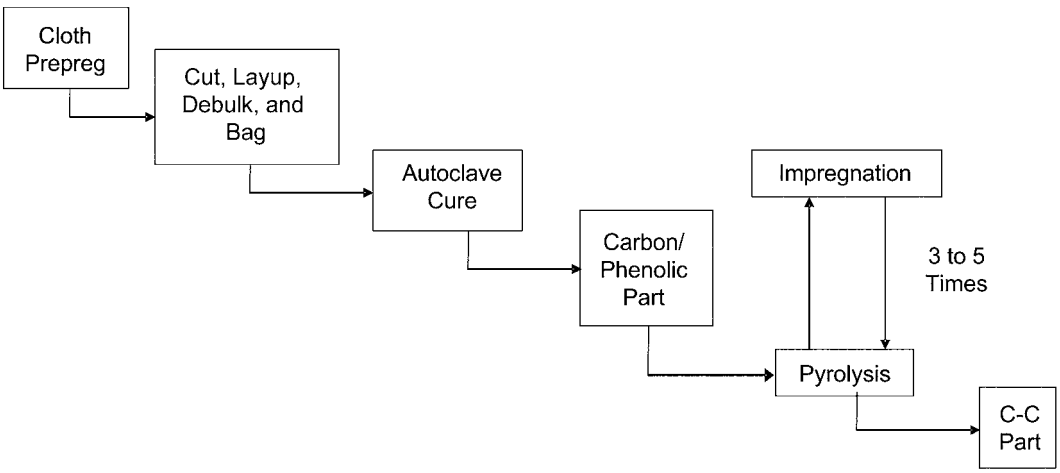


Fig. 21.12 Fabrication sequence for space shuttle carbon-carbon parts. Carbon-carbon (C-C)

(815 °C) and held for 70 hours to facilitate conversion of the phenolic resin to a carbon state. During pyrolysis, the resin forms a network of interconnected porosity that allows volatiles to escape. This stage is extremely critical. Adequate volatile escape paths must be provided, and sufficient times must be provided to allow the volatiles to escape. If the volatiles become trapped and build up internal pressure, massive delaminations can occur in the relatively weak matrix. After this initial pyrolysis cycle, the carbon is designated *reinforced carbon-carbon-0* (RCC-0), a state in which the material is extremely light and porous, with a flexural strength of only 3000 to 3500 psi.

Densification is accomplished in three infiltration and pyrolysis cycles. In a typical cycle, the part is loaded into a vacuum chamber and impregnated with furfural alcohol. It is then autoclave cured at 300 °F (150 °C) for two hours

and postcured at 400 °F (205 °C) for 32 hours. Another pyrolysis cycle is then conducted at 1500 °F (815 °C) for 70 hours. After three infiltration/pyrolysis cycles, the material is designated RCC-3, with a flexural strength of around 18,000 psi (125 GPa).

To allow usage at temperatures above 3600 °F (1980 °C) in an oxidizing atmosphere, it is necessary to apply an oxidation-resistant coating system. The coating system consists of two steps: (1) applying a silicon carbide diffusion coating to the C-C part and (2) applying a glassy sealer to the silicon carbide diffusion coating. The coating process (Fig. 21.13) starts with blending of the constituent powders, consisting of 60 percent silicon carbide, 30 percent silicon, and 10 percent alumina. In a pack cementation process, the mix is packed around the part in a graphite retort. The retort is loaded into a vacuum furnace, where it undergoes a 16-hour cycle that includes drying at 600 °F (315 °C) and then a coating reaction up to 3000 °F (1650 °C) in an argon atmosphere. During processing, the outer layers of the C-C are converted to silicon carbide. The silicon carbide–coated C-C part is removed from the retort, cleaned, and inspected. During cool-down from 3000 °F (1650 °C), the silicon carbide coating contracts slightly more than the C-C substrate, resulting in surface crazing (coating fissures). This crazing, together with the inherent material porosity, provides paths for oxygen to reach the C-C substrate.

To obtain increased life, it is necessary to add a surface sealer. The surface sealing process involves impregnating the part with tetraethylorthosilicate (TEOS). The part is covered with a mesh and placed in a vacuum bag, and the bag is filled with liquid TEOS. A five-cycle TEOS impregnation process is then performed on the bagged part. After the fifth impregnation cycle, the part is removed from the bag and oven cured at 600 °F (315 °C) to liberate hydrocarbons. This process leaves SiO_2 in all of the microcracks and fissures, greatly enhancing the oxidation protection.

21.8.2 Conventional PIP Processes

For ceramic matrices other than carbon, silicon-based organometallic polymers are the most common precursors, including silicon-carbon, silicon-carbon-oxygen, silicon-nitrogen, silicon-oxygen-nitrogen, and silicon-nitrogen-carbon-oxygen precursors. Aluminum-oxygen and BN have also been studied. The polymeric precursor should produce a high char yield to obtain the desired density in as few polymer infiltration and pyrolysis cycles as possible. Polymers containing highly branched and crosslinked structures,

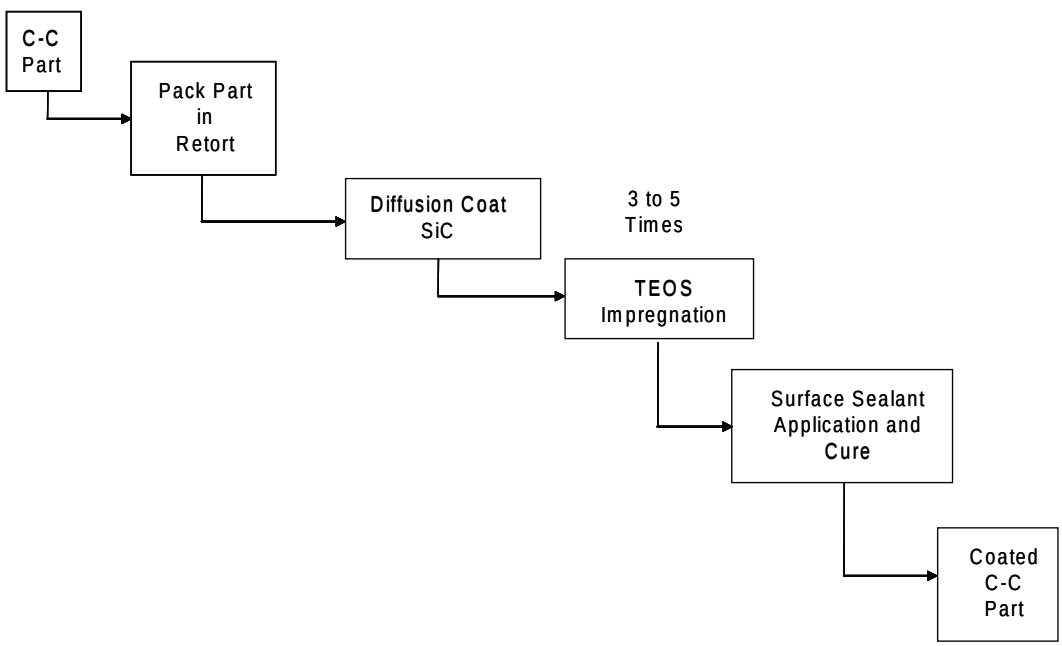


Fig. 21.13 Coating sequence for space shuttle carbon-carbon parts. Carbon-carbon (C-C), silicon carbide (SiC), tetraethylorthosilicate (TEOS)

and those with high percentages of ring structures, are good candidates. Those that contain long chains tend to break up into low-weight volatiles and are poor choices. Polymer branching and crosslinking increases the ceramic yield by inhibiting chain scission and the formation of volatile silicon oligomers during pyrolysis. Initial pyrolysis produces an amorphous ceramic matrix, while high-temperature treatments lead to crystallization and shrinkage as the amorphous matrix develops small domains of crystalline structures. Fillers, such as silica or ceramic whiskers, can improve matrix properties by reducing and disrupting the matrix cracks that form during shrinkage. Typical filler loadings are 15 to 25 volume percent of the matrix.

If prepreg is going to be used, the first step is to impregnate the reinforcement with the precursor matrix material. Another option is to use a dry preform and to infiltrate the precursor resin directly into the preform before pyrolysis. Resin transfer molding, vacuum impregnation, fiber placement, and filament winding have all been used to impregnate and form preceramic preforms. The composite part is initially autoclave cured at 300 to 500 °F (150 to 260 °C) and 50 to 100 psi. The part is then put through the first pyrolysis cycle to convert the precursor matrix to ceramic. Pyrolysis in either argon or nitrogen atmospheres of at least 1300 °F (705 °C) is required, with typical processing temperatures in the range of 1700 to 2200 °F (925 to 1205 °C).

During pyrolysis, large amounts of organic volatiles, such as H_2 and carbon monoxide, are released. Therefore, pyrolysis cycles must be done slowly to allow the volatiles to escape without causing part delamination. As a result of pore formation and growth, pyrolysis gases can produce both micro- and macrocracking. In addition, there is an extremely large reduction in volume during the matrix conversion from polymers to ceramics. Cycles as long as one to two days are not uncommon.

Subsequent infiltrations are conducted with a low-viscosity prepolymer. Infiltration is best done by vacuum impregnation in a vacuum bag. After the first pyrolysis cycle, the matrix is amorphous and highly porous, with multiple matrix cracks and a void content of 21 to 30 percent. The infiltration and pyrolysis process is repeated, often between five and ten times to reduce the porosity, fill the cracks, and obtain the desired density. After the last pyrolization cycle, the part can be heat treated at higher temperatures to convert the amorphous matrix to a crystalline phase, relieve residual stresses, and provide final consolidation.

The biggest advantage of the PIP process is the use of the familiar methods employed in organic matrix composite fabrication. However, the multiple infiltration and pyrolysis cycles required to obtain high-density parts are expensive and the lead times are long. In addition, it is almost impossible to fill all of the fine matrix cracks, which degrades mechanical properties.

21.8.3 Sol-Gel Infiltration

Sol-gel infiltration is a lower-temperature infiltration and pyrolysis process that can be used for oxide-based ceramic matrix composites. Densification still requires pressure and high temperatures, but the densification temperatures are usually less than those required in the slurry infiltrated matrices. Sol-gel techniques require minimal exposures to temperatures above 1800 °F (980 °C), which helps to reduce thermal damage to the fibers. Infiltration can be performed at temperatures below 600 °F (315 °C), using either vacuum infiltration or autoclave molding. In addition, sintering aids, such as boria, are not required due to the lower processing temperatures.

In sol-gel infiltration, a chemical precursor is hydrolyzed, polymerized into a gel, and then dried and fired to produce a glass or ceramic composition. The precursors range from mixtures of water, alcohols, and metal oxides to commercially available stabilized colloids containing discrete ceramic particles. Hydrolysis reactions form an organometallic solution, or sol, composed of polymer-like chains containing metallic ions and oxygen. Amorphous oxide particles form from the solution, producing a rigid gel. The gel is then dried and fired to provide sintering and densification of the final ceramic part.

As an example, in the sol-gel process for alumina, an organometallic precursor is hydrolyzed, converted to colloidal solution that is peptized with hydrochloric acid, and then fired at increasing temperatures to produce first γ-alumina and eventually α-alumina as follows:

$$Al(OC_4H_9)_3 + H_2O \rightarrow Al(OC_4H_9)_2 + C_4H_9OH \quad \text{(Hydrolysis)}$$

$$2Al(OC_4H_9)_2(OH) + H_2O \xrightarrow{HCl} C_4H_9O\text{–}AlOH\text{–}O\text{–}AlOH\text{–}OC_4H_9 + 2C_4H_9OH \quad \text{(Peptization)}$$

$$2AlO(OH) \rightarrow \gamma\text{-}Al_2O_3 + H_2O \rightarrow \alpha\text{-}Al_2O_3 \quad \text{(Firing)}$$

The ideal sol should have as high a ceramic content greater than 30 weight percent if possible, a low viscosity (15 to 20 cps), and a small particle size less than 30 nm if possible. A neutral pH helps minimize fiber degradation. The sol should be capable of being processed at room temperature for several hours and should be stable enough to allow shipping and storage.

Again, fillers can be used to help reduce shrinkage and subsequent matrix cracking. Ceramic filler powders can: (1) reduce shrinkage and matrix cracking as the matrix loses water and alcohols, (2) provide sites for the nucleation of grains, and (3) maximize matrix densification during the infiltration. Typically, alumina particles are added to alumina sols. However, loading the liquid precursor with powder increases the viscosity considerably and hinders the reimpregnation step.

Impregnation of fiber tows can be accomplished by several methods: (1) the tows can be passed through a bath containing the sol and then hydrolyzed in humid air; (2) the tows can be passed through a bath containing a partially hydrolyzed sol and then wet wound; or (3) the tows can be dry wound and then pressure infiltrated with the sol. For woven two- and three-dimensional fiber architectures, it is normal practice to weave the fabric first and then infiltrate the woven preform with the sol. For two-dimensional woven fabrics that will require lay-up, polymeric binders are often used to provide tack and drape but require burnoff prior to densification.

A typical fabrication sequence is to weave a preform and then impregnate it with the sol. Impregnation can be conducted by immersing the preform in the sol and pulling a vacuum to facilitate impregnation. An autoclave can also be used to provide positive pressure, resulting in better impregnation. The sol is then gelled by heating. Temperatures in the range of 200 to 400 °F (95 to 205 °C) will remove water and alcohols, while higher temperatures of 550 to 750 °F (285 to 400 °C) can be used to drive off any organics.

The infiltration and gelling cycle is repeated until the desired density is obtained. Processing under vacuum pressure usually yields a composite with about 20 percent porosity. Lower porosity levels can be achieved by using 50 to 100 psi (345 to 690 kPa) autoclave pressure. After the desired density is achieved through multiple infiltration cycles, the part is fired at high temperatures to obtain the final ceramic microstructure.

While lower processing temperatures can be used in the sol-gel process, the disadvantages are high shrinkage, which results in matrix cracking; low yield, which requires multiple infiltrations; and high precursor costs. High shrinkage of the gelled sols results from the large volume of water and alcohols that must be removed, often resulting in significant levels of porosity and extensive matrix micro- and macrocracking. Excess water is typically used to ensure complete hydrolysis, but large amounts of water also reduce the yield of the dried matrix obtained per infiltration cycle. In some cases, the polymeric precursor chemicals are very expensive, and most metal-organic compounds are very sensitive to moisture, heat, and light.

21.9 Chemical Vapor Infiltration (CVI)

Chemical vapor deposition (CVD) is a well-established industrial process for applying thin coatings to materials. When it is used to infiltrate and form a ceramic matrix, it is called *chemical vapor infiltration* (CVI). In CVI, a solid is deposited within the open volume of a porous structure by the reaction or decomposition of gases or vapors. A porous preform of fibers is prepared and placed in a high-temperature furnace, as shown in Fig. 21.14. Reactant gases or vapors are pumped into the chamber and flow around and diffuse into the preform. The gases decompose or react to deposit a solid onto and around the fibers. As the reaction progresses, the apparent fiber diameter increases and eventually fills the available porosity, as depicted in Fig. 21.15. Since this is essentially a deposition process, there is very little mechanical stress on the fibers. The primary processes involved are mass and heat transfer, with the objective of maximizing the rate of matrix deposition while minimizing density gradients.

One of the problems with CVI is that the reactions occur preferentially at or near the first surfaces contacted by the reactant gases, resulting in sealing off the interior pores in the preform. To minimize this effect, it is necessary to run the process at low temperatures and reduced pressures and use dilute reactant concentrations, all of which translate into long processing times.

The most important uses of CVI are to produce carbon and silicon carbide matrix composites. A carbon matrix can be formed by the decomposition of methane for example, CH_4 + nitrogen + hydrogen, on a hot fibrous preform. For a silicon carbide matrix, methyltrichlorosilane (CH_3SiCl_3) is used, along with hydrogen at

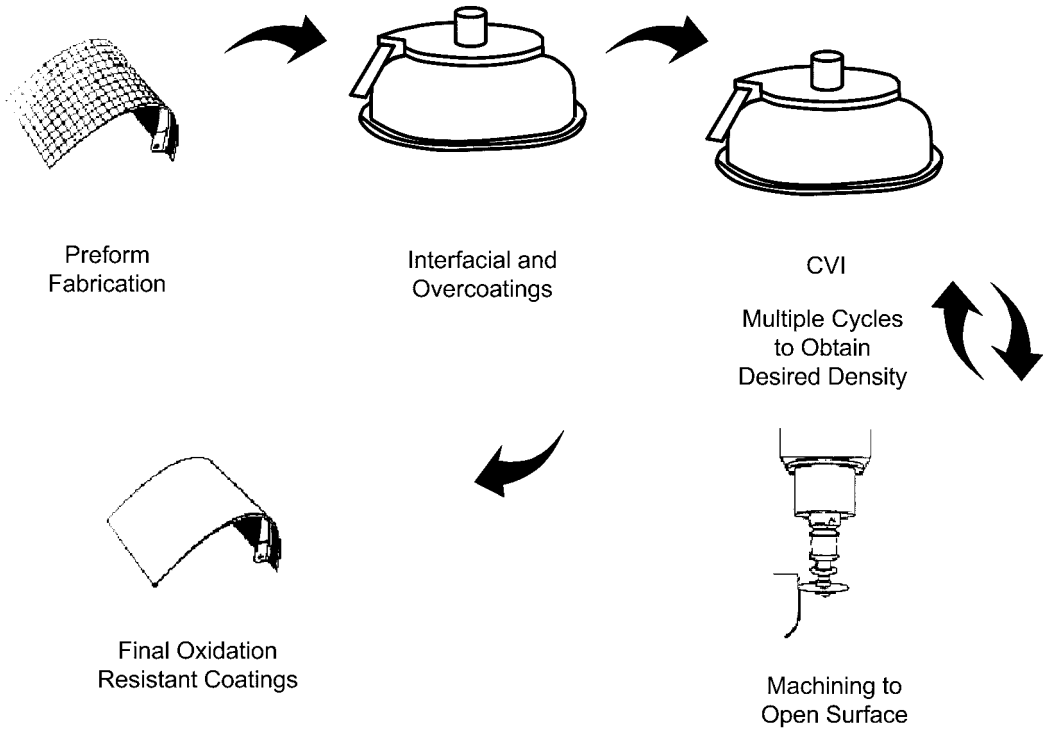


Fig. 21.14 Chemical vapor infiltration fabrication sequence. Chemical vapor infiltration (CVI)

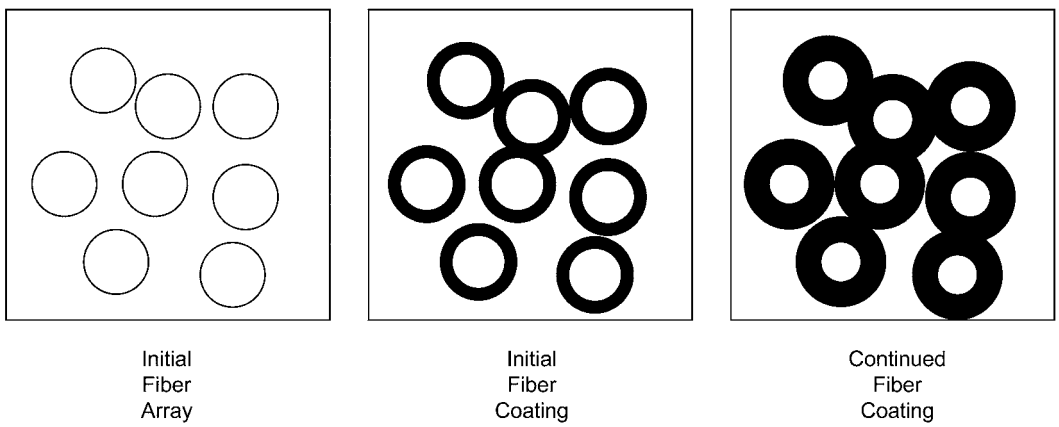


Fig. 21.15 Chemical vapor infiltration growth. Source: Ref 1

1800 °F (980 °C), according to the following reaction:

$$CH_3SiCl_3\,(g) \rightarrow SiC(s) + 3HCl(g)$$

To obtain the desired microstructure and delay the closing of porosity at the preform surface, it is important to control parameters such as the temperature, pressure, flow rate of the gases, and preform temperature. It should be noted that the microstructure produced by CVI is normally not as fine as that produced by hot pressing. In addition, carbon fiber and silicon carbide are incompatible from a coefficient of thermal expansion standpoint, and the silicon carbide matrix will develop microcracks, allowing oxygen pen-

etration into the structure during service. Therefore, silicon carbide fibers are often used with silicon carbide matrices.

The equipment used for CVI includes gas handling and distribution equipment, a reactor or furnace to heat the substrates, a pressure control system, and scrubbers or traps to remove hazardous materials from the effluent gases. The details of a reactor are shown in Fig. 21.16, and a schematic of the equipment layout is given in Fig. 21.17. Reactants may be gases, liquids, or solids at room temperature. Direct evaporation of liquids and solids can be accomplished; however, liquids are usually swept through the reactor as vapors by bubbling carrier gases such as hydrogen, argon, nitrogen, or helium through the reactant liquid. The reactors are normally heated by either resistance or induction. Graphite fixtures are used to support the preforms during the initial stages of infiltration. Vacuum pumps are used to control the process pressure.

There are a number of variations on the CVI process, the most important being the isothermal, forced gradient, and pulse flow processes. The objectives of the forced gradient and pulse flow processes are to utilize temperature (or temperature and pressure) gradients or, by pulsing the reactant gases, to reduce the long cycle times inherent in the isothermal process.

The isothermal process is by far the most common process and the only one widely used commercially. The gases flow outside the preform by convection and inside the preform by diffusion. To delay sealing off the interior of the preform by surface crusting, deposition is performed at relatively low temperatures and reduced pressures. The relatively low temperatures result in lower reaction rates, with the reduced pressures favoring diffusion. Since pore sealing on the surface occurs (sometimes called *crusting* or *canning*), it is necessary to periodically remove the part and machine the surface to allow further densification. An advantage of the isothermal process is that a furnace can be loaded with a number of parts with different configurations for processing at the same time.

In forced gradient CVI, a graphite tool that holds the preform is placed in contact with a

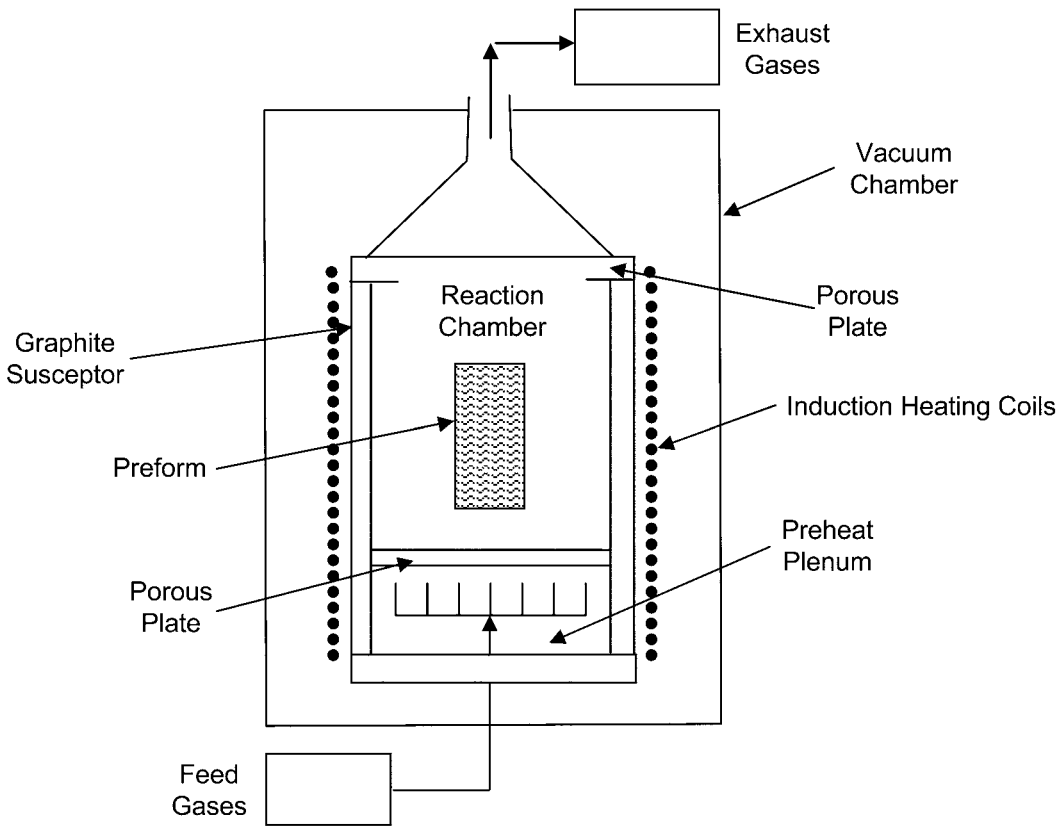


Fig. 21.16 Chemical vapor infiltration reactor

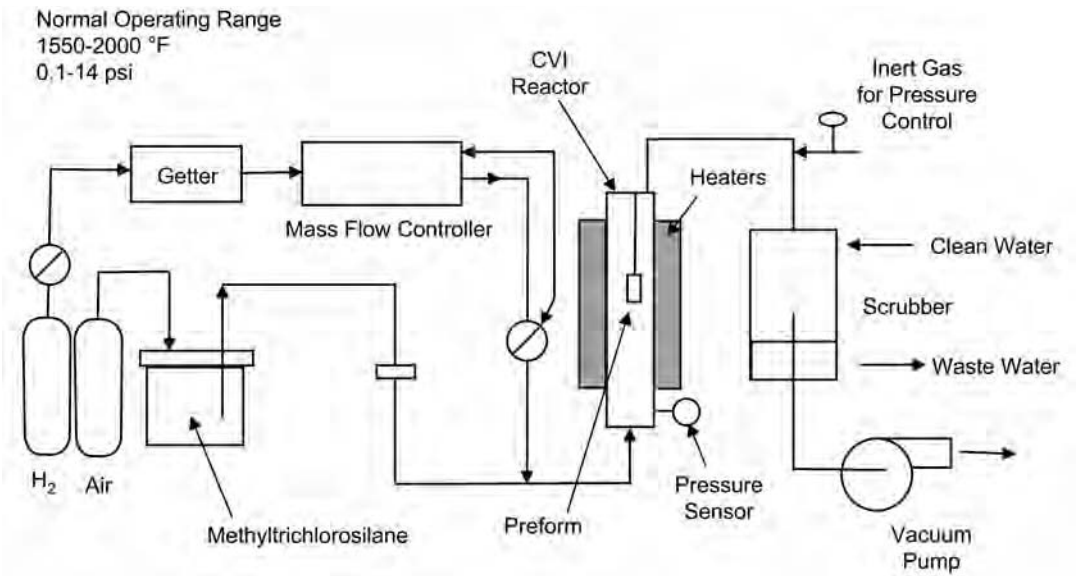


Fig. 21.17 Chemical vapor infiltration (CVI) equipment

water-cooled metallic gas distributor. The preform is heated on one side and the reactant gases are injected through the cooler side, where almost no deposition occurs under pressure. The reactant gases pass unreacted through the preform because of the lower temperature. When the gases reach the hot zone, they decompose and deposit on the fibers to form the matrix. As the matrix material is deposited in the hot portion of the preform, the preform density and thermal conductivity increase and the hot zone moves progressively from the hot side toward the cooler side. This process reduces the number of machining cycles required to obtain a dense part.

In the pressure pulse CVI process, the chamber is evacuated, and reactant gases are then injected for a very short time followed by another evacuation. This cycle is repeated until the part is fully dense. The pulsing action speeds the deposition process by continually removing spent gases and supplying fresh reactant gases, but it still does not eliminate all of the machining operations.

The CVI method offers several advantages. First, it is conducted at relatively low temperatures, so damage to the fibers is minimal. Since most interfacial coatings are applied using CVD, matrix infiltration can be conducted immediately after the interfacial coatings are applied. It can also be used to fabricate fairly large and complex near-net shapes. The mechanical and thermal properties are good because high-purity matrices with controlled microstructures can be obtained. In addition, a large number of ceramic matrices can be formed using CVI; a few of these are listed in Table 21.4. The major disadvantage of the CVI process is that it is not possible to obtain a fully dense part since the amount of residual porosity (Fig. 21.18) is around 15 to 20 percent, which adversely affects the mechanical and thermal properties, particularly after matrix cracking occurs in an oxidizing atmosphere at elevated temperatures. The other big disadvantage is that long processing times, often greater than 100 hours, and multiple machining cycles result in high costs.

21.10 Directed Metal Oxidation (DMO)

Directed metal oxidation (DMO), or reactive melt infiltration, uses liquid aluminum that is allowed to react with air (oxygen) to form alumina (Al_2O_3) or with nitrogen to form aluminum nitride (AlN). A fiber preform, which has been precoated with a BN interfacial coating and a silicon carbide protective overcoating, is brought in contact with molten aluminum alloy held in a suitable container, along with air or nitrogen, for the growth of an alumina or aluminum nitride matrix according to the following reactions:

$$2Al\ (l) + 3O_2\ (g) \rightarrow Al_2O_3\ (s)$$

$$Al\ (l) + N_2\ (g) \rightarrow AlN\ (s)$$

Table 21.4 CVI reactions for ceramic matrices

Ceramic matrix	Reactant gases	Reactant temperature, °F
C	CH_4-H_2	1800–2200
TiC	TiC_4-CH_4-H_2	1650–1800
SiC	CH_3-$SiCl_3$-H_2	1800–2550
B_4C	BOI_3-CH_4-H_2	2200–2550
TiN	$TiCl_4$-N_2-H_2	1660–1800
Si_3N_4	SiCl-NH_3-H_2	1800–2550
BN	BCl_3-NH_3-H_2	1800–2550
AiN	$AiCl_3$-NH_3-H_2	1475–2200
Ai_2O_3	$AlCl_3$-CO_2-H_2	1650–2010
SiO_2	SiH-CO_2-H_2	400–1110
TiO_2	$TiCl_3$-H_2O	1470–1830
ZiO_2	$ZrCl_4$-CO_2-H_2	1650–2200
TiB_2	$TiCl_4$-BCl_3-H_2	1470–1830
WB	WCl_6-BBi_3-H_2	2550–2900

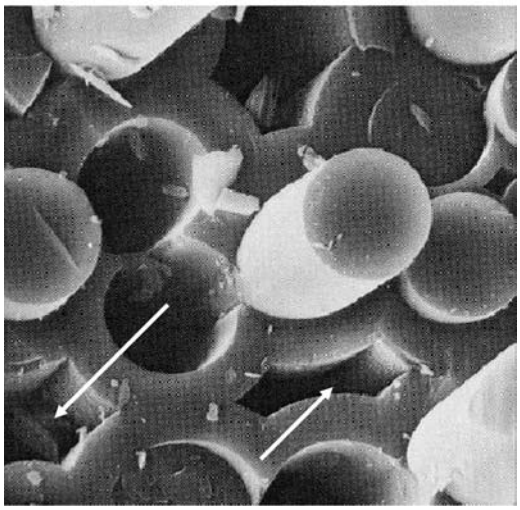


Fig. 21.18 CVI residual porosity

When the liquid aluminum is heated to 1650 to 2200 °F (900 to 1205 °C) in air, the alumina matrix grows by a complex process involving the dissolution of oxygen and the precipitation of alumina. Wicking of the molten aluminum along interconnected microscopic channels in the reaction product sustains the reaction, promoting outward growth from the original metal surface. To form near-net-shaped parts, the preform surface is coated on all surfaces except the surface in contact with the molten metal. The coating is a gas-permeable barrier layer that is applied by either spraying or dipping. Since the barrier layer is not wetted by the molten aluminum, an impervious barrier is formed when the growth front comes in contact with the barrier. The process flow for fabricating a part by DMO is shown in Fig. 21.19.

Important process parameters include alloy composition, growth temperature, oxygen partial pressure, and the presence of fillers, which can be used to control grain size and act as nucleation sites for the reaction. Magnesium, added as a minor alloying element, forms a thin layer of magnesia at the molten interface that prevents the formation of a dense protective scale of alumina that would otherwise stop the in-depth diffusion of oxygen. The matrix slowly builds up approximately 1 in. (25.4 mm) per day within the fiber preform and fills in the space between the fibers. Since the reaction product is not continuous and contains microscopic channels, the liquid metal wicks to the surface and reacts with the gaseous atmosphere.

For discontinuous composites, preforming can be conducted using conventional ceramic processes such as slip casting, pressing, and injection molding. For continuous-fiber composites, fabric lay-up, weaving, braiding, or filament winding can all be used. Since thin layers of both carbon and BN oxidize rapidly during matrix growth of alumina-based composites, a duplex coating of BN/silicon carbide is used to protect the fiber and provide the necessary weak interface. The overcoating of silicon carbide at 0.1 to 0.2 mil (3 to 4 μm) protects the thin inner BN layer of 0.01 to 0.02 mil (0.2 to 0.5 μm) from attack by the molten aluminum during processing.

This process is relatively low in cost, with near-net-shape capabilities, and complex shaped parts can be fabricated. Only small dimensional changes occur during processing since the matrix fills the pores within the preform without disturbing the reinforcement. A disadvantage is the presence of residual aluminum phase, approximately 5 to 10 percent, in the matrix that must be removed if the part is to be used above the melting point of aluminum 1220 °F (660 °C). The residual metal can be leached away by an acid treatment that leaves behind open porosity with a residual metal content of approximately one percent. Matrix cracking also occurs due to the thermal expansion mismatch between the alumina matrix and the protective silicon carbide overcoating. This cracking and the residual porosity from the removed aluminum phase reduce the strength and thermal conductivity. This process is conducted commercially as the proprietary Dimox process, which stands for directed metal oxidation.

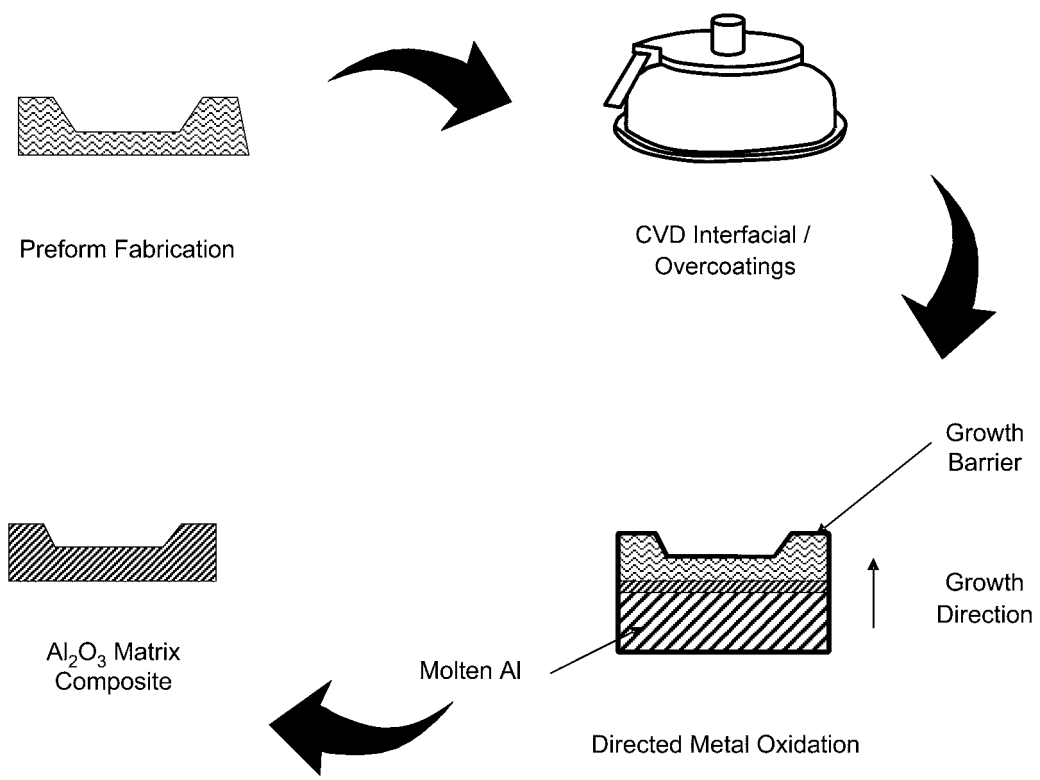


Fig. 21.19 Directed metal oxidation process. Aluminum (Al), chemical vapor deposition (CVD)

21.11 Liquid Silicon Infiltration (LSI)

Liquid silicon, or one of its lower melting point alloys, is used to infiltrate a fibrous preform to form a silicon carbide matrix. The fibers must contain an interfacial coating, along with a SiC overcoating, to protect them from the liquid silicon. Before infiltration, a fine-grained silicon carbide particulate is slurry cast into the fiber preform. After removal of the slurry carrier liquid, melt infiltration is usually done at 2550 °F (1400 °C), or higher, and is usually complete within a few hours, as illustrated in Fig. 21.20. The liquid silicon bonds the silicon carbide particulates together and forms a matrix that is somewhat stronger and denser than that obtained by CVI. Since the resulting matrix can contain up to 50 percent unreacted silicon, the long-term use temperature is limited to about 2200 °F (1205 °C). The amount of unreacted silicon can be reduced by infiltrating the preform with carbon slurries prior to the silicon infiltration process. However, some unreacted or free silicon will always be present in the matrix.

In another variant of the liquid metal infiltration process, liquid silicon is reacted with unprotected carbon fibers to form a silicon carbide matrix. After the initial step of using prepreg to form a highly porous carbon matrix part, liquid silicon is infiltrated into the structure, where it reacts with the carbon to form silicon carbide along with unreacted silicon and carbon. Since the carbon fibers are intended to react with the liquid silicon, no coatings are used on the fibers. However, the poor oxidation resistance of the carbon fibers means that the entire part will require an oxidation-resistant coating.

The liquid metal infiltration processes have several advantages: (1) they produce a fairly dense silicon carbide–based matrix with a minimum of porosity; (2) the processing time is shorter than for most ceramic matrix composite fabrication processes; and (3) the dense and closed porosity on the surface can often eliminate the need for a final oxidation-resistant coating. The major disadvantage is the high temperatures greater than 2550 °F (1400 °C) required for liquid silicon infiltration that expose the fibers

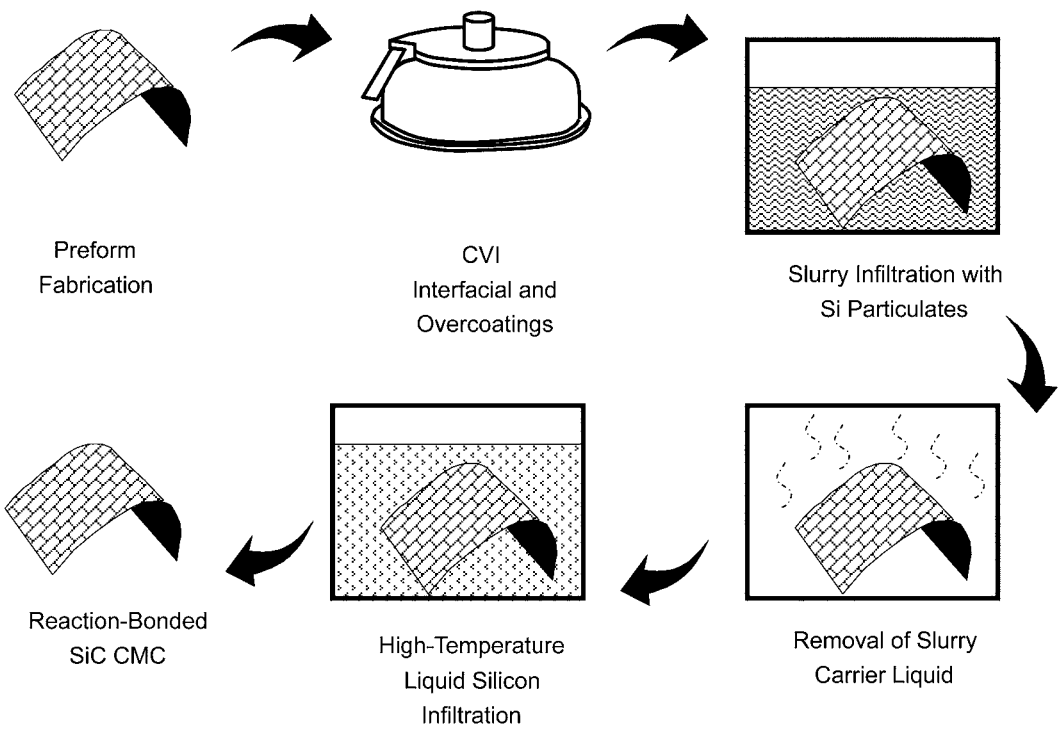


Fig. 21.20 Liquid silicon infiltration process. Chemical vapor infiltration (CVI), silicon (Si), silicon carbide (SiC), ceramic matrix composite (CMC)

to possible degradation due to the high temperatures and corrosive nature of liquid silicon. In addition, the temperatures can be even higher due to the possibility of an exothermic reaction between silicon and carbon.

REFERENCES

1. W.J. Lackey and T.L. Starr, Fabrication of Fiber-Reinforced Ceramic Composites by Chemical Vapor Infiltration: Processing, Structure and Properties, *Fiber Reinforced Ceramic Composites: Materials, Processing and Technology*, Noyes Publications, 1990, p 397–450

SELECTED REFERENCES

- M.F. Amateau, Ceramic Composites, *Handbook of Composites*, Chapman & Hall, 1998, p 307–332
- P.F. Becher, T.N. Tiegs, and P. Angelini, Whisker Reinforced Ceramic Composites, *Fiber Reinforced Ceramic Composites: Materials, Processing and Technology*, Noyes Publications, 1990, p 311–327
- J.D. Buckley, Carbon-Carbon Composites, *Handbook of Composites*, Chapman & Hall, 1998, p 333–351
- K.K. Chawla, Processing of Ceramic Matrix Composites, *Ceramic Matrix Composites*, Chapman & Hall, 1993, p 126–161
- *Composites*, Ceramics Information Analysis Center, 1995, p 1–31
- G.H. Cullum, Ceramic Matrix Composite Fabrication and Processing: Sol-Gel Infiltration, *Handbook on Continuous Fiber-Reinforced Ceramic Matrix Composites*, Ceramics Information Analysis Center, 1995, p 185–204
- J.A. DiCarlo and N.P. Bansal, "Fabrication Routes for Continuous Fiber-Reinforced Ceramic Composites (CFCC)," NASA/TM-1998-208819, National Aeronautics and Space Administration, 1998
- J.A. DiCarlo and S. Dutta, Continuous Ceramic Fibers for Ceramic Matrix Composites, *Handbook on Continuous Fiber-Reinforced Ceramic Matrix Composites*, Ceramics Information Analysis Center, 1995, p 137–183

- A.S. Fareed, Ceramic Matrix Composite Fabrication and Processing: Directed Metal Oxidation, *Handbook on Continuous Fiber-Reinforced Ceramic Matrix Composites*, Ceramics Information Analysis Center, 1995, p 301–324
- J.E. French, Ceramic Matrix Composite Fabrication and Processing: Polymer Pyrolysis, *Handbook on Continuous Fiber-Reinforced Ceramic Matrix Composites*, Ceramics Information Analysis Center, 1995, p 269–299
- W.J. Lackey and T.L. Starr, Fabrication of Fiber-Reinforced Ceramic Composites by Chemical Vapor Infiltration: Processing, Structure and Properties, *Fiber Reinforced Ceramic Composites: Materials, Processing and Technology*, Noyes Publications, 1990, p 397–450
- F.F. Lange et al, Powder Processing of Ceramic Matrix Composites, *Material Science and Engineering*, A144, 1991, p 143–152
- D. Lewis III, Continuous Fiber-Reinforced Ceramic Matrix Composites: A Historical Overview, *Handbook on Continuous Fiber-Reinforced Ceramic Matrix Composites*, Ceramics Information Analysis Center, 1995
- R.A. Lowden, D.P. Stinton, and T.M. Besmann, Ceramic Matrix Composite Fabrication and Processing: Chemical Vapor Infiltration, *Handbook on Continuous Fiber-Reinforced Ceramic Matrix Composites*, Ceramics Information Analysis Center, 1995, p 205–268
- K.L. Luthra and G.S. Corman, "Melt Infiltrated (MI) SiC/SiC Composites for Gas Turbine Applications," GE Research and Development Center, Technical Information Series, 2001
- T. Mah et al, Ceramic Fiber Reinforced Metal-Organic Precursor Matrix Composites, *Fiber Reinforced Ceramic Composites: Materials, Processing and Technology*, Noyes Publications, 1990, p 278–310
- A. Marzullo, Boron, High Silica, Quartz and Ceramic Fibers, *Handbook of Composites*, Chapman & Hall, 1998, p 156–168
- R.R. Naslain, Ceramic Matrix Composites: Matrices and Processing, *Encyclopedia of Materials: Science and Technology*, Elsevier Science Ltd., 2000
- R. Naslain, Design, *Preparation and Properties of Non-Oxide CMCs for Application in Engines and Nuclear Reactors: An Overview*, *Compos. Sci. Technol.*, Vol 64, 2004, p 155–170
- "3M Nextel Ceramic Textiles Technical Notebook," 3M Ceramic Textiles and Composites, 2003
- State of the Art in Ceramic Fiber Performance, *Ceramic Fibers and Coatings: Advanced Materials for the Twenty-First Century*, National Academy of Sciences, 1998, p 21–36
- R. Zolandz and R.L. Lehmann, Crystalline Matrix Materials for Use in Continuous Filament Fiber Composites, *Handbook on Continuous Fiber-Reinforced Ceramic Matrix Composites*, Ceramics Information Analysis Center, 1995, p 111–136

Copyright © 2010, ASM International®
All rights reserved.
www.asminternational.org

APPENDIX A

Metric Conversions

Conversion factors

To convert from	to	multiply by
Area		
$in.^2$	mm^2	6.451 600E+02
$in.^2$	cm^2	6.451 600E+00
$in.^2$	m^2	6.451 600E–04
ft^2	m^2	9.290 304E–02
Force		
lbf	N	4.448 222E+00
kip (1000 lbf)	N	4.448 222E+03
Fracture toughness		
ksi $(in.)^{1/2}$	MPa $(m)^{1/2}$	1.098 800 E+00
Length		
mil	μm	2.540 000E+01
in.	mm	2.540 000E+01
in.	cm	2.540 000E+00
ft	m	3.048 000E–01
yd	m	9.144 000E–01
Mass		
oz	kg	2.834 952E–02
lb	kg	4.535 924E–01
Mass per unit area (areal weight)		
$oz/in.^2$	kg/m^2	4.395 000E+01
$oz/ft.^2$	kg/m^2	3.051 517E–01
oz/yd^2	kg/m^2	3.390 575E–02
lb/ft^2	kg/m^2	4.882 428E+00
Mass per unit volume (density)		
$lb/in.^3$	g/cm^3	2.767 990E+01
$lb/in.^3$	kg/m^3	2.767 990E+04
lb/ft^3	g/cm^3	1.601 846E–02
lb/ft^3	kg/m^3	1.601 846E+01
Pressure (fluid)		
$lbf/in.^2$ (psi)	Pa	6.894 757E+03
in. of Hg (60 °F)	Pa	3.376 850E+03
atm (Standard)	Pa	1.013 250E+05
Stress (force per unit area)		
$lbf/in.^2$ (psi)	MPa	6.894 757E–03
ksi (1,000 psi)	MPa	6.894 757E+00
msi (1,000,000 psi)	MPa	6.894 757E+03
Temperature		
°F	°C	5/9 (°F–32)
K	°C	K–273.15
Thermal conductivity		
$Btu/ft \cdot h \cdot °F$	$W/m \cdot K$	1.730 735E+00
Thermal expansion		
$in./in. \cdot °F$	$m/m \cdot K$	1.800 000E+00
$in./in. \cdot °C$	$m/m \cdot K$	1.000 000E+00
Velocity		
in./s	m/s	2.540 000E–02
ft/s	m/s	3.048 000E–01
ft/min	m/s	5.080 000E–03
ft/h	m/s	8.466 667E–05
Viscosity		
poise	$Pa \cdot s$	1.000 000E–01
Volume		
$in.^3$	m^3	1.638 706E–05
ft^3	m^3	2.831 685E–02

"*This page left intentionally blank.*"

Copyright © 2010, ASM International®
All rights reserved.
www.asminternational.org

Index

4,4' methylene dianaline (MDA), 72, 74

A

A286 iron-nickel, 320, 323, 467
adhesive bonding, 193–194
  adhesion, theory of, 235
  advantages of, 463, 468(F)
  aluminum primers, 243–244(F)
  design guidelines, 506
  disadvantages of, 463–464
  epoxy adhesives, 244–249(F,T)
  overview, 235, 236(F)
  surface preparation
    aluminum, 239–242(F)
    composite, 237–239(F)
    overview, 235–237(F)
  titanium surface preparation, 242–243
adhesive bonding procedures
  adherends, prekitting of, 249
  adhesive application, 250–251(F)
  bonding, 252–253
  bondline thickness control, 251–252(F)
  prefit evaluation, 249–250(F)
  steps in, 248–249(T)
adhesive peel testing
  climbing drum peel test (ASTM D 1781), 367, 370(F)
  floating roller bell peel test (ASTM D 3167), 367, 369(F)
  overview, 364, 367
adhesive shear testing
  double lap shear test (ASTM D 3528), 364, 367(F)
  single lap shear test (ASTM D 1002), 364, 366(F)
  thick adherend test (ASTM D 5656), 364, 368(F), 369(F)
aerodynamic smoothing compounds, 517
aerospace
  Airbus A380, 195
  applications, 19, 21(F), 22(F), 27, 29(F)
  automated drilling, 315–316(F)
  Boeing 757 (weight of water per spoiler), 508
  composite materials, advantages of, 14–15(F)
  continuous-fiber aluminum MMCs, 551
  corrosion, 331(F), 332, 385(F)
  epoxy resins, 67
  F-14, 551
  F-15, 551
  F/A-18 fighter aircraft, 481, 483(F), 484(F)
  fasteners, 307 (*see also* fasteners)
  fluids, 411, 412(T)
  imide corrosion, 71, 72(F)
  lightning strikes, 412–415(F,T)
  materials, fatigue properties of, 16(F)
  materials, structural efficiency of, 14–15(F)
  S-2 glass, 376, 377(T)
  space shuttle C-C process, 585–587(F)
  trade study, aircraft control surface, 498–499(F)
aluminum
  A356, 542, 543
  adhesive bonding primers, 243–244(F)
  adhesive bonding surface preparation, 239–242(F)
  adhesive shear stress-strain, 474–475
  aluminum nitride (AlN), 546
  autoclave curing, 103
  bonded joint design considerations, 477–478
  caul plates, 133
  composite laminate, through-the-thickness tensile strength versus, 11, 12–13(F)
  continuous-fiber aluminum MMCs, 550–554(F,T), 555(F)
  corrosion, 262
  discontinuously reinforced aluminum (DRA), 537, 540–541, 546
  drilling, 313
  form block tools, 103, 105(F)
  honeycomb core, 262
  imide corrosion, 71, 72(F)
  integrally cocured unitized structure, 273–278(F), 279–283(F)
  matrix composites, 540–542(F,T)
  sealing, 331
  7075-T6, 14, 15(F), 391(F)
  spray deposition, 548
  stir casting, 543–544
  thermal management, 105, 107(F), 108–111(F)
aluminum nitride (AlN), 546, 592
American Society for Testing Materials (ASTM), 351
amorphous bonding, 195
amorphous polyetherimide (PEI), 195
amorphous thermoplastic HTA, 409
anhydride curing agents, 70, 409, 410(F)
anisotropic materials, 4–7(F)

applications
  aerospace, 19, 21(F), 22(F), 27, 29(F)
  automakers, 20, 23(F)
  construction, 21, 23, 26(F)
  infrastructure, 21, 25(F)
  marine industry, 20–21, 24(F)
  metal and ceramic matrix composites, 26–27, 28(F)
  overview, 18–19
  sporting goods, 24–25
  wind power, 23–24, 27(F)
aramid, 39, 153
aramid composites
  impact performance of, 391
  impact resistance, 391(F)
  mechanical properties, 376–379(F,T)
  standard high-speed steel (HSS) drills, 317
  sustained high compressive loading, 40
  ultraviolet radiation, prolonged exposure to, 41
aramid fibers, 18, 39–41(F)
aspect ratio, 1
assembly
  considerations, 309–311(F)
  determinant assembly, 310
  fastener selection and installation (*see* fasteners)
  hole preparation (*see* hole preparation)
  overview, 307
  painting, 332
  sealing, 329, 331–332(F)
ASTM, 351
  ASTM 2344 (interlaminar shear test), 357
  ASTM C297 (flatwise tension test), 367, 371(F)
  ASTM D 1002 (single lap shear test), 364, 366(F)
  ASTM D 1781 (climbing drum peel test), 367, 370(F)
  ASTM D 3039, 354
  ASTM D 3167 (floating roller bell peel test), 367, 369(F)
  ASTM D 3410, 354–355, 356(F)
  ASTM D 3518, 356
  ASTM D 3528 (double lap shear test), 364, 367(F)
  ASTM D 3672 (wedge-crack propagation test), 241–242(F)
  ASTM D 5379, 357
  ASTM D 5528, 362
  ASTM D 5656 (thick adherend test), 364, 368(F), 369(F)
  ASTM D 5766, 357
  ASTM D 6272 (four-point loading), 352, 356
  ASTM D 6484, 357
  ASTM D 6641, 355, 356(F)
  ASTM D 7136, 361
  ASTM D 7137, 361
  ASTM D 7291, 361
  ASTM D 790 (three-point loading), 352
  mechanical property test methods, 351
  modified ASTM D 695, 354, 355(F)
attenuation
  definition of, 36
  ultrasonic inspection, 335, 336, 339, 340(F), 394–395, 397(F)
autoclave curing, 133–135(F)
autoclave process, 122
autoconsolidation, 185–186, 187(F), 206
autohesion, 89–90(F), 205–206
automakers, applications for, 20, 23(F)
automated tape laying (ATL), 125–127(F), 128(F), 129(F)
average stress criteria, 455
Avimid K-III, 86, 87
Azzi-Tsai-Hill maximum work theory, 442–443(F), 444(F)

B

back counterboring, 315(F)
ballistic protection, 40
band, definition of, 31–32
barely visible impact damage, 389
biaxial strain gage, 357
biaxially oriented polyethylene teraphthalate (boPET), 120, 132
bismaleimide resins (BMIs), 70–71(F), 72(F)
Boeing
  757 spoilers, average weight per spoiler, 508
  787, 19, 22(F)
  PAA process, 239–241(F)
  resin film infusion (RFI), 174–175(F)
bolt shearing strength
  double shear, 360, 361(F)
  overview, 358, 360
  single shear, 361, 362(F)
bond testers, 341, 343(T)
boron
  aerospace applications, 537, 551
  aluminum assemblies, 533
  batching, 36
  boron trifluoride mono ethyl amine (BF_3-MEA), 68, 70, 203, 221
  ceramic matrix composites, 574
  continuous-fiber aluminum MMCs, 550–552(F), 553(F), 554(F), 555(F)
  continuous-fiber reinforcements, 537
  epoxy resins, 68, 70
  fiber, 32, 490, 551, 552
  fiber selection, 490
  interfacial coatings, 580
  monofilament boron/aluminum composite, 555(F)
  overview, 32
  particle-reinforced TMCs, 567
  slurry casting—compocasting, 544
  Sylramic-iBN, 578
  thermoplastic injection molding, 303
boron nitride (BN), 580
Borsic, 537, 552
braiding, 153–156, 157(F), 158(F), 159(F), 160(F)
broadgoods, 54, 123
B-staging, 146
building-block approach, 499–501(F)
bulk molding compounds (BMCs), 293, 305, 492–493

C

canning, 549, 591
carbon fibers
  overview, 42–43(F), 44(F)

PAN-based, 43–47(F)
pitch-based, 47–49
rayon-based, 43
carbon-carbon (C-C) composites, 573(F), 574–575, 577(T)
carbon/epoxy (C/E), 313, 329
carbon-nitrogen (C-N) bond, 67
carboxyl terminated butadiene-acrylonitrile (CTBN) rubber, 79
caul pad, 116–117(F)
caul plates, 117(F), 133, 142, 146
cellular polymer, 271
ceramic matrix composites
carbon-carbon (C-C) composites, 573(F), 574–575, 577(T)
chemical vapor infiltration (CVI), 589–592(F), 593(F,T)
directed metal oxidation (DMO), 592–594(F)
fabrication methods, 581
fiber architectures, 580–581, 582(F)
glass-ceramic systems, 579
interfacial coatings, 580, 581(F)
liquid silicon infiltration (LSI), 594–595(F)
matrix materials, 578–580(T)
overview, 373–375(F), 376(F), 377(T)
polymer infiltration and pyrolysis (PIP), 584–589(F)
powder processing, 581–583(F), 584(F)
reinforcements, 575–578(T)
slurry infiltration and consolidation, 583–584(F)
certification considerations. *See also* design considerations
building-block approach, 499–501(F)
chemical vapor infiltration (CVI), 589–592(F), 593(F,T)
chopped fibers, 52
chopped strand mat (CSM), 375, 376(T)
chromic acid anodize (CAA), 239, 241(F), 242
cobonding, 278, 283(F), 506
cocured hats, 276, 280(F)
cocuring, 156–157, 193, 255, 267–269(F), 506, 510(T). *See also* integrally cocured unitized structure
coefficient of thermal expansion (CTE), 103, 226, 227–228, 229, 230, 580
coefficients of mutual influence, 424
combined loading compression (CLC) test, 355, 356(F)
combined loading test. *See* combined loading compression (CLC) test
compocasting, 544
composite materials
advantages of, 14–15(F), 16(F)
anisotropic materials, 4–7(F)
applications, 18–27(T), 28(F), 29(F)
composites versus metallics, 10–14(F,T)
defined, 1
delamination, 16–18, 20(F)
disadvantages of, 15–18(F), 20(F), 27
fabrication processes, 2, 3(F)
impact damage, resistance to, 11, 15, 17–18, 20(F)
isotropic materials, 4–6(F)
laminates, 7–8(F,T), 9(F)
orthotropic materials, 6–7(F)
overview, 1–4(F)
property relationships, 8–10(F), 11(F)
reinforcement, 1–4(F)
composite mechanical properties
aramid fiber composites, 376–379(F,T)
barely visible impact damage, 389
carbon fiber composites, 379–383(F,T)
defects, effects of
effect of defects test program, 397
fastener hole defects, 398, 400(T)
fiber distortion, 397–398(F), 399(F)
fiber marcelling, 397
overview, 393
tool mark-off, 397, 398(F), 399(F)
voids and porosity, 393–397(F)
delaminations, 388–392(F), 393(F)
fatigue
overview, 383–386(F)
phase 1: matrix cracking, 386(F)
phase 2: fiber fracture, crack coupling, and delamination, 386–387(F)
phase 3: delamination growth and fracture, 386(F), 387–388(F)
glass fiber composites, 374–376(T), 377(T)
impact resistance, 389–392(F), 393(F)
overview, 373–374(T)
compression molding
discontinuous-fiber processes, 496
overview, 290(F)
thermoplastic
glass mat thermoplastics (GMTs), 295–296(F)
long-fiber thermoplastic (LFT) process, 296, 297(T)
thermoset
bulk molding compound (BMC), 293
compounds, 291
overview, 290–291
preforming, 293–294(F), 295(F)
sheet molding compound (SMC), 291–293(F,T)
transfer molding, 295, 296(F)
compression strength after impact (CAI), 381, 391–392(F)
compression testing
ASTM D 3410, 354–355, 356(F)
ASTM D 6641, 355, 356(F)
modified ASTM D 695, 354, 355(F)
overview, 354
computer-aided design (CAD), 123, 131, 489
computer-aided manufacturing (CAM), 489
construction applications, 21, 23, 26(F)
contour tape-laying machines (CTLMs), 127
corduroy texture, 219
corrosion
advanced composites, 27
aluminum honeycomb assemblies, 262, 508
bismaleimide resins (BMIs), 71
bolted repairs, 521, 527
bolts, 323
bondline thickness control, 252
composite materials, 14
composite materials, trade-offs when selecting, 492(T)
composites versus metals comparison, 11(T)
composite-to-metal joints, 450
E-glass, 490
fatigue, 385(F)

corrosion (continued)
galvanic, 247 (*see also* galvanic corrosion)
imide, 71, 72(F)
impact damage, 391
infrastructure, 21
inhibiting primer, 242, 243–244(F), 568
marine industry, 20, 21
mechanical fastener material, 320, 326
mechanically fastened joints, 467(T)
phosphoric acid anodize (PAA) core, 262, 263(F)
radiographic inspection, 345
resistant primer, 239(F)
salt, 578
sandwich structures, 513
sealing, 329, 331(F)
thermoplastic molding compounds, 300
thermoset matrix systems, comparison of, 495(T)
coupling agents, 37–38, 47, 163(T), 197
crack coupling, 386–387
critical fiber length l_c, 285–286
crosslinking
description of, 63(F)
epoxy resins, 67
polyester resins, 65–66(F)
toughened thermosets, 76, 77
crusting, 591
C-scan displays, 339–340(F)
CTBN rubbers, 79
curing
addition, 135, 136(F)
autoclave, 133–135(F)
condensation curing systems, 135–137(F)
low-temperature curing/vacuum bag (LTVB) systems, 137–141(F), 142(F), 143(F)
cyanate ester resins, 71–72, 73(F)
Cycom 5215, 381, 382(T)
Cycom 5320, 381
Cycom 977-3, 379(T)

D

damage tolerance considerations, 510–512(F)
debulking
bagging schematic, 140(F)
double-bag method, 530(F)
hot, 124, 136, 205, 275–276
vacuum, 115, 124
debulks, definition of, 152
decibels (dB), 335
defects, effects of
defects test program, effect of, 397
fastener hole defects, 398, 400(T)
fiber distortion, 397–398(F), 399(F)
overview, 393
voids and porosity, 393–397(F)
Defence Evaluation and Research Agency (UK), 556
delaminations
bearing failures, 451, 454
bond testing, 343(T)
bonded repairs, 524
bonded-bolted joints, 482, 484
composite mechanical properties, 388–392(F), 393(F)
composite surface preparation, 237
countersinking, 317
design guidelines, 503, 505(T)
edge, 333–334, 365(F), 519
fabrication tooling, 104
fastener hole defects, 398
fatigue, 386
foam cores, 272
gaps, 310–311, 323
growth and fracture, 387, 388
impact resistance and, 388–392(F), 393(F)
initiation, 387
injection repairs, 517–520(F), 521(F), 522(F)
interference-fit fasteners, 329
interlaminar free-edge stresses, 440
interlayering, 80
low-velocity impact damage (LIVID), 510
machining, 307, 308
mechanical fastening, 450
melt fusion, 195
moisture absorption, 401, 410
nondestructive inspection (NDI), 333
overview, 16–17, 20(F)
phenolic resins, 74–75
pin and collar fasteners, 323
residual curing stresses, 231
resin flow, 213
single-layer, 511
Space Shuttle nose cap, 586
stiffener, 506–507, 508(F)
tap testing, 335
thermal management, 105
thermographic inspection, 346
TMC processing defects, 563
toughened thermosets, 75, 76
ultrasonic inspection, 335
visual inspection, 333–335
denier, 37
design considerations
allowables, 501–503(F)
building-block approach, 499–501(F)
damage tolerance considerations, 508, 510–512(F)
design limit load (DLL), 503
design ultimate load (DUL), 503
environmental sensitivity considerations, 512–514(F,T)
fabric process selection
continuous-fiber processes, 497–498
discontinuous-fiber processes, 496–497
overview, 496(T)
fiber selection, 490–491
guidelines, 503–508(F,T), 509(F), 510(T)
material selection, 489
matrix selection, 494–496(T)
overview, 489
product form selection
continuous-fiber product forms, 493–494
discontinuous-fiber product forms, 492–493
overview, 491–492(F,T), 493(T)
trade studies, 498–499(F)
design limit load (DLL), 503

design ultimate load (DUL), 503
determinant assembly, 310
diaminodiphenyl sulfone (DDS), 68, 69, 70, 92(F), 94
differential scanning calorimetry (DSC), 94–95(F)
differential scanning calorimetry (DSC) curves, 203
diffusion
  autoconsolidation, 186
  autohesion, 89
  chemical vapor infiltration (CVI), 591
  dry spinning, 43
  environmental sensitivity considerations, 513
  Fickian (*see* Fickian)
  moisture, 404
  powder metallurgy (PM) methods, 549
  reinforcements, 576–577
  space shuttle C-C process, 587(F)
  TMC consolidation procedures, 561
  trade study, aircraft control surface, 498, 499(F)
diffusion bonding, 561–562(F)
  continuous-fiber aluminum MMCs, 551, 552, 554(F), 555(F)
  continuous-fiber TMC processing methods, 557–558, 560
  solid state processes, 540
  superplastic forming and diffusion bonding (SPF/DB), 563, 564(F)
  TMC consolidation procedures, 560–562(F)
  TMCs, secondary fabrication of, 562–563(F)
  trade study, aircraft control surface, 498, 499(F)
diglycidyl ether of Bisphenol A (DGEBA), 67–68(F,T)
dimethylactamide (DMAC), 72
dimethylformamide (DMF), 72
dimethylsufoxide (DMSO), 72
Dimox™ process, 593
directed metal oxidation (DMO), 592–594(F)
discontinuous-fiber composites
  compression molding (*see* compression molding)
  fabrication methods, 289
  fiber length, 285–286(F), 287(F)
  fiber orientation, 286, 288(F)
  injection molding (*see* injection molding)
  mechanics of, 287–289(F)
  overview, 279–283(F), 285(T)
  reaction injection molding (RIM), 296–297(F), 298(F)
  reinforced reaction injection molding (RRIM), 297, 298(F)
  spray-up, 289–290(F)
  structural reaction injection molding (SRIM), 297, 298(F)
discontinuously reinforced aluminum (DRA), 537, 540–541
drawing (manufacturing process), 31
dual resin bonding, 193, 195, 198(F)
dummy part, 117
dynamic mechanical analysis (DMA), 99

E

Eddie-Bolt, 323, 325(F)
edge delamination, 333–334, 365(F), 519
effect of defects test program, 397
eggcrate support, 108, 111, 115
E-glass, 32, 33
  batching, 36
  corrosion resistance, 490
  fiber selection, 490
electrical discharge machining (EDM), 564–565
elevated temperature dry (ETD), 245
elevated temperature wet (ETW), 245
end, definition of, 31
environmental degradation
  diffusion, 404–405
  erosion, 411
  Fickian diffusion, 404
  flammability, 417–418, 420
  fluids, 411, 412(T), 413(T)
  heat damage, 416–417, 418(F), 419(F)
  indirect effects, 412, 413(F)
  lightning strikes, 412–415(F,T)
  moisture absorption, 401–410(F), 411(F), 412(F)
  overview, 401
  thermal spiking, 409–410, 411(F)
  thermo-oxidative stability (TOS), 415–416(F), 417(F)
  ultraviolet (UV) radiation, 411
environmental sensitivity considerations, 512–514(F,T)
epoxy adhesives
  epoxy film adhesives, 247–248(T), 249(T)
  overview, 244–245(T), 246(F)
  two-part room-temperature curing epoxy liquid and paste adhesives, 245, 247(T)
epoxy resins, 67–70(F,T), 71(F)
extensional mode, 380

F

fabrication tooling
  general considerations, 101–104(F), 105(F)
  overview, 101
  thermal management, 104–111(F)
  tool fabrication, 111–117(F,T)
  tooling materials, properties of, 103(T)
fasteners
  blind fasteners, 326–327(F), 328(F)
  bolts, 323, 325, 326, 326(F), 327(F)
  composite joints, 320, 322(F)
  gang channels, 326(F)
  hole defects, 398, 400(T)
  interference-fit fasteners, 328–329(F), 330(F)
  material selection, 320
  nut plates, 326(F), 327(F), 523
  nuts, 323, 325–326
  overview, 319–321(F)
  pin and collar fasteners, 323, 324(F), 325(F)
  screws, 326, 327(F)
  solid rivets, 322
  washers, 323
fatigue
  crack coupling, 387
  overview, 383–386(F)
  phase 1: matrix cracking, 386(F)
  phase 2: fiber fracture, crack coupling, and delamination, 386–387(F)

fatigue (continued)
phase 3: delamination growth an fracture, 386(F), 387–388(F)
spectrum loading, 383, 385
fiber, definition of, 31
fiber areal weight (FAW), 54
fiber marcelling, 397
fiber metal laminates, 567–570(F,T)
fiber orientation angle, 421
fiber placement machine, 127–130(F)
fiber wash, 171
fibers
aramid, 39–41(F)
carbon, 42–49(F)
chopped, 52
glass, 33–34, 36–39(F)
graphite, 42–49(F)
milled, 52
overview, 31
prepreg manufacturing, 52–58(F,T), 59(F), 60(T)
reinforced mats, 52
relative costs and performance, 35(F)
strength of, 32–33, 35(F)
terminology, 31–32(F,T), 34(F), 35(F)
ultra-high molecular weight polyethylene (UHMWPE), 41–42(F)
woven, 49–52(F), 53(F), 54(F,T)
Fickian, 404–405, 406(F)
Fickian diffusion, 404
filament, definition of, 31
filament winding
autoclave curing, 146
B-staging, 146
glass fiber composites, 375–376(T)
helical winding, 143–144
hoop winding (circumferential or circ winding), 144–145
mandrel material and design, 146
overview, 141–143, 144(F), 145(F)
polar winding, 144
resin systems, 145
towpreg winding, 146
wet winding, 145
wet-rolled prepreg winding, 145–146
film stacking, 184
finish, definition of, 47
first generation epoxies, 391
flags, 125
flammability, 417–418, 420
flat ply collation, 124–125, 126(F)
flat tape-laying machines (FTLMs), 127
flaws
bond flows, 476(F)
definition of, 37
NDI methods, 333, 334(F)
pitch-based fibers, 48–49
strength of fibers, 33
ultrasonic inspection, 335
foil-fiber-foil method, 557–558(F)
Forest Products Laboratory, FPL, 239–241(F), 242
forging, 542, 548, 550
form block tools, 103
Fourier transform infrared spectroscopy (FTIR), 91

G

galvanic corrosion
adhesive bonding, 247, 463
carbon fiber composites, as a cause of, 14, 490
Gr/Al MMCs, 553
imide linkage, mechanism for, 72(F)
lightning protection, 414, 514
mechanical fastener material, 320
sealing to prevent, 331
shim material, 311
galvanized steel, 513(T)
gang channels, 326(F)
gel coat, 120–121
gel permeation chromatography (GPC), 91
gellation, 92–93
general orthotropic lamina ($\theta \neq 0°$ or 90°), 7
glass fibers
batching, 36
coating, 37–38
coupling agents, 38
drying/packaging, 38–39
fiberization, 36–37(F), 38(F)
melting, 36
overview, 33–34, 36
product forms, 38(F)
Glass Laminate Aluminum Reinforced (GLARE), 568–570(F,T)
glass mat reinforced thermoplastic, 82
glass mat thermoplastics (GMTs), 90, 295–296(F)
glass-ceramic matrix composite (GCMC), 573(F)
glass-ceramic systems, 579
glass-ceramics, 574–575, 579(T), 583
glycidyl amine, 67(F), 68(F)
glycidyl ether, 67
graphite fibers
overview, 42–43(F), 44(F)
PAN-based, 43–47(F)
pitch-based, 47–49
rayon-based, 43
green body, 549
green fiber, 48
green tape method, 551–552, 555(F), 558–559

H

heated platen press, 135
High Speed Civil Transport program, 74
High Temperature Amorphous (HTA), 409
high-performance liquid chromatography (HPLC), 91
high-speed steel (HSS) drills, 317
high-temperature/ high-temperature (HT/HT) prepregs, 115
Hi-Lok fasteners, 323, 324(F)
Hi-Nicalon, 578
HOBE, 258
hole preparation
automated drilling, 315–316(F), 317(F), 318(F)

back counterboring, 315(F)
countersinking, 317–318, 319(F)
drill bit geometries, 316–317, 319(F)
high-speed steel (HSS) drills, 317
manual (freehand) drilling, 311–314(F)
numerically controlled drill jigs, 315–316(F)
overview, 311
peck drill, 314–315(F)
polycrystalline diamond (PCD) drills, 317
power feed drilling, 314–315(F)
reaming, 317
honeycomb core sandwich structure
cell configurations, 257, 260(F)
comparative properties of, 258, 261(T)
corrosion protection system, 262, 263(F)
details of, 259(F)
durability problems, 262–264(F)
fabrication methods, 257–258, 260(F)
facesheets, 255
HOBE, 258
honeycomb processing (*see* honeycomb processing)
materials, 256
node bond adhesive, 256
strength retention at temperature, 258, 261–262(F)
terminology, 259(F)
honeycomb processing
cleaning, 266
cocured honeycomb assemblies, 267–271(F)
core migration, 268–270(F)
crushing, 268–270(F)
drying/packaging, 266
forming, 264
honeycomb bonding, 266–267(F), 268(F)
machining, 266
overview, 264(F)
potting, 266(F)
splicing, 265–266(F)
trimming, 264
hot isostatic pressing (HIP), 549, 559–560(F), 562–563(F), 582, 584
hot pressing
continuous-fiber aluminum MMCs, 553
continuous-fiber TMC processing methods, 558, 559
matrix materials, 579
powder metallurgy (PM) methods, 549
powder processing, 582–583, 584(F)
TMC consolidation procedures, 560
vacuum hot pressing (VHP), 558, 559
hot rolling, 542, 549–550
hot-wet condition, 512–513(F)
hybrids, 494
hygroscopic, 300

I

Illinois Institute of Technology Research Institute (IITRI), 354, 356(F)
imide corrosion, 71, 72(F)
impact damage
barely visible impact damage, 389
carbon fiber designs, 386
composites resistance to, 11, 13(F), 14, 15
delaminations, 389–391(F)
low-velocity, 17, 20(F), 75, 81, 389
low-velocity impact damage (LVID), 510(T)
thermographic inspection, 345
thermoplastics, 81
thin-skinned honeycomb assemblies, 507
tolerance to, 17–18
toughened thermosets, 75, 76
in situ composites, 566–567
in situ MMCs, 567
Inconel 718, 320, 323
indirect effects, 412, 413(F)
infrared (IR), 185
infrared (IR) spectroscopy, 91
infrared spectrum, 91, 92(F)
infrastructure applications, 21, 25(F)
injection molding
discontinuous-fiber processes, 496
machine, 301–303(F)
overview, 297–298
runner designs, 302(F)
schematic, 301(F)
sequence, 299(F)
thermoplastic, 298–304(T)
thermoset, 304–305
injection pultrusion, 178
in-motion x-ray, 343, 347(F)
inner moldline (IML) surface, 101, 102(F)
integrally cocured unitized structure, 273–278(F), 279–283(F)
integrated product definition (IPD) team, 489, 498
interlaminar free-edge stresses, 439–440, 441(F)
internally pressurized bag (IPB) curing, 223–225(F)
interply slip, 190, 191(F), 192(F), 194(F)
intraply slip, 190, 191(F), 192(F)
Invar 42, 115, 168, 184
Invar alloys, 103(T), 104, 170, 184
Invar/Nilo, 103(T)
Invar-type tools, 111, 115, 130
isothermal rolling, 550
isotropic materials, 4–6(F)

J

joints, mechanically fastened
advantages of, 449–450
analysis, 450–455(F)
average stress criteria, 455
disadvantages of, 450
failure modes, 451–453(F)
point stress criteria, 455

K

Kapton, 133, 184
Kevlar
adhesive bonding, 194
epoxy strength, 379(F)

Kevlar (continued)
honeycomb, 261
Kevlar/epoxy composites, 391
manufacturing process, 39
properties of, 32(T), 40, 41, 490
yarn weights, 153
Kevlar 29, 41, 153, 175, 178(F)
Kevlar 49
comparison: Kevlar 49 and S-2 glass epoxy, 378(T)
effect of temperature and moisture on Kevlar/ epoxy strength, 379(T)
Kevlar honeycomb, 261
properties of, 32(T), 41, 378
weave styles in high-performance products, 54(T)
Kevlar 149, 32(T), 41
K-IIIB, 223–225(F), 227(F)
kink bands, 377
knit lines, 285–286

L

lamina, 4, 5(F), 7(F)
laminate notations, 430. *See also* laminates
laminates, 7–8(F,T), 9(F), 429–430
angle-ply laminates, 430
balanced laminates, 430
cross-ply laminates, 430
defined, 7
hybrid laminates, 430
lay-ups, 7(F)
other laminate notations, 430
quasi-isotropic laminate, 8, 430
symmetric laminates, 430
unidirectional laminates, 430
laser projection, 123–124, 125(F), 154, 310(F)
length-to-diameter *(l/d)* ratio, 1
lightning strikes, 412–415(F,T), 514
liquid metal infiltration
overview, 545(F)
pressure infiltration casting (PIC), 545–546
pressureless infiltration, 546
squeeze casting, 545(F)
liquid molding
continuous-fiber processes, 497–498
overview, 146–148(F,T)
preform technology
advantages, 156–157, 160(T)
braiding, 153–156, 157(F), 158(T), 159(F), 160(F)
disadvantages, 157, 158, 160(T)
fibers, 148–149
multiaxial warp knits (MWKs), 151–152, 153(F), 154(F), 155(F)
overview, 148(F)
preform lay-up, 158–161(F), 162(F)
random mat, 156
stitching, 152–153, 156(F)
three-dimensional woven fabrics, 149–151(F), 152(F)
woven fabrics, 149
Priform process, 164–166(F), 167(F)
resin injection, 162–164(F,T), 165(F)
RTM curing, 166–167, 168(F)
RTM defects, 170–172(F)
RTM tooling, 167–170(F)
vacuum-assisted resin transfer molding (VARTM), 172–174(F)
liquid shim, 247, 310–311, 315(F), 504(T)
liquid shimming, 311
liquid silicon infiltration (LSI), 594–595(F)
Lockbolt, 323, 325(F)
long-fiber thermoplastic (LFT) process, 296, 296(F), 297(T)
low velocity impact damage (LVID), 17, 75, 81, 510
low-temperature curing/vacuum bag (LTVB) systems, 137–141(F), 142(F), 143(F), 380–381
low-temperature/high-temperature (LT/HT) prepreg, 115
low-viscosity resins
aircraft assemblies, damaged, 247
bonded repairs, 533
comparison: low-viscosity and paste epoxy adhesives, 245–246, 247(T)
injection repairs, 517, 518–519(F)
PIP processes, 588
resin transfer molding, 497–498
RTM process, 147, 162
thermoset, 2
thermoset injection molding, 305
voids and porosity, 226
wet lay-up, 119
low–volatile organic compound coatings, 332

M

machining. *See also* assembly
machining, 307, 309(F)
trimming, 307–308(F), 309(F)
Malaysia, environmental exposure in, 407, 409(F)
marbles, 36
marine industry applications, 20–21, 24(F)
Material Safety Data Sheet (MSDS), 99
matrix resin systems
bismaleimide resins (BMIs), 70–71(F), 72(F)
cyanate ester resins, 71–72, 73(F)
epoxy resins, 67–70(F,T), 71(F)
overview, 63–64(F)
phenolic resins, 74–75(F)
polyester resins, 65–67(F)
polyimide resins, 72–74(F)
quality control methods
chemical testing, 91–92(F)
glass transition temperature, 97–99(F)
overview, 90–91
rheological testing, 92–94(F)
thermal analysis, 94–96(T), 97(F)
summary, 99
thermoplastics, 81–90(F)
thermosets, 64–65(F,T)
thermosets, toughened, 75–81(F)
vinyl esters, 66–67
mechanical fastening, 194, 505–506
melt fusion, 194–195

mesophase, 47
metal and ceramic matrix composites applications, 26–27, 28(F)
metal matrix composites (MMCs)
  aluminum matrix composites, 540–542(F,T)
  aluminum nitride (AlN), 546
  compocasting, 544
  continuous-fiber aluminum MMCs, 550–554(F,T), 555(F)
  continuous-fiber reinforced (TMCs), 554–557(F,T)
  continuous-fiber TMC processing methods, 557–560(F)
  discontinuous composite processing methods, 542(F)
  discontinuous MMCs, secondary processing of, 549–550
  discontinuously reinforced aluminum (DRA), 537, 546
  fiber metal laminates, 567–570(F,T)
  hot isostatic pressing (HIP), 549
  liquid metal infiltration, 545–546(F)
  Osprey method, 547(F)
  overview, 337–340(F)
  particle-reinforced TMCs, 566–567(T), 568(F)
  powder metallurgy (PM) methods, 548–549(F)
  rheocasting, 544
  in situ MMCs, 567
  slurry casting, 544
  spray deposition, 546–548(F)
  stir casting, 542–544(F)
  TMC consolidation procedures, 560–562(F)
  TMCs, secondary fabrication of, 562–566(F), 567(F)
metallics, composites versus, 10–14(F,T)
microcracking, 226, 227(F)
milled fibers, 52
Mobile Automated Ultrasonic Scanning (MAUS) system, 342, 344(F)
monolithic graphite, 103(T), 115, 116, 184, 579
monotapes, 551
multiaxial warp knits (MWKs), 151–152, 153(F), 154(F), 155(F)
Mylar, 120, 132

N

NASA Composite Wing Program, 174–175, 176(F), 177(F), 178(F)
National Aeronautics and Space Administration (NASA), 74, 174–175(F)
net-resin-content prepregs, 54
Nextel, 577–578
Nicalon fibers, 578
nickel
  A286 iron-nickel, 320, 323
  electroformed, 103(T), 111
  electroformed tools, 105, 108, 109(F), 497
  galvanic series in seawater, 513(T)
  iron-nickel alloys, 103 (*see also* Invar alloys; Nilo alloys)
  MP159 (nickel-cobalt-chromium multiphase alloy), 320
  MP35N (nickel-cobalt-chromium multiphase alloy), 115, 320
  nickel-plated aramid fiber, 414, 467(T)
nickel tools, 112, 114(F)
Nilo alloys, 103(T), 104
N-methylpyrrolidone (NMP), 72
node bond adhesive, 256
nondestructive inspection (NDI)
  bond testing, summary of, 343(T)
  common core defects detected by radiography, 347(F)
  damage in composite parts, potential for, 334(F)
  in-motion x-ray, 343, 347(F)
  Mobile Automated Ultrasonic Scanning (MAUS) system, 342, 344(F)
  overview, 333, 334(F)
  portable equipment, 341–342(F), 343(T), 344(F)
  pulse echo inspection, 336
  radiographic inspection, 342–345(F), 346(F), 347(F), 348(F), 349(F)
  tap testing, 334–335
  thermographic inspection, 345–346, 349(F), 350(F)
  ultrasonic inspection, 335–341(F)
  visual inspection, 333–334
nondestructive testing (NDT), 223
non-Fickian, 404, 409, 410(F)
nonhydroscopic, 300
novolacs, 74
numerical control (NC) machined, 105, 170
numerically controlled drill jigs, 315–316(F)
nylon, 39, 122, 123, 133, 238, 285(T), 335

O

open, definition of, 251
original equipment manufacturer (OEM), 525
orthotropic, 421
orthotropic materials, 6–7(F)
Osprey method, 547(F)
out time, 66, 71, 138, 251, 493, 494
outer moldline (OML) surface, 101, 102(F)
oxy-PAN, 44

P

PAN-based carbon fibers, 43–47(F)
peck drill, 314–315(F)
peel ply, 123, 131, 237–239, 332
PETI-5, 74
phenolic resins, 74–75(F)
phosphoric acid anodize (PAA), 239–241(F)
phosphoric acid anodize (PAA) core, 262, 263(F)
physical vapor deposition (PVD), 559
pillowing, 268(F)
pitch, definition of, 47
pitch-based carbon fibers, 47–49
plasma spraying, 559
plastic-faced plaster (PFP), 112, 113(F), 115
plasticizing unit, 301
PMR-15, 73–74(F), 136–137(F), 415(F), 416(F)
point stress criteria, 455
polyacrylonitrile (PAN), 42
polycrystalline diamond (PCD) drills, 317
polyester resins, 65–67(F)
polyetheretherketone (PEEK), 82, 83(F), 85–86, 185, 195, 382(T)

polyetherimide (PEI), 82, 83(F)
polyetherketoneketone (PEKK), 82, 83(F), 382(T)
polyimide resins, 72–74(F)
polymer foam, 271
polymer infiltration and pyrolysis (PIP)
  conventional processes, 587–588
  overview, 584–585(F)
  sol-gel infiltration, 588–589
  space shuttle C-C process, 585–587(F)
polymer matrix composites
  cure monitoring techniques, 232–233
  heat transfer, 207–209(F)
  kinetics, 202–206(F)
  overview, 201–202(F)
  residual curing stresses, 226–232(F)
  resin flow
    hydrostatic resin pressure studies, 214–217(F), 218(F)
    overview, 209–214(F)
    resin flow modeling, 217–219
  thermoset cure model framework, 201(F)
  viscosity, 206–207(F), 208(F)
  voids and porosity
    condensation-curing systems, 226, 227(F)
    overview, 219–226(F)
polymeric monomer reactants, 72
polymethylmethacrylimides, 272
polyphenylene sulfide (PPS), 82, 83(F)
polypropylene (PP), 82, 83(F)
polytetrafluoroethylene (PTFE) film, 252
polyvinyl chloride (PVC) foam, 262, 272
porosity (use of term), 219, 393. *See also* voids and porosity
pot, definition of, 251
pot life, 247
powder coating, 88
powder metallurgy (PM) methods, 7, 548–549(F)
prepreg lay-up
  automated methods
    automated tape laying (ATL), 125–127(F), 128(F), 129(F)
    fiber placement, 127–131(F)
    overview, 125
  curing
    addition curing, 135, 136(F)
    autoclave, 133–135(F)
    condensation curing systems, 135–137(F)
  flat ply collation and vacuum forming, 124–125, 126(F)
  manual lay-up, 123–124(F), 125(F)
  overview, 122–123
  roll wrapping, 125
  tape wrapping, 125
  vacuum bagging, 131–133(F)
prepreg manufacturing
  advanced composite manufacturing, 54, 56(F)
  fiber areal weight (FAW), 54
  hot melt impregnation, 57, 58(F)
  net-resin-content prepregs, 54
  overview, 52
  prepreg rovings or tows, 54–56(F)
  resin filming process, 57, 59(F)
  resins, 52–54, 55(F)
  solvent impregnation, 57–58, 60(F)
pressure bag process, 122
pressure infiltration casting (PIC), 545–546
Priform process, 164–166(F), 167(F)
principal material axes system, 421
principal material coordinate system, 6
process control test specimens, 90–91
pulling (manufacturing process), 31
pull-winding process, 177
pulse echo inspection, 336
pultrusion, 175–181(F), 375–376(T), 498
pultrusion die, 178–179(F)
pyrolysis, 585–587, 588

Q

quartz fibers, 32(T), 33–34, 36
quasi-isotropic laminate, 8

R

race tracking, 164
ratcheting, 329
rayon-based carbon fibers, 43
reaction injection molding (RIM), 296–297(F), 298(F), 374, 496–497
reaction injection pultrusion, 178
reinforced carbon-carbon-0 (RCC-0), 586
reinforced mats, 52
reinforced reaction injection molding (RRIM), 297, 298(F), 374–375(T), 497
reinforcements, 575–578(T). *See also* fibers
relative humidity (RH), 368, 378
repairs
  aerodynamic smoothing compounds, 517
  bolted, 520–521, 523(T), 524(F), 525(F), 526(F), 527(F)
  bonded, 523–533(F), 534(F)
  fill, 517
  injection, 517–520(F), 521(F), 522(F)
  metal-bonded assemblies, 533
  metallic details, 533
  method selection, 523(T)
  overview, 517, 518(F)
resin film infusion (RFI), 174–175, 176(F), 177(F), 178(F), 179(F)
resin injection, 162–164(F,T)
resin transfer molding (RTM)
  bismaleimides (BMIs), 71
  continuous-fiber processes, 498
  curing, 166–167, 168(F)
  defects, 170–172(F)
  process, 146–148(F,T)
  resin injection, 162–164(F,T), 165(F)
  tooling, 167–170(F)
  voids, 171–172
resins. *See also* matrix resin systems
  epoxy, 67–70(F,T), 71(F)
  prepreg manufacturing, 52–54, 55(F)
  resin filming process, 57, 59(F)

resistance spot welding, 566
resoles, 74
rheocasting, 544
rheological testing, 92–94(F)
rivets, 322
roll wrapping, 125
room temperature dry (RTD), 245
rosette strain gage, 357
roving, definition of, 31
rovings, 37, 39
RTM curing, 166–167, 168(F)
RTM defects, 170–172(F)
RTM tooling, 167–170(F)
rubber elastomer system, 79
rubbers, 79–80
rule of mixtures, 8

S

S-2 glass
  advantages of, 18, 33
  aerospace applications, 376, 377(T)
  batching, 36
  costs, 32
  fiber metal laminates, 568
  fiber selection, 490
  Glass Laminate Aluminum Reinforced (GLARE), 568(F)
  impact resistance, 391(F)
  overview, 33
  wet lay-up, 119
sandwich cocured structure
  foam cores, 271–273(F,T)
  honeycomb core (*see* honeycomb core sandwich structure)
  overview, 255
  structure, 255, 256(F), 257(F), 258(F)
  syntactic core, 272–273(F)
sandwich structure
  guidelines for design of, 510(T)
  honeycomb core, 255–264(F,T)
  impact damage, 507, 510(T)
  moisture ingression, 507, 510(T)
  overview, 255
  PVC foams, 272
  radiographic inspection, 345
  repairs, 508
self-forming technique (SFT), 568–570(F)
shear testing
  ± 45-degree tensile test, 356, 357(F)
  interlaminar shear test, 357, 360(F)
  Iosipescu shear test, 357, 359(F)
  overview, 356
  rail shear test, 356–357, 358(F)
  short beam shear, 357, 360(F)
sheet molding compounds (SMCs), 291–293(F,T), 374(T), 492
shims, 310–311
short beam shear, 357, 360(F)
shot size, 299
Sigma, 556–557(F)
size, 47
sizing, 37, 38, 47
slurry casting—compocasting, 544
sol-gel infiltration, 588–589
sol-gel process, 577–578
sonotrode, 196
SP Resin Infusion Technology (SPRINT), 175
space shuttle C-C process, 585–587(F)
specially orthotropic lamina ($\theta = 0°$ or 90°), 7
specially orthotropic ply, 424
spectrum loading, 383, 385
sporting goods applications, 24–25
spray deposition, 546–548(F)
spray-up, 289–290(F), 496
spring in, 276, 279(F)
squeeze casting, 545(F)
stainless steel, 71, 407, 467(T), 513(T), 560
stair-step ply terminations, 130
steel
  adhesively bonded joints, guidelines for, 486(T)
  autoclave curing, 103
  caul plates, 133
  composite design, guidelines for, 504(T)
  continuous-fiber aluminum MMCs, 554
  countersinking cutters, 318
  dies, 168
  discontinuous-fiber processes, 497
  fabrication tooling, 101, 103(T)
  fasteners, 320
  fiber placement, 130
  4330 steel, 391(F)
  galvanic series in seawater, 513(T)
  galvanized, 513(T)
  laminate distortion, effects of tool material, orientation, and thickness on, 170, 231, 232(F)
  matched metal dies, thermoplastic production runs, 303
  matched metal molds, 168
  mechanically fastened joints, guidelines for, 467(T)
  preforming, 294
  pultrusion die, 178–179(F)
  RTM tooling, 168
  standard high-speed steel (HSS) drills, 317
  structural reaction injection molding (SRIM), 297
  thermal management, 104, 108–111(F)
  TMC, generating holes in, 565
  tool fabrication, 111, 112(F), 115
stir casting, 542–544(F)
stitch bonding, 151
stitching, 152–153, 156(F)
strand, definition of, 31
stress-strain curves, 11, 12(F), 32, 34(F), 468–469, 470–471, 472(F)
structural analysis
  coefficients of mutual influence, 424
  failure theories
    Azzi-Tsai-Hill maximum work theory, 442–443(F), 444(F)
    maximum strain theory, 442
    maximum stress criterion, 440, 442

structural analysis (continued)
overview, 440
Tsai-Wu failure criterion, 443–444, 445(F)
fiber orientation angle, 421
interlaminar free-edge stresses, 439–440, 441(F)
lamina fundamentals, 421–425(F)
laminate analysis—classical lamination theory
example 16.3, 433–437(F)
example 16.4, 437–439(F)
overview, 430–433(F)
laminate failure, predicting
limited discount method, 445
overview, 444–446
residual property method, 445
total discount method, 444
laminates and laminate notations, 429–430
overview, 421
ply fundamentals, 421–425(F)
principal material axes system, 421
specially orthotropic ply, 424
stress-strain relationships for a single ply loaded off-axis to the material axes ($\theta = 0°$ or 90°), 427–429(F)
stress-strain relationships for a single ply loaded parallel to the material axes ($\theta = 0°$ or 90°), 425–427
structural joints—bolted and bonded
adhesive bonding, 463–464, 468(F)
adhesive shear stress-strain, 466, 468–475(F)
bonded joint design, 464, 466, 469(F), 470(F)
bonded joint design considerations, 475–479(F), 480(F), 481(T)
bonded-bolted joints, 481–482, 484–486(F,T)
failure modes, 451–453(F)
mechanically fastened joint analysis, 450–455(F)
mechanically fastened joints, 449–450, 467(T)
multirow bolted composite joints, 459, 461–463(T), 464–465(F), 466(F), 467(F)
overview, 449
single-hole bolted composite joints, 455–459(F,T), 460(F)
stepped-lap adhesively bonded joints, 479–481, 482(F), 483(F), 484(F)
structural reaction injection molding (SRIM), 297, 298(F), 497
stump Lockbolts, 323
superplastic forming and diffusion bonding (SPF/DB), 563
Suppliers of Advanced Composites Manufacturers Association (SACMA), 351
SACMA SRM-3, 357
SACMA SRM-5, 357
SACMA SRM-7, 356
SACMA SRM-8, 357
SACMA SRM-13, 354
Supral sheet, 192
Sylramic, 578

T

tackifier, 160–161
tagalong test specimens, 91
tap testing, 334–335
tape, definition of, 32
tape casting, 559
tape wrapping, 125
Tedlar, 132
Teflon, 132
test methods, mechanical property, 355
adhesive peel testing, 364, 367, 369(F), 370(F)
adhesive shear testing, 364, 365–366(F), 367(F), 368(F), 369(F)
bolt shearing strength, 358, 360–361(F), 362(F)
compression strength after impact, 361–362, 363(F)
compression testing, 354–355(F), 356(F)
data analysis, 369–371(T)
double cantilever beam test, 362, 364, 365(F)
environmental conditioning, 367–369, 372(F)
flatwise tension test, 361, 362(F)
flexure testing, 352–353(F)
fracture toughness testing, 362, 364(F), 365(F)
honeycomb flatwise tension, 367, 371(F)
open-hole compression testing, 357–358
open-hole tension test, 357, 360(F)
overview, 351
shear testing, 356–357(F), 358(F), 359(F), 360(F)
specimen preparation, 351–352(F)
tension testing, 353–354(F)
tetraethylorthosilicate (TEOS), 587
tetraglycidyl methylene dianiline (TGMDA), 67, 68(F), 70, 92(F), 94, 95
tetraglycidyl-4,40-diaminodiphenylmethane (TGGDM), 67, 68(F)
tex, 37
Thermabond process, 195
thermal analysis, 94–96(F), 97(F)
thermal mechanical analysis (TMA), 97–99(F)
thermal spiking, 409–410, 411(F), 416
thermoforming
continuous consolidation process, 192, 196(F)
diaphragm forming, 191, 195(F)
dies for, 188
heating methods, 188
interply slip, 190, 191(F), 192(F), 194(F)
intraply slip, 190, 191(F), 192(F)
press, 189, 190(F)
resin percolation, 189, 191(F), 192(F)
roll forming process, 192, 197(F)
rubber block forming, 188–189(F)
setup, 186–188(F)
springs, 191, 194(F)
transverse squeeze flow, 189–190, 191(F), 192(F), 193(F)
thermogravimetric analysis (TGA), 96
thermo-oxidative stability (TOS), 415–416(F), 417(F)
thermoplastic composite fabrication processes
thermoforming (*see* thermoforming)
thermoplastic consolidation, 183–186(F), 187(F)
thermoplastic joining (*see* thermoplastic joining)
thermoplastic consolidation, 183–186(F), 187(F)
thermoplastic joining
adhesive bonding, 193–194
dual resin bonding, 195, 198(F)

induction welding, 197–198, 200(F)
mechanical fastening, 194
melt fusion, 194–195
overview, 192–193
resistance welding, 195–196, 199(F)
ultrasonic welding, 196–197
thermoplastics
overview, 81–82
thermoplastic composite matrices, 82–87(F), 88(F)
thermoplastic composite product forms, 87–90(F)
thermoset composite fabrication processes
filament winding, 141–146(F)
lay-up processes
overview, 119
prepreg lay-up (*see* prepreg lay-up)
wet lay-up, 119–122(F)
liquid molding (*see* liquid molding)
low-temperature curing/vacuum bag (LTVB) systems, 137–141(F), 142(F), 143(F)
overview, 119
pultrusion, 175–181(F)
resin film infusion (RFI), 174–175, 176(F), 177(F), 178(F), 179(F)
thermosets, 64–65(F,T)
thermosets, toughened
interlayering, 80–81(F)
network alteration, 76–77, 78(F)
overview, 75–76(F), 77(F)
rubber elastomer second phase toughening, 77–80(F)
thermoplastic elastomeric toughening, 80(F)
thixotropy, 120–121
titanium
adhesive bonding primers, 243–244(F)
adhesive bonding surface preparation, 242–243
drilling, 313
Ti-6Al-4V, 14, 15(F), 313, 320, 557, 566, 567(T)
Ti-6Al-4V pin, 322, 323
Ti-15Mo-2.8Nb-3Al-0.2Si, 557
Ti-15V-3Cr-3Sn-3Al (Ti-15- 3-3-3), 557
titanium matrix composites (TMCs)
consolidation procedures, 560–562(F)
continuous-fiber reinforced (TMCs), 554–557(F,T)
continuous-fiber TMC processing methods, 557–560(T)
particle-reinforced, 566–567(T), 568(F)
secondary fabrication of, 562–566(F), 567(F)
in situ composites, 566–567
tool mark-off, 397, 398(F), 399(F)
tow placement machine, 127–130(F)
tows, 31, 49
tracer yarns, 51–52
trade studies, 498–499(F)
transfer molding, 295, 296(F)
triglycidyl derivative of p-aminophenol (TGAP), 68, 69(F)
trimming
abrasive water jet trimming, 308, 309(F)
edge trimming, 307
manual edge-trimming, 307–308(F)
Tsai-Wu failure criterion, 443–444, 445(F)
turbostatic graphite, 45
Tyranno, 577(T), 578

U

ultra-high molecular weight polyethylene (UHMWPE), 41–42(F), 490
ultrasonic horn, 196
ultraviolet (UV) radiation, 411
Upilex, 184
Upilex-R, 192
Upilex-S, 192

V

V50 parameter, 391
vacuum bag process, 122
vacuum bagging, 131–133(F), 528
vacuum bags, 121, 133, 173, 529, 531(F)
vacuum debulk, 115, 124, 140. *See also* debulking
vacuum forming, 124–125, 126(F)
vacuum hot pressing (VHP), 559–560(F)
vacuum pressure
bonded repairs, 523, 526
condensation curing systems, 136
continuous-fiber processes, 497
honeycomb bonding, 267
LTVB systems, 139
pressure infiltration casting (PIC), 546
resin injection, 163
sol-gel infiltration, 589
VARTM, 170, 172, 173
vacuum-assisted resin transfer molding (VARTM), 166, 170, 172–174(F), 498
veil, 490
verifilm, 249
viscosity
addition curing thermoset composites, 135, 136(F)
anhydride curing agents, 70
autohesion, 90
comparison: low-viscosity and paste epoxy adhesives, 247(T)
comparison: toughened and untoughened epoxy, 166(F)
condensation curing systems, 135
cure monitoring techniques, 232
DGEBA resins, 67–68(T)
epoxy resins, 67, 68(T)
high-viscosity thixotropic epoxy adhesives, 517
injection repairs, 518–519(F)
low-temperature curing/vacuum bag (LTVB) systems, 139
LTVB systems, 139
matrix resin systems, 63
polyester resins, 66
polymer matrix composites, 206–207(F), 208(F)
powder processing, 582
prepreg manufacturing, 57
resin, 162–163(T)
resin viscosity, determinant of, 121
RFI process, 174
rheological testing, 92–94(F)
shear thinning, 88
slurry casting—compocasting, 544
sol-gel infiltration, 589

viscosity (continued)
stir casting, 543, 544
thermal analysis, 95–96
thermoplastic composite matrices, 87
thermoplastic elastomeric toughening, 80
thermoplastics, 81
thermoset injection molding, 305
VARTM, 173
wet winding, 145–146
whiskers, 582
voids (use of term), 219, 393. *See also* voids and porosity
voids and porosity
carbon fiber composites, 383
composite mechanical properties, 393–397(F)
condensation curing systems, 135
continuous-fiber processes, 497
filament winding, 146
heat transfer, 209
matrix selection, 495
polyimide resins, 72, 74
polymer matrix composites, 219–226(F)
resin flow, 213, 214
resin injection, 162, 163, 164
thermosets, 65
void submodel, 201
wet lay-up, 122

W

warp, 49
washers, 320, 323
weaves
basket, 50
leno/mock leno, 50–51
overview, 49
plain, 49–50
satin, 50
styles, 54(T)
twill, 50
welding
induction welding, 197–198, 200(F)
resistance welding, 195–196, 199(F)
ultrasonic welding, 196–197
wet lay-up, 496, 497
bonded repairs, 523
composite tool fabrication, 115
continuous-fiber processes, 496
fabrication process selection, 496
glass fiber composites, 375
laminates, 503
low-temperature curing/vacuum bag (LTVB) systems, 138, 141
thermoset composite fabrication processes, 119–122(F)
vacuum bag cures, 531
wet lay-up patches, 523, 527, 530(F)
whiskers. *See also* reinforcements
ceramic matrix composites, 575, 577(T)
discontinuous MMCs, secondary processing of, 549
MMCs, 537
PAA process, 239, 240(F), 241
PIP processes, 588
powder metallurgy (PM) methods, 548(F), 549
powder processing, 582
reinforcements, 31
silicon carbide, 539(F), 542
slurry casting—compocasting, 544
stir casting, 543(F)
wind power applications, 23–24, 27(F)
winding. *See* filament winding
working life, 251
woven cloth, definition of, 32
woven fabrics, 49–52(F), 53(F), 54(F,T), 149
three-dimensional, 149–151(F), 152(F)

Y

yarn, 31, 39